



UNIVERSITY OF NIŠ
FACULTY OF MECHANICAL ENGINEERING
Department for Production, IT and Management



34th INTERNATIONAL CONFERENCE ON PRODUCTION ENGINEERING

PROCEEDINGS



Sponsor General

Ministry of Education and Science, Republic of Serbia

September 28-30 2011,
Niš
Serbia

PROCEEDINGS OF THE 34th INTERNATIONAL CONFERENCE ON PRODUCTION
ENGINEERING NIŠ, 2011.

Izdavač: Univerzitet u Nišu, Mašinski
fakultet u Nišu
Aleksandra Medvedeva br 14
18000 Niš
Srbija

Publisher: UNIVERSITY OF NIŠ,
FACULTY OF MECHANICAL
ENGINEERING IN NIŠ
Aleksandra Medvedeva br 14
18000 Niš
Serbia

Za izdavača:
For publisher:

Prof.dr Vlastimir NIKOLIĆ, dekan fakulteta

Glavni i odgovorni urednik:
Editor:

Prof.dr Miroslav TRAJANOVIĆ

Tehnička obrada:
Technical treatment:

Milan Zdravković
Nikola Vitković
Marko Veselinović
Dalibor Stevanović

Rukopis predat u štampu:
Manuscript submitted for publication:
Izdanje:
Printing:
Tiraž:
Circulation:

20.09.2011. godine
Septembar 20.2011
prvo
1st
150

Štampa:
Printed by:

UNIGRAF – X – COPY
18000 Niš, Vojvode Putnika

ISBN: 978 – 86 – 6055 – 019 – 6



Izdavanje zbornika radova, organizovanje i održavanje 34 Međunarodne konferencije proizvodnog mašinstva Srbije pomogao je pokrovitelj
Ministarstvo prosvete i nauke Republike Srbije
Financing of the Proceedings was sponsored by the **Ministry of Education and Science of the Republic of Serbia**



34th INTERNATIONAL CONFERENCE ON
PRODUCTION ENGINEERING
29. - 30. September 2011, Niš, Serbia
University of Niš, Faculty of Mechanical Engineering



ORGANIZING INSTITUTIONS:

Association of production engineering scientific research institutions of Serbia

- Unverzitet u Nišu, Mašinski fakultet u Nišu – Katedra za proizvodno informacione tehnologije i menadžment
- Mašinski fakultet, Beograd
- Mašinski fakultet, Kragujevac
- Fakultet tehničkih nauka – Departman za proizvodno mašinstvo, Novi Sad
- Fakultet tehničkih nauka – Departman za industrijsko inženjerstvo i menadžment, Novi Sad
- Tehnički fakultet, Čačak
- Mašinski fakultet, Kraljevo
- Fakultet tehničkih nauka, Kosovska Mitrovica
- LOLA Institut, Beograd

ORGANIZERS:

UNIVERZITET U NIŠU
MAŠINSKI FAKULTET U NIŠU
Katedra za proizvodno informacione tehnologije i menadžment
Aleksandra Medvedeva br 14
18000 Niš
Tel. +381 (18) 500 – 669; Fax. +381 (18) 588 – 244
Web: <http://www.masfak.ni.ac.rs>
email: spms@masfak.ni.ac.rs

CONFERENCE VENUE:

Niš
Hotel Tami residence
18000 Niš, Durmitorska – prilaz bb
Tel. +381 (18) 505 – 800, 282 – 222
Web: <http://www.tamiresidence.com>
email: info@tamiresidence.com



34th INTERNATIONAL CONFERENCE ON
PRODUCTION ENGINEERING
29. - 30. September 2011, Niš, Serbia
University of Niš, Faculty of Mechanical Engineering



SCIENTIFIC COMMITTEE

1. Prof. dr Velibor MARINKOVIĆ, MF, Niš, SRB, president
 2. Prof. dr Sergey ALEKSANDROV, RA of S, Moscow, RUS
 3. Prof. dr Miroslav BADIDA, ME, Košice, SK
 4. Prof. dr Nikolai BOBYR, KPI, Kiev, UA
 5. Prof. dr Pavao BOJANIĆ, MF, Beograd, SRB
 6. Prof. dr Alan BRAMLEY, University Bath, UK
 7. Prof. dr Aleksandar BUKVIĆ, MF, I. Sarajevo, RS, BIH
 8. Prof. dr Miodrag BULATOVIĆ, MF, Podgorica, MNE
 9. Prof. dr Ilija ČOSIĆ, FTN, N. Sad, SR
 10. Prof. dr Cristian DOICIN, TU, Bucharest, RO
 11. Prof. dr Dragan DOMAZET, FIT, Beograd, SRB
 12. Prof. dr Ljubodrag ĐORĐEVIĆ, VTMŠ, Trstenik, SRB
 13. Prof. dr Kornel EHMANN, Northwestern U., Chic., USA
 14. Prof. dr Miloš GLAVONJIĆ, MF, Beograd, SRB
 15. Dr Peter HARTLEY, University Birmingham, UK
 16. Prof. dr Janko HODOLIĆ, FTN, N. Sad, SRB
 17. Prof. dr Vid JOVIŠEVIĆ, MF, Banja Luka, RS, BIH
 18. Prof. dr Milan JURKOVIĆ, MF, Bihać, BIH
 19. Prof. dr Klaus KABITZSCH, TU, Dresden, D
 20. Prof. dr Damir KAKAŠ, FTN, N. Sad, SRB
 21. Prof. dr Mochael KHEIFETZ, PSU, Novopolotsk, BY
 22. Prof. dr Sergey KLIMENKO, ISM, Kiev, UA
 23. Prof. dr Pavel KOVAČ, FTN, N. Sad, SRB
 24. Prof. dr Karl KUZMAN, FS, Ljubljana, SLO
 25. Dr Vladimir KVRGIĆ, LOLA Institut, Beograd, SRB
 26. Prof. dr Miodrag LAZIĆ, MF, Kragujevac, SRB
 27. Prof. dr Ljubomir LUKIĆ, MF, Kraljevo, SRB
 28. Prof. dr Vidosav MAJSTOROVIĆ, MF, Beograd, SRB
 29. Prof. dr Miodrag MANIĆ, MF, Niš, SRB
 30. Prof. dr Ostoja MILETIĆ, MF, Banja Luka, RS, BIH
 31. Prof. dr Dragan MILUTINOVIĆ, MF, Beograd, SRB
 32. Prof. dr Bogdan NEDIĆ, MF, Kragujevac, SRB
 33. Prof. dr Mircea NICOARA, FM, Temisoara, RO
 34. Prof. dr Herbert OSANNA, TU, Wien, A
 35. Prof. dr Zoran PANDILOV, MF, Skopje, MK
 36. Prof. dr Miroslav PILIPOVIĆ, MF, Beograd, SRB
 37. Prof. dr Miroslav PLANČAK, FTN, N. Sad, SRB
 38. Prof. dr Snežana RADONJIĆ, TF, Čačak, SRB
 39. Prof. dr Bela SABO, FTN, N. Sad, SRB
 40. Prof. dr Mirko SOKOVIĆ, FS, Ljubljana, SLO
 41. Prof. dr Bogdan SOVILJ, FTN, N. Sad, SRB
 42. Prof. dr Victor STARKOV, Stankin, Moscow, RUS
 43. Prof. dr Milentije STEFANOVIĆ, MF, Kragujevac, SRB
 44. Prof. dr Ljubodrag TANOVIĆ, MF, Beograd, SRB
 45. Prof. dr Tomislav TODIĆ, FTN, K. Mitrovica, SRB
 46. Prof. dr Velimir TODIĆ, FTN, N. Sad, SRB
 47. Prof. dr Dragiša VILOTIĆ, FTN, N. Sad, SRB
 48. Prof. dr Frank VOLLERTSEN, BIAS, Bremen, D
 49. Prof. dr Radomir VUKASOJEVIĆ, MF, Podgorica, MNE
 50. Prof. dr Miomir VUKIĆEVIĆ, MF, Kraljevo, SRB
 51. Prof. dr Milan ZELJKOVIĆ, FTN, N. Sad, SRB
-

Members of the Honorary Committee

1. Dipl. ing. Mile BENEDETIĆ, LOLA Institut, Beograd
2. Prof. dr Branislav DEVEDŽIĆ, MF, Kragujevac
3. Prof. dr Ratko GATALO, FTN, Novi Sad
4. Prof. dr Branko IVKOVIĆ, Mašinski fakultet, Kragujevac
5. Prof. dr Ratomir JEČMENICA, Tehnički fakultet, Čačak
6. Prof. dr Milenko JOVIČIĆ, Mašinski fakultet, Beograd
7. Prof. dr Milisav KALAJDŽIĆ, Mašinski fakultet, Beograd
8. Prof. dr Vučko MEČANIN, Mašinski fakultet, Kraljevo
9. Prof. dr Vladimir MILAČIĆ, Mašinski fakultet, Beograd
10. Prof. dr Dragoje MILIKIĆ, FTN, Novi Sad
11. Prof. dr Mihajlo MILOJEVIĆ, Mašinski fakultet, Kraljevo
12. Prof. dr Predrag POPOVIĆ, Mašinski fakultet, Niš
13. Prof. dr Jožef REKECKI, FTN, Novi Sad
14. Prof. dr Sava SEKULIĆ, FTN, Novi Sad
15. Prof. dr Joko STANIĆ, Mašinski fakultet, Beograd
16. Prof. dr Vojislav STOILJKOVIĆ, Mašinski fakultet, Niš
17. Prof. dr Sreten UROŠEVIĆ, Tehnički fakultet, Čačak
18. Prof. dr Svetislav ZARIĆ, Mašinski fakultet, Beograd
19. Prof. dr Dragutin ZELENOVIĆ, FTN, Novi Sad

ORGANISATIONAL COMMITTEE

1. Dr Miroslav Trajanović, president
 2. Dr Miodrag Stojiljković
 3. Dr Dragan Temeljkovski
 4. Dr Miroslav Radovanović
 5. Dr Peda Milosavljević
 6. Dr Predrag Janković
 7. Dr Vladislav Blagojević
 8. Mr Nikola Korunović
 9. Mr Milan Zdravković
 10. Nikola Vitković
 11. Dr Dragoljub Lazarević
 12. Dr Bojan Rančić
 13. Dr Goran Radenković
 14. Dr Saša Randelović
 15. Dr Dragan Mišić
 16. Mr Miloš Stojković
 17. Mr Jelena Milovanović
 18. Dušan Petković
 19. Milan Trifunović
-



34th INTERNATIONAL CONFERENCE ON
PRODUCTION ENGINEERING
29. - 30. September 2011, Niš, Serbia
University of Niš, Faculty of Mechanical Engineering



*ORGANIZER OF CONFERENCE ON PRODUCTION ENGINEERING OF
YUGOSLAVIA / SERBIA AND MONTENEGRO / SERBIA 1965-2011*

I	Beograd	Mašinski fakultet	1965.
II	Zagreb	Fakultet za strojarstvo i brodogradnju	1966.
III	Ljubljana	Fakultet za strojninstvo	1967.
IV	Sarajevo	Mašinski fakultet	1968.
V	Kragujevac	Mašinski fakultet	1969.
VI	Opatija	Fakultet za strojarstvo i brodogradnju Zagreb	1970.
VII	Novi Sad	Mašinski fakultet	1971.
VIII	Ljubljana	Fakultet za strojninstvo	1973.
IX	Niš	Masinski fakultet	1974.
X	Beograd	Mašinski fakultet	1975.
XI	Ohrid	Mašinski fakultet Skoplje	1977.
XII	Maribor	Visoka tehnička skola	1978.
XIII	Banja Luka	Mašinski fakultet	1979.
XIV	Čacak	Pedagosko-tehnički fakultet	1980.
XV	Novi Sad	Fakultet tehničkih nauka	1981.
XVI	Mostar	Mašinski fakultet	1982.
XVII	Budva	Mašinski fakultet Podgorica	1983.
XVIII	Niš	Mašinski fakultet	1984.
XIX	Kragujevac	Mašinski fakultet	1985.
XX	Beograd	Mašinski fakultet	1986.
XXI	Opatija	Tehnički fakultet Rijeka	1987.
XXII	Ohrid	Mašinski fakultet Skoplje	1989.
XXIII	Zagreb	(nije održano)	1991.
XXIV	Novi Sad	Fakultet tehničkih nauka	1992.
XXV	Beograd	Mašinski fakultet	1994.
XXVI	Podgorica	Mašinski fakultet	1996.
XXVII	Niš	Mašinski fakultet	1998.
XXVIII	Kraljevo	Mašinski fakultet	2000.
XXIX	Beograd	LOLA Institut	2002.
XXX	Čacak	Tehnički fakultet i Viša tehnička škola	2005.
XXXI	Kragujevac	Mašinski fakultet	2006.
XXXII	Novi Sad	Fakultet tehničkih nauka	2008.
XXXIII	Beograd	Mašinski fakultet	2009.
XXXIV	Niš	Univerzitet u Nišu, Mašinski fakultet u Nišu	2011.

FOREWORD

The first Scientific conference on production engineering of ex Yugoslavia was held in Belgrade, in 1965, initiated by Prof. Vladimir Šolaja. This also marked the forming of the Association of scientific and research institutions in production engineering, which included faculties of mechanical engineering and research institutes of almost all major cities of the former federation. The Association of scientific and research institutions in production engineering was reinstated, under new circumstances, in 1994. In 2009, the Executive Board of the Association delegated the organization of 34rd Conference to the University of Niš, Faculty of Mechanical Engineering in Niš.

The organizer of this Conference, the Department for Production, IT and Management of the Faculty of Mechanical Engineering, University of Niš, has ambitiously approached the task of organizing this Conference, setting two primary goals: (1) to point to the current state of research in the area of production engineering in the region of SEE as well as rest of Europe, (2) to use presence of highly competent professionals to initiate discussions on boosting of production in SEE.

In order to meet these goals, the organizing committee has made efforts to attract production engineering community to present the results of their research. A total of 180 papers were registered. All papers submitted for presentation passed through a double blind review process and were evaluated by two reviewers. After peer review process 119 papers were accepted for presentation. Those authors whose papers were chosen for presentation at the conference submitted manuscripts to be published in these Proceedings. The authors are from 16 European countries: Austria, Bosnia and Herzegovina, France, Germany, Montenegro, Slovenia, Slovakia, Czech, Croatia, Poland, Romania, Belarus, Macedonia, Greece, United Kingdom and Serbia.

Also, four invited lectures will be given by distinguished professors. One of these lectures is an introduction to a roundtable on the theme: "Boosting production in SEE".

The Ministry for Education and Science of Serbia, together with donors from industry, have financially supported the organization of this Conference, for which the organizer wishes to express gratitude on this occasion.

On behalf of the organizing committee, I wish to express my gratitude to all domestic and foreign contributors, as well as the editing board for the performed reviews.

Niš

September 20, 2011

*President of the organizing
committee*

Prof. Dr. Miroslav Trajanović

*President of the Executive Board
of the Association*

Prof. Dr. Velibor Marinković



Contents

PLENARY PRESENTATIONS:

Invited lets to res

Herve Panetto SYSTEM ENGINEERING FOR SYSTEMS INTEROPERABILITY IN MANUFACTURING ENVIRONMENT.....	3
Vidosav Majstorović QUALITY MANAGEMENT – STATE OF THE ART AND FUTURE DEVELOPMENT.....	5
Dorian Marjanović DESIGN RESEARCH – THE MOMENTUM AND EXPECTATIONS.....	13
Petar Petrović, Vladimir Milačić NATIONAL TECHNOLOGY PLATFORMS OF SERBIA.....	15

SECTION A:

Machining technologies

Uros Zuperl, Franc Cus NEURAL NETWORK ALGORITHM FOR ON-LINE TOOL BREAKAGE DETECTION.....	29
Milan Milutinović, Ljubodrag Tanović THE EFFECTS OF TOOL FLANK WEAR ON TOOL LIFE.....	33
Obrad Spaić, Zdravko Krivokapić, Rade Ivanković MATHEMATICAL MODELLING OF CUTTING FORCE AS THE MOST RELIABLE INFORMATION BEARER ON CUTTING TOOLS WEARING PHENOMENON.....	37
Ljubodrag Tanović, Pavao Bojanić, Radovan Puzović, Mihajlo Popović, Goran Mladenović ANALYSIS OF STONE MICRO-CUTTING MECHANISM USING THE EXAMPLE OF GRANITE AND MARBLE GRINDING.....	41
Marko Kovačević, Miloš Madić, Velibor Marinković SOFTWARE PROTOTYPE FOR ANALYZING MANUFACTURING PROCESS MODELS.....	45
Diana Baila CONTRIBUTIONS TO MANAGEMENT SWARF HIGH-SPEED MACHINE TOOLS.....	49



Dijana Nadarević, Mirko Soković STEEL VALVE PLATE GRINDING.....	53
Milenko Sekulić, Miodrag Hadžistević, Zoran Jurković, Pavel Kovač, Marin Gostimirović APPLICATION OF TAGUCHI METHOD IN THE OPTIMIZATION OF FACE MILLING PARAMETERS.....	57
Jozef Peterka, Martin Kováč, Marek Zvončan INFLUENCE OF TOOL BALANCING ON MACHINED SURFACE QUALITY IN HIGH SPEED MACHINING.....	61
Aco Antić, Milan Zeljković, Aleksandar Živković FEM MODELING AND EXPERIMENTAL VERIFICATION OF CUTTING TOOL VIBRATIONS.....	65
Miloš Madić, Goran Radenković, Miroslav Radovanović PREDICTION OF MECHANICAL PROPERTIES AND MACHINABILITY OF CAST COPPER ALLOYS USING ANN APPROACH.....	69

SECTION B:

Surface engineering and nanotechnologies

Ilare BORDEASU, Mircea Octavian POPOVICIU, Ion MITELEA, Alin Dan JURCHELA RESEARCH ON CAVITATION EROSION BEHAVIOR OF STAINLESS STEELS WITH CONSTANT CHROMIUM AND VARIABLE NICKEL CONTENT.....	75
Damir Kakaš, Branko Škorić, Aleksandar Miletić, Pal Terek, Lazar Kovačević, Marko Vilotić INFLUENCE OF SUBSTRATE ROUGHNESS ON ADHESION STRENGTH OF HARD TiN FILMS.....	79
Damir Kakaš, Branko Škorić, Pal Terek, Aleksandar Miletić, Lazar Kovačević, Marko Vilotić MECHANICAL PROPERTIES OF TiN COATINGS DEPOSITED AT DIFFERENT TEMPERATURES BY IBAD.....	83
Bogdan Nedić, Desimir Jovanović, Gordana Lakić Globočki SCRATCH TESTING OF Zn COATING SURFACES.....	87
Sebastian Baloš, Lepasava Sidanin, Dragan Rajnović, Olivera Erić ADI MATERIALS FOR BALLISTIC PROTECTION.....	91
Jasna Radulović, Predrag Petrović OBSERVATION ON THE USE OF THIN FERROMAGNETIC PLATES IN PRESENCE OF EXTERNAL MAGNETIC FIELD.....	95



Aleksandar Todić, Dejan Čikara, Tomislav Todić, Branko Pejović, Bogdan Ćirković, Ivica Čamagić THE EFFECT OF VANADIUM CONTENT ON MECHANICAL PROPERTIES AND STRUCTURE OF SELF-TEMPERED STEEL X160CrMo12-1.....	99
Radovan Ćirić, Emil Veg, Biljana Savić, Zvonimir Jugović, Radomir Slavković ANALYSIS OF THE IMPACT OF EXPLOSION HARDENING PROCEDURE ON CHARACTERISTICS OF SURFACE LAYER OF ELEMENTS EXPOSED TO ABRASION.....	103
SECTION C:	
Production engineering – new technologies and globalisation of engineering	
Mijodrag Milošević, Velimir Todić, Dejan Lukić WEB-BASED COLLABORATIVE ENVIRONMENT FOR PROCESS PLANNING	109
Slobodan Tabaković, Cvijetin Mladenović, Milan Zeljković, Ratko GATALO ANALYSIS OF KINEMATIC CHARACTERISTICS OF MACHINE TOOLS USING A VIRTUAL MODEL.....	113
Đorđe Čiča, M. Zeljković, G. Lakić-Globočki, B. Sredanović, S. Borojević MODELING OF DYNAMICAL BEHAVIOR SPINDLE – HOLDER – TOOL ASSEMBLY.....	117
Bogdan Ćirković, Ivica Čamagić, Nemanja Vasić COMPOSITE MATERIALS SUCH APSORPTION MATERIALS FOR SUPPORTING STRUCTURES OF MACHINES.....	121
Predrag Ćosić, Dragutin Lisjak, Valentina Latin MULTIOBJECTIVE OPTIMIZATION – POSIBILITY FOR PRODUCTION IMPROVEMENT.....	125
Vladimir Kvrgić, Miroslav Vasić, Vladimir Čarapić, Jelena Vidaković, Velimir Komadinić C RESEARCH AND DEVELOPMENT OF THE NEW GENERATION FIVE AXIS VERTICAL TURNING CENTRES.....	129
Robert Cep, Jan Strbka, Lenka Cepova DEPENDENCE OF SURFACE ROUGHNESS FOR SHAFT PACKING.....	133
SECTION D:	
Metrology, quality systems and quality management	
Milan Blagojević, Miroslav Živković, Ana Pavlović QUALITY CONTROL OF CONTOUR VERIFIER USING PHOTOGRAMMETRIC MEASURING SYSTEMS.....	139



Miodrag Hadžistević, Janko Hodolič, Igor Budak, Đorđe Vukelić, Branko Štrbac RESULTS OF THE ANALYSIS ON STYLUS CALIBRATION OF COORDINATE MEASURING MACHINE (CMM).....	143
Krzysztof Stepień RESEARCH ON INFLUENCE OF THE SENSOR POSITION ON THE RESULT OF THE V-BLOCK CYLINDRICITY MEASUREMENT.....	147
Milan Kolarević, Branko Radičević, Miomir Vukićević, Mišo Bjelić, Ljubinko Cvetković IMPROVING PRODUCT QUALITY OF SECURITY EQUIPMENT USING SPC...	151
Vladan Radlovački, Radmila Jovanović, Bato Kamberović, Milan Delić, Srđan Vulanović THE ROLE OF MANAGERS IN IMPLEMENTING QUALITY MANAGEMENT STANDARDS.....	155
Peđa Milosavljević, Dragoljub Živković, Predrag Janković, Srđan Mladenović THE POSSIBILITIES FOR IMPROVEMENT OF THE MAINTENANCE PROCESSES IN THE COMPANIES.....	159
Bojan Rančić, Predrag Janković, Srđan Mladenović, Slaviša Planić DESIGN AND TENSIOMETRIC ANALYSIS OF THE C-CLAMP FOR RAILROAD TRACKS.....	163
Slavenko Stojadinović, Vidosav Majstorović METROLOGICAL PRIMITIVES IN PRODUCTION METROLOGY – ONTOLOGICAL APPROACH.....	167
Remigiusz Labudzki THE USE OF MACHINE VISION TO RECOGNIZE OBJECTS.....	171
Jelena Micevska, Zoran Spiroski, Jasmina Čaloska, Atanas Kočov PRODUCT QUALITY CONTROL BY USING REVERSE ENGINEERING.....	175

SECTION E:

CAx technologies (CAD/CAM/CAPP/CAE systems) and CIM systems

Jozef Novak-Marcincin, Miroslav Janak, Ludmila Novakova-Marcincinova, Veronika Fecova, Jozef Barna APPLICATION OF THE COMPUTER AIDED SELECTION OF OPTIMAL CNC MILLING STRATEGY.....	181
Janko Hodolič, Tatjana Puškar, Igor Bešić CURRENT STATUS AND FUTURE TRENDS IN DENTAL CAM RESTORATIVE SYSTEMS.....	185



Goran Devedžić, Sasa Ćuković, Branko Ristić, Suzana Petrović, Michele Fiorentino, Tanja Luković COMBINED REGISTRATION OF HUMAN MUSCULOSKELETAL SYSTEM...	189
Radomir Slavković, Zvonimir Jugović, Ivan Milićević, Marko Popović, Radomir Radiša OPTIMIZATION OF CAD/CAM/CAE DESIGN OF THE CONNECTING PART OF EXCAVATOR'S TOOTH THROUGH THE SIMULATION OF MANUFACTURING TECHNOLOGY.....	193
Stevo Borojević, Vid Jovišević, Gordana Globočki Lakić, Đorđe Čiča, Branislav Sredanović IDENTIFICATION OF FACE FUNCTIONALITY WITH PROGRAM SYSTEM FOR PURPOSE OF MODULAR FIXTURE DESIGN.....	197
Dragan Marinković, Manfred Zehn FEM IN VIRTUAL REALITY CONCEPT.....	201
Ionut Ghionea, Ioan Tanase, Adrian Ghionea, Cristian Tarba APPLICATIONS BY CAM AND FEM SIMULATIONS IN ESTABLISHING THE MILLING CONDITIONS FOR PARTS WITH THIN WALLS.....	205
Nikola Korunović, Miroslav Trajanović, Miloš Stojković, Nikola Vitković, Milan Trifunović, Jelena Milovanović TIRE TREAD MODELING FOR FEA	209
Ivan Matin, Miodrag Hadžistević, Janko Hodolič, Đorđe Vukelić AN INTERACTIVE CAD/CAE SYSTEM FOR MOLD DESIGN.....	213
Miroslav Pilipović, Ivan Danilov, Nikola Lukić, Petar Petrović VIRTUAL MANUFACTURING – ADVANCED MANUFACTURING EXAMPLES.....	217

SECTION F:

Education in the field of production engineering

Engineering ethics

Product development – product design

Production system management

Revitalization, reengineering and maintenance of manufacturing systems

Miloš Ristić, Miodrag Manić, Boban Cvetanović MANUFACTURABILITY ANALYSIS OF DIE-CAST PARTS.....	223
Sofija Sidorenko, Jelena Micevska, Ile Mircheski DESIGN OF MODULAR WHEELCHAIR FOR CHILDREN WITH CEREBRAL PALSY.....	227



Dragan Rajnović, Olivera Erić, Milica Damjanović, Sebastian Baloš, Leposava Sidanin THE CRACK PROPAGATION STUDY IN ALLOYED ADI MATERIALS.....	231
Suzana Petrović, Milan Erić, Goran Devedžić, Miodrag Manić, Saša Ćuković, Miloš Ćirović COLLABORATION AND COMMUNICATION IN INTEGRATED SYSTEM OF DIGITAL MANUFACTURING.....	235
Vladimir Simić, Branka Dimitrijević MODELLING OF PRODUCTION SYSTEMS FOR END-OF-LIFE VEHICLES PROCESSING.....	239
Dragan Mišić, Nikola Vitković, Miloš Stojković, Milan Zdravković, Miroslav Trajanović RESOURCES MANAGEMENT IN WORKFLOW MANAGEMENT SYSTEMS...	243
Nedim Ganibegović, Sandira Eljsan STEAM TURBINE CASINGS REVITALIZATION.....	249
Tadej Tasner, Darko Lovrec COMPARISON OF MODERN ELECTROHYDRAULIC SYSTEMS.....	253
Goran Slavković, Žarko Spasić HYBRID CONTROLLER FOR SYSTEM MANAGEMENT OF INTEGRATED UNIVERSITY.....	257
Guenther Poszvek ESTABLISHMENT OF A LECTURE SERIES ON LIFE CYCLE DESIGN – ECODESIGN.....	263
Dragan Temeljkovski, Predrag Popović, Bojan Rančić, Petar Đekić EVALUATION OF PRODUCT AND PRODUCTION TECHNOLOGIES QUALITY METHOD OF SUPERIORITY AND INFERIORITY.....	267

SECTION G:

Forming and shaping technologies

Neculai Nanu, Gheorghe Brabie THE INFLUENCE OF RESIDUAL STRESS DISTRIBUTION ON THE SPRINGBACK PARAMETERS IN THE CASE OF CYLINDRICAL DRAWN PARTS.....	273
Srbislav Aleksandrović, Tomislav Vujinović, Milentije Stefanović, Vukić Lazić, Dragan Adamović VARIABLE CONTACT PRESSURE AND VARIABLE DRAWBEAD HEIGHT INFLUENCE ON DEEP DRAWING OF Al ALLOYS SHEETS.....	277



Bojan Rančić, Predrag Janković, Dragan Temeljkovski DETERMINING SOME PARAMETERS IN THE OIL HYDRAULIC PROCESS OF SQUARE CUPS DEEP DRAWING.....	281
Bojan Rančić, Predrag Janković, Velibor Marinković ASSESSMENT THE NUMBER OF DEEP DRAWING STEPS OF CYLINDRICAL CUPS WITHOUT CALCULATION.....	285
Dragan Adamović, Milentije Stefanović, Srbislav Aleksandrović, Miroslav Živković, Zvonko Gulišija, Slaviša Đačić THE INFLUENCE OF TOOL SURFACE CONDITION ON IRONING PROCESS EXECUTION.....	289
Zdravko Božičković, Ranko Radonjić, Ranko Božičković THE SIMULATION OF DISCONTINUOUS TIN BENDING IN THE PROCESS OF FORMING ROUND CONICAL TUBE.....	293
Milan Jurković, Zoran Jurković, Asim Jušić, Vesna Mandić EXPERIMENTAL ANALYSIS AND MATHEMATICAL MODELLING OF THE ROLLING FORCE.....	297
Dragiša Vilotić, Miroslav Plančak, Sergei Alexandrov, Aljoša Ivanišević, Dejan Movrin, Mladomir Milutinović NUMERICAL SIMULATION OF UPSETTING OF PRISMATIC BILLETS BY V- SHAPE DIES WITH EXPERIMENTAL VERIFICATION.....	301
Milan Lazarević, Dejan Lazarević, Miloš Jovanović, Saša Randelović THE APPLICATION OF ADAPTIVE FEM METHOD TO STRESS AND STRAIN ANALYSIS OF COLD FORGING PROCESS.....	305
Mladomir Milutinović, Dragiša Vilotić, Tatjana Puškar, Dubravka Marković, Aljoša Ivanišević, Michal Potran METAL FORMING TECHNOLOGIES IN DENTAL COMPONENTS PRODUCTION.....	309

SECTION H:

Rapid prototyping

Reverse engineering

Miroslav Plančak, Tatjana Puškar, Ognjan Lužanin, Dubravka Marković, Plavka Skakun, Dejan Movrin SOME ASPECTS OF RAPID PROTOTYPING APPLICATION IN MEDICINE...	315
Nenad Grujović, Jelena Borota, Milan Šljivić, Dejan Divac, Vesna Ranković ART AND DESIGN OPTIMIZED 3D PRINTING.....	319
Nenad Grujović, Milan Radović, Vladimir Kanjevac, Jelena Borota, Đorđe Grujović, Dejan Divac 3D PRINTING TECHNOLOGY IN EDUCATION ENVIRONMENT.....	323



Nikola Milivojević, Nenad Grujović, Dejan Divac, Vladimir Milivojević, Jelena Borota AUGMENTED REALITY ASSISTED PART REMOVAL FOR POWDER-BASED 3D PRINTING SYSTEMS.....	327
Dalibor Nikolić, Branko Ristić, Milovan Radosavljević, Nenad Filipović APPLIED RAPID PROTOTYPING TECHNOLOGY AND MODELING IN THE SPECIFIC PATIENT DAMAGE HIP REPLACEMENT.....	331
Milan Trifunović, Jelena Milovanović, Miroslav Trajanović, Nikola Korunović, Miloš Stojković APPROACHES TO AUTOMATED CREATION OF TISSUE ENGINEERING SCAFFOLDS.....	335
Radomir Vukasojević, Simo Saletić, Željko Raičević 3D DIGITIZING FREE FORM SURFACES BY OPTICAL TRIANGULARING LASER SCANNING.....	339
Milan Blagojević, Miroslav Živković, Bojana Rosić QUALITY 3D SURFACE RECONSTRUCTION BASED ON POINT CLOUD GENERATED BY OPTICAL MEASURING TECHNIQUES.....	343
Goran Devedžić, Suzana Petrović, Saša Ćuković, Branko Ristić, Zoran Jovanović, Miloš Ćirović TOWARDS DIGITAL TEMPLATE FOR ARTIFICIAL HIP IMPLANTS SELECTION.....	347
Nikola Vitković, , Jelena Milovanović, Miroslav Trajanović, Nikola Korunović, Miloš Stojković, Miodrag Manić METHODS FOR CREATING GEOMETRICAL MODEL OF FEMUR ANATOMICAL AXIS.....	351
Marko Veselinović, Dalibor Stevanović, Miroslav Trajanović, Miodrag Manić, Stojanka Arsić, Milan Trifunović, Dragan Mišić METHOD FOR CREATING 3D SURFACE MODEL OF THE HUMAN TIBIA...	355
Dejan Petrović, Marko Anđelković, Ljiljana Tihaček-Šojić, Nenad Filipović COMPUTER BIOMECHANICAL ANALYSIS OF SPECIFIC TOOTH FOR DIFFERENT APPLIED LOADING.....	359

SECTION I:

Automatization, robotization and mechatronics IT and artificial intelligence in production engineering

Živana Jakovljević, Miroslav Pajić, Dragan Aleksendrić, Dragan Milković WIRELESS SENSOR NETWORK APPLICATION IN MONITORING OF MACHINING OPERATIONS.....	365
---	-----



Dušan Kravec, Marian Tolnay, Ondrej Staš, Michal Bachraty IMPLEMENTATION OF PALLET LOADING METHODS AND VIRTUAL REALITY TO THE NEW SOFTWARE PRODUCT.....	369
Jan Slamka, Marian Tolnay, Michal Jedinak LAYOUT DESIGN OF VACUUM EFECTOR HEAD FOR MANIPULATION WITH FLOPPY MATERIALS.....	373
Vladislav Blagojević, Miodrag Stojiljković, Milorad Rančić DC SERVO MOTORS CONTROL OF CNC MACHINES BY SLIDING MODE...	377
Dragan Milutinović, Miloš Glavonjić, Nikola Slavković, Saša Živanović, Branko Kokotović, Zoran Dimić COMPLIANCE MODELING AND IDENTIFICATION OF 5-AXIS VERTICAL ARTICULATED ROBOT FOR MACHINING APPLICATIONS.....	381
Dalibor Petković, Nenad Pavlović INVESTIGATION AND ADAPTIVE NEURO-FUZZY ESTIMATION OF MECHANICAL /ELECTRIAL PROPERTIES OF CONDUCTIVE SILICONE RUBBER.....	385
Milica Petrović, Zoran Miljković, Bojan Babić, Najdan Vuković, Nebojša Čović TOWARDS A CONCEPTUAL DESIGN OF AN INTELLIGENT MATERIAL TRANSPORT BASED ON MACHINE LEARNING AND AXIOMATIC DESIGN THEORY.....	389
Milan Erić, Miladin Stefanović, Branko Tadić, Slobodan Mitrović SOFTWARE SOLUTION OF REENGINEERING MODEL OF TECHNOLOGICAL PROCESSES OF SMALL ENTERPRISES.....	393
Milan Zdravković, Miroslav Trajanović, Herve Panetto, Alexis Aubry, Mario Lezoche ONTOLOGY-BASED SUPPLY CHAIN PROCESS CONFIGURATION.....	399
Vesna Ranković, Nenad Grujović, Dejan Divac, Nikola Milivojević, Konstantinos Papanikolopoulos, Jelena Borota PREDICTION OF THE NONLINEAR STRUCTURAL BEHAVIOUR BY DIGITAL RECURRENT NEURAL NETWORK.....	403
Darko Stefanović, Andraš Anderla, Cvijan Krsmanović, Aleksandar Ivić ERP IMPLEMENTATION STRATEGIES FOR MANUFACTURING COMPANIES IN E-BUSINESS ENVIRONMENT.....	407

SECTION J:

Nonconventional technologies (Advanced machining technologies)

Laurențiu Slatineanu, Margareta Coteata, Miroslav Radovanović, Stefan Potarniche, Lorelei Gherman, Irina Besliu SURFACE ROUGHNESS AT ABRASIVE JET ENGRAVING OF GLASS PARTS	413
--	-----



Marin Gostimirović, Pavel Kovač, Milenko Sekulić, Borislav Savković THE RESEARCH OF DISCHARGE ENERGY IN EDM PROCESS.....	417
Dragan Adamović, Milentije Stefanović, Branislav Jeremić, Srbislav Aleksandrović THE EFFECTS OF SHOT PEENING ON THE FATIGUE LIFE OF MACHINE ELEMENTS.....	421
Anđela Lazarević, Miodrag Manić, Dragoljub Lazarević ENERGY BALANCE OF THE PLASMA ARC CUTTING PROCESS.....	425
Srđan Mladenović, Miroslav Radovanović MODEL FOR OPERATING COSTS OF PLASMA CUTTING.....	431
Predrag Janković, Miroslav Radovanović, Jelena Baralić CUT QUALITY IN ABRASIVE WATER JET CUTTING.....	435
Bogdan Nedić, Jelena Baralić, Miroslav Radovanović THE COMPLEXITY OF DEFINING THE QUALITY OF LASER CUTTING.....	439
Jelena Baralić, Bogdan Nedić, Predrag Janković MACHINING PARAMETERS EFFECT ON THE JET RETARDATION IN ABRASIVE WATER JET MACHINING.....	443

SECTION K:

Joining and casting technologies

Processing of nonmetal materials (plastic, wood, ceramics, ...)

Michael Kheifetz, Natalia Pozilova, Alexander Pynkin, Leonid Akulovich ANALYSIS AND DESIGN OF HIGHLY EFFICIENT METHODS OF TREATMENT.....	449
Vladimir Borodavko, Gaiko Victor, Viacheslav Kroutko, Michael Kheifetz, Elena Zeveleva DESIGN OF TECHNOLOGICAL COMPLEXES FOR HIGHLY EFFICIENT TREATMENT.....	453
Radivoje Mitrović, Dejan Momčilović, Olivera Erić, Ivana Atanasovska INFLUENCE OF PRODUCTION PROCESS ON FATIGUE PROPERTIES OF HEAVY CASTINGS - A CASE STUDY.....	457
Dušan Jovanić, Željko Eremić, Miloš Jovanović MODELLING DATABASE OF QUALIFIED WELDERS ACCORDING TO STANDARD SRPS EN 287-1:2008.....	461
Andreja Ilić, Danica Josifović, Vukić Lazić, Lozica Ivanović MECHANICAL PROPERTIES OF WELDED JOINTS AT STEEL TUBES WITH SQUARE CROSS SECTION.....	465



Vukić Lazić, Dragan Milosavljević, Srbislav Aleksandrović, Rajko Čukić, Božidar Krstić, Gordana Bogdanović DETERMINATION OF OPTIMUM TEMPERING TEMPERATURE IN HARD FACING OF THE FORGING DIES FOR WORKING AT ELEVATED TEMPERATURES.....	469
Vukić Lazić, Dragan Milosavljević, Srbislav Aleksandrović, Rajko Čukić, Božidar Krstić, Gordana Bogdanović SELECTION OF THE WELDING TECHNOLOGY OF RELIABLE ASSEMBLIES USING GMAW PROCESS.....	473
Dragan Milčić, Aleksandar Živković, Miroslav Mijajlović AN OVERVIEW ON FRICTION STIR WELDING OF THE AL 2024 T351.....	477
Nenad Gubelj, Bojan Međo, Jozef Predan, Marko Rakin, Goran Radenković, Aleksandar Sedmak DETERMINATION OF TENSILE PROPERTIES OF WELDED JOINTS – INFLUENCE OF SPECIMEN GEOMETRY.....	481
Anka Trajkovska Petkoska MANUFACTURING AND CHARACTERISATION OF FLAKES MADE BY SOFT LITHOGRAPHY TECHNIQUE.....	485
Rok Justin, Davorin Kramar, Janez Kopač, Mirko Soković INDUSTRIALIZATION OF EASY BOOM.....	489

SECTION L:

Tribology

Miroslav Plančak, Igor Kačmarčik, Dejan Movrin, Đorđe Čupković PROPOSAL OF A NEW FRICTION TESTING METHOD FOR BULK METAL FORMING.....	495
Plavka Skakun, Igor Kačmarčik, Tomaž Pepelnjak, Ognjan Lužanin, Aljosa Ivanišević, Mladomir Milutinović COMPARISON OF CONVENTIONAL AND NEW LUBRICANTS FOR COLD FORMING.....	499
Milentije Stefanović, Slaviša Đaćić, Srbislav Aleksandrović, Dragan Adamović IMPORTANCE OF TRIBOLOGICAL CONDITIONS AT MULTI-PHASE IRONING.....	503
Vito Tič, Darko Lovrec EVALUATION OF PHYSICAL AND CHEMICAL CHANGES IN HYDRAULIC OIL USING ON-LINE SENSORS.....	507
Darko Lovrec, Vito Tič USE OF ON-LINE CONDITION MONITORING SYSTEM ON HYDRAULIC MACHINES.....	511



34th INTERNATIONAL CONFERENCE ON
PRODUCTION ENGINEERING
29. - 30. September 2011, Niš, Serbia
University of Niš, Faculty of Mechanical Engineering



Dragoljub Lazarević, Predrag Janković, Miloš Madić, Andjela Lazaravić STUDY ON SURFACE ROUGHNESS MINIMIZATION IN TURNING OF POLYAMIDE PA-6 USING TAGUCHI METHOD.....	515
Slobodan Mitrović, Miroslav Babić, Dragan Adamović, Fatima Živić, Dragan Džunić, Marko Pantić WEAR BEHAVIOUR OF Cr HARD COATINGS FOR COLD FORMING TOOLS UNDER DRY SLIDING CONDITIONS.....	519
Ivan Sovilj-Nikić, Bogdan Sovilj, Stanislaw Legutko, Sandra Sovilj-Nikić, Ivan Samaržić, Ivan Kolev INFLUENCE OF WEAR OF CUTTING ELEMENTS OF CONVEX MILLING CUTTERS ON PROCESSED SURFACE TOPOGRAPHY.....	523
Marko Vilotić, Damir Kakaš, Aleksandar Miletić, Lazar Kovačević, Pal Terek INFLUENCE OF FRICTION COEFFICIENT ON WORKPIECE ROUGHNESS IN RING UPSETTING PROCESS.....	527
Božica Bojović, Dušan Kojić, Zoran Miljković, Bojan Babić, Milica Petrović FRICTION FORCE MICROSCOPY OF DEEP DRAWING MADE SURFACES...	531
Previous winners of the charter and plaque "Professor dr Pavle Stanković".....	537
AUTOR INDEX.....	545

34th INTERNATIONAL CONFERENCE ON PRODUCTION ENGINEERING



PLENNARY PRESENTATIONS



34th INTERNATIONAL CONFERENCE ON
PRODUCTION ENGINEERING
September 28-30 2011, Niš, Serbia
University of Niš, Faculty of Mechanical Engineering



SYSTEM ENGINEERING FOR SYSTEMS INTEROPERABILITY IN MANUFACTURING ENVIRONMENT

Prof. Dr. Hervé PANETTO

Chair of IFAC TC 5.3 « Enterprise Integration and Networking »

Centre de Recherche en Automatique de Nancy (CRAN - UMR 7039),
Nancy-University, CNRS,
F-54506 Vandoeuvre les Nancy, France,
Herve.Panetto@cran.uhp-nancy.fr
<http://www.panetto.fr>

Abstract: *Recent advances in information and communication technologies have allowed manufacturing enterprise to move from highly data-driven environments to a more cooperative information/knowledge-driven environment. Enterprise knowledge sharing (know-how), common best practices use, and open source/web based applications are enabling to achieve the concept of integrated enterprise and hence the implementation and interoperability of networked enterprises. Enterprise Integration and Interoperability in Manufacturing Systems is a key concept to face the challenges of these new environments. Integration in Manufacturing (IiM) is the first systemic paradigm to organise humans and machines as a whole system, not only at the field level, but also, at the management and corporate levels, to produce an integrated and interoperable enterprise system. Business process software and Manufacturing Execution Systems are now available to meet the requirements of this fully computerised and automated integration. Major problems remain with respect to the interface between the enterprise corporate level and the manufacturing shop floor level, so that management and operation decisions within a closed loop are facilitated to pace the production according to the life-cycle dynamics of the products, processes and humans inside and outside the enterprise. Today, networked business encounters recurrent difficulties due to the lack of interoperability between enterprise systems. The role of research in the field is to create upstream conditions of technological breakthrough to avoid that enterprise investment be simply pulled by the incremental evolution of IT offer. However, the future relies on collaboration networks that can be created among companies, people and societies in order to generate shared knowledge and wealth. System Engineering paradigm, from an architecture point of view, is an enabler to better specify systems requirements with a focus on systems interoperability. The keynote presents challenges, trends and issues that must be addressed in order to support the generation of new technological solutions and modelling paradigms for systems interoperability with a system engineering perspective.*

Key words: *System Engineering, Systems Interoperability, Manufacturing enterprise*



QUALITY MANAGEMENT – STATE OF THE ART AND FUTURE DEVELOPMENT

Prof. Dr. Vidosav D. MAJSTOROVIĆ,

University of Belgrade, Faculty of Mechanical Engineering, Kraljice Marije 16, Belgrade, Serbia.

vidosav.majstorovic@sbb.rs

Abstract: *Development of the theory and practice of quality management, taking place simultaneously in two directions: (i) systems approaches to quality improvement based on the use of different techniques and models of quality management, and (ii) integration of manufacturing technology with quality control technology. The first approach involves the quality control approach to the concept of sustainable development and integrated business, while the second refers to the range of conventional metrology systems to intelligent quality models. This paper provides an overview of both these approaches, with special reference to some research results from new approaches to quality management, where for the Laboratory for production metrology and TQM, Mechanical Engineering Faculty in Belgrade.*

Keywords: *Quality, Quality Management, Digital Quality, CMM.*

1. INTRODUCTION

Total Quality Management (TQM), a framework for generating and applying ideas, concepts and tools with which to improve quality throughout the organization, in all its functions and the various aspects of products and services. The word *total* is related to all elements and activities in an organization, directly or indirectly affect the quality and the word *management* implies that the technical aspect of quality generalizes and extends to the organizational and business factors of the organization [10].

1.1. Development and definition of quality

Today there is no universal definition of quality, but the quality gurus¹ promote the quality of different formulations [7, 8].

A. Feigenbaum defines quality as: "*total composition of product² characteristics in terms of marketing, engineering, production and maintenance, which in its use will ensure that customer expectations*". From this definition we can conclude that we are assuming that the requirements of the customers are absolutely satisfied. **P. Crosby** quality products defined as: "*compliance with requirements*", and **J. Juran** quality in its definition uses the phrase "*fitness for purpose*". Some other researchers

share the characteristics of product quality and perception of the facts. Aspects of product quality, viewed through the prism of the facts are right, the right features, the true function at the right time and on time delivery. Perception of quality in terms of customer is defined as: it is the best, this is what I expected, the fulfillment of all requirements, relationship with customers with respect, courtesy and respect. It is interesting to note, as **J. Juran**, now defines product quality as its multi-dimensional feature, such as: features, performance, competitiveness, speed (ready), kindness, ability to process work without errors, compliance with specifications, standards and procedures, user-oriented, safety for employees, customers and the environment, reliability, maintainability, including the availability of spare parts, durability, aesthetics, non-quality costs, cycle time, costs (manufacturing, non-production, quality), customer satisfaction, employee satisfaction, social responsibility towards employees and society. This example illustratively shows a complex understanding of the concept and understanding of quality products today.

Theoretical assumptions and frameworks that are the basis for the development of systematic approaches to quality, and that led to the evolution and application of TQM as a model of business excellence, they were formed and evolved in the second half of the twentieth century [6, 10-17].

Scientific management theory, a theoretical concept of the organization, as defined at the beginning of the industrial revolution that is still followed by the development of production. Quality function is then defined model inspection (quality control), and **F. Taylor** author of scientific organization of work, defined the model of work organization and production, in that the plant looked like a closed system of work processes, facing the achievement of maximum effect. This approach is considered the beginning of scientific and technical

¹ It is a world recognized quality leaders who are in their theoretical, professional and practical contributions in this area gave a personal contribution to the science of quality. These are: *E. Deming (USA), J. Juran (USA), A. Feigenbaum (USA), P. Crosby (USA), K. Ishikawa (Japan) and G. Taguchi (Japan).*

² The latest definition of the product according to ISO 8402 (Quality System Dictionary) includes four categories: hardware, software, process materials and services. It is called a generic product, to be here in after referred to as the term considered all the products mentioned above.

development of the management concept. The same conclusion applies to the inspection, the first systematic approach to quality management.

Movement for productivity, is formulated and a result of research studies, performed forties of last century, the Western Electric Company. They determine the impact of the working environment to increase productivity. So the researchers: *F. Roethlisberger, E. Mayo and W. Dickson*, foundations of scientific productivity, which is in their approach was integrated with the quality of production.

Control charts were created based on the theoretical works of English statisticians *R. Fisher*, who laid the foundations of the theory of statistics. They represent one of the most important tools for quality improvement, and they defined the *W. Shewart*, a physicist who worked thirties of last century, ATT Bell Laboratories. He has his own model of control charts, designed and used for quality management in Western Electric Company. Some time later, the forties of this century, he and *W. Edwards* and *J. Juran*, developed a special scientific and technical discipline, statistical quality control.

Economic statistics are created surveys conducted by *A. Makprang*, a Danish economist, as part of his doctoral thesis at the beginning of the 20th century. He has applied statistical evaluation and regression analysis, and later *I. Tenbergen and R. Frisch* (the first Nobel laureate in economics), define econometrics as a discipline, which has contributed to the monitoring and development of the economic parameters affecting the quality of products.

Mathematical tools for simulating decision-making, have been developed and applied during World War II. Russian mathematician, *L. Kantorovich*, a Nobel laureate in economics, has developed a linear programming, as the most popular method for optimization in Operations Research. After World War II, many companies, particularly in the U.S., has used this tool for quality improvement.

Taguchi method, the developer has already specified the quality gurus, *G. Taguchi*, as a new concept of designing for quality, the eighties. He defined Taguchi loss function, which based on the theory of experiments, defines the optimal cost of quality in the product life.

New concept of quality, defined by *E. Deming* and *J. Juran* and implemented in the Japanese economy after World War II. Its basic characteristic is that they are responsible for quality functions in an organization. It was the foundation for creating a worldwide movement of quality, which has now evolved into a model of quality management standards ISO 9000.

Quality costs as a method for quality management, real inaugurated *A. Feigenbaum*, 1956. year. He then argued that a high quality product, should not mean its high price. Then set up the model to track the cost of quality, and through them to monitor the effects of quality management.

Systems theory, developed after World War II, and by *H. Simon*, a Nobel laureate, applied to the modeling of business systems through hierarchical decomposition with feedback, was used for the modeling of quality. Modeling the organizational structure, defined as input, process and output, with feedback, and thus related management processes and processes for quality.

Quality circles, defined by the professor. *K. Ishikawa* and applied since 1962. vol., were the main organizational innovation model for quality improvement in Japanese companies. They constitute a small group of volunteers who are directly or indirectly involved in the underlying quality problem. They are particularly contributed to the development of the TQM concept in Japan, and now used as a model for quality improvement in Europe and America.

Benchmarking is a model for designing products and processes, based on a set of goals that represent the best world practices. This approach was first developed and applied in Japan, at Toyota, under the slogan "be the best of the best." In America, the benchmark model is first applied Xerox, and today this model is applicable worldwide.

Lean system is the organizational technical system, established in Japan, which is based on the "flat" organizational structure, where a special place quality management. QM activities is regulated by a "cross-functional teams".

Supply chains are also a contribution to the QM model of the supply chain. They form a network company that connects suppliers and buyers in the product lifecycle, from raw material to his exclusion from the process of use. Supply Chain Management integrates all aspects of development and design and a competitive production and use of the product in its lifetime. This model optimizes and synchronizes the material, process, information flows from raw material to products delivered to customers, optimizing inventory and reducing costs of product life. The rule is: to deliver the product at the right time to the right place with the right (affordable) cost for the customer. Each Organization of the supply chain can initiate the program and realize the benefits of it. However, the organization that is closest to the end user, as a rule it is best positioned in the supply chain.

Good Manufacturing Practice (GMP) are procedures that must be applied manufacturers of medical devices and drugs, who want to be placed on the market USA. They are prescribed by the American agency FDA (Food and Drug Administration), and the organization is required to establish a quality assurance program for its medical devices, according to the specifications that ensure control over their safe and effective use. CGMP complete the program of quality assurance in the organization, buildings, equipment, components, manufacturing and production processes, packaging and labeling, distribution and installation, maintenance and cleaning equipment and records. The auditors assessed the FDA approval of bills with CGMP quality assurance plan. Besides this, the pharmaceutical industry, food and beverage industry is luck and good: Laboratory Practice, practice packages, and others. In addition to these systems for certification of management practices, products or processes, based on national and / or international standards, there are many others like: IECQ-CECC CEN mark, GOST R mark, mark RADMAC, ASTA gold mark, BEAB mark, S mark, mark GS, ETL and CCC mark, which in fact represent a sign of quality products and relate to the fulfillment of specific standards of these products. Today, all of them, as a rule, applied in pairs with ISO 9001:2008.

Digital quality of the QM model for quality management in the lifecycle. The whole concept is based on the integrated digital product model, where the digital model of quality, one of a number of product models, which are generated for different life stages. It is developed and used for the digital factory.

Virtual quality is a concept advanced the concept of digital-quality technology for intelligent systems. It developed as a simulation model for intelligent model quality in IMS.

Exposed to concepts as a framework for development - application of the latest systematic approach to quality improvement, which is now in the industry based on the TQM model.

2.2. Development of quality management as a systematic approach

Theory and practice of Japanese scientists and engineers, has enabled the translation of models of *quality control*³, on the basis of quality control based on statistics (*statistical quality control*), the model of quality control across the company (*company-wide quality control - CWQC*). *Total Quality Control - TQC*, is a term that Japan has the same meaning as CWQC.

This model (TQC)⁴, widely used in Japanese industry, has enabled the achievement of the following effects [15]: (i) reducing costs, especially manufacturing, (ii) increasing productivity, (iii) timeliness of delivery, (iv) ensuring the safety of using this product and (v) radically increase product quality.

After 1980, this model is increasingly came into operation in non-production areas, such as transportation, manufacturing and distribution of electricity and gas, air transportation, hotels, restaurants, etc., which is only fueled the rapid growth of Japanese economy. During this period, quality management in Japan has undergone major changes in theory and practice. The first changes were made in the term "*management-control*". In the initial stage of development and application CWQC models, "*management*" meant "*care*" designed and applied model and, later, now it means "*improvement-improvement (kaizen)*". Today the terms "*control*" and "*improvement*", replaces the term "*management*", which is based on the PDCA⁵ model. It is expected that in the future this model (PDCA), be extended to activities such as "*development*" and "*creativity*".

Extended the concept of "*quality*". At the beginning he meant "*the degree of compliance with technical standards*". Its extension, which was later followed, the term "*fitness for purpose*", to expand the circle of responsibility for quality management. From suppliers, through producers, and service and maintenance.

³ Namely, it is considered under the term - quality control, to the fifties, involved and explained the model of classical quality control (inspection). After that, the first in Japan, and later in other countries, under this term is meant a model for quality management.

⁴ TQC model started to develop and implement the seventies in the Japanese industry, but later expanded to other industries.

⁵ PDCA – Plan, do, check, act the Deming model of continuous improvement.

However, the buyer was not satisfied with the time, but he wanted more: high quality products, reliable and prompt service and reasonable price. So there has been integration of the three requirements: quality, price, time (delivery service). In this way, defined the *total quality of products*, which are integrated: quality, cost and delivery (time, service). Thus, the limit extended to the quality management of technological processes and other processes in an organization (research and development, design, management, administration, business functions). This causes a revolution in quality management, which is the industry spread to other industries, first in Japan and later in America and Europe. and ISO 8402 (1986. vol.) defined product quality, to the 2000th year, he⁶ gave a new definition: "*a set of characteristics that an entity possesses that would satisfy all the requirements, and even anticipated customer needs and preferences.*" The term "*entity*" means: product, service, process, activity, organization, systems, staff or any combination of these elements with each other. Finally, the concept of "*total*" has also seen the evolution. At first, he meant an "*integrated*" in the TQM model A. Feigenbaum, but sustained changes in the concept of "*across*" the company (*company-wide*), it meant the participation of all employees. This was true at all levels of the organizational structure of an organization, and it was first applied in Japan. The fact is that quality circles (QC circle), here played an important role. Decisive contribution to the development of these approaches, given the different methods and techniques for quality control [3], developed and applied in practice. It started from the basic statistical methods (charts, plans of receipt), in order to proceed with the seven basic tools of quality management (B7)⁷, then the seven new tools for quality management (N7)⁸, to talk today about the seven management tools Quality Management (M7), and other quality engineering techniques: QFD (Quality Function Deployment), CE (Concurrent Engineering), and others. All these methods are facing a man (the designer, manufacturer, user, customer), which created an additional motivating factor for all employees in Japanese companies. Especially important were the quality circles, because they have become a place where ideas and suggestions of individuals to promote and resolved. This was the evolution of Japanese TQC model, which is the eighties turned into TQM, based on further development of corporate management. Top management in any company defined development strategy based on

⁶ It is a TC 176 International Organization for Standardization ISO, which was brought to the ISO 9000 series, and officially is called the ISO Technical Committee 176 for Quality Management and Quality Assurance. ISO organization headquarters in Geneva.

⁷ Basic Tools for Quality Management (B7) are: *list for data collection, cause-effect diagram (Ishikawa diagram), histogram, ABC (Pareto) analysis, scatter diagrams, charts and flow chart.*

⁸ New tools for quality management (N7) are *a diagram of similarity, relational diagram (diagram of interconnections), the tree diagram, matrix diagram, matrix data analysis method, map-making process and techniques of network planning (CPM).*

quality, which is in practice at such companies⁹ increased sales volume, profit and its overall image in the global international market.

All the above facts speak clearly and illustrate the genesis and development of TQM, today the most modern model for quality management.

2. TQM MODELS

Total Quality Management is still no universally accepted definition, and here is one of the possible states: "*TQM is a management approach to continuous process improvement for the quality of the business system, which is derived on the basis of a defined strategy, vision and mission-oriented fully meet customer requirements in order achieving world class quality products*". From this definition it can be concluded that the bullets are the key words: continuous improvement, meeting customer requirements and world-class quality¹, which actually represents the basic aspects of TQM.

Former world theory and practice has made the next generation of TQM [13, 18-22]: (i) The first generation refers to the global *gurus of TQM models for quality*, (ii) the second generation of these models is related to the *world famous prize for applied TQM model*, (iii) the third generation of TQM represents a *new model of TQM and EFQM*¹⁰ based on self-assessment (self-assessment), and a new Japanese model of business excellence, and (iv) the latest generation of TQM and it seems his model, which is the subject of *research, and is known as RE-TQM*.¹¹

3. JAPANESE MODEL FOR BUSINESS EXCELLENCE - TQM NEW MODEL¹²

The new model has emerged TQM training and development [15, 16] in particular the following areas and approaches in the existing TQC model: (i) the basic essence of TQM is customer satisfaction with products and services, through continuous development and improvement of relations with stakeholders such as employees, company, suppliers and shareholders, (ii) improvement of these relations, TQM contributes to strengthening the power base of the organization as a key

⁹ Includes only some of them: Sony, Panasonic, Toyota, Komatsu, Honda, Nissan.

¹⁰ EFQM – European Federation Quality Management based in Brussels.

¹¹ With great pleasure to be here to say, that this author, this concept RE-TQM (Re-engineering of TQM) among the first in the world, set up as a possible model of TQM for virtual manufacturing system. Details of this concept are given in [9, 23].

¹² JUSE (Japanese Scientists and Engineers Union), in April 1996. years, formed the TQM Committee: prof. Dr. Y., Iizuka, The University of Tokyo (President), and members: prof. Dr M. Inohara, Osaka Electro-Communication University, prof. Dr. T. Enkawa, Tokyo Institute of Technology, Dr. H. Kubota, Hiroshima Institute of Technology, prof. Dr. H. Shindo, Yamanashi University, prof. Dr M. Munechika, Waseda University, prof. Dr. S. Yatsu, Tamagawa University, and Professor. Dr. T. Yoshizawa, Tsukuba University. On in 1997. Here we present the first draft of the new TQM model, in 1999. year, its final version.

technology, vitality and building a prestigious reputation, (iii) the best response to change, TQM provides over medium and long term vision and strategy under the leadership of top management, and (iv) the management of resources, TQM attaches special importance to people and information, the efforts of building an organization with excellence in management, learning, flexibility, speed and creativity. Based on this defined approach, the basic definition of a new TQM model, reads: TQM is a model of quality improvement, which under the leadership management of the organization, in any business environment seeks the following: (i) top management establishes a clear medium-and long-term vision and strategy, (ii) clear use of concepts, values and scientific methods in the established TQM model, (iii) acceptance of the fact and its application to the human resources and information, vital elements of organizational infrastructure, (iv) under appropriate management systems, effectively implemented quality assurance and cross functional management system that includes cost, delivery, environment and security, (v) with the support of major organizational power, such as a key technology, speed and vitality, providing a mutually excellent relationship with customers, employees, the company, suppliers and shareholders, and (vi) the continuous realization of corporate goals of the organization through its mission, building its respected reputation and ensure continuous profits.

3.1. Basic features

Changes in the environment in which the transformation will be performed in TQC TQM, is characterized by [15]: (i) requires the evolution of business management, in the direction required to ensure product and service quality with maximum effective business results and build a business reputation of the organization, (ii) the future development of business management infrastructure in terms of reducing the temporal and physical proximity, as a result of progress in information and transport technology, (iii) changes in the social systems of the companies require a high level of transparency of the organizational structure, maintenance of acceptable prices and respect the norms of business, (iv) changes in working conditions in the direction required for their continuous improvements, and (v) increasing uncertainty (frequency change), to accelerate the changes that are occurring within the political, economic, social and technological changes in the world.

Before we define what are the requirements for a new model of TQM, we must consider what are the expectations of organizations for tomorrow, so that their expectations related to the TQM model.

Expectations and requirements for business management in the restructuring. Japanese economy and Japanese society developed the management demands to industry provide products and services of maximum quality and efficiency, and organization to be respectable. TQC contribution relates to the improvement of physical product quality and improving the efficiency of systems that provide this quality. However, as the economy and society continue to evolve, growing demands for a greater

diversity of product quality. Now, more and more each entity of the organization, its mission, becoming responsible for their own building and overall reputation. Re-engineering existing TQC and, for its translation into a new TQM model include: (i) *defining the objectives of TQM, namely:* (a) construction of a respected organization through the aspect of the product and the name of the organization, which will have a wider reputation, (b) building the system right (bilateral) values in relations with customers, employees, society, suppliers and shareholders, and (c) develop a "force" organizations based on key technology, the speed (corresponding to the demands of the market / customer) and vitality (the constant changes) (ii) *highly diversified quality concept that is based on:* (a) highly sophisticated requirements of customers, (b) diversification of customers, and (c) widely covered by the quality, and (iii) *a highly sophisticated management, which includes:* (a) expansion and expansion of management (vision, strategy, transformation, speed and prevention), and (b) people and information as an important resource management.

Respectable presence. TQM must allow the organization to be respectable. If the application of TQM as an effective management tool, the company will build such a system that will give the respectable products. In other words, companies do not expect a simple production produce better products at an affordable price. They expect that their mission and maintain their integrity be the basis for the establishment of corporate responsibility and a respectable presence. Because of this organization with the reputation in the market, have an extra incentive for further improvement and TQM should be seen as an effective management tool for establishing, maintaining and improving their reputation in the eyes of stakeholders.

Relations. Those organizations that want to be leaders of a respectable reputation, must have excellent relations with all stakeholders. Keeping customers satisfied products and services, as well as the most important element of overall relations with stakeholders, the organization must develop good relationships with: employees, society, suppliers and shareholders. Organizations today are exposed to demands for improved working conditions, knowing that employees are important management resources, a large social responsibility in the narrower and wider community, particularly in terms of increasing globalization and the abolition of various barriers. TQM tomorrow must all take this into account and build the best relationships with stakeholders, we are not the aspect of quality products and services.

Power organization. In the process of building operational excellence, strength of the organization lies in its key technology, speed, responsiveness and vitality. Every organization has key technology that is the basis of its existence. What is the key technology complex and unique style, it's reputation and leadership of the organization increased. Speed is the next essential feature of the organization today. In an environment where the speed of political, economic, social and technological change bigger and bigger, and the vagueness of these changes, the speed of activities that an organization takes must also be greater. Additionally, organizations also need to have vitality for each level of your organization.

Top management must have the spirit of change towards the environment, middle management changes within the spirit and the third level of management and employees must have high internal morale to implement these changes in their workplace. TQM tomorrow must become a concept and methodology that will build organizational strength, as the source of its growth and development.

Highly sophisticated requirements. TQM model must enable the acceptance of requests for high and widely diversified, comprehensive concept of quality. Customer requirements are becoming more sophisticated (more subtle) and more mature. TQM has provided a methodology for product planning, in order to meet these demands. TQM also needs to define more sophisticated and quality objectives.

Diversification of customers. Particular attention should be paid to the fact that the expanding range of customers. Development of society leads to progressive divisions of the market. TQM must have a methodology for product planning, which will economically meet different customer groups. Soon, the main characteristics of quality to meet customer demands for which the respective products and services implemented. But the quality of products and services must have such characteristics, which will meet the standard requirements of our customers. The expanded concept of quality includes all employees of the company, and TQM must support this approach.

Widely covered by the quality. Quality is a term for defining product characteristics. The new concept of TQM must explicitly express the new "widely covered by the concept of quality, or value of products, which include cost, time (delivery, use, ...) and service. Especially in the area of new product development, TQM must develop a methodology for total management and quality assurance, achieving at the same: high quality, reasonable price (cost) and defined the time of delivery.

The expansion of management. New TQM model requires more sophisticated management. First of all TQM should extend the existing concept of management. Increasing uncertainty in the business environment, rapid changes and different market demands, the management of new demands, such as vision, strategy, speed and prevention. Extremely important role in these processes of planning, a concept that enables the "strategy and vision" in the field of management, translated into the domain of management. Future plans must undergo radical changes, and instead of extrapolation of the past, have improved the quality of the planning process in the future. All this, as well as speed, flexibility, and increasing uncertainty in the business environment, indicate that the new TQM model must provide the basic concept and applicable methodology for the management of all these activities.

People and information. Another very important aspect of a new management style is the recognition of the importance of people and information as a management resource. In the past, aspects of "people-to-staff" is considered from various angles. Changes have occurred in this area, primarily in the direction of increased demands for improved working conditions and requirements for improving intellectual productivity. Therefore, attention is focused on how to provide staff development, motivation and high moral and professional values. TQM must

provide answers to these questions. Management system is essential information system for decision making. The rapid development of information technology, these requirements, but TQM must give answers to the effective use of information technology in management quality.

3.2. Methodologies and tools that support implementation of the new TQM model

Development and application of new TQM model, based on a number of methodologies and tools that support it.

The integration of management strategies and policy management. Policy management has emerged as an excellent management tool in the TQC model for planning and managing the annual operating policies and goals. However, improvements in the defined policies and goals are the most important step in the implementation of policy management. The best method for overview of business management strategies, based on annual policies and objectives, need for improvements. On the other hand is facing policy management and strategic planning. In practice, however, these dimensions TQC is limited. TQM requirements include concepts and methodologies for the management of business strategies, which are mostly developed in the U.S., but without the involvement of all employees. So, the new TQM model integrates policy management with strategic planning.

The integration of technology marketing with the development of new products. Understanding of the requirements of customers is central to the model of quality management. However TQC model has no knowledge of the methodology and the substantial marketing and technology, now applied, understood as the customer's requirements. On the one hand, TQC uses table quality, they represent a powerful tool to support the activities in the correct understanding and translating customer requirements into product quality characteristics. On the other hand, this methodology is quite rigid in the process of generating customer requirements. In the field of marketing, using many methods, which may be in support of TQM, such as: defining and exploring marketing requirements, market research, analysis of data studied. All this analysis and data are crucial for planning and development of new products. Because of this, a new model of TQM attaches particular importance to the integration with marketing technologies.

Comprehensive quality management, cost and delivery in developing new products. In poor and underdeveloped countries, people look at the quality of the product in other ways. For example, they say: "The price is more important than quality." And also notes: "We can not sell our products only if they improve quality." Quality are reduced only to the technical characteristics of products, which are identified with the demands of customers, but they do not result in a relationship relationships of customer satisfaction. But today the quality determined by customers, so it is inevitable that it is constantly improving, so they can meet. The concept of TQM concept of quality is the most widely observed, and is now defined as the product value based on factors such as price, time and services.

Therefore, TQM must develop a methodology to optimize the quality and costs, in particular the methodology for comprehensive management of quality, cost and delivery in developing new products.

Quality assurance in a global society. Present-day globalization trends raise the question, how to achieve quality assurance in the new situation. Methodology for quality assurance can be effective and efficient in terms of Japan. From all over the world come to implement the requirements of ISO 9000 series. Those from the perspective of the customer provide the following: procurement of materials at an affordable price and with a single test, engineering design technology and production processes where required and under control, decentralization of development (the organization), and development in different areas (geographically), where for this suitable conditions exist.

Coordination, fusion and integration with the international trends in quality. ISO 9000 gave the biggest contribution to improving quality throughout the world. TQM, as specific Japanese style of management, may be included in the western management style, supported with ISO 9000, which would be given universal methodology for quality management, today in the world. Some possibilities are: elements of management functions such as planning, implementation and validation can be divided so clearly defined authority and responsibility; suitable communication systems (not just using documentary information system, but direct communication between employees) method to include ISO 9000 in a model of quality assurance is defined in the TQM-in, understanding the importance of documentation as well as infrastructure TQM.

Quality information systems and technologies based on the latest technologies. Progress in development of information technology today is spectacular. Not only does the amount and speed of information are growing constantly, but the business support and work in the network, open access, and multimedia. In the field of quality, current information technologies enable the development of new information systems for quality, which had not existed. Some examples are: the integration of information for quality and technological information, integration of information relating to quality, cost and delivery, promotion of customer relationships, effective use of databases in the network. Information technologies also enable the integration process of product design and technology, and manufacturing (DNC). So, before the new information technologies are very wide possibilities for an effective quality management.

Management of equipment maintenance. It is quite clear that the technological (production) is directly dependent on the quality of the equipment. Previously, the TPM (Total Productive Maintenance) gave the biggest contribution to improving the technological quality and productivity. But TPM has a strong planning function of management equipment. TQM requires a developed methodology for assessing the state of the equipment, which is being held, with respect to necessary accuracy of the process (production), upon which it feeds. This methodology must be defined and established in the design of equipment, and that in the process of

exploitation involved in the management plan for the quality and maintenance.

TQM methodology to improve the technology. TQM is principally focused on developing management systems that will best use of installed production technology. Improving the quality of installed technologies and products that they provide, is one of the most important task management system. Since the task of TQM is to increase the level of established technologies in each area. In all TQM improvement processes should involve all employees.

New SQC (Statistical Quality Control) for analysis and management processes. The development of information technology has also enabled the improvement of management methodology for technological processes. What processes are more automated, more and more data is collected, by which it is managed. For example, automatic control devices, enabling automatic inspection of parts in process and finished parts. TQM proposes a new methodology for the management process, from the aspect of quality management. Particularly effective use of on-line, real-time data for management and analysis process. TQM is open for development and application of new statistical methods, such as for example time series.

Methodology for solving various problems. In applying the model of quality management, there are several problems that need to be addressed. "The QC Story" is the most famous scientific method suitable for solving the problem, which is based on the structure of the "cause - consequence" and a detailed analysis of the problem. Therefore, in the field of TQM, must give the following reply: how different types of problems identified and to establish their solution? The solution to this problem is the standard procedure for identifying and solving any type of problem or task.

Employed to support changes in production. As a rule, managers and executives in the direct production, more are required for specific knowledge in the field of manufacturing and maintenance, the aspect of technological quality. Also today workplaces equipped with hardware / software equipment, which provides a "data management". In response to these trends, TQM must be for these changes define the training methodology and training of employees across various levels of the structure of jobs.

Human resource development and encouraging creativity. Changes in the development of society and lead to changes in the workplace. All these changes can be defined as requests for more respect for the man. Management must accept the fact that change is inevitable in this area and that TQM must provide answers to how to further develop the quality circles (QC circle).

4. OUR RESEARCH

The last our research result is the hybrid intelligent system (IS) model presents a generic and integrative approach to a multiresponse process design based on experimental data. It is composed of three stages: the design of experiment, the factor effects approach, and the process modelling and optimisation [24 – 31].

The objective of the developed intelligent model is to incorporate customers' specifications for several (possible

correlated) responses in order to find the optimal process parameter settings and reduce the influence of noise factors. The effectiveness of the proposed generic knowledge-based system is illustrated in brief with five case studies, emphasising the possibility to use the model for solving various types of multiresponse problems in manufacturing processes.

In order to contribute to 'knowledge-based' and 'zero-defect' manufacturing paradigm, an integrative, generic and intelligent model for multiresponse process design was developed. The presented model does not imply any assumptions regarding the type of process or process parameters, type of responses, type of relations between responses and process parameters and existence of interactions among them.

The most important feature of the developed model, in comparison the existing artificial intelligence-based models from the literature, are: (i) The vast majority of GA-based approaches found in the literature are designed to solve a particular problem and they are suitable for general application. In contrast to this, in order to consider the specifics of each particular problem and to enhance the generality, several GAs with different basic functions are tested for each problem in the proposed model; (ii) The initial population in the GA is formed in the neighbourhood of the potentially good solution – the solution of the factor effects approach. This feature significantly advances the convergence to the global solution, which means that the probability of finding the actual global solution in the given number of generations is significantly improved. None of GA-based approaches for multi-response process design found in literature discuss the initial population at such way; and (iii) the quality loss function is the essential part of this approach, because it directly presents a relative financial significance of each response, hence no assumptions or assigned response weights are required. This significantly improves the objectivity of the analysis and the application of the model in a real world.

The analysis of the application of the proposed model indicated that it showed better results, in terms of the optimal parameter settings that yield the maximal synthetic multiresponse performance measure, than the other four commonly used methods. Drawing on the above, it might be expected that the model implementation could contribute to the transition from the 'experience or assumption-based' to the 'knowledge-based' decision making in a multiresponse design of manufacturing processes.

5. CONCLUSION

Today, the most popular models for improving quality: ISO 9000, TQM and re-TQM [1 - 5]. Their comparison, by type of improvement and Deming applied model, we get the following facts - ISO 9000 provides quality control, which is realized through the SDCA cycle. In this way it creates a basis for improvement of TQM, which are carried out incrementally, through the PDCA cycle. Finally, discontinuous improvement is a hallmark of RE-TQM model, which is realized through the SECI cycle. Therefore, TQM is a model of quality improvement, which gave the best results in improvement of the world,

while the RE-TQM can say that he is a research approach to improving quality.

REFERENCES

- [1]. Geyer, A., *The Future of Manufacturing in Europe The Future of Manufacturing in Europe 2015 2015-2020: 2020 - The Challenge for Sustainable The Challenge for Sustainable Development Development*, DG Research, Brussels, 2010.
- [2]. Haug, G., *Education and training in the Lisbon strategy, European Commission DG Education and Culture*, Brussels, 2010.
- [3]. Flegel, H., *MANUFUTURE – a vision for 2020 Assuring the future of manufacturing in Europe*, Brussels, 2010.
- [4]. Leitner, K., Green, L., Malik, K., *Measuring, Precision and Process Control in Manufacturing*, Case Sector Report, Brussels, 2010.
- [5]. Benson, G., et all, *The Effects of Organizational Context on Quality Management an Empirical Investigation*, *IJ Management Science*, Vol. 37. No. 9. September 2001.
- [6]. Feigenbaum, A., *Quality's Worldwide Direction, The Quality Anniversary Magazine*, pp. 6-9, Frankfurt at Main, 1996.
- [7]. Feigenbaum, A., *Total Quality Control*, Fourth Edition, McGraw-Hill, New York, 2001.
- [8]. Hundy, B., *A History of Quality*, *Journal of "Manufacturing Engineer"*, pp. 49-59, 2007.
- [9]. Majstorović, V., *Virtual Quality in Agile Manufacturing Systems, The 4th International Seminar "Intelligent Manufacturing Systems – Theory and Practice"*, pp. 29-31, Belgrade, 1998.
- [10]. Fujita, Sh., *Recommending Creative Type TQM*, NTT Data Corporation, Tokyo, 1998.
- [11]. Ivanović, M., Majstorović, V., (2005), *Research on the Quality Management Level in the certified organisations in our country, Balkans Conference on Quality "The Balkans as a region of quality"*, Proceedings, pp. 12- 16, Belgrade.
- [12]. Ivanović, M., Majstorovic, V., (2006), *Model developed for the assessment of quality management level in manufacturing systems*, *The TQM Magazine*, Vol.18 No. 4, pp. 410-418.
- [13]. Conti, T., *The Evolution of International Quality Standards Versus the Evolution of TQM*, Proceedings of IAQ Preconference Workshop, pp. 1-10, Yokohama, 2006.
- [14]. Dale, B., *A National Quality Culture For World Competitiveness*, Quality Management Centre, UMIST, Manchester, 2008.
- [15]. Imai, K., Akao, Y., Koura, K., *Systematization of TQC in Japan*, Tamagawa University, Machida, 2009.
- [16]. Izuka, Y., *Re-Recognition of the Japanese Way of TQM*, Proceedings of ICQ, pp. 21-26, Yokohama, 2008.
- [17]. Kano, N., *Business Growth and TQM*, Proceedings of IAQ Preconference Workshop, pp. 21-32, Yokohama, 2008.
- [18]. Majstorović, V., *Research in advanced quality concept (on Serbian language)*, *Journal "Total Quality Management"*, No. 1, pp. 129-133, 1998.
- [19]. Majstorović, V., *Total Quality Concept – advanced approaches for manufacturing systems (on Serbian language)*, Mechanical Engineering Faculty, Belgrade, 1995.
- [20]. Majstorović, V., *From QS to TQEM*, Introduction paper (on Serbian language), XXIV Jupiter Conference, pp. PS-19/PS-24, Zlatibor, 1998.
- [21]. Majstorović, V., *Base of TQM (on Serbian language)*, Proceedings – 23rd Annual Conference of JUSK-a, pp. 150-156, Belgrade, 1996.
- [22]. Majstorović, V., *Trends in TQM (on Serbian language)*, *Journal "Total Quality Management"*, No. 1-2, Vol. 25, pp. 55-59, Belgrade, 1997.
- [23]. Majstorović, V., *Virtual quality (on Serbian language)*, *Journal "Total Quality Management"*, No. 3-4, pp. 87-96, Belgrade, 1996.
- [24]. Majstorović, V., Šibalija, T., *EU / Serbia Manufuture Excellence*, Introduction paper, Proceedings of Manufuture Conference, Tampere, 2007.
- [25]. Majstorović, V., *Center of Excellence for Manufacturing Engineering and Management (CEMEM)*, Facts – Objectives – Goals - Researches Framework, Mechanical Engineering Faculty, Belgrade, 2008.
- [26]. Majstorović, V., *Manufuture Serbia – Strategic Research Agenda*, Mechanical Engineering Faculty, Belgrade, 2008.
- [27]. Šibalija, T., Majstorovic, V., *An integrated approach to optimise parameter design of multi-response processes based on Taguchi method and artificial intelligence*, *Journal of Intelligent Manufacturing*, doi: 10.1007/s10845-010-0451-y, 2010.
- [28]. Šibalija, T., Majstorovic, V., Miljkovic, Z., *An intelligent approach to robust multiresponse process design*, *International Journal of Production Research*, doi: 10.1007/s00170-010-2945-3, 2010.
- [29]. Šibalija, T., Petronic, S., Majstorovic, V., Prokic-Cvetkovic, R., Milosavljevic, A., *Multi-response design of Nd:YAG laser drilling of Ni-based superalloy sheets using Taguchi's quality loss function, multivariate statistical methods and artificial intelligence*, *International Journal of Advanced Manufacturing Technology*, doi: 10.1007/s00170-010-2945-3, 2010.
- [30]. Šibalija, T., Majstorovic, V., Sokovic, M., *Taguchi-based and intelligent optimisation of a multi-response process using historical data*, *Strojnicki Vestnik – Journal of Mechanical Engineering*, april 2011.
- [31]. Šibalija, T., Majstorovic, V., *Multi-response optimisation of thermosonic copper wire-bonding process with correlated responses*, *International Journal of Advanced Manufacturing Technology*, Vol.42, pp.363-371, 2009.



34th INTERNATIONAL CONFERENCE ON
PRODUCTION ENGINEERING
28. - 30. September 2011, Niš, Serbia
University of Niš, Faculty of Mechanical Engineering



DESIGN RESEARCH – THE MOMENTUM AND EXPECTATIONS

Prof. Dr. Dorian MARJANOVIĆ

University of Zagreb,
Faculty of Mechanical Engineering and Naval Architecture,
Chair of Design and Product Development

dorian@fsb.hr

Humankind's way of life depends on technology since the very first tool was used by the unknown. Statements like „civilization began when humans first used technologies“ have been argued in different occasions. Technologies have been thought, applied, tested and improved by experience gained through time. Through time technologies have been designed with the same methodology the artefacts which resulted as benefits of those technologies have been designed. Everything around us is designed. Design enabled us to go beyond mere existence, to take advantage of intellectual capital, to design a way of life we know.

Over the past 30 years, engineering designers have witnessed revolutionary change in design methods— from pen and paper to two-dimensional software and now to 3-D computer-aided design, from dedicated problem oriented programming to nowadays simulation software. New technologies and skills change the profession as it seeks to fit to changes. The definition of engineering design and designers profession has stretched over the disciplinary boundaries. Mechanical engineers have actively participated in analyzing the workings of biomechanical systems, creating virtual reality environments, building nanomachines or medical nanodiagnosics. A significant part of today's CAD, CAE tools have been coded by mechanical engineers. Today, projects combine mechanical with electronic, materials, chemical, and biomechanical engineering.

The cycle of technological change grows faster than ever before. Successful engineering has always been on the leading edge of technology thus forcing beyond the dominant designs of the moment. In the moment when the bubble of unrealistic expectations has exploded we will have to rethink the way that we live to be more sustainable. In a whole all aspects of our civilisation will be redesigned the transportation systems, food processing, energy management, buildings, office and household equipment and manufacturing facilities that are less polluting and less demanding of natural resources.

Engineers will continue to improve existing and develop new technologies. The challenge to rebuild the world we know will promote a need for creativity and new thinking to generate new ideas. Design was and will continue to be the bridge between the world we know and the world that will be. Building that bridge is an engineering design issue which we need to address by new research.



34th INTERNATIONAL CONFERENCE ON
PRODUCTION ENGINEERING
28. - 30. September 2011, Niš, Serbia
University of Niš, Faculty of Mechanical Engineering



NATIONAL TECHNOLOGY PLATFORMS OF SERBIA

Petar B. PETROVIC, Vladimir R. MILACIC

Faculty of Mechanical Engineering, Belgrade University, Kraljice Marije 16, 11120 Belgrade, Serbia
pbpetrovic@mas.bg.ac.rs, vmilacic@mas.bg.ac.rs

Abstract: *This plenary paper presents general information about the Program of National Technology Platforms of Serbia (NTPS), which is initiated and implemented by Academy of Engineering Sciences of Serbia. This program is based on European Technology Platforms (ETP) which was developed ten years ago by European Commission as new political instrument focused on three main targets: 1) Provide a framework for stakeholders, led by industry, to define research and development priorities, 2) Ensuring an adequate focus of research funding on areas with a high degree of industrial relevance, and 3) Address technological challenges that can potentially contribute to a number of key policy objectives which are essential for Europe's future competitiveness. Following the ETP approach AINS was developed an original program of National Technology Platforms of Serbia which is closely related to specific situation of Serbian industry, national research and technology priorities, as well as the European integration processes of Serbia. This paper covers general information about NTPS program, its structure, organization and implementation plan, and in particular, development of network of individual platforms carefully designed to optimally support industry recovery process and its future sustainable development.*

Key words: *Industry, Technology, Development*

1. INTRODUCTION

Serbian industry is facing serious problems that last almost two decades. The new industry policy [1], as well as the strategy for growth and economical development of Serbia (Serbia 2020 document, [2]) are both focusing on industrial development, recognizing industry as a vital element of the national economy. In the past decade Serbia has adopted market economy and privatization process is almost finished. The key element of the current industrial development practice is providing the ambient, almost exclusively dedicated to the foreign investors, which is based on low wages, financial stimulations for every newly opened workplace as well as other types of financial measures that stimulate business. However this approach has not shown its effectiveness in practice as expected. Even more, deeper analysis shows that this approach is not sustainable on a long-term basis. Focusing only on the financial supporting instruments is necessary but not sufficient.

As Serbia cannot compete on the costs alone, knowledge has a central role to play in helping industry to recover, especially to recover its technological and structural foundations and adjust to the pressures of globalization, in all sectors regardless of their technology intensity, including low-technology sectors where traditional industry is located mainly. In this context, fostering innovation and retaining and developing highly skilled human resources are essential.

Economic globalization refers to increasing economic interdependence of national economies across the world through a rapid increase in cross-border movement of

goods, service, technology and capital. It is paradox that in a globalised economy location remains a crucial factor for research and innovation. This is the chance for Serbia, especially for Serbia in future when it becomes a part of European community.

At the Lisbon European Council on 23 and 24 March 2000, the Heads of State or Government resolved to make Europe's economy the most competitive knowledge-based economy in the world, working on increasing jobs, greater social cohesion, and on economic growth until 2010. Following the Lisbon agenda, and later stated Barcelona target of 3% GERD (Gross Domestic Expenditure on R&D) by 2010, European Commission has developed new instrument with the mandate of helping to further mobilize private and public R&D investments in research and innovation. This instrument is named European Technology Platforms (ETPs).

This paper starts with general information about European technology platforms. Then the text is focused to the Program of National Technology Platforms of Serbia (NTPS), providing the information on its general concept, its rationale as well as its roadmap for the future actions, together with pilot actions which are already initiated or which should be started in close future. In particular, in this paper is presented the first individual national platform NTPS-Production, which is focused on recovery of Serbian industry and make it ready, in technological sense, for European integration processes. The paper is structured as follows: 1) General notes on European Technology platforms, 2) National Technology Platforms of Serbia, 3) NTPS-Production and 4) Concluding remarks.

2. EUROPEAN TECHNOLOGY PLATFORMS

ETPs were first introduced officially in the EC Communication “Industrial Policy in an enlarged Europe” [3] in December 2002. In this document is exactly stated: “Technological platforms could be considered to foster marketplaces for cooperation among stakeholders and work out a long-term strategic plan for R&D for specific technologies involving major economic or societal challenges, such as the advent of hydrogen as a new source of energy. They would ensure synergy among public authorities, users, regulators, industry, consumers, and poles of excellence viewed as places where basic research and technology transfer are closely linked. There is a need for coherence between research, which can create new opportunities, and the downstream regulatory framework in which these technologies can be developed and marketed.”

The ambition was to bring together R&D-relevant stakeholders with various backgrounds (e.g. regulatory bodies at various geo-political levels, industry, public authorities, research institutes and the academic community, the financial world and civil society) who would develop a long-term R&D strategy in areas of interest to Europe. The set up of an ETP follows a bottom-up approach in which the stakeholders take the initiative and where the European Commission evaluates and guides the process, [4].

After almost ten years of existence, and systematically collected experience from development of respective number of individual platforms, each of them targeted to specific EU societal challenges, the concept of ETP that was outlined in its very beginning has been largely confirmed, [5], [7], [8]. Recent development activities are focused into two directions, both straightening the role of ETP concept, [8], [9]:

1. Tackling the grand societal challenges – ETP and European research community must focus on the challenges (such as global warming, tightening supplies of energy, water and food, ageing societies, public health, pandemics and security, as well as the overarching challenge of turning Europe into an eco-efficient economy) that European society faces in the 21st century, moving beyond currently present rigid RTD thematic approaches, and
2. Straightening interaction between European Technology Platforms and national research actors.

The later one is of high importance for Serbia, because it makes a room for setting-up a comprehensive national program of establishing technology platforms that is well concentrated on Serbian societal challenges and well aligned with national specificities, starting from historical and geographical aspects, up to the current economy situation as well as adopted priorities within actual research and industry policies.

2.1. Bottom-up three stage process

European Technology Platforms are an effective means of defining research and development priorities, timeframes and action plans on a number of strategically important issues where achieving future growth, competitiveness

and sustainability objectives is dependent on major research and technological advances in the medium to long term. ETPs focus on areas of significant economic impact and high societal relevance where there is high public interest. ETPs are focused on three main targets:

1. Provide a framework for stakeholders, led by industry, to define research and development priorities, timeframes and action plans on a number of strategically important issues where achieving Europe's future growth, competitiveness and sustainability objectives is dependent upon major research and technological advances in the medium to long term,
2. Ensuring an adequate focus of research funding on areas with a high degree of industrial relevance, by covering the whole economic value chain and by mobilizing public authorities at national and regional levels,
3. Address technological challenges that can potentially contribute to a number of key policy objectives which are essential for Europe's future competitiveness.

The development of European Technology Platforms is essentially a “bottom-up” process, [4]. Hence, it is the stakeholders themselves who take the initiative to set up a European Technology Platform, with the support and guidance of the European Commission, as appropriate.

In practice, the ETP concept is performing as a set of individual technology platforms. Each individual platform has its own origins and approach and its own particular way of working. In most cases individual technology platforms follow a three-stage process and that successful completion of each is a prerequisite for effective implementation of the subsequent stages (Figure 1).

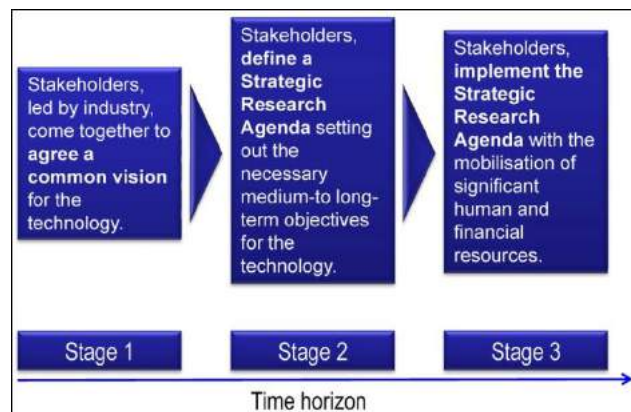


Fig.1. Evolution stages in setting-up individual technology platforms, [6]

Stage 1: Emergence and Setting Up: In this stage, stakeholders are brought together. Industry plays an initiating role in this regard with the aim of achieving consensus on the way forward. The main deliverable is a strategic vision document reflecting this consensus and endorsed by top executives from leading companies in the sector. The vision document explains the strategic importance of the activity and gives an outline of the desired medium and long term development objectives of the platform. It also explains why action at European level

is required. At this stage, the main principles for the governance of the platform have to be established.

Stage 2: Definition of a Strategic Research Agenda: The Strategic Research Agenda is the key deliverable of a technology platform. It should set out research and technological development priorities for the medium to long term, including measures for enhancing networking and clustering of the RTD capacity and resources in Europe. The definition of a Strategic Research Agenda is commonly co-ordinated by an advisory council that includes representation from a wide range of stakeholders. In many cases, the active involvement of Member States is channeled through a “mirror group” that reflects their views as the Strategic Research Agenda takes shape. Steering panels undertake the detailed work of defining the Strategic Research Agenda, often supported by specialized working groups.

In parallel with the definition of a Strategic Research Agenda, European Technology Platforms begin to specify a deployment strategy at this stage. The deployment strategy anticipates the key elements required in order to implement the Strategic Research Agenda effectively with the aim of bridging the gap between the current state of development of a given technology and its eventual deployment. It should take into account, for example, the need for mechanisms to mobilize private and public investments, strategies to implement optimal demonstration activities, actions related to education and training and the establishment of an ongoing communication process. It should also capitalize on possible synergies with other European Technology Platforms and address any possible overlap or duplication of activities across platforms.

Stage 3: Implementation of the Strategic Research Agenda: During this phase, the Strategic Research Agendas defined within European Technology Platforms are implemented with the support of Community research programs as appropriate, where they are compatible with the objectives of European research and competitiveness policies, together with other policies where relevant. At the same time, the Strategic Research Agendas will make an important contribution to the preparation of the Commission’s proposals for future research programs. It is, however, important to stress that the implementation of Strategic Research Agendas is likely to involve support from a range of sources, including the Framework Program, other sources of European funding, national research programs, industry funding and third-party private finance.

As the shape of a European Technology Platform evolves through these three stages, it remains flexible and open to entities joining or leaving the platform as well as to the integration of new initiatives. Thus, as it moves from the vision and strategy phases to the implementation phase, its character and structure can also change.

There are currently 36 individual technology platforms at various stages of development (ref. ETP web-site):

ACARE -	Advisory Council for Aeronautics Research in Europe
ARTEMIS -	Embedded Computing Systems
Biofuels -	European Biofuels Technology Platform
ECTP -	European Construction Technology Platform
eMobility -	Mobile and Wireless Communications
ENIAC -	European Nanoelectronics Initiative Advisory Council
EPoSS -	European Technology Platform on Smart Systems Integration
ERRAC -	European Rail Research Advisory Council
ERTRAC -	European Road Transport Research Advisory Council
ESTEP -	European Steel Technology Platform
ESTP -	European Space Technology Platform
ETP SMR-	European Technology Platform on Sustainable Mineral Resources
EuMaT -	Advanced Engineering Materials and Technologies
EUROP -	European Robotics Technology Platform
FABRE TP -	Farm Animal Breeding and Reproduction Technology Platform
Food -	Food for Life
Forestry -	Forest based sector Technology Platform
FTC -	Future Textiles and Clothing - FTC
GAH -	Global Animal Health
ETPIS -	Industrial Safety ETP
ISI -	Integral Satcom Initiative
Manufuture -	Future Manufacturing Technologies
NanoMedicine -	Nanotechnologies for Medical Applications
NEM -	Networked and Electronic Media
NESSI -	Networked European Software and Services Initiative
Photonics21 -	European Technology Platform for Photonics
Photovoltaics -	European Photovoltaic Technology Platform
Plants -	Plants for the Future
RHC -	Renewable Heating & Cooling
SmartGrids -	European Technology Platform for the Electricity Networks of the Future
SNETP -	Sustainable Nuclear Energy Technology Platform
SusChem -	European Technology Platform for Sustainable Chemistry
TPWind -	European Technology Platform for Wind Energy
Waterborne -	Waterborne European Technology Platform

¹ **Petar B. Petrovic**, Professor Dr., *Faculty of Mechanical Engineering, Belgrade University, Kraljice Marije 16, 11120 Belgrade, Serbia, pbpetrovic@mas.bg.ac.rs.*

² **Vladimir R. Milacic**, Professor Dr., *Faculty of Mechanical Engineering, Belgrade University, Kraljice Marije 16, 11120 Belgrade, Serbia, vmilacic@mas.bg.ac.rs..*

WSSTP -	Water Supply and Sanitation Technology Platform
ZEP -	Zero Emission Fossil Fuel Power Plants

2.2. The role of European commission

In the course of the development of the technology platforms, the European Commission has the role which is defined by following clarifications [11]:

- The Commission is not the owner of technology platforms, nor is it directing the way in which they are undertaking their activities.
- The Commission is however encouraging bottom-up, industry-led approach to defining medium to long-term research needs through:
 - Its active participation as an observer in many of the platforms;
 - Playing a guiding role where necessary;
 - Providing limited Community financial support for operational entities (for example a Secretariat) to some of the platforms where their objectives and activities correspond closely with the thematic areas of actual research programs; and
 - Maintaining the Community's sponsoring role through the continued funding, where appropriate, of collaborative research projects in many of the areas concerned.
- Whilst not bound by the views of technology platforms, the Commission services are closely co-ordinating their activities in this area, monitoring developments on an ongoing basis and, where appropriate, using their deliverables in the course of developing research policy.

2.3. Openness and transparency

The issue of openness and transparency has been identified as of crucial importance for the successful development of technology platforms. At a seminar held on 15, December 2004 in Brussels, the industrial leaders of the existing and emerging platforms committed themselves to respect a voluntary code of conduct on openness and transparency. For their individual platforms, they will set and make public clear and transparent rules of participation (including rotation of members in key bodies) and ensure full transparency (web-site, conferences, reports and other documentation).

Each platform is free to decide for itself how to implement these principles and a range of initiatives have been taken in this respect.

An open and transparent platform is one which respects three key principles [10]:

Openness refers to the degree to which a European Technology Platform encourages and allows the participation of a broad range of stakeholders in its activities. It also relates to the level of cooperation with national and regional public authorities, as well as with other platforms.

Accountability refers to the existence and clarity of rules and procedures within the European Technology Platform

structure, as well as to the process for monitoring and adapting platforms' activities according to changing priorities and circumstances.

Transparency refers to the measures taken by European Technology Platforms to communicate openly with their target audiences, including the general public, and to provide full and up-to-date information about their current status and activities.

Openness and transparency are key to the success of European Technology Platforms. The involvement of a broad range of stakeholders in defining their common vision and research agendas will increase commitment to these objectives and, hence, the platforms' effectiveness.

2.4. National and regional dimension

Using Mirror Groups instrument, ETP concept was extended to the national level. Member States deployed Mirror Groups widely. Mirror Groups are normally composed of experts nominated by the Member States and aim to facilitate coordination and provide an effective two-way interface between ETPs and complementary activities at a national level. Parallel to the Mirror groups, national platforms started to emerge based on NRTP mechanism, typically focusing on a part of the research agenda of interest to national research players. Currently, national TPs exist in different forms. In most cases they have been set up following a national call for proposals, with varying degrees of involvement of European TPs in the process. Some national TPs operate as national branches of the corresponding ETP, but other are mainly coordinated with their national government. Some countries have a very high number of national TPs because they have decided that the concept serves them well for national policy purposes. Other countries, however, have chosen a limited number of research and social priorities and have promoted the establishment of the corresponding TPs. In this way, public authorities are actively involved in ETPs in their roles as policy-makers and funding agencies, and as promoters and consumers of technologies, focusing on those ETPs which are more relevant for their national industries, research organizations and academia..

3. NATIONAL TECHNOLOGY PLATFORMS OF SERBIA

The program of the national technology platforms was initiated and developed by the Serbian Academy of Engineering Sciences with the aim of introducing technological dimensions and engineering to the process of recovery and development of Serbian industry, as a vital element of the national economy. This process is planned to be achieved through comprehensive and interdisciplinary set of activities within the development triangle consisting of industry, research and investment.

The development triangle (Figure 2) can actually be seen as a special kind of a machine, with extreme complexity, which transforms money into knowledge, knowledge into innovation and innovation into money. This circular mechanism of functioning is the very essence of this machine. Full functionality of the development triangle provides the basis for achieving industrial growth,

creating a helix of development and maintaining sustainability of such processes on a long-term basis. Environment, in which the nodes of this triangle are equally developed, functional and mutually interactive, renders the development triangle functional, i.e., the machine which generates social welfare and prosperity.

NTPS Program is nested within the development triangle and its mission is to harmonize its internal processes, focusing on the engineering and technological aspects only. At the moment, the development triangle of Serbian economy is unbalanced and nonfunctional. Its nodes are asymmetrically developed, and the interconnections between them are weak or even broken. The dysfunctionality of the development triangle is one among the reasons for stagnation of the Serbian economy, especially the Serbian industry, creating economic difficulties, social problems and poverty that Serbia faces a number of years.

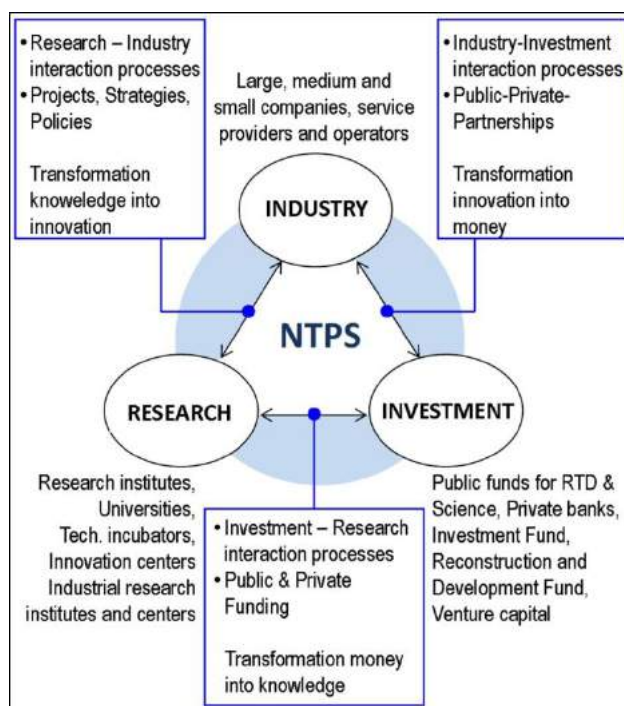


Fig.2. Technology development triangle

NTPS Program was formally launched in the year 2010 and for its development and implementation is responsible the AINS Committee for technology platforms, i.e. NTPS Committee, which has multidisciplinary engineering structure, composed of eminent professors and researchers appointed by the Council of the Serbian Academy of Engineering Sciences. NTPS Committee has the mandate to conceptualize the basic framework of the NTPS program, taking into account both national and international aspects, and also to stimulate and monitor the implementation of this program in the research and industrial area of Serbia. NTPS program is generally based on the concept of European Technology Platforms and in all aspects of its activity is tightly focused on establishing and developing various forms of cooperation, especially with individual

technology platforms having strategic research agendas complementary with research and development priorities of Serbia. The NTPS program is a link to the European Technology Platforms.

NTPS Program is recognized by Serbian Ministry of Science and Education as a program of strategic importance for technology development, technology transfer and innovation system development. Moreover,

NTPS Program is incorporated in Serbian industrial policy 2020 as a pillar of strategic importance for rising high technology content in Serbian industry through extensive cooperation between scientific institutions and industry [1].

3.1. Basic objectives

NTPS program has four basic objectives:

- Providing a new formal framework for smart and systemic transformation of technological basis of Serbian industry;
- Strengthening Science - Industry interaction by focusing of RTD programs and funding to areas of high relevance to Serbian industry and stops the situation in which investment in R&D often produces fewer than expected;
- Focus on technology as important component for European integration process;
- Recognition of technology challenges that can potentially contribute to the realization of key societal priorities and challenges and delivers benefits to the Serbian citizen.

Regarding the methodological framework, NTPS program draws its foundations from the respective national potential for technology research and development (well developed educational system and extensive RTD infrastructure), the respective industrial tradition that spreads out for nearly two centuries, and also cultural and regional specificities. Besides previously mentioned, the methodological framework of action of the NTPS Program includes as follows:

1. Transfer of ETP concept into Serbian industry, ETP scaled down to the national level;
2. Synergies with the EU level through a extensive cooperative relationships with the individual ETPs;
3. Broad mobilization of industrial companies, industry associations, RTD institutions and universities, public authorities and the holders of investment capital;
4. Partnership with Government and other state regulatory bodies in creating a stimulating environment for industry recovery and growth - strong political support;

3.2. Structure and guiding principles

Although the European technology platforms are designed as bottom-up instrument, experience shows that pure bottom-up approach is not quite suitable for its use in the economies of Eastern European countries (Polish

¹ Petar B. Petrovic, Professor Dr., Faculty of Mechanical Engineering, Belgrade University, Kraljice Marije 16, 11120 Belgrade, Serbia, pbpetrovic@mas.bg.ac.rs.

² Vladimir R. Milacic, Professor Dr., Faculty of Mechanical Engineering, Belgrade University, Kraljice Marije 16, 11120 Belgrade, Serbia, vmilacic@mas.bg.ac.rs..

Technology platforms for instance). To make it really effective it is necessary to ensure sizeable participation of state regulatory bodies and other state institutions. That is the essential difference and this difference is very important. Therefore, from the beginning, when AINS started to consider how to establish the program of national technology platforms which will be truly functional and capable to generate benefit to Serbian industry and research community, decision was made that this program should be a compromise, combination between top-down and bottom-up approach. It means that the program must have one strong central entity which will define the general framework and later on continuously supervise implementation of this framework, ready to react immediately if the development of the program starts to decline from its general principles. However, it doesn't mean that the bottom-up approach is not still dominant and top-down activities hinder the freedom of stakeholders to play an essential role and act autonomously.

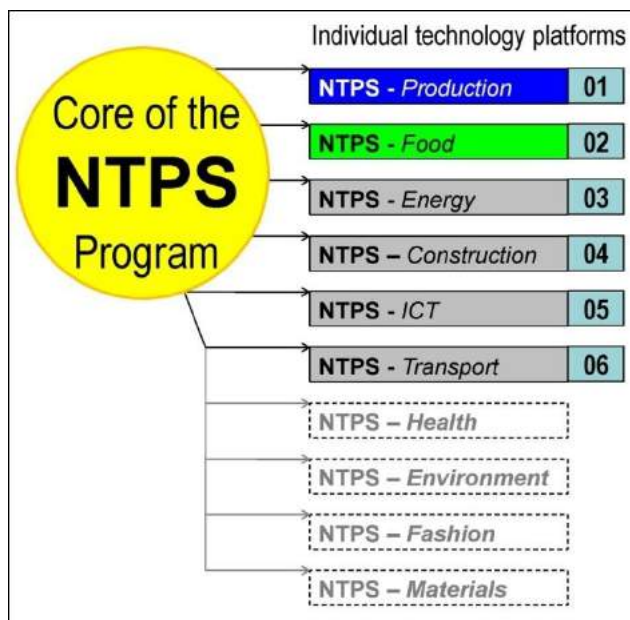


Fig.3. NTPS organizational structure

As a result of such approach, the NTPS program was conceptualized as a structure that is composed of two hierarchical levels: NTPS Core, which is located in the Serbian Academy of Engineering Sciences and governed by NTPS Committee, and NTPS Individual Platforms, a set of up to 10 individual platforms (in order to maintain a critical mass of resources to be representative) that emerges from NTPS Core as a network of mutually complementary, highly networked and interacting entities. These individual platforms are in their construction and principles of operation very similar to European individual technology platforms. Figure 3 shows the general functional structure of NTPS Program.

There are five guiding principles which are adopted by NTPS program that should be used to decide whether an individual platform should be established or not. These guiding principles are of equal importance for stakeholders, i.e., industry, research and educational institutions, investors, but also for national regulatory bodies that are

in some way responsible for the issue of technological development, research, education and other aspects related to industrial development. Any of the NTPS individual technology platform should be:

1. **A Response to Major National Challenges:** The Platforms are mission oriented and address major national economic – environmental – technical – social challenges. NTPS is not a short-term, problem solving instrument.
2. **A Strategic National Initiative:** Platforms should be set up only when there is a well-defined, national strategic need for such an instrument, and national added value can be clearly justified.
3. **Politically Highly Visible:** To affect change across national, industrial, technological boundaries, the NTPS individual platforms must create strong political support and be highly visible at a national, European, and even at a global level.
4. **Industry Led:** To be effective, the NTPS individual platforms must be driven by actors from the applications / problem end of the innovation process. Individual platforms should not become too academic and the most relevant stakeholders in the sector should be included. The governing bodies of the platforms must be lead by a person who is coming from industrial domain.
5. **Well planned and executed:** There must be a Road Map with a long-term vision, a sound strategy for achieving this vision and a detailed action-plan for carrying out the necessary activities. The platform must be big enough to be representative.

The NTPS program in whole is not and in any case or under any circumstances should not become a new vehicle for personal promotion of any scientist or institution. This program also should not become isolated from the industry in its implementation, especially in terms of satisfying its needs and decision-making on matters affecting the industry on any issue.

3.3. NTPS rationale – Serbian industry data

Due to the crisis that has lasted almost continuously for two decades, Serbian industry is currently in very difficult situation. Stagnation in all sectors has been present since the nineties, and this process is associated with the aftermath of the disintegration of former socialist Yugoslavia and all related causes that have had serious impact on the overall economy, especially industry.

Quantification of this process can be achieved based on the analysis of three main indicators: 1) The index of industrial production, 2) The number of industrial workers, and 3) The share of industry in GDP creation. The Index of Production (IoP) measures the volume of production of the manufacturing, mining and quarrying, and energy supply industries. The IoP is a major contributor to the National Accounts. GDP measures the sum of the value added created through the production of goods and services within the economy.

Contrary to common practice to analyze above mentioned indicators quarterly, yearly or for a short period of several years, in a study which was carried out by the NTPS

Committee, a significantly broader time period of fifty years was considered. This approach stems from the fact that all industrial processes are very complex, mostly asynchronous, and inherently slow. Industry is intrinsically very inert system. Therefore, for their full understanding it is necessary to consider very broad time frames. Such standpoint holds even in the case of new and emerging technologies. Time dependences of considered industry indicators are shown graphically in Figure 4 (source: Republic Development Bureau, Republic of Serbia).

Statistical trends given in Figure 4 show the evidence for sudden collapse of industry output, huge loss of human resources, and marginalization of the role of industry. In fact, the crisis from the nineties has triggered the process of intensive deindustrialization of Serbian economy. To figure out these graphs objectively it is important to consider the information related to the socio-political ambient in which the industry was operated. In the period of five decades, it is possible to identify three characteristic stages:

1960 – 1990 The context before the crisis: Serbia in the former socialist Yugoslavia; Stable industry development; Rapid industrial development, average growth rate for 3 decades: 7.8% per year.

Basic data: IoP₁₉₉₀ = 100, 998.000 workers, 28.6 % GDP;

1990 – 2000 Collapse of former Yugoslavia: Massive disintegration processes and ethnic conflicts; Severe economic downturn, enormous inflation and collapse of national fiscal system, extensive fragmentation of the industrial system, UN economic sanctions, etc., all together was created serious consequences and severely damaged the industry.

Basic data: IoP₁₉₉₀ = 43.3, 643.000 workers, 24.7 % GDP;

2000 – 2010 Democratic changes: Emerging Republic of Serbia; Economic liberalization process / market economy; Extensive privatization process (almost completed); Openness for foreign direct investments; Global economy crisis in 2008.

Basic data: IoP₁₉₉₀ = 45.9, 312.000 workers, 15.9 % GDP;

For more comprehensive insight in the industry condition it is necessary to introduce another indicator that refers to the quantification of industry sectoral technology content, i.e., industry technological profile. Industry technological profile is defined by the sectoral classification of investment intensity in research and development (products, processes and / or business systems), i.e., R&D expenditure as defined in [12] and [13]. This indicator is not systematically monitored in Serbia, but it can be derived from the industry statistical data that are collected regularly. Figure 4 shows the sectoral technological

profile of Serbian industry for year 2008 (source: Republic Development Bureau, Republic of Serbia). For comparison, in Figure 5 are also given the sectoral technological profiles for two leading world economies, the U.S. and EU, expressed through R&D investment of industrial companies (the investment funded by the companies themselves and for their own technological development, [14]). The differences are almost dramatic, and clearly show high degree of technological erosion that was occurred. It is clear that in past two decades the process of technological development had inverse character, i.e., downward development helix that has transformed former highly dynamic and technology intensive industry into recourse based and low adding value industry.

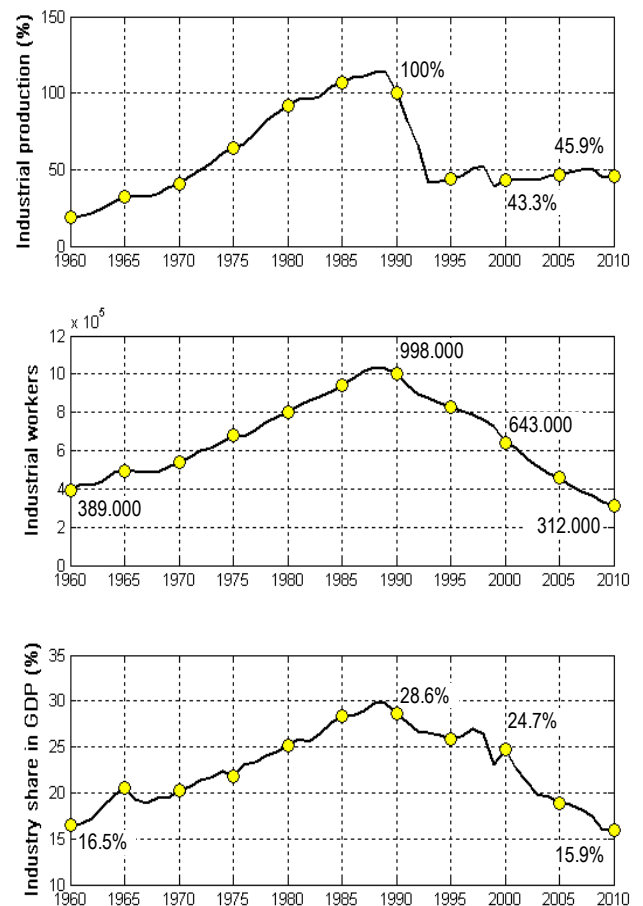


Fig.4. The index of production (indexed to 1990), industrial workers, and total industry share in GDP creation within the past five decades

3.4. NTPS-Production

NTPS-Production is the first individual platform that is derived from NTPS program and put into operation. It is an industry-lead voluntary association of stakeholders in the field of industrial production in Serbia.

The NTPS-Production platform was launched in May 2011 as a pilot action with the twofold mission: 1) to constitute a functional system, i.e., association, composed

¹ Petar B. Petrovic, Professor Dr., Faculty of Mechanical Engineering, Belgrade University, Kraljice Marije 16, 11120 Belgrade, Serbia, pbpetrovic@mas.bg.ac.rs.

² Vladimir R. Milacic, Professor Dr., Faculty of Mechanical Engineering, Belgrade University, Kraljice Marije 16, 11120 Belgrade, Serbia, vmilacic@mas.bg.ac.rs..

of referent national actors in the field of manufacturing industry and production engineering (leading industrial companies and systems, leading RTD institutions in the field of production engineering, and investors) that should provide strategic support to the national regulatory bodies in facing with the one of the most important and the most urgent grand societal challenges of Serbia, i.e., industry recovery and systematic revitalization / reinforcement of its technological foundations, and 2) to prove practical applicability of the NTPS concept in general and improve it if necessary.

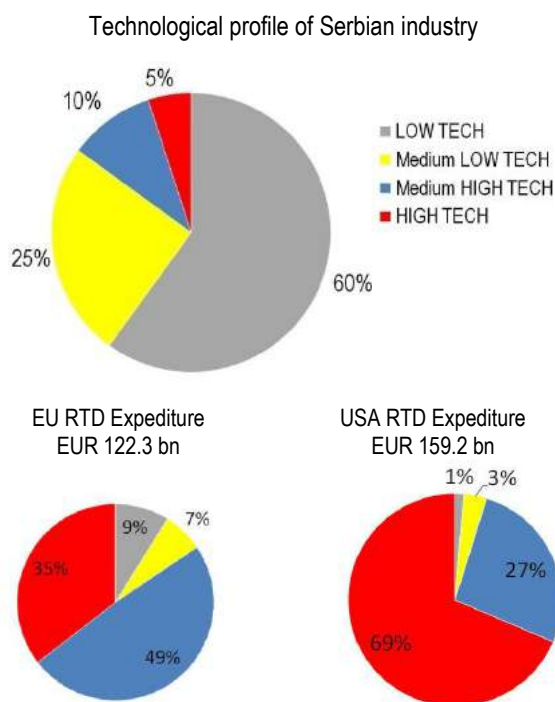


Fig.5. Sectoral profile of Serbian industry in accordance to technology intensity for the year 2008 (up), and RTD technology investment profile of industrial companies in EU and USA (down)

The overall mission of the NTPS-Production platform is the concerted strategic planning, the coordination and the facilitation of pre-competitive industrial and research activities in the field of production technologies, encompassing education, basic research, applied / industrial research and development. To this end, NTPS-Production platform will discuss industrial, scientific, technical, political, social and economic objectives.

Referring to the ETP implementation model, development of the NTPS-Production platform is planned as three-stage process:

Stage I: Action plan for year 2011

- Set-up a stakeholders consortia and associated Business Interest Groups (BIG)
- Consultation process and preparing the Platform Vision document,
- Constitution of the Platform structure and governance bodies,
- Setting up NTPS Production WEB Portal,
- Promotion activities, Community support, Industry support,

- Official contacts with relevant ETPs at EU level + Regional collaboration,
- Cooperative actions with industry; focus on the priorities stated in the Serbian industry policy 2020 document.
- Formal Launch of NTPS Production and clear political visibility.

Stage II: Action plan for year 2012

- Producing Strategic Research Agenda document: Methodology, Time lines, Targets / Priorities / Strategic pillars, Collaboration with relevant ETP SRAs, Establishing or confirmation of the Platform Working Groups, Wide industry and research Consensus / consultations,
- Financing and budgeting issues,
- Involvement of interested Public Authorities and Government, Political visibility,
- Communication, NTPS Production WEB Portal,
- Promotion activities, Community support, Industry support,
- Dissemination and similar issues,
- Cooperative actions with industry; focus on the priorities stated in the Serbian industry policy 2020 document.

Stage III: Action plan for year 2013

- Implementation of SRA,
- Rising Commitment and effective involvement of stakeholders and members of the associated Business Interest Groups (BIG);
- Building a long-term public-private partnership models and cooperative actions / initiatives,
- Cooperative actions with industry; focus on the priorities stated in the Serbian industry policy 2020 document.

In addition to activities that are planned to be carried out at the national level, intensive cooperation activities are also planned at the regional and EU level. A key activity is to establish synergistic relationships with relevant individual technology platforms at EU level, including membership and close collaboration. This vertical action is of highest importance to the NTPS Program in general. For NTPS Production platform of special importance is the cooperation with the following ETPs:

- **ManuFuture:** Future Manufacturing Technologies, [18],
- **EUROP:** European Robotics Platform,
- **MINAM:** European Platform on Micro- and Nanomanufacturing,
- **ARTEMIS:** The European Technology Platform for Advanced Research and Technology for Embedded Intelligence and Systems,
- **EPoSS:** European Platform on Smart Systems integration.

The organizational model of the NTPS-Production platform is shown in Figure 6. This model has four hierarchical strata:

- Level 1 - Stakeholders / members level,
- Level 2 - Operational core level,
- Level 3 - Decision-making level, and
- Level 4 - Managing level of TP.

The **stakeholder level** in form of General Assembly composed of representatives of the platform member organizations and associated representatives of Business Interest Groups (BOS) forms the basis of the technology platform. Business Interest Groups are composed of partner organizations with goals synergistic with the goals of the NTPS-Production platform or representatives of public bodies, organizations or initiatives whose activities have a bearing on meeting the goals of NTPS-Production but who are not members of NTPS-Production platform.

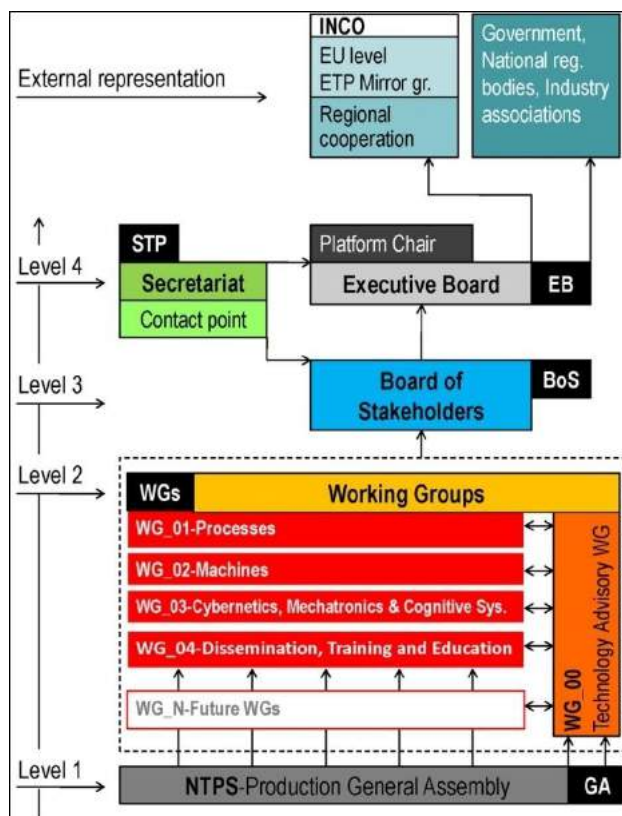


Fig.6. Organizational structure of NTPS-Production individual technology platform

Membership in NTPS-Production platform is open to all organizations or entities concerned with industrial or research activities in the field of the production, in particular: manufacturing and associated services, robotics, automation, ICT supporting production including mechatronics, Web and Internet-based services, and cognitive systems enabling the concept of Factories of Future – FoF (launched under the European Economic Recovery Plan in November 2008), [16], [17]. Particularly important in this respect are those activities that have a great potential to affect innovation in many different industrial sectors and fields of application, i.e., key enabling technologies (KETs) that include a high demand for RTD, skills and capital expenditure, a

multidisciplinary approach cutting across many technology areas, and long time horizons between basic research results and implementable innovations, [15], [17].

Members shall contribute to the mission and to the activities of the technology platform, participating actively in the Working Groups (each member is assigned to at least one Working Group according to his/her preference). A complete list of the NTPS-Production membership will be publicly available on the official NTPS-Production platform website.

The **operational core level** is composed of the NTPS-Production Working Groups (WGs) that are the main centres of activities within the technology platform. They are focused on domain-specific or cross-disciplinary, technological or application-oriented issues, or on specific tasks related to production technologies, including various forms of dissemination outcomes produced by Platform activities. The following issues are related to the Platform operational core level:

- Working Groups can be established or discontinued by the Board of Stakeholders on request of the Working Group itself, NTPS-Production Stakeholders, or the associated Business Interest Groups (BIG);
- The Working Group Chairs (WG Chairs) are elected within the Working Group from NTPS-Production Members participating in the Working Group;
- The composition of a Working Group will be established under the responsibility of its Chairperson, who will represent the Working Group at the Executive Board and report annually and upon request to the Executive Board.
- Working Group Chairs become members of the EB and become BoS members, unless his/her election is opposed by the NTPS-Production General Assembly.

At the current stage of the Platform development the Executive Board has been adopted initial set of working groups that should be constituted and put in operation immediately. This set of working groups consists of:

- WG_00 – Technology advisory working group;
- WG_01 – Production Processes working group;
- WG_02 – Machines and Equipment working group;
- WG_03 – Cybernetics, Mechatronic and Cognitive Systems working group;
- WG_04 – Dissemination, Training and Education working group.

This is the initial set of working groups and is subject to modifications if the need for different solutions arises through its implementation in practice.

The **decision making level** consists of Board of Stakeholders (BoS) that is the main decision-making body of the platform. In particular, the BoS bears responsibility for:

¹ Petar B. Petrovic, Professor Dr., Faculty of Mechanical Engineering, Belgrade University, Kraljice Marije 16, 11120 Belgrade, Serbia, pbpetrovic@mas.bg.ac.rs.

² Vladimir R. Milacic, Professor Dr., Faculty of Mechanical Engineering, Belgrade University, Kraljice Marije 16, 11120 Belgrade, Serbia, vmilacic@mas.bg.ac.rs..

- The determination of all matters related to NTPS-Production platform, unless otherwise stated within the Platform constitutive documents;
- Defining, pursuing and implementing the objectives of NTPS-Production according to its mission;
- Establishing or discontinuing Working Groups;

The BoS will appoint an organization to establish a platform office, i.e., the NTPS-Production Secretariat, which shall provide organizational and operational support to the BoS, to the EB and to the WGs. The NTPS-Production Secretariat acts on behalf of, and reports to, the EB.

The **managing level** consists of Executive Board (EB) that is the main managing body of the platform. The EB is responsible for the coordination and execution of the platform operations, for the preparation and the implementation of the decisions of the BoS and for the external representation of the platform (national and international collaborative actions and initiatives). The EB is composed of the Chair, the Working Group (WG) Chairs and the SME representative. The EB Chair will be elected by the BoS from amongst its own members. At least one representative of the Secretariat will be delegated as non-voting member of the EB.

With minor variations, this model should be applied in future for other individual platforms that emerge within the NTPS Program.

4. CONCLUDING REMARKS

In this paper are presented basic aspects of European technology platforms, as a new instrument that was established by the European Commission with the aim to strengthen interaction of industry and research area which was recognized as the key factor for the creation and development of knowledge-based society. European technological platform has demonstrated their full effectiveness and potential in practice.

Serbian economy is faced with crisis that lasts almost two decades. Its excessive length hardly destroyed the national economy, especially industry. Industry data show horrifying consequences. Industrial growth and technological development that existed in the period before the crisis were almost completely stopped. The industrial production volume has been reduced to the level of the seventies, the contribution of industry to national GDP was halved, and the number of industrial workers has been reduced to 1/3. The way out of the crisis requires economic growth, but the economic growth is impossible without a strong, productive and competitive industry. The strong industry requires a strong and dynamic technological base. Recognizing these needs, the Academy of Engineering Sciences of Serbia has conceptualized and developed a program of national technology platforms, i.e., NTPS Program. In its basis, NTPS Program is derived from the concept of European technology platforms. Although it is in its beginning, significance of the NTPS Program was recognized by the relevant public authorities and embedded in the industrial policy 2020 as one of strategic pillars, dedicated for recovering of technological basis of Serbian industry and for rising high technology content in all industrial

activities. The NTPS Program was started its implementation stage by launching the first individual technology platform NTPS-Production as a pilot action, aimed to show practical value of the NTPS concept and to prove potential of the NTPS Program in whole under the real industrial scenario.

REFERENCES

- [1] STRATEGY AND POLICY OF INDUSTRIAL DEVELOPMENT 2011-2020, Ministry of Economy and Regional Development of Republic of Serbia, Belgrade, 2011, (in Serbian).
- [2] SERBIA 2020 – A Strategy for Development and Growth of Republic of Serbia, Prepared by ad-hoc working group appointed by President of Republic of Serbia, Belgrade, 2010, (in Serbian).
- [3] Commission of the European communities: INDUSTRIAL POLICY IN AN ENLARGED EUROPE - Communication from the commission to the council, the European parliament, the economic and social committee and the committee of the regions, Brussels, 12.2.2002, COM(2002) 714 final.
- [4] European commission, TECHNOLOGY PLATFORMS - From Definition to Implementation of a Common Research Agenda, Report compiled by a Commission Inter-Service Group on Technology Platforms, Directorate-General for Research, Directorate B - Structuring the European Research Area, 2004, EUR 21265.
- [5] Commission of the European communities, REPORT ON EUROPEAN TECHNOLOGY PLATFORMS AND JOINT TECHNOLOGY INITIATIVES - Fostering Public-Private R&D Partnerships to Boost Europe's Industrial Competitiveness, Brussels, 10.6.2005, SEC(2005) 800.
- [6] European Commission Inter-Service Group on European Technology Platforms, SECOND STATUS REPORT ON EUROPEAN TECHNOLOGY PLATFORMS - Moving to Implementation, Directorate-General for Research, Directorate B – Structuring the European Research Area, 2006, ISBN 92-79-01019-0.
- [7] European Commission, THIRD STATUS REPORT ON EUROPEAN TECHNOLOGY PLATFORMS - At the Launch of FP7, Directorate-General for Research, Directorate C – European Research Area: Knowledge-based economy, Unit C1 – European Research Area Policy, 2007, EUR 22706 EN
- [8] European Commission, FOURTH STATUS REPORT ON EUROPEAN TECHNOLOGY PLATFORMS - Harvesting the Potential, Directorate-General for Research, 2009, EUR 23729 EN
- [9] European commission, Directorate-General for Research, European Research Area Knowledge-based economy, STRENGTHENING THE ROLE OF EUROPEAN TECHNOLOGY PLATFORMS IN ADDRESSING EUROPE'S GRAND SOCIETAL CHALLENGES - Report of the ETP Expert Group, October 2009, EUR 24196 EN.

- [10] European commission, EUROPEAN TECHNOLOGY PLATFORMS – Ensuring Openness and Transparency, 2006, ISBN: 92-79-02486-8
- [11] Commission of the European Communities, DEVELOPMENT OF TECHNOLOGY PLATFORMS - Status report, 2005, ISBN 92-894-8985-5
- [12] Hatzichronoglou, T. (1997), “Revision of the High-Technology Sector and Product Classification”, OECD Science, Technology and Industry Working Papers, 1997/2, OECD Publishing. doi: 10.1787/134337307632
- [13] Organization for Economic Cooperation and Development - OECD, Frascati Manual: THE MEASUREMENT OF SCIENTIFIC AND TECHNOLOGICAL ACTIVITIES - Proposed Standard Practice for Surveys on Research and Experimental Development, 2002, ISBN 92-64-19903-9.
- [14] European Commission Joint Research, Centre Institute for Prospective Technological Studies, Monitoring Industrial Research: The 2009 EU Industrial R&D Investment Scoreboard, 2009, EUR 24079 EN, ISBN 978-92-79-14058-7.
- [15] Aschhoff, B., Crass, D., Cremers, K., Grimpe, C., and Rammer, C., European Competitiveness in Key Enabling Technologies - FINAL REPORT, Centre for European Economic Research (ZEW), Mannheim, Germany, 2010.
- [16] European commission, Directorate-general for research, Directorate G – Industrial technologies, FACTORIES OF THE FUTURE - PPP Strategic Multi-annual Roadmap, 2010, ISBN 978-92-79-15227-6.
- [17] Communication from the Commission to the European Council, A EUROPEAN ECONOMIC RECOVERY PLAN, Brussels, 26.11.2008, COM(2008) 800 FINAL.
- [17] Communication from the Commission to the European Parliament, the Council, the European economic and social committee and the Committee of the regions: AN INTEGRATED INDUSTRIAL POLICY FOR THE GLOBALISATION ERA - Putting Competitiveness and Sustainability at Centre Stage, 2010, Brussels, COM(2010) 614.
- [18] Jovane, F., Westkämper, E., and Williams, D., THE MANUFUTURE ROAD - Towards Competitive and Sustainable High-Adding-Value Manufacturing, 2009, Springer-Verlag Berlin Heidelberg, ISBN 978-3-540-77011-4.

¹ **Petar B. Petrovic**, Professor Dr., *Faculty of Mechanical Engineering, Belgrade University, Kraljice Marije 16, 11120 Belgrade, Serbia, pbpetrovic@mas.bg.ac.rs.*

² **Vladimir R. Milacic**, Professor Dr., *Faculty of Mechanical Engineering, Belgrade University, Kraljice Marije 16, 11120 Belgrade, Serbia, vmilacic@mas.bg.ac.rs..*

34th INTERNATIONAL CONFERENCE ON PRODUCTION ENGINEERING



SECTION A

MACHINING TECHNOLOGIES



NEURAL NETWORK ALGORITHM FOR ON-LINE TOOL BREAKAGE DETECTION

Uros ZUPERL, Franc CUS

Production Engineering Institute, University of Maribor, Smetanova 17, Maribor, Slovenia
uros.zuperl@uni-mb.si, franc.cus@uni-mb.si

Abstract: *The original contribution of the research is the developed monitoring system that can detect tool breakage in real time by using a combination of neural decision system and ANFIS tool wear predictor. The ANFIS method uses the relationship between flank wear and the resultant cutting force to estimate tool wear. Therefore, the ANFIS method is used to extract the features of tool states from cutting force signals. A neural network is used in tool condition monitoring system (TCM) as a decision making system to discriminate different malfunction states from measured signal. A series of experiments were conducted to determine the relationship between flank wear and cutting force as well as cutting parameters. The forces were measured using a piezoelectric dynamometer and data acquisition system. Simultaneously flank wear at the cutting edge was monitored by using a tool maker's microscope. The experimental force and wear data were utilized to train the developed simulation environment based on ANFIS modelling. By developed tool condition monitoring system (TCM) the machining process can be on-line monitored and stopped for tool change based on a pre-set tool-wear limit.*

Key words: *END-milling, tool condition monitoring (TCM), wear estimation*

1. INTRODUCTION

The main goal of development of tool condition monitoring systems (TCM) is to increase productivity and hence competitiveness by maximizing tool life, minimising down time, reducing scrappage and preventing damage. The traditional ability of the operator to determine the condition of the tool based on his experiences and senses is now the expected role of the monitoring system. Each tool condition monitoring (TCM) system consists of: sensors, signal conditioners/amplifiers and a monitor. The monitor uses a strategy to analyse the signals from the sensors and to provide reliable detection of tool and process failures. It can be equipped with some signal visualisation system and is connected to the machine control.

Many studies have been conducted on the monitoring of malfunctions and abnormal cutting states of machine tools [1]. With regard to the monitoring of cutting tool states, two main factors are tool wear and failure. Tool failure has become more important recently since hard tools are frequently used in the cutting process.

There are two techniques for tool wear sensing: direct and indirect. Generally direct measurements are avoided because of difficulty of online measurements. For indirect methods of TCM, the following steps are followed: use of single or multiple sensors [2] to capture process information; use of signal processing methods to extract features from the sensor information; use of decision-making strategy to utilise extracted featured for prediction of tool failure. Indirect technique includes measuring of cutting forces, torque, vibration, acoustic emission (stress wave energy), sound, temperature variation of the cutting tool, power or current consumption of spindle or feed

motors and roughness of the machined surface [3]. The recent trend in TCM is multisensory approach which is termed as sensor fusion /sensor integration/sensor synthesis. The idea is to gather information from several sensors to make a comprehensive estimate of tool wear. The application of TCM in industry have relied mostly on robust and reliable sensor signals such force, power and AE. They are relatively easy to install in existing or new machines, and do not influence machine integrity and stiffness.

The recent studies show that force signals contained the most useful information for determining the tool condition [4]. However, in many cases the use of force sensors is not practical for retrofit applications and spindle power signal is often used as an alternative. Several different approaches have been proposed to automate the tool monitoring function. These include classical statistical approaches as well as fuzzy systems and neural networks. For instance Iqbal [5] developed an approach based on the least-squares regression for estimating tool wear in machining while. The capacity of artificial neural networks to capture nonlinear relationships in a relatively efficient manner has motivated Chien and Tsai [6] to apply these networks for developing tool wear prediction models. But in such models, the nonlinear relationship between sensor readings and tool wear embedded in a neural network remains hidden and inaccessible to the user. In this research we attempt to solve this situation by using the Adaptive Neuro-Fuzzy Inference System (ANFIS) to predict the flank wear of the tool in end-milling process. This model offers ability to estimate tool wear as its neural network based counterpart but provides an additional level of transparency that neural networks fails

to provide. Then a neural network is used as a decision making system to predict the condition of the tool. In this study, the cutting forces are used as the indicator of the tool flank wear variation.

2. PROBLEM DEFINITION

End-milling is interrupted cutting process, which means that each cutting tooth generates a cyclic cutting force ranging from negative to maximum force, and back to negative. This force is graphed as a series of peaks (Fig. 1).

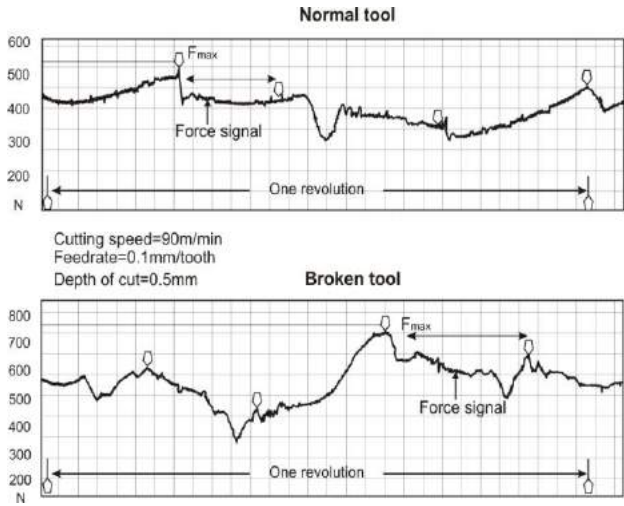


Fig.1. Cutting force signal of a good and damaged cutter

Cutting parameters and tool conditions affect the magnitude of resultant force.

herefore, the resultant force F_R , generated from X and Y directions, is used in this experiment for detecting tool state. If the tool condition is good, the peak measurement of each tooth's force should be roughly the same during one revolution of the cutter. If a tooth is broken, it generates a smaller peak force because it carries a smaller chip load.

As a result, the tooth that follows a broken tooth generates a higher peak force as it extracts the chip that the broken tool could not. One main force principle can be used to detect tool condition:

Maximum peak force in each revolution should differ between good and broken tools. Maximum peak force of a broken tool must be larger than that of a good tool; Applying these principles, an in-process tool breakage monitoring system was developed for end milling operations. The cutting forces and machining parameters were selected as input factors.

3. TCM METHODOLOGY AND STRUCTURE

The proposed approach consists of two main steps: First, an ANFIS model of tool wear is developed from a set of data obtained during actual machining tests performed on a Heller milling machine using a Kistler force sensor.

The trained ANFIS model of tool wear is then subsequently merged with a neural network for estimating tool wear condition (fresh, worn). Fig. 2 shows the basic architecture of the proposed system.

This is a typical TCM system where the sensor is used to collect the signals during milling through a data acquisition module. The signal processing module analyses the machining signals for extracting features sensitive to tool wear.

The features together with the machining parameters constitute the data set to be used as input to the decision system and estimator. The main purpose of the decision system and estimator is to map the input features to the current state of tool .i.e. the amount of tool wear.

A multi-layer perceptron neural network with backpropagation algorithm is used in TCM as a decision system due to its ability of learning, noise suppression and parallel processing.

A random pattern classifier module divides the data into training and testing set. The training set is used for learning purpose while the testing set is used for testing the decision system performance.

3.1. ANFIS Based Tool Wear Predictor

The relationship between the machining parameters/sensor signals and flank wear is first captured via a network and is subsequently reflected in linguistic form with the **help of a fuzzy** logic based algorithm.

The estimation design process consists of a linguistic rule construction, partition of fuzzy subsets and the definition of the membership function shapes.

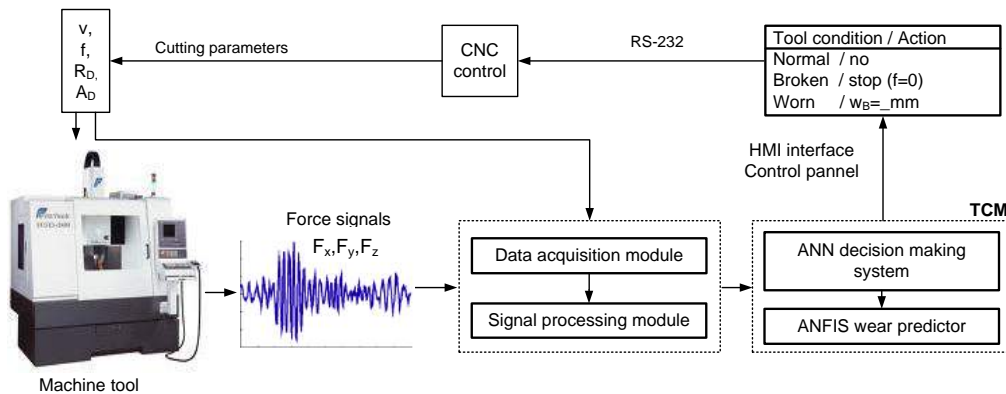


Fig.2. Architecture of tool condition monitoring system

It uses training examples as input and constructs the fuzzy if-then rules and the membership functions (MF) of the fuzzy sets involved in these rules as output. This process is called a training phase. In this model, we adopted two different types of membership functions for analysis in ANFIS training and compared their differences regarding the accuracy rate of the flank wear prediction. After training the estimator, its performance was tested under various cutting conditions. The performance of this method turned out to be satisfactory for evaluating of flank wear, within a 5% mean percentage error.

Fig. 3 shows the fuzzy rule architecture of ANFIS when the triangular membership function is adopted. The architectures shown in Fig. 3 consist of 31 fuzzy rules. ANFIS applies Hybrid Learning method for updating parameters.

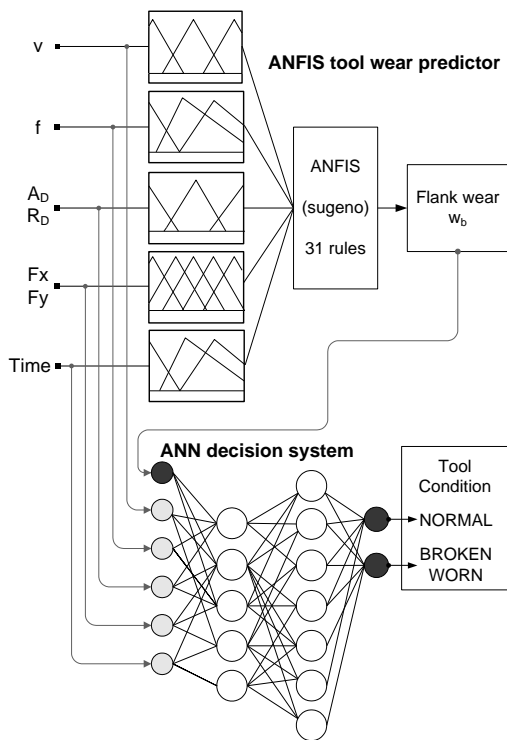


Fig.3. Components of TCM

For premise parameters that define membership functions, ANFIS employs gradient descent to fine-tune them. For consequent parameters that define the coefficients of each output equations, ANFIS uses the least-squares method to identify them. This approach is thus called Hybrid Learning.

3.2. Neural Decision System Development

A neural decision-making system was developed in Matlab software. The neural network used to predict the cutting tool condition is shown in Fig. 3. It has tool-breakage detection capability and is based on pattern recognition. The neural network stores a number of reference force patterns that are characteristic of tool breakage. When a tool tooth breaks, cutting force suddenly rises for a while, and then drops to zero. The system continuously monitors the signal for the break pattern. If pattern is identified, a break is declared within

10 ms of the breakage. Four steps are required to develop a neural decision system. In step one, network architecture and prediction factors were selected. Network has two hidden layers and uses a set of 5 normalized inputs for tool condition prediction: (1) cutting speed, (2) feed rate, (3) depths of cut, (4) forces, (5) tool wear. Output layer consist of only two neurons: (1) normal and (2) broken/worn. In steps two the learning rate, momentum factor and the number of hidden layers/hidden neurons were defined. The number of hidden neurons was set at 12, the learning rate was set at 1, and the momentum item was 0.4. The number of training/testing cycles was 1700. In step 3 the data set was divided into training and testing set. 200 data points were used in this research. Good tools collected half of these and broken tools collected the rest. In step 4 the training and testing faze is accomplished. Finally in the last step the trained neural network was used to predict tool conditions

4. EXPERIMENTAL DESIGN

Monitoring experiments were performed on a HELLER machine tool (type BEA1) with FAGOR CNC controller. It involved an end milling process of steel parts using two end mill cutters: normal and on tooth broken. The cutting tool used in the machining test was a solid end-milling cutter (R216.24-16050 IAK32P) with four cutting edges. The tool diameter was 16 mm. Its helix angle was 10°. The corner radius of the cutter was 4 mm. The insert had an outer coated layer of TiN featuring low friction and welding resistance. The workpiece material used in the machining test was Ck 45 and Ck 45 (XM) with improved machining properties. The workpiece was mounted in a 3 component piezoelectric dynamometer (Kistler 9255) to monitor the cutting forces in the X and Y directions. Force dynamometer was mounted on the machining table and connected to a 3-channel charge amplifier. The signals were monitored using a fast data acquisition card (National Instruments PC-MIO-16E-4) and software written with The National Instruments CVI programming package. The experimental set-up is shown in Fig. 2. The flank wear was observed during the experiments. The cutting tool flank wear was discontinuously measured with a tool microscope of 0.01 mm accuracy. The machining tests were carried out in two types of end milling operations: down milling and up milling operations. The experiments were carried out for all combinations of the chosen cutting parameters and tool wear.

5. RESULTS AND DISCUSSION

In-process sensing technique in connection with decision-making system is essential for successful working of TCM. The neural network was capable of detecting tool conditions accurately in real time. The accuracy of training data was 98.1%, and the accuracy of testing data was 94.9%. The results of neural network testing are shown in Table 1. The output node value of a back-propagation neural network was mapped as 0.01 for the normal cutting state, and 0.99 for the tool breakage. When

Table 1. Partial results of TCM testing

Tool condition s	Input factors					ANN outputs		ANN Prediction	ANFIS Prediction W_B [mm]
	F [N]	N (min^{-1})	F [mm/rev]	A_D [mm]	R_D [mm]	ANN ₁	ANN ₂		
Normal	427.2	440	0.17	1.2	8	0.9	0.1	Normal	0.11
Broken	777.9	440	0.17	1.2	8	0.02	0.98	Broken	0.24
Normal	433.9	440	0.13	1.4	8	0.3	0.7	Broken	0.17
Broken	729.6	440	0.13	1.4	8	0	1	Broken	0.26
Normal	650.5	440	0.20	1.4	8	0.89	0.11	Normal	0.13
Broken	925.7	440	0.20	1.4	8	0	1	Broken	0.27
Normal	614.4	480	0.20	1.4	8	0.88	0.12	Normal	0.15
Broken	751.9	480	0.20	1.4	8	0.03	0.97	Broken	0.23
Normal	904.3	360	0.22	1.6	8	0.89	0.11	Normal	0.14
Broken	991.9	360	0.22	1.6	8	0	1	Broken	0.31

the neural network outputs are over 0.9 (tool breakage), it sends the signal “Tool broken” to the PC. When both the neural network outputs are below 0.9, it sends the signal “Tool condition Normal”. Figs. 4a and 4b represent the cutting force signals for the normal and broken cutter. Developed decision system incorporates simple fixed limits for tool breakage detection. Limits are: L1 (collision), L2 (tool fracture), L3 (worn tool) and L4 (missing tool limit).

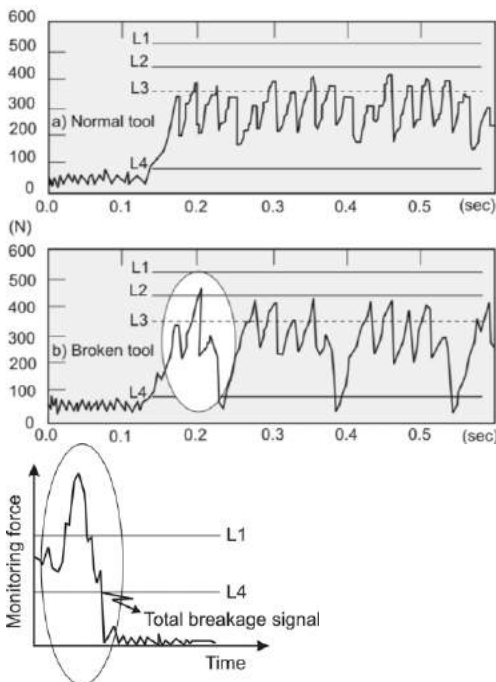


Fig.4. Thrust force of normal (a) and broken (b) tool in real time monitoring; (c) Indicative tool breakage force pattern with limits

In future it will be appropriate to replace fixed limits with self-adjusting limits. The detection system demonstrated a very short response-time to tool conditions. Because tool conditions could be monitored in a real-time, the worn tool could be replaced immediately to prevent damage to the product and machine.

6. CONCLUSION

We developed a system for monitoring tool condition in real time and obtained the following result through verification experiments:

- (1) The proposed monitoring system of cutting process may be very useful because of its parallel processing capability;
- (2) It enables monitoring of the cutting process with high reliability; ANFIS component can estimate flank wear progress very fast and accurately, once the maximum cutting forces are known.

A monitoring system using a neural network is able to classify the various cutting states such as tool breakage, and tool wear.

REFERENCES

- [1] MULC, T., UDILJAK, T., CUS, F., MILFELNER, M. (2004) *Monitoring cutting- tool wear using signals from the control system*, Journal of Mechanical Engineering, Vol.50, No.12, pp 568-579
- [2] KUO, R.J. (2003) *Multi-sensor integration for on-line tool wear estimation through artificial neural networks and fuzzy neural network*, Engineering Applications of Artificial Intelligence, Vol.3, pp 49-261
- [3] ACHICHE, S., BALAZINSKI, M., BARON, L., JEMIELNIAK, K. (2008) *Tool wear monitoring using genetically-generated fuzzy knowledge bases*, Engineering Applications of Artificial Intelligence, Vol.15, pp 303-314
- [4] KOPAC, J. (2002) *Cutting forces and their influence on the economics of machining*, Journal of Mechanical Engineering, Vol.48, No 3, pp 72-79.
- [5] IQBAL, A., HE, N., DAR, N.U., LI, L. (2009) *Comparison of fuzzy expert system based strategies of offline and online estimation of flank wear in hard milling process*, Expert Systems with Applications, Vol.33, pp 61-66
- [6] CHIEN, W.T., TSAI, C.S. (2005) *The investigation on the prediction of tool wear and the determination of optimum cutting conditions in machining 17-4PH stainless steel*, Journal of Materials Processing Technology, Vol.140, pp 340-345



THE EFFECTS OF TOOL FLANK WEAR ON TOOL LIFE

M. MILUTINOVIĆ, Lj. TANOVIĆ

Tehnikum Taurunum, High Enigineering School of Vocational Studies, Nade Dimić 4, Zemun, Serbia
Department of Production Engineering, Faculty of Mechanical Engineering, University of Belgrade, Kraljice Marije 16,
Belgrade 11120, Serbia
mmilutinovic@tehnikum.edu.rs, ltanovic@mas.bg.ac.rs

Abstract: *The development and application of cutting tools made of superhard materials as a precondition for increasing the productivity of machining requires higher costs of tools. Since tool life is closely related to tool wear, it can be influenced by the knowledge about the tool – workpiece interaction mechanism. Starting from the Merchant’s model of orthogonal cutting and by introducing the effects of the tool flank wear height B_L and the concentrated force on the cutting edge, it is arrived at the novel concept of consideration of the forces acting in the chip formation process. The increase of the radial force developed as a consequence of tool flank wear is taken for the tool wear criterion. The mentioned concept makes possible the prediction of tool flank wear height as well as tool life under manufacturing conditions with concrete values of cutting parameters.*

Key words: *Tool life, Flank wear, Orthogonal cutting*

1. INTRODUCTION

Tool wear is an important factor that directly affects the productivity and surface quality. Traditionally, at the production environment, a tool change was based on experience or the quality of machined surface. In the early nineties of the last century there was a transition from traditional to automated tool change with the idea that implies possibility of monitoring the amount of wear on the cutting tool edges during the cutting process. With the development of computer this on-line monitoring of the tool wear is gaining more importance [2].

Previous studies in the field of monitoring tool wear in a metal cutting process where based on measurement of the: cutting forces, stress/strain measurement, work piece dimensions, spindle motor torque and the surface finish quality.

The paper emphasizes the influence of the flank wear height at the clearance face on tool life and the forces that appear. The starting point is basic Merchants model of chip formation in orthogonal cutting. As the cutting forces increase with increasing of the flank wear height it is necessary to complete Merchants model that would include: flank wear, forces caused by flank wear, concentrated force acting at the cutting edge and force for chip formation. The presence of wearland has been found to have no effect on the basic model of chip formation and basic cutting quantities such as: shear angle, shear stress on the shear plane and friction angle. Existence of flank wear in the vicinity of the cutting edge resulting in an additional force of rubbing or ploughing at the clearance face results in increased thrust force. Based on completed Merchant’s model and predominant adhesion wear mechanism it is possible to define tool life using

cutting speed, feed and flank wear height, which is the efficient mathematical model that predicts tool life in production environment.

Prediction of the tool life in production environment is important because it provides good machined part in manned factories so that a new tool may be introduced at the instant at which the existing tool is worn out, thus preventing any hazards occurring to the machine or deterioration of the surface finish.

Forms of the tool wear occurring during metal cutting

When mating surfaces of the tool and workpiece are brought together as the result of their contact the following forms of tool wear occur: adhesion, abrasion, diffusion and oxidant wear [2].

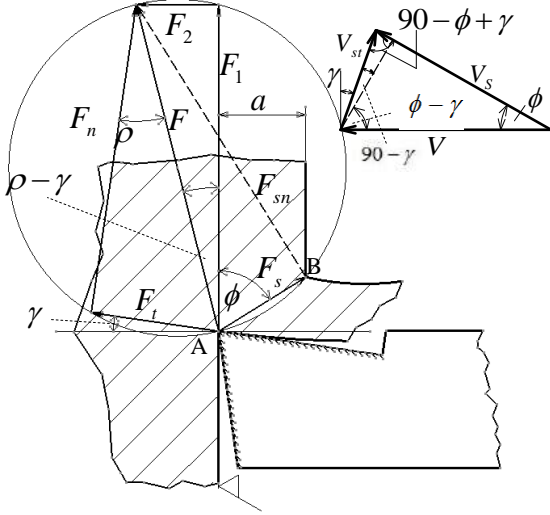
The more predominantly occurring forms of cutting tool wear often identified as the principal types of tool wear in metal turning using single-point tools are nose, flank, notch and crater wear. Nose wear or edge rounding occurs predominantly through the abrasion wear mechanism on the cutting tool’s major edges. Flank wear arises due to both adhesive and abrasive wear mechanism from the intense rubbing action of the two surfaces in contact, i.e. the clearance face of the cutting tool and the newly formed surface of the workpiece. Increasing the height of the flank wear leads to deterioration of the surface finish and to increased heat generation [3].

2. ORTHOGONAL CUTTING ANALYSIS

Tool’s cutting wedge penetrates in the workpiece under the influence of the resultant force F acting on the back of the chip and opposite to the resultant force F' acting on the shear plane (cutting resistance). In Fig. 1 is shown orthogonal cutting-Merchants model. A single straight

$$\phi = \frac{\pi}{4} - \frac{1}{2}(\rho - \gamma) \quad (4)$$

cutting edge with a plain face and flank is used to cut a workpiece of constant width at a constant cut thickness.



- F_1 - primary cutting force, F_2 - radial force,
 F_t - tangential force, F_n - normal force,
 F_s - shearing force, F_{sn} - normal force in the
shearing plain, F - resultant cutting force,
 γ - normal rake angle, ρ - friction angle,
 ϕ - shear angle, V - resultant cutting
velocity,
 V_s - shearing velocity,
 V_{st} - chip flow velocity.

Fig. 1. Orthogonal cutting-Merchant's model

Orthogonal cutting-Merchant's model assume the following: perfectly sharp tool with no concentrated edge force on the cutting edge, a continuous chip, plane strain, uniform shear stress distribution on the shear plane, and equilibrium of the under the action of equal and opposite resultant force acting at the shear zone and tool-chip interface, resultant cutting velocity V and chip flow

$$F_1 = \frac{tb \cos(\rho - \gamma)}{\sin \phi \cos(\phi + \rho - \gamma)} \quad (1)$$

velocity V_{st} are perpendicular to the cutting edge.

$$F_2 = \frac{tb \sin(\rho - \gamma)}{\sin \phi \cos(\phi + \rho - \gamma)} \quad (2)$$

$$\rho = \arctan \mu = \gamma + \arctan \left(\frac{F_2}{F_1} \right) \quad (3)$$

$$\tau = \frac{(F_1 \cos \phi - F_2 \sin \phi) \sin \phi}{bt} \quad (5)$$

Further development to the thin shear zone analysis, in addition to the force for chip formation R_s , is the introduction of the following forces: concentrated force acting at the cutting edge R_l and wearland force R_h representing the completed Merchant's model, Fig.2. Concentrated force acting at the cutting edge is manifested by the positive force intercepts when the measured force is extrapolated to zero cut thickness [4]. When Merchant's model includes concentrated force R_l equations (1), (2), (3), (5) have been modified when evaluating ρ and τ , i.e.

$$\rho = \arctan \mu = \gamma + \arctan \left(\frac{F_{2izm} - F_{2l}}{F_{1izm} - F_{1l}} \right) \quad (6)$$

$$\tau = \frac{[(F_{1izm} - F_{1l}) \cos \phi - (F_{2izm} - F_{2l}) \sin \phi]}{bt} \cdot \sin \phi \quad (7)$$

where: F_{1l} - concentrated force component in the direction of the primary cutting force for extrapolated zero cutting thickness, F_{2l} - concentrated force component in the direction of the radial force for extrapolated zero cutting thickness, F_{1izm} - as measured primary cutting force, F_{2izm} - as measured radial force.

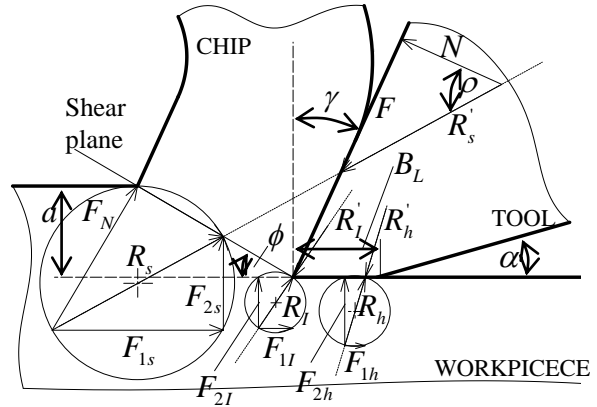


Fig. 2. Completed Merchant's model of orthogonal cutting [4]

Total cutting force can be represented by

$$F_1 = F_{1s} + F_{1l} = \frac{tb \cos(\rho - \gamma)}{\sin \phi \cos(\phi + \rho - \gamma)} + k_1 b \quad (8)$$

$$F_2 = F_{2s} + F_{2l} = \frac{tb \sin(\rho - \gamma)}{\sin \phi \cos(\phi + \rho - \gamma)} + k_2 b \quad (9)$$

where: F_{1s} - chip formation force component in primary cutting force direction, F_{2s} - chip formation force component in radial force direction, k_1 i k_2 are concentrated edge force intensity factors.

Equations (6) and (7) describe correlation between friction angle and shear stress considering concentrated edge force. Since the cutting edge is perfectly sharp only at the very beginning of the cutting process the question posed on the trend of the basic cutting quantities such as: friction angle, shear stress and shear angle when completed Merchant's model would include wear land height B_L . It has been suggested by many researchers that since the cutting edge is not perfectly sharp, a rubbing or ploughing process could occur in the vicinity of the cutting edge increasing total cutting force, in addition to the force for chip formation and the concentrated edge force. If the tool wear land height B_L does not affect the basic cutting quantities: friction angle, shear stress, shear angle etc., its effect on the cutting process will be an additional ploughing or rubbing forces that can be introduced in a similar way as the edge force and the force for chip formation.

Wang's experimental results have proved that the wear land height does not affect the values of the basic cutting quantities (shear stress, friction angle and shear angle) [4]. During the turning of carbon steel with cutting tool grade P20 carbide flat-top insert on CNC lathe machine at various cutting parameters (depth of cut, cutting speed, tool geometry and flank wear height) cutting force components, friction angle and shear angle were measured considering depth of cut a , Fig. 3.

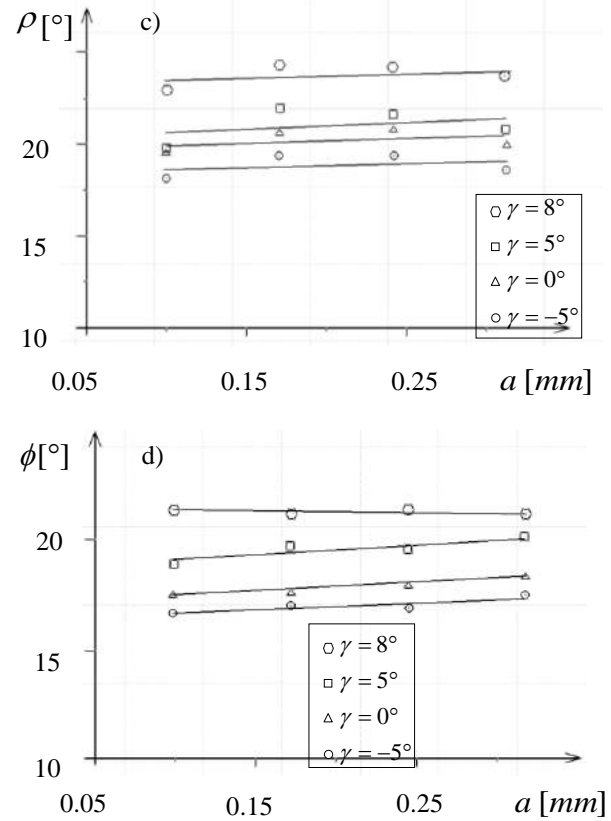
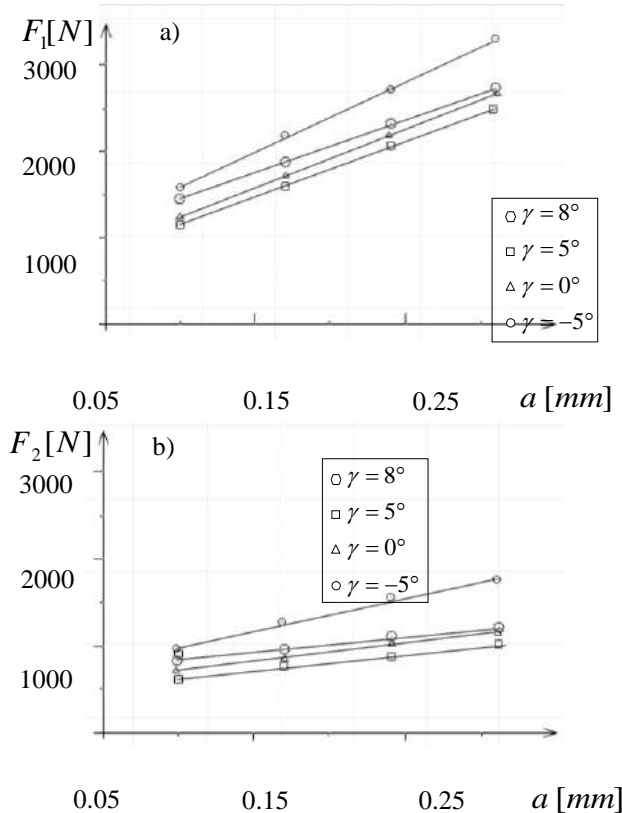
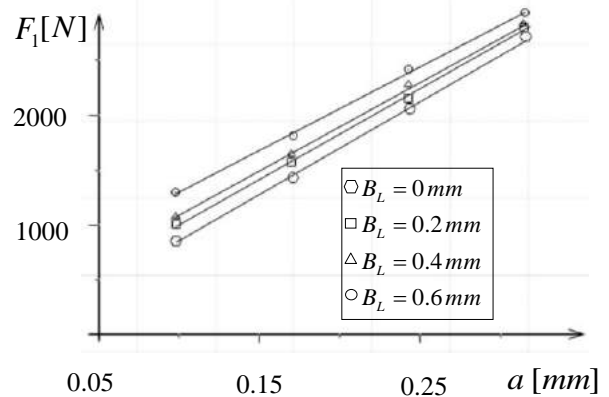


Fig. 3. Experimental trends in orthogonal cutting with tool wear ($V = 200m/min$, $B_L = 0.6mm$) [4]

Figure 3. shows that increase of rake angle γ results in a decrease of two force components, while the shear angle ϕ and friction angle ρ are independent of the cutting depth a . Fig. 4. shows the measured force components with respect to the depth of cut at different wearland sizes B_L . Flank wear results in a substantial increase in two force components F_1 and F_2 because of the increased ploughing or rubbing action on the wearland.



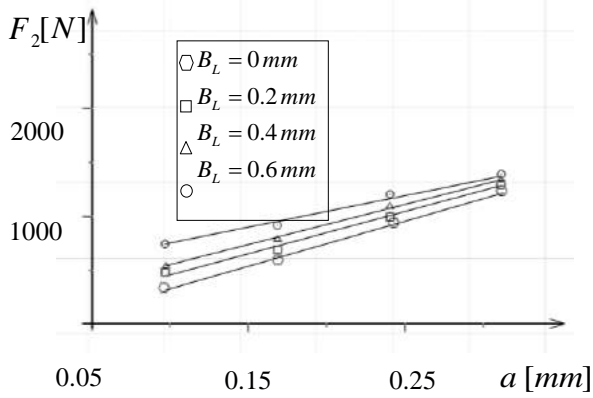


Fig. 4. Influence of tool flank wear height on the force components ($V = 100\text{m/min}$, $\alpha = 5^\circ$) [4]

Experimental results show that there is no effect of the wearland height B_L and depth of cut a on the shear angle ϕ and friction angle ρ which means that the forces generated by increase of the flank wear can be treated in the same way as the concentrated edge force and force for chip formation.

From the previous considerations, the overall cutting force for cutting with tool flank wear may be a result of the forces required for chip formation in the shear zone and tool-chip interface, the concentrated edge force and the rubbing forces on the wearland generated due to friction between the clearance face of the cutting tool and the newly formed surface of the workpiece. Based on the completed Merchant's model, the overall cutting force components can be established based on Eqs. (8) and (9), i.e.

$$F_1 = F_{1s} + F_{1l} + F_{1h} = \frac{\tau b t \cos(\rho - \gamma)}{\sin \phi \cos(\phi + \rho - \gamma)} + k_1 b + F_{1h} \quad (10)$$

$$F_2 = F_{2s} + F_{2l} + F_{2h} = \frac{\tau b t \sin(\rho - \gamma)}{\sin \phi \cos(\phi + \rho - \gamma)} + k_2 b + F_{2h} \quad (11)$$

where: F_{1h} - rubbing force between the clearance face of the cutting tool and the newly formed surface of the workpiece in the primary cutting force direction, F_{2h} - rubbing force between the clearance face of the cutting tool and the newly formed surface of the workpiece in the radial force direction.

Completed Merchant's model includes force analysis occurring in orthogonal cutting with special reference to rubbing forces generated between the clearance face of the cutting tool and the newly formed surface of the workpiece which is typical for adhesion wear model.

According to the fundamental law of adhesion wear, adhesion flank wear volume per unit length is proportional to the rubbing force between the clearance face of the cutting tool and the newly formed surface of

the workpiece in the radial force direction F_{2h} , which leads to the following equations [1]:

$$F_{2h} = K v^a s^b B_L^c \quad ; \quad F_{1h} = K_1 v^a s^b B_L^c \quad (12)$$

$$t = \left(\frac{B_L}{K_1 v^a s^b} \right)^{\frac{1}{c}} \quad (13)$$

where: $a', b', c', a, b, c, \alpha, \beta, \gamma, K, K_1$ are constants to be evaluated by the experiment; v - cutting velocity; s - feed, B_L - flank wear height, t - tool life.

According to ISO3685 tool is worn when flank wear height reaches threshold criterion $B_L = 0.6\text{mm}$. Based on equation (13) tool life can be determined in production environment.

3. CONCLUSION

The paper emphasizes the influence of the flank wear height at the clearance face on tool life and the forces that appear in two ways. The first one represents the completed Merchant's model of orthogonal cutting which, in addition to force for chip formation, comprises concentrated edge force and rubbing or ploughing force generated by increase of the flank wear or rubbing between clearance face of the cutting tool and the newly formed surface of the workpiece. The second way represents mathematical model that defines the correlation between tool life, cutting velocity, feed and flank wear height. Mathematical model is based on the fundamental law of adhesion wear. This leads to efficient prediction of tool life in production environment which is very important because it provides good machined part in manned factories so that a new tool may be introduced at the instant at which the existing tool has been worn out, thus preventing any hazards occurring to the machine or deterioration of the surface finish.

REFERENCES

- [1] CHOUDHURY, S., K., APA RAO, I. (1998) *Optimization of cutting parameters for maximizing tool life*, Journal of Machine Tools & Manufacture, 39, pp 343-353.
- [2] DIMLA, E., DIMLA, SNR. (2000) *Sensor signals for tool-wear monitoring in metal cutting operations-a review of methods*, Journal of Machine Tools & Manufacture, Vol. 40, pp 1073-1098.
- [3] SALGAM, H., YALDIZ S., UNSACAR, F. (2005) *The effect of tool geometry and cutting speed on main cutting force and tool tip temperature*, Materials and design, Vol.28, pp 101-111.
- [4] WANG, J., HUANG, C.Z. (2003) *The effect of tool flank wear on the orthogonal cutting process and its practical implications*, Journal of Materials Processing Technology, 142, pp 338-346.



MATHEMATICAL MODELLING OF CUTTING FORCE AS THE MOST RELIABLE INFORMATION BEARER ON CUTTING TOOLS WEARING PHENOMENON

Obrad SPAIĆ, Zdravko KRIVOKAPIĆ, Rade IVANKOVIĆ

Production and Management Faculty in Trebinje, East Sarajevo University, Trg palih boraca 1, Trebinje, Republika Srpska, Bosna i Hercegovina

sobrad1@teol.net, zdravkok@ac.me, rade.ivankovic@gmail.com

Abstract: *Being one of their prominent exploitative characteristics, cutting tools durability depends on the character, intensity and the speed of wearing. Identification of tool wearing is of great significance for the purpose of avoiding sooner or later replacement of tools. The parameters of tool wearing can be measured by out-process and in-process-measuring systems. Given the extremely limiting role of the former in modern production lines, development of the latter (the indirect measuring systems) has gained prominence. The basis of indirect measuring systems comprises a set of various signals originating from the units of the system under treatment which stand in certain correlations with the wearing parameters. The paper presents mathematical models of axial force designed on the basis of experimental research in drilling tempered steel by twist drills made of high-speed steel manufactured by powder metallurgy.*

Key words: *tool, durability, wear, cutting force, mathematical model*

1. INTRODUCTION

Identification of cutting elements wear is of high practical importance because, apart from allowing for timely replacement of tools, it also allows for management of wearing processes as well as for automation of treatment and technological processes. Production lines, in particular those of mass and large scale automated production benefit from timely replacement of cutting tools as it eliminates the low quality of final products and reduces production costs arising from sooner and later replacement of tools.

As in modern production lines the out-process methods of measuring tool wear have become a significantly limiting factor, development of online process measuring systems are gaining prominence. The process methods most frequently applied are the indirect ones whose basis comprises a set of various signals originating from the units of the system under treatment which stand in certain correlations with the wear parameters. The information bearers (signals) of tools wear in cutting process that are most often used by researchers are cutting force and resistance. Thus, J. Sheikh-Ahmad and R. Yadav [1] designed a force model at milling composite materials by applying regression analysis. [B. Lotfi](#), [Z. W. Zhong](#) and [L. P. Khoo](#) [2] designed a model to predict cutting force at milling dependent on tool orbit. J. T. Lin, D. Bhattacharyya and V. Kecman [3] showed that measuring cutting force enables for tool wear to be monitored without interruption of cutting process. Based on the comparative analysis of the assessment of wear of a 8 mm diameter twist drill, C. Sanjay, M. L. Neema and C. W. Chin [4] showed that modified regression equations could be used to assess the value of tool wear.

2. AXIAL CUTTING FORCE IN DRILLING

Axial cutting force in drilling (the auxiliary movement resistance), F_3 , along with other conditions unaltered, is in the function of cutting regime (the twist drill nominal diameter, the spindle speed and feed):

$$F = f(D, n, s) \quad (1)$$

By way of experimental-analytical method, i.e. the theory of experiment planning and the theory of regression analysis, the cutting force can be expressed in the form of a degree function:

$$F = C_F \cdot D^{b_{1F}} \cdot n^{b_{2F}} \cdot s^{b_{3F}} \quad (2)$$

where:

C_F , b_{1F} , b_{2F} , b_{3F} – are the constants dependent on the type of material,

D [mm] – is the drill nominal diameter,

n [rev/min] – is the spindle speed, and

s [mm/rev] – is the feed.

3. EXPERIMENT PLANNING

With the aim to design a mathematical model of axial force as the information bearer on the wear phenomenon, the paper contains experimental research on the basis of which the constants C_F , b_{1F} , b_{2F} , b_{3F} were determined within the assumed mathematical model (2). Given that the axial force is in the function of three parameters (D , n , s), the experiment was conducted in line with the complete three-factor orthogonal first-order plan, i.e. the Box-Wilson's plan, repeating the experiment four times in the central plan point ($n_0=4$) as illustrated in Table 1.

Table 1. The three-factor plan matrix

Experi- mental points	Coded values								Real values				The output vector [F]
	x ₀	x ₁	x ₂	x ₃	x ₁ x ₂	x ₁ x ₃	x ₂ x ₃	x ₁ x ₂ x ₃	d [mm]	n [rev/min]	s		
											[mm/rev]	[mm/min]	
1	+1	-1	-1	-1	+1	+1	+1	-1	6.0	250	0.027	6.67	F ₁
2	+1	+1	-1	-1	-1	-1	+1	+1	10.0	250	0.027	6.67	F ₂
3	+1	-1	+1	-1	-1	+1	-1	+1	6.0	500	0.027	13.33	F ₃
4	+1	+1	+1	-1	+1	-1	-1	-1	10.0	500	0.027	13.33	F ₄
5	+1	-1	-1	+1	+1	-1	-1	+1	6.00	250	0.107	26.67	F ₅
6	+1	+1	-1	+1	-1	+1	-1	-1	10.0	250	0.107	26.67	F ₆
7	+1	-1	+1	+1	-1	-1	+1	-1	6.0	500	0.107	53.33	F ₇
8	+1	+1	+1	+1	+1	+1	+1	+1	10.0	500	0.107	53.33	F ₈
9	+1	0	0	0	0	0	0	0	7.75	355	0.053	18.67	F ₉
10	+1	0	0	0	0	0	0	0	7.75	355	0.053	18.67	F ₁₀
11	+1	0	0	0	0	0	0	0	7.75	355	0.053	18.67	F ₁₁
12	+1	0	0	0	0	0	0	0	7.75	355	0.053	18.67	F ₁₂

3.1. Experiment conditions

The experiment was conducted by means of twist drills (TD) DIN 338, nominal diameter Ø6.0; Ø7.75 and Ø10.0 mm, made of high-speed steel with 8% of Co, manufactured by powder metallurgy, used for drilling blind hole in tubes made of chrome-molybdenum alloy steel for enhancement, Č.4732, thermally treated to 43-45 HRC hardness.

The chemical composition, thermal treatment conditions and microstructure of the TD steel and test tubes are shown in References [5].

Construction of twist drills followed the recommendations in References pertaining to drilling hard treatable materials (tempered steel) as well as previous experience. The drills were manufactured by grinding technology. The geometrical elements of TD are shown in References [5].

The experiment was conducted using test tubes, Ø60 mm in diameter, with the thickness adjusted to the blind hole drilling depth $l=3xd$.

Test tubes' hardness was evenly distributed along longitudinal and cross cut and within the prescribed limits.

Cutting regimes were defined in line with the recommendations stated in References [5], adhering to the interval limits of variations of influential factors ($n_{sr}^2 = n_{min} \cdot n_{max}$, and $s_{sr}^2 = s_{min} \cdot s_{max}$) and are shown in the three-factor plan matrix (Table 1).

The experiment was conducted in the laboratory of the Faculty of Mechanical Engineering in Podgorica, University of Montenegro, on the universal milling machine Typ: FGU-32. Integrated with the milling machine was the equipment for measuring axial force and torque manufactured by KISTLER.

During the experiment, the 8% solution of Teolin H/VR in the quantity of 1 l/min was used for cooling and lubrication.

3.2. Axial force measuring

Axial force measuring was conducted by means of a three-component dynamometer manufactured by "Kistler", TYP 8152B2, with the measurement range

from 100 to 900 kHz, integrated with the universal milling machine and Global Lab software.

For the data acquisition during the experiment, the KISTLER high-frequency amplifier, type AE-Piezotron Coupler 5125B was used while a two-channel DAQ Scope PCI-5102 was used as an AD convertor. The acquired signals were processed by means of a virtual instrument, aided by Global Lab software. The data acquisition schema is illustrated in Figure 1.

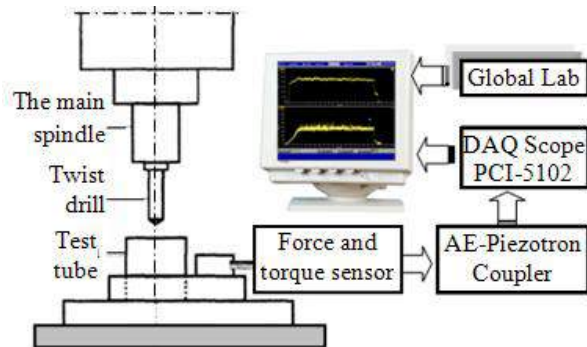


Figure 1. Data acquisition schema during the experiment

4. EXPERIMENT RESULTS

Measurement of axial force was conducted in line with the stated Plan matrix in five measuring points. The first measurement was conducted during drilling of a blind hole, $l=3d$, with sharp twist drills while the fifth (the last) measurement was conducted subsequent to the achieved lengths of drilling (in mm) during which the twist drills wear reached the following maximally allowed (defined in advance) values:

- for TD Ø6.0 mm – 0.25 mm
- for TD Ø7.75 mm – 0.30 mm
- for TD Ø10.0 mm – 0.35 mm

The mean value of the wear band width of the back surfaces was taken to represent the maximum wear value ($B \approx 0.04D$), at the edge of regular area which is at 0.025mm distance from outer fibres (Figure 2).

At different cutting regimes (the nominal diameter, the spindle speed and the feed), TD reached the maximally

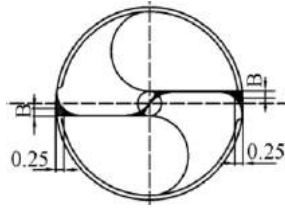


Figure 2. Twist drill wear

allowed wear value at different drilling lengths. The measured axial force value at maximal wear is shown in Table 2.

Table 2. Axial force values at maximal TD wear

Exp. points	D [mm]	n [rev/min]	s [mm/rev]	I_{\max} [mm]	F_{\max} [N]
1.	6.0	250	0.027	1265.40	956.50
2.	10.0	250	0.027	2700.00	594.50
3.	6.0	500	0.027	1533.00	1090.50
4.	10.0	500	0.027	2340.00	1139.00
5.	6.0	250	0.107	999.00	955.50
6.	10.0	250	0.107	4800.00	638.50
7.	6.0	500	0.107	1800.00	1925.50
8.	10.0	500	0.107	756.00	1579.70
9.	7.75	355	0.053	2569.13	783.30
10.	7.75	355	0.053	2336.63	682.90
11.	7.75	355	0.053	2569.13	655.50
12.	7.75	355	0.053	2801.63	754.80

5. MATHEMATICAL MODELLING OF AXIAL FORCE

The pattern of axial cutting force (2) subsequent to linearisation can be expressed in the following form:

$$y = b_0 + b_1x_1 + b_2x_2 + b_3x_3 \quad (3),$$

where:

$$y = \ln F, \quad b_0 = \ln C_F, \quad x_1 = \ln(D), \quad x_2 = \ln(n) \quad \text{and} \quad x_3 = \ln(s).$$

The orthogonal first-order plan with constant members can be applied to the above pattern with coding performed by means of the equations of transformation:

$$\begin{aligned} X_1 &= 2 \frac{\ln(D) \cdot \ln(D_{\max})}{\ln(D_{\max}) \cdot \ln(D_{\min})} + 1, \\ X_2 &= 2 \frac{\ln(n) \cdot \ln(n_{\max})}{\ln(n_{\max}) \cdot \ln(n_{\min})} + 1, \quad \text{and} \\ X_3 &= 2 \frac{\ln(s) \cdot \ln(s_{\max})}{\ln(s_{\max}) \cdot \ln(s_{\min})} + 1 \end{aligned} \quad (4).$$

By applying regression analysis, the parameter of the model b_0 is determined on the basis of results of all $N = 2^k + n_0$ plan points, in line with the pattern [6]:

$$b_0 = \frac{1}{N} \sum_{i=0}^N x_{0i} \cdot y_i \quad (5),$$

while parameters b_j are determined on the basis of results of $N = 2^k$ points arranged along the vertexes of hypercube according to the pattern:

$$b_j = \frac{1}{N} \sum_{i=0}^N x_{ji} \cdot y_i, \quad (j=1,2,3) \quad (6).$$

Assessment of the significance of the first-order model was done by means of application of F-criteria, for the adopted level of significance $q=0.05$, according to the pattern:

$$F_{ij} = N \frac{b_j^2}{S_E^2}, \quad (j=1,2,3) \quad (7).$$

Dispersion of experiment results in the multi-factor space is as follows:

$$S_E^2 = \frac{1}{f_E} \sum_{i=0}^{n_0} (y_{0i} - \bar{y}_0)^2 \quad (8).$$

$$S_E^2 = 0.007,$$

where:

$f_E = n_0 - 1 = 3$ – is the degree of freedom of experimental error.

The degrees of freedom of parameters b_j , ($j = 0, 1, 2, 3$) are:

$f_{b_j} = 1$, which results in the tabled value of the dispersion relation $F_{\alpha, 1-q/1, 3} = 10.10$ [7].

The parameters of the model and assessments of significance are listed in Table 3, which shows that all parameters of the first-order model (b_0, b_1, b_2 i b_3) are significant.

Table 3. Model parameters

Model parameters	Disper. relations (F_{ri})	Assesments	
b_0	6.820	F_{b_0} 76831.617	sign.
b_1	0.121	F_{b_1} 16.813	sign.
b_2	-0.129	F_{b_2} 19.112	sign.
b_3	0.298	F_{b_3} 102.457	sign.
b_{12}	-0.021	$F_{b_{12}}$ 0.575	not sign.
b_{13}	0.103	$F_{b_{13}}$ 12.214	sign.
b_{23}	0.091	$F_{b_{23}}$ 9.484	not sign.
b_{123}	-0.039	$F_{b_{123}}$ 1.724	not sign.

On the basis of listed parameters the empirical model was deduced of axial force at maximal TD wear:

$$\hat{y} = 6.820 + 0.1215x_1 - 0.121x_2 + 0.612x_3 \quad (9).$$

Revisiting the original coordinates by means of the equations of transformation (4) provided for deduction of a concrete empirical axial force model:

$$F = \frac{5.358 \cdot D^{0.822} \cdot s^{0.433}}{n^{0.372}} \quad (10).$$

Testing of adequacy of the defined model was done according to Fisher's criterium [6]:

$$F_{rLF} = \frac{S_{LF}^2}{S_E^2} \quad (11).$$

$$F_{rLF} = 15.061.$$

Dispersion of experiment results in the multi-factor space is as follows:

$$S_{LF}^2 = \frac{1}{f_{LF}} \left[\sum_{u=1}^N \left(y_u^2 - N \sum_{i=0}^k b_i^2 - \sum_{u=1}^{n_0} (y_{0u} - \bar{y}_0) \right)^2 \right] \quad (12).$$

$$S_{LF}^2 = 0.1048.$$

The degree of freedom of model adequacy is:

$f_{LF} = N - k - 1 - (n_0 - 1) = 5$, thus entailing the tabled value of dispersion relation of $F_{(5\%;5;3)} = 9.0$ [7].

Given the $F_{LF} > F_{(5\%;5;3)}$ the mathematical model fails to describe the correctly observed function of response, which implies existence of effects of mutual action among the model parameters.

Three-factor orthogonal first-order plans allow for assessment of basic effects as well as the effects of mutual action of the first and second order on the empirical model of the response function. Should the complete three-factor first-order model be applied, the pattern to describe the (axial force) response function becomes non-linear and can be expressed in the form of the equation:

$$y = b_0 + b_1x_1 + b_2x_2 + b_3x_3 + b_{12}x_1x_2 + b_{13}x_1x_3 + b_{23}x_2x_3 + b_{123}x_1x_2x_3 \quad (13).$$

On the basis of values of the model parameters corresponding to mutual action effects (see Table 4) and taking into account the assessment of significance, while also revisiting the original coordinates by means of the equations of transformation (4), the following non-linear empirical model of axial force is deduced:

$$\ln F = 6.82 + 2.187 \cdot \ln(D) + 0.737 \cdot \ln(n) - 2.994 \cdot \ln(s) + 0.586 \ln(D) \cdot \ln(s) + 0.38 \cdot \ln(n) \cdot \ln(s) - 7.536 \quad (14).$$

Given that the dispersion relation value of the parameter b_{13} (9.484) is approximate to the tabled value (10.10), its influence has been included in the model. The modelled values of axial force, as well as the relative error in relation to the experimental results are shown in Table 4.

Table 4. Modelled values of axial force

Exp. points	Modelled values	Error %	Exp. points	Modelled values	Error %
1	830.47	-13.19	5	1024.26	-6.07
2	860.2	-9.97	6	1602.63	-16.75
3	535.15	-9.98	7	948.21	-16.75
4	554.3	-13.19	8	1483.64	-6.08
9-12	907.81	26.24			

If we compare the modelled and experimental values of axial force in the experimental points, we can see that maximal deviation of experimental points from modelled surface is 16.75%, thus providing for the model (14) to be considered a mathematical interpretation of the goal function. However, in the central plan point the deviation of modelled results from the experimental ones is 26.24%, which means that mathematical model fails to properly describe the response function within the boundaries of the covered multi-factor space. Therefore, the null hypothesis that the effects of squared elements in the model equal zero must be jettisoned.

For the purpose of designing a mathematical model in order to properly describe axial force within the boundaries of the covered multi-factor space it is necessary to apply the second-order polynomial model which necessitates additional amount of information on the diffusion system, i.e. additional number of experiments.

6. CONCLUSION

The mathematical models designed by means of orthogonal first-order plan and regression analysis fail to properly describe the response function, i.e., axial cutting force within the boundaries of the covered multi-factor space due to mutual action of the model parameters, the squared elements action effects, as well as the action of a series of parameters whose source, nature and span of action are unknown.

This points to the fact that highly complex processes that take place in the zone of drilling tempered steel and which are conditioned by actions of numerous influential and mutually collinear factors, cause difficulties for mathematical models to be applied so as to describe the behaviour of mechanical, thermo-dynamical, tribological, chemical and other phenomena in the cutting zone.

REFERENCES

- [1] Sheikh-Ahmad J., Yadav R. (2008) *Model for predicting cutting forces in machining CFRP*, International Journal of Materials and Product Technology, Vol. 32, Number 2-3, 152 – 167
- [2] Lotfi B., Zhong Z. W., Khoo L. P. (2009) *Prediction of cutting forces along Pythagorean-hodograph curves*, The International Journal of Advanced Manufacturing Technology, Vol. 43, Numbers 9-10, 872-882
- [3] Lin J. T., Bhattacharyya D., Kecman V. (2003) *Multiple regression and neural networks analyses in composites machining*, Composites Science and Technology, Vol. 63, 539–548
- [4] Sanjay C., Neema M. L., Chin C. W. (2005) *Modeling of tool wear in drilling by statistical analysis and artificial neural network*, Journal of Materials Processing Technology, Vol. 170, 494–500
- [5] Spaić O. (2006) *Uporedna analiza habanja zavojnih burgija od brzoreznog čelika proizvedenog konvencionalnom metalurgijom i metalurgijom praha*, MSc thesis, University of East Sarajevo, Faculty of Production and Management Trebinje
- [6] Stanić J. (1986) *Metod inženjerskih mjerenja*, Faculty of Mechanical Engineering Beograd
- [7] Laković R., Nikolić B. (1999) *Primijenjena statistika 2. dio – eksperiment*, University of Montenegro, Faculty of Electrical Engineering, Podgorica



34th INTERNATIONAL CONFERENCE ON
PRODUCTION ENGINEERING
28. - 30. September 2011, Niš, Serbia
University of Niš, Faculty of Mechanical Engineering



**ANALYSIS OF STONE MICRO-CUTTING MECHANISM USING THE EXAMPLE OF
GRANITE AND MARBLE GRINDING**

Ljubodrag TANOVIĆ, Pavao BOJANIĆ, Radovan PUZOVIĆ, Mihajlo POPOVIĆ, Goran MLADENOVIC
Department of Production Engineering, Faculty of Mechanical Engineering, University of Belgrade, Kraljice Marije 16,
Belgrade 11120, Serbia

ltanovic@mas.bg.ac.rs, pbojanic@mas.bg.ac.rs, rpuzovic@mas.bg.ac.rs, mpopovic@mas.bg.ac.rs,
gmladenovic@mas.bg.ac.rs

Abstract: *The paper presents the results of to date investigations in the field of ornamental stone micro-cutting using the examples of granite and marble originating from the stone varieties of Serbian location. The diamond grain - machined stone (the 'Josanica' granite and the 'Plavi tok' marble) interaction was analyzed. The analysis also embraced the changes of the normal cutting force as a function of cutting speed and grain penetration depth in the chosen stone. Based on grain traces (cracks) that occurred on the surface of the machined stone, the critical cutting depths, at which brittle cutting occurs, were established for the mentioned stones. The presented analysis is to be used for the grinding process optimization as a dominant ornamental stone machining technology with the aim of obtaining quality machined surfaces and preserving the stone surface structure and color.*

Key words: *micro-cutting, grinding, diamond grain, granite, marble*

1. INTRODUCTION

Rock materials are widely used in construction industry for lining the aesthetic surfaces. Of all the materials, the most used rocks are granite and marble that high quality surface finish is required from, however, the accuracy of measures and shapes to a lesser degree. Considering the stone surface finish technologies, the most utilized are grinding and polishing technologies that enable preservation of the structure and high gloss surface. The rock structure characteristics depend on the conditions of its formation, and they are defined by textural and structural properties. The structure is determined by the crystallinity degree and grain size, but also by the shape and mutual relations of the breed components. By the grain size, rocks can be distinguished as: coarse-grained, medium-grained and fine-grained. The texture, the totality of attributes, defines the location and distribution of the one rock components relative to another within the space they cover. The specificity of surface finish technology demands a good knowledge of all the rock's characteristics including its structural-textural (continuum, homogeneity and isotropy), physico-mechanical (specific gravity, porosity, moisture, water-permeability, hardness, toughness and abrasiveness) and mineralogical-petrography (grain size, type and content of colored components, etc) properties. It is well-known that tool wear intensity, as the consequence of granite and marble abrasiveness, is related to friction and cutting speed and cutting resistance, respectively.

2. OVERVIEW OF CHIP FORMATION MECHANISMS

Machining by grinding occurs as the sum of effects of all abrasive grains, expressed through the development of deformation and fracturing. However, the mechanisms of micro-deformation and micro-fracturing in the grinding zone differ, depending on the grinding parameters and non-homogeneity of the machining material. A large number of researchers dealing with the development of model for deformations and fracturing regarded the cutting action of a diamond grain in the grinding wheel as being identical to the indentation effects caused by a diamond indenter during hardness measurements. Considering the investigations on brittle materials, they go into two directions: by how the force acts during the indentation (dynamic and static) and by the shape of the indenter. Lawn and Wilshaw [1] think that fracture patterns in brittle materials, under blunt indenters of a larger radius, usually occur as a result of cracks' presence immediately outside the contact zone. By increasing the normal load, these surface cracks evolve into the so-called Hertzian cone cracks. Anton and Subhash [2], unlike the traditional static indentation models, which do not capture the strain rate effects, consider that the current dynamic indentation can provide a more realistic picture of the influence of loading rate on the material removal mechanisms during a dynamic process. Conway and Kirchner [3] analyzed the mechanics of crack initiation and propagation beneath a moving of sharp indenter. A fracture mechanics solution for a single embedded penny-shaped crack was used to predict the propagation depth of pre-existing defects. The second group of researchers, though to a lesser extent, performed the cutting process in

a variety of brittle materials by a single diamond grain. Mishnaevsky [4] performed the real cutting process in brittle materials and observed different physical mechanisms involved in material destruction (deformation, crushing, cracking and spalling). He considers that neither Hertzian cone cracks nor circumferential cracks are formed. Instead, penny-shaped cracks in the cutting force vector direction are formed. Chiaia [5] provides a system analysis for the current approaches to the issues of micro-cutting processes in brittle and quasi-brittle materials. It was shown that various interaction mechanisms beneath the tools during the penetration process are essentially reduced to plastic deformation and brittle fracturing. The third group of researchers analyzed the crack formation and development in brittle materials. Labuz et al. [6] studied crack propagation in granite and concluded that a large number of micro-cracks occur around the crack tip covering the fracture process zone and together with the fracture free length defines the effective crack length. Germanovitch et al. [7] investigated brittle material fracturing in uniaxial compression which is manifested through spalling or shearing (oblique fracture) as the consequence of a multitude of existing cracks. Abe et al. [8] investigated the formation and proliferation of cracks in the granite and their effects on the fracture process zone. The fourth group of researchers performed the real cutting and grinding processes in brittle materials and analyzed the crack propagation and chip brittle fracturing mechanisms. They measured the cutting forces, and the cutting strength and tool wear in ceramics and granite with the aim to recommend the efficient abrasive machining [9-15].

3. MICRO-CUTTING EXPERIMENTAL SCHEMES

The cutting ability of a single diamond grain in the process of its acting upon the machined material (granite and marble) is primarily determined by the physico-mechanical properties and geometrical parameters, conditions and strength of its gracing into the bond and also by the kinematic and thermodynamic conditions of the grain's operation. The grain strength characteristics, as opposed to the action of forces and temperature effects, cause significant differences in tool cutting properties. The diamond grain shape influences the basic parameters of the grinding wheel cutting properties: tool life, productivity, cutting forces, grinding temperature, surface layer state, etc. Unlike the tools with geometrically defined cutters, the geometry and shape of diamond grains is complex and undefined to some extent. The analysis of work of such grains includes experimental determination of the size, shape and geometry with the aim of replacing such non-defined grains, in the final calculations, with the grains of equivalent shape. The micro-cutting process was performed in two modes:

The first model (Fig. 1): cone shaped diamond grain, a 120° tip angle, a 0.1 mm tip radius, was placed and rigidly fastened to an aluminium disc 150 mm in diameter that was statically and dynamically balanced. On a cutting table of a HMC 500 machine, a dynamometer was mounted with a fixture for clamping the stone specimens

(granite, marble). The fixture enables the rotation of the stone specimens (granite and marble) under an inclination relative to the axial motion of the cutting grain (v_w), thereby achieving varying depth of cut. The 1:200 inclination enables achieving varying grain penetration depth up to 0.28 mm.

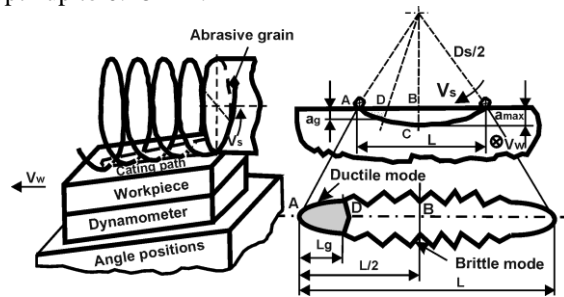


Fig. 1 Micro-cutting with diamond grain rotary and radial motion – scheme 1

The second model of the cutting process is reduced to the principle of the peripheral milling with a single grain, with the grain penetration depth adjustment by moving the disc in the z-direction (Fig. 2). The chip formed in the process is a space between the two epicycloids.

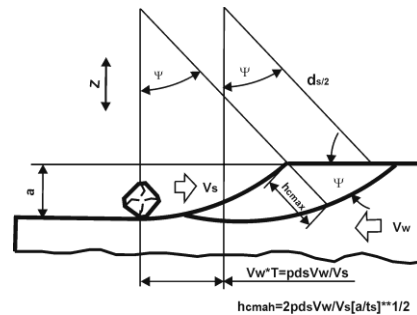


Fig. 2 Micro-cutting with diamond grain rotary and radial motion – scheme 2

4. EXPERIMENTAL RESULTS

The micro-cutting process was performed on two types of stone: the 'Josanica' granite (GJ) and the 'Plavi tok' marble (PT) whose physico-mechanical properties were examined and presented in Tab. 1. The values of the listed properties were determined as mean values obtained from a larger number of measurements, depending on the petrography nature of the stones (granite and marble). The measurements indicate pronounced differences in physico-mechanical properties of the examined stones (GJ granite and PT marble).

Table 1. Physico-mechanical properties of stones

Properties	Granite	Marble
	Jošanica GJ	Plavi tok PT
Specific gravity, KN/m ³	29.70 ± 0,3	26.65 ± 0,2
Micro-hardness, HK75/HK25	3.1	1.9
Compressive strength, MPa	185 ± 20	75.04 ± 3.5
Ultimate strength, MPa	16.6 ± 1	8.20 ± 0.3
Cohesion, MPa	31.8	14.10
Abrasion coefficient, %	21.5-23.0	29-30.5

Experiments were carried out using the following measuring equipment: a two-component piezo-electric

dynamometer (Kistler 9271), a data acquisition card ED2110-AD, a laser microscope (Carl Zeiss – LSM 510) with an Axioscope F32. Figs. 3 and 4 show diagrams of changes in the normal cutting force (resistance) during machining of stones (granite and marble) as a function of grain penetration depth at cutting speeds $v_s = 7.85, 11.1, 15.7$ and 22 m/s.

The results presented are mean values of 40 measurements, with the standard deviation of $\pm 10\%$ for GJ and $\pm 5\%$ for PT. On the basis of the dependences obtained, it is concluded that as the grain penetration speed increases the cutting resistance increases in both types of stone (granite and marble), being higher in the granite (GJ) machining than in the marble (PT) machining, due to the granite's higher hardness and strength compared to the marble. If analysis is performed of the changes of forces in both schemes of loading, it is observable that both types of stone have approximately identical values for the same grain penetration depth, which confirms the correctness of the measurements concept and the accuracy of the obtained results. The non-linearity in the change of F_n is the consequence of the stones' non-uniformity (granite and marble). Also, as the grain penetration depth increases, the cutting force increases. It can be stated that at places where the force decreases this is the result of a soft phase presence in the stone (granite and marble). The processing of the experimental results makes possible to arrive at a mathematical model of the force for a range of changes in speed (v_s) and grain penetration depth (a):

$$F_n = 52,04 \cdot v_s^{0,738} \cdot a^{1,237} \rightarrow GJ \quad (1)$$

$$F_n = 15,7 \cdot v_s^{0,68} \cdot a^{0,78} \rightarrow PT \quad (2)$$

The analysis of the traces from the stone micro-cutting (granite – Fig 5 and marble – Fig.6) can provide the description of the chip formation mechanism. When entering into the material, the diamond grain establishes strain and deformations followed by radial and lateral cracks that increase as the cutting depth increases. At a certain cutting depth, the mentioned cracks become interconnected, causing the detachment of the machined material in the form of blocks with non-equal dimensions. On the grain's leaving the contact, median cracks emerge too. At smaller cutting depths, there occurs the diamond grain's trace that causes elastic and afterward plastic deformations followed by lateral, radial and median cracks that are smaller in intensity. At larger cutting depths, the mentioned cracks enlarge and become interconnected, causing the fracturing of blocks of the machined surface. In this zone, fracturing, crushing or detachment of the entire stone grains (granite and marble) is noticeable, which causes the non-uniform fracturing along the channel formed by the diamond grain. Beneath the machined surface there remain the cracks formed not only during the stone formation process (granite and marble) but also during the machining process, so they can essentially influence the work piece hardness. This indicates that cracks formed during the machining process should be of as small dimensions as possible, because the detachment of blocks of the machined material will be smaller in volume and the corresponding characteristics

of the machined surface quality ($Ra, Rz, Rmax$) lower, respectively. In stone (granite and marble) micro-cutting two regions are observable, which can be restricted by the grain penetration depth (critical grain penetration depth) that separates the region of plastic deformation followed by crack formation from the region of fracture-induced detachment of the machined material.

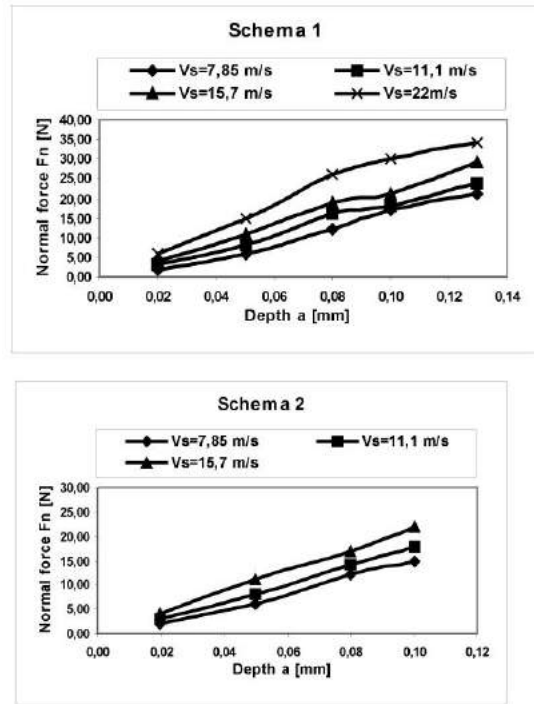


Fig. 3. Change of the normal force as a function of grain penetration depth in GJ granite micro-cutting: (a) Scheme 1 (b) Scheme 2

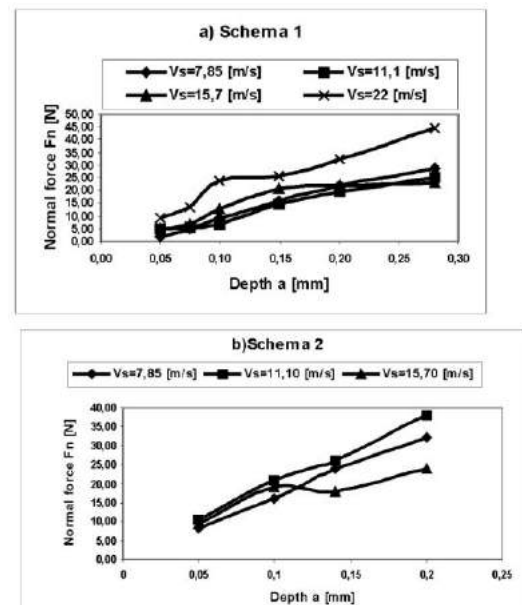


Fig. 4. Change of the normal force as a function of grain penetration depth in PT marble micro-cutting: (a) Scheme 1 (b) Scheme 2

The critical penetration depth can be used as one of the criteria for the optimization of the grinding process. The measurements established the critical grain penetration

depth in the GJ granite of 0.020 mm ($v_s = 7.85$ m/s) and that the critical depth declines to 0.015 mm as the speed increases to 15.7 m/s. The lengths of the radial cracks at the critical depth are 0.35 – 0.30 mm for the range of penetration speeds given above. In the PT marble machining as early as at grain penetration depth of 0.02 there occurs fracturing along the grain trace. In both types of stone (granite and marble) the increase of speed leads to the increase of radial cracks and fracturing along the grain trace, resulting in decrease of the critical grain penetration depth.

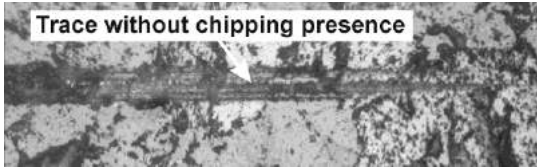


Figure 5. Micro-cutting trace on GJ granite, scheme 2. ($v_s=15.7$ m/s, $a=0.025$ mm), $x100$

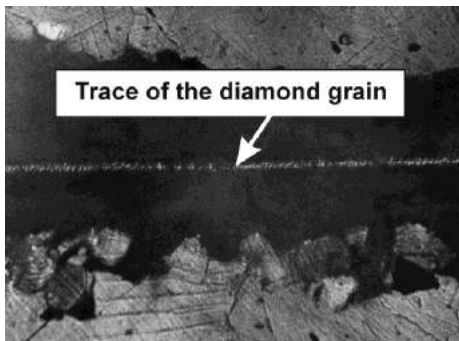


Figure 6. Micro-cutting trace on PT marble, scheme 2. ($v_s=7.85$ m/s, $a=0.1$ mm), $x125$

5. CONCLUSION

The development and application of new diamond tools for ornamental stone (granite and marble) machining implies the knowledge of processes that take place at the point of interaction between the abrasive grain-granite and the abrasive grain-marble, respectively. The choice of the cutting mode and tool characteristics are greatly affected by granite and marble physico-mechanical properties, primarily abrasiveness (wear resistance) that directly influences tool wear. Fine-grained and medium-grained varieties of granite and marble are more suitable for machining, because the fracturing phenomenon is also less pronounced than in coarse-grained structures. Beneath the machined surface there remain cracks formed not only in the granite formation process but also during the machining process, so they can essentially influence the work piece hardness. This indicates that cracks formed during the machining process should be of as small dimensions as possible, because the fracturing of blocks will be smaller in volume and the corresponding characteristics of the machined surface quality lower, respectively. The investigations carried out provided for establishing the critical grain penetration depth, thereby micro-cutting at stone (granite and marble) machining as well as the components of cutting resistance as a function of cutting speed and grain penetration depth.

REFERENCES

- [1] LAWN, B.R., WILSHAW, R. (1975) Indentation Fracture: principles and Applications, *J. Mater. Sci.*, 10: 1049-1081.
- [2] ANTON, R.J., SUBHASH, G. (2000) Dynamic Vickers Indentation of Brittle Materials, *Wear*, 239/1: 27-35.
- [3] CONWAY, J.C., KIRCHNER, H.P. (1980) The mechanics of crack initiation and propagation beneath a moving sharp indenter. *J. Mater. Sci.*, 15: 2879–2883.
- [4] MISHNAEVSKY, L.L. (1994) Investigation of the cutting of brittle materials, *Int. J. Mach. Tools Manufact.*, 34: 499–505.
- [5] CHIAIA, B. (2001) Fracture Mechanisms Induced in a Brittle Material by a Hard Cutting Indenter, *International Journal of Solids and Structures*, 38/44-45: 7747-7768.
- [6] LABUZ, J.F., SHAH, S.P., DOWDING, C.H. (1987) The Fracture Process Zone in Granite: Evidence and Effect, *International Journal of Rock Mechanics and Mining Sciences*, 24/4: 235-246.
- [7] GERMANOVICH, L.N., SALGANIK, R.S., DYSKIN, A.V., LEE, K. K. (1994) Mechanisms of Brittle Fracture of Rock with Pre-existing Cracks in Compression, *Journal Pure and Applied Geophysics*, 143; 117-149.
- [8] ABE, H., SAKA, M., OHBA, S. (1992) Does the Process Zone Control Crack Growth, *Applied Mechanics Reviews*, 45/8: 367-376.
- [9] XU, X., LI, Y., MALKIN, S. (2001) Forces and Energy in Circular Sawing and Grinding of Granite, *Trans. ASME, Journal of Manufacturing Science and Engineering*, 123/1: 13-22.
- [10] XIE, J., TAMAKI, J. (2007) Parameterization of Micro-Hardness Distribution in Granite Related to Abrasive Machining Performance, *Journal of Materials Processing Technology*, 186/1-3: 253-258.
- [11] HUANG, H., Li, Y., SHEN, J.Y., Zhu, H.M., Xu, X.P. (2002) Micro-Structure Detection of a Glossy Granite Surface Machined by the Grinding Process, *Journal of Materials Processing Technology*, 129/1-3: 403-407.
- [12] YANG, S.Q., DAI, Y.H., HAN, L.J., JIN, Z.Q. (2009) Experimental Study on Mechanical Behavior of Brittle Marble Samples Containing Different Flaws Under Uniaxial Compression, *Engineering Fracture Mechanics*, 76: 1833-1845.
- [13] CHANDRA, A., WANG, K., HUANG, Y., SUBHASH, G., MILLER, M.H., Q, W. (2000) Role of Unloading in Machining of Brittle Materials, *Trans. ASME, J. Manuf. Sci. Eng.*, 122: 452- 462.
- [14] TANOVIC, LJ., BOJANIC P., PUZOVIC, R., KLIMENKO, S. (2009) Experimental Investigation of Micro-cutting Mechanisms in Marble Grinding, *J. Manuf. Sci. Eng.*, ASME Trans., 131/6: 064507_1-5.
- [15] TANOVIC, LJ., BOJANIC P., PUZOVIC, R., MILUTINOVIC, S. (2011) Experimental Investigation of Micro-cutting Mechanisms in Granite Grinding, *J. Manuf. Sci. Eng.*, ASME Trans., Vol. 133/024501_1-5.



SOFTWARE PROTOTYPE FOR ANALYZING MANUFACTURING PROCESS MODELS

Marko KOVAČEVIĆ¹, Miloš MADIĆ², Velibor MARINKOVIĆ²

¹Faculty of Electronic Engineering in Niš, University of Niš, A. Medvedeva 14, Niš, Serbia

²Faculty of Mechanical Engineering in Niš, University of Niš, A. Medvedeva 14, Niš, Serbia
marko.kovacevic@elfak.ni.ac.rs, madic@masfak.ni.ac.rs, velmar@masfak.ni.ac.rs

Abstract: In this paper, the software prototype “Function Analyzer” for analyzing manufacturing process models is presented. Based on a loaded mathematical model and possible values of inputs, the developed prototype is able to perform the following tasks. Firstly, the prototype is able to determine extreme points of the process model and corresponding input values. Secondly, the prototype is able to determine optimal input values that satisfy the specified requirements for output: value and accuracy. The developed prototype was successfully tested on a mathematical model of the turning process.

Key words: manufacturing processes, software prototype, optimization

1. INTRODUCTION

Process modeling and optimization are two important issues in manufacturing [1]. Manufacturing processes are characterized by a multiplicity of dynamically interacting process variables, and usually too complicated to warrant appropriate analytical models [2]. Therefore manufacturing process models are often developed empirically using the regression analysis (RA) and in recent years by means of artificial neural networks (ANNs). To ensure high quality products, reduce manufacturing costs and increase the manufacturing effectiveness, it is very important to select the optimal process parameters. There are numerous methods and algorithms applied for the process optimization, such as ANNs [1], regression analysis [3], response surface method (RSM) [4], Taguchi method [4, 5], mathematical iterative search methods [5], meta-heuristic algorithms such as genetic algorithm (GA) [6], simulated annealing (SA) [7], particle swarm optimization (PSO) [8].

Also there are hybrid approaches that integrate two or more methods or algorithms. Most of aforementioned methods and algorithms can handle single and multi-objective optimization problems. However, despite numerous optimization methods, every method has certain advantages and disadvantages for implementation in real-life. There exists no universal method which is the “best” choice for optimization of all kinds of manufacturing processes.

Above all, optimization methods can be difficult to use for engineers, who are not experts on optimization theory [9].

The motivation of this paper is to develop the software prototype Function Analyzer, which can be used for manufacturing process optimization and control. Based on the loaded mathematical model, the prototype is able to determine optimal input values of the process model that satisfy the specified requirements. Figure 1 describes the potential usage of the software for optimization and control of manufacturing processes.

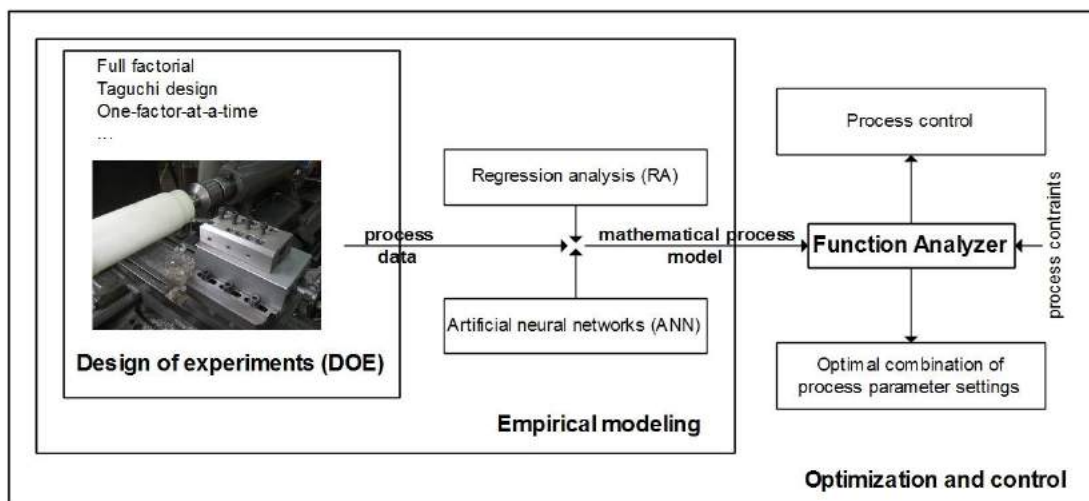


Fig.1. Possible application of software prototype Function Analyzer

Function Analyzer is based on iterative search of all input values combinations, and is able to solve two types of optimization problems: to determine input values that correspond to output extremes (minimum or maximum) and to determine input values that correspond to user defined output with desired accuracy. It enables simple and flexible way of defining lists of possible input values and mathematical model functions. Due to user-friendly application interface, Function Analyzer simplifies solving engineering optimization problems and requires no expert knowledge on optimization theory. Software architecture is flexible and extendible, thus it can be improved for solving multi-objective optimization problems.

2. FUNCTION ANALYZER

2.1. Software functionalities

The software prototype Function Analyzer enables users to define following parameters:

- o lists of possible input values V_1, V_2, \dots, V_n , where $V_1=(v_{11}, v_{12}, \dots, v_{1p})$, $V_2=(v_{21}, v_{22}, \dots, v_{2q}), \dots, V_n=(v_{n1}, v_{n2}, \dots, v_{nr})$, and
- o mathematical model function $F:R^n \rightarrow R$ where $n \in N$.

Using defined parameters and defined mathematical model function F , Function Analyzer calculates output f_b for all input combinations $C_b=(v_{1b}, v_{2b}, \dots, v_{nb})$, where $i=1, \dots, p, j=1, \dots, q, \dots, k=1, \dots, r, b=1, \dots, p \cdot q \cdot r$. As a result we get a list of ordered pairs $P_b=(f_b, C_b), b=1, \dots, p \cdot q \cdot r$.

By iteratively searching a list of ordered pairs P_b , valuable information about the mathematical model can be extracted. Function Analyzer is able to extract following information:

- o for user defined number of minimums (maximums) l , determine l ordered pairs $P_u=(f_u, C_u)$, that correspond to l minimal (maximal) values f_u , and
- o for user defined output value f_{user} and output value accuracy Δ , determine all ordered pairs $P_u=(f_u, C_u)$, where $|f_u - f_{user}| \leq \Delta$.

2.2. Software architecture

The architecture of the software prototype Function Analyzer is designed to satisfy the following crucial requirements:

- o basic functionalities described in section 2.1 are implemented,
- o simple and flexible way of defining lists of possible values V_1, V_2, \dots, V_n is enabled,
- o matrix calculus is supported,
- o implementing new mathematical model function requires no changes in software architecture and minor changes in software code, and
- o due to user-friendly application interface, operating on Function Analyzer does not require a domain expert.

Figure 2 shows UML (unified modeling language) logical model of the developed software prototype. The programming language used for implementation is C#.

Class *MainForm* implements user interface of the software prototype. Software logic is implemented in class *MathModelOutputManager*. Method *SetPossibleInputValues()* is used to load lists of possible input values V_1, V_2, \dots, V_n from XML (extensible markup language) file, which is passed as a parameter of this method. As a result, an instance of the class *PossibleInputValues* is created (attribute member *mInputValues*). One instance of the class *PossibleInputValuesItem* corresponds to one list of possible input values. Each list of possible input values can be specified in two ways in XML file:

1. name (attribute member *Name* of class *PossibleInputValuesItem*), start value (*StartValue*), end value (*EndValue*) and step (*Step*),
2. name (*Name*) and list of possible values (*Values*).

Method *SetMatrices()* is used to load matrices from text file, if mathematical model function contains matrices in its formula. As a result an attribute member *mMatrices* is filled. Method *SetNetworkOutputFunction()* is used to select one of the implemented mathematical model functions.

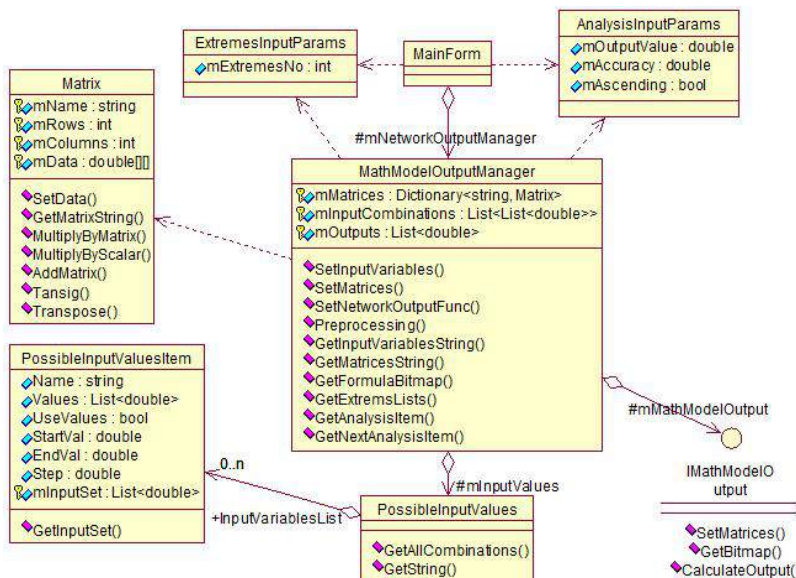


Fig. 2. Logical model of software prototype Function Analyzer

Method **Preprocessing()** is used to fill lists *mInputCombinations* (list of all input combinations C_b) and *mOutputs* (corresponding list of output values f_b), based on loaded parameters. List *mInputCombinations* is obtained by using method *GetAllCombinations()* of attribute member *mInputVariables*. List *mOutputs* is obtained by using method *CalculateOutput()* of attribute member *mMathModelOutput*, for each input combination from the list *mInputCombinations*. Method **GetExtremesList** is used to determine l ordered pairs $P_u=(f_{iw}, C_{iu})$ for minimums and l ordered pairs $P_u=(f_{iw}, C_{iu})$ for maximums. A parameter of this method is an instance of the class *ExtremesInputParams*, that contains user defined number of extremes l (attribute member *mExtremesNo*). Methods **GetAnalysisItem** and **GetNextAnalysisItem** are used to determine ordered pairs $P_u=(f_{iw}, C_{iu})$ for which inequality $|f_u - f_{user}| \leq \Delta$ is satisfied. A parameter of this method is an instance of the class *AnalysisInputParams*, that contains user defined output value f_{user} (attribute member *mOutputValue*), output value accuracy (*mAccuracy*) and search order of list of all input combinations (*mAscending*).

Every mathematical model function is modelled by a class that implements an interface *IMathModelOutput* (Fig. 3). Three methods must be implemented:

- o *SetMatrices()* – defines matrices if necessary,
- o *GetBitmap()* – provides bitmap of the formula for display in user interface, and
- o *CalculateOutput()* – calculates output f_b for input combination C_b , which is passed as a parameter of this method.

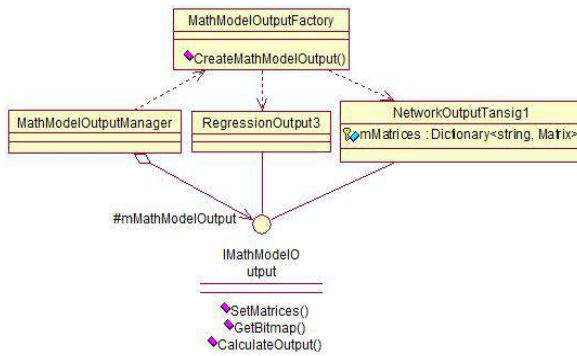


Fig. 3. Mathematical model functions implementation

At the moment, two mathematical model functions are implemented, modelled by classes *RegressionOutput3* and *NetworkOutputTansig1*. Class *MathModelOutputFactory* realizes factory pattern, and is used by the class *MathModelOutputManager* to obtain one of the implementations of interface *IMathModelOutput* (class *MathModelOutputManager* is not aware of which implementation of interface *IMathModelOutput* is obtained). As a consequence, implementing new mathematical model function is very simple and requires no changes in software architecture. It only requires adding new class that implements interface *IMathModelOutput*, and minor changes in classes *MathModelOutputFactory* and *MainForm*.

3. A CASE STUDY

An illustrative example is used to demonstrate the ability of Function Analyzer for machining process optimization and control. In this paper, the process of dry turning of cold rolled alloy steel using coated tungsten carbide inserts is considered [3]. Three major cutting parameters (factors, independent variables, inputs), cutting speed (V_c), feed rate (f), and depth of cut (a_p) were varied in the experiment. The average surface roughness (R_a) was chosen as a measure of surface quality and as target function (dependent variable, response, output).

For the purposes of regression analysis, coding of independent variables by means of the transforming equation was carried out:

$$x_i = 2 \frac{X_i - X_{i\min}}{X_{i\max} - X_{i\min}} + 1; \quad (i=1,2,3) \quad (1)$$

where x_i are coded factors, X_i are natural factors, from $X_{i\max}$ to $X_{i\min}$ (in the design space of interest to the experimenter), $X_{i\max}$ and $X_{i\min}$ are the highest and the lowest values of the natural factors X_i respectively, and i is the index of the input factor. In this case, the following relationships are valid: $X_1 = V_c$; $X_2 = f$; $X_3 = a_p$.

Based on experimental data and adopted non-linear (quadratic) mathematical model, by means of the regression analysis, the following multiple regression equation (in coded factors) was obtained [3]:

$$R_a = 3.844 - 2.811 \cdot x_1 + 1.036 \cdot x_2 + 1.02 \cdot x_3 + 0.498 \cdot x_1^2 + 0.055 \cdot x_2^2 - 0.081 \cdot x_3^2 - 0.12 \cdot x_1 \cdot x_2 + 0.057 \cdot x_1 \cdot x_3 - 0.162 \cdot x_2 \cdot x_3; \quad x_i \in [1, 2, 3] \quad (2)$$

The fitted multiple regression equation in terms of the natural factors (V_c , f , and a_p) may be obtained by substituting the transforming equation (1) into the equation (2). This equation is not given in the paper.

3.1. Optimization

The purpose of the optimization is to determine such a set of the cutting conditions (V_c , f and a_p) that satisfies the cutting parameters ranges to minimize the R_a . Within this range, there are multiple near optimal solutions, i.e. the combination of cutting parameter settings which software can find and sort. With Function Analyzer, using the step $\delta = 0.01$, the following results were obtained: $x_{1opt} = 2.88$ ($V_{copt} = 136.4$ m/min); $x_{2opt} = 1$ ($f_{opt} = 0.071$ mm/rev); $x_{3opt} = 1$ ($a_{popt} = 0.5$ mm), and $y_{min} = R_{a(min)} = 1.586$ μm . An identical result was obtained in the work [3].

3.2. Process control

In the turning process, there can be various requirements for surface finish of machined part. For example, high quality surface finishes are often required, while rough surface finishes are sometimes sufficient for the machined part. Therefore, it is very important to control the turning process, so that for the required surface finish one can determine suitable cutting parameter settings.

The selection of cutting parameter settings (input values) is based on control algorithm implemented in Function Analyzer. Based on predefined input values ranges,

desired output and desired accuracy Δ (max. difference between desired and computed output values) the control algorithm iterates through all combinations of input values until optimal input values are determined.

Consider a situation when one needs to determine cutting parameter settings so the required surface roughness of $R_a = 4.77 \mu\text{m}$ is achieved. Using the $\Delta = 0.01$ and starting the iteration process from the upper limits of cutting parameter values ranges, because this ensures high material removal rate, the following was obtained: $x_1 = 1.62$ ($V_{\text{copt}} = 98.64 \text{ m/min}$); $x_2 = 3$ ($f_{\text{opt}} = 0.321 \text{ mm/rev}$); $x_{3\text{opt}} = 3$ ($a_{\text{popt}} = 2 \text{ mm}$).

Figure 4 illustrates the usage of Function Analyzer for the discussed case study. The software was run on Intel Core2Duo T5800 with 4 GB RAM. Computational time is given in Table 1. Note that there was $8 \cdot 10^6$ of possible input values combinations. Preprocessing (determination of all combinations of input values and corresponding outputs) enables efficient algorithms execution.

Table 1. Computational time for the case study

Preprocessing	Optimization algorithm	Process control algorithm
12.06 s	0.29 s	0.20 s

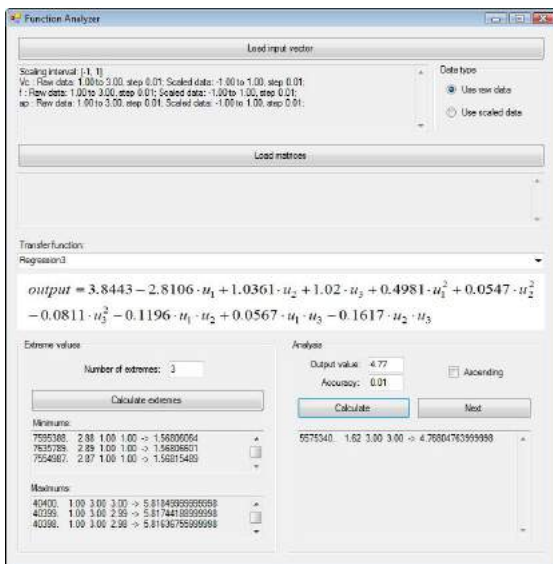


Fig. 4. Function Analyzer applied to turning process

4. CONCLUSION

In this paper, the software prototype Function Analyzer for single objective optimization of manufacturing processes parameters is proposed. Function Analyzer is based on iterative search of all input values combinations, and is able to solve two types of optimization problems: to determine input values that correspond to output extremes (minimum or maximum) and to determine input values that correspond to user defined output with desired accuracy. Function Analyzer enables a simple and flexible way of defining lists of possible input values. It provides working with mathematical models based on RA and ANN, but additional models can easily be implemented. Due to user-friendly application interface, Function Analyzer simplifies solving engineering optimization

problems and requires no expert knowledge on optimization theory. Although based on iterative search, the developed software prototype is efficient even for large possible input values sets. Additionally, setting numerous optimization parameters and initial search points is avoided.

The ability of Function Analyzer for optimization and control of the turning process was demonstrated using an illustrative example.

Future work could be directed toward solving multi-objective optimization problems in manufacturing processes and implementation of the software to real-time problems.

ACKNOWLEDGMENTS

This paper is part of project TR35034 and III41017, funded by the Ministry of Education and Science of the Republic of Serbia.

REFERENCES

- [1] ČUŠ, F., MILFELNER, M., BALIČ, J. (2006) *An intelligent system for monitoring and optimization of ball-end milling process*, Journal of Materials Processing Technology, Vol.175, No 1-3, pp. 90–97
- [2] LIAO, T.W., CHEN, L.J. (1998) *Manufacturing process modeling and optimization based on multi-layer perceptron network*, Journal of Manufacturing Science and Engineering, Vol.120, No 1, pp. 109-119
- [3] TANIKIĆ, D., MARINKOVIĆ, V. (2011) *Modelling and optimization of the surface roughness in the dry turning of the cold rolled alloyed steel using regression analysis*, Journal of the Brazilian Society of Mechanical Sciences and Engineering, (in press)
- [4] BAJIĆ, D., JOZIĆ, S., PODRUG, S. (2010) *Design of experiment's application in the optimization of milling process*, Metalurgija, Vol.49, No 2, pp. 123-126
- [5] JURKOVIĆ, Z., BREZOČNIK, M., GRIZELJ, B., MANDIĆ, V. (2009) *Optimization of extrusion process by genetic algorithms and conventional techniques*, Technical Gazette, Vol.16, No 4, pp. 27-33
- [6] LEE, B.J., TARNG, Y.S. (2000) *Cutting-parameter selection for maximizing production rate or minimizing production cost in multistage turning operations*, Journal of Materials Processing Technology, Vol.105, No 1-2, pp. 61-66
- [7] YANG, S.-H., SRINIVAS, J., MOHAN, S., LEE, D.-M., BALAJI, S. (2009) *Optimization of electric discharge machining using simulated annealing*, Journal of Materials Processing Technology, Vol.209, No 9, pp. 4471–4475
- [8] KARPAT, Y., ÖZEL, T. (2007) *Multi-objective optimization for turning processes using neural network modeling and dynamic-neighborhood particle swarm optimization*, International Journal of Advanced Manufacturing Technology, Vol.35, No 3-4, pp. 234-247
- [9] HIMMELBLAU, D.M. (1972) *Applied Nonlinear Programming*, McGraw-Hill Book Company, New York



CONTRIBUTIONS TO MANAGEMENT SWARF HIGH-SPEED MACHINE TOOLS

Baila DIANA

University Politehnica of Bucharest, Splaiul Independentei 313, Bucharest, Romania
baila_d@yahoo.com

Abstract: *The transition from traditional manufacturing with machine tools and CNC machine tools at high speeds requires modification on the technological concept of steel, machinery, tools and cutting regimes. This paper aims to draw attention to changes in management and management swarf. It also presents some additional tests designed to increase the life of tools used at high speeds.*

Key words: *traditional machine tools, CNC machine tools and high speed, conical swarf, semi swarf, SIM analysis.*

1. INTRODUCTION

Development of manufacturing with high-speed machine tools previously claimed, the development of techno-economic study further the research and management chip.

In general, chip generation and management problems have made practical activities in workshops, which resulted in finding technical solutions and safety, as correct.

In this respect, with the evolution of machine tools have diversified and expanded research objectives, as follows:

-the traditional machine tools (lathes, milling machines) with cutting speeds of 35-70 m/min was used Merchant model to calculate the optimum cutting conditions and chip evacuation recommendations were included in the STAS:

- chip-shape and characteristics;
- how to remove the chip from the workpiece;
- compression chip-evacuation and transportation are provided by the factory.

-the NC machine tools and CNC machining centers at speeds of 60-120 m / min was used Oxley model [7], [10] to calculate the optimum cutting conditions and chip evacuation is included in STAS.

-the high-speed machine tools 150-480 m / min, is used at present, the american way [1] to calculate rough cutting regimes. Household chips are discharged inside the car and involves the following elements:

- detached from the workpiece chips should have taper type IIIB;
- to remove chips from the workpiece is recommended to use 4 way chip clearance with turning chips into each cup to get seated properly so called conical fragment (fig. 1) and compression chip is inside the machine frame.

Chip not detached from the workpiece, due to high speeds necessary to make three additional tests, namely:

- determination of thickness of the resistance of semi-chips;

- analysis of the microstructure of white strip in the middle section cutting;
- finding the diffusion of metallic elements (Cr, Mo, V, Ti) on the lower surface of the chip.

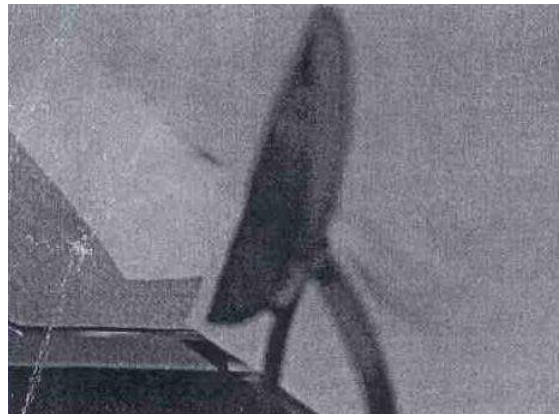


Fig.1. Conical swarf

2. RESEARCH ON THE PROCESSING OF LOW ALLOY STEELS TEMPERED

Programme of work uses a test bench from ENI Tarbes laboratories where they planned the following actions:

2.1. Choice of workpiece material

In the last decade, most research contracts aimed at economic reasons, the use of tempered low alloy steels, which in case of high speed machine tools, provides:

- obtain workpiece with high strength and toughness;
- processing of these components is done with some hard cutting regimes provides hard-schemes:
 - workpieces with fine-structure (give up to rectification);

-in the case of precision parts after cutting take electroerosion apply to $Ra = 0.2 \mu m$.

Consequently, taking into account the provisions of the agreement, a group of steels commonly used in cars with high speeds (table 1), choose low-alloy steel 32CrMoV13 quality and delivered in the form of bar.

Table 1. Tempered low alloy steels

Symbol	Steel grade	Metallurgical state
15CrMoV6	mechanical and structural steel heat treatment	annealed
32CrMoV13	nitrided steel used in aerospace	hardened and tempered
15CrNiTi1703	ferritic stainless steel	hardened and tempered
16NiCrMo13	hardening steel bearings and shafts	hardened and tempered



Fig.2. General appearance of the CNC lathe

Researching test equipment (fig.2.) is provided as follows:

- normally a lathe's working where the gearbox was adapted to achieve cutting speeds between 60-480 m/min;
- were chosen ceramic plates mineral ceramics type TP-200-TNM-160412-M5;
- cooling-medium: air stationary.
- pot type samples (fig. 3) are obtained from steel bar 32Cr MoV13 delivered at dimensions of $\phi 100 \times 150 \text{ mm}$.
- it uses front turning scheme (fig.4)
- hard cutting regimes are scheduled:
 - cutting speed $v = 100 \text{ m/min}$;
 - cutting thickness $t_1 = 0.1, 0.2, 0.3 \text{ mm}$;
 - cutting width $w = 7 \text{ mm}$;
 - rake angle $\chi = 0$.

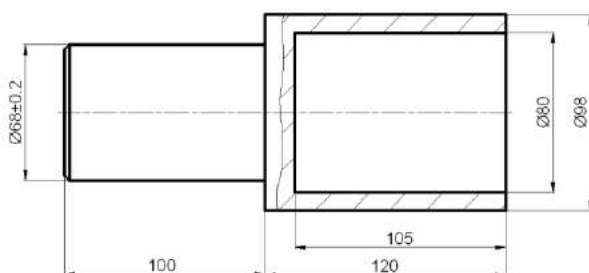


Fig.3. Pot workpieces

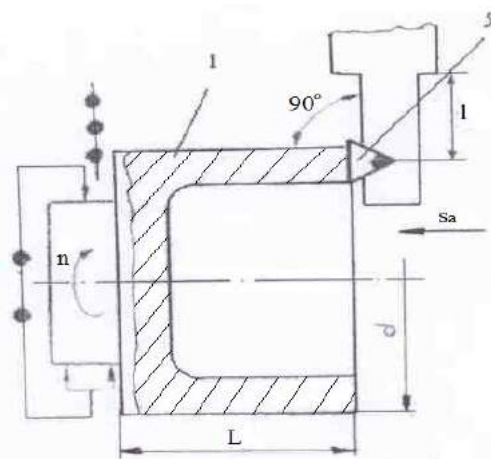


Fig.4. General appearance of the CNC lathe

Preparing the way for chip evacuation is taking these measures IIB in the workspace:

Since adopting the ISO chip clearance mode 4:

- for outside the sample pot;
- advance movement in the opposite direction (fig.5).

By positioning curled cup ensure proper reception cone chips IIB as shown in fig.6.

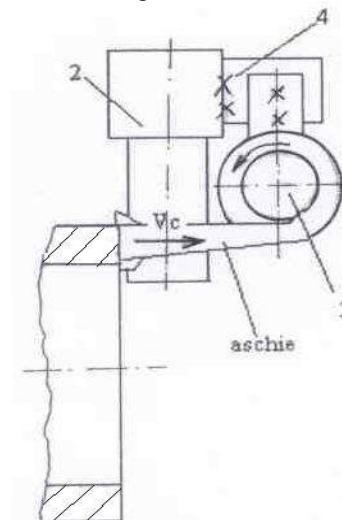


Fig.5. Working in the opposite direction of advance movement

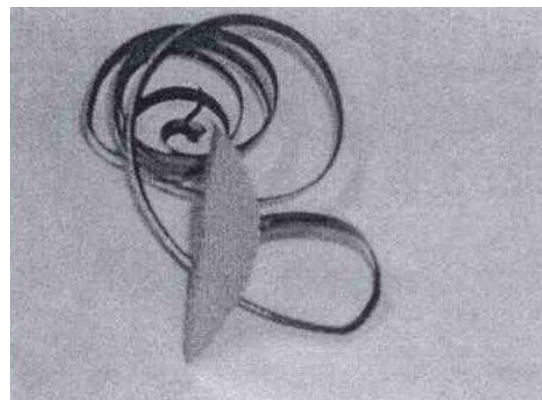


Fig.6. Working cup

Results of tests on three samples pot are shown in Table 2 .

Table 2.

No	v [m/min]	chip features					
		t1	t2	Δt2	h2	h1	Cr
1	100	0.1	0.58	12	26	22	18.2
2		0.2	0.7	18	30	27	11.1
3		0.3	1	26	46	43	7

2.2. Processing results

When processing the results through two objectives:
 -processing results in photomicrography;
 -processing of the results obtained with a complex apparatus.

2.2.1. Processing results in photomicrography

To process the results using an optical microscope to Carl Zeiss Jena type MM3 and φ38 mm respectively three cylindrical samples, from which:
 -fragment is positioned for measurements (fig. 7);

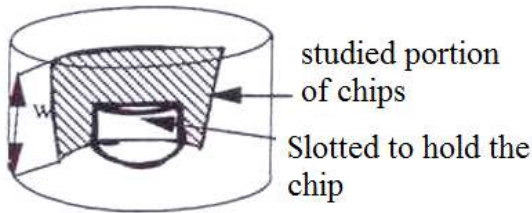


Fig.7. Positioned fragment for measurements

-symbolizes the chip with a plastic paste;
 -leave a hole in the center centering cylindrical sample and measurement system.

Microphotographs obtained by consulting with hard cutting regimes in table 2, we can determine the characteristics of the chips from chip geometry of fig. 8, namely:

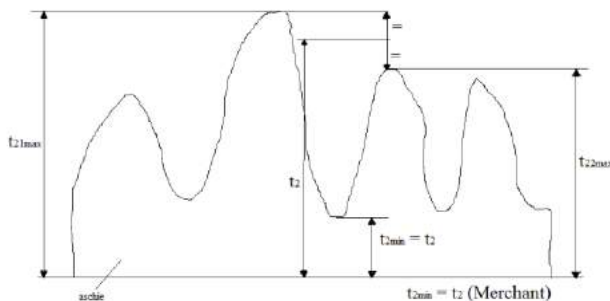


Fig.8.Geometry chip

- t_2 -chip thickness is calculated using the formula:

$$t_2 = \frac{t_{21max} + t_{22max}}{2} \quad (1)$$

-chip-thickness resistance is on the lower Δt_2 chips and are measured directly, knowing the scale of magnification photomicrography (fig. 9).

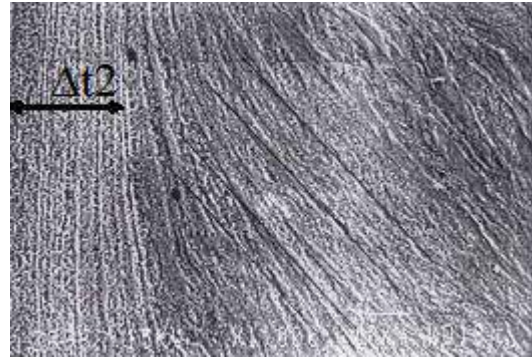


Fig.9. Photomicrography

Basically, the objective of the consultation paper aimed at three photomicrography made for $t_1 = 0.1, 0.2, 0.3$ mm and obtaining Δt_2 values in table 2 (fig.10. a, b, c). With these results demonstrate that there is a linear dependence between the advance work using (t_1) and the resistance of the chip thickness (Δt_2). The degree of segmentation of chips (G_s) is measured on a peak period T by identifying deep hole h_1 and h_2 . It uses the formula:

$$G_s = \frac{h_2 - h_1}{h_2} \quad (2)$$

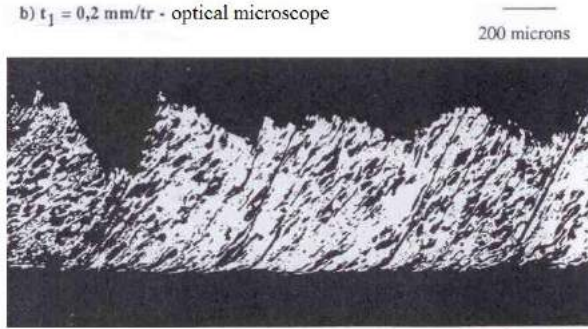
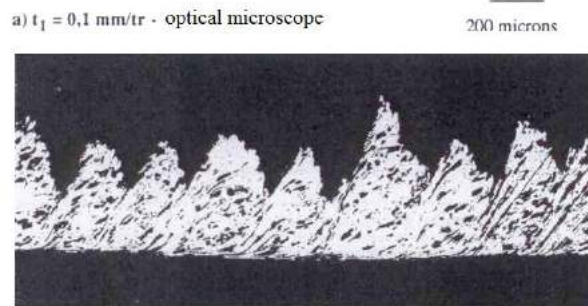
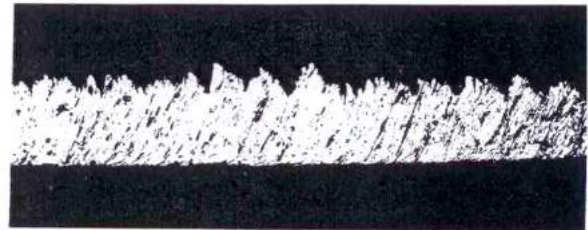


Fig.10.Microstructure with different chip advances

Finally, the characteristic features of the chips allow us to note the following:

- thickness of chip resistance (Δt_2) should represent an indication that detached fragment of the piece is right in the cup reception coils (fig. 6). Any fragment breaks minimum thickness $\Delta t_2 = 12 \mu\text{m}$ to stop driving the car, which must be kept fully closed during operation;
- chip-level segmentation (G_s) highlights the instability of the operating regimes of cutting hard and is an indicator for evaluating the workability of the steel cutting study.

2.2.2. Processing of the results obtained with complex equipment

The management can be demanding two more additional analysis:

- 1-white middle-width strip characterization chips conical IIB;
- 2-identification of metal-broadcast on the lower surface of the chip.

Characterization of white middle band width chips:
 -Chips in the middle white band width corresponds to the secondary shear zone at the interface tool-fragment. In this area the large amount of heat determines the chip surface but also deep changes in phase austenite/martensite.

-Interferometer is used to analyze Cr anticathode each other as positioned. To see in depth the structure, the lower surface of the chip is polished electrochemically, as follows: Cr-anticathode initially be scheduled for a depth of $6 \mu\text{m}$ where noted: γ -Fe austenite existing in the 111 plane angle of 65° α -Fe martensite present in the 110 plane at the angle of 68° .

-At depths greater austenite disappears almost completely highlighting excessive hardness of the strip of white conical fragment IIB. Given the dependence between hardness and strength, hardness white band offers safe technology that will not break chip cone, even if chip thickness Δt_2 resistance is small.

2.2.3. Identifying running on the lower surface of the metal chips

It's used semi chips obtained by cutting a tough regime: $v = 100 \text{ m/min}$, $t_1 = 0.2\text{mm}$ and pleasant mineral ceramics TNM-TP-200-160412-M5.

After crossing the interface tool-fragment in the presence of oxygen in the air, freshly detached fragment is finding an oxide layer of Fe, Cr, Mo, V, Ti.

SIMS depth analysis on chips made using reverse mechanism, the underlying oxidation process, as follows: To interface of chip at a distance of 0.1 mm from the edge tool, breathe a jet of oxygen, under certain conditions:

- adjustable pressure-controlled;
- pressure-stabilized;
- at certain times-blasting.

This near-interface layers of oxygen, metal ions cause excitement Fe^+ , Cr^+ , Mo^+ , V^+ , Ti^+ , and excitation of ions in the form of oscillations is recorded on a diagram (fig.11)

Processing the results show the following:
 elements of the charge-steel (Cr, V, Mo) is in large quantities on the surface of the tool-fragment interface and decrease with depth;

Ti-derived chemical element of the tool material and decreases in concentration, with depth.

Basically, the elements Cr, Mo, V, Ti strongly emphasizes the tool wear in particular crater on the surface of the recess.

Finally, knowledge of the elements Cr, Mo, V, Ti allows taking measures that:

- use another type of plate cutting;
- correcting the chemical composition of the cast-steel 32 Cr MoV13.

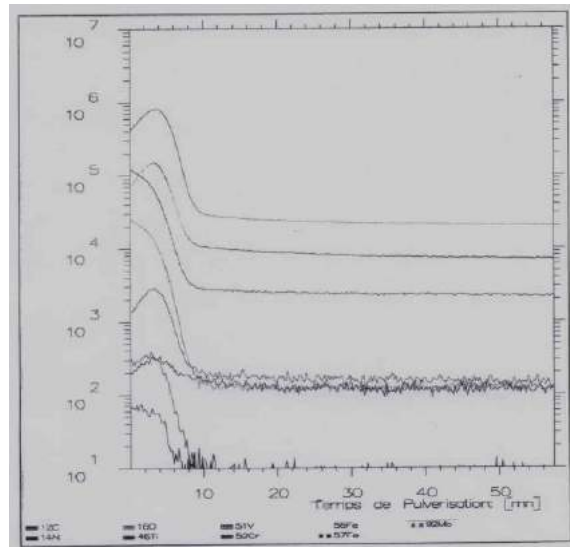


Fig.11. Depth profile SIMS realized in fragment

3. CONCLUSION

The traditional machine tools with NC machine tools, management of special chips not allowing it to raise a lot of types of chips, according to STAS.

In contrast, the high-speed machine tools, the problems are complicated because:

- the frame is required in the management of the car chip;
- tough regime to accommodate the claims cutting conditions for obtaining a cone chips IIB;
- during processing, workspace is locked and an accidental breaking of the chip would interfere with proper operation of the machine;
- further analysis shows that it can take steps to increase the lifetime of the tool, even with some tough cutting conditions.

REFERENCES

- [1] ALTINTAS Y: *Manufacturing automation*, Cambridge University Press, 2000;
- [2] LE CALVEZ C: *Etude des aspects thermiques et métallurgiques de la coupe orthogonale d'un acier au carbone*. Thèse. Centre de Paris, 1995.



STEEL VALVE PLATE GRINDING

Dijana NADAREVIĆ, Mirko SOKOVIĆ

University of Niš, Faculty of Mechanical Engineering

dijana.nadarevic@secop.com, mirko.sokovic@fs.uni-lj.si

Abstract: In the optimization of the process of steel valve plate grinding it is necessary to take into consideration different processing parameters. This paper is going to describe the production of a steel valve plate with the focus on flat-grinding. It is also going to present the method of choosing grinding wheels and parameters, as well as their impact on the processing quality parameters (roughness, surface flatness and seat width). The optimization of the grinding process ensures acceptable quality of the final product applying the smallest possible changes in parameters at non-uniform quality levels of the tools. Here we have to make sure that the machining process is acceptable in terms of processing cost as well. We are going to use the G-factor as the efficiency indicator for different tools.

Key words: valve plates, flat-grinding, G-factor

1. INTRODUCTION

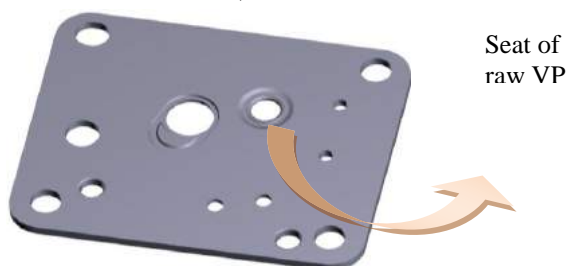
At the beginning of the planning of the grinding process it is first of all necessary to collect the data about the workpiece, about the available machine, processing operations, types of grinding wheels etc. Based on these starting points (input parameters) and on the already known output parameters (the surface flatness and roughness, the seat width, the process costs etc.) it is possible to optimize the flat-grinding process to such degree that the quality of the product is acceptable even at minimum production costs.

In continuation the process of the high-serial production of a steel valve plate, a part of a household compressor, is described. A particularity of such valve plate is in the difficulty of production both for the geometric shape and its low hardness.

Due to the above mentioned difficulties the further focus is set on the choice of processing parameters and grinding tools necessary for the efficient grinding.

2. VALVE PLATE PRESENTATION

Picture 1 presents a valve plate made of steel St20, dimensions 56 x 60 x 2,1mm.



Picture 1. Steel valve plate

Low hardness of 117 to 170 HV is typical for a steel valve plate. The seat of raw material is rather inadequate for the automatic feeding, a consequence of the pressed material

of the seat. Due to the rapid corrosion of the raw material, a supplier has to protect the material from corrosion, which causes plate gluing and makes the automating feeding difficult.

The product designing is complex both for the possibility of the primary burr (resulting from the stamping process, especially at the intersection of two smaller radii) and for the secondary burr (resulting from the grinding process). The following section discusses only those grinding wheels and parameters which have given acceptable results in terms of secondary burrs.

3. PRODUCTION OF STEEL VALVE PLATES

After the verification of the raw material (stamped valve plate) in the "Incoming inspection" section the plates are transported to the store for the flat-grinding operation. The grinding process is performed on the machine for two-sided flat-grinding: Diskus, Germany.

After that the grinding operator transports the valve plates in boxes to the brushing operation. The plates travel from the load via a conveyer belt to the magnet plates of the machine and are brushed first from one side at the first station Rotex 1 (a station with three brushes $\phi 150$ mm) and then they are rotated and brushed on the other side at the second station Rotex 2, Switzerland. The aim of this operation is primarily to remove the secondary, as well as the primary, burr from the valve plates and to even the sharp edges, especially the ones on the seats of the surface of a valve. After the brushing process the valve plate is rotated by 90° (vertical position) and is transported to the washing operation.

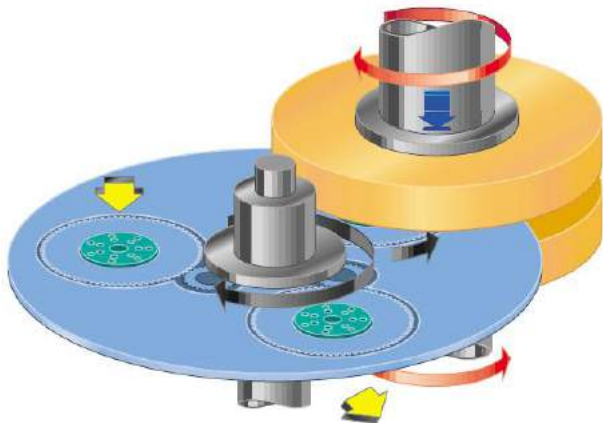
After the washing the operator first visually inspects the valve plates, then stacks them in cardboard boxes and puts them onto the shelves for the finished valve plates. The last operation includes the valve system assembly. The operator impresses the suction valve bolts (1) and rivets (4) the discharge valve (2) together with the stop-plate (3), as shown in Picture 2.



Picture 2. Valve plate with valve plate system

3.1 Steel valve plate grinding

Flat-grinding is a process of material subtraction, in which a high accuracy and a high surface quality can be achieved. The main movement is performed by two grinding wheels rotating very fast. In this case the feeding is performed by a wheel or a transport plate with planets, as shown in Picture 3.



Picture 3. Movement of grinding wheels and feeding plate

Double-sided flat-surface grinding is a process in which the material is removed from the workpiece from both sides simultaneously. The uniformity of the removal of material is guaranteed by setting optimal grinding parameters.

The grinding process itself is conducted so that the operator manually puts the valve plates onto the planets of the transport plate which then carries them between the grinding wheels and the grinding process begins. During the work the operator monitors the thickness of the valve plates (consequently also the seat width), the roughness and the flatness of the surface. On the basis of these control variables he decides about his further action: changing the thickness of the raw valve plate, more

frequent wheel dressing, changing the speed of the wheels...

4. CHOICE OF STEEL VALVE PLATE GRINDING PARAMETERS

In the selection of optimal parameters in flat-grinding the major part of the problems arose from the instability of the quality of grinding wheels. Table 1 shows the parameters that remain mainly unchanged despite the unstable quality of grinding wheels.

Table 1. Unchanging grinding parameters

Grinding parameters	Values
Transport plate grinding speed	8000 rpm
Planet rotation speed	80 rpm
Planet rotation direction	To the right (1)
Partial shift of the z-axis	0,040 mm
Spindle rotation	counter direction

Besides the above given unvarying parameters we also have the adjustable parameters, such as the wheel rotation speed, the thickness of the raw material, the number of the transitions in dressing, etc. The speed of the feeding plate has no significant influence on the product quality.

The process analyses have shown that the wheel rotation speed has a big importance in the quality of grinding.

The optimal value is determined and it is also the maximum value permitted by the machine (32 m/s). According to the machine manufacturer it is possible to specify the optimal planet rotation speed (approximate values) from the speed ratio, as shown in Table 2:

$$q_s = 60 \cdot \frac{v_s}{v_w} = \frac{n_s \cdot d_s}{n_w \cdot d_w} \quad (1)$$

Where:

- n_s – the number of rotations of grinding wheels,
- v_s – the peripheral speed of wheels in m/s,
- n_w – the number of rotations of the workpiece,
- v_w – the peripheral speed in m/s of the workpiece (planets with the diameter of $\phi 230$ mm).

Recommended values of speed ratios are presented in Table 2.

Table 2. Recommended values of speed ratios

Process	Indicator – orientation values
Rough grinding	40 - 60
Fine grinding	25 - 40

Other important processing parameters include the dressing parameters. Namely, the quality of the finished product (especially the flatness of the valve plate) depends on the quality of dressing. These parameters are: the speed of dressing wheels, the number of dressing transitions and the thickness of the raw material during the dressing.

Based on the performed tests it was found that the quality parameters were satisfied (the roughness and the flatness of the surface) in terms of the material removal of 0.02 mm and at the 5 dressing wheel transitions.

The optimal processing parameters for flat-grinding have been shown in Table 3.

Table 3. The optimal valve plate grinding parameters

Grinding parameters	Values
Grinding wheel rotation speed	32/28 m/s
Thickness of raw material	0.1 mm
Number of dressing transitions	5
Dressing frequency	1 h

The ratio of 32/28 m/s has been taken for the rotation speed of grinding wheels since this combination ensures a uniform material removal on both sides of a workpiece. Depending on the speed of the grinding wheel wear the frequency of the manual shift of the bottom grinding wheel is determined.

5. CHOICE OF WHEELS FOR THE GRINDING OF VALVE PLATES

The suppliers of grinding wheels can only hardly ensure equal resistance of grinding wheels, even though the process of their production is the same for each pair with the same specifications.

Grain size is selected on the basis of the required surface quality of the workpiece. For the roughness of $R_a < 0.3 \mu\text{m}$, recommended by the producer, we can choose the medium granulation of grinding grains. The tests have shown that in the area of fine granulation better results have been achieved, especially in the case of smaller thickness of the raw material. Some producers also use double marks for granularity, for example 150/2. This code means that one third of the grain mixture has the granulation of 150, one third has one level lower granulation (120), and the last third of the mixture has one level higher granulation (180).

In the choice of hardness and structure of wheels, we considered the advice that it is necessary to choose harder grinding wheels to grind softer material. The problem occurred in the determination of the structure of wheels. In a more open structure we had problems with scratches on the valve plate. Selecting the wheels with lower hardness and more closed structure we the grinding wheels started "levelling", what means that the grains were wearing out and were not pushing, which resulted in the loss of the cutting capacity of grinding wheels.

Experiments have shown that the medium hard and hard wheels are the most suitable in grinding a steel valve plate.

Ceramic bound grinding wheels are normally used at the operating speed of 40 m/s; they maintain the form very well and are useful for all types of grinding (from very rough to the finest).

Bakelite has proved to be a better solution for the burr, but there were many problems with so-called "watering of wheels" (change of the characteristics of wheels after a certain period of time). This phenomenon is observed especially in the period when the space is unheated or in case of a longer machine failure.

It should be stressed that each analysis had to be performed for each supplier separately since the grinding wheels with the same marks are quite different at different suppliers.

Experiments have shown that we get similar results with the following grinding wheels:

- 58A150/1R8B25
- 52A150/2L5B22
- 50A180J5AV217

That means that we are talking about a mixture of the corundum of 150, 120 and 180 granulation (depending on the specified ratio), the medium (L) or high (R) hardness, and the closed structure with the Bakelite binder (exceptionally ceramic).

A more detailed analysis has been made for Bakelite wheels since they are used the most frequently. The results of Bakelite grinding wheels with the granulation of 120 and 150 (mixture), hardness R (hard) and closed structure (8) have been compared to the grinding wheels with the mixture of grains with the granulation of 120, 150 and 180, medium hardness (L) and closed structure.

The dressing of grinding wheels have been performed in all cases using the diamond dressing tool in dimensions of $\phi 120 \times 20 \times 51 \text{ mm}$, mark 119D126-30MB02.

6. ANALYSIS OF THE RESULTS

The analysis is based on the optimal process parameters (Table 3) for grinding wheels of two different suppliers (supplier A and supplier B).

As a criterion for the suitability of individual tools the G-factor has been chosen and it represents the ratio between the volume of raw materials and the grinding wheel wear, as shown in the equation (2):

$$G = \frac{V_w}{V_s} \quad (2)$$

Where:

- V_s – the volume of the grinding wheel wear and
- V_w – the volume of the raw material.

The volume of the grinding wheel wear is calculated using the equation (3):

$$V_s = \frac{\pi \cdot (D^2 - d^2)}{4} \quad (3)$$

Where:

- D – the outer diameter of wheels,
- d – the inner diameter of wheels.

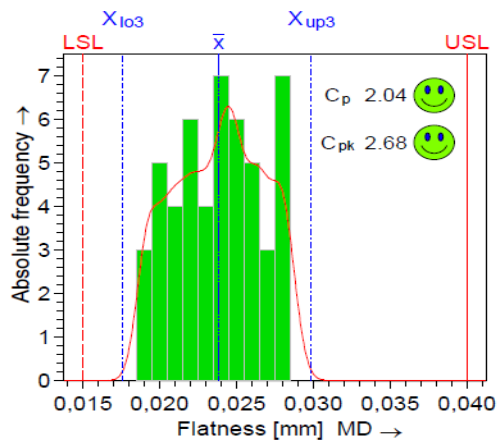
The volume of the raw materials is:

$$V_w = n \cdot l \cdot h \cdot \delta \quad (4)$$

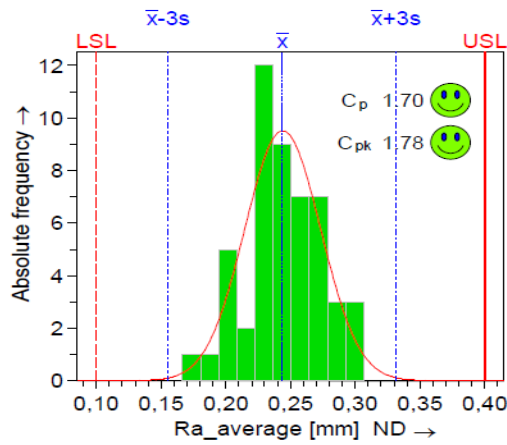
Where:

- n – the number of valve plates ground by one pair of grinding wheels,
- l – the length of the workpiece,
- h – the width of the workpiece,
- δ – the thickness of the raw material.

Before we check the value of the G-factor it is necessary to verify the capability of the valve plate grinding process for selected grinding tools and parameters. The process capability index (C_p , C_{pk}) has been chosen as the indicator of quality.



Picture 4 shows the process capability index for both quality parameters: the flatness and the roughness of a valve plate.



Picture 4: Process capability index

According to the values obtained for both parameters (C_p and $C_{pk} > 1.33$) we can claim that the process is capable. The lower tolerance limit is presented by the value which can be reached in a real process. In case the value 0 is taken as the lower limit the process centring is worse, this in our case can also be accepted.

In continuation we are going to compare the performance of two different grinding wheels (GW):

- GW 1 = 58A150/1R8B25 (supplier A),
- GW 2 = 52A150/2L5B22 (supplier B).

Table 4 presents an example of the efficiency of two wheels with different features.

Table 4: Comparison of G-factors of grinding wheels (GW) taken from different suppliers

Type of grinding wheel	GW 1 (supp. A)	GW 2 (supp. B)
Outer diameter of GW D [mm]	456	455
Inner diameter of GW d [mm]	220	220
GW height T [mm]	45	45
Length x width of workpiece l [mm]	60x56	60x56
Raw material thickness δ [mm]	0.1+0.03	0.1+0.03
Nr. of valve plates n	40 446	32 175
Volume of GW V_s [mm ³]	5635509	5603428
Volume of raw valve plate V_w [mm ³]	10569888	10810800
G-factor	2.41- 3.13	1.93- 2.51

G-factor for hard wheels (1) is a little higher. This result was expected since the softer wheels (2) require more frequent measure corrections (the removal of the raw

material). Due to the manual adjustment of the quantity of subtraction it is not possible to specify the G-factor exactly. However, we can define the area in which it is located.

7. CONCLUSION

Due to the unequal quality of grinding wheels the major part of tests performed include the choice of the optimal type of wheels.

Since the requirements included lower roughness of the processed surface at higher material removal certain difficulties have been encountered. An incorrect choice of grinding wheels has also caused an increased wheel wear. This resulted in smaller cutting capability and in fast wheel dressing, which means that the processing costs were higher.

The automation in setting the material removal, the possibility to choose higher speed of grinding wheels and the provision of stability in the quality of wheels have a great influence on both the quality and the cost optimization of the steel valve plate grinding process.

In case of satisfaction of the mentioned requirements the G-factor would improve, as well, mainly due to the decrease in the frequency of the grinding wheel dressing.

REFERENCES

- [1] Swaty, tovarna umetnih brusov d.d; Interni priročnik, 2010
- [2] <http://diskus-werke.dvs-gruppe.com/index.php?id=19&L=1>
- [3] Malkin, S. (2008) Changsheng Guo: Grinding Technology, New York.
- [4] DISKUS WERKE, Double-Face-Grinding-Machines, 2001, Germany
- [5] Diskus Werke – Technische Dokumentation, 2001, Germany



APPLICATION OF TAGUCHI METHOD IN THE OPTIMIZATION OF FACE MILLING PARAMETERS

Milenko SEKULIĆ¹, Miodrag HADŽISTEVIĆ¹, Zoran JURKOVIĆ², Pavel KOVAČ¹, Marin GOSTIMIROVIĆ¹

- 1) Faculty of Technical Sciences, University of Novi Sad, Trg D. Obradovica 6, Novi Sad, Serbia
- 2) Faculty of Engineering, University of Rijeka, Vukovarska 58, Rijeka, Croatia
milenkos@uns.ac.rs

Abstract: This paper examines the influence of cutting parameters on cutting forces in face milling when machining hardened steel Č3840 (EN 90MnCrV8). The milling parameters evaluated are cutting speed, feed rate and depth of cut. The experiments have been carried out in accordance with a Taguchi method. An orthogonal array, signal-to-noise (S/N) ratio and analysis of variance (ANOVA) are employed to analyze the effect of these milling parameters. The analysis of the results shows that the optimal combination for low cutting force are high cutting speed, low feed rate and low depth of cut. The study shows that the Taguchi method is suitable to solve the stated problem with minimum number of trials as compared with a full factorial design.

Key words: Taguchi method, face milling, cutting force

1. INTRODUCTION

Cutting of hardened steel is a topic of high interest for today's industrial production and scientific research. In fact, hard cutting operations can seriously be regarded as an alternative for grinding operations under certain conditions. Hard milling is a viable alternative for machining materials with hardness from 45 to 64 HRC. The common disadvantages of hard milling are excessive tool wear and high cutting forces.

Reliable prediction of milling forces is significant for the simulation of the machinability, cutter breakage, cutter wear, chatter and surface quality. The subject of this study is to analyse dependence of main cutting force F_v on three cutting parameters in face milling when machining hardened steel (cutting speed v , feed rate s and dept of cut a). The Taguchi method, based on orthogonal arrays, has been used for determining the influence of particular cutting parameters.

2. TAGUCHI METHOD

Classical experimental design method, i.e. rotatable central composite design, is too complex and not easy to use. A large number of experiments have to be carried out especially when the number of process parameters increases. To solve this problem, the Taguchi method uses a special design of orthogonal arrays to study the entire parameter space with a small number of experiments. This is an engineering methodology for obtaining product and process condition, which are minimally sensitive to the various causes of variation, and which produce high-quality products with low development and manufacturing costs. Signal to noise ratio and orthogonal array are two major tools used in robust design.

The S/N ratio characteristics can be divided into three categories when the characteristic is continuous: nominal is the best, smaller the better and larger is better characteristics. For the minimal main cutting force F_v , the solution is „smaller is better“, and S/N ratio is determined according to the following equation:

$$\frac{S}{N} = -10 \log \left(\frac{1}{n} \sum_{i=1}^n y_i^2 \right) \quad (1)$$

where n is the number of replication and y_i is the measured value of output variable. The minimal F_v is achieved using the cutting parameters where S/N ratio is maximal. The influence of each control factor can be more clearly presented with response graphs. The experimental layout for the machining parameters using $L_9(3^4)$ orthogonal array was used in this study. This array consist of four control parameters and three level (fourth parameter D was used to estimate the experimental error). The experimental results were analyzed with Analysis of Variance (ANOVA), which is used for identifying the factors significantly affecting the performance measures.

3. EXPERIMENTAL DETAILS

The experimental work was carried out at the Department for Production Engineering, the Faculty of Technical Sciences in Novi Sad. The machining was conducted on a Vertical-spindle Milling Machine („Prvomajska“ FSS-GVK-3) in dry condition. A face milling cutter with $\varnothing 125$ mm diameter („Jugoalat“ G.717), with cemented carbide inserts („Sandvik Coromant“ type SPKR 12 03 ED R-WH 3040) with tool cutting edge angle $\kappa=75^\circ$ and rake angle $\gamma=7^\circ$ was used as a tool. All of the experiments were conducted with one insert by orthogonal arrays with three levels (coded by:1,2 and 3), Table 1.

Table 1. Machining parameters and their levels

Symbol	Parameters	Levels		
		1	2	3
A	Cutting speed v , m/min	27,86	35,32	43,96
B	Feed s , mm/rev	0,223	0,280	0,352
C	Depth of cut a , mm	0,2	0,32	0,5

Workpiece material was pre-annealed tool steel Č3840 (EN 90MnCrV8) (hardness 57 HRC). Material composition of workpiece is as follows: C-0,9%; Si-0,3 %, Mn-2%; Cr-0,3%; V-0,15% by wt. Dimensions of experimental probe is 200x104,7 x50 mm.

The instrumentation package includes a three-force component dynamometer Kistler (model 9257), based on the piezoelectric effect and PC based data acquisition system with LabView 8.0 software. The samples were sent to a multichannel amplifier for analogical signals for a better integrity of F_x , F_y and F_z . Then the data was transferred to a computer with an AD card to convert the analogical signals to digital format for analysis. The photograph of the experimental set-up is shown in Fig. 1.



Fig.1. Experimental set-up [1]

4. EXPERIMENTAL RESULTS

Fig. 2 presents the cutting forces scheme in one-tooth face milling.

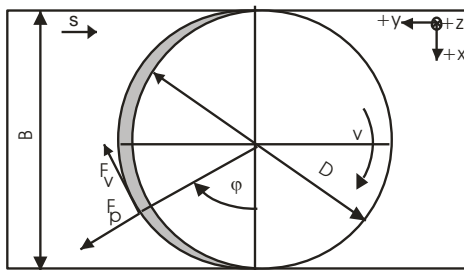


Fig.2. The scheme of cutting forces [1]

To eliminate the influence of random factors on change forces F_x , F_y and F_z during one revolution of cutter, requested their average value. The middle value

was based on the values of cutting force for series of three full revolution of cutter (Figure 3).

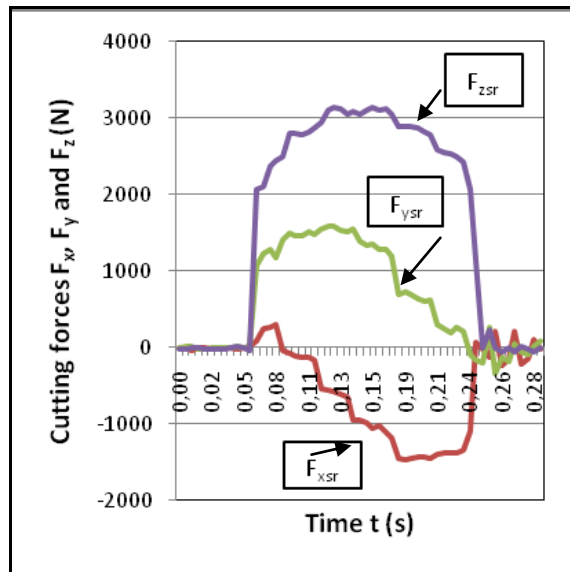


Fig.3. Average value of cutting forces [1]

The measured orthogonal force components can be converted to the instantaneous cutting force components in the tangential direction by equation:

$$F_v = -F_x \cdot \sin \varphi + F_y \cdot \cos \varphi \quad (2)$$

Equation (2) is used to describe the main cutting force on a single tooth. Experimental results, together with their transformations into signal-to-noise ratios are given in Table 2.

Table 2. Orthogonal array $L_9(3^4)$ with experimental results and calculated S/N ratio

№	Factors				F_v, N	S/N
	A	B	C	D		
	v	s	a	Exp. error		
1	1	1	1	0	506,58	-54,094
2	1	2	2	0	635,10	-56,059
3	1	3	3	0	1218,81	-61,741
4	2	1	2	0	566,87	-55,071
5	2	2	3	0	1008,81	-60,086
6	2	3	1	0	573,54	-55,187
7	3	1	3	0	828,86	-58,371
8	3	2	1	0	639,52	-56,125
9	3	3	2	0	777,26	-58,169

5. ANALYSIS OF RESULTS

In this study all the analysis based on the Taguchi method is done by Qualitek-4 software to determine the main effects of the cutting parameters. From Table 2 it can be determined which control factor have strong influence on main cutting force in face milling. Optimal cutting conditions of these control factors can be very easily determined from the S/N response graphs in Figures 4, 5 and 6. The response graphic of main cutting force has been shown for all three control factors. The best main

cutting force is at the higher S/N values in the response graphs. Parameter influence on output process variable shows angle of inclination of the line which connects different parameter levels. It can be seen from the presented graphs that depth of cut has the greatest influence on the main cutting force. Feed has certain influence and cutting speed has insignificant influence on main cutting force.

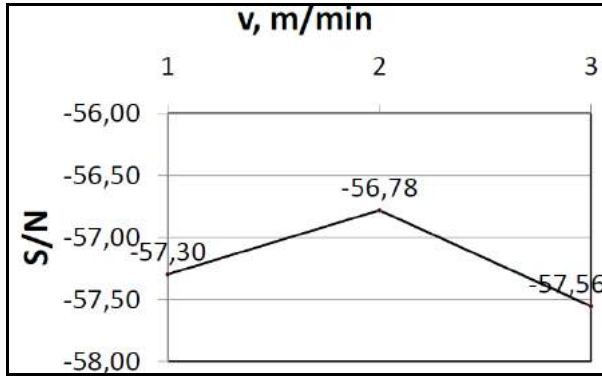


Fig. 4. S/N response graphs for cutting speed

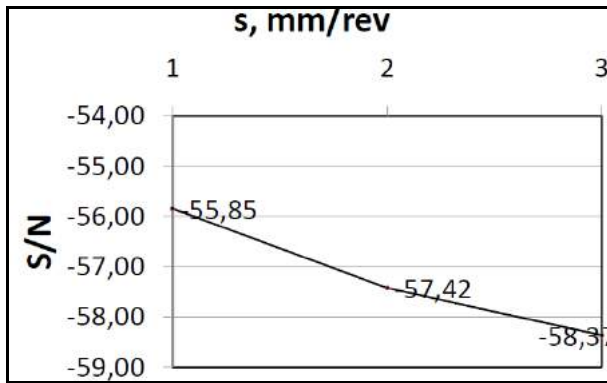


Fig. 5. S/N response graphs for feed

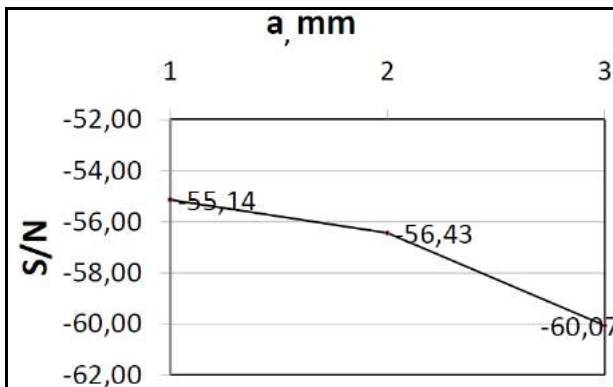


Fig. 6. S/N response graphs for depth of cut

Optimal cutting conditions are shown in Table 3. The optimization of cutting parameters inside offered factors levels, with regard to criterion „smaller is better“, gives the combination of control factors: A=2, B=1, C=1. This combination enables the lowest main cutting force. A verification test has to be performed after optimal settings of control factors have been determined with the goal to approve the calculated value of the quality characteristic. Difference between the calculated and yielded value of main cutting force is very small.

Table 3. Optimal settings of control parameters

Control parameters	Level	Setting		F _v obtained using Taguchi method	F _v obtained using verification
v, m/min	2	35,32	Require add. exp.	S/N=-53,771 F _v =488,46 N	F _v =495,54 N
s, mm/rev	1	0,223			
a, mm	1	0,20			

5.1. Analysis of Variance (ANOVA)

Analysis of variance (ANOVA) and F test (standard analysis) are used to analyse the experimental data as follows [2]:

The first step: Summary table

Table 4. Summary table

Factor	Level	Total	Middle value
A	1	$Y_{A1}=Y_1+Y_2+Y_3$	$y_{A1}=\frac{Y_{A1}}{3}$
	2	$Y_{A2}=Y_4+Y_5+Y_6$	$y_{A2}=\frac{Y_{A2}}{3}$
	3	$Y_{A3}=Y_7+Y_8+Y_9$	$y_{A3}=\frac{Y_{A3}}{3}$
B	1	$Y_{B1}=Y_1+Y_4+Y_7$	$y_{B1}=\frac{Y_{B1}}{3}$
	2	$Y_{B2}=Y_2+Y_5+Y_8$	$y_{B2}=\frac{Y_{B2}}{3}$
	3	$Y_{B3}=Y_3+Y_6+Y_9$	$y_{B3}=\frac{Y_{B3}}{3}$
C	1	$Y_{C1}=Y_1+Y_6+Y_8$	$y_{C1}=\frac{Y_{C1}}{3}$
	2	$Y_{C2}=Y_2+Y_4+Y_9$	$y_{C2}=\frac{Y_{C2}}{3}$
	3	$Y_{C3}=Y_3+Y_5+Y_7$	$y_{C3}=\frac{Y_{C3}}{3}$
Total		$Y = \left(\sum_{i=1}^3 y_{Ai} + \sum_{i=1}^3 y_{Bi} + \sum_{i=1}^3 y_{Ci} \right)$	$y = Y/3$

The second step: Total sum of squares to total variation

$$S_T = \sum_{i=1}^n Y_i^2 - \left(\frac{\left(\sum_{i=1}^n Y_i \right)^2}{n} \right) \quad (3)$$

Where:

n-total number of experiments,

Y_i-value of results of each experiment (i=1 to 9)

The third step: Sum of squares due to parameter (A,B,C)

$$S_p = \sum_{j=1}^t \frac{\left(\sum Y_{ij} \right)^2}{t} - \frac{1}{n} \left(\sum_{i=1}^n Y_i \right)^2 \quad (4)$$

Where:

p-some of the parameters (A, B, C)

t-repeating number of each level (1, 2, 3) of parameter p

ΣY_{ij}-value of results of each level (1, 2, 3) of parameter p

Sum of squares due to error:

$$S_{error} = S_T - S_A - S_B - S_C \quad (5)$$

The fourth step: Degree of freedom (DOE)

Degree of freedom of parameter p:

$$DF_{factor} = n_e - 1 = 3 - 1 = 2 (= DF_A = DF_B = DF_C) \quad (6)$$

Where:

n_e-number of levels of parameter p

Total degree of freedom:

$$DF_{total} = n - 1 = 9 - 1 = 8 \quad (7)$$

Degree of freedom of error term:

$$DF_{error} = DF_{total} - \sum DF_{factor} = 8 - 6 = 2 \quad (8)$$

The fifth step: Variance of parameter p and error term

$$V_p = \frac{S_p}{DF_{factor}} \quad (9)$$

$$V_{error} = S_{error} / DF_{error} \quad (10)$$

The sixth step: F ratios of parameter p

$$F_p = \frac{V_p}{V_{error}} \quad (11)$$

The seventh step: Beginning ANOVA table

Table 5. Beginning ANOVA table

Factor	DOF	Sum of squares	Variance	F-ratio
	DF	S	V	F
A	2	7458,33	3729,17	0,288
B	2	74712,77	37356,38	2,886
C	2	334999,17	167499,58	12,941
Error	2	25887,19	12943,59	
Total	8	558727,73		

The eighth step: Pooling

The value of F-ratio for factor A is less than 1, it means that factor is not significant and this factor is rejected. This process is called pooling. The calculation of pooling is determined according to the following equations:

$$DF_{error(pooling)} = DF_{error} + DF_A = 4 \quad (12)$$

$$S_{error(pooling)} = S_{error} + S_A = 33345,53 \quad (13)$$

$$V_{error(pooling)} = \frac{S_{error(pooling)}}{DF_{error(pooling)}} = 8336,38 \quad (14)$$

F-ratios for factors which not included in the pooling must be re-calculated by new variance of error:

$$F'_p = \frac{V_p}{V_{error(pooling)}} \quad (15)$$

For these factors must be obtained pure sum of square:

$$S'_p = S_p - (V_{error(pooling)} \times DF_{faktor}) \quad (16)$$

$$S'_{error} = S_{error} + ((DF_{total} - DF_{error(pooling)}) \times V_{error(pooling)})$$

Percentage contribution of parameter is obtained by dividing the sum of squares (re-calculated) for each parameter with total sum squares:

$$P_p = \left(\frac{S'_p}{S_T} \right) \times 100\% \quad (18)$$

The ninth step: Final ANOVA table

Table 6. Final ANOVA table

Factor	DOF	Sum of squares	Variance	F-ratio	Pure Sum	Percent %
B	2	74712,77	37356,38	4,48	58040,01	13,1
C	2	334999,17	167499,58	20,09	318326,41	71,85
Error	4	25887,19	12943,59		59232,72	15,05
Total	8	435599,14			435599,14	100

The influence of errors in the amount of 15.05% indicates a significant effect of all those parameters that are not included in the experiment (old machine tool, tool wear, cutting tool material ...).

6. CONCLUSION

This paper has discussed dependence of the main cutting force on three cutting parameters, namely the cutting speed, feed and depth of cut in the face milling hardened steel. Taguchi method has been used to determine the main effects, significant factors and optimum machining conditions to the value of main cutting force. From the analysis using Taguchi's method, results indicate that among the all-significant parameters, depth of cut is the most significant parameter. Results obtained from Taguchi method closely match with ANOVA.

REFERENCES

- [1] SEKULIC, M., KOVAC, P., GOSTIMIROVIC, M., HADZISTEVIC, M., SAVKOVIC, B. (2010) *Prediction of cutting forces in face milling of hardened steel*, Proceedings of the International Conference of Sustainable Life in Manufacturing SLIM2010, Isparta, Turkey, pp 36-39
- [2] MAJSTOROVIC, V., SIBALIJA, T., SOKOVIC, M., PAVLETIC, D. (2009) *Six Sigma Model and Application*, Tempus project number IB_JEP-41120-2006, FTN, Novi Sad, Serbia
- [3] CUKOR, G., JURKOVIC, Z., SEKULIC, M. (2011) *Rotatable central composite design of experiments versus Taguchi method in the optimization of turning*, Metalurgija, Vol.50, No 1, pp 17-20



INFLUENCE OF TOOL BALANCING ON MACHINED SURFACE QUALITY IN HIGH SPEED MACHINING

Jozef PETERKA, Martin KOVÁČ, Marek ZVONČAN

Institute of Production Technologies, Faculty of Materials Science and Technology, Slovak University of Technology,
Paulínska 16, Trnava, Slovakia

jozef.peterka@stuba.sk, martin.kovac@stuba.sk, marek.zvoncan@stuba.sk

Abstract: High speed machining has some differences according to conventional milling. The main difference is higher rotational speed of the spindle (40 000min⁻¹ and higher). During high speed spindle rotations more dynamic forces are rising, which are affecting bearings, frame and the whole machine. The forces are efforting vibrations furthermore causes worse quality of machined surface and may damage the spindle. Minimization of these forces is essential. According to that, the tool balancing machines are used. Tool balancing should provide better mass set out around the tool axis. Machining with balanced tool will provide better surface quality and less tool and machine wear. To verify theoretical knowledge, an experiment was realized. Two identical tools were balanced according to ISO 1940-1 standard at two different levels. Aluminum plate was used as an experimental part. Both milled surfaces were scanned with 3D microscope and surface roughness was evaluated. Results showed High speed machining with balanced tool provided better surface quality than conventional milling as well as worse balanced tool.

Key words: Tool balancing, unbalance, high-speed machining, 3D microscope, surface quality

1. INTRODUCTION

The key-stone in high-speed milling is to reach higher surface quality and removal rate with high cutting speed and in the same way reach lower tool wear a lower cutting forces. Large amount of heat generated at the cutting edge is minimally transferred to a material and tool at high-speed milling. In order to reach high surface quality, adequate chip removing rate is an important parameter [5]. By high-speed milling it is possible to achieve surface roughness at level Ra 0, 2 μm [6]. Important parameter affecting achieved surface roughness is run out, caused by unbalance of the tool, tool holder and the spindle. Importance of run out is rising with frequency of spindle rotation, furthermore with rising of centrifugal forces affecting tool in high-speed milling.

2. OUT - OF - BALANCE

Unbalance of a rotational part comes from its geometric shape depending on its functionality. Unbalance of parts symmetrical by axe like tools and tool holders are, is caused by inaccuracy of shape and size, non-homogeneity of material, nonsymmetrical parts e.g. clamping screw in some types of tool holders, clamping slot on some tool shanks and run out of a tool holder. Unbalanced tool arrangement can be explained as a rotational part, where momentum central axis is not identical with axis of rotation (Fig.1). Balancing is a process of mass correction around the central momentum axis by loading or unloading of mass. The aim is to reach identical position of momentum and rotational axis of the tool arrangement

as well as it is possible. That preserves dynamic forces and vibrations in bearings in allowed limits when required rotations are reached [3].

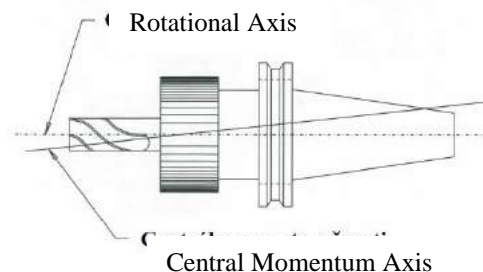


Fig.1. - Central momentum axis and rotational axis [2]

2.1 Calculation of unbalance

In High Speed Cutting, the maximum unbalance is characterized in ISO 1940-1 standard. This standard presents levels of G for certain rotational frequencies and rotational parts. For rotational tool arrangements, G level should be at least 2,5 ms⁻¹ at maximum spindle rotational speed. According to unbalance G level, rotational speed and tool arrangement weight, maximum allowed unbalance can be calculated as [4]:

$$U_{zv} = \frac{G \cdot 9549 \cdot m}{n} \quad [\text{gmm}] \quad (1.1)$$

Where: U_{zv} is remaining unbalance [gmm],
 G –level of balancing ($G1,0$; $G2,5$; $G6,3$) [ms^{-1}],
 m – Tool arrangement weight [kg],
 n – Rotational speed [min^{-1}],
 9549 – Constant [-].

2.2 Ways of tool arrangement balancing

Ways of tool arrangement balancing can be divided as following:

1. Balancing in one balancing level: static and rotational unbalance
2. Balancing in two balancing levels: momentum and dynamic unbalance

Balancing in one balancing level is used when gravity center is out of rotational axis (Fig.2). The aim is to move the gravity center of tool arrangement into rotational axis. When rotational balancing is employed, centrifugal force perpendicular to axis is raising. Rotational unbalance is eliminated in one level; balancing level position is irrelevant in this case. In practice, balancing in one level is enough. It can be said, this is valid for rotational parts, where the ratio of length to diameter is smaller than 0.2 [3].

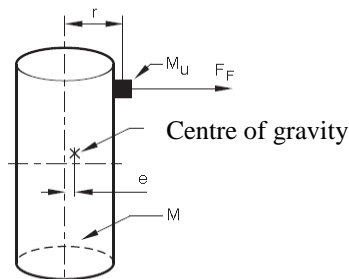


Fig.2. Balancing in one level

M_u , unbalance rate [gmm]; r distance of unbalanced mass from rotational axis [mm]; M weight of rotating mass [g];
 e distance of gravity center of mass from rotational axis [mm],
 C_n centrifugal force [N][1]

After balancing in one level, momentum unbalance may remain. In momentum unbalance center of gravity is identical with rotational axis and two unbalances are rotated 180° degrees to each other (Fig.3). This caused vibrations characterized by swinging movement. In order to eliminate the unbalance it is necessary to use momentum with contradictory direction and balancing in two levels.

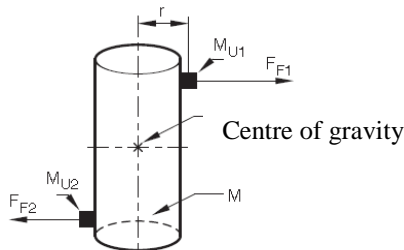


Fig.3. Balancing in two levels

M_{u1} , M_{u2} unbalance rate [gmm]; r distance of unbalanced mass from rotational axis [mm]; M weight of rotating mass [g]; e distance of gravity center of mass from rotational axis [mm], F_{F1} , F_{F2} centrifugal force [N]; $M_{u1} = M_{u2}$; $F_{F1} = F_{F2}$ [1]

Dynamic unbalance is caused by two unbalances with different angle position. Dynamic unbalance can be divided into static and moment unbalance.

3. EXPERIMENTAL

Experimental part is a plate made of aluminum according to standard EN6061 with dimensions 80 x80 10 mm divided into 3 areas, as is figured out in Fig.4. For experiments DMG Sauer Ultrasonic 20 linear machine tool was used and Seco JV 40 HEMI carbide monolith cutting tools with diameter 8mm. Both tools were clamped into shrink fit holders and the arrangement were balanced by Haimer Tool Dynamic 2009 with G levels according to Table 1.

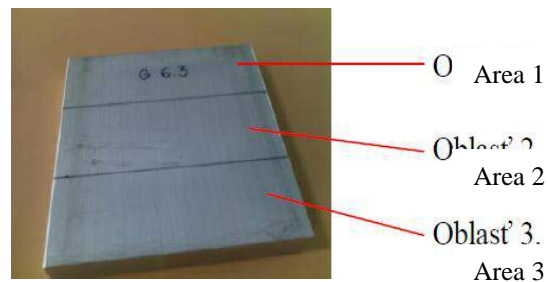


Fig.4. –Experimental part

3.1 Cutting conditions

Stability of cutting process was one of the most important conditions in cutting conditions setup. Feed f_z was considered as a constant and rotations were selected based upon balance level G and cutting parameters were obtained through analytical calculation (for cutting speed and feed). Selected values for feed velocity and rotations are in Table 2. According to selected cutting parameters and tool diameter, standard ISO 1940-1 were selected for tool balancing. At nowadays machine tools and tool shanks producers start using standard DIN 69888 especially for small diameters and weights of tools, where ISO 1940 -1 standard is not adequate.

Table 1. Cutting conditions

G 1,6		G 6,3	
Rotations (min^{-1})	Feed vf ($mm. min^{-1}$)	Rotations (min^{-1})	Feed vf ($mm. min^{-1}$)
18 000	2016	6 000	672
24 000	2688	12 000	1344
30 000	3360	18 000	2016
Cutting depth $ap = 0,5$ mm			

3.2 Experiment realization

Surface of experimental part were divided into three areas, where each of them were machined under different cutting conditions (different rotations and feed velocity) according to a Table 1 with a tool arrangement balanced to a G level of 1.6. The other side of a part was machined under different cutting conditions with tool arrangement balanced to a G level of 6.3. Surface quality of machined surface was analyzed by confocal microscope LSM 700

with ZEISS optics. Results are shown in Table 3; the cutting process is in Fig.5; the output from 3D microscope is shown in Fig. 6.



Fig.5. Cutting process on DMG Ultrasonic 20 linear machine tool with balanced tool arrangement by eccentric balancing rings on shrink fit tool holder with HSK 32 adaptor for high-speed milling.

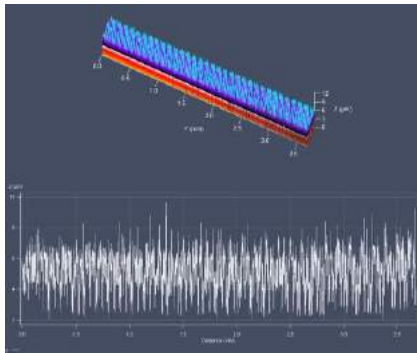


Fig.6. 3D profile map of milled surface with rotations of 18 000 min⁻¹

Table.2 Measured Ra values

Surface area		Ra [μm]
G1,6	Area 1. (18 000 min-1)	1,031
	Area 2. (24 000 min-1)	0,945
	Area 3. (30 000 min-1)	0,76
G6,3	Area 4. (6 000 min-1)	0,882
	Area 5. (12 000 min-1)	1,03
	Area 6. (18 000 min-1)	0,979

4. CONCLUSION

Based upon measured values, shown in Table 2 following charts (Chart 1, Chart 2.) were created for better imagination according to equations written below.

For both charts creation, method of ordinary least squares was used. The calculation for experiment with tool arrangement balanced to a G level of 6.3 is as following:

Table 3 Ordinary Least Squares input values for G 6,3

Meas. N.	zi [min-1]	xi	xi2	wi [μm]	yi	xi, yi
1.	6 000	3, 778	14, 273	0, 882	-0, 054	-0,204
2.	12 000	4, 079	16, 638	1, 031	0, 012	0, 048
3.	18 000	4, 255	18, 105	0, 979	-0, 009	-0, 038
$\Sigma n = 3$	$\Sigma zi = 36000$	$\Sigma xi = 12,11$	$\Sigma xi2 = 49, 016$		$\Sigma yi = -0,051$	$\Sigma xi \cdot yi = -0,194$

$$(\Sigma xi)^2 = 12, 1122 = 146, 7; xi = \log zi; yi = \log wi$$

Regression coefficients:

$$b_0 = \frac{\Sigma yi \cdot \Sigma xi2 - \Sigma xi \cdot \Sigma xi \cdot yi}{n \cdot \Sigma xi2 - (\Sigma xi)^2} =$$

$$\frac{-0,051 \cdot 49,016 - 12,112 \cdot (-0,194)}{3 \cdot 49,016 - 146,7} = -0,43.$$

$$b_1 = \frac{n \cdot \Sigma xi \cdot yi - \Sigma xi \cdot \Sigma yi}{n \cdot \Sigma xi2 - (\Sigma xi)^2} =$$

$$\frac{3 \cdot (-0,194) - 12,112 \cdot (-0,051)}{3 \cdot 49,016 - 146,7} = 0,101.$$

$$b_0 = \log c \rightarrow \begin{array}{ll} c = 10^{b_0} & w = c \cdot z^k \\ c = 10^{-0,43} & k = b_1 \\ c = 0,37 & k = 0,101 \end{array}$$

Then Ra calculation is as following:

$$w(Ra) = c \cdot z(n)^{0,101} \quad (4.1)$$

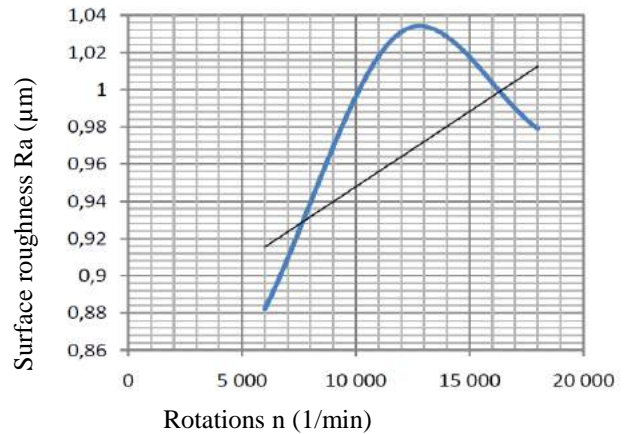


Chart 1 Surface roughness flow on a surface machined with tool balanced to a G level of 6,3

Chart 1 shows relation between surface roughness characterized by Ra and rotations where the G level of balanced tool was 6.3. The chart may be explained as following: surface roughness, represented by Ra was rising until the rotations reached approximately 13 000min⁻¹, since that we can see decreasing of roughness. This effect may be caused by the transformation of cutting conditions from conventional to high speed milling conditions. According to tool manufacturer's recommendations, rotations for selected tool should reach a value of 19890min⁻¹.

The calculation for experiment with tool arrangement balanced to a G level of 1.6 is as following:

Table 4 Ordinary Least squares input values for G 1.6

Meas. N.	zi [min-1]	xi	xi2	wi [μm]	yi	xi, yi
1.	18 000	4, 255	18, 105	1, 031	0, 013	0, 055
2.	24 000	4, 380	19, 184	0, 945	-0, 024	-0, 105
3.	30 000	4, 477	20, 043	0, 760	-0, 119	-0, 532
$\Sigma n = 3$	$\Sigma zi = 72 000$	$\Sigma xi = 13, 082$	$\Sigma xi2 = 57, 332$		$\Sigma yi = -0,13$	$\Sigma xi \cdot yi = -0,582$

$$(\Sigma xi)^2 = 13, 0822 = 171, 13; xi = \log zi; yi = \log wi$$

Regression coefficients:

$$b_0 = \frac{\sum y_i \cdot \sum x_i^2 - \sum x_i \cdot \sum x_i \cdot y_i}{n \cdot \sum x_i^2 - (\sum x_i)^2} = \frac{-0,13,57,332 - 13,082 \cdot (-0,582)}{3.57,332 - 171,13} = 0,18$$

$$b_1 = \frac{n \cdot \sum x_i \cdot y_i - \sum x_i \cdot \sum y_i}{n \cdot \sum x_i^2 - (\sum x_i)^2} = \frac{3 \cdot (-0,582) - 13,082 \cdot (-0,13)}{3.57,332 - 171,13} = -0,05$$

$$b_0 = \log c \rightarrow \begin{matrix} c = 10^{b_0} & w = c \cdot z^k \\ c = 10^{0,18} & k = b_1 \\ c = 1,51 & k = -0,05 \end{matrix}$$

Then Ra calculation is as following:

$$w(Ra) = c \cdot z(n)^{-0,05} \quad (4.2)$$

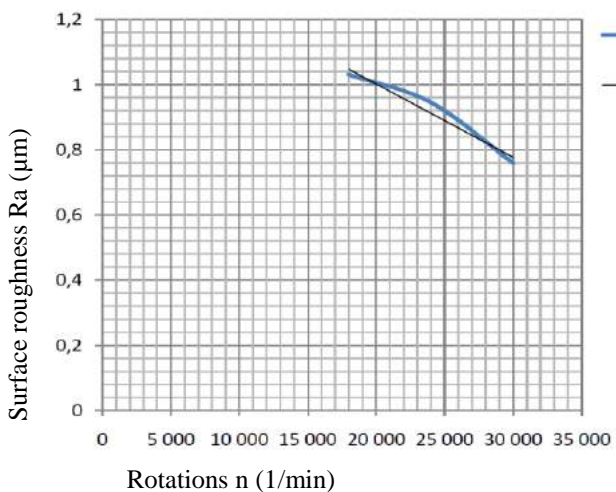


Chart 2 Surface roughness flow on a surface machined with tool balanced to a G level of 1,6

Chart 2 Shows surface roughness flow in High speed milling with tool balanced to a G level of 1.6. Explanation of chart is as following: decreasing of surface roughness is caused by cutting speed rising, where in high speed machining, cutting conditions are changing. In High speed machining various changes are raising especially heat transfer and chip removing, which caused surface roughness declination. Surface quality is one of the most important benefits of high-speed machining.

The influence of tool balancing is possible to evaluate according to a surface roughness characterized by Ra and its relation to rotations at level of 18 000. This rotation speed was used both for G level of 6.3 and G level of 1,6. From Charts 1 and 2 or Table 2 it is clear that better G level provided better surface quality, however the difference at this rotation speed level is not very high. We can assume that the difference of surface roughness will rise with rotation speed. According to a ISO 1940 -1

standard it is not possible to use tool arrangement with balance level G of 6.3 for higher rotational speed like it was used, it will produce high centrifugal and dynamic forces and may cause breakage of spindle bearings or the whole spindle. Due to we can only suppose that surface quality decreasing in relation with rotational speed raising is valid.

REFERENCES

- [1] Tool Dynamic, Manual Haimer Tool Dynamic 2009
- [2] Mickelson, D. *Guide to Hard Milling & High Speed Machining*. New York : Industrial Press Inc., 2007. s. 227. ISBN 978-0-8311-3319-1
- [3] Záhorec, O., Caban, S. *Dynamika*. Košice : OLYMP, 2002. s. 512. ISBN 80 - 7099 - 825 - 3
- [4] Marek, J., et al. *Konstrukce CNC obráběcích strojů*. Praha : MM publishing, 2010. s. 420. ISBN 978-254-7980-3
- [5] Kopešek, T., Vodička, J., Pahl, P., Herkner, V. 2005. *Fundamentals of high speed cutting – HSC*. Plzen: Západočeská univerzita v Plzni, 2005. S. 132. ISBN 80-7043-344-2
- [6] Erdel, B. 2003. *High speed machining*. USA: Society of Manufacturing Engineers, 2003. s. 177. ISBN 0-87263-649-6
- [7] Novák, M. 2011. *Vplyv vyváženia držiakov nástrojov na rezný proces*. Diploma thesis, MTF STU Trnava

Tento článok vznikol vďaka podpore v rámci OP výskum a vývoj pre projekt Centrum excelentnosti 5 -osového obrábania - experimentálna báza pre high - tech výskum, ITMS 26220120045, spolufinancovaný zo zdrojov Európskeho fondu regionálneho rozvoja.



Podporujeme výskumné aktivity na Slovensku / Projekt je spolufinancovaný zo zdrojov ES

This article has been realized under the research and development OP for project Centre of Excellence of Five axis Machining Experimental Base for High Tech Research ITMS 26220120045 co-financed by European Fund for Regional Development.



Supporting research activities in Slovakia/ Project is co-financed by European Community

FEM MODELING AND EXPERIMENTAL VERIFICATION OF CUTTING TOOL VIBRATIONS

Aco ANTIC, Milan ZELJKOVIC, Aleksandar ŽIVKOVIĆ

University of Novi Sad, Faculty of Technical Sciences, Trg dositeja Obradovica 6, 21000 Novi Sad, Serbia
antica@uns.ac.rs, milanz@uns.ac.rs, acoz@uns.ac.rs

Abstract: The paper presents a comparative survey of the oscillations calculated by utilizing the finite element method (FEM) and the measured vibrations of the cutting system elements during the machining operation. The analysis of the microscopic structure of the chip generated in the turning process is employed to determine the chip segmentation frequency and the agreement with the measured system vibrations. There presents a segment of research results concerned with the identification of the influence of the chip segmentation process during the turning process and the “free” segment of the vibration acceleration signal specter with the aim of creation and laboratory verification of the proposed method for recognizing tool wear condition in turning. The aim of the paper is to prove that there exists a dominant influence of the chip formation process in the high-frequency specter segment with the neglectable participation of the proper higher frequencies of the cutting system.

Key words: FEM modeling, tool wear, chip forming frequency

1. INTRODUCTION

The sources of vibrations appearing on a tool are of diverse origin, while their causes can be classified into deterministic and non-deterministic. Among the deterministic ones are: material deformation, friction of the tool and workpiece and chip separation. Their main feature is the inherent nonlinearity, having as a consequence the appearance of self-induced vibrations in the cutting process [1].

The increased loads lead to the pass over the material elastic point, which can be observed in the leap into the plastic deformation zone and material failure. In the process, the accumulated energy that appears impulsively each time the lamella shearing process occurs i.e. a chip is being formed, is released. This can be explained by the fact that in the material that has the crystal structure, the micro crack occurs during the crystal breakage and it rapidly moves creating the material failure i.e. breaking the inter-crystal connections and releasing the energy. These short-term individual events induce the elastic-viscous element structure of the workpiece system that generates vibrations in a wide frequency specter.

The friction on the contact areas between the tool and the workpiece creates the “stick-slip” effect. This effect introduces the aperiodic oscillatory induction into the workpiece system, which, same as in the case of the formation of chip segmentation can be observed as a set of discrete energy impulses inducing the elements of the workpiece system in the wide frequency specter as well.

2. CHIP SEGMENTATION

Segmented appearance of chip lamellas comprises of two phases in which the workpiece material is plastically

deformed in front of the tool causing the material convexas on the free chip surface. The result of the material deformation in the process of chip segmentation occurrence is composed of the moderately deformed chip segments separated by detached narrow band with the intensive material deformation. The described model of chip segmentation is presented in Figure 1 [2].

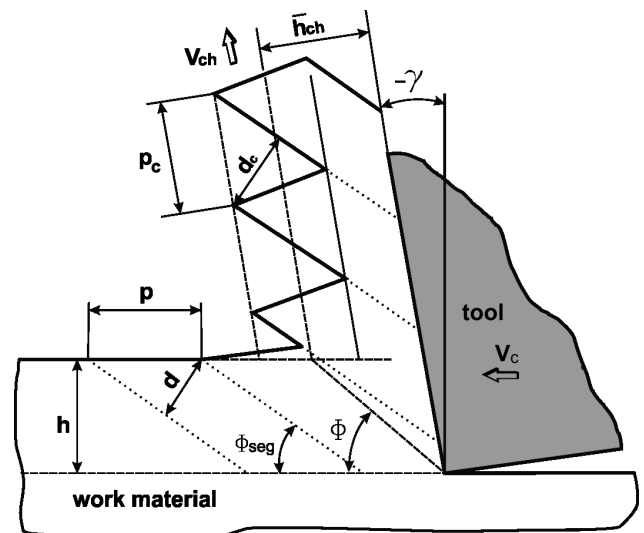


Fig. 1 Chip formation model [2]

One of the important induction mechanisms causing the vibrations in the machining process is the creation of chip lamellas. In their research, Cotterell and Byrne [3] have determined the frequency of the occurrence of a lamella f_{seg} by analyzing the video material with chip formation. The frequency of chip segmentation formation linearly increases with the increase of the cutting speed, and

decreases with the increase in depth. Chip frequency can occur in the range from 3.8 kHz to 250 kHz in hard material turning [4, 1], leading to great variations in the frequency of forces in a tool. The influence of chip segmentation onto the tool wear and processed surface quality has not yet been explained in detail, although it has been determined that it influences the intensity of force in the cutting process and the tool condition [5, 8]. Crater wear and wear band are the primary processes in tool wear with the cutting speed in the range between 80-800 m/min [6].

Lamella formation in the cutting process is characterized by their occurrence frequency. The frequency of chip segmentation formation can be calculated on the basis of the lamella formation steps p_c , cutting depth (thickness of the undeformed chip part) h , height of the deformed chip part h_{ch} and cutting speed v_c , applying the expression:

$$f_{lam} = \frac{v_{ch} \cdot h_{ch}}{h \cdot p_c} = \frac{v_{ch}}{\lambda \cdot p_c} \quad (1)$$

Based on the expression (1), one can observe that the increase of the thickness of the undeformed chip leads to the decrease in the lamella formation frequency which is directly observed in the decrease of the chip deformation coefficient [1].

$$f_{lam} = \frac{v_c \cdot f \cdot \sin \kappa}{h'_c \cdot p_c} \quad (2)$$

The relation 2 comprises parameters linked to the tool cutting geometry and technological parameters speed, feed and depth of cutting. On that basis, it can be concluded that the lamella formation frequency is directly proportional to the machining speed and feed, and indirectly proportional to the depth. The increase in the cutting speed directly influences the chip segmentation formation frequency, the increase in the energy that is reflected in the intensified heat release and the decrease in lamella steps; in a word, the overall wear dynamics is being increased. In the performed experimental research with the plate made of hard metal and the cutting speed range between 200 and 250 m/min, the frequencies of the chip segmentation were around 8 – 100 kHz. The area of the lamella formation frequencies, based on the mathematical calculations following the Bähre formula, approximates the measured frequencies of the tool holder oscillations, i.e. its natural frequencies, between 8.5 kHz and 88 kHz.

3. ANALYSIS OF GEOMETRICAL PARAMETERS OF FREQUENCY CHIP FORMATION

Most researches in material processing are directed towards the chip formation mechanism and tool wear characterization. Significant for the research in the tool wear effects and chip formation morphology are also cutting conditions. It has been observed that the alteration

in the tool wear degree and cutting conditions alters the shape of the occurring chip lamellas [6].

Tool wear, cutting process parameters and their influence on the chip appearance and shape have been monitored in the experimental research. The shape of the chip has been measured by a microscope depending on the tool wear degree, in diverse cutting conditions (cutting speed, feed and cutting depth). During the processing, the vibrations on the tool holder have also been measured, while the segmentation frequency has been calculated on the basis of the measured parameters for the chip cross section in an electronic microscope.

Figure 2 presents the morphology of the sawtooth chip with characteristic dimensions: lamella step (p_{sb}), height of the continual (compressed) chip part (h'_c), height of lamella shearing (d_c), shearing zone band (δ_{sb}), angle in the direction of the initial crack (Φ_{seg}) and angle of the free lamella part (ρ_{seg}) [5].

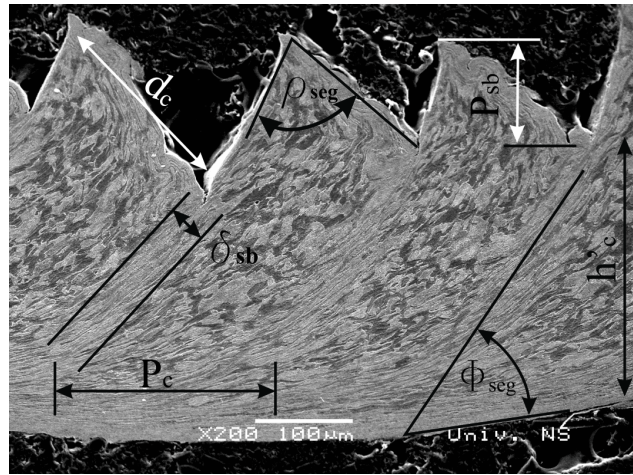


Fig. 2 Characteristic dimensions for calculating the chip formation frequency

Based on the processed results of the experimental research, the following conclusions can be drawn as a result of monitoring the chip morphology and tool wear condition:

- The medium value of the segmentation of the free chip part (lamella step) (p_c) and the height of the free part (tooth) (p_{bs}) are increased with the increase of tool wear.
- Segmentation step, distance between lamellas (p_c), increases with the cutting speed.
- Height of the continual chip part (h'_c) is greater with a new tool.
- Segmentation frequency increases with the increase in the cutting speed and decreases with the increase of tool wear degree.

The research in the chip segmentation formation contributes to determining chip segmentation formation mechanisms, as well as defining the most suitable processing technology. The crater increase on a front tool surface has a very significant influence on the chip segmentation formation mechanism, same as on the frequency of lamella formation and chip shape.

Crater wear directly influences the basic initial structure of chip segmentation formation that always tends to have

the character of a continual indefinite chip. Rear chip side in an extremely formed crater leads to the beginning of the occurrence of layers on the tool cutting edge.

4. MODELLING THE DYNAMIC TOOL BEHAVIOUR

4.1 Modeling tools using finite element method

Within the research, the dynamic behavior of a turning cutting tool has been analyzed by applying the FEM - finite element method, [8].

FEM model of cutting tool holder and tool insert had 5940 degrees of freedom (DOF) and it is formed as one two-part model. All DOFs for the support part of the handle have been removed, while the loads responding to cutting loads are set as parallel to the long axis of tool (Figure 3). Model is built by use of nine-node heterosis thick shell FE (from steel) and special link FE in connection between handle and cutting cutting tool (hard material) parts.

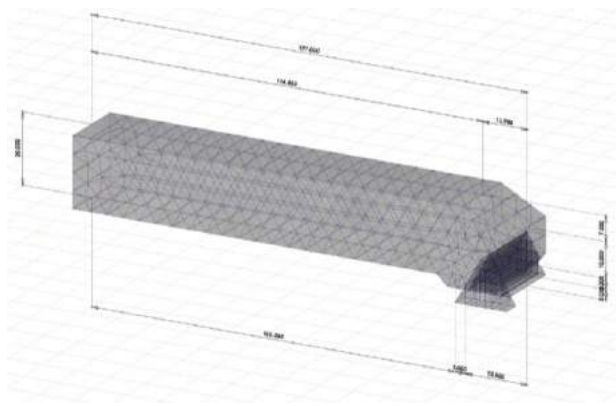


Fig. 3 FEM model of the cutting tool device

Analysis of the dynamic behavior of a turning cutting tool generates a very important a priori feeding set which can be utilized for building a neural-fuzzy system for the intelligent recognition of the tool wear condition [8]. The presence of the tool's natural frequencies in the upper part of the specter, in the concrete example over 10 kHz, presents a problem in monitoring the tool wear condition, since this is the part of the specter where the frequencies occurring in the process of the chip segmentation formation are also situated. In such a "deformed figure", the monitoring of the chip formation process by analyzing the adjoining frequency content will be significantly harder, if not even disabled. Presumptive information on the dynamic behavior of the tool can be utilized for separating the specter part that is not contaminated and whose monitoring can, with high precision, establish an unambiguous correlation between tool condition and tool vibration signal measured by an adequate sensor.

It is important to note that, due to the features of the tool carrier and other elements of the workpiece system linked to the mass, their influence on the dynamic behavior of the workpiece system measured on the tool holder is not critical. The frequencies of these elements are situated in the lower specter part which is significantly distant from the specter part where the frequencies generating the chip

formation process are situated. Hence, the dynamic behavior analysis of the mechanical structure of the workpiece system is limited only to the tool behavior analysis.

Vibration signals originating from the cutting process are difficult to be measure by direct methods, and they are technically and practically rather inaccessible for measuring in order to define the real influence. In the practical sense, what can be measured are the reactions of the overall system "tool-workpiece-machine" on the tool. In measuring, certain limitations occur in identifying and separating the induction mechanisms and transferring vibrations from other machine elements. It practically means that for certain processing operations only the phenomenological explanation is possible. Determining the precise content of the measured vibrations from the cutting process in the output sensor signal presents a very important task. Dominant influences of natural tool frequencies in the signal specter can be relatively precisely calculated by applying certain calculation methods.

The analysis of the dynamic behavior of the turning cutting tool holder, utilizing the finite element method, has an objective to determine natural frequencies and oscillation amplitudes of the cutting tool holder in the machining process. Furthermore, the analysis by finite element method enables the establishment of connections between experimental research and certain models in the machining process linked to tool wear and cutting geometry alteration.

The analysis of vibration signals tends to identify the difference between natural and self-induced tool vibrations during the cutting operation and the entire system vibrations.

4.2 Calculation of natural tool oscillation frequencies

The calculated natural frequencies of the cutting tool are presented by broken lines. Within the experimental research, apart from the turning cutting tool holder acceleration, the simultaneous measuring of the cutting forces has also been performed, and hence the turning cutting tool has been fixed to a dynamometer whose rigidity is lower than the tool carrier rigidity.

The turning has been done on the lathe „POTISJE Ada“, type PH 45.

The machining is done with combination of cutting speed and feed show in table 1. Combinations are selected in order to achieve progressive tool wear.

Table 1: Cutting parameters

Material:	42CrMo4, SRPS CR 10260 hardened to HRC30
Workpiece diameter:	100 mm
Cutting speed:	200 m/min
Feed:	0.25 mm/rev
Tool type:	„Sandvik Coromant" PTGNL tool holder cross-sect. 20x20
Insert coated with TiN:	TNMG 110408 PGP-415 P15, PP-CORUN

Vibration alternation is measured using the accelerometer

set up at the lateral tool side and oriented towards the longitudinal Workpiece axis.

Based on the presented results, one can observe that almost all natural frequencies of tool oscillation are situated in the upper domain of the frequency specter. This confirms the feasibility of the adopted approach in modeling and analyzing the dynamic tool behavior. In this case, significant approximations in setting the model have not reduced the dominant vibration effects in the machining process.

For calculating the characteristic oscillation amplitudes of the cutting tool holder, the method of harmonic analysis of oscillations has also been utilized. Harmonic analysis comprises the frequency range from 4 to 60 kHz. Figure 4 presents the amplitude frequency cutting tool characteristics in the direction of the axes X, Y and Z. The analysis of the obtained results can argue that the oscillation amplitudes in the directions of the axes Y and Z are of the same size order in the larger number of natural frequencies, while they are significantly smaller in the direction of X axis, even at the frequency 46.6 kHz which presents the largest frequency in the direction of this axis.

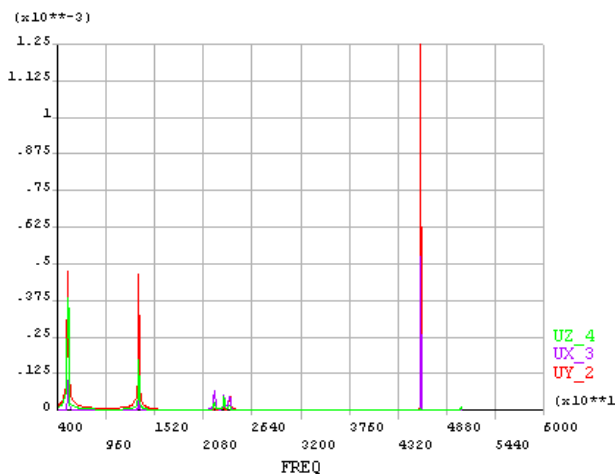


Fig. 4 Amplitude frequency characteristic of the cutting tool in the directions of X, Y and Z axes

The analysis of the experimental results and the results obtained by the calculation from the finite element method can be utilized to connect the oscillation modes on calculated and measured frequencies with the conditions of their occurrence:

1. At 14 kHz there is cutting tool oscillation in the directions of Y and Z axes where the largest amplitudes occur on the cutting tool top and they are around 30 to 35 [μm];
2. At 22.95 kHz the amplitudes of movement in the direction of the stated axes are around 10-20 [μm] and occur on the cutting tool holder (neck);
3. At other frequencies 23 and 42.5 kHz the maximal movement amplitudes also appear on the turning cutting tool neck.

The mentioned natural frequencies entirely cover the part of the frequency range in which there are dominant components of induction generated by discontinuities during the chip segmentation formation.

5. CONCLUSION

In the range between 10 and 50 kHz there are a larger number of the tool's natural frequencies, creating a space for the appearance of the resonance under the action of induced force generated by chip segmentation formation. The increase in the oscillation intensity induced by the tool resonance on a larger number of frequencies has a greater intensity and deforms the signal content occurring in the process of chip segmentation formation. Vibration output is variable, with distinctive peaks in individual frequencies overlapping with the chip segmentation frequency. The alteration in chip type stipulates the appearance of new frequency components (harmonics) which are close to lamella formation frequency, with the occasional appearance of self-induced vibrations in the moments when the tool is at the end of its life span.

ACKNOWLEDGEMENTS

This paper presents a segment of the research on the project "Contemporary approaches in the development of special solutions bearing in mechanical engineering and medical prosthetics", project number TR 35025. financed by the Ministry of Education and Science of the Republic of Serbia. University of Novi Sad, Faculty of Technical Sciences.

REFERENCES

- [1] Antić, A., Hodolić, J., Soković, M., (2006) *Development of a neural-network tool-wear monitoring system for a turning process*, Strojniški vjestnik - Journal of Mechanical Engineering, Vol. 52(11), pp 763-776
- [2] Gente, A., Hoffmeister, H.W., (2001) *Chip formation in machining Ti6Al4V at extremely high cutting speeds*, Journal Annals of the CIRP 50(1), pp 49-52.
- [3] Cotterell, M., Byrne, G., (2008) *Dynamics of chip formation during orthogonal cutting of titanium alloy Ti-6Al-4V*, CIRP Annals - Manufacturing Technology 57, pp 93-96.
- [4] Calamaz, M., Coupard, D., Girod, F., (2008) *A new material model for 2D numerical simulation of serrated chip formation when machining titanium alloy Ti-6Al-4V*, International Journal of Machine Tools & Manufacture 48, pp 275-288.
- [5] Morehead, M.D., Huang, Y., Luo, J., (2007) *Chip morphology characterization and modeling in machining hardened 52100 Steels*, Machining Science and Technology 11, pp 335-354.
- [6] Katuku, K., Koursaris, A., Sigalas, I., (2009) *Wear, cutting forces and chip characteristics when dry turning ASTM Grade 2 austempered ductile iron with PcBN cutting tools under finishing conditions*, Journal of Materials Processing Technology 209, pp 2412-2420.
- [7] Kovačević, D., (2006) *FEM Modelling in structural analysis* (in Serbian), Građevinska knjiga, Belgrade.
- [8] Antić, A., Zeljković, M., Klančnik, S., Živković, A., (2011) *Influence tool wear condition on cutting process and tool vibrations*, Machine Design, Vol. 3, No 4, pp 259-262.



PREDICTION OF MECHANICAL PROPERTIES AND MACHINABILITY OF CAST COPPER ALLOYS USING ANN APPROACH

Miloš MADIĆ, Goran RADENKOVIĆ, Miroslav RADOVANOVIĆ

Faculty of Mechanical Engineering of Niš, University of Niš, A. Medvedeva 14, Niš, Serbia
madic@masfak.ni.ac.rs, rgoran@masfak.ni.ac.rs, mirado@masfak.ni.ac.rs

Abstract: Artificial neural networks (ANNs) have been used in many application areas of engineering. Their flexibility and robustness enables them to model very complex relationships between large number of parameters with complex interdependencies. In this paper, an ANN approach is applied to predict the mechanical properties and machinability of Cu–Sn–Pb–Si–Ni–Fe–Zn–Al cast alloys. ANN having 8 neurons in input layer for representing alloy chemical composition (wt%), 4 neurons in hidden layer, and 3 output neurons for prediction of yield strength, ultimate tensile strength and machinability rating was developed. For evaluating the predictive performance of the proposed ANN model the statistical methods of mean absolute percentage error (MAPE) and correlation coefficient (R) are used. It has been shown that the proposed ANN architecture trained with 51 data patterns and tested on 12 unknown data patterns is capable of successful prediction.

Key words: Artificial neural network, mechanical properties, machinability, Cu–Sn–Pb–Si–Ni–Fe–Zn–Al cast alloys

1. INTRODUCTION

The mechanical properties of cast alloys mainly depend on the weight fractions of alloying elements, applied heat treatments, microstructures, morphologies of the various phases constituting [1]. Similarly, it has been widely reported that machinability of selected material, besides cutting conditions, depends on the chemical composition. Recently, the application of artificial intelligence (AI) methods for modeling complex relationships among a large number of variables, confirms the validity of these methods for developing predictive models in material science and engineering. The application of artificial neural network (ANN) for prediction of mechanical properties can be found in numerous sources including [1–3]. The prediction of machinability of steel using the genetic programming (GP) can be found in [4]. The aim of this paper is to predict both mechanical properties, namely, tensile strength and yield strength, and machinability of Cu–Sn–Pb–Si–Ni–Fe–Zn–Al cast copper alloys on the basis of the chemical composition (wt%) of alloying elements using the ANN approach.

2. ARTIFICIAL NEURAL NETWORKS

Artificial neural networks (ANNs) are massive parallel systems made up of numerous simple processing units called neurons that are linked with weighted connections. ANNs are characterized by their topology, weight vectors and biases, and activation functions that are used in hidden and output layers of the network [5]. Among various types of ANNs multi-layer perceptron (MLP) with back propagation (BP) training algorithm, is the most commonly used. The BP MLP is designed to operate

as a multilayer fully-connected feed-forward network, with a particular BP training algorithm for supervised learning [6].

The feed-forward ANN is composed of many interconnected neurons which are grouped into input, hidden, and output layer. The number of input neurons of the ANN is equal to the number of independent variables, while the number of output neurons is equal to the number of functions being approximated by the ANN. The number of hidden layers and the number of neurons in each of them is not defined in advance. The number of hidden neurons can change during the ANN training until the optimum topology is defined, namely, the one that produces the best performances of ANN [6].

In a feed-forward architecture, information flows only in the forward direction, i.e. from input to output neurons. Each neuron in the ANN is interconnected with all neurons in the preceding and following layers. There are no interconnections within neurons of the same layer. The input neurons are used to introduce the data in the ANN. Through neurons interconnections each input data is processed with weights to be used in the hidden layer. The j -th hidden neuron receives an activation signal which is the weighted sum from the neurons in input layer:

$$h_j = \sum_i w_{ji} \cdot x_i + b_j \quad (1)$$

where w_{ji} is input to hidden units weights, and b_j biases (thresholds) of hidden neurons. This sum is then passed through an activation (transfer) function (f) to produce the neurons output (H_j). The activation function introduces a degree of nonlinearity. Transfer function in hidden layer

is most commonly sigmoid function whose general form is:

$$H_j = f(h_j) = \frac{1}{1 + e^{-h_j}} \quad (2)$$

Finally, the output neurons receive the following signals from the hidden neurons:

$$y_k = \sum_j w_{kj} \cdot H_j + b_k \quad (3)$$

where w_{kj} is the weight of the connection between hidden and output neurons, and b_k biases of output neurons. These activation signals can be transformed again, using the sigmoid transfer function to give the outputs of the ANN. However, for prediction, it is sufficient to use linear activation function (identity) for output neurons.

Once the ANN architecture is developed, the ANN must be trained in order to learn the relationships between inputs and output(s).

Before the ANN training, all the weights and biases must be initialized. The selection of initial weights is very important in ANN training. There are a number of method for weights initialization but it is typical to set weights and biases to small random numbers (e.g., between -0.5 and 0.5 or between -1 and 1). Weights initialization according to Nguyen-Widrow method is also one of the most popular methods and this is the default initialisation method for the feed-forward ANNs that are created through the ANN toolbox of the MATLAB software package.

In order to improve the converge speed, the input and output data should usually be normalized (scaled). The normalization range depends largely on the activation function. Normalizing to [-1,1] for the hyperbolic tangent transfer function and to [0,1] for the sigmoid transfer function is often applied.

3. ANN PREDICTIVE MODEL FOR MECHANICAL PROPERTIES AND MACHINABILITY

3.1. Data collection

Chemical compositions, mechanical properties and machinability ratings of cast copper alloys were collected from related standards, ASM Hand books [7], [8], and [9]. Cast copper alloys are classified into alloy groups according to chemical composition [8]. In the present study 63 data was collected for Cu–Sn–Pb–Si–Ni–Fe–Zn–Al cast alloys.

Although the properties of copper materials are mainly determined by the composition of the alloy, categorizing materials according composition to their machinability is unsuitable, because alloys in the same alloy group often exhibit different machinability properties [9]. However, ANNs have proven to be a very powerful tool in data mining. In order to provide practitioners with a basic overview of the machinability of the copper alloys, a machinability rating was proposed in the literature [7], [8]. The machinability rating of copper alloys goes from 20 (hard to machine) to 100 (excellent machinability), with step 10. According to [9] copper and copper alloys are classified into three main machinability groups:

1. Machinability group I, with $70 < \text{machinability rating} < 100$,
2. Machinability group II, with $40 < \text{machinability rating} < 60$,
3. Machinability group III, with $20 < \text{machinability rating} < 30$.

3.2. ANN model development

The ANN model was aimed to predict the mechanical properties (yield and tensile strength) and to classify the alloys to above-mentioned machinability groups by predicting the machinability ratings. The ANN model has eight input neurons for representing Cu–Sn–Pb–Si–Ni–Fe–Zn–Al (wt%) contents and three output neurons for prediction of yield strength, tensile strength, and machinability rating. In developing an ANN model, the available data set is divided into two sets, one to be used for training of the ANN model, and the remaining is to be used to verify the generalization capability of the ANN model. Therefore, 51 data patterns were used for ANN model training, and 12 data patterns for ANN model testing. The selection of training and testing data was done by random method. The upper limit of number of hidden neurons was determined knowing that the number of weights doesn't exceed the number of data for training. Though the ANN can still be trained, the case is mathematically undetermined [10]. For 51 training data patterns available, eight inputs and three outputs, the maximum allowed number of hidden neurons is four. Hence, the architecture of ANN model becomes 8-4-3 as shown in Figure 1.

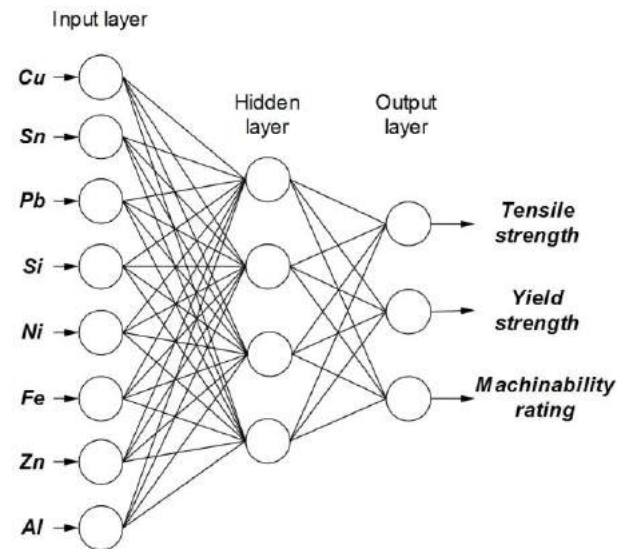


Fig.1. ANN model proposed in present study

Linear transfer function and hyperbolic tangent transfer function were used in the output and hidden layer, respectively. In order to stabilize and enhance ANN training the whole data was normalized between 0.1 and 0.9 using the following equation:

$$x_{norm} = 0.8 \cdot \frac{(x_i - x_{min})}{(x_{max} - x_{min})} + 0.1 \quad (4)$$

where x_{norm} and x_i represent the normalized and original (raw) data, and x_{min} and x_{max} are minimum and maximum values of the raw data.

Prior to ANN training, the initial values of weights were set according to Nguyen-Widrow method.

The MATLAB's Neural Network Toolbox software package was used for training and testing the ANN model. BP algorithm with adaptive learning rate and momentum, "traingdx", was used for ANN training. The ANN's performance during training was measured according to the mean of squared error (MSE), Figure 2. The training was stopped after 50000 iterations since no further improvement in ANN performance was achieved.

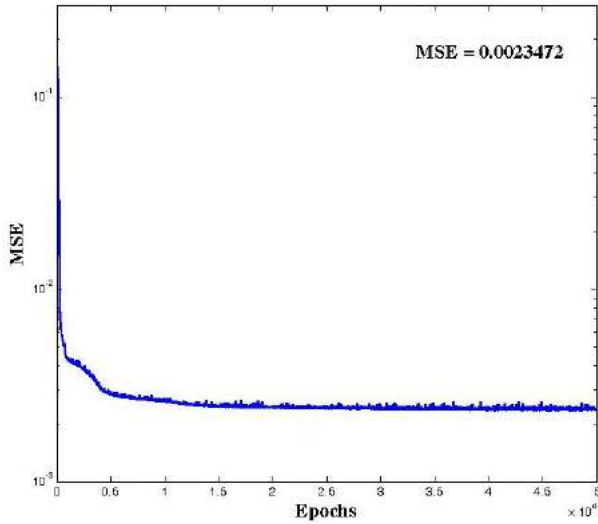


Fig.2. ANN performance during training

3.3. Statistical evaluation of ANN model

In order to estimate the generalization ability of the developed ANN model, the test data set is used. Before estimating the performance of the ANN model all the ANN outputs were denormalized using the equation:

$$x_{denorm} = \frac{(o_i - 0.1) \cdot (x_{max} - x_{min})}{0.8} + x_{min} \quad (5)$$

where o_i is the i -th predicted value by ANN model.

Statistical methods were used to compare the results predicted by the ANN model on both testing and entire data (training+testing). In addition to the correlation coefficient (R), the statistical method of mean absolute percent error (MAPE) has been used for estimating the prediction errors. These values are mathematically defined by the following equation:

$$R = \frac{\sum_{i=1}^N (t_i - \bar{t}) \cdot (p_i - \bar{p})}{\sqrt{\sum_{i=1}^N (t_i - \bar{t})^2} \cdot \sqrt{\sum_{i=1}^N (p_i - \bar{p})^2}} \quad (6)$$

$$MAPE = \frac{1}{N} \cdot \sum_{i=1}^N \left| \frac{t_i - p_i}{t_i} \right| \cdot 100\% \quad (7)$$

where: t is the i -th target value, p is the i -th predicted value where the bars indicate mean values, and N is the number of data. A comparison of the target and predicted yield strength, tensile strength and machinability rating, are presented in Figs. 3 and 4.

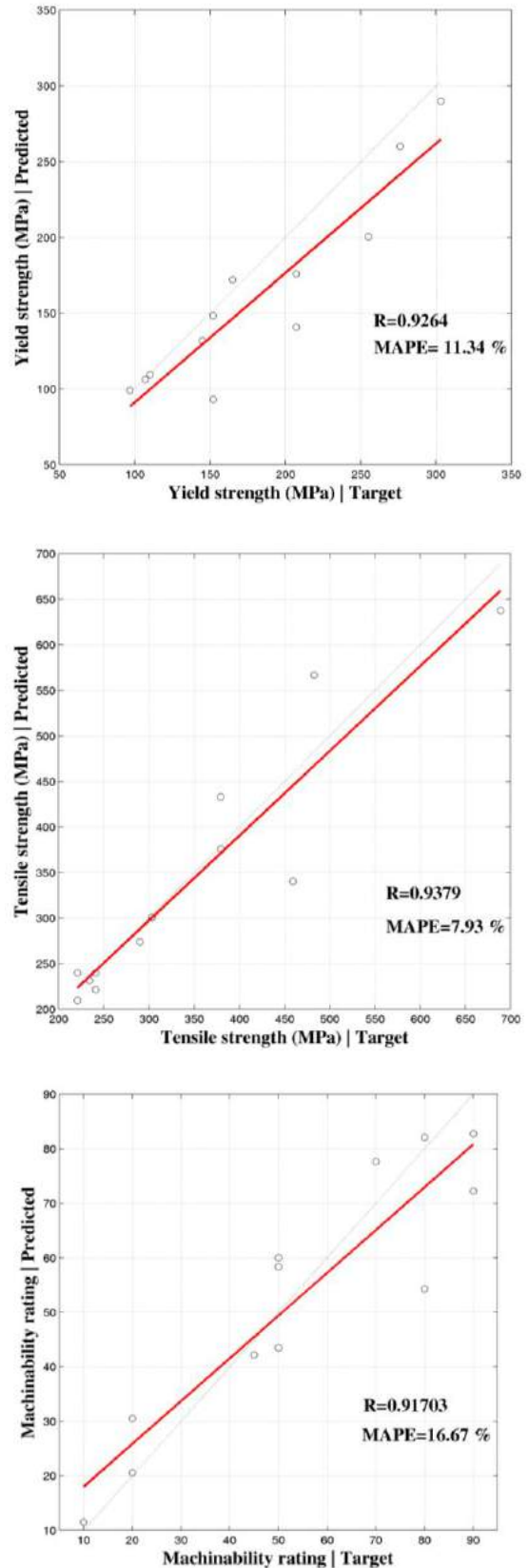


Fig.3. Comparison of target and predicted for testing data

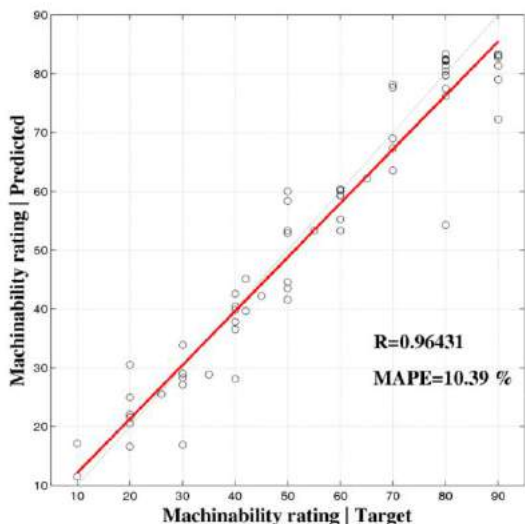
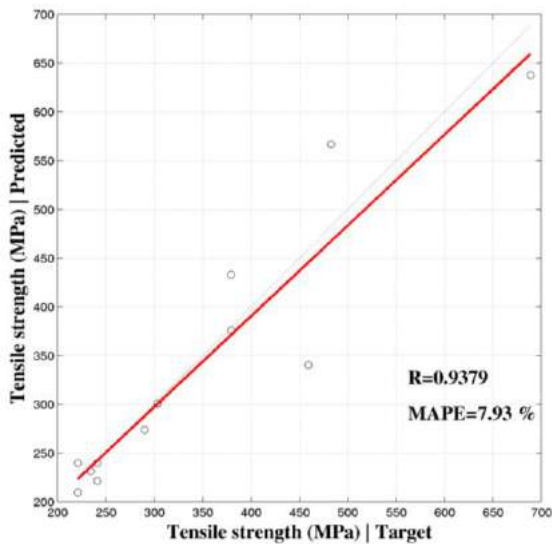
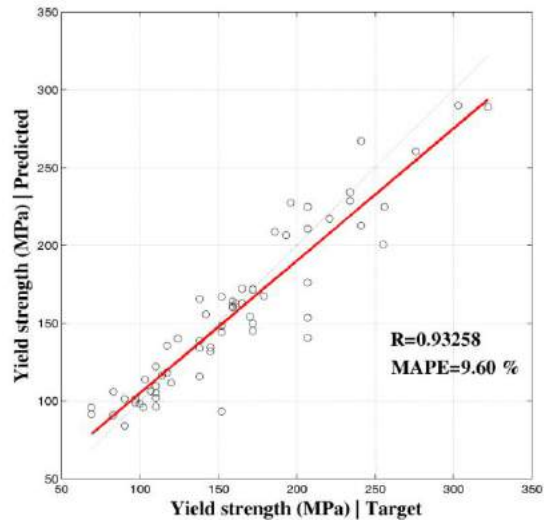


Fig.4. Comparison of target and predicted for entire data

From Figs. 3 and 4 it is evident 8-4-3 ANN model trained on 51 data patterns is capable of successful prediction of yield strength, tensile strength and machinability.

4. CONCLUSION

In this paper, an ANN approach has been used to predict the mechanical properties (namely, yield strength and tensile strength) and machinability as a function of chemical composition of Cu–Sn–Pb–Si–Ni–Fe–Zn–Al cast alloys. It has been shown that ANN having 8-4-3 architecture trained with BP algorithm is capable to accurately predict multiple characteristics. High values of R and MAPE around and below 10 % confirm the validity of the developed ANN model.

Further improvement of the ANN model can be achieved by using more data patterns which would enable using additional hidden neurons, i.e. developing ANN model with more expressive power. Similarly, one would expect improved results by developing the ANN models for each output characteristic separately.

Also it would be advantageous to develop ANN model for prediction of machinability which would include as ANN inputs, in addition to chemical composition, mechanical properties of the alloy.

REFERENCES

- [1] OZERDEM, M.S., KOLUKISA, S. (2009) *Artificial neural network approach to predict the mechanical properties of Cu–Sn–Pb–Zn–Ni cast alloys*, Materials and Design, Vol.30, No 3, pp. 764-769
- [2] JANČIKOVÁ, Z., ROUBÍČEK, V., JUCHELKOVA, D. (2008) *Application of artificial intelligence methods for prediction of steel mechanical properties*, Metalurgija, Vol.47, No 4, pp. 339-342
- [3] DOBRZANSKI, L.A., KROL, M. (2009) *Application of neural network for Mg-Al-Zn mechanical properties modelling*, Journal of Achievements in Materials and Manufacturing Engineering, Vol.37, No 2, pp. 549-555
- [4] BREZOČNIK, M., KOVAČIČ, M., PŠENIČNIK, M. (2006) *Prediction of steel machinability by genetic programming*, Journal of Achievements in Materials and Manufacturing Engineering, Vol.16, No 1-2, pp. 107-113
- [5] RADOVANOVIĆ, M., MADIĆ, M. (2010) *Methodology of neural network based modeling of machining processes*, International Journal of Modern Manufacturing Technologies, Vol.II, No 2, pp 77 -82
- [6] MADIĆ, M., MARINKOVIĆ, V. (2010) *Assessing the sensitivity of the artificial neural network to experimental noise: a case study*, FME Transactions, Vol.38, No 4, pp 189-195
- [7] SCHMIDT, R., SCHMIDT, D., SAHOO, M. (1988) *Copper and Copper Alloys*, ASM Handbook: volume 15, ASM International.
- [8] TYLER, D., BLACK, W. (1990) *Introduction to Copper and Copper Alloys*, ASM Handbook: volume 2, ASM International.
- [9] *Recommended Machining Parameters For Copper And Copper Alloys*, Deutsches Kupferinstitut, (2010)
- [10] SHA, W. EDWARDS K. L. (2007) *The use of artificial neural networks in materials science based research*, Materials and design, Vol.28, No 6, pp 1747–1752

34th INTERNATIONAL CONFERENCE ON PRODUCTION ENGINEERING



SECTION B

SURFACE ENGINEERING AND NANOTECHNOLOGIES



RESEARCH ON CAVITATION EROSION BEHAVIOR OF STAINLESS STEELS WITH CONSTANT CHROMIUM AND VARIABLE NICKEL CONTENT

Iliare BORDEASU, Mircea Octavian POPOVICIU, Ion MITELEA, Alin Dan JURCHELA
Politehnica University of Timisoara, Bvd. Mihai Viteazul, no.1, Timisoara, Romania
ilarica59@gmail.com, mpopoviciu@gmail.com, ionel.mitelea@yahoo.com, alindantm@yahoo.com

Abstract: Paper analyses the cavitation erosion behavior of four stainless steels used for details heavy subjected to cavitation, such as hydraulic turbine runners and pump impellers. Those steels have the same chromium content (12%) and variable nickel content (2...8%). According with the tendencies to reduce the carbon content under 1%, this element was maintained at 0.036%. The experimental researches undertaken in the Cavitation Laboratory of the Timisoara Polytechnic University used a vibratory facility and respected the conditions of the ASTM G32-2006 Standard. The steel behavior was evaluated both on the ground of microstructure erosion (through optic and electronic microscopy) and by comparisons with other reference steels. One of them, symbolized OH12NDL was used in Romania and other countries for manufacturing turbine blades and assured over 20 years of good running, with normal repair works.

Key words: stainless steel, cavitation erosion, microstructure, characteristic curves, maximum depth of erosion

1. INTRODUCTION

The damages produced by cavitation, especially to the turbine runners, pump impellers and ship propellers, determined the researchers to analyze the erosion causes and to establish the materials that can give the best resistance to this erosion. Although multiple researches were carried out [2], [3], the best solution was not found till now because cavitation is a complex physical phenomenon. So, important damages continue to take place in our days. That is way, the researchers analyses damaged structures produced in laboratory conditions [4], [5] and look for models to estimate the cavitation resistance [3]. Toward this purpose were directed also the researches presented in this paper and obtained in the Cavitation Laboratory of Timisoara Polytechnic University, using stainless steels with the same content of chromium (12%) and variable content of nickel. These steels were chosen similar to those used for refurbishing some Romanian power plants. The studies put into evidence similarities and differences for steels with various microstructures and found new elements for the evaluation of cavitation erosion behavior on the ground of the rate "Equivalent Chromium/Equivalent Nickel" which permits to establish the types of the microstructure with the Schöffler diagram [2].

2. RESEARCHED MATERIALS

The researched steels were obtained as 300 g stocks in a multiple chamber melting furnace, with an EMO 80 electronic beam for melting, alloying and casting in vacuum, equipped with an electron gun having a power of 80 kW (producer Electric Factory for Locomotives

Building "HANS BEIMLER", Henningsdorf, Germany) possessed by GIROM Giurgiu. The effective realized chemical composition, shown in Table 1, was determined using an optical emission spectrometer with sparks, of the type "Foundry Master" produced by the German Firm WAS at the Laboratory for Optic and Fluorescent X Ray Emission Spectrometry (LISEOFRX) of the Center for Special Materials (Bucharest Polytechnic University).

Table 1 Chemical Composition

Chemical Element	Symbol stainless steel			
	12/2	12/4	12/6	12/8
	% Chemical Element			
C	0.036	0.036	0.036	0.036
Si	0.642	0.510	0.461	0.696
Mn	0.204	0.271	0.028	0.427
Cr	11.957	11.840	12.059	12.206
Ni	1.97	4.009	5.597	7.847
Mo	0.036	0.029	0.039	0.041
Nb	0.010	0.012	0.009	0.018
Al	0.062	0.073	0.064	0.044
Co	0.000	0.010	0.002	0.035
Ti	0.080	0.149	0.073	0.024
V	0.011	0.013	0.009	0.010
W	0.083	0.076	0.153	0.146
Al	0.062	0.073	0.064	0.044
Cu	0.046	0.075	0.077	0.09
P	0.007	0.007	0.007	0.009
S	0.013	0.015	0.012	0.020

Fe-rest

The heat treatment of the steels was done with the help of a UTTIS furnace at Bucharest Polytechnic University. They consisted in a process annealing followed by quenching in water from 1050 °C.

Taking into account the equivalent coefficients of chromium (Cr)_e and nickel (Ni)_e obtained with the relations (1) and using the Schöffler diagram the microstructure constitution was determined. In Table 2 are listed the approximate proportions of constituents.

$$(Cr)_e = \%Cr + 1.5x\%Si + \%Mo + 0.5x\%(Ta+Nb) + 2x\%Ti + \%W + \%V + \%Al$$

$$(Ni)_e = \%Ni + 3x\%C + 0.5x\%Mn + 0.5x\%Co$$

(1)

Table 2 Prediction of the microstructure constitution in conformity with the Schöffler diagram

Steel (Cr/Ni)	(Cr) _e	(Ni) _e	≅ M %	≅ A %	≅ F %
12/2	13,272	3,152	55	-	45
12/4	13,1	5,23	86	-	14
12/6	13,166	6,692	100	-	-
12/8	13,548	9,158	90	10	-

M-Martensite, A-Austenite, F-Ferrite

Finally, the microstructure analyze of the steels was done with a Reichert metallographic microscope and is presented in Figure 1. The analyzed microstructure is in agreement with the data established using the Schöffler diagram, the steels presenting characteristics structures for the casting procedure, with coarse grains. The steels with controlled chromium (12%) have martensite as major constituent (steel 12/6) at which is added either ferrite (in equal proportion for the steel 12/2 or only 14% for the steel 12/4) or austenite (with insular arrangement for the steel 12/8).

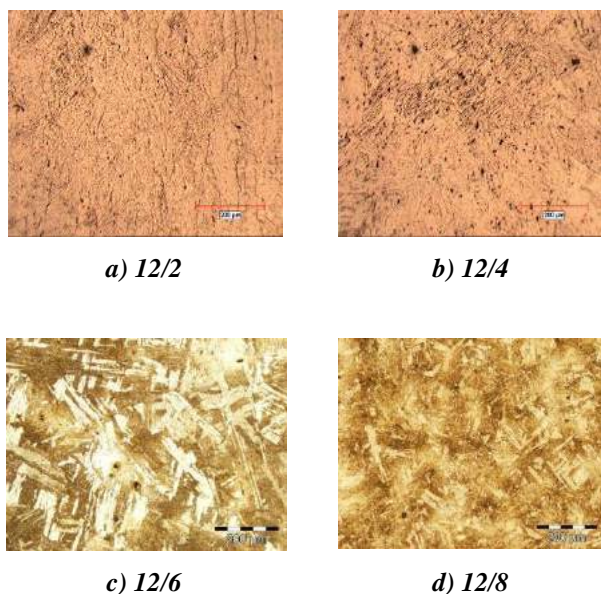


Fig. 1 Microstructure aspect of the used stainless steels (attack with acid nitromuratic with glycerin, x100)

3. TEST FACILITY AND PROCEDURE

The cavitation erosion tests were performed using the vibratory device presented in Figure 2, realized by taking into account the ASTM G32 Standard [7]. The device parameters are: power 500 W; vibration frequency 20 kHz; double amplitude of vibrations 50 μm; specimen diameter 15.8 mm; supply voltage 220V/50Hz; vibratory specimen type. The working agent was double distilled water, having a constant temperature of 23±1°C. In conformity with the procedure of our laboratory, the total test exposure was 165 minutes, divided in 12 periods (one of 5 minutes, one of 10 minutes and 10 of 15 minutes [6]. At the beginning and the end of each period each specimen was washed successively with tap water, double distilled water, alcohol and acetone and afterward weighted.

During the inter-test periods the specimens were maintained in desiccators to avoid any influence of the environment upon the specimen surface.

From each material were tested three specimens. After the erosion tests there were analyzed two surfaces situated in perpendicular planes. The first was the surfaces exposed to cavitation attack. The second was obtained by cutting the specimen and was necessary to determine the maximum penetration depth and the state of material under the eroded area. In order to establish the structural characteristics the analyzes were accomplished by: the optic stereomicroscope OLYMPUS SZX 7 equipped with the program quickMicrophoto 2.2 for image processing; the REICHERT Univar metallographic microscope with an automatic table and a video camera with adaptor and a system for image acquisition; and the scanning electronic microscope XL-30-ESEM TMP.



Fig. 2 T2 standard vibratory device

4. EXPERIMENTAL RESULTS

Relaying on the mass losses recorded at the end of each testing period there were realized the time dependence of the cumulate mass losses as well as the erosion velocities, Fig. 3a and 3b. The values of mass losses and erosion velocities presented in diagrams are the averages obtained from the three specimens tested for each material. In order to evaluate the behavior of the tested steels in the diagrams are presented also the results for the OH12NDL

steel, used in the past, for manufacturing numerous hydraulic turbines runners.

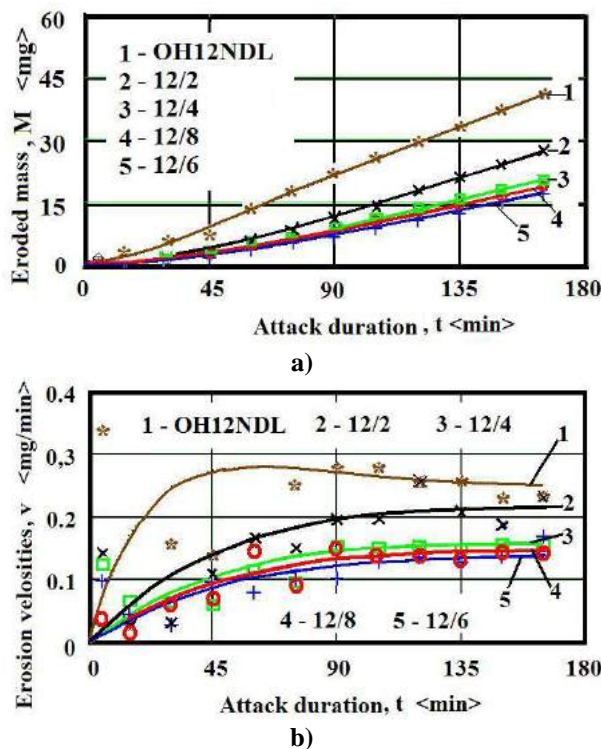


Fig. 3 Cavitation erosion characteristic curves for steels with constant chromium
 a) Cumulative mass losses against time,
 b) Erosion rate against time
 (Steel symbols represent chromium concentration over nickel concentration)

The cavitation erosion evolution and the comparisons of the specific structural aspects for different microstructure constituents was put into evidence both at the macrostructure level with the stereomicroscope and for the microstructure level accomplished with the metallographic optic microscope as well as the scanning electronic microscope. The macrostructure analyze on the surface subjected to cavitation realized with the stereomicroscope is presented in the Figure 4. The eroded surfaces, regardless of the structure, have an irregular outline and the eroded area (P) occupies between 83.1% (for the steel 12/6) and 88.75% (for the steel 12/4) from the whole area subjected to cavitation. The maximum penetration depth (DP_{max}), determined after cutting the specimens has values between 116.8 μm (for the steel 12/4) and 267,40 μm (for the steel 12/2), as can be seen in Figure 5.

In the cut section there were put into evidence, the damages suffered by the metal in the hardened zone, damages produced by the repetitive actions of the imploding bubbles [1, 5, 6] as can be seen from Figure 6.

5. RESULTS ANNALYSE. DISCUSIONS

In comparison with the OH12NDL martensitic steel (0.1 %C, 12.8 %Cr, 1.25 %Ni; 88% martensite, 12% ferrite) [2] all the studied steels have better cavitation erosion resistance.

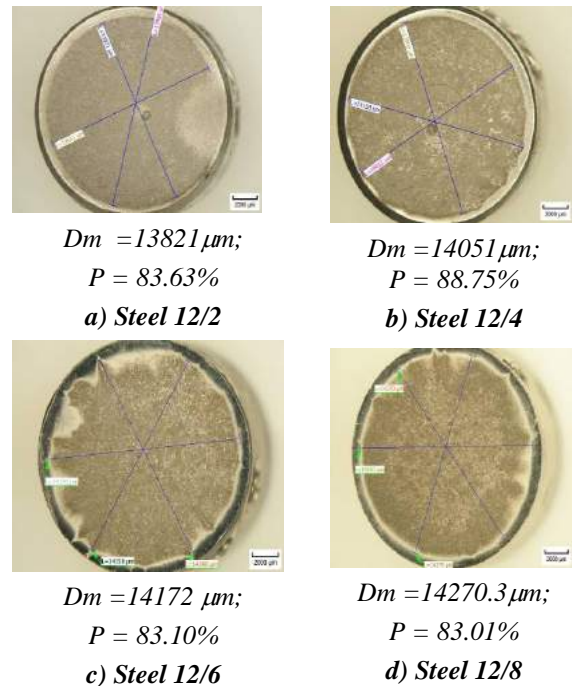


Fig. 4 Stereo microstructure of specimens and measurements of the eroded area (x8)

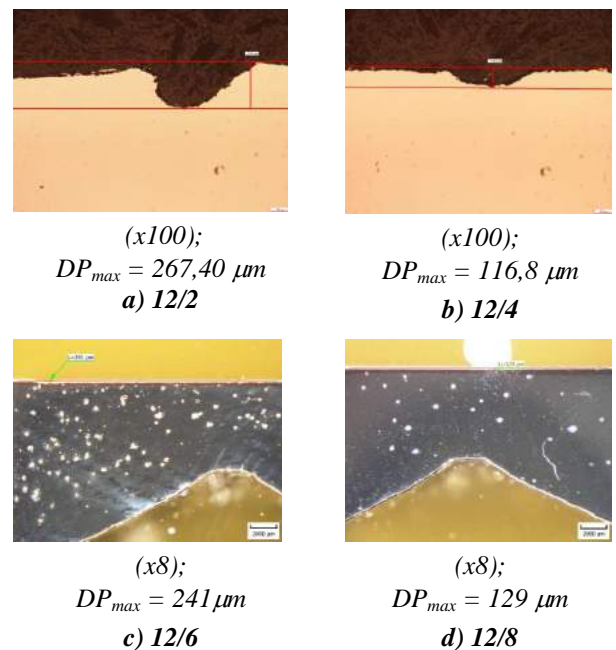


Fig. 5 Erosion maximum penetration depth (images at the stereomicroscope)

From the Figures 3 it can be seen that the steels 12/4, 12/6 and 12/8 have similar behavior at cavitation erosion although the microstructure (see Table 2) is a little dissimilar (different proportions of martensite and ferrite) but with the martensite as the main structure constituent. The scatter of the measured points (Figures 3b) is the result of the coarse grains obtained through the casting and entirely expelled during the cavitation attack. This conclusion is sustained also by the images in Figures 5 (maximum penetration depth) and 6 (aspects of microstructure damages).

Comparing the values of maximum erosion depth given in Figure 5 with the characteristic curves shown in Figure 3 we can see substantial discrepancies. While the parameters of the vibrating device were the same for all the tests, we appreciate that the depth depends in great measure on some local conditions, such as the expelled grain dimension. Consequently, we believe that the maximum penetration depth is not an adequate method to compare the material resistance. Eventually, it can be used to appreciate the cavitation behavior for different manufacturing procedures. This conclusion is sustained by the incongruities between this value and the evolution of lost masses (Figures 3a) as well as the evolution of the erosion velocities (Figures 3b). On the contrary, the experience accumulated in our laboratory during forty years of researches in the domain lead us to the conclusion that the mean penetration erosion is an adequate parameter for comparisons of the cavitation erosion for various materials.

In the images presented in Figure 6 it can be seen a narrow zone in which appear local deformations. This situation is the effect of the phenomena created by the implosion of bubbles [2], [3]. A more careful examination shows that this hardened zone is greater for the steels with austenitic structure (12/8).

Examinations by electronic microscopy put into evidence the following aspects of the microstructure damages, see Fig.6.

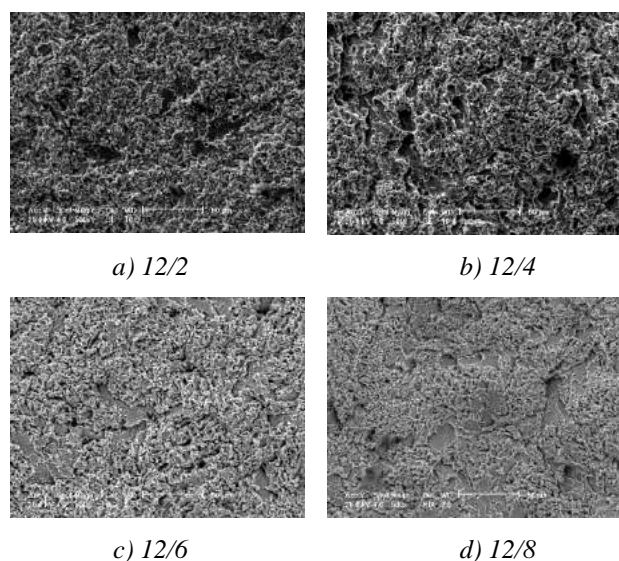


Fig. 6 SEM image of the specimen after cavitation (x500)
a) Inter grain fragile cracks produced by cavitation; caverns with inter grain propagation, dimensions 2-8 μm .
b) Cleavage fracture with fragile aspect, with inter grain propagation; caverns disposed between grain with great dimensions (10-15 μm) alternating with small caverns;
c) Combinations of caverns 1...5 μm and cleavage cracks with fine inter grain cracks;
d) Minute caverns and non-metallic inclusions; mixture of caverns and cleavages and evident fine inter grain cracks

6. CONCLUSIONS

1. The tested steel present good and very good behaviors to cavitation erosion, better than the reference steel OH12NDL. The cavitation affected area represents $\cong 83\%$ till $\cong 88\%$ from the exposed surface and the maximum penetration depth varies between 116.8 μm and 267.4 μm .
2. All the four steels can be used for manufacturing or repair works of the pieces heavy affected by cavitation.
3. Studies upon steels with controlled contents of chromium and variable nickel offer the possibilities to put into evidence the correlation of cavitation erosion resistance with the steel structure.
4. Our opinion is that the use of the maximum depth penetration, measured for the final testing period (see Figure 5), being dependent on the dimension of the expelled grains, does not represent a suitable parameter to compare materials. This statement is sustained by the incongruity between the maximum depth and the evolution of material losses or erosion velocities (see Figures 3). Eventually it can be used to appreciate some manufacturing procedures. If necessary we recommend the use of mean depth erosion, computed for the final eroded volume.

Acknowledgments

The present work has been supported from the National University Research Council Grant (CNCSIS) PNII, ID 34/77/2007 (Models Development for the Evaluation of Materials Behavior to Cavitation)

REFERENCES

- [1] BORDEASU, I., POPOVICIU, M. O., BALASOIU, V., JURCHELA, A. D., KARABENCIOV, A. (2010) *Influence of the Vibratory Test Facility Type and Parameters upon the Cavitation Erosion Evolution*, 25th IAHR Symposium on Hydraulic Machinery and Systems, Timisoara, Romania, vol. 121, pp. 282-290
- [2] BORDEAȘU, I. (2006) *Eroziunea cavitațională a materialelor*, Editura Politehnica, (2006)
- [3] FRANC, J.P., MICHEL, J.M. (2004) *Fundamentals of Cavitation*, Kluwer Academic Publishers, P.O.Box, 322, 3300 AH Dordrecht, The Netherlands
- [4] HEATHCOCK, C.J., PROTHEROE, B.E., BALL, A. (1982) *Cavitation erosion of stainless steels*, Wear, Volume 81, Issue 2, 1 October (1982), pp. 311-327
- [5] HATTORI, S., Ishikura, R. (2010) *Revision of cavitation erosion database and analysis of stainless steel* Wear, Volume 268, Issues 1-2, pp. 109-116
- [6] POPOVICIU, M. O., BORDEASU, I. (1998) *Considerations Regarding the Total Duration of Vibratory Cavitation Erosion Test*, Third International Symposium on Cavitation, Grenoble, France pp.221-226
- [7] *** Standard Test Method for Cavitation Erosion Using Vibratory Apparatus ASTM G-32-08



INFLUENCE OF SUBSTRATE ROUGHNESS ON ADHESION STRENGTH OF HARD TiN FILMS

Damir KAKAŠ, Branko ŠKORIĆ, Aleksandar MILETIĆ, Pal TEREK, Lazar KOVAČEVIĆ, Marko VILOTIĆ
Faculty of Technical Sciences, University of Novi Sad, Trg D. Obradovica 6, Novi Sad, Serbia
kakasdam@uns.ac.rs, miletic@uns.ac.rs

Abstract: Ion beam assisted deposition was used to prepare hard TiN coatings. In order to provide appropriate adhesion of TiN film, a titanium nano-interfacial layer was introduced between coating and base material. The interfacial layer was produced by ion beam mixing of titanium atoms with atoms of steel substrate. The influence of substrate surface roughness on adhesion properties of TiN coatings was studied in this research.

Adhesive strength of the coatings was characterized by commonly used scratch test technique. Coating adhesion and toughness were evaluated qualitatively by HRC adhesion test. Optical microscopy was implemented in order to examine channels generated during scratch test. Atomic force microscopy was employed to determine sample roughness prior and after the deposition of TiN films. It has been found that critical load of coating detachment increases with increase in substrate roughness.

Key words: Adhesion strength, Roughness, TiN, IBAD

1. INTRODUCTION

Hard coatings are used to improve surface properties of components in a great number of applications, e.g. plastic injection moulding, die casting tools, cutting and forming tools, and others.

The most important parameter in practical application of coated elements is adhesion between a coating and a substrate. Regardless of its importance, there is no widely accepted characterization technique for quantitative measurement of adhesion strength of thin coatings. Adhesion is usually evaluated by generally accepted scratch test technique. During the scratch test a diamond tip is dragged over the surface with the normal force increasing linearly with the traveled distance. The critical load, the load at which the coated film is removed from the substrate, is influenced by many factors such as film thickness, substrate hardness, substrate roughness, interface bonding, and intrinsic properties of the deposited film [1-3].

Thin hard coatings can be produced by great number of different deposition techniques. Among them ion beam assisted deposition distinguishes as a promising to produce highly adherent films [4,5]. This technique combines physical vapor deposition with ion beam bombardment of growing films. Careful selection of process parameters such as the ion angle of incidence, ion energy, ion current and ion to atom ratio provides a possibility to prepare thin film with desired properties.

This article presents the study of the effect of substrate roughness on the adhesion of TiN coatings deposited on carburized steel substrates. The references reporting on influence of substrate roughness on adhesion of hard coatings are scarce. While Bromark et al [6] did not find any significant influence several researches [7-9] have

shown a decrease of the critical load with increase in substrate roughness.

2. EXPERIMENTAL

TiN coatings were produced by using the Ion Beam Assisted Deposition (IBAD) technique. The used IBAD system is equipped with a Kaufmann ion source and an e-beam evaporation source. All depositions were performed in a system with a base pressure of 1.5×10^{-6} mbar. The coatings were deposited in mixed Ar and N₂ atmosphere with partial nitrogen pressure between 1.1 and $1.2 \cdot 10^{-5}$ mbar, while substrate temperatures were kept at 400 °C. Hot Work Tool Steel (X38CrMoV5-1) was used as a base material. Substrate roughness was varied by varying grating of the sand paper used during grinding procedure. The studied samples were denoted as *sample 400*, *sample 1500*, and *sample 2000* where substrates were prepared using 400, 1500, and 2000 grit silicon carbide sandpaper respectively. The sample 2000 was additionally polished by using a 3 μm diamond polishing paste. Prior to deposition, all substrates were sputter-cleaned by using an argon ion beam.

In order to provide appropriate adhesion a Ti interfacial layer was introduced between TiN film and steel substrate. The layer was produced by ion beam mixing of atoms of base material with titanium atoms.

A scratch test was employed to characterize adhesion properties of TiN coatings. During the test, the diamond tip moved at a velocity of 10 mm/min, the load applied was progressively increased from 1 to 100 N at rate of 100 N/min over the scratching distance of 10 mm.

Optical microscopy was used to identify failures along scratch channels and to determine the critical loads at which these failures occur.

Additionally, the friction coefficient curves were used to determine the critical load for coating detachment. In addition to scratch test, adhesion was quantitatively evaluated by standard HRC adhesion test. Rockwell indentations were made by applying 140 kg force. Atomic force microscopy (AFM) was applied to measure sample surface roughness prior and after the deposition. All images were acquired in contact AFM mode using a symmetrically etched silicon-nitride probe. The scan area was $90 \times 90 \mu\text{m}^2$ while scan rate and set point were kept at 0.5 Hz and 225 nN respectively.

3. RESULTS AND DISCUSSION

Table 1. Surface roughness before and after the coating deposition

Sample	Sa (nm)		Sq (nm)	
	Uncoated	Coated	Uncoated	Coated
400	25	38	33	48
1500	11	15	15	19
2000	3	9	4	12

The surface topography of uncoated and coated samples has been imaged by using an atomic force microscope.

The surface roughness was characterized by arithmetic mean (Sa) and root mean square roughness (Sq). The values of roughness parameters are given in Table 1. The AFM images of samples with and without TiN coating are shown in Figure 1.

It can be seen from the Table 1 that surface roughness of all samples increases after applying TiN coating. Change in surface roughness can be attributed to several effects directly connected with ion bombardment, among which are adatom mobility, sputtering and ion incorporation. There is a great number of parameters which influence the roughness after the deposition such as the ion beam energy [10,11], ion to atom arrival ratio [11], film thickness [12-14], grain size [13,14], coating texture [12,14], and others. In this study all process parameters were kept constant for all samples. The coating thickness was around $1 \mu\text{m}$ for all samples; therefore it should not have influence on surface roughness of studied coatings. During the deposition growing film was bombarded by argon ion beam with energy of 1keV. Such ion bombardment induces enough energy into growing film to enhance the mobility of the surface atoms. Increased adatom mobility leads to aggregation of large crystal grains which results in increased surface roughness [15].

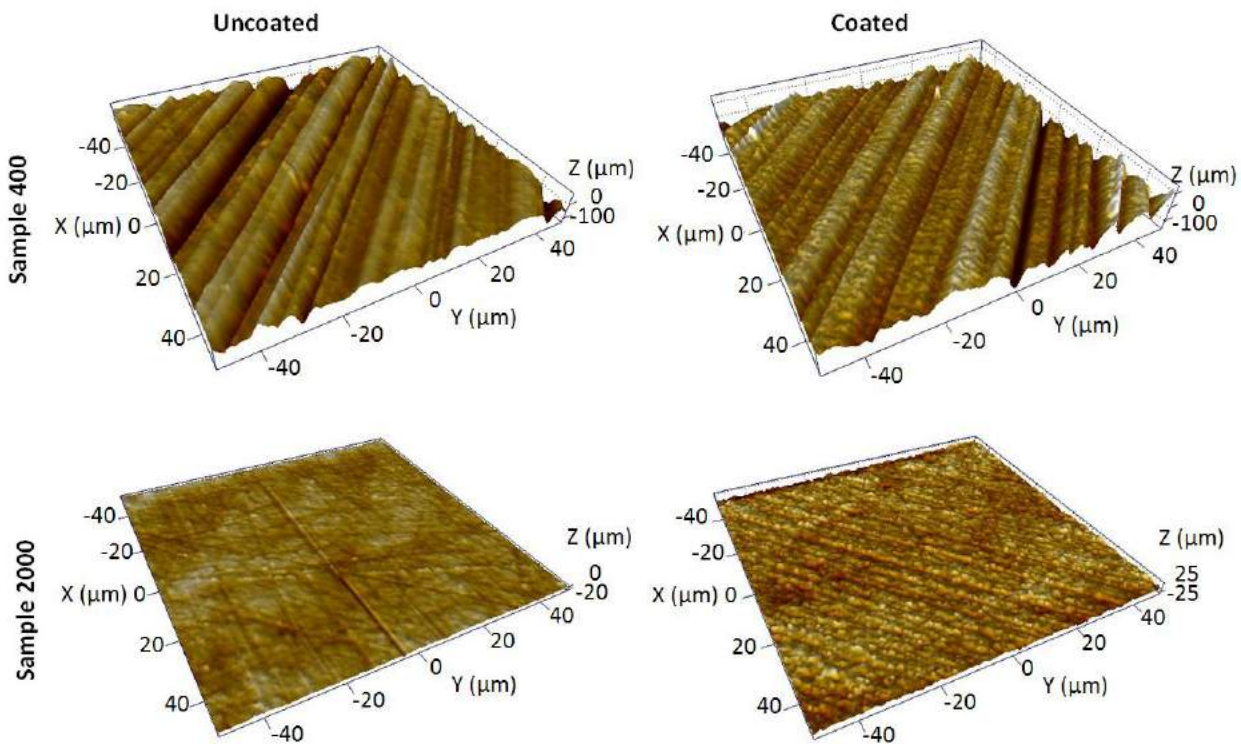


Fig.1. AFM images of samples 400 and sample 2000

In order to find a relation between substrate roughness and coating adhesion all samples were subjected to scratch test. During this test a critical load which leads to coating failure is determined. In the present study three critical loads were identified: L_{c1} - is the normal load at which the first chipping of the film occurs, L_{c2} - is the normal load at which the substrate is exposed for the first

time, and L_{c3} - is the normal load at which the complete removal of the film occurs. Optical microscopy of generated scratch channels was used to determine all three critical loads. In addition, friction and acoustic emission curves (Figure 2) were examined in order to evaluate the critical load of complete coating detachment.

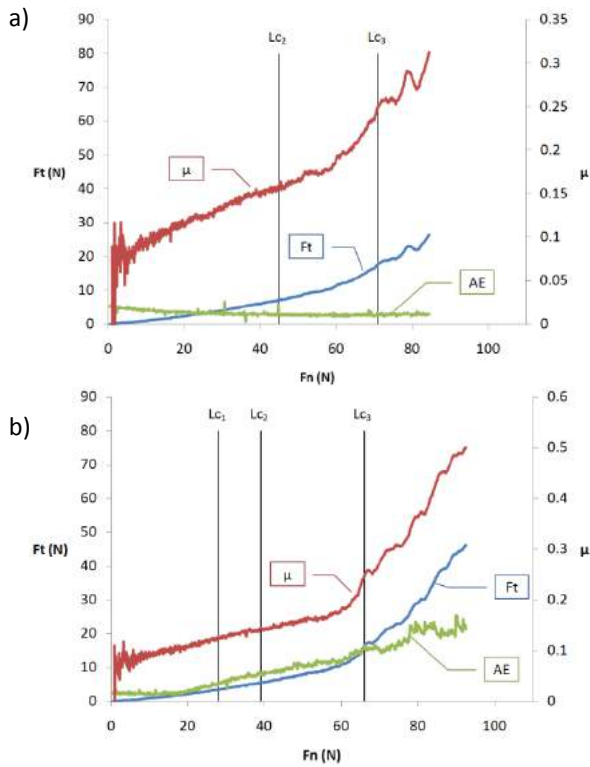


Fig.2. Friction and AE curves recorded during scratch tests a) sample 400, b) sample 2000. Vertical lines indicate the critical loads (Lc)

Figure 3 shows critical loads Lc_1 , Lc_2 and Lc_3 in a function of the substrate roughness. There was no formation of chipping failure along the scratch channel of the sample 400; therefore the critical load Lc_1 for this sample is not presented in the Figure 3. The highest critical load Lc_3 of 71 N was recorded for the coating deposited on the roughest substrate. Decreasing trend of the critical load with decrease in surface roughness was observed.

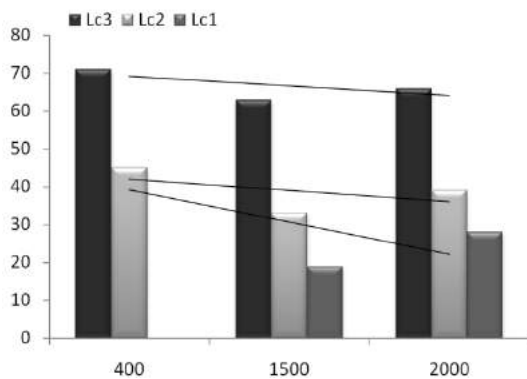


Fig.3. Critical load of TiN coatings in function of substrate roughness

Optical micrographs of generated scratch channels are presented in Figure 4. All samples show remarkable adhesion, with damage localized to do edge of the scratch track. Buckling failure mode was observed for the samples. Buckling failures appear as a result of the compressive stress field in front of the moving slider.

Curved, concentric, through - thickness cracks extending to the edge of the scratch track or beyond are typical for this type of failure [16]. Usually chipping failure occurs around previously formed crack in the region of high tensile stress within the coating. However, there was only minor chipping formation on the two smoother samples, while there was no coating chipping on the roughest sample (sample 400). First coating delamination (substrate exposure) occurs earlier on the smooth samples, and is present on a much larger scale comparing to the roughest sample.

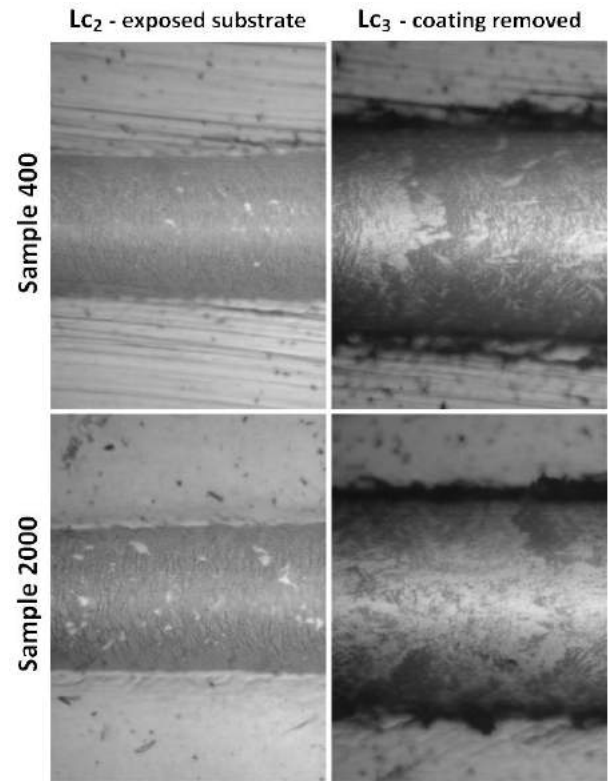


Fig.4. Optical micrographs of scratch tracks of TiN coatings, a) sample 400, b) sample 2000

High adhesion of studied coating was confirmed by employing standard HRC adhesion test. Optical micrograph of produced indents is shown in Figure 5. There was no visible coating delamination for all samples. According to the HRC test, there are six grades of adhesion strength quality HF1 - HF6 (HF1 being the best). All samples were characterized by high adhesion strength of HF2. High adhesion might be explained by the presence of ion beam mixed layer between TiN coating and steel substrate.

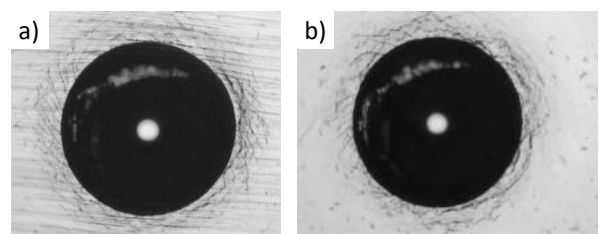


Fig.5. HRC indents made on TiN coatings applying standard 140 kg load, a) sample 400, b) sample 2000

The increase of the critical load with an increase of substrate roughness can be explained by different deformation modes of samples with different surface morphology. Rougher coating resists a greater amount of plastic deformation before formation of the damage. As substrate roughness increases, the amount of energy required for plastic deformation of surface asperities increases as well. Therefore, higher normal load is required to develop the same type of failure on rougher samples. The increase of roughness induces growth of interface surface area resulting in lower shear stress values and an apparent increase in adhesion strength [17]. The adhesion trend found in this study is contrary to the results reported by other authors [7-9] who studied influence of substrate roughness on coating adhesive properties. According to cited articles, the ridges on rough substrates generate the stress concentration which leads to easier crack formation and to decrease in adhesion. The different trend can be explained by the difference in absolute roughness of studied samples. Comparing to cited articles this study was conducted on generally smooth substrates. Apparently, there is an upper value of roughness after which coating adhesion starts to decrease.

4. CONCLUSION

The surface roughness of all studied samples increases after applying TiN coating. High scratch resistance was observed for all samples. Evidently, the ion beam mixed interlayer introduced between the coating and steel substrate plays important role in increasing the adhesion of TiN coatings. Increase of adhesion strength with increase in substrate roughness was found. This is contrary to previous findings from studied area. It appears that there exists a peak roughness after which adhesion starts to decay. In order to confirm observed adhesion trend further investigation should be directed to other types of hard coatings applied to samples with surface roughness from larger domain.

5. ACKNOWLEDGMENT

This research was supported by the Serbian Ministry of Science and Technological Development which authors gratefully acknowledge.

REFERENCES

- [1] SKORIC, B., KAKAS, D., RAKITA, M., BIBIC, N., PERUSKO, D. (2004) *Structure, hardness and adhesion of thin coatings deposited by PVD, IBAD on nitrated steels*, Vacuum, Vol. 76, pp 169-172
- [2] KAKAS, D., SKORIC, B., MILETIC, A., VILOTIC, M., KOVACEVIC, L. (2008) *Influence of substrate hardness on friction coefficient of TiN films deposited by IBAD technique*, Proceedings of the International Conference "THE" Coatings, Greece, pp. 433-438
- [3] KAMMINGA, J.-D., ESSEN, P., HOY, R., JANSSEN, G. (2005) *Substrate dependence of the scratch resistance of CrNx coatings on steel*, Tribology Letters, Vol. 19, pp 65-72
- [4] SKORIC, B., KAKAS, D., M., BIBIC, RAKITA, M. (2004) *Microstructural studies of TiN coatings prepared by PVD and IBAD*, Surface Science, Vol. 566-568, pp 40-44
- [5] HIRVONEN, J. (1991) *Ion beam assisted thin film deposition*, Materials Science Reports, Vol. 6, pp 215-274
- [6] BROMARK, M., LARSSON, M., HEDENQVIST, P., OLSSON, M., HOGMARK, S. (1992) *Influence of substrate surface topography on the critical normal force in scratch adhesion testing of TiN-coated steels*, Surface and Coatings Technology, Vol. 52, pp 195-203
- [7] SUBRAMANIAN, C., STRAFFORD, K.N., WILKS, T.P., WARD, L.P., MCMILLAN, W. (1993) *Influence of substrate roughness on the scratch adhesion of titanium nitride coatings*, Surface and Coatings Technology, Vol. 62, pp 529-535
- [8] TAKADOUM, J., BENNANI, H. (1997) *Influence of substrate roughness and coating thickness on adhesion, friction and wear of TiN films*, Surface and Coatings Technology, Vol. 96, pp 272-282
- [9] JEONG, G.H., HWANG, M.S., JEONG, B.Y., KIM, M.H., LEE, C. (2000) *Effects of the duty factor on the surface characteristics of the plasma nitrated and DLC coated high-speed steels*, Surface and Coatings Technology, Vol. 124, pp 222-227
- [10] ŠIKOLA, T., SPOUSTA, J., DITRICHOVÁ, L., BENEŠ, L., PEŘINA, V., RAFAJA, D. (1997) *Ion beam assisted deposition of metallic and ceramic thin films*, Nuclear Instruments and Methods In Physics Research Section B, Vol. 127-128, pp 673-676
- [11] OLESZKIEWICZ, W., ROMISZOWSKI, P. (2003) *Characteristics of surface and film morphology in the IBAD deposition process: a Monte Carlo simulation study*, Vacuum, Vol. 70, pp 347-352
- [12] Ji, H., Was, G.S., (1999) *Linkage between crystallographic texture and surface roughness in niobium films synthesized by ion beam assisted deposition*, Nuclear Instruments and Methods In Physics Research Section B, Vol. 148, pp 880-885
- [13] HE, Y., ZHANG, J., YAO, W., LI, D., TENG, X. (2009) *Effect of temperature on residual stress and mechanical properties of Ti films prepared by both ion implantation and IBAD*, Applied Surface Science, Vol. 255, pp 4484-4490
- [14] LÓPEZ, J., GORDILLO-VÁZQUEZ, F.J., BÖHME, O., ALBELLA, J.M. (2001) *Low grain size TiN thin films obtained by low energy IBAD*, Applied Surface Science, Vol. 173, pp 290-295
- [15] XU, J., SHAO, T., WEI, S., QIN, L (2010) *Effect of ion beam bombardment on the properties of Ni films deposited on polyimide by IBAD*, Surface and Coatings Technology, Vol. 204, pp 3443-3450
- [16] BULL, S., BERASETEGUI, E. (2006) *An overview of the potential of quantitative coating adhesion measurement by scratch testing*, Tribology International, Vol. 39, pp 99-114
- [17] WEISS, H. (1995) *Adhesion of advanced overlay coatings: mechanisms and quantitative assessment*, Surface and Coatings Technology, Vol. 71, pp 201-207.



MECHANICAL PROPERTIES OF TIN COATINGS DEPOSITED AT DIFFERENT TEMPERATURES BY IBAD

D. KAKAŠ, B. ŠKORIĆ, P. TEREK, A. MILETIĆ, L. KOVAČEVIĆ, M. VILOTIĆ
Faculty of Technical Sciences, University of Novi Sad, Serbia, Trg Dositeja obradovica 6
kakasdam@uns.ac.rs, skorich@uns.ac.rs

Abstract: TiN coatings were deposited on hot working steel substrates by ion beam assisted deposition technique. The deposition process was conducted at two different temperatures 50 and 400°C. The influence of applied deposition temperature on the mechanical properties, adhesion strength and surface morphology of TiN coatings was studied. The mechanical properties, i.e. hardness, modulus of elasticity and coating strength were characterized by nano-indentation technique. Adhesion strength was evaluated by generally accepted scratch test technique. In addition, HRC adhesion test was utilized to compare adhesion of different coatings qualitatively. Surface morphology was analyzed by atomic force microscopy before and after the film deposition. The coating deposited at higher temperature displayed higher hardness, and also higher critical loads were obtained during scratch test when compared to coating deposited at lower temperature. The ion bombardment during the deposition process enhances the adatom mobility allowing the deposition of coatings with high hardness and adhesion strength even at low temperatures.

Key words: TiN, IBAD, deposition temperature, AFM, surface roughness

1. INTRODUCTION

Hard coatings are deposited by a large variety of PVD deposition techniques where a lot of process parameters are controllable in order to produce a desirable coating. The process parameter that is distinctive for all these techniques and withal one of the most important is the deposition temperature. Deposition temperature is one of the key parameters affecting the coating growth and the one that also affects the substrate properties [1-4]. Coating mechanical properties like hardness, elastic modulus and coating/substrate adhesion are dependent on the deposition temperature, [1]. It is well documented that most of the coating mechanical properties are improved as the deposition is carried out at higher temperatures, [1]. When coatings are deposited onto heat sensitive substrates the control of heat that is introduced by the deposition process is crucial. Lowering the deposition temperature raises another difficulty since the coating grows in condition with less energy – lower adatom mobility, [3]. The lack of energy is compensated when a low temperature deposition process is carried out under constant ion beam bombardment what is feasible with Ion Beam Assisted Deposition, [4, 5]. This implies that such process conducted on a high temperature can result with coatings exhibiting great properties.

The goal of this research was to investigate the influence of deposition temperature on the structure and properties of TiN coatings deposited by IBAD technology.

2. MATERIALS AND EXPERIMENTAL

Studied TiN coatings were produced in an Ion Beam Assisted Deposition (IBAD) chamber with a base pressure of 1.5×10^{-6} mbar. The coatings were deposited at two substrate temperatures: Sample 1 - low temperature $\sim 50^\circ\text{C}$ and Sample 2 - high temperature 400°C . Hot-working steel (X27CrMoV51) disks were used as a substrate material. Prior to coating the substrates were carburized and prepared to the same grade of surface roughness. Samples were grounded using a 2000 grit paper before the process of fine-polishing with $1\mu\text{m}$ grain diamond paste. Thickness of the coatings was calculated after abrading the coatings using CSEM "Calotest" instrument. The coating hardness was assessed by the Hardness Agilent Nano Indenter G200. Hardness was calculated for the two indentation load applied, 5mN and 10mN. The Coating adhesion was evaluated by the "Revetest" scratch tester. The tests were carried out by sliding the diamond tip against the coatings at rate of 10mm/min and by progressive increasing the load with 100N/min rate until the full delamination of the coating occurred. Critical loads which led to typical coating failures were determined by light optical microscopy. Those critical loads are denoted as followed: L_{c1} - first crack formation, L_{c2} - more serious crack formation, L_{c3} - first chipping, L_{c4} -coating detachment L_{c5} -full delamination. Standard HRC adhesion test were carried out by utilizing standard Vickers hardness tester. In order to compare the coatings produced, Rockwell indents were qualitatively analyzed by light optical microscopy (LOM). Surface roughness of the samples was evaluated before and after the deposition process by VEECO di-CPII atomic force microscope (AFM). All images were

acquired in contact AFM mode using a symmetrically etched silicon-nitride probe. In the case of surface roughness determination the scan size used was $90 \mu\text{m}^2$. On the other side, in order to determine the grain size the scans were taken on the areas of $5 \mu\text{m}^2$. Scan rate and set point were kept at 1 Hz and 225 nN respectively.

3. RESULTS AND DISCUSSION

3.1. Hardness

The hardness of both coatings was determined at two different loads with respect to the penetration depth which was kept below 10% of the coatings thickness. Considering the hardness of commercially deposited TiN coating both coatings examined in this study exhibited very high hardness. Such high hardness is achieved by additional ion bombardment during the film growth. Argon ions deliver energy to adatoms on the growing surface increasing their mobility thus enabling them to achieve the state with lowest energy [4]. Additional heat induced to the substrates, improves the deposition process taking it closer to the thermodynamic equilibrium [5]. The hardness results obtained for both coatings are presented in Fig1. and modulus of elasticity is depicted by Fig2. Depositing the coating at 400°C temperature resulted with considerably harder coating (29GPa) than the low temperature one. It is also evident that a high temperature coating showed less sensitivity on the indentation load increase.

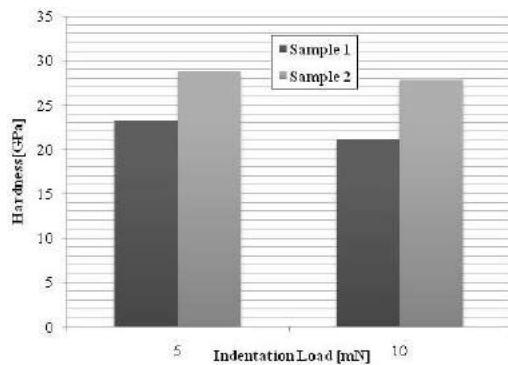


Fig.1. Hardness comparison of coatings deposited at different temperatures

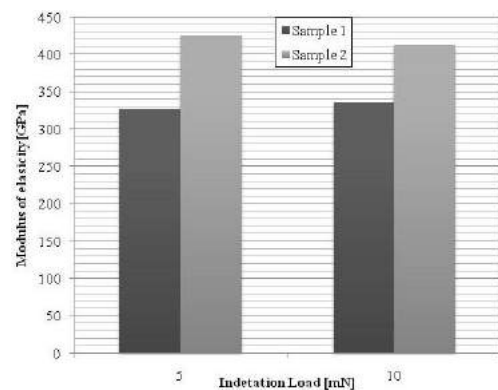


Fig.2. Comparison between modulus of elasticity of coatings deposited at different temperatures

If considering that the Sample1 coating grew in less favorable conditions then the hardness achieved in this process is outstanding.

3.2. Adhesion

Sample1 coating showed generally good adhesion (Fig.3.a), although the moments when the first cracks formed occurred fairly earlier than in the case of Sample2. First cracks were quickly followed by coating chipping (L_{c3}) that also occurred considerably earlier than in the case of Sample2, compare Fig.3.a) and b). Surprisingly the coating detachment occurred somewhat earlier at the Sample2 but this coating resisted a longer period before full delamination, which occurred at higher forces than at Sample1. It must be pointed out that adhesion is dependent on the coating thickness in a way that thicker coatings more adhere than the thinner ones, [6]. Although the Sample1 coating thickness with value of 1600nm is larger than of Sample2 that is 1050nm it displayed lower adhesion. Further, this proves the previous findings that the coating deposited at lower temperature has generally lower adhesion. As it is expected the higher adhesion is in direct relation with coating hardness.

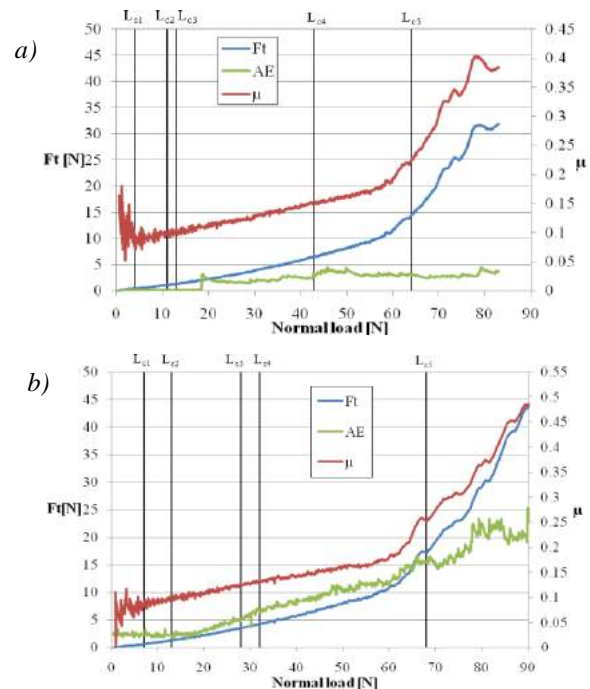


Fig.3. Scratch test plots: a) Sample1 - deposited at low temperature ($\sim 50^\circ\text{C}$), b) Sample2 - deposited at 400°C

In order to depict the different behavior between two coatings, during the scratch test, the morphology of the wear tracks were investigated at the same scratching load of 30N. Examination of the scratch tracks by LOM is presented in Fig.4. a) and b). In this stage, ductile tensile cracking along the scratch track is evident in both cases but the extent of its appearance is different. The cracks are more frequent and the coating chipping is much more severe at low temperature deposited coating – Sample1. This means that the Sample2 coating resists greater plastic deformation before chipping formation what is additionally proved by folded coating with fewer cracks on the scratch track edge Fig.4. b). In both cases none of the cracks extends outside the wear track what is a sign

that their origin is not a buckling failure in front of indenter. Both coatings displayed ductile failure modes during the scratch testing. The wear track morphology undoubtedly confirms that the higher deposition temperature enhanced the adhesion of TiN coating.

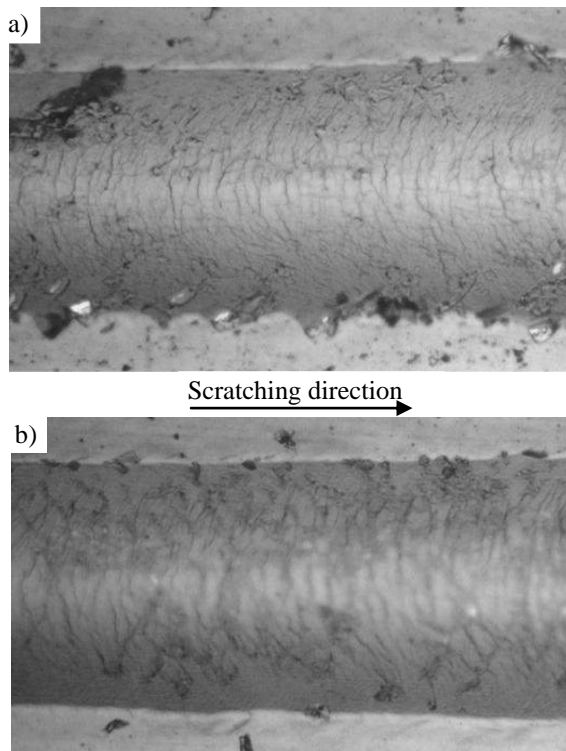


Fig.4. Scratch tracks morphology at 30N load: a) Sample1-deposited at low temperature (~50°C), b) Sample2-deposited at 400°C

In Fig.5. HRC indents are presented in order to evaluate the coatings according to HRC adhesion test standard. Crack pattern and extent of chipping indicate that both coatings falls into the HF2 group of adhesion strengths quality.

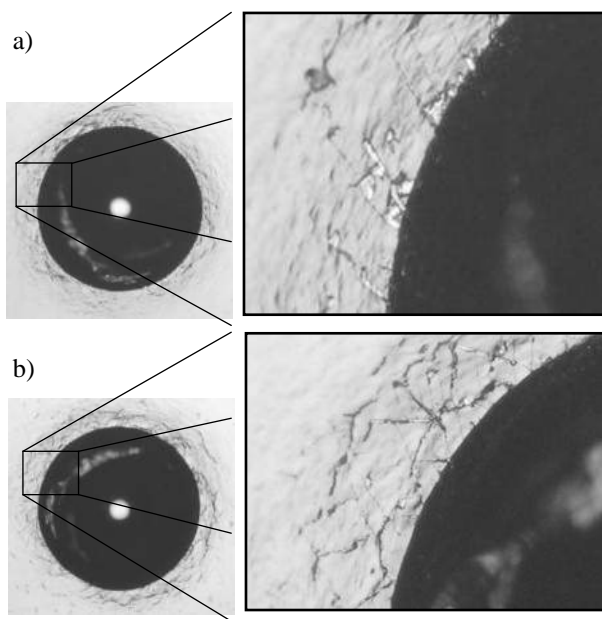


Fig.5. HRC indent: a) Sample1, b) Sample2

This is a group of coatings with very good adhesion to the substrate. Examining the HRC indents additionally proves the conclusions drawn from the scratch test results. The coating deposited at 400°C (Sample2) exhibited higher adhesion. Under applied load Sample2 coating plastically deformed what prevented chipping formation on the folded edges of the indent, as it was not the case with Sample1 coating, presented in Fig.5a.

3.3. Coatings morphology and structure

After both deposition processes increase in surface roughness was observed. The higher the deposition temperature was the more the surface roughness increased, see Table1.

Table1. Surface roughness of the samples before and after the deposition process

	R_a [nm]	R_q [nm]
Samples before the deposition	3.96	3.02
Sample 1 (~50°C)	9.3	7.2
Sample 2 (400°C)	12.06	9.04

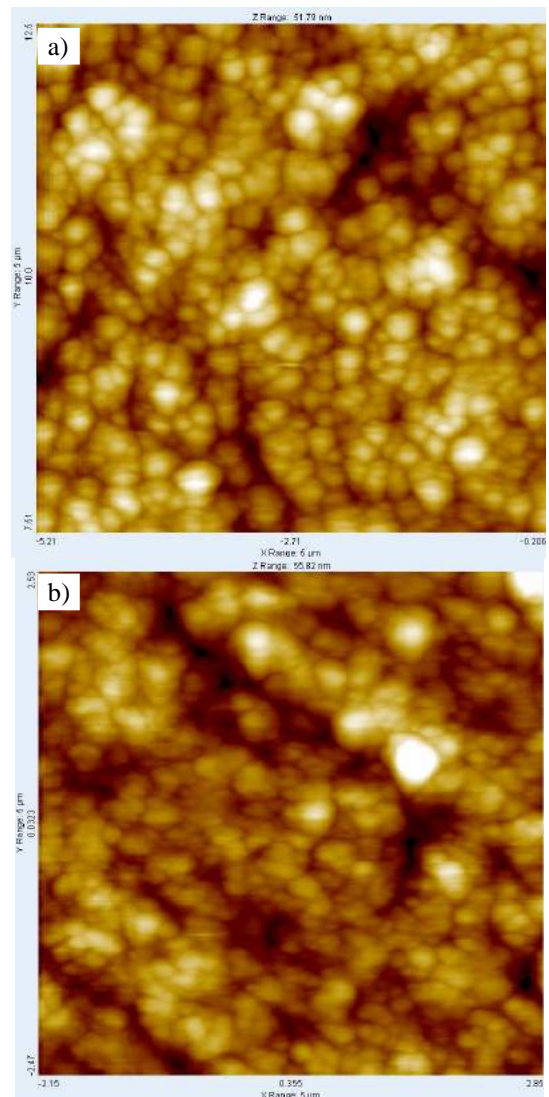


Fig.6. AFM images of coatings morphology a) Sample1, b) Sample2

¹ Kakaš D., prof.dr, Faculty of technical sciences, Novi Sad Trg Dositeja Obradovića 6, kakasdam@uns.ac.rs

² Škorić B., prof.dr, Faculty of technical sciences, Novi Sad Trg Dositeja Obradovića 6, skoricb@uns.ac.rs

There is a great number of parameters which influence the roughness after the deposition such as the ion beam energy [5],[7], ion to atom arrival ratio [7], film thickness [8],[9],[10], grain size [9],[10], coating texture [8],[10], and others. In this study all process parameters were kept constant except the temperature (heat) which directly affects the adatom mobility. Increase in surface roughness can be attributed to increased adatom mobility which leads to aggregation of large crystal grains [11].

Different heat input during the process of deposition resulted not only with different surface roughness but also with different TiN grain sizes. The 5 μm^2 scan of the coating surface revealed that Sample 1 consists of larger grains, see Fig.6. It is well known that increase in adatom mobility increases the grain size of the deposited coating. However, this was not the case in this study because exists a limit in this process. When the energy becomes greater than the surface energy the process of desorption appears and the adatoms are desorbed, [12]. This suggests that there exist a maximum in temperature when the grain size of TiN is maximal. A maximum temperature is obviously below 400°C. Determining exact temperature is a subject of our future research. Higher hardness and higher adhesion strength is clearly a consequence of denser coating structure comprised of smaller grains.

4. CONCLUSION

From the present study the following conclusions are drawn:

- The deposition process carried out at 400°C resulted with TiN coating exhibiting very high hardness up to 28,5GPa. This coating has higher hardness than the one deposited in the same conditions but at low temperature (~50°C)
- For both coatings ductile failure modes were observed during scratch testing. Such behavior is preferred in applications of highly loaded wear resistant coatings. The coating deposited at higher temperature displayed higher adhesion, withstanding a greater amount of plastic deformation before cohesive and adhesive cracking
- Both deposition processes increased the surface roughness. It was found that surface roughness increased in a greater extent when the coatings were deposited at high temperatures (400°C). Generally when coatings are deposited by IBAD technology it is expected that increase in process temperature will result with increase in surface roughness.
- AFM microscopy revealed that the higher hardness and the higher adhesion of a high temperature deposited coating can be attributed to the coating finer grained structure.

A high temperature deposited TiN coating exhibited better mechanical properties comparing to the one deposited at low temperature. The properties of TiN coating achieved by a low temperature deposition are substantially better when compared to the same coatings produced by other techniques. This makes IBAD low temperature deposited TiN coatings favorable in a field of wear protection of thermally sensible base materials.

REFERENCES

- [1] Combadiere L., Machet J., *Reactive magnetron sputtering deposition of TiN films. I. Influence of substrate temperature on structure, composition and morphology of the films*, (1996), Surface and coatings technology, Vol. 88, pp17-26
- [2] Patsalas P., Charitidis C., Logothetidis S., (2000), *The effect of substrate temperature and biasing on the mechanical properties and structure of sputtered titanium nitride thin films*, Surface and coatings technology, Vol. 123, pp335-340
- [3] Gåhlina R., Bromark M., Hedenqvista P., Hogmarka S., Håkansson G., (1995), *Properties of TiN and CrN coatings deposited at low temperature using reactive arc-evaporation*, Surface and Coatings Technology, Vol. 76-77, Part 1, pp174-180
- [4] Ensinger W., *Ion bombardment effects during deposition of nitride and metal films*, (1998), Surface and coatings technology, Vol. 99. pp1-13
- [5] Šíkola T., Spousta J., Ceska R., Zlámál J., Dittrichová L., Nebojsa A., Navrátil K., Rafaja D., Zemek J., Perina V., (1998), *Deposition of metal nitrides by IBAD*, Surface and coatings technology, Vol. 108-109, pp284-291
- [6] Burnet P.J., Rickbery D.S., (1987), *The relationship between hardness and scratch adhesion*, Thin Solid Films, Vol.154, pp403-416
- [7] Oleszkiewicz W., Romiszowski P., (2003), *Characteristics of surface and film morphology in the IBAD deposition process: a Monte Carlo simulation study*, Vacuum. Vol. 70, pp347-352
- [8] Ji H., Was G.S., (1999), *Linkage between crystallographic texture and surface roughness in niobium films synthesized by ion beam assisted deposition*, Nuclear Instruments and Methods In Physics Research Section B: Beam Interactions With Materials and Atoms, Vol. 148, pp880-885
- [9] He Y., Zhang J., Yao W., Li D., Teng X., (2009), *Effect of temperature on residual stress and mechanical properties of Ti films prepared by both ion implantation and ion beam assisted deposition*, Applied Surface Science, Vol. 255, pp 4484-4490
- [10] López J., Gordillo-Vázquez F.J., Böhme O., Albella J.M., (2001), *Low grain size TiN thin films obtained by low energy ion beam assisted deposition*, Applied Surface Science, Vol.173, pp290-295
- [11] Xu J., Shao T., Wei S., Qin L., (2010), *Effect of ion beam bombardment on the properties of Ni films deposited on polyimide by ion beam assisted deposition*, Surface and Coatings Technology, Vol.204, pp3443-3450
- [12] Jiménez H., Restrepo E., Devia A., (2006), *Effect of the substrate temperature in ZrN coatings grown by the pulsed arc technique studied by XRDH*, Surface & Coatings Technology, Vol.201, pp1594-16



SCRATCH TESTING OF Zn COATING SURFACES

Bogdan NEDIĆ¹⁾, Desimir JOVANOVIĆ²⁾, Gordana LAKIĆ GLOBOČKI³⁾

¹⁾ Mašinski fakultet, Kragujevac, Srbija, nedic@kg.ac.rs

²⁾ Zastava oružje AD, Kragujevac, Srbija, zo.tehnologija@open.telekom.rs

³⁾ Mašinski fakultet, Balja Luka, Republika Srpska, BiH, gordana.globocki@gmail.com

Abstract: Galvanic Zn coatings are applied to the base material surface in order to obtain some of the characteristics: resistance to corrosion, chemical inertness, better aesthetic impression, etc. Most studies of Zn coatings focuses on the characterization of coatings and their links to the basic material, while very little is known about the effects of substrate on the characteristics of the coating. Surface finish has a great influence on determination of the physical and mechanical properties and structure of the surface layer. This paper presents the preliminary results scratch testing of the depending on the thickness of Zn coating. The research was performed with samples of different hardness and different previous grinding.

Key words: Zn coating, galvanic coating, scratch test, adhesion testing

1. INTRODUCTION

Creating metal coatings on the surface of another metal has a dual role, corrosion protection and changing characteristics of the metal surface, such as hardness, electrical conductivity, decoration and so on. But when the metal coatings are damaged, they can not simply be fixed, that makes them different from the organic coating.

The effect of processing procedure and conditions of pre-treatment and preparation of surfaces to which coatings are applied, technological heritage, is very little explored. Surface layers of machined surfaces obtained by different treatment processes and regimes may have a different structure, which only in the period of exploitation may be experienced. Therefore, it can be said that the characteristics of surface layers are formed as a result of different processing conditions in the technological chain of production of the finished part. The basic parameters that are inherited through the process of technological development can be divided into two groups. On the one hand there are parameters related to properties of materials: their composition, structure, stress state, etc., while on the other hand are parameters related to macro and micro geometry of the surface (geometrical parameters). This indicates the complexity of the problem and the need for further studies [9].

Surface finish has a great influence on determining the physical - mechanical properties and structure of the surface layer. In this paper is investigation of the influence of the previous surface treatment and coating thickness on the characteristic scratch testing Zn coating.

2. GALVANIC ZN COATING

Galvanic plating and metals are crystalline in nature. Therefore, the electrodeposition process is called crystallization. In the crystallization process - there are three independent processes:

- 1) formation of seeds (centers) or crystal nuclei,
- 2) crystal growth rate,
- 3) increase the speed of crystals on account of their merger.

These processes run in parallel. The creation and quality of metal coatings are influenced by many factors: The concentration of ions significantly affects the quality of the coating, the composition of the electrolyte affect the properties and appearance of the coatings. Current density has a large impact on the formation rate of crystal nuclei, mixing is performed to maintain constant concentration of metal ions, the temperature plays a significant role in the speed of chemical reactions. Metals are polycrystalline particles, so the characteristics of the coating are affected by the structure of the substrate [9].

Zinc coatings are used for corrosion protection of machinery parts, steel plates, wire, etc.. located in different climate conditions, in closed environments with moderate humidity, at the polluted gases areas, flue gases area and in atmosphere containing sulfur vapor. These coatings are used to protect pipes, tanks and other parts, which are in contact with water at temperatures up to 70°C. Color of zinc coating is usually light gray, become dark during time, and therefore does not provide a decorative look. Zinc also protects the iron from corrosion when the coating is porous or damaged, because it forms a couple in which the iron is cathodically protected [3, 4].

Life of the protective effect of the coating depends on its thickness. For metal objects, which are used in relatively dry air in closed rooms, sufficient thickness of zinc coating of 10-15 µm. For items that are outside the room, in the air that is polluted by industrial gases, the thickness increases to 20 - 25 µm, and for articles intended for use in industrial environments, in terms of enhanced effects of moisture, sea water or water vapor, the thickness of zinc coating moving to 50 µm. Coating is more resistant if the zinc cleaner [1, 2, 3].

The hardness of metal coatings of zinc is 45 to 120 HB. Galvanic corrosion resistance of zinc coating can be improved by after-treatment - the application of phosphate or various types of chromate coatings: colorless – A, bluish – B, yellow - C, olives – D, and black - F coating. Chromate conversion coatings should not be applied to surfaces of elements that are in contact with flammable and explosive environments, [6, 7].

Requirements for quality zinc coatings are contained in the applicable standards and the most important are [6, 7]:

The external appearance of galvanized zinc coating is defined by color.

Allowable defects of zinc coatings without post-processing are darker color of the coating on the inside surface elements, the presence of shiny and matte places on the same element, the absence of coating in blind holes, channels, and the like. at a depth of more than one diameter and in the openings that pass through the entire element at a depth greater than two diameters, slightly peeling in places of weld for molded parts, color change of coating after heating with aim to the remove of hydrogen and the existence of traces of the inflow of water.

Unacceptable defects coatings without the occurrence of subsequent processing and dendrites and spongy coating, dark stripes on the edges of elements, (burned sites), uncovered places, except for points given to technical documentation, bubbles, layer removal and peeling of coating, appearance of grains and hard spots that interfere with the function of element, the black points and corrosion of zinc, traces of unwashed salts existence and mechanical damages of the coating.

The thickness of zinc coating is usually: 5, 8, 12 and 25 μm . Depending on the needs designer may define other values of thickness, allowing a greater thickness than the prescribed, if at the same time increasing the dimensions of the element does not affect its function. Smaller thickness of zinc coating is allowed on the inside surface, in holes and hollows, where the thickness of the coating must not be less than 60% of the prescribed level.

Adhesion. Galvanic zinc coatings shall not peel off of base metal and chromic or phosphate conversion coatings must not wash off from the zinc coating.

Corrosion resistance. Galvanic zinc coatings on steel must be corrosion resistant. When examining the chamber with a neutral salt fog 5% zinc coating without subsequent processing, does not allow the occurrence of red-brown dots (representing the corrosion of the base material) visible with the naked eye.

3. EKSPERIMENTAL INVESTIGATIONS

For the purpose of testing the samples were made 15 x 6.3 x 10 mm (Figure 1). On samples from the front side were embedded serial numbers of the sample, and through lateral surfaces were drilled openings designed to mounting each sample individually for coating.

Samples are made of spring steel 67SiCr5 (Č4230). After the sample design, milling, heat treatment was done by improving the different hardness (Table 1).

Grinding of samples was carried out with two regimes, A and B. Grinding of samples labeled A was performed with two passes with 0.02 mm depth and speed of 11 m/s and

two passes with 0.01 mm and the speed of 22 m/s, and grinding of samples B was performed with two passes of depth 0.02 mm and speed 22 m/s. In this way they obtained different characteristics of the surface layer and the surface topography of various samples. Application of metal coatings was performed at the facility for electroplating factory "Zastava Arms", Kragujevac in production conditions, with different times in order to obtain different thicknesses of Zn.

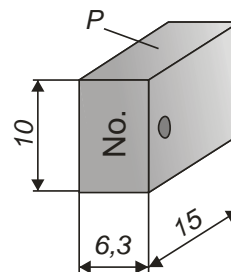


Fig. 1. Sample

Zinc coating was carried out as follows:

- I. alkaline degreasing without cyanides with industrial detergent,
- II. rinse with water,
- III. pickling in diluted hydrochloric acid in a 1:1 ratio,
- IV. rinse with water,
- V. electro-chemical coating of zinc,
 - temperature coating-room,
 - strength of current $I = 3 \text{ A/dm}^2$,
 - time 8 - 35 min,
- VI. enlightening in 2% HNO_3 for a period of 50 seconds,
- VII. rinse with water,
- VIII. blowing.

Table 1 shows the data on the tested samples: marking of grinding, the hardness after heat treatment and obtained layer of Zn. Coating thickness measurement was performed in a laboratory galvanizing area of factory "Zastava Arms" in Kragujevac. Samples with coatings of Zn in which the thickness were up to 4 μm were not further analyzed.

Table 1 Hardness and thickness of Zn samples

Sample number	Grinding	Time, min	Hardness samples, HRC	Thickness μm
2	A	8	47,6	2
5	A	25	46,5	12
6	A	35	33	16
8	A	25	19,1	12
9	A	35	35,4	15
22	A	25	20,0	10
4	B	8	35,5	4
10	B	16	35,9	9
11	B	8	48,3	2
13	B	25	45,8	14
16	B	25	36,9	12,7
17	B	35	21,7	20
31	B	16	24,2	6,5
34	B	16	21,1	6

4. EQUATIONS

After grinding the samples, before applying the coatings, were measured hardness and surface topography parameters and the longitudinal and transverse direction. Measurements were taken at the surface of the sample P (Fig. 1). The appearance of ground surface of one of the samples before applying the coating is shown in figure 2. The value of the basic parameters of roughness in the longitudinal and transverse direction is approximately the same. significant differences were observed in additional parameters, for example, uneven steps. ra value ranges from 0.26 to 0.4 μm .

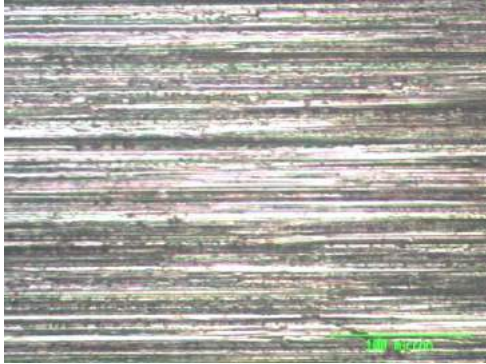


Figure 2 The appearance of ground surface of the sample before application of coatings

Applying Zn coatings leads to a deterioration of surface quality and roughness increases significantly. Class roughness of Zn coating can deteriorate for one, even for the two classes.



Fig. 3 Surface of the sample 31 with Zn coating

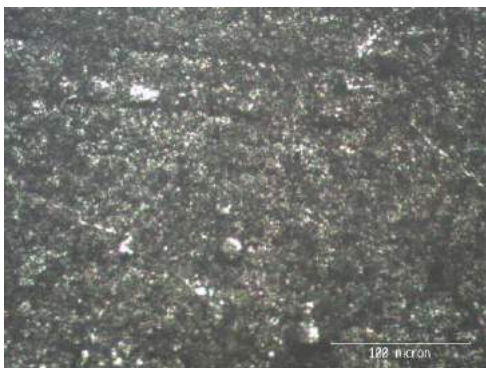


Fig. 4 Surface of the sample 9 with Zn coating

Tests adhesive properties of coatings was carried out to help Scratch Tester ST-99, Figure 5 The analysis of measurement results in terms of traces of wear and tear of constant increase in normal load ($vF_n = 10 \text{ N/min}$) and constant sliding velocity ($v = 10 \text{ mm/min}$) obtained data on adhesive resistance or strength adhesive link between the coating and base material. By monitoring changes in force and the coefficient of friction with the change of the load for the duration of contact, it is possible to determine the "critical value of force F_{NC} " at which the change in their values [5].

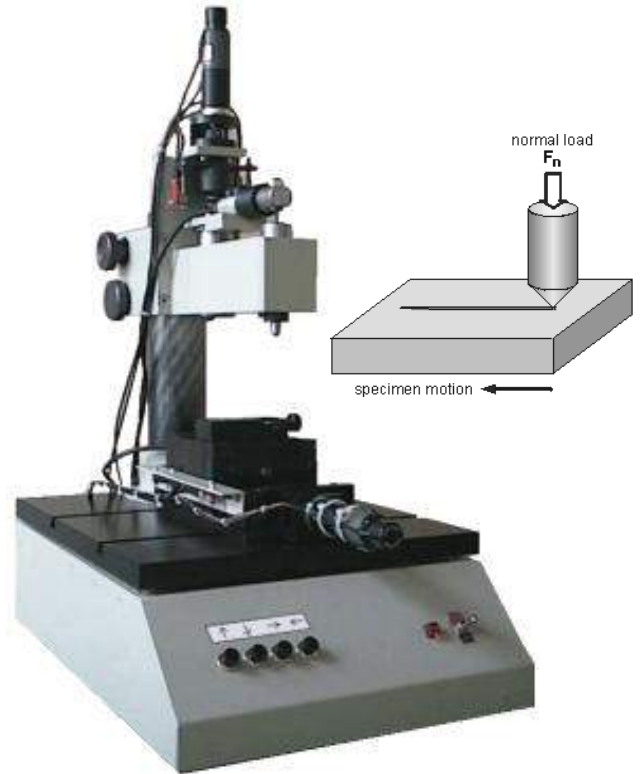
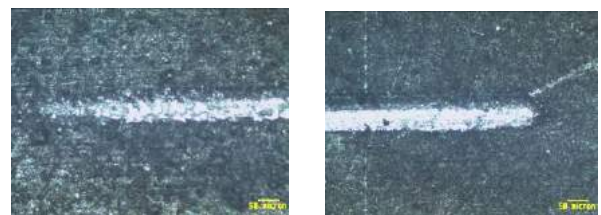


Fig. 5. Scratch tester ST-99



Start

End

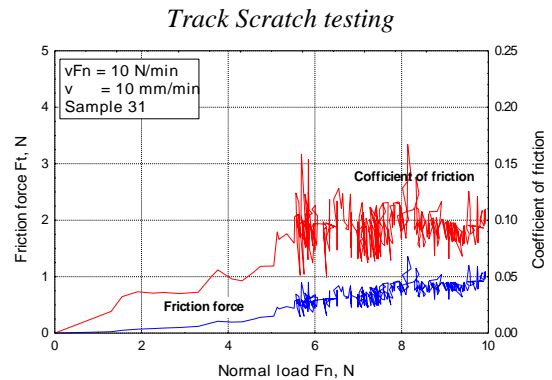


Fig. 6. Track Scratch testing and change in the coefficient of friction of the sample 31, thickness Zn coating 6,5 μm

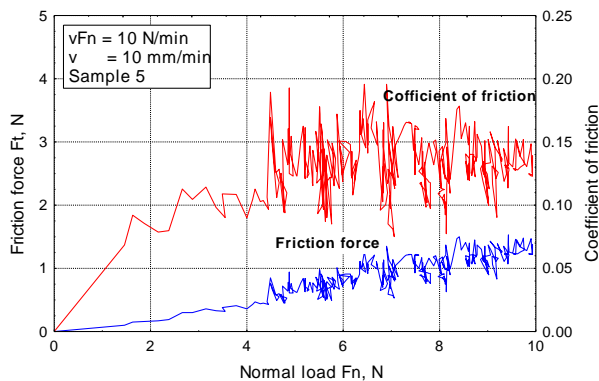
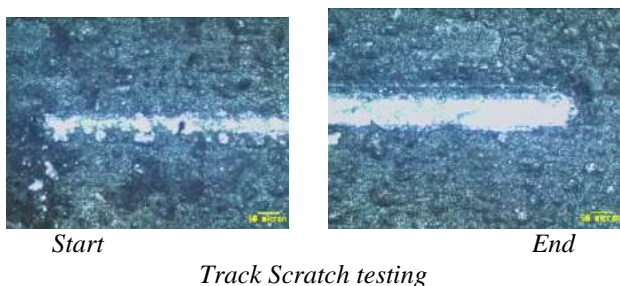


Fig. 7. Track Scratch testing and change in the coefficient of friction of the sample 5, thickness Zn coating $12 \mu\text{m}$

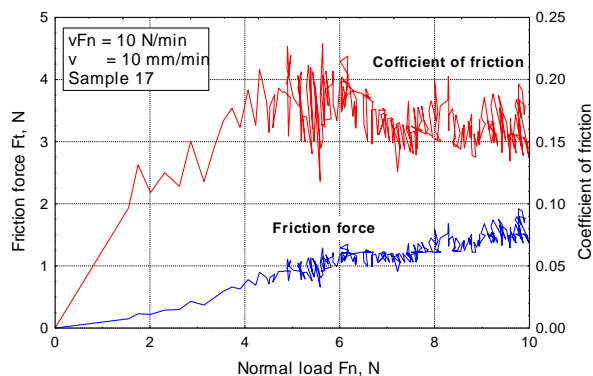
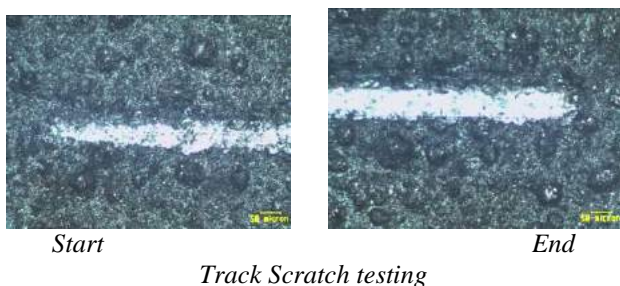


Fig. 8. Track Scratch testing and change in the coefficient of friction of the sample 17, thickness Zn coating $20 \mu\text{m}$

Performing the scratch test on the Zn coating cause additional problems. Firstly, it was not possible to reveal the iron substrate directly under a reflected light optical microscope due to the absence of colour contrast. The max. load was set to a sufficiently high value of 10 N.

Secondly, the ductile character of the Zn coatings implies that the stylus simply ploughs through and perforates the Zn coating at a certain normal load, into the iron the substrate. The load at perforation of the coating was assumed to be critical load.

However, as the observed failure mode is not related to coating spallation events, it was concluded that the scratch test method cannot be used to characterise the

adhesion properties of conventional electro deposited Zn coatings.

Analysis of signals for the friction force and coefficient of friction have shown the existence of certain differences. Until the advent of significant oscillation signal occurs at different values of normal load. This value is directly related to the hardness of the substrate and coating thickness.

5. CONCLUSION

The main parameters that are inherited through the technological process of making the parameters related to properties of materials: their composition, structure, stress state, etc., and parameters related to macro and micro-geometry area (geometrical parameters).

When using the Scratch test on the Zn coating, a perforation of the coating was obtained without any failure mode related to the adhesion. the stylus is ploughing through the coating material. the scratch test method thus can not be used to characterise the adhesion properties of conventional ductile electro deposited zn coatings. The results are consistent with [8].

Preliminary Scratch test results Zn coatings have shown that there is a significant change in surface topography and differences in the signals measured coefficient of friction. In order to establish the necessary correlations are very extensive research.

REFERENCES

1. ĐORĐEVIĆ, S. MAKSIMOVIĆ, M., PAVLOVIĆ, M. G., POPOV, K. I., *Galvanotehnika*, Tehnička knjiga, Beograd, 1998.
2. PROSKURKIN, E. V., POPOVIĆ, V. A., MOROZ, A. T., *Cinkovanje*, "Metalurgija", Moskva, 1988.
3. CREUTZ, H. G., MARTIN, S., *Plating and Surface Finishing*, 62, 7, 681, 1975.
4. KUNZ, V., *Zintek-Techseal-Tri-Coat Catalouge*, Trebur 2001.
5. IVKOVIĆ, B., NEDIĆ, B., JEŠIĆ, D., *Scratch test - merenje abrazione otpornosti materijala i kvaliteta prevlaka*, DEMI 2001, Banja Luka,, RS, BiH, 2001.
6. SRPS C.T7.111-117:1991
7. ISO 4539
8. http://www.belspo.be/belspo/home/publ/pub_ostc/NOrNOB018_en.pdf
9. NEDIĆ, B., JOVANOVIĆ, D., LAKIĆ GLOBOČKI, G., Influence Of Previous Machining On Characteristics Of Galvanic Coatings, Serbiantrib - 12th International Conference on Tribology, Kragujevac, 2011.

ACKNOWLEDGEMENT

This paper is part of project TR35034 The research of modern non-conventional technologies application in manufacturing companies with the aim of increase efficiency of use, product quality, reduce of costs and save energy and materials, funded by the Ministry of Education and Science of Republic of Serbia.



ADI MATERIALS FOR BALLISTIC PROTECTION

Sebastian BALOS¹, Leposava SIDJANIN¹, Dragan RAJNOVIC¹, Olivera ERIC²

¹ Department of Production Engineering, Faculty of Technical Sciences, University of Novi Sad, Trg Dositeja Obradovica 6, 21000 Novi Sad, Serbia

² Institute „Kirilo Savic“, Vojvode Stepe 51, 11000 Belgrad, Serbia
sebab@uns.ac.rs, lepas@uns.ac.rs, draganr@uns.ac.rs, olivera66eric@gmail.com

Abstract: Perforated plates offer a very convenient combination of properties: ballistic protection, combined with a high multi – hit resistance, making them very attractive for mounting at some distance from the basic armour of the armoured vehicle. Although the traditional material for making perforated plates has been the high strength steel, there are some alternatives. One of them is the ADI (Austempered Ductile Iron) material. ADI possessed a unique microstructure – ausferrite, obtained after heat treating of ductile iron. This material is an attractive replacement for steels for a number of reasons: adequate mechanical properties for a number of applications and lower cost of production and machining. Mechanical properties of ADI are similar to high strength steels, except for ductility, which is lower to some extent, but the specific geometry of perforated plates allow the arrest of the propagated crack, overcoming this drawback. On the other hand, ADI is cheaper to produce as well as machine than high strength steels, due to a smaller volume of material removed and higher machinability due to the presence of graphite nodules.

Key words: ballistic protection, add-on armour, ADI materials

1. INTRODUCTION

The end of Cold war influenced the dramatic diminishing of military funds, leading to an ever increasing need for modernization of various armoured vehicles in order to keep them updated [1]. However, their armour protection levels proved inadequate in many occasions, which led to the wide adoption of add – on armour protection. This type of armour is mounted on top of the basic armour, offering a higher protection level. Many types of add – on armour have been used, where the majority is based on metallic or ceramic components. The simplest way of increasing ballistic protection is to bolt a high hardness rolled homogenous armour, however, this type of armour although cheap, offers a less convenient mass efficiency [2, 3]. Therefore, ceramics were used, offering twice the hardness and mass efficiency. On the other hand, it is well known that ceramics in general suffer from a relatively low fracture toughness and ductility, leading to problems regarding multi – hit resistance. This drawback refers to all types of advanced ceramics: although the first shot is stopped, other subsequent shots, if hit near the first may penetrate due to the cracked and weakened ceramic material. This influences a careful optimization of ceramic tile size, which, in turn, if is small enough may offer a longer overall edge length [4 - 6]. If the projectile impacts the edge, mass efficiency drops by the free edge effect [7]. However, free edge effect may be turned in favor of the add – on armour, by applying a different type of armour,

non – homogenous armour. This comprises the use of fences and perforated plates. Namely, when the projectile impacts the edge, or near the edge, a non – homogenous stress develops, which can induce yaw, or even fracture the projectile, as projectiles or penetrating cores tend to have relatively high hardness, but low ductility as well. A yawed or fractured penetrating core has a dramatically lowered penetration, in some cases lower than the basic armour protection level [8]. To achieve this, a certain distance between the basic and add-on armour must exist, to allow the yaw to induce, or, in case of penetrating core fragmentation, to allow a sufficient fragment separation to spread their kinetic energy on a larger area of basic plate [9].

In this paper, some results of ballistic testing perforated plates made from steel are shown, with a special attention to some aspects that may influence the application of a novel generation of ADI (Austempered Ductile Iron) materials for the same purpose.

ADI material is a heat treated ductile iron. By heat treating, a special microstructure is obtained, called ausferrite. Ausferrite is a mixture of ausferritic ferrite, and carbon enriched retained austenite [10 - 12]. ADI material possesses a wide range of mechanical properties, combining high strength and fracture toughness similar to high strength steels, while its ductility is notably higher than that of other cast irons, albeit lower than high strength steels. Furthermore, one of ADI material's advantages over steel is its lower density, which may influence a higher mass efficiency, or similar mass efficiency at lower cost, which is another benefit.

2. PERFORATED PLATES

2.1 Ballistic testing

The basics of the free-edge-effect has been defined in the excellent work of Chocron et.al. [8]. They proved the existence of bending stresses as the penetrating core impacts the add-on armour plate edge, Fig.1. Furthermore, the minimum perforated plate thickness for a given armour piercing ammunition was defined as absolutely necessary for inducing sufficient bending stresses for core fracture in two parts. This effectively lowers the kinetic energy approximately in half, lowering the cores penetrating performance.

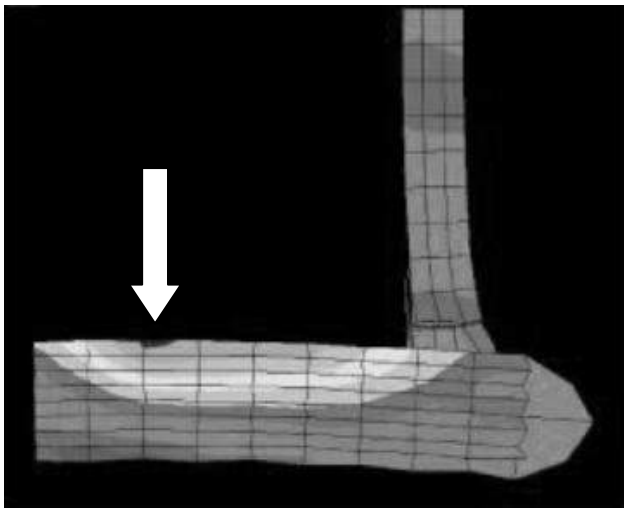


Fig.1. Penetrating core bending at edge impact – maximum stress is marked with an arrow[8].

In Balos [9] and Balos et. al. [1, 13], where the experimental setup shown in Fig.2 was used, it was found that when an optimized material and geometry of an add-on perforated plate is used, a larger, heavy machinegun/sniper rifle armour piercing incendiary (API) ammunition can be defeated by the application of the basic armour only half the usual thickness. The results for an optimized perforated plate are shown in Table 1.

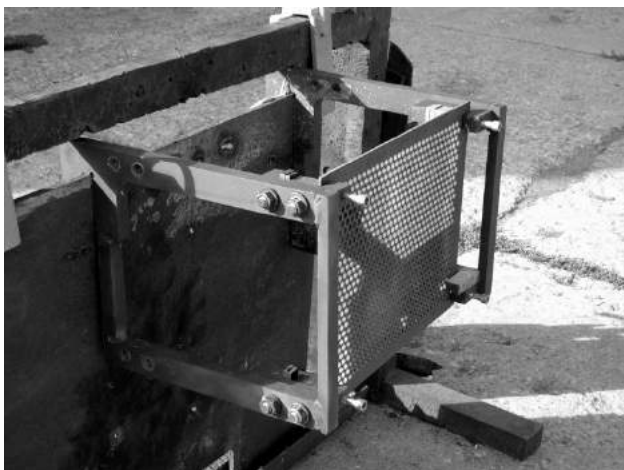


Fig.2. Ballistic testing target: add-on perforated plate mounted on the basic plate by a frame [9].

The result shown in Table 1, show the influence of perforated plate thickness, which, if sufficiently thin, may not result in a successful induction of yaw or penetrating core bending stresses to cause fracture. Furthermore, it can be seen that penetrating core can fracture not only in two, but in three, four and even five parts. Such phenomenon is documented by the number of impacts on the basic plate, Fig.3, dramatically lowering the kinetic energy of the penetrating core. Although the basic plate thickness has not been varied, it is likely that a thinner than the used 13 mm plate would certainly stop those fragments. This result proves that perforated plate is a highly effective add-on armour.

Table 1 Ballistic testing results of perforated plates made from Hardox 450 steel (0.22C-0.69Si-1.62Mn-0.8Cr), hole diameter 9 mm, plate thickness 6 and 4 mm [9].

No.	v_{10} [m/s]	Description of basic plate damage
6 mm perforated plate		
1	867.7	Smooth bulge – core fractured in 4 parts
2	859.2	Smooth bulge
3	881.7	Smooth bulge – core fractured in 3 parts
4	862.7	Smooth bulge – core fractured in 5 parts
5	863.0	Smooth bulge
4 mm perforated plate		
1	865.6	Hole normal
2	866.7	Hole normal
3	879.2	Hole normal
4	880.5	Hole normal
5	872.0	Cracked bulge (two cracks)



Fig.3. Five penetrating core fragments made smooth bulges on the basic plate [9].

2.2 Macroscopic characterization

After impact, it was noted that the damaged area near the impact point is fairly limited. This phenomenon is in contrast to the already mentioned free-edge-effect that degrades the protection level if used on an armour added directly (without air gap) on top of the basic plate.

Namely, even ductile materials such as steels, after a certain number of impacts catastrophically shatter due to the crack propagation and linking. Although crack nucleation in perforated plates does exist as well, their propagation is arrested by the nearest hole, where the crack sinks. This behavior is shown in Fig.4. The arrest of the crack prevents a further crack propagation and crack linking, leading to a high multi hit resistance of perforated plates, Fig. 4.

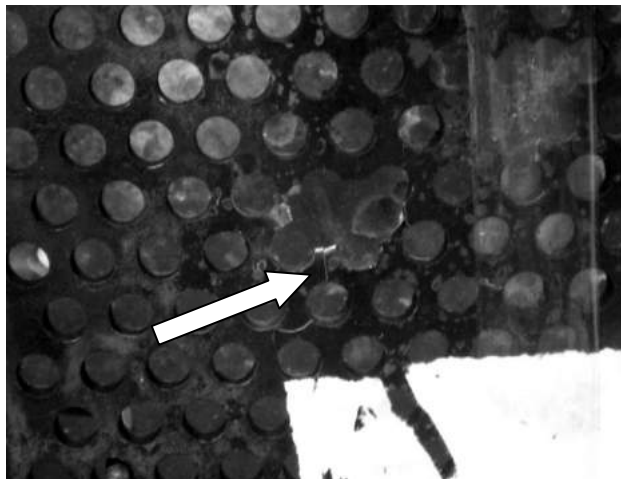


Fig.4. Perforated plate impact damage showing cracking between holes [9].

3. ADI MATERIALS FOR PERFORATED PLATES

3.1 Mechanical properties of ADI

Mechanical properties of ADI make this novel material similar to steel in some aspects. Namely, in accordance with ASTM A897M-03 standard [14], there are five grades of ADI materials, Table 2.

Table 2 Standard ADI material grades according to ASTM A897M-03 and Hardox 450 (H450) mechanical properties as shown in [9].

Grade	Min. R_m [MPa]	Min. $R_{p0.2\%}$ [MPa]	A [%]	K0 [J]	BHN
1	900	850	9	100	269-341
2	1050	750	7	80	302-375
3	1200	850	4	45	341-444
4	1400	1100	2	25	388-477
5	1600	1300	1	15	402-512
H450	1450	1255	11	60*	445

*V-notch specimen (KV)

From Table 2, it can be seen that ultimate tensile stress (R_m), yield strength ($R_{p0.2\%}$) and hardness of Hardox 450 steel closely corresponds to Grade 4 ADI. On the other

hand, its elongation (A) and Charpy impact strength are higher. However, these mechanical properties may be of secondary importance for this particular application, due to specific geometrical characteristics of perforated plates, where, as shown in Fig.4, crack propagation is stopped by the nearest hole. Crack nucleation may be initiated only by another impact, while damaged area remains relatively limited to five or six interconnected holes [9].

3.2 Density of ADI materials

In addition to convenient key mechanical properties, which are similar to some kind of steels, ADI materials possess lower density. Namely, as mass percent of carbon amounts to 3,5 – 4 % [15]. The typical microstructure of ADI showing spheroidal graphite is shown in Fig.5. As a result, an ADI component will be 10 % lighter than steel, if the geometry will be retained [16]. This means that a perforated plate may be lighter if made from ADI, having a higher mass effectiveness when made from steel.

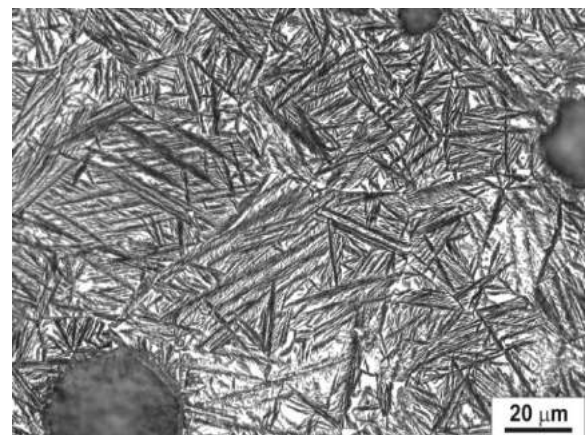


Fig.5. A typical ADI microstructure containing spheroidal graphite and ausferrite metal matrix [17].

3.3 Technological advantages

As the ADI material is in effect a heat treated ductile iron, it is fundamentally obtained by casting. It is well known that per given mass of product, cast parts are cheaper [11]. Furthermore, hole shape and profile may not be cylindrical, but rather specially suited for various types of ammunition. Namely, hole dimensions must be finely tuned to various types of penetrating core dimensions to obtain sufficient ballistic protection of the armour system [9]. As the hole becomes smaller, the free – edge effect is diminished or totally lost since such plate behaves like a homogenous plate, while if the hole size is too large, the projectile may pass through it, without contact, or with an insufficient contact to induce bending stresses and cause fracture. The application of cores of various shape and dimensions (step or conical shape), may make such a perforated plate effective against different ammunition types and calibers. Although hole sides will nevertheless have to be finished by machining, the volume of the material removed is much smaller than in the case of drilling the whole hole. In addition to this, machinability of ADI material is higher than that of heat treated steels,

due to a lubricating effect of graphite, resulting in further savings in time and cost [18]. This way, the machining of ADI perforated plate may be both shorter and cheaper compared to steel, resulting in a cheaper product. For crankshafts, if forged steel is replaced by ADI, an overall cost may be lowered by 30 % [19]. However, for the purpose of perforated plates, an even higher savings may be expected.

Testing of ADI materials for this application is already undergone in UK [20, 21] and Serbia on the behalf of Ministry of Defence [22].

4. FINAL REMARKS

For common engineering purposes, it can be said that more ductile grades of ADI can compete with medium-strength steels, while high strength grades of ADI compete less effectively with the high-strength steels. These high strength grades may replace high strength steels for purposes that demand primarily high wear resistance and moderate ductility. Furthermore, ballistic protection in form of perforated plates may be another attractive application of high strength ADI for a number of reasons:

- Lower density offers higher mass effectiveness, that can be utilized in two basic ways: lowering the weight of add-on armour and increasing ballistic resistance.
- Optimizing the geometry to cover more different calibers with one perforated plate.
- Lowering cost of production due to cheaper production process and machining.

Therefore, ADI material may be a feasible alternative to high strength steels for production of an advanced perforated plates for ballistic protection.

ACKNOWLEDGEMENT

This study is supported by the Ministry of Education and Science of the Republic of Serbia, through technology development project TR34015.

REFERENCES

[1] BALOS, S., GRABULOV, V. SIDJANIN, L. (2010) *Future armoured troop carrying vehicles*, Defence Science Journal, Vol. 60, pp. 483-490

[2] OGORKIEWITZ, R., (2002) *Armor for Light Combat Vehicles* *Advances in armour materials*, International Defence Review July Vol. 6, pp. 41-45

[3] OGORKIEWITZ, R., (1991). *Advances in Armour Materials*, International Defence Review, Vol. 4, pp. 349-352

[4] HAZELL, P., ROBERSON, C., MOUTINHO, M. (2008) *The design of mosaic armour: The influence of tile size on ballistic performance*, Materials & Design 29, 2008, pp. 1497-1503

[5] BLESS, S., JURICK, D. (1998) *Design for multi-hit capability*, International Journal of Impact Engineering 21, 1998, pp. 905-908

[6] DE ROSSET, W. (2005) *Patterned armor performance evaluation*, International Journal of Impact Engineering 31, pp. 1223-1234

[7] GOLDSMITH, W. (1999), *Review: Non-ideal Projectile Impact on Targets*, International Journal of Impact Engineering Vol. 22, pp. 95-395

[8] CHOCRON, C., ANDERSON JR, C., GROSCH, D., POPELAR, C. (2001), *Impact of the 7.62-mm APM2 projectile against the edge of a metallic target*. International Journal of Impact Engineering Vol. 25, pp. 423-437

[9] BALOS, S. (2010) *Nehomogeni dodatni razmaknuti metalni oklop za oklopna vozila*, PhD Thesis, Faculty of technical sciences, Novi Sad, Serbia

[10] SIDJANIN, L., SMALLMAN, R.E. (1992) *Metallography of bainitic transformation in austempered ductile iron*, Materials Science and Technology, Vol.8, pp 1095-1103

[11] HARDING, R.A. (2007) *The production, properties and automotive applications of austempered ductile iron*, Kovove Materialy, Vol.45, pp 1-16

[12] ERIC, O., RAJNOVIC, D., ZEC, S., SIDJANIN, L., JOVANOVIC, M.T. (2006) *Microstructure and fracture of alloyed austempered ductile iron*, Materials Characterization, Vol.57, pp 211-217

[13] BALOS, S., GRABULOV, V. SIDJANIN, L. (2009) *50CrV4 steel as a material for perforated plates in ballistic application*, Proceedings of the 10th International Scientific Conference on Flexible Technologies - MMA 2009, Novi Sad, Serbia, October 9-10, 2009, pp. 274-277

[14] ASTM A897M-03 standard, West Conshohocken, USA

[15] SMALLMAN, R., NGAN, A. (2007) *Physical Metallurgy and Advanced Materials*, Elsevier Ltd., Oxford, UK, 458

[16] RIMMER, A., (2004), *ADI solutions aid vehicle design*, FTJ, pp. 54-56

[17] RAJNOVIĆ, D., ERIĆ, O., SIDJANIN, L. (2008) *Transition temperature and fracture mode of as-cast and austempered ductile iron*, Journal of Microscopy Vol. 232, pp. 605-610

[18] KOVAČ, P., SIDJANIN, L., FIŠL, J., RAJNOVIC, D., STOJAKOVIĆ, D. (2003) *Machinability of ADI Materials on Microstructure - Level*, 2nd International Congress of Precision Machining, Prague, Czech Republic, pp. 175-179

[19] SIDJANIN, L. (1996), *Cast Iron – A Real Advanced Material, Towards the Millenium – A Materials Perspective*, The University Press, Cambridge, UK, 335-350

[20] <http://newsimg.bbc.co.uk>

[21] <http://ArmyRecognition.com>

[22] BALOS, S. (2008) *Add-on Armor for Light Combat Vehicles*, Y Report Vol. 25, pp. 47 - 53



OBSERVATION ON THE USE OF THIN FERROMAGNETIC PLATES IN PRESENCE OF EXTERNAL MAGNETIC FIELD

Jasna RADULOVIĆ, Predrag PETROVIĆ

University of Kragujevac, Faculty of Mechanical Engineering, Sestre Janjić 6, Kragujevac, Serbia
jasna@kg.ac.rs, predrag.petrovic@mfg.rs

Abstract: The thin arbitrary shaped ferromagnetic plates in the external magnetic field will be observed. In order to determine magnetic field distribution the integral equation governing magnetic scalar potential is formed with induced magnetic charges on the plate surface as unknowns. The obtained integral equations will be numerically solved using Equivalent electrodes method. The basic idea of the proposed theory is that an arbitrary shaped electrode can be replaced by a finite system of equivalent electrodes. Application of ferromagnetic plates as biomedical implants will be observed. Also, possible risk of interaction of these implants and medical devices is analyzed.

Key words: thin ferromagnetic plates, external magnetic field, equivalent electrodes method, biomedical implants

1. INTRODUCTION

Equivalent electrodes method is a numerical method for approximate solving of non-dynamic electromagnetic fields and other potential fields of theoretical physics. In recent years, this method became popular in computational electromagnetics problem solving [1-4].

The basic idea of the proposed theory is: an arbitrary shaped electrode can be replaced by a finite system of equivalent electrodes (EE). Thus it is possible to reduce a large number of complicated problems to equivalent simple systems. Depending on the problem geometry, the flat or oval strips (for plan-parallel field) and spherical bodies (for three-dimensional fields), or toroidal electrodes (for systems with axial symmetry) can be commonly used. In contrast to the charge simulation method [5], when the fictitious sources are placed inside the electrodes volume, the EE are located on the body surface. The radius of the EE is equal to the equivalent radius of electrode part which is substituted. Also the potential and charge of the EE and of the real electrode part are equal. So it is possible, using boundary condition that the electrode is equipotential, to form a system of linear equations, with charges of the EE as unknowns. By solving this system, the unknown charges of the EE can be determined and, then, the necessary calculations can be based on the standard procedures. It is convenient to use Green's functions for some electrode, or for stratified medium, in case when the system has several electrodes, or when the multilayer medium exists, and after the remaining electrodes to substitute by EE. In the formal mathematical presentations, the proposed EEM is similar to the moment method form [6], but very important difference is in the physical fundamentals and in the process of matrix establishments. So it is very significant to notice that in the application of the EEM an integration

of any kind is not necessary. In the moment method solutions the numerical integration is always present, which produces some problems in the numerical solving of nonelementar integrals having singular subintegral functions.

One of possible application of ferromagnetic plates is as biomedical implants. A significant risk to some patients undergoing Magnetic resonance imaging (MRI) is the way implanted or internal ferromagnetic material can react to the strong magnetic field and RF impulses. When implanted ferromagnetic material is exposed to the magnetic field, it can be subjected to torque and translational forces strong enough to tear surrounding tissues. MR compatibility of these devices must be demonstrated by manufacturer's declaration, [7].

2. SHORT THEORETICAL APPROACH

Let an ideal ferromagnetic body ($\mu \rightarrow \infty$) be placed in the external static magnetic field. $H_0 = -\text{grad}\varphi$, where $\varphi = \varphi(r)$ is the existing magnetic scalar potential, 'Fig.1'. Then the total magnetic scalar potential,

$$\varphi = \varphi_p + \varphi \quad (1)$$

satisfies Laplace's equation, $\Delta\varphi = 0$, and boundary condition $\varphi = C^{te}$ or $\hat{n} \times H = 0$ on the body surface, S . \hat{n} is unit vector normal to the body surface, $H = -\text{grad}\varphi$, is the total magnetic field strength and φ_p denotes the perturbed component of the magnetic scalar potential, which can be expressed as

$$\varphi_p = \oint_S \eta(r') G(r, r') dS' \quad (2)$$

where η defines the unknown induced magnetic charge surface density of the body surface and $G(r, r')$ is the corresponding Green's function. For example, Green's function of single point magnetic charge placed in the point having radius vector r' is

$$G(r, r') = \frac{1}{4\pi|r - r'|} \quad (3)$$

Using boundary condition $\varphi = C^{te}$ on the body surface, $r - r_0$, the following integral equation governing the surface charge density distribution can be formed

$$\varphi + \oint_S \eta(r') G(r_0, r') dS' = C^{te} \quad (4)$$

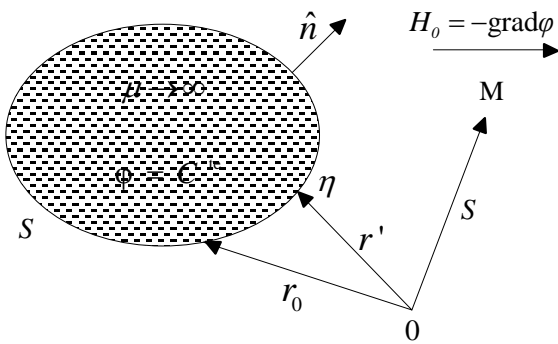


Fig.1. Ideal ferromagnetic body in an external magnetic field

The condition that the total magnetic charge of the body surface is always equal to zero,

$$\oint_S \eta(r') dS' = 0 \quad (5)$$

must be added to the integral equation (4).

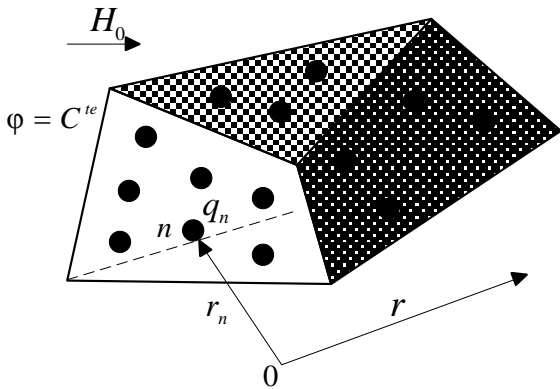


Fig.2. Application of EEM

Although an exact solution of the integral equation (4) does not exist in the general case of arbitrary shaped bodies, some numerical method can be used for solving this problem approximatively. Then is very useful the moment method [6]. In the moment method application the numerical integration is always present, which produces some problems in the numerical solving of nonelementar integrals having singular or quasi-singular subintegral functions.

The application of EEM is more convenient, because the numerical integration is not necessary. In the case of three dimensional ferromagnetic bodies the equivalent electrodes are small perfect ferromagnetic spheres having equivalent radius determined in respect to the electrode surface elements which they substitute, 'Fig. 2'. Now the perturbed component of the magnetic scalar potential (2) can be approximatively expressed as

$$\varphi_p = \sum_{n=1}^N q_n G(r, r_n) \quad (6)$$

where:

r is the field point radius vector,

r_n is the radius vector of the electrical middle point of the body surface element, or of the EE and

$q_n, n = 1, 2, \dots, N$ are the unknown magnetic charges of the EE governing the condition (5) in the following form

$$\sum_{n=1}^N q_n = 0 \quad (7)$$

N is the total number of the EE.

So the resulting magnetic scalar potential is

$$\varphi = \varphi + \sum_{n=1}^N q_n G(r, r_n). \quad (8)$$

In order to determine the unknown magnetic charges of the EE the following linear equations system, governing boundary condition on the electrode surface, can be put

$$\varphi(r_m) + \sum_{n=1}^N \frac{q_n}{4\pi\sqrt{|r_n - r_m|^2 + a_{en}^2}} = C^{te} \quad (9)$$

$$m = 1, 2, \dots, N$$

where a_{en} denotes the EE equivalent radius and δ_{nm} is Kronecker's symbol.

3. EXAMPLES

3.1. Example 1

The thin rectangular plate with sides $a, b, c \ll a, b$ in homogeneous external magnetic field, $H_0 = H_0 \hat{x}$, will be treated. Because of the existing symmetry the EE are placed only in the region $x > 0$ and $y > 0$, as 'Fig.3' shows. The approximative value of magnetic scalar potential is

$$\varphi = -H_0 x + \sum_{n=1}^N \frac{q_n}{4\pi} \left(\frac{1}{R_1} + \frac{1}{R_2} - \frac{1}{R_3} - \frac{1}{R_4} \right), \quad (10)$$

where:

$$\begin{aligned} R_1 &= \sqrt{(x - x_n)^2 + (y - y_n)^2}, \\ R_2 &= \sqrt{(x - x_n)^2 + (y + y_n)^2}, \\ R_3 &= \sqrt{(x + x_n)^2 + (y - y_n)^2}, \\ R_4 &= \sqrt{(x + x_n)^2 + (y + y_n)^2}. \end{aligned} \quad (11)$$

In order to determine the unknown magnetic charge the zero value of the potential of the plate is realized.

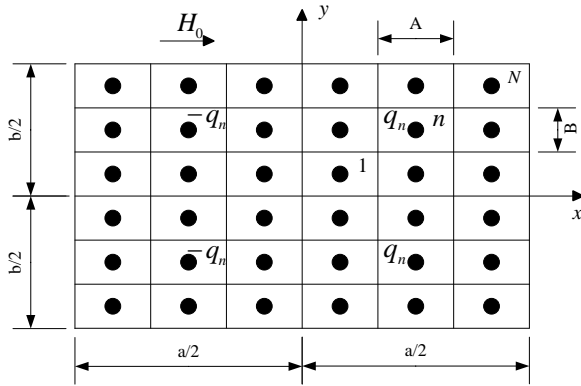


Fig.3 - Thin square plate in homogeneous external magnetic field

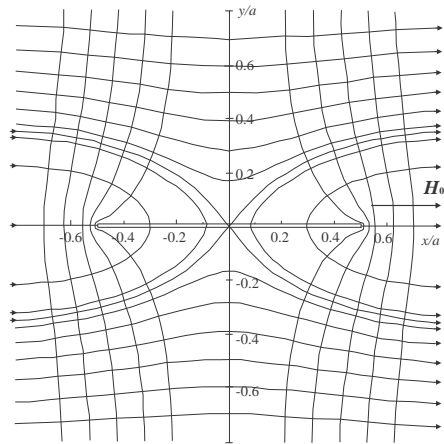


Fig.4 - Equipotential lines and lines force of thin square plate in homogeneous external magnetic field

The EE are small spheres replacing the rectangular elements with sides A and B. The equivalent radius is determined using EEM [1] with the following approximative formula

$$\frac{A_e}{A} = \begin{cases} 0.373(B/A)^{0.3882}, & 0.5A < B \leq A \\ 0.404(B/A)^{0.5}, & 0.3A < B \leq 0.5A \\ 0.696(B/A)^{0.957}, & 0 < B \leq 0.3A \end{cases} \quad (12)$$

For example, in the 'Fig.4' are shown equipotential lines and lines force of thin square plate in homogeneous external magnetic field, $H_0 = H_0 \hat{x}$. The plate with sides having length a is placed in plane $y=0$, so it is $|x| \leq a/2$ and $|z| \leq a/2$.

The formula (12) gives the value $A_e = 0.373A$ for equivalent radius of thin square plate with sides A. Using moment method [6], the equivalent radius of thin square plate with side A is $A_e = 0.37A$, which agrees very well with the presented results.

If the thickness of the square plate is not neglectable and the external magnetic field is homogeneous, $H_0 = H_0 \hat{z}$, 'Fig. 5' shows the equipotential lines and lines force.

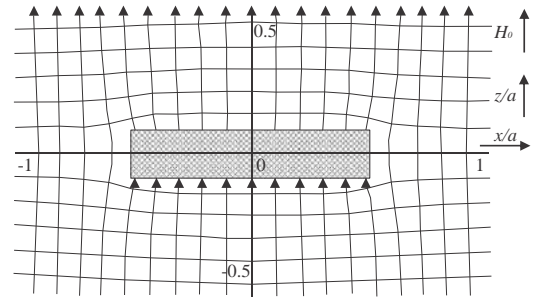


Fig. 5 - Equipotential lines and lines force of square plate in homogeneous magnetic field, for $a = b = 10c$

3.2. Example 2

The thin ideal ferromagnetic square plate with side a is placed by the side of infinite linear conductor having current I , 'Fig. 6'.

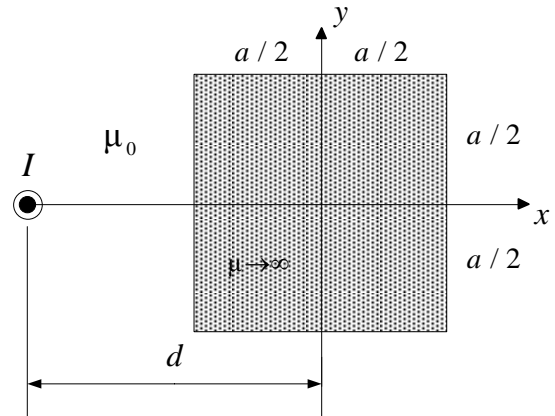


Fig. 6 - Linear conductor by the side of thin square ferromagnetic plate

The external magnetic scalar potential is

$$\varphi = -\frac{I}{2\pi} \arctg \frac{y}{x+d}. \quad (13)$$

The ratio H/H_s , for $a = 0.8d$, is presented in 'Fig. 7'. H is magnetic field strength on the upper half plate surface and $H_s = I/2\pi d$. d is the distance between the linear conductor and square plate middle point.

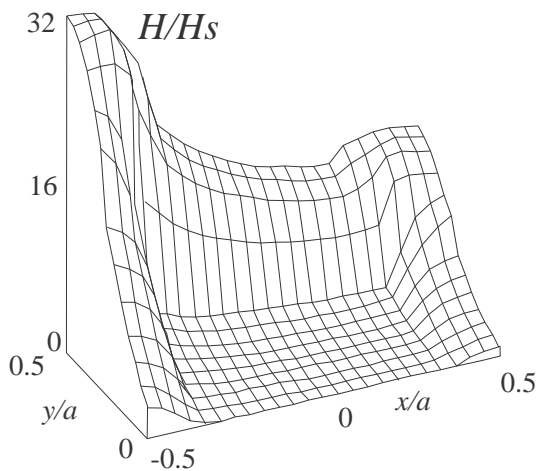


Fig. 7 - The ratio H/H_s , $H_s = I/2\pi d$, for thin square plate ('Fig.6') for $a = 0.8d$

4. APPLICATION IN MEDICINE

Bioimplants are used in dentistry, orthopedics, plastic and reconstructive surgery, ophthalmology, cardiovascular surgery, neurosurgery, immunology, histopathology, experimental surgery, and veterinary medicine. Various classes of materials such as metals, alloys, polymers, ceramics and composites have been widely used to fabricate the bioimplants [8]. Metals that are currently being used as biomaterials are gold (Au), cobalt-chromium (CoCr) alloys, type 316 stainless steel, titanium (Ti), titanium-nickel alloys (TiNi -Nitinol) and silver-mercury alloys (AgHg). These metals are chosen based on their material properties and biocompatibility. Many factors have to be considered before any particular material can be chosen, fabricated and used as a biomedical material.

For example, the aneurysm clip, placed to prevent bleeding from an intracranial aneurysm, usually contains ferromagnetic components. One possible use of a ferromagnetic implant is when they are placed near an artery to assist the collection of magnetic drug carrier particles [9]. Also, some of orthopedic implants are made from ferromagnetic materials.

The presence of a metallic implant in a patient or individual in the magnetic resonance (MR) environment may create a hazardous situation primarily due to excessive magnetic field interactions [10]. The MR environment may be unsafe for patients or individuals with certain biomedical implants or devices, primarily due to movement or dislodgment of objects made from ferromagnetic materials [10].

5. CONCLUSION

In order to determine magnetic field distribution by the side of thin ferromagnetic plates in the external magnetic field the EEM is used. Then integral equation governing magnetic scalar potential is adopted with induced magnetic charges on the plate surface as unknowns. The method is very useful in practice. Thin ferromagnetic plates in the external magnetic field can be observed like biomedical implants in presence of medical devices (MRI scanner), in sense of MR-compatibility.

6. ACKNOWLEDGEMENT

This paper is part of project III41017 Virtual human osteoarticular system and its application in preclinical and clinical practice, funded by the Ministry of Education and Science of Republic of Serbia (<http://vihos.masfak.ni.ac.rs>).

7. REFERENCES

- [1] VELIČKOVIĆ, D.M. (1996) *Equivalent Electrodes Method*, Scientific Review, Belgrade, pp 207-248
- [2] ČEŠELKOSKA, V.C. (2004) *Interaction Between LF Electric Fields and Biological Bodies*, Serbian Journal Of Electrical Engineering Vol. 1, No. 2, pp 153 - 166
- [3] VELIČKOVIĆ, D.M., RADULOVIĆ, J.J. (1998) *Thin Ferromagnetic Plate in External Magnetic Field*, Oradea, Romania, pp 24-29
- [4] RAIČEVIĆ, B.N., ALEKSIĆ, R.S. (2010) *One method for electric field determination in the vicinity of infinitely thin electrode shells*, ELSEVIER, Engineering Analysis with Boundary Elements 34, pp 97-104
- [5] SURUTKA, J.V., VELIČKOVIĆ, D.M. (1981) *Some Improvements of the Charge Simulation Method for Computing Electrostatic Fields*, Bulletin LXXIV de l'Academie Serbe des Sciences et des Arts, Class des Sciences technique, No 15, pp 27-44
- [6] HARRINGTON, R.F. (1968) *Field Computation by Moment Method*, Macmillan, New York.
- [7] DEMPSEY, M.F., CONDON, B., HADLEY, D.M. (2002) *MRI safety review*, Semin Ultrasound CT MRI 23, pp 392- 401
- [8] MANIVASAGAM, G., DHINASEKARAN, D., RAJAMANICKAM, A. (2010) *Biomedical Implants: Corrosion and its Prevention - A Review*, Recent Patents on Corrosion Science 2, pp 40-54
- [9] AVILES, M.O., EBNER, A.D., CHEN, H., ROSENGART, A.J., KAMINSKI, M.D., RITTER, J.A. (2005) *Theoretical analysis of a transdermal ferromagnetic implant for retention of magnetic drug carrier particles*, Journal of Magnetism and Magnetic Materials 293, pp 605-615
- [10] SHELLOCK, F.G. (2002) *Biomedical Implants and Devices: Assessment of Magnetic Field Interactions With a 3.0-Tesla MR System*, Journal Of Magnetic Resonance Imaging 16, pp 721-732



THE EFFECT OF VANADIUM CONTENT ON MECHANICAL PROPERTIES AND STRUCTURE OF SELF-TEMPERED STEEL X160CrMo12-1

Aleksandar TODIĆ¹, Dejan ČIKARA¹, Tomislav TODIĆ¹, Branko PEJOVIĆ¹, Bogdan ĆIRKOVIĆ¹, Ivica ČAMAGIĆ¹

¹Faculty of Technical Sciences, University of Priština, Kosovska Mitrovica, street Kneza Miloša no. 7, 38220 Kosovska Mitrovica, Serbia

todics@open.telekom.rs, dcikare@sezampro.rs, todics@infosky.net, cirkovicb@ptt.rs, icamagic@verat.net

Resume: The objective of this research was to examine the influence of vanadium on structure, hardness and strength of self-tempered steels. The tests were performed on steel type X160CrMo12-1. It is obvious that vanadium affects on the process of solidification of these alloys on such a way that narrows temperature interval of crystallization whereby from melt form V_6C_5 carbides which blocking further growth of austenite dendrite and thus helps obtaining of small-grained structure. Vanadium as an alloying element moves liquidus and solidus to higher temperatures, forms V_6C_5 carbides, partially is distributed between phases present in steel, carbide $(Cr, Fe)_7C_3$ and austenite. The existence of vanadium allows forming $(Cr, Fe)_{23}C_6$ carbides and his deposition into austenite during cooling process, in local areas around fine carbide particles transform into martensite. This means that vanadium reduces the amount of retained austenite and thereby improves the hardenability of steel.

Key words: vanadium, impact toughness, hardness, microstructure

2. INTRODUCTION

Self-hardening steels belong to the group of wear resistant steels which, makes them usable in a wide area of application. The basic characteristic of these steels is high hardness, and strength, due to its high carbon content, and relatively small impact toughness. Research carried out on one type of these steels was aimed to investigate the effect of some alloying elements on mechanical properties of materials (strength). For our investigations we used high-alloyed, high carbon steel in which chromium, molybdenum and vanadium were the alloying elements. Research has aimed to improve the characteristics of these steels, through increased resistance to abrasive and impact-fatigue wear. The main aim of this research was to obtain appropriate structure of the metallic matrix of steel and increase the tensile strength. Such a compromise can be achieved by appropriate heat treatment, to obtain a martensitic structure with lower content of retained austenite.

3. EFFECT OF CHROMIUM AND MOLYBDENUM ON THE STRUCTURE AND PROPERTIES OF STEEL

Chromium is an essential alloying element in steel with increased hardness and wear resistance. Chromium is a carbide maker element that reacts with carbon and forms hard, wear resistant carbides. Besides that, chromium prevents the transformation of austenite into pearlite during cooling, and affects the structure of the metallic matrix of steel, closing γ -area in the phase diagram. The best structure, regarding a combination of toughness and hardness, is the structure with carbides $(Cr, Fe)_7C_3$, which are formed in steel that contains more than 8% of chromium. Chromium does not increase hardenability but,

in combination with higher carbon content, has a beneficial effect on depth of hardened layer. The important parameter for hardening is the ratio Cr / C and, the higher the ratio, the higher the hardenability. Molybdenum prevents the formation of pearlite, and the transformation of austenite moves in bainitic and martensitic area. For this reason, molybdenum in small contents increases hardenability. In this way he provides obtaining hard and solid martensitic steel matrix that holds alloy carbides. Molybdenum builds interstitial phase Mo_2C having a hardness approximately 1800HV, and the increased content of molybdenum forms certain amount of this phase in the structure of steel.

3. INFLUENCE OF VANADIUM

By adding vanadium to the high alloy chromium steels, structure becomes finer. Structure refining by adding of vanadium is explained by the influence of vanadium on the crystallization process. In addition, vanadium changes the morphology of proeutectic $(Cr, Fe)_7C_3$ carbides. With increasing of the vanadium content, the radial distribution of carbides becomes dominant, but the share of long oriented lamellas and plates does not decrease, [2]. Presence of vanadium in small percentage has a positive effect on high-alloy Cr-Mo steels. It affects the process of solidification of these alloys by narrowing of the temperature interval of crystallization. Besides that, during growth of primary austenite from the melt, V_6C_5 carbides are formed in the steel structure. They block further growth of the austenite dendrites and so help to obtain the fine grain structure. In high chromium steels with the content of 12% Cr, 1.4–2.0% C and over 2.5% vanadium, the vanadium carbide, VC type, with a BCC lattice is formed [7]. VC-carbides have the globular shape and are very often associated with eutectic M_7C_3 carbides.

VC carbides can also appear in the form of rods, which grow radial from the nucleus, to form spherical eutectic cells together with the austenite grains. Higher content of vanadium enhances the formation of $(Cr, Fe)_{23}C_6$ carbides and their precipitation in the austenite grains, during the cooling process. Austenite, in local areas, around these fine carbide particles, transformed into martensite. In other words, vanadium reduces the amount of retained austenite and thus improves the hardenability of steel, [3], [4], [5].

4. DESCRIPTION OF EXPERIMENT

Research are based on self-hardening steel, with the chemical composition of 12.5% Cr, 1.2% Mo, while the

content of carbon change in the range 1.4% to 2.2%, and vanadium in the range from 0.5% to 3%.

Test samples were cast in the form of standard test samples for testing the hardness and tensile strength. Melting of steel, is carried out in the middle frequency, induction furnace *ABB type ITMK-500*. We used wooden patterns for mold making, and molds for casting are made by standard CO_2 and *Shell Molding* process. After cleaning, the castings were heat treated by hardening with subsequent tempering at a temperature of 250°C and 400°C. For all samples period of tempering was 1 hour. This type of heat treatment is characteristic for high-alloy Cr-Mo steels. For each single carbon content vanadium content is changed in the range from 0.5% to 3%. In this work, representative samples with carbon content of 1.6% were considered. Their chemical compositions are shown in the Table 1.

Table 1. Chemical composition of steel samples

Number	Group of the samples	Chemical composition				
		C (%)	Cr (%)	Mo (%)	S (%)	V (%)
1	I	1,542	11,831	1,115	0,03	0,554
2	II	1,536	11,562	1,111	0,03	1,053
3	III	1,521	11,311	1,094	0,032	1,976
4	IV	1,624	10,076	1,062	0,026	2,992

Surface of cast and heat treated samples was rough, and for this reason they were machined to the standard dimensions. Processing of samples intended for hardness testing was carried out on mechanical grinder for flat grinding. In order to eliminate any change in the microstructure of the samples, they are cooled by emulsion during grinding. Samples for tensile test are processed with ceramic tiles for processing of the hard metal surface, type *SANDVIK CNGA*, on universal lathe, and also with emulsion cooling. Dimensions of specimens for tensile tests are made according to the standard SRPS ISO 10002-1 (EU 18:1979). The tests were performed on the universal testing machine with maximum force of 200 KN. Hardness testing was performed on samples, dimensions 10x10x50, by a Rockwell-C method on the *Otto Wolpert-Werke* hardness testing machine. Testing of microstructure of steel samples was carried out with the light microscope *Olympus GX41*, equipped with a digital camera and software for image processing.

5. RESEARCH RESULTS

The research results of heat treated samples, tempered at a temperature of 250°C and 400°C, with different contents of vanadium are shown in Table 2.

5.1. Influence of vanadium on hardness and tensile strength

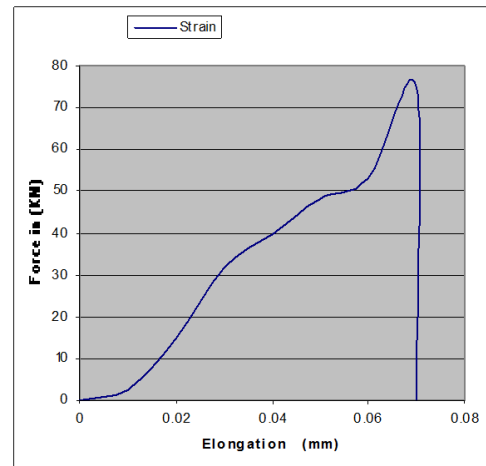
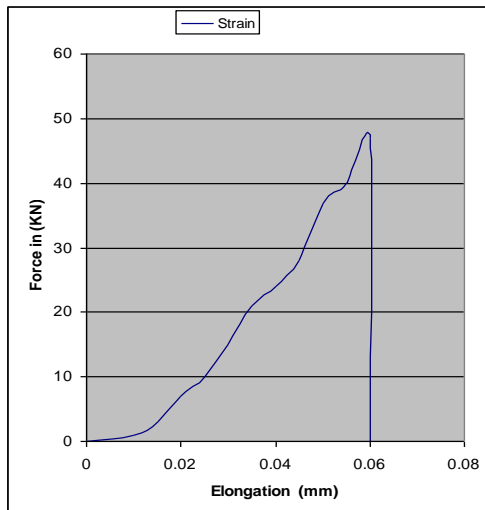
Measurement of hardness was carried out in six points in the sample, and average value is taken as authoritative. From the presented data it is evident that, with increasing of the vanadium content in the alloy, hardness decreases respectively. However, the reduction is law and the hardness remains at a relatively high level. This decrease of hardness clearly shows the increase in impact toughness. Tensile test was performed on three samples from each batch, and average value is taken as authoritative. Table 2 shows the results of tensile strength and hardness. For the illustration, characteristic diagram of tensile strength alternation in elongation is presented on the Figure 1. Analysis of the data shows that vanadium does not affect significantly on tensile strength and it remains approximately constant. In general, it could be concluded that vanadium, in that content of carbon, has no significant effect on tensile strength.

5.2. Influence of vanadium on structure

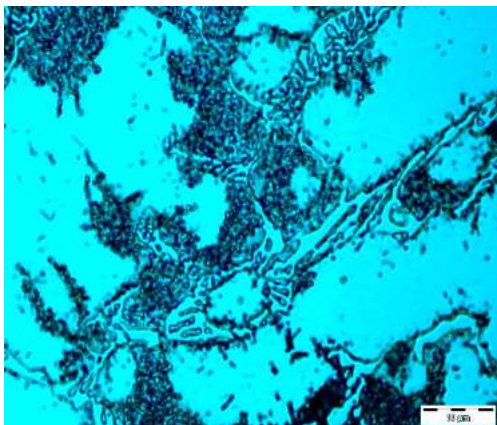
The samples are heat treated by hardening and subsequent low temperature tempering. To complete the austenitisation of the structure, the samples are previously homogenized by the annealing on 1000°C. Hardening (quenching) was performed by cooling the cold air stream, and the rate of cooling was greater than critical. On the Figures 2 and 3 are shown the microstructure of samples after heat treatment.

Table 2. Hardness and tensile strength of the samples

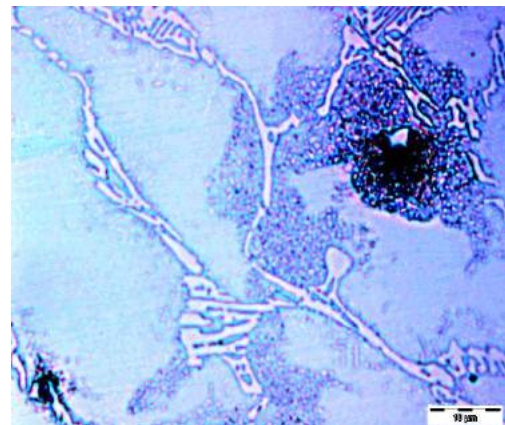
Chemical composition		Hardness [HRC]		Tensile strength [N/mm ²]	
Content C [%]	Content of V [%]	Tempered at 250°C	Tempered at 400°C	Tempered at 250°C	Tempered at 400°C
1,6	0,5	56,5	56,0	528,2	533,3
	1,0	56,0	55,4	631,2	587,0
	2,0	56,2	54,8	676,7	673,6
	3,0	55,5	53,6	645,1	641,5



Picture 1. Diagram of force change and elongation



Picture 2. Microstructure of alloys, group I



Picture 3. Microstructure of alloys, group II

In general, the structures of the samples consists of martensitic metal matrix in which are clearly visible islands of retained austenite and dispersed carbides, type $(Cr,Fe)_7C_3$, deployed mainly as a network on the boundaries of metal grains. Carbide phase, formed during solidification of eutectic, has a very oriented growth. The proeutectic austenite has been transformed into martensite and it can be seen as a dark field between carbide needles. During quenching process, primary austenite crystals and austenite from eutectic are transformed into martensite. In the process of tempering, oversaturated martensite solid solution has been transformed into cubic martensite, and carbides have remained deployed in the form of network upon the grain boundaries of metal matrix. In the Figures 2 and 3 are shown the microstructure of tested samples. The

pictures shows that with increasing of the vanadium content up to 2%, the distribution of carbides remains the same, but their size and stereologic shape are changed. Namely, the vanadium affects on the refining of structure components both, the metal matrix and the carbide network. The increasing of vanadium content in the alloy, also reduces the dispersion of carbide particles, and increases the number of finer carbides in the structure, shown on Figures 2 and 3. Vanadium is a typical carbide-maker so that built carbide V_6C_5 with the present carbon, whose content in the structure grows with increase of vanadium content in the alloy. In alloys that contain 3% V, during cooling of austenite is partly transformed into beneit, which remains unchanged during low-temperature tempering, neither in form nor in size. After heat

treatment, in structure are present small amounts of cubic martensite and retained austenite. Martensite is distributed mainly along the grain boundary of the eutectic carbide. Distribution of carbides is changed, carbide network is no more clearly expressed, and besides carbide V_6C_5 , in structure appears very hard carbide VC in a significant percentage. Changes in the volume fraction, size and morphology of the phases present in the microstructure of Fe-C-Cr-V alloy, indicate that with the increase of vanadium content, alloy composition approaches the eutectic composition in four-component Fe-C-Cr-V system, causing a decrease of temperature interval of solidification.

6. POSSIBILITY OF APPLICATION

Adding 3% vanadium in steels, quality X160CrMo12-1, forms the alloy that have very good combination of hardness and tensile strength and thereby may have wide area of application. Therefore, this steel with addition of 3% V can be successfully used for making parts and components that are exposed to abrasion, corrosion-abrasion, and impact-fatigue wear or combined type of wear. Assortment of these parts are: construction and mining machinery parts (excavators teeth and teeth covers), parts of grinders and mills for stone, ore, coal and minerals (balls, hammers, impact plates, mill linings and separation grids), wear resistant parts in process plants (mill rods for abrasive materials, blades of wheel-abrators, mud pumps bodies, molds for coal and steel scrap briquetting, tanks caterpillars etc.), [1], [6].

7. CONCLUSION

In this work were considered the effect of vanadium on hardness, tensile strength and micro structure of steel with 1.6% of carbon, 12% chromium and 1.3% molybdenum. With increasing vanadium content, structure becomes finer, which affects on the mechanical properties of steel, i.e. on the hardness and tensile strength as well as on the impact toughness. In the tested samples content of vanadium was increased; in first series 0.5% V, was added, in second 1% V, in third 2% V and in fourth 3% V. It is evident that higher vanadium content of 3% does not lead to improved properties of this steel, and for this reason, research with a greater percentage of vanadium are not included in this work. Discussion of the results given in paragraphs 5.1 and 5.2 indicates that an increased amount of vanadium has positive influence on characteristics of steel and its microstructure. Testing of samples group, with 0.5% vanadium have shown great hardness. With the increase of vanadium content up to 2.0%, the hardness slightly decreases, and tensile strength remains approximately constant. The presence of hard carbides type $(Cr,Fe)_7C_3$, V_6C_5 and VC, their content, favourable distribution and morphology, provides good abrasive wear resistance, even in cases when they are in contact with extremely abrasive materials such as silica, feldspar and others.

REFERENCES

- [1] ČIKARA D., ČIKARA D., (2001) *Otpornost na habanje, struktura i mogućnosti primene visokohromnih legura železa otpornih na habanje*, Journal of metallurgy, Vol 7 (1), pp. 45-59
- [2] RADULOVIĆ, M., (1991) *Uticao vanadijuma na mikrostrukturna i mehanička svojstva visokohromnog belog gvožđa*, Doktorska disertacija, Tehnološko-metalurški fakultet, Beograd.
- [3] FILIPOVIĆ, M., KAMBEROVIĆ, Ž., KORAC, M., (2008) *Uticao termičke obrade na žilavost i otpornost na habanje Fe-C-Cr-Nb legura*, Journal of Metallurgy, Vol 14 (4), pp. 243-252
- [4] FILIPOVIĆ, M., MARKOVIĆ, S., KAMBEROVIĆ, Ž., KORAC, M., (2005) *Uticao titana i cerijuma na mikrostrukturnu i svojstva Fe-C-Cr-Nb legura*, Journal of Metallurgy, Vol 11 (4), pp. 345-351
- [5] FILIPOVIĆ, M., (2004) *Uticao sadržaja vanadijuma i brzine hlađenja na stereološke parametre faza u strukturi Fe-C-Cr-V legura*, Journal of Metallurgy. Vol 10 (2), pp. 127-138
- [6] ČIKARA, D., RAKIN, M., ČIKARA-ANIĆ, D., (2006) *Quality optimization of steel milling balls*, Proceedings of 18th International Conference on material handling, constructions and logistics, Belgrade, pp. 131-138
- [7] YAMANAKA, N KUSAKA, K., (1955) *Influence of vanadium and molybdenum on the properties of air-hardening die steel containing 1.5% carbon and 12% chromium*, The Iron and Steel Institute of Japan, Vol 41 (6), pp. 613-620



ANALYSIS OF THE IMPACT OF EXPLOSION HARDENING PROCEDURE ON CHARACTERISTICS OF SURFACE LAYER OF ELEMENTS EXPOSED TO ABRASION

Radovan ĆIRIĆ, Emil VEG, Biljana SAVIĆ, Zvonimir JUGOVIĆ, Radomir SLAVKOVIĆ

Higher Education Technical School of Professional Studies, Svetog Save 65, Čačak, Serbia

Faculty of Mechanical Engineering, University of Belgrade, Kraljice Marije 16, Beograd, Serbia

Higher Education Technical School of Professional Studies, Svetog Save 65, Čačak, Serbia

Technical Faculty, Svetog Save 65, Čačak, Serbia

Technical Faculty, Svetog Save 65, Čačak, Serbia

radovan.ciric@vstss.com, emilveg@eunet.rs, biljana.savic@vstss.com, zvonko@tfc.kg.ac.rs, slavkovic@tfc.kg.ac.rs

Abstract: In this paper, we have presented the results of studying the characteristics of surface layer of mills hammer with explosion hardening. Based on metallographic analysis and testing the hardness, it was determined that explosion hardening leads to extreme increase of surface layer hardness and microstructure change. Results show that a hardened layer up to 10 mm depth can be obtained by this procedure. The biggest effect of hardening (hardness up to 593 HV02) and the formation of martensitic structure are achieved in surface layers of cast steel.

Key words: wear-resistant steel, abrasion, explosion hardening, hardness, microstructure.

1. INTRODUCTION

Austenitic manganese steels have high resistance to abrasive wear and a rather tough core. Toughness of this steel is achieved by austenitization with subsequent rapid cooling in water (quenching). The aim of this process is to achieve the dissolution of carbide phase in solid austenite solution. Resistance of these steels to abrasion is increased with the increase of hardness, which is achieved by the process of plastic deformation of surface layers, where martensitic structure occurs [1, 2, 3].

In accordance with vertical cross-section of the system diagram Fe-Mn-C, Fig. 1., steel with 1,2-1,3% C and 13% Mn in cast condition at temperatures above 940°C has a stable austenitic structure. Below that temperature field, complex carbide particles $(FeMn)_3C$ are extracted from solid solution, while at the temperatures below 600°C, there is also a ferrite phase. Below 400°C, the structure consists of ferrites and carbides $(FeMn)_3C$ [4].

Mechanism of these steels hardening under the impact of cold plastic deformation is still not completely explored. There are opinions that this mechanism is not significantly different than the conventional deformation mechanism. It is considered that the deformation takes place by doubling mechanism, but there are the views that hardening mechanism of these steels with fine grain is based on the interaction of doubling and dislocation changes. According to [5], with these steels exposed by explosion, the presence of ϵ -martensite and α -martensite was determined.

Method of surface layer hardening of high alloy manganese steels by explosion is a relatively new technological procedure [2].

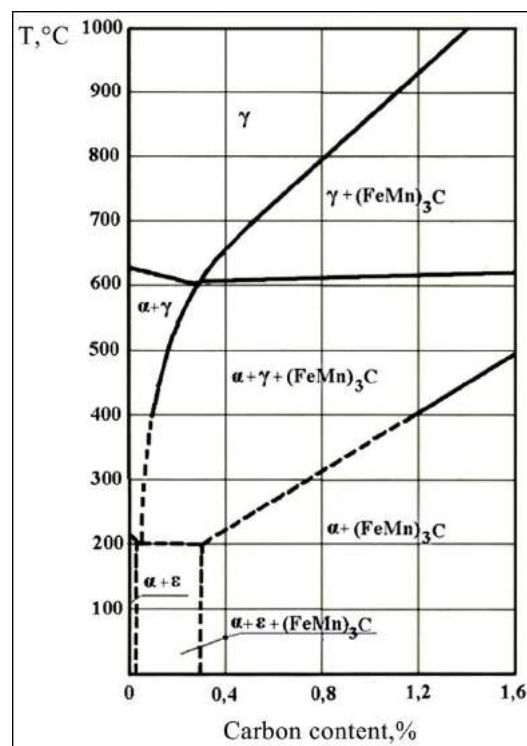


Fig.1. Vertical cross-section of system diagram Fe-Mn-C for steel with 13% Mn [4]

According to literature sources, hardened layer, up to 25 mm thickness, can be obtained. Main parameters of the regime are type and quantity of explosives. As a result of the explosion, there is an impact tension of order size of tens GPa that affects the hammer surface layer.

Process takes place at extremely high deformation rates. Effects of explosion hardening can be quantified by examination of mechanical properties and materials microstructure. The same [1] can be followed during the process itself with the assistance of very rapid cameras, as well as after the deformation on the basis of displacement analysis and other defects.

Mechanical systems in mining (elements of working and walking part of the excavator, mills and other systems that are in contact with tailing and ore) are exposed to abrasive wear. As a rule, mechanical parts on these systems are subject to shock loads, and in their case, in addition to high resistance of surfaces to wear, tough core is also required [6, 7, 8].

Hammer of the mill for grinding ore works in the conditions that can lead to a catastrophic failure. In its case, high resistance of the working part to impact abrasion is required, as well as high resistance of the core to brittle fracture. Usual solutions are the development of the same of high alloy Mn-steel or low alloy steel with improved core and high hardness of the working part. In literature, there are also data about hammer development of bimetallic materials.

The aim of this paper is the analysis of microstructure change and hardness of surface layer of mill's hammer of 120Mn12 (ČL 3160) explosion hardened steel.

2. DATA ON MATERIAL AND EXPERIMENT

Experimental explosion hardening is done on the hammer of the mill for grinding coal in slacked condition, Figure 2.

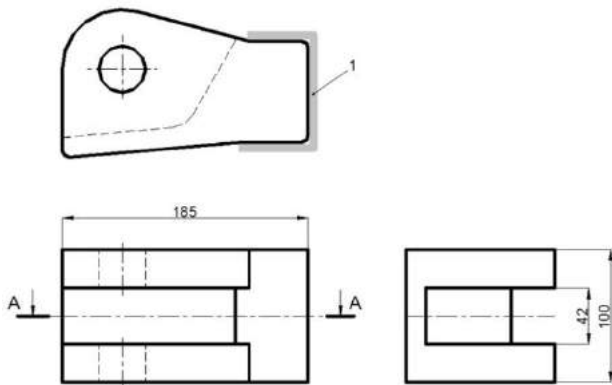


Fig.2. Mill hammer of cast steel 120Mn12
1-layer of explosive

Hardened working surfaces are coated with a layer of plastic explosive that is 5 mm thick, 1 in the Figure 2.

As a means of causing the explosion, plastic high explosive of filled weight from 0,5 – 0,7 g/cm³. Detonation velocity of explosives is 7000 – 8000 m/s, where the stresses of the size order of tens GPa are achieved.

After explosion hardening, there was a detailed examination of hardness in characteristic cross-sections (directions), metallographic analysis and non-destructive testing.

3. RESULTS AND DISCUSSION

3.1. Hardness of 120Mn12 after explosion hardening

Hardness of 120Mn12 after explosion hardening is measured in the cross-section A-A (plane of hammer's longitudinal symmetry), fig.2 in selected directions I – VII, fig. 3.

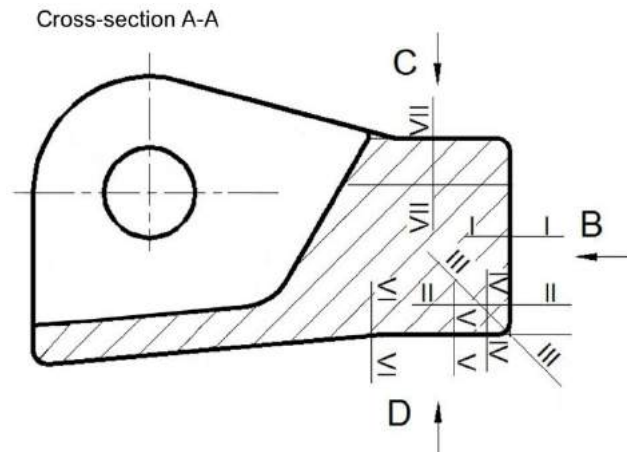


Fig.3. Schematic view of the place of hardness measurement (directions I-I to VII-VII)

Results of hardness measurements, according to Vickers method in measurement direction according to fig. 3, are given in fig. 4.

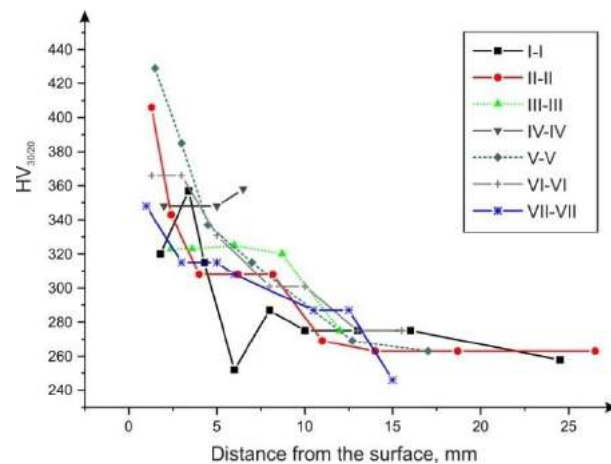


Fig.4. Hardness of explosion hardened surface layer of hammer made of 120Mn12 cast steel

Based on the results, it was determined that the greatest hardness was achieved close to the frontal area B (406 HV). Depth of hardened layer with hardness greater than 300 HV in the direction I-I is 4,3 mm, and in the direction II-II - 8,2 mm.

The greatest hardness measured on lateral surface is C (VII-VII) is 348 HV, while the depth of layer with hardness above 300 HV is 6 mm.

On the lateral surface D, directions IV-IV, V-V i VI-VI, a hardness up to 366 HV was achieved. Depth of hardened layer of hardness above 300 HV is more than 6,5 mm (IV-IV), more than 7 mm (V-V) and about 10 mm (VI-VI). In general, the highest hardness on working surfaces B, C and D is achieved in zones close to angles. Results of micro-hardness measurement in cross-section VII, fig. 5., show that micro-hardness of surface layer is significantly higher than the hardness determined by the method HV₃₀.

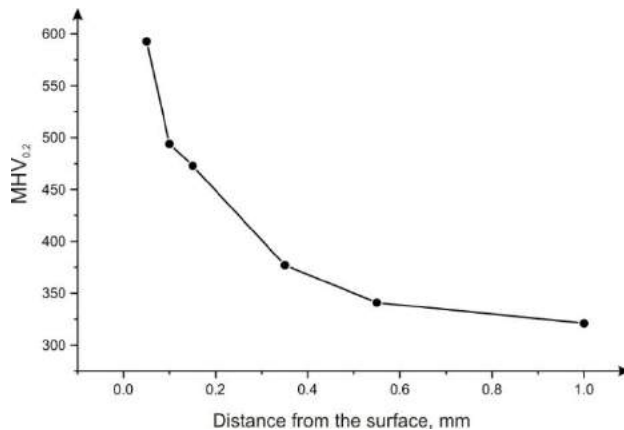


Fig.5. Microhardness of 120Mn12 after explosion hardening in the function of distance from the surface

The results given in fig.6 show that maximum measured hardness is 593 MHV_{0.2}, and that the hardness above MHV_{0.2} is achieved to the depth of 0,15 mm minimum.

3.2. Examination of microstructure

Microstructure of surface layer in which there came to explosion hardening is given in Fig. 6. Basic micro-constituent in the structure is martensite (dark needles). In microstructure, there is also a significant proportion of retained austenite (fields with no martensite needles) and carbides. The dark zones in Fig. 6 are gas pores or non-metal inclusions.

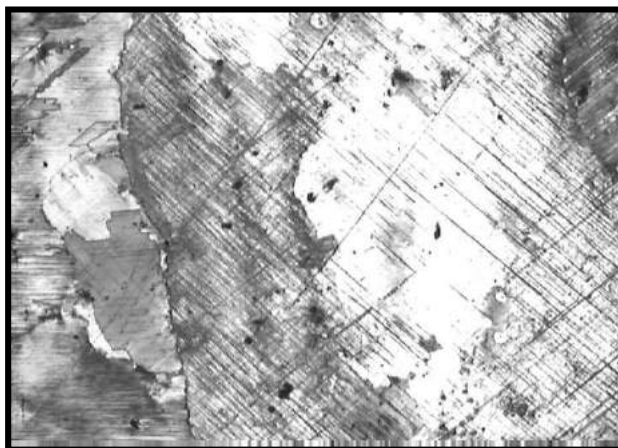


Fig.6. Microstructure of hammer made of 120Mn12 cast steel in the explosion hardened field

Austenitic structure of hammer outside of the field where explosion hardening occurred is given in fig. 7.

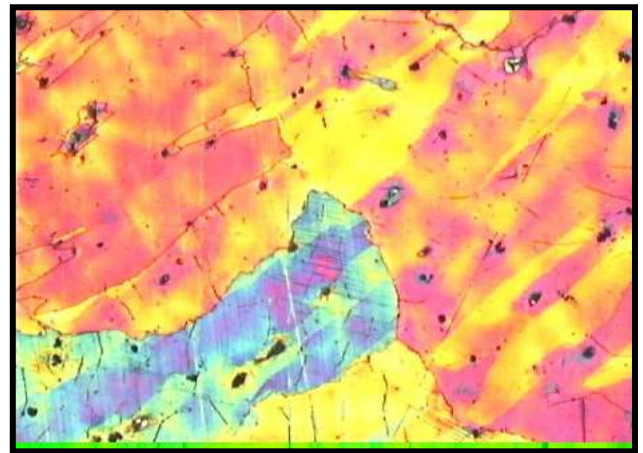


Fig.7. Microstructure of basic material (core) of the 120Mn12 hammer

At particular samples in the core of the impact part of the hammer, there are macroscopic defects present, such as cracks due to shrinkage during hardening, non-metallic inclusions in grain boundaries and grain, gas pores. Determined macroscopic defects have occurred during the casting in the process of hardening the central part of the drip moulding. High presence of non-metallic inclusions, even gas pores, in central part of drip moulding, and the other zones to a certain extent, as well as big austenitic grain, indicate that casting process is not optimally performed.

4. CONCLUSION

The process of explosion hardening leads to big changes of mechanical characteristics and microstructure of surface layer. Main effects that lead to the increase of hardness are cold plastic deformation and the occurrence of martensitic structure. Due to the shape of hammer, and with the same thickness of the explosive used, the effects of hardening are significantly different in different zones. Measured depths of hardened layer are, depending on measurement zone, within the limits of 4,3 – 10 mm. The highest micro-hardness of hardened layer of 593 HV_{0.2} was measured in surface layer of the sample. Micro-hardness above 400 HV_{0.2} is reached to the depth of 0,15 mm, minimum.

The applied process of explosion hardening has not caused cracks in surface layer, as well as the expansion of the existing macroscopic defects in the central part (core) of the hammer.

5. ACKNOWLEDGEMENTS

This paper is a result of the project with the serial number 35037, founded by the Ministry of Science and Technological Development. Writing the paper helped Concern "Farmakom M.B.", IKG – "Guča".

REFERENCES

- [1] EFSTATHIOU, C., SEHITOGLU, H. (2010) *Strain hardening and heterogeneous deformation during twinning in Hadfield steel*, Acta Materialia 58, pp 1479–1488.
- [2] ZHANG, F., LV, B., WANG, T., ZHENG, C., ZHANG, M., LUO, H. and LIU, H. (2008) *Microstructure and Properties of Purity High Mn Steel Crossing Explosion Hardened*, ISIJ International, Vol. 48, No. 12, pp. 1766–1770.
- [3] KOPAČ, J. (1982) *Težavnost obdelave obrabno odpornih avstenitnih jekel – 12 Mn*, Zbornik radova XVI Savetovanja proizvodnog mašinstva Jugoslavije, Mostar, s. 67-70.
- [4] http://www.nbu.gov.ua/portal/natural/Ptz/2008_50/64-69%20Text.pdf, maj 2011.
- [5] ВЕРЕЗИНАЈ, В. Н. и др. (1981) *Физика и химија обработки материјалов*, 1, с. 60.
- [6] JUGOVIĆ, Z., ĆIRIĆ, R., KATANA, R. (1996) *An investigation of double layer metallic materials used for elements that wear*, Science of Sintering, 28 spec. Issue, s.197-202.
- [7] ĆIRIĆ, R., JUGOVIĆ, Z., RADOŠEVIĆ, M. (2002) *Primena navarivanja u reparaturi elemenata izloženih abrazivnom habanju i udarnim opterećenjima*, Zavarivanje i zavarene konstrukcije, 1, str.17-21.
- [8] ĆIRIĆ, R., JUGOVIĆ, Z., RADOŠEVIĆ, M. (1999) *Vозможности примененија наплавки дјла востановленіја детаљ испитивајућіх абразивни износ*, The 3-rd International Conference MET-99, June 1999, Riga, Latvia.

34th INTERNATIONAL CONFERENCE ON PRODUCTION ENGINEERING



SECTION C

**PRODUCTION ENGINEERING – NEW TECHNOLOGIES AND GLOBALISATION OF
ENGINEERING**



WEB-BASED COLLABORATIVE ENVIRONMENT FOR PROCESS PLANNING

Mijodrag MILOŠEVIĆ, Velimir TODIĆ, Dejan LUKIĆ

Department of Production Engineering, Faculty of Technical Sciences, Trg D.Obradovića 6, Novi Sad, Serbia
mido@uns.ac.rs, todvel@uns.ac.rs, lukicd@uns.ac.rs

Abstract: Advances in information technologies have enabled designers to more effectively communicate, collaborate, obtain, and exchange a wide range of design resources during development. Web-based design environment is a new design paradigm for product development.

This paper presents a framework for distributed and collaborative environment, which could assist manufacturing organizations to evaluate, optimize, and select process plans for groups of manufacturing parts. The proposed system emphasizes the integration of the software tools and the resources involved in the design process to enable collaboration of geographically dispersed design teams and process planning experts.

Key words: Digital Manufacturing, e-Manufacturing, Collaborative Engineering, Process planning, CAPP

1. INTRODUCTION

Shortening of product life-cycle and frequent changes in production programs have influenced the need for ever-faster and efficient transfer of information between engineers and other participants in design and manufacturing process.

In recent years, the Internet and local area networks have greatly increased the integration of engineering work, equipment, and other components which are required for design and manufacture. Introduction of digital documents has led to a novel, modern way of operation, vastly contributing to modern society. Digitalization has introduced numerous innovations into the area of product development.

Within the modern environment, manufacture of complex products often takes place in a number of small and medium enterprises, taking the form of distributed manufacture. Single enterprises are specialized in partial manufacturing processes. Complex products consisting of a large number of parts, components, and modules, are assembled into functional units within a single enterprise but need not necessarily be produced under a single roof. Therefore, better coordination is in order between geographically dispersed teams collaborating on the same project.

2. DIGITAL MANUFACTURING

Digital manufacturing represents a technology, or discipline which offers strategic approach to development, implementation, and optimization of all elements of manufacturing process. The term 'digital manufacturing' implies a network of digital models and methods which define all aspects of manufacturing process. Digital manufacturing environment represents a combination of digital product and digital processes and

resources [1]. This requires a common framework which integrates virtual model of manufacturing with its real physical counterpart. Digital manufacturing allows efficient monitoring and improvement of manufacturing process through utilization and control of data pertaining to development, planning, and validation of manufacturing processes. The goal is to integrate the data from various departments in the domain of product design and manufacture.

Exchange of information and engineering collaborative processes are crucial for digital manufacturing, as well as for optimization of manufacturing [2], Fig. 1.

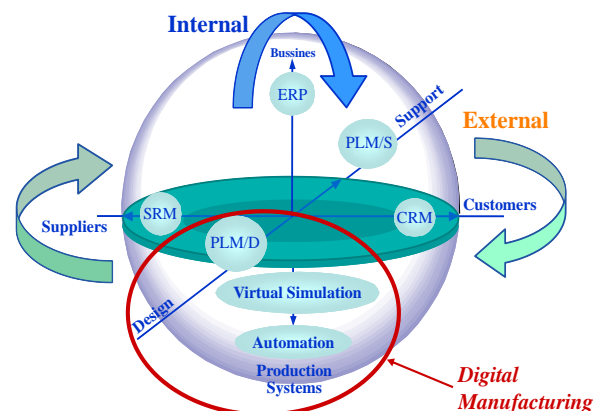


Fig. 1: Digital manufacturing's position in the collaborative manufacturing management model [3]

Today's trend of accelerated advancement of Internet technologies allows development of distributed software applications which surpass traditional physical and chronological limitations, helping us to connect geographically dispersed users, systems, resources, and services. By means of web-based collaborative systems, designers and engineers can exchange and share tasks and

knowhow on a global level, using Internet/intranet networks, Fig. 2.

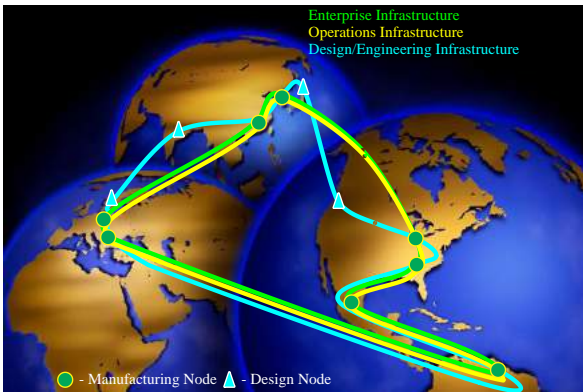


Fig. 2: An example of a global manufacturing infrastructure [4]

3. e-MANUFACTURING

3.1. The concept of e-Manufacturing

In a wider sense, electronic manufacturing (*e-Mfg*) can be described as an **application of Internet in manufacturing**. Electronic manufacturing integrates buyers, systems, electronic shops, and suppliers in a single manufacturing process, thus creating a strategic framework for manufacture which is based on Internet technologies. This concept is most often applied in hi-tech industries, but is also common in companies which integrate the Internet into their manufacturing processes in order to boost profits. Modern companies utilize Internet for various forms of e-Commerce and e-Business, but also to create manufacturing environment, i.e., the e-Manufacturing. Various Internet services allow the transfer of information regardless of distances, as well as the control of manufacturing processes which involves manipulators, robots, CNC machines, and other similar industrial equipment. The synthesis of Internet

technologies and the concept of digital factory constitutes a framework for e-Manufacturing.

From the aspect of global hierarchical levels within e-Manufacturing one can discern between two primary groups of activities: engineering, and manufacturing, Fig. 3. On an inter-company level, the engineering aspect includes a so called *Engineering Chain* which allows realization of required engineering tasks.

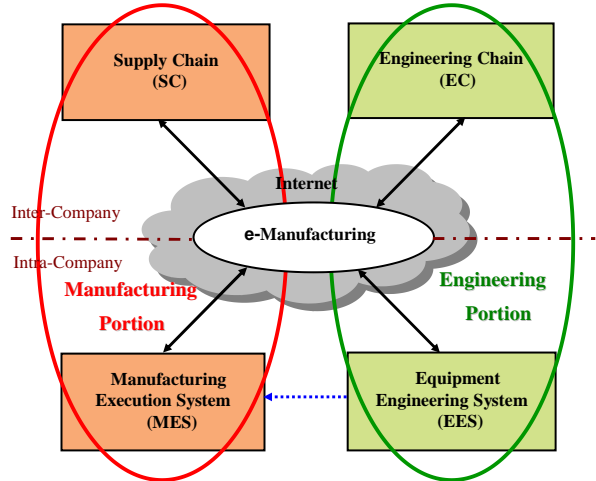


Fig. 3: e-Manufacturing components [5]

3.2. Engineering Chain

The Engineering Chain on an inter-company level, and the in-house systems of engineering equipment represent the basic infrastructure necessary for execution of engineering processes within e-Manufacturing. This Engineering Chain represents a network of engineering objects and services, Fig. 4, which allow product design and process planning based on valid engineering data. In addition, manufacturing process is monitored by means of the systems of engineering equipment and executive manufacturing systems.

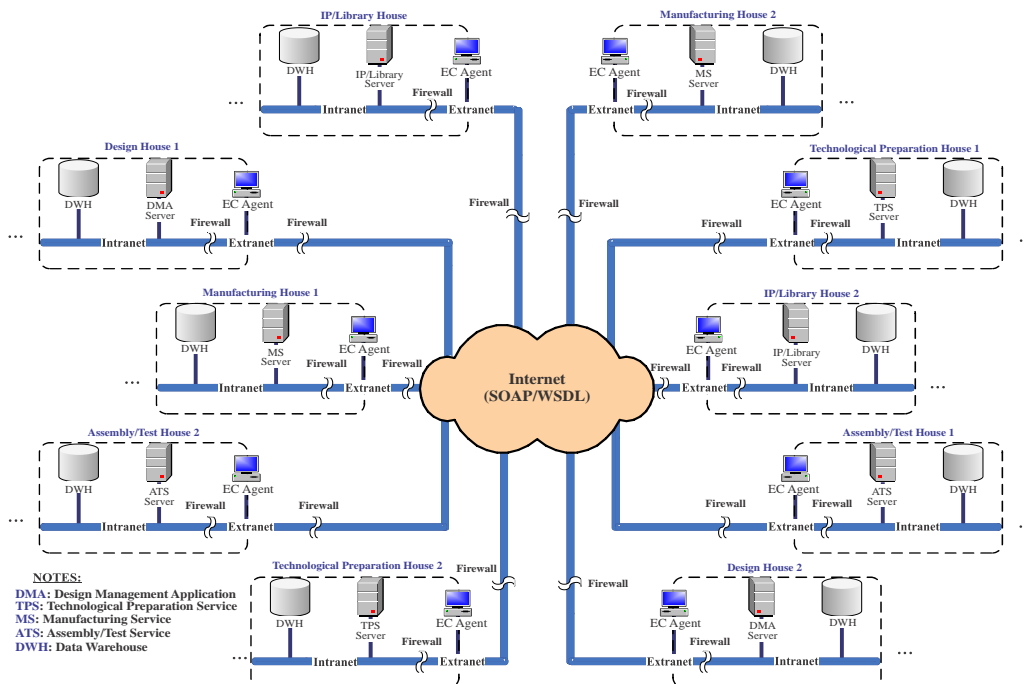


Fig.4: Vision of global Engineering Chain system [6]

4. COLLABORATIVE PROCESS PLANNING

4.1. Collaborative design environment

Collaborative environments for integrated design allow various groups involved in design process to work together on the development of an efficient digital model which pertains to a product or process. Such approach opens new possibilities in the domain of marketing analysis, multi-criteria product design assessment, and manufacturing process plan variants, optimization of product characteristics with the aim to increase quality, reliability, productivity, easy assembly and maintenance.

Shared virtual environments allow engineers in remote locations to analyze a virtual prototype together and simultaneously in a center where the product is being developed, Fig. 5. Moreover, such environments allow engineers and designers to gain better understanding of products, increasing the quality and providing design for manufacture from the very beginning, thus reducing the need for expensive re-work during later stages of development.



Fig. 5: Global collaborative design environment

Present-day CAD/CAPP/CAM and CAE systems incorporate Internet support for collaborative engineering. This support allows designers to compare and harmonize their model with those of other designers which share the common collaborative environment.

4.2. Process planning collaborative environment

Process planning for manufacturing is one of key tasks which need to be solved in a distributed manufacturing environment in which various companies and engineers take part in collaborative product development. In such environments, the activities related to process planning are often realized by means of CAPP systems. Thereby, procedures are applied which take engineering drawings, bills of materials, and other manufacturing specifications to identify and select appropriate machining processes, resources, sequences and other parameters necessary to transform a blank into a finished product. However, the knowledge implemented into a typical CAPP system is subject to frequent updates with newly acquired expert knowledge. Market conditions are constantly changing, while the prices, terms of delivery, and production volumes require modifications of current process plans [3]. In order for these modifications to be of high quality and as efficient as possible, expert knowledge is required [7].

Shown in Fig. 6 is an example of a web-based collaborative process planning environment within a company which manufactures a group of products. Beside various CAX systems and human resources within the company, the collaborative environment also includes geographically dispersed experts which are nevertheless included in the collaborative process via Internet. External associates cooperate in the process planning and evaluation, on a par with in-house experts and engineers.

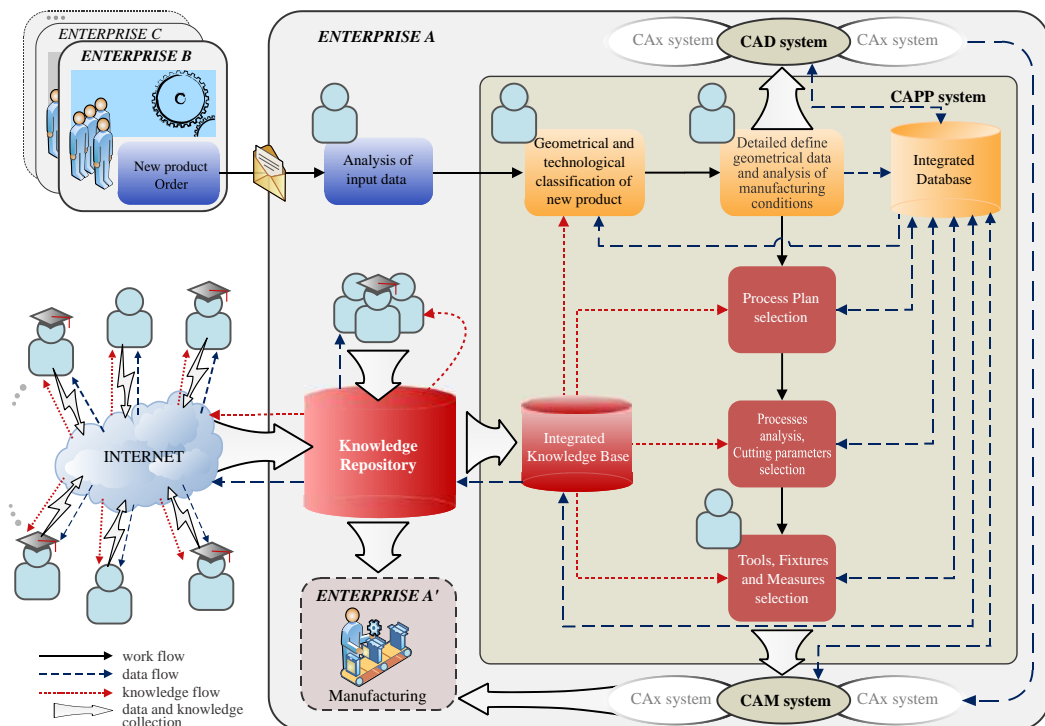


Fig. 6: Workflow activities and information flow in the web-based process planning collaborative environment

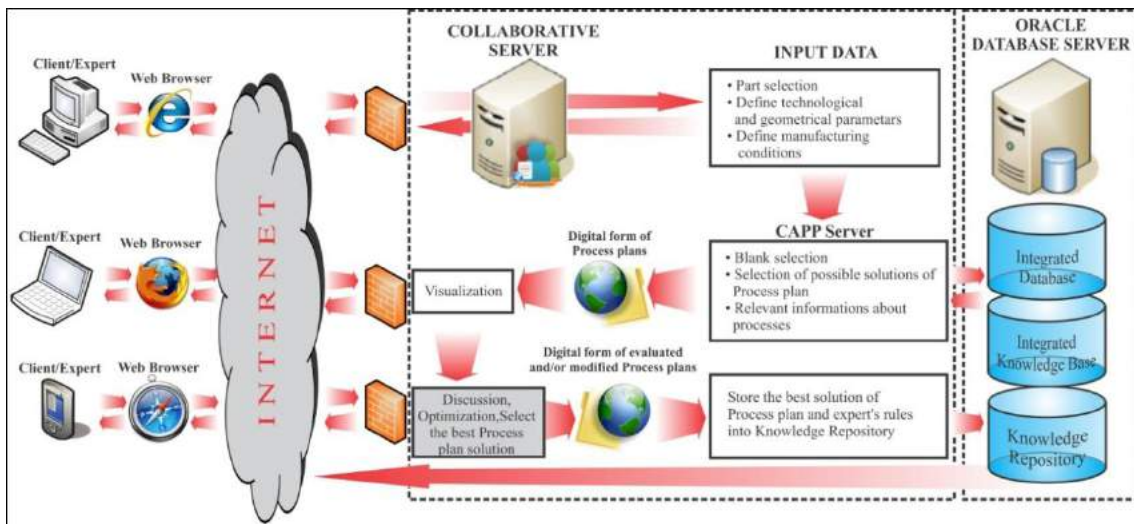


Fig. 7: Architecture of the web-based process planning collaborative system

Figure 7 shows the proposed three-tier architecture of a process planning collaborative system. In addition to clients, i.e., experts whose number is not limited, also includes collaborative- and database servers. This collaborative system provides expert analysis, discussion, and evaluation, which results in an optimal process plan for the given production conditions. Furthermore, experts are not expected to use any of the commercially available software systems for process planning or interaction with collaborative environment, due to the fact that the collaborative process takes place exclusively through a web browser, Fig. 8.

overwhelmingly changing the traditional way of thinking and doing business within the manufacturing industries. The proposed web-based environment, dedicated to collaborative process planning for manufacturing, represents another step in the direction of advancement of modern distributed manufacturing.

REFERENCES

- [1] VELASQUEZ, J., NOF, S. (2009): *Collaborative e-Work, e-Business, and e-Service*, Springer Handbook of Automation, pp.1549-1573.
- [2] WANG, L., NEE, Y.C.A. (2009) *Collaborative Design and Planning for Digital Manufacturing*, ISBN 978-1-84882-286-3, Springer-Verlag London Ltd.
- [3] SILLER, H.R., ESTRUCH, A., VILA, C., ABELLAN, J.V., ROMERO, F. (2008): *Modeling Workflow Activities for Collaborative Process Planning with Product Lifecycle Management Tools*, Journal of Intelligent Manufacturing, Vol.19, No.6, pp.689-700.
- [4] SLANSKY, D. (2007) *PLM & Digital manufacturing: Integrating PLM with the Shop Floor - vision experience*, The Organization for Machine Automation and Control - OMAC
- [5] CHENG, K., BATEMAN, R.J. (2008): *e-Manufacturing: Characteristics, Applications and Potentials*, Progress in Natural Science, Vol.18, No.11, pp.1323-1328.
- [6] CHANG, Y.C., CHENG, F.T., WANG, T. LI (2007) *Novel Semiconductor BusinessModel - Engineering Chain for the Semiconductor Industry*, IEEE International Conference on Robotics and Automation, Roma, pp. 1597-1602
- [7] MILOŠEVIĆ, M., TODIĆ, V., LUKIĆ, D. (2009) *Model Development of Collaborative System for Process Planning*, Journal of Production Engineering, Novi Sad, ISSN 1821-4932, Vol.12, No.1, pp. 95-98.



Fig. 8: Access to the online process planning collaborative system through a web browser

5. CONCLUSION

Efficient exploitation of novel design and manufacturing technologies is possible only within a flexible and collaborative working environment. In addition, the Internet technologies are rapidly and



ANALYSIS OF KINEMATIC CHARACTERISTICS OF MACHINE TOOLS USING A VIRTUAL MODEL

Slobodan TABAKOVIĆ, Cvijetin MLAĐENOVIĆ, Milan ZELJKOVIĆ, Ratko GATALO

Faculty of Technical Sciences, Trg Dositeja Obradovića 6, Novi Sad, Serbia
tabak@uns.ac.rs, mladja@uns.ac.rs, milanz@uns.ac.rs, gatalora@uns.ac.rs

Abstract: Designing of modern machine tools is a procedure which requires great effort of the designer, and which includes quick and detailed analysis of their kinematic and dynamic characteristics in exploitation. Thus, in recent times, design and analysis of machine tools is performed by using a virtual models that describe the geometric and kinematic structure of the machine.

This paper presents the kinematic analysis of the elements of machine tools in its virtual model formed in the module of program system Matlab, SimMechanic. The analysis was done on the example of machine tools based on parallel mechanisms.

Key words: Machine tools, parallel mechanism, virtual model, kinematic analysis, SimMechanic

1. INTRODUCTION

In the conditions imposed by a contemporary market for a long time period, the behaviour estimation of the product in the exploitation creates requirements for its improvement from the very development process. In the prior periods, physical prototypes of a product were maximally utilized for the verification of the theoretical exploitation characteristics. Considering the fact that their manufacturing is rather expensive and long, virtual prototypes originating from the integration of diverse specialized disciplines into the engineering process for the product's design and manufacturing have been more and more utilized with the same purpose in recent times.

Observing machine tools, the increase in market demands from the aspects of productivity and accuracy of the machining process makes it necessary to employ new methods and tools during their improvement. As an efficient means for achieving the set requirements in the shortest time period possible, the solution proved to be a concept of designing a virtual model, i.e. virtual prototype, a machine tool describing the geometric and kinematic structure of the machine itself.

Figure 1 illustrates the time saving achieved by applying virtual prototypes in the process of machine tool design.

The application of a virtual model of a machine tool during its design process greatly simplifies the testing of a great number of proposed design solutions in the early design phase. Likewise, it also enables: fast and detailed analysis of kinematic and dynamic characteristics of a machine in exploitation; estimations of functionality, efficiency and safety of a machine tool; basic operator training; or the presentation of the designed machine for marketing purposes. Modelling, testing and alterations of physical prototypes for the above mentioned purposes are very costly and impractical.

The paper presents certain analyses of the virtual model of a machine tool performed during the design process.

2. PROCEDURE FOR FORMING THE VIRTUAL MODEL OF A MACHINE TOOL

A virtual model of a machine tool presents its geometric or symbolic description that can be utilized for the analysis of the product it represents by applying adequate programme systems. The analysis most often implies the simulation of the behaviour of the machine tool elements in exploitation conditions.

This research describes the procedure for forming a symbolic model of a machine tool by applying a functional module of the programme system Matlab, known as SimMechanic.

For the analysis, a machine tool with a hybrid, parallel – serial, kinematic structure of the type biglajd has been selected. This mechanism type has been chosen due to its specific kinematic structure made of a planar parallel mechanism that is translated along one axis providing a basis for a simple three-axes machine tool (Figure 2).

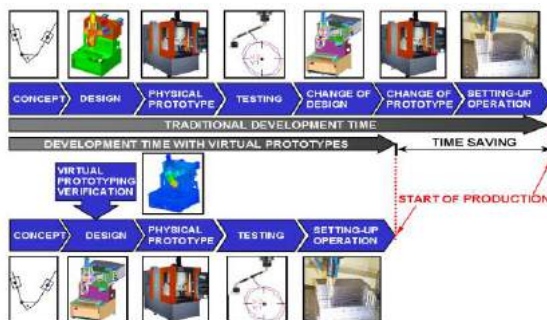


Fig. 1. Shortening the machine tools design process by applying virtual prototypes [1]

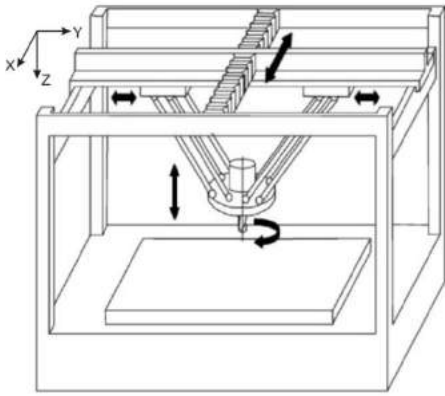


Fig. 2. Machine tool with a hybrid kinematic structure of the type biglajd [8]

2.1. Symbolic modelling

Symbolic modelling refers to the description of a physical model by connecting adequate symbolic blocks. Each of the mentioned blocks contains information on the following:

- Physical properties of the machine elements (inertia matrices, mass matrices, coordination systems, etc.),
- Connections between them (joints),
- Environment influences (stimuli), and
- Management – monitoring elements (mutual influences and monitoring elements, feedbacks, etc.)

In order to use a certain block to describe a physical element of a machine tool (platform, rod, guide, etc.), it is necessary to define its: dimensions, physical characteristics, and spatial orientation. Connections between elements are describes by connections that, depending on demands, can be of guide, joint and rigid connection types, and with them it is possible, on a virtual model, to present any connection between two elements of a machine tool. To obtain as authentic results as possible, during the process of analysing a virtual model, it is also necessary to define the environment influence on a machine tool, friction and resistance between moveable elements, power engines that perform stimuli, as well as segments presenting the obtained results [5].

As an illustration, Figure 3 presents a series of blocks to describe a simple mechanism of a physical swing type comprising a single body that is linked to the fixed base with a universal joint.

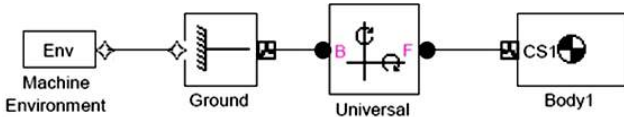


Fig. 3. An example of a mechanism model formed in Matlab SimMechanic

2.2. Visualisation of a virtual model

For a better insight into the movements that the formed model exhibits in space, there is a segment for the model visualisation in the programme system Matlab. It can be employed in two manners:

1. Generating the VRML model of the mechanism in the SimMechanic. In this manner, the geometry of individual elements of the kinematic structure of a machine tool is generated on the basis of information on dimensions and moments inertia input into individual blocks. Hence a simple VRML model made of fundamental geometric shapes – primitives (cylinder, sphere, slab, etc.) is generated. Figure 4 presents a VRML model of a biglajd mechanism formed for further analyses in this paper.

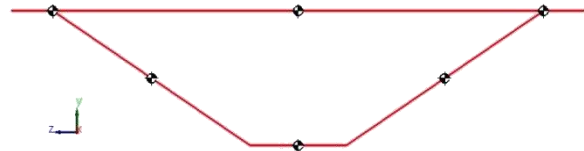


Fig. 4. VRML model of a biglajd mechanism

2. Linking a detailed geometric mechanism model formed in one of the CAD programme packages with the adequate blocks of the virtual model created in SimMechanic. In such a manner, one obtains a virtual model that is geometrically more similar to the physical model of the machine tool with a more complete and realistic visualisation.

3. DEFINING A VIRTUAL MODEL OF A PARALLEL MECHANISM OF THE BIGLAJD TYPE

For defining a model of a hybrid mechanism of the type biglajd and for its engineering analysis, the method of symbolic modelling with the visualisation of mechanism elements by generating the VRML model in Matlab SimMechanic has been applied.

The generation of the virtual model of the biglajd mechanism is performed in such a manner that all mechanism elements are described by appropriate blocks forming a scheme adequate to the biglajd mechanism. This scheme, actually, presents its virtual model illustrated in Figure 5.

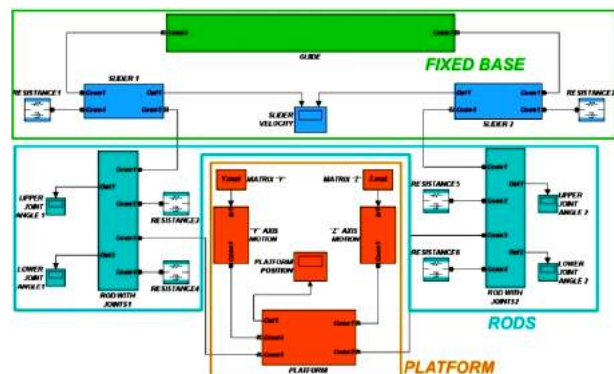


Fig. 5. Virtual model of the mechanism type triglajd formed in Matlab SimMechanic

In the figure, one can observe three units that represent individual complex elements of the biglajd mechanism. These are the mechanism base made of a guide and sliders, moveable platform, and rods connecting the base and the moveable platform. Inside these subunits there are also complex blocks originating from the integration of simpler elements; e.g. rods, beside the rod itself, also have two joints on its ends.

3.1 Realized analyses

As already stated, one can perform several types of analyses on virtual models of machine tools (and mechanisms in general), providing an insight into the behaviour of individual elements, as well as the entire mechanism in exploitation. In this case, virtual models are used for analysing the following:

- Position and orientation of individual mechanism elements in the entire working space of the mechanism
- Kinematic characteristics of the vital moveable elements

3.1.1 Working space analysis

During the conducted research, one of the main goals has been the set demand to examine the behaviour of all vital mechanism elements (sliders, joints and rods) in the overall working area (Fig. 6). Dimensions and the shape of the working space of the mechanism were obtained by analytical methods in earlier research phases, and they were subsequently expressed in a discrete form (as an adequate matrix) to simplify further analyses.

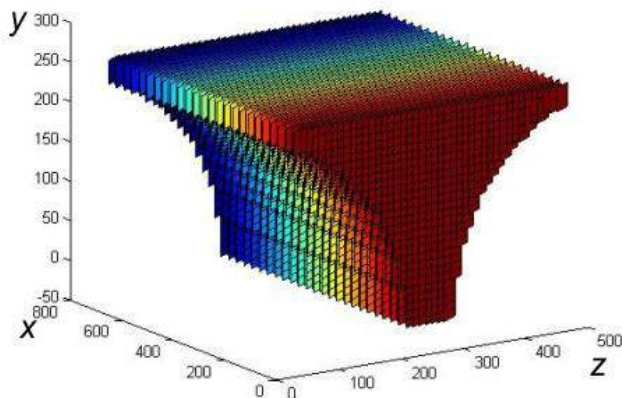


Fig. 6. Theoretical working space of the biglajd parallel mechanism

The analysis of the theoretical working space has enabled the elimination of singular points, inadequate slider positions and joints and the formation of an efficient useable working space of a mechanism.

Furthermore, the conducted analysis of the working space of the virtual model is employed for determining minimal and maximal angles occupied by rods in relation to the base and the moveable platform.

In the concrete case, the current values of the angles of mechanism joints at the position of connections between rods and sliders, i.e. rods and moveable platform, have been monitored (Fig. 7), as well as the position of sliders at the mechanism base.

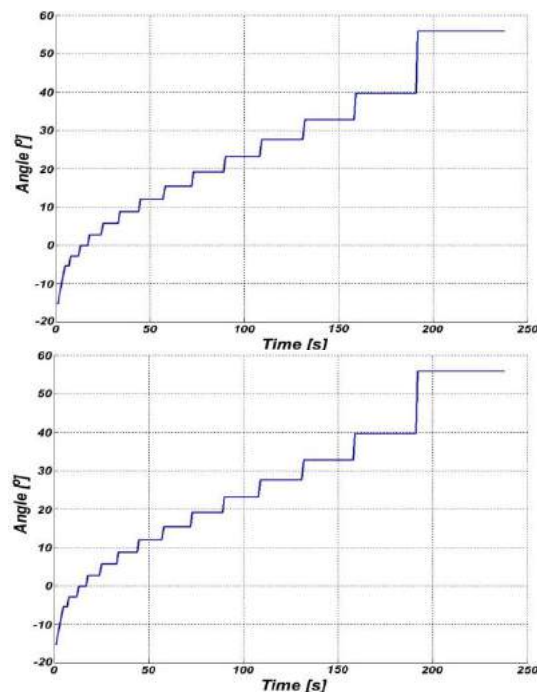


Fig. 7. Alteration in the joint angle between the rod and sliders, i.e. moveable platform, respectively

From the figure, it can be observed that the values of angles in the mechanism joints during movement alter in the total range of 70° . The determination of these values enables a selection of adequate joints for the mechanism of demanded dimensions and characteristics, together with the optimization of individual elements, if necessary.

3.1.2 Kinematic analysis of the mechanism

Apart from the analysis of the working space, to design a certain machine tool it is necessary to perform the analysis of kinematic factors in the process of mechanism movement as well. In this case, it implies the analysis of the velocities of individual mechanism elements for the maximal values achieved by the moveable platform in the machine tool.

On the other hand, to select guides, sliders, joints, power elements of the machine tool and the like, it is necessary to analyse accelerations appearing on these elements in exploitation conditions with the maximal loading of the moveable platform.

The kinematic analysis of the parallel mechanism has been conducted by utilizing the inverse kinematic chain, referring to setting the movement of a moveable platform and monitoring the behaviour of all joint mechanism elements. As a result, one can obtain velocities and accelerations of transverse sliders for the movement of the moveable platform across the theoretical working space defined by velocity and acceleration.

In the conducted analysis, the moveable platform was assigned the velocity of 1 m/s and the acceleration of 10 m/s^2 with the definition of friction between sliders and the guide, and friction in joints.

Figures 8 and 9 illustrate functional dependencies between velocities and accelerations of mechanism sliders and time, respectively, originating in linear movement of the moveable platform in various positions, for the defined movement conditions of the moveable platform.

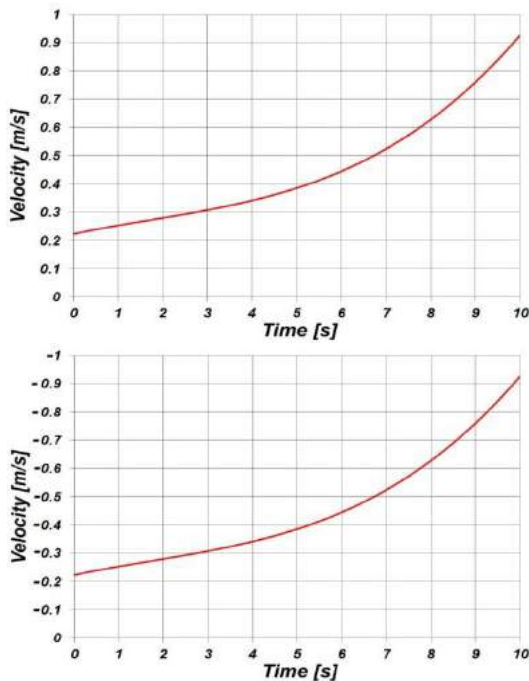


Fig. 8. Velocity of mechanism sliders for the set values of the platform velocity

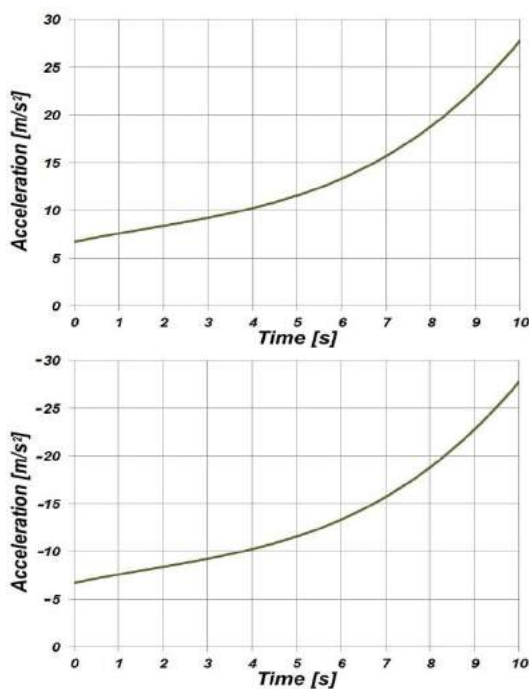


Fig. 9. Acceleration of mechanism sliders for the set values of the platform acceleration

Based on the obtained results, the adequate power engines, guide dimensions and mechanism slider characteristics are adopted, significantly simplifying the design process.

4. FINAL CONSIDERATIONS

As it can be observed from the presented diagrams, the application of virtual models in this phase of the machine

tool design process enables a continual monitoring and the analyses of all relevant movements on a machine. In such a manner it enables, on one hand, to form a conclusion on the possibilities of applying the mechanism itself in machine tools and hence of determining the feasibility of further improvements; on the other hand, it enables the realization of individual phases of the design by optimizing dimensions and characteristics of its elements.

The paper presents a model of a machine tool and the obtained results of its analyses, which is a segment of the research being conducted at the Department for Production Engineering, Faculty of Technical Sciences in Novi Sad, with the objective of improving the procedures in machine tool design and the analyses of exploitation possibilities of the existing solutions for machine tools based on parallel and hybrid kinematic structures.

REFERENCES

- [1] ALTINTAS, Y., BRECHER, C., WECK, M., WITT, S. (2005), *Virtual Machine Tool*, CIRP Annals - Manufacturing Technology, Vol 54, Issue 2, pp. 115-138.
- [2] DOMBRE, E., KHALIL, W. (2007), *Modeling, Performance Analysis and Control of Robot Manipulators*, ISTE Ltd, ISBN-13: 978-1-905209-10-1.
- [3] KADIR, A.A., XU, X., HAMMERLE, E., (2011) *Virtual machine tools and virtual machining — A technological review*, Robotics and Computer-Integrated Manufacturing 27, pp 494–508
- [4] MERLET, J.-P., (2006), *Parallel Robots*, Springer, ISBN-10 1-4020-4132-2.
- [5] MLAĐENOVIĆ, C., TABAKOVIĆ, S., ZELJKOVIĆ, M., GATALO, R. (2011), *Virtual model as a base for machine tools kinematic analysis*, 37-th Jupiter conference, Proceedings, pp 3.1-3.6, ISBN 978-86-7083-724-9
- [6] NEUGEBAUER, R. (2006), *Parallelkinematische Maschinen, Entwurf, Konstruktion, Anwendung*, Springer, ISBN 10 3-540-20991-3.
- [7] TABAKOVIĆ, S. (2008), *Development of The Programme System for Automated Design of Parallel Mechanism-Based Machine Tools and Optimal Selection of Their Components* Ph. D. thesis, Faculty of technical sciences, Novi Sad
- [8] ZOU, P. (2003), *Kinematic analysis of a biglide parallel grinder*, Jurnal of Materials Processing Technology, Vol.138, pp.461-463, Elsevier, ISSN: 0924-0136

Acknowledgement: This paper presents a segment of the research results on the project “Contemporary Approaches in the Development of Special Solutions Bearing in Mechanical Engineering and Medical Prosthetics”, TR 35025, financed by the Ministry of Education and Science of the Republic of Serbia.

MODELING OF DYNAMICAL BEHAVIOR SPINDLE – HOLDER – TOOL ASSEMBLY

Đ.ČIČA, M. ZELJKOVIĆ, G. LAKIĆ-GLOBOČKI, B. SREDANOVIC, S. BOROJEVIC

University of Banja Luka, Faculty of mechanical engineering, Vojvode Stepe Stepanovića 75, Republika Srpska
 djordje@urc.rs.ba, milanz@uns.ns.ac.rs, gnm@urc.rs.ba, sredanovic@gmail.com, stevoborojevic@hotmail.com

Abstract: The paper describes the complete procedure of mathematical modeling dynamic behavior spindle – holder – tool assembly. Developed mathematical model includes rotational degrees of freedom and can be used for prediction the tool point frequency response function. In order to verify the proposed mathematical model of spindle – holder – tool assembly and method for identifying rotational degrees of freedom, the numerical analysis of the above systems is carry out. Furthermore, the model is experimentally verified on a free-free spindle – holder – tool system.

Key words: mathematical model, spindle, dynamics

1. INTRODUCTION

Most of the research related to machine tools are connected to the machine tools spindle, since the characteristics of the spindle, such as static and dynamic behavior, strength, speed, among many others, have a significant impact on machine tools performance. Emphasized the importance of spindle assembly is based on the fact that the essence of the machining process is reduced to relative motion of the tool in relation to workpiece, so the accuracy of the spindle movement directly reflects the accuracy of the tool motion relative to the workpiece, and thus the accuracy of the final product . The most important requirements of spindle assembly exploitation are parameters of the dynamic behavior, so the main aim of this paper is development of mathematical model for modeling dynamical behavior spindle - holder – tool assembly.

2. MATHEMATICAL MODEL OF SPINDLE – HOLDER – TOOL ASSEMBLY

Spindle – holder – tool assembly is one of a major machine tool components, because its static, dynamic and thermal behavior mainly characterized the behavior of the entire mechanical system of machine tools. Components of spindle – holder – tool assembly should be coupled elastically due flexibility and damping introduced by the contacts at spindle – holder and holder – tool interfaces. Furthermore we are applying the approach [1], where the part of the holder inside the spindle is considered as integrated to the spindle (Figure 1). Some authors [2] applied somewhat different approach, where the spindle and holder are connected with a series of parallel springs. However, the approach presented in [1] provides a more realistic model, because only the dynamics due to the masses of these subsystems will be included into the model or it will be required to include their stiffness effects with distributed springs.

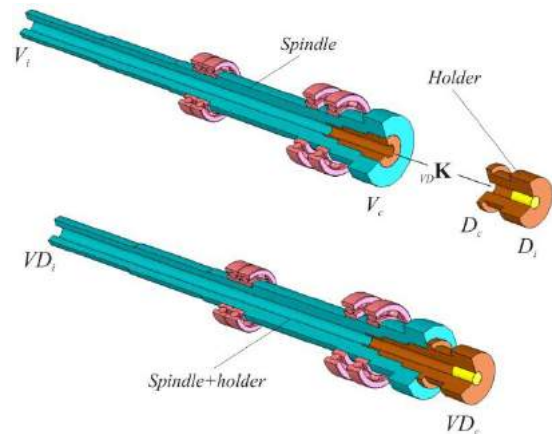


Fig.1. Elastically coupling spindle – holder system

Complex stiffness matrix, which representing the spindle – holder interface dynamics has the following form:

$${}_{VD} \mathbf{K} = \begin{bmatrix} {}_{VD}k_t + i \cdot \omega \cdot {}_{VD}c_t & 0 \\ 0 & {}_{VD}k_r + i \cdot \omega \cdot {}_{VD}c_r \end{bmatrix} \quad (1)$$

where: ${}_{VD}k_t$ – translational stiffness, ${}_{VD}c_t$ – translational damping, ${}_{VD}k_r$ – rotational stiffness and ${}_{VD}c_r$ – rotational damping at the spindle – holder interface. Assuming that matrix of response subsystem V (spindle with bearings) and subsystem D (holder) are known, then it is possible by using method of receptance coupling to obtain the global system response matrix VD (spindle – holder) at the holder tip:

$$\mathbf{VD}_{ii} = \mathbf{D}_{ii} - \mathbf{D}_{ic} \cdot (\mathbf{D}_{cc} + \mathbf{V}_{cc} + {}_{VD} \mathbf{K}^{-1})^{-1} \cdot \mathbf{D}_{ci} \quad (2)$$

Similarly, the part of the tool inside holder is considered as rigidly joined to the holder, so the receptance matrix of the tool can be coupled with the rest of the the system, as depicted Figure 2.

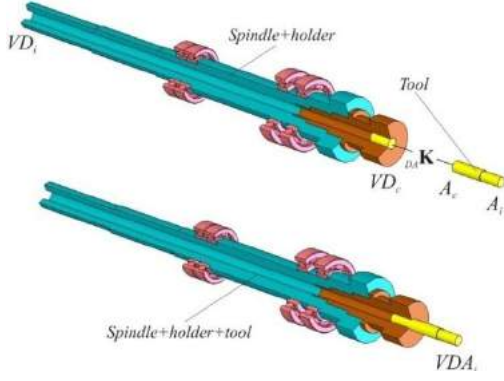


Fig.2. Elastically coupling spindle – holder – tool system

Receptance matrix of the global system VDA (spindle – holder – tool) at the tool tip has the following form:

$$\mathbf{VDA}_{ii} = \mathbf{A}_{ii} - \mathbf{A}_{ic} \cdot (\mathbf{A}_{cc} + \mathbf{VD}_{cc} + {}_{DA}\mathbf{K}^{-1})^{-1} \cdot \mathbf{A}_{ci} \quad (3)$$

In the above equation \mathbf{A} is a subsystem of a tool and ${}_{DA}\mathbf{K}$ is the complex stiffness of holder – tool interface dynamics:

$${}_{DA}\mathbf{K} = \begin{bmatrix} {}_{DA}k_t + i \cdot \omega \cdot {}_{DA}c_t & 0 \\ 0 & {}_{DA}k_r + i \cdot \omega \cdot {}_{DA}c_r \end{bmatrix} \quad (4)$$

where: ${}_{DA}k_t$ – translational stiffness, ${}_{DA}c_t$ – translational damping, ${}_{DA}k_r$ – rotational stiffness and ${}_{DA}c_r$ – rotational damping at the holder – tool interface.

If equation (3) is been used to predict the frequency response function of the tool tip we need to know translational and rotational dynamic response each of the components of spindle - holder – tool assembly. Response matrix of tool and holder can be obtained by analytical method, using some of the beam theory or through the FEM analysis. The problem is defining the response of the spindle, because data regarding the dimensions, material, the manner of bearing, the number and type of bearings, are unknown so the their modeling is critical. On the other hand, experimentally we can only measured translational dynamic response of the spindle, and to complete the receptance matrices we need rotational response. The following section presents the methodology for identification of rotational dynamic response of the spindle – holder – tool assembly.

2.1. Calculation of rotational degrees of freedom

The second chapter emphasized the importance RDOF in receptance coupling, as well the difficulties that accompany their direct measurement. Silva [3] presented a method to determine the rotational response of an arbitrary system without their direct measurements. It is assumed that a spindle assembly (Figure 3) consist subsystems A and B. The objective is receptance coupling these two subsystems with the inclusion of RDOF in synthesis. The assumption is that a subsystem A can be modeled using one of the FEM system, and thus determine the complete FRF response matrix with translational and rotational dynamic responses, while the

subsystem B can not be modeled, but only experimentally measured. So, with FEM simulation of subsystem A we can obtain the dynamic response ${}^A\mathbf{H}_{tt}$, ${}^A\mathbf{H}_{tr}$, ${}^A\mathbf{H}_{rt}$, ${}^A\mathbf{H}_{rr}$ to be completed the following FRF matrix: ${}^A\mathbf{H}_{ii}$, ${}^A\mathbf{H}_{ic}$, ${}^A\mathbf{H}_{ci}$ and ${}^A\mathbf{H}_{cc}$. For the subsystem B, the only reliable way of experimentally measured is translational response ${}^B\mathbf{H}_{tt}$, because responses ${}^B\mathbf{H}_{tr}$ and ${}^B\mathbf{H}_{rr}$ are related to RDOF and practically it is impossible to measure. The methodology presented in [3] defines the rotational responses of only one FRF, and in this case exist two FRF to be determined as follows: ${}^B\mathbf{H}_{tr} = {}^B\mathbf{H}_{rt}$ and ${}^B\mathbf{H}_{rr}$. In this sense, the equations presented in this paper extend the system of two equations with two unknowns.

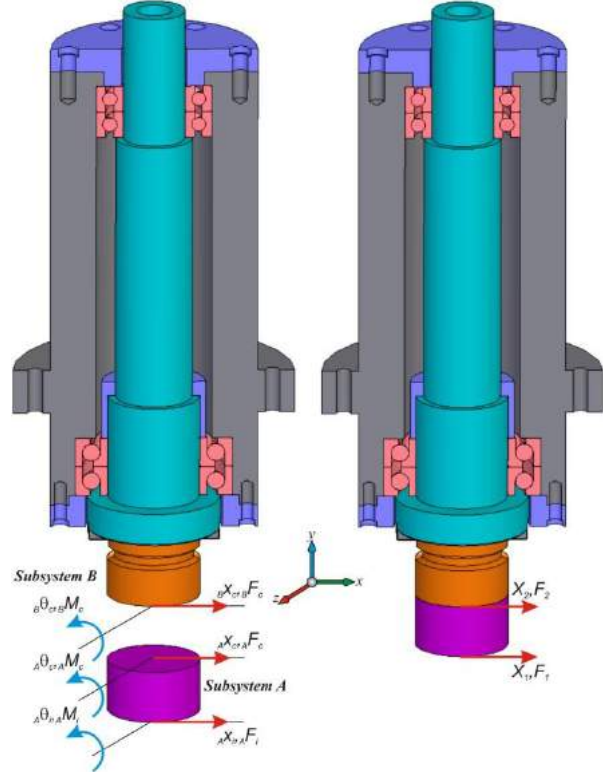


Fig.3. Substructuring spindle assembly

After appropriate mathematical transformations and with rotational responses of subsystems A using a finite element method, we can derive expressions for the rotational dynamic responses of subsystem B:

$${}^B\mathbf{H}_{rt}^{cc} = \mathbf{B}_{rt} - {}^A\mathbf{H}_{rt}^{cc} \quad (5)$$

$${}^B\mathbf{H}_{rr}^{cc} = \mathbf{B}_{rr} - {}^A\mathbf{H}_{rr}^{cc} \quad (6)$$

where:

$$\mathbf{B}_{rt} = \frac{(kfv - kug + kag - kfb + fdb - cbg)}{(ad - ud - cb + cv)} \quad (7)$$

$$\mathbf{B}_{rr} = \frac{1}{(ad - ud - cb + cv)^2} \left[kf^2v^2 + (2kagf + bf^2d - 2kugf - ec^2g + decf - 2bkf^2 - bfcg)v - d^2efu + d^2efa + g^2ka^2 - decga + decgu + g^2ku^2 + bdgfa - 2g^2kua + bec^2g - bdgfu - bdefc + 2bkugf + b^2kf^2 - 2bkagf + bg^2cu + b^2fcg - b^2f^2d - bg^2ca \right] \quad (8)$$

where: $a = {}_A\mathbf{H}_t^{ii}$, $b = {}_A\mathbf{H}_t^{ic}$, $c = {}_A\mathbf{H}_t^{ci}$, $d = {}_A\mathbf{H}_t^{cc}$,
 $e = {}_A\mathbf{H}_t^{ri}$, $f = {}_A\mathbf{H}_t^{ci}$, $g = {}_A\mathbf{H}_t^{cc}$, $k = {}_A\mathbf{H}_t^{cc} + {}_B\mathbf{H}_t^{cc}$, $u = \mathbf{G}_t^{11}$,
 $v = \mathbf{G}_t^{12}$.

Equations (5) and (6) define calculated RDOF responses of subsystem B, or in this case the system spindle – holder (VD). To get response at the tip of the spindle is necessary to use inverse receptance coupling to subtraction holder from the spindle – holder system. Returning to the notation, in which tags VD, V and D denote subsystems spindle – holder, spindle and holder, respectively, we get the desired response at the top of the spindle:

$$\mathbf{V}_{cc} = \mathbf{D}_{ci} \cdot (\mathbf{D}_{ii} - \mathbf{VD}_{ii})^{-1} \cdot \mathbf{D}_{ic} - (\mathbf{D}_{cc} + \mathbf{VD}_{cc} \mathbf{K}^{-1}) \quad (9)$$

3. NUMERICAL SIMULATION AND VERIFICATION OF PROPOSED MODEL

The geometry of the spindle – holder – tool assembly used for numerical simulation is shown in Figure 4, while the dimensions of subsystems, bearings and interface dynamics properties are given in [4]. The material is steel with Young's modulus $E = 2.1 \cdot 10^{11} \text{ N/m}^2$, mass density $\rho = 7800 \text{ kg/m}^3$ and Poisson's ratio $\mu = 0.3$. The assembly analysis was carried out using finite element software ANSYS. For modeling the components of assembly we use beam element BEAM188, which is based on Timoshenko beam theory. Additional restrictions are given by the stiffness of supports. For representing the dynamics of bearings and spindle – holder and holder – tool interface we use finite elements with spring and damping (COMBIN14).

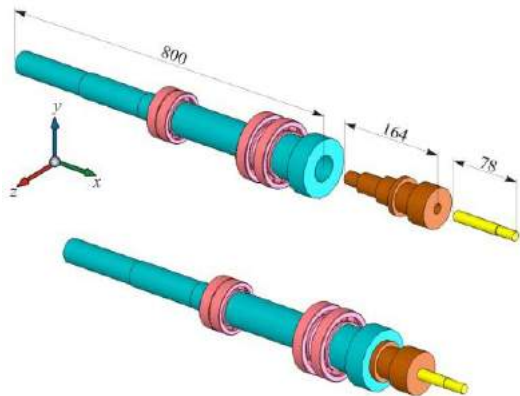


Fig.4. Components for the FEM analysis and their assembly

Figure 5 shows the comparison between calculated and simulated rotational dynamic responses of the spindle – holder system \mathbf{VD}_{rt}^{ii} and \mathbf{VD}_{rr}^{ii} .

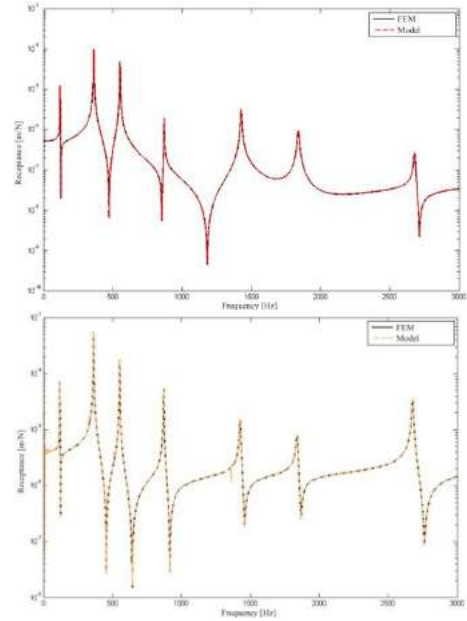


Fig.5. Comparison between substructured and simulated responses \mathbf{VD}_{rt}^{ii} (above) i \mathbf{VD}_{rr}^{ii} (below)

As can be seen in figure 5 the simulated and substructured FRF is identical. Error between subtracted and simulated values of \mathbf{VD}_{rt}^{ii} and \mathbf{VD}_{rr}^{ii} ranges up to a maximum of 10^{-5} . Between predicted and obtained response of the FEM simulation are no significant differences, which lead us to conclude that the proposed method is accurate and can therefore be used to identify RDOF.

4. EXPERIMENTAL TESTS

In this chapter, an evaluation of the method describe above will be done, combining real measurement with FE data. The spindle – holder – tool assembly shown in Figure 6. is suspended to obtain free - free end conditions for performing impact test. First, the FRF of spindle (with and without holder part in his cone) is measured and then is measured FRF of spindle – holder system. Finally, it was performed measurement of the spindle – holder – tool assembly. Modeling dynamics of tool subsystem was performed by using FEM.



Fig.6. Measuring chain for the identification of dynamic system behavior spindle - tool holder - tool

According to the presented mathematical model spindle – holder – tool assembly, for accurate prediction of the dynamic response it is necessary accurate knowledge of the complex stiffness of spindle – holder and holder – tool interface dynamics. Matrix elements are stiffness and damping and how these values can not be experimentally measured, it is required to define them in a another way. Problems of identification unknown parameters of spindle – holder – tool interface dynamics is presented in detail in [5]. First, with Levenberg-Marquardt method we identified complex stiffness matrix of the spindle – holder dynamics: ${}_{VD}k_t = 2.971 \cdot 10^8$ N/m, ${}_{VD}k_r = 5.811 \cdot 10^6$ Nm/rad, ${}_{VD}c_t = 135$ Ns/m, ${}_{VD}c_r = 35$ Nms/rad. Figure 7 show the result of receptance coupling of spindle and holder with identified spindle – holder interface dynamics. It can be concluded that the accuracy of identified parameters is satisfactory.

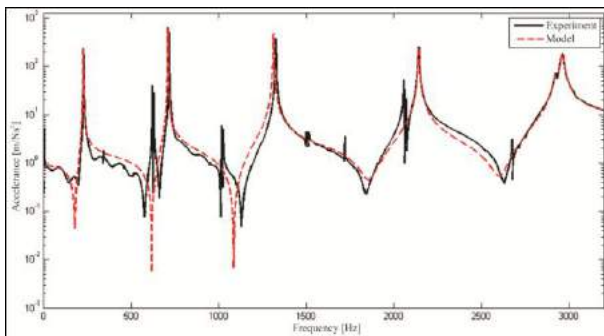


Fig.7. The measured FRF and the FRF with the identified spindle – holder interface dynamics

Afterwards, the identification of holder – tool interface dynamics is carried out. For a system combination of spindle – holder – tool with a diameter of tool $D = 20$ mm and tool overhang $L = 40$ mm, we identified the following parameters: ${}_{DA}k_t = 3.337 \cdot 10^7$ N/m, ${}_{DA}k_r = 1.571 \cdot 10^6$ Nm/rad, ${}_{DA}c_t = 63$ Ns/m, ${}_{DA}c_r = 10$ Nms/rad. Figure 8 show the receptance coupling results of the spindle – holder system with tool. And in this case can be concluded that the accuracy of identified holder – tool interface dynamics is satisfactory.

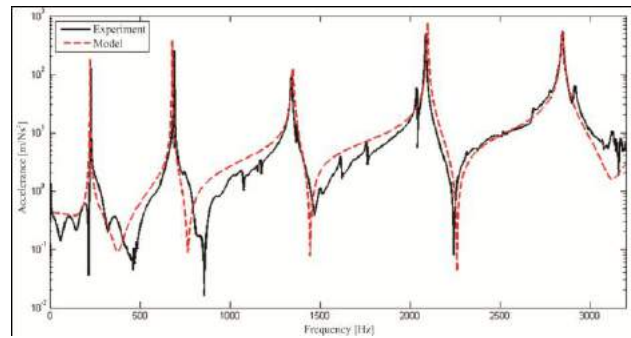


Fig.8. The measured FRF and the FRF with the identified holder – tool interface dynamics

5. CONCLUSION

The research of static and dynamic behavior of spindle assembly is a constant challenge for many researchers and designers of modern machining systems. In exploitation of spindle assembly one of the most important requirements is its dynamic behavior, so the main aim of this study was to develop a mathematical model for modeling dynamic behavior spindle – holder – tool assembly. In order to verify the proposed mathematical model numerical simulations and experimental tests of the system spindle –holder – tool was carried out.

REFERENCES

- [1] ERTURK, A., OZGUVEN, H.N., BUDAK, E. (2006) *Analytical modeling of spindle-tool dynamics on machine tools using Timoshenko beam model and receptance coupling for the prediction of tool point FRF*, International Journal of Machine Tools & Manufacture, vol. 46, pp 1901-1912
- [2] NAMAZI, M., ALTINTAS, Y., ABE, T., RAJPAKSE, N. (2007) *Modeling and Identification of Tool Holder-Spindle Interface Dynamics*, International Journal of Machine Tools & Manufacture, vol. 47, pp. 1333-1341
- [3] SILVA, J.M.M., MAIA, N.M.M., RIBEIRO, A.M.R. (1999) *Estimation of Frequency Response Functions Involving RDOFs Using an Uncoupling Technique*, International Conference on Applications of Modal Analysis
- [4] Chae, J., Park, S.S., Lin, S.: *Substructure Coupling with Joint Identification for Reconfigurable Manufacturing Systems*, The 2nd CDEN International Conference on Design Education, 2005.
- [5] ČIČA, Đ. (2010) *Modeling dynamic behavior spindle - tool holder – tool assembly*, Ph.D. thesis, Faculty of Mechanical Engineering, Banja Luka



COMPOSITE MATERIALS SUCH ABSORPTION MATERIALS FOR SUPPORTING STRUCTURES OF MACHINES

Bogdan ĆIRKOVIĆ, Ivica ČAMAGIĆ, Nemanja VASIĆ

Fakultet tehničkih nauka, ul. Kneza Miloša br.7 Kosovska Mitrovica
bogdancirkovic555@hotmail.com, icamagic@verat.net

Abstract: Conduct research supporting structures of machinery, it was concluded that composite materials can be applied to a change in their composition can significantly influence the size of authoritative for the normal operation of the machine, such as the amplitude of displacement in the horizontal and vertical direction, the rigidity of the structure and the like.

Today, composite materials can be done in several layers, in addition to fiber and dispersion strengthened. Composite materials from multiple layers are widely used, and to reduce vibration and amplitude of displacement can be applied and the calculation methods of dynamic behavior. This is done by calculating the damping coefficient for different compositions of composite materials with a graphical interpretation of results. I still damping coefficient is taken in the calculations of the dynamic behavior of the supporting structure of the machine and thus obtain new solutions in the construction of the supporting structure of the machine.

Key words: composite materials, amplitude of displacement, damping coefficient, vibration, supporting structure

1. INTRODUCTION

Term composite materials today refers to the narrow range of materials that must satisfy next criterions:

1. composite materials must be product human work, so thus no natural materials as example tree can't be considered such.

2. composite materials must be made of two or more chemically dissimilar materials with clear boundaries of separation between them.

3. integral components of the composite have their volumetric content to form a composition, so thus in this group of materials can not fall any layer of the composition or sandwich materials.

4. composite materials must have qualities that do not exhibit a single component separately.

Given the above criteria can be summarized to give a definition:

Under the composite materials include artificially created materials made of two or more chemically dissimilar materials, that according to their physical - chemical and mechanical characteristics perform new material, and in his integrity exist clearly defined borders separate between integral components /1/.

Today, composite materials can be done in several layers, in addition to fiber and dispersion strengthened.

Conduct research supporting structures of machinery fiber composite material of iron-concrete (reinforced concrete), it was concluded that composite materials can be applied to a change in their composition can significantly influence the size of authoritative for the normal operation of the machine, such as amplitude shift in the horizontal and vertical direction, the rigidity of construction and the like / 2, 3 /.

This paper presents the calculation of the coefficient of damping in structures that are used reinforced concrete as a composite material. Under construction in this case involve two or more layers of different materials / 4 /, which is not a layered composite material, but one of the layers of fiber reinforced concrete as a composite material.

In addition to calculate the resulting coefficient of such structures and such structures can be applied in the construction of supporting structures of machines.

2. ABSORPTION LINING AND CONSTRUCTION

Today is elaborated many different forms and construction of absorbing lining.

2.1. Plates with simple lining

At simple lining absorbing material applied to one side of plate whose oscillations need to weaken (fig.1). Figure 1.a shows the unloaded plate with simple lining, and figure 1.b process of folding plate and a built absorbent material.

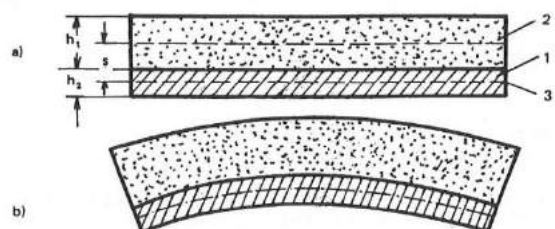


Figure 1, Base plate with a simple coating

Basic quantities at simple plates are coefficient of damping and elasticity modules (η_1) and (E_1) materials of basic plate, (η_2) and (E_2) absorbent material and (η) and (E) resulting coefficient of damping and elasticity modul of plate with simple lining.

Resulting coefficient of damping, depending on the elasticity modul and lining thickness, calculated with the help of equations:

$$\eta = \eta_2 \frac{E_2 \cdot h_2 \cdot s^2}{B}$$

and the resulting flexion stiffness (B) by the equation:

$$B = \frac{E_1 \cdot h_1^2}{12} + E_2 \cdot h_2 \cdot s^2$$

where is h_1 -basic plate thickness, h_2 -lining thickness, and

$$s = \frac{1}{2}(h_1 + h_2) \text{ distance between neutral axis.}$$

By introducing some simplifications, previous equations can be written as:

$$\eta \approx \eta_2 \frac{E_2 h_2}{E_1 h_1} \text{ or } \frac{\eta}{\eta_2} \approx \frac{E_2 h_2}{E_1 h_1}$$

In the diagram fig.2 presents the relationship η / η_2 the functions h_2/h_1 and E_1/E_2 .

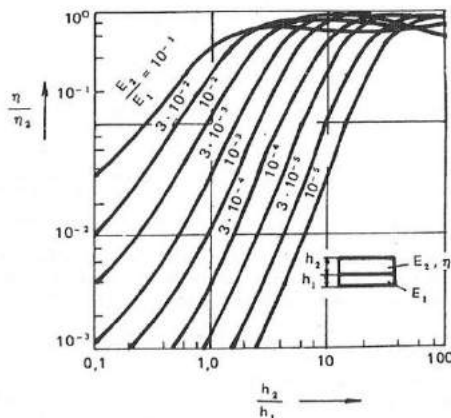


Figure 2, The dependence of damping coefficient of the coefficient of elasticity and thickness of layers

To achieve the higher damping coefficient method simple coating should adhere to the following guidelines:

1. For use as much damping material with a high damping factor. Material that is commonly used is the $\eta_2 = 0,5 \dots 2$
2. Modulus of elasticity absorbent material should preferably higher. Materials such as rubber, felt, etc. are not good. Modulus of elasticity absorbing material are the order of $E_2 = 10^8 - 10^9$, while for example, elastic modulus steel $E_1 \approx 2,1 \times 10^{11}$ [N/m²].
3. Applied absorbing material should be as thick. On the basis of practical experience should be 2-3 times thicker than the thickness of which should quell oscillations.

4. Damping coefficient, can be significantly increased if the achieve a greater distance between the neutral axis of the base plate and absorbing lining. This separation is achieved by increasing the coating thickness. For this reason absorbing material should be applied only on one side of the board. The distance between the neutral axis can be increased if the base plate and put an extra layer of coating, preferably with great strength, in the form of hollow holders.

2.2. Plates with various and multiple linings

a) The board covered absorption materials

This coating method is shown in figure 3 it differs from simple coverings because of absorbing material applied as a layer of metal foil with a small coefficient of damping $\eta_3 \approx 0$. It is practically the same material as the base plate.

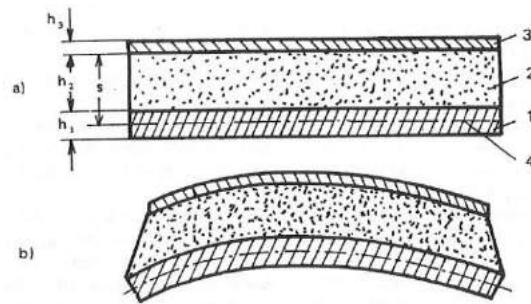


Figure 3, Base plate in conjunction with absorbing material and a thin cover: 1. base plate ($E_1, \eta_1 \approx 0$); 2. absorption linings (G_2, η_2); 3. cover in the form of thin films ($E_3, \eta_3 \approx 0$); 4. neutral line.

In this method, absorbing material in addition to bending loads in addition to suffering the burden of shear. Because the elastic properties of absorbent material characterized by shear modulus

$$\bar{G}_2 = G_2(1 + j \cdot \eta_2)$$

that depending on the elastic modulus can be calculated by the equation

$$G = \frac{E}{2(1 + \mu)}$$

The basic characteristics of this method is that the absorption coefficient depends on the frequency. Maximum damping coefficient (η_{\max}) occurs at a frequency:

$$f_{\max} = \frac{1}{2\pi} \frac{G_2}{E_3} \frac{\sqrt{1 + \eta_2^2}}{h_2 h_3} \sqrt{\frac{B}{m_s}}$$

and is

$$\eta_{\max} = \frac{E_3 h_3 s^2}{B} \frac{\eta_2}{2(1 + \sqrt{1 + \eta_2^2})}$$

For the base plate with a thickness $h_1 \gg h_2, h_1 \gg h_3$ i

$$B \approx \frac{E_1 \cdot h_1^3}{12} s = \frac{h_1}{2}$$

obtained

$$\eta_{\max} = \frac{3 E_3 h_3}{2 E_1 h_1} \left(\frac{\eta_2}{1 + \sqrt{1 + \eta_2^2}} \right)$$

Provided that the base plate and the protective cover of the same material $E_1 = E_3$ and that the damping coefficient of absorption material $\eta_2 = 0,8$, is obtained

$$\eta_{\max} \approx 0.5 \frac{h_3}{h_1}$$

This analysis shows that this method is suitable for damping noise of thick plates. It is the thickness of absorbent material is of minor importance. Compared to the simple trim, the maximum damping coefficient (η_{\max}) does not depend on elastic modulus (E_2) and shear modulus (G_2) of absorbent material. However, it is important that the frequency at which it can be expected (η_{\max}) lies in the frequency range that can be realized with the available materials of small modulus (E) and (G). In this method uses a material with a high η .

In figure 4 are shown the comparative coefficient obtained by theoretical analysis for simple and covered with absorptive lining.

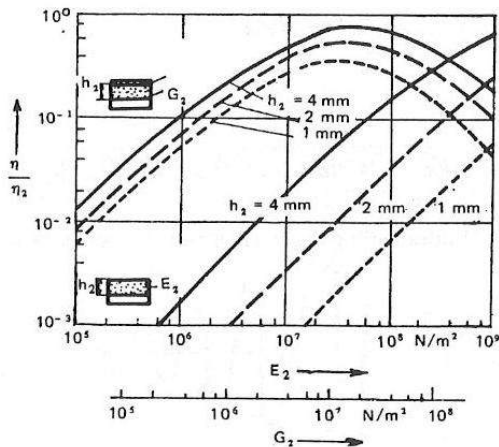


Figure 4, Comparative diagram

The diagram shows that the coating covered achieved a coefficient with soft materials whose modulus

$$E_2 = 10^6 - 10^9 \text{ N/m}^2 \text{ i } G_2 = 4 \cdot 10^5 - 4 \cdot 10^8 \text{ N/m}^2.$$

Benefits covered in relation to simple coverings are as follows:

1. Can be used materials with low modulus of elasticity.
2. Effective noise reduction of thick plates.
3. Receives a large damping coefficient, and with it the greatest noise reduction at low consumption of material, or a small increase in weight machines.
4. Can be achieved selective noise reduction at a particular frequency range.

For practical sizing covered absorbing coating is recommended following the plate thickness (h) and damping coefficient (η) (table 1).

Table 1, Recommended panel thickness and damping coefficients

h_2	h_3	η
$0.5 h_1$	$(0.05 - 0.1) h_1$	0.05
$1 h_1$	$(0.05 - 0.1) h_1$	0.1

For example, a thin steel sheet for car bodies for $h=1\text{mm}$ has $\eta \approx 2 \times 10^{-2}$, while steel plates for ship armor have $\eta \approx 10^{-3}$.

b) Two panels of the same thickness with a thin interlayer

Figure 5 shows the principle design solution absorption of two plates of the same thickness, with a thin interlayer absorption.

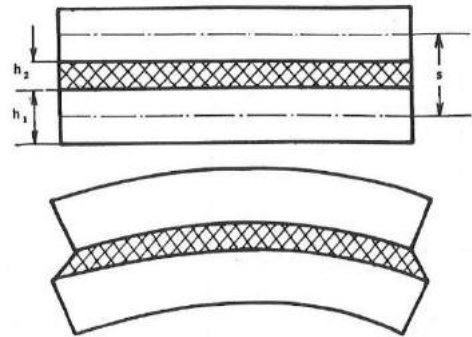


Figure 5, Two panels of the same thickness with a thin interlayer

c) Arbitrary forms of plates and other structural elements

Figure 6 shows the principal construction solutions vibration absorption of different geometric shapes of elements and systems.

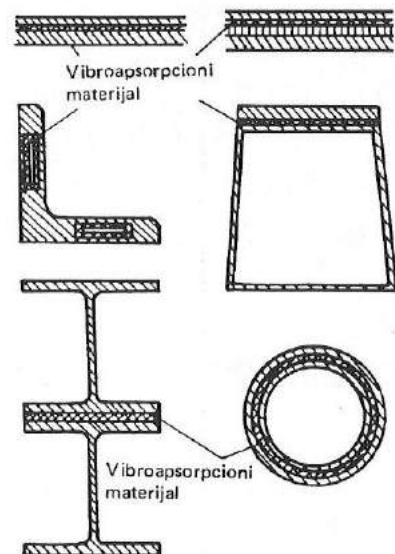


Figure 6, Arbitrary forms of plates and other structural elements

3. COEFFICIENT DAMPING OF COMPOSITE MATERIAL

Using the previous mentioned possibilities of absorption material, as well as the possibility to change the initial values of the mechanical properties of the base material, which in this case reinforced concrete (a composite material), we obtained the results shown in Figure 7.

For both variants was done by changing the thickness of plate, which is the ratio of the image data $h1/h2$ (first version) and the ratio $h1/h3$ (for the second variant) and for ten different values. The highest ratio, $h1: h2 = 1:10$, giving the highest value of damping coefficient and it is in the picture numbered 1, and further reducing the ratio 1:1, where the increase in the minimum damping coefficient (marked by numbered 10). The same was done with the relationship $h1/h3$, noting that such large differences can

not be practically used, but are less value for variant 2 (1:2, 1:3) larger than the first variant.

See that, for the variant 1, when we have only one record get lower values of total attenuation coefficient. We can observe the impact characteristics of reinforced concrete, for whom he has previously proven that he can easily modify the change in concentration of reinforcement, ie, fibers in a matrix of concrete.

For version 2, when we have a coating of two plates of composite materials is negligible, but the ease of application of concrete in construction and a large increase in damping coefficient of the whole structure is taken as a good opportunity for the design of supporting structures and machines in general for the construction of any use. It should be emphasized that this variation is good and the reason for the lower mechanical properties of concrete are compensated by a large increase in damping coefficient.

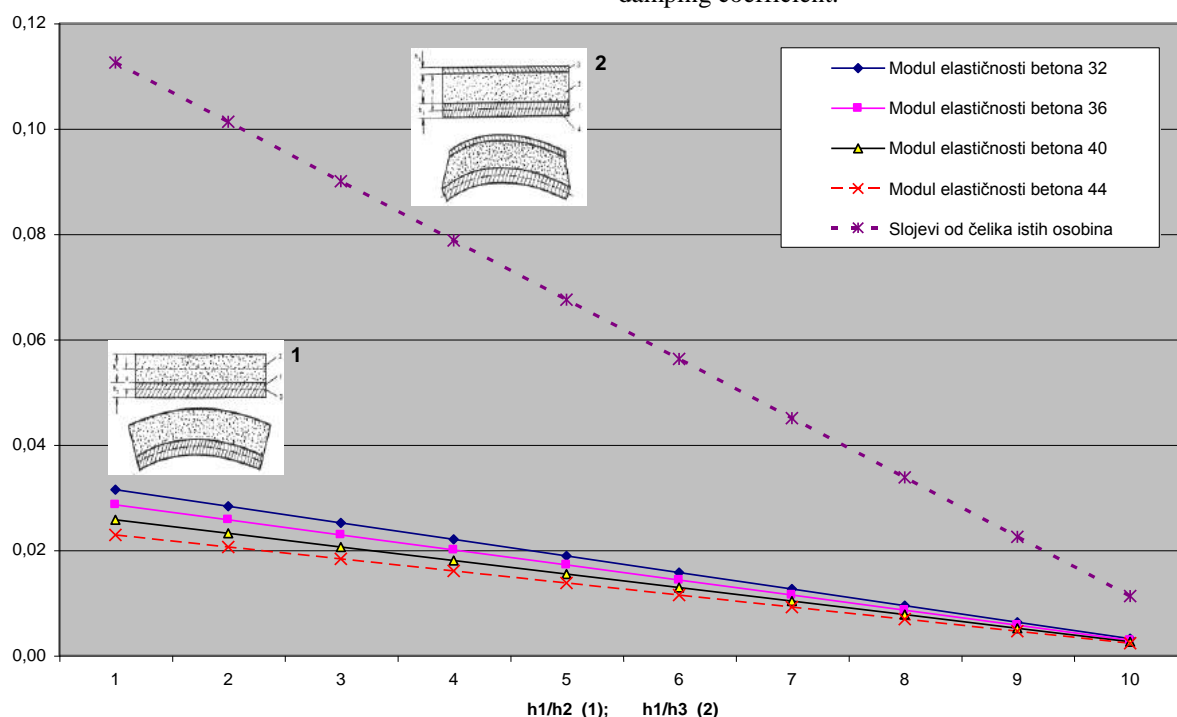


Figure 7, Coefficient of damping plates, with cladding of composite material, iron - concrete

After analysis of the possibility of such changes in material properties, it is clear that in all calculations where the same use, we can get a wide range of results. In the area of dynamic behavior of machine support structure, with the balance of the amplitude of movement of supporting structures of machines for forming / 2,3 /, the ability to change input parameters, ie. characteristics of the material provides great opportunities for a different number of constructive solutions.

CONCLUSION

Looking at these examples and taking into account the proven possibility of using composite materials in load-bearing structure of the machine, we found results that suggest an increasing possibility of using them.

In addition to ease of construction, there is a relatively low price of this composite material, and ease of change of its features is the best feature. Small changes to content of steel fibers in a matrix of concrete, which in itself can

be stronger or weaker in mechanical terms, we get the composite material with a very wide range of mechanical properties and damping coefficients, which are so essential for the absorption of vibration and dynamic behavior of machine support structure.

REFERENCES

1. R.Kristensen, Uvod u kompozitne materijale, Mir, Moskva, 1982.
2. Ćirković B., Todić T., Ljamić D., Analiza uticaja materijala na dinamičko ponašanje konstrukcije alatne mašine, IMK-14 - Istraživanje i razvoj, vol. 12, br. 1-2, str. 15-23, 2006.
3. Ćirković B., Todić T., Todić A., Dinamičko ponašanje alatne mašine u zavisnosti od kompozitnih materijala, IMK-14 - Istraživanje i razvoj, vol. 13, br. 1-2, str. 37-42, 2007.
4. D.Veličković, Buka i vibracije II, Univerzitet u Nišu, Niš, 1990.



34th INTERNATIONAL CONFERENCE ON
PRODUCTION ENGINEERING
28. - 30. September 2011, Niš, Serbia
University of Niš, Faculty of Mechanical Engineering



**MULTIOBJECTIVE OPTIMIZATION – POSSIBILITY FOR PRODUCTION
IMPROVEMENT**

Predrag ĆOSIĆ, Dragutin LISJAK, Valentina LATIN

FSB, Department of Industrial Engineering, University of Zagreb, Ivana Lučića 5, Zagreb, Croatia
predrag.cosic@fsb.hr, dragutin.lisjak@fsb.hr, valentina.latin@fsb.hr

Abstract: *In the previous research strong correlation was discovered between the features of the product drawing and production time, which has resulted with 8 regression equations. They were realized using stepwise multiple linear regressions. Since the optimization of these regression equations did not fully define the most frequent requirements, multiobjective optimization was applied. The applied criteria included: minimum production time, maximum work costs/total costs ratio for a group of workpieces. The group was created using specific classifiers that defined similar workpieces. A STEP model with seven decision variables within a group was applied, and the groups with a high index of determination were selected. Independent values that maximize the work costs/total costs ratio and minimize production times were determined. The obtained regression equations of time production parts and work costs/total costs ratio are included in the objective functions to reduce production time and increasing, work costs/total costs at the same time. The values of decision variables that minimize production time and maximize work costs/total costs ratio were determined. As the solution of the described problem, multicriteria interactive STEP method was applied.*

Key words: *stepwise multiple linear regression, multiobjective optimization, STEP method*

1. INTRODUCTION

Our numerous experiences and experience of others as well, and following of economic trends in Croatia and wider have motivated us to start research in this area. Since a considerable number of research works and papers are dealing with optimization of technological parameters, we have decided to focus our attention on the relationship between product features (geometry, complexity, quantity,..) and production times and costs [1,2,3,4]. It has been proved that it is possible to make estimation of production time applying classification, group technology, stepwise multiple linear regression as the basis for accepting or rejecting of orders, based on 2D [1, 2] drawings, and the set basis for automatic retrieval of features from the background of 3D objects (CAD: Pro/E, CATIA) and their transfer to regression models [5]. Of course, certain constraints have been set: application of standardized production times from technical documentation or estimations made using CAM software (CATIA, PRO/E, CamWorks); type of production equipment/technological documentation determines whether it will be single- or low-batch production. Initial steps have been taken regarding medium-batch, large-batch or mass production.

It has been assumed (relying on experience) that small companies (SMEs) in Croatia make decision about acceptance of production (based on customer's design

solution of the product, delivery deadlines and manufacturing costs imposed by the customer - PICOS concept) on the basis of free intuitive assessment due to the lack of time and experts. This often results in wrong estimates.

If the optimization of regression curves is to be applied (independent variables - product features, dependent variable – production time), it is hard to explain what it would mean for the minimum or maximum production time for a given group of products. The minimum production time could mean a higher productivity, but we do not know about the profit. The maximum production time could suggest that a higher occupancy of capacities may mean higher earnings, although it may not be so. This dual meaning has led us to introduce multiple objective optimizations for a new class of variables that differently classify our products. A response variable (dependent variable) can assume several meanings: maximum profit per product, minimum delivery time (related to production time, and also to organizational waste of time, production balancing...), ratio of the production cost and the costs of product materials, ratio of the production cost and the ultimate production cost. Thus, the problem-solving approach has become more complex, and is no longer a mere result of intuition and heuristics, but more exact assessment of 'common' optimum for more set criteria.

2. THEORETICAL BACKGROUND

TABLE 1. Minimum and maximum values of selected variables

PRODUCT TYPE - 41113									
min	2.90	0.100	1.00	11.21	0.22	0.0132	0.001	6.00	0.92
max	100.00	0.400	5.00	19.63	12.50	0.3972	0.820	33.00	1.00
variable	x_1	x_2	x_3	x_4	x_5	x_6	x_7	Z_1	Z_2
Variable description	Workpiece outer diameter	Narrowest tolerance of measures	Scale of the drawing	Material mass/strength ratio	Wall thickness/length ratio	Product surface area	Material mass	Production time	Ratio of Work costs/total costs
unit of measure	mm	mm	number	number	number	10^4 mm ²	kg	h/100	number

Used technological documentation for conventional machining tools (420 positions) is from INAS Company, a successful producer of machine tools in Croatia. The main grouping criteria were the features (geometrical, tolerance, hardness) from technical drawings and for each workpiece production time was used (technological and auxiliary time).

It was found that the optimization of regression equations, in order to obtain minimum or maximum production times was insufficient with respect to the needs in real production. Thus, the aim was to obtain, by considering a series of regression equations, the optimum for multiobjective optimization (minimal production time, labor cost/material cost ratio or labor cost/total cost ratio for the selected group of products. As multiobjective optimization requires the same variables (x_1 , x_7), it was necessary to make new grouping of the basic set (302 workpieces) using new classifiers. New classifiers were defined W (1-5), based on 5 basic features:

W1-material: 1(polymers)-5(alloy steel), W2-shape: 1(rotational)-5(complex), W3- max. workpiece dimension: 1(mini $V < 120$ mm)-5($V > 2000$ mm), W4-complexity, BA – number of dimension lines: 1(very simple $BA \leq 5$)-5(5 –very complex $BA > 75$), W5-treatment complexity: 1(very rough)-5) very fine). The conditions were defined based on the range of data about the number of dimension lines on the considered sample

of 415 elements. A classifier that is being developed is based on 5 basic workpiece features. For the purpose of the research, a group of workpieces (W1-W5) 41113 was selected for further analysis. The code 41113 means: steel – rotational – small – very simple – commonly complex - workpieces. From the available database, the minimum and maximum values for independent variables, and dependent variable (Z_1 -production time), and derived variable Z_2 was taken (Table 1.).

Two regression equations, Z_1 (production time) and Z_2 (labor cost/total cost ratio), were selected. For them multiobjective optimization was also performed. In order to use the same types of variables, new grouping was made using specifically adjusted classifiers. *Workpiece classification according to the criterion of complexity* was done semi-automatically by setting conditions on certain features of drawings (basic roughness, the finest roughness requirement, the narrowest tolerance of measures, the narrowest tolerance of shape or position (geometry), number of all roughness and geometry requirements in the drawing. Each of these 6 criteria based on its specific conditions is assigned a value ranging from 1 to 5. The obtained result (Table 2.) is rounded to integer (e.g. 3.49 is $W=3$, and 3.51 is $W=4$), and this integer (in the range from 1 to 5) becomes complexity criterion coefficient (the fifth digit in the code).

TABLE 2. Results of stepwise multiple linear regression

Regression Statistics	Dependent variable -production time	Regression Statistics	Dependent variable- work costs/ultimate costs ratio
	Z_1		Z_2
Multiple R	0.92212166	Multiple R	0.99207
R Square	0.85030835	R Square	0.984202
Adjusted R Square	0.78481826	Adjusted R Square	0.977291
Standard Error	4.09742037	Standard Error	0.002725
Observations	24.0	Observations	24.0
	<i>Coefficients</i>		<i>Coefficients</i>
Intercept	-13.490042	Intercept	0.990439
X Variable 1	0.86652065	X Variable 1	0.000238
X Variable 2	-0.1993556	X Variable 2	-0.0039

X Variable 3	0.75343156	X Variable 3	0.00046
X Variable 4	1.41593567	X Variable 4	0.000794
X Variable 5	-1.8669075	X Variable 5	-0.00107
X Variable 6	4.83640676	X Variable 6	-0.04466
X Variable 7	-51.274031	X Variable 7	-0.08551

3. THE MULTIOBJECTIVE MODEL

The general multiobjective optimization problem with n decision variables, m constraints and p objectives is [6]:

$$\text{maximize } Z(x_1, x_2, \dots, x_n) = [Z_1(x_1, x_2, \dots, x_n), Z_2(x_1, x_2, \dots, x_n), \dots, Z_p(x_1, x_2, \dots, x_n)] \quad (1)$$

$$\text{s.t. } g_i(x_1, x_2, \dots, x_n) \leq 0, \quad i = 1, 2, \dots, m \quad (2)$$

$$x_j \geq 0, \quad j = 1, 2, \dots, n$$

where $Z(x_1, x_2, \dots, x_n)$ is the multiobjective objective function and $Z_1(\cdot)$, $Z_2(\cdot)$, $Z_p(\cdot)$, are the p individual objective functions. The step method [7] is based on a geometric notion of best, i.e., the minimum distance from an ideal solution, with modifications of this criterion derived from a decision maker's (DM) reactions to a generated solution. The method begins with the construction of a payoff table. The table is found by optimizing each of the p objectives individually, where the solution to the k th such individual optimization, called x^k , gives by definition the maximum value for the k th objective, which is called M_k (i.e., $Z_k(x^k) = M_k$). The values of the other $p - 1$ objectives implied by x^k are shown in the k th row of the payoff table. The payoff table is used to develop weights on the distance of a solution from the ideal solution. The step method employs the ideal solution, which has components M_k for $k = 1, 2, \dots, p$. The ideal solution is generally infeasible. The λ , metric is used to measure distance from the ideal solution. The distance is scaled by a weight based on the range of objective Z_k and the feasible region is allowed to change at each iteration of the algorithm. The basic problem in the step method is:

$$\text{Min } \lambda \quad (3)$$

$$\Pi_k [M_k - Z_k(x)] - \lambda \leq 0, \quad k = 1, 2, \dots, p \quad (4)$$

$$x \in F_d^i \quad \lambda \geq 0 \quad (5)$$

where F_d^i is the feasible region at the i th iteration and λ is used to indicate that the original metric has been modified. Initially, $F_d^0 = F_d$; i.e., at the start of the algorithm the original feasible region is used in Eq.5 The weights π_k in Eq.4 are defined as:

$$\Pi_k = \frac{\alpha_k}{\sum_k \alpha_k} \quad (6)$$

$$\alpha_k = \frac{M_k - n_k}{M_k} \left[\sum_{j=1}^n (c_j^k)^2 \right]^{\frac{1}{2}} \quad (7)$$

where n_k is the minimum value for the k th objective; i.e. it is the smallest number in the k th column of the payoff table. The c_j^k are objective function coefficients, where it is assumed that each objective is linear.

4. RESULTS

On the basis of considerations of regression functions in previous sections, the problem of multiobjective optimization with minimization of the objective functions Z_1 and Z_2 with related constraints (Eq.8 to Eq.10) is defined.

$$\text{Min } Z_1 = -13.49004192 + 0.866520652 * \mathbf{x}_1 + 0.199355601 * \mathbf{x}_2 + 0.753431562 * \mathbf{x}_3 + 1.415935668 * \mathbf{x}_4 - 1.866907529 * \mathbf{x}_5 + 4.836406757 * \mathbf{x}_6 - 51.27403107 * \mathbf{x}_7 \quad (8)$$

$$\text{Min } Z_2 = -0.990438731 - 0.000238475 * \mathbf{x}_1 + 0.003897645 * \mathbf{x}_2 - 0.00045981 * \mathbf{x}_3 - 0.000794225 * \mathbf{x}_4 +$$

$$0.0010738 * \mathbf{x}_5 + 0.044664232 * \mathbf{x}_6 + 0.085514412 * \mathbf{x}_7 \quad (9)$$

$$\mathbf{x}_1 \leq 100; \quad \mathbf{x}_2 \leq 0.4; \quad \mathbf{x}_3 \leq 5.0; \quad \mathbf{x}_4 \leq 19.63; \quad \mathbf{x}_5 \leq 12.50; \quad \mathbf{x}_6 \leq 0.3972; \quad \mathbf{x}_7 \leq 0.820 \quad (10)$$

In Eq.12 and Eq.13 Z_1 represents variable T , and Z_2 variable TU/TR . It should be mentioned that for the needs of consistency of the objective functions Z_1 and Z_2 , for the objective function Z_2 (Eq.9) the signs of the coefficients of variables and of the free member have been changed. The values of objective functions Z_1 and Z_2 in the extreme points of the set of possible solutions (feasible region) are given in Table 3. It is visible from the table that there is no common set of points ($x_1 \dots x_7$) where both functions Z_1 and Z_2 have extreme (maximum) values, and thus the need for optimization of the given problem is justified.

In accordance with Eq.6 and Eq.7 coefficients of equation Eq.4 are calculated as follow: $\alpha_1 = 0.0197$, $\alpha_2 = 10.1974$, $\Pi_1 = 0.0019$, $\Pi_2 = 0.9981$. The results of the first compromise solution given in Table 4. Since in the given problem there are two objective functions, it is necessary to make calculation of the second compromise solution. It has been decided that the previous value for $M_1 = 73.1620$ is to be reduced for the value of 33.1620, and thus the new value for $M_1 = 40$.

In accordance with Eq.6 and Eq.7 coefficients of equation Eq.4 are calculated as follow: $\alpha_1 = 0.0199$,

$\alpha_2=10.1974$, $\Pi_1=0.0019$, $\Pi_2=0.9981$. The results of the second compromise solution given in Table 5.

5. CONCLUSION

The paper presents research on the development of a model for the estimation of production time for unit production or medium size batch production. As a result, eight regression equations were obtained. They show estimation of the production time as a function of geometrical and technological characteristics of a homogeneous group of products that were grouped using logical operators. Using specifically developed 5 classifiers at 5 levels, on the sample taken from the real production a homogenous group was formed which resulted in a regression equation showing dependence between production time (Z_1) and 7 independent variables (x_1, \dots, x_7). After that, the dependence between the work costs/total costs ratio (Z_2) and independent variables (x_1, \dots, x_7) is shown in another regression equation. The

optimization part of the work considers the possibility of application of standard STEP method as multiobjective optimization approach in optimization of production problems, where the objective functions are obtained by regression model. The results obtained by application of STEP method indicate that its application is possible in the optimization of decision variables of the given objective functions. It is evident that the results of both objective functions are within the statistical range, i.e. $Min Z_1(x_1, x_7) = 19.0013$ and $Max Z_2(x_1, x_7) = 0.9915$, and thus it is not necessary to introduce a new payoff table to find a new compromise (feasible) solution. The following can be concluded: it is cost-effective to manufacture products with minimum outside diameter (x_1), maximum (wider range) tolerance (x_2), maximum scale (x_3), maximum strength/mass ratio (x_4), minimum of wall thickness/length ratio (x_5), maximum product surface area (x_6) and minimum mass of material (x_7).

TABLE 3. Values of the decision variables and the objective functions

Extreme point	Decision variables							Objective functions	
	x_1	x_2	x_3	x_4	x_5	x_6	x_7	$Z_1(x_1, \dots, x_7)$	$Z_2(x_1, \dots, x_7)$
A	100	0	0	0	0	0	0	73.1620	-1.0143
B	0	0.4	0	0	0	0	0	-13.5698	-0.9889
C	0	0	5	0	0	0	0	-9.7229	-0.9927
D	0	0	0	19.63	0	0	0	14.3048	-1.0060
E	0	0	0	0	12.50	0	0	-36.8264	-0.9770
F	0	0	0	0	0	0.3972	0	-11.5690	-0.9727
G	0	0	0	0	0	0	0.820	-55.5347	-0.9203

TABLE 4. Results of the first compromise solution

$x_1=100$; $x_2=0.4$; $x_3=1.0$; $x_4=12.0428$; $x_5=12.5$; $x_6=0.3962$; $x_7=9999998E-4$; $\lambda=7.128304E-2$ Min $Z_1(x_1, \dots, x_7) = 69.4161$; Min $Z_2(x_1, \dots, x_7) = -0.9915$; Max $Z_2(x_1, \dots, x_7) = 0.9915$

TABLE 5. Results of the second compromise solution

$x_1= 3.37147$; $x_2= 0.3711865$; $x_3= 4.553035$; $x_4= 18.92068$; $x_5= 0.2269908$; $x_6= 0.2826709$; $x_7= 2.965111E-2$; $\lambda = 7.682257E-2$ Min $Z_1(x_1, \dots, x_7) = 19.0013$; Min $Z_2(x_1, \dots, x_7) = -0.9915$; Max $Z_2(x_1, \dots, x_7) = 0.9915$
--

REFERENCES

- [1] COSIC, P., ANTOLIC, D., MILIC, I. (2007), *Web Oriented Sequence Operations.*, 19th International Conference on Production Research, ICPR-19, July 29-August 2, 2007, Valparaiso, Chile, on CD
- [2] ANTOLIC, D. (2007) *Estimation of production times by regression models (in Croatian language)*, Master's thesis, University of Zagreb, Faculty of Mechanical Engineering and Naval Architecture, FSB, Zagreb
- [3] VOLAREVIC, N., COSIC, P. (2005) *Shape Complexity Measure Study*, 16th International DAAAM Symposium, University of Rijeka, 19-22nd October 2005, Opatija, Croatia, pp. 375-376
- [4] LISJAK, D., COSIC, P., MILIC, D., (2011), *Two Approaches for Estimation of Production Time: Robust Regression Analysis and Neural Networks*, 21th International conference on Flexible Automation and Intelligent Manufacturing FAIM 2011, Taichung, Feng Chia University, Taiwan, pp. 27-35
- [5] COSIC, P., MILIC, D., KOVACIC, I. (2008), *Production Time Estimation as the Part of Collaborative Virtual Manufacturing*, International Centre for Innovation and Industrial Logistics -. ICIL 2008, International, March 9 – 15, 2008, Tel Aviv, Israel, pp. 93-100
- [6] COHON, J. L., (1978), *Multiobjective programming and planning*, Academic Press, Inc. New York
- [7] BENAYOUN, R., deMONTGOLFIER, J., TERGNY, J., LARITCHEV, O., (1971), *Linear Programming with Multiple Objective Functions: Step Method (STEM)*, Vol. 1 Num. 1, 366-375, Springer Berlin/Heidelberg



RESEARCH AND DEVELOPMENT OF THE NEW GENERATION FIVE AXIS VERTICAL TURNING CENTRES

Vladimir KVRGIĆ, Miroslav VASIĆ, Vladimir ČARAPIĆ, Jelena VIDAKOVIĆ, Velimir KOMADINIĆ
Lola Institute, Kneza Višeslava 70a, Belgrade, Serbia

vladimir.kvrgic@li.rs, miroslav.vasic@li.rs, vladimir.carapic@li.rs, jelena.vidakovic@li.rs, velimir.komadinic@li.rs

Abstract: Turning, 5-axis milling, drilling and boring in only one setup is very useful, which is possible on 5-axis turning centres. In this paper, we present the solution for forward and inverse kinematics of this type of machine with two linear and three rotational axes. The solution allows for programming the machine motion as if the machining were performed on a 5-axis gantry milling machine. With given control algorithm we facilitated machine programming, because tool positions and orientations required for programming are determined disregarding the workpiece swivelling during machining and current positions and orientations taken by the tool during machining relative to the workpiece.

Key words: Vertical five-axis turning center, programming, control algorithm

1. INTRODUCTION

Currently, the precision and productivity that users demand from the 5-axis machining of complex workpiece surfaces is gradually increasing. To satisfy these requirements, different structures of 5-axis machines were developed. The aim of this paper is focused on the development of a multifunctional vertical 5-axis turning centre that allows for turning and 5-axis milling and drilling and threading at the displaced work table centre and at various angles. To provide the possibility for the machine to perform more types of machining in a single setup, time can be saved by relocating the work piece from one machine to another. This significantly increases the machining productivity and accuracy.

With regard to the vertical lathes, the best 5-axis milling and drilling performances on these machines are achieved by placing a rotary turning table on the Y -axis slider, which has an overall travel that is longer than the maximum diameter of turning [1]. Here, the work table becomes the axis of auxiliary motion (C_y swivelling axis). For 5-axis machining, the machine has turning, milling and drilling units, with the possibility of accepting a single-axis head with a B_t axis. In this way, the vertical lathe becomes a vertical 5-axis gantry milling machine with X , Y , Z , B_t and C_y axes. Using such a machine presents great possibilities. One drawback, however, is the complicated, long and heavy base of the Y -axis slider. In addition, these machines are very expensive. They also require a large workshop space.

Moreover, there are also lathes with the C_y axis and a small Y axis (up to 200 mm), which are placed on the ram and carry an angular head along the B_t axis. These machines cannot achieve 5-axis milling across the entire work table.

The present paper deals with the development of a vertical 5-axis turning centre, where the work table becomes the C_y axis. The swivelling of this axis, with a

cutting tool motion along the X axis according to the corresponding law, produces motion corresponding to the motion along the Y axis. The turning, drilling and milling units can accept the replaceable 2-axis angular head. In this way, a machine with 2 linear and 3 rotational axes can be obtained. This is a machine with C_y , X , Z , B_t and C_t axes. The working mechanism of this machine is illustrated in Fig. 1.

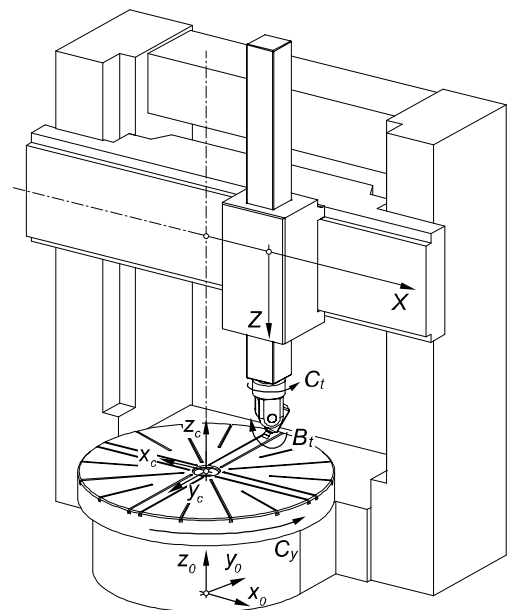


Fig. 1. 3D model of the vertical 5-axis turning centre

The forward and inverse kinematics for different kinds of 5-axis milling machines have been presented and discussed in many papers, such as in [2] or [3]. Kinematic chain design and the utility of different kinds of 5-axis machines are discussed in [4]. In this work, the forward and inverse kinematics have been solved for the vertical

lathe with 2 linear and 3 rotational axes, which, for the 5-axis milling, should realise the motion accomplished by 3 linear and 2 rotational axes. Consequently, the given control algorithm enables programming tool locations in milling or drilling as if it were machining on a 5-axis gantry milling machine. This has been done for a machine with an angular head, with axes that do not intersect, as shown in Fig. 2.

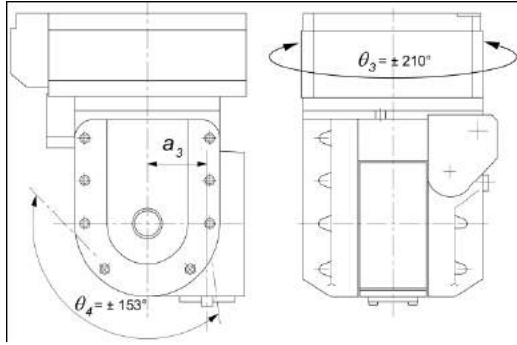


Fig. 2. Two-axis angular head with non-intersecting axes

The angular head increases the machining possibilities and helps to avoid some singular positions of the machine work table. The control algorithm for the work table axis, C_y , and the angular head axis, C_r , has been given, eliminating a number of their singular positions. All of the above have additionally made solving the forward and inverse kinematics more complex.

2. COORDINATE FRAMES OF MACHINE COMPONENTS AND MATRICES DETERMINING THEIR RELATIONS

This section defines the coordinate frames for the components of a vertical 5-axis turning centre and the matrices determining their relations. The machine components, their links and their coordinate frames are denoted using the Denavit-Hartenberg convention (D-H) [5, 6]. The machine is viewed as a system with two entities performing a cooperative motion; one entity comprises a swivelling work table with a work piece, and the other is a serial mechanism with four links carrying the cutting tool. The machine base is denoted by 0, the serial components are denoted by 1 for the X axis, 2 for the Z axis, 3 for the C_t axis and 4 for the B_t axis, and the work table axis (C_y) is denoted by 5. The first two serial links are translational, and the other two are rotational; therefore, the corresponding axis variables are $d_1=d_x$, $d_2=d_z$, $\theta_3=\theta_{C_t}$ and $\theta_4=\theta_{B_t}$. The angle of the work-table rotation is denoted by $\theta_5=\theta_c$. This angle is the fifth axis variable. The adopted convention specifies that the angle θ_3 is positive when the component's 3 rotation is in the negative mathematical direction, and the angles θ_4 and θ_c are positive when the component's 4 rotation and the rotating table are in the positive mathematical direction. The thermal dilatation along the X and Y axes are denoted by δ_{xc} and δ_{yc} . Fig. 3 shows the frames for machine components.

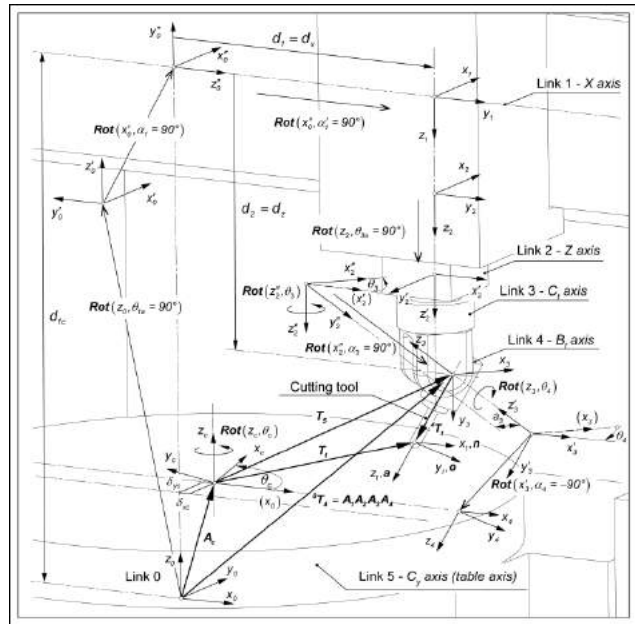


Fig. 3. Coordinate frames of the vertical 5-axis turning centre components

Parameters D-H of the machine components are given in Tab. 1.

Table 1. D-H parameters of vertical 5-axis turning centre components

Link	1-X	2-Z	3- C_t	4- B_t	5- C_y
Variable	d_1	d_2	$(-)\theta_3 = \theta_{C_t}$	θ_4	C
a [mm]	0	0	a_3	0	δ_{xc}
ay [mm]	0	0	0	0	δ_{yc}
d [mm]	d_{1c}	0	0	0	0
α [°]	$\alpha_1=-90$	0	$\alpha_3=90$	$\alpha_4=-90$	0
θ [°]	$\theta_{1a}=90$	0	$\theta_{3a}=90$	0	0

The homogenous matrix that transforms the coordinates of a point from frame $x_n y_n z_n$ to frame $x_m y_m z_m$ is denoted by ${}^n T_m$. This matrix, which describes the relation between one link and the next, is called $A_i = A(i-1, i)$ [6]. The following homogenous matrices for the relation between the coordinate frames of the machine links are defined to derive the kinematic equations for the machine. By using the convenient shorthand notation, $\sin(\varphi) = s_\varphi$ and $\cos(\varphi) = c_\varphi$, the transformation matrices defined above are written as follows:

$$A_1 = \begin{bmatrix} 0 & 1 & 0 & d_x \\ 1 & 0 & 0 & 0 \\ 0 & 0 & -1 & d_{zc} \\ 0 & 0 & 0 & 1 \end{bmatrix} \quad (10)$$

$$A_2 = \begin{bmatrix} 1 & 0 & 0 & 0 \\ 0 & 1 & 0 & 0 \\ 0 & 0 & 1 & d_z \\ 0 & 0 & 0 & 1 \end{bmatrix} \quad (11)$$

$$\mathbf{A}_3 = \begin{bmatrix} s_3 & 0 & c_3 & s_3 a_3 \\ c_3 & 0 & -s_3 & c_3 a_3 \\ 0 & 1 & 0 & 0 \\ 0 & 0 & 0 & 1 \end{bmatrix} \quad (12)$$

$$\mathbf{A}_4 = \begin{bmatrix} c_4 & 0 & -s_4 & 0 \\ s_4 & 0 & c_4 & 0 \\ 0 & -1 & 0 & 0 \\ 0 & 0 & 0 & 1 \end{bmatrix} \quad (13)$$

$$\mathbf{A}_c = \begin{bmatrix} c_c & -s_c & 0 & \delta_{xc} \\ s_c & c_c & 0 & \delta_{yc} \\ 0 & 0 & 1 & 0 \\ 0 & 0 & 0 & 1 \end{bmatrix} \quad (14)$$

2.1. Forward kinematics

Forward kinematics are used to calculate the tool position and orientation, X , Y , Z , B_t and C_t , with respect to the machine axis variables, d_1 , d_2 , θ_3 , θ_4 and θ_c . It is obvious from Fig. 3 that the component 4 position and orientation relative to the machine base is given by the equation:

$$\mathbf{T}_5 = \mathbf{A}_c^{-1} \mathbf{A}_1 \mathbf{A}_2 \mathbf{A}_3 \mathbf{A}_4 \quad (15)$$

The tool location relative to the rotating work piece is determined by the matrix:

$$\mathbf{T}_t = \mathbf{T}_5 {}^4\mathbf{T}_t = \mathbf{T}_5 \begin{bmatrix} 1 & 0 & 0 & -r_t \\ 0 & 1 & 0 & 0 \\ 0 & 0 & 1 & l_t \\ 0 & 0 & 0 & 1 \end{bmatrix} \quad (16)$$

Here, ${}^4\mathbf{T}_t$ is tool position matrix relative to the component 4, l_t is the length and r_t is the radius of the tool (Fig. 3). By using the tool orientation matrix, $[\mathbf{n} \ \mathbf{o} \ \mathbf{a}]$, and Eq. (7), the tool orientation angles can be determined.

2.2. Inverse kinematics

Inverse kinematics are used to determine the axes variables d_1 , d_2 , θ_3 , θ_4 and θ_c by using the desired cutter location, X , Y , Z , $-a_{x5}$, $-a_{y5}$ and $-a_{z5}$, given in the CL data file, or using X , Y , Z , C_t and B_t given in G code. The control unit, during machining in each interpolation period, determines the tool locations and corresponding positions of the machine axes.

The given control algorithm eliminates some of the singular positions of the rotating table and the head axis, C_t .

By virtue of the tool position and the orientation relative to the rotating table and given by the matrix, \mathbf{T}_t , Eq. (7), we will determine the machine components positions. The position of component 4, with respect to the rotating table, is defined by the expression:

$$\mathbf{T}_5 = \mathbf{T}_t {}^4\mathbf{T}_t^{-1} \quad (17)$$

If we program the machine using G code, we could, using parameters X , Y , Z , C_t and B_t , calculate the matrix, \mathbf{T}_5 . If we program the machine by a CAM system, we could first calculate C_t and B_t then calculate the matrix, \mathbf{T}_5 .

By multiplying both sides of Eq. (6) by matrix \mathbf{A}_c on the left side, we obtain:

$$\mathbf{A}_c \mathbf{T}_5 = {}^0\mathbf{T}_4 = \mathbf{A}_1 \mathbf{A}_2 \mathbf{A}_3 \mathbf{A}_4 \quad (18)$$

In Eq. (9), we calculate the terms of matrix \mathbf{T}_5 by Eq. (8). Multiplying Eq. (9) consecutively by \mathbf{A}_1^{-1} , then by \mathbf{A}_2^{-1} and lastly by \mathbf{A}_3^{-1} on the left side, we obtain:

$$\mathbf{A}_3^{-1} \mathbf{A}_2^{-1} \mathbf{A}_1^{-1} \mathbf{A}_c \mathbf{T}_5 = {}^3\mathbf{T}_4 = \mathbf{A}_4 \quad (19)$$

From the previous equations one can easily calculate axes variables d_1 , d_2 , θ_3 , θ_4 and θ_c .

3. ALGORITHM FOR CALCULATION OF THE TABLE ROTATION ANGLE θ_c

The X axis feed will be limited so that the cutting tool moves from the table centre to the maximum positive value. To achieve this, and also taking into consideration that the value of X_5 can be negative, the table swivelling angle θ_c should be in the minimum range of $[-180^\circ, 180^\circ]$. To reduce the additional positioning of the table and the angular head during milling, the table swivelling angle θ_c will be adopted in the range of $[-360^\circ + \theta_{c90}, 360^\circ + \theta_{c90}]$. Hence, it is necessary to extend the range of angle θ_c , from $[-90^\circ, 90^\circ]$ to $[-360^\circ + \theta_{c90}, 360^\circ + \theta_{c90}]$. To achieve this, but also to avoid the uncontrolled work table swivelling in singular positions by approximately $\pm 180^\circ$ or $\pm 360^\circ$, this paper proposes a novel algorithm for calculating angle θ_c . It consists of three steps, presented below.

Step 1. Step 1 involves the calculations of angle θ_c . The range of angle θ_c obtained here is $[-180^\circ, 180^\circ]$. Let angle θ_c be denoted by θ_{cprev} for the previous interpolation period. The angle θ_c increment for the next interpolation period will be:

$$\Delta\theta_c = \theta_c - \theta_{cprev} \quad (20)$$

Step 2. In Step 2, we check if the value of angle θ_c , calculated in Step 1 for a single interpolation period, changes by approximately $\Delta\theta_c = \pm 180^\circ$ or $\Delta\theta_c = \pm 360^\circ$. The procedure, presented below, makes this changing impossible and, if necessary, extends the range of the angle θ_c from $[-180^\circ, 180^\circ]$ to $[-360^\circ, 360^\circ]$. For calculation of angle θ_c in the next interpolation step, the value will be assigned as $\theta_{cprev} = \theta_c$.

Step 3. In Step 3, angle θ_c is determined for the case of . First, by using expression (9), the value of angle θ_{c90} is calculated. Using this and the value of angle θ_c obtained in Step 2, the range of angle θ_c is extended from $[-90^\circ, 90^\circ]$ to $[-360^\circ + \theta_{c90}, 360^\circ + \theta_{c90}]$.

The difference between angle θ_{c90} , obtained by expression (9), and angle θ_c as calculated in Step 2 will be denoted by:

$$\Delta\theta_{c90} = \theta_{c90} - \theta_c \quad (21)$$

4. PROGRAMMING OF THE 5-AXIS VERTICAL TURNING CENTRE

The programming of the 5-axis milling, drilling and boring operations on the vertical turning centre are performed by a CAM system or by G code [1] in the machine base coordinates $x_0y_0z_0$ (Fig. 3) as if it were machining on a 5-axis gantry milling machine, where the work piece is fixed. This is possible because the solutions for the forward and inverse kinematics proposed in this work allow for the tool locations relative to the swivelling work piece to be identical to the tool locations relative to

the fixed work piece. This will essentially facilitate machine programming. Using G code, the tool direction is given in the X , Y , and Z coordinates, and the tool orientation is given in Euler or RPY angles or by the tool direction vector, which points from the tool tip towards the tool holder. If we define the approach vector as $\mathbf{a}=a_{x5}\mathbf{i}+a_{y5}\mathbf{j}+a_{z5}\mathbf{k}$, which lies in the z_t direction from which the tool approaches the work piece (Fig. 3), the tool direction vector components will be $-a_{x5}$, $-a_{y5}$ and $-a_{z5}$. Here, \mathbf{i} , \mathbf{j} and \mathbf{k} are unit vectors along the x_0 , y_0 and z_0 machine base coordinates. Using a CAM system, the output is the tool-path, which is defined by the cutter locations, X , Y , Z , $-a_{x5}$, $-a_{y5}$ and $-a_{z5}$, which define the tool positions and the tool direction vectors with respect to the work piece coordinate system, given in the CL data file [2, 3, 5]. The tool-path between two CL points is a straight line relative to the work piece.

The following step after the tool-path generation is post-processing, where the program is translated to a specified machine and control unit [2]. The postprocessor converts the CL motion commands from the CL data file to the motion commands of the NC program (in G code).

Finally, the tool-path is converted into a sequence of consecutive positions of machine axes that will produce the desired tool locations (inverse kinematics). The controller used in this work calculates the path interpolation and the inverse kinematics in real-time [7].

5. CONCLUSION

It has been shown that, on a 5-axis turning centre with 2 linear and 3 rotational axes, in addition to the turning, it is possible to achieve 5-axis milling, drilling and boring identical to that of a milling machine with 3 linear and 2 rotational axes. A control algorithm to achieve this was presented. Using this algorithm, machine programming is possible in the same way that it is done for a 5-axis milling machine, which essentially simplifies writing the machining program or taking over the CL data file from CAM systems developed for the milling machines.

Forward and inverse kinematics, based on the D-H formulation, has been solved for the case of utilising the 2-axis angular head with non-intersecting axes. The proposed control algorithm was tested on the off-line programming system of the controller developed at the Lola Institute. This controller was obtained by extending the Lola-Industrial Robot Language [7] with the commands for a machine tool by integrating the new solutions for the forward and inverse kinematics of a vertical 5-axis turning centre in it and by adapting its trajectory planner to novel tool-motion commands.

The control algorithm for the angular head with intersecting axes is simplified. Also, this algorithm extends the table swivelling angle range to approximately $\pm 360^\circ$. Thus, additional positioning of the work table and the angular head during machining is decreased.

ACKNOWLEDGEMENTS

This research is supported by the Ministry of Science and Technological Development of Serbia under the project:

Research and development of the new generation of vertical 5-axis turning centre (2008-2010), no. 14026.

REFERENCES

- [1] López de Lacalle, L.N., Lamikiz, A. (2008) *Machine Tools for High Performance Machining*, Springer Verlag, ISBN: 978-1-84800-379-8
- [2] Lee, R.S., She, C.H., (1997) *Developing a postprocessor for three types of five-axis machine tools*, Int J Adv Manuf Technol, 13(9) 658–665
- [3] Sørby, K., (2007) *Inverse kinematics of five-axis machines near singular configurations*, Int J of Machine Tools & Manufacture, 47 299–306
- [4] Bohez, E.L.J., (2002) *Five-axis milling machine tool kinematic chain design and analysis*, Int J of Machine Tools and Manufacture. 42 505–520
- [5] Lee, R.S., Lin, Y.H. (2010) *Development of universal environment for constructing 5-axis virtual machine tool based on modified D–H notation and OpenGL*, Robotics and Computer-Integrated Manufacturing, 26 253–262
- [6] Paul, R.P., (1984) *Robot manipulators: Mathematics, Programming and Control*, The MIT Press, Cambridge MA
- [7] Pavlović, M., Kvrđić, V., Velašević, D., (1994) *L-IRL: High Level Programming Language for Robots*, In Proc of the European Robotics and Intelligent Systems Conference, Malaga, Spain

DEPENDENCE OF SURFACE ROUGHNESS FOR SHAFT PACKING

Robert CEP, Jan STRBKA, Lenka CEPOVA

Department of Machining and Assembly, Faculty of Mechanical Engineering,
 VSB – Technical University of Ostrava, 17. listopadu 15/2172, 708 33 Ostrava, Czech Republic
robert.cep@vsb.cz, jan.strbka.st@vsb.cz, lenka.cepova@vsb.cz

Abstract: This paper is about determination of change of roughness character under rotary shaft packing for increase of operation life of packing point at preservation of packing property. A part of paper is comparison of roughness sizes of shaft at centre grinding and determination of optimal characteristic.

Key words: Roughness, Packing, Grinding, Wearing, Friction.

1. INTRODUCTION

The functional properties of parts and machine surfaces depend in a large extent on the surface character. Optimum choice and observance of surface character requirements during product evaluation affects surface performance characteristics, liability and working life of frames and mechanism, including environment effect resistance [1].

Similarly is it with the surface character of the shaft in the sealing bushing, where the shaft and sealing bushing edge active area prevent the external environment impacts on functional parts of the equipment.

2. PROBLEM DEFINITION

The issue of the surface under the sealing bushing and sealing bushing working life is very complex. Determination of the optimum solution of the issue between these two parts is difficult, because there interact different tribological factors that by some means depend on each other. See fig.1.

From the point of view of tribology on the sealing system, the friction and sealing working life are in the sealing system interconnected. The mutual influence of these properties depends on the parameters interaction (temperature, pressure and velocity).

Since this issue is quite extensive, we focused in this article on the determination of the optimum shaft surface profile.

The sealing effect which should ensure the sealing bushing basic required parameters and the quality requirement of shaft surface as well as lubrication oil.

The friction effect of two adjacent sliding surfaces is minimized if the two friction surfaces are separated by lubricant layer.

The lubrication oil is used for the friction reduction. This lubricant must be able to resist various conditions e.g. ambient temperature, feed rate, normal force. The sealing bushing wearing depends extensively on the shaft surface profile.

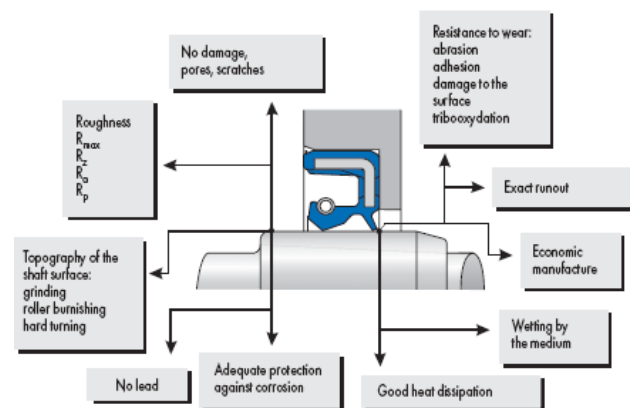


Fig.1. Factors incoming into the sealing process

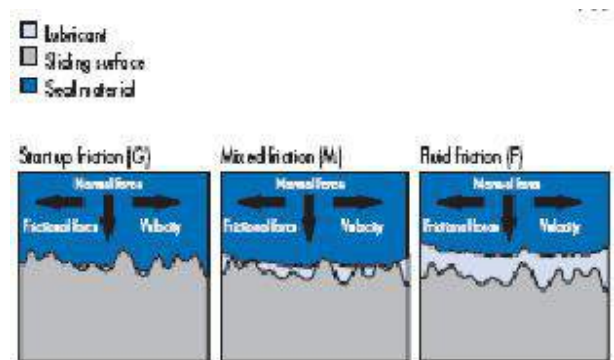


Fig.2. Friction types

2.1. Surface quality

The evaluation of the sealing mechanism surface quality depends on the surface profile and values R_z , R_a . The shaft surface structure is effected by the technological method of processing during finishing.

For reaching of the high sealing effect it is necessary to provide the most optimum size of roughness with the lubrication oil. The peaks of R_z must be as periodical as possible.

However this is by the recessing method difficult to achieve. Using the recessing method on the shaft surface generates the same surface profile as on the grinding wheel.

For the sealing effect it is necessary that there isn't any line on the shaft surface after the machining. If there such line appears e.g. in the direction out of the device, it would occur lubrication oil discharge. On the other hand the line towards the device would cause the supply of impurities from the environment and the impurities would get into the contact with device and result in damage of the sealing.

That's why recess grinding method is used for finishing. For the shaft guidance control we use „ thread method“, where on the shaft with oil film is a line marked with pencil. Weight on thread is then hung on the shaft. (Fig. 5)

The shaft is twisted in one and then in another direction and the thread would in case of the movement on surface wipe the oil film.

That's why the surface profile depends substantially on the grinding wheel type, its composition and grain size. The tests proved, that another important aspect for the surface forming is the removed layer thickness (ap.).

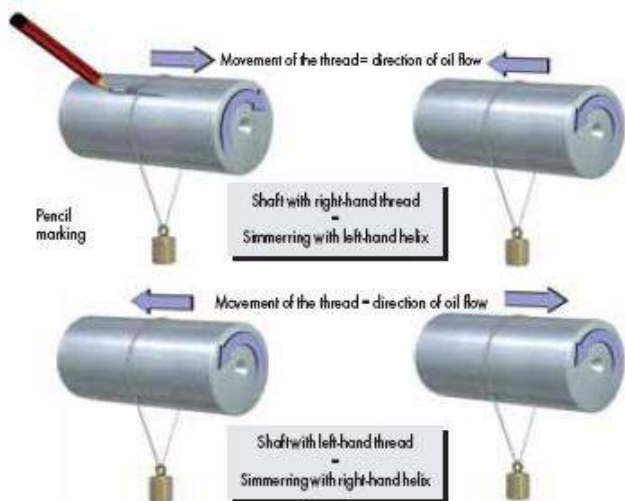


Fig.3. Determining lead on the shaft

2.2. Lubrication oil

The lubrication oil creates on the shaft surface the oil film which separates the sealing surface from the shaft surface and reduce the friction.

For this effect it is important to have certain dimensions of the shaft surface Ra, Rz. It is due to the fact, that if the surface is too smooth, it would prevent the lubrication oil from making an even oil film (Fig.4).

In such case there would negative operation of sealing occur.

On the surface with created cutting marks (after tool) which are within the limits the conditions are perfect for the lubrication oil to get into the grooves and this way create coherent oil film (Fig.5).



Fig.4. Non-wettable surface

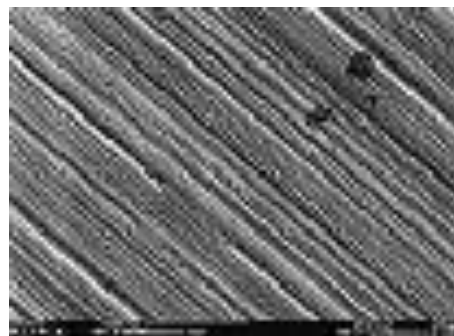


Fig.5. Ground surface

Too rough shaft surface cause the friction against the tops of the profile asperity which then lead to the wearing in the sealing tip contact area and enlargement of the contact area of the sealing and shaft surface. In this area high friction and temperature occur and the functionality and service life of the sealing is significantly decreasing.

3. RECOMMENDED VALUES OF THE SEALING SYSTEM FOR THE SHAFT QUALITY

Tolerance ISO h11
 Roundness IT 8
 Ra = 0,2 to 0,8 μm
 Rz = 1 to 4 μm
 Material 42CrMoS4
 Hardness 45 to 60 HRC
 Grinding wheel: 60 to 100

3.1. Testing procedure and testing conditions

In the test of the ideal surface profile we examined the abrasivity, it means the sealing material wearing. For comparison we chose 4 types of sealing materials which were proper for the stated conditions.

PTFE - polytetrafluoroethylene
 PTFE C104. carbon fibre alloy
 PTFE B602 bronze alloy
 PTFE GM201 glass fibre mixture MoS2
 By achieved roughness Ra = 0,3 μm .

For the achieving of the required roughness we used grinding wheels of Winterthur producer marked 57A80J7V, 57A60J7V and 57A100J7V

3.2. Test parameters

Wheel speed 45 m.s-1
 Complete spark out.

Mesh depth 0,03mm
 Recess method.
 Shaft material 42CrMoS4, high-frequency hardened for hardness 53+7 HRC
 Sealing internal diameter 63,400 mm

3.3. Test procedure

The shaft surface was machined using the grinding wheel for the roughness $Ra=0,3 \mu m$ with the identical cutting parameters.

In the next phase, the wearing on these surfaces was examined by inspected sealings. The wearing took place in the real conditions where the given shaft was used and that was in hydraulic device, where we used the shaft with sealing and loaded for 50 % using 10 000 cycles.

1 cycle- start up- pressure 14 bar.- shutdown, start up in opposite direction -pressure 14 bar- shutdown.

After finishing the load test the change of the sealing internal diameter size using 3D measuring device Mitutoyo was measured. From this test two best materials of the sealing (subjected to the load test with testing time 336 hours with 60 % load and pressure 5 bar) were chosen.

4. MEASURING RESULTS

Table 1. Results for 10000 cycle

Ra=0,3	PTFE	PTFE B602	PTFE C104	PTFE GM 201
57A80J7V	63,309	63,379	63,372	63,314
57A60J7V	63,378	63,394	63,393	63,385
57A100J7V	63,295	63,341	63,338	63,301

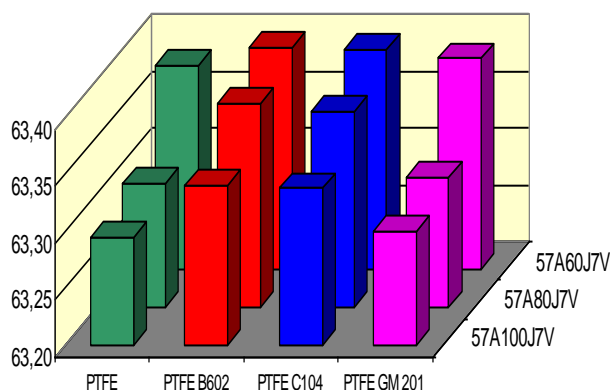


Fig.6. Results for 10000 cycle

Table 2. Results for 336 hours

Ra 0,3	PTFE B602	PTFE C104
57A60J7V	63,358	63,343

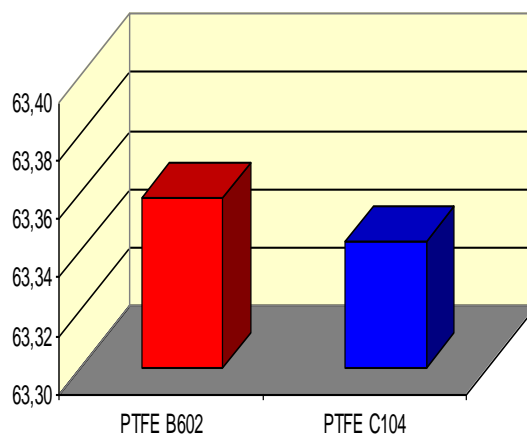


Fig.7. Results for 336 hours

5. CONCLUSIONS

From the obtained values and diagram it is visible, that the minimum wearing reached the sealing using the grinding wheel with the grain size of 60, and the worst with the grain size 100.

For all types of grinding wheels the least wearing got the material with bronze alloy and then material with the carbon fiber alloy.

For the next test the sealing materials PTFE B602 and PTFE C104 with the surface profile which was left by the grinding wheel 57A60J7V, consequently will be chosen. In this test the best results had the material with bronze alloy.

From the test results suggestion is to use, under stated conditions, the sealing made from PTFE B602 material, because it passed the test with the best results from all tested materials.

REFERENCES

- [8] NESLUŠAN M., TUREK S., BRYCHTA J., ČEP R., TABAČEK M. *Experimentálne metódy v trieskovom obrábaní*. Žilina : Edis 2007, 311-346s. ISBN 978-80-8070-711-
- [9] VASILKO, Karol. *Technológia dokončovania povrchov*. Prešov : Cofin 2004, 114s. ISBN 80-8073-124-1
- [10] BEČKA, Jan. *Tribologie*. Praha : ČVUT 1997. 211s. ISBN 80-01-01621-8
- [11] www.simrit.com
- [12] SADÍLEK, M.; ČEP R.; GREGUŠOVÁ M. *Vliví řezné rychlosti na drsnost povrchu při frézování tvarových ploch*. Zborník referátov z 8. medzinárodnej vedeckej konferencie „Nové smery vo výrobných technológiách 2006“, Fakulta výrobných technológií Technickej univerzity v Košiciach so sídlom v Prešove, 2006, s. 109 – 113. Prešov, Slovenská republika. ISBN 80-8073-554-09.

34th INTERNATIONAL CONFERENCE ON PRODUCTION ENGINEERING



SECTION D

METROLOGY, QUALITY SYSTEMS AND QUALITY MANAGEMENT



QUALITY CONTROL OF CONTOUR VERIFIER USING PHOTOGRAMMETRIC MEASURING SYSTEMS

Milan BLAGOJEVIĆ¹, Miroslav ŽIVKOVIĆ¹, Ana PAVLOVIĆ²

¹ Faculty of Mechanical Engineering, University of Kragujevac, Sestre Janjić 6, Kragujevac, Serbia
blagoje@kg.ac.rs, zile@kg.ac.rs

² Department of Mechanical Engineering-DIEM, University of Bologna, via Risorgimento 2, 40126 Bologna, Italy
ana.pavlovic@unibo.it

Abstract: Photogrammetric measuring systems provide precision compatible or better than the accuracy achieved by the coordinate measurement systems for high-precision measurement of large volumes. Quality control by contour verifier is carried out using method of light gap. Therefore, it is important that the contours of the equipment have made precise geometric entities. Objects' size of control devices is varying from a few tens of millimeters to a few meters. Sometimes it is necessary to perform on site measurements which give photogrammetric measuring systems a great advantage compared to conventional systems.

Optical measuring system TRITOP was performed very precisely position measuring of coded and uncoded reference points and adapters. Reference objects were placed on the measured geometric entities. The paper reviews the procedure of obtaining measurement results and results processing. Good interfaces to conventional CAD/CAM and numerical simulation systems made optical measuring systems a part of process chains. Using optical systems considerably decreases the production time while improving the quality.

Key words: Optical measuring systems, Photogrammetry, CMM, Quality Control, Contour Verifier, CAD/CAM/CAE

1. INTRODUCTION

Optical measuring technology have become a standard tool within almost all industries. This is the most cost-effective and affordable way to do accurate 3D scanning, measurement and surveying. Measuring tasks that traditionally were performed by tactile 3D coordinate measuring machines can now easily be carried out with the optical CMM systems. It does not require any complex, heavy and maintenance-intensive hardware. This contactless method is suitable, because the measuring instruments are robust and mobile. Also, the measuring machine comes to the object.

Foundation of optical measuring technology is photogrammetry. Photogrammetry is the science of making measurements from photographs. In practice, photogrammetry is tool for determining the geometric properties of objects from photographic images as the main metrology medium.

Photogrammetry uses methods from many disciplines, including optics and projective geometry. The data model of photogrammetry show what type of information can go into and come out of photogrammetric methods. It consists of four main (n exterior orientations, image coordinates from views, camera model(s), 3D coordinates) and ancillary variables. Each of the main variables can be an input or an output of a photogrammetric method.

Photogrammetry can be classified a number of ways but one standard method is to split the field based on camera location during photography. On this basis we have Aerial

Photogrammetry, and Close-Range Photogrammetry. In Close-range Photogrammetry the camera is close to the subject and is typically hand held, mounted on robot or tripod. Also, non-contact optical scanners can be categorized by the degree to which controlled illumination is required. Passive scanners do not require direct control of any illumination source, instead relying entirely on ambient light. Active optical scanners overcome the correspondence problem using controlled illumination. For a detailed history of active methods, we refer the reader to the survey article by Blais [1] **Error! Reference source not found.**

Photogrammetry is used in different fields, such as topographic mapping, architecture, police investigation, geology, as well as in archaeology. In field of Mechanical and Civil Engineering photogrammetry offers an accurate and cost-effective solution in a number of different application areas including: Quality Control, Reverse Engineering, Rapid Prototyping, Rapid Milling, Digital Mock-Up, etc.

2. MODEL OF TRIANGULATION

The fundamental principle used by photogrammetry is triangulation. By taking photographs from at least two different locations, so-called lines of sight can be developed from each camera to points on the object, as depicted in Figure 1. Since light moves along straight lines (in a homogeneous medium such as air), we derive 3D reconstruction equations from geometric constructions

involving the intersection of lines and planes, or the approximate intersection of pairs of lines (two lines in 3D may not intersect).

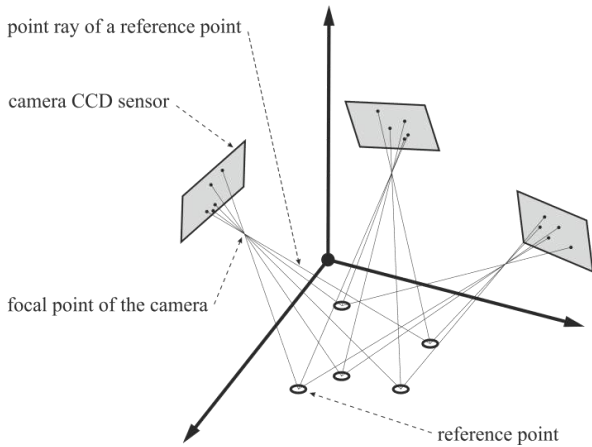


Fig.1. Affiliation of photogrammetric images

These lines of sight (sometimes called rays owing to their optical nature) are mathematically intersected to produce the 3D coordinates of the points of interest. A point is reconstructed by intersecting two or more corresponding lines, Figure 2. After establishing correspondences across two or more views (measurement images taken from different spatial locations), triangulation recovers the scene depth.

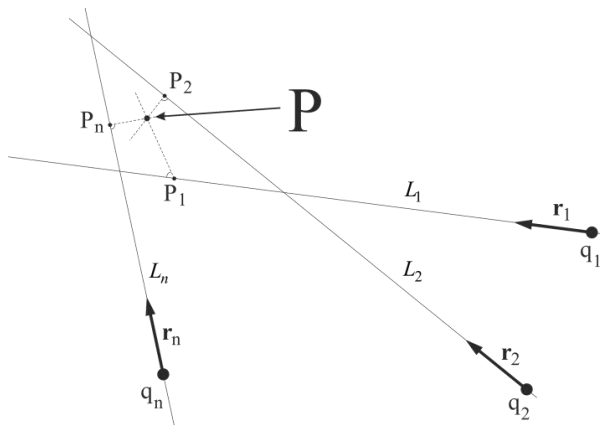


Fig.2. Triangulation by line-line intersection

A simple and popular geometric model for a camera is the pinhole model [2], composed of a plane and a point external to the plane. We refer to the plane as the image plane, and to the point as the center of projection. In a camera, every 3D point (other than the center of projection) determines a unique line passing through the center of projection. If this line is not parallel to the image plane, then it must intersect the image plane in a single image point. In mathematics, this mapping from 3D points to 2D image points is referred to as a perspective projection. That is, given a 2D image point in the projector's image plane, there must exist a unique line containing this point and the center of projection, since the center of projection cannot belong to the image plane. Let us assume that the locations and orientations of camera are known with respect to the global coordinate system. Under this assumption, the equations of camera rays corresponding to illuminated points, are defined by parameters which can be measured. From these measurements, the location of illuminated points can be

recovered by intersecting the rays of light. Through such procedures the depth ambiguity introduced by pinhole projection can be eliminated, allowing recovery of a 3D model.

Let us consider here the intersection of n arbitrary lines of sight $L_i, i = 1, \dots, n$, as shown in Figure 2.

$$\begin{aligned} L_1 &= \{p = q_1 + \lambda_1 r_1 : \lambda_1 \in \mathbf{R}\} \\ L_2 &= \{p = q_2 + \lambda_2 r_2 : \lambda_2 \in \mathbf{R}\} \\ L_n &= \{p = q_n + \lambda_n r_n : \lambda_n \in \mathbf{R}\} \end{aligned} \quad (1)$$

If the two lines intersect, the intersection contains a single point. Since two lines may not intersect, we define the approximate intersection as the point which is closest to the two lines. We define the approximate intersection as the point P which minimizes the sum of the square distances to lines

$$\phi(P, \lambda_1, \lambda_2, \dots, \lambda_n) = \sum \|q_i + \lambda_i r_i - P\|^2 \quad (2)$$

Let us assume $r_i, i = 1, \dots, n$ are linearly independent, such the approximate intersection is a unique point.

3. PHOTOGRAMMETRIC MEASUREMENT

Photogrammetric measurement was performed by optical measuring system TRITOP [3], [4], [5].

3.1. Overview of the measuring system

TRITOP is an industrial, non-contact optical measuring system for exact 3D coordinate acquisition of discrete object points. This mobile technology supports time-optimized measurements for on-site quality control and deformation analysis. System consists of coded and uncoded reference points, reference scale bars, adapters, high-resolution DSLR camera, and high-end computer. The coded reference points provide an automated method for obtaining the location of a camera during measurements. Each point has its own ID in order to generate an image set that can be automatically evaluated in TRITOP and to allow for calculating the camera positions. Uncoded reference points enable system to get 3D coordinates of the measuring-relevant parts of the object to be measured. Reference scale bars are made of alloys that have a negligible coefficient of linear expansion at a certain temperature range. Scale bars has role to give dimension - scale to photogrammetric measurements, by known distance between the coded reference points on the bar. Always, when possible, should be used more than one lengths for measurements scaling.

Complete 3D measuring machine with minimum hardware requirements consists of 3 cases with a total weight of 23 kg. The object is not touched during measuring. Very high accuracy is achieved for large objects. Measuring equipment is independent of environmental conditions, except light conditions. TRITOP allows for measuring objects up to some 20 m. The TRITOP software interprets the images and generates 3D measuring data. The measuring data can be evaluated

in the TRITOP system (CAD comparison, inspection, ...) or made available to subsequent systems like ATOS. Configuration and photo of Optical Measuring System TRITOP is provided in Table 1 and Figure 3.

Table 1. Configuration of Measuring System

Item	Property
Optical Measuring System	TRITOP
Photogrammetric Camera	NIKON D200 12Mpx
Scale Bars	Optical Scale Bar 1000mm SG00243, Dist.0/1: 906.351mm, CrNi Steel na 20°C 16.2x10 ⁴ K ⁻¹ SG00244, Dist.2/3: 907.577mm, CrNi Steel na 20°C 16.2x10 ⁴ K ⁻¹
Coded Reference Points	15bit Coded Reference Points
Application software	TRITOP v602



Fig.3. Photogrammetric system TRITOP

3.2. System calibration

Reliable measurement requires the calibration of measuring equipment. Calibration is a process during which the measuring system, with or without the calibration target, perform auto-tuning which provides dimensional accuracy. Every time the optical measuring system TRITOP is assembled, in fact, we work with a unique and non-repeatable configuration of an optical measuring system. Characteristics of the system components are changing over time. Also, changing of the lighting conditions during measurements and in different points of measurement volume are not neglectable.

Camera calibration requires estimating the parameters of the general pinhole model. This includes the intrinsic parameters, being focal length, principal point, and the scale factors, as well as the extrinsic parameters, defined by the rotation matrix and translation vector mapping between the world and camera coordinate systems. In total, 11 parameters (5 intrinsic and 6 extrinsic) must be estimated from a calibration sequence. In practice, a lens distortion model must be estimated as well. Natively, one would simply need to optimize over the set of 11 camera

model parameters so that the set of 2D-to-3D correspondences are correctly predicted [2], [6].

The ability to calibrate the camera as one of the components of measuring process is called self-calibration. This means that the camera is calibrated during the measurement in environmental conditions (temperature, humidity, ...) that ruled during the measurements. This is an important feature in relation to laboratory conditions calibrated systems, which may differ significantly from the conditions under which the measurement is done. For system TRITOP is recommended to make four initial calibration images, from the same place and same target direction, while the camera turns about 90 degrees to the previous snapshot. If self-calibration process is not done, we rely on pre-defined calibration that is slightly less reliable and less accurate.

3.3. Measurement

In order to meet defined requirements by TRITOP optical measuring system, object is properly prepared for 3D digitization process, Figure 4. Measuring project must provide a precise determination of the coordinates of geometrical features, by placing the plane adapter, and appropriate number of uncoded reference points defining these features. Each uncoded reference point must be captured in at least three measuring images.

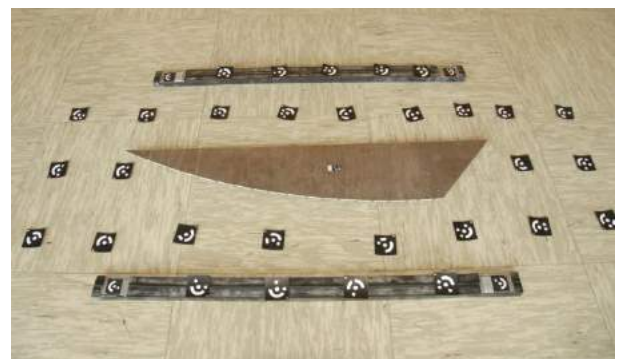


Fig.4. Properly prepared measuring volume

In order to obtain high quality measurements, a few requirements have to be satisfied. Above all, measuring volume need to be well prepared. The highest precision is achieved when reference scale bars is the same size as the dimensions of the measuring object. The scale distance(s) should be as long as practical because any inaccuracy in the scale distance(s) is magnified by the proportion of the size of the object to the scale distance. Next, to achieve the orientation of the camera in relation to the measuring volume reference points should be properly placed in the measuring volume. Each measuring image must contain at least five coded reference points recorded in at least three measuring images in order to enable its orientation.

Making a measurement image is essential for making high-quality photogrammetric measurements. In order to get photos of great accuracy, reliability, and benefit from the opportunities provided by the system, photos must be of the highest quality, Figure 5. Images are recorded from various angles of view. During the acquisition of an image set it is the goal to record reference points from multiple different directions that show the largest possible angle to each other. Then, the software provides image-

based modeling, for accurate measurement and engineering 3D models.

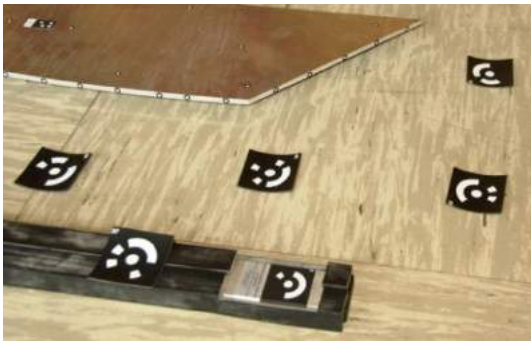


Fig.5. One of the measuring images

Software automatically calculates the 3D coordinates of the adhesive markers and object characteristics from these digital images. Software has two operating modes: Project and Evaluation. Project Mode (a) creates a measuring project (define camera, scale bars, coded markers ...), (b) load photogrammetric images into the measuring project, (c) computes project (images are oriented automatically, 3D coordinates of the reference points are calculated, ...), (d) Check the result, and if required, add not identified points and compute the project again. Evaluation Mode (a) transforms the measuring data into a defined coordinate system, (b) carry out inspection tasks, load CAD data for comparison, (c) creates a result in form of snapshots and documentation.

4. RESULTS

The obtained model, generated by optical measurement was compared by the CAD model. Figures 6 and 7 show some typical measures of sample contour verifier.

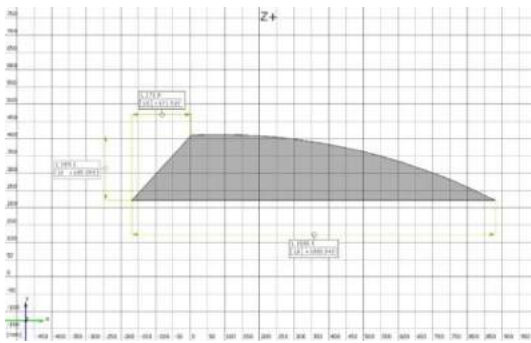


Fig.6. Example of measurement report

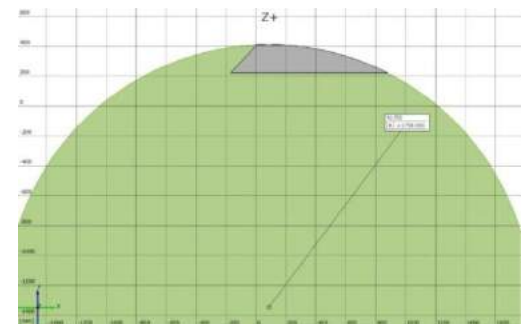


Fig.7. Example of measurement report

Moreover, these results can be presented in diagrams, directly on CAD data or superimposed onto the recorded

camera images providing an easy to understand and intuitive result presentation. The measured and aligned data is used for various tasks: CAD comparison, verification of shape and position tolerances, verification of specifications from drawings, files or tables, initial measurements.

5. CONCLUSION

The paper presents the use of photogrammetric system in geometry control and measuring tasks of contour verifier. Photogrammetric measurement accuracy can fluctuate significantly, because it depends on several interrelated factors. The most important factors are: quality and resolution of the camera used to measure, size of measured object, the number of recorded images, the geometric arrangement of photographs in relation to the object, and in relation to each other photos. Photogrammetry is more accurate in the x and y direction than in the z direction. Compared with tactile measuring systems, typically measuring optical measuring system provides significant benefits, especially for complex geometry. When comparing the measuring data with CAD data, the corresponding measuring reports are created in the familiar formats: false-color representation, deviation of individual points as labels, sections, angles and distances, diameters and flatness, tables and lists. Based on large number of performed measurements, it can be said that these systems are an excellent tool for the contour verifier geometry control. Presented results of measurements show that the optical measuring systems are powerful tool for quality control, analysis and debugging. A good interface to important CAD/CAM systems was introduces these systems in complex production chains. Using the optical measuring system significantly reduces the time required to develop and manufacture products, while increasing quality.

ACKNOWLEDGMENTS

The part of this research is supported by Ministry of Education and Science, Republic of Serbia, Grant TR32036.

REFERENCES

- [1] BLAIS, F., (2004) *Review of 20 years of range sensor development*, Journal of Electronic Imaging, Vol.13, No 1, pp 231–240
- [2] BOUGUET, J., Y., (1999) *Visual methods for three dimensional modeling*, PhD Dissertation, California Institute of Technology, Pasadena, California
- [3] TRITOP User Information, *TRITOP Adapters*
- [4] TRITOP User Manual - Software, *TRITOP v6*,
- [5] BLAGOJEVIC, M (2009) *Application of optical measuring systems in modeling and simulation (in Serbian)*, Faculty of Mechanical Engineering in Kragujevac, University of Kragujevac
- [6] LANMAN, D., TAUBIN, G., (2009) *Build Your Own 3D Scanner: 3D Photography for Beginners*, SIGGRAPH 2009 Course Notes



RESULTS OF THE ANALYSIS ON STYLUS CALIBRATION OF A COORDINATE MEASURING MACHINE (CMM)

Miodrag HADZISTEVIC, Janko HODOLIC, Igor BUDAK, Djordje VUKELIC, Branko STRBAC
Department of Production Engineering, University of Novi Sad, Trg Dositeja Obradovića 6, Novi Sad, Serbia
miodrags@uns.ac.rs, hodolic@uns.ac.rs, budaki@uns.ac.rs, yukelic@uns.ac.rs, strbacb@uns.ac.rs

Abstract: *The result of the measurement on a coordinate measuring machine (CMM) depends on many factors. Calibration accuracy of the styli is one component of inaccuracy. The exact calibration of the styli is the basic requirement for all measurements. Inaccuracies occurring during the calibration and verification have an effect on all measuring results. Influential factors in the calibration process, such as the accuracy of the calibration sphere and the environmental conditions in this study will be ignored. This paper analyses the results of the calibration depending on the calibration sphere direction on the machine table and the displacement of calibration contact starting point in the positive direction of the x axis. The appropriate conclusions will be made based on the analysis of the results.*

Key words: *calibration styli, probe, accuracy, CMM.*

1. INTRODUCTION

Coordinate measurement machines are complex machines with a large number of error sources affecting the accuracy of measurement results. Many factors have been identified as the source of measurement errors on CMM and can be summarized in five groups: measuring machine (measuring range, reference sphere, machine geometry, linear measuring system, etc.), environment (room temperature, thermal radiation, humidity, floor vibration, etc.), workpiece (soiling of the workpiece, linear stability, roughness, elasticity, etc.), measurement strategy (stylus selection, measuring method, number of probing, evaluation method, etc.) and operator training (further training, shaft probing, measuring run planning, stylus calibration, etc.). [2] One of the errors includes the probing system calibration (stylus calibration) and it has a critical role in the CMM measurement, not only in terms of its functionality, but also its contribution towards the overall measurement error. The probing system in CMM includes a stylus and a stylus tip which have their own dynamic characteristics during the measuring process [4]. The stylus tip contact with the detected surface is the source of signals that will develop the pattern on the working objects. Hence, the performance of the CMM overall system is very much dictated by the motion precision of the probe tip and its actuator. Therefore, the probe stylus tip is laterally at the centre of the CMM operation and a key element of coordinate measurements [5]. The exact calibration of the styli is the basic requirement for all measurements. Any deviation caused by an inadequate or not correctly performed calibration process will affect every measurement to be done with the probing system, i.e. the measurement results could have significant errors.

This paper analyses the results of the calibration contact starting point in the positive direction of the x axis and the

orientation reference sphere. The standard deviation is considered as a calibration value. Influential factors in the calibration process, such as the accuracy of the calibration sphere and the environmental conditions will be ignored in this study.

The experimental tests have been carried out on a CMM "Carl Zeiss CONTURA G2 RDS" in the Metrology Laboratory of the Department of Production Engineering at the University of Novi Sad.

2. CALIBRATION STYLUS

The position of the tip ball centre point related to the reference point of the probing system and the radius of the tip ball must be known in order to perform correct measurements. These parameters are dependent on the probing force (magnitude and direction), elastic behaviour of a probing system, styli, workpiece and other influences. Their origin can be materials, components, arrangement of components in the probing system, dimensions like length, diameter of styli, material properties, and elastic flexibility of stylus joints, including suspension and roundness deviations of the tip ball.

Due to the necessary accuracy and the complexity of interactions, they cannot be calculated. They can be determined experimentally for a virtually ideal probing system with a virtually stiff stylus with an effective tip ball diameter using a calibrated artefact under the same conditions as the performance of the subsequent measurement. This procedure is called the probing system calibration (Figure 1).[3]

Calibration is a fundamental action in the management of sensors and of the entire measuring cycle. Calibration consists in the identification of diameter and of the position of the centre artefact with respect to the origins of the CMM reference system. In essence, calibration

defines where the probe (stylus) is located in space, and nullifies the effect of probing forces on accuracy. It is very important that the correct reference sphere is used and that its latest calibrated size is entered into the software. It is also essential that the stylus tip and calibration artefacts are scrupulously clean. The smallest amount of dust can lead to an incorrect probe calibration. Measuring the length of a known artefact e.g. a calibrated block or plain setting ring, is a simple check on the probe calibration. If the difference between the calibrated size of the gauge block and the length you measure is not within the machine uncertainty at this length, the probe should be recalibrated and the check repeated [6]. For reliable calibration 25 to 50 touch points are recommended for each stylus tip.

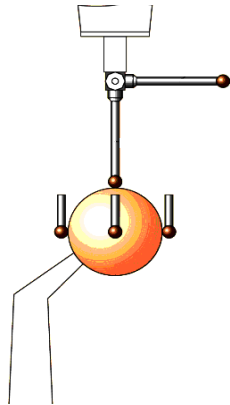


Figure 1. Probing system calibration

2.1. Calibration of the styli of CMM "Carl Zeiss CONTURA G2 RDS"

The CONTURA G2 is a mid-range bridge type CMM with advanced features and design strengths. All axes have 4-sided Carl Zeiss air bearings providing maximum stability and a very precise measurement. Ceramic guideways are thermally stable, minimizing the effect of temperature variation. The calibration process of the measuring stylus depends on the type of the measuring head with the inserted probing system. This experiment utilizes the RDS turning measuring head with the combination of VAST XXT scanning measuring sensor. As a replacement for trigger sensors, the VAST XXT offers the unmatched measurement capability, reliability, and accuracy. With a large deflection range and a low measuring force, it is a very robust scanning sensor. It uses the styli lengths up to 250 mm, side and star styli, and a minimum ball radius of 0.3 mm. The VAST XXT has very low measuring forces and there is little influence when swivelling. When the RDS head is used, the CMM can probe the workpiece from a large number of different directions by adjusting A and B angles. Every RDS position wanted to be utilized for probing is considered to be its own stylus and must be calibrated separately. A stylus must be qualified when and if there is a new stylus system installed and there is a need for the re-calibration of a stylus system, for example after a collision or due to thermal changes. The calibration of the measuring stylus is performed with the reference sphere. The reference sphere of the CMM is a sphere of a known diameter mounted on the measuring table via a stem. The software (Calypso) must know the exact

position of this reference sphere for the orientation and in order to analyze the calibration correctly. The position of the reference sphere on a measuring table is determined by the calibration of the master measuring stylus. After this calibration is performed, the next step is the calibration of measuring styli. In order to decide whether the calibration result is acceptable, standard deviation can be used as a basic for the decision. Acceptable standard deviation depends at least on the following factors: quality of the calibration, length and stability of the styli and extensions used, value of the temperature deviations and temporal thermal fluctuations on the CMM, degree of soiling, wear, damage of the reference spheres, existence of loose or damaged stylus and/or extension elements. The standard deviation should lie in the range of a few micrometers. The first calibration of a stylus must be done manually. Once the stylus has been calibrated for the first time, future calibration can be done automatically [7].

3. EXPERIMENTAL WORK

The calibration of the measuring stylus is an obligatory procedure preceding every measuring task. The procedure is performed automatically, although with the first calibration, the operator has to provide the contact between the measuring stylus and the reference sphere. This contact should happen at the point at the top of the calibration sphere, passed through by the axis line of the measuring sensor containing the measuring stylus centre and the axis line of the reference sphere. Since this is relative, this paper determines the dependence of the calibration results in relation to the deviated contact point in the positive direction of the x axis (Figure 2). Previous researches have determined that, for the deviation value larger than 3.5 mm, there is an angle deviation during the calibration, i.e. the software will signal an error and the value of the standard deviation reaches even the tenth part of the millimetre [1]. Changing the angle to zero tells Calypso to rotate the stylus system path by the deviation angle, ensuring that the sphere measurement path follows the centre line of the sphere and does not touch the shank of the stylus [9]. Software uses the information to calculate the centre of the sphere, which, relative to this centre, will look at the first point. If the first point lies within an internal tolerance of where it should be, the full sphere is measured.

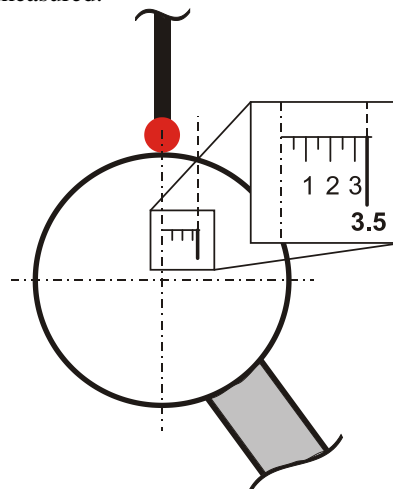


Figure 2. Experiment performance procedure

After the calibration of the master stylus, the next calibration is the one of the styli with the radius of 3 mm (Figure 3). The calibration process for the styli is performed in every contact point of the measuring stylus and the reference sphere with the deviation of 0.5 mm in the positive direction of the x axis until the value of 3.5

mm (Figure 2). The value of the standard deviation is monitored for every deviation of the contact point that begins the calibration process. For static analysis of the results to be performed, the same procedure has been repeated six times.

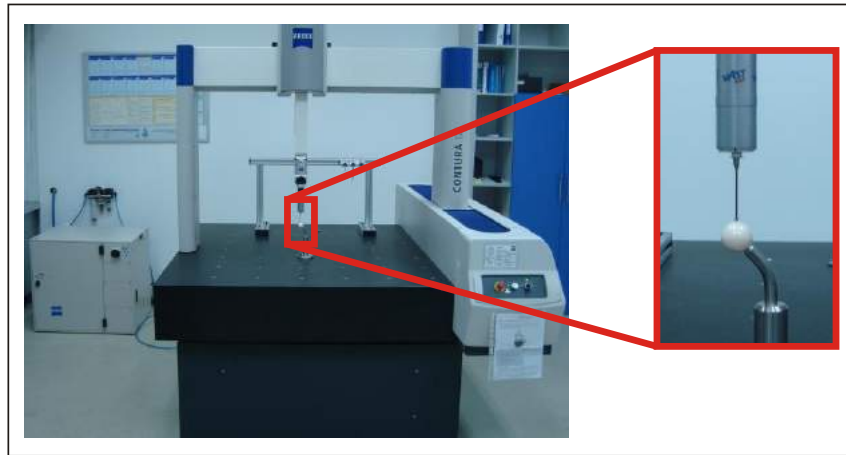


Figure 3. CMM Carl Zeiss CONTURA G2 RDS, reference sphere and styli

The second variation parameter in the experiment is the orientation of the reference sphere. Reference sphere has four different orientations, while the position on the measuring table of the machine remains unchanged (Figure 4). Previously described calibration procedure has been repeated for all four diverse orientations.

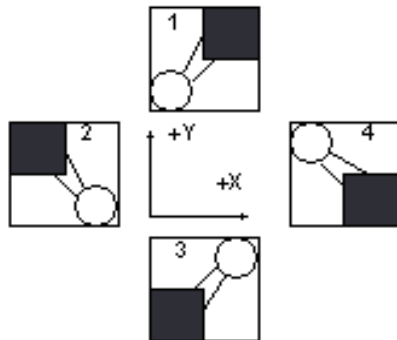


Figure 4. Different orientations of the reference sphere[7]

As a calibration method, all cases utilize the qualify passive stylus method. Four points are first probed for

position determination, followed by the required number of points for stylus calibration.

The paper presents the influence of the calibration results by varying the starting point calibration and the orientations reference sphere. Other influential factors determining the standard deviation value are neglected or maintained at a constant level. The ambient environmental conditions during the experiments in the laboratory have been recorded. The room temperature is maintained within the range $20.0 \pm 0.5^\circ\text{C}$; while the humidity is maintained at $50 \pm 2\%$.

3.1. Calibration results

It has been observed that in the total of 192 calibration procedures, the standard deviation did not have the value larger than the tenth part of millimetre. Results are presented by the number of different orientations reference sphere. The table overview is presented for standard deviations for the first orientation calibration sphere (Table 1).

Table 1. Standard deviation for first orientation reference sphere [mm]

No. of measurement	1	2	3	4	5	6
Starting point calibration						
0.0 [mm]	0.0000	0.0001	0.0001	0.0000	0.0000	0.0001
0.5 [mm]	0.0000	0.0001	0.0000	0.0000	0.0001	0.0001
1.0 [mm]	0.0000	0.0001	0.0000	0.0001	0.0000	0.0001
1.5 [mm]	0.0000	0.0001	0.0001	0.0000	0.0001	0.0001
2.0 [mm]	0.0000	0.0000	0.0000	0.0001	0.0000	0.0001
2.5 [mm]	0.0001	0.0001	0.0001	0.0001	0.0001	0.0001
3.0 [mm]	0.0001	0.0001	0.0001	0.0001	0.0000	0.0001
3.5 [mm]	0.0002	0.0003	0.0002	0.0003	0.0005	0.0001

The software package MiniTab is used for the static data processing. The influence of the contact point between the measuring stylus and the reference sphere in initiating the calibration procedure and the orientation reference sphere onto the standard deviation is presented in a Multi-Vari chart (Figure 5). Multi-Vari charts are powerful graphical representations for the analysis of variance. A Multi-Vari chart allows the user to observe patterns of variation in

the output of a process that can correlate with simultaneous multiple potential input variables. The advantage of a Multi-Vari chart over other graphical methods is that it allows the graphical representation multiple families of variation on a single chart. A Multi-Vari analysis can help narrowing a list of potential causes down to a precious few by focusing the attention on the sources of variation that need further study [8].

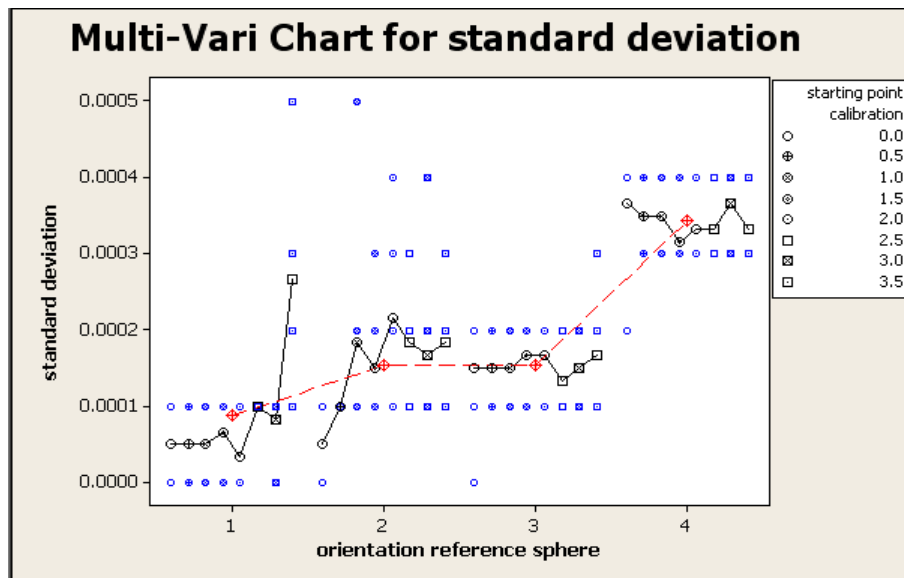


Figure 5. Multi-Vari chart for standard deviation by starting point calibration-orientation reference sphere

The presented diagram refers that the starting calibration contact point between the stylus and the reference sphere does not have any influence on the standard variation value until the measure of 3.5 mm. It can be observed that with the first orientation reference sphere there appears a greater result dispersion, while with the other three, the standard deviation values are constant. However, it can be concluded that even the diverse orientation reference sphere at the same position on the measuring machine table does not influence the calibration value.

4. CONCLUSION

From all the above it can be concluded that the parameters like starting calibration point and the orientation reference sphere insignificantly influence the standard deviation. The confirmation of this hypothesis should be presented by mathematical values, which is the objective of future research, same as the research aimed at the position deviation of the reference sphere on a machine's measuring table and the usage of diverse stylus configurations.

REFERENCES

[1] STRBAC, B., HADZISTEVIC, M., HODOLIČ J., VRBA, I. (2010) *Influence of Stylus Calibration on Overall CMM Error*, International Scientific Conference "Mechanical Engineering", Bratislava, Vol. 1, pp 80-86.
 [2] CARL ZEISS 3D AKADEMIE. (2009) *Measurement Strategies in Contact Coordinate Metrology*, Aalen.

[3] WECKENMANN, A., ESTLER, T., PEGGS, G., MCMURTRY, D. (2004). *Probing System in Dimensional Metrology*. CIRP Annals-Manufacturing Technology, 53 (2), 657-684.
 [4] SCHWENKE, H., KNAPP, W., HAITJEMA, H., WECKENMANN, A., SCHMITT, R., DELBRESSINE, F (2008). *Geometric Error Measurement and Compensation of Machines-An Update*. CIRP Annals-Manufacturing Technology, 57, 660-675.
 [5] SALAH H. R. ALI (2010). *Probing System Characteristics in Coordinate Metrology*. Measurement Science Review. Vol. 10, No 4.
 [6] DAVID FLACK (2001). *Cmm Probing*. Measurement Good Practice Guide No. 43. National Physical Laboratory Queens Road, Teddington, Middlesex, United Kingdom.
 [7] CARL ZEISS (2008). *Calypso Basics*, Operating Instruction. Revision 4.8. Oberkochen, Germany.
 [8] WALTER W. MCLNTYRE (2009). *Lean and Mean Process Improvement*. United States of America.
 [9] http://www.cms-home.com/Applications_Tip_2.pdf

Acknowledgement

Results of investigation presented in this paper are part of the research realized in the framework of the project "Research and Development of Modelling Methods and Approaches in Manufacturing Dental Recoveries with the Application of Modern Technologies and Computer Aided Systems" – TR 035020, financed by the Ministry of Science and Technological Development of the Republic of Serbia.



RESEARCH ON INFLUENCE OF THE SENSOR POSITION ON THE RESULT OF THE V-BLOCK CYLINDRICITY MEASUREMENT

Krzysztof STĘPIEŃ

Chair of Mechanical Technology and Metrology, Kielce University of Technology, Al. 1000-lecia P. P. 7,
25-314 Kielce, Poland
kstepien@tu.kielce.pl

Abstract: At the Kielce University of Technology a new method for in situ cylindricity measurement has been developed. It has been called a V-block method and its fundamental is using a set of two connected V-blocks. Along the element connecting V-blocks the measuring sensor moves. The method is characterized by so-called detectability coefficient that is responsible for detection of the harmonic components in observed profile. The value of the coefficient depends on the V-blocks angle and the position of the sensor. The paper presents fundamentals of the V-block method and results of the research work on influence of the sensor position on the results of measurements of out-of-cylindricity.

Key words: cylindricity, measurement, method, error, V-block

1. INTRODUCTION

Cylindrical elements belong to a numerous and important group of machine parts. Cylindricity measurement of small elements has reached a high metrological level, with instruments of high accuracy [1]. For accurate cylindricity measurements radius change methods are usually applied [2]. In these methods the workpiece should be placed on the measuring table of the instrument. However, in shipbuilding, power industry, paper industry, metallurgical industry, etc., there are large-size cylinders that cannot be placed on the table of the measuring instrument. Therefore producers operating in these areas of industry need methods that would enable in-situ measurement of cylindricity profiles of large cylindrical workpieces during the manufacturing process and during its exploitation [3]. The solution of this problem can be the V-block method [4, 5].

In V-block methods a signal is obtained in relation to a physical reference, which is constituted by points of support of the workpiece and contact points of the measuring sensor and the workpiece [6, 7]. In V-block methods the difference between the maximum and minimum value of the sensor reading is considerably different from the real deviation. It is because the measured value of the signal depends not only on the value of the real deviation measured at the contact point of the sensor and the workpiece but also on the value of deviation at the contact point of the workpiece and the supports. Thus, the difference between the sensor readings and the real profile is usually quite large.

The research work on this subject, of which some were supported by the Polish National Committee for Scientific Research (Project No 7T07D04008) [8], show that the V-block methods can be applied to exact measurements of roundness profiles, if one performs a mathematical

transformation of the sensor readings. The easiest way to do that is to use FFT (Fast Fourier Transform) algorithm. The results of the research work on V-block methods presented in [8] show that the results of measurement of the roundness deviation by the traditional V-block method ranges from 22 % to 63 % in relation to the result obtained by a highly accurate radius change method (for assumed probability level $P=0,95$). However, thanks to applying computer-aided measurements (FFT algorithm) this difference between the result of the V-block and the radius change method lies within the interval of 13÷15 %.

Successful finish of the research work on computer-aided V-block roundness measurement resulted in design and construction of measuring instruments allowing in-situ measurements of roundness profiles. In authors opinion similar measuring instrument allowing V-block cylindricity measurement can be designed and constructed.

In hitherto practice the V-block method was used usually to measure simplified cylindricity. Katsurada et al. in [9] describe the V-block measurement of simplified cylindricity of parallel rollers (roundness profiles in three cross-sections of the workpiece are measured : two cross-sections were defined by the V-blocks and one cross-section in the middle). Such approach allows only rough evaluation of cylindricity if measured element is long.

Considering the requirements of the Geometrical Product Specifications standards [10, 11], the measuring instrument should allow evaluation of the entire surface of the element.

2. CONCEPT OF V-BLOCK CYLINDRICITY MEASUREMENTS

Taking to account needs of producers of large cylinders and guidelines of Geometrical Product Specification

standards authors have developed concept of V-block cylindricity measurement presented in Fig. 1 [12].

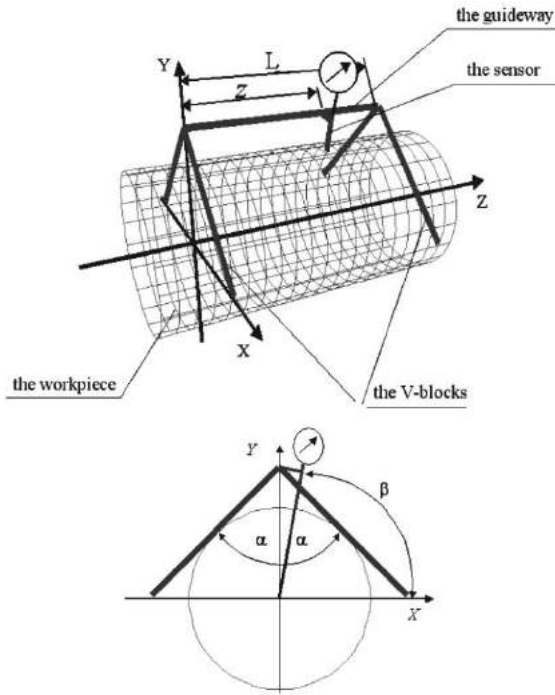


Fig.1. Concept of the V-block cylindricity Measurement [13]

The proposed concept assumes that the measured object is placed on a machine tool or on the working stand. Two interconnected V-blocks adhere to its surface. The connecting element of the V-block functions additionally as a guide, along which an induction sensor is shifted. The V-blocks are slightly pressed down to the measured object by means of a set of springs, which ensures their stable contact with the object in rotation. In the measuring instrument, both the object's angle of rotation and the sensor's displacement are controlled by means of a computer controller. The cylindricity measurement of an object implies appropriate scanning of the object's surface with a measuring sensor, along the suitably designed trajectory, through appropriate steering of the object's angle of rotation and sensor's displacement. Values α and β are the angular parameters of the V-block method for cylindricity measurement. They are responsible for detecting particular harmonic components of the measured cylindricity profile [14].

The cylindricity deviation for each sample element was determined with two methods: the investigated V-block method and the highly accurate radial method. The conducted tests, the results of which were published in [15], showed that the difference between the results of cylindricity deviation measured by the V-block and the highly accurate radius change method lies within the interval $\pm 19\%$ (for a probability level $P=0.95$).

The next step in investigation on the application of V-block method to accurate cylindricity measurements was to look for its improvement and measurement accuracy

enhancement. The work mainly involved the analysis of potential sources of measurement errors, and their elimination or compensation through specially developed procedures. One of the factors that can influence measurement results is the position of the measuring sensor.

3. INFLUENCE OF THE SENSOR POSITION ON MEASUREMENT RESULT

The position of the measuring sensor is defined by the value of angle β , which is one of the method parameters, as it was shown in Fig. 1. Values of the angles α and β are responsible for detecting the particular harmonic components of a profile. Therefore, it is very important to identify and establish their real values as well as to investigate the influence of the difference between the real and nominal values on measurement results [16]. This is the reason why, a computer simulation was performed so as to determine the interdependence of the nominal and the real values of the angle β and their influence on measurement results. The simulation required:

- generating a model cylindricity profile $R(\varphi, z)$,
- generating sensor readings $F_{\beta_n}(\varphi, z)$ for the nominal value of the angle $\beta = \beta_n = 90^\circ$,
- generating sensor readings $F_{\beta_r}(\varphi, z)$ for the real value of the angle β (for the simulation purposes, the real value was assumed to be $\beta = \beta_r = 89^\circ$),
- transforming the profiles $F_{\beta_n}(\varphi, z)$ and $F_{\beta_r}(\varphi, z)$ into the processed profiles $R_{\beta_n}(\varphi, z)$ and $R_{\beta_r}(\varphi, z)$,
- calculating the orientation of the mean cylinders axes for the profiles $R_{\beta_n}(\varphi, z)$ and $R_{\beta_r}(\varphi, z)$,
- calculating the deviations for the profiles $R_{\beta_n}(\varphi, z)$ and $R_{\beta_r}(\varphi, z)$ from the mean cylinders,
- comparing the deviations of the profiles $R_{\beta_n}(\varphi, z)$ and $R_{\beta_r}(\varphi, z)$.

The simulation made it possible to establish the difference between the profiles. A change in the angle β causes a change in the detectability coefficient. The diagram in Fig. 2 was plotted to illustrate how the change in β affects the change in the detectability coefficients.

The values of the detectability coefficient K_n for the nominal values of the angles α and β ($\alpha = \alpha_n = 60^\circ$ and $\beta = \beta_n = 90^\circ$) are plotted in blue, and the values of K_n for the simulated values of α and β ($\alpha = \alpha_n = 60^\circ$ and $\beta = \beta_r = 89^\circ$) are plotted in red. In a general case, the values of K_n are complex numbers, therefore in the X axis there are values of $\Re(K_n)$ and in the Y axis we have values of $\Im(K_n)$. For each value of the coefficient K_n , in the range of harmonic components $2 \div 15$, a segment was plotted. The initial point of the segment lies at point (0,0) and the end of the segment was the point with coordinates $(\Re(K_n), \Im(K_n))$. The end of each segment was

marked with a star and the number next to the star corresponds to the number of a respective harmonic component.

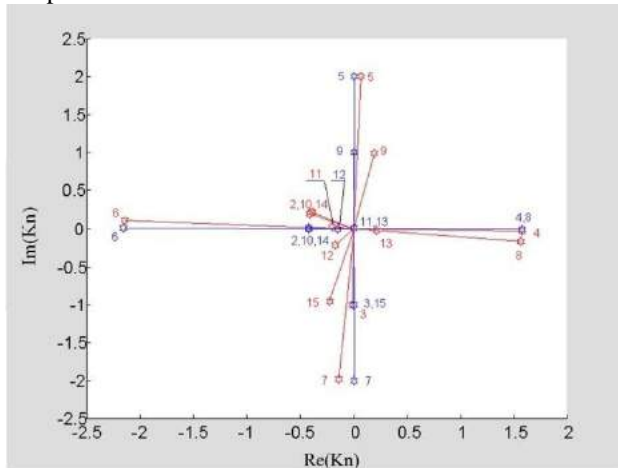


Fig. 2. The values of the detectability coefficient for $\alpha = 60^\circ$ and $\beta = 90^\circ$ (in blue) and for $\alpha = 60^\circ$ and $\beta = 89^\circ$ (in red) – the range of harmonic components: $2 \div 15$

From the diagram in Fig. 2 it is clear that a one-degree change in the angle β causes a change in the detectability coefficient, this change being different for different harmonic components. For example, for $n = 3$ the change in K_n is very small, but for $n = 12$ the value of K_n changes significantly. We can also see that if the angular combination is $\alpha = 60^\circ$ and $\beta = 89^\circ$, then the values of K_n for $n = 11$ and $n = 13$ are not equal to zero, and therefore the eleventh and thirteenth harmonic components can be detected. Results of work presented in [17] show that these harmonic components cannot be detected if the combination is $\alpha = 60^\circ$ and $\beta = 90^\circ$. Analysing the change in the detectability coefficient, we report that for $\alpha = 60^\circ$ and $\beta = 90^\circ$ the imaginary or the real part of K_n is equal to zero, and for the combination $\alpha = 60^\circ$ and $\beta = 89^\circ$ both parts are different from zero.

The different values of the detectability coefficient cause a change in the profile values $R_{\beta_n}(\varphi, z)$ and $R_{\beta_r}(\varphi, z)$, calculated for $\beta = \beta_n = 90^\circ$ and for $\beta = \beta_r = 89^\circ$, respectively. Figure 3 shows the coinciding profiles $R_{\beta_n}(\varphi, z)$ and $R_{\beta_r}(\varphi, z)$ and Figure 4 presents roundness profiles in one of the cross-sections of the generated cylinder. In Figures 3 and 4 the coincidence of compared profiles is high. Figure 5 shows the difference between the profiles illustrated in Fig. 4.

Then, Figure 6 shows a 3D diagram of the difference between the profiles on the entire surface of the inspected cylinder.

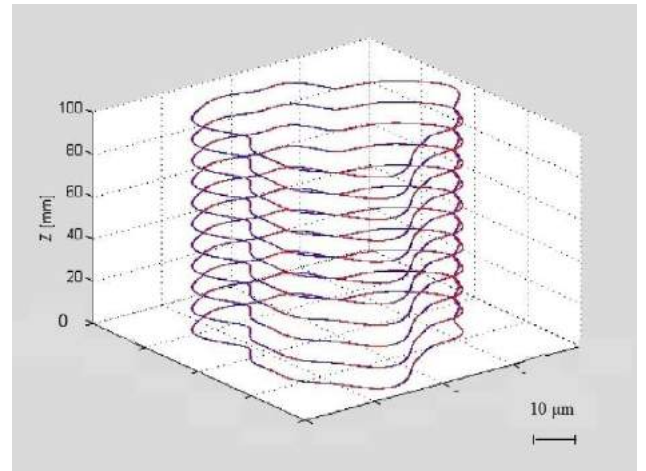


Fig. 3. Cylindricity profiles $R_{\beta_n}(\varphi, z)$ (in blue) and $R_{\beta_r}(\varphi, z)$ (in red)

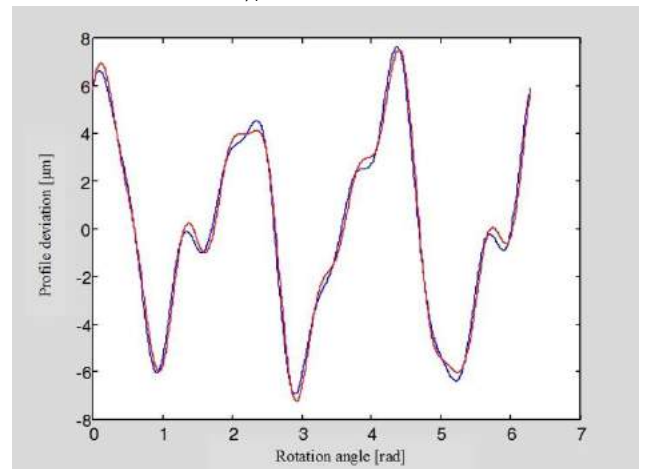


Fig. 4. Roundness profiles in one of the cross-sections of the generated cylinder for the profiles $R_{\beta_n}(\varphi, z)$ (in blue) and $R_{\beta_r}(\varphi, z)$ (in red)

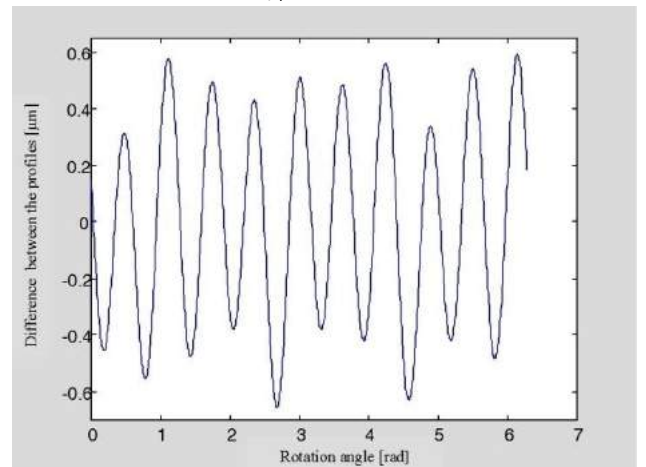


Fig. 5. The difference between the profiles $R_{\beta_n}(\varphi, z)$ and $R_{\beta_r}(\varphi, z)$ in one of the cross-sections of the analyzed cylinder

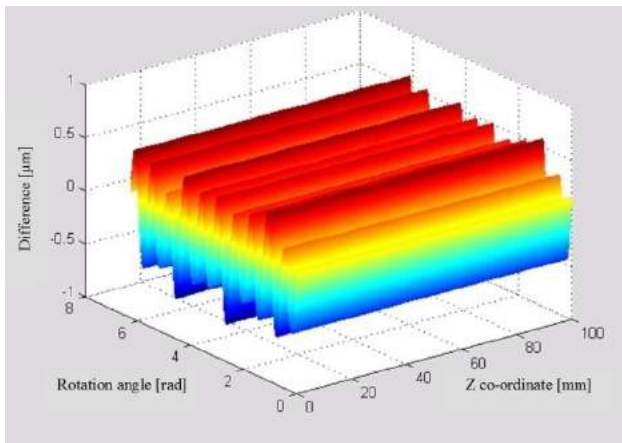


Fig. 6. The difference between the profiles $R_{\beta_n}(\varphi, z)$ and $R_{\beta_r}(\varphi, z)$ on the entire surface of the analyzed cylinder.

The maximum value of the difference between the profiles equals $0.63 \mu\text{m}$, which constitutes about 4.5 % of the cylindricity deviation. Considering the fact that both profiles were calculated for the angles β_n and β_r , whose difference is rather large ($\beta_n - \beta_r = 1^\circ$), we can assume that the influence between a real and nominal value of the angle β on the result of the reference cylindricity measurement is rather small.

4. SUMMARY

Developed concept of cylindricity measurements by the V-block method meets requirements of modern technological processes. Described method allows accurate in situ measurements of form deviations of large cylinders that are used in electric, paper or naval industry. The main disadvantage of the method is that some harmonic components of the profile cannot be detected by the measuring system. Detection of harmonic components of roundness profiles depends on values of angles α and β , that are the method parameters. Position of the sensor is defined by the angle β . Results of the research work presented in Chapter 3 show that the influence of the change of the value β on the measurement result is quite small. Change of the angle equal to 1° results in the difference of the sensor readings that is about 4.5 %. However, in order to increase the accuracy of the method, real value of the angle β should be determined. It can be made by the optimization method with use of reference and real measurement data. Development of the special procedure allowing determination of the real position of the sensor will be the aim of next stage of research work on cylindricity measurements by the V-block method.

REFERENCES

[1] ZHAO W.Q., XUE Z., TAN J.B., WANG Z.B. (2006) *SSEST: A new approach to higher accuracy cylindricity measuring instrument*, International Journal of Machine Tools and Manufacture, Vol. 46, No (14), pp. 1869-1878.
 [2] OSANNA P. H. et al. (1992) *Cylindricity – a well known problem and solution*, International Journal of Machine Tools and Manufacture, Vol. 32, No 1/2, pp. 91-97.

[3] DAWSON D. J. W. (1992) *Cylindricity and its measurement*, International Journal of Machine Tools and Manufacture, Vol. 32, No. 1/2, pp. 247-253.
 [4] KAKINO Y., KITAZAWA J. (1978) *In Situ Measurement of Cylindricity*. Annals of the CIRP, Vol. 27, No. 1, pp. 371-375.
 [5] OKUYAMA E., GOHO K., MITSUI K. (2003), *New analytical method for V-block three-point method*. Precision Engineering, Vol. 27, No. 3, pp. 234-244.
 [6] SONOZAKI S., FUJIWARA H. (1989) *Simultaneous measurement of cylindrical parts profile and rotating accuracy using multi-three-point method*, Bulletin of Japan Society. of Precision Engineering, Vol. 23, No. 4, pp.286-291.
 [7] B. MURALIKRISHNAN, S. VENKATACHALAM, J. RAJA, M. MALBURG (2005), *A note on the three-point method for roundness measurement*, Precision Engineering, Vol. 29, No. 2, pp. 257-260.
 [8] ADAMCZAK S. et al (1997) *Concept of reference methods for accurate measurements of roundness of machine elements (in Polish)*. Science report KBN no. 7T07D04008, Kielce University of Technology, Kielce.
 [9] KATSURADA K., GOHO K., MITSUI K, HAYASHI A. (2003) *Cylindricity measurement of parallel rollers based on a V-block method*, Nippon Kikai Gakkai Ronbunshu, C Hen/Transactions of the JSME, Vol. 69, No. 11, pp. 3124-3129.
 [10] ISO/DIS 12180-1, 2: 1999, *Geometrical Product Specifications (GPS) – Cylindricity*.
 [11] JIAN MAO, YANLONG CAO, JIANGXIN YANG (2009) *Implementation uncertainty evaluation of cylindricity errors based on geometrical product specification (GPS)*, Measurement, Vol. 42, No. 5, pp. 742-747.
 [12] ADAMCZAK S., JANECKI D., STĘPIEŃ K. (2003) *Concept of reference measurements of cylindricity profiles of machine parts*, XVII IMEKO World Congress, Dubrovnik, pp. 201.
 [13] JANECKI D., STĘPIEŃ K. (2008) *A study of the effects of the sensor guideway slope on the results of the reference measurement of cylindricity deviations*, Pomiar Automatyka Kontrola, Vol. 5, pp. 258– 262.
 [14] ADAMCZAK S., JANECKI D., STĘPIEŃ K. (2006) *An analysis of errors of V-block cylindricity measurement with a regard to the method parameters*, XVIII IMEKO World Congress, Metrology for a Sustainable Development, Rio de Janeiro, Brazil.
 [15] JANECKI D., STĘPIEŃ K. (2004) *Applying the normalized cross correlation function to the comparison of cylindricity profiles*. Metrology and Measurement Systems, Vol. 9, No. 3, pp. 209 – 220.
 [16] ADAMCZAK S., JANECKI D., STĘPIEŃ K. (2010) *Qualitative and quantitative evaluation of the accuracy of the V-block method of cylindricity measurements*, Precision Engineering, vol. 34, No. 3, pp. 619-626.
 [17] STĘPIEŃ K. (2006) *An analysis of errors of the cylindricity measurements by the V-block method*. PhD dissertation. Kielce University of Technology, Kielce, Poland, 2006.



IMPROVING PRODUCT QUALITY OF SECURITY EQUIPMENT USING SPC

Milan KOLAREVIĆ¹, Branko RADIČEVIĆ¹, Miomir VUKIĆEVIĆ¹, Mišo BJELIĆ¹, Ljubinko CVETKOVIĆ²

¹Faculty of Mechanical Engineering Kraljevo, University of Kragujevac, Dositejeva 19, Kraljevo, Serbia

²Primat oprema D.O.O, Milutina Vujovića bb, Baljevac, Serbia

kolarevic.m@mfkv.kg.ac.rs, radicevic.b@mfkv.kg.ac.rs, vukicevic.m@mfkv.kg.ac.rs,
bjelic.m@mfkv.kg.ac.rs, po.cvetkovic@open.telekom.rs

Abstract: *There are some basic quality characteristics and some basic unconformity of Security Equipment (Safes, Deposit safes, ATM Safes, Vault Rooms) that occurs during production process and which should be controlled. The stability of the process for variable sample size is controlled using *u*-chart, which shows the average number of defects (failures) per product. Quality improvement of products is carried out by determination of the critical failures using Pareto analysis and by determination of corrective actions that should be taken.*

Key words: *Security Equipment, *u*-chart, Quality improvement, Pareto analysis*

1. INTRODUCTION

Unlike developed countries, statistical process control in our country have not yet reached the true extent of use even for companies that are certified according to standard ISO 9000. The reason is certainly insufficient knowledge of mathematical statistics which is basis of the SPC and the insufficient use of computers.

The essence of the application of these methods is the rapid spotting of errors and selection of parameters that influence to the process instability. This provides opportunity for corrective measures to be taken in order to countionously improve quality of products and processes and thereby achieve high customer expectations and ensure competitiveness in the increasingly demanding global market.

Below is an example of application of SPC methods in the process of producing the security equipment that is manufactured in the company PRIMAT EQUIPMENT - Baljevac.

2. PRODUCTION OF SAFETY EQUIPMENT IN THE COMPANY PRIMAT EQUIPMENT - Baljevac

Company PRIMAT EQUIPMENT LTD - Baljevac produces metal security equipment that is used to store valuables such as important documents, cash, jewelry and others. Product range includes:

- commercial safes - type STARPRIM and STARPRIM/N,
- specific purpose safes such as deposit safes and components for ATM safes,
- vault rooms - MODULPRIM type,
- vault doors – DOORPRIM type,
- security doors,
- Fireproof doors

- Wall and furniture safes type PT and ZT and
- Cabinets for weapons of type A, B and C.

Security equipment products are certified by the German Institute Verband der Schadenversicherer Köln (VdS) in accordance with European standards EN 1143-1. This standard defines the anti - intrusion levels of security which anti burglary security grade is measured in units of resistance RU (Resistant Unit). Commercial and specific purpose safes are made in sizes from 15 to 780 liters and with security grade from 1 to 5 while the vault rooms in modular construction ModulPrim and vault doors DoorPrim are made with security grade from 0 to 9.

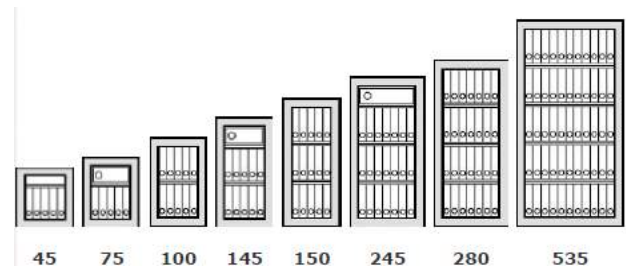


Fig.1. Models of commercial and specific purpose safes

Company PRIMAT EQUIPMENT LTD - Baljevac has introduced QMS (Quality Management System) in compliance with the requirements of ISO 9001:2008. Processes and production technologies of metal security equipment are based on our own experience and business and technical collaboration with partner PRIMAT Inc. from Maribor, who is also the majority owner of the company.

Method of product inspection and method of recording the results of inspection to ensure product quality in accordance with the requirements of the QMS is defined by procedure for controlling product POB-824-101. This procedure implies use of attribute quality control charts and Pareto analysis. Integral part of procedure are control

plans that are developed for all types of security equipment. They defined sampling method ie. the sample size and frequency of control process.

3. ERROR CLASSIFICATION

The basic feature of these products is reflected in the provision of security of valuable items stored in them and it is therefore necessary that the quality characteristics that provide this functional demand are full controlled and that the same measures are critical to the products of this type. Conformity of products is documented by plan / record of product checking which include the value of functional measures.

Since these safes are used in banks and offices, it is necessary to satisfy the aesthetic appearance and ease of functioning, ie. opening, closing and locking. It is therefore necessary to monitor errors that affect to these quality characteristics and to take corrective measures for elimination of the causes and for prevention of their recurrence.

The technological process is divided in three parts: safe shell assembly by welding, door assembly and black assembly. Depending on the safe security grade and a size range, there are different control plans and the requirements that products have to satisfy.

Production form of commercial safes - type STARPRIM is a small-series from 5 to 50 pieces. On the other hand, there are 44 different models of this safes based on the size and grade of security.

Table 1. Error classification

<i>i</i>	Controlled error
1	Removing residue from welding
2	Control of the welds on the armor system
3	Fine grinding of corners and welds on the armor system
4	Fine grinding of doors
5	Location of safety pin
6	Holes for the rack mounts
7	Dorr flatness
8	Control if hinge is welded
9	Positioned and grinded fabric number
10	Flatness of armour system plates
11	Control of locking parts
12	Control of welds at door housing
13	Easy opening of doors
14	Straightness and angularity of envelope
15	Removing concrete residue from housing
16	Gap between door and casing
17	Alignment between housing and doors
18	Control of parts for piles admission
19	Alignment of the pipe with the bottom

For the implementation of statistical process control and comparison of products with different models and different levels of security, it is necessary to group similar

errors in order to eliminate difference in the names of errors and to provide a sufficient number of samples for monitoring process stability. Thus, for example error No. 11 - "Control of lock parts" includes the following errors:

- wrong position of sound beeper
- error of locking mechanism,
- improperly installed rail guides and
- lack of dividers.

Errors in the process of making commercial safes type STARPRIM are classified into 19 groups and are shown in Table 1.

4. U- CONTROL CHART

U - control chart for variable sample size was chosen for statistical process control. Basic parameter of **u**-chart is the average number of defects per unit in the sample:

$$u_i = \frac{\sum_{j=1}^{n_i} c_{ij}}{n_i} \quad (1)$$

where: n_i -size of i -th sample

The average number of defects / errors of entire population ie. central tendency of the process is:

$$CL_u = \bar{u} = \frac{\sum_{i=1}^s \sum_{j=1}^{n_i} c_{ij}}{\sum_{i=1}^s n_i} \quad (2)$$

The position of the control limits is variable and depends on sample size so the value of the control limits have to be calculated for each point in the control chart

$$GKG_u = \bar{u} + \frac{3 \cdot \sqrt{\bar{u}}}{\sqrt{n_i}} \quad (3)$$

$$DKG_u = \bar{u} - \frac{3 \cdot \sqrt{\bar{u}}}{\sqrt{n_i}} \quad (4)$$

During the period from 30.12.2010. to 07.04.2011. total number of errors is monitored using **u**-chart according to the classification shown in Table 1. The results are shown in Table 2.

The average number of defects per unit is calculated on the basis of the equation (1).

The value of the central line is:

$$CL_u = \bar{u} = \frac{\sum_{i=1}^s \sum_{j=1}^{n_i} c_{ij}}{\sum_{i=1}^s n_i} = \frac{538}{341} = 1.578$$

Control limits are calculated using following equations:

$$GKG_u = 1.578 + \frac{3 \cdot \sqrt{1.578}}{\sqrt{n_i}} = 1.578 + \frac{3.768}{\sqrt{n_i}}$$

$$DKG_u = 1.578 - \frac{3 \cdot \sqrt{1.578}}{\sqrt{n_i}} = 1.578 - \frac{3.768}{\sqrt{n_i}}$$

All points on **u**-chart (Fig.2) are within the control limits and can be considered that the previous process was stable. Data processing and graphical representation of was performed using MS Excel. By locking unnecessary

cells, chart can be used by executives who do not have specific knowledge of SPC and MS Excel. It is enough to enter the measured values in the provided fields and the program will automatically performs all necessary

processing. In case of deviation points which are outside the control limits, measures are taken according to a procedure that monitors the implementation of control charts to prevent occurrence of nonconformities.

Table 2. Measured data and calculated parameters for u-karte

<i>i</i>	1	2	3	4	5	6	7	8	9	10	11	12	13	14	15	16	17	18	19	20	21	22	23	24	25	Σ
n_i	15	10	10	10	15	10	10	6	10	10	30	10	50	30	10	6	9	10	15	10	5	10	10	15	15	
G1	15			14	3				10	9	26															77
G2	8	1			5	9	10																			33
G3	11	4	8	7	14	8	9	2	7	3	29	8	18	28	2	1	4	4	3	10	2	7	3	10	3	205
G4								2																		2
G5																		2								2
G6															2		3	6		8				11		30
G7	1			2									1													4
G8																1										1
G9				1												1										1
1G0		1																					6			7
G11																				1				3		4
G12								1																		1
G13												2					2	1		8			3			16
G14																										0
G15															3	5	9	6		8		5		4	13	53
G16												3	33	14	1	6	4		1		1	5	10	7	1	86
G17																						5	2			7
G18					2	4	1																			7
G19																	1	1								2
Σc_i	35	6	8	8	35	22	23	6	17	12	55	13	52	42	8	16	22	18	12	27	3	22	24	35	17	538
$U_i = \Sigma c_i / n_i$	2,33	0,60	0,80	0,80	2,33	2,20	2,30	1,00	1,70	1,20	1,83	1,30	1,04	1,40	0,80	2,67	2,44	1,80	0,80	2,70	0,60	2,20	2,40	2,33	1,13	
CLu	1,58	1,58	1,58	1,58	1,58	1,58	1,58	1,58	1,58	1,58	1,58	1,58	1,58	1,58	1,58	1,58	1,58	1,58	1,58	1,58	1,58	1,58	1,58	1,58	1,58	
GKGu	2,55	2,77	2,77	2,77	2,55	2,77	2,77	3,12	2,77	2,77	2,27	2,77	2,11	2,27	2,77	3,12	2,83	2,77	2,55	2,77	3,26	2,77	2,77	2,55	2,55	
DKGu	0,60	0,39	0,39	0,39	0,60	0,39	0,39	0,04	0,39	0,39	0,89	0,39	1,04	0,89	0,39	0,04	0,32	0,39	0,60	0,39	0,00	0,39	0,39	0,60	0,60	

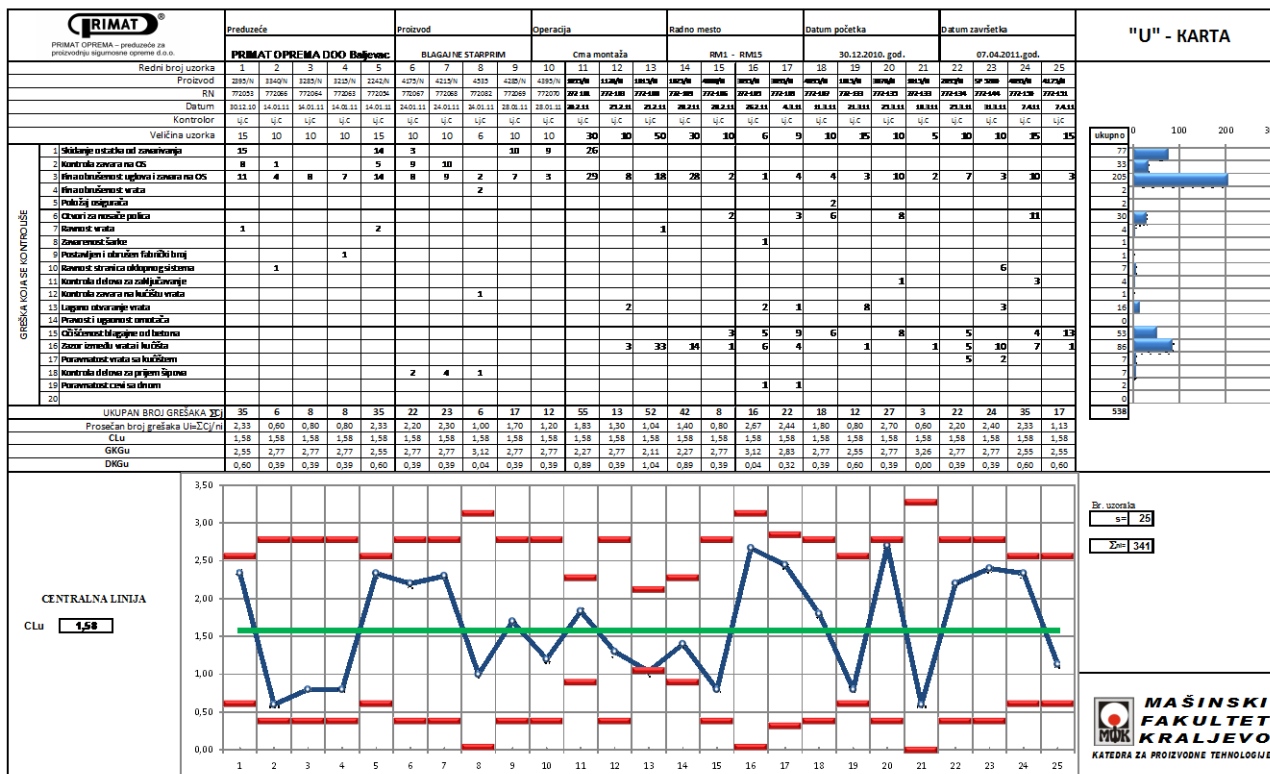


Fig.3. U-chart for variable sample size

5. PARETO ANALYSIS

The number of occurrences for each observed error is shown on the right side by adequate histogram. If ranking of errors is made by its number, ie. the percentage of participation (Table 3) we can notice that the most common error is G3- Fine grinding of corners and welds on the armor system (38.1%) which does not belong to the line of critical errors, but from the aesthetic aspect is very important. Errors G3, G16, G1, G15 and G2 are \approx 85% of all errors (Group A in Table 3 and area A in Figure 3) and therefore is necessary to provide corrective actions for their elimination. In addition, it is necessary to consider errors from group B (error G6, G13, G10 and G17) that make \approx 10% of and take steps to reduce them in the next stage. Other errors (class C) are less than 5% of all errors and at this stage it is not necessary to analyze them.

Table 3. Classification of errors according to the the number of occurrences

G_i	n_i	cum	n_i (%)	cum (%)	Group
G3	205	205	38,10%	38,10%	A
G16	86	291	15,99%	54,09%	
G1	77	368	14,31%	68,40%	
G15	53	421	9,85%	78,25%	
G2	33	454	6,13%	84,39%	
G6	30	484	5,58%	89,96%	B
G13	16	500	2,97%	92,94%	
G10	7	507	1,30%	94,24%	
G17	7	514	1,30%	95,54%	
G18	7	521	1,30%	96,84%	C
G7	4	525	0,74%	97,58%	
G11	4	529	0,74%	98,33%	
G4	2	531	0,37%	98,70%	
G5	2	533	0,37%	99,07%	
G19	2	535	0,37%	99,44%	
G8	1	536	0,19%	99,63%	
G9	1	537	0,19%	99,81%	
G12	1	538	0,19%	100,00%	
G14	0	538	0,00%	100,00%	
Σ	538				

6. CONCLUSION

Companies that want to improve quality of their products and reduce the costs of quality must constantly work to improve the quality system which includes the necessity of applying statistical methods to control the manufacturing process.

Control charts are highly applicable tools to determine the ability of the manufacturing process. Although attribute control charts provide smaller insight into the state of the process than is possible by using numerical control charts, their application is very useful and economically justified. On the basis of performed analysis we can conclude that the process of making safes from the program of security equipment in the company PRIMAT EQUIPMENT-Baljevac is stable but that there are significant opportunities to improve quality. The data analysis allows the selection of parameters that influence on the occurrence of errors in the production process and gives opportunity to eliminate the causes of errors in order to ensure a higher level of product quality.

7. ACKNOWLEDGEMENT

Authors wish to acknowledge their gratitude to Ministry of Education and Science od Republic of Serbia for the support to the research through project grant TR37020.

REFERENCES

- [7] Oakland, S. J.: *Statistical Process Control*, Fifth Edition, Butterworth Heinemann, 2003.
- [8] Chandra, J. M.: *Statistical Quality Control*, ©2001 CRC Press LLC
- [9] Stanić, J.: *Upravljanje kvalitetom proizvoda, Metodi I*, Mašinski fakultet, Beograd, 1989.
- [10] Kolarević, M.: *Upravljanje kvalitetom I-praktikum*, Mašinski fakultet, Kraljevo, 2008.

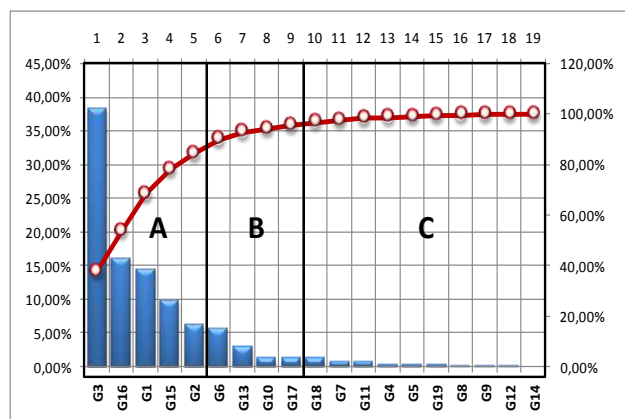


Fig.3. Pareto graph



THE ROLE OF MANAGERS IN IMPLEMENTING QUALITY MANAGEMENT STANDARDS

Vladan RADLOVAČKI¹, Radmila JOVANOVIĆ², Bato KAMBEROVIĆ¹, Milan DELIĆ¹, Srđan VULANOVIĆ¹

¹Faculty of Technical Sciences Novi Sad, Department of Industrial Engineering and Engineering Management, Trg Dositeja Obradovića 6, Novi Sad, Serbia

²Blood Transfusion Institute of Vojvodina, Medical Faculty of Novi Sad, Hajduk Veljkova 9a, Novi Sad, Serbia
rule@uns.ac.rs, radajov@yahoo.com, bato@uns.ac.rs, milan@uns.ac.rs, srdjanv@uns.ac.rs

Abstract: Using the sample of 51 organization in Serbia (as a part of a complex project), a pilot study is carried out about the role of managers in implementing requirements of various management system standards. The aim of this research is to provide basic information on most important elements of management systems using only ISO 9001 standard requirements and organizations that implemented requirements of other management standards. Determined differences should indirectly point out to fulfilled and unfulfilled roles of managers, because the current state is the result of managers' work. Research is based exclusively on managers' subjective estimates.

It is authors' belief that results of this research should shed light on basic characteristics of our organizations related to implementation of management systems, as seen from managers' perspective. This would pave the way for new studies that would encompass a number of elements and wider constructs. Results thereof might provide guidelines for managers in our organizations for effective application of management systems.

Key words: Quality management system, role of managers, effective application

1. INTRODUCTION

Manager that is aware of his or her role in the process is valuable to the firm he or she works in, and top managers should be able to recognize such qualities when employing new managers, estimating the work of present managers or planning improvements and making teams to carry them out.

Subject of this research are not routine manager roles present at everyday work process activities. Managers, of course, have, as anyone else in a work process, such routine tasks. Here, the subject are, let's say, strategic tasks, carried out to improve some very important elements of QMS (like understanding how QMS works by employees, teamwork, raising conscience about user satisfaction importance and similar) which can not be improved in one day or week, which take long time of patient work to show clear impact on performance and which have to be maintained. However, it is known that once properly activated, these elements can be very useful in many ways (they can ease decision making in complex situations, make favorable employees interrelations raising employees' satisfaction with the result of improving performance, etc).

To the knowledge of authors, it is likely that there are several general problems present in a significant number of Serbian quality management systems (QMS):

- managers often do not transfer enough information to employees to complete their tasks,

- managers do not organize appropriate trainings for employees to gain knowledge and skills enabling the improvement of efficiency/efficacy,
- managers often do not involve employees in decision making and similar.

Authors made an assumption (hypothesis) that understanding of described processes by quality managers in quality management systems vary by number and types of management systems applied in the QMS. Namely, integrated management systems covered by the research had QMS with ISO 9001 requirements applied. Besides ISO 9001, they could have applied: environmental management system (requirements of ISO 14001), occupational health and safety management systems (requirements of OHSAS 18001), food safety management system (requirements of ISO 22000), quality management system in laboratory/ies (requirements of ISO/IEC 17025), or requirements of other organizational standards (ISO 27001, GMP, GLP, HACCP strictly, other branch organizational standards, etc). Some organizations could have applied several of these standards. Differences in estimating elements considered relevant for the research at organizations applying different standards lead to appropriate conclusions.

2. SAMPLE AND METHOD USED

Basis for this research is a part of results of a survey carried out in year 2010 for purposes of a wider research of a TQM practice in Serbia.

The survey is carried out using a questionnaire.

The questionnaire was sent to management representatives (quality managers) in 204 certified firms. 51 completed questionnaires (25%) were returned back.

Among organizations that returned questionnaires, 12 are production firms (23%), 14 organizations (28%) are mixed production and services firms and 25 organizations (49%) exclusively providing services.

Seven organizations (13.73%) are micro organizations (1 to 9 employees), 17 firms (33.33%) are small (10 to 49), 23 firms (45.10%) are middle organizations (50 to 249) and 4 firms (7.84%) have 250 or more employees (large organizations).

The average age of QMS in the sample is 4.07 years, while σ is 2.78. Youngest is 1 year old and the oldest has 13 years. Organizations in the sample apply different organizational systems. The distribution of these systems within the sample is given in Figure 1.

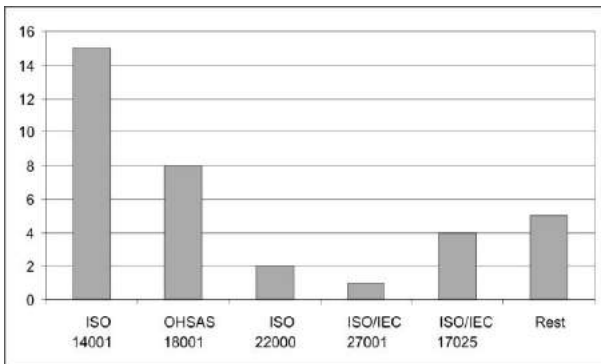


Fig.1. Various organizational systems in firms in the sample

This diverse structure makes the described sample representative for the Republic of Serbia.

Respondents were asked to sign their subjective estimate on its items according to the discrete 5 point Likert-type scale. 1 stands for 'I disagree' estimate, while 5 stands for 'I fully agree'.

Validity test of the questionnaire was made by calculating Cronbach α coefficients. One item was eliminated from the research (see appendix).

Hypothesis was tested using the one-way ANOVA at the confidence level of 95%.

In this research 23 items from the questionnaire were used (see appendix). Cronbach α was 0.9127 ($\alpha > 0.7$) which indicates to the validity of items.

Items P2-P7 were included in the research to estimate the overall satisfaction with the QMS and the satisfaction with individual changes brought to organization with the QMS.

Items P8-P11 are items treating basic leadership characteristics of organization management (authors consulted [1], [4], [5], [6]).

Items P12-P15 are treating some elements of human resource management [1], [7], [8], [9], while items P16-P18 are related to process management ([1], [3], [4], [7], [9]).

Some items are treating learning of an organization (P19-P23). These items are treated in [2], [3], [4], [10].

3. RESULTS

For testing the validity of a hypothesis, a series of ANOVA tests were carried out. 22 items were tested for variations between estimations in systems that have or not implemented standards: ISO 14001, OHSAS 18001, ISO/IEC 17025, ISO 22000 or other organizational standards (ISO/IEC 27001 systems were not examined because there was only one system with ISO/IEC 27001 standard implemented). This means that total of $22 \times 5 = 110$ ANOVAs were carried out to come to the findings of this research.

Only 4 (out of 110) estimates were found to significantly vary by implementation of organizational standards. These are items P3, P9, P22 and P23 (see appendix). The only system causing variations (at all four of the items) is ISO/IEC 17025.

Table 1 ANOVA - variation of P3 vs. impl. of ISO/IEC 17025

Source	DF	SS	MS	F	P
ISO 17025	1	2.670	2.670	3.85	0.055
Error	49	33.957	0.693		
Total	50	36.627			

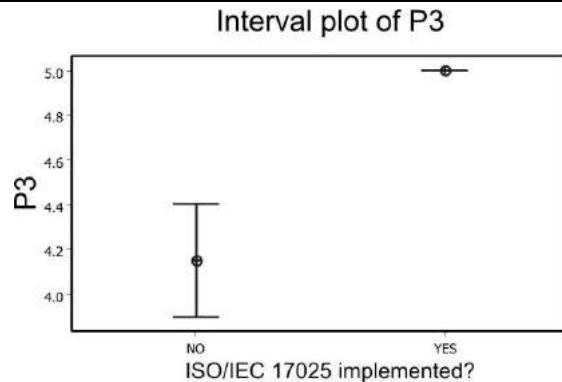


Figure 2: Interval plot of P3 vs. implementation of ISO/IEC 17025

Calculated p-value is not less than 0.05 (table 1), but is near to that value - formally we couldn't consider variations of P3 significant, but difference of two means are obvious (figure 2).

Table 2 ANOVA - variation of P9 vs. impl. of ISO/IEC 17025

Source	DF	SS	MS	F	P
ISO 17025	1	4.007	4.007	4.59	0.037
Error	48	41.913	0.873		
Total	49	45.920			

It also is the case with items P22 and P23 (tables 3-4).

It is indicative that all items P3, P9, P22 and P23 in all 4 systems running ISO/IEC 17025 are estimated by mark 5 (figures 2-5).

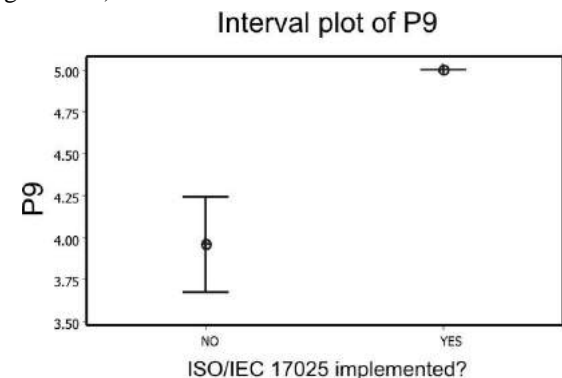


Figure 3: Interval plot of P9 vs. implementation of ISO/IEC 17025

Table 3 ANOVA - variation of P22 vs. impl. of ISO/IEC 17025

Source	DF	SS	MS	F	P
ISO 17025	1	2.538	2.538	3.59	0.064
Error	49	34.638	0.707		
Total	50	37.176			

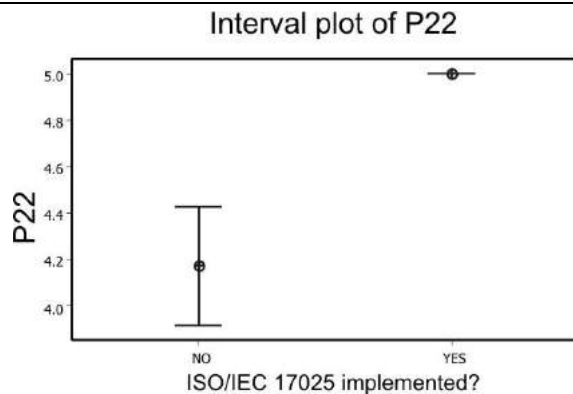


Figure 4: Interval plot of P22 vs. implementation of ISO/IEC 17025

Table 4 ANOVA - variation of P23 vs. impl. of ISO/IEC 17025

Source	DF	SS	MS	F	P
ISO 17025	1	4.87	4.87	3.98	0.052
Error	49	59.96	1.22		
Total	50	64.82			

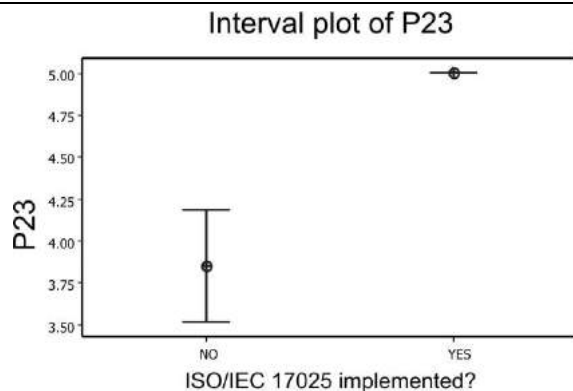


Figure 5: Interval plot of P23 vs. implementation of ISO/IEC 17025

4. DISCUSSION

Implementing organizational systems brings changes to QMS. It is proven that estimates of almost all observed changes do not vary by implemented systems. All except for one: responsibility for quality. It turns out that employees in systems implementing ISO/IEC 17025 are estimated more responsible for quality.

Quite logical is, then, the finding that systems implementing ISO/IEC 17025 encourage staff to initiate/support changes in the organization. These systems do more to involve people in improving processes.

Environment and its support for on-the-job training are estimated higher in systems applying ISO/IEC 17025 than in others.

At the end, according to quality managers, participation of managers in specialized trainings is higher estimated in systems applying ISO/IEC 17025.

These findings point out to the conclusion that quality managers in observed systems not applying ISO/IEC 17025 should review their roles in context of involving people in improvement process, training and human resource management. It might bring them some ideas

how to plan and carry out improvements to raise employee satisfaction and performance.

5. CONCLUSION

This research uncovered variations of implementing various quality management obligations set by ISO 9001 and similar standards, by standards implemented within the integrated management system in an organization (or QMS, if organization applies only ISO 9001 requirements). Observed elements are listed in appendix.

Authors made an effort to extract most of managers' obligations not considered as routine, but rather as goals to be reached and maintained as a continuous task.

Conclusions about these roles are made upon estimates provided by quality managers. They are not made directly, but as an attempt of diagnosing relevant QMS elements. Any time when manager's diagnosis is not favorable, manager should be aware of the fact that he (or she) is the one (more or less, alone or as a member of a team, by direct action or by providing supporting and/or by its coordination) to make effort directed towards improvement. This is one of prerequisites for a manager to become a leader or, at least, to try to be closer to a leader.

Why is ISO/IEC 17025 making a difference in completing observed tasks and fulfilling the roles? It might be a question for a new research. It could be because laboratory staff is in average more committed to their jobs, or it might be a result of different aspects like education or perception of responsibility, quality of service, clarity of tasks, or some other element.

As for the others, it is clear we now have a reason to believe that laboratories are best in implementing organizational standards - if something goes wrong, maybe it is not a bad idea to use knowledge of successful managers. At solving general problems, maybe managers in laboratories know the answer.

REFERENCES

- [1] Tarí, J. J., Molina, J. F., Castejón, J. L. (2007). The relationship between quality management practices and their effects on quality outcomes, *European Journal of Operational Research*, vol. 183, no. 2, pp 483-501.
- [2] Martínez-Costa, M.; Jiménez - Jiménez, D. (2008). Are companies that implement TQM better learning organisations? An empirical study, *Total Quality Management & Business Excellence*, 19, no. 11, pp 1101-1115.
- [3] Anderson, J., Rungtusanatham, M., Schroeder, R. O., Devaraj, S. (1995). A Path Analytic Model of a Theory of Quality Management Underlying the Deming Management Method: Preliminary Empirical Findings, *Decision Sciences*, vol. 26, no. 5, pp 637-658
- [4] Grandzol, J. R., Gershon, M. (1997). Which TQM practices really matter: an empirical investigation, *Quality Management Journal*, vol. 4, no. 4, pp 43-59.
- [5] Dow, D., Samson, D., Ford, S (1999). Exploding the myth: do all quality management practices contribute to superior quality performance?, *Production and Operations Management*, vol. 8, no. 1, pp 1-27.
- [6] Samson, D., Terziovski, M. (1999). The relationship between total quality management practices and

- operational performance, *Journal of Operations Management*, vol. 17, no. 4, pp 393–409.
- [7] Wilson, D. D., Collier, D. A., (2000). An empirical investigation of the Malcolm Baldrige National Quality award causal model, *Decision Sciences*, vol. 31, no. 2, pp 361-390
- [8] Powell, T. C. (1995). Total quality management as competitive advantage: a review and empirical study, *Strategic Management Journal*, vol. 16, no. 1, pp 15–37.
- [9] Forza, C., Flippini, R. (1998). TQM impact on quality conformance and customer satisfaction: a causal model, *International Journal of Production Economics*, vol. 55, no. 1, pp 1–20.
- [10] Adam Jr., E. E., Corbett, L. M., Flores, B. E., Harrison, N. J., Lee, T. S., Rho, B. H., Ribera, J., Samson, D., Westbrook, R. (1997). An international study of quality improvement approach and firm performance, *International Journal of Operations and Production Management*, vol. 17, no. 9, pp 842–873.

Appendix 1

ITEMS USED

- P1 Certificates other than ISO 9001 (not a Likert scale item)
- P2 I am satisfied with the way the QMS operates in the company
- P3 One of the changes brought in by the QMS implementation is responsibility for quality
- P4 One of the changes brought in by the QMS implementation is importance of the certificate(s) to customers[†]
- P5 One of the changes brought in by the QMS implementation is more efficient processes
- P6 One of the changes brought in by the QMS implementation is true leadership of top management
- P7 One of the changes brought in by the QMS implementation is employee satisfaction
- P8 Managers actively communicate with employees about a quality commitment
- P9 Employees are encouraged to initiate/support changes in the organization
- P10 Managers encourage employees to take responsibilities
- P11 Managers motivate employees to perform their tasks at the best possible way
- P12 Managers are trained about quality principles
- P13 Vertical and horizontal communication is effective
- P14 Organization insists on teamwork and team spirit
- P15 Organization provides safe and healthy work environment
- P16 Organization carries out continuous control and improvement of key processes
- P17 Performance of all processes is measured in the organization
- P18 Organization departments share the experience in process improvement with other departments or units
- P19 Organization reinforces improvement of all its products, services and processes
- P20 Most employees in this organization have sufficient knowledge of the basic aspects of our sector
- P21 Most employees in the organization understand the basic processes used to create our products/services
- P22 Top management has developed an environment that supports on-the-job training
- P23 Managers participate in specialized trainings
- [†] *This item proved to be invalid*



THE POSSIBILITIES FOR IMPROVEMENT OF THE MAINTENANCE PROCESSES IN THE COMPANIES

Pedja MILOSAVLJEVIĆ, Dragoljub ŽIVKOVIĆ, Predrag JANKOVIĆ, Srđan MLADENOVIĆ
University of Niš, Faculty of Mechanical Engineering, Aleksandra Medvedeva 14, 18000 Niš, Serbia
pedja@masfak.ni.ac.rs

Abstract: *Only the companies capable of constant and quick adapting to fast changing conditions can survive on the global market nowadays. The customers expect an excellent quality of services, and pay only the prices that are better than those from the competition. To keep the company competitive and to maintain the maximum efficiency of the facilities, an approach different from the traditional concept of maintenance is required. The concept that can facilitate the maximum efficiency of installed capacities must take into consideration the whole system: man-facility-environment and must apply the continuous measures to avoid losses, in this way constantly improving the maintenance process.*

The classical approach to the maintenance process does not permit achieving the maximum efficiency of the facility, because it is based on the technical efficiency factor of the facility. Thus, the total approach to man-production facility surrounding is required in order to achieve the high availability and capability of facility performance and its optimal status. The maintenance that applies to the process comprises taking suitable maintenance measures, needed for the process stability, detecting and elimination of the weak points and constant improvement of facility considering handling and maintenance. In order to achieve such a goal, the entire operational life of the facility should be considered, from designing, manufacturing, installing and using to replacing or retiring.

Key words: *maintenance, improvement, processes, management*

1. INTRODUCTION

The management in a company has a task to organize the system and supervise its functioning, and to make decisions to improve the critical processes according to the business results. Improving the process means that the current status should be assessed. The process improvement teams have a key role in this enterprise. The analysis of the process reveals what is not functioning properly in the process, i.e. what the causes for inefficiency of the process are, so the suggestions for the process improvement are made. In the end, the improved process is being measured and observed. The processes of the company are identified, described and adjusted to the customers demands, and so the customers' satisfaction is increased. The processes that have a particular impact on the customers' satisfaction are significant processes. Among them, there may be some very important processes for realizing the mission and vision of the company which are inefficient. Those are critical processes that require improvement, redesign or reengineering [1].

Firstly, the significant processes in maintenance should be recorded and fully arranged. The public utility systems consist of a large number of processes and activities, that in most of the cases offer numerous opportunities for improvement. However, every initiative of such activities is almost doomed unless all the processes are not treated simultaneously. A much better approach is the improvement of the most significant processes, that will be the solution model for the less important processes.

Almost none of the improvement processes can be imagined without its user. The user is at the beginning and at the end of every process, the one providing evaluation and guidelines for the future work. On the basis of the users' satisfaction the efficiency of the applied tools, quality or management, as well as methodology of improvement are evaluated. On the basis of the evaluation of the end user, the size of the problem is analyzed and the corrective action is being initiated accordingly. The complexity of the processes in public utility systems can be seen through their connection and mutual conditioning with the users of their services [2].

2. MAINTENANCE PROCESS IN PUBLIC UTILITY COMPANIES

Public utility companies have an important role in the economy of every country, because the satisfaction of vital needs of population, such as supplying electricity, water, heating, waste removal and other, depend on their unhindered functioning. Therefore, an on-time, effective and efficient maintenance process is crucial for the successful work of public utility companies. Users of their services have very high requirements concerning the satisfaction of their needs, thus a high availability, reliability and optimal facility state can only be achieved through the interaction of people who work at the facilities and the facilities themselves. Conducting specific maintenance measures, needed for a stable process, discovery and removal of weak spots and constant improvement of a facility in relation to handling

and maintenance are the characteristics of the maintenance directed towards constant process improvement [4].

Maintenance of engineering systems in utility systems presents a following activity, that is, a group of activities and relations between each of them on securing the functionality of engineering system elements as well as the viability of the entire system, and all with the aim of reaching a desired level of functioning security and usable quality of a public utility or service business system. In the process of engineering systems maintenance in public utility service companies, very significant savings can be achieved by applying modern technologies and maintenance concepts, with the reduction in spare parts and materials supplies in warehouses, by using a lesser number of workers in maintenance tasks, by shortening maintenance time and reducing outsourcing in maintenance activities.

Successful business activities of public service companies requires adequate arranging and improvement of engineering systems maintenance process, where preventive measures can be conducted in order to avoid major losses and reduce the number of inactive working hours. This implies the qualification and training of workers in maintenance, according to assumed and prescribed procedures, so that they can conduct the simple ongoing interventions and repairs on engineering systems, replace used elements, construct simple element positions, and other. Using this approach, the maintenance system becomes independent from partner services and interventions, which can cause lengthy delays in critical situations and absence of mechanization from significant processes [3].

Having in mind the unequal usage of engineering systems and equipment in companies by immediate agents, there is a need for specific technical-technological reconstructions and modernizations. These requirements can be carried out after a detailed check of prescribed parameters and collecting actual data from the equipment in the exploitation phase. This will help to record the capacities which are not being used sufficiently, that is, which are overloaded and which require necessary constructive changes [5].

Through measurements and analysis of mechanical values, it is possible to propose corrective measures for improving the working conditions of immediate agents. By training workers who are in immediate danger in their workplaces and encouraging them to give constructive suggestions for working conditions improvement, one can have a better insight into the immediate problems and choose the possibility for their solution. It is also necessary to make working instructions at workplaces, which will describe a workplace, work means and work actions, work actions corrections (corrective measures and activities) and influential factors in detail.

A lower level of engagement of outside agents in conducting maintenance interventions, shorter times of specific corrective and preventive maintenance interventions, as well as the engagement of a smaller number of better trained maintainers, could be an efficient indicator of the achieved level of engineering systems maintenance process improvement in public service companies [5].

3. MAINTENANCE PROCESS IN PUBLIC UTILITY COMPANY "GORICA" NIS

The process of maintenance in "Gorica" include: preventive maintenance, corrective maintenance and technical control [6].

3.1. Preventive Maintenance

Preventive maintenance consists of daily and weekly inspections of vehicles and agricultural machinery and execution of technical review (semi-annual and annual). Managers are required to conduct daily inspection of vehicles and agricultural machinery on the list of daily care, which includes washing of vehicles and machinery, control of oil in the aggregate and control coolant. On the basis of the plan, norms and fuel consumption lubrication is done (upgrade and complete vehicles). By law, the inspection is done annually for all vehicles [7].

3.2. Corrective Maintenance

Corrective maintenance is performed on the application of the driver, when the transfer vehicle, which defines an order for corrective maintenance work or through user's claims.

There is also an unscheduled inspection of vehicles that are returned due to defect from the field and point to the technical sector of maintenance, or for vehicles due to malfunction or damage requiring major intervention on the field [8].

3.3. Technical control

Technical control process includes visual inspection activities, control of braking systems and vehicle diagnostics. According to a monthly maintenance plan, the vehicles are directed to preventive maintenance checks.

4. IMPROVEMENT OF MAINTANANCE PROCESS

Improving the maintenance process involves [8]:

- failure analysis
- cost analysis;
- introduction of computer system;
- check list application;
- preparation of working instructions.

Failure analysis and **cost analysis** is done by team responsible for improving. This imply the collection and processing costs of preventive maintenance and corrective maintenance, and analysis of the causes of failures.

Introduction of computer system imply creating a database of preventive and corrective maintenance, supporting documentation, spare parts and failure analysis and cost.

Check list application and preparation of working instructions makes the team responsible for improving. It is composed of existing workers, a team leader is the maintenance engineer. All they have to undergo certain training [9].

4.1. Preventive maintenance process improvement

Figure 1 shows the chart of the improved preventive maintenance process [9].

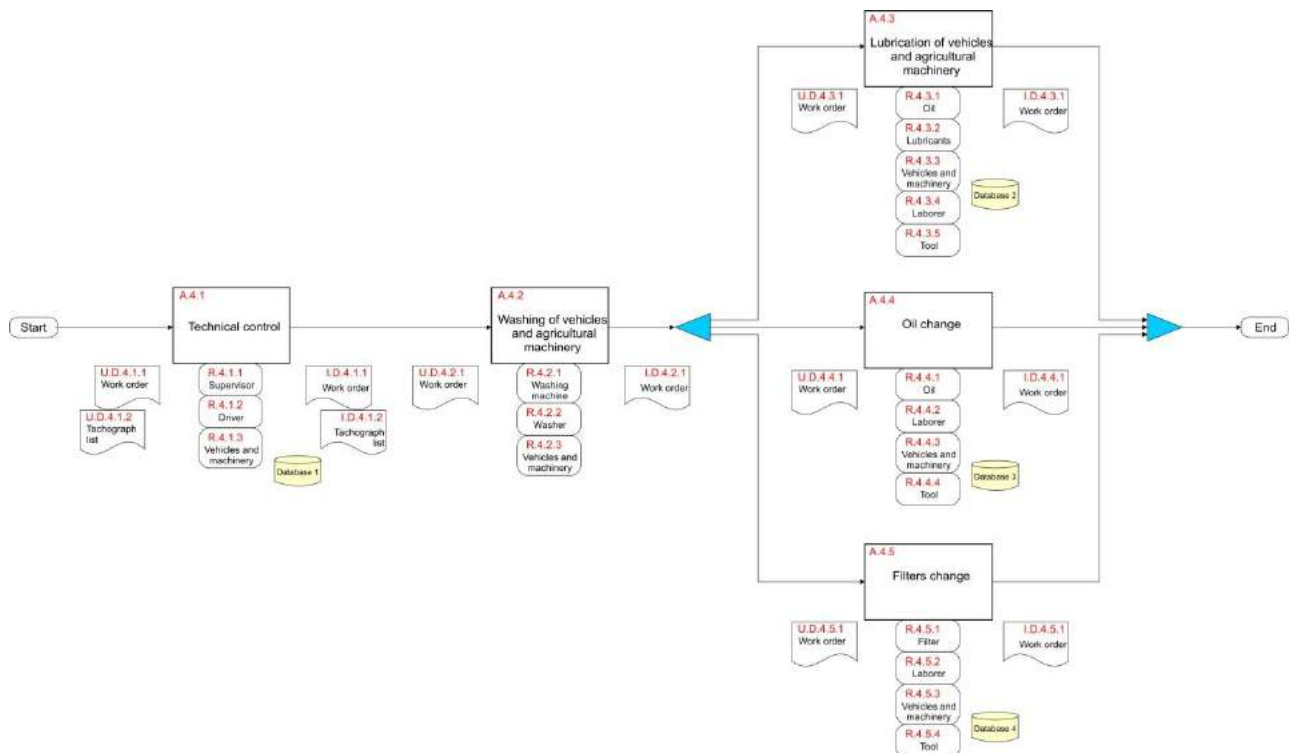


Figure 1: The Chart of the Improved Preventive Maintenance Process

4.2. Control process improvement

Figure 2 shows the chart of the improved control process [9].

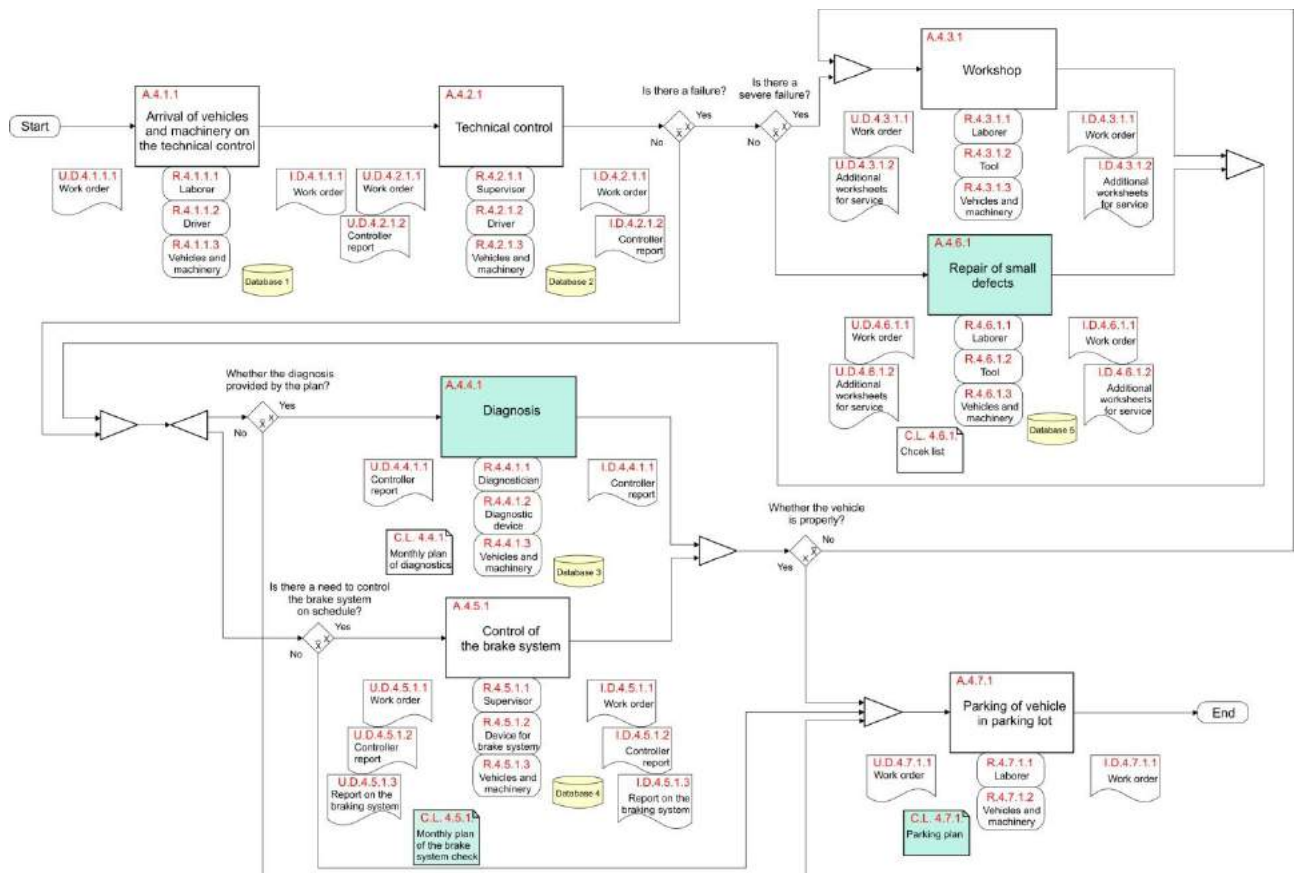


Figure 2: The Chart of the Improved Control Process

5. CONCLUSION

After collecting and analyzing data of cleared up, improved and standardized processes, it can be concluded that there is room for improvement. By implementing these improvements, one can save both time and money, improve the quality in providing services, connect all sectors into one whole, reduce idling and speed up communication between sectors. By constant review and continuous improvement of all processes, a quicker, better quality and just in time service is achieved.

By introducing integrated management systems, work injuries risk is reduced, as well as the adverse effects of waste material on the environment. By prescribing working instructions, it is determined who and in which way can do the specific job. This provides for a better organized work, time savings and reduction of possible errors.

The key results of the maintenance process improvement in the observed public service company are [4]:

1. Increase in end user satisfaction.

An active inclusion of the end user at the input and output of a process is a guarantee that the business system will be able to survive and sustain itself on the market in the future. In that way, the management is constantly receiving information on where the company is at and what is needs to be done in order to make it better.

2. Increase in the level of arrangement of public city areas.

As the result of all improvements and activities, the entire social community in the city ends up with a better quality environment based on the highest standards and requirements. This is the first step that guarantees the continuous improvement and advancement.

3. More efficient use of existing capacities and loss reduction.

The economic conditions on a global level are a warning to large economic systems that they must be more efficient and effective in their business activities. The great economies are first in line because of the excessive expenses and investments. This points to the fact that the existing capacities should be used entirely and that the costs should be reduced wherever it is possible.

4. Greater performance of employees and improved working conditions.

This demands greater responsibility from employees for the entire business system, in accordance with the position they occupy. It helps increase the level of activity in employees, which contributes to the overall performance and process improvement. By process improvement and redistributing available human resources into teams, a necessary control function will be reached, as well as the possibility to compare teams based on their performance.

5. Reduction of means for own resources maintenance by adopting simple procedures of manufacturing and replacement of critical elements and parts.

These business systems are based on the application of mechanization in their fundamental activities. If the maintenance of these resources is planned as outsourcing, it can quickly come to the dependence on the maintainer, time deadlines, spare parts, outsourcing, which make the

business system inflexible. For these reasons, the foundation of smaller workshops for significant processes support is predicted, where these workshops would have the capacity to manufacture, repair or replace certain parts of engineering systems.

REFERENCES

- [1] STOILJKOVIC V., MILOSAVLJEVIC P., RANDJELOVIC S. (2010) *Industrial management*, practicum, Faculty of Mechanical Engineering University of Niš, Niš, pp 368
- [2] STOILJKOVIC V., VELJKOVIC B., STOILJKOVIC P., JEVREMOVIC D. (1998) *With chances to world class: improvement and re-engineering of process*, CIM College and Mechanical Faculty of Niš, Niš, pp 346
- [3] MILOSAVLJEVIC P. (2007) *Maintaining technical systems according to concept TPM and Six Sigma.*, monograph, Library Dissertatio, Endowment Andrejević, Belgrade, pp 125
- [4] MILOSAVLJEVIC P., RANDJELOVIC S., RADOICIC G. (2010) *The possibilities for improvement of the maintenance process in the public utility service companies*, Proceedings of International Maintenance Conference & Exhibition: Euromaintenance 2010, Verona, Italy, pp 330-334
- [5] MLADENOVIC S., MILOSAVLJEVIC P. (2010) *The road towards a Lean Six Sigma company*, International Journal „Total Quality Management & Excellence“, Vol. 38, No. 3, pp 71-78
- [6] MILOSAVLJEVIC P., MLADENOVIC S., JOVANOVIC M., TODOROVIC M. (2010) *Improvement of Production Process and Providing Services in the Company „Hidrokontrol“ ltd. Niš*, International Journal „Total Quality Management & Excellence“, Vol. 38, No. 3, pp 179-186
- [7] MILOSAVLJEVIC P., MILOJEVIC A., KRSTIC D. (2010) *Improvement of plastic coating and sheet metal treatment process in the company „Interlemind“ a.d. Leskovac*, Proceedings of International Conference: "Mechanical Engineering in XXI Century", Faculty of Mechanical Engineering, Niš. pp 225-228
- [8] MILOSAVLJEVIC P., RALL K. (2005) *Six Sigma Concept in the Maintenance Process of Technical Systems*, Facta Universitatis, Series: Mechanical Engineering, Vol. 3, No 1, pp 93-108
Students projects from the course Industrial management
Faculty of Mechanical Engineering in Niš, Niš.



DESIGN AND TENSIOMETRIC ANALYSIS OF THE C-CLAMP FOR RAILROAD TRACKS

Bojan RANČIĆ, Predrag JANKOVIĆ, Srđan MLADENOVIĆ, Slaviša PLANIĆ
Faculty of Mechanical Engineering, University of Niš, A. Medvedeva 14, 18000 Niš, Serbia
bojanr@masfak.ni.ac.rs, jape@masfak.ni.ac.rs, maki@masfak.ni.ac.rs, splanic@sezampro.rs

Abstract: In factory "MIN-DIV" Svrlijig new product is developed. This product (C-clamp) find his use for quickly joint of railroad tracks in cases of specific situations, like high differences of daily and night temperatures. C-clamp probes are produced by casting technology from two different materials: low alloyed steel C45E (EN), and cast iron GS-70. Because of complex form of C-clamp, in program CosmosWorks finite element method (FEM) analysis are accomplished in order to find relation between moment of a force and tightening force, and also identification of C-clamp endings displacements. Tensometric method is used for verification of theoretical results. By these measurements good coincidence of theoretical and experimental results are observed.

Key words: C-clamp, design, tightening force, displacement, measurement

1. INTRODUCTION

The track joint assembly (manufacturer "MIN-DIV" Svrlijig from Svrlijig) is used to connect railway tracks rapidly.

Such connection is performed in the following cases:

- assembly of a parallel railway track, when there has been damage to the main one;
- when one must wait for optimal temperature conditions for welding rails, and
- for rails that are subject to extreme differences between day and night temperatures.

Since the C-clamp is the basic support element in the railroad tracks joint assembly, full attention is paid to the construction of this element.

The design of a C-clamp 3D model (Figure 1) was performed in the "SolidWorks" program.

On the basis of the model, in the same program, the technical drawing of the clamp was also done, which is given in Figure 2.

Aside from the model, shown in Figure 2, two more models were constructed, which differed from the presented model only in their shape and the size of groove for reducing clamp mass (contours marked with 2 and 3 in Figure 2).

This was done due to customer demand that the mass of the clamp was less than 8 kg.

"SolidWorks" program also includes an option for determining the volume of the model, which made it easy to determine the mass of the clamp.

The mass of the basic model (contour 1, Fig. 2) is the smallest and it amounts to 6.8 kg, the mass of the second model (contour 2) is 7.6 kg, and of the third (contour 3) 8.2 kg.

After this check, the second and third models were removed from further examination.

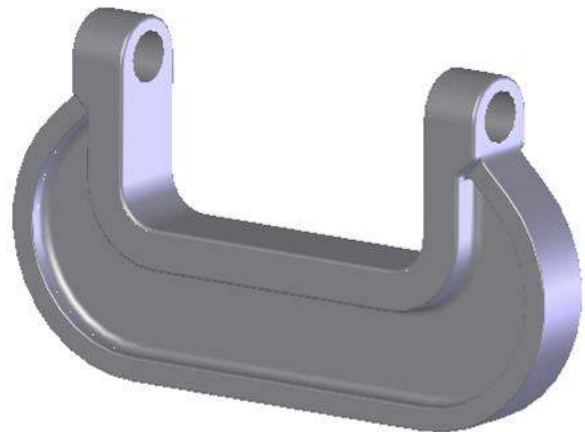


Figure 1. 3D model of C-clamp

2. STRESS AND DISPLACEMENT ANALYSIS

Stress and displacement analysis was performed using the finite element method (FEM) in the "COSMOSWorks" program [1].

For the purpose of simpler calculations, tightening force was approximated to act on the cylindrical surface of the opening, 27 mm in diameter, which corresponded to the average diameter of the inner thread.

Due to the symmetry of the C-clamp, only one half of this part was analyzed. The first restraint was in the plane section of clamp symmetry, and it had the freedom of movement along the Y axis, while the second was on the cylindrical surface with the freedom of movement along

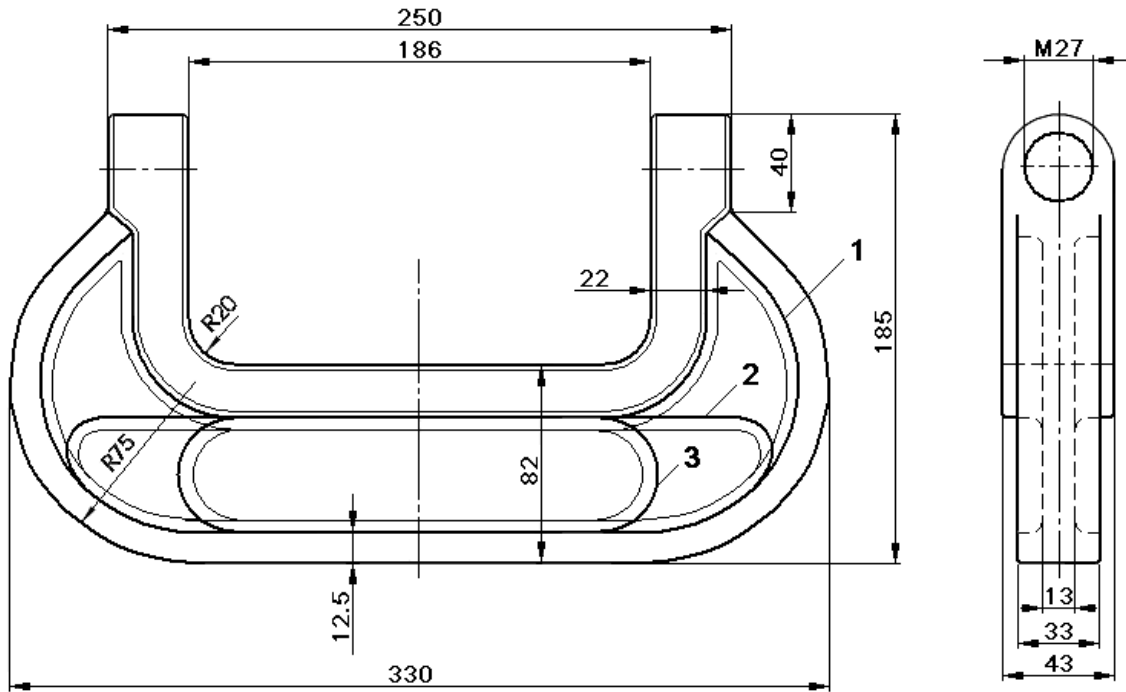


Figure 2. Technical drawing of C-clamp

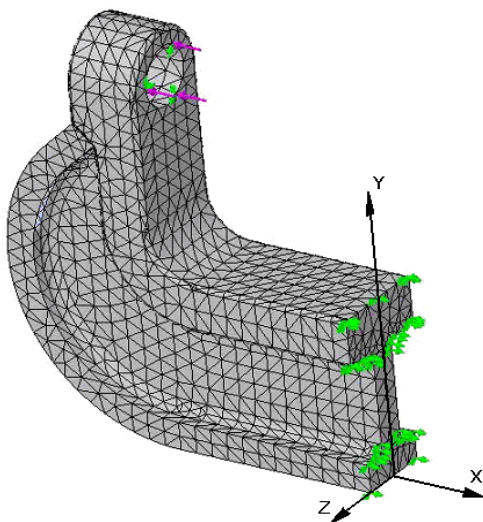


Figure 3. Basic model of C-clamp

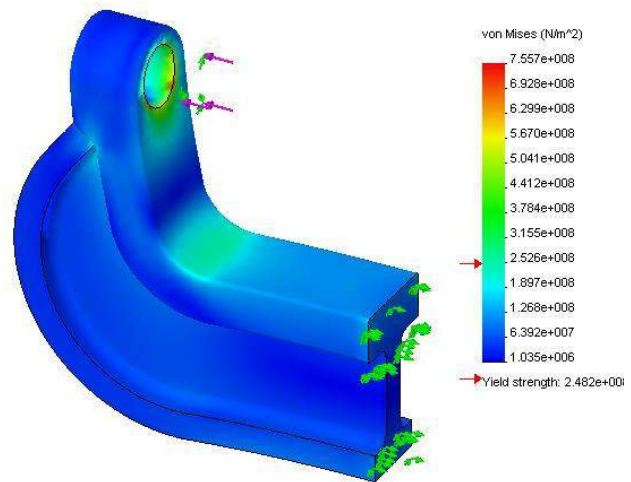


Figure 4. Stress distribution by moment of tightening of 250 Nm for basic model

Figure 4 and 5 show the distribution of stress and displacement for the basic (above) and corrected (below) model, respectively, obtained using the FEM analysis, while the moment of tightening was 250 Nm.

It is obvious from Figure 4 that the most tightened areas are the area of transitive radius R20 and the area of inner thread M27. Furthermore, the stresses in the basic model are greater in terms of the von Mises plasticity condition [2].

C-clamp displacements were greatest in the places subjected to the tightening force and they were directed outwards, causing the opening of the clamp. There was a certain displacement upwards in the middle part (in the plane of transverse symmetry).

A force transmitter was assembled in such a way as to have a cylindrical steel (42CrMo4, EN) body, $\varnothing 50 \times 35$ mm in dimension with a central $\varnothing 9$ opening, to which four strain gauges were connected into a full Wheatstone bridge, [3].

The calibration line was obtained after loading and calibration.

$$(y = 0.0626 \cdot x + 16.278).$$

Screw tightening was performed manually using a torque wrench "Dremometer" from 0 to 300 Nm ("Gedore").

Dial indicators were used to determine the values of C-clamp openings.

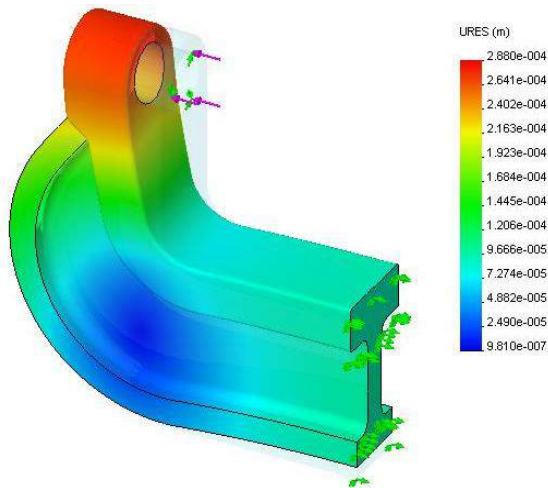


Figure 5. Layout of displacements under the moment of tightening of 250 Nm for the basic model

The results obtained using the FEM analysis can be verified by the classical theoretical analysis, [3].

3. EXPERIMENTAL RESEARCH

The manufacturer chose the basic model of the C-clamp due to lesser usage of material. Clamps were made by casting using C45E (EN) steel and GS-70 (DIN) cast steel. On the basis of stress-strain state analysis, strain gauges were positioned in the arrangement shown in Figure 6, 7 and 8. Strain gauges 10/120 LY11 were used (“Hottinger Baldwin Messtechnik”, [4].

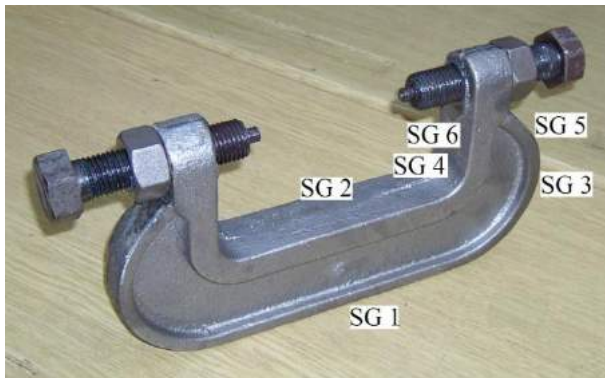


Figure 6. Strain gauges position on C-clamp

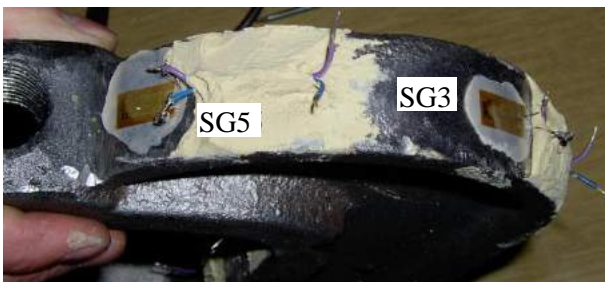


Figure 7. Strain gauges SG3 and SG5

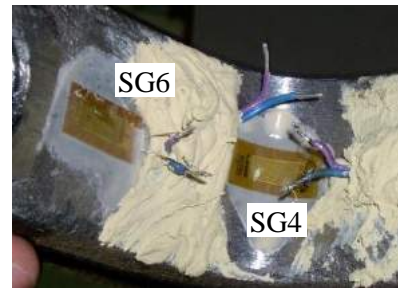


Figure 8. Strain gauges SG4 and SG6

4. PRESENTATION AND ANALYSIS OF MEASUREMENT RESULTS

The diagrams of change in relative deformation in relation to the moment (force) of tightening are shown in Figure 9a for strain gauges SG1, SG3 and SG5, and in Figure 9b for strain gauges SG2, SG4 and SG6 (under the load up to $M = 300$ Nm).

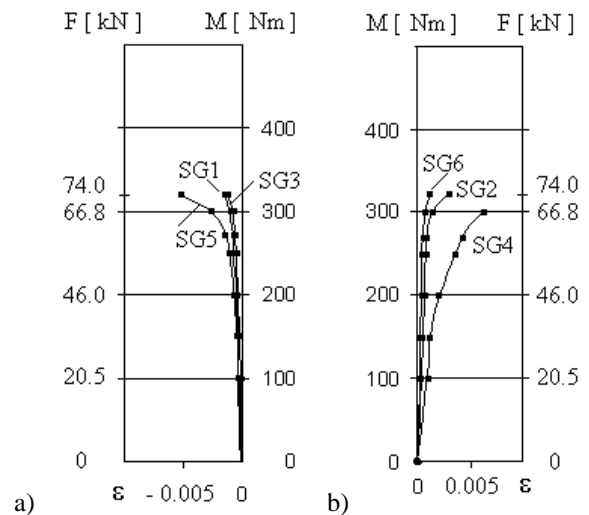


Figure 9. Diagrams of relative strain

It is obvious from the diagram in Fig. 9a that the outer side of the clamp body (SG1, SG3 and SG5) is subjected to pressure and that it is in the state of elasticity up to the moment of 270 Nm. Under the load of 300 Nm plastic deformation occurs in the vicinity of the thread (SG5).

Deformations on the inner side of the clamp are tension deformations. Relative deformations in SG2 and SG6 are in the region of elastic deformation up to the moment of tightening of 270 Nm, while both the middle of the central part of the clamp body (SG2) and the spot in the vicinity of the inner thread on the arm of the clamp body (SG6) are plastically deformed under higher loads.

Using the FEM for clamps made of C45E (EN) and GS-70 (DIN) showed that they were in the state of elasticity under all moments up to, which was further verified by measurements.

Recorded values of the clamp arm displacement (for appropriate values of the moment of tightening), both in the loaded and unloaded state, are given in Table 1.

Table 1. C-clamp arms displacement

Moment [Nm]	C-clamp arms displacement			
	C45E (EN)		GS-70 (DIN)	
	load	unload	load	unload
100	0.71	0	0.68	0
150	1.05	0	0.98	0
200	1.43	0	1.41	0
250	1.67	0	1.67	0
270	1.87	0	1.88	0
300	2.10	0	2.15	0

Table 1 implies that C-clamps made of both materials are in the region of elasticity under all given moments.

Values of given moments of tightening and measured tightening forces for clamps made of C45E (EN) and GS-70 (DIN) are given in Table 2.

Processing of measurement results was performed in the "Microsoft Excel" program.

In C-clamps (made of both materials), the linear dependence between the tightening moment and force existed up to the moment of tightening of 300 Nm (maximum moment that could be achieved with the used torque wrench), that is, the brace holder assembly was in the state of elasticity.

By comparing the obtained equation for change in the one-sided tightening force (according to Table 2) in the function of the moment of tightening for C45E:

$$y = 0.1953 \cdot x - 1.6091,$$

where: y – the one-sided tightening force in [kN] and x – the moment of tightening in [Nm],

with the analogue equation for clamps made of GS-70:

$$y = 0.1995 \cdot x - 0.8974$$

it becomes apparent that, from the aspect of carrying power, it is the case of C-clamps with similar characteristics, thus clamps should be made from less expensive or more easily machined material.

Comparing the results obtained by FEM and measurement (see Figures 4 and 5 and Tables 1 and 2), it was determined that the values obtained by finite element method are higher 5 - 8 percent.

While clamps were cast, there was a deviation in certain measures from the dimensions in the drawing. By measuring the dimensions of the clamp body, the following deviations were determined: in the opening diameter (190 mm in the drawing, and 186 mm in the mold) and in the clamp body thickness (45, 34 and 14 mm

Table 2. Moment of tightening and measured tightening forces

Moment, [Nm]	Measured tightening force [kN]	
	C45E (EN)	GS-70 (DIN)
100	16.2	18.3
150	26.8	28.3
200	37.6	37.0
250	46.5	46.3
270	51.7	52.7
300	58.0	59.4

in the drawing, and 43, 33 and 13 mm in the mold). Figure 2 shows the mold measures.

5. CONCLUSION

Clamps made of C45E (EN) and GS-70 (DIN) are of almost same characteristics and they satisfy conditions for all given loads.

The testing was performed under the static load, while the brace holder assembly works under the one-sided dynamic load in real conditions (the movement of railroad car wheels over the assembly).

Experimental testing showed that the measured values of deformation and displacement were in good agreement with the values obtained using the FEM analysis.

Special attention should be paid to the tightening of the M27 screw to prevent the screw from coming loose during the exploitation of the brace holder assembly.

Thermal processing of the clamp body mold is recommended.

If it is not allowed to manufacture the clamp body by casting, it is recommended to manufacture it by forging, which will improve the working characteristics of the entire railroad track joint assembly

REFERENCES

- [1] PAUL KUROWSKI, (2006), *Engineering Analysis with COSMOSWorks Professional 2006*, SDC Publication, Canada.
- [2] V. STOILJKOVIĆ, (1984), *Teorija obrade deformisanjem*, Univerzitet u Nišu, Niš,.
- [3] BOJAN RANČIĆ, (2005), *Sistemi za merenje, prikupljanje i obradu podataka*, I deo, Mašinski fakultet u Nišu, Niš.
- [4] HOFFMAN., (1987), *Eine Einführung in die Technik des Messens mit Dehnungsmeßstreifen*, Hottinger Baldwin Messtechnik GmbH, Darmstadt.

METROLOGICAL PRIMITIVES IN PRODUCTION METROLOGY – ONTOLOGICAL APPROACH

Slavenko M. STOJADINOVIC, Vidosav D. MAJSTOROVIC

Faculty of Mechanical Engineering, University of Belgrade, Kraljice Marije 16, Belgrade, Serbia
 sstojadinovic@mas.bg.ac.rs, vmajstorovic@mas.bg.ac.rs

Abstract: The paper defines the metrological primitives as concepts of engineering ontology in the field of production metrology. The proposed is the process acquisition of individuals and properties, as one of the main components of engineering ontology, suitable for implementation in the appropriate software for development of the engineering ontology. The results indicate that is justified further development of engineering ontology methodology in the field of production metrology and its implementation in the appropriate software.

Key words: production metrology, metrological primitives, engineering ontology, Protégé

1. INTRODUCTION

Measuring parts whose measurement or inspection are perform on the CMM (Fig. 1. (1a)) are determine by the ideal (Fig. 1. (2)) and the real (Fig. 1. (2a)) geometry. Ideal geometry from the aspect production metrology is defined by the CAD model of the measuring parts and describe the basic metrology primitives: point, line, circle,

ellipse, plane, sphere, cylinder, cone, and torus. Complex and derived of the metrology primitives are obtaining composing of the basic metrological primitives. On the other hand, the real geometry presents of the real shape of the measuring parts.

Describing the dimensional tolerancing and geometrical tolerancing (form, orientation and location) are perform across of the basic metrology primitives ideal geometry.

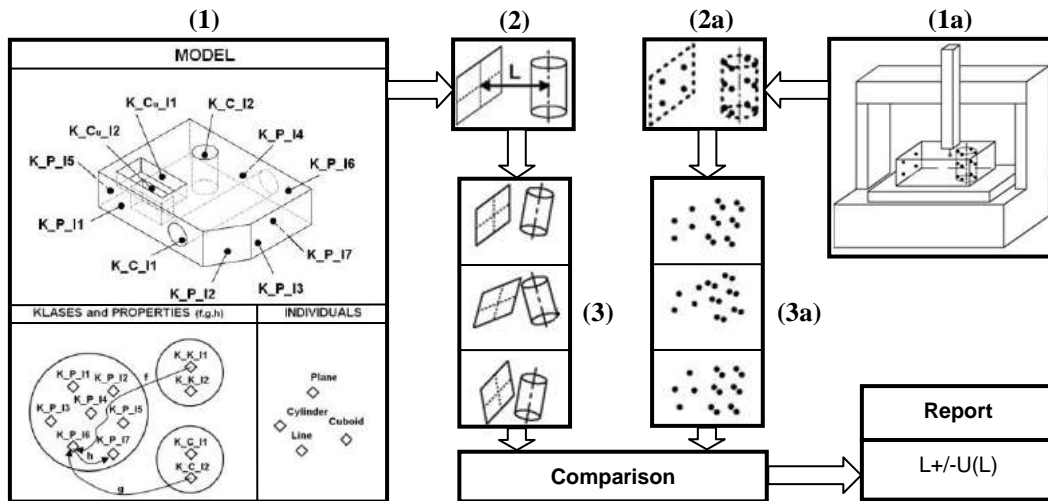


Fig. 1. The principle of measurement on the CMM - based of the engineering ontology (EO)

The real dimensions are obtained as a result of comparing the real and the ideal geometry (Fig. 1). Comparison of these two geometries is the basis of software development for CMM. Geometric grounds on which are basing software's for CMM are basic metrology primitives (Table 1), which is detail discussed in [1]. The essence of the metrology software is an interpretation of primitive metrology primitives (the ideal (3) and real (3a)) in a form suitable for their identification. This analysis is a starting point for defining the ontological approach to the identification of ideal metrology primitives (Fig. 1 (a)),

which is discussed in this paper an example of a machine part.

As is known, the measurement process at the CMM allow and coordinate systems (KS) such as KS measuring machines, KS measuring sensor and KS measuring part. For the analysis in this work is an essential KS measurement part, which is to the holder of a part metrological information, because it is using to describe the position and orientation of the ideal metrology primitives based on parameters given in Table 1.

Table 1. Parameters of the ideal geometric features [2]

Characteristics	Parameters		
	Coordinates $X_0 Y_0 Z_0$	Normal vector $E_x E_y E_z$	Parameters $D D_1 D_2 W$
Point	+ + +		
Line	+ + +	+ + +	
Circle	+ + +	+ + +	+
Ellipse	+ + +	+ + +	+ +
Plane	+ + +	+ + +	
Sphere	+ + +		+
Cylinder	+ + +	+ + +	+
Cone	+ + +	+ + +	+
Torus	+ + +	+ + +	+ +

2. THE METHOD FOR MODELING THE METROLOGICAL PRIMITIVES – ONTOLOGICAL APPROACH

As it is said, the ideal geometry of the metrological model is obtained by using basic metrology primitives or the ideal geometric shapes, which are certain the appropriate parameters (Table 1.). These parameters uniquely determine every metrological primitive in regard to the coordinate system of the measuring part. This set of parameters presents a set of metrological information

about ideal geometry in the coordinate system of the measuring part.

Starting from the assumption that the basic metrological primitives can be represented as a class engineering ontology, on the example of metrological model (Fig. 2.) that contains all the basic metrology primitive, represented is its description from aspect of the engineering ontology. To other words, given is the mini - ontology or the ontology simpler metrological part, in order to test what are the potential characteristics and individuals if we know what the classes or concepts.

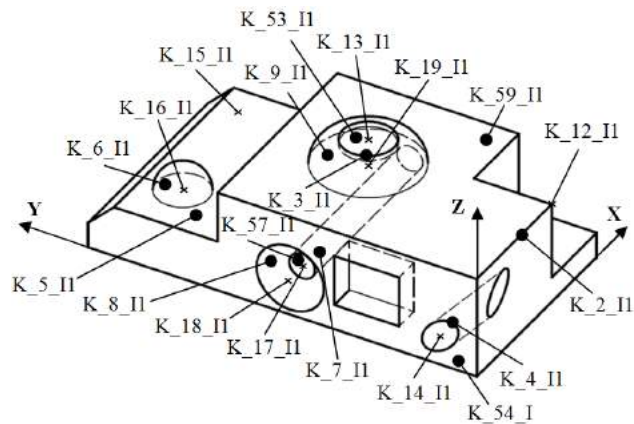


Fig. 2. A representation metrological primitives as an individuals EO

Table 2. A representation of classes, individuals ($i=1,2,3,\dots,n$) and parameters

Classes	Mark	Individuals	Parameters			n	Subclasse K_1	Subclasse K_5
			Coordinates $X_0 Y_0 Z_0$	Normal vector $E_x E_y E_z$	Parameters $D D_1 D_2 W$			
Point	K_1	K_1-I_i	$X_{1i} Y_{1i} Z_{1i}$			28	K_{11}	
Line	K_2	K_2-I_i	$X_{2i} Y_{2i} Z_{2i}$	$E_{2Xi} E_{2Yi} E_{2Zi}$		40	K_{12}	
Circle	K_3	K_3-I_i	$X_{3i} Y_{3i} Z_{3i}$	$E_{3Xi} E_{3Yi} E_{3Zi}$	D_{1i}	7	K_{13}	K_{53}
Ellipse	K_4	K_4-I_i	$X_{4i} Y_{4i} Z_{4i}$	$E_{4Xi} E_{4Yi} E_{4Zi}$	$D_{41i} D_{42i}$	2	K_{14}	K_{54}
Plane	K_5	K_5-I_i	$X_{5i} Y_{5i} Z_{5i}$	$E_{5Xi} E_{5Yi} E_{5Zi}$		17	K_{15}	K_{55}
Sphere	K_6	K_6-I_i	$X_{6i} Y_{6i} Z_{6i}$		D_{6i}	1	K_{16}	
Cylinder	K_7	K_7-I_i	$X_{7i} Y_{7i} Z_{7i}$	$E_{7Xi} E_{7Yi} E_{7Zi}$	D_{7i}	3	K_{17}	K_{57}
Cone	K_8	K_8-I_i	$X_{8i} Y_{8i} Z_{8i}$	$E_{8Xi} E_{8Yi} E_{8Zi}$	W_{8i}	1	K_{18}	K_{58}
Torus	K_9	K_9-I_i	$X_{9i} Y_{9i} Z_{9i}$	$E_{9Xi} E_{9Yi} E_{9Zi}$	$D_{91i} D_{92i}$	1	K_{19}	K_{59}

Information model about the ideal geometry based on the ontological approach can be divided into:

- Set of metrological information about the ideal geometry in relation to the coordinate system of measurement,
- Set of metrological information about the derived geometric characteristics of the measuring parts (a set of information about the relations between of the coordinate system task and coordinate system measuring part).

An approach to modeling the metrology information is presented in [3], while others in [4]. The first concerns the integration of inspection activity while others on the integrated design and manufacturing based on STEP.

In order to get a set of metrological information about the ideal geometry in relation to the coordinate system of measuring part, based on EO, we have to define what are the classes, individuals and properties (Table 2). Classes,

individuals and properties are the main components of the EO and as such are detail described in [5]. Given that everything viewed in relation to the coordinate system of the measuring part, it is necessary to introduce one more additional class (K_{10}) that will be the superclass of all other class.

From Table 2. can see that point as the metrology primitive participate in the creation of other primitive, which resulting in the existence of subclasses that correspond to other metrology primitives, including herself. Also, the table shows that in describing the metrological primitive such as Line, Circle, Ellipse, Cylinder, Cone and Torus participate metrology primitive plane, as well as for itself. This results in the existence of subclasses that match superclass plane, and which are containing the planes for description of the listed primitives metrology. Parameters given in Table 2. represent properties of the individual and in developing

the information model they can be loaded as an input data.

By proposed method are covered all the basic metrology primitives, so in accordance with those, measuring part (Figure 3.) contains all the basic metrology primitives. The proposed hierarchy of classes based on the choosing of metrology primitives is the same for each the metrology part, except that will change individual number depending on the complexity of metrology part.

3. IMPLEMENTING THE METROLOGICAL PRIMITIVES IN THE SOFTWARE PROTÉGÉ

Software Protégé is a free, open source ontology editor and knowledge – base framework, based on Java. At its core, Protégé implements a set of knowledge – modeling structures and actions that support the creation, visualization, and manipulation of ontologies in various representation formats [6]. In this paper is used Protégé – OWL editor that supports the Web Ontology Language,

as most recent development in standard ontology language. An OWL ontology include description of classes, properties and instances.

In this chapter, will be performed implementation of the proposed method of ontological modeling of metrology primitives, which is given in the previous chapter, according to the modeling principles set out in [7, 8].

The implementation of metrology primitives of the part shown in Figure 3 in Protégé includes: 1) modeling classes, 2) modeling of class hierarchy, 3) modeling of the individual, 4) modeling properties classes and individuals. Classes are represented metrological primitives (Fig. 2), which are organized in a hierarchy shown on Fig. 3. Individuals are represented in Protégé as a specific class (e.g. class of points consists of more individual, which are also points that are defined across the properties). In Fig. 3. is shown a number of individuals that make up the class K_2. Between individuals from the class lines are also present in the individual classes of points, because the proposed model class of points used to describe the class lines.

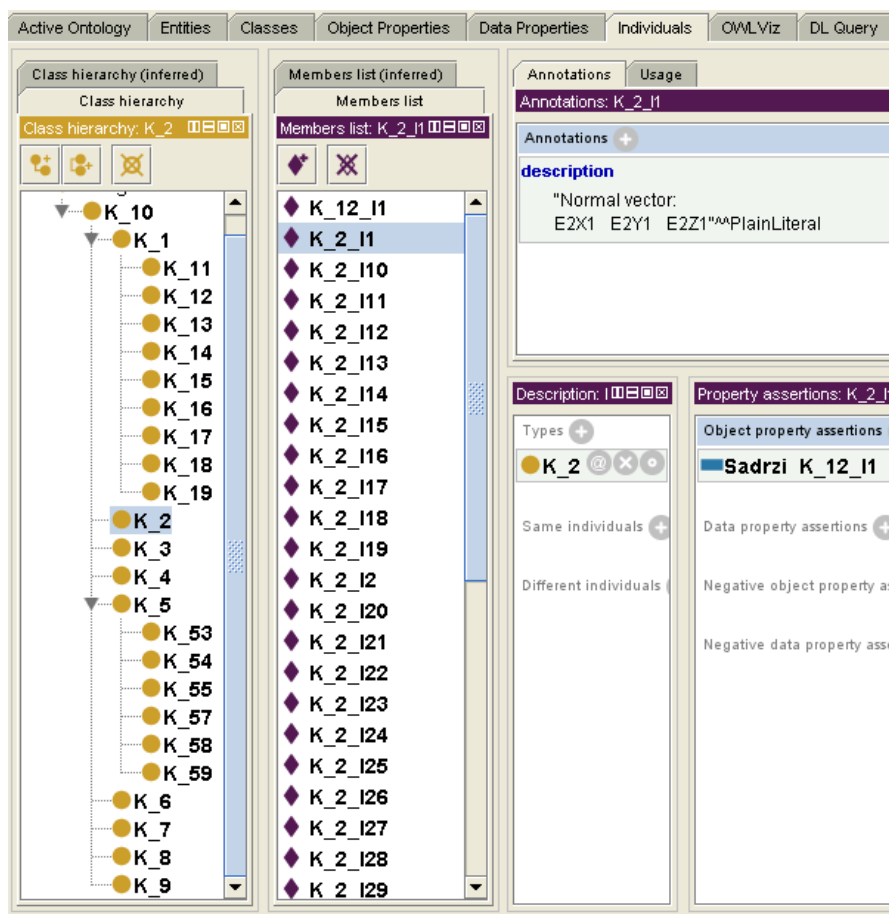


Fig. 3. A representation of classes, properties and individuals in Protégé

This occurs as a consequence of existence a subclass K_{1i} , $i = 1, 2, 3, \dots, 9$, class K_1 . Also, K_5 class consists of subclasses K_{53} , K_{54} , K_{55} , K_{57} , K_{58} , K_{59} and as a result of the fact that individuals plane (K_{5i} , I_i) take part in the description of other classes such as K_3 , K_4 , K_5 , K_7 , K_8 and K_9 . In Fig. 3. are shown two characteristics that fully describe the individual K_{2_I1} :

the normal vector as the first properties and second properties that K_{2_I1} include K_{12_I1} .

The advantage of defined class hierarchy, for the case to describing the geometry which consists of basic metrology primitives, is that the same for all parts. In contrast, the number of individual changes and depends on the metrological complexity of measuring part.

4. CONCLUSION

The paper defines the metrological primitives as class of the engineering ontology in the field of production metrology in order to develop an information model for the CAI, based on the EO as an armature around which to build a knowledge base for metrology information about the ideal geometry in relation the coordinate system of measuring part. Defined method of modeling metrological primitives as classes, individuals and properties fully provides all the information about the ideal geometry of measuring part. The result of the proposed method is a unique of class's hierarchy for all metrology parts that consist from the basic metrological primitives. Implementation in Protégé showing that with the optimization of individuals within classes on the basis of metrological information about the measuring part, quite justified further develop of EO in the field production metrology.

ACKNOWLEDGEMENT

Some research results presented in this paper refer to the Projects supported by the Ministry of Education and Science of the Republic of Serbia, whose support are here emphasizes and expressing acknowledgement to it.

REFERENCES

- [1] SOURLIER, D., *Three Dimensional Feature Independent Bestfit in Coordinate Metrology*, (1995), Doctoral dissertation, Swiss Federal Institute of Tehnology Zurich
- [2] MAJSTOROVIĆ, V., HODOLIČ, J. (1998) *Numerički upravljane merne mašine*, Fakultet tehničkih nauka, Institut za proizvodno mašinstvo – Novi Sad, ISBN 86-499-0091-7
- [3] BARREIRO, J., LABARGA, J.E., VIZAN, A., RIOS, J., (2003) *Information model for the integration of inspection activity in a concurrent engineering framework*, International Journal of Machine Tools & Manufacture 43, pp. 797-809. doi: 10.1016/S0890-6955(03)00060-9
- [4] ZHAO, F., HABEEB, S., XU, X., (2009) *Research into integrated design and manufacturing based on STEP*, International Journal of Advance Manufacturing Technology 44, pp. 606–624, DOI 10.1007/s00170-008-1841-6
- [5] USCHOLD, M., GRUNINGER, M. (1996) *Ontologies: Principles, Methods and Applications*, Knowledge Engineering Review 11(2)
- [6] <http://protege.stanford.edu/>
- [7] MATTHEW, H. et al, (2009) *A Practical Guide to Building OWL Ontologies Using Protégé 4 and CO-DE Tools*, Edition 1.2, The University Of Manchester
- [8] NOY, N.F., MCGUINNESS, D.L. (2001) *Ontology Development 101: A Guide to Creating Your First Ontology*, Tech. Rep. KSL-01-05 and SMI-2001-0800. Stanford, CA: Stanford University, Knowledge Systems Laboratory and Stanford Medical Informatics



THE USE OF MACHINE VISION TO RECOGNIZE OBJECTS

Remigiusz LABUDZKI

Institute of Mechanical Engineering, Poznan University of Technology, Piotrowo 3, Poznan, Poland
remigiusz.labudzki@put.poznan.pl

Abstract: *Machine vision (system vision) it's a apply computer vision in industry. While computer vision is focused mainly on image processing at the level of hardware, machine vision most often requires the use of additional hardware I/O (input/output) and computer networks to transmit information generated by the other process components, such as a robot arm. Machine vision is a subcategory of engineering machinery, dealing with issues of information technology, optics, mechanics and industrial automation. One of the most common applications of machine vision is inspection of the products such as microprocessors, cars, food and pharmaceuticals. Machine vision systems are used increasingly to solve problems of industrial inspection, allowing for complete automation of the inspection process and to increase its accuracy and efficiency. This paper presents the possible applications of machine vision in the present and show analysis results of the presence a tin alloy on copper elbow.*

Key words: *machine vision, image processing, inspection*

1. INTRODUCTION

The introduction of the automation has revolutionized the manufacturing in which complex operations have been broken down into simple step-by-step instruction that can be repeated by a machine. In such a mechanism, the need for the systematic assembly and inspection have been realized in different manufacturing processes. These tasks have been usually done by the human workers, but these types of deficiencies have made a machine vision system more attractive. Expectation from a visual system is to perform the following operations: the *image acquisition* and *analysis*, the *recognition* of certain features or objects within that image, and the *exploitation* and *imposition* of environmental constraints.

Scene constraint is the first consideration for the machine vision system. The hardware for this subsystem consists of the light source for the active imaging, and required optical systems. Different lighting techniques such as the structured lighting can be used for such purpose. The process of vision system starts with the image acquiring in which representation of the image data, image sensing and digitization is accomplished. Image sensing is the next step in order to obtain a proper image from the illuminated scene. Digitization is the next process in which image capturing and image display are accomplished. The last step in this process is the image processing in which a more suitable image is prepared [1]. The first aim of this article is to show typical examples of the visions systems in the automated manufacturing systems.

2. OPERATION OF A MACHINE VISION SYSTEM

A visual system can perform the following functions: the image acquisition and analysis, the recognition of an object or objects within an object groups. The light from a source illuminates the scene and an optical image is generated by image sensors. Image acquisition is a process whereby a photo detector is used to generate and optical image that can be converted into a digital image. This process involves the image sensing, representation of image data, and digitization. Image processing is a process to modify and prepare the pixel values of a digital image to produce a more suitable form for subsequent operations. Pattern classification refers to the process in which an unknown object within an image is identified as being part of one particular group among a number of possible objects.

3. THE COMPONENTS OF MACHINE VISION SYSTEM

A typical machine vision system consists of several components of the following:

- one or more digital or analogue camera (black and white or colour) with optical lenses,
- interface the camera to digitize the image (the so-called frame grabber),
- processor (this is usually PC or embedded processor such as DSP),
- device I/O (input/output), or communication links (e.g. RS-232) used to report the results of system,
- lens for taking close-ups,
- adapted to the system, specialized light source (such as LEDs, fluorescent lamps, halogen lamps,

- software to the imaging and detection of features in common image (image processing algorithm) (fig. 2),
- sync-sensor to detect objects (this is usually an optical or magnetic sensor), which gives the signal for the sampling and processing of image,
- the regulations to remove or reject products with defects.

Sync-sensor determines when a product (eg. running on a conveyor) has reached the position in which it can be inspected. The signal from the sensor starts the camera, which starts downloading the image of the product, and sometimes (depending on the system) gives a signal to synchronize the lighting in order to obtain a good image sharpness. Light sources are used in vision systems for lighting products in order to offset the dark places and to minimize the adverse effects of the emergence of conditions for the observation (such as shadows and reflections). Most of the panels to be used with LEDs.

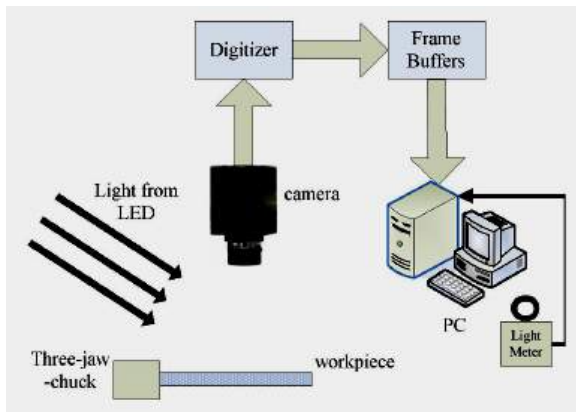


Fig.1. A typical vision system operation [2]

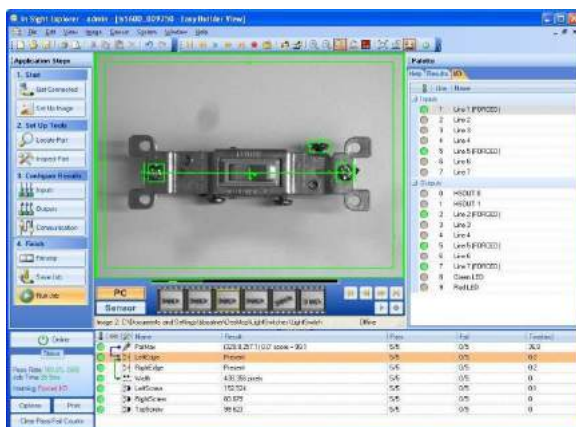


Fig. 2. The latest software Easy Builder (Cognex) for total analysis of image

The image from the camera is captured by frame grabber, which is a digitalize device (included in each intelligent camera or located in a separate tab on the computer) and convert image from a digital camera to digital format (usually up to two-dimensional array whose elements refer to the individual image pixels). The image in digital form is

saved to computer memory, for its subsequent processing by the machine vision software. Define abbreviations and acronyms the first time they are used in the text, even if they have been defined in the abstract. Abbreviations such as IEEE, SI, CGS, ac, dc, and ms do not have to be defined. Do not use abbreviations in the title unless they are unavoidable. Depending on the software algorithm, typically executed several stages, making up the complete image processing. Often at the beginning of this process, the image is noise filtering and colours are converted from the shades of gray on a simple combination of two colours: white and black (binarization process). The next stages of image processing are counting, measuring and/or identity of objects, their size, defects, or other characteristics. In the final stage of the process, the software generates information about the condition of the product inspected, according to pre-programmed criteria. When does a negative test (the product does not meet the established requirements), the program gives a signal to reject the product, the system may eventually stop the production line and send information about this incident to the staff.

4. APPLICATION OF MACHINE VISION

Machine vision systems are widely used in the manufacture of semiconductors, where these systems are carrying out an inspection of silicon wafers, microchips, components such as resistors, capacitors and lead frames [3].

In the automotive machine vision systems are used in control systems for industrial robots, inspection of painted surfaces, welding quality control [4, 5], rapid-prototyping [6, 7], checking the engine block [8] or detect defects of various components. Checking products and quality control procedures may include the following: the presence of parts (screws, cables, suspension), regularity of assembly, of the proper execution and location of holes and shapes (curves, circular area, perpendicular surfaces, etc.), correct selection of equipment options for the implementation of the quality of surface markings (manufacturer's numbers and geographical detail), geometrical dimensions (with an accuracy of a single micron) [2] the quality of printing).

Beside listed above are other area to implement machine vision. Fig. 3 shows the simplest arrangement of the machine vision measuring olive oil bottles on production lines. The online defect inspection method based on machine vision for float glass fabrication is shown in Fig. 4. This method realizes the defect detection exactly and settles the problem of miss-detection under scurriness fabricating circumstance. Several digital line-scan monochrome cameras are laid above float glass to capture the glass image. The red LED light source laid under the glass provides illumination for grabbing the image. High performance computers are used to complete the inspection based on image processing.

Another interesting proposition is use the machine vision system to validation of vehicle instrument cluster [10]. The machine vision system (Fig. 5) consists of a camera, lighting, optics and image processing software. A Cognex In-sight CCD vision sensor was selected for image acquisition and processing, which offers a resolution of 1600 x 1200 pixels and 64 MB flash memory. The acquisition rate of the vision sensor is 15 full frames per second. The image acquisition is through progressive scanning. The camera can work in a partial image acquisition mode, which provides flexibility for selecting image resolution and acquisition rate.

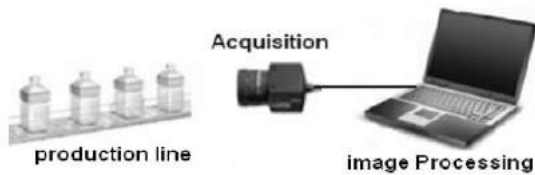


Fig. 3. The simplest arrangement of the machine vision measuring olive oil bottles on production lines [9]

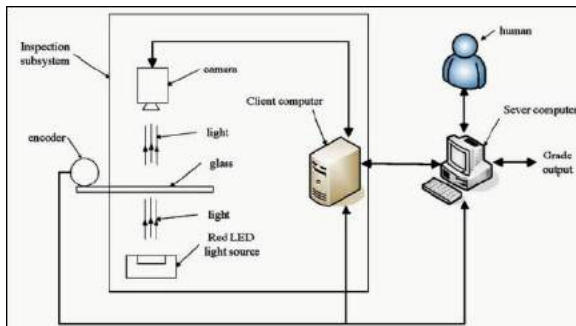


Fig. 4. Float glass inspection system [10]

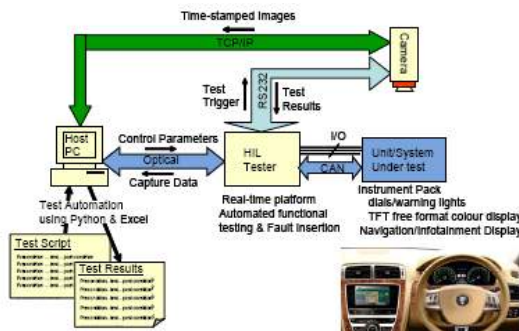


Fig. 5. System configuration for validation testing of vehicle instrument cluster [11]

The image processing software provides a wide library of vision tools for feature identification, verification, measurement and testing applications. The PatMax™ technology for part fixturing and advanced OCR/OCV tools for reading texts are available within the software. The primary source of illumination is from LED ring lights with directional front lighting, which provides high contrast between the object and background. The selection of optical lens depends on the field of view and the working

distance. In this setting, a lens with a focal length of 12 mm is used.

5. IDENTIFICATION OF SELECTED CHARACTERISTICS OF ELBOW

The author made an attempt to identify the fill tube copper tin alloy. To realize this purpose the appropriate test bench was built. The identification was carried out using Basler camera connected to the computer with NI software. Using the capabilities of NI's software author decided to perform detection in three variants.

5.1. Pattern matching with distinguishing shades of gray

Pattern matching using image processing black and white, which gives each of the points of one of 256 shades of gray, and then recognize the pattern. For comparison - the processing of binary images are treated as black or white.

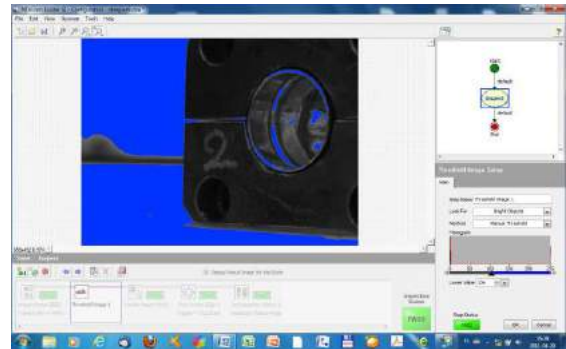


Fig. 6. Distinguishing shades of gray

5.2. Pattern Matching with color images

The basis for recognizing the pattern in the image is the original process of storing the image pattern. Remembering the pattern may cover the entire recorded image, or part of a limited manually to a fragment. Separation of the standard windows can accelerate the process of searching the entire image in the search for a pop. The window scans the specified search area, starting from the upper left corner, ending at the bottom right to find a place that best suits the saved model.



Fig. 7. Creating a pattern on a workpiece without tin

¹ Remigiusz LABUDZKI, PhD, Poznan University of Technology, Piotrowo 3, 60-965 Poznan, remigiusz.labudzki@put.poznan.pl

5.3. Matching patterns with circles

This method involves finding the edge on which to draw a circle. If the program will recognize a few points, after which the connection may be formed circle - draws him. The program searches for these points in a strictly defined by the user environment. In the case of an experiment carried out if the program recognized points in the test piece was a tin. Then, in the place where the tin was found by points, which belonged to the edge of the circle. If, however, does not detail the groove was filled with tin program does not draw a circle, which meant a defect part. The status of the inspection is set to FAIL if the program could not draw a circle and a PASS if the circle has been drawn.

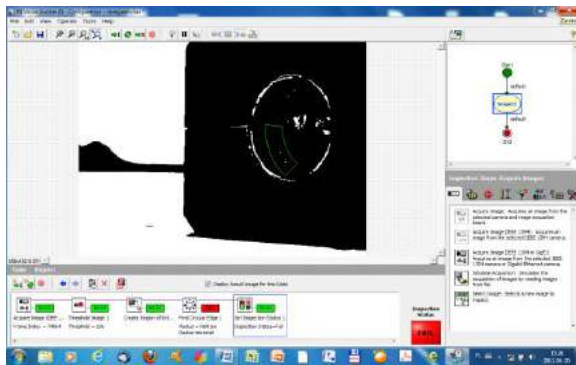


Fig. 8. Lack of recognition of an appropriate amount of edge

6. CONCLUSION

Analyzing test results is not difficult to choose the best solution. The results obtained for a method which involves drawing a circle on the basis of the edge is definitely the best. 48 tests performed in this method were positive, that is, agree with reality. This represents as much as 96%. Only in two cases, the program poorly studied object recognized. The reason for this could be for example, inadequate lighting. However, the error rate is so low that the solution can be applied on the machine.

Otherwise the case is when it comes to pattern matching. In this case, as many as 10 of 50 attempts resulted in an erroneous analysis. 20% error is too many to be the solution to enter the production hall. One can estimate that a similar margin of error in the control of units have a man. There would therefore make sense to use the vision system, which would improve substantially no audit details. Negative results of measurement may arise from the fact that we do not find two identical connectors filled with tin. Each of the surface, which creates the tin has a different structure. Therefore, the pattern was not always correctly compared to subsequent test details. Ended in complete failure to distinguish between degrees of greyness. Here, in comparison to previous methods, the number of correct negative diagnoses exceeds the diagnosis. As many as 32 attempts (64%) gave a negative result, which excludes this solution.

Too many factors can influence the outcome of the experiment, because it is not suitable for use. The shade of tin is relatively similar, while the color of copper fittings may be in a significantly different.

The results show that the analysis of the presence of an alloy of tin to copper tubes can join the many already existing machine vision applications such:

- biometrics,
- positioning,
- industrial production on a large scale,
- small-lot production of unique objects,
- safety systems in industrial environments,
- intermediate inspection (e.g. quality control),
- visual control of inventory in the warehouse and management systems (counting, reading bar codes, storage interfaces for digital systems),
- control of autonomous mobile robots,
- quality control and purity of food products,
- exploitation of bridges,
- retail automation,
- agriculture,
- vision systems for blind people.

REFERENCES

- [1] Golnabi H, Asadpour A.: Design and application of industrial machine vision systems. *Robotics and Computer-Integrated Manuf.*, 23 (2007), 630–637.
- [2] Zhang Z., Chen Z., Shi J., Jia F., Dai M.: Surface roughness vision measurement in different ambient light conditions. 15th Int. Conf. Mechatronics and Machine Vision in Practice, Auckland, 2008.
- [3] Bhuvanesh A., Ratnam M.: Automatic detection of stamping defects in lead frames using machine vision. *Int. J. Adv. Manuf. Technology*, 2007, pp 1201-1210.
- [4] Tsai M., Ann N-J.: An automatic golf head robotic welding system using 3D machine vision system. Workshop on Advanced Robotics and Its Social Impacts, Taipei, 2008, pp 1-6.
- [5] Liao G., Xi J.: Pipeline weld detection system based on machine vision. 9th Int. Conf. on Hybrid Intelligent Systems, Shenyang, 12-14 August 2009, pp 325-328.
- [6] See A.: Rapid prototyping design and implementation of a motion control integrated with an inexpensive machine vision system. *Instrumentation and Measurement Technology*, 3, Ottawa, 2005.
- [7] Cheng Y., Jafari M.: Vision-based online process control in manufacturing applications. *Trans. on Automation science and engineering*, 5, 2008, 140-153.
- [8] Yradley E.: New generation machine vision: coping with changes in light and surface quality. *Computing & Control Engineering Journal*, 16(2005)6, pp 26-31.
- [9] Taouil K., Chtourou Z., Kamoun L.: Machine vision based quality monitoring in olive oil conditioning. *Image processing theory, tools and applications*, Sousse, 2008, 1-4.
- [10] Peng X., Chen Y., Yu W., Zhou Z., Sun G.: An online defects inspection method for float glass fabrication based on machine vision. *Int. J. Adv. Manuf. Techn.*, 39(2008), pp 1180-1189.
- [11] Huang Y., Mouzakitis A., McMurran R., Dhadyala G., Jones R.: Design validation testing of vehicle instrument cluster using machine vision and hardware-in-the-loop. *Int. Conf. on Vehicular Electronics and Safety*, Columbus, 2008, pp. 265-270.

PRODUCT QUALITY CONTROL BY USING REVERSE ENGINEERING

Jelena MICEVSKA, Zoran SPIROSKI, Jasmina ČALOSKA, Atanas KOČOV

Faculty of Mechanical Engineering, Karpos II bb, Skopje, R.Macedonia

jelena@cirko-mes.com; zspiroski@technologica.com;

jasmina.chaloska@mf.edu.mk; atanas.kochov@mf.edu.mk

Abstract: In the production process of every product, engineers are faced with different kind of problems. Most of these problems are caused by external factors which cannot be taken in consideration during the design, construction and production process. The produced part often differs from the CAD model, designed by the engineer. In this paper, technology of reverse engineering is used in order to control the quality of the final product produced by injection molding. Measurements and scans are made by using the optical device from the producer Gom, ATOS II. The necessary corrections of the die are made as a result of comparative analysis of the CAD models.

Key words: reverse engineering, die design, injection molding

1. INTRODUCTION

Reverse Engineering is a technology that is used for transformation of the produced physical models into 3D CAD models. This technology has vast use in the field of mechanical engineering, but at the same time in many different fields as medicine, architecture, art, cultural inheritance. Purpose of the reverse engineering is not just simple scanning on the models and making their copies in computer environment, but it is much more. With the help of this technology we can get any physical model that we want in computer environment, and after that make changes and analysis directly on the model or include it in any part of the CAD/CAM/CAE system.

One of the many uses of this technology in the mechanical engineering is conduction of dimensional comparison between two models, where one is the actual scanned data from the physical model and the other one is designed CAD model. The dimensional comparison of the scanned model is done by receiving point cloud, which has to be segmented aligned. This way the surfaces are identical with the produced part and can be compared with the given CAD model for determination of the deviations.

Reverse engineering in the tooling is used for reconstruction or reparation of the parts, tools and dies (Figure 1-1; 1-2).



Fig. 1-1. Tool reparation

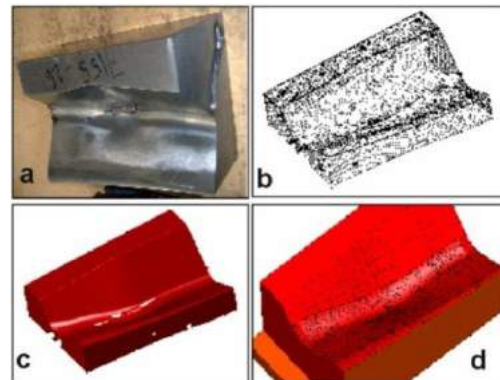


Fig. 1-2. Part reparation
 (a – damaged part, b – point cloud,
 c – STL model, d – CAD model)

Softwares that are used in the reverse engineering have the possibility to compare the scanned model with the CAD model. Usually the CAD model is imported as STL or IGES model, and is placed in the same coordinated system as the scanned model and the comparison is run (Figure 1-3).

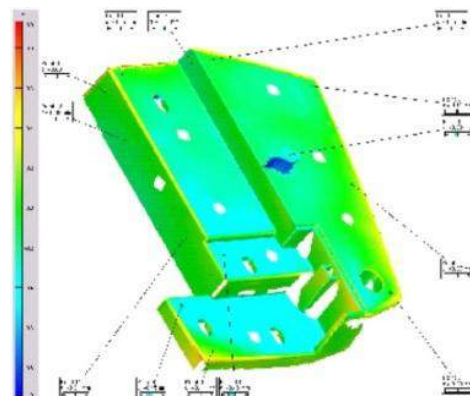


Fig. 1-3. Comparison of scanned and CAD model

2. USE OF THE REVERSE ENGINEERING FOR QUALITY CONTROL OF TOOL

Reverse engineering enables fast control of the dimensions, as well as the surfaces of the produced model with the technology of injection molding of polymer material. Some of the dimensions (diameters of holes, lengths, widths etc.) can be controlled with classical measuring instruments but everything gets complicated when it should be controlled and determined if the quality of the surfaces is in the defined tolerance range. In cases like this, the technology of the RE is irreplaceable.

2.1. Description of the product – housing for star

The product – housing for star is compound of the ridge switch – type BS (Figure 2-1), made from – ULTRAMID B3S. This product has a very responsible role in the hole assembly since it is used as a switcher of the electromotors, transformer stations, welding apparatuses, resistors, heaters. The product has also high built-in power, long electric durability and safety from contact voltage. The characteristics of this product are completely regulated with the international standard IEC 60947-3.



Fig. 2-1. Ridge switch - type BS

Housing of this product has to satisfy many requirements. At the same time it has to be made from a certain material and has to have certain precision of the functional and built-in dimensions, given in the technical documentation (Figure 2-2).

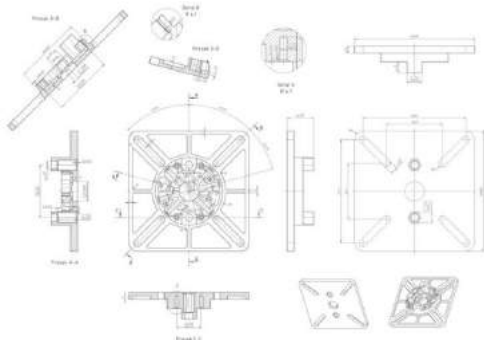


Fig. 2-2. 2D drawing of the part- housing for star

Ridge switches typical are produced in many different sizes. In this case the process of the reverse engineering is used for quality control of the tool, or more precise for determination of the deviations of the produced model from its 3D model. The control is conducted with the 3D model (design in Solid Works 2010, figure 2-3), created from the 2D technical documentation (fig. 2-2), and 3D scan (made with ATOS II) of the produced model (figure 2-4). After creating CAD models of the two models they are joined in same virtual environment and comparative analysis is conducted.



Fig. 2-3. 3D model made in SolidWorks 2010

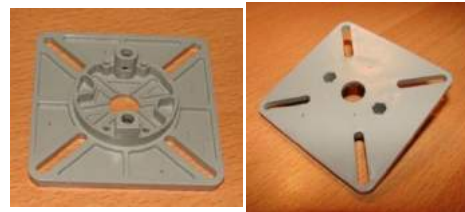


Fig. 2-4. Produced model

2.2. Process of creating 3D scanned data with Atos II

ATOS II (Figure 2-5) is a 3D scanner that is characterized with high precision, fast work and mobility. It has a light source – projector (pos. 2, figure 2-5) and two photosensitive devices – cameras (pos. 1 and 3, figure 2-5). The possession of two cameras puts this 3D scanner in advantage before the competition.



Fig. 2-5. ATOS II – contact-less device for collecting data

ATOS II works on the same principle as the human eyes. Same way as the human registers only the information seen by the both eyes, the camera collects the data that is seen by the both cameras (Figure 2-6).



Fig. 2-6. Working principal of the ATOS II

ATOS II can scan models with vast volume range from 35x28x20 mm to 1700x1360x1360 mm. It has digital camera that is working with 1.300.000 pixels. Time needed for one scan is 0,7 seconds. Distance of the points in the cloud point is from 0,08 to 1 mm. Accuracy of the 3D scanner is 0,002 mm, which makes it optical measuring device.

Phases of the process of scanning:

1st phase – preparation of the 3D scanner and the model

Before the scanning is started, the volume of the model needs to be calculated. This is important step because according to the volume of the part the 3D scanner is prepared. This means that the adequate size of the lenses is chosen and put on the two cameras and the projector. Next step is calibration of the equipment, step very important for the accuracy of the final results. During the calibration, except setup of the optics, setup of the temperature and the humidity is made.

Also according to the volume of the model, the size of the referent points is chosen. These referent points are important because they are the link between the model and the 3D scanner. The 3D scanner captures the surface of the model through these points and also merges all of the scanned data through them.

2nd phase – process of scanning

Scanning is the process in which the data collected with the 3D scanner is transfer into the computer. The scanning of the whole model is done scan by scan (Figure 2-7), which are well merged through the referent points.



Fig. 2-7. Scanning process

The process of 3D scanning should be conducted in highly controlled conditions (temperature, lighting, movement) since the precision of the device is very high and with only a slight change of the conditions there is a possibility of incorrect results. When the whole process of collecting data is finished, in the software we have one point cloud (Figure 2-8) which resemble of the model that is scanned but it is useless for many operations and has to be finished adequate, depending of the purpose of the scanning.

This process of scanning the model is done in Project mode which is finished with the process of polygonization.



Fig. 2-8. Housing for star – point cloud

3rd phase – polygonization

This is the phase in which from point cloud we get polygon model (Figure 2-9). The polygonization is automatically run, but there are some aspects of it that can be controlled, as precision and size of the polygons.



Fig. 2-9. Housing for star – polygon model

These modifications are controlled manually because they depend on the precision of the finishing surface that we need.

After the polygonization, we automatically enter into new mode in the software, called Evaluation mode. In this mode slight changes can be made on the geometry of the model. First thing, that is necessary to be done is to remove the places were markers used to be because of the irregular finishing. These surfaces are cut off, and then are replaced with new ones. If the whole surface is a little bit noisy, smoothing can be applied. In this mode, model can be presented with sections by the desired axis and the desired distance between the sections. In this mode also comparisons between scans or models can be made.

3. COMPARATIVE ANALYSIS

The comparative analysis in conducted in the software Atos v5.1.1. CAD model from the 2D drawings is drawn in Solid Works 2010 and it is exported as STL file, so it can be imported in this software for the analysis. The imported model is set as a reference, which means that the analysis is going to be according to it. The polygonized model from the scans is also imported in the software in the same window as the CAD model. When the both models are imported, they are overlapped by the coordinate systems. The overlapping of the model is very important because the validity of the whole analysis is in risk. So before importing the models we assure that the coordinate systems of the both models are identical actually that the both models are set identically in the space. The analysis of the deviation

is run automatically but the analyzed degree of the deviation is set manually by the operator. This means that we can determine how precise should be the analysis depending on what is our final goal. Since we wanted to see if the deviations of the dimensions and surfaces are higher than 10^{-4} mm, we set the scale that way, so the deviations less than 10^{-4} mm will not be shown on the screen. The results of the analysis can be seen on the figure 3-1.

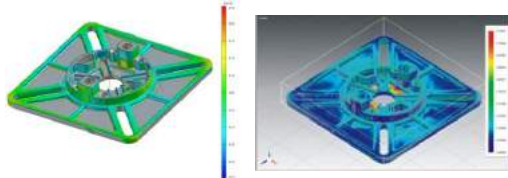


Fig. 3-1. Analysis of the deviations

4. DISCUSSION

From the comparison between the two models it is clear that there are some deviations in the geometry, bigger than the permitted ones. Deviations can be caused by two groups of problems:

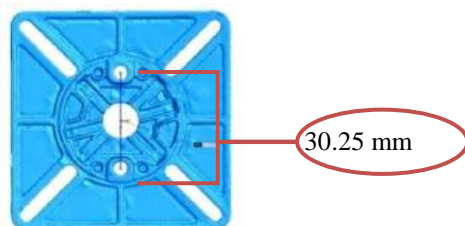
- Deviations from the shape,
- Deviations from the tolerance dimensions.



Fig. 4-1. Deviation from the shape

Unformed places of the model, shown on the figure 4-1 with red colour (position 1) are as a result of trapped air in the tool. Crack, shown on the figure 4-1, with yellow colour, (position 2) is a result of so called “cold joint” which is caused by early hardening of the melted polymer. Deviations of the surface are caused by the uneven cooling.

Correction of these imperfections can be made by changing the technological parameters in the process of injection molding or by changing the tool. Bigger deviations than the ones permitted by the constructor can be solved only by correction of the segments of the tool.



Measured dimension is 30.25mm
Tolerance dimension is $30^{+0.05}$ mm \Rightarrow **Deviation is 0.2 mm.**

Fig. 4-2. Deviation from the dimensions

5. CONCLUSION

Unlike the use of classic coordinate measuring machines, here, with only one quick session of scanning, we can detect and define all the deviations and irregularities of the produced part:

- Of the all free and tolerant dimension,
- Geometric tolerances of the shape and form etc,

Irregularity of the complex surfaces indicates on incorrect values of the technological parameters. With their change and by re-scanning and re-comparing produced part with 3D model, we shall determine the optimal values of technological parameters. This way we perform optimization of production process, to obtain correct product.

It is important to notice that this is not just simple measurement of one part but it is much more. Use of the reverse engineering is part from a whole process of development and adaptation of a technology for serial production of a certain part. Through analysis of the dimensions and the form of one product produced with the technology of the injection molding of polymer materials, we can make conclusions not only for the tool itself but also for the technological parameters within the process. This results in increasing the quality of the overall process of production.

Apart from the scanning of the part it is good to scan the tool/mold, which in this case it is not done. By conducting analysis on the tool itself we can get additional information, which can be used for better optimization of the whole process.

The whole system ATOS II is adequate for transportation and change of the working environment.

REFERENCES

- [1] Training Tutorial ATOS v5.1.1
- [2] Vesna Mandic,; *Virtuelni inženering*, Masinski fakultet u kragujevcu, Centar za virtuelnu proizvodnju, 2008
- [3] W. Dealey: The magic, art and science, Modern mold&tooling, Vol.3 No.3 2001
- [4] Kim G. J. Designing Virtual Reality Systems, Springer, London, 2005
- [5] Lee K., Principles of CAD/CAM/CAE Systems, Addison-Wesley Longman 1999
- [6] Kalpakjian S., Manufacturing Processes for Engineering Materials, Pearson Education Inc, New Jersey 2003

34th INTERNATIONAL CONFERENCE ON PRODUCTION ENGINEERING



SECTION E

CAX TECHNOLOGIES (CAD/CAM/CAPP/CAE SYSTEMS) AND CIM SYSTEMS



APPLICATION OF THE COMPUTER AIDED SELECTION OF OPTIMAL CNC MILLING STRATEGY

Jozef NOVAK-MARCINCIN, Miroslav JANAK, Ludmila NOVAKOVA-MARCINCINOVA,
Veronika FECOVA, Jozef BARNA

Faculty of Manufacturing Technologies, Technical University of Kosice, Bayerova 1, Presov, Slovakia
jozef.marcincin@tuke.sk, miroslav.janak@tuke.sk, ludmila.marcincinova@tuke.sk, veronika.fecova@tuke.sk

Abstract: Goal of this paper is to describe manufacturing strategies used in 3D milling and possibilities to simplify the choice of manufacturing strategy, especially for inexperienced user. Main attention is directed to creation of simple software tool for optimization of suitable milling strategy selection, functional principles of this program and conditions related to its creation.

Key words: computer aid, milling strategies, software application, Delphi

1. INTRODUCTION

Currently in the field of CAD/CAM systems there is need of using such systems for improvement of production's efficiency, production time shortening, simplification of production, saving of energies and materials and that also in implicated form of better exploitation of production devices and lesser tools consumption. This request of productivity improving concerns all the participants from the field of tool, automobile and aero-industry, producers of moulds and different parts of variable shapes in various usage areas.

Optimization of suitable manufacturing strategy selection is important matter mainly for new and inexperienced users of CNC technique, for the acquirement of knowledge about strategies and their importance and utilization of new software tools would present barrier from economical and time aspect. Simple but helpful software product should assist in faster decision about strategy fitness and produce positive impacts of this decision correctness. Further chapters consist briefing of computer aid of manufacturing strategies and creation method of software which mitigates the selection of milling strategy.

2. CA MANUFACTURING STRATEGIES

There are a huge number of products offering computer aid in different production spheres including manufacturing strategies area. Common effort of these CAM systems is to simplify the work of NC programmer and to ensure the correctness of his decisions or even to substitute his own decision by software process and so to ensure best possible milling efficiency. To most used CAD/CAM systems solving the problems of manufacturing strategies currently belong: EdgeCAM, Pro/ENGINEER, ProTOOLMAKER, CADD5, CAM-TOOL, Catia, FeatureCAM, SurfCAM, Unigraphics, MasterCAM, PowerMILL, ESPRIT, VX CAD/CAM and other.

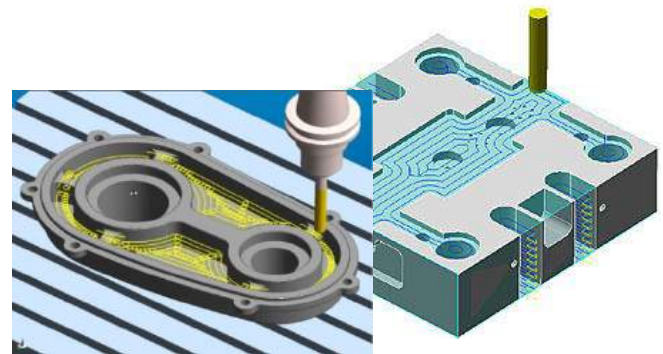


Fig.1. Milling strategies in different CAM systems

These software systems concern milling in the scope of 2 – 5 axis machining. They offer section designing for roughing, which is machining with goal of cutting as much material as possible considering additional material for further operations. They also offer finishing, which means the process of removing residual material left on workpiece after some previous technology [1].

To main roughing strategies supported in CAD/CAM systems belongs:

- raster milling – tool path is parallel with coordinate system axis, tool is moving upright with minimal steps,
- contour milling – tool path copies the contour of machined element,
- profiling – tool path copies the contour of machined element while keeps moving with defined steps,
- raster and profiling – combination of two previous strategies.

To finishing strategies offered in CAD/CAM systems usually belongs [2]:

- projection milling – means projection of 2D predefined motion to the model,
- constant Z-height milling – mill moves in certain height while copying model's contours,
- corner milling – for removing the residual material after previous tool or in between two surfaces,

- nib milling – mill moves down the model continuously like a pen,
- rotary milling – tool moves linear, workpiece rotates around its axis.

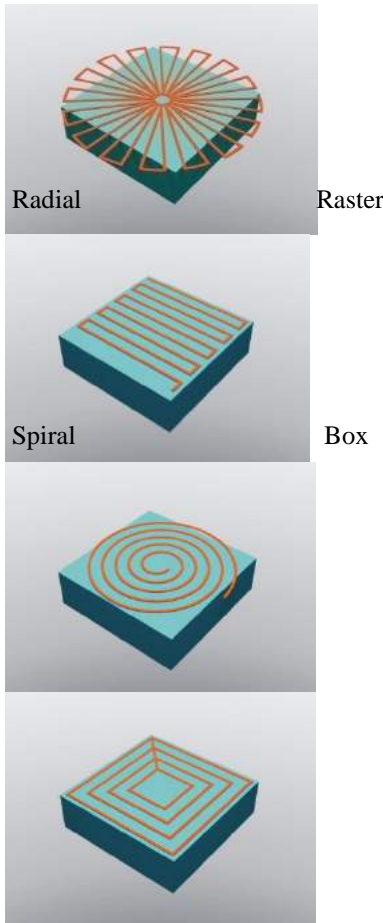


Fig.2. Projection strategies of finish cutting

In most software concerning manufacturing strategies NC programmer has an option to choose suitable strategy, which would allow surface machining in shortest possible time while preserving requested quality. However only few programs select optimal strategy without choice process of its user.

3. SOFTWARE FOR OPTIMAL MILLING STRATEGY SELECTION

For creation of application we use program language Object Pascal and its visual implementation called Delphi. Every application created in Delphi is based on components. They generate its design and executive kernel. Most of necessary components are implied with an installation pack of Delphi, other can be created by user or downloaded from web [3].

Application should terminate optimal strategy after consideration of certain criteria such as machining time, residual stresses volume and tool wear. To do so it will compare the output values of computations for each strategy (length of absolved trajectory, number of contours, etc). To perform these computations program needs input data given by user corresponding with cutting

conditions. That concern tool diameter, feed rate, side motion and sizes of machined surface.

User's environment consists out of 4 main parts:

- *Geometry selection section* – buttons for choice of machined surface type according to its geometrical characteristics.
- *Input information section* – space for writing of cutting parameters related to suitable strategy selection.
- *Graphical information section* – visual information giving user a view of planned strategy and dimensions.
- *Output information section* – space for quoting the results of computations and final strategy selection. For comparison, numerical values of results are shown for each strategy. Optimal variant will be highlighted.

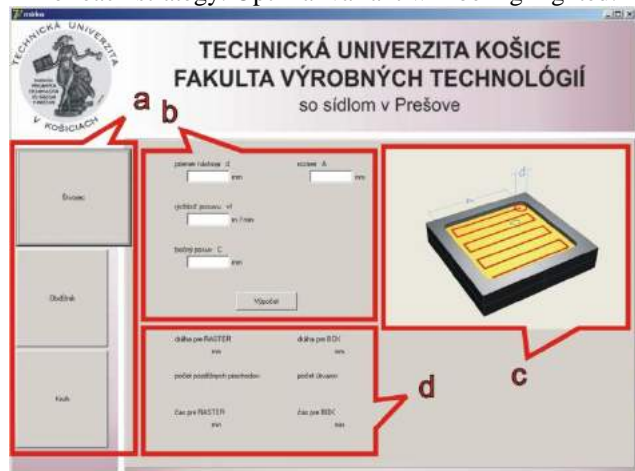


Fig.3. User's environment of software – a) geometry selection, b) input information, c) graphical information, d) output information section

Program for its computation uses mathematical operations summarizing length of tool trajectory. When entering input data into the editable labels, it assigns them to relevant variables. Numerical dimensions of machined surface and tool diameter serves as limit borders decisive about stopping of tool motion. After pressing the COMPUTATION button program starts the procedures that calculate the length of tool path for each strategy according to input data received from user. Optimal solution presents the variant with lowest value of machining time criteria.

4. CONCLUSION

From programmer point of view, application uses events control of particular visual components – panels, edit fields, labeled edit fields, buttons, images. From the aspect of computation, main part of program code consists of cycles, that ensure computing determination in case of reaching the borders of machined surface. Final border contouring of machined element is added to result in order to make the final faces and edges smooth.

Slovak Ministry of Education supported this work, contract VEGA No. 1/0036/09, KEGA No. 047-004TUKE-4/2010 and ITMS project code 26220220125.



REFERENCES

- [1] CHANG, T. CH., WYSK, R. A., WANG, H. P.: *Computer-Aided Manufacturing*. Prentice-Hall, New Jersey, 1998, 748 p.
- [2] LEE, K.: *Principles of CAD/CAM/CAE Systems*. Addison-Wesley, Reading, 1998.
- [3] MARCINCIN, J. N., JANAK, M. (2009). *Software support for selection of suitable milling strategy*. Buletin Stiintific, Vol. 23, p. 119-122.



34th INTERNATIONAL CONFERENCE ON
PRODUCTION ENGINEERING
28. - 30. September 2011, Niš, Serbia
University of Niš, Faculty of Mechanical Engineering



CURRENT STATUS AND FUTURE TRENDS IN DENTAL CAM RESTORATIVE SYSTEMS

Janko HODOLIČ¹, Tatjana PUŠKAR², Igor BEŠIĆ³

^{1,3}University of Novi Sad, Faculty of Technical Sciences, Trg Dositeja Obradovića 6, 21000 Novi Sad

²University of Novi Sad, Medical Faculty, Hajduk Veljkova 3, 21000 Novi Sad, 21000 Novi Sad

hodolic@uns.ac.rs, tatjanapuskar@yahoo.com, besic@uns.ac.rs

Abstract: This article presents recent developments in dental computer aided design and manufacturing systems for fabrication of custom inlays, onlays, crowns and fixed partial dentures from perspective of different materials, manufacturing technologies and digitization methods. The use of dental CAD/CAM systems is promising in terms of minimising time and effort made by dentists, technicians and patients for restoring and maintaining patients oral function and aesthetic, while delivering high quality end result. Components and methodologies of the existing commercial dental CAD/CAM systems as well as systems in development are analyzed and discussed in detail.

Key words: CAD, CAM, crowns, inlays, onlays, bridges, digitizing

1. INTRODUCTION

Automation of the production process or computer aided manufacturing (CAM) can be regarded in two ways: as a computer aided system which purpose is to support activities in manufacturing; or as software which is used to develop control programs for the numerically controlled systems.

CAM systems evolved historically in the industrial metal manufacturing environment with beginnings in 1950's as concept of numerically controlled machine tools. A major milestone in the development was in 1970's with introduction of microprocessors. This enabled broader and more intensive development of CAM. In the 1980's complex systems for automation of product design – computer aided design (CAD) and manufacturing emerged. These systems were named CAD/CAM systems (IDEAS; CADAM, CATIA). In the 1990's six major corporations were dominating available CAD/CAM choices: Computervision, EDS/Unigraphics, SDRC, PTC, Matra Datavision and Dassault Systems. Software systems developed by these corporations were made from modules for various areas in engineering and are still dominating the choice of CAM software solution until present [1].

With computer hardware getting more available, the CAM systems also made it to manufacturing areas and users other than industrial metalworking.

The first steps in dental CAM application were made in 1980's with first concept of the CEREC system. The concept evolved to functional CAD/CAM system CEREC-1 five years later [2].

2. DENTAL COMPUTER AIDED MANUFACTURING PROCESS MODEL

The overall quality of recovering patient's oral function and maintaining their oral health has been largely dependant on technology and materials used for fabrication of crowns and fixed partial dentures (FPDs). The classical fabrication process relies heavily on manual labor and its quality is resulting in part from craftsmanship, skill and experience of dentists and dentist technicians.

In terms of the manufacturing engineering, fabrication of dental crowns and FPDs can be considered highly complex and low in production volume, driving the fabrication method selection towards CAM, i.e. the usage of CAM can be recognized as an immediate benefit for improving the quality of the restorations.

2.1. Traditional process

The traditional fabrication process is presented in detail in Figure 1. The process starts with the tooth or teeth preparation and ends with aesthetically and functionally restored tooth or teeth (*restoration*). The algorithm shows the process steps grouped to form three main phases: a) stone model fabrication, b) custom restoration design and manufacturing, and c) final restoration *in vivo* testing, fitting and *cementing*.

Stone model fabrication starts with placing viscous fluid into the mouth with prefabricated tray and, optionally, using customized tray. After some time, the liquid hardens to become an elastic solid. After removal from the mouth, the material retains shape of the preparation, and is referred to as *the impression*. Custom dental model cast (also known as work model) is then made based on the impression. A wax pattern is then applied to the surface of the model and hand-modeled to have desired

¹ Prof. dr Janko Hodolič, University of Novi Sad, Faculty of Technical Sciences, Trg Dositeja Obradovića 6, 21000 Novi Sad, hodolic@uns.ac.rs

² Doc. Dr. Tatjana Puškar, University of Novi Sad, Faculty of Medicine, Hajduk Veljkova 3, 21000 Novi Sad, tatjanapuskar@yahoo.com

³ Igor Bešić, University of Novi Sad, Faculty of Technical Sciences, Trg Dositeja Obradovića 6, 21000 Novi Sad, besic@uns.ac.rs

shape of the future restoration. A lost wax or investment casting process is then used to produce metal restoration. This investment casting method is time consuming and comprised of many manual steps including manual post-processing or finishing. Post processing includes: veneering, thermal processing, grinding and pre delivery quality control. This functional quality control is being done utilizing specialized mechanical device (*articulator*) to check interaction of the restored teeth to adjacent teeth and the occluding teeth.

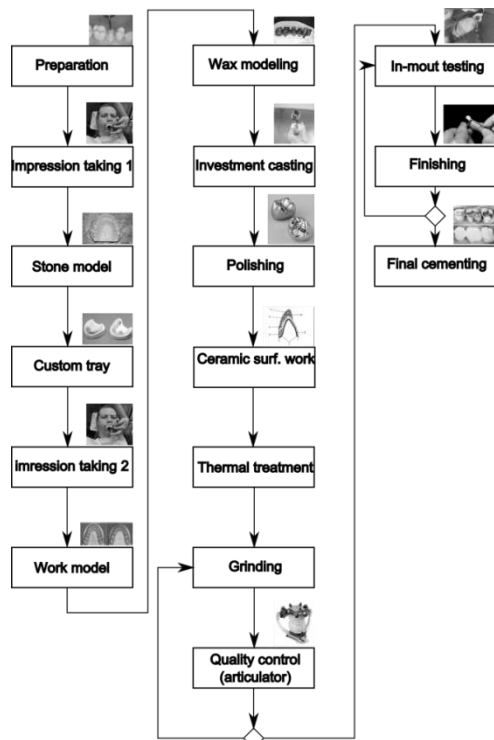


Fig.1. Traditional wax modeling based fabrication process flow for metal ceramic crowns

Final adjustments are being made *in vivo* and require extensive experience.

2.2. Computer aided manufacturing process

With the simultaneous introduction of numerically controlled machining and fast digitization techniques a major breakthrough has been achieved in: application of new materials, reducing labor, cost effectiveness and quality control [3]. This concept has been named *dental CAD/CAM*.

Figure 2 shows the flow of a typical dental CAD/CAM fabrication process. The wax and investment casting phase has been replaced with three new functional components: data capture, restoration design and fabrication.

Digitization is a data acquisition process of the oral environment (tooth preparation, adjacent teeth and occluding teeth geometry). This data capturing step differs between commercially available systems [4]. Extraoral 3D scanning systems capture data from models, using mechanical or optical methods. With few exceptions, extraoral digitizers use technologies that prevent them from being used intraorally [5].

Intraoral digitizers capture data from the patients mouth directly. When having this capability, the model making

and impression taking phase is avoided (Figure 2). Consequently, this digitization technique is also referred to as *digital impression taking*.

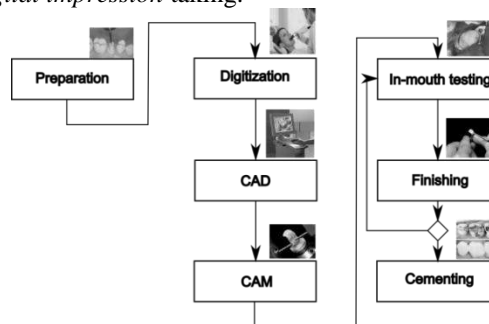


Fig.2. CAD/CAM fabrication process flow in case of intra oral digitization

The device used for data acquisition is an integral part of the CAD/CAM system and can be used only in combination with the CAD software [5]. In contrast to these *closed systems*, there are systems available that allow such type of component interchange. These systems are referred to as *open systems*. For the digitizer component, this usually means that the digitized result can be exported in one of the common data formats: ASCII, DXF, IGES, STEP or STL for use in CAD software.

The CAD software is used for restoration design based on data captured in digitizing stage. The purpose of the dental CAD software is to enable *individual design* of the restoration. This digital design replaces traditional restoration shaping in wax.

There are many CAD software choices available for this activity [6]. Like the data acquisition systems, software component is usually proprietary and cannot be interchanged among systems.

In case of the full crown restoration, the restoration design consists of inner face and the outer face. The inner face is modeled based on the preparation digitization, while the outer face is retrieved from the CAD software internal database of teeth shapes. The line where those two surfaces meet is called *margin line*. The gap between the preparation and restoration must be designed to leave space for adhesive material (cement) as shown in Figure 3. This gap can be viewed as one of the components of error budget for the digitization, design and fabrication process. Acceptable marginal opening for full crowns for instance is 50 μm up to 75 μm [7].

The degree of interaction in the CAD stage varies, ranging from substantial to no required user operations. Even in the most automated systems, the user generally has the option to modify the automatically designed restoration to fit his or her preferences [5].

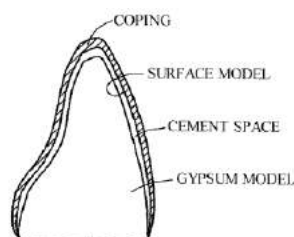


Fig.3. The position of the cement space relative to model and restoration [8]

Finally the CAD modeled shape is transformed to physical crown or a bridge by means of computer aided manufacturing. During the last years, a spectacular amount of production systems has been developed and made commercially available. These advanced systems use a subtractive or an additive approach.

The subtractive approach usually implies usage of dedicated milling or grinding NC systems. The NC codes are calculated by the CAM software and transferred to these systems. One approach is to have fully automated system capable of one-appointment restoration fabrication. The other possibility is that the dentists handle only the data capturing and CAD issues, while central production centers deal with the CAM issues and NC milling .

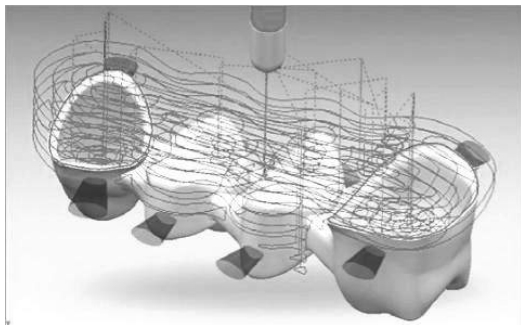


Fig.4. An example of calculated milling tool path resulting from the dedicated CAM software module [9]

Grinding/milling systems subtract the material from prefabricated ceramic blocks. These ceramic blocks are machined mostly in pre-sintered state because of their mechanical properties. This means that the restorations need to be heat treated in furnace after machining. One example is dense zirconia-based ceramics which is very hard for machining [10]. The NC milling approach is also being successfully used in machining of metal alloys and composites.

Rapid prototyping processes like selective laser sintering (SLS), stereolithography (SLA), ink jet printing (IJP) and 3D-Printing are successfully used to produce wax or resin based master patterns for mould fabrication [11]. Rapid manufacturing approach such as selective laser melting (SLM) is used for direct manufacturing of crowns/bridges from cobalt-chromium and precious metal alloys. The CAM task here is to position the parts virtually in the build volume of the SLM machine, slice this positioned CAD model and set the optimal process parameters.

3. EXISTING SYSTEMS

The commercially available systems vary dramatically in their advantages and limitations. Table 1 gives an overview of few selected systems.

The **CEREC** system was the first successful implementation of integrated intraoral digitizer and numerically controlled grinding system for restoration fabrication. The development started 30 years ago and is continued with the latest version that uses the “step-bur” diamond tool for 5-axis grinding (Figure 6) and a blue light fringe projection system for intraoral digitizing (Figure 5). This highly integrated system is intended to be single-visit chairside restoration system.

Table 1 Dental CAD/Cam systems overview

CAD/CAM system (reference)	Data acquisition method	Material options	Production technology
CEREC [12]	intraoral/extraoral (optical – blue light)	Al, Zr ceramics, composites	NC milling
LAVA [13]	intraoral/extraoral (optical – blue light)	Zr ceramics	NC milling
Medifabricating [14][15]	extraoral (optical – white light)	Zr cer., Titanium alloys	SLM
Evolution 4D [16]	intraoral (optical-laser)	*	NC milling

* The system is in development; no information about the material options has been specified.



Fig.5. CEREC acquisition center: intraorally projected fringe pattern of short frequency visible light [12]



Fig.6. CEREC: 5-axis double tool milling system [12]

Lava system is a two option system with intraoral or extraoral digitizing capability. The both options can be integrated with the dedicated Lava CNC milling unit, or used in standalone mode (Figure 7).



Fig.7. LAVA intra oral scanner (left), 3shape extraoral scanner (right) [13] [14]

The **BEGO Medifabricating** uses alternative method of direct restoration fabrication - SLM. The available materials include: titanium alloys, precious metals and CoCr alloys. The digitizing option is the “open” **3shape** extraoral scanner (Figure 7). **Sirona infiniDent** uses the similar SLM approach. Because of the high price of the

laser sintering machines, they are rarely seen in in-office dental applications (such as CEREC). The pragmatic approach taken by both companies is to centralize the production of the restorations while leaving data capturing and CAD issues to the dentists.

Evolution 4D CAD/CAM system uses intraoral laser stripe scanning system for data capturing. The E4D milling system is a double tool with a tool magazine. This complete system is still in development stage.

4. FUTURE TRENDS AND CHALLENGES

As already mentioned in the article, there are several directions to develop CAD/CAM systems in dentistry. One of them is further integration of the CAD/CAM system, including intraoral digitization phase, design phase and manufacturing phase in the dental office. With doing so, a single-visit treatment approach is made available. While this approach has advantages of shorter treatment and patients convenience, it has drawbacks in terms of skills required for its deployment (dentists should have additional training in CAD/CAM) and the price of investment and maintenance. This approach implies further improvements of intraoral scanners (which are less accurate than their extraoral counterparts). Higher automation and simplification CAD user interface may lead to an integration of virtual articulators, which would facilitate automatic design of the occlusal surface.

Because of these limitations, centralized approach has been introduced. By using this alternative approach, only digital equipment needed in dental office is a digitizer. The digitized result is sent from the office electronically and final physical restoration is being received after fabrication in centralized manufacturing center. This business model is being used in both CNC milling and SLM manufacturing approaches.

An introduction of industrial CT digitization of cast models is likely, because it has already been used in orthodontic applications (Invisalign [17]). Utilization of medical CT technology can also be an interesting development since the optical scanning or impression taking techniques can't capture sub gingival structures.

Another opportunity could also be in improving of the accuracy of the restoration, tackling errors being made in digitization, design and fabrication stage. This may enable, e. g., fabrication of thicker and more durable restorations while retaining the same preparation depth and decreasing the cement space.

5. CONCLUSION

The application of dental CAD/CAM is promising not only in the fields of dental prosthetics, but also in other fields of dentistry. The available CAD/CAM systems have been contributing to improvement of patient's quality of life. Emerging technologies and further engineering developments will expand capabilities of future systems and also may lead to less required training for their use in full capacity.

The automated CAD/CAM concept taken from the industrial metalworking may completely substitute the traditional manually intensive wax based method.

ACKNOWLEDGEMENT

Results of investigation presented in this paper are part of the research realised in the framework of the project "Research and development of modelling methods and approaches in manufacturing of dental recoveries with the application of modern technologies and computer aided systems" – TR 035020, financed by the Ministry of Science and Technological Development of the Republic of Serbia.

REFERENCES

- [1] Kuric, I.; Košturiak, J.; Janač, A.; Peterka, J.; Marcinčin, J.: Počítačom podporovane sistemi v strojarstve, Knižna publikacija, Univerzitet u Žilini, 2002.
- [2] Mormann, W.: The evolution of the CEREC system, The Journal of the American Dental Association, Am Dental Assoc, Vol. 137(1), pp.7S, 2006
- [3] Miyazaki, T., Hotta, Y., Kunii, J., Kuriyama, S. & Tamaki, Y.: A review of dental CAD/CAM: current status and future perspectives from 20 years of experience, Dental materials journal, Vol. 28(1), pp. 44-56, 2009
- [4] Budak, I., Trifković, B., Puškar, T., Hadžistević, M., Vukelić, DJ., Hodolič, J.: Application and accuracy of 3D-digitization systems in the field of dentistry., 6th International Working Conference "TOTAL QUALITY MANAGEMENT - ADVANCED AND INTELLIGENT APPROACHES", Belgrade, 2011.
- [5] Strub, J.R., Rekow, E.D. & Witkowski, S.: Computer-aided design and fabrication of dental restorations: Current systems and future possibilities, The Journal of the American Dental Association, , Vol. 137(9), pp. 1289-12962006
- [6] Rudolph, H., Quaas, S. & Luthardt, R.: CAD/CAM--Neue Technologien und Ent-wicklungen in Zahnmedizin und Zahntechnik, Deutsche Zahn\ärztliche Zeitschrift, , Vol. 58, pp. 10, 2003
- [7] Beuer, F., Naumann, M., Gernet, W. & Sorensen, J.: Precision of fit: zirconia three-unit fixed dental prostheses, Clinical Oral Investigations, Springer Berlin / Heidelberg, , Vol. 13, pp. 343-349, 2009
- [8] Matsuda, Y.; Doumoto, T.; Ebihara, Y.; GC Corporation Patent no EP 1895471: Program to make of cutting data for inner face of dental prosthesis, 2008
- [9] DELCAM dental CAD/CAM system : <http://www.dental-cadcam.com/>
- [10] Luthardt, R.; Sandkuhl, O. & Reitz, B.: Zirconia-TZP and alumina--advanced technologies for the manufacturing of single crowns. The European journal of prosthodontics and restorative dentistry, 1999
- [11] Plančak, M., Puškar, T., Lužanin, O., Marković, D., Skakun, P., Movrin, D.: Some aspects of rapid prototyping applications in medicine, 34th International conference on production engineering, Faculty of Mechanical Engineering, Nis, 2011.
- [12] Sirona CEREC system: <http://sirona.com/>
- [13] 3M Lava system: <http://www.3m.com/>
- [14] 3shape system: <http://www.3shape.com/>
- [15] BEGO Medifactory solution: <http://www.bego-medical.de/>
- [16] Evolution 4D system: <http://www.e4dsky.com>
- [17] Invisalign orthodontics: <http://www.invisalign.com>



COMBINED REGISTRATION OF HUMAN MUSCULOSKELETAL SYSTEM

Goran DEVEDŽIĆ¹, Saša ČUKOVIĆ¹, Branko RISTIĆ², Suzana PETROVIĆ¹, Michele FIORENTINO³, Tanja LUKOVIĆ²

¹Faculty of Mechanical Engineering, Sestre Janjić 6, Kragujevac, Serbia

²Faculty of Medicine, Svetozara Markovića 69, Kragujevac, Serbia

³Polytechnic of Bari, Department of Mechanical and Management Engineering, Viale Japigia 182, Bari, Italy

devedzic@kg.ac.rs, cukovic@kg.ac.rs, branko.ristic@gmail.com, suzana.petrovic@mfgk.rs,

fiorentino@poliba.it, tanjalukovic_kg@yahoo.com

Abstract: The need for accurate shape measurement and modeling of human musculoskeletal system appears to be important for both, clinical practice and incorporating emerging technologies to orthopedic and rehabilitation devices and systems. Particularly important emphasis is set on non-invasive, i.e. radiation-free approaches. The contemporary optical and probe-based measurement systems, together with 3D modeling and computer graphics techniques, provide the key platform for methodology development. We present the generic algorithm for reconstruction of patient's back surface from clouds of points in the case of female spinal deformities. Basic registration methods that enable comparative analysis before and after applied therapy are described too. The key benefits of the global and local 3D registration methodology are shown through the matching analysis of the reconstructed surfaces and illustrated by the sample case study of spinal deformity diagnostics.

Key words: Complex shape registration, clouds of points, global and local registration, spinal deformity diagnostics

1. INTRODUCTION

Combined registration of a 2D/3D shapes is critical to various medical imaging modalities and clinical applications. There are numerous shape alignment methods which are proposed to address global and local registration and combination. Also, the registration problems can be under constrained, especially in the case of non-rigid or deformable registration when reliable correspondence is needed in order to determine the local deformation parameters of contours or surfaces [1, 4]. Global registration method is also known as shape alignment. It aims to realize a global transformation that has source image or shape as close as possible to a target one by optimization algorithm (Fig.1) [2, 5].

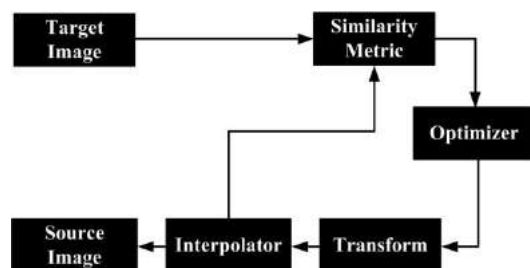


Fig.1. Main components of a 2D/3D image registration framework (adapted from [5]).

Methods of a rigid or non-rigid 2D and 3D registration of pre- and intra- interventional data sets are one of the key technologies for image guided therapies and minimally invasive surgery procedures [3].

Furthermore, non-rigid local registration of the object of interest is needed to achieve appropriate correspondences over the basic deformable elements of shapes, such as points, curves, etc.

2. MEDICAL IMAGING MODALITIES

Modeling of anatomical structures (bones and soft tissues) is a critical component of 3D medical image analysis process. Precise and compact representation that can describe the variation in an anatomical structure of interest across individuals requires establishing local and global correspondences across a set of scans (2D slices). Contemporary medical imaging modalities employ noninvasive methods to retrieve images from inside the human body for diagnosis, to study of normal and abnormal anatomy, and plan therapeutic procedures. Most of these methods involve exposing the patients to harmful ionizing radiation, since the properties of internal structures are inferred from the observed X-rays [3, 5]. The most common types of medical image modalities are:

- Computed Tomography (CT),
- Single Photon Emission Computed Tomography (SPECT),
- Positron Emission Tomography (PET),
- Magnetic Resonance Imaging (MRI),
- Ultrasonography Methods (US).

These modalities record valuable information about the patient's state and they are part of standard daily diagnostic procedures for many fields of medicine. In this paper we present noninvasive optical diagnostic method

for patients with scoliosis deformities and introduce methods for 3D registrations.

3. 3D RECONSTRUCTION AND ANALYSIS OF PATIENT'S BACK SURFACE

3.1. 3D reconstruction

In order to create 3D CAD anatomical model of spinal deformities, patients' back surfaces are digitalized using optical 3D measurement system FORMETRIC 3D/4D (Diers, Germany). This optical system is based on the spatial triangulation and rasterstereography principle. As a result of surface scanning, clouds of points, which fully represent deformed shapes, are generated.

Using adequate reverse engineering software (Raindrop Geomagic Studio) and reconstruction algorithms for free form modeling, we have created 3D surfaces (Fig.2). The reconstruction process goes through the following characteristic phases: (a) Acquisition of clouds of points, (b) Generation of a polygonal model, (c) Grid and NURBS (Non-Uniform Rational B-Spline) surface model fitting [7, 8].

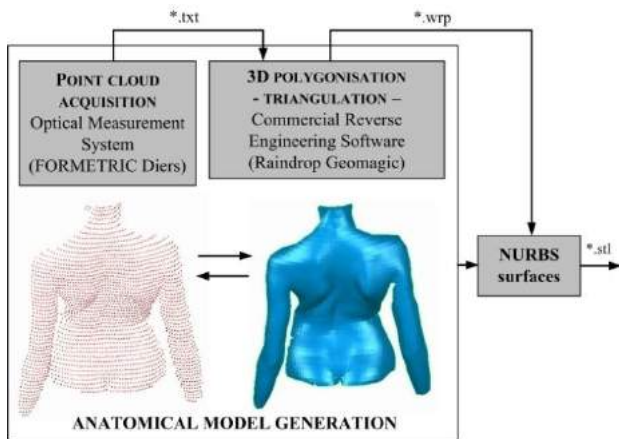


Fig.2. 3D reconstruction of the back shape from clouds of points

3.2. Shape analysis

The aim of the back shape analysis is to obtain relevant parameters of deformities from the reconstructed shape and to relate them to other findings, e.g. x-rays. When the recording and reconstruction are complete, the results are initially available as three-dimensional coordinates (x, y, z) for all the measured clouds of points [6]. There are several reasons why this representation is unsuitable for a direct interpretation and relation:

- The coordinate values are dependent on the random position of the patient relative to the recording system,
- The measurement points are distributed more or less irregularly over the surface of the skin,
- In contrast to the technical objects, the surface of the body has an irregular and variable shape.

The advent of rasterstereography methods, based on Moiré topography and common mathematical principles of surface analysis (e.g. Gaussian curvature distribution), opened a new field in medical diagnosis, which aim

specifically lay in the three-dimensional recording of trunk deformity (Fig.3).

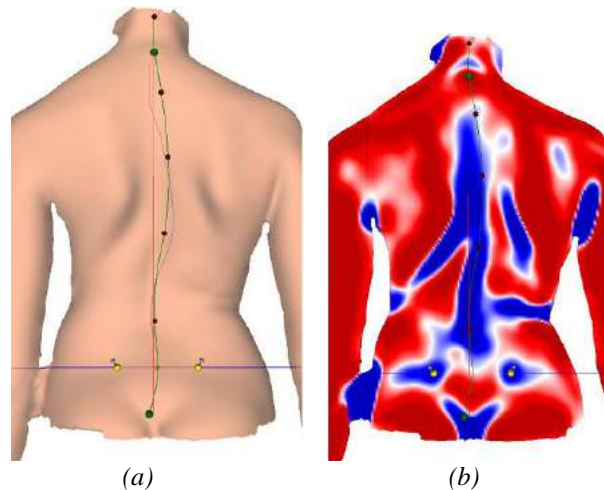


Fig.3. Reconstructed shape: (a) 3D cloud of points of the back shape, (b) medial spinal line created by Gaussian method

In a healthy state the central spinal line has a two-dimensional shape, which is modified into a three-dimensional through vertebral rotations and lateral deviations of the vertebrae, with trunk and back shape asymmetry [9] (Fig.4).

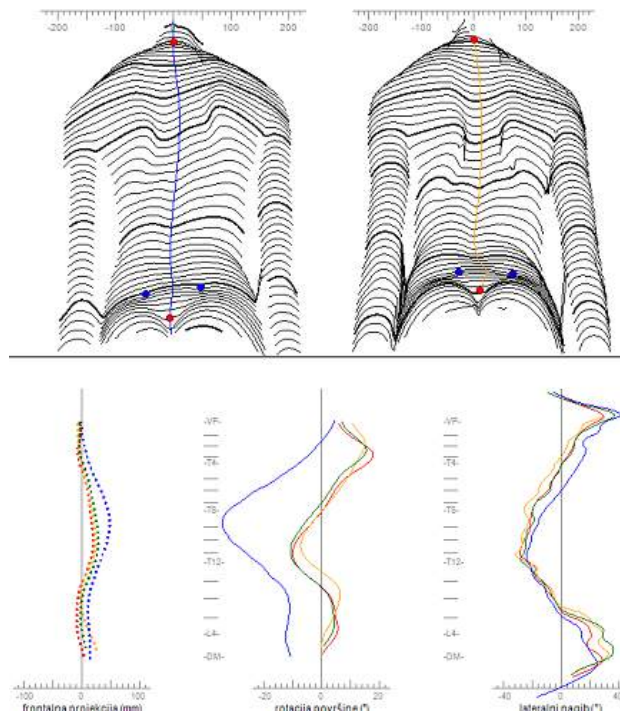


Fig.4. 3D analysis of back shape before and after applied kinesitherapy

In case of spinal deformities, rotational movements of the spinal segments are different from normal range of motion. Such abnormal rotations cause spinal deformity (kyphosis, lordosis and scoliosis) or a combination of these deformities. It is thus desirable to measure and confirm such three-dimensional pathological deformities objectively. Until recently this has been possible only by

using supplementary two-dimensional methods (x-rays films on two planes) [9].

4. 3D SURFACE REGISTRATION

4.1. Registration Framework

In a typical image registration framework, it is necessary to define the source images (point clouds as well as polygonal surfaces) as $f(x)$ and the target images as $g(x)$, where x is a current position in n -dimensional space. By considering the registration process as an optimization problem in medical imaging, main task is to find the optimal transformation function, defined as $t(x)$, which matches the source image to the target image.

A similarity indicator is used to measure how well the transformed source image $t(f(x))$ aligns to the target image $g(x)$. Since most medical images have different sizes in discrete pixel space, as well as in the level of voxels, all computation which is performed in continuous space requires some interpolation [5].

4.2. 3D surface shape registrations

There are innovative tools for registering and merging multiple unaligned clouds of points or polygonal models using a variety of automatic and semi-automatic methods. Surface registration allows easy steps to create a single polygonal model from unaligned scans. It is necessary to perform global, tolerance based alignment to minimize deviation between scans [1, 5, 10]. In the case of spinal deformities, we performed global and local registrations over two polygonal models of back surface of one female patient to determine progress or stagnation of the scoliosis deformity. Second optical scanning is done two months later in the same condition. Figure 5 shows overlay of globally transformed source shape on the target shape.

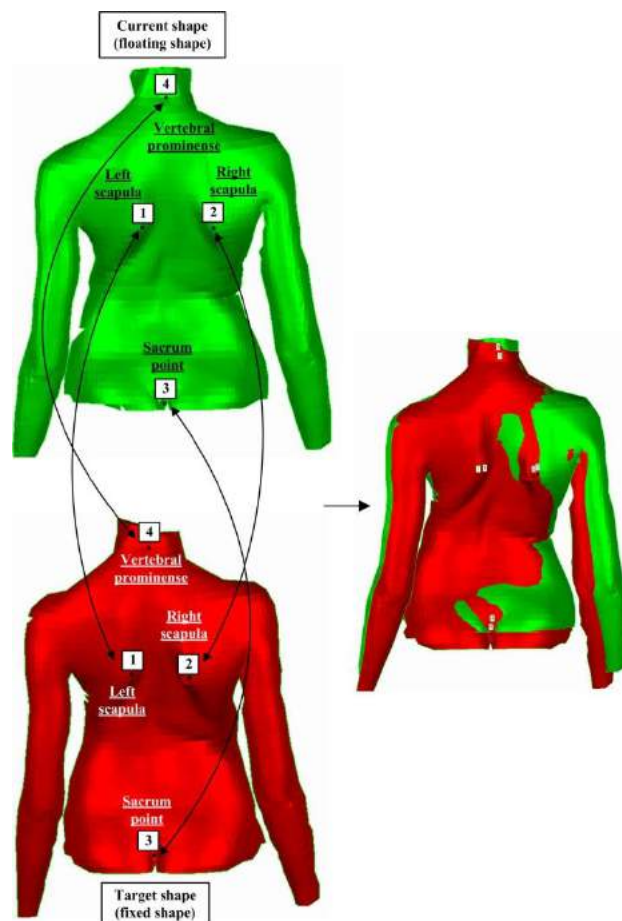


Fig.5. Global registration using the similarity transformation model

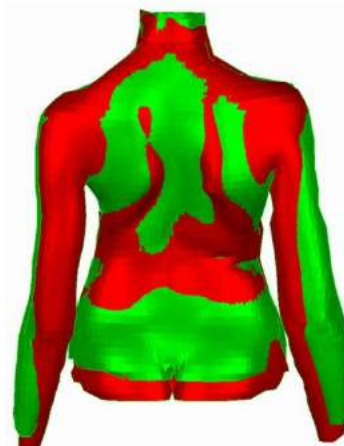
Registration methods have ability to align and merge point data that is tremendous advantage and allows

compatibility with any scanner, digitizer or medical image modalities.

Manual registration is done by selecting local anatomical landmarks on target and current shapes (n -points registration). In this case we use vertebral prominences and sacrum points, as well as points on left and right patient's scapula.



(a)



(b)

Fig.6. Local registration for 3D polygonal back shape scan data (source and target shapes) using 4 anatomical reference points (a) matching (b) registration

¹ Goran Devedžić, PhD, Faculty of Mechanical Engineering, Sestre Janjić 6, Kragujevac, devedzic@kg.ac.rs

² Saša Ćuković, PhD candidate, Faculty of Mechanical Engineering, Sestre Janjić 6, Kragujevac, cukovic@kg.ac.rs

³ Branko Ristić, PhD, Faculty of Medicine, Svetozara Markovića 69, Kragujevac, branko.ristic@gmail.com

⁴ Suzana Petrović, PhD student, Faculty of Mechanical Engineering, S. Janjić 6, Kragujevac, suzana.petrovic@mfgk.rs

⁵ Michele Fiorentino, PhD, Polytechnic of Bari, Viale Japigia 182, Bari, Italy, fiorentino@poliba.it

⁶ Tanja Luković, PhD, Faculty of Medicine, Svetozara Markovića 69, Kragujevac, tanjalukovic_kg@yahoo.com

Figure 6 shows that locally deformed source shape after registration overlay on the target establishing point-by-point correspondence between the source and target shapes. The registration process is finished when one of the main conditions is satisfied [10]:

1. The desired tolerance is achieved,
2. The number of maximum iterations is performed,
3. A specified number of iterations are run without convergence.

One of the most important applications of 3D surface registration is for matching a cloud of points acquired at one time-point during a treatment to another one from a different time-point. 2D registration procedures are known as intra-patient registration, which is often used to monitor progress during treatment of non-visible structures. Matching set of images or clouds of points from different patients can be used for generating a model of motion across a population of patients, or to match an image to a PACS atlas. In the case of spinal deformities, registration can be significant to show possible postures and shapes of patients' back.

Having in mind that image registration is the process of transforming different images into a single coordinate space, the data obtained from the different image modalities can be compared by pixel-to-pixel or a voxel-to-voxel level. The most important features to address global registration are:

1. Rigidity (shape translation and rotation),
2. Similarity (shape translation, rotation, and isotropic scaling),
3. Affinity (shape translation, rotation, isotropic or anisotropic scaling, shearing).

Surface registration frameworks feature the choice of best transformation between two anatomical surfaces of the same object and involve spatially transforming the source image to accurately align with the target image. Registration can be performed as a single operation between images from a single-modality or from multiple modalities. The voxel-based registration algorithms have been utilized mostly for the registration of soft tissues images from various medical modalities based on 2D slices.

5. CONCLUSION

Several techniques have been proposed for automatic medical image registration. In this paper we demonstrate a complete application for main types of registration between optical scans of back surfaces. The results demonstrate superior performance compared to surface-based or landmark-based deformable registration methods. We firstly apply global registration to align polygonal model to target one in order to compare progress of deformity. Local registration based on free-form deformations demonstrates non-rigidity of surface registration over common anatomical landmarks. We used single-modality registration method which tends to register optical scans acquired by the same scanner. Further development of the methodology is directed to the

multi-modality registration that processes images acquired by different scanners (sensors).

ACKNOWLEDGMENT

The research is supported by the Serbian Ministry of Science and Technology under the grant of III-41007: "Application of Biomedical Engineering in Preclinical and Clinical Practice".

REFERENCES

- [1] Simon Flöry, Michael Hofer: "Surface Fitting and Registration of Point Clouds Using Approximations of the Unsigned Distance Function", *Journal of Computer Aided Geometric Design*, Vol.27, pp.60-77, 2010.
- [2] Yunbao Huang, Xiaoping Qian, Shiliang: "Multi-Sensor Calibration Through Iterative Registration and Fusion", *Journal of Computer-Aided design*, Vol.41, pp.240-255, 2009.
- [3] Said Benameur, Max Mignotte, Stefan Parent, Hubert Labelle, Wafa Skalli, Jacques de Guise: "3D/2D Registration and Segmentation of Scoliotic Vertebrae Using Statistical Models", *Journal of Computerized Medical Imaging and Graphics*, Vol.27, pp. 321-337, 2003.
- [4] Zhi-Quan Cheng, Wei Jiang, Gang Dang, Martin, R.R., Jun Li, Honghua Li, Yin Chen, Yanzhen Wang, Bao Li, Kai Xu, Shiyao Jin: "Non-rigid Registration in 3D Implicit Vector Space", *Proceeding of IEEE International Conference on Shape Modeling and Applications (SMI)*, pp. 37-46, ISBN: 978-1-4244-7259-8, 2010.
- [5] Ayman El-Baz, Rajendra Acharya U., Andrew F. Laine, Jasjit S. Suri: "*Multi Modality State-of-the-Art Medical Image Segmentation and Registration Methodologies*", Volume II, Springer, ISBN 978-1-4419-8203-2, 2011.
- [6] M. D'Amico, A. Merolli, G.C. Santambrogio: "*Three dimensional Analysis of Spinal Deformities*", *Proceedings of the 8th Symposium on Surface Topology and Spinal Deformity*, IOS Press, ISBN 90-5199-181-9, 1995.
- [7] Devedzic G., Ristic B., Stefanovic M., Cukovic S., Lukovic T.: "Development of 3D Parametric Model of Human Spine and Simulator for Biomedical Engineering Education and Scoliosis Screening", *Journal of Computer Applications in Engineering Education*, Vol. 19, DOI: 10.1002/cae.20411, 2010.
- [8] Cukovic S., Devedzic G., Ivanovic L., Lukovic T., Subburaj K.: "Development Of 3D Kinematic Model of the Spine for Idiopathic Scoliosis Simulation", *Journal of Computer Aided Design and Applications*, Vol. 7, No.1, pp.153-161, DOI: 10.3722/cadaps.2010.153-161, ISSN 1686-4360, 2010.
- [9] DiCAM Diers Manuals, www.diers.de.
- [10] Raindrop Geomagic Studio, www.geomagic.com.



OPTIMIZATION OF CAD/CAM/CAE DESIGN OF THE CONNECTING PART OF EXCAVATOR'S TOOTH THROUGH THE SIMULATION OF MANUFACTURING TECHNOLOGY

Radomir SLAVKOVIC¹, Zvonimir JUGOVIC¹, Ivan MILICEVIC¹, Marko POPOVIC¹, Radomir RADIŠA²

¹Technical Faculty Cacak, University of Kragujevac, Svetog Save 65, Cacak, Serbia

²Lola Institute, Kneza Višeslava 75a, Belgrade, Serbia

slavkovic@tfc.kg.ac.rs, zvonko@tfc.kg.ac.rs, ivanmil@tfc.kg.ac.rs, marko@tfc.kg.ac.rs, radomir.radisa@li.rs

Abstract: Simulation of the casting process of dynamically loaded drip moulding in engineering is widely accepted as technological activity in almost all world foundries in recent years. This methodology significantly reduces the time of the products manufacturing, in relation to traditional methods of testing the prototypic product. However, reliability of simulation results imposes a good knowledge of both technical and technological parameters and boundary conditions of simulation application. This paper presents an example of the application of MAGMASoft software system for simulation of casting process of split tooth connecting part of the excavator of continuous action in open pit "Kolubara".

Key words: casting, designing, final elements, simulation, software

1. INTRODUCTION

The most important changes in the field of drip moulding construction have emerged by introduction of **CAD** (Computer Aided Design) technologies. New current computer technologies, such as simulation of the development process of **CAM** (Computer Aided Manufacturing), computer optimization of drip moulding's construction and optimization of casting process **CAE** (Computer Aided Engineering) have significantly improved casting environment. With the products obtained by casting, there are constant requirements for the reduction of price, increase of quality and performances, i.e. requirements for their optimal construction. Optimal form of drip moulding with walls that have required thickness and appropriate mechanical characteristics that will meet necessary loads and stresses must be predicted in the phase of drip moulding construction as a product. These requirements can only be met by applying an integrated **CAD/CAM/CAE** approach in the development of the product. In many cases of construction optimization, the aim is to save materials, minimize the mass, maximize the allowed load, even distribution of stress, optimization of rigidity and dynamic behaviour during the vibration of machine systems.

2. CAD/CAE DESIGNING

By the analysis of the conditions of exploitation and wear of the mentioned tooth (fig.1), maximum wear of the cutting part to 30% of total mass of the tooth was observed. As cost-effectiveness in production is an important factor of all studies (coal production, in this case), having in mind the geometry of cutting tooth, the goal of designing is to develop split tooth whose cutting

part is changed after the wear, and the connecting part is reusable. In addition, through technical and technological parameters of the cutting part of tooth, we can influence its operating characteristics (wear resistance, toughness, hardness, dynamic solidity etc.) that can be adapted to the conditions of working environment and thus, significant reduction of the costs of coal mining.



Figure 1 Split tooth and working wheel of rotary excavator

Construction of cutting and connecting part of split tooth fig. 1 is done in **SolidWorks** that implies **3D CAD** software with an integrated package of programmes that have solutions offered for a series of industries. SolidWorks includes advanced tools for defining complex geometry and surfaces, creating alternative solutions for family products and simulating working conditions, which enables the realization of highly complex products. In addition, it contains an integrated software model for calculations by finite elements method (**FEM- Metod**). The paper presents an example of identification of the solidity of cutting and connecting part of the split tooth modelled by finite elements in trihedral shape by applying

COSMOSWorks. Stresses and changes of stresses are the main cause of the fatigue of material structure of cutting teeth, their deformation, formation of cracks and fractures. Intensities of stresses and their distribution are exceptionally significant for development and analysis of the state and working ability of cutting teeth. By applying integrated approach, simultaneous analysis is provided, which has a goal to generate the shape of cutting tooth and its dimensions, and based on the analysis of results obtained about size and distribution of stress. In that way, it is possible to perform adequate changes on virtual model very rapidly and optimize the shape and dimensions, until optimal distribution and size of stress and deformation is achieved. In Figure 2, there is one of the analyses that are done for the purpose of developing modular cutting tooth TF14038 for rotary excavator.

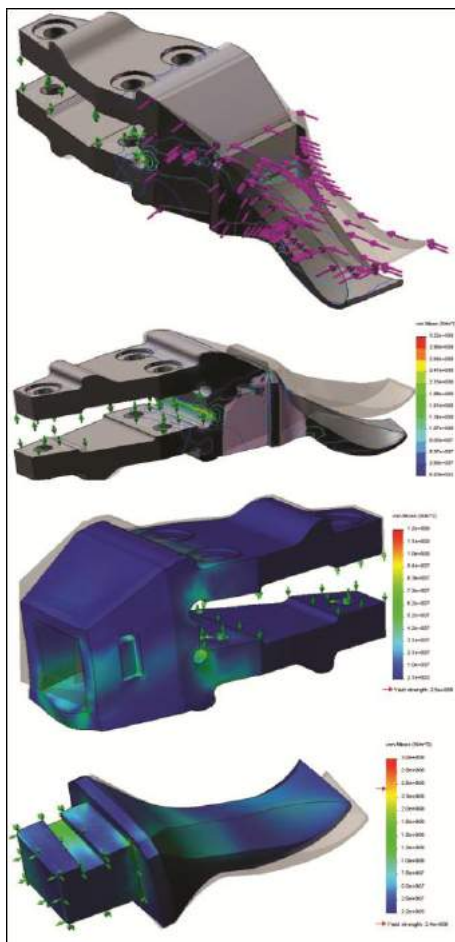


Figure 2 Stress analysis of split tooth

3. CAD/CAM CASTING SIMULATION

3.1. Basic CAD elements of casting process

For the simulation of casting process by applying MAGMASoft [3],[6], it is necessary to do 3D CAD model of all elements of the mould cavity that is filled by liquid metal, i.e. pouring system (pouring basin, sprue, collector, distributor and ingates), risers and dischargers of gases. Correctly constructed pouring system should provide for liquid metal to flow into moulding cavity rapidly and without any turbulence. Turbulent flow can cause entrance of gases, air and slag into the moulding, which is

the main cause of defect drip moulding's appearance. In addition, we should provide the entering of non-metal inclusions in the moulding, provide the extraction of gases from moulding cavity and ensure a rapid enough filling of moulding cavity. Volume shrinkage of liquid metal during cooling causes the reduction of drip moulding's volume. This effect causes the creation of shrinkage porosity (cavities) in places that solidify the rear ones. In such cases, riser with main function to provide enough liquid metal are designed for the most massive sections of drip moulding, which provides solidification without shrinkage porosities. Place of the riser is determined empirically. For optimal cooling, it is necessary to provide the inflow of liquid metal on the basis of "directed solidification", from thinner to more massive parts of drip moulding. Risers are set on the top or at the side of the drip moulding, so that the last part of liquid metal should solidify in risers themselves. Place of the riser is mostly limited by the shape of drip moulding (its most massive part). Dischargers of gases prevent the creation of air pockets in moulding cavity and they are set at appropriate places to vent them. They are always set at the highest places of drip moulding. Places of air pockets' appearance are defined on the basis of the analysis of liquid metal flow through moulding cavity. Figure 3 shows basic elements of the usual pouring system for one drip moulding.

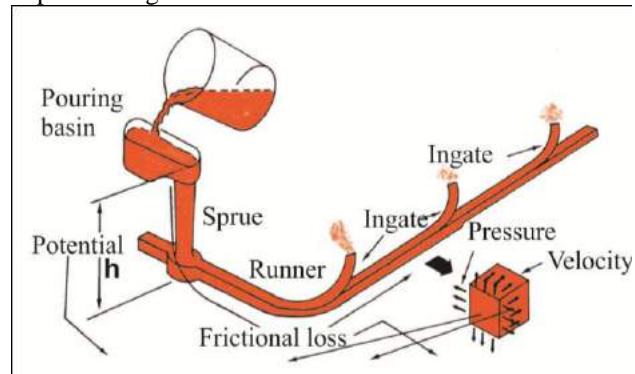


Figure 3 The usual basic elements of pouring system

Calculation of the elements of pouring system is based on laws on fluid flow and application of Bernoulli equation:

$$mh + mpv + (mV^2) / 2g + mF = C \quad (1)$$

where: mh - Potential head, mpv - Pressure head, $(mV^2) / 2g$ - Velocity head, mF - Friction loss of head, C - Constant.

3.2. Basic CAD elements on the example of cutting part of continuous action excavator teeth

Split teeth [7] are connected by cutting part to the bucket of working wheel that performs the excavation in certain time intervals, by cutting tops. As a consequence of periodical entrance of teeth into the digging grab, cutting and connecting elements of teeth are exposed to significant dynamic loads. In mentioned conditions of exploitation, both of connecting and cutting elements, the possibility of appearance of internal voids (cavities), which are rather sensitive to stress concentration and often are the cause of fracture, must be eliminated. In

such cases, it is very important, prior to developing the tools necessary for shaping the mould, to perform the simulation of casting process, i.e. perform virtual casting process, based on which a wide range of technical and technological characteristics of drip moulding can be tested. Fig.4 presents *CAD* model [4] of the system drip moulding, pouring system and riser for the simulation of casting of the connecting part, by *MAGMASoft* software system.

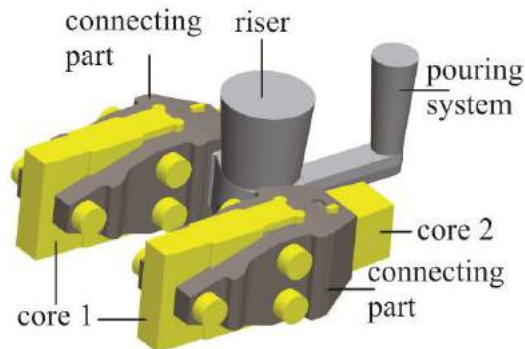


Figure 4 CAD model of the system connecting element, pouring system, riser with cores

MAGMASoft software system is a computer tool that enables the simulation of casting and solidification of drip moulding. That is a very powerful and reliable simulation software used when studying parameters of improvement and optimization of casting process. It provides a rapid and efficient testing of a series of possibilities and alternatives within the limits of casting process and selection of optimal combination of technological parameters. Potential problems are easily discovered and eliminated in the phase of designing the shape of drip moulding, which allows the designer/technologist to optimize the casting process. Simulation results are shown in 3D graphical environment, where, by X-ray view into the mould, we can see the process of filling the mould cavity, velocity of filling the mould, as well as temperature field. With cross-sections of drip moulding, we get the front of solidification and possible places of porosity due to metal solidification. The input data necessary for simulation are: 3D geometric model of drip moulding and other components (pouring system, riser, filter, bench etc.), parameters of casting technology (starting temperature of casting, mould material, coating type, drip moulding material, type of foundry ladle – tilt/with a stopper) etc. *MAGMApre* module uses 3D models in standard graphical formats (*STL* or *STEP*). After processing the casting, recommendations and conclusions are given. Based on them, new simulations with changed parameters are performed when necessary. In addition, when observing the results of simulation, the pictures of critical and interesting ideas, necessary to the user of simulation results, are done.

4. RESULTS OF CASTING SIMULATION OF SPLIT TOOTH'S CONECTING PART

For conceptual solution of two drip mouldings in one mould, fig. 4, and based on theoretical assumptions given

in [1],[2], as well as having in mind symmetrical arrangement of drip mouldings in relation to the axis of casting, it is predicted that the riser should be above the pouring system, fig. 4. Material for drip moulding is C0545, mould and cores are obtained by CO₂ procedure and protected by zirconium coating. Casting is gravitational from tilt foundry ladle. Group *FILLING* of software package *MagmaSoft* has many modules, among which there are: module "*Fill Press*" for showing the arrangement of pressure in metal during the casting, module "*Fill Velo*" for showing the velocity of metals during the casting and module "*Fill Temp*" for showing the change of temperature during the casting. In figure 5, the time of filling the moulds is shown t(s). Simulation shows in which moment the elements of mould cavity are filled.



Figure 5 Time of filling the mould

In Figure 6, the velocity of filling the moulds v (cm/s) with 35% of mould impletion is given. This simulation gives the possibility of the flow of liquid metal in particular moments of mould impletion.

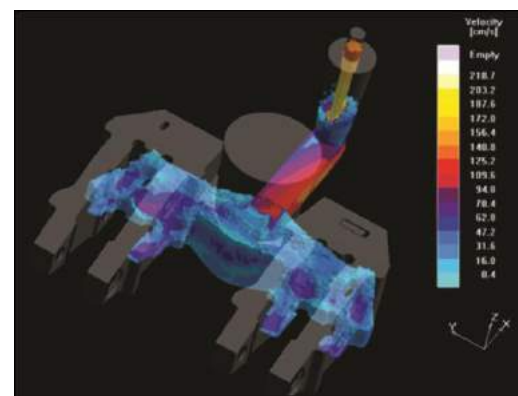


Figure 6 Velocity of filling the mould

Module *SOLIDIFICATION* is used for showing the results of solidification with isotherms and temperature fields. Figure 7 shows the time of solidification of connecting parts of split tooth with shown temperature fields. This test provides the detection of critical spots in drip moulding, both in 3D overview of drip moulding and in the cross-sections by the requirement of technologist. The figure shows directed solidification, i.e. the riser is the last one to solidify, which prevents the cavities.

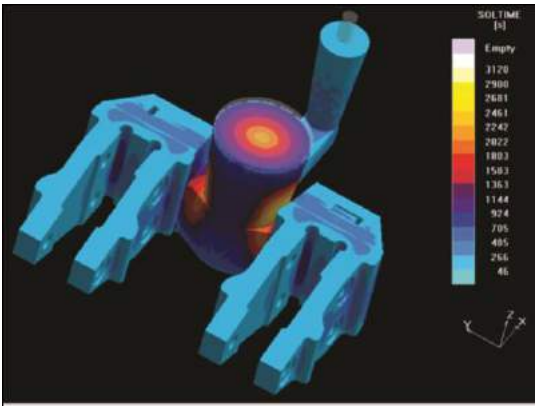


Figure 7 Time of solidification of metals in mould

Figure 8 shows hot spots in drip moulding that show the volumes of metals that are solidified in the end. In addition, the simulation shows the places at which cavities (blue places) may appear.

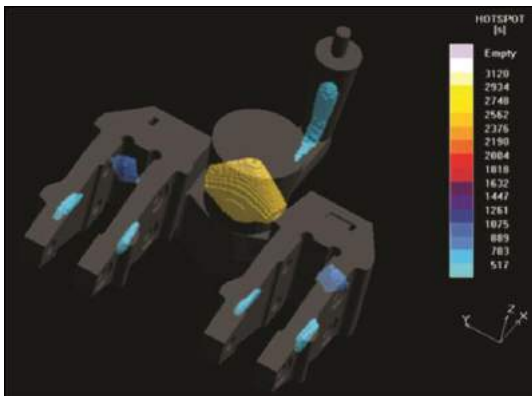


Figure 8 Hot spots in drip moulding with possible errors

Module **POROSITY** enables the analysis of porosity, cavities, as well as phase structure in drip moulding. Figure 9 shows a completely solidified drip moulding with two connecting parts of the tooth. The overview of simulation through cross-sections does not imply the possibility of porosity in drip moulding.



Figure 9. Porosity in drip moulding

5. CONCLUSION

Figures 7 and 9 show that, according to designed technology, connecting part has no porosity, and temperature fields are properly arranged, which is a precondition for good drip moulding. Figure 8 shows possible places of porosity, so the extension of additional risers with the reduction of cross-section of the existing riser is recommended. MAGMASoft package, within enormous database, includes many world experiences from the field of casting that are used for testing the technologies in foundries. Its use shortens the time of product development cycle. This, together with today's strict requirements of the market and with the lack of experienced staff in foundries, presents very important segment, both in winning new positions and optimization of the existing ones.

6. ACKNOWLEDGEMENTS

This paper is a result of the project with the serial number 35037, financed by the Ministry of Science and Technological Development. Concern "Farmakom M.B.", IKG – "Guca". Writing supported the paper.

REFERENCES

- [1] ASM INTERNATIONAL (2009), Casting design and performance, (Materials Park, Ohio).
- [2] BISHOP, H., TAZLOR, H & POWELL, R., Riser of Steel Castings with Exothermic Sleeves, Foundry, June 1958, 50-54
- [3] MAGMASoft, Manual Part One, www.MAGMASOFT.COM
- [4] LOMBARD, M.(2009), SolidWorks Surfacing and Complex Shape Modeling Bible, Wiley Publishing, Inc., (Indianapolis).
- [5] MARKOVIĆ, S., MATIJAŠEVIĆ, S., JOSIPOVIĆ, Ž & OCOKOLJIĆ, S. (1994), Collection of solved tasks in the metal casting process, (Faculty of Technology and Metallurgy, Belgrade).
- [6] STURM J. C, HANSEN P. N, HARTMANN G, & ACHIM E. W. (2002), (Magma Giebereitechnologie GmbH, Achen, Germany), Optimized Development for Castings and Casting Processes, World Foundry Congress, (Korea).
- [7] SLAVKOVIĆ, R., JUGOVIĆ, Z., MILIĆEVIĆ, I., POPOVIĆ, M. (2009), Design of cutting teeth of excavators using CAD/CAM/CAE technology, IMK „14. October“, Research and development, Year XI, No(32-33) -4/2009.



IDENTIFICATION OF FACE FUNCTIONALITY WITH PROGRAM SYSTEM FOR PURPOSE OF MODULAR FIXTURE DESIGN

Stevo BOROJEVIĆ, Vid JOVIŠEVIĆ, Gordana GLOBOČKI LAKIĆ, Đorđe ČIČA, Branislav SREDANOVIĆ
Faculty of Mechanical Engineering, University of Banjaluka, Stepe Stepanovića 75, Banjaluka, B&H
stevoborojevic@hotmail.com, vid.jovisevic@blic.net, globocki@blic.net, djordje@urc.rs.ba, sredanovic@gmail.com

Abstract: An automated programming system was developed in SolidWorks environment in order to design modular fixtures. This paper presents identification of face functionality for positioning and clamping purposes using production rules and specifically developed software tool. Verification of developed software system was carried out on a workpiece which is a subject of modular fixture design.
Key words: face functionality, API, application, SolidWorks

1. INTRODUCTION

In this paper, a software application for identification of planar face functionality of a 3D workpiece model was introduced. Developed application was integrated into the SolidWorks environment and it was part of the overall program system for automation of modular fixture design that has been developed at the Faculty of Mechanical Engineering in Banjaluka. Automating modular fixture design, one of the activities of the CAPP system, belongs to the class of knowledge that is hard to formalize and mathematically describe [5]. With application of production rules, SW tools and APIs in the SolidWorks software system [7] as well as integration with object-oriented programming, modeling, development and verification of application for identification of the face functionality using 3D workpiece model were executed. The identification of the face functionality was implemented for automation of positioning and clamping of the workpiece using modular fixture [6].

2. DEVELOPMENT OF SOFTWARE APPLICATION

A software application was developed within the SolidWorks software system (Fig. 1) using production rules, VB6 programming language and MS Excel. The basic structure [1] of developed application for identification of face functionality of the 3D workpiece model is shown in Fig. 2 and detail structure is shown at Fig. 3.



Fig. 1 User interface in the SW environment

Developed applications are primarily used for identification of planar face functionality of CAD models, i.e. face that have a constant normal vector different from (0,0,0).

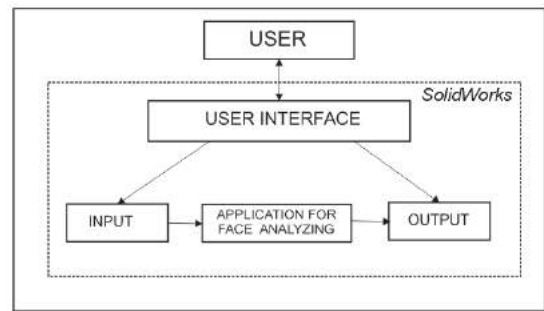


Fig. 2 The basic structure of developed application

The basic idea that is implemented through the application for identification of face functionality of the CAD model is based on an examination of configuration of the face from the point of occurrence of openings (holes) or new contours (boss) on it.

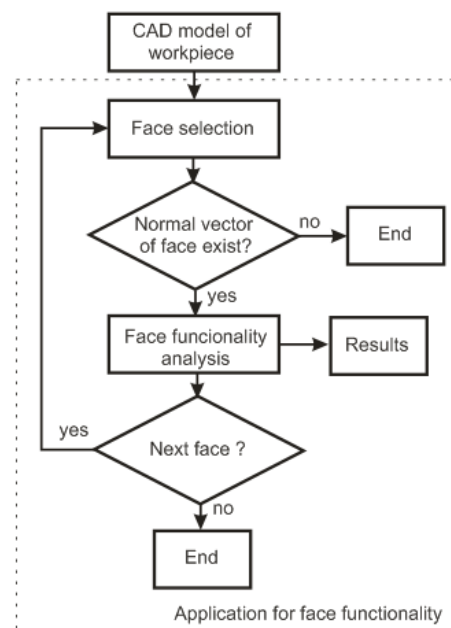


Fig. 3 The detail structure of developed application

Existence of such features prevents modular fixture component to be placed on observed face of the workpiece.

In developed application, according to Fig. 3, as first step is necessary to import CAD model of workpiece, than user execute selection of face at interactive manner. Developed application check does selected face has normal vector, if yes application calculate face functionality at automated manner, if no application stop the procedure of functioning. After calculation of face functionality, application generates results. If we need results for face functionality of another face, it is necessary to select desired face. After analyzing of faces functionality for import CAD model of workpiece, application ends its processes.

Mathematical apparatus upon which the application is based was presented in detail in [2], while the basic parameters that are necessary to understand functioning of the application are presented in this paper.

The software application for identification of face functionality provides output in the form of accessibility coefficient (AC - accessibility coefficient) for corresponding segment of the face in the form of a numeric value between 0 and 2. Calculation of accessibility coefficient (AC) consists of four coefficients i.e. [2]:

- The coefficient of the position of the test area in relation to the selected face - S_1 ;
- The obstruction coefficient of the test area - S_2 ;
- The coefficient of matching test area to the selected face in mm^2 - S_3 ;
- The coefficient of accessibility of neighboring points - PST which takes into account the result of the S_3 coefficient for all neighboring positions of the test area;

Calculation of accessibility coefficient for the observed face is done using relation (1):

$$AC = S_3 + PST \quad (1)$$

Depending on the position of the test area in comparison to the face of the CAD workpiece model, S_1 coefficient generates values for three respective cases, as shown in Fig. 4 [2]:

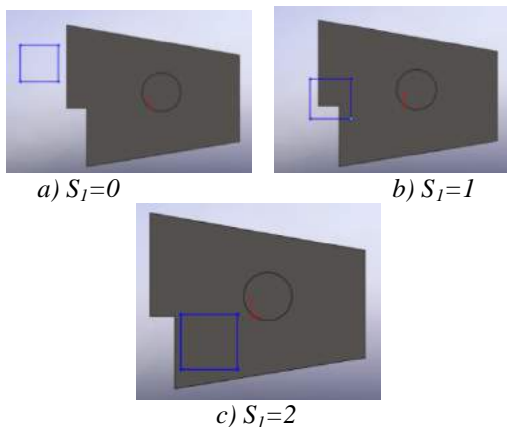


Fig. 4 Positions of the test area and limit values of the coefficient S_1

The coefficient of the test area position in relation to the selected face gives value $S_1 = 0$ when a position of the contour of the test area is outside the outer contour of the observed face (Fig. 4a). The value $S_1 = 1$ is generated when the contour of the test area intersects the contour of the observed face (Fig. 4b), and $S_1 = 2$ is generated when the whole contour of the test area is inside contours of the observed face of the CAD workpiece model (Fig. 4c).

Two boundary cases exist for the obstruction coefficient of the test area. The first case (Fig. 5a) is defined by a state when the test area is not obstructed from other faces, bodies or workpiece model. In this case, the obstruction coefficient obtains value $S_2 = 0$. Otherwise, when the test area is obstructed by the workpiece model/body, the obstruction coefficient is $S_2 = 1$ (Fig. 5b). Identification of obstruction for an observed face with respect to the test area is performed using SW tools Extrude and Interface detection.

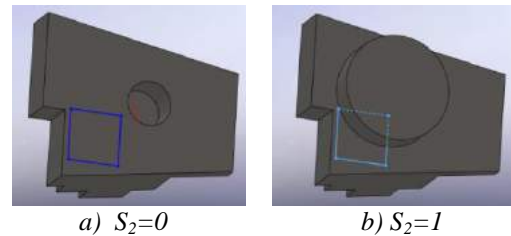


Fig. 5 Positions of the test area and the limit values of coefficient S_2

The coefficient of matching test area to the selected face in mm^2 - S_3 only exists in the case when the coefficients S_1 and S_2 have values $S_1 \neq 0$ and $S_2 = 0$. In this case, the calculation of coefficient S_3 is based on relation (2) [2]:

$$S_3 = \frac{POV}{T^2} \quad (2)$$

Where

POV is Value of test area which matches observed face
T is Length of the side of the test area

The case in which a coefficient of matching test area to the selected face exists is shown in Fig. 6 as a hatched area.

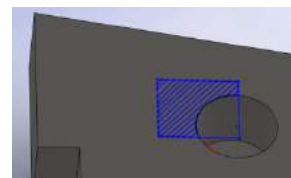


Fig. 6 The case when coefficient S_3 exists

In all other boundary cases, coefficient S_3 does not exist or it is equal to 0. It results in the fact that the respective position of the test area in comparison to the face of a CAD model is not available for placement of modular fixture component.

The coefficient of accessibility of neighboring points (PST) shows the state of accessibility of observed face in

the vicinity of respective point P_c (Fig. 7). The space around the point P_c is 3×3 test area which contains 8 points from P_1 to P_8 . After identification and calculation of coefficients S_1 , S_2 and S_3 , the coefficient of accessibility of neighboring points is calculated on the basis of relation (3):

$$PST(u, v) = \frac{1}{8} \sum_{i=1}^8 S_{3,i} \quad (3)$$

P_4 ○ ($u-1, v+1$)	P_3 ○ ($u, v+1$)	P_2 ○ ($u+1, v+1$)
P_5 ○ ($u-1, v$)	P_c ○ (u, v)	P_1 ○ ($u+1, v$)
P_6 ○ ($u-1, v-1$)	P_7 ○ ($u, v-1$)	P_8 ○ ($u+1, v-1$)

Fig. 7 3×3 area for calculation purpose of coeff. PST [2]

If the sum of all accessibility coefficients is higher, the observed face for positioning or clamping has greater facility for realization of automated process of positioning and clamping using modular fixture components.

Identification of face functionality for bottom positioning is carried out with a standard 50×50 mm test area. The reason for using this area lies in the fact that the contact area of modular fixture components for positioning, in most cases, can enter the selected test area.

The process of identification of face functionality for bottom positioning follows four characteristic steps [4] that are shown in Fig. 8. In the first stage, an analysis is performed with initial coordinates (0.0) corresponding to the initial position of the test area. In the second step, initial coordinates of the test area are moved into the position (0.25), then in the third step in (25.0), and in the last step in the position (25.25). The reason for introducing four steps of analysis lies in the fact that the application is developed for modular fixture with standard 50 mm distance between hole centers. Developed application can easily apply arbitrary distances.

After obtaining results for each of the four cases, further analysis for the evaluation of these cases was performed. The evaluation aiming to determine which one of the four cases generates greater value of face functionality is based on relation (4):

$$FC_u = \sum_{i=1}^n ACv_i \quad (4)$$

Where

FC_u is Functionality coefficient of the entire observed face

ACv_i are Accessibility coefficients whose values exceed 50% of the maximum value of AC for each of the points on the observed face.

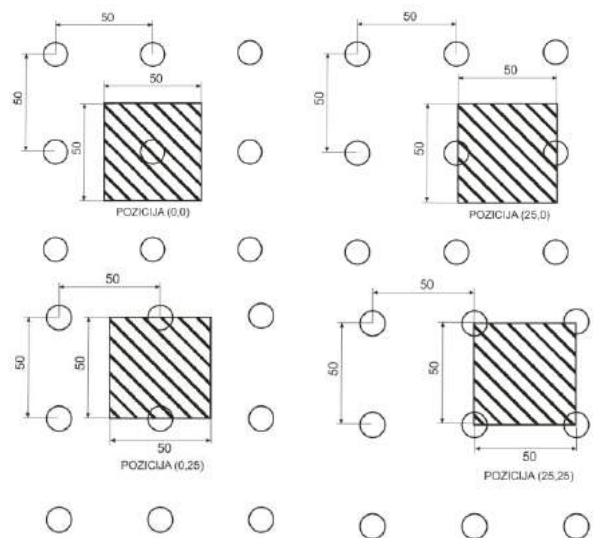


Fig. 8 Typical cases in the face analysis

The respective case where value for FC_u is maximal has been adopted as a case whose coordinates give the greatest chance for placement of modular fixture components on the observed face. In other words, the selected case means that for the corresponding coordinates of a workpiece moving relative to the starting position, functionality of the analyzed face has the highest value.

After executing functionality analysis of face(s) for bottom positioning and obtaining the analysis results, an algorithm for point selection is applied on selected points on the observed face. As algorithm output, selected points become points of contact with a modular fixture component for positioning.

An analysis of face functionality for side positioning and for clamping is done after points for bottom positioning have been selected and after the workpiece relative to a base plate of the modular fixture has been fixed.

Developed application for identification of face functionality allows the user to adjust and select the necessary distance and dimensions of the test area used for analyses of the selected face of the workpiece.

3. VERIFICATION OF DEVELOPED APPLICATION

Developed application for identification of planar face functionality of the CAD model was verified using the example of the workpiece shown in Fig. 9. In this case, the selected face of the CAD workpiece model is a face for bottom positioning.

Face selection, starting of developed applications and identification of face functionality are performed in an automated manner (Fig. 10). With further analysis of the selected face according to Table 1, "case no. 3" is chosen as the best functionality case with coordinates of displacement (0.25). For the selected case, the functionality coefficient for observed face has the highest value.

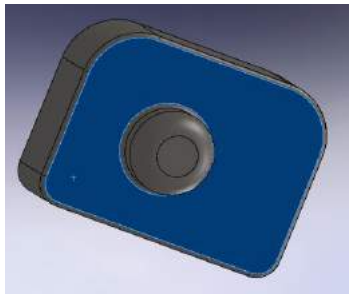


Fig. 9 A workpiece example

Table 2 shows the values of accessibility coefficients for “case 3” for each of the analyzed points. In Table 2, AC values are emphasized which have been included in further analysis for selection of specific points on the workpiece which are in contact with modular fixture components.

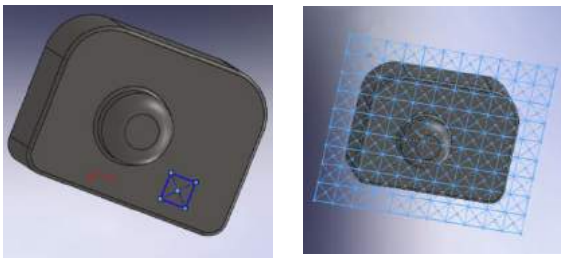


Fig.10 Details of the functionality analysis process

The analysis given in this paper has not covered how many points may be chosen depending on the model and standard schemes for positioning and clamping.

Table 1. Cases and values of FC_u for the observed face

No. of case	$FC_u = \sum_{i=1}^n ACv_i$	Coordinate of a moving workpiece
1.	26,293	(0,0)
2.	24,342	(25,0)
3.	27,876	(0,25)
4.	21,470	(25,25)

Table 2. Values of accessibility coefficients for case 3

PA	u									
	0.000	0.000	0.000	0.000	0.000	0.000	0.000	0.000	0.000	0.000
	0.000	0.000	0.256	0.525	0.582	0.583	0.583	0.566	0.363	0.000
	0.000	0.256	0.945	1.139	0.936	0.937	0.937	1.420	1.464	0.552
	0.000	0.525	0.743	0.722	0.250	0.250	0.750	1.245	1.789	1.025
v	0.000	0.582	0.790	0.250	0.000	0.000	0.250	1.250	1.836	1.082
	0.000	0.583	1.042	0.500	0.000	0.000	0.500	1.250	1.837	1.083
	0.000	0.510	1.310	0.446	0.446	0.446	0.446	1.587	1.688	0.788
	0.000	0.252	0.885	0.830	0.508	0.508	0.833	1.083	0.988	0.404
	0.000	0.000	0.000	0.000	0.000	0.000	0.000	0.000	0.000	0.000

Calculated results are also generated using MS Excel application in the form of a Table 2 and a diagram shown in Fig. 11.

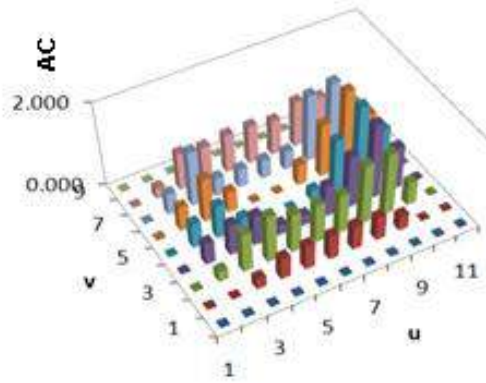


Fig. 11 Histogram of accessibility coefficients for case 3

4. CONCLUSION

Identification of planar face functionality using developed application generates results in the form of diagrams and tables. Based on the results, functionality of the observed face for the purpose of modular component positioning can be identified. The results can also be interpreted in a form of histogram of accessibility coefficients for each analyzed point. In this way, developed application gives mathematical record of face functionality for previously defined conditions and restrictions. The obtained results can be further analyzed and used for different purposes. Thus, contribution to the development of CAPP technology was given in the form of identification of planar face functionality of a CAD model for the purpose of automating modular fixture design.

5. REFERENCES

- [1] JOVIŠEVIĆ, V. (2002) *Automatizacija projektovanja tehnoloških procesa*, Mašinski fakultet Banjaluka.
- [2] RONG Y., ZHU Y. (1999) *Computer-Aided Fixture Design*, Marcel Dekker, New York.
- [3] AN Z., HUANG S., RONG Y., JAYARAM S., (1999) *Development of automated dedicated fixture configuration design systems with predefined fixture component types: Part 1, Basic design*, Int. J. of Flexible Automation and Integrated Manufacturing, Vol. 7. 168 - 176.
- [4] RONG Y., HUANG S. H., and HOU Z. (2004), *Advanced Computer-aided Fixture Design*, Elsevier Science & Technology.
- [5] SHOKRI M., AREZOO B. (2008), *Computer-aided CMM modular fixture configuration design* International Journal of Manufacturing Technology and Management, Volume 14, Number 1-2, 174 - 188
- [6] BOROJEVIĆ S. (2011), *Automatizacija projektovanja modularnih pomoćnih pribora*, Magistarski rad, Mašinski fakultet Banjaluka.
- [7] *SolidWorks program system*, Concord, Massachusetts, USA / Dassault Systèmes S.A. France



FEM IN VIRTUAL REALITY CONCEPT

Dragan MARINKOVIC^{1,2}, Manfred ZEHN¹

¹Institute of Mechanics, Berlin Institute of Technology, Strasse des 17. Juni, Berlin, Germany,

²Faculty of Mechanical Engineering, University of Nis, A. Medvedeva 14, Nis, Serbia

Dragan.Marinkovic@TU-Berlin.de, Manfred.Zehn@TU-Berlin.de

Abstract: Virtual reality (VR), as a novel technology, represents one of the most powerful tools to assist or even play the major role in many areas, such as development of new designs, training medical practitioners or assembly operators, entertaining industry, etc. On the other hand, the finite element method (FEM) imposed itself as an essential technical support for the needs of computing flexible bodies' deformational behavior. FEM together with CAD are important ingredients of VR. In the VR applications that imply interactive simulations with flexible bodies included, the efficiency of FEM formulations is of crucial importance. The paper presents features of some existing as well as some recently developed FEM formulations designed to meet this important requirement.

Key words: virtual reality, finite element method, interactive simulation

1. INTRODUCTION

In the last several decades, classical computer aided engineering (CAE) software packages have offered invaluable assistance to engineers. For years, they have represented the maximum in terms of performance and reliability in a variety of engineering tasks. The initial development of virtual reality (VR) technology aimed primarily at displaying models previously made in other CAE applications, thus facilitating the review process of developed design. However, the strong development of advanced visualization systems, followed by further development of already existing components (CAD, FEM, etc.) and necessary hardware, have enabled the integration of VR technology into the very core of engineering tasks. And further more, the possibility of application of VR concept in a number of other fields has also been recognized.

With the VR concept, the user is offered the possibility of manipulating and analyzing a 3D virtual world, as if the objects were right in front of him. In certain applications, it suffices to incorporate rigid-body behavior in the VR environment. But in many areas of application, VR requires simulation of deformable object's behavior, quite often involving large or moderately large deformations. An example of such a requirement is found in some special applications of VR technology, such as various surgical simulators, especially those involving soft tissues.

A number of methods have been developed with the aim of predicting physical behavior of deformable objects with very high level of accuracy. The finite element method (FEM), as dominant one in the field, has deservedly gained the reputation of the 'state-of-the-art method'. Typical engineering tasks rely on the so-called "off-line" FEM calculations, which pose the accuracy as the primary simulation objective, as it is aimed at

authentic representation of the real world. Numerical efficiency, i.e. the CPU time needed for the calculation, always plays an important role, of course. But regarding the VR concept, the efficiency of applied FEM formulation gains in importance and may even become the primary objective, thus reducing the accuracy requirement to "plausible deformational behavior". This, of course, strongly depends on the field of application. The paper presents features of some already existing as well as some recently developed FEM formulations that may find their application in different fields, VR technology being only one of them. The solutions for high efficiency have been sought in modal reduction technique, but also in some novel simplified geometrically nonlinear formulations based on full FEM models. Examples are given to illustrate the proposed formulations.

2. MODAL SPACE BASED FORMULATIONS

One of the basic ideas on how to reduce the computational burden required to determine flexible bodies' deformational behavior consists in model reduction. Actually, this idea enables to perform a large portion of computation in a pre-step, i.e. prior to interactive simulation. Among different approaches for model reduction, the one that has established itself as the method of choice for simulation of dynamic behavior is modal reduction. It implies that orthogonal mode shapes, calculated in a step prior to simulation, determine modal degrees of freedom, in terms of which the elastic behavior of the body is described. Not only is the number of degrees of freedom in this manner significantly reduced, but the equations for elastic behavior are also decoupled, i.e. the generalized mass and stiffness matrices are diagonal.

This method is already a common choice in a number of Multi-Body System (MBS) software packages. The

solution used by commercial software package like ADAMS is the Component Mode Synthesis (CMS) technique, particularly the Craig-Bampton method. The method requires to partition the flexible body degrees of freedom (DOFs) into boundary DOFs and interior DOFs, the former belonging to the nodes of the FE-model that the user wants to retain in the simulation model mainly for the purpose of defining (kinematic or dynamic) boundary conditions. In the next step, the method requires to determine two sets of modes: 1) *constraint-modes*, which are static shapes obtained by giving each boundary DOF a unit displacement, while all other boundary DOFs are fixed; 2) *fixed-boundary normal modes*, which are obtained by fixing all boundary DOFs and computing an eigensolution. Since the so-obtained Craig-Bampton modes are not a usual orthogonal set of modes, they are not suitable for direct use in MBS dynamics and are, therefore, orthonormalized prior to simulation.

Fig. 1 depicts an interactive deformable model of a car rear axle, with interaction programmed by the authors. The full FEM model contains approximately 300,000 DOFs, involving over 44,000 shell elements and almost 5,000 solid elements with altogether over 50,000 nodes. At the present hardware technology level, such a model is not suitable for simulations at interactive frame rates. But once reduced to modal space, a reasonable number of mode shapes, found to be adequate for the purpose of interactive simulation, can be determined and the simulation can run effectively enough to be used in combination with a VR environment.

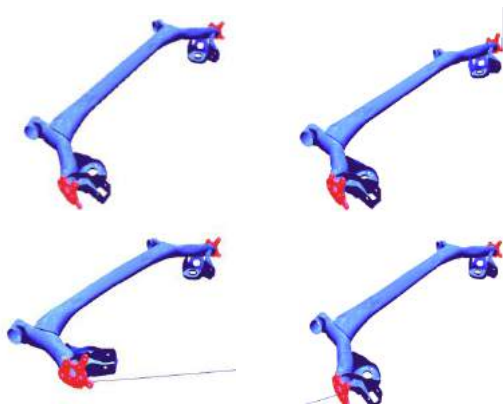


Fig.1. An interactive deformable car rear axle model

2.1. Geometrical nonlinearities

MBS programs apply the approach denoted as floating reference-frame. The idea behind the approach is to decompose the overall motion into a large rigid-body motion, which is described by the motion of the reference-frame, and a small deformational motion, described in modal space with respect to the floating reference-frame. This enables consideration of nonlinearities resulting from large rigid-body motion, which was actually the original aim of programs for MBS dynamics. Depending on flexible body topology and the exerted deformational behavior, this approach might yield satisfying results even for deformations that would typically be described as moderately large and that would require geometrically nonlinear FEM formulation to determine the deformational behavior with satisfying

accuracy. But quite generally speaking, the approach based on modal reduction is meant for linear deformational behavior, as the used degrees of freedom (mode shapes) are characteristics of the FEM model linearized in its original configuration. The authors have recently developed original methods to resolve up to certain extend the issue of geometrically nonlinear behavior computed in modal space. Those methods are only briefly mentioned below, as more details are already available in published literature.

2.2. Geometric stiffness matrix based approach

The idea is based on the assumption of relatively small displacements, similar to the assumption of linearity. But, while linear models consider only the linear stiffness matrix, the proposed formulation extends the linear approach so that the stress stiffening effects are additionally accounted for through a simplified computation of the geometric stiffness matrix. The formulation keeps the advantages of computation in modal space. This is done by computing the geometric stiffness matrices for each of the used mode shapes and using the principle of their superposition to determine the overall geometric stiffness matrix. The method needs to be used with caution since it is suitable for specific cases of deformational behavior characterized by small displacements and large stiffening effects. More details about the approach can be found in [1, 2].

2.3. Partial rotation of displacements

The approach denoted as *partial rotation of displacements* aims at consideration of geometrically nonlinear effects caused by relatively large rotation of single sub-domains of the structure with respect to the structure as a whole. The method consists in partitioning a complex structure into segments that perform relatively large rigid-body rotations with respect to the rest of the structure. Upon deformation, the average rigid-body rotation of the segments is determined and this amount of rotation is used to rotate the part of displacement field (determined in modal space) belonging to the segments. More details about the approach can be found in [2, 3].

What should be noticed here is that this approach is rather complementary to the previously described one. As a matter of fact, the two approaches can be combined in order to meet the requirement to simultaneously account for both causes of geometrical nonlinearities.

3. FORMULATIONS BASED ON FULL FEM MODELS

Linear FEM-models are known for high efficiency and stability. Furthermore, as long as deformations remain in the realm of materially linear behavior, translations of elastic bodies are easily handled with linear models. However, already moderate rotations suffice to deteriorate the accuracy of the linear FEM results beyond the limit of applicability, even if only visual representation of deformation is of interest. On the other hand, geometrically nonlinear formulations, in their theoretically pure form, offer more than a satisfying

degree of accuracy, but are rather expensive and may also exhibit problems with simulation stability. A relatively simple but therefore efficient formulation that is supposed to combine the advantages and avoid the drawbacks of the previous two has been recently developed [3, 4].

The developed formulation is of corotational type. Its essence consists in extension of the already mentioned floating reference frame approach. Whereas in the floating reference frame approach, as used in MBS systems, a single local reference frame is assigned to the whole body in order to describe its rigid-body motion, in the developed FEM-formulation the idea is extended so that each single finite element is assigned a local coordinate system. Furthermore, it is assumed that the element behavior with respect to the local coordinate system remains purely linear. This allows the computation of linear stiffness matrices of single elements prior to interactive simulation. Over the course of simulation, it is necessary to use the information about the last determined and the original configuration in order to extract the rigid-body rotation for each single element, described by the rotational matrix \mathbf{R}_e . Once the rotation is known, the last determined configuration of the element is rotated back, i.e. through \mathbf{R}_e^{-1} . The so-obtained configuration is compared with the initial configuration to determine the displacements free of rigid-body rotation. Multiplication of the element stiffness matrix with rotation-free displacements yields internal elastic forces of the element in the original frame of the element. What remains is to rotate the forces to the current element frame, i.e. through \mathbf{R}_e , which yields internal forces in the current configuration.

Another important aspect is the time integration scheme and solver. Since the formulation aims at high efficiency and low frequency behavior, the authors take advantage of an implicit time integration scheme, which is indeed more expensive regarding the necessary computational effort for a single time-step, but, on the other hand, allows significantly larger time-steps compared to an explicit solver. The implicit time integration scheme keeps the coupled system of equations and, thus, requires forming the complete stiffness matrix of the structure and solving the system. Instead of commonly used direct solvers, the authors use an iterative solution procedure – the preconditioned conjugate gradient method (more information in [5]), which benefits from the system matrix in the sparse form. The method is very convenient for real-time simulations. First of all, the conjugate gradient method involves one matrix-vector product, three vector updates, and two inner products per iteration, which makes it computationally very attractive for nonlinear systems. Furthermore, it provides a very easy way of performing a trade-off between the solution accuracy and computational effort by limiting the number of performed iterations.

The applicability of the developed formulation is quite wide. In following, a several possible applications are tackled.

3.1. Example of models for entertaining industry

Although the quality of the animation and rendering determines the very first impression in entertaining

industry, it is actually the displayed physical behavior of deformable objects that eventually determines the degree of realism. The main objective here is plausible behavior, which allows certain model manipulations. One of the very effective techniques to achieve a plausible behavior of very complex geometries in combination with the presented formulation is the coupled mesh technique. The idea consists in introducing two meshes – a volumetric FE-mesh, which is used to calculate the deformation and a detailed triangularized surface mesh, which is used to represent the actual, complex geometry of the object. As a pre-step of interactive simulation, the two meshes are coupled to each other. For each vertex of the surface mesh a corresponding finite element is found and the surface vertex is assigned to this element.

A model of a dog shown in Fig. 2 illustrates the above described approach. The FE-mesh (700 elements, 314 nodes) of the model is given in Fig. 2a. Fig. 2b depicts 12520 surface vertices, which are connected to form the topology of triangularized surface – 24835 faces (Fig. 3c), which can be covered by a texture to provide a realistic appearance (Fig. 3d).

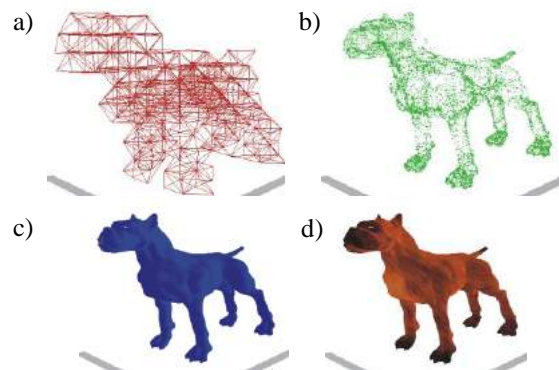


Fig.2. Model of a dog: a) FE-mesh; b) surface vertices; c) triangularized surface, d) texture

Fig. 3 shows large deformations of the dog model during an interactive simulation. The combination of the corotational FEM-formulation with the coupled mesh technique yields plausible deformational behavior.



Fig.3. Large plausible deformations of the dog model during an interactive simulation

3.2. Examples of models for surgery simulators

Certain types of surgeries, such as laparoscopic surgery, are performed under very difficult conditions, thus requiring very special skills from the surgeon, which can only be gained with extensive training. This is where surgery training devices come into account.

If soft tissues are involved in the surgery, then models need to provide a satisfactorily accurate representation of the internal organ mechanics, while still allowing real-

time computation – two requirements which are not easy to conciliate. The presented FEM formulation in combination with the above described coupled mesh technique is applicable here just as well. A model of a liver in Fig. 4 illustrates the approach once again. The FE-mesh (2640 elements, 660 nodes) of the model is given in Fig. 4a, with Fig. 4b showing 2598 surface vertices, which are interconnected to form the topology of triangularized surface – 5192 faces (Fig. 4c).

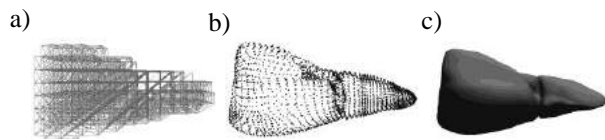


Fig.4. Liver model: a) FE-mesh; b) surface vertices; c) triangularized surface

Similar to Fig. 3, Fig. 5 depicts deformations of the liver model over the course of an interactive simulation.



Fig.5. Liver model deformations during an interactive simulation

Bone tissue is, however, pretty stiff and deformation of a bone would typically not require a geometrically nonlinear computation (with respect to the local reference frame). On the other side, interaction with bones in a surgery simulator imposes the need for large rigid-body motion. Hence, the above described FEM formulation may be simplified so as to take a single rigid-body motion into account. In fact, that would be essentially the already mentioned floating reference frame based approach, however with the slight modification that the rigid-body motion is not determined based on physics of rigid-body behavior, but rather on physics of elastic-body behavior. This means that the “rigid-body” rotation is computed by averaging rotations of single finite elements. Of course, this is only one of possible approaches to extract the rotational part of motion which is further used to rotate the stiffness matrices of all elements. But the major difference between this approach and the floating reference frame approach as used in MBS systems is that this one retains the FEM model in its full extent, i.e. no model reduction is performed. This offers a greater flexibility and accuracy in interaction with the model.

Fig. 6 depicts an FEM model of a femur containing nearly 8,000 tetrahedral elements and which supports large rigid-body rotation. An important difference compared to the

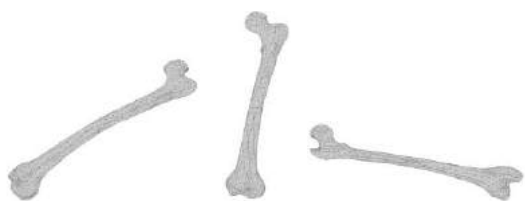


Fig.6. Femur model in an interactive environment

liver model is that the FEM model now reflects the actual femur geometry. In other words, models of bone structures should principally avoid the approach based on coupled mesh technique. The reason for this resides in the fact that an acceptably accurate prediction of stress fields excited in bones through various external stimuli is of crucial importance. The FEM meshes used with the coupled mesh approach are just unacceptably rough from the point of view of structural mechanics. Having at hand an acceptably accurate stress prediction in bones allows surgery planning, optimal choice of implant geometry, design of adequate scaffold for bone reconstruction, etc.

4. CONCLUSION

Virtual reality technology calls for a multidisciplinary approach. Mechanics of deformable objects is only one segment of it, but in certain applications very important one. The paper presents some existing as well as some originally developed FEM-formulations for efficient computations of flexible bodies’ deformation. The features of those formulations, such as high efficiency combined with possibility of accounting for geometrical nonlinearities, render them suitable for applications in the field of VR technology.

The presented models demonstrate applicability of the development in a variety of fields, such as training assembly operators and medical practitioners, or entertainment industry. This certainly does not exhaust the potential of the development, as new ideas for possible applications are coming out each and every day.

Acknowledgment

This paper is part of project III41017 Virtual human osteoarticular system and its application in preclinical and clinical practice, funded by the Ministry of Education and Science of Republic of Serbia. (<http://vihos.masfak.ni.ac.rs>)

REFERENCES

- [1] MARINKOVIC, D., ZEHN, M. (2010) *Geometric stiffness matrix in modal space for multibody analysis of flexible bodies with moderate deformations*, Proceedings of ISMA, Leuven, Belgium.
- [2] MARINKOVIC, D., ZEHN, M. (2010) *FE-formulations for fast computation of large and moderately large deformations*, Proceedings of 10th International Conference on Computational Structures Technology (CST2010), Valencia, Spain.
- [3] MARINKOVIC, D., ZEHN, M. (2011) *Geometrical nonlinearities in elastic body behaviour for multi-body system dynamics*, Proceedings of NAFEMS World Congress 2011, Boston, USA.
- [4] MARINKOVIC, D., ZEHN, M. (2009) *FE-formulations for real-time simulations of large deformations*, Proceedings of NAFEMS World Congress 2009, Crete, Greece.
- [5] BATHE, K. J. (1996) *Finite element procedures*, Prentice Hall, New Jersey.



APPLICATIONS BY CAM AND FEM SIMULATIONS IN ESTABLISHING THE MILLING CONDITIONS FOR PARTS WITH THIN WALLS

Ionuț GHIONEA, Ioan TĂNASE, Adrian GHIONEA, Cristian TARBĂ

University Politehnica of Bucharest, Faculty of Engineering and Management of Technological Systems,
Spl. Independenței nr. 313, sector 6, Bucharest, Romania

ionut76@hotmail.com, tanase.ioan@yahoo.com; adrianghionea@yahoo.com, ticris@gmail.com

Abstract: *The paper presents some results of the CATIA application in milling simulations of parts with thin walls using end mill tools. The considered surfaces have linear and curved directories – concave and convex and low stiffness or a high ratio for width/thickness. These situations are met in large number of parts for moulds, rotor blades, aerospace assemblies, etc. The simulations offer numerical values of the elastic deformations and stresses, these results being very helpful in the establishment of the working regime parameters in real conditions, in the adaptation of the technological processes to CNC machine-tools.*

Key words: CAM milling, CNC manufacturing, FEM analysis, stress, simulation

1. INTRODUCTION

The use of modern CAD/CAM/FEM techniques in the manufacturing processes has a large application in the mechanical, automotive or aerospace industry domains. The specialty literature [1], [3] highlights remarkable results of FEM applications used to determine the elastic deformations values and the stresses induced in parts by the contact with the machining tools during the working processes. The influences of the technological system (machine-tool precision, tools, fixture devices) determine dimensional variations and irregularities of the processed surfaces, dynamical behaviour of the machine-tool in the cutting process and also the premature wear of the cutting edges [5]. The results of the surfaces generation by simulation, with the aid of CAM techniques (tool path, division pattern of the stock left for machining, different working strategies, etc.) offer a large number of data: machining times, surface accuracy (roughness size), behavior of the machine-tool in working conditions (power and cutting torque), both for roughing and finishing operations. For the optimization of the technological process there are considered and applied various criteria, software environments, tables of data.

2. THE CAM SIMULATION

Preparing the part for processing on a machine-tool with numerical control involves the generation of command information, all data is then stored in a preset order within a storage device. Programs can be generated directly on the machine using a CAD-CAM program and a virtual model of the part [2], [3], [4].

Defining the part in a CAD environment is an important entry date to generate the NC program with one of the complex existing programming languages. Thus, the simulation is justified to optimize the process because

CAM programs elaborate the NC code. Each program, compatible with the machine, consists of a group of sentences written in a logical sequence based on a specific syntax (words, numbers, addresses) [4]. On the modern CNC equipments the user may program, in addition to coordinates, other geometrical information regarding the compensation of length and tool diameters. Thus, it is possible to do various corrections on the dimensions, clearances and vibrations that may appear in the fixture devices of the part on the machine-tool, etc.

For the purposes of this paper, it is considered a part having its 3D model made in CATIA Part Design module and presented in figure 1. The overall dimensions of the stock part are 100×100×32 mm.

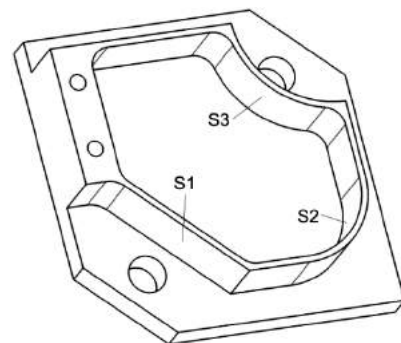


Fig.1. The part's 3D model

From the analysis of the part's surfaces it is identified the cavity delimited by a closed contour whose walls have thickness of 2 mm and 20 mm height. To express (by comparison) the material influence over the part's stiffness in manufacturing conditions, there are considered two materials: high-alloyed steel and aluminium alloy, having the yield strength of 2.5×10^8 N/m², respectively, 9.5×10^7 N/m².

To manufacture the part it is used a 3-axis CNC vertical milling machine-tool having the following main characteristics: spindle speed: 20000 rpm with infinite variable speed range (direct drive spindle), movement on axes X = 1020 mm, Y = 550 mm, Z = 560 mm, the power of the main electric drive: P = 15 kW (continuous rating), cutting feedrate max: 8000 mm/min and rapid traverse rate: 30000 mm/min. The machine-tool has a CNC Sinumerik controller.

The tools used in manufacturing simulation are chosen from a company catalogue [6]. Also, the toolholders are in correspondence with the spindle nose and with the holding system of the machine-tool.

Below are presented (as parameters) the main steps of the CAM simulation in the case of aluminium alloy working, with 75 HB.

a. *Face mill*, one pass, $D_c = 50$ mm - tool diameter, $h_m = 0.08$ mm - average chip thickness, $v_c = 960$ m/min - cutting speed, $n_c = 5600$ rpm - spindle speed, $v_f = 3400$ mm/min - feed speed, $P_c = 4.6$ kW - cutting power for removal of chips, $M_c = 7.7$ Nm - cutting torque, $f_z = 0.1$ mm - feed per cutting edge, $a_p = 2$ mm - cutting depth, $z_c = 5$ - number of teeth, $t_m = 9$ s - machining time, $t_t = 11$ s - total time.

b. *External roughing profile contouring mill*, one pass, $D_c = 25$ mm, $h_m = 0.04$ mm, $v_c = 1000$ m/min, $n_c = 12000$ rpm, $v_f = 2600$ mm/min, $P_c = 13$ kW, $M_c = 11$ Nm, $f_z = 0.04$ mm, $a_p = 20$ mm, $z_c = 5$, $t_m = 19$ s, $t_t = 20$ s.

c. *External finishing profile contouring mill*, two passes, $D_c = 16$ mm, $h_m = 0.02$ mm, $v_c = 1000$ m/min, $n_c = 14000$ rpm, $v_f = 2400$ mm/min, $P_c = 11$ kW, $M_c = 5.3$ Nm, $f_z = 0.02$ mm, $a_p = 20$ mm, $z_c = 6$, $t_m = 50$ s, $t_t = 52$ s.

d. *Internal roughing profile pocketing mill*, one pass, $D_c = 16$ mm, $h_m = 0.02$ mm, $v_c = 1000$ m/min, $n_c = 14500$ rpm, $v_f = 1300$ mm/min, $P_c = 13$ kW, $M_c = 6.4$ Nm, $f_z = 0.02$ mm, $a_p = 20$ mm, $z_c = 4$, $t_m = 24$ s, $t_t = 27$ s.

e. *Internal finishing profile contouring mill* (fig. 2), two passes, $D_c = 12$ mm, $h_m = 0.03$ mm, $v_c = 735$ m/min, $k_{c1} = 700$ N/mm² - specific cutting force, $m_c = 0.25$ - exponent, $n_c = 19500$ rpm, $v_f = 8000$ mm/min, $P_c = 4.4$ kW, $f_z = 0.11$ mm, $a_p = 20$ mm - cutting depth, $a_e = 1$ mm - working engagement, $z_c = 4$, $t_m = 27$ s, $t_t = 31$ s.

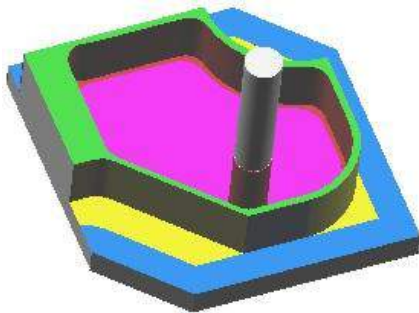


Fig.2. Profile contouring mill, finish surface

f. *Drill Ø12 two holes*, $D_c = 12$ mm, $v_c = 200$ m/min, $n_c = 5300$ rpm, $v_f = 2100$ mm/min, $P_c = 3.5$ kW, $M_c = 6.4$ Nm, $f_z = 0.02$ mm, $a_p = 6$ mm, $z_c = 2$, $t_m = 5$ s, $t_t = 7$ s.

g. *Drill Ø5 two holes*, $D_c = 5$ mm, $v_c = 140$ m/min, $n_c = 8900$ rpm, $v_f = 1800$ mm/min, $P_c = 0.7$ kW, $M_c = 0.6$ Nm, $f_z = 0.02$ mm, $a_p = 2.5$ mm, $z_c = 2$, $t_m = 16$ s, $t_t = 18$ s.

Figure 3 presents the part after its final simulation operation; it can be observed all the machined surfaces and also the drill tool.

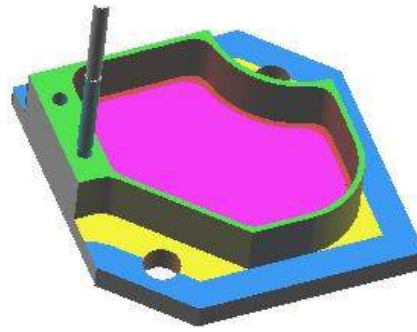


Fig.3. The part's machined surfaces

In the case the part would be processed of high-alloyed steel, with 200 HB, all the data above will be modified. For the operation e. *Internal finishing profile contouring mill* the parameters become: two passes, $D_c = 12$ mm, $h_m = 0.03$ mm, $v_c = 235$ m/min, $k_{c1} = 1950$ N/mm², $m_c = 0.25$, $n_c = 6235$ rpm, $v_f = 2750$ mm/min, $P_c = 4.3$ kW, $f_z = 0.11$ mm, $a_p = 20$ mm, $a_e = 1$ mm, $z_c = 4$, $t_m = 30$ s, $t_t = 34$ s. To determine the cutting power for this operation, it is used the next equation:

$$P_c = \frac{a_p \cdot a_e \cdot v_f \cdot k_c}{60 \cdot 10^6 \cdot \eta}, \text{ [kW]} \quad (1)$$

where: $k_c = k_{c1} \cdot h_m^{-m_c} = 4685$ N/mm² and $\eta = 1$.

```

N10 G0 G90 G40
N20 G40 M8
N30 G17
N40 G0 X0 Y0 Z25
N50 ;= TOOL CHANGE =
N60 ; DESC :
N70 ;=====
N80 T5 M06
N90 D5
N100 G0 G90 G40 G17
N110 F0 S0
N120 G64 SOFT
N130 S6250 M3
N140 G1 X18.5 Y-18.5 Z10 F8000 G94
N150 Z-22
N160 Y-51.479 F2700
N170 X48.521 Y-81.5
N180 X65
N190 G3 X81.5 Y-65 I0 J16.5
N200 G1 Y-47.55
N210 G2 X52.45 Y-18.5 I8.5 J37.55
N220 G1 X18.5
N230 Y-18 F500
N240 G3 X18 Y-18.5 I0 J-0.5
N250 G1 Y-51.479
N260 X18.146 Y-51.833
N270 X48.167 Y-81.854
N280 X48.521 Y-82
N290 X65
N300 G3 X82 Y-65 I0 J17
N310 G1 Y-47.55
N320 X81.909 Y-47.262
N330 X81.61 Y-47.062
N340 G2 X52.938 Y-18.39 I8.39 J37.062
N350 G1 X52.785 Y-18.129
N360 X52.45 Y-18
N370 X18.5
N380 Z10 F6000
N390 M5
N400 M5 M9
N410 M30

```

Fig.4. CNC code for the internal finishing profile contouring mill, high-alloyed steel case

After the CNC simulation of the considered operation, the resulted code is shown in figure 4.

3. THE FEM SIMULATION AND ANALYSIS

The Finite Element Method (FEM) is one of the best existing approaches that accomplish a vast range of engineering calculus and simulation [1]. The method and FEM based programs becomes a main constituent of modern engineering computer-aided design. A FEM based analysis is now mandatory for high performance engineering tasks.

The FEM analysis of a structure is in fact a numeric computation review. Hence, for a specific geometrical model, particular loads and constraints will result the required values of the deformation, stress, bearing reaction and natural frequency [1], [2].

In this FEM simulation it is considered a finishing end mill with the diameter $D_c = 12$ mm, number of cutting edges $z_c = 4$, pitch of the helical cutting edge $P_{hc} = 37.4$ mm, helix angle $\omega = 45^\circ$. On the contact line between the mill and the part there are created four cutting spots placed on the height of the helix pitch. Two of the spots corresponding to the cutting depth ($a_p = 20$ mm) are shown in figure 5.

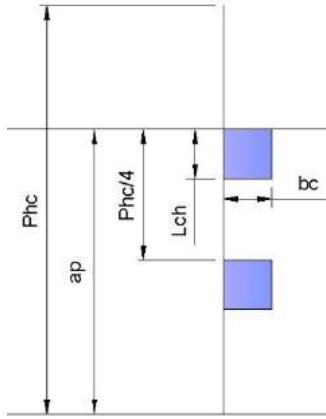


Fig. 5. Positioning of the cutting spots

In order to establish these spots where the tangential medium cutting force is applied it was necessary to determine the contact length of each helical edge with the part. The dimensions of these spots and also the contact angle φ between the part and the cutting edge are calculated with the following equations:

$$b_c = \sqrt{\frac{D_c^2}{4} - \left(\frac{D_c}{2} - a_e\right)^2} = 3.32, [\text{mm}] \quad (2)$$

$$L_{ch} = \frac{\sqrt{D_c \cdot a_e}}{\text{tg } \varpi} = 3.46, [\text{mm}] \quad (3)$$

$$\varphi = 2 \cdot \sqrt{\frac{a_e}{D_c}} = 0.577, [\text{rad}] \quad (4)$$

The medium cutting force acting on a contact spot for the contact angle φ is determined by the relation:

$$F_{m\varphi} = L_{ch} \cdot h_m \cdot k_c \cdot [\text{N}] \quad (5)$$

With the previously determined values for cutting power (aluminium alloy and high-alloyed steel) it is calculated the tangential medium cutting force:

$$F_{m\varphi} = \frac{60000 \cdot P_c}{v_c}, [\text{N}] \quad (6)$$

and it has the values: 360 N, respectively, 1098 N.

The medium radial cutting force (which is practically applied on the two spots) is $F_{rm} = (0.3 \dots 1) \cdot F_{m\varphi}$, considered $F_{rm} = 0.45 \cdot F_{m\varphi}$.

As follows, there are presented some results of FEM simulations and analysis in the cases of the part being processed of aluminium alloy and high-alloyed steel. Thus, the medium radial cutting force is different for each case ($F_{rm} = 164$ N – aluminium alloy and $F_{rm} = 536$ N – high alloyed steel).

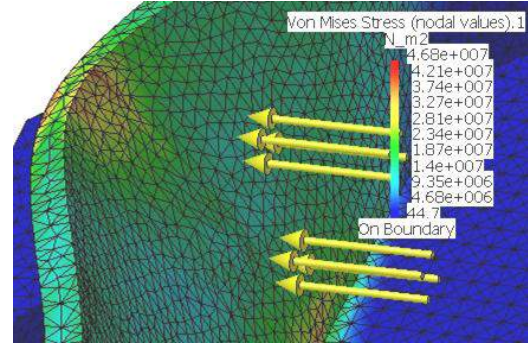


Fig. 6. Example of Von Mises Stresses for the flat milled surface S1

Figure 6 shows the Von Mises Stresses calculated by the FEM analysis in the case of aluminium alloy and flat surface. For a force of 164 N applied on the two spots the results are: max. stress = 4.68×10^7 N/m² and max. elastic deformation = 0.062 mm with an error of 48.8 %.

The error is too high, so a new analysis is done after a refinement of the part structure. Although CATIA software defines a default net of nodes in a process named digitization, it is highly recommended for experienced users to edit this net and establish the dimension of the finite element, the maximum deviation of the virtual digitized model from the real model and the type of the finite element. After the refinement, the error is 32.7 % and the values become: max. stress = 6.22×10^7 N/m² and max. elastic deformation = 0.083 mm.

In the high-alloyed steel case (flat surface S1, $F_{rm} = 536$ N), for an error of 48.8 % the max. stress = 1.53×10^8 N/m² and max. elastic deformation = 0.07 mm. Also, for an error of 31 % the values are: max. stress = 2×10^8 N/m², max. elastic deformation = 0.09 mm.

In the FEM practice, an error of 20 - 35% is acceptable and it's very close to the real case. Anyway, in both situations for the flat surface S1, the max. stresses are lower than the materials' yield strengths, so the surface is deformed only in the elastic domain.

On the convex surface S2 it is applied the same force for each considered material. In the aluminium alloy case, for an error of 38.3 %, the max. stress is 3.47×10^7 N/m² and the max. elastic deformation is 0.014 mm.

After the refinement, the error is 25.5 % and the values become: max. stress = 5.35×10^7 N/m² and max. elastic deformation = 0.0175 mm.

Figure 7 shows an example of the Von Mises Stresses determination in the high-alloyed steel case. Thus, for an

error of 38.13 % the max. stress is $1.12 \times 10^8 \text{ N/m}^2$ and the max. elastic deformation = 0.016 mm.

After the refinement is applied, the error is 25.3 % and the values are: max. stress = $1.34 \times 10^8 \text{ N/m}^2$ and max. elastic deformation = 0.02 mm.

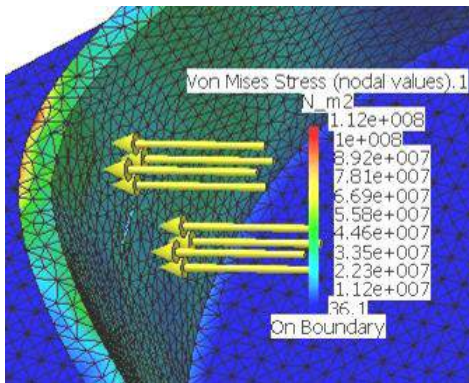


Fig. 7. Example of Von Mises Stresses for the convex milled surface S2

The last analysis simulations consider that the radial cutting force is applied on the concave surface S3. In the aluminium alloy case, for an error of 34.4 % the max. stress = $3.39 \times 10^7 \text{ N/m}^2$ (fig. 8) and the max. elastic deformation = 0.0214 mm (fig. 9).

After the refinement, the error is 22.3 % and the values become: max. stress = $4.28 \times 10^7 \text{ N/m}^2$ and max. elastic deformation = 0.0245 mm.

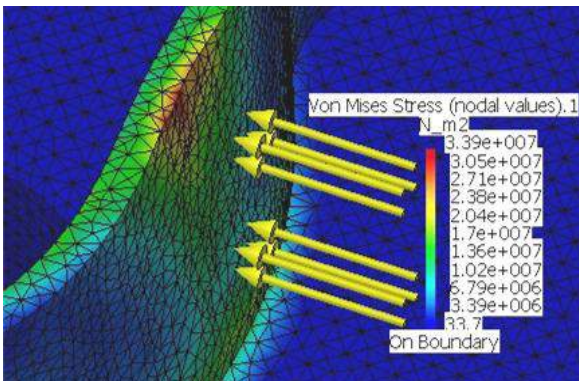


Fig. 8. Example of Von Mises Stresses for the concave milled surface S3

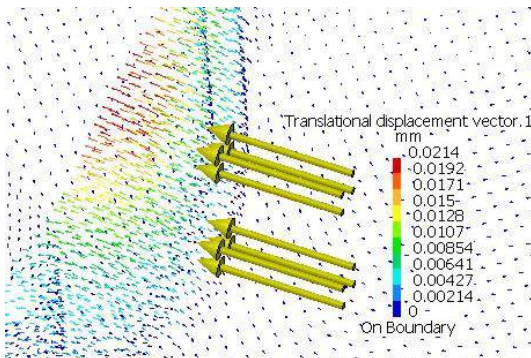


Fig. 9. Example of wall deformation for the concave milled surface S3

In the high-alloyed steel case, for an error of 35.1 % the max. stress = $1.11 \times 10^8 \text{ N/m}^2$ and the max. elastic deformation = 0.024 mm.

After the refinement is applied, the error is 22.2 % and the values are: max. stress = $1.47 \times 10^8 \text{ N/m}^2$ and max. elastic deformation = 0.027 mm.

For an increased precision and higher improved model for each simulation, the user may continue an iterative analysis and to refine the model to decrease the error. Such errors like those obtained in the previous simulations seem to be high, but they indicate in fact all the differences between the proposed virtual model and the real structure.

The user is interested in the outputs of the maximum stress that must not exceed the admissible material yield strengths.

4. CONCLUSION

The determination of the cutting forces with which the cutting edges action on the machined surface was accomplished using the values of the cutting power, of the chip thickness and of the specific cutting force. The radial cutting force is distributed on the contact spots between the cutting edges and the part. These spots have calculated dimensions corresponding to the cutting parameters.

The simulations' results show that the stresses induced in the part's thin walls do not exceed the elastic domain. The maximum elastic deformations of the machined surfaces are greater in the case of the high-alloyed steel than in the case of the aluminium alloy.

It can be distinguished the dependence of the stresses and of the deformations with the shape of the machined surface. The elastic deformations are greater in the case of the flat surfaces than in the case of the convex or concave surfaces.

Also, these deformations corresponding to the considered working regime (max. 0.09 mm) seem to be unacceptable, influencing the dimensions of the processed surfaces. If the aim is a higher precision, the parameters of the working regime should be decreased and the process simulation resumed.

REFERENCES

- [1] CONSTANTINESCU, N. I., SOROHAN, ȘT., PASTRAMĂ, ȘT. (2006) *The practice of finite element modeling and analysis*. Editura Printech, București, ISBN 978-973-718-511-2, 2006.
- [2] GHIONEA, I. (2009) *CATIA v5. Aplicații în inginerie mecanică*. Editura Bren, București, ISBN 978-973-648-843-6.
- [3] GHIONEA, I. (2010) *Cercetări privind optimizarea prin simulare a concepției produselor industriale*. Phd thesis, University Politehnica of Bucharest.
- [4] KIEF, B. H. (2001) *NC/CNC Handbuch*. Carl Hanser Verlag Wien, ISBN 3-446-21756-8.
- [5] TRENT, E., WRIGHT, P. (2000) *Metal cutting*. Butterworth Heinemann, Oxford, Boston.
- [6] *** (2008) *Cutting tools from Sandvik Coromant Catalogue. Turning Milling Drilling Boring Toolholding C2900*, 6 Eng/01, Sweden, www.coromant.sandvik.com.



TIRE TREAD MODELING FOR FEA

**Nikola KORUNOVIĆ, Miroslav TRAJANOVIĆ, Miloš STOJKOVIĆ,
Nikola VITKOVIĆ, Milan TRIFUNOVIĆ, Jelena MILOVANOVIĆ**
Faculty of Mechanical Engineering in Niš, University of Niš, Niš, Serbia
nikola.korunovic@masfak.ni.ac.rs

Abstract: *This paper deals with creation of finite element tire models with detailed tread pattern. Such models are necessary when interaction between the tire and the surface is going to be analyzed in detail. Different methods for creation of tire tread mesh are systematized by two different criteria: the most common approaches and the finite element analysis type. Some of the representative approaches found in literature are described in more detail and their advantages and disadvantages are discussed. An example from author's experience, which describes the creation of finite element tire model with detailed tread for steady-state rolling analysis, is also given.*

Key words: *tire, tread pattern, FEA, steady-state rolling*

1. INTRODUCTION

Tire tread provides the necessary grip or traction for driving, braking and cornering. Both tread pattern and tread compound must be designed to provide effective performance in various driving conditions, while also meeting customer expectations for acceptable wear resistance, low noise, and good ride quality. Tread pattern is designed to provide uniform wear, to channel water out of the footprint, and to minimize pattern noise on a variety of road surfaces [1].

Typical features of tread pattern design are described in [1]. They are combined in order to primarily satisfy the function of tire tread and also to conform to aesthetic trends, which form the customer's perception of product performance. Parametric and knowledge-based design systems may efficiently be used to streamline the process of tread design, as may be seen from [2], [3] and [4]. They help in merging the strict constraints, determined by tread function and manufacturability, with tacit knowledge of tire designer. This paper, however, does not deal with the rules of tread design but with tire tread modeling for use in finite element analysis (FEA). FEA is often deployed in tire design to predict the behavior of the tire during its service life, as described in [5], [6] and [7]. Depending on the type of results that tire FEA should yield, tire tread is modeled in different level of detail, using different approaches, of which the most common ones are:

1. **Simplified tread modeling:** the tire is modeled as a smooth one or only the circular channels are included in the finite element (FE) model while the other features of tire tread are omitted. If the goal of the analysis is to find the tire forces and moments during cornering or braking, or to find the first approximation of footprint shape, size and contact pressure distribution, such a model is often sufficient [5], [6], [7].

2. **Global-local approach:** at first a simplified (global) tire model is built and analyzed. Then the portion of the tire is modeled in detail (local model) and displacements and stresses are transferred from global to local model as boundary conditions [8], [9].
3. **Detailed tread modeling:** tire tread is modeled in detail and assigned a dense mesh of finite elements. The rest of the tire is modeled in less detail and assigned a relatively coarse mesh. Then the two meshes are tied along the contacting surface. If the contact pressure on tread surface is to be analyzed in detail, the FE model with detailed tread will produce the output which is closest to the experimental values [7], [10].

The level of detail in tire tread modeling is also determined by the type of FEA. If tire behavior on dry and stiff surface is considered, three different cases may be identified:

1. **Static FEA** - only the behavior of the tire subjected to static loads is considered [5]: finite element mesh on tire tread may be of arbitrary density; very large densities are possible; the most important consideration is how to merge the dense mesh in the vicinity of the footprint with the mesh on the rest of FE model [8], [10].
2. **Steady-state rolling analysis:** the behavior of steady-state rolling tire is analyzed using mixed Eulerian-Lagrangian formulation [6], [7], [11]; until recently only the circular channels could be modeled with the benefit of having the dense mesh only in the vicinity of the footprint; the method is now expanded to include detailed tread modeling where an identical tread segment is patterned and scaled in circular direction [11], [12]; the approach of typical segment patterning necessarily implies the approximation of tread

shape; mesh density is limited by model size, i.e. the time needed for the analysis to finish.

3. **Implicit FEA using purely Lagrangian approach or explicit FEA [7]:** tread pattern may be modeled without approximation of tread geometry; FE mesh may be of arbitrary density, which is limited by model size, nevertheless this limitation is very significant for those analysis types.

In this paper, the generation of finite element tire model with detailed tread is described through literature review and an example from author's experience.

2. TREAD MODELING – EXAMPLES FROM LITERATURE

This section does not bring a detailed literature review of tire tread modeling, but rather presents some typical examples that illustrate the cases mentioned in the introduction.

In [13] an attempt is made to model the influence of tread pattern to behavior of steady-state rolling tire by assigning orthotropic material properties to simplified tread tire model. Material properties are obtained by FEA of a flat portion of tire tread, containing several tread blocks. This approach had been introduced before the mixed Eulerian-Lagrangian formulation was expanded to include detailed tread modeling. The analyses were performed on two FE tire models, with isotropic and orthotropic tread properties, and then compared to each other and to experimental results. The results showed that introduction of orthotropic tread properties brought the results closer to experimental ones.

A global-local approach is used in [8] and [9] to analyze the behavior of tire model with detailed tread pattern in the vicinity of footprint area. In order to transfer the solution results from global to local model, a tying algorithm for the linking of two originally geometrically incompatible finite element meshes with different degrees of refinement is proposed in [8], and applied to FEA of the model of an automobile tire with a simplified tread. Consideration of tread profile is restricted to the anticipated region of contact with the road surface and to its vicinity. For the remaining part of the analysis model a coarser finite element mesh is used (Fig. 1).

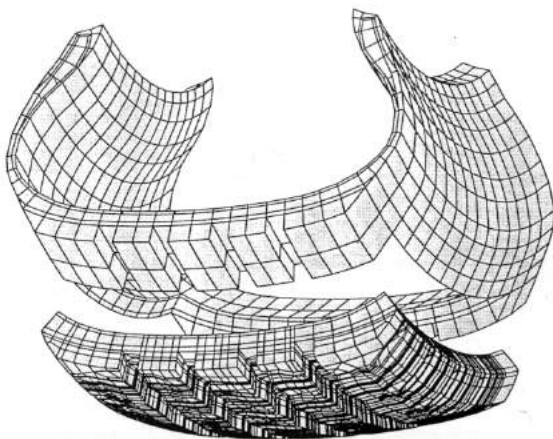


Fig.1. Global-local approach to tire tread modeling [8]

Simplified and global-local tire models are roughly criticized in [10]. It is said that simplified tire models may produce poor numerical results because some of the major tire interactions, such as footprint shape and size, contact pressure distribution, frictional energy and rolling resistance are characterized by the deformation of tread blocks and the interaction between belts and adjacent parts of tire. Considering the global-local approach, it is claimed that even though the local model is able to provide the numerical results associated with tread block, its accuracy is strongly influenced by the reliability of simplified model. The reason for this claim is found in the fact that the local model uses the results obtained by the simplified model as boundary conditions and it also ignores any interaction between the tread blocks and the belts and the adjacent parts of tire.

The approach to detailed mesh generation described in [10] is based on a method for tying of two incompatible meshes: coarse regular mesh of tire body and dense tread pattern mesh, which is inserted either partially or fully, depending on analysis purpose (Fig. 2). Tread mesh is constructed from 2D 1-pitch pattern, which is multiplied and transformed into 3D pattern by the subroutines coded in Fortran. When partial mesh is used, a transitional area must also be added, which serves to relax the abrupt density change in overall tread mesh and to avoid problems in assembling the tread mesh and body mesh. Resulting tire model is shown in Fig. 3. The paper also compares footprint stresses obtained numerically and experimentally, confirming the quality of proposed approach.

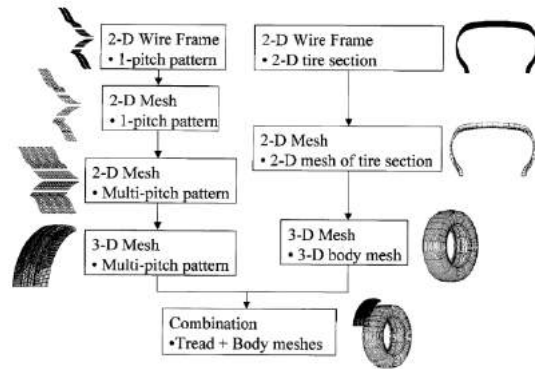


Fig.2. Tire meshing process considering detailed tread blocks [10]

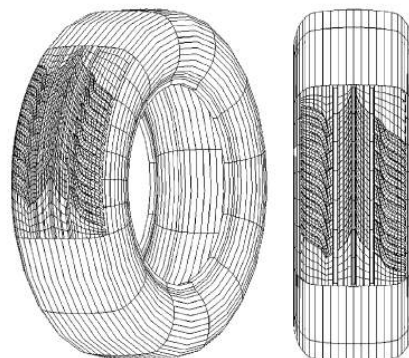


Fig.3. 3D tire model with partial tread mesh [10]

An example of detailed tread generation for use in steady-state rolling analysis is given in [12]. Similar to method described in [10], tread pattern mesh is created by multiplying and scaling of a repeating tread section and assembled to body mesh (Fig. 4). The main difference between the two approaches is that the latter requires that the repeating section is bordered by two planar surfaces, which contain the tire axes. Such an approach is described in more detail in the next section.

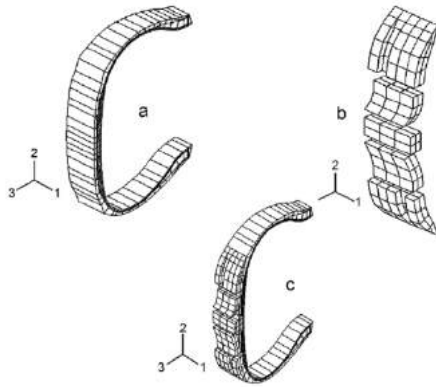


Fig.4. Finite element meshes of the (a) symmetric part without tread pattern, (b) tread pattern and (c) symmetric part + tread pattern [12]

3. AN EXAMPLE OF DETAILED TREAD MODELING FOR FEA OF STEADY-STATE ROLLING TIRE

In this section the finite element tire model with detailed tread, developed by the authors for steady-state rolling analysis, is described. The nature of mixed Eulerian-Lagrangian formulation, which is used for tire FEA, implies that the mesh is composed of typical segments ("slices") that are topologically equal. The segments have to be chosen in such way that by their multiplication and scaling in circular direction the best approximation of tire tread geometry is obtained. In this way a certain level of approximation of initial geometry is inevitably introduced, but it is a consequence of requirements dictated by the finite element formulation. The initial geometry of the tire which is modeled in this example is shown in Fig. 5.



Fig.5. 3D parametric model of an existing tire type, dimensioned 165/70R13 [2]

It is obvious that a typical segment of tire geometry would be easily created if the tire was cut along the bottom of lateral grooves. However, the FE method requires that the slices are cut along the planes that contain the tire axes [11]. Thus, the tread geometry was idealized by removing of smaller features, sipes and kerfs, and then the optimal location of cutting planes was identified and typical segment produced (Fig. 6).

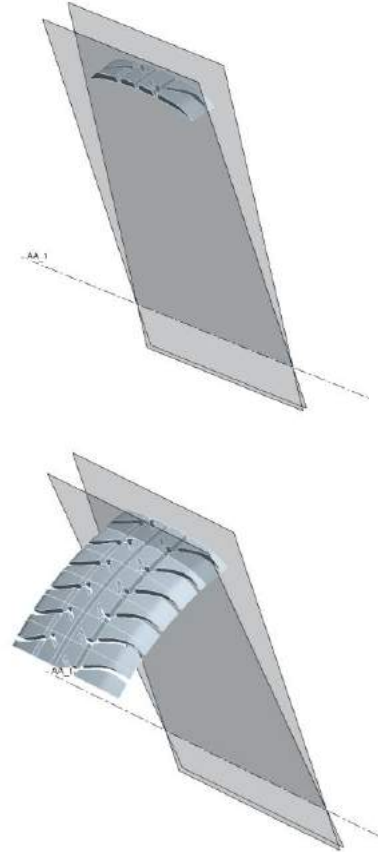


Fig.6. Identification of typical tread segment. The multiplication of the segment is shown for better visualization of resulting approximated tread geometry

Independently from the tread segment, the typical segment of tire body (without tread) was created, which spanned the identical angle of 5.6° (the angle of intermediate pitch). The two segments were then assembled to form the complex typical segment of the tire (Fig. 7).



Fig.7. Typical mesh segment formed by assembling of body and tread segments. Nodes on contacting surface are tied by DOF coupling

Finally, the FE model of the tire was created by rotation of complex typical segment along circular direction (Fig. 8). The segment was multiplied and scaled in such a way that a realistic disposition of tread blocks was achieved, which corresponds to a predefined pitch sequence (Fig.9).

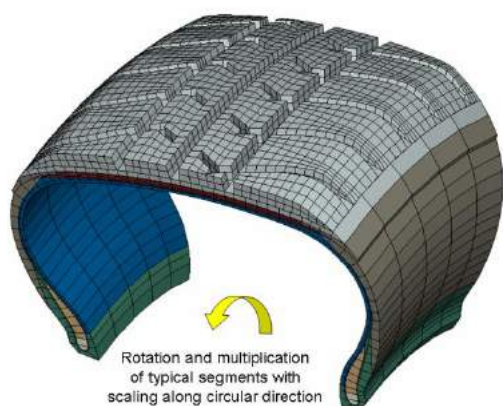


Fig.8. FE tire model creation by multiplication of complex typical segment



Fig.9. Final 3D FE model of the tire

4. CONCLUDING REMARKS

Various methods for creation of finite element tire model with detailed tread were systematized and discussed in the paper. The systematization was introduced by two criteria: the common approaches and the type of finite element analysis. In this way the understanding and the choice of tire tread meshing methods are facilitated. Some of the most important meshing approaches found in literature were also described, along with the criticism of their quality. Detailed tread modeling approach with node tying between tread and body meshes was identified as the best one. Such a method, performed by the authors

and adapted for steady-state rolling analysis was presented in more detail in the last section.

REFERENCES

- [1] GENT, A. N., Walter J. D. (2006) *The Pneumatic Tire*, National Highway Traffic Safety Administration, U.S. Department of Transportation.
- [2] STOJKOVIĆ, M., TRAJANOVIĆ, M. (2001) *Parametric design of automotive tyre*, Proceedings of First Nat. Conf. on Recent Advances in Mech. Eng., Patras, Greece, pp ANG1/P046
- [3] STOJKOVIĆ, M., MANIĆ, M., TRAJANOVIĆ, M., KORUNOVIĆ, N. (2004) *Functional Model of the Tire Tread*, 23rd Annual Meeting and Conference on Tire Science and Technology, Akron, Ohio
- [4] STOJKOVIĆ, M., MANIĆ, M., TRIFUNOVIĆ, M., MIŠIĆ, D. (2009) *Semantic Interpretation of Geometrical Features*, International Journal - Total Quality Management & Excellence, Vol.37, No 3, pp 75-80
- [5] KORUNOVIĆ, N., TRAJANOVIĆ, M., STOJKOVIĆ, M. (2007) *FEA of tyres subjected to static loading*, Journal of Serbian Society for Computational Mechanics, Vol.1, No 1, pp 87-98
- [6] KORUNOVIĆ, N., TRAJANOVIĆ, M., STOJKOVIĆ, M. (2007) *Finite element model for steady-state rolling tire analysis*, Journal of Serbian Society for Computational Mechanics, Vol.2, No 1, pp 63-79
- [7] KABE, K., KOISHI, M. (2009) *Tire cornering simulation using finite element analysis*, Journal of Applied Polymer Science, Vol.78, No 8, pp 1566-1572
- [8] MESCHKE, G., PAYER, H. J., MANG, H. A. (1997) *3D Simulations of Automobile Tires: Material Modeling, Mesh Generation, and Solution Strategies*, Tire Science & Technology, Vol.25, No 3
- [9] MUNDL, R., FISCHER, M., WAJROCH, M., LEE, S. W. (2005) *Simulation and validation of the ply steer residual aligning torque induced by the tyre tread pattern*, Vehicle System Dynamics: International Journal of Vehicle Mechanics and Mobility, Vol. 43, No 1 supp 1, pp 434 - 443
- [10] CHO, J. R., KIM, K. W., YOO, W. S., HONG, S. I. (2004) *Mesh generation considering detailed tread blocks for reliable 3D tire analysis*, Adv. Eng. Softw., Vol.35, No 2, pp 105-113
- [11] ABAQUS Version 6.9 HTML Documentation (2009) Dassault Systèmes
- [12] GHOREISHY, M. H. R. (2009) *Finite Element Modelling of the Steady Rolling of a Radial Tyre with Detailed Tread Pattern*, Iranian Polymer Journal, Vol. 18, pp 641-650
- [13] CHO, J. R., KIM, K. W., YOO, W. S., HONG, S. I. (2006) *Finite element analysis of a steady-state rolling tire taking the effect of tread pattern into account*, International Journal of Automotive Technology, Vol. 7, No 2, pp 101-107



AN INTERACTIVE CAD/CAE SYSTEM FOR MOLD DESIGN

Ivan MATIN, Miodrag HADZISTEVIC, Janko HODOLIC, Djordje VUKELIC

Department for Production Engineering, Faculty of Technical Sciences, Trg Dostiteja Obradovica 6, Novi Sad, Serbia
matini@uns.ac.rs, miodrags@uns.ac.rs, hodolic@uns.ac.rs, vukelic@uns.ac.rs

Abstract: In injection molding, the design of the molds is of critical importance for the product quality and efficient processing. This paper describes a knowledge-based parametric design system for mold design, which requires only a minimum set of injection molding parameters to be established before being able to complete the design of the main components of a mold. This CAD/CAE system contains of Pro/E and special developed modules for calculation, selection, modification and design. Developed CAD/CAE system can greatly improve the design quality while reducing the development time and cost.

Key words: CAD/CAE system, injection molding, mold design

1. INTRODUCTION

The highly competitive environment makes it necessary to reduce the time and money spent on mold design while maintaining high standards for product quality. Therefore, using computer-aided systems has become one of the most important manners to increase productivity. Most CAD software offers only simple geometrical modeling function. However, they fail to provide users with the sufficient design knowledge, which is of great help in most design tasks. Therefore, the design of automatic, knowledge-based, and intelligent systems has been an active research topic for a long time. Regarding the construction of a dedicated system, Deng et al. [1] developed an expert mold design system based on the configuration design method. This system allows users to design a mold in the CAD/CAE environment. Kong et al. [6] developed a Windows-native plastic injection mold design system based on the Solid Works using Visual C++. Lou et al. [7] utilized the set-based design approach with the parametric modeling technique to handle the uncertainties that are intrinsic at early stages of the mold design. In the stamping tool design area, authors [8, 9] developed a knowledge-based strip layout integrated design system in Pro/E. An interactive mold design systems were developed for dividing the mold design into four major steps, as well as for parting surface design, core and cavity design, runner system design, and mold base design [2,7]. It also provided the ability to control and manage projects, and assist designers in completing projects correctly. Systems have been constructed using the experience and knowledge of a product design and mold manufacturers. The researchers first determine the parting line for the plastic part, followed by the calculation of the number of cavities required. The cavity layout is created based on the input information of the layout pattern and the orientation of each cavity. The mold base is loaded automatically to accommodate the layout. Alternatively, Low and Lee [8,9,10] proposed a methodology of standardizing the cavity layout design system for plastic injection mold such that only standard

cavity layouts are used. When only standard layouts are used, their layout configurations can be easily stored in a database for fast retrieval later in the mold design stage. Other mold design system was developed by Ma [11], offering collaborative design systems, a standard mold base, and a decision-making system to improve the concurrent mold design efficiency in CAD software. Constructing standard components is an efficient manner to shorten the mold design cycle in the mold development. The advantages of using standard components include the ability to ensure the consistency of mold development and the reduction of manufacturing costs and time. The most important purpose of an interactive CAD/CAE environment's standard mold base is to assist designers in managing and using standard components correctly and efficiently. A mold base controls components via a three-level classification by class, type, and order number. Using the standard components library, designers browse for the components they need and save valuable time lost in searches. The standard components library includes three techniques for constructing models: general type, program type, and family table type [14]. General type components are typically complicated and invariant. Users need only to specify the component needed, and are not required to specify any dimensions, such as slide groups. Program type components have similar shapes but different features, such as date-code inserts. Family table type components, such as ejector pins, have variable dimensions. There are two ways to find components in the mold base by class and type, or by directly linking to the window containing the desired components.

2. KNOWLEDGE-BASED APPROACH

A knowledge-based approach broadly means to build up a system, usually called a knowledge-based system (KBS), for solving complex decision problems in a specific domain. A KBS, normally in the form of an intelligent computer program, uses knowledge and inference procedures to solve problems that are difficult enough to

require significant human expertise for their solution. The typical structure of a knowledge-based system is shown in Fig. 1. [11, 14]

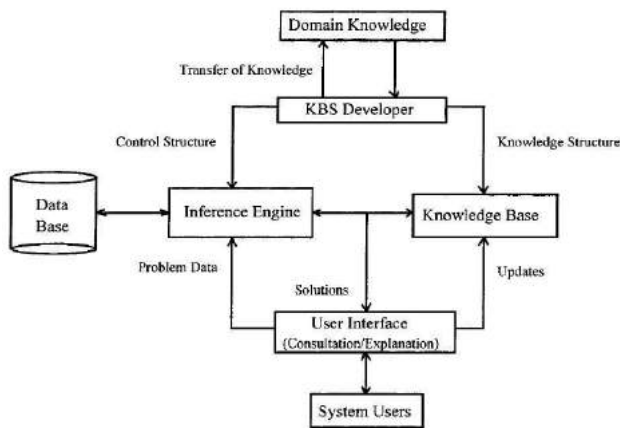


Fig. 1. The typical structure of a knowledge-based system

The developed interactive CAD/CAE system is based on a typical structure of a knowledge-based system. It comprises of the knowledge base, containing encoded expertise from the expert. The inference engine on the other hand provides strategies for processing the encoded knowledge in order to reach KB solutions. The KB system also provides a user interface for the KB system/user interaction. Links to a traditional database provide the KB system with the opportunity to import and use data in the inference or reasoning process. Knowledge is represented by a set of primitive components. Such primitive component is called a knowledge object, and it consists of a functional features and associated data. Mold design represents a generic sequence of activities, and each activity is represented by a mold function. A function defines effects on associated data, and it is represented by various forms, such as mathematical formula, decision tables, constraints and logical formula. Data types include simple data types, such as numerals and their aggregation, and also complicated data types, such as geometry and other objects.

3. GENERAL STRUCTURE OF AN INTERACTIVE CAD/CAE SYSTEM FOR A MOLD DESIGN

Generally, plastic injection molding design includes a plastic part design, a mold design, and an injection molding process design, all of which contribute to the quality of the molded product as well as the production efficiency. The developed program system makes possible to perform: 3D modeling of the parts, analysis of part designs, numerical simulation of injection molding, and mold design with calculation [3,4]. By the realization of the proposed integrated system, this problem could be solved. The main part of the system consists of a knowledge base. The knowledge base is organized by knowledge objects, and practically managed by a commercial database system. A knowledge engine accesses to the knowledge base, and invokes appropriate applications. General structure of a developed interactive

CAD/CAE system for a mold design is presented in Fig. 2. [4,13]

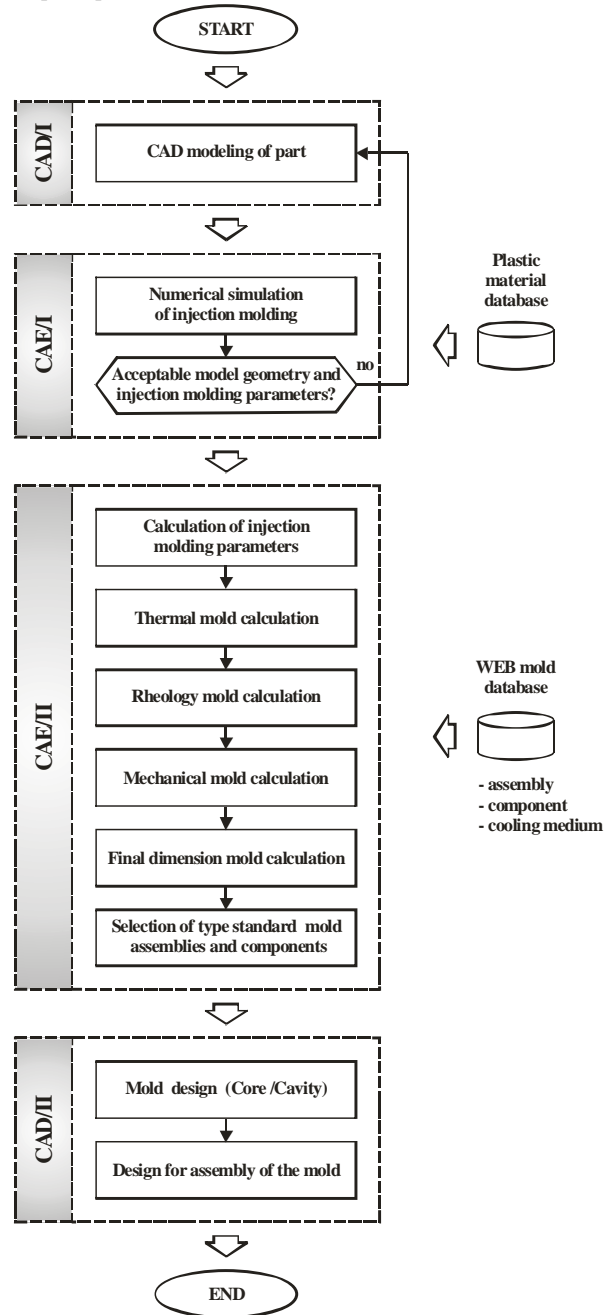


Fig.2. General structure of an interactive CAD/CAE system for a mold design

System consists of four foundation modules. These are:

- CAD/I module for the solid modeling of the part,
- CAE/I module for the numerical simulation of the injection molding process,
- CAE/II module for the calculation of parameters of the injection molding and mold design,
- CAD/II module for the final mold modeling (Core and Cavity design and the design of all residual mold components).

CAD/I module is the first module in an interactive CAD/CAE system for a mold design. This module is used for generating the CAD model of the plastic products. The

result of this module is a solid model of a plastic part with all necessary geometrical specifications. CAE/I module is utilized for the numerical simulation of the plastic injection molding. Using Pro/Plastic Advisor, a user can optimize the injection molding parameters and optimize the part geometry and a plastic material. CAE/II module has been developed to solve the problem of a mold thermal, rheological and mechanical calculations and the mold selection. The next section shows the details of the general structure of the CAD/II module.

3.1. Structure of the CAD/II module

CAD/II module is used for the final CAD modeling of the mold (core and cavity design). This module uses additional software tools for the automation, creating a core and a cavity from the CAD model, including the shrinkage factor of plastic materials and the automation splitting mold volumes of the stationary and movable plates. The product information standard in a CAD/CAE system has different types which deal with the geometry representation, the feature representation and the integrated representation. The integrated representation can incorporate some kinds of non-geometry information, such as expert experience and knowledge, into product modeling, resulting in an efficient manner to realize the intelligence and the automation of a product design and a mold design.

Additional capability of the CAD/II module are software tools that:

- Apply a shrinkage that corresponds to the designed plastic part, geometry, and molding conditions, which have been computed in the CAE/I and CAE/II module for the automation of core and cavity design;
- Make a conceptual CAD model for non-standard plates and mold components;
- Design core and cavity inserts, sand cores, sliders, lifters, and other components that define a shape of a molded part;
- Populate a mold assembly with standard components such as standard D-M-E mold base, and CAD modeling ejector pins, screws, and other components creating the corresponding clearance holes;
- Create runners and waterlines, whose dimensions have been calculated in the CAE/II module;
- Check the interference of components during the mold opening, and check the draft surfaces.

After applying the dimensions and selecting the mold components, the CAD/II module generates a 3D model of the fixed and movable plates. Geometry mold specifications, which are calculated in the CAE/II module, are automatically integrated into the CAD/II module; as a result, the CAD/II outcomes are an assembly of mold plates. Features and specifications of the CAD/II module are as follows: specialized 2D GUI enables the instant customization of a mold base and components; automatic assembly of components – ‘pick and place’; necessary clearance holes, threads, counter bores, etc. are automatically added to plates; part-level features are already fully dimensioned; custom components can be created, saved and reused; mold base consists of „D-M-E“ mold components. The structure of the CAD/II module is presented in the Fig.3.

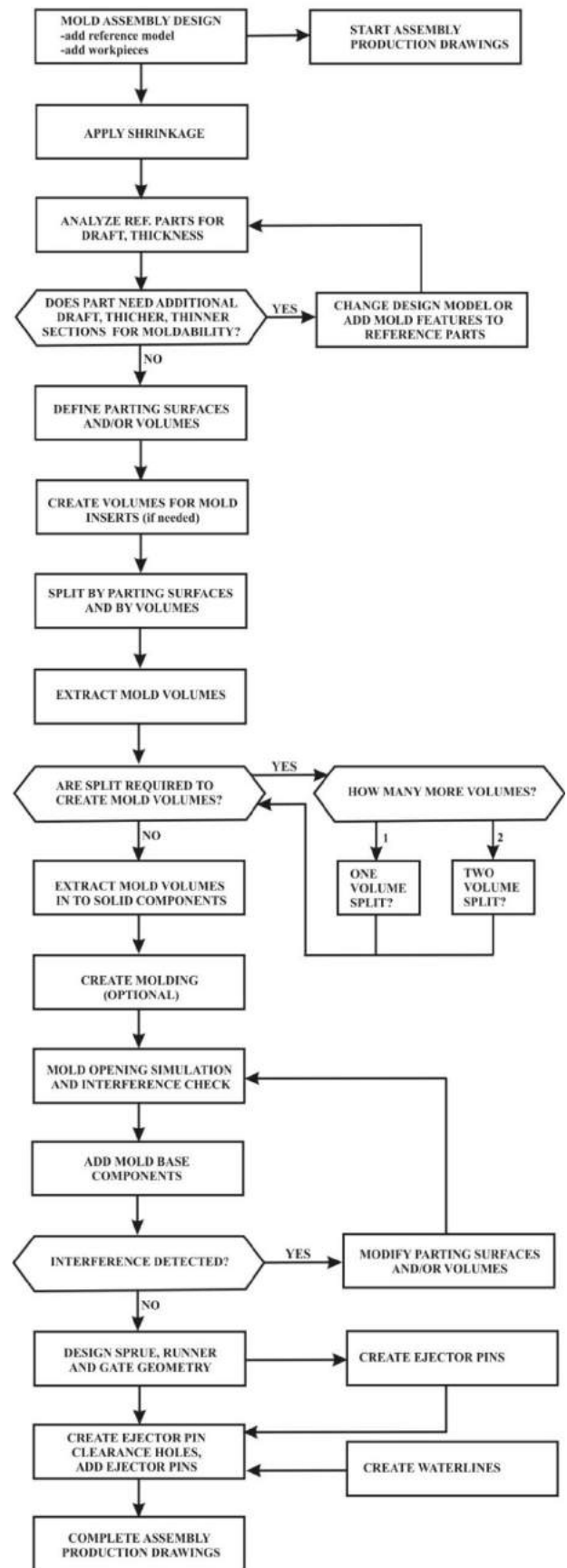


Fig.3. Structure of the CAD/II module

Mold base assemblies and components with automatic functions, such as the on-the-fly customization

component, sizing, placement, trimming, and clearance cut and thread creation, are provided for the following: Complete Mold Base Assemblies, Plates, Leader and Return Pin Assemblies, Locating Rings and Sprue Bushing, Screws and Washers, Automatic Drawing, and BOM Creation. The drawings of the mold assembly and plates, completed with hole charts, are created automatically. Mold opening simulation, completed with the slider and ejector simulation is created automatically.

4. CONCLUSION

Completing the mold design stage in the shortest possible time is the goal of every mold designer. Design automation substantially increases the overall efficiency of the design process, reducing the occurrence of the design flaws as well as the time-to-market reduction. An interactive CAD/CAE system proves to be a confident software tool for the plastic industry for the injection molding dental parts whose material is an integral part of the plastic material database. All modules of the CAD/CAE system are 3D solid-based, feature oriented, and parametric. Plastic flow simulation product is in the CAE/I and allows engineers to determine the injection molding parameters. CAD/II module also enables engineers to capture their own unique design and best practices directly within the database components. The module for the calculation of the mold specification and the parameters of injection molding (CAE/II) improves the design efficiency, reduces the mold design errors, and provides the full information needed for the mold selection. The future work of this research can focus on two issues. The first one is to analyze the market to define which plastic parts used in dental laboratories are in deficit and to determine the commercial for the injection molding in the Serbian industry. The second one are research possibilities for the full application of an interactive CAD/CAE system for the mold design for plastic parts, which is used in the dentistry.

REFERENCES

[1] DENG, Y.M., Lam, Y.C., Tor, S.B., Britton G.A. (2002) *A CAD-CAE Integrated Injection Molding Design System*, International Journal of Engineering with Computers, Vol.18, pp 80-92

[2] CHAN, WM., YAN, L., XIANG, W., CHEOK, BT. (2003) *A 3D CAD knowledge-based assisted injection mould design system*, International Journal of Advanced Manufacturing Technology, Vol.22, pp 387–395

[3] HODOLIC, J., MATIN, I., HADZISTEVIC, M., KOVACEVIC, I., KURIC, I. (2008) *Mold Design and Simulation of Plastic Injection Moulding Process in CAD/CAE software*, Proceedings of 10th International Conference on Mechanical Engineering.

[4] HODOLIC, J., MATIN, I., HADZISTEVIC, M., VUKELIC, DJ. (2009) *Development of Integrated CAD/CAE System of Mold Design for Plastic*

Injection Molding, International Journal of Materiale Plastique, Vol. 46, No 3, pp. 236-242

- [5] HODOLIC, J., MATIN, I., VUKELIC, DJ., ANTIC, A. (2006) *Using Complex Surfaces for Core and Cavity Design of mold*, Proceedings of 7th International Scientific Conference, University of Kosice, Slovakia, 2006.
- [6] KONG, L., FUH, J. Y. H., LEE, K. S., LIU, X. L., LING, L. S., ZHANG, Y. F., NEE, A. Y. C. (2003) *A Windows-native 3D plastic injection mold design system*, Journal of Materials Processing Technology, Vol. 139, pp 81-89
- [7] LOU, Z., JIANG, H., RUAN, X. (2004) *Development of An Integrated knowledge-based System for Moldbase Design*, Journal of Material Processing Technology, Vol.150, pp 194-199,
- [8] LOW, MLH. LEE, KS. (2003) *A parametric-controlled cavity layout design system for a plastic injection mould*, International Journal of Advanced Manufacturing Technology Vol. 21, pp. 807–819
- [9] LOW, MLH., LEE, KS. (2003) *Application of standardization for initial design of plastic injection moulds*. International Journal of Production Research Vol.41, pp 2301–2324.
- [10] LOW, MLH., LEE, KS. (2004) *3D rapid realization of initial design for plastic injection moulds*, Journal of Institution of Engineers Singapore, Vol. 44., pp 15–30
- [11] MA, Y.S., TOR, S.B., BRITTON, G.A. (2003) *The development of a standard component library for plastic injection mould design using an object-oriented approach*, International Journal of Advanced Manufacturing Technology, Vol.22, pp 611-618.
- [12] MATIN, I., HODOLIC, J., BUDAK, I. (2004) *Injection moulding simulation in the automated product designing systems*, International Journal of Simulation Modeling, Vol.3, pp 69-79
- [13] MATIN, I., HADZISTEVIC, M., HODOLIČ, J., VUKELIĆ, DJ., TADIĆ, B. (2010) *Development CAD/CAE system for mold design*, Journal of Production Engineering, Vol.12, No 1, pp 222-225
- [14] MOK, C.K., CHIN, KS., HO, J.K.L. (2001) *An Interactive Knowledge-Based System for Mould Design in Injection Moulding Processes*, International Journal of Advanced Manufacturing Technology, Vol.17, pp 27-38.

ACKNOWLEDGMENTS

Results of the investigation presented in this paper are a part of the research realized in the framework of the project “Research and Development of Modeling Methods and Approaches in the Manufacturing of Dental Recoveries with the Application of Modern Technologies and Computer Aided Systems”– TR-035020, financed by the Ministry of Education and Science of the Republic of Serbia.



34th INTERNATIONAL CONFERENCE ON
PRODUCTION ENGINEERING
28. - 30. September 2011, Niš, Serbia
University of Niš, Faculty of Mechanical Engineering



VIRTUAL MANUFACTURING – ADVANCED MANUFACTURING EXAMPLES

Miroslav PILIPOVIĆ¹, Ivan DANILOV², Nikola LUKIĆ³, Petar PETROVIĆ⁴

University of Belgrade, Faculty of Mechanical Engineering, Kraljice Marije 16, Belgrade, Serbia
mpilipovic@mas.bg.ac.rs, idanilov@mas.bg.ac.rs, nlukic@mas.bg.ac.rs, pbpetrovic@mas.bg.ac.rs

Abstract: *Virtual manufacturing as concept applied in the design of advanced manufacturing systems, enables realization of manufacturing processes in synthetic computer environment in the same way as under real conditions. The paper describes the concept and architecture of the Control-Centered virtual manufacturing environment defined by integration of different tools for products, manufacturing processes and manufacturing resources modeling. The applications of developed concepts and environment for the advanced manufacturing system modeling are also given with an example of the robotized welding and industrial and truck tires manufacturing.*

Key words: *Virtual manufacturing, Robots, Welding, Tires manufacturing*

1. INTRODUCTION

The globalization of the market of today requires the manufacture of increasingly complex products, with a great range of project design variants to adjust with and meet the specific needs of the end buyer. This imposes the need for as short as possible manufacturing cycle, as well as the distribution of design, development and manufacturing tasks to several geographically distant sites. In order to achieve success in this context, manufacturing company need to develop capabilities to quickly respond to customers needs and to make correct decision as earlier as possible during the product development process. Advanced manufacturing systems, however, require an increasing use of computer for accomplishing of a large number of activities for computer information processing, CAD/CAM or process control. Such intensive changes in the field of manufacturing and computer technologies demand continuous development of existing concepts and the creation of new concepts. In the design field a new concept is being defined - Virtual Manufacturing (VM). This paper presents the concepts and architecture of the virtual manufacturing environment, developed in the last ten years for domestic industry. The applications of developed concepts for the pellet stove robotized welding and industrial and truck tires manufacturing are given.

2. VIRTUAL MANUFACTURING AND INDUSTRY

Leading industries in many sectors use VM to support many of the stages of their product development process. Automotive industries identified very early VM as the emergency technology. For example, USCAR (United States Council for Automotive Research) in the project PNGV (Partnership for the new generation of vehicles) identified in advanced manufacturing technology, among all, agile manufacturing, rapid prototyping and virtual

manufacturing as technological areas where improvements and innovation are needed [1]. Exactly, VM has its roots in the automotive industry, where the need to shorten time to market, reduce costs, and improve product quality are especially acute, and today is being widely used in the worlds leading automobile manufacturers.

In the last ten years, there are lot examples of the research in areas of VM from major automakers [2]. One of the examples is DaimlerChrysler, which announced its Digital Factory plans, a project to reducing the company s new-vehicle cycles by up to 30%. DaimlerChrysler began using the Digital Factory approach as part of the project to build new engine-manufacturing plant in Koellada, Germany (February 2002). Basic of the project is the simulation of the entire production process – from initial drawings of facilities to final functioning assembly line, with plan to design, retrofit all of its plants by 2005. Another example is car company Rover. Rover has introduced an electronic build (E-build), process that enables prototype vehicles to be built, component-by-component, in the virtual world. During the E-build process, a multi-disciplined team of engineers and managers meets in specially built E-Build Theater where they don stereoscopies glasses to view the assembly process in full 3D stereo.

Others industry see the benefits of technology and today customers of VM includes most of the world leading manufacturers in the aerospace, automotive, electronics, and heavy machinery industries.

At the same time, there are trends for fundamental changes and transformation of the manufacturing industry from traditional, vertically integrated value-chain to collaborations between specialized independent companies. These trends are resulting in global manufacturing virtual networks and the meaning of 'virtual manufacturing' has been extended to signify inter-firm relationships used to form a temporary supply chain [3].

¹Prof. dr Miroslav Pilipović, ²M.Sc. Ivan Danilov, ³M.Sc. Nikola Lukić, ⁴Prof. dr Petar Petrović
University of Belgrade, Faculty of Mechanical Engineering, Kraljice Marije 16, Belgrade, Serbia

In production engineering, virtual manufacturing concept is used in design of complex advanced products. For example, in [4], a virtual machine tool is defined as a complex mechatronical system and the paper presents the design, analysis, optimization and operation of machine tools in virtual environment. The concept is complex and includes kinematics, dynamics, Finite-Elements-Analysis, optimization of structural components and coupled simulation of structural dynamic and control loops of machine tools, simulation of CNC control with a virtual model, NC-path simulation, optimization of NC programs for five-axis machines, simulation of metal cutting processes and integrated simulation at the machine and process.

3. VIRTUAL MANUFACTURING DEFINITIONS

According to the professional literature virtual manufacturing (VM) system may be defined in several ways. According to [5], this concept executes and estimates manufacturing processes in computers, without the use of real facilities. Computer system entitled as "virtual and informational system" simulates real and information system, and generates control commands for the real and physical system. On the basis of an analysis dealing with the information dependence between the tasks, [5] proposes that VM system architecture should be defined with seven types of the following activities: device model preparation, service development, virtual shop floor definition, operation definition, product handling, virtual shop simulation and simulation interface. The core idea of the other concept given by [6] is that a parallel to the real world of CIM enterprise is a modeled virtual world comprised from product model, virtual prototype model, manufacturing resource model and manufacturing environment model. According to [7] VM system is an integrated, synthetic manufacturing environment, whose purpose is to enhance all levels of decision and control comprising design-centered VM, production-centered VM and control-centered VM. According to [8], virtual manufacturing proposes the creation of a synthetic and integrated environment, composed by many software tools and systems as simulation and virtual reality (VR), offering turnkey solutions for the entire product development process from design to manufacturing. VM represents an important step toward the factory of future providing ability to make changes in a virtual environment, saving money and time, and resulting in better design.

As with most emerging technology, VM goes by many names: digital factory, digital plant, digital manufacturing, virtual factory, and others; some experts feel the term computer-aided production engineering (CAPE) is perhaps best. Just as an integrated CAD/CAM/CAE system can allow an organization to make a change in one place, VM permits production engineers to study the effects of the change, whether they are made in an individual operation, or the entire facilities, or even in the CAD model.

4. APPROACH OF CONTROL-CENTERED VIRTUAL MANUFACTURING

Three paradigms defining specific view of the VM, were proposed at the "Virtual Manufacturing User Workshop" held in Dayton, Ohio on 12-13 July 1994 and published in the "Technical Report, Compiled and Edited by Lawrence Associates Inc." These three paradigms, Design-Centered VM, Production-Centered VM and Control-Centered VM, have been analyzed in more detail by other authors as well, and particularly in [7]. Design-Centered VM uses manufacturing-based simulation to optimize the design of products and processes for specific manufacturing goals such as: design for assembly, quality, lean operations, and/or flexibility. Production-Centered VM provides an environment for generation of process plans, production plans and resource requirement planning. Simulation is used to allow inexpensive, fast evaluation of many processing alternatives. Control-Centered VM provides information for optimizing manufacturing processes and improving manufacturing systems with the use in simulation of control models and actual processes as well. Taking into consideration the above mentioned paradigms with further development of virtual manufacture for extended CIM enterprise [9], the authors of this paper have built the concept and the architecture of control-centered VM.

The basic concept of this model illustrated in Figure 1 was made with IDEF0 methodology for functional modeling. The main inputs are product and process models. For the established production planning/scheduling model different variants of shop floor and machine control models may be defined and modeled, so that control optimization elements (control strategy, process performances and possible shop floor layout) may be obtained through distributed simulation process. For this model, in agreement with the previous concept, detailed architecture and functional models of the control-centered virtual manufacturing system are defined in several MSc and PhD thesis.

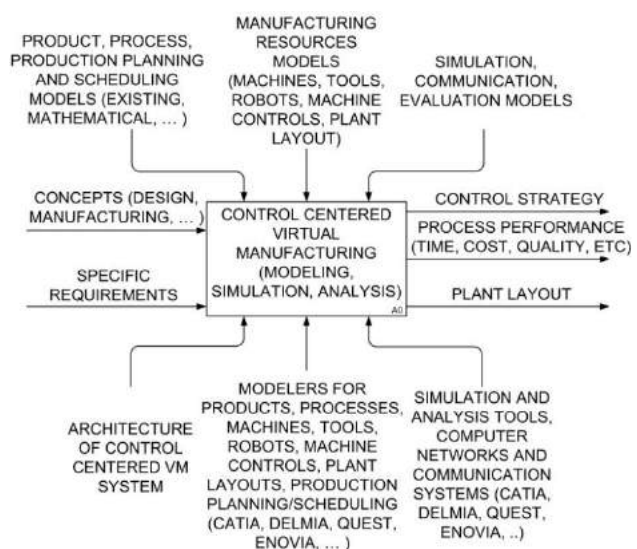


Fig. 1. Control-centered VM concept

5. VIRTUAL ENVIRONMENT FOR ADVANCED MANUFACTURING - EXAMPLES

According to the basic functional concept (Figure 1), activities and life cycle of the virtual manufacturing system are modeled. Four stages are defined: product design, processes planning, manufacturing resources modeling, simulation and analysis.

Main supports of the presented concept are modelers for the system components. The "big four" CAD/CAM/CAE/PDM vendors--Dassault Systems/IBM Corp., Parametric Technology Corp. (PTC), SDRC, and Unigraphics Solutions Inc.--all claim to offer "design-through-manufacturing solutions." As such, all have ties into the virtual manufacturing world [10].

According to that, virtual products, virtual processes and virtual resource are mainly modeled using standard advanced CAD/CAM/CAE systems (Catia [11] and Reengineer), with models based on STEP and other data files types. In same case own developed software was used. For further developing of the system, other software tools will be used (Delmia, Enovia, Quest, etc.). Examples are made for the advanced manufacturing automation, Automotive, Aerospace's and other manufacturing industries in several projects.

This paper presents the modeling of virtual manufacturing heat exchanger for pellet stoves and modeling the plant for industrial and truck tires manufacturing.

The modeling of virtual products is first phase in realization of the virtual manufacturing for pellet stove heat exchanger. Main components of the pellet-stove heat exchanger are: base, bottom, special mounts and ribs. Without entering into detail about design, in the Fig. 2 Catia 3D model for the pellet stove heat exchanger is given and exploded view in the Fig. 3.

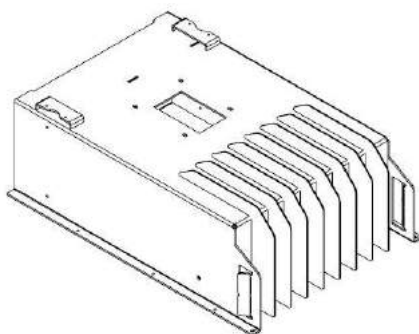


Fig. 2 Pellet stove heat exchanger

All parts are obtained by cutting on the machine for laser cutting, and then bent on the press. After that, the worker put all the pieces together. The special grooves on the parts help him to do the job much easier and efficient. The robot Yaskawa Motoman SAA2000 is used for welding heat exchanger subassembly in two operations. The robot is equipped with a special gooseneck that gives it much more freedom in positioning and orientation. Utilizes a MIG welding process. We have two robotic welding operations: outer welding to fix the base with the bottom, special mounts and ribs and inner welding to enforce the

base with bottom. Fig. 4. presents simulation of outer robotized welding.

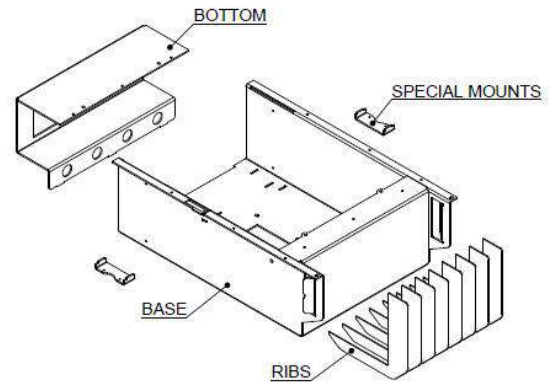


Fig. 3. Pellet stove heat exchanger – exploded view

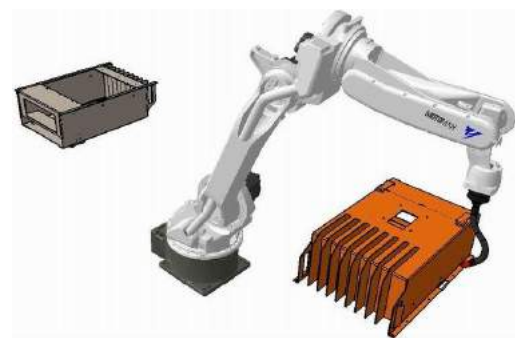


Fig.4. Outer robotized welding of the heat exchanger

Virtual Programming is used for programming robot for welding. All welds are defined in the 3D CAD model of the heat exchanger subassembly. In NRL Teach (Native Robot Language Teach box) robot is virtually programmed for welding of all defined welds. Positions and welding speed are set here as well Simulation of robotic welding is used to verify the existence of the collision, and then export program in the programming language for the specific control unit. Example of the dialogues in the robot programming is given in Fig. 5.

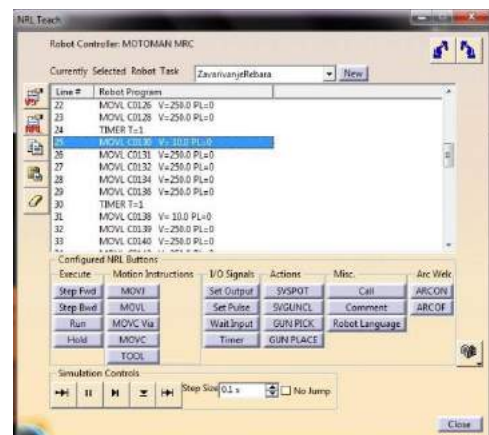
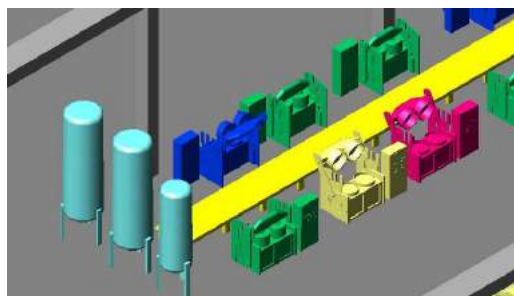


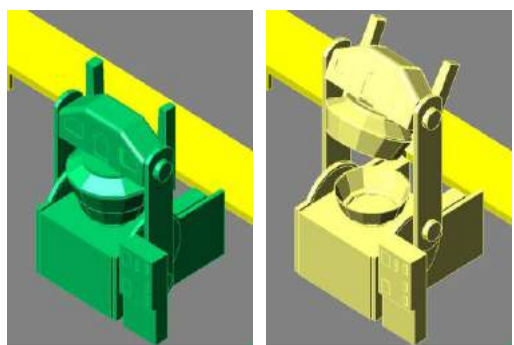
Fig. 5. Robot programming dialogues

The other approach, with special own developed software, was applied in modeling virtual manufacturing for the

industrial and truck tires manufacturing. Example is the plant for elastomer (rubber) vulcanization. Digital model of the manufacturing plant is build with the main goal – optimization, control and monitoring of the vulcanization process and reduction of the energy consumption [12]. Developed system is complex and contains: special developed SCADA system, process parameters data base, dynamic graphical interface, 3D manufacturing resources models (vulcanization presses, transport system, energy flow, etc.), plant layout and MMI interface. The example of the plant model and the vulcanization presses detail models are shown in Fig. 6. The entire virtual models are developed in AutoCAD environment using AutoLISP functions.



a) Part of the plant layout



b) Vulcanization press model

Fig. 6. Example of the plant layout modeling

6. CONCLUSION

The new paradigm in the design of advanced manufacturing systems - virtual manufacturing is presented in the paper with examples of applied concepts, research and development in the world. It is emphasized that the virtual manufacturing, by definition, is a great challenge and of great importance for production engineering. Different virtual environment and the software tools where used for the particular cases. For example, modeling of virtual manufacturing of the heat exchanger for pellet stoves uses the standard CAD/CAM systems for products and processes modeling, Application for the elastomer vulcanization plant use different CAD system and AutoLISP function together with the object oriented programming languages and standard data base systems. These experiences open the problem of the integration of different software tools and virtual environments subsystems. The further research will be

directed to the integration of current and new technologies in integrated virtual environment solutions.

ACKNOWLEDGMENT

We wish to thank to the Ministry of Science and Technological Development of the Republic of Serbia for their support of this research undertaken within the project 35007.

REFERENCES

- [1] USCAR (1997) *Partnership for the New Generation of vehicles - Technology Areas*, United States Council for Automotive Research - USCAR, www.uscar.org,
- [2] HOFFMAN, T. (2002) *Automakers Goes Digital*, *Computer World*, Vol. 36, Issue 49, pp 1-2.
- [3] SHI, Y., GREGORY, M. (2005) *Emergency of Global Manufacturing Virtual Network and Establishment of New Manufacturing Infrastructure for faster Innovation and Firm Growth*, *Production Planning & Control*, Vol. 16, No 4, pp 621-631.
- [4] ALTINTAS, Y., BRECHER, C., WECK, M., WITT, S., (2005) *Virtual Machine Tool*, *Annals of the CIRP*, Vol. 54/2, pp 115-138.
- [5] IWATA, K., ONOSATO, M., TERAMOTO K., OSAKI, S. (1997) *Virtual Manufacturing Systems for Integrating Manufacturing Resources And Activities*, *Annals of the CIRP*, Vol. 46/1, pp 335-338.
- [6] KIMURA, F. (1993) *Product and Process Modeling as a Kernel for Virtual Manufacturing Environment*, *Annals of the CIRP*, Vol. 42/1, pp. 147-150.
- [7] LIN, E., MINIS, I., NAU, D., REGLI, W. (1995) *Contribution to Virtual Manufacturing Background Research Phase I & Phase II, Final Report*, Institute for System Research - University of Maryland.
- [8] SOUZA, M., PORTO, A., SACCO, M. (2006) *Virtual manufacturing as a way for the factory of the future*, *J. Intelligent Manufacturing*, Vol. 17, pp 725-735.
- [9] PILIPOVIĆ, M., SPASIĆ, Ž (2006) *Virtual Environment for Extended CIM Enterprise*, *Proceedings of the 18 International Conference on Material Handling, Construction and Logistics*, Belgrade, Faculty of Mechanical Engineering, pp 289-292.
- [10] MILLS, R., SCHMITZ, B. (1998) *Manufacturing Goes Virtual*, *Computer-Aided Engineering*, Vol. 17, Issue 12, pp 30-34.
- [11] DASSAULT SYSTEMS (2003) *Catia Version 5 Release 11 - Documentation*, Dassault Systems.
- [12] PETROVIĆ, P., JAKOVLJEVIĆ, Ž., MIKOVIĆ, V. (2008) *Real Time Interactive Monitoring and Control of Enterprise Production Resources Based on Dynamical 3D Virtual Model*, *Proceedings of the 34. Jupiter Conference*, Belgrade, Faculty of Mechanical Engineering, pp 4.28-4.34.

34th INTERNATIONAL CONFERENCE ON PRODUCTION ENGINEERING



SECTION F

EDUCATION IN THE FIELD OF PRODUCTION ENGINEERING
ENGINEERING ETHICS
PRODUCT DEVELOPMENT – PRODUCT DESIGN
PRODUCTION SYSTEM MANAGEMENT
REVITALIZATION, REENGINEERING AND MAINTENANCE OF MANUFACTURING SYSTEMS

MANUFACTURABILITY ANALYSIS OF DIE-CAST PARTS

Miloš RISTIĆ¹⁾, Miodrag MANIĆ²⁾, Boban CVETANOVIĆ¹⁾

¹⁾ Higher Technical School of Professional Studies – Niš, Aleksandra Medvedeva 20, 18000 Nis, Serbia

²⁾ Faculty of Mechanical Engineering, University of Niš, Aleksandra Medvedeva 14, 18000 Nis, Serbia
milos.ristic@vtsnis.edu.rs, miodrag.manic@masfak.ni.ac.rs, boban.cvetanovic@vtsnis.edu.rs

Abstract: Manufacturability analysis of a product is used at early stages of a design process in order to assess the possibilities of product realization, reduce the number of design iterations, thus also reducing the cost. One of the conditions for the automated manufacturability analysis is parametric modeling and feature-based design. This paper presents the concept of the system for the manufacturability analysis of die-cast parts. It presents the way to create knowledge basis containing recommendations and restrictions used for die-casting of a part. The paper also describes advice CA system gives the designer during the design process by means of which the design process itself is upgraded and the concurrent engineering environment is created.

Key words: manufacturability analysis, die-casting, part attributes, feature recognition.

1. INTRODUCTION

Die-casting is a method of producing finished castings by forcing molten metal into a hard metal die, which is arranged to open after the metal has solidified so that the casting can be removed (Fig.1).

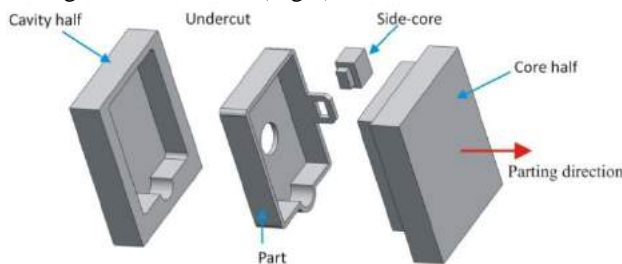


Fig. 1. Die-casting process terminology

Die-casting is a ‘near net shape’ manufacturing process extensively used for realizing quality products required in many engineering applications [1]. Advantages of die-casting process are higher production rate, lower cost, better quality and process automation. A part to be made with die-casting should be designed keeping in mind many process considerations. Involving production engineers in the product development during the design phase is the process of concurrent engineering which has the aim to get critical suggestions and advices related to part design which is, in fact, manufacturability analysis. Industries today are striving to achieve lower product development time, higher productivity and efficiency. In large enterprises, where design and manufacturing personnel may be stationed at different locations, the concept of Design for Manufacture (DFM) is preferred [2]. Implementing DFM will have the benefits of improved manufacturability of product design, shorter time-to-market and reduced cost. Three areas where DFM can be applied are: Verification; Quantification and Optimization [3]. Gupta et al [4] have classified DFM into

direct or rule based approaches. In rule based approach, rules are used to identify design attributes which are beyond process capabilities, while in direct based approach the first step is to generate feasible process plan and to find most suitable plan in order to reduce time or cost. Shah and Wright [5] have identified DFM metrics which include qualitative (good practice rules etc.) and quantitative (cost and time estimates etc.) methods. Most of the work in DFM has been done in the machining [4,6] or sheet metal processing [7,8] domain, while little attention has been given to die casting. In die-casting, implementation of DFM is important as production lead times are significantly longer. This is due to greater number of iterations required between design and manufacturing teams; die design and manufacturing, and process simulation and testing are required before production is started [1]. Certain progress in reducing production lead time has been achieved in the area of mold design. [9, 10]. Manufacturability analysis of feature based model has great importance during virtual product development [11].

2. FEATURE-BASED DESIGN AS A PREREQUISITE FOR MANUFACTURABILITY ANALYSIS

Manufacturability analysis requires the application of feature-based modeling techniques which, besides geometrical descriptions, contain technological recommendations and restrictions [12]. Depending on the manufacturability analysis moment, two approaches can be defined: analysis during the design process itself (on-line); analysis done upon the completion of the constructing process (off-line).

If the term “feature based design” [13] is used and if the product database, in a specific CAD system, is object-oriented, then we can perform on-line analysis. One of the

possible ways to do it is to do it during the constructing process, i.e. during the process of inserting certain elements in the product model and to automatically correct inserted value of a certain parameter if necessary. Another approach to manufacturability analysis is the analysis after the design process completion. Using this approach the whole product model would be analyzed and, if certain illogicalities are observed the report could be sent to the designer. This report may take the form of a warning, or alternatively the model could be changed and this changed model sent back to the designer. This off-line analysis approach is implemented using an expert system with the expert shell where, as in the case of an on-line analysis, the product model is object-oriented. Both analyses are based on parametric design and feature based project modeling. In order for a feature to be functional its attributes and characteristics have to be thoroughly described. Feature attributes carry the information about specific feature characteristics important for a current application and they can be determined at different levels- from the feature level, or feature set level to the level of describing part or an assembly [14]. Attributes can also be used to determine characteristics of a relationship between features and feature sets. Feature attributes can be position, orientation, dimensions, shape or tolerances. Assembly attributes can, besides other things, contain the information such as: assembly surface, overlaps/gaps, relative orientation.

3. PROCESS CONSTRAINTS AND DESIGN GUIDELINES

A part to be die-cast should possess certain design characteristics to make it suitable for manufacturing with die-casting process. Following sub-sections elaborate these constraints and guidelines.

3.1 Part Geometry Limitations

Hui [15] has discussed some of the geometric aspects related to mouldability of a part. According to Madan et al [1] some features which cause accessibility problems are not allowed in die-casting. These are explained in the following paragraph with the help of figure 2 (a-f):

- Internal undercuts are not allowed in die-casting.
- Features with reverse draft and void features.
- Partially visible depression features like holes with smaller opening diameter and larger diameter at the base.

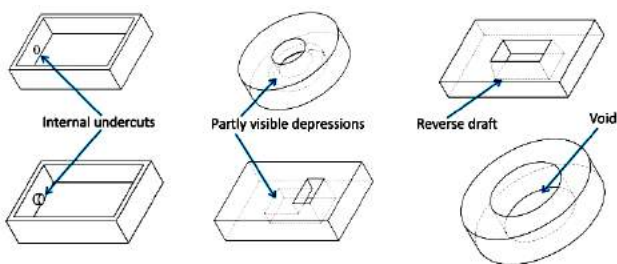


Fig. 2: Part geometrical limitations.

3.2 Overall Part Attributes

Die casting process has limitations on overall part characteristics, such as part weight, surface area, wall thickness, material, size, tolerance and surface finish. These limitations depend on the type of material which makes it necessary for the designer to evaluate part against material specific process constraints. Table 1 shows representative database of material specific process capabilities.

Tab. 1: Die-casting material and process constraints (source: [15, 16])

Attribute		Material			
		Zn	Al	Mg	Cu
Weight (kg)		30	45	16	7
Effective projective area (m ²)		0.77	0.77	0.77	0.77
Recommended minimum wall thickness (mm)					
surface area (cm ²)	<25	0.38-0.75	0.75 - 1.3	1.5-2.0	
	25 - 100	0.75-1.3	1.3 - 1.8	2.0-2.5	
	100 - 500	1.3-1.8	1.8 - 2.2	2.5-3.0	
	500 - 2000	1.8-2.2	2.2 - 2.8	-----	
	2000 - 5000	2.2-4.6	2.8 - 6.0	-----	
Minimum wall thickness		6	6	6	6

3.3 Good practice rules

There are certain rules in die-casting part design which should be followed in order to make a good part. There are many such good practice rules, some of which are shown in Figure 3.

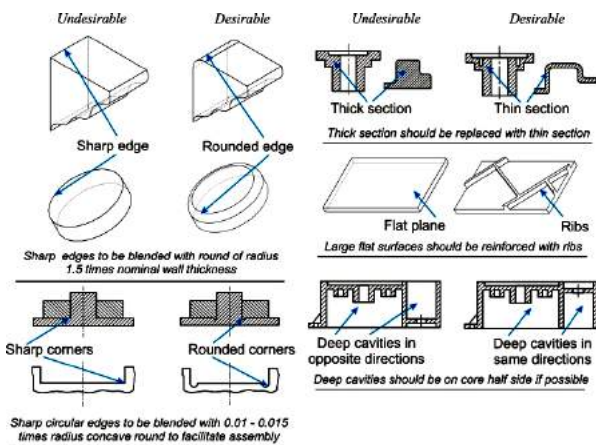


Fig. 3: Good practice rules in die-casting (Source: [16, 17]).

3.4 Manufacturability of Individual Features

Some recommendations regarding individual feature characteristics in die-casting should be followed in order to make a good part. Design rules for ribs in die-casting, limitations on hole diameter and their relationship with core length, as well as tolerance limitations for a die-casting part, are described in the following sections of this paper.

4. PART ATTRIBUTES AND FEATURE RECOGNITION

Feature recognition is a key for automation of any automated manufacturability evaluation system and that also applies to die-casting process [1]. Geometric reasoning or feature recognition rules are applied to get and store required information of die-casting features. Feature recognition is done in following domains: Non-manufacturability features, Features requiring side-cores, Part attributes, Wall thickness, Sharp edges, and Rib features.

Any features or regions of the part which pose molding tool disengagement problems are identified so that same can be reported to the designer. Side-core diameter and maximum length limitations depend on the type of alloy used. Recommended tolerances for die-casting part [16,17] also depend on material.

During manufacturability analysis of die-casting parts, determination of parting direction is important for identifying those die-casting features which require a side-core for molding.

Overall attributes of the part such as volume, surface area are directly extracted from the part CAD model, while tolerance and surface finish evaluation is performed interactively because of non availability of this data in machine readable format.

It is important to identify regions of the part which violate thickness constraints like minimum and maximum allowed wall thickness and even sharp thickness variations [18]. It is very critical in die-casting process to obtain parts with uniform wall thickness and smooth variations.

Die-casting process requires that, as much as possible, sharp edges be rounded or smooth, therefore the process of edges identification is important in the whole manufacturability analysis assessment. It is important to identify both sharp edges and smooth edges with insufficient round radius.

Rib features are those protrusion features in die casting which have wall thickness comparable to the nominal wall thickness and much larger length.

Taking into consideration part attributes and feature recognition, we can create rules and give advices to the designer. Depending on the available computer aided systems for manufacturability analysis, we opted to include necessary rules into parametrically designed gear housing (fig. 4).

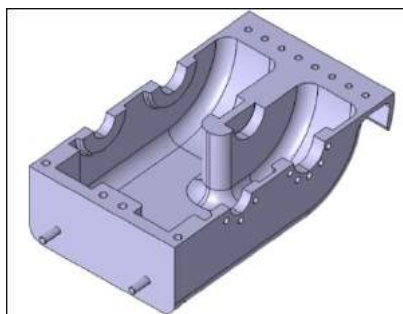


Fig. 4: Parametrically designed redactor housing.

Considering the fact that during the parametric designing each feature was defined and related, we can include adequate relations. This was done by defining features

using CATIA V5 (Knowledgeware) software. Using CAX Template, which contains information and inserted knowledge necessary to the expert, we define Knowledge Embedded Template – KET [19]. For example, sharp corners are undesirable because they become a localized point of heat and stress built-up in the die steel, which can cause die cracking and early failure. This is done by using rounding off sharp edges of the part. Manufacturability restrictions are directly inserted in parametrically designed product model in the form of rules. Radius of this round depends on the wall thickness of the part and is generally 1.5 times wall thickness. This rule can be of a great importance when a designer modifies parametrically defined product. If he wants to change radius user defined feature at the same time keeping the wall thickness, he will get an advice stating “radius r_2 should be 1.5 times greater than the wall thickness”.

The rule was inserted in CATIA V5 Knowledgeware in the following form:

```

If 'Fillet_Radius_Value' < '1.5*Wall_Thickness'
{
    Message (“Radius should be 1.5 times greater
    than the wall thickness !
    Modify a parameter according to the rule.”)
}

```

And as such was tested at a redactor housing. The figure 5 presents the advice in the form of information given by knowledgeware to a user who wants to change the described radius outside restrictions.

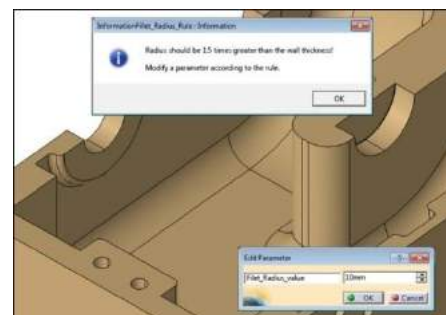


Fig. 5: Knowledgeware gives advice on the basis of previously defined rule.

Knowledge based technologies enable a user to define object-oriented product model and to include material characteristics, technological process requirement, standards and rules necessary for rule based design. It is important to note that these rules are not unchangeable, but can be customized to a user.

If we use relational dependency to connect, for example, rib thickness with the wall thickness and set the requirement using if/then relations to emphasize that the rib thickness has to be equal to the wall thickness, we get manufacturing restriction that a designer will use as an advice during product designing (Tab. 2).

Previously stated rule, along with some other rules, were described in table 2 where manufacturability evaluation of each rule was also described. In addition, adequate advices were given in order to help designer during the continuation of product development.

Tab. 2: Part manufacturability evaluation and advice.

Part attribute / feature	Manufacturability evaluation and advice
Weight: 4.12 kg	Is within limits of process.
Maximum wall thickness: 30mm	Maximum wall thickness should be reduced below 6.3 mm.
Number of side-cores: = 4	Number of side-cores required is high and should be reduced.
Rib with = 8mm	Thickness of the rib is high and should be made equal to wall thickness.
Sharp edges	Sharp edges in the part should be rounded or smoothed.

Nowadays, different methods [20] are developed for assessing manufacturability of parts created during die-casting process.

1. CONCLUSION

Specificities of die casting processes and the available resources have to be taken into consideration during manufacturability analysis and presented to the designer in the form of either on-line or off-line advices, depending on the chosen process chosen. Previously presented on-line process is parametrically modeled part with inserted rules according to the if/then relations. The advice designer gets is the result of the set of experiential rules (examples of good practices) inserted during previous phrases of project design. Advice received aims at final product being produced more easily, distributed more cheaply, at the same time following the product life-cycle.

In general, working with knowledgware systems provides control and monitoring reduction during designing process and unites product development phases raising a concurrent engineering to a higher level, which is extremely important in terms of manufacturability.

ACKNOWLEDGEMENT

This research is sponsored by the Ministry of Science and Technology of the Republic of Serbia - project id III 41017 for the period of 2011-2014.

REFERENCES

[1] MADAN, J., RAO, P.V.M., KUNDRA, T.K. (2007) *Computer Aided Manufacturability Analysis of Die-cast Parts*, Computer-Aided Design & Applications, Vol.4, Nos. 1-4, pp 147-158.

[2] BOOTHROYD, G., DEWHURST, P., KNIGHT, W., (1994) *Product Design for Manufacture and Assembly*, Marcel Dekker Inc., New York.

[3] VAN VLIET, J. W., VAN LUTTERVELT, C. A., KALS, H. J. J., (1999) *State of the art report on design for manufacturing*, Proceedings of ASME DETC, September 12-15, Las Vegas.

[4] GUPTA, S. K., DAS, D., REGLI, W. C., NAU, D. S., (1997) *Automated manufacturability analysis: A survey*, Research in Engineering Design, 9(3), pp 168-190.

[5] SHAH, J. J., WRIGHT, P. K., (2000) *Developing*

theoretical foundations of DFM, DETC2000/DFM 14015, September 10- 14, Baltimore, MD.

[6] SRIKUMARAN, S., SIVALOGANATHAN, S., (2005) *Proving manufacturability at the design stage using commercial modeling software*, Computer-Aided Design and Applications, 2 (1-4), 507-516.

[7] RAMANA, K. V., RAO, P. V. M., (2005) *Automated manufacturability evaluation system for sheet metal components in mass production*, International Journal of Production Research, 43 (18), pp 3889–3913.

[8] ZHAO, Z., SHAH, J. J., (2005) *Domain independent shell for DFM and its application to sheet metal forming and injection molding*, Computer-Aided Design, 37, pp 881–898.

[9] SONG, I. –H., PARK, J. –M, CHUNG, S. –C, (2005) *Web based interference verification system for injection mold design*, Computer-Aided Design and Applications, 3 (1-4), pp 129-138.

[10] NI, Q., LU, W. F., YARLAGADDA, P.K.D.V., (2006) *A PDM-based framework for Design to Manufacturing in mold making industry*, Computer-Aided Design & Applications, Vol. 3 Nos. 1-4, pp 211-220.

[11] MANIĆ, M., MILTENOVIĆ, V., STOJKOVIĆ, M., BANIĆ, M., *Feature Models in Virtual Product Development*, Strojniški vestnik - Journal of Mechanical Engineering 56(2010)3.

[12] SHUKOR, S.A., AXINTE D.A. (2009) *Manufacturability analysis system: issues and future trends*, International Journal of Production Research, Vol. 47, No. 5, pp 1369-1390.

[13] MANIĆ, M., MILTENOVIĆ, V., STOJKOVIĆ, M., *Feature Models in Virtual Product Development*, The scientific journal FACTA UNIVERSITATES, Ser. Mechanical Engineering, Vol. 1, No 10, p.p. 1327-1337, 2003, 2003.

[14] STOJKOVIĆ, M. (2010), *Analysis of the Manufacturability Parameters Based on Semantic Structures of the Digital Product Model*, Doctoral dissertation, Faculty of Mechanical Engineering, Niš.

[15] HUI, K. C., (1997) *Geometric aspects of the mouldability of parts*, Computer aided design, 29 (3), pp 197-208.

[16] BRALLA, J.G. (1999) *Design for Manufacturability Handbook*, McGraw Hill, New York.

[17] (1998) *Product Design for Die Casting*, North American Die Casting Association (NADCA), Rosemont, USA.

[18] MADAN, J., RAO, P. V. M., KUNDRA, T. K. (2006) *An automated cost estimation system for die-cast parts*, Transactions of ASME Journal of Computing and Information Science in Engineering.

[19] STOJKOVIC, M., MANIC, M., TRAJANOVIC, M. (2005) *Knowledge-Embedded Template Concept*, CIRP Journal of Manufacturing Systems, Vol.34 No1.

[20] BIDKAR, R. A., McADAMS, D. A. (2010) *Methods for automated manufacturability analysis of injection-molded and die-cast parts*, Research in Engineering Design, Vol. 21, No. 1, pp 1-24.



DESIGN OF MODULAR WHEELCHAIR FOR CHILDREN WITH CEREBRAL PALSY

Sofija SIDORENKO, Jelena MICEVSKA, Ile MIRCHESKI

Faculty of Mechanical Engineering, Sts Cyril and Methodius University, Karpos II bb, Skopje, Republic of Macedonia
sofija.sidorenko@mf.edu.mk, jelena.micevska@gmail.com, ile.mircheski@mf.edu.mk

Abstract: Patients with cerebral palsy have to spend almost all their life in the wheelchair. They need different wheelchairs for inside and outside use. On the other hand, children are growing up and necessity for bigger wheelchairs becomes economic problem. In order to meet the needs of these children we propose a model of adjustable modular wheelchair. Using ergonomic methods and appropriate anthropometric measurements of children we established the ranges of adjustable dimensions for seat for children of age between 7 and 14 years. According to these dimensions a model of an adjustable seat for wheelchair has been made. Using the principle of modularity the seat is designed to be adjustable in several dimensions: seat height, backrest height, headrest height, armrests height and distance and footrests height and distance. The principle of modularity is also applied in the possibility to place the seat on different driving structures. Virtual model of the wheelchair was examined by virtual mannequins.

Key words: anthropometrics, ergonomics, modularity, virtual mannequin, wheelchair.

5. INTRODUCTION

Cerebral palsy is a result of brain injury, which produces impairments of the locomotion system, balance and coordination of the body [1]. Most of the patients with cerebral palsy have different kinds of spasms of the body. Almost all of them are characterized with individual physical and intellectual conditions. Every patient has to be treated with different types of medical treatments. One of the most important treatments is positioning of the patient's body in stable and regular posture. This is possible with a special seat with accessories for stabilization of the patient's body. In most of the cases, these treatments are very successful. Because of this fact, design of the seat is of a great importance for these patients. On the other hand, the fact is that these children are growing up from their birth until the end of teenage, so they need bigger seats almost every year. This is a big economic problem for their families.

The main goal of our research, made in cooperation with "Slavej AD" Center for orthopedic prosthetics from Skopje, was to find the best solution of wheelchair design, in order to meet the needs of the children with cerebral palsy. After the considerable anthropometric and ergonomic researches we propose concept of modular wheelchair consisted of two main parts: seat and driving structure. The advantage of this concept is possibility for combining of seat with different driving structures in order to provide better flexibility of use in different spaces. We also propose modular seat consisted of several adjustable parts in order to follow the changes of the child's body and with possibility to put other accessories for performing different tasks.

2. DESIGN REQUIREMENTS

At the beginning we established the target group of users: children with cerebral palsy on age between 7 and 14 years. We defined that the main purpose of the wheelchair is performing as much as possible activities of the children with cerebral palsy. The main goal of the proposed idea for modular wheelchair is improvement of the life of the children with cerebral palsy.

In order to provide the best solution we made several surveys: survey of the market requirements, anthropometric survey of the target group, survey of the ergonomic requirements.

2.1 Market survey

There are many kinds and types of wheelchairs with different driving systems and different purposes on the market. According to the experience of the staff of "Slavej AD" Center for orthopedic prosthetics from Skopje and medical staff of the Orthopedic Department at the Faculty of medicine in Skopje, we established the design requirements on the base of three different aspects: Medical requirements:

- the wheelchair should provide firm posture of the spine;
- the angle between the body and lower limbs must be 90°;
- the head must have support for obtaining proper position;
- the seat must be soft in order to avoid wounds;
- possibility to add medical treatment accessories;
- dimensions of the seat must be appropriate for the child's dimensions.

Customer requirements:

- low price;
- low weight;
- easy to use;
- easy to put in vehicle;
- easy to change positions;
- easy to disassemble;
- comfortable enough for all day seating;
- possible to use it in different spaces;
- suitable for performing as much as possible activities;
- good and pleasant design;
- possibility to buy and add different accessories for everyday tasks;
- long period of exploitation;
- possibility to change parts because of damaging.

Requirements of manufacturer:

- low production price;
- low market price;
- modular parts for better and easier reparation;
- modular accessories for extra activities which could be sold separately.

2.2 Anthropometric analysis of sitting in wheelchair

In order to solve the problem of seat design it was necessary to make anthropometric analysis of the target group: children with cerebral palsy on age between 7 and 14 years. Definition of dimensions and the ranges of adjustability for all wheelchair parts was the main goal of the anthropometric analysis that we performed. One of the biggest problems was how to find proper sources of anthropometric measurements. There are many anthropometric sources for children without disabilities, but very few for disabled. Because of great variability of dimensions of children with cerebral palsy [3] in different conditions, we decided to use measurements for children without disabilities on age between 7 and 14 years [2]. The measurements found in accepted source are for the 50 percentile children. The fact is that the children with cerebral palsy are usually closer to the lower percentiles, so we accepted data for 50 percentile as appropriate for definition of the seat dimensions and adjustment ranges.

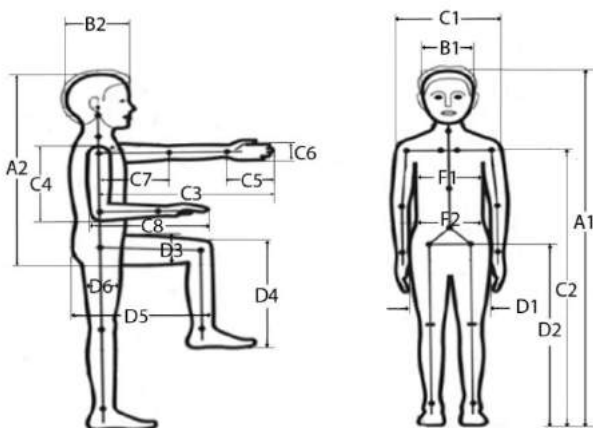


Fig. 1 Required measurements for seat design

Table 1. Estimation of the ranges of adjustability

Kind of measurement	Measure for 7 years old child in cm	Measure for 14 years old child in cm	Difference in cm
A1	1212	1594	382
A2	657	823	166
B1	140	148	8
B2	181	191	10
C1	291	383	92
C2	966	1244	278
C3	488	665	177
C4	245	335	90
C5	132	172	40
C6	61	79	18
C8	317	427	110
C7	193	264	71
D1	223	311	88
D2	618	848	230
D3	100	137	37
D4	372	505	133
D5	388	543	155
D6	105	150	45
F1	186	247	88
F2	187	257	70

According to accepted source [2] of anthropometric measurements, we made table of required measurements for seat design (fig. 1). The first column in Table 1 shows the symbols for different measurements, measurements of 7 old children are in the second column and measurements of 14 old children are in the third column. Differences between the measurements are presented in the fourth column. The differences are actually necessary ranges of adjustability for all required measurements for the seat.

2.3 Ergonomic requirements

As a result of the anthropometric survey we decided to apply the principle of adjustability in order to design seat that could be adapted according to the needs of the patients. Due to the changes of the child's body during the childhood, there is a necessity for more space on the seat, and additional adjustments.

We established ergonomic requirements for the wheelchair and the seat.

Ergonomic requirements for the wheelchair:

- possibility to change driving system:
 - for use at open space - manual system with big wheels or electrical one;
 - for use at home – system with small wheels with appearance like home furniture;
- possibility for having of storage space;
- good suspension system;
- adjustable handles for companion's manipulation.

Ergonomic requirements for the seat:

- the angle between seat and backrest must be 90° (usual active position);
- the seat must have a possibility to change the angle of the backrest in order to provide rest position (90° - 120°);

- the seat must have a possibility to be transformed into support for standing (rotation of the seating surface into vertical position) ;
- the seat must have armrests for placing the arms in rest position;
- the seat must have additional supports from both sides of the chests for providing vertical position of the spine;
- the seat must have foot support for stabilization of the body;
- the seat must have additional support for legs for stabilization of the body in standing position;
- the seat must have additional support between the legs of the patient to prevent of spasms;
- the seat must have headrest with special shape as a support for obtaining proper position of the head;
- the seat must be soft in order to avoid wounds;
- dimensions of the seat must be appropriate for the child's dimensions.

Additional requirements:

- possibility to install small table for performing different activities: writing, drawing, having a meal, working on computer etc.;
- possibility to install additional medical equipment.

3. DESIGN CONCEPT

In order to solve the problem of wheelchair design we applied two main design principles: principal of modularity [4] and principal of adjustability [5].

3.1 Concept of modular wheelchair

The principal of modularity [4] is applied on the main concept, where we propose the wheelchair to be consisted of two main parts: seat and driving structure. We propose three different driving structures: manual with big wheels for outside use, manual with small wheels for inside use and electrical one. The seat has to obtain maximum comfort for the patient. It is independent part that could be placed on any of these structures and it could be also placed on the back seat in any vehicle.

Driving system for outdoor use could be manual or electrical (fig. 2). Driving system for indoor use is usually manual (fig. 3). The design of the whole wheelchair for indoor use should be adapted on the home ambient. This is especially important for the children from psychological viewpoint.



Fig. 2 Seat with driving system for outdoor use



Fig. 3 Seat with driving system for indoor use

3.2 Concept of adjustable seat

Both principals, principal of modularity and principal of adjustability, are applied on the concept of the seat. In order to follow the changes of children dimensions during their childhood, we propose design of modular seat with several adjustable parts: seat, backrest, headrest, armrests and footrests. All of these parts could be adjusted according to the child's dimensions. The other advantage of the applied modularity is possibility to replace parts because of changes in medical treatment, damaging or because of necessity for better one.

The other advantage of the modular adjustable seat is possibility to be transformed into a device for supporting of standing of the disabled child (fig. 4). The best fit of the seat for performing of this function is in combination with driving system for indoors use, because it is usually performed in home environment.

The seating surface must be with maximum width and maximum depth. In order to follow the dimensions of smaller patients the width could be adjusted with armrests position and the depth could be adjusted with backrest position.

Seating surface could be rotated around the axis in the back edge in order to achieve vertical position for obtaining standing position of the patient.

Foot rest must be adjustable along the distance between the set surface and lower foot surface and also the grips for legs.

Armrests must be adjustable in vertical direction and also in horizontal in order to adjust the width of the seat. Headrest must be adjustable in vertical direction.



Fig. 4 Transformation of the seat into standing support



Fig. 5 Seat with additional equipment – table for playing, writing

3.3 Additional equipment

The principal of modularity [4] and adjustability [5] is also applied on the possibility to obtain extra accessories for performing different tasks: having a meal, writing, drawing, playing, working on computer, standing etc (fig. 5, 6, 7). Sometimes there is a need to put additional medical accessories for obtaining stable posture. The advantage is possibility for the users to supply them according to their needs.



Fig. 6 Additional adjustable equipment for leg support



Fig. 7 Additional adjustable equipment for foot support

4. WHEELCHAIR COMFORT EVALUATION

At the end of design process it is necessary to make appropriate evaluation of product. The best way to make evaluation is through real model, prototype. But, there are many software products with virtual mannequins, used mostly in automotive design. We applied one of them in our research in order to check some of the properties of the model in the early phase of design process.

We used software module Human Builder of CATIA to make appropriate analysis. The biggest problem was to find appropriate mannequin because the data base of the software does not have data for children. With comparison of the children data and data for different nationalities and percentiles we found as convenient data for 5th percentile woman from Korea as data for 7 years old child and 50th percentile man from France as data for 14 years old child.



Fig. 8-11 Comfort analyses with Human Builder virtual mannequins

Several important analyses were performed with Human Builder: patients' comfort in the seat (appropriate dimensions), zones of convenient reach, vision zones (fig. 8-11). An analysis of comfort for the companion person's manipulation with the wheelchair was also performed.

5. CONCLUSION

The main goal of presented research was to find the best solution for wheelchair comfort for children with cerebral palsy and obtaining of multifunctional exploitation. For the patient's families this means economic advantage.

The anthropometric and ergonomic researches were of a great importance for the design process. The result was a new modular design of wheelchair. Analyses of the 3D model of designed wheelchair are significant, but they are not viable enough. Our next step will be to make prototype which will be evaluated with real patients.

Our next researches in the field of ergonomic design will be also applied in the area of medical devices for upgrading of life of people with illnesses and disabilities. The principals of modularity and adjustability will also be applied because of their great importance in the serial production.

REFERENCES

- [1] Frischhut B., Krismer M., Butschek R., Luze Th., Gedik A., Haberfellner H., Orthopedic Treatment in Infantile Cerebral Palsy, Paediatrica Paedol 30, 1995, pg.23-27
- [2] Tilley A., Henry Dreyfuss Associates: The measurements of man and woman: Human factors in design, Whitney Library of design 1993.
- [3] PhD Bradmiller B: Anthropometry for persons with disabilities: needs in the 21st century, Antrotech, Yellow Springs, Ohio, RESNA 2000 Annual Conference Research Symposium
- [4] Lindwell W., Holden K., Butler J.: Universal Principels of design, Rackport Publishers, 2003
- [5] Bridger R.S.: Introduction to ergonomics, Taylor & Francis, 2003



THE CRACK PROPAGATION STUDY IN ALLOYED ADI MATERIALS

Dragan RAJNOVIC¹, Olivera ERIC², Milica DAMJANOVIC¹, Sebastian BALOS¹, Leosava SIDJANIN¹

¹ Department of Production Engineering, Faculty of Technical Sciences, University of Novi Sad, Trg Dositeja Obradovica 6, 21000 Novi Sad, Serbia

² Institute „Kirilo Savic“, Vojvode Stepe 51, 11000 Belgrad, Serbia

draganr@uns.ac.rs, olivera66eric@gmail.com, damica@uns.ac.rs, sebab@uns.ac.rs, lepas@uns.ac.rs

Abstract: The ADI (Austempered Ductile Iron) is a real advanced material with a unique microstructure – ausferrite. It is produced by austempering of ductile iron, where by varying austempering parameters, a wide range of properties can be obtained. As the ADI might be further shaped by production engineering technologies, such as machining or plastic deformation, the study of ADI material behavior under load is of great interest. Because of that, in present study crack initiation and propagation in two ADI materials alloyed with 0.45% of copper and 1.5% of copper and nickel were observed. The materials used have been isothermally transformed at different temperatures in order to produce different morphologies of ausferrite microstructure. Consequently, the influence of graphite nodules, metal matrix microstructure and alloying elements on crack propagation generated by squeezing was studied. It was founded that process is similar for all tested ADI materials. The cracks originate from graphite nodules while the propagation path in metal matrix depends on the orientation of ausferritic ferrite sheaves.

Key words: ADI materials, microstructure, cracks, squeezing

1. INTRODUCTION

The ADI (Austempered Ductile Iron) is a type of cast iron with spheroidal graphite embedded in the ausferrite metal matrix obtained after heat treatment. The ausferrite is unique microstructure, distinctive for ADI, it is a mixture of ausferritic ferrite, and carbon enriched retained austenite [1-3]. The ADI possesses remarkable combination of high strength, ductility and toughness together with good wear, fatigue resistance and machineability [2]. For that reason, ADI material is used for many wear resistant and engineering parts in different sectors including automotive, trucks, construction, earthmoving, agricultural, railway and military [2].

During the austempering process, the ADI undergoes a two stage transformation. In the first stage, the austenite (γ) decomposes into mixture of ausferritic ferrite (α) and carbon enriched retained austenite (γ_{HC}), a product known as ausferrite. If the casting is held at the austempering temperature too long, then the carbon enriched retained austenite (γ_{HC}) transform into ferrite (α) and carbides (bainite) [1-3]. These carbides make material more brittle and therefore, that reaction must be avoided [1, 3]. The optimum mechanical properties can be achieved upon completion of the first reaction, but before second reaction started [2, 3].

As the ADI might be further shaped by production engineering technologies, such as machining or plastic deformation, the study of ADI material behavior under load is of great interest. Because of that, in present study crack initiation and propagation in two ADI materials alloyed with 0.45% of copper and 1.5% of copper and nickel were observed.

The materials used have been isothermal transformed at different temperatures and times of holding in order to produce different morphologies of ausferrite microstructure. Consequently, the influence of graphite nodules, metal matrix microstructure and alloying elements on crack propagation generated by squeezing was studied.

The obtained results might be further utilized in machining modeling as well as for other production engineering shaping technologies of ADI materials.

2. EXPERIMENTAL PROCEDURE

The ductile irons alloyed with Cu and with Cu+Ni have been examined in as-cast and austempered condition. The chemical compositions of as cast materials are given in Table 1.

In order to produce an ADI material, the samples were first austenitized at 900°C for 2 hours in protective atmosphere of argon and then rapidly quench in salt bath at an austempering temperature of 350°C. The holding times at austempering temperature were different and were chosen in order to produce different microstructures. For fully ausferrite microstructure with high amount of retained austenite, 2 and 3 hours for ADI Cu and ADI Cu+Ni were used, respectively. On the other hand, for microstructure where a second stage of reaction started, i.e. decomposition of ausferrite in ferrite and carbides appear; the 6 hours for both alloys were used.

Conventional metallographic preparation technique (mechanical grinding and polishing; and etching with nital) was applied prior to light microscopy (LM) examinations of samples cut from Charpy impact specimens.

Table 1. Chemical composition of as-cast material [mass %]

Material	C%	Si%	Mn%	Cu%	Ni%	Mg%	P%	S%
DI Cu	3.64	2.49	0.30	0.46	-	0.066	0.014	0.014
DI Cu+Ni	3.48	2.19	0.26	1.57	1.51	0.060	0.020	0.012

For microstructural characterization, a “Leitz-Orthoplan” metallographic microscope was used. The volume fraction of retained austenite in ADI material (V_γ) was determined by x-ray diffraction technique using “Siemens D 500” diffractometer with nickel filtered Cu $K\alpha$ radiation.

For all samples mechanical properties, namely, tensile properties (R_m -ultimate tensile strength, $R_{p0.2\%}$ -proof strength, A_5 -elongation, EN 10002), impact energy (K0, EN 10045) and Vickers hardness (HV10, ISO 6507) were determined at room temperature.

In order to study crack nucleation and growth a “squeezing” samples given in Fig.1 were produced from Charpy impact specimens, also [4]. By squeezing the samples at one side, a tensile stress state was induced at the opposite side, thus favoring a crack initiation. The squeezing was performed by pressing at universal tensile testing machine in several small steps. The crack initiation and propagation were observed at light microscope and further at scanning electron microscope JEOL “JSM 6460LV” operated at 20 kV.

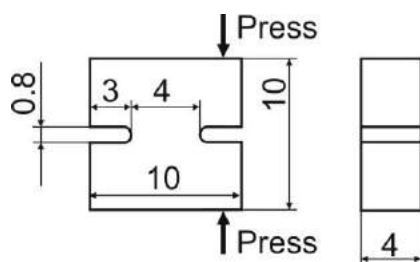


Fig.1. Squeezing sample (mm)

3. RESULTS AND DISCUSSION

1. Microstructure and mechanical properties

Light micrographs of ductile iron and ADI alloyed with Cu and with Cu+Ni are given in Fig. 2 to 4. The graphite spheroidisation for all specimens was more than 90%, with average graphite volume fraction of 10.5%, nodule size of 40 to 55 μm and nodule count of 50 to 80 per mm^2 , Fig.2.

As-cast microstructure of ductile iron alloyed with Cu was dominantly pearlitic with up to 10% of ferrite, whereas ductile iron alloyed with Cu+Ni was fully pearlitic.

The representative microstructure of the ADIs alloyed with Cu austempered at 350°C for 2 and 6 hours is shown in Fig.3. The microstructure is fully ausferritic consisting of mixture of ausferritic ferrite and carbon enriched retained austenite. However, after 6 hours a decrease in retained austenite amount can be detected, Table 2. This indicates that a second stage of transformation has begun even the microstructure change cannot be distinguished on light microscope.

The microstructure of ADI alloyed with with Cu+Ni for 3 hours is fully ausferritic (Fig.3), too. However, alloying the ADI with Cu+Ni cause that the acicular appearance of microstructure obtained in ADI alloyed with Cu (Fig.3a) has change to more plate-like morphology of ausferritic ferrite (Fig.4a). Furthermore, alloying austempered ductile iron with Cu+Ni delays the transformation kinetics of austenite, shifting the maximum of retained austenite from 2 hours to 3 hours and promotes the increase of retained austenite volume fraction, Table 2. After 6 hours of holding in the ausferrite microstructure of ADI Cu+Ni a presence of bainite as a product of second reaction can be observed, Fig.4b. This is a positive proof that the second stage of transformation is in progress.

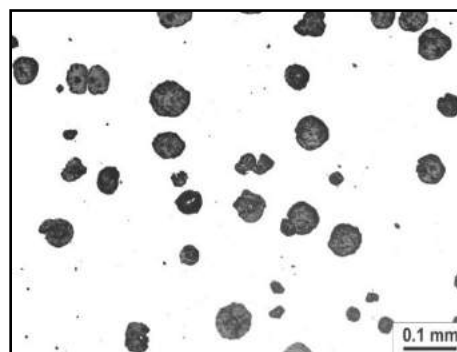


Fig.2. Microstructure of ductile iron (polished surface)

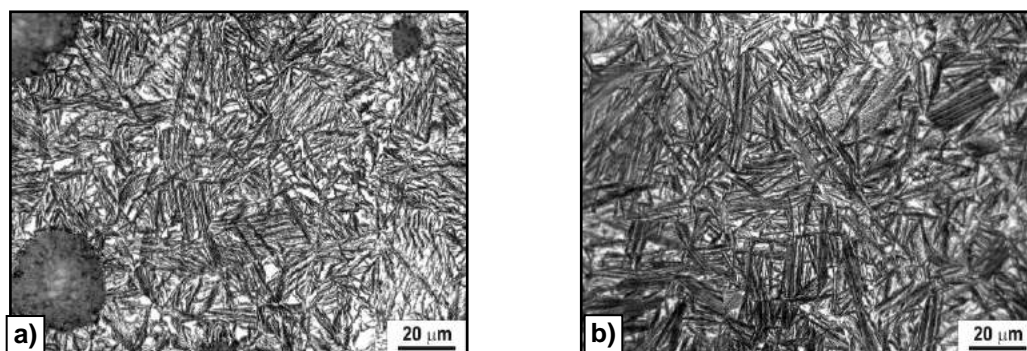


Fig.3. Microstructure of austempered ductile iron alloyed with Cu (etched surface):
a) austempered at 350°C for 2h, b) austempered at 350°C for 6h

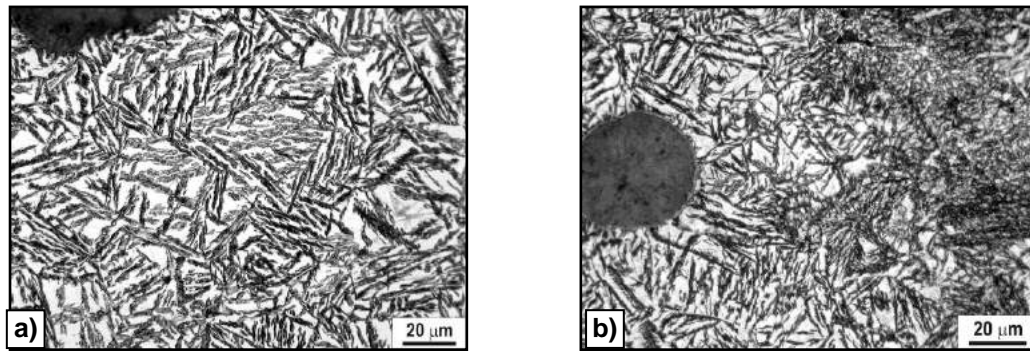


Fig.4. Microstructure of austempered ductile iron alloyed with Cu and Ni (etched surface):
a) austempered at 350°C for 3h, b) austempered at 350°C for 6h

Table 2. Mechanical properties of as-cast and ADI material

Material	R _m [MPa]	R _{p0,2%} [MPa]	A ₅ [%]	KO [J]	HV10	V _γ [%]	SRPS EN 1563:2005
DI Cu	770	514	4.9	21.4	270	-	EN-GJS-700-2
ADI Cu 350°C/2h	1112	998	7.9	106.1	373	16.6	EN-GJS-1000-5
ADI Cu 350°C/6h	1160	1066	5.3	91.6	420	11.8	EN-GJS-1000-5
DI Cu+Ni	880	677	3.2	20.5	296	-	EN-GJS-800-2
ADI Cu+Ni 350°C/3h	1070	901	11.1	122.1	308	18.9	EN-GJS-1000-5
ADI Cu+Ni 350°C/6h	1042	822	6.1	50.3	380	14.2	EN-GJS-1000-5

The mechanical properties of tested materials are given in Table 2. The starting strength and ductility of as-cast material have been increased significantly after austempering. Comparing two ADI materials it can be noticed that the strength is somewhat higher for ADI alloyed with Cu, while the ductility is higher ADI alloyed with Cu and Ni. This behavior is attributed to influence of Cu and Ni on transformation kinetics, resulting in microstructure and retained austenite volume differences [3].

2. Crack nucleation and growth

The process of crack nucleation and growth is shown at Fig. 5 to 8. The process is similar for all tested ADI materials and might be divided on following steps:

- Graphite-metal matrix decohesion;
- Initiation of microcracks on free surface, along ferrite-austenite interface;
- Propagation of microcracks formed on graphite nodules into metal matrix;
- Internodular linkage of microcracks and formation of main crack;
- Linkage of main crack and favorable microcracks to form a final fracture.

Under low stress the first decohesion between graphite nodule and metal matrix can be noticed, Fig.5. The extent of decohesion depends on plastic deformation of matrix. The higher plasticity, the higher decohesion and vice versa. This behavior is similar to ductile irons with ferrite (ductile matrix) or pearlite (brittle matrix) and it is reported in literature [5]. At the same time, the first crack initiation sites appear on graphite-metal matrix surface. On Fig.5, at least five different initiation sites can be seen. The cracks initiation in all cases was on ausferritic ferrite – retained austenite (F-A) interface. There is an atomic mismatch at the F-A interface, and the tensile stress that it can withstand is not as great as that of ausferritic ferrite or

retained austenite [6]. Furthermore, the presence of carbides at interface could lead to additional weakness of A-F interface [7]. The observed cracks along F-A interface is represented in Fig.6. After nucleation, the crack will further propagate at the site where the necessary energy is minimal, Fig.5. However, due to complex microstructure where ausferrite sheaves are oriented in all direction the crack in this stage can continue its propagation along F-A interface, as well perpendicular or inclined by different angle on ausferritic shaves. Furthermore, the crack could branch and change direction. The initial cracks usually form on opposite sides of graphite nodule and have a tendency to interconnect with other cracks formed on neighboring nodules thus forming the main crack, Fig.7. The final step is linkage of main crack and favorable microcracks in order to form a final fracture, Fig.8. The different microstructure of tested ADI samples does not have a significant influence on crack initiation and propagation path, but it strongly influence the fracture mode. The presence of carbides in bainite structure of ADI Cu+Ni 350°C/6h decrease the toughness and favor brittle fracture by decreasing the plastic zone ahead of crack tip [7].

Under tension, beside decohesion of graphite-metal matrix interface, a cracking of graphite nodules might appear, also, Fig.8. As the graphite strength is low it can easily brake and do not represent a crack arrest site, but at contrary it is established that cracks originate from graphite nodules. The cracking of graphite is consequence of interface strength between nodule and metal matrix. If the interface strength is low the nodule is pullout and it appears that crack follows interface around nodule. On other hand, if the interface strength is high the graphite nodule break apart and it appears that crack propagate through nodule.

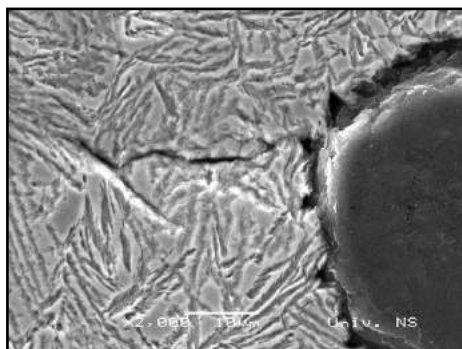


Fig.5. Graphite-matrix decohesion and crack initiation (ADI Cu+Ni 350°C/3h)

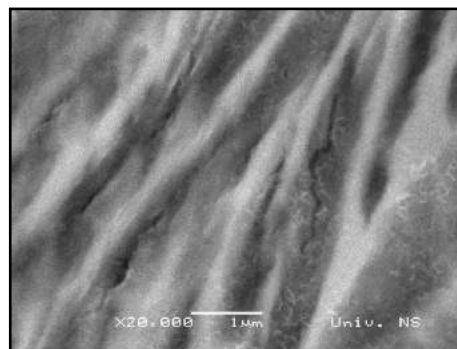


Fig.6. Cracks along F-A interface (ADI Cu+Ni 350°C/3h)

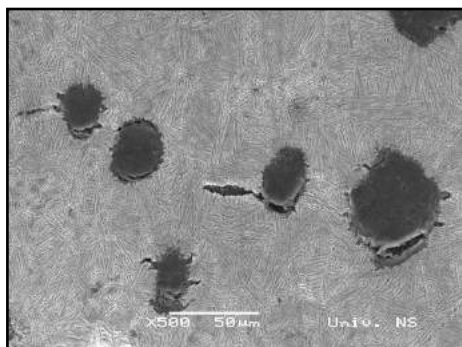


Fig.7. Internodular linkage of microcracks (ADI Cu 350°C/2h)

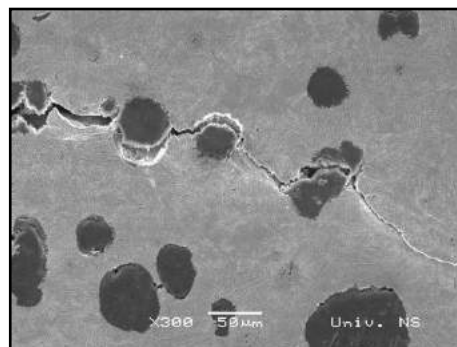


Fig.8. Formation of main crack (ADI Cu 350°C/6h)

4. CONCLUSIONS

The crack nucleation and growth is similar for all tested ADI materials.

The first cracks nucleate along the ausferritic ferrite-retained austenite interface from the decohesed graphite nodules-metal matrix surfaces.

The further crack propagation proceed by internodular linkage of the initial microcracks.

In this step, the cracks can propagate through F-A interface (favored propagation direction), perpendicular on ausferritic shaves or inclined by different angle on ausferritic shaves.

The different ADI microstructure does not significantly influence the cracks propagation direction, however its strongly influence the fracture mode.

ACKNOWLEDGEMENT

This study is supported by the Ministry of Education and Science of the Republic of Serbia, through technology development project TR34015.

REFERENCES

- [1] SIDJANIN, L., SMALLMAN, R.E. (1992) *Metallography of bainitic transformation in austempered ductile iron*, Materials Science and Technology, Vol.8, pp 1095-1103
- [2] HARDING, R.A. (2007) *The production, properties and automotive applications of austempered ductile iron*, Kovove Materialy, Vol.45, pp 1-16

- [3] ERIC, O., RAJNOVIC, D., ZEC, S., SIDJANIN, L., JOVANOVIC, M.T. (2006) *Microstructure and fracture of alloyed austempered ductile iron*, Materials Characterization, Vol.57, pp 211-217
- [4] SHIH, T.S., LIN, P.Y., CHANG, C.H. (1990) *A Study of the Austempering of a Ni-Cu Alloyed Ductile Iron*, AFS Transactions, Vol.142, pp 609-630
- [5] IACOVIELLO, F., DI BARTOLOMEO, O., DI COCCO, V., PIACENTE, V. (2008) *Damaging micromechanisms in ferritic-pearlitic ductile cast irons*, Materials Science and Engineering A, Vol.478, pp 181-186
- [6] DAI, P.Q., HE, Z.R., ZHENG, C.M., MAO, Z.Y. (2001) *In-situ SEM observation on the fracture of austempered ductile iron*, Materials Science and Engineering A, Vol.319, pp 531-534
- [7] SIDJANIN, L., SMALLMAN, R.E., BOUTORABI, S.M. (1994) *Microstructure and fracture of aluminium austempered ductile iron investigated using electron microscopy*, Materials Science and Technology, Vol.10, pp 711-720



34th INTERNATIONAL CONFERENCE ON
PRODUCTION ENGINEERING
28. - 30. September 2011, Niš, Serbia
University of Niš, Faculty of Mechanical Engineering



**COLLABORATION AND COMMUNICATION IN INTEGRATED SYSTEM OF DIGITAL
MANUFACTURING**

Suzana PETROVIĆ¹, Milan ERIC¹, Goran DEVEDŽIĆ¹, Miodrag MANIĆ², Saša ĆUKOVIĆ¹, Miloš ĆIROVIĆ¹

¹ Faculty of Mechanical Engineering, Sestre Janjića 6, Kragujevac, Serbia

² Faculty of Mechanical Engineering, Aleksandra Medvedeva 14, Niš, Serbia

suzana.petrovic@mfkg.rs, ericm@kg.ac.rs; devedzic@kg.ac.rs; cukovic@kg.ac.rs; cirovicmilos@kg.ac.rs,
mmanic@masfak.ni.ac.rs

Abstract: *The paper presents a short overview of the tools and technologies for product data interoperability and management in digital manufacturing environment. The concept of digital manufacturing requires a reference model implemented within infrastructure of information and communication technologies. Reference model of collaborative process planning is based on merging of virtual organizations focused on product design and development. Such approach provides process planning activities at meta, macro, and micro levels. Usual web platform that supports this kind of work, implemented as a part of a collaborative environment, is the CORE platform. From a technological point of view, the concept of this platform is based on synchronous usage of Internet and services of virtual and augmented reality. Full collaboration assumes extensive application of neutral data formats.*

Key words: *digital manufacturing, IC technologies, CORE platform, Web platform*

1. INTRODUCTION

Product Data Management (PDM) systems are the most important component of the Product Lifecycle Management (PLM) systems, which provide us with monitoring of product lifecycle activities. Therefore, the information storage may be very complex because many organizations and users are involved, causing some activities to overlap, while others to run in parallel [1], [3], [4].

Access to different types of data must be allowed to all users, but at the same time, the data have to be protected from non – authorized access. This implies that different types of users will be interested in having access to different types of data, i.e. the data they understand and require for their tasks. For instance, designer will understand the technical drawing of a component, and the programmer the code that describes the technical drawing. In fact, the core of corresponding data should follow the capability of adaptation to the appropriate application. Modifications made by one user should be saved in the data kernel, so that the same change could be seen and accessed by other users as well [1], [2].

2. MANAGING COLLABORATIVE PROCESS PLANNING ACTIVITIES

The result of transformation of certain business strategies is the concept of extended enterprise. This concept is influenced by the expansion of Internet technologies, consequently affecting the simultaneity and availability of information related to the process planning.

The concept of extended enterprise is more than just the merging of different enterprises connected by a product supply chain. It is based on an organizational paradigm in satisfying not only clients' needs, but also the needs of people involved in all stages of the product lifecycle, such as product design, manufacturing or recycling [1,7,8].

However, in addition to many advantages of concept of extended enterprise, several disadvantages still persist in the industry. They refer to the problems related to different organization of business, differences in the usage of PLM systems, data incompatibility, rules, methods etc. Some disadvantages can be overwhelmed by the usage of distributed, opened and intelligent systems for collaborative work, which implementation depends on technological and economic support of industries that want to introduce them.

Systems for collaborative process planning should enable the users to work at different levels, i.e. these should enable meta-, macro and micro planning. Meta planning refers to process planning on global level. From production point of view, meta-planning determine production process, quality, product cost, etc. Macro planning refers to identification of major turning points and does not include detailed tasks and activities. In other words, corresponding procedures and activities define production equipment, optimum (minimal) number of machines for parts production, and operational sequence. Micro planning assumes detailed definition of tasks and activities, i.e. tooling, tool paths, and the parameters associated to shop floor operations, providing that productivity, quality of the parts and manufacturing costs are optimized [2,3].

2.1 The reference model of collaborative process

Product development and process planning in extended enterprise imply the existence of reference model, which should be implemented in IC technology infrastructure that supports collaborative work within PLM systems. These models are mostly used to provide the reference for different enterprises within the same industrial sector [2,3,7,8].

The basic structure of a reference model implies the definition of needs, resources and criteria (Fig.1). The requirement for development of extended enterprise is to provide development from the basic supply chain to the higher level of cooperation and collaboration in order to achieve greater efficiency and agility. Such needs are seen from the inside of the enterprise network, resulting in closer collaboration between enterprises and suppliers or partners and clients.

The available resources define the level of satisfaction of the expressed needs, presenting the basic indicators for establishment of the criteria and for placing the limits for development of an extended enterprise [3].

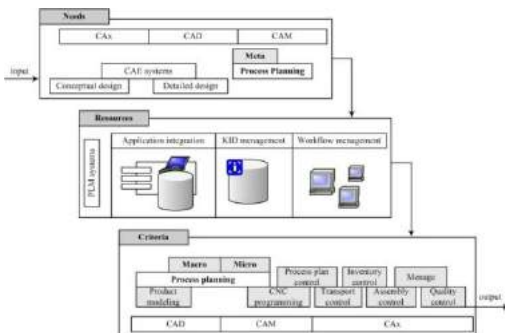


Fig.1. The reference model of collaborative process planning in extended enterprise

Criteria that define the main characteristics of extended enterprise are setting through macro and micro level planning.

2.1 Implementation of IC technologies

From functional point of view, IC technologies, which provide collaborative process planning, should have a client – server architecture (Fig.2) [1,2,3].

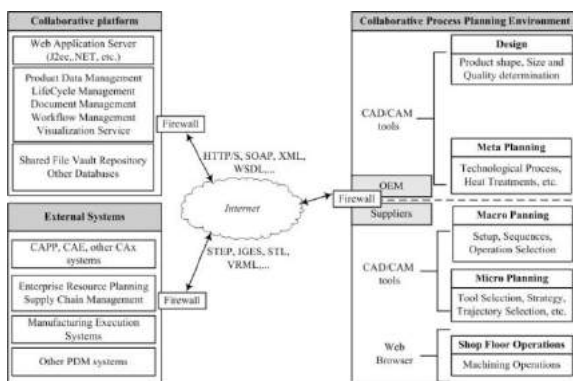


Fig.2. The implementation of IC technologies for collaborative process planning in extended enterprise [2]

Basic server's components support data, lifecycle, documents, and workflow management, as well as the visualization of a common database. On the other side, the client platform should provide connection with server applications using Web browser or CAD/CAM tools. Such concept of a server enables realization of data exchange, design, analysis, and decision making processes [4].

Client-server communication is performed via Internet by using communication standards, such as HTTP/S (Hypertext Transfer Protocol Secure), SOAP (Simple Object Access Protocol), XML (Extensible Markup Language), WSDL (Web Service Description Language), RMI (Remote Method Invocation), etc. Data exchange is conducting using standards like STEP (Standard Template for Electronic Publishing), IGES (Initial Graphics Exchange Specification), DXF (Drawing Exchange Format), etc. Unauthorized data access is prevented as well.

Most enterprises use PLM systems that are limited for working in heterogeneous environment. In such conditions, it is necessary to analyze PLM systems that are feasible in an environment of extended enterprise.

3. WEB PLATFORM

Data exchange is a very important issue that relates distributed users working on product development. The application of Web oriented PDM systems enables the large number of collaborative activities. A number of issues that concern the product and process complexity are resolved using Virtual Reality (VR) and Augmented Reality (AR) technologies. Web platform that supports this kind of work, implemented within Collaborative Manufacturing Environment (CME) is called Collaborative Product Reviewer – CORE [1]. From technological point of view, the CORE platform concept relies on synchronized usage of Internet, VR and AR services.

3.1 The architecture of CORE platform

Design of CORE platform is based on open architecture and browsing technologies. The architecture involves three layers (Fig.3):

- data layer,
- business layer, and
- presentation layer.

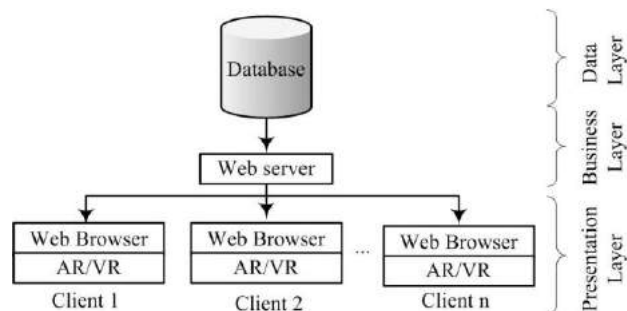


Fig.3. The architecture of the CORE platform

These layers communicate through the Internet or an Intranet, depending on the type of communication [1].

Data layer relates to external databases that store and update the project related data, and provide their stability, consistency, integrity, etc.

Business layer defines business logic, and consists of a number of connection mechanisms that contain algorithms for business distribution and database interaction.

Presentation layer supports the work with clients, where some standard browsers are involved (Internet Explorer, Opera, etc.), as well as the VR and AR applications.

CORE platform architecture suggests that creation, modification, and management of the environment requires establishment of communication between an appropriate Web platform and the VR and AR applications (Fig.4).

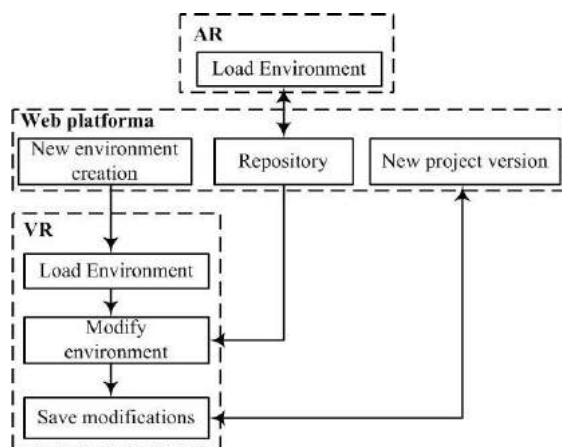


Fig.4. Communication between Web platform and VR and AR applications

This kind of communication is provided by XML technology. It creates data formats that are independent of a platform (Windows, Unix, Linux, etc.) and facilitates data sharing within information system, in particular for web-based systems.

Implementation of the CORE platform architecture is schematically shown in Fig.5. Database stores all essential data that refer to projects and processes. Users (internal or external) access the database via server.

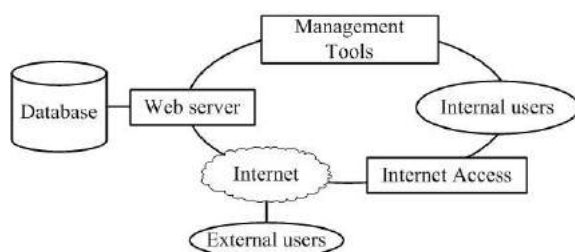


Fig.5. CORE environment [1]

All users can manipulate with a virtual product at any time, without restrictions concerning the number of simulations. When user performs any modification of the product it is instantly seen by all other users.

4. INFORMATION EXCHANGE IN DIGITAL PRODUCTION

The information exchange of the products and processes between different systems or/and applications should include total product definition. PLM systems that are built on the same kernel have similar data format, providing complete data exchange with no information loss. However, in the heterogeneous PLM environments data exchange is prone to errors or incomplete data and information transfer [2,5,6].

4.1 Review of standards for data exchange

Product information and data exchange in heterogeneous production environments most commonly uses standard exchange formats, such as STEP and XML.

STEP standard contains the data of the complete product lifecycle. The possibility of describing models in text format provides the access to any type of information that the text includes. Manipulation with STEP model can be performed by using appropriate CAD/CAM system or by user-defined application.

The architecture of STEP standard (Fig. 6) contains three levels:

- application level – contains all the information about model,
- logical level – maintain the consistency of data structure which are exchanged, and
- physical level – generates the file sharing. [5,7,9]

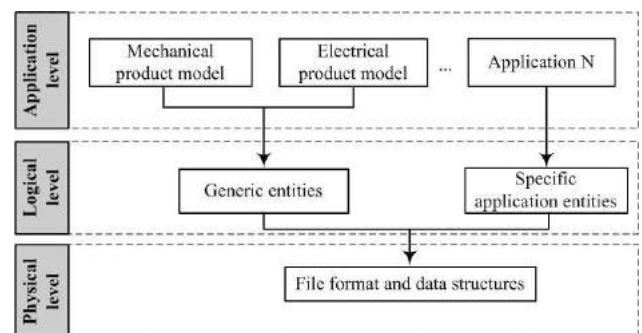


Fig.6. The architecture of STEP standard

Data specification described by STEP standard is performed by descriptive and implementation method. The descriptive method contains the EXPRESS language for formalization of STEP models, and implementation method contains techniques for structuring information defined by STEP standard [9], [5].

¹ Suzana Petrović, PhD student, Faculty of Mechanical Engineering, Sestre Janjić 6, Kragujevac, Serbia, suzana.petrovic@mfgk.rs

¹ Dr Milan Erić, PhD, Faculty of Mechanical Engineering, Sestre Janjić 6, Kragujevac, Serbia, ericm@kg.ac.rs

¹ Dr Goran Devedžić, PhD, Faculty of Mechanical Engineering, Sestre Janjić 6, Kragujevac, Serbia, devedzic@kg.ac.rs

² Dr Miodrag Manić, PhD, Faculty of Mechanical Engineering, Aleksandra Medvedeva 14, Niš, Serbia, mmanic@masfak.ni.ac.rs

¹ Saša Ćuković, PhD student, Faculty of Mechanical Engineering, Sestre Janjić 6, Kragujevac, Serbia, cukovic@kg.ac.rs

¹ Miloš Ćirović, PhD student, Faculty of Mechanical Engineering, Sestre Janjić 6, Kragujevac, Serbia, cirovicmilos@kg.ac.rs

STEP Data Access Interface (SDAI) represents the standard for the low-level data access applications using EXPRESS language. The binding can be early and late. The difference is in accessibility to data libraries in some applications. Early binding generates the specific data structure according to EXPRESS schemas and definitions of programming language. Defined entities within EXPRESS schema are converted into classes of programming language C, C++ or Java. Late binding is using the low level library for the access to some simple functions in order to assume or define parameter values [6].

XML contains different rules for defining semantic description of product model aimed for classification and identification of document's entities. Although XML is very easy to use, there are potential conflicts between flexibility and easiness of usage. Elimination of conflict situations is provided by Document Type Definition (DTD) formalism for document structure description. It defines constraints in XML document structure and declares all types of elements, attributes, entities, processing instructions, etc.

5.1 The architecture of digital production

Modern PLM systems (such as, Catia, Pro/Engineer, SolidWork, etc.) have the ability to save or load STEP AP203 standard files. In order to ensure working with Web oriented applications that integrate distributed users, the transformation of STEP AP203 document into XML documents is being performed. The architecture of a system that supports such procedure is shown in Fig. 7.

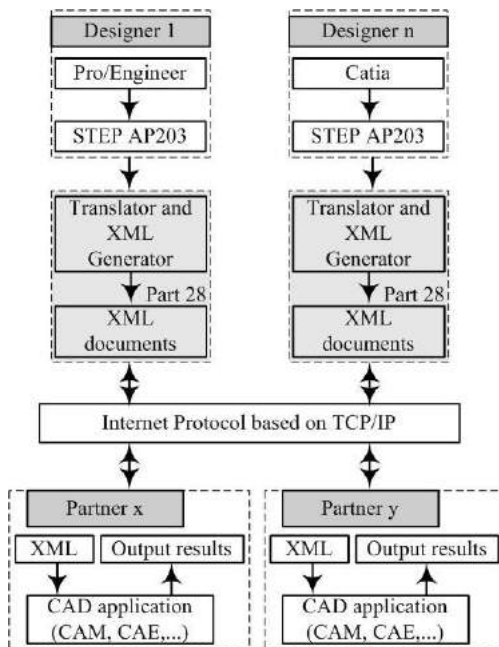


Fig.7. System architecture [1]

As this is a multi-user environment, which implies multi-application environment, it is necessary to save product models in STEP AP203 format. Distributed users may download these models as XML documents by using appropriate Internet protocols. The models stored in this format are appropriate for usage in different applications.

5. CONCLUSION

The reference model of collaborative process planning is based on merging virtual organizations that are focused on product design and development. The companies that make an integral part of the extended enterprise should use these tools to reduce costs and time-to-market. This is particularly evident within planning activities, which are often crucial for product development.

Complete collaboration includes the application of a neutral file format. Nowadays STEP standard file formats are in common. The conventional methods of implementation are inflexible for the complete model manipulation via Internet. This deficiency is eliminated by the description of product models using programming languages, such as Java, C++, XML, etc. In such cases XML and STEP are considered as the complementary technologies.

ACKNOWLEDGEMENT

This research is supported by Ministry of Science and Technological Development, grants III-41007 and III-41017.

REFERENCES

- [1] WANG L., NEE Y.C.A. (2009) *Collaborative Design and Planning for Digital Manufacturing*, Springer
- [2] SILLER H.R., ESTRUCH A., VILA C., ABELLAN J.V., ROMERO F. (2008) *Modeling workflow activities for collaborative process planning with product lifecycle management tools*, Springer, pp 689-700
- [3] ADESTA E.Y.T. (2002) *A reference model for extended enterprise*, PhD thesis, University of Huddersfield
- [4] HOU J., SU C., WANG W. (2008) *Knowledge Management in Collaborative Design for Manufacture*, International Conference on Computer Science and Software Engineering, IEEE, pp 1031-1034
- [5] DEVEDŽIĆ G. (2009) *CAD/CAM tehnologije*, Mašinski fakultet, Kragujevac
- [6] LI W.D., ONG S. K., NEE Y.C.A., McMAHON C. (2007) *Collaborative Product Design and Manufacturing Methodologies and Applications*, Springer, London
- [7] LIANDONG Z., QUIFENG W. (2009) *Integrated Collaborative manufacturing Management System for Complex Product*, Second International Conference on Future Information Technology and Management Engineering, IEEE, pp 206-209
- [8] OBERWEIS A., PANKRATIUS V., STUCKY W. (2006) *Product lines for digital information products*, Elsevier, Information Systems, Elsevier B.V., No 20, pp 909-93
- [9] KEMMERER S. *STEP: The Grand Experience*, NIST Special Publication 939, National Institute of Standards and Technology, Gaithersburg, MD, 1999.



MODELLING OF PRODUCTION SYSTEMS FOR END-OF-LIFE VEHICLES PROCESSING

Vladimir Simić, Branka DIMITRIJEVIĆ

Faculty of Transport and Traffic Engineering, University of Belgrade, Vojvode Stepe 305, Belgrade, Serbia
vsima@sf.bg.ac.rs, brankad@sf.bg.ac.rs

Abstract: *The treatment of end-of-life vehicles (ELVs) and the environmental impact of discarding the resulting residues are subjects of global concern. This paper focuses on the material selection problem in vehicle recycling factories (VRFs). It describes a VRF optimization model for processing ELVs in the EU legislative environment as well as global business environment. The problem is formulated as a linear program, which provides optimal procurement, storage, processing and recovery, recycling and landfill disposal route decisions. Process configuration is designed as highly flexible. Its structure directly depends from predominate ecological and economical parameters. All calculations of recycling, energy recovery and overall recovery rates are performed according to ISO 22628 standard, which defines calculation method of recyclability and recoverability of road vehicles. In addition, the type of EOL operation (recovery, recycling or disposal) is determined according to definitions from the new EU Directive on waste (2008/98/EC). The developed model can help VRFs improve their eco-efficiency and profitability, and also give answers to many important and current issues. Finally, we ran our model with different compositions of incoming procurements and prescribed quotas. All created test problems were solved to optimality using the CPLEX 12.2 solver.*

Key words: *Production planning; Material selection; End-of-Life Vehicles; Recycling.*

1. INTRODUCTION

The treatment of End-of-Life Vehicles (ELVs) and the environmental impact of discarding the resulting residues are subjects of worldwide concern [1]. ELVs are the priority in the EU waste flow. The latest data shows that 6.34 million ELVs were processed in 2008, with the average weight of 949.38 kg [2]. Particularly in an attempt to reduce waste that originates from ELVs, in 2000 the EU enforced the ELV Directive (2000/53/EC). It aims at preventing waste from ELVs and protecting the environment through promoting the collection, re-use and recycling of their components [3]. According to the Directive, beginning on the 1st of January 2006, vehicle recovery must reach a minimum of 85% by weight per vehicle (with energy recovery maximum 5%), of which a minimum of 80% will have to be reuse and material recycling. By the 1st of January 2015, recovery will rise to a minimum of 95% (with energy recovery maximum raised to 10%), of which minimum 85% will have to be reuse and material recycling.

Efficient processing of automobile shredder residue (ASR) or auto fluff fraction represents a major concern for VRFs. ASR is the waste generated during the shredding process, and consists of three parts: light ASR, heavy ASR, and soil/sand. It is a by-product of the recycling procedure and makes up 20-25% weight of the average ELV, i.e. approximately 200kg. The development of technology for recycling ASR is complicated because it is a very heterogeneous waste material; its composition, density, and moisture content change from site to site, and

from day to day at the same site. In addition, factors that prevent the total recovery of ASR are its physical nature, frequent contamination, poor development of certain secondary markets and substantial processing costs.

This paper focuses on the on the material selection problem in the VRF. It presents a tactical production planning problem for vehicle recycling factory in the EU legislative environment as well as global business environment. The problem is formulated as a linear program, which provides optimal procurement, storage, processing, and recovery, recycling and landfill disposal route decisions.

This paper is organized as follows. Section two describes flow sheet of the contemporarily equipped VRF. Case study is placed in the Section three, and the Last section presents the main conclusions of the paper.

2. PRODUCTION PROCESSES IN VEHICLE RECYCLING FACTORY

A detailed flow sheet is the starting point for the formulation of the VRF production planning model, and it is represented in Figure 1. It contains a network of various unit operations necessary for processing numerous material flows, ranging from shredding to metal producing processes and therefore gives configuration of the contemporarily equipped VRF. Process configuration is designed as highly flexible and its structure directly depends on specific environmental requirements imposed by a specific ELV recycling policy (i.e. reuse/recycling and recycling/recovery quotas from the ELV Directive)

and present economical factors. In addition, any possible vehicle hull quantity and processing route can be viewed and assessed as a potential solution of the analysed problem.

A number of procurement classes are available for a VRF, each of which has more than one type of hulks present. Since each type of hulks is characterised by specific composition of materials, general material composition of each class will obviously depend exclusively on the share of hulk type belonging to it (Figure 1). When procurements arrive, they are unloaded from transportation vehicles and forwarded to storage. Vehicle hulks planned for processing are taken over from there and transported to shredder, which is the core element of every VRF. It shreds them into mostly fist-size chunks to liberate metals from everything else. A heavy duty cyclone is installed on top of the shredder to vacuum the light automobile shredder residue (ASR) fraction. This fraction can be further sorted or shipped to advanced thermal treatment (ATT) plant. If the first option is chosen, then the second magnetic sorter separates this material flow to ferrous metals 2 and NF mix fractions. NF mix can also be further sorted to isolate NF metals

from it, sent to selected ATT plant or disposed on landfill. If the first option is chosen, then the second eddy current sorter (ECS) separates this material flow to NF metals 2 and non-metals 2, which will then be routed to the optimal destination. Heavy materials fraction passes through the first magnetic sorter which diverts the ferrous metals 1 from the heavy ASR fraction. Market requirements dictate that both fractions of ferrous metals are firstly manually treated along a conveyor for possible impurities (above all, for insulated Cu wires), and only then sold to steel industry. As for the fraction of insulated Cu wires, two routes are possible, export and (manual) recycling in low cost labour countries, and landfill disposal. Heavy ASR fraction is forwarded to the first ECS which separates it to NF metals 1 and of non-metals 1. The first and the second fraction of NF metals are then routed to HMS, which separates those to Al-rich and Cu-rich fractions. Al-rich fraction can be sold as is, or routed to the third ECS for further refinement from rubber, plastics and rest fraction (RPR). Isolated RPR fraction can be either incinerated in a municipal solid waste incinerator (MSWI) or disposed on landfill.

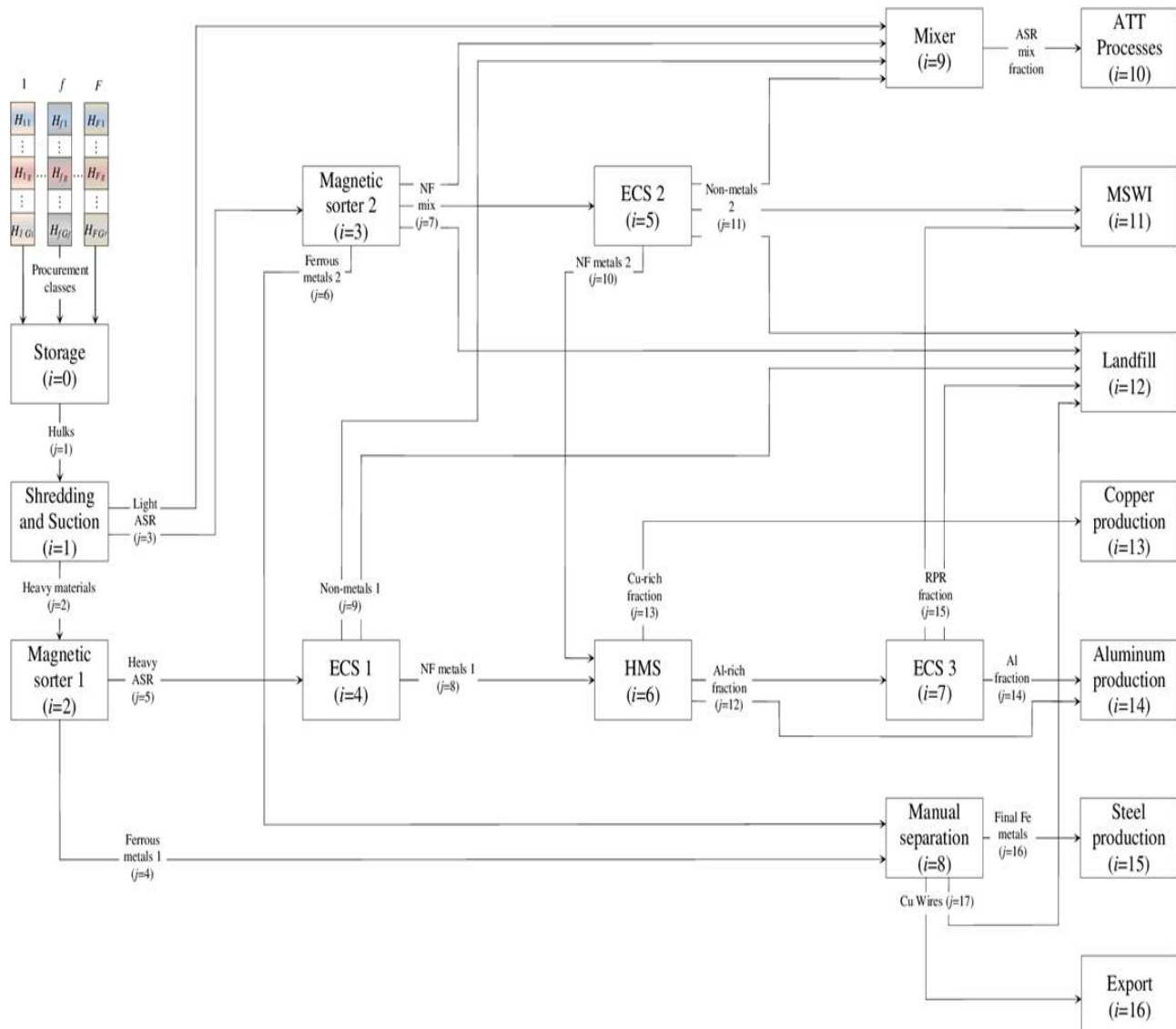


Fig. 1. Flow sheet of the contemporarily equipped vehicle recycling factory.

3. CASE STUDY

In this case study, the following scenarios were investigated:

- *Scenario 1 - Valid quotas* (valid since 1 January 2006). The VRF has to guarantee that recycling rate and recovery rate do not fall under 80 and 85% respectively, as well as that the energy recovery rate does not exceed 5% [3]; and
- *Scenario 2 - Future quotas* (will be valid from 1 January 2015). The VRF has to guarantee that recycling rate and recovery rate do not fall under 85 and 95% respectively, as well as that the energy recovery rate does not exceed 10% [3].

ELV Directive simply defined “vehicle” as any vehicle designated as class M_1 (passenger vehicles with less than eight seats in addition to the driver's seat) or N_1 (vehicles used for the carriage of goods whose maximum weight does not exceed 3.5 tonnes), and three wheel motor vehicles [3]. In this case study we analysed 2 prevailing types of M_1 and N_1 vehicle hulk classes: steel-intensive (SI) and aluminium-intensive (AI). Therefore, we will be looking at the special case of vehicle design change influencing VRFs business, i.e. the influence of the reduction of its weight by substituting ferrous metals with aluminium. As a result, the above mentioned scenarios formed 121 test problems each by varying the share of SI type hulks in each procurement class in the interval of 0-100% with the step of 10%.

1. Case study results

The optimal decisions for all test problems were solved using the CPLEX 12.2 solver on a Toshiba Qosmio with Intel Core i5-430M mobile technology processor. Testing of the developed model showed that during every planning period the quantity of procured vehicle hulks is exactly the same as the maximum capacity of shredding mill and that VRF aims at attaining as higher level of quantity and quality of sorted metal flows as possible regardless of the hulk category. So, for example, Al-rich fraction is always additionally purified because the additional income always exceeds the costs of its sorting and additional manipulation of RPR fraction. On the other hand, export possibilities of insulated Cu wires have primacy over landfill disposals as expected.

In reference to scenario 1, valid eco-efficiency quotas were reached in all created test problems, while the rates of recovery, recycling and energy recovery were on average 85.07, 83.15 and 1.92% respectively. The resulting functional dependence of profit made from general material compositions of vehicle hulk classes is presented in Figure 2. It should be noted that in previously mentioned figure, the H_{11} and H_{21} stand for the share of SI vehicle hulks of the first and the second procurement class respectively. As it is visible in Figure 2 the change in M_1 -SI category share will have more significant influence ($>5\%$) on VRF profitability only when SI type attains larger share in the N_1 class procurement. On the other hand, the change in N_1 -SI category share always influenced the level of profit, while its effect is noticeably limited by the quality improvement of the first class procurement (i.e. by the reduction of M_1 -

SI category share). The same figure leads to conclusion that NF metal share in certain vehicle hulk categories was actually the basis for creating the optimal procurement plan, as well as production plan. This is entirely logical, and since isolated NF metals can be sold at 4.5 (Al-rich fraction) to almost 8 (Cu-rich fraction) times higher price than isolated ferrous metals, their share in vehicle hulks and the situation on the metal market will evidently present only drivers of production planning process of the analysed contemporarily equipped VRFs. In compliance with the above mentioned conclusions, and based on the material composition of certain vehicle hulk categories, from the NF metal share aspect (i.e. “profitable” aspect) the most desired category is N_1 -AI (with 19.65% share) and the least desired category is M_1 -SI (with 10.54% share). For the exact same reason, the highest profit was made in test problem 1 (€2,947,013.93 or 206.95 €/tonne of processed hulk), when the second procurement class consisted exclusively of AI type hulks. Conversely, the lowest profit was recorded in test problem 11 (€2,375,890.98 or 166.85 €/tonne of processed hulk), when both offered classes consisted exclusively of SI type hulks. Ultimately, as hulk types belonging to the second procurement class have “profit” rank of 1 and 3, this class dominated throughout scenario 1 (average share of 70.71%) and was ordered more in 88 test problems.

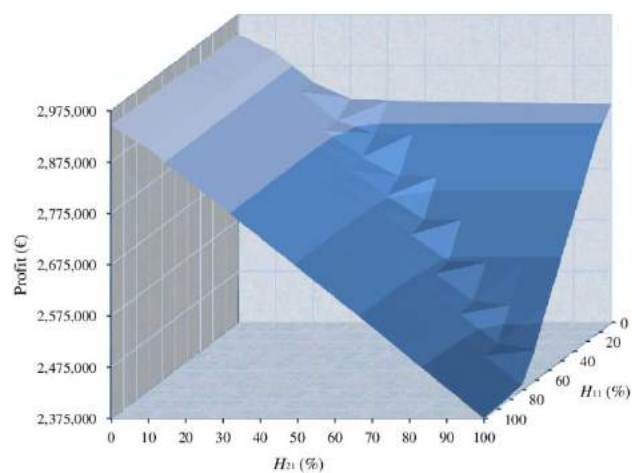


Fig. 2. Functional dependence of profit made from general material compositions of vehicle hulk classes in case of valid quotas.

In reference to scenario 2, future eco-efficiency quotas were reached in all created test problems, so we are led to conclude that the success of the ELV Directive implementation phase 2 was not jeopardized. The average rate of energy recovery was 9.87%, whereof MSWI and ATT plant contributed with 7.08 and 2.79% respectively. During this process, 5.36% of the production total went through the advanced thermal treatment, and 9.33% was combusted. Figure 3 presents the obtained functional dependence of profit made from general material compositions of vehicle hulk classes. As it is visible in Figure 3, the change in N_1 -SI category share has always significantly influenced ($>5\%$) the level of made profit, while its effect is noticeably limited by the quality improvement of the first class procurement. On the other hand, the change in M_1 -SI category share will have more

significant influence on the VRF profitability only when the N_1 -SI category share is not lower than 70%. In reference to the analysis of the optimal procurement plan, the second class procurement was ordered more even in 98 test problems, with the average share of 78.41%. The change in procurement plan is obvious, meaning that the even more dominant second class procurement came as a direct consequence of introducing more rigorous eco-efficiency quotas. That is why, when determining the optimal procurement plan, special attention must be paid not only to the mentioned NF metal share and the situation on the metal market, but also to the ASR share (i.e. plastics, rubber and rest materials fraction) in the analysed hulk categories. In accordance with material composition and ASR share aspect (i.e. "ecological" aspect) the most desired category is N_1 -SI (with 13.39% share) and the least desired category is M_1 -AI (with 18.60% share). Speaking of profitability, the highest profit was made in test problem 1 (€2,787,360.34 or 195.74 €/tonne of processed hulk) when the second procurement class consisted exclusively of AI type hulks (with the profit rank 1). On the other hand, the lowest profit was recorded in test problem 11 (€2,297,337.41 or 161.33 €/tonne of processed hulk), as well as the best ecological result (recycling rate value of 86.17%), when both offered classes consisted exclusively of SI type hulks (with a low profit and high ecology rank).

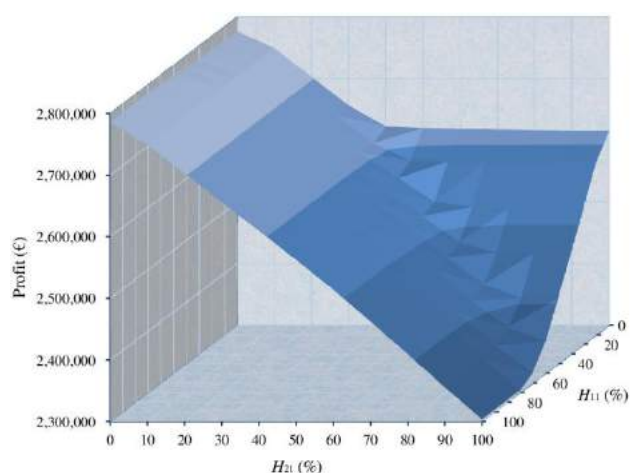


Fig. 3. Functional dependence of profit made from general material compositions of vehicle hulk classes in case of future quotas.

4. CONCLUSION

Analysis of testing results of the developed model leads to the following conclusions:

- Contemporarily equipped VRF can do profitable business even in strictly controlled and legally rigorous production conditions. Testing the developed model showed that in such conditions VRF will continuously procure the maximum quantity of hulks that it is able to process according to the planning period, as well as aim at achieving the highest quantity and the best quality of sorted metal flows regardless of the hulk category being processed.

- All eco-efficiency quotas are attainable, but only if VRF has contemporary sorting equipment and a possibility to forward certain waste fractions to MSWI and/or ATT plant for their further treatment. Moreover, availability of plants of this type will be additionally important starting 1 January 2015, which is evident from the data that in case of future quotas the average energy recovery rate increased to 9.87%.

- The change in vehicle design, which was observed from the aspect of substituting ferrous metals with aluminium, will not jeopardize VRFs. In both examined scenarios, analysis of the optimal procurement plans identified the NF metals share as one of the main drivers of production planning process. However, only contemporarily equipped VRFs will be able to use high value of NF metals to their advantage, because compared to traditional VRFs (so called shredding facilities), they are able to isolate them successfully.

As a result, all three conclusions clearly point out that VRFs investing in the procurement of contemporary sorting equipment is an absolutely valid decision and also that the final success of ELV Directive is realistic.

REFERENCES

- [1] SIMIC, V., DIMITRIJEVIC, B. (2010) *Perspectives for Application of RFID on ELV CLSC*, Proceedings of the 1st International Scientific Conference on Supply Chains, Katerini-Olympus, Greece
- [2] EU Environmental Data Centre on Waste (Eurostat) (2010) *End of live vehicles data - 2008*. Available from: http://epp.eurostat.ec.europa.eu/portal/page/portal/waste/documents/ELV_year_2008_ref_2010_09_30_published_04_10_2010.xls [Accessed 10 June 2011]
- [3] EU. (2000) *Directive 2000/53/EC of the European Parliament and of the Council of 18 September 2000 on end-of-life vehicles*, Official Journal of the European Union, L269, pp 34-42

ACKNOWLEDGMENT

This work was partially supported by Ministry of Science and Technological Development of the Republic of Serbia through the project TR 36006 for the period 2011-2014.



RESOURCES MANAGEMENT IN WORKFLOW MANAGEMENT SYSTEMS

Dragan MISIC, Nikola VITKOVIC, Milos STOJKOVIC, Milan ZDRAVKOVIC, Miroslav TRAJANOVIC
Faculty of Mechanical Engineering, Nis, Aleksandra Medvedeva 14, Nis, Serbia
draganm@masfak.ni.ac.rs, vitko@masfak.ni.ac.rs, milos.stojkovich@gmail.com, milan.zdravkovic@gmail.com,
traja@masfak.ni.ac.rs

Abstract: *Workflow management systems manage business processes within an organization. In order to be successful, the systems must have ability for efficient management of resources which are used in processes. One of the shortcomings that have been noticed in the most of the workflow management systems is weak support for resource management. In this paper it is shown how to manage resources in MD system, which is developed on the Faculty of Mechanical Engineering Nis. This system tries to exceed shortcomings of the existing systems.*

Key words: *workflow management systems, resource management*

1. INTRODUCTION

From the aspect of the workflow management system, resource is an entity related to a specific activity and required at the time of execution for the activity to be done. Model of resources should contain definition of human and technical resources that will be used during the execution of the activity. Division into a process model on the one hand and a resource model on the other hand, enables separated evolution for both models. The process life cycle is usually different from the resources life cycle. If those two models are separated, the workflow management system designer can create process models which are independent of changes in the organization structure. Besides, if the resource model is separated, its division is allowed within the company and it simplifies managing of the model and avoids its redundancy.

If the model is given by WfMC coalition, managing information about resources is the task of the workflow system. Consequently, some workflow management software vendors add appropriate routines for resource management into their products. Those routines can be part of process molding environment (IBM MQSeries, Carnot) or special applications (Organization and Resource Manager – Siemens-Nixdorf). This way of implementation in which more than one workflow management system participates in the execution of complex processes might cause problems in large organizations. Namely, such systems cannot share information about resources which leads to redundancy of data. In addition, information such as occupation of resources can be marked out only if data from separate component for handling resources is integrated. Access to the data might be difficult, in which case resources can be managed only at the local level.

2. RESOURCES IN XPDL SPECIFICATION

In MD system, the model is consistent with XPDL specification [3]. In the domain of resources, this model is not complete and it is necessary to expand it with new constructions. XPDL model recognizes only human resources performing certain activities. There are processes and activities performed by participants with pre-defined roles.

Connecting a given defined role and specific participant in the process is done at the time of the process execution by the execution engine. It is possible that there is no participant with the role required, or that there is more than one appropriate participant. Both these cases are resolved in the specific implementation of the execution engine.

XPDL specification observes resources only from the aspect of the performer of a certain activity, which is inadequate for the production business system, as well as for most other systems. Availability of other resources is also very important for the execution. For example, the mere presence of a worker is insufficient for cutting, the machine must function properly, and there must be necessary tools. Even the electricity, which is necessary for the machine, can be considered as resource.

In accordance with the necessity to express the possible complexity of resources required for the execution of a certain activity, the basic XPDL scheme is expanded to include some additional elements.

The attribute MdResources describing all resources that are used during the execution of activity, is added to the element Activity which describes everything that refers to some process activity. The part of the activity definition, with the added element MdResources looks like this:

```
<xsd:element name="Activity">  
<xsd:complexType>  
<xsd:sequence>  
...  
<xsd:element ref="xpdl:MdResources" minOccurs="0"/>
```

```
</xsd:sequence>
```

```
...
```

```
</xsd:complexType>
```

```
</xsd:element>
```

The MdResources element is the list of all resources used in the activity and it should enable grouping of all the resources so as to facilitate approaching and manipulating them. It is the set of MdResource type elements which describe specific resources. XPD L definition of this element is:

```
<xsd:element name="MdResource">
```

```
<xsd:complexType>
```

```
<xsd:sequence>
```

```
<xsd:element ref="xpdl:Description" minOccurs="0"/>
```

```
<xsd:element ref="xpdl:MdResourceAttributes" minOccurs="0"/>
```

```
</xsd:sequence>
```

```
<xsd:attribute name="Id" type="xsd:NMTOKEN" use="required"/>
```

```
<xsd:attribute name="Name" type="xsd:string"/>
```

```
</xsd:complexType>
```

```
</xsd:element>
```

The element has two attributes and two sub elements. The attributes are Id, which is used for unique identifying of resources, and Name, which defines the name of the resource which is used for virtual display of the resource. Sub elements that closely describe resource are called Description used for defining textual description of the resource and MdResourceAttributes.

The workflow management system can be used for different processes in various domains. As the activities in those processes can be very different, the resources necessary for their execution can be manifold. In accordance with possible and expected diversity of resources, the describing is done by indefinite number of attributes. The list of the attributes that describes certain resource is defined by the resource itself and it can be arbitrary in size. Attributes themselves can also be various, either by name or content.

The element MdResourceAttributes represents a list of all attributes describing one resource. There can be one or more elements of MdResourceAttribute type. The basic purpose of this element is to enable grouping of all resource attributes and thus facilitate approaching and manipulating them.

Resource attributes make one resource different from another. There are no mandatory attributes, and it is up to the person describing a certain resource to choose attributes that will describe the resource in question best. XML definition of this element looks like this:

```
<xsd:element name="MdResourceAttribute">
```

```
<xsd:complexType>
```

```
<xsd:sequence>
```

```
<xsd:element ref="xpdl:Description" minOccurs="0"/>
```

```
<xsd:element ref="xpdl:RangeOfValue" minOccurs="0"/>
```

```
<xsd:element ref="xpdl:Value" minOccurs="0"/>
```

```
</xsd:sequence>
```

```
<xsd:attribute name="Id" type="xsd:NMTOKEN" use="required"/>
```

```
<xsd:attribute name="Name" type="xsd:string"/>
```

```
<xsd:attribute name="Required" type="xsd:string"/>
```

```
<xsd:attribute name="ValueType" type="xsd:string"/>
```

```
</xsd:complexType>
```

```
</xsd:element>
```

The resource attribute is described by a few elements and a few attributes. Two common attributes are Id, which is used for exact identifying of the attribute, and Name, which defines the name of the attribute that is used for its visual display.

Apart from Id and Name elements, there are two more attributes: required and value type. The attribute Required may have two values – YES and NO. This attribute is used for managing resources in order to highlight the importance of a resource. Some attributes are of great importance and they have to be satisfied, while others which are less important, can be satisfied (which is better), but if they are not, it does not entail that the resource is useless. This can be exemplified by the processing part on the lathe.

One of required resources is a turning tool. This tool is described by a line of attributes that defines its geometry and required characteristics. From the aspect of mandatory and required attributes, the tool type can be observed. It is better if the tool has hard metal plates for the process itself, but in the lack of such a tool, it is possible to use the high-speed steel blade. That means that the tool with hard metal plates is desirable but not also a necessary attribute. It will be used later on in the algorithm for selection of a particular resource.

On the other hand, if it is turning, then the attribute which defines the tool for turning has to be satisfied. If the attribute is not satisfied, the tool is not a possible resource for that activity.

The final attribute of the MdResourceAttribute element is the Value Type attribute. This attribute defines the value type that is given as the attribute value. Generally, the value can be numerical or it can be a string. Testing and regulation of required and given values are possible only if the values are of the same type and if this type is known. If values are numerical, comparisons operators can be used, while sets of characters can be compared only by the equivalence.

The XPD L specification may contain a description of resources. The resource description can be specific, which means that it is precisely indicated which resource is to be used, or the description can be schematic, in which case the list of required characteristics the resource should satisfy is given in order to use the resource for the activity.

Data about the existing resources in a company are placed in an independent database. Resources from a database are described by their characteristics. For every resource, there is information in database whether it is inoperative or whether it is engaged in a business.

Resources are characterized by their features which qualify the resource to perform certain activities.

3. HANDLING RESOURCES IN THE MD SYSTEM

3.1 Module for resource defining

The workflow management system, among other things, should monitor and assign the existing resources and assign to them some activities in the process. To make

this possible, the resources ought to be represented in an adequate way.

Resources which system has available are described in the database that is mentioned before. Data in this database could come in two ways. The first one is entering them directly with appropriate interface.

The other way for filling the database could be used if there is already another system for handling resources. In that case, it would be necessary to create an interface for connecting that system and the MD system with appropriate protocols for data transfer. This interface should be made in accordance with the specific case because its appearance and functions depend on the system which is used.

Currently, a separate module for resource managing is used in the MD system. The module is part of the system, so not only the system administrator can manage resources, but also a person that is not connected to the workflow management system. By system of permissions, it is regulated that the other person cannot access options provided only for the administrator.

This system enables entering new resources, updating the existing ones, defining new attributes, connecting attributes with resources, connecting resources with each other, defining occupancy and availability of resources.

3.2 Distribution of work in the MD system

Precondition for resource managing is an adequate resource description. As stated above, there is a database which contains resource data. Due to this database, it was possible to build a system that will manage resources within the business processes in a more sophisticated way.

Most authors who deal with workflow management systems regard those systems as a way for a complete automation of the processes. That means that most activities should be done by a computer program. That is the reason why so little attention is paid to manual activities done by people using appropriate tools. In the production environment is not often possible to have a completely automated process. There always remain some islands which are impossible to automate. As it often happens, those islands represent the major part of the process.

In processes based on manual activities, the first task is to distribute the work. In the existing systems, an activity is sent to all participants in the process which have defined ability to do it, so that it appears in the worklists of each appropriate participant. When it is taken over by one participant, it is removed from others worklists. In real terms it is not so simple to distribute the work which is received for execution.

Resources data contained in the database are precondition for improving the work distribution and resource managing. In the MD system, work distribution is done by an algorithm which takes into account the occupancy of resources and competence for execution of some works and priorities in executions of activities.

The algorithm starts when there is a new activity for the execution. Before the activity is assigned to a process participant, it is examining whether the participant can perform the activity, analyzing several options.

If resources and their attributes are not defined in XPDL definition, the work distribution is done in accordance with recommendations of the WfMC coalition. The roles are used most commonly, when the work is assigned to everyone in the organization with that role.

In the MD system, the activity is not put in the worklist of all participants that have the same role or belong to the same organizational units. Before putting an activity to a worklist, it is has to be checked whether that person has already taken up some activity. If no priorities have been defined, the activity is assigned only to those participants who are currently not occupied by any other activity. Thus, the more equal distribution of work is provided and each participant has a task to perform. If all the participants are occupied, the activity is put on each of the worklists.

Even if a participant in a process is unoccupied (the participant is not doing any activity at the moment), that does not mean that the participant is available. The participant might not have come to work or it might not be working hours, etc. The activity is not assigned to such participants unless there are not other participants that can perform the activity.

If the resource definitions for certain activities are given in the XPDL process definition, those definitions have the highest priority. In the previous text, the elements added to XPDL definition are described.

The moment the activity starts, it has to be checked whether the resources for the activity are available. This testing should only determine if there is a worker able to do the activity, as now it is only a matter of work distribution at this point. If there is more than one, the algorithm should decide which one is the most appropriate. If it is determined that there is no participant that can perform the activity, it is up to the exception handling system to take over solving the problem.

The process of determining the best participant is done in the following way:

After finding the resource which describes the participant that should do the activity, the set of attributes which the participant should satisfy is loaded. The set of attributes is loaded from XPDL process definition and it is defined by the process manager during creating the process definition.

XPDL definition contains a description of required resources. On the other hand, there is set of available resources, which are described in the database. In addition to their characteristics, in the database the information about the availability of the resources is given as well. Characteristics of all available resources are compared to required characteristics. The mandatory characteristics are checked first. If a resource (a person in this case) satisfies all mandatory characteristics, it becomes one of possible executors. If there is more than one member in the group of possible executors, a procedure for choosing the best one is started. The choice is based on desirable attribute values. All desirable attributes are being tested and the one with most of them becomes the executor. If there is more than one equally good executor, the activity will appear in worklist of all of them.

By choosing the best executor from the group, the work distribution is finished. The described procedure is used in case executors are not connected in any other way with

other resources required for the activity. Cases when other resources are connected with executors, best illustrated by examples, also have to be taken into consideration.

For the processing part on the lathe a worker whose task is to do it (a turner) is required. On the other hand, there has to be a lathe with certain characteristics. For example, if the part has a large diameter, the lathe where is possible to process large diameters is required. Workers in facility usually have machines that they are working on. That means that a certain machine, which is a resource, is tied with the worker who is also a resource. In such cases, it is necessary to consider the whole connection, which means the worker and the machine should be observed together. Thus the procedure of work distribution is a bit different.

The connection between the resources is implemented and is situated in the database.

The procedure of finding the work executor in the MD system is run by finding all the resources which satisfy conditions given in the XPDL process definition. Those resources represent the set of possible resources (resources which could be used for the activity). When the set of possible resources is formed, the connections between the subparts of the group are tested. In the final ranking, the best ranked will be a set of connected resources (if such exists). The group of connected resources will be chosen rather than single resources. For the previous example with a worker and a machine, it means that if the specifications of obliged attributes are satisfied, the priorities in choosing a resource are the worker and the machine which both satisfy the conditions. Although it may happen that other workers or machines are better, the priority is the connection between them.

After the work executor is chosen in one of those mentioned ways, the activity is assigned to the executor's worklist. The work executor's task is to take it over. If that does not happen in a pre-defined period, it may lead to an exception. In such cases, the exception handling mechanism is started. If the executor takes over the activity, his status is immediately changed to busy in the database. When the activity is finished, the executor signalizes that and in the resource database his status is changed to available.

4. DETECTION OF EXCEPTIONS RELATED TO RESOURCES

During the execution of a process, different exceptions may occur. In the manufacturing business processes, the most common exception is lack of resources for a certain activity. It is mentioned earlier that a resource may be defined within the definition of a process. In order to make that possible, the XPDL scheme is expanded with elements for defining resources. These elements are, as it was said, part of a definition of an activity.

Defining resources for every activity of every process might be hard. According to that, the engineer who creates processes should define only the resources that might be critical. For example, if there are ten lathes with similar characteristics, in defining activities of turning (which is done on one of those lathes), it is not necessary to define that for the activity of turning is required a lathe with those characteristics. On the other hand, if a lathe

with special characteristics is required, such as carousel with numerical control, intended for processing of parts with large dimensions, which can be done only on that machine, then it is required to define that machine as a necessary resource. It is considered here that there is only one such machine in a factory (which is the usual case because those machines are very expensive, and they are supplied individually).

If the resources are not defined for an activity, the resource exceptions cannot occur. In that case, there is no need to monitor the activity from the aspect of availability of required resources.

The other possibility is defining required resources for an activity. As it was mentioned earlier, the resources can be defined descriptively or specifically. Descriptive resource defining is done by defining attributes that should be satisfied. There are mandatory and desirable attributes as already described earlier. Specifically resource defining is done by giving a specific resource. For example, it has to be specified that for the activity to be performed the carousel with precisely defined mark is needed.

All activities for monitoring resources in the MD system are separated into a special module. The task of this module is to detect any exception, based on monitoring of resources. Information connected with a specific exception is sent to the expert system that tries to solve the problem.

Collecting information by the mentioned module for monitoring resources can be done in two ways. The information can be reached at the initiative of the modules for monitoring or they may originate from a system for resources handling. The first way is used during the execution of regular activities of the workflow management system. Because resources are defined in the activity itself, it is natural to check whether the appropriate resources are available before the activity starts. This check is done just in case that the resources for the activity are defined. If that is not the case, the process goes without any influence of the module for monitoring. However, if it finds that a resource for execution of the activity is missing, that information is sent to the expert system [2] the task of which is to do appropriate, corrective actions.

The process of checking availability of necessary resources is done in two ways. Which method is used depends on how the connection between resources and activities is defined. If the resource is defined specifically, the definition of the activity should clearly state that this specific resource is required (for example, the machine labeled SK-22). In this case, it is checked in the database if the adequate resource is available and if it is not busy. If a specific resource is unavailable, other data are downloaded from the database and with the process definition they are sent to the expert system. The other data here means a time when the resources will be available (if they will be available at all). For example, if the machine is out of order, there should be the time when it was broken in the database and also assessment when it will be fixed. Another option in checking availability of resources is that the resource is defined descriptively within the activity. The procedure of finding an appropriate resource in this case is conducted in the same manner as determined which participant will perform the

activity. If an adequate resource is not found, the expert system takes over solving the problem.

The other way for detecting possible exceptions is that the resource handling system, which is external system in regard to the workflow management system, sends the other one information that some resource is not available. In the resource handling system, there is an option to indicate that a certain resource will not be available in specific time interval.

The moment when it is specified that a resource is not available is the time to check whether the resource is necessary to carry out an activity. This is done by the message about unavailability of resources which is sent to the workflow management system. After that, the module for resource handling checks if the resource will be used anywhere.

At first, the module for monitoring resources checks activities of the processes which are already initiated. The check starts from the current activity onwards. If it is found that for some of the activities to be carried out in the future needed resource is not available, it is tried to determine the moment when the activity will be carried out. The resulting execution time is compared with the moment when the resource will be available (if that moment is defined). If the activity's execution time is after provided resource's repair, nothing will happen in the system. If that time is shorter, or it is not known when and if the resource will be available again, that is considered as an exception and all data are sent to the expert system to take corrective actions. A resource which is not available could be used in instances of processes that are yet to start. To enable the examination of the process, information about unavailability of resources is stored in a separate table in the database. This table contains information about unavailable resources. It is used to check the resources for new processes which are just starting. When a new instance of a process is being started, all unavailable resources are moved out from this table and it is checked if they are necessary for the process. If they are, the previously described procedure for time determination will be started. If they are not, the process runs its usual course.

5. CONCLUSION

The problem of WfMS resources management is an issue which has not been adequately solved. This paper has shown how resources are managed in MD system developed at the Faculty of Mechanical Engineering in Nis.

To define a process model in MD system XPDL specification is used. As this particular specification is not directly concerned with resources, it has been expended to include novel elements which make possible proper defining of resources required for the performance of an activity.

ACKNOWLEDGEMENT

This paper is part of project III41017 Virtual human osteoarticular system and its application in preclinical and clinical practice, funded by the Ministry of Education and

Science of Republic of Serbia (<http://vihos.masfak.ni.ac.rs>).

Defining resources within XPDL specification and the advanced module for resources management make it possible to evade some of the problems which may occur in the course of the workflow execution. Distribution of activities is more efficient (if manual activities are in question), and the activities themselves are performed using the most adequate resources.

Should any resources-related problems occur during the execution of activities, they are to be solved by the expert system, which has been described in detail in [2].

6. References

- [1] Misić, D., Stojković, M., Domazet, D., Trajanović M., Manić, M., Trifunović, M. (2010) Exception detection in business process management systems. *Journal of Scientific and Industrial Research*, pp. 188-193.
- [2] Mišić, D., Domazet, D., Trajanović, M, Manić, M., Zdravković, M. (2010) Concept of the exception handling system for manufacturing business processes, *Computer Science and Information Systems (ComSIS)*
- [3] WfMC (XPDL): Workflow Process Definition Interface - XML Process Definition Language. Document Status - 1.0 Final Draft. Document Number WfMC-TC-1025. Workflow Management Coalition 2002
- [4] Weber, B., Rinderle, S., Reichert, M. (2007) Change Support in Process-Aware Information Systems - A Pattern-Based Analysis, Tech. Rep. TR-CTIT-07-76, CTIT, University of Twente, The Netherlands.
- [5] Wu, S., Guo, B. (2008) Design of an exception handling algorithm of workflow. *ISECS International Colloquium on Computing, Communication, Control, and Management*, pp.281-284.
- [6] Hwang S & Tang, J. (2004) Consulting past exceptions to facilitate workflow exception handling, *Decision Support Systems* 37, pp. 49– 69



STEAM TURBINE CASINGS REVITALIZATION

Nedim GANIBEGOVIĆ, Sandira ELJŠAN

Thermal Power Plant Tuzla, University of Tuzla, Faculty of Mechanical Engineering, Tuzla, Bosnia and Herzegovina
nedim.ganibeg@gmail.com, sandira.eljsan@untz.ba

Abstract: Many year's operation, but especially a big number of shut downs and starts of turbo sets under operation in power industry caused degradation of their elements. Such elements are steam turbine casings.

The paper presents results of an extensive inspection and revitalization of 100 MW steam turbine casing in Thermal Power Plant Tuzla that was performed during overhaul in 2008. After 290.000 hours in exploitation changes in the microstructure of the cast steel had occurred and degradation of the mechanical properties of high pressure casing was confirmed.

Revitalization of casing allows obtaining operational features (plasticity limit, impact strength, transition temperature into brittle state and geometry) which do not differ from the new one.

Key words: revitalization, heat treatment, steam turbine, cast steel.

1. INTRODUCTION

Many year's operation, but especially a big number of shut downs and starts of turbosets under operation in power industry caused degradation of their elements. One of such elements are steam turbine casings.

During operation turbine casings are subject to action of different agents that cause their damage.

After long-term operation of cast steels at elevated temperatures (500-550⁰ C), casings show the changes, which make further utilization impossible. These changes include significant deformation, technological cracks and cracks caused by utilization and structural changes, causing decrease of material mechanical properties.

By reason of great dimensions and weight of casings their material may be already in initial state characterised by non-homogeneous structure and cracks, what considerably decreases mechanical properties of metal, mainly of its plasticity.

As a result of that, it is probable that damages will appear, especially in case of unfavourable conditions of utilizing.

The above mentioned changes do not limit further usability of casings, on condition that their revitalization will be executed. Otherwise, it is necessary to replace casings with the new ones.

Revitalization is a complicated process required to each repair the elaboration of separate technology, use of high-specialist machine tools, appropriate welding equipment and heat treatment equipment including furnace.

The paper presents results of an extensive inspection and revitalization of 100 MW steam turbine casing in Thermal Power Plant Tuzla that was performed during overhaul in 2008. After 290.000 hours in exploitation changes in the microstructure of the cast steel had

occurred and degradation of the mechanical properties of high pressure casing was confirmed.

2. TECHNICAL STATE OF MATERIAL BEFORE REVITALIZATION

The material of investigation was G21CrMoV4 – 6 (L21HMF) low alloy cast steel taken from the down and up steam turbine casing, chamber of regulation valves and HP nozles serviced for 290.000 hours at the temp. of 535 °C and the pressure of 9 MPa.

Table 1. Chemical composition

No	C	Si	P	S	Cr	V	Ni
1	0,21	0,31	0,015	0,017	0,99	0,26	0,11
3	0,17	0,32	0,016	0,018	1,15	0,21	0,20
5	0,23	0,30	0,020	0,019	1,10	0,20	0,33
6	0,24	0,28	0,019	0,016	1,07	0,21	0,34
7	0,21	0,31	0,016	0,012	1,13	0,27	0,19
8	0,20	0,33	0,019	0,019	1,03	0,24	0,12
9	0,25	0,32	0,012	0,011	1,08	0,27	0,24
10	0,25	0,32	0,013	0,014	1,09	0,28	0,24
11	0,20	0,33	0,16	0,020	1,13	0,28	0,12
12	0,19	0,32	0,015	0,019	1,13	0,27	0,12
13	0,21	0,31	0,021	0,030	-	-	0,10
14	0,26	0,20	0,024	0,019	0,26	-	0,15

Scope of destructive testing was:

1. Chemical composition with spectral method
2. Metallographic investigation
3. Definition of mechanical properties

Chemical composition of the investigated cast steel is given in Table 1.

Aim of estimation with destructive method was:

- Determination of material properties before revitalization
- Definition of appropriate heat treatment parameters in laboratory conditions.

Results of destructive testing obtained in laboratory conditions for appropriate kind of materials are presented in Table 2.

Table 2. Results of destructive testing

No. Of sample	Hardness HV ₃₀	Impact resistance KCV [daJ/cm ²]	Grain size
1	147	0,6	6
2	146	0,9	6
3	158	1,3	6/7
4	159	1,5	6/7
5	157	3,3	6/7
6	169	1,1	6/7
7	146	2,1	5/7
8	152	1,0	5/7
9	157	1,8	5/7
10	201	0,8	4/7
11	156	1,0	4/7
12	187	0,9	4/7
13	126	1,5	4/6
14	132	3,1	6

From these results it is obvious that the impact resistance satisfactory in only one sample. Impact resistance of all other samples was significantly lower than the standard prescribed amount of 3 [daJ/cm²] at the temperature of 20⁰ C.

3. METHODOLOGY OF REPARATION AND HEAT TREATMENT

Extending the operation time of long-term serviced cast steels is possible through the process of cast steel revitalization.

Repair starts with cleaning of casing, making of geometry measurements and carrying out of comparative analysis of real measurements with nominal measurements.

Magnetic tests are the next stage. After their performance it can begin elimination of cracks through grinding and milling, and next pad welding of losses. In case of extensive damages (through and through cracks) it is carried out inserts from proper material. It is necessary to initially heat material which casings are made of, because it easily yields to hardening at cooling rates typical of welding process. The induction and conductive heaters are used for this purpose. HP turbine casing after magnetic tests and after elimination of cracks are presented on Fig. 1.



Fig 1. HP turbine casing, outer side

Next very important stage is heat treatment in the furnace. The way of treatment performance is contingent upon material structure and their plastic properties. Heat treatment reaches target of removal of stresses, removal of internal stresses forming during exploitation, geometry correction, structure regeneration and amelioration of plasticity. In the end it is performed verification of planes and borings on the way of heat treatment.

Heat treatment for certain elements was performed in furnace in the separate cycles.

Regenerative heat treatment of steel casts, which is currently applied in industry, consists in normalizing or full annealing from austenitizing temperature with subsequent high-temperature tempering or under annealing. Ferritic – pearlitic or ferritic – bainitic structure, obtained as a result of such a heat treatment, ensures required impact energy KV > 27J and mechanical properties comparable to those after service. In the post operational condition the cast steel G21CrMoV4 – 6 (L21HMF) revealed degraded ferritic – pearlitic structure with numerous carbide precipitations located on grain boundaries and inside ferrite grains. Carbides precipitated on grain boundaries often formed „continuous grid“ of precipitates. [2].

State of material microstructure after heat treatment are presented on Fig 2. and Fig 3.

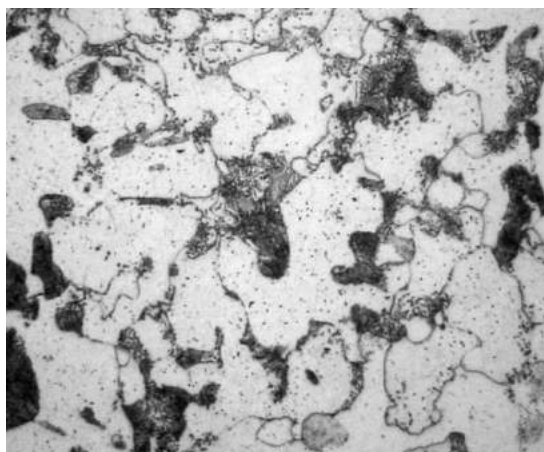


Fig. 2. HP casing, upper half, the steam entrance

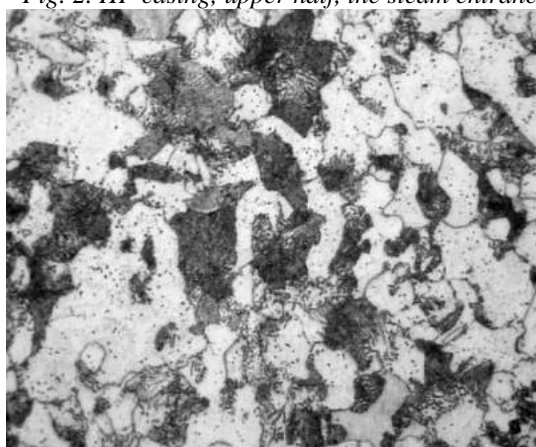


Fig. 3. HP casing, upper half, the steam exit

This picture shows the Ferrite-perlite structure with a grain size no. 7 ÷ 8 by the scale of PN-EN ISO 643.

4. RESULTS AND DISCUSSION

The survey consisted of 100% of the inner and outer surfaces of elements.

Results of destructive testing obtained in laboratory conditions for taken samples after heat treatment are presented in Table 3.

Steel castings tested samples, as shown in the Table 3 has a higher impact resistance than the required standard. Also, it can be seen that the hardness after heat treatment is higher compared to those measured after operation. During defectoscopic tests revealed a large number of cracks on all the elements covered by tests. Cracks was damaged internal and external surfaces of the elements studied. The character flaw is technology - exploitation. In areas of the entrance steam on the inside and the outer surface prevailed as the cracks which have exploitation character. Surface discontinuities that were present in other areas were substantially caused by technological reasons (overhaul and structural connections, and the casting surface defects below the surface).

Table 3. Cast steel properties after heat treatment in laboratory conditions

Position of sample	Hardness HV ₃₀	Impact resistance KCV [daJ/cm ²]
HP housing, the lower half, the steam entrance	160	5,5
HP housing, the lower half, the steam exit	160	4,1
HP housing, upper half, the steam entrance	160	4,3
HP housing, upper half, the steam exit	162	3,4
HP control valve, lower left	157	6,5
HP control valve, lower right	155	3,9
Box nozzle, right upper	156	4,5
Box nozzle, left upper	157	5,5

Due to the use of appropriate heat treatment parameters was obtained by regeneration through the creation of uniform structures and grinding grain size. Plasticity was improved: impact resistance is increased to a level that significantly exceeds 3,5 [daJ/cm²]. Also, the stresses was removed after operation and welding.

The table 4 presented the properties of steel castings L21HMF subject to standard (as a new element) and properties of cast steel L21HMF obtained after revitalization.

Table 4. Properties of cast steel L21HMF obtained before and after revitalization

Material	The properties of cast steel by PN-89/H-83157		The properties of cast steel after revitalization	
	Impact resistance KCU2 [daJ/cm ²]	Hardness [HB]	Impact resistance KCU2 [daJ/cm ²]	Hardness [HB]
L21HMF	3,0	140÷197	7,9÷9,5	143÷147

5. CONCLUSION

A basic aim of an adequate maintenance of power units is to increase their reliability and efficiency as well as to extend their service life at minimized expenditures. The above objective can be reached by performing the overhauls undertaken on the basis of either predetermined work time or the condition of the equipment.[3]

Revitalization of casing allows obtaining operational features (plasticity limit, impact strength, transition temperature into brittle state and geometry) which do not differ from the new one. Thus we can lengthen exploitation of casing about at least 100.000 hours with considerably lower costs.

HP turbine casing of steam turbine VK100 LMZ after heat treatment and revitalization is presented on Fig.4.



Fig. 4. HP turbine casing after revitalization

In this moment 100 MW steam turbine in Thermal Power Plant Tuzla has over 300.000 hours in service. As exploitation experiences show us, the turbine casings which has been constructed, tested and maintenance in appropriate manner, can be in exploitation for a long time.

REFERENCES

- [1] INSTITUT PRO NOVUM, Katowice (2009): *Estimation of technical state of HP casing of steam turbine type VK100-90-6 LMZ (TG-3) in Thermal Power Plant Tuzla*, Raport nr.132.2256/2008.
- [2] GOLANSKI, G. (2007) *Influence of tempering temperature on mechanical properties of cast steels*, Archives of Foundry Engineering, Vol. 8, Issue 4/2008, pp 47 – 50

- [3] BRUNNE, W., ZBROINSKA-SZCZUCHURA. E. (2010) *Recommendations for the examination and condition assesment of power generating equipment subject to official technical inspection, whose service life is expected to exceed 300000 hours*, XII Sympozjum Informacyjno-Szkoleniowe,(Pro Novum Katowice), pp 43-51



COMPARISON OF MODERN ELECTROHYDRAULIC SYSTEMS

Tadej TAŠNER^{1,2}, Darko LOVREC²

¹HAWE hidravlika d.o.o., Petrovče, Slovenia

²Production Engineering Institute, Smetanova ulica, Maribor, Slovenia
t.tasner@hawe.si, d.lovrec@uni-mb.si

Abstract: One of the main requirements of modern industrial systems is efficiency. Greater efficiency can be achieved by minimizing required energy, improving reliability and eliminating break-downs needed for maintenance. Due to increased usage of electrohydraulic systems in industrial applications, such systems have to be improved. Most of the systems use motor coupled with variable displacement pump. With cost-effective gear pumps driven by variable speed electric motor, another drive concept is becoming more popular. There are some questions posed by system designers: “What are the advantages and disadvantages of both concepts?” and “What would be the benefits when combining variable displacement pump with variable speed motor?”. All three systems will be described and compared by simulation results.

Key words: electrohydraulics, variable speed drive, constant pump, variable displacement pump

1. INTRODUCTION

Electrohydraulic systems are mostly used in machines or production lines which require big forces and power in order to operate as desired. Big forces result in big energy consumption which can be optimized by lowering losses in the electrohydraulic systems. Therefore, improved efficiency and reduced energy consumption are two of the main goals in modern electrohydraulic drive systems design.

Hydraulic energy can be controlled in two main ways: with throttling principle (by throttling on the directional valve) or with volumetric principle (by adjusting the pump displacement volume). The throttling principle has good dynamic behaviour, but its energy losses are substantial. The volumetric principle is energy friendlier, but has worse dynamic response. [1] Due to better efficiency, the volumetric principle is mostly used.

The hydraulic energy can be controlled by changing the flow and consequently pressure, which is achieved by adjusting the pumps' displacement volume. This can be done directly by using a variable displacement pump or indirectly by using a constant displacement pump coupled with a speed controlled motor. The second, indirect, principle is becoming more and more popular due to low prices of constant gear pumps and frequency inverters that are used to control motor speeds. [2, 3] When thinking in the way of improving efficiency of the electrohydraulic system an idea of using variable speed motor and variable displacement pump arises (Figure 1).

The main goals of this paper are to design a mathematical model and compare all three mentioned drive concepts by simulation results. The simulation results will give a rough estimation of performance differences between the drive concepts. The concepts will be evaluated by comparing settling time and overshoot of step response and ability to track a sine wave and a ramp.

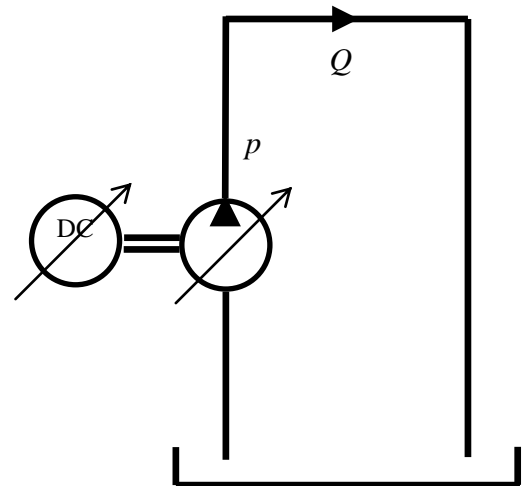


Figure 1: Combined drive concept – variable displacement pump coupled with variable speed DC motor

2. SIMULATION MODEL

The simulation model consists of a DC motor coupled with a variable displacement vane pump. The vane pump pumps the hydraulic fluid from a hydraulic tank through small diameter flexible hoses (equiv. higher resistance), which represents the load, and back to the tank. The flow through the hoses causes a pressure drop which is measured directly after the pump by an ideal pressure sensor. The pressure after the pump is controlled by all three different drive concepts to match the reference pressure as precisely as possible.

To be able to perform the simulation all the components used in the electrohydraulic circuit are modelled.

2.1. Variable displacement vane pump

The simulation model uses relatively simplified model of a variable displacement vane pump. The main parameter of a hydraulic pump is displacement – volume of fluid pumped in one revolution of the pump's shaft. If the displacement (V_D) is multiplied by pump's rotational speed (n) and pump setting ($k_p \in [0,1]$), we get the pump's flow rate (Q) (1) [4].

$$Q = k_p \cdot n \cdot V_D \quad (1)$$

Table 1: Variable displacement vane pump parameters

Displacement	$V_D = 6 \text{ cm}^3/\text{rev.}$
Cut-off frequency	$f = 50 \text{ Hz}$
Pump efficiency	$\eta = 0.8$

Because the flow cannot be changed as soon as the pump's setting changes, the pump's delay is approximated as a low pass filter with a cut-off frequency (f) and can be expressed in Laplace's frequency domain (2).

$$\frac{\alpha_D}{\alpha} = \frac{1}{\frac{1}{2 \cdot \pi \cdot f} \cdot s + 1} \quad (2)$$

The flow produced by the pump creates a pressure difference in the flexible hoses due to resistance between hydraulic fluid and hose wall. When the pump is creating pressure difference (Δp) the pump's shaft is loaded with torque (T_p) which is proportional to it (3)




$$T_p = \frac{k_p \cdot V_D \cdot \Delta p}{2 \cdot \pi \cdot \eta} \quad (3)$$

2.2. Hydraulic tubing

The dynamic behaviour of the fluid in the pipeline can be modelled in more different ways. The most exact model is based on the Navier-Stokes equations and the law of mass conservation, which results in a system of partial differential equations which are too much time consuming for such simulations.

Such an exact model of hydraulic pipeline is not needed, because all three drive concepts will be tested on the same pipeline system. Therefore more appropriate – discrete model also known as model with concentrated parameters was chosen. The discrete model is analogous to electrical circuits used by electrical engineers, where the properties of a circuit are represented by resistance, capacitance and inductance. In hydraulics the properties of a pipeline system are hydraulic resistance R_H (pressure drop in a tube due to flow), hydraulic capacitance C_H (pressure drop in a tube due to tube volume increase/decrease) and hydraulic inductance L_H (pressure drop due to fluid acceleration/deceleration). The analogy between electronics and hydraulics is presented in Table 2. [4]

Table 2: Electrical-hydraulic analogy

Electrical symbol	Electrical equation	Hydraulic equation
	$U = R \cdot I$	$p = R_H \cdot Q$
	$U = L \frac{dI}{dt}$	$p = L_H \frac{dQ}{dt}$
	$U = \frac{1}{C} \int I dt$	$p = \frac{1}{C_H} \int Q dt$

Using the electrical symbols the hydraulic pipeline system can be then represented by n segments as shown in Figure 2. Each segment represents part of a pipeline with a length of, l/n where l is total length of the pipeline. The number of segments also equals the number of possible pressure measurement points (ex. if the tube is modelled as one segment, the pressure in the middle of the tube cannot be calculated.)

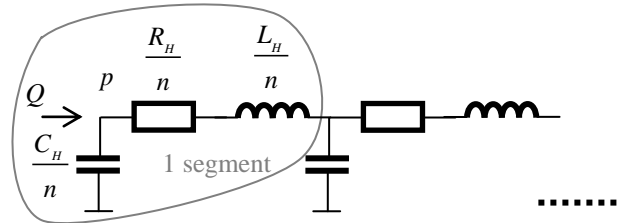


Figure 2: Hydraulic tubing represented by electric symbols

Because the pressure will be measured only at the pump outlet, the model will use a tube represented by only one segment. Such segment can be described using two differential equations; first one for hydraulic capacitance (4) and second one for resistance and inductance (5). If Q_c -flow through the capacitor is expressed out of the first equation and inserted into the second equation, a second order ordinary differential equation is obtained (6). Converting that equation to Laplace's frequency domain and expressing p/Q yields the transfer function of the hydraulic tubing represented by one segment.

$$p = \frac{1}{C_H} \int Q_c dt \quad (4)$$

$$p = R_H \cdot (Q - Q_c) + L_H \frac{d(Q - Q_c)}{dt} \quad (5)$$

$$p = R_H \cdot \left(Q - C_H \frac{dp}{dt} \right) + L_H \frac{d \left(Q - C_H \frac{dp}{dt} \right)}{dt} \quad (6)$$

$$\frac{p}{Q} = \frac{L_H \cdot s + R_H}{L_H \cdot C_H \cdot s^2 + R_H \cdot C_H \cdot s + 1} \quad (7)$$

In the simulation a model of MINIMESS® flexible hose with inner diameter of 2 mm was used. All other hose parameters crucial for the simulation are described in Table 3.

Table 3: Flexible hose and oil parameters

Hose length	$l=10$ m
Hose inner diameter [5]	$d_i=2$ mm
Hose outer diameter [5]	$d_o=5$ mm
Pressure loss for mineral oil with viscosity of $30 \frac{\text{mm}^2}{\text{s}}$ [5]	$R_H = 1 \frac{\text{MPa/m}}{\text{l/min}}$
Hose's Young's modulus	$E_R=1$ GPa
Density of oil	$\rho = 900 \frac{\text{kg}}{\text{m}^3}$
Bulk modulus of oil	$E_{oil} = 1$ GPa

The hydraulic oil plays an important role in the hydraulic transfer function. Its influence on the pipeline transfer function is hidden in the hydraulic resistance, capacitance and inductance, which can be calculated with the following equations (8, 9). [6]

$$C_H = \frac{V_0}{E_{oil}} = \frac{\frac{\pi \cdot d_i^2 \cdot l}{4}}{E_{oil}} = 2,41 \cdot 10^{-6} \frac{1}{\text{bar}} \quad (8)$$

$$L_H = \frac{l \cdot \rho}{\pi \cdot d_i^2} = 0,080 \frac{\text{bar}}{\text{min}^2} \quad (9)$$

2.3. DC motor

In the electrohydraulic system model a brushed DC motor was used. The DC motor was chosen because its model and control is relatively simple. The motor parameters used in the model are shown in Table 1.

Table 4: DC motor parameters

Armature resistance	$R_a = 2.5+2*0.38 \Omega$
Armature inductance	$L_a = 0.3+2*1.5 \text{ mH}$
Back EMF constant	$K_e = 0.0195 \text{ Vs/rad}$
Torque constant	$K_m = 0.0195 \text{ Nm/A}$
Rotor inertia	$J = 9.87\text{e-}6 \text{ kg.m}^2$
Friction coefficient	$B = 1.42\text{e-}6 \text{ Nm s/rad}$

The dynamic behaviour of a DC motor can be split into electrical (10) and mechanical (11) part. Both parts can be modelled by differential equations (10, 11) which are interconnected by torque (12) and back EMF constant (13).

$$U_a = I_a \cdot R_a + L_a \cdot \frac{dI_a}{dt} + E_b \quad (10)$$

$$T_E = B \cdot \omega + J \cdot \frac{d\omega}{dt} + T_L \quad (11)$$

$$T_E = K_m \cdot I \quad (12)$$

$$E_b = K_e \cdot \omega \quad (13)$$

Armature current (I_a) is controlled by controlling the armature voltage (U_a) and armature current is proportional to the electrical torque (T_E). The rotational speed of the motor is therefore dependent on the motor load (T_L) and the voltage applied to the armature. [7] Therefore the flow through the hydraulic pump coupled with the motor can be controlled by changing the voltage applied to the motor.

3.IMPLEMENTED CONTROL STRATEGY

Pressure is controlled by either DC motor in the indirect concept (variable motor, constant pump), or variable vane pump in the direct concept (constant motor, variable pump) or by both motor and pump in the combined concept (Figure 3). All controllers used in the simulation are PI type with internal (integrator) and external limits. PI controllers are known to be able to eliminate the steady state error and are more invulnerable to noise than controllers with the derivative (D) part. [8]

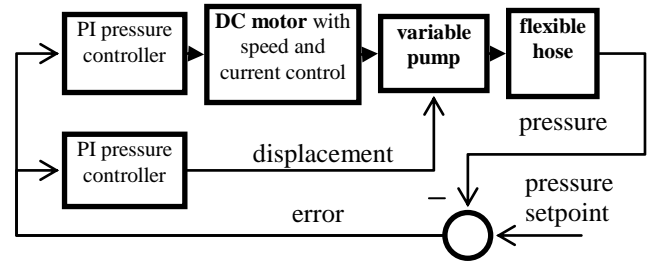


Figure 3: Control strategy of combined drive concept

3.1. DC motor controller

The control structure of the motor has a triple closed loop or with other words cascaded control. The innermost loop is current control loop which controls the armature current by changing the armature voltage; the middle loop controls rotational speed of the motor by setting a desired current value to the current controller; and the outermost controller controls pressure in the pipeline, by changing the rotational speed.

Integral gain of the current controller is chosen to compensate the poles of the electrical part and integral gain of the rotational speed controller to compensate the poles of the mechanical part.

3.2. Pump controller

The pump is controlled by a single closed loop and controls pressure by changing the displacement. Integral gain is chosen in the way that the controller's zero eliminates the pump's pole.

4.SIMULATION RESULTS

Simulations were performed on simulation model described above using Matlab/Simulink software. Dynamics of each drive concept were compared by responses to a combined cycle (sine, ramp and step) and a step. Simulation results are presented in Figures 4 to 7.

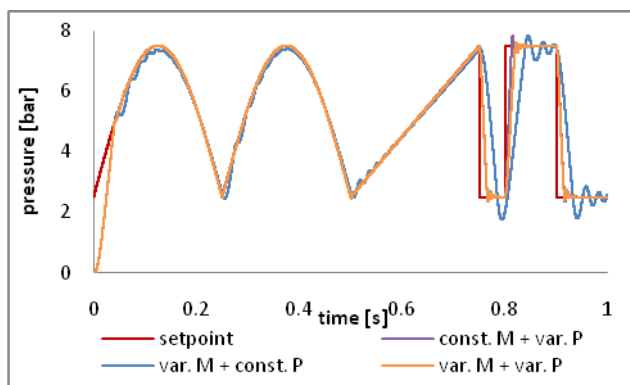


Figure 4: Pressure control performance – combined cycle

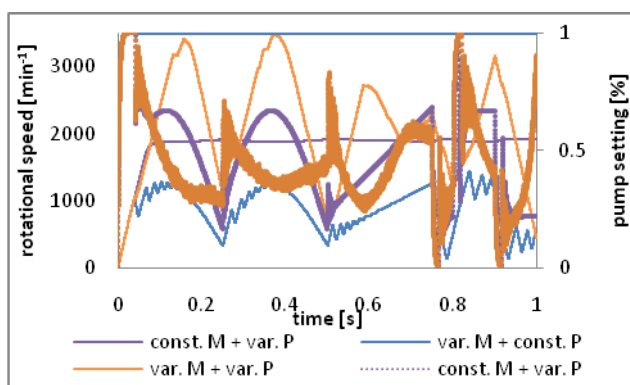


Figure 5: Rotational speed and pump setting – combined cycle

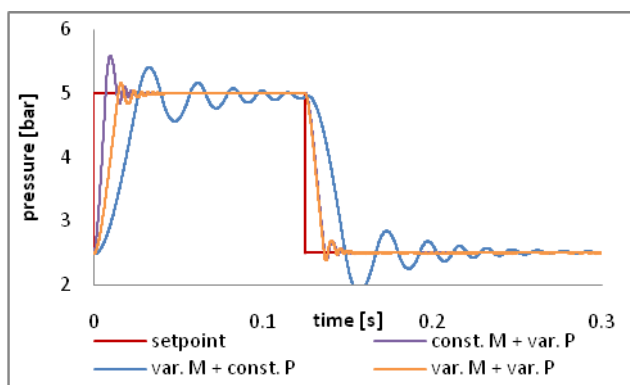


Figure 6: Pressure control performance - step

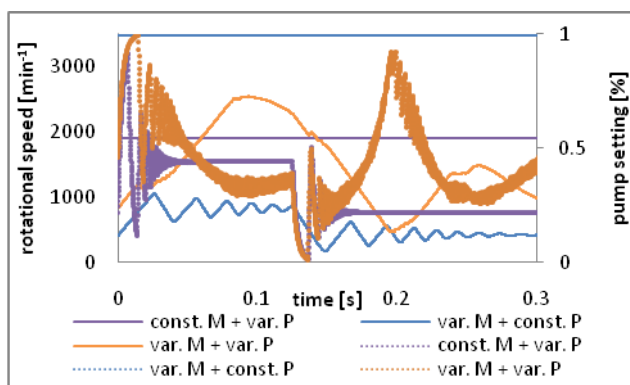


Figure 7: Rotational speed and pump setting - step

5. CONCLUSION

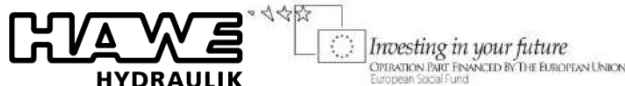
The concept of variable motor coupled with constant pump has the slowest dynamics. It is about 5 times slower than the other two concepts. Other two concepts (variable motor + variable pump and constant motor + variable pump) are very hard to separate. On rising steps the concept with variable motor and pump is a bit slower, but on falling edges it's sometimes slightly faster. The following two systems are very hard to compare, because the concept with variable pump and variable motor has two controllers which sometimes interfere with each other, resulting in poorer dynamics.

5.1. Future work

The control strategy for the concept with variable motor and variable pump should be improved, to minimize unnecessary changes (ex. lowering the rotational speed and increasing pump's displacement which cancel each other out). Further task is to create a controller which will maintain the maximum possible efficiency for current operating conditions and comparison of the simulation model with a real-world measurement.

6. ACKNOWLEDGEMENT

Operation part financed by the European Union, European Social Fund. Operation implemented in the framework of the Operational Programme for Human Resources Development for the Period 2007-2013, Priority axis 1: Promoting entrepreneurship and adaptability, Main type of activity 1.1.: Experts and researchers for competitive enterprises.



REFERENCES

- [1] MAJUMDAR, S. R. (2003) *Oil hydraulic systems: principles and maintenance*, McGraw-Hill.
- [2] LOVREC, D., ULAGA, S. (2007) *Pressure control in hydraulic systems with variable or constant pumps*, Experimental techniques, Vol.31, pp 33-41.
- [3] LOVREC, D., KASTREVC, M., HRIBERNIK, D. (2005) *Primerjava prilagodljivih elektrohidravličnih napajalnih sistemov na primeru regulacije tlaka*, Ventil, Vol. 11, pp 153-160.
- [4] LOVREC, D., HRIBERNIK, D., KIKER, E. (2002) *Model elektrohidravlične regulacije tlaka - osnova za načrtovanje in optimiranje pogona*, Ventil, Vol.3, pp 136-146.
- [5] MINIMESS®-Technical data on DN2 and DN4 microbore hose.
- [6] MURRENHOFF, H. (1998) *Grundlagen der Fluidtechnik - Teil 1: Hydraulik*, IFAS-RWTH, Aachen.
- [7] KAMARUDIN, N., ROZALI, S. (2008) *Simulink implementation of digital cascade control DC motor model - a didactic approach*, Power and Energy Conference 2008, pp 1043-1048.
- [8] SCHLEICHER, M., BLASINGER, F. (2004) *Control Engineering; A guide for beginners*, JUMO.



HYBRID CONTROLLER FOR SYSTEM MANAGEMENT OF INTEGRATED UNIVERSITY

Goran SLAVKOVIĆ, Žarko SPASIĆ

Faculty of Mechanical Engineering, BELGRADE University, Kraljice Marije 16, Belgrade, Serbia
gslavkovic@mas.bg.ac.rs, zpasic@mas.bg.ac.rs

Abstract: Hybrid controller is a major element in the projected system management of integrated university. University is seen as a complex system in partnership synergy with educational, research and business environment. There are shown characteristics that define a model of hybrid controller presented with appropriate block diagrams. Defined quality procedures are an essential part of an integrated quality assurance system for integrated university. For selected quality procedures, relating to the activities of teaching, research and management, the functions of the hybrid controller are shown. Especially is shown the quality procedure for Alumni Association feedback on the quality of teaching to degree programs, accredited one-semester courses and modules according to the Principles of Bologna Declaration. This means that the role of Alumni Association is adapted to the new way of studying and communicating with the university environment.

Key words: university, hybrid, controller, quality procedure

1. INTRODUCTION

Quality assurance in the CIM enterprise of integrated production, information and communication technologies is an essential function that requires the integration of information from all levels of the production company to make quality products and services to be competitive in the market of goods, capital and knowledge [1]. Internal and external exchange of information is enabled by description of digital products and services, compatible with all computerized systems and standards.

Projected solutions for system management of university in synergy with educational and business environment resulting from the analysis of the results of research in the fields of complex systems and education [2, 3, 4]. Based on the analyzed objects of control and management models it is possible to define the characteristics of a complex system of university for which is needed to design components that will contribute to the integrated operations of digital university with information and communication infrastructure and with a unique information resource. The university is an educational-research-business institution of higher education with many features that are related to systems management:

- A complex system with many components (subsystems and modules);
- A hierarchical system integrated with goals and objectives of individual sub-modules and subsystems;
- A system of multi-criterion decision-making;
- A system with dynamic changes (changes over time);
- A system of integrated disciplines of different expertise areas;
- A system with information feedback loop of educational and business environment;
- A system of integrated information of organizational units;
- A system of integrated internal and external activities and communications between university and environment;
- A system connected with users of education and research;
- A system with optimal adaptation to changes and demands (the Bologna process, the reform of higher education, competence in the knowledge market in Europe and in the world);
- A system of integrated information resources (an unique database/knowledgebase);
- A system with coordinate management, optimization and harmonization of conflicting demands;
- A system with advanced information and communication infrastructure of high technology;
- A system with built-in mechanism of gradual but steady improvement of the quality of all academic activities;
- A system which apply European and world standards for academic institutions;
- A system which is part of an integrated European area of education and research (EHEA¹ + ERA²).

¹ EHEA – European Higher Education Area

² ERA – European Research Area

2. INTEGRATED MODEL OF UNIVERSITY

Many university functions during the operations are dynamically changing over time, indicating that the university is system with dynamic changes. Data and information appearing in higher education are not signals with rules known in advance. There are various dynamic discrete data generated during the regular academic and management activities of the university. Unlike static systems whose condition does not change over time, the university is a dynamic system over time with tends to growth and development and there is a need for constant change. An important feature of the university is: that is a system with time delay. In modern systems management information delay occurs when information measure of variable and its further processing does not occur in the same place [5]. The existence of systems with time delay is a consequence of the presence of delays inherent in the object and/or in individual components of the control system, or of deliberate introduction of delays in the system, structure or process (e.g. using feedback in order to achieve better management or other improvements). The functioning of the university is based on multiple feedback loops that introduce delay into the system management. The university is a deterministic system because during the work exactly specifies what is required from the output of the education system (e.g. qualifications, certifications, profiles of expertise). It is also a stochastic system because different responses in the system include random variables, as components defined with some probability (for example, unpredictable results of research that do not always provide new products or new technologies).

The university is a nonlinear system with multi-dimensional state space in which a large number of inputs during the regular activities of the university, transformed into a large number of outputs using algorithms for managing, monitoring and prediction of system behavior [2, 4]. The most of the output signal through feedback loops are used for analyzing and improving management based on programmed controller algorithms. Adaptive systems with the functions of filtering, prediction and management are also responsive to the needs of managed digital university, because they have the ability to compensate unforeseen changes in the dynamics of processes or disorders affecting the system. Business of universities is followed by definition of business performances and quality indicators that represent discrete functions rather than continuous functions of time. The university is a complex system because the operations within the university produce a large number of processes (social, technical, economic, chemical and biological), that is characterized by the time-continuous, time-discrete, deterministic, stochastic, autonomous and non-autonomous. Annual reports on operations of the university and the evaluation reports in the accreditation procedures usually contain tabular and diagram displays

which should be designed in a unique way for comparability at the university level.

The data and knowledge of university are mostly deterministic nature, but in many activities with the valuation is embedded fuzzy logic. Database/knowledgebase as a unique information source of the university, a repository of information as an archive resource information, and control algorithms of controller should be designed for deterministic variables and fuzzy systems. Meaning of existence of multi-level and hierarchical relationship between them is explained by the principle of priority management actions. Management actions of subsystems at a higher level have priority over the execution of management actions at a lower level. At the higher level (faculty) there are decisions of strategic character (whose implementation took some time), while at the lower level (department) there are decisions largely with operational character.

3. SPECIFICATIONS FOR DESIGN OF HYBRID CONTROLLER OF INTEGRATED UNIVERSITY

The university is a complex educational-research-business system with many components that need to be integrated into a manageable system that operates effectively in a narrowly defined mission in society. The central place in the management of digital university belongs to the integrated system of quality assurance (Fig. 1) as part of an integrated information and communication system of university with also integrated information resources [4, 6].

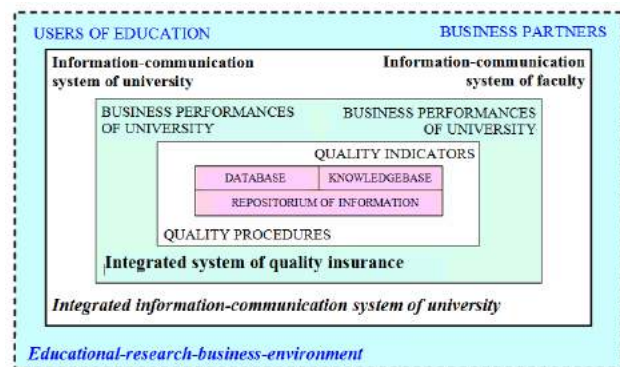


Fig.1. Integrated and partial systems of university and faculty

In order to define the characteristics of the hybrid controller for the integrated management of activities of universities starts with the role of each element in the block diagram that models the management of the university. Hybrid controller processes the input and feedback information containing data and knowledge of different types (signal, numerical data, diagrams, tables, fuzzy variables, etc.), as well as criteria for decision-making built-in algorithms that determine the size of the output controller to the next block of the adopted management model (Fig. 2).

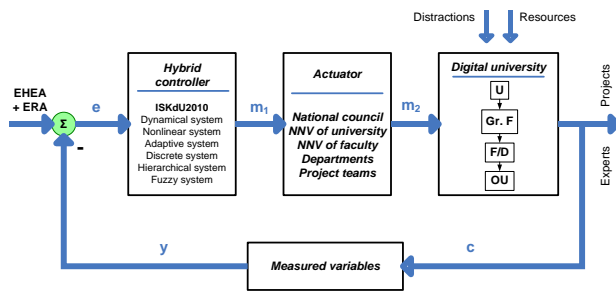


Fig.2. Hybrid controller and management of integrated university

The control unit of control system contains an error detector or a comparator and a unit that determines the way of management. Error detector calculates the difference of the current value of controlled variable and set reference value, determining the current deviation to make decisions that lead the management system in that way that these discrepancies are minimal and that seek to improve the quality of managed system, subsystem or module [2, 4, 7, 8]. Component for determining the control mode convert found deviation in control or corrective action or in controlled output to reduce the deviation. Adaptive control systems and processes ensure their optimal and adaptive behavior and movement through the state space based on adaptive management in space and time.

Actuator is an element of system management that converts the output of the hybrid controller and implements executive action of the controlled element. Manipulating element is using output control units and components for immediate regulation of necessary actions. Actuators translate controlled outputs in final execution of controlled elements which directly alter the value of controlled variables. In context of activities of integrated university these are professional and governing bodies which make appropriate business decisions (Serbian Conference of Universities, Educational Council, Council, Senate, Board of Directors, Supervisory Board, Council Chair, Consortium Projects, Student Parliament, Union of Universities, Council for development of Higher education and other bodies) [2, 4].

Block diagram of the hybrid controller shown in Fig. 2 in more detail is shown in Fig. 3. Input block in hybrid controller is block for analyzing of input signals and information. The mechanism of decision making in the next block processes the input signals and information using an appropriate algorithm for a given class of problems for which it was designed. In the same time is used a database/knowledgebase and programs upon which is possible to generate reports for decision making. If a collision occurs when processing data, feedback is used for corrections. At the exit of the hybrid controller are formulated proposals taking into account the limitations of the system. The particular feedback line performs the measurement and evaluation of relevant parameters and control variables, based on which appropriate action is taken.

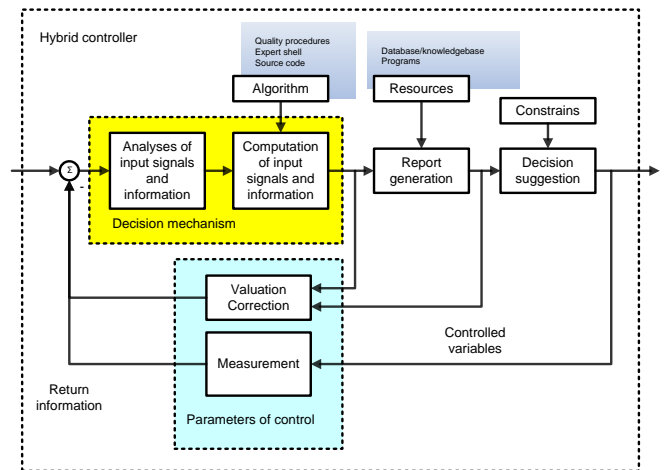


Fig.3. Block diagram of hybrid controller

4. QUALITY PROCEDURES FOR UNIVERSITY

Quality procedures are the basis for the implementation of an integrated system of quality in an institution of higher education. A procedure in a standardized manner that complies with the specifications of ISO 9000 describes the activities of education, research and management of universities, colleges or institutes. Each institution of higher education (university, college or institute) should define a coherent system of internal and external quality procedures that are part of the adopted policy of improving quality and determining the codex of business behavior all individuals and all organizational units with clearly defined activities and responsibilities in their implementation [2, 4]. In that way the development and improvement of culture quality of institutions and strategy of continuous quality improvement of education and research at the university is achieved. Quality procedures should be documented in a manner that involves employees in institution of education to understand them and their simple and uniform application in business. This means that the digital description of the procedures should be in accordance with the specifications of applicable standards, where quality procedures are part of an integrated quality assurance system with a unique database/knowledgebase.

It is believed that the university has introduced and implemented an integrated quality assurance system if its own documentation is translated into a uniform database/knowledgebase and in repository of information.

1. Quality Procedures of Hybrid Controller

For purpose of development of the hybrid controller functions for integrated management of the university is given an overview of several quality procedures. Each of the quality procedures should include:

- Description of quality procedure of an integrated university;
- Block diagram of the functions of the controller for quality procedure;
- The algorithm operation of quality procedure;

- Program code for defined controller's function.

Description of quality procedures in short explains the role of standardized procedures in an integrated quality assurance system that which is part of the overall information and communication system of digital university. Block diagram is showing the direct role of particular block in some standardized procedure. The algorithm operation of quality procedure provides graphically order of execution of the immediate tasks and perpetrators in the process. Program code is a software solution of a hybrid controller for a given quality procedure.

Below is given an overview of block diagram some of projected quality procedures [4]. These are: the procedure of monitoring the progress of students through the semester (QP-111014), the procedure for applying for research programs (QP-231024), and important procedure for feedback from *Alumni Association* (QP-331079). Identification numbers displayed quality procedures are determined on the basis of the adopted classifier for university activities of teaching, research and management.

2. The Procedure of monitoring the progress of Students through the Semester (QP-111014)

Description of the procedure for monitoring the progress of students through the semester (QP-111014)

The procedure for monitoring student progress through the study involves continuous recording of completed pre-examination and test obligations for each subject and calculate the current number of points, passed exams and current average of marks. Based on unfulfilled obligations it is possible to calculate the current study success because of ranking which is necessary to set priorities in the selection (e.g. selection of subjects, modules and directions, accommodation in student dormitories, etc.). Monitoring the progress of students through the process of university education is possible only by applying an integrated information system of the university with unique and integrated database/knowledgebase. Fig. 4. shows the initial database with information content of some entities and relations. Only on the basis of consistent and reliable database it is possible to define the correlation between the input quality and output quality in the process of university education.

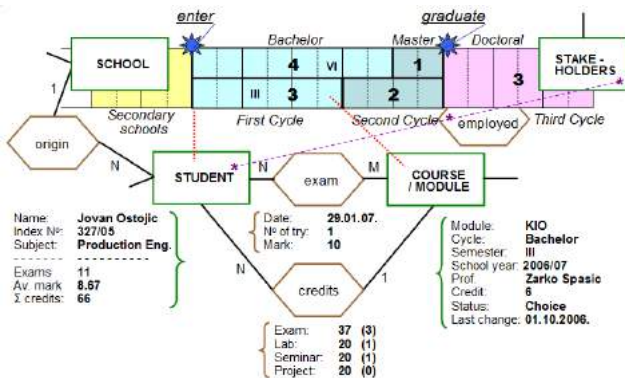


Fig.4. Initial database to track students progress

Efficacy studies can not be measured directly and depends on the number of subjects, length of study programs, quality teaching materials, use of equipment and software in teaching, studying and other. Taking into account the two available quality indicators that should accompany in the faculty's student services, it is possible to determine the relationship of these indicators as a simplified value of effectiveness studies. The first indicator determined student success to acquire a programmed quantum of knowledge, while the second indicator defines the time during which the performance is achieved. In other words, the coefficient of effectiveness study would be a ratio of two indicators, average mark during study and length of study.

Block diagram of the procedure for monitoring the progress of students through the semester (QP-111014)

Block diagram of the quality procedure to monitor the progress of students through courses and semesters is shown in Fig. 5. The decision mechanism involves blocks related to the pre-examination activities and the final exam of each course. Points from pre-examination activities and results of the final exam are added to the previous success of students by providing current success of student and defining variables for feedback which are used for analysis and ranking of classes, students and professors.

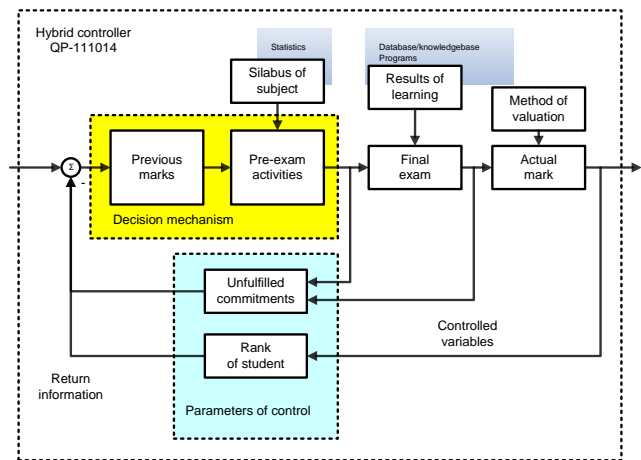


Fig.5. Block diagram of the controller's function for QP111014

3. The Procedure for application for Research programs (QP-231024)

Description of the procedure for application for research programs

Quality procedure for applications for research programs define the way of making proposals and the procedure for application of the competition of the Ministry for Technological Development, European Commission and other institutions responsible for funding. Universities and faculties based on development strategies and programs of scientific-research areas apply with projects in consultation with users of research. The research results

are implemented with business of users of research. With feedbacks are defined the control variables that determines the effects of implementing the results in business-research environment of universities.

Block diagram of the procedure for application for research programs (QP-231024)

Block diagram of the quality procedure for proposal for research programs is shown in Fig. 6. The decision mechanism involves blocks that define elements of the proposal whose are immediately entered into a database of appropriate software for project management. Each project has several phases in the life cycle, where the control points of execution and the quality of the results the most important parameters of successful research. Expected results of which are listed in the proposed project are compared with the results obtained, which must be acceptable to all users of research.

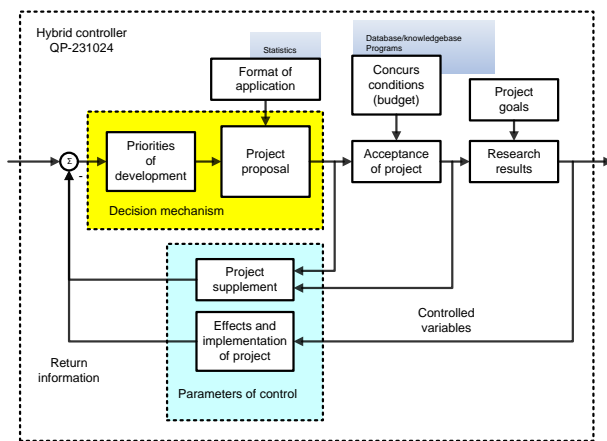


Fig.6. Block diagram of the controller's function for QP231024

4. The Quality procedure for feedback from Alumni Association (QP-331079)

Description of quality procedure for feedback from Alumni Association (QP-331079)

The main role of the Alumni Association is to provide feedback to improve teaching at faculties and universities. In that way Alumni Association represent one of the important subsystems of an integrated quality assurance system in the business of higher education. Reform of European's universities according to the principles of Bologna declaration is stopped the role of older generation of Alumni to affect the quality of teaching of new one-semester subjects. Newer generation must take over the role of the older generation, but for that part of the procedure should be enough time elapsed to obtain relevant feedback. Quality procedure QP-331079 establishes that possibility, so universities and faculties have enough time for younger generation to develop a sense of belonging to academic institutions which degree have acquired.

Block diagram of the procedure for feedback from Alumni Association (QP-331079)

Block diagram of the quality procedure for feedback form Alumni Association is shown in Fig. 7. The decision mechanism involves blocks that define the fields of teaching and teaching disciplines.

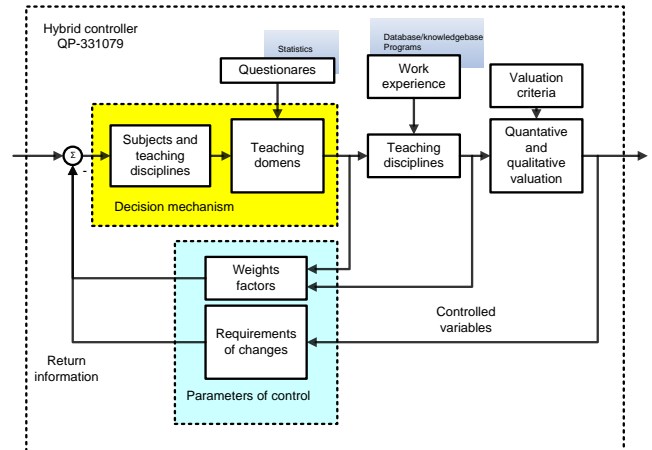


Fig.7. Block diagram of the controller's function for QP331079

5. CONCLUSION

Application of information-communication technologies in university management or in production-business enterprise is an essential precondition for the competitiveness of products and knowledge that requires constant change and adaptation. The elements of designed integrated information resource must to meet the requirements of modern and intelligent business and make decisions in real time, because the university and industry are very important to each other as business environment. Together they make up the world markets of products, technologies, and knowledge and expert services. Facility management is a university with its educational and business environment as a complex system that can be organized and managed in different ways. The integrated digital information system of university should to integrate all the partial information systems of faculty and other organizational units. Prerequisites for this long and complex task, which requires also a systematic approach, are: the integrated quality system, the classification of the elements of business, design of a unique database/knowledgebase, and define communication infrastructure and good organization of work.

REFERENCES

- [1] SPASIĆ, Ž., DIMITRIJEVIĆ-MARKOVIĆ, Lj., PILIPOVIĆ, M. (1994) *Informaciona integracija preduzeća – CIM integracija menadžmenta i kvaliteta*, Naučna knjiga, Beograd.
- [2] SPASIĆ, Ž., (2007) *Integrirani sistem kvaliteta digitalnog univerziteta*, Mašinski fakultet, Beograd.
- [3] SLAVKOVIĆ, G., SPASIĆ, Ž., (2010) *Hibridni kontroler za kompleksne sisteme na primeru univerziteta*, 36. JUPITER konferencija, 29. simpozijum CIM u strategiji tehnološkog razvoja industrije prerade metala, Zbornik radova na CD-u, str. 1.68-1.72, Beograd.
- [4] SLAVKOVIĆ, G., (2011) *Primena teorije upravljanja kompleksnim sistemima na integrirani sistem kvaliteta u sinergiji univerziteta sa obrazovno-poslovnim okruženjem*, doktorska disertacija, Mašinski fakultet, Beograd.
- [5] DEBELJKOVIĆ, Lj. D., (2010) *Linearni singularni sistemi sa čistim vremenskim kašnjenjem*, Mašinski fakultet, Beograd.
- [6] SPASIĆ, Ž., (2006) *Modelling of Quality Assurance System in the Relation „University-Industry“*, IFNANS International Journal, Problems of Nonlinear Analysis in Engineering Systems, No. 2 (26), Vol. 12, pp. 117-127.
- [7] HAIMES, Y. Y., KYOSTI, T., SHIMA, T., THADATHIL, J., (1990) *Hierarchical Multiobjective Analysis of Large-Scale Systems*, Hemisplan Publishing Corporation, New York.
- [8] LUNZE, J., (1992) *Feedback Control of Large-Scale Systems*, Prentice Hall, New York.

ESTABLISHMENT OF A LECTURE SERIES ON “LIFE CYCLE DESIGN – ECODESIGN”

Guenther POSZVEK

Institute of Mechatronics, UAS Technikum Wien, Höchstädtplatz 5, 1200 Wien, Austria
 poszvek@technikum-wien.at

Abstract: *The present work shows how the lecture "Life Cycle Design - Ecodesign" was implemented didactic at the UAS Technikum Wien. Under Ecodesign we can subsume all activities that attempt, the negative environmental impacts of products to be minimized. The Brundtland Commission defines it as "the capacity to meet the needs of the present without compromising the ability of future generations to meet their own needs." Green is another way in which sustainability has been expressed. As energy costs increase, so too does the demand for environmentally friendly products and services, including energy and environmentally friendly designs. There doesn't exist any kind of "eco" thinking or teaching at the UAS Technikum Wien and the great challenge was to implement a course like this. The course has been designed and new content, like the following key issues have been incorporated: "Sustainability", "Ecodesign", "Life Cycle Assessment of products", "Life Cycle Thinking" and "Ecodesign - examples". Using different software tools the students learn more than one perspective of sustainability. The final layer is the evaluation of a mechatronic product with the help of learned tools.*

Key words: Sustainability, Ecodesign, Life Cycle Design

1. INTRODUCTION

If the speech is about "Ecodesign" inevitably emerges the concept of sustainability on. It originally comes from forestry, and states that the ratio of replanting and clearing at the present time must be in a steady relationship, so that the next generation the same amount of trees available [1].

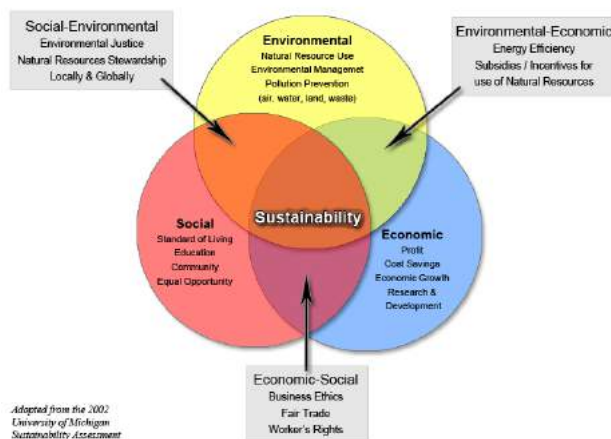


Fig.1. The Three Spheres of Sustainability

This state of equilibrium is the natural state of the earth. The aim is to ensure sustainable development. As part of the course work implemented should help to promote sustainable development through Ecodesign.

2. ASSIGNMENT OF TASKS

One of the main tasks was to build for the course "Life Cycle Design" a base and find out what were the basics for it. Subsequently, the lecture will be analyzed and improved. Besides the slides a script was written and implement in an uniform with the presentation slides.

3. ECODESIGN

Sustainability can be specifically influenced by an appropriate design and development and environmentally friendly products will be promoted. For this reason, the term ECODESIGN appeared. In this area can also be other terms with the same statement, like "DfE" - Design for the Environment, "LCD" - Life Cycle Design, "DFS" - Design for Sustainability and many more.

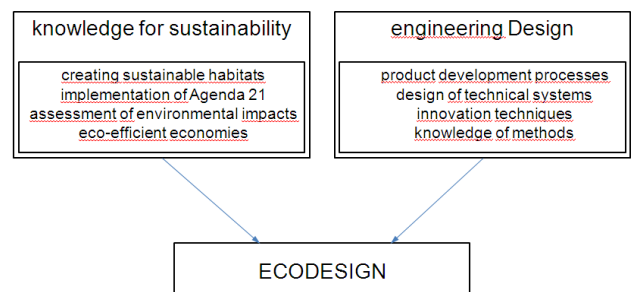


Fig.2. Term assignment ECODESIGN

3.1 IMPLEMENTATION OF SUSTAINABLE TECHNICAL SOLUTION

In the design of sustainable technical solutions within the framework of ECODESIGN there are three points which are of crucial importance. These three points are the efficiency of technology, organizational effectiveness and the sufficiency of the culture. The following chart shows the interaction.

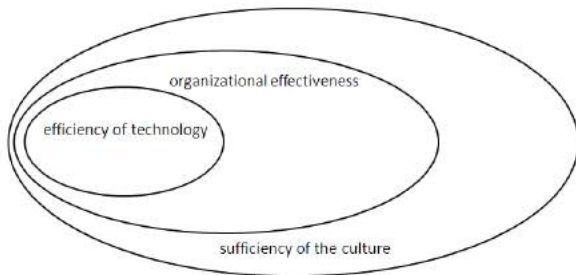


Fig.3. The three points of a sustainable technical solution

3.2 Benefits of ECODESIGN

ECODESIGN brings numerous advantages. These are located along the entire product life cycle.

- 1st New product ideas can be found, they will best fit the needs of the customer. This will optimize the product in its function and the quality is improved.
- 2nd The environmental performance of its products is increased. This environmental damage caused by waste and emissions are reduced.
- 3rd Favorable cost structures can be achieved, since material and disposal costs are saved. Additionally, supplies can be saved.
- 4th The company's future is secured. The responsibility is assumed active and the company image and increase customer confidence by the integrated product policy (IPP).

The integrated product policy is a synonym for the environmentally friendly product and process development and was launched by the European Union into being. It relies on a point in two and three above-mentioned measures and concerns the entire product life cycle

4. LIFE CYCLE STUDY OF PRODUCTS

An essential step for improving the product through its life cycle is ECODESIGN consideration. As the life cycle after the EuP Framework Directive [2]

"... the totality of the consecutive and interlinked stages of an EuP from raw material use to final disposal" [2] (EuP Directive 2005/32/EC 2005) understood.

At the beginning of this cycle is the clarification of the market, defining the future operational area of the product, deriving from the concepts and the appearance of the product. As a result of these initial steps are obtained including parts lists, construction plans and operation plans. Following are the product manufacturing, transportation to site, use and recycling or disposal, etc. In essence, the product life cycle can thus in five phases (Wimmer and Züst 2001) divide. These are shown in the figure below.

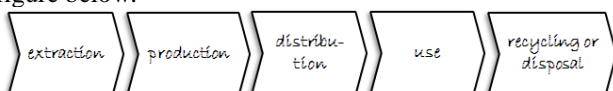


Fig.4. The five phases of the product life cycle [3] (Wimmer and Züst 2001, p. 21)

The figure shows the entire product life cycle. Based on the resources used and their transformation through the following stations [3]:

- **extraction of raw materials:** it will provide the necessary energy. This usually happens by the extraction and conversion of natural resources. Oil must be encouraged to produce plastic and metal ores to be mined to produce steel.
 - **production:** the products are manufactured from the produced commodities. In this step, assembly machines, tools, equipment, supplies and transportation systems are necessary.
 - **distribution:** following the production is transported to the place of deployment.
 - **use:** within this phase there may be an additional consumption of energy, materials, emissions, effluents and waste. It also can repair cycles to come to life and to extend the operational status of the product.
 - **after use:** after using the product must be disposed of or if there is a recycling of the substances.
- Of an ecologically solution we talk when all five phases of the product life cycle as a whole are considered and optimized. It is then of "Life-Cycle Thinking" mentioned. Not all products go through the life cycle in a linear sequence, as just described. There may be unplanned processes within or between the five steps described above (eg repair).

5. ECODESIGN Example

As part of the implementation of the Manuscript ECODESIGN one example was prepared that shows the product improvement of a CD case. As a product developer of CD cases have different product requirements into account. The aim is to achieve an optimization and environmentally improved product.

5.1 MATERIAL SAVINGS STRATEGY

As a recommended measure is to save material by the ECODESIGN PILOT proposal, preferably recycled (secondary materials) of polystyrene use. Furthermore, the amount of material to be reduced by a strength-optimized design. This could be achieved by minimizing the amount of housing (Slim-Case). This would increase the strength and prolong life. In addition, the amount of material could be reduced by a functional integration, for example by a lever mounted for closing and holding the CD in the package.

5.2 GROWTH STRATEGY OF PRODUCT LIFE

To increase product life by the ECODESIGN PILOT recommended design of usable interface design [4]. Through the use of semi-transparent polystyrene could be achieved.

5.3 STRATEGIC REUSE OF MATERIALS

Finally, for the recycling of used materials, a Standard-compliant marking of the materials is considered. For this reason, the CD case with a PS-marking be provided

REFERENCES

- [1] KOPLIN, J.(2005) *Nachhaltigkeit im Beschaffungsmanagement. Ein Konzept zur Integration von Umwelt- und Sozialstandards.* Oldenburg: Deutscher Universitätsverlag
- [2] EuP-Rahmenrichtlinie 2005/32/EC – *Directive for energy using products. Art.2 Abs. 13. 2005.*
- [3] WIMMER, W., ZÜST R. (2001) *ECODESIGN PILOT, Produkt- Innovations-, Lern- und Optimierungs-Tool für umweltgerechte Produktgestaltung.* Zürich: Verlag industrielle Organisation
- [4] ECODESIGN PILOT, 1996. *Ecodesign Pilot* <http://www.ecodesign.at/index.en.html> [Stand: 20. Juni 2011].



EVALUATION OF PRODUCT AND PRODUCTION TECHNOLOGIES QUALITY METHOD OF SUPERIORITY AND INFERIORITY

Dragan TEMELJKOVSKI¹, Predrag POPOVIĆ², Bojan RANČIĆ³, Petar ĐEKIĆ⁴

University of Niš, Mechanical Engineering Faculty, Aleksandra Medvedeva 14, 18000 Niš, Serbia
temelj@masfak.ni.ac.rs, bojanr@masfak.ni.ac.rs, petardjekic@masfak.ni.ac.rs,

Abstract: *The method of superiority and inferiority is used for evaluating superiority or inferiority of some natural or engineering-technological value with respect to some other one or of many values of the same kind with respect to one another. It has come into being as a result of the research done by the author of this paper. In order to qualitatively compare two or more values (that can be technologies, processes, products, methods, services or events or any other assessable states or phenomena), it is for them that we must determine respective exact value indicators which are in this paper defined by variables. By using a relatively simple mathematical apparatus in addition to a systematized tabular instruction, we determine the qualities of the observed values as well as superiority or inferiority among them.*

Key words: Product, Technology, Quality, Superiority, Inferiority

1. INTRODUCTION

The method of superiority and inferiority is used for evaluating superiority or inferiority of some natural or engineering-technological value with respect to some other one or of many values of the same kind with respect to one another. It has come into being as a result of the research done by the author of this paper, [1], [2].

Our task is to qualitatively compare two or more values (that can be technologies, processes, products, methods, services or events or any other assessable states or phenomena) for which we can determine qualitative or quantitative characteristics given in the form of exact parameters, variables, by which a given value can be competently assessed. The characteristics of the comparable values or variables of the observed value given in the form of qualitative or quantitative parameters by which a given variable is evaluated can be determined, depending on the variable's character, in one of the following ways, [3], [4], [5]:

- By exact mathematical calculation,
- By applying qualitative statistical methods,
- By collecting and processing information about the observed variable,
- By surveying, and,
- By researching referential literature, and the like.

The variable's characteristic in the form of the evaluation parameters must be given in the form of numerical qualitative or quantitative value as well as percentage value. The quality of the comparative value in the function of characteristic assessing variables can be given in the form:

$$KV_j = \sum_{k=1}^m q_{kj} \cdot p_{kj} \quad (k=1,2,3... \dots m, j = 1,2,... \dots n) \quad (1)$$

where: KV_j - quality of j-th comparative value,
 q_{kj} - k-th coefficient of involvement of qualitative or quantitative variable k in evaluating comparative value j,
 p_{kj} - k-th variable of comparative value given in the form of qualitative or quantitative value of comparative value j,
 j - j-th comparative value,
 m - number of characteristics of variable j given in the form of qualitative or quantitative parameters, and
 n - number of comparative values whose quality is being evaluated.

The very process of calculating and evaluating the values to be compared by this method is taking place in four steps by making respective decision-making matrices.

2. FIRST STEP

In the prepared table, the first column is to comprise the names of respective selected variables by which we evaluate the comparative values input into the first row. The sequence of inputting comparative values as well as that of their variables is irrelevant. The number of variables directly affects the value quality evaluation and it is necessary to tend to as many variables as possible so that the observed value can be evaluated from as many aspects as possible. However, we should not exaggerate with the number of variables. It is far more important to exactly calculate or determine, by some other method, the value of the observed variable for the analyzed evaluation of the comparative value so that its evaluation of the observed value could be as best and as of higher quality and competence as possible.

		COMPARATIVE VALUES V _j						
VARIABLES P _{kj}	OPTIMIZA. CRITERIA	V ₁	V ₂	...	V _j	...	V _n	SUM
1	2	3	4	...	j+2	...	n+2	n+3
P _{1j}	max	P ₁₁	P ₁₂	...	P _{1j}	...	P _{1n}	$\sum_{j=1}^n P_{1j}$
P _{2j}	min	P ₂₁	P ₂₂	...	P _{2j}	...	P _{2n}	$\sum_{j=1}^n P_{2j}$
.....
P _{kj}	max	P _{k1}	P _{k2}	...	P _{kj}	...	P _{kn}	$\sum_{j=1}^n P_{kj}$
.....
P _{mj}	min	P _{m1}	P _{m2}	...	P _{mj}	...	P _{mn}	$\sum_{j=1}^n P_{mj}$
	SUM	$\sum_{k=1}^m P_{k1}$	$\sum_{k=1}^m P_{k2}$...	$\sum_{k=1}^m P_{kj}$...	$\sum_{k=1}^m P_{kn}$	$\sum_{k=1}^m \sum_{j=1}^n P_{kj}$

		COMPARATIVE VALUES V _j						
VARIABLES P _{kj}	OPTIMIZA. CRITERIA	V ₁	V ₂	...	V _j	...	V _n	SUM
1	2	3	4	...	j+2	...	n+2	n+3
P _{1j}	max	$\frac{P_{11}}{P_{12}^{\max}}$	1	...	$\frac{P_{1j}}{P_{1j}^{\max}}$...	$\frac{P_{1n}}{P_{1n}^{\max}}$	$\sum_{j=1}^n \frac{P_{1j}}{P_{1j}^{\max}}$
P _{2j}	min	$\frac{P_{21}^{\min}}{P_{21}}$	$\frac{P_{22}^{\min}}{P_{22}}$...	1	...	$\frac{P_{2n}^{\min}}{P_{2n}}$	$\sum_{j=1}^n \frac{P_{2j}^{\min}}{P_{2j}}$
.....
P _{kj}	max	1	$\frac{P_{k2}}{P_{k2}^{\max}}$...	$\frac{P_{kj}}{P_{kj}^{\max}}$...	$\frac{P_{kn}}{P_{kn}^{\max}}$	$\sum_{j=1}^n \frac{P_{kj}}{P_{kj}^{\max}}$
.....
P _{mj}	min	$\frac{P_{m1}^{\min}}{P_{m1}}$	$\frac{P_{m2}^{\min}}{P_{m2}}$...	$\frac{P_{mj}^{\min}}{P_{mj}}$...	1	$\sum_{j=1}^n \frac{P_{mj}^{\min}}{P_{mj}}$
	SUM	$\sum_{k=1}^m \frac{P_{k1}}{P_{k1}^{\max}}$	$\sum_{k=1}^m \frac{P_{k2}}{P_{k2}^{\max}}$...	$\sum_{k=1}^m \frac{P_{kj}}{P_{kj}^{\max}}$...	$\sum_{k=1}^m \frac{P_{kn}}{P_{kn}^{\max}}$	$\sum_{k=1}^m \sum_{j=1}^n \frac{P_{kj}}{P_{kj}^{\max}}$

Into columns V₁ and V_n we input quantitative numerical values or percentages for the given variable of the value under observation.

In the column SUM we sum up the values of the evaluations made for the given parameter of the observed row with all the variables that participate in the evaluation

$$\text{of observed value } \sum_{k=1}^m P_{kj}$$

In the row SUM we sum up the values of the evaluations of all the parameters of the observed row with the given

$$\text{variable of observed row } \sum_{k=1}^m P_{kj} . \text{ In the last row SUM}$$

we sum up the values of each comparative parameter determined by all the variables in given column $\sum_{k=1}^m P_{kj} .$

SUM in the last row of the observed table represent qualities of the observed values with the coefficient of the variable's participation, that is, characteristics of comparative value $q_{kj}=1$ which means that the given variable in the form of evaluation parameter participates with 100% of its value in the evaluation of the observed comparative value. This evaluation is rough and frequently even incorrect since the greatest impact in evaluating the observed value is that of the variable with the highest nominal value while the impact of the variables with small nominal values – which are, in essence, quite relevant – on the evaluations of the comparative values is minor and negligible.

In order to avoid all these and other shortcomings that may arise while evaluating quality of the observed value we take the following step.

3. SECOND STEP

In this step we unify the characteristics of the variable and classify them according to the criterion of their characteristics' optimality given in the column two of the first step table or in the same column two of the second step table (OPTIMITAZION CRITERERION). Unification and ranking of the characteristics' values is done in the following way:

- If in the observed row of the given matrix (OPTIMIZATION CRITERION) is minimum, then the minimal order of the given row is divided by each member in the observed row. Where the minimal member of the given row used to be, there is now value 1 and this characteristic in evaluating the quality of the observed value in this column participates with 100% of its value.
- The last member of the observed j-th row $\sum_{j=1}^n \frac{P_{kj}}{P_{k1}^{\max}}$ represents the SUM of percentage participation of j-th variable in the summary evaluation of all observed values V_j.
- Parameters in the last row represent the evaluation of the quality of the observed value $\left(\sum_{k=1}^m v_{kj} = \frac{P_{1j}}{P_{12}^{\max}} + \frac{P_{2j}^{\min}}{P_{21}} + \dots + \frac{P_{k1}}{P_{k1}^{\max}} + \dots + \frac{P_{mj}^{\min}}{P_{mj}} \right)$ in the function of percentage participation of all m characteristics, namely variables p_{mj} .

If the quality evaluation were to be made in this step, we would face the same problems that we did in the first step. In this case as well certain characteristics, although they have 100% participation in the evaluation of the observed variable, due to their small nominal value, have an impact upon the total quality evaluation of the observed variable which is minor and negligible.

4. THIRD STEP

In this step we determine optimal values of coefficient of participation of quantitative kth variable in evaluating observed value j.

The coefficients of the optimal participation of k-th variable in evaluating j-th value are determined by dividing every member of the matrix from the previous step by the SUM of the row in which the given member is located; then, the obtained value is divided by the SUM from the column in which the given member is located.

$$\text{If we use } r_{kj} = \frac{P_{kj}}{P_{k1}^{\max}}$$

to denote k-th member of the second step matrix, then the formula for calculating the coefficient of the characteristic in the third step is:

$$q_{kj} = \frac{\left(\frac{r_{kj}}{p_{kj}} \right)}{\left(\frac{\sum r_{kj}}{p_{kj}} \right)} \cdot \left(\frac{r_{kj}}{p_{kj}} \right)$$

where P denotes the previous member, PR denotes the previous row and PK the previous column.

The calculated coefficient q_{kj} represents the value of the percentage participation of k-th characteristic in evaluating quality of j-th of the comparative value.

The value of the sums in the last row of the given matrix for each comparative value is 1 and it represents the total participation of all m variables in evaluating the observed j-th comparative value.

		COMPARATIVE VALUES V_j						
VARIABLES p_{kj}	OPTIMIZA CRITERIA	V_1	V_2	...	V_j	...	V_n	SUM
1	2	3	4	...	$j+2$...	$n+2$	$n+3$
p_{1j}	max	q_{11}	q_{12}	...	q_{1j}	...	q_{1n}	$\sum_{j=1}^n q_{1j}$
p_{2j}	min	q_{21}	q_{22}	...	q_{2j}	...	q_{2n}	$\sum_{j=1}^n q_{2j}$
.....
p_{kj}	max	q_{k1}	q_{k2}	...	q_{kj}	...	q_{kn}	$\sum_{j=1}^n q_{kj}$
.....
p_{mj}	min	q_{m1}	q_{m2}	...	q_{mj}	...	q_{mn}	$\sum_{j=1}^n q_{mj}$
SUM		$\sum_{k=1}^m q_{k1} = 1$	$\sum_{k=1}^m q_{k2} = 1$...	$\sum_{k=1}^m q_{kj} = 1$...	$\sum_{k=1}^m q_{kn} = 1$	$\sum_{k=1}^m \sum_{j=1}^n q_{kj} = n$

5. FOURTH STEP

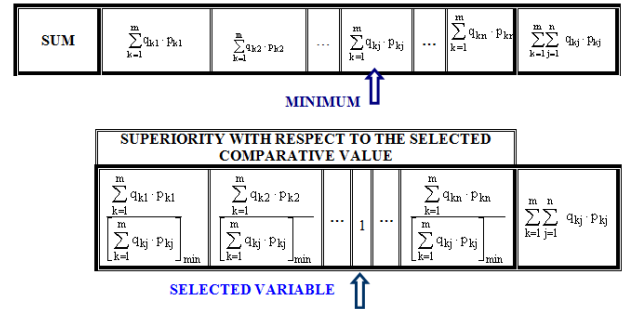
As can be seen from equation (1), in order to obtain quality evaluation of some comparative value, it is necessary to multiply each coefficient of observed variable q_{kj} from the third step matrix with its respective numerical value of the variable in quantitative form p_{kj} given in the first step table.

The sum in the last row of this matrix table (fourth step) represents quality measuring parameter expressed in exact numerical form.

		COMPARATIVE VALUES V_j						
VARIABLES p_{kj}	OPTIMIZA CRITERIA	V_1	V_2	...	V_j	...	V_n	SUM
1	2	3	4	...	$j+2$...	$n+2$	$n+3$
p_{1j}	max	$q_{11} \cdot p_{11}$	$q_{12} \cdot p_{12}$...	$q_{1j} \cdot p_{1j}$...	$q_{1n} \cdot p_{1n}$	$\sum_{j=1}^n q_{1j} \cdot p_{1j}$
p_{2j}	min	$q_{21} \cdot p_{21}$	$q_{22} \cdot p_{22}$...	$q_{2j} \cdot p_{2j}$...	$q_{2n} \cdot p_{2n}$	$\sum_{j=1}^n q_{2j} \cdot p_{2j}$
.....
p_{kj}	max	$q_{k1} \cdot p_{k1}$	$q_{k2} \cdot p_{k2}$...	$q_{kj} \cdot p_{kj}$...	$q_{kn} \cdot p_{kn}$	$\sum_{j=1}^n q_{kj} \cdot p_{kj}$
.....
p_{mj}	min	$q_{m1} \cdot p_{m1}$	$q_{m2} \cdot p_{m2}$...	$q_{mj} \cdot p_{mj}$...	$q_{mn} \cdot p_{mn}$	$\sum_{j=1}^n q_{mj} \cdot p_{mj}$
SUM		$\sum_{k=1}^m q_{k1} \cdot p_{k1}$	$\sum_{k=1}^m q_{k2} \cdot p_{k2}$...	$\sum_{k=1}^m q_{kj} \cdot p_{kj}$...	$\sum_{k=1}^m q_{kn} \cdot p_{kn}$	$\sum_{k=1}^m \sum_{j=1}^n q_{kj} \cdot p_{kj}$

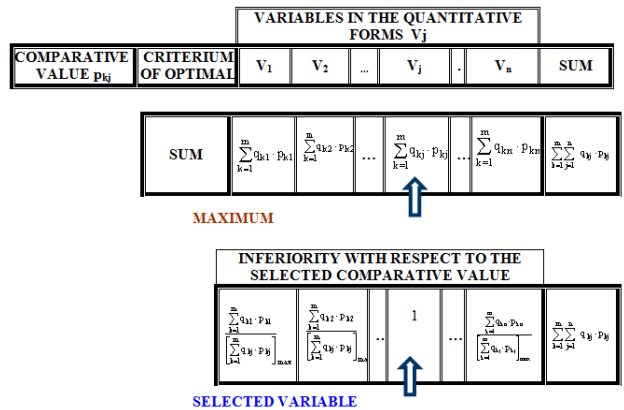
6. SUPERIORITY CRITERION

If as a condition for evaluation we select the smallest comparative value (last row of the fourth step table) with the smallest nominal value, then by simply dividing all the comparative values by the selected measuring value, we obtain SUPERIORITY of the given comparative value over the selected value while at the place of the selected variable there is one.



7. INFERIORITY CRITERION

If as a condition for evaluation we select the comparative value with the highest nominal value, then each comparative value is divided by the selected maximal value thus obtaining INFERIORITY of the observed comparative values with respect to the selected one while the place of the selected variable is taken by one since in this column the value is divided by itself.



8. CONCLUSIONS

The variables of the observed value given in the form of qualitative or quantitative parameters by which a given variable is evaluated can be determined, depending on the variable's character, in one of the following ways:

- By exact mathematical calculation,
- By applying qualitative statistical methods,
- By collecting and processing information about the observed variable,
- By surveying,
- By direct informing, and,
- By researching referential literature, and the like.

¹Dragan Temeljovski, full prof., Faculty of Mech. Eng. A. Medvedeva 14, 18000 Niš, Serbia, temelj@masfak.ni.ac.rs

²Predrag Popović, full prof. in retirement, Faculty of Mech. Eng. A. Medvedeva 14, 18000 Niš, Serbia.

³Bojan Rančić, full professor, Faculty of Mech. Eng. A. Medvedeva 14, 18000 Niš, Serbia, bojanr@masfak.ni.ac.rs.

⁴Djekić Petar, M.Sc. Eng, Faculty of Mech. Eng. A. Medvedeva 14, 18000 Niš, Serbia, petardjekic@masfak.ni.ac.rs.

The variable in the form of the evaluation parameter must be given in the form of numerical qualitative or quantitative value or as a percentage value.

The very process of calculating and evaluating the observed values, by this method, is taking place in four steps by making respective decision-making matrices.

As a condition for evaluation, we can select any observed value while taking care that, if it is to be compared with a higher value, we should use the INFERIORITY rule while, if it is compared with that of a smaller nominal value, the rule of SUPERIORITY should be used.

In order to successfully carry out the given research and to apply the given method, a respective program package named "Program Tools for Design and Analysis of Profile Making Technologies" or PAPTIP is made; within this package, a module for evaluating comparative values by the method of superiority and inferiority is developed, [6].

REFERENCES

- [1] Zrilić R.: Istraživanje zavisnosti tehno-ekonomske i energetske efikasnosti od naponskog stanja pri izradi profila, Doktorska disertacija, Mašinski fakultet, Banja luka, septembar 2004.

- [2] Zrilić R.: Matematički model elastičnih deformacija okvira valjačke mašine, Obrada deformisanjem u mašinstvu, godina 12, broj 1-2, strana 73-83, Novi Sad, septembra 1987.
- [3] Popović B., Kamberović B.: Upravljanje kvalitetom – zbirka rešenih zadataka sa objašnjenjima, Naučna knjiga, Beograd, 1987.
- [4] Stanić J.: *Metod inženjerskih merenja – osnovne matematičke teorije eksperimenta*, Mašinski fakultet, Beograd, 1986.
- [5] Popović P.: *Ukuni stepen tehničko-tehnološkog iskorišćenja mašina za obradu materijala deformisanjem kao pokazatelj stanja i perspektive razvoja sredstava rada za obradu materijala deformisanjem*, BIAM '78, Zagreb, 1978.
- [6] Norton P.: *Visual Basic 6*, Kompjuter biblioteka, Četvrto izdanje, SAMS publishing, Svetlost, Čačak, 2001

ACKNOWLEDGEMENT

This paper is part of project TR33040 Revitalization of Existing and Design of New Micro and Mini Hydroelectric Power Plants (from 10 to 1000 kW) on the Territory of Southern and Southeastern Serbia, funded by the Ministry of Education and Science of Republic of Serbia.

34th INTERNATIONAL CONFERENCE ON PRODUCTION ENGINEERING



SECTION G

FORMING AND SHAPING TECHNOLOGIES

THE INFLUENCE OF RESIDUAL STRESS DISTRIBUTION ON THE SPRINGBACK PARAMETERS IN THE CASE OF CYLINDRICAL DRAWN PARTS

Neculai NANU, Gheorghe BRABIE,

IMT Centre of Research, Bacau University, Marasesti Street, Bacau, Romania
nicu.nanu@ub.ro, g-brabie@ub.ro

Abstract: In the case of deep drawing process, the springback is an important phenomenon that leads to the modification of the part shape and dimensions after the tools removing. For this reason, in order to obtain a drawn part with a good accuracy of the shape and dimensions, this phenomenon must be controlled. The main cause of the springback phenomenon is represented by the residual stress distribution on the sheet thickness of the drawn part. Hence, in order to control the springback, the residual stress distribution on sheet thickness must be known and controlled. In this paper an analysis was made concerning the influence of the residual stress distribution on the springback intensity in the case of cylindrical drawn parts made from steel sheet.

Key words: deep drawing, residual stresses, springback.

1. INTRODUCTION

The springback phenomenon leads to the modification of the dimensional and shape parameters of the drawn parts after the tools removing. In order to obtain an accurate drawn part, the minimisation of the springback effects must be performed. The researches performed in order to minimise the springback have been focused on *reduction* or *compensation* of their effects. The *reduction* of the springback effects suppose the knowledge of it causes and the influence factors that affects it intensity. The researches performed concerning the generating causes of the springback shows that the main cause of this phenomenon is the *uneven distribution* of residual stresses in thickness of the deformed part generated before tools removing [1], [2], [3]. Hence, in order to control the springback effects, the residual stress distribution in the sheet thickness must be controlled. In the case of deep drawing processes, the material is subjected to a complex loading, the stresses varying on the part region and in the sheet thickness [4], [5], [6]. In order to *compensate* the springback, the study was focused on the optimisation of the process parameters in order to minimisation of the springback effects. The compensation is based on such algorithms that use the results from experiment, finite element simulation and different models of calculation. This aim of this paper is to study the influence of residual stress distribution on the springback intensity in the case of cylindrical drawn parts.

2. GEOMETRY OF PART AND MATERIAL

The determination of residual stress distribution was performed on cylindrical drawn parts made from steel sheets. The blank diameter was equal to 200 mm; the sheet thickness was equal to 0.75 mm. The part geometry is shown in fig.1 and the material properties in table 1.

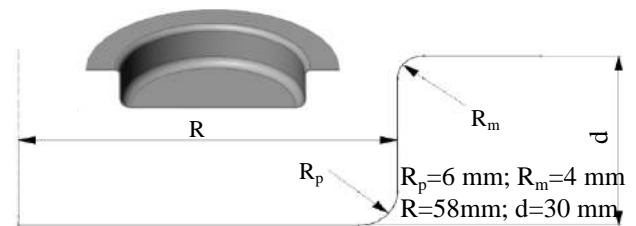


Fig. 1 Geometry of cylindrical drawn part

Table 1. Material properties

Material properties	Measuring unit	Value
Young's modulus	[MPa]	144120
Yield strength	[MPa]	156
Strength coefficient	[MPa]	531
Uniform elongation	%	21.42
Total elongation	%	38.84
Anisotropy coefficients	r_0	1.25
	r_{45}	1.90
	r_{90}	2.02
Hardening exponent n		0.248

3. DETERMINATION OF RESIDUAL STRESS DISTRIBUTION AND SPRINGBACK PARAMETERS

3.1 Simulations methodology

The distribution of residual stresses was determined from simulation by using the ABAQUS finite element software and its implicit solver. In order to reduce the analysis time, a quarter of the geometric model was used and two symmetry conditions were applied (symmetry to the plane xOz and yOz). The friction coefficient between blank and tools was equal to 0.13. The simulations were performed by using three values of blankholder forces: 30 kN, 40 kN and 50 kN. The blank was modelled as deformable body

and meshed with S4 elements having 31 integration points in the sheet thickness. The tools were modelled as rigid bodies and meshed with R3D4 elements. The elastic material properties were: Young's modulus and Poisson's ratio. The plastic material behaviour was described by introducing in the program a series of values obtained from stress-strain curve. In order to describe the material anisotropy, the Hill plasticity criterion was used. The geometrical model used in simulation is shown in fig. 2.



Fig. 2 Tools geometry and blank used in the finite element simulation

The residual stress distribution was determined along the deformed part profile (profile A) that correspond, (in non-deformed configuration) to rolling direction of blank (fig. 3). The springback parameters in the case of cylindrical drawn part were chosen as it is shown in fig. 3.

In the flange-wall connection zone the geometrical parameters affected by the springback phenomenon are the flange wall connection radius ρ_m and the angle between flange and wall α_m . In the wall zone the geometrical parameters affected by springback phenomenon are the part radius determined in the points B, C and D (R_1 , R_2 and R_3). The positions in which the part radius was determined are as follows: $d_1=7$ mm, $d_2=16$ mm and $d_3=25$ mm. In the wall bottom connection zone the geometrical parameters affected by the springback phenomenon are the wall-bottom connection radius ρ_p and the angle between wall and bottom α_p .

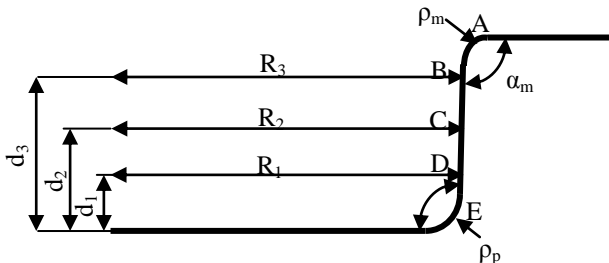


Fig. 3 Position of points chosen on the part profile of the drawn part and the springback parameters

3.2 Analysis of the obtained results

In the flange-wall connection zone (point A), the residual stresses have an important variation in the sheet thickness, the radial stresses having positive values and circumferential stress, negative value. The increase of blankholder force leads to increase of radial stresses and decreases in absolute values of circumferential stresses (figs. 4 and 5). For each point the distribution of stresses in the sheet thickness generates a bending moment that depends on the stress distribution in the sheet thickness.

The most important deviation of geometrical parameters of the part after springback was observed in the bending zones (point A, points B, C and D, point E). Fig. 6 shows the variation of the bending moment and the variation of springback parameters as a function of blankholder force. By analysing the diagram from fig. 6 it can be shown that in the flange wall connection zone the bending moment

decreases with the increase of the blankholder force. The decrease of the bending moment determines the decrease of the deviations of springback parameters from nominal values. The variation of bending moment and springback parameters are the same as a function of blankholder force.

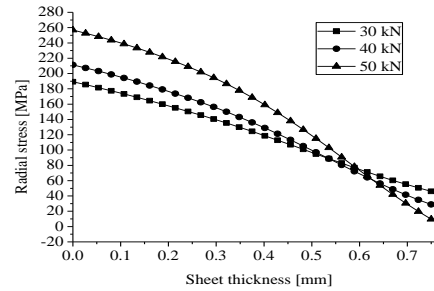


Fig. 4. Distribution of radial stresses in sheet thickness in the point A

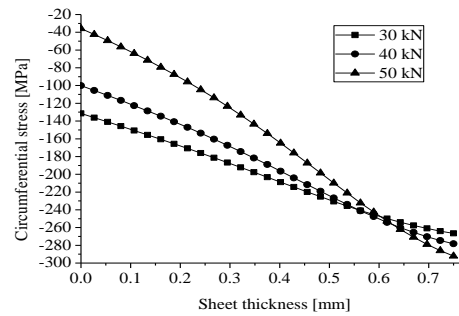


Fig. 5. Distribution of circumferential stresses in sheet thickness in the point A

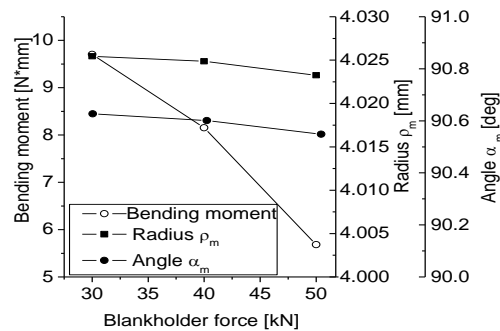


Fig. 6. Variation of bending moment and springback parameters as function of blankholder force in the point A

The variation of the stresses in the sheet thickness, the variation of the bending moment and of springback parameters as function of the blankholder force in the (points B, C and D) are shown in figs. 7- 15. The wall region shows an important variation of stresses that is not monotonic, as in this zone the material loading is more complex due to bending over the punch profile and unbending in the wall zone. The increase of blankholder force leads to increase of radial stresses and circumferential stresses. In the point B the increase of the blankholder force leads to decrease of the bending moment in circumferential direction and of the deviation of the part radius. It can be observed that the bending moment and the deviations of the part radius present the same variation as function of the blankholder force.

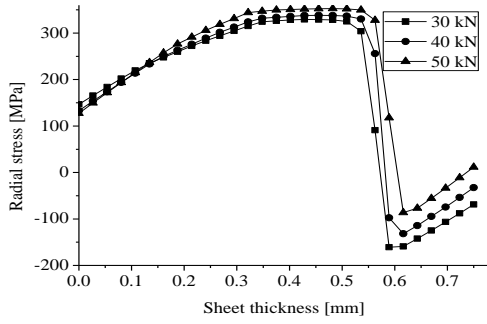


Fig.7. Distribution of radial stresses in sheet thickness in the point B

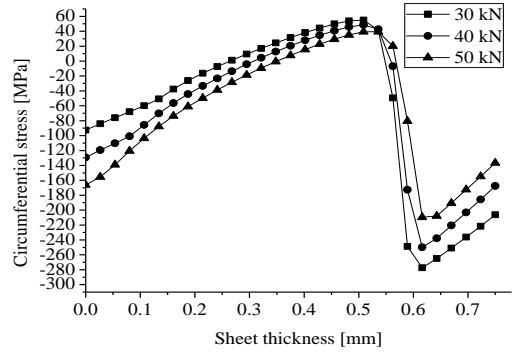


Fig.11. Distribution of circumferential stresses in sheet thickness in the point C

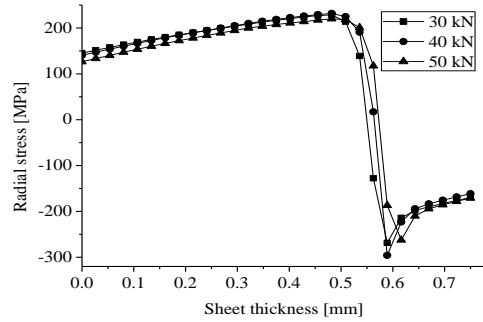


Fig.8. Distribution of circumferential stresses in sheet thickness in the point B

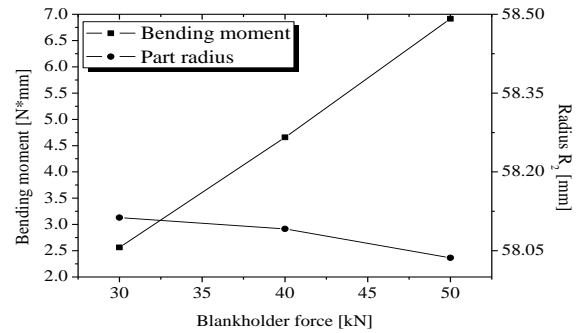


Fig.12. Variation of bending moment and springback parameters as function of blankholder force

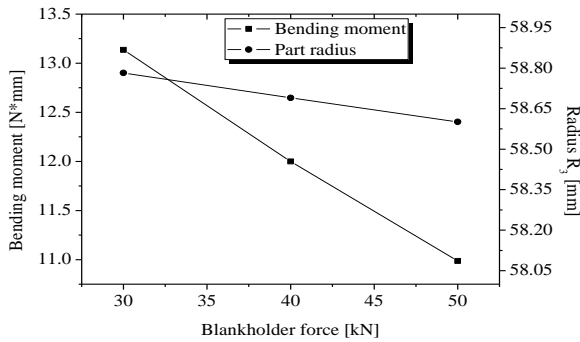


Fig.9. Variation of bending moment and springback parameters as function of blankholder force in the point B

In the point C the increase of the blankholder force leads to increase of bending moment and the decrease of deviation of part radius (fig. 12).

In the point D the increase of the blankholder force leads to the increase of the bending moment in the circumferential direction. The deviation of part radius decreases with the increase of the blankholder force.

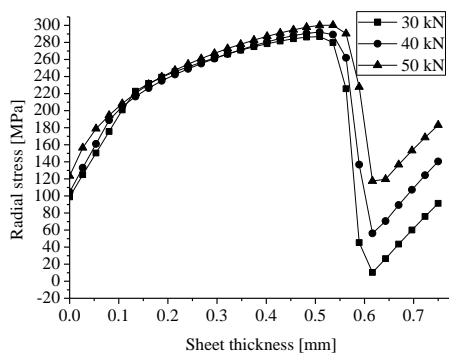


Fig.10. Distribution of radial stresses in the sheet thickness in the point C

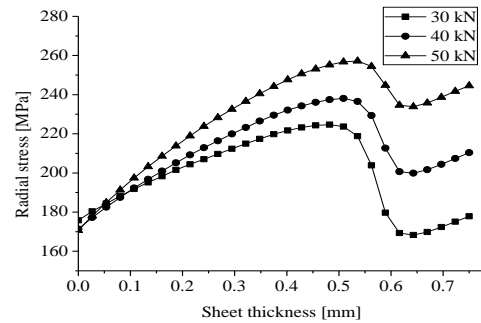


Fig.13. Distribution of radial stresses on sheet thickness in the point D

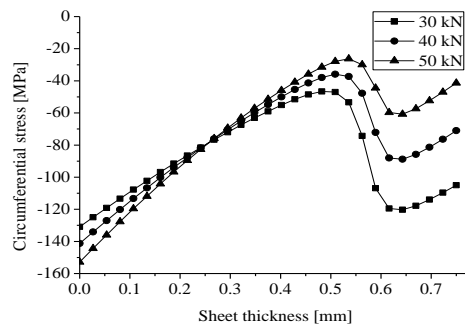


Fig.14. Distribution of circumferential stresses on sheet thickness in the point D

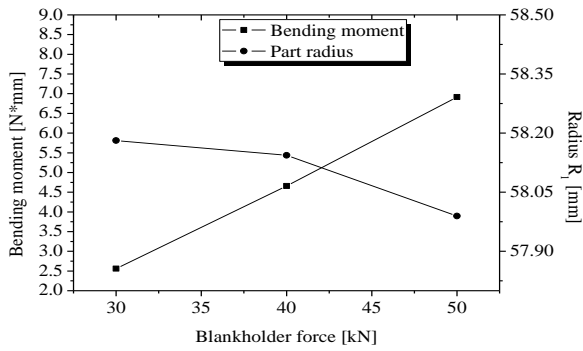


Fig.15. Variation of bending moment and springback parameters as function of blankholder force in the point D

In the wall-bottom connection zone, the radial and circumferential stresses have positive values and present a significant variation in sheet thickness. The increase of blankholder force leads to a small increase of radial stresses and have a little influence on circumferential stresses (figs. 16 and 17). Fig. 18 shows the variation of the bending moment and the deviation of springback parameters as function of blankholder force. By analysing the diagram from fig. 18 it can be shown that in the wall bottom connection zone the bending moment decrease with the increase of the blankholder force. The decrease of the bending moment determines the decreases of the deviations of springback parameters. The variation of bending moment and springback parameters are the same as function of blankholder force.

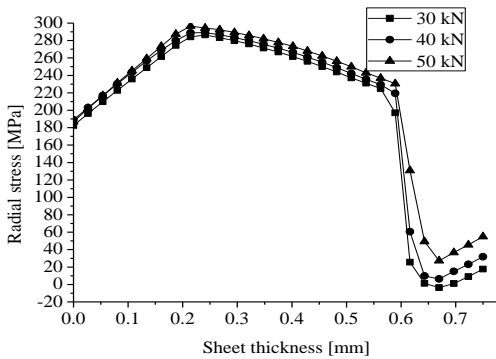


Fig.16. Distribution of radial stresses in sheet thickness in the point E

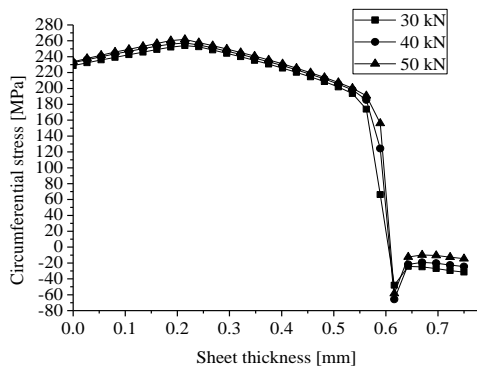


Fig.17. Distribution of circumferential stresses in sheet thickness in the point E

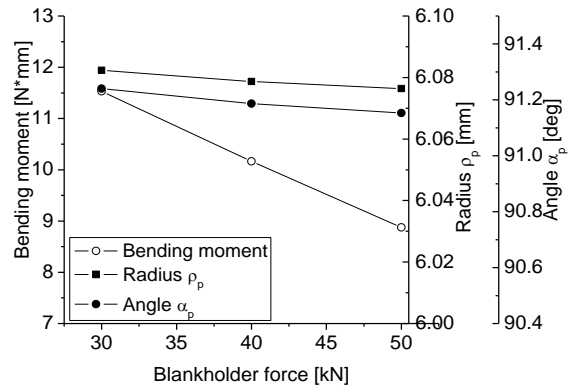


Fig.18. Variation of bending moment and springback parameters as function of blankholder force in the point E

4. CONCLUSIONS

In this paper a study concerning the influence of residual stress distribution on the springback intensity was performed by using the finite element simulations. By analyzing the results it can be shown that the deviations of the geometric parameters of the drawn parts determined by springback depend on the bending moment generated in the drawing stage. But this bending moment is determined by the distribution of residual stresses in the sheet thickness. Hence the distribution of residual stresses in the sheet thickness determines the springback intensity.

Acknowledgments

The present research was performed with the financial support from the Romanian CNCIS, PNII - IDEI programme, project no.595.

REFERENCES

- [1] BRABIE, G., a.o. (2005) *Cold forming of metal sheets. Instability phenomena of the shape and dimensions of part (In Romanian)*, Ed. Junimea, Iași, ISBN 973-37-1098-9
- [2] BURCHITZ, I. A. (2008) *Improvement of Springback Prediction in Sheet Metal Forming*, PhD Thesis Rotterdam, p 14, 28-30
- [3] WITHERS, P. J., BHADSHIA H. (2001) *Residual stress – Measurement techniques*, Materials Science and Technology, Vol. 17, pp 355-365
- [4] BRABIE, G., NANU, N. (2008) *Analysis of the stress distribution in the case of drawn parts made from steel sheets*, 17th Int. Sci. Conf. “Design and Techn. of Drawpieces and Die Stamping, Polland, pp 269-282
- [5] BRABIE, G., CHIRITA, B., NANU, N., CIUBOTARIU, V. (2009) *Analysis of the springback and residual stresses generated by cold plastic forming in drawn round parts made from steel sheets*, Metalurgia International, Vol.14-12, pp 21-27
- [6] BRABIE, G., NANU, N., RADU, M. (2009) *Analysis by simulation of the state of strains during the drawing process of parts made from metal sheets*, Proc. of the „Int. Conf. On Manufacturing Systems, ICMAS 2009”, Romanian Academy, pp 83-86



VARIABLE CONTACT PRESSURE AND VARIABLE DRAWBEAD HEIGHT INFLUENCE ON DEEP DRAWING OF Al ALLOYS SHEETS

Srbislav ALEKSANDROVIC¹, Tomislav VUJINOVIC², Milentije STEFANOVIĆ¹, Vukic LAZIC¹,
Dragan ADAMOVIĆ¹

¹ Faculty of Mechanical Engineering, Kragujevac, Serbia

² FAM Jelsingrad, Banja Luka, BiH, RS

srba@kg.ac.rs, stefan@kg.ac.rs, vlazic@kg.ac.rs, adam@kg.ac.rs

Abstract: *The process of deep drawing is influenced by many factors. During the forming process, only two of those factors can be controlled. They are blank holding force and drawbead height. Realisation of such control requires rather complex computerised apparatus.*

For this investigation, electro-hydraulic sheet-metal strip sliding device has been constructed. Basic capacity of realized device is obtaining contact pressure and drawbead height as functions of time or stripe displacement. Additional features consist of the ability to measure drawing force, contact pressure, drawbead displacement etc.

Presented in the paper are the first results of influencing of increasing and decreasing function of drawbead height in combination with increasing-decreasing function of contact pressure. Stripe material is aluminium alloy AlMg4,5Mn0,7 0,9 mm sheet metal. Contact condition are additionally influenced by application of mineral oil or completely dry tool and stripe surfaces. Drawbead geometry, with rounding radii of 2 and 5 mm, is also varied.

The accomplished results indicate that simultaneous effects of variable drawbead height, variable contact pressure, tool geometry and appropriate friction conditions can influence the plastic flow process in line with desired change of forming force.

Key words: *deep drawing, stripe sliding, variable drawbead height, variable contact pressure.*

1. INTRODUCTION

Deep drawing process is widely applied in modern industry, which makes it extremely important. That is the reason for ongoing tendencies to accomplish total control of forming process. In order to succeed in that, it is necessary to select, out of a large number of influential factors, the ones which can be influenced throughout the forming process, thus correcting it until it is completed successfully. There are only two such factors: contact pressure and drawbead height [1].

Process control through active complex (closed-loop) systems requires constant dynamic feedback between the given function of the objective, controlled and controlling variables [2]. The functions of the objective and controlled variable can be different: wrinkle height, thinning in critical zone, flange motion, flange thickness change, friction force, forming force, stress in work piece wall etc. The given objective functions are defined either by computer simulations or by previous experiments. Pressure on flange and drawbead height present the controlling effects. High velocity of reacting to controlled values change and robust controlling hardware and software apparatus are required, which all implies significant investments [3, 4].

There is also the alternative – a much simpler approach – used in this paper. However, first it is necessary to define optimal functions of pressure and drawbead height

according to proper criterion (drawing depth, piece quality etc.). This often requires comprehensive experiments [5, 6] in order to identify the character of specified factors influence. With such information, it is possible to form the controlling apparatus for practical application whose main objective is to realise previously defined optimal functions of pressure and drawbead height. Such equipment requires considerably smaller investments regarding hardware and software and is far more accessible to a wide range of users.

Application of constant height drawbeads is still most often applied and well known [7, 8]. The same goes for application of constant blank holding force on flange. The main reasons for this are smaller forming process costs. However, due to the development of new materials of more complex formability properties, in most cases it is not possible to accomplish the satisfactory results by classical methods.

The application of blank holding force without draw beads is the subject of separate researches based on the same aforementioned principles [9].

In this paper, the emphasis is on investigation of the character of the connection between drawing force and various influences combinations. They include friction conditions (dry, application of lubricant), drawbead geometry (two rounding radii), one variable function of pressure of increasing-decreasing character, two functions of drawbead of decreasing and increasing character and

corresponding constant values of both pressure and drawbead height. The significance of the physical model applied in actual experiments is clearly seen in [8].

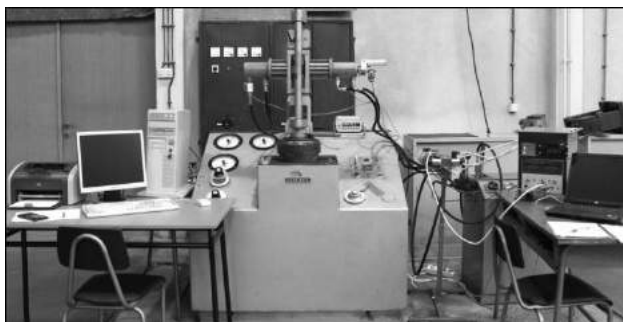


Fig. 1. Physical appearance of experimental apparatus

2. EXPERIMENTAL CONDITIONS

2.1 Material

The material of which the stripes used in the experiment are made is Al alloy sheet metal from series 5000, AlMg4,5Mn0,7. Its thickness is 0.9 mm. Main mechanical properties and properties of formability are given in table 1 (R_p – yield strength, R_M – tensile strength, A – elongation at fracture, n – strengthening exponent, r – coefficient of normal anisotropy, K – effective stress in plastic zone). Material properties are related to the condition after the following thermal treatment: glowing at temperature of 350°C in duration of 3 hours.

In one case, the friction conditions are dictated by dry surfaces – completely degreased and cleaned by acetone. In the other case, the contact surfaces were richly covered (by sponge) with oil for deep drawing of the following properties at 40°C: kinematic viscosity 45 mm²/s, dynamic viscosity 42 mPas and density 0,93 kg/dm³.

Dimensions of applied stripes were: length 250 mm, width 30 mm and thickness 0,9 mm.

Table 1. Material properties

AlMg4.5Mn0.7 s=0.9 mm				
R_p , MPa	R_M , MPa	A, %	n, -	r, -
120.5	276.6	26.2	0.26	0.715
$K = 443.6 \cdot \varphi^{0.26}$, MPa				

2.2 Experimental device

The physical appearance of the apparatus is shown in figure 1. Sheet metal stripe is positioned vertically between contact pairs, drawbead and die, which are variable. Drawing force is obtained from laboratory press ERICHSEN 142/12 in range 0-20 kN, as well as voltage signal for measuring the force of proper sensor. Hydro-cylinders for drawbead displacement and pressure realization are fed by aggregate ERICHSEN of nominal pressure 100 bars and flow 1,5 l/s. The oil from the

aggregate runs through the series of controllable proportional hydro valves to both cylinders.

Measuring and pressure controlling branch consists of pressure sensor which gives the current true value signal and control unit (micro-controller) which receives the given desired value from the software and sends signal D/A to the convertor. The received analogous signal is transmitted to the control card of the proper hydro-valve connected to the pressure cylinder.

In controlling branch, due to drawbead motion, the current true drawbead position is read by rotational encoder. After processing, the signals are sent to the control unit (micro-controller), and then to the card for control of hydro-valve for drawbead cylinder. One signal is related to the direction change, and the other one to the value of drawbead motion function. For measuring and reading the true drawbead position, supporting branch with inductive sensor and proper amplifier is made.

All true values signals are brought into PC computer with integrated A/D card and proper original software, which enables monitoring of all values, their memorizing, presentation as well as generating of pressure and drawbead motion functions necessary for micro-controller performance.

Drawbead is 10 mm thick and is applied with two radii: 2 mm and 5 mm. Die rounding radius is 2 mm, and die opening is 12 mm. Both drawbead and die can be varied with the aim of monitoring the influence of drawbead geometry change. Active surfaces of drawbead and die are fine grinded and polished.

3. RESULTS AND DISCUSSION

3.1 Pressure and displacement functions

For the needs of planned comprehensive experiment, 6 variable dependencies of both pressure and drawbead motions on time, as given functions, were defined. Those functions are marked with numbers 1 to 6. Dependencies 5 and 6 are linear (fig. 2 and 3), and 1, 2, 3 and 4 non-linear – parabolic. Functions were defined based on empiric values of minimal and maximal pressure (0-20 MPa) and drawbead height (0-8 mm). Process duration was conditioned by limited stripe displacement and adopted sliding velocity of 20 mm/min. This conditioned maximal process duration of 3 min.

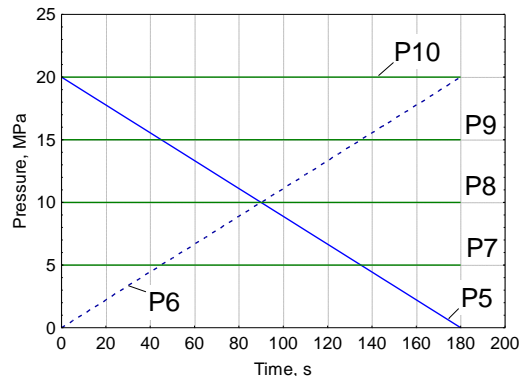


Fig. 2. Dependencies of contact pressure on time

The purpose of so defined functional dependencies, which have different characters, is the inclusion of wide range of

possible influences: decreasing, increasing, combined decreasing-increasing and increasing-decreasing, linear and non-linear. Monitoring of the response of drawing force regarding the performance of such dependencies together with friction conditions and drawbead geometry is the most important part of this research.

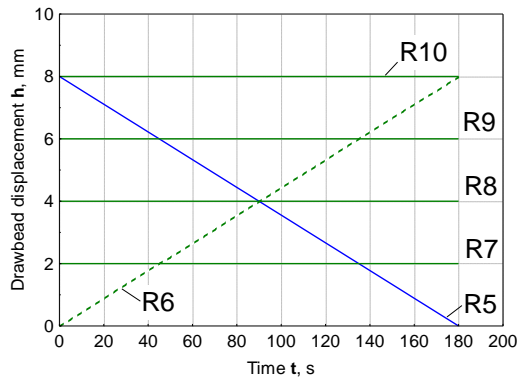


Fig. 3. Dependencies of drawbead height on time

3.2 Experimental values of drawing force

Fig. 4 shows given and truly achieved dependence of pressure P3 change. Fig. 5 shows given and truly achieved dependencies of drawbead height. Truly achieved constant dependencies of pressure according to schemes P7, P8, P9, P10 and constant drawbead height according to scheme R9 are corresponding, with insignificant deviations to fig. 2 and fig. 3 and are not shown here. Such a combination was selected with the purpose of checking the response of drawing force to complex increasing- decreasing dependence of contact pressure during the process together with decreasing and increasing functions of drawbead height. The investigation of the following combinations was also carried out: constant pressure P7 to P10 – constant drawbead height R9, variable pressure P3 – constant drawbead height R9, as well as constant pressure P8 – variable drawbead height R1 and R2. The purpose of such combinations is the evaluation of separate influences of variable pressure and drawbead height influence. In addition to that, it was necessary to estimate the influence of friction conditions. Drawbead geometry was defined by rounding radius of 5 mm and it was not varied.

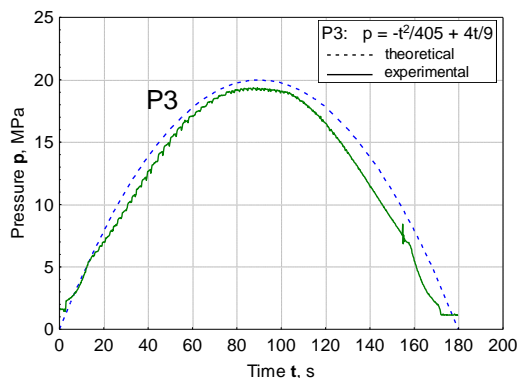


Fig. 4. Real dependence of pressure on time

Fig. 6 confirm the known dependencies of drawing force on stripe travel at constant pressures and constant drawbead height [8]. In figure 6, contact pressures are 5,

10, 15 and 20 MPa, and drawbead height is 6 mm. Dependencies were obtained in conditions of dry friction. The influence of extremely intensified friction is obvious. The intensity of force increases. In addition to that, stripe fracture before the end of process in 3 cases can be noticed, at pressures P8, P9 and P10. The combination of unfavourable friction conditions and contact pressures leads to critical sliding conditions and forming, which results in stripe fracture. At pressure P7, the process runs successfully until the end in both cases, and at extremely high pressure P10, fractures occur for both friction types.

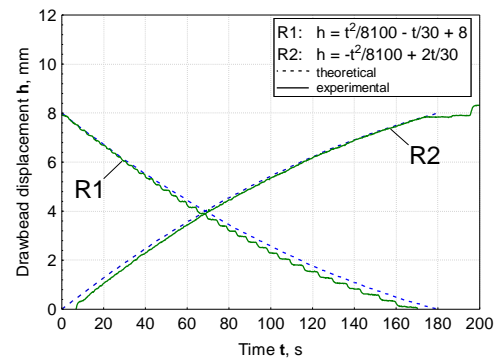


Fig. 5. Real dependencies of drawbead height on time

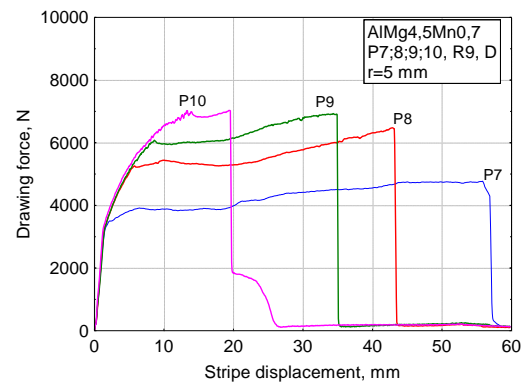


Fig. 6. Drawing force dependencies on stripe travel

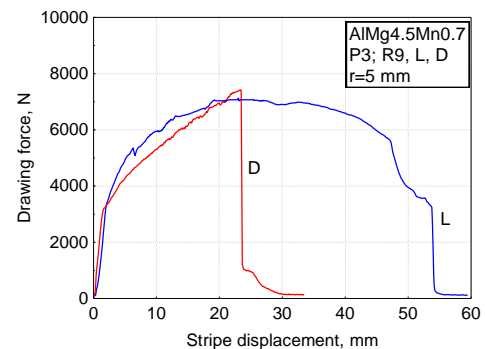


Fig. 7. Drawing force dependencies on stripe travel

Fig. 7 shows drawing force at combination of influence of variable pressure P3 and constant drawbead height R9. Drawing force response is, in a way, in line with pressure function P3. At smaller friction (L) such a conclusion is valid until the end of the entire stripe travel, while unfavourable conditions of strong friction (D) lead to fracture in travel smaller than half of the total travel. If constant pressure value is fixed at 10 MPa, and drawbead height is varied (R1 i R2), dependencies in fig.

8 will be obtained, at oil lubrication. Due to the initial drawbead height of 8 mm for function R1, drawing force increases and only after approximately 10 mm of travel it begins to decrease less intensively than drawbead height decrease. In the case of increasing drawbead function (R2), drawing force increases almost proportionally to the increase of drawbead height. The initial force increase is conditioned by pressure P8.

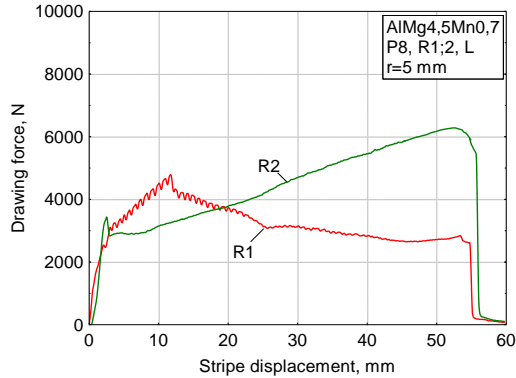


Fig. 8. Drawing force dependencies on stripe travel

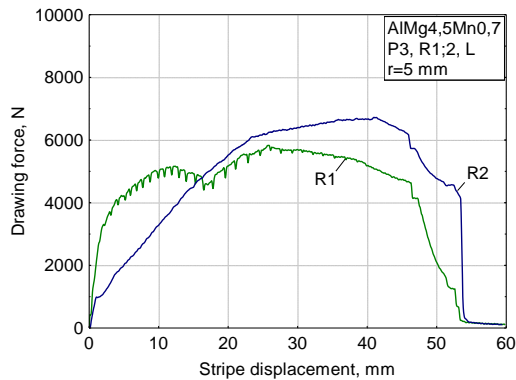


Fig. 9. Drawing force dependencies on stripe travel

Finally, in fig. 9, the effects of simultaneous influence of variable pressure (P3) and variable drawbead height (R1 i R2) at oil lubrication can be seen. According to the intensity and shape of drawing force curves, it can be seen that the intensity of influence of pressure P3 and change of drawbeads height R1 and R2 is equal. At the beginning of travel, combination P3R2 has small values of pressure and drawbead height, which results in weak intensity of drawing force which increases slowly. On the contrary, when function R2 is replaced with R1, large initial height of drawbead causes initial increase of force which lasts until drawbead height decreases sufficiently and sliding process enters a rather stable phase, with smaller oscillatory changes.

4. CONCLUSION

Computerised device for testing the various influences on drawing force in the process of stripe sliding over drawbead at variable contact pressure and variable drawbead height enables accurate registering of the influence of pressure action, drawbead height, drawbead geometry and friction conditions on drawing force. This paper presents a part of experimental results for the sliding test for aluminium alloy AlMg4,5Mn0,7 stripe.

Based on the presented results, the following conclusions can be made:

- the response of drawing force is approximately equally influenced by simultaneously applied functions of variable pressure and drawbead height in milder sliding conditions, at larger drawbead rounding radius and smaller friction,
- reaction of drawing force is registered even at relatively small differences in drawbead height change during the process,
- the character of drawing force response shows that the favourable combination of simultaneous performance of contact pressure change, change of drawbead height and friction conditions makes it possible to influence precisely the course of sheet metal forming process according to the desired forming force criterion,
- by such investigations, with relatively simple apparatus, it is possible to define significant data for numerical simulations and immediate application in practice at deep drawing of complex geometry parts.

REFERENCES

- S. WAGNER (1998) *Tribology in drawing car body parts*, 11th International colloquium: Industrial and automotive lubrication, Technische Akademie Esslingen, Proc. Vol. III, pp. 2365-2372.
- S. ALEKSANDROVIĆ, M. STEFANOVIĆ (2006) *Significance of blank holding force in realization of deep drawing process control*, 31. Conference on production engineering of Serbia and Montenegro, Kragujevac, Proceedings pp. 139-146. (in Serbian).
- M. LIEWALD (2008) *Current Trends in Research on Sheet Metal Forming at the Institute for Metal Forming Technology (IFU) at the University Stuttgart*, Papers of the International Conference on "New Developments in Sheet Metal Forming", IFU Stuttgart, pp. 263-288.
- C. BLAICH, M. LIEWALD (2008) *New Approach for Closed-Loop Control of Deep Drawing Processes*, Papers of the International Conference on "New Developments in Sheet Metal Forming", IFU Stuttgart, pp. 363-384.
- J. R. MICHLER, K. J. WEINMANN, A. R. KASHANI, S. A. MAJLESSI (1994) *A strip-drawing simulator with computer-controlled drawbead penetration and blankholder pressure*, Journal of Materials Processing Technology, 43, pp. 177-194.
- S. G. HU, M. L. BOHN AND K. J. WEINMANN (1998) *Drawbeads and their Potential as Active Elements in the Control of Stamping*, Papers of the International Conference on "New Developments in Sheet Metal Forming", IFU Stuttgart, pp. 269-303.
- J. A. WALLER (1978) *Press Tools and Presswork*, Portcullis Press Ltd, Great Britain.
- M. STEFANOVIĆ (1994) *Tribology of deep drawing, monograph*, Yugoslav Society for Tribology and Faculty of Mechanical Engineering, Kragujevac, (In Serbian).
- S. ALEKSANDROVIĆ (2005) *Blank holding force and deep drawing process control*, monograph, Faculty of Mechanical Engineering, Kragujevac, (In Serbian).



DETERMINING SOME PARAMETERS IN THE OIL HYDRAULIC PROCESS OF SQUARE CUPS DEEP DRAWING

Bojan RANČIĆ, Predrag JANKOVIĆ, Dragan TEMELJKOVSKI

Faculty of Mechanical Engineering, University of Niš, A. Medvedeva 14, 18000 Niš, Serbia

bojanr@masfak.ni.ac.rs, jape@masfak.ni.ac.rs, temelj@masfak.ni.ac.rs

Abstract: At deep drawing of cylindrical cups, blanks are circular, while at cups with rectangular cross section blank can have different shape (octagonal, dodecagonal, elliptical, circular). In this article are given various methods for determining the shape and size of blanks for hydraulic forming process of square cups. Also, accomplished is and experimental check of blank shape influence on oil pressure needed for drawing of square cups.

Siebel's analytic-experimental expression has given good results in industry applications. This paper presents an adjustment of Siebel's expression to the purpose of square cups deep drawing in hydraulic forming process. The values of blank holder pressure obtained by the suggested expression are within the range of boundary limits of a good area. The precise stress distribution in the focus of deformation, i.e. in the square cup flanges (of non-axis-symmetric parts), during the process of their forming three characteristic areas appear on the flange: corner area, side zone and the transitional area between them. Different stress-strain states appear in the above mentioned areas. This paper provides both a derivation of the expressions leading to the determining of a transitional area value. Practical experimental results have confirmed the validity of the expression enabling determining the value of transitional area.

Key words: blank size, blank holder, transitional area, square cup, oil-hydraulic forming process

1. INTRODUCTION

Parameters for oil-hydraulic forming process of square cups include ([1], [2]): blank shape and size, blank holder pressure i.e. blank holder load, oil-pressure needed for deep drawing i.e. drawing force, cup bottom holder, stripper force, die lip radius, punch nose radius.

With certain sheet metal thickness and also taking into account the size of the initial blank and the size of a drawn cup, there is some instability of the sheet metal in the cup flange resulting in wrinkles formation.

To prevent wrinkles occurrence the sheet metal is exposed to the effect of cup bottom holder. In this case, the cup flange is affected by the blank holder pressure p_{bh} , i.e. the force F_{bh} exerted by the holder. This force brings about the friction force on the contact surfaces between the sheet metal and blank holder and between the sheet metal and the die as well.

This paper presents experimental check up results and shows whether it is possible to apply the Siebel's expression [3], to calculate the blank holder pressure in the process of square cups drawing with the indirect influence of the working fluid exerted on the sheet metal with the use of a movable cup bottom holder.

For experimental research is used three sheet materials: electrolytic copper (E Cu 58), brass (CuZn37, EN CW508L) and steel (DC03, EN 10027-1). For this three materials sheet thickness was same and are 1.0 mm.

2. BLANK SHAPE AND SIZE FOR SQUARE CUPS

Methods for determining of blank shape and size for square cups with rectangular and square cross section based on knowledge of displacement of metal in drawing and assumption about equality blank and cup surface. Most applied are: Oehler-Kaiser method, [4], Romanovskii method, [5], and slip line method, [6].

2.1. Oehler-Kaiser method

By this method, corner areas, united herself at fictive, cylindrical part (assigned with thin line in Fig. 1), with diameter $d=2r_u$ and radius r_i (at drawing with rigid tool set), i.e. r_d (at oil-hydraulic forming process). For this part, toward already known formula [4], blank diameter D_0 is defined, subsequently and radius $R_0 = D_0/2$. By reason of displacement of metal from corner areas to sides areas, radius R_0 is enlarged on R_1 . Calculation of radius R_1 does toward expression:

$$R_1 = x \cdot R_0 \quad (1)$$

where: $x = 0.074 \cdot (R_0/d)^2 + 0.982$

From center of arc with radius r_u (point O), quarter of circle is drawn with radius R_1 .

By assumption that side areas are only bends, blank size here is equal to initial bend length. Above longer and shorter parts side segments AB and DC are drawn on

distances q_b respectively q_a from cup walls. q_b and q_a can be determined by formula:

$$q_b = h + 0.43 \cdot r_i - y \cdot R_0^2 / (b - 2 \cdot r_0) \quad (2)$$

and

$$q_a = h + 0.43 \cdot r_i - y \cdot R_0^2 / (a - 2 \cdot r_0)$$

where is: $y = 0.785 \cdot (x^2 - 1)$, while other geometrical parameters are defined in Fig. 1

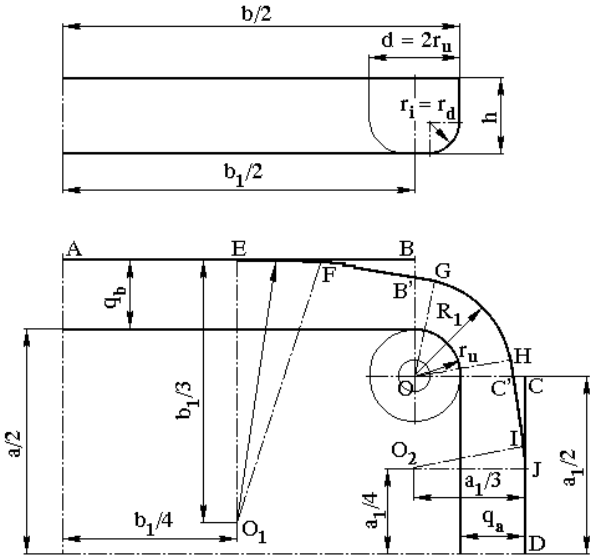


Fig. 1. Blank shape and size for square cup with rectangular cross section

Pointed peaks on B, B' and C, C' need to be replaced with arcs, considering that surface area which is added is equal to surface area which is subtract.

Tool making for piercing of this blank shape is payable only in case of large production. For experimental research it is not rational and because of that desirable blank shape is obtained on shears by hand. In this case blank shape is transformed at dodecagon (Fig. 5,a) or octagon (Fig. 5,b), considering that surface area which is added is equal to surface area which is subtract.

2.2. Romanovskii method

With change of reduced cup height (h/a) and reduced corner radius (r_u/a), there is, also, change in displacement of metal form corner areas to sides areas. This method taking at consideration this fact.

By Romanovskii method there are three cases:

1. - relatively shallow drawn cups, with relatively small corner radius (difference between Romanovskii method and Oehler-Kaiser method is negligible small),
2. - cups with middle height, with relatively large corner radius (Romanovskii method and Oehler-Kaiser method are identical) and
3. - relatively deep cups, with relatively large corner radius.

Only at third case there is difference at blank shape and size determined by Romanovskii and Oehler-Kaiser method. More about Romanovskii method can be found at literature [5].

2.3. Slip line method

More about slip line method can be found at literature [6].

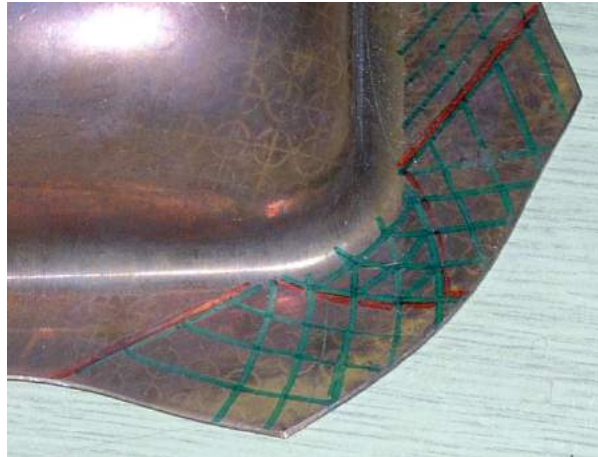


Fig. 2. Slip line field

3. BLANK HOLDER PRESSURE

By square cup forming, flange area can be divided into three zones: corner zone, side zone and transitional zone (Fig. 3, [2]).

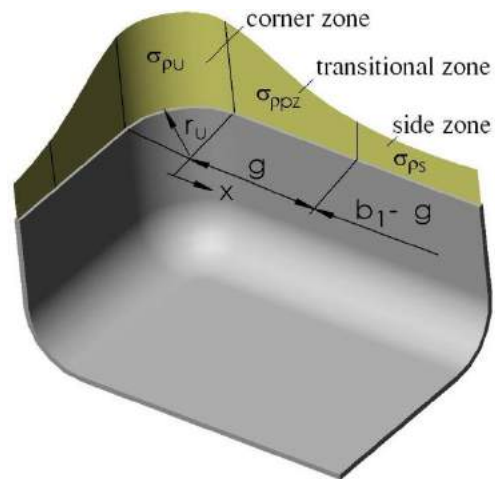


Fig. 3. Characteristic zones in cup flange

For assignment of blank holder specific pressure by forming of axisymmetrical cups, original Siebel's expression is used, [3]:

$$p_d = (0.002 \div 0.003) \cdot \left[\left(\frac{D_0}{d_{un}} - 1 \right)^2 + \frac{d_{un}}{200 \cdot s} \right] \cdot R_m \quad (3)$$

where: D_0 - blank diameter, [mm],
 d_{un} - internal cup diameter, [mm],
 s - sheet thickness, [mm] and
 R_m - blank material tensile strength, [N/mm²].

For square cup forming with rectangular and square cross section, we can use Siebel's expression, except in expression (3) shall to put D_{of} (fictive blank diameter)

and d_{unf} (fictive inside cup diameter), instead of D_0 and d_{un} . Fictive blank diameter d_{unf} , is determined on equality of inside square cup cross section and corresponding area of circle:

$$d_{unf} = \sqrt{\frac{4}{\pi} [a_{un} \cdot b_{un} - (4 - \pi) \cdot r_{uun}^2]} \quad (4)$$

where: a_{un} , b_{un} and r_{uun} - internal width, length and corner radius.

For determining of blank size (area of surface), inverse method is used. Namely, start point is final cup with ideal flange (cup flange with constant width over whole flange circumference), and then it follow determination of area of cup flange:

$$A_v = b_v \cdot a_v - b_{un} \cdot a_{un} - (4 - \pi) \cdot (r_{uv}^2 - r_{uun}^2)$$

and diameter of fictive circular ring:

$$d_{vf} = d_{unf} + \sqrt{\frac{4}{\pi} \cdot A_v}$$

Then, for known expression [2] can be determined diameter of fictive circular blank:

$$D_{of} = \sqrt{d_{vf}^2 + 4 \cdot d_{unf} \cdot [h + 0.57 \cdot (R + r)]} \quad (5)$$

4. DETERMINING OF TRANSITIONAL AREA MAGNITUDE

The transitional area (Fig. 3, [2]) does not have the same width. It is larger over the outward than the inward flange edge. The assumption that the flange outward and the inward transitional areas are of the same width will make it possible to determine its magnitude.

An elementary volume within the transitional area is observed (Fig. 4, a, b). The origin of coordinate system O_2 is located in the middle of side zone.

The following expression is obtained to determine the magnitude of the transitional area [2]:

$$g = \frac{\ln \left(\frac{f \cdot \mu \cdot s}{2 \cdot p_{bh}} \cdot K_{mid} + 1 \right)}{f \cdot \mu} \quad (6)$$

where: f – damping factor, including damping of normal stresses caused by the pressure in the circumferential direction σ_θ , occurring in the corner area;

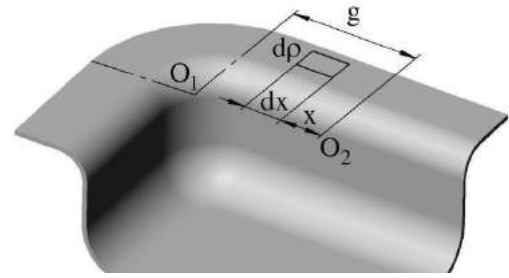
μ – coefficient of friction in the flange, ($\mu = 0.1$);

p_{bh} – blank holder pressure, equation (3);

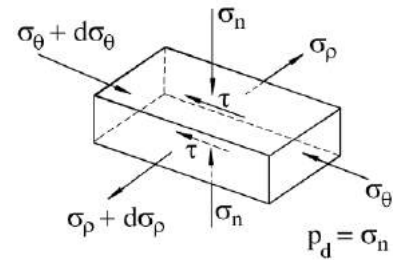
s - sheet metal thickness, ($s = 1$ mm), and

K_{mid} - mean value of plastic yield.

The only problem in equation (6) is to determine the damping factor f . Experimental results have shown that the value of $f = 0.3$ taken in standard deep drawing of square cups is sufficient for the smaller punch radii ($r_p = 8 \div 10$ mm) and sheet metal thickness $s_0 < 2.0$ mm, [7].



a)

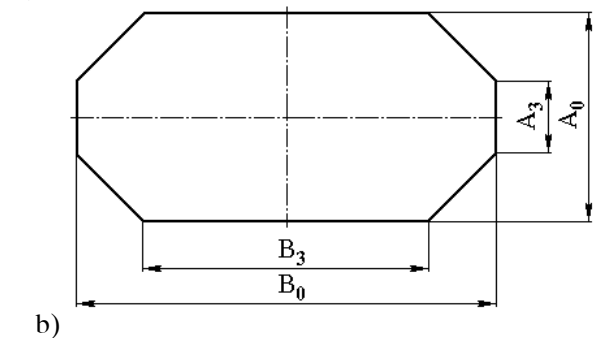
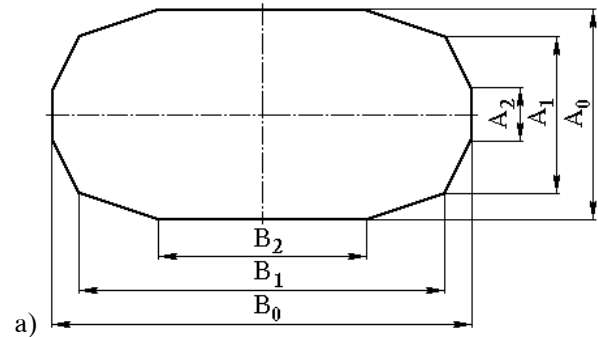


b)

Fig. 4. The elementary volume within the transitional area

5. EXPERIMENTAL RESEARCH

Because of verification of theoretical expression, experimental research are done on rectangular and square cup cross sections, by oil-hydraulic forming process, and with use of moving cup bottom holder, [2].



b)

Fig. 5. Dodecagonal (a) and octagonal (b) blank

For experimental research are used blanks, which shape and size are defined by Oehler-Kaiser method (Fig. 1). Since making tool for piercing of this blank shape is payable only in case of large production, advantage is given to dodecagonal (Fig. 5,a) and octagonal (Fig. 5,b) blanks, at whose rounds are changed with straight lines.

Numerical values of blank sizes are afford at articles [8], [9].

Corner radius (Fig. 3.) has values: $r_u = 16.0$ mm, and $r_u = 12.5$ mm. Lower level for cup depth (height) is $h = 30$ mm, and upper level is $h = 45$ mm (assumption is that oil-hydraulic forming process with movable cup bottom holder, is equal to conventional deep drawing, in sense of achieving same cup heights, [4], [5].

For cup cross section size, is taken: $c = b/a = 80/80 = 1.0$, $c = 120/80 = 1.5$ and $c = 160/80 = 2.0$ (in respect of recommendations given in literature [2], [4], [10]).

From practice is known that in certain interval of blank holder pressure values (p_d), "good" cups can be made. When pressure is over this value interval, it comes to cup fracture. In case when pressure is below this interval, material begins to wrinkle. By experimental research is determined lower and higher limit for blank holder pressure, "good" cups can be made with. One result is given on Fig. 6.

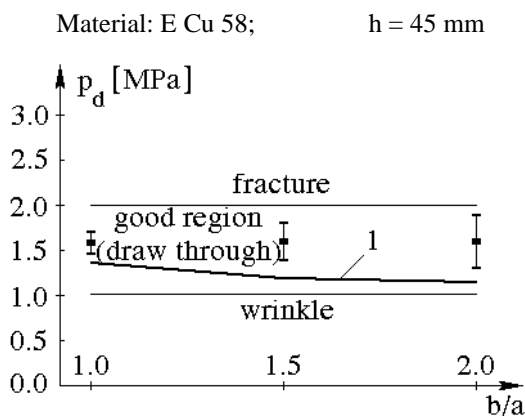


Fig. 6. Experimental values of blank holder pressure

On Fig. 6. are, also, given and curves (assigned with 1), what are calculated by Siebel-s expression (3), beside correction toward expressions (4) and (5). On this Figure, are assigned, also, intervals for blank holder pressure, by which "good" cups can be made.

On Fig. 6. can be notice that is good according between analytical and experimental results. And, also, analytical curves (curve assigned with 1) lies near by lower limit of "good" interval.

Experimental check up of the expression determining the working fluid pressure, including the transitional area magnitude g and the damping factor $f = 0.3$ has shown a satisfying discrepancy between the calculated and experimental values. The relative error was less than 15%.

6. CONCLUSION

Dominant process parameter (oil pressure needed for square cup drawing p_i) is practically same for both blank shapes (octagonal and dodecagonal). Yet, flange width is a few bigger in cups drawn from octagonal blank shape. Cutting direction of blanks form sheet, nor placement of blanks at tool, have not considerable influence on maximum oil pressure needed for square cup drawing.

Therefore, we can conclude that sheet anisotropy have not considerable influence on maximum value of p_i .

Siebel-s expression for calculation of blank holder pressure by forming of cylindrical and conical cups, can be applied, with some modifications, for square cups oil-hydraulic forming process.

Value of blank holder pressure for square cup forming, calculated by Siebel-s expression lies near by lower limit of value interval, determined by experiment.

Value of blank holder pressure, determined by expression (3), on lower limit of interval, guarantee that no inhibit flow of sheet material on cup flange, i.e. no cup fracture will occur. Even in case of material wrinkling, in small magnitude, this phenomenon can be eliminated by higher blank holder pressure.

It is necessary to be familiar with the transitional area magnitude in order to determine the flange stress-strain state of the cups of both square and rectangular cross section, as well as to determine the pressure of the working fluid required for their forming.

REFERENCES

- [1] K. SIEGERT, M. HÄUSSERMAN, B. LÖSCH, R. RIEGER, (2000), *Recent developments in hydro-forming technology*, Journal of Materials Processing Technology, 98, pp 251-258.
- [2] B. RANČIĆ, (2005), *Oblikovanje delova od lima nestišljivim fluidom*, monografija, Mašinski fakultet u Nišu, Univerzitet u Nišu, Niš.
- [3] H. OETTINGER, (1953), *Untersuchungen über das Tiefziehens elliptischer Teile im Anschlag*, Dr.-Ing. Dissertation, Technische Hochschule, Stuttgart.
- [4] G. OEHLER, F. KAISER, (1973), *Schnitt-, Stanz- und Ziehwerkzeuge*, Springer Verlag, Berlin-Heidelberg - New York.
- [5] В.П. РОМАНОВСКИЙ, (1979), *Справочник по холодной штамповке*, Машиностроение, Ленингр.
- [6] V. HASEK, (1986), *Bestimmung des Zieverhältnisses beim Ziehen von Blechteilen mit komplizierten Formen*, Blech Rohre Profile, 2, pp 57-61.
- [7] W. STRACKERJAHN, (1982), *Die Voraussage des Versagenfalls beim Tiefziehen rechteckiger Teile*, Dr.-Ing. Dissertation, der Fakultät für Maschinenwesen der Universität Hannover.
- [8] B. RANČIĆ, P. JANKOVIĆ, V. STOILJKOVIĆ, (2006), *An expression suggested to determine the blank holder pressure in the oil hydraulic process of square cups deep drawing*, Journal for Technology of Plasticity, Vol. 31, No 1-2, pp. 91-100.
- [9] B. RANČIĆ, P. JANKOVIĆ, V. STOILJKOVIĆ, (2006) *Determining the transitional area of square cups in oil hydraulic forming process*, Journal for Technology of Plasticity, Vol. 31, No 1-2, pp. 45-55.
- [10] A. ASSEMPUR, M. R. EMMAMI, (2008), *Pressure estimation in the hydro-forming process of sheet metal pairs with the method of upper bound analysis*, Journal of Materials Processing Technology.



ASSESSMENT THE NUMBER OF DEEP DRAWING STEPS OF CYLINDRICAL CUPS WITHOUT CALCULATION

Bojan RANČIĆ, Predrag JANKOVIĆ, Velibor MARINKOVIĆ

Faculty of Mechanical Engineering, University of Niš, A. Medvedeva 14, 18000 Niš, Serbia
bojanr@masfak.ni.ac.rs, jape@masfak.ni.ac.rs, velmar@masfak.ni.ac.rs

Abstract. It is well-known from practice that only some cups whose height is less than diameter can be successfully drawn in one step. Many steps require more tools and larger total manufacturing costs. The aim of the paper is to offer, to engineers-designers, a reliable way of determining the minimal number of deep drawing steps practically with no prior calculations at all. The determination of the number of step without inter-step annealing given in this paper is valid for steel sheet metals and it is done only on the basis of the drawing of a finished part.

The design of the deep drawing computer-aided process via the DDCP program is done for over 100 diverse forms of the finished part. The analysis of the calculation results shows that the number of drawing steps is decisively affected by relative height of the given part, while the impact of relative radius is smaller.

Key Words: forming process, deep drawing, number of steps, cylindrical cups

1. INTRODUCTION

The deep drawing of cylindrical elements is done, as a rule, in many steps. It is well-known from practice that only some cups whose height is less than diameter can be successfully drawn in one step. Many steps imply more tools for each step. Along with increasing the number of steps, also increasing is the time needed for designing the technological process and tools as well as the total costs for manufacturing such parts.

It is clear that productivity and economic benefits of steel elements manufacture can be, to a great extent, increased by reducing the number of drawing steps. On the other hand, the prior knowledge of the needed number of steps reduces the design efforts and shortens the whole procedure. The usual procedure for determining the number of steps for deep drawing of cups without flange is given in Fig. 1. Some recommendations for the choice of the number of steps that are not sufficiently precise can be found in the referential literature. The aim of the paper is to offer, to engineers-designers, a reliable way of determining minimal number of deep drawing steps practically with no prior calculations at all.

2. METHOD FOR DETERMINING THE NUMBER OF DEEP DRAWING STEPS

Fig. 2 gives a cylindrical cup without flange obtained in many deep drawing steps. The given geometric parameters affect the blank diameter size and thus the number of drawing steps since draw-reduction ratios (DRR) are defined as:

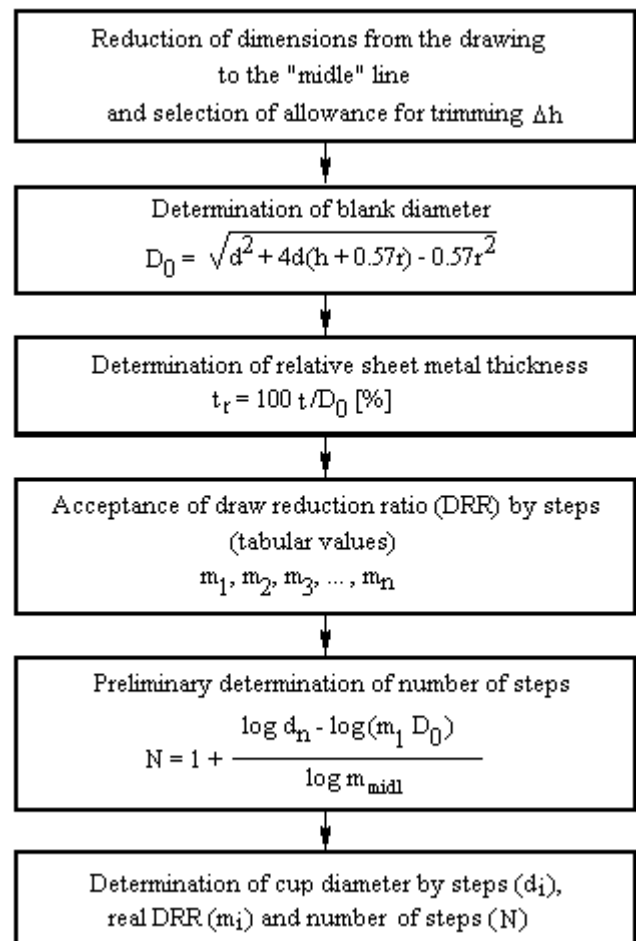


Fig.1 - Determining the number of deep drawing steps

$$m_1 = \frac{d_1}{D_0}; m_2 = \frac{d_2}{d_1}; \dots\dots\dots m_N = \frac{d_N}{d_{N-1}} \quad (1)$$

where: d_i - cup diameters by steps,
 D_0 - blank diameter,
 N - number of drawing steps.

The values of draw-reduction ratios are given in Table 1 taken over from References [1] and [2].

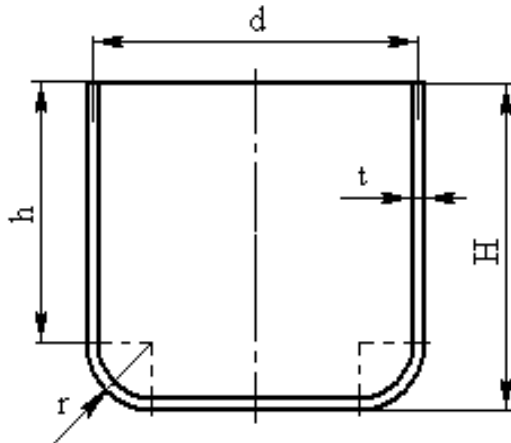


Fig. 2. Cylindrical cup without flange

The problem in question can be simplified by introducing relative geometric parameters H/d and r/t . Thus, on the basis of formula for blank diameter of cylindrical cup with flat bottom we can determine the theoretically maximal relative height of the drawn cup in one drawing step:

$$\frac{H}{d} = \frac{1}{4} \left[\left(\frac{1}{m_1} \right)^2 + 1.72 \frac{r}{d} + 0.57 \left(\frac{r}{d} \right)^2 - 1 \right] \quad (2)$$

$$(0 \leq r/d \leq 0.5d)$$

If the limit value of the draw-reduction ratio in the first step is $m_1 \cong 0.48$, from relation (2) we obtain that $H/d \cong 0.84 \div 1.09$.

Steel sheet cups can be drawn in 3 to 5 steps without any inter-step annealing.

A very detailed analysis of the effects of the above-given parameters can help us determine the sufficient number of drawing steps, only on the basis of the drawing of a finished part.

For this purpose, we have carried out the deep drawing process design by means of computer and the DDCP (Deep Drawing of Cylindrical Parts, [3]) program for over 100 forms of finished parts.

For engineers in practice the most suitable way of presenting these results is a diagram (Fig. 3).

The analysis of the calculation results shows that the most decisive effect upon the number of deep drawing steps is that of the cup's relative height H/d while the impact of relative radius r/t is smaller.

3. RESULTS AND DISCUSSION

Analyzing the diagram from Fig. 3 the following conclusions can be drawn:

- increase of H/d ratio brings about increasing number of steps, at first rapidly and then much slowly;
- there are transition intervals of H/d ratio when the number of steps is not unambiguously determined. Since it is generally desirable for the number of deep drawing steps to be as small as possible, the diagram suggests that for the given metal sheet thickness the cup radius should be increased (when allowed).

Moreover, it is well known from practice that the DRRs are also influenced by others (not only geometric) factors.

In that sense, a more favorable DRRs, and thus a smaller number of drawing steps, can be realized by:

- choosing a larger die (r_d) and/or punch radius (r_p), [2], [4], [5];
- reducing trimming allowance (Δh);
- choosing metal sheets with greater normal anisotropy (R) and/or greater strain hardening coefficient (n) [1];
- heat treatment of sheet metal and inter-step annealing;
- local heating blank flange in deep drawing [1], [2].

By applying one or more of the above suggested actions, the number of deep drawing steps can be reduced which should be especially kept in mind in the above mentioned situations of indecision. On the other hand, it is clear that some of the proposed actions cannot be always and everywhere applied for technical reasons or lack of economic benefits of such production.

Here we should also mention that some deviations of the theoretical values of the relative drawing heights for the first drawing step, according to equation (2), from the values given in Fig. 2 are consequent upon real prior calculations that takes into consideration allowance for trimming as well.

4. A CASE STUDY

The cylindrical cup manufactured in real deep drawing process in industry is shown in Fig. 4. The sheet metal material was SPCC (a kind of cold forging steel). The total number of drawing steps was four with the trimming process inserted between the first and the second drawing steps [6].

The same results was obtained by applying the DSS (Design Support System) program [6].

After running the DDCP 3 program for the given cup, the sequence of steps and the cup dimensions by the drawing steps are shown in Fig. 5. The DDCP program suggests four drawing steps with added trimming process.

The comparison DRRs between the real process and the output from the DSS and DDCP is given in graphical form in Fig. 6, which shows that the DRR in the first drawing step is the lowest in the real process and vice versa; in the other drawing steps, DRR is the highest in the real process.

It is known that the first drawing step is a critical one due to a higher possibility for failure (breakage) and wrinkling, [7]. In that sense we could expect the DDCP designed deep drawing process to be the most successful (with the least scrap).

Table 1. Draw reduction ratio for the cylindrical cup without flange

Draw-Reduction Ratio m_i	Blank relative thickness $t_r=100 t/D_0$ (%)				
	2.0-0.50	1.5-1.0	1.0-0.5	0.5-0.2	0.2-0.06
$m_1=d_1/D_0$	0.46-0.50	0.50-0.53	0.53-0.56	0.56-0.58	0.58-0.60
$m_2=d_2/d_1$	0.70-0.72	0.72-0.74	0.74-0.76	0.76-0.78	0.78-0.80
$m_3=d_3/d_2$	0.72-0.74	0.74-0.76	0.76-0.78	0.78-0.80	0.80-0.82
$m_4=d_4/d_3$	0.74-0.76	0.76-0.78	0.78-0.80	0.80-0.82	0.82-0.84
$m_5=d_5/d_4$	0.76-0.78	0.78-0.80	0.80-0.82	0.82-0.84	0.84-0.86

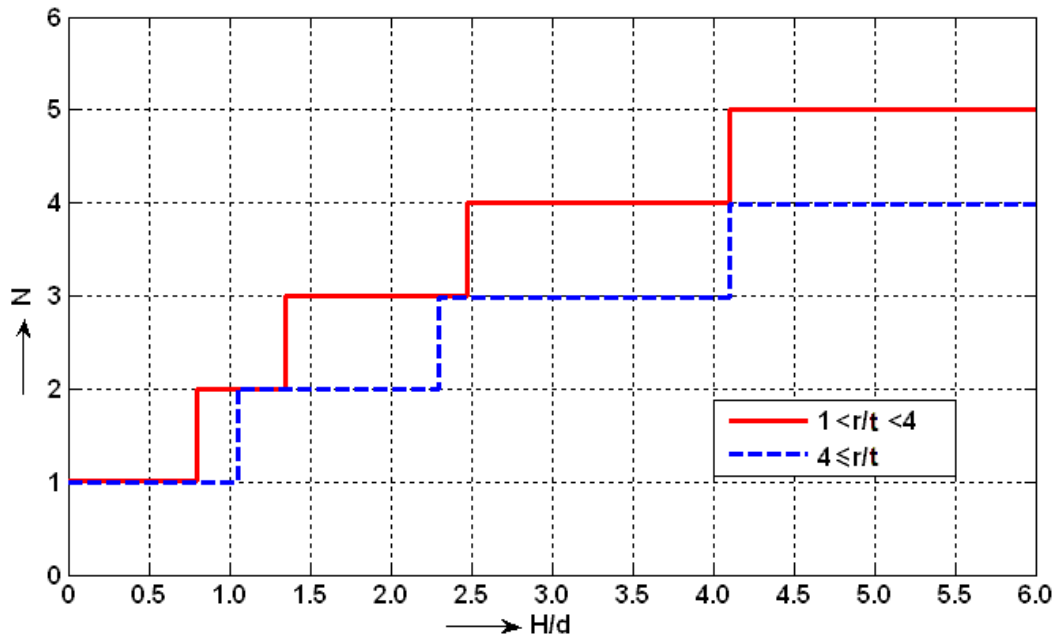


Fig. 3. Number of deep drawing steps vs. relative cup height

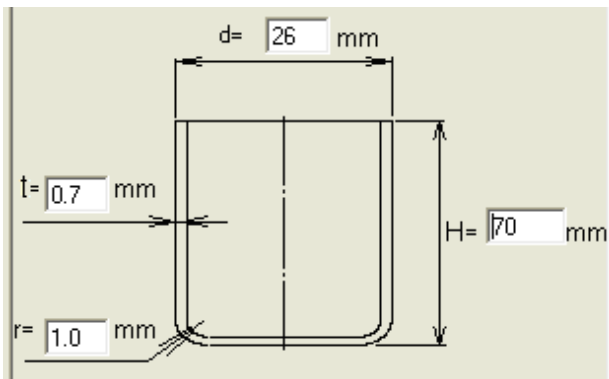


Fig. 4. Cylindrical cup after deep drawing process

5. CONCLUSION

One step drawing can be carried out only with the ratio being $H/d \leq 1$.

The result variability could be considerably affected by allowance for trimming. Namely, for the cups of the same diameter and of different heights, the trimming allowances are also different.

By reducing the trimming allowance we can also reduce the number of drawing steps.

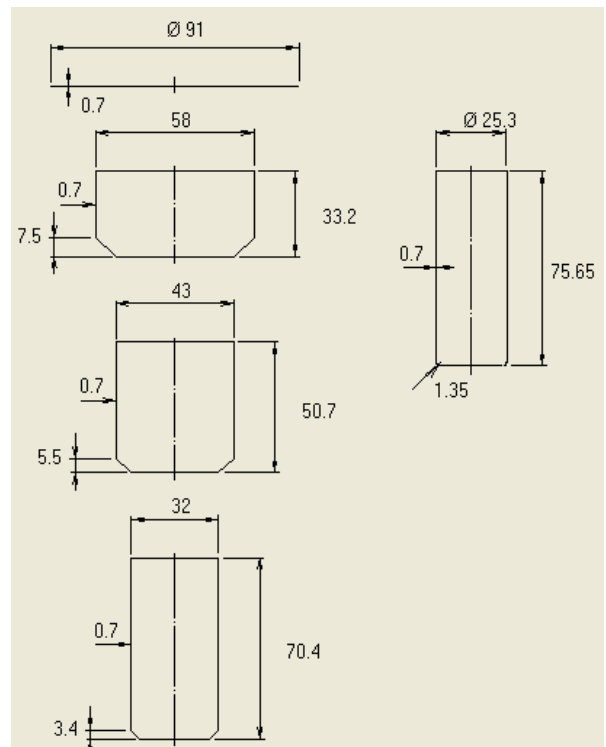


Fig. 5. Deep drawing process displayed in the DDCP

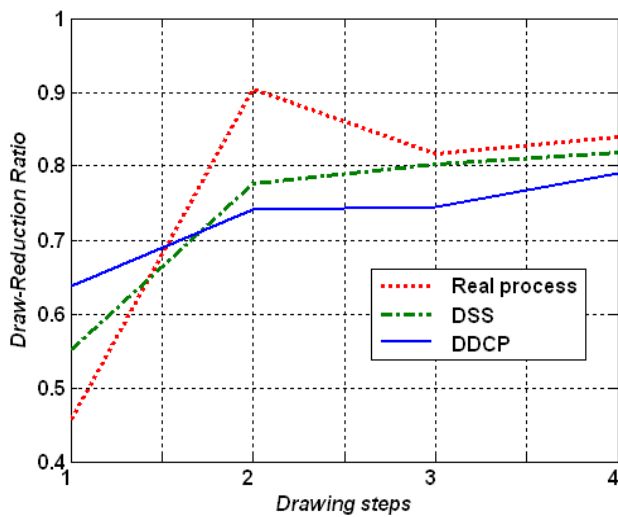


Fig. 6. Graphical comparison of DRR between real process and output from the DDCP and DSS: ($D_0 = 91.9$ mm (real process). $D_0 = 91.0$ mm (DDCP, [3]). $D_0 = 92.4$ mm (DSS, [6]).

While choosing the limiting DRR it is desirable to choose, in the die design, larger radii. This does not affect the geometry of the drawn cylindrical cup.

The choice of some other actions for reducing the number of drawing steps implies a comprehensive analysis.

The advantage of the diagram given in this paper lies in the fact that “critical” spots can be noticed, namely the places where the proposed actions are most likely to reduce the number of drawing steps.

Some deviations are possible since the number of drawing steps is interruptive and integer function of the given parameters. In the cases in which there is a dilemma about the number of steps, we should rely on our practical experience and/or results of the numerical simulation of the deep drawing process.

It is assumed that the given recommendations are valid for optimal unilateral clearance ($1 < f \leq 1.3$, [8]) and optimal blank holding pressure ($1 \leq p_{bh} \leq 3$ Mpa).

REFERENCES

- [1] ROMANOVSKIY, V.P. (1979) *Handbook of cold stamping*, Mashinostrenie, Leningrad, (In Russian).
- [2] MUSAFIA, B. (1972) *Metal forming*, Svjetlost, Sarajevo, (In Serbian).
- [3] MANIĆ, M., MARINKOVIĆ, V., PANTOVIĆ, A. (2004) *Technology designing for the multi-step deep drawing of the cylindrical cups*, Research and Design in Commerce and Industry, No 6, pp 35-42, (in Serbian).
- [4] HARPEL, E.T. et al. (2000) *Numerical prediction of the limiting draw ratio for aluminium alloy sheet*, Journal of Materials Processing Technology, Vol. 100, pp 131-141.
- [5] HUANG, Y.M., CHEN, J.W. (1995) *Influence of the die arc on formability in cylindrical cup-drawing*, Journal of Materials Processing Technology, Vol. 55, pp 360-369.
- [6] CHOI, T.H. et al. (2002) *Application of intelligent design support system for multi-step deep drawing process*, Journal of Materials Processing Technology, Vol. 130-131, pp 76-88
- [7] AGRAWAL, A. et al. (2007) *Determination of optimum process parameters for wrinkle free products in deep drawing process*, Journal of Materials Processing Technology, Vol. 191, pp 51-54.
- [8] HUANG, Y.M., CHEN, J.W. (1996) *Influence of the tool clearance in the cylindrical cup-drawing process*, Journal of Materials Processing Technology, Vol. 57, pp 4-13.



THE INFLUENCE OF TOOL SURFACE CONDITION ON IRONING PROCESS EXECUTION

**Dragan ADAMOVIĆ¹, Milentije STEFANOVIĆ¹, Srbislav ALEKSANDROVIĆ¹, Miroslav ŽIVKOVIĆ¹,
Zvonko GULIŠIJA², Slaviša ĐAČIĆ³**

¹Faculty of Mechanical Engineering in Kragujevac, s. Janjic 6, 34000 Kragujevac, Serbia

²Institute for Technology of Nuclear and other Raw Materials (ITNMS), Franše d' Eperea 86, 11000 Belgrade, Serbia

³Coal Mine A.D., Pljevlja, Montenegro,

adam@kg.ac.rs, stefan@kg.ac.rs, srba@kg.ac.rs, zile@kg.ac.rs, z.gulisija@itmms.ac.rs, djale@t-com.me

Abstract: Friction has significant influence, both on geometrical, kinematic and dynamic conditions of metals forming execution and on tool life; in that way, it influences the continuity of production.

One of the methods for enabling the reduction of friction resistance (and in that way the influence on product quality) is the selection of properties of outer layers of the tool. Unlike machine elements, where it is possible to select a wide range of contact couples materials, in the case of ironing process one of contact couples elements – strained material – is determined in advance. The only thing that can be changed here, in certain limits, is tool material (die and punch) or various thermo-chemical forming procedures can be applied, as well as hard coatings etc., by which chemical content of surface layers is changed.

In this paper, we will present the experimental results obtained by modelling ironing process by application of proper technological lubricants, use of anti-adhesion coatings on tools (coating TiN and hard coating Cr), selection of suitable type of tool materials (tool steel, hard metal) etc. The obtained results indicate that friction resistance can be reduced to a large extent, which will also minimize tool wear.

Key words: Ironing, Coatings, Friction, Wear, Tools

1. INTRODUCTION

High intensity of tool wear in metal forming (MF) is the reason why tool life problem is getting the increasing attention. Together with the advancement of tool wear process, which mainly reflects the change of dimensions and form, the product quality deteriorates, and the obtained products have major dimensional deviations, worse surface quality and even visible errors in the form of notches and nodes. Tool life also influences the reliable functioning of the machines or forming systems. Frequent replacements of tools lead to unavoidable standstill of machines which also influences productivity decrease, and therefore the production costs. Tool wear process is very complex, and, and tool fracture can be caused by several reasons which act together. Tool wear process is influenced not only by friction appearance, but also by other processes, such as: fatigue (thermal and mechanical), corrosion and oxidation. Therefore, tool wear for MF will be the result of the superposition of all physical processes which act upon the tool; consequently it will be more intense than it would have been if it were influenced only by friction process course.

In tools intended for cold MF, the following types of wear are dominant:

- adhesive,
- abrasive and
- fatigue (crumbling).

However, abrasive wear is considered as the significant process which determines tool life for MF.

Intensive tool wear in ironing processes results from the fact that the entire work surface of the tool is in constant contact with the material being formed. From that reason, wear intensity is higher when compared with other tools. Wear cases for this kind of tools can be divided into following types:

- adhesive wear which manifests as the appearance of glued particles ("bulges"),
- micro and macro cracks,
- crumbling and
- the appearance of material loss in the form of ring, which is the effect of abrasive wear.

The most influential type of wear for this kind of tools is the appearance of so called annular damage on work (conic) surface for compression, which eliminates the conditions for normal forming and causes the appearance of additional friction resistance and significant increase of drawing force.

Such mechanism of tool wear is the consequence of material flow kinetics and distribution of pressures in cone for compression. The material being compressed achieves the largest straining in the entrance cone zone, which is why the highest unit pressures are created there. Furthermore, all impurities, oxides etc. remain on work edges at the entrance into the cone tool part; those impurities can act as abrasives which cause abrasive wear

characterised by high intensity; therefore the contact of partly formed material of released oxide and tool material occurs in the central part of the cone.

The increase of tool life for MF can be accomplished by:

- replacement of tool steels used so far with materials with better resistance properties, which are also much more expensive,
- application of properly selected methods of surface forming which enable the obtaining of desired surface layer properties, especially higher resistance to wear,
- application of suitable technological lubricants.

The deficit of alloying elements and, particularly, their high price are the reasons why high-alloyed steels are applied only in special cases and for heavily loaded tool elements. That is why effective and efficient increase of tool durability can be accomplished by surface forming.

By using this solution for the problem of short durability of productive tools, friction and wear processes, as well as processes of fatigue, oxidation and corrosion are mainly localised on surface layers, so they are the only ones required to have higher resistance to wear, thermal fatigue, oxidation, corrosion etc.; thus, it is not necessary that the entire tool has those properties.

In the course of searching for optimal properties of surface layers, nowadays we have at our disposal several forming methods which enable accomplishment of useful contact couples properties. In addition to the mechanical forming where the improvement of tribological properties is achieved, mainly, as the result of increase of outer layers hardness (e.g. pressing procedures), in other cases one of the important goals of surface forming is the change of chemical content (e.g. by enriching with ingredients, such as: carbides Cr, carbides B, nitrides Al, Ti, Cr, Mo, V etc.) due to which a significant increase of resistance to abrasive wear is accomplished. It has been determined, as the result of many investigations, that finely-dispersed hard phases (e.g. carbides, nitrides etc.) are the most resistant to abrasive wear [1].

Galvanic forming represents a special group of surface layers modifications. It includes the procedures such as: hard chromium-coating, phosphating etc.

Coating obtained by hard chromium-coating is characterised by relatively high hardness (1000-1200HV), as well as by characteristic grid which represents natural canals for lubrication. The result of such surface layers forming is the significant increase of resistance to wear.

With the aim of obtaining good tribological properties, both at room and at increased temperature, plasma technologies were developed which involve applying coatings of hard soluble metals such as: Cr, W, Co, Ti or their compounds TiN, TiC etc. [2].

The group of methods for surface forming which are also worth the attention also includes also electro-polishing and chemical polishing. The result of polishing is the removal of defective surface layers made at preceding forming (e.g. forming by cutting) and new surface layers are obtained which are characterised by significantly less roughness and lower or very low levels of their own stresses. Surface layers obtained as the result of these processes are characterised by considerably smaller friction coefficient, increase of resistance to abrasive wear and to corrosion.

2. EXPERIMENTAL INVESTIGATIONS

Experimental investigations in this paper were conducted on the original model of ironing, which is characterised by a double sided simulation of the contact zone with the punch and die [3]. This model enables realization of the high contact pressures and respects the physical and geometrical conditions of the real process (die and punch materials, topography of the contact surfaces, the die cone angle (α) etc.). The scheme of the mentioned model is shown in Fig. 1.

The dies are placed in holders, where the left hand holder is fixed and the right hand holder is moving together with the die. The punch consists of the body 3 and the front 4, which are mutually connected by the pickup with the strain gauges 5.

The bent strip of thin sheet 7, in the U shape, (test-piece) is being placed on the "punch". The strip is being acted upon by "dies" 2 with force F_D . Test-piece is passing (sliding) between dies, by the action of the force F_{ir} on the punch front, when the sample wall is being ironed. During passing through, the external surface of the sample is sliding along the die surface, which is inclined for an angle α , while the internal surface of the sample is sliding over the plates 6, which are fixed to the punch body.

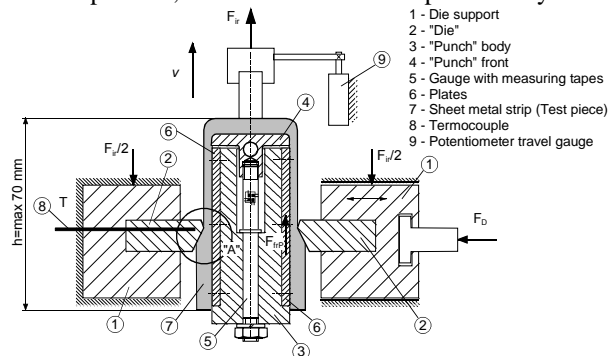


Fig. 1. Scheme of model used in this paper

The device was made with the possibility for an easy substitution of the contact – pressure elements (die 2 and plates 6), easy cleaning of the contact zones and convenient placing of samples.

Plates 6 and dies 2 can be made of various materials, as well as with various roughnesses, while dies can have various slope angle α .

On the mentioned device it is also possible to simulate consecutive (multi-phase) ironing, when one sample is passing between the contact pairs several times.

The device for ironing is installed on a special machine for thin sheet testing ERICHSEN 142/12.

For experimental investigations in this paper, the low carbon steel sheet, tempered by aluminium, Č0148P3 (WN: 1.0336; DIN: DC 04 G1/Ust 4, Ust 14) was chosen. It belongs into a group of high quality sheets aimed for the deep drawing and it has properties prescribed by standard SRPS EN 10130:2004.

For the die and punch material, the alloyed tool steel (TS) Č4750 (WN: 1.2601; DIN17006: X165CrMoV12; EN: X 160 CrMoV 12 1) was selected, while one set of dies was made of the hard metal. In order to improve the surface, a certain number of dies and of punches – their working surfaces – were coated by chromium (Cr) or titanium

nitride (TiN). In experiments, pairs of dies and punches made of the same materials were always used, e.g., D-TS/P-DS or D-TS+Cr/P-TS+Cr, with exception of the hard metal die, which was always used with the punch made of tool steel.

The special attention was devoted to material characteristics in the sheet rolling direction (0°), since the tested samples were cut in that way, (SRPS C.A4.002:1986) which was applied using specimens in rolling direction. Material characteristics for test-piece were determined. Values are shown in Tab. 1. Tests have been performed under laboratory conditions ($v=20\text{mm/min}$, $T=20^\circ\text{C}$).

Table 1. Properties of tools and test piece materials

		Material	Mechanical properties
Tool	Die (D)	TS* TS + Cr plate TS + TiN plate HM**	TS Hardness 60÷63 HRC
	Punch plate (P)	TS* TS + Cr plate TS + TiN plate * - TS – Tool steel, Č4750 (DIN17006: X165CrMoV12)	
Test-piece		Č0148P3 (WN: 1.0336; DIN: DC 04 G1/Ust 4) Thickness: 2,0 mm width: 18,6 mm	$R_p = 186.2\text{ MPa}$ $R_m = 283.4\text{ MPa}$ $A_{80} = 37,3\%$ $n = 0,2186,$ $r = 1,31915$
		* - TS – Tool steel, Č4750 (DIN17006: X165CrMoV12) ** - HM – Hard metal, WG30 (DIN4990: G30)	

3. EXPERIMENTAL RESULTS

The investigations performed on tribo-model of the ironing process made it possible to estimate the influence of surface tool layers (die and punch) on the progression of ironing process (drawing force, friction coefficient on die and punch, wall tension stress etc.).

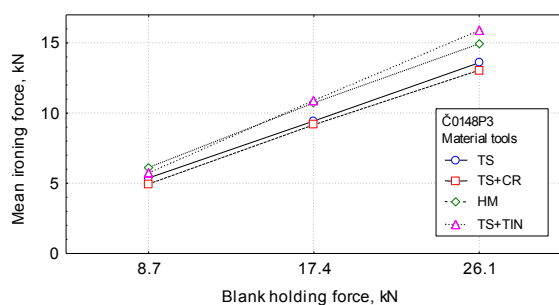


Fig. 2. The change of mean value of drawing force in dependence on blank holding force at various tool materials

The change of mean value of drawing force in dependence on blank holding force at various surface states of the tool is given in figure 2. The increase of blank holding force leads to the increase of the mean value of drawing force similarly for all the states. Application of both the tool without coating (TS) and with chromium coating (TS+Cr) leads to similar values of drawing force, which are somewhat smaller than the ones obtained by tools with coating TiN (TS+TiN) and hard metal (HM).

The change of mean value of drawing force in dependence on die gradient angle, when tool material is the parameter, is given in figure 3. Drawing force increases with the increase of die gradient angle. At smaller die cone angles, that increase is more intensive than at bigger angles.

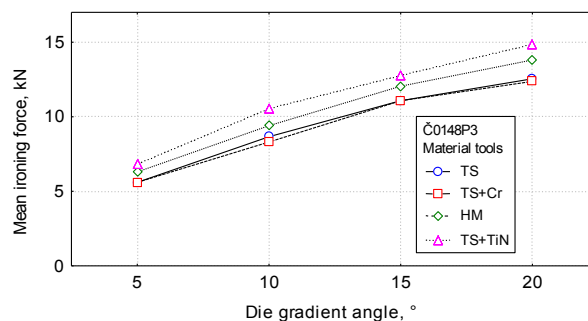


Fig. 3. The change of mean value of drawing force in dependence on die gradient angle for various tool materials

Mean values of drawing force for various tool materials are given in figure 4. The tool with hard chromium coating (TS+Cr) proved to be the best (the smallest value of drawing force). Somewhat worse results were obtained by using the tool of alloyed tool steel (TS), hard metal (HM) and coating TiN (TS+TiN, respectively).

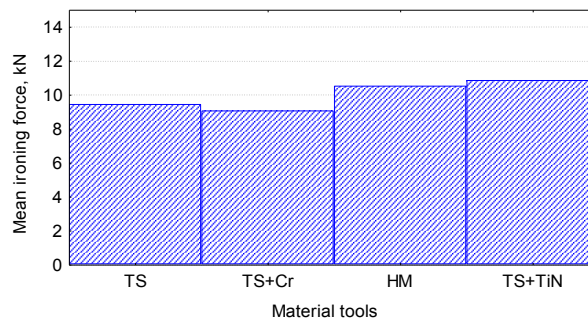


Fig. 4. Mean value of drawing force for various tool materials

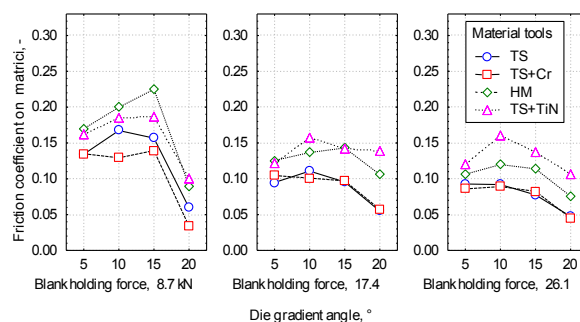


Fig. 5. Change of friction coefficient on die in dependence on die gradient angle and blank holding force for various tool materials

Figure 5 shows the change of friction coefficient on die side in dependence on blank holding force and die gradient angle at various tool materials. The smallest friction coefficient was obtained by using the tool with hard chromium coating at all angles of die gradient. Somewhat higher values were obtained with alloyed tool steel, and the highest values were obtained with tools of hard metal and titan-nitride coating.

The examples of change of friction coefficient on die side on sliding path at ironing with various tool coatings are given in figure 6.

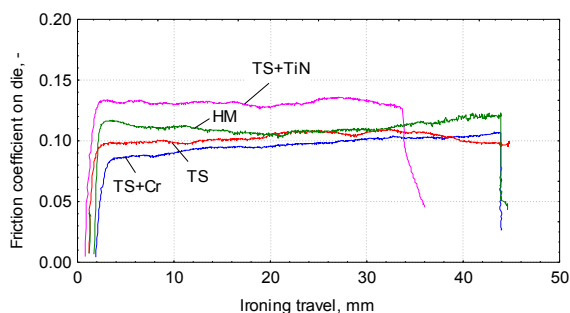


Fig. 6. Friction coefficient for various tool materials

The change of friction coefficient on punch in dependence on blank holding force, for various tool materials, is shown in figure 7. For steel samples, for all tool materials, friction coefficient will decrease in the beginning, with the increase of blank holding force, and then it will start increasing with further increase of blank holding force. The highest value of friction coefficient is obtained by using the tool with titan nitride coating (TiN).

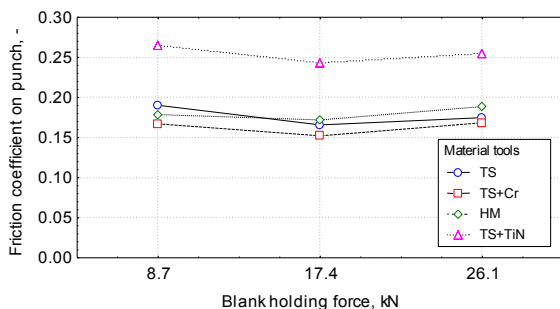


Fig. 7. Change of friction coefficient on punch in dependence on blank holding force at various tool materials

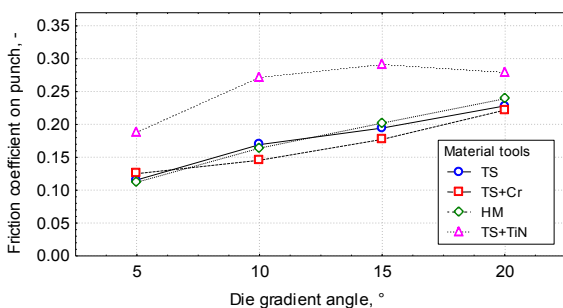


Fig. 8. The change of friction coefficient on punch in dependence on die gradient angle at various tool materials

The influence of tool material on friction coefficient on punch at various die gradient angles is shown in figure 8. By using the tool of tool steel (TS), with chromium coating (TS+Cr) and hard metal (HM) at the increase of angle α , friction coefficient constantly increases and that connection is almost linear. The values for TS and HM are almost identical, which is understandable, because the tool is marked with HM, i.e. HM/TS, i.e. Punch plate is made of tool steel. The tool with hard titan nitride coating (TS+TiN) gives significantly higher values of friction coefficient.

Figure 9 shows the change of wall tension stress in dependence on die gradient angle and blank holding force

for various tool materials. The smallest values of wall tension stress are obtained with tools with TiN coating, and the highest values are obtained with tools of HM. Regarding aluminium alloy samples, the smallest wall tension stress is obtained by using the tool of alloyed tool steel (TS), and the largest one is obtained with tool of hard metal (HM).

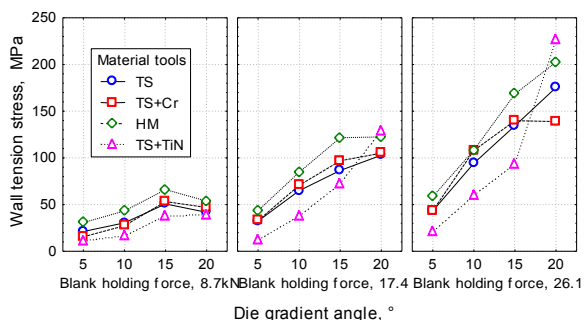


Fig. 9. Change of wall tension stress independence on die gradient angle and blank holding force for various tool materials

The specified diagrams show that at small blank holding forces, with the increase of die gradient angle above 15° , the decrease of wall tension stress occurs. At larger blank holding forces and larger die gradient angles, stress differences become more significant compared with the ones obtained at small blank holding forces and small die gradient angles.

ACKNOWLEDGMENT

The part of this research is supported by Ministry of Education and Science, Republic of Serbia, Grant TR32036 and TR34002.

4. CONCLUSION

One of the methods which enable the reduction of friction resistance (and in that way the influence on product quality) is the selection of properties of tool surface layers. However, it should be emphasised that, unlike machine elements for which it is possible to select the a wide range of contact couples materials, in the case of MF process, one of the contact couple elements – strained material – is determined in advance. The only thing that can be changed, in certain limits, is the tool material or various procedures of thermo-chemical forming, galvanisation etc. can be applied, which change the chemical content of surface layers.

REFERENCES

- [1] GIERZYNSKA M. (1983) *Tarcie zużycie i smarowanie w obrobce plastycznej metali*, WNT, Warszawa,
- [2] DOHDA K. (1990) *Tribological properties of thin hard coatings used in metal forming*, Proceedings of the Japan International Tribology Conference, Nagoya, pp 1973-1980
- [3] ADAMOVIC D. (2002) *Conduct of materials in contact at processes of plastic forming with high working pressures*, Doctoral thesis, The Faculty of Mechanical Engineering, Kragujevac, (in Serbian).



THE SIMULATION OF DISCONTINUOUS TIN BENDING IN THE PROCESS OF FORMING ROUND CONICAL TUBE

Zdravko BOŽIČKOVIĆ¹, Ranko RADONJIĆ², Ranko BOŽIČKOVIĆ³

¹University of East Sarajevo – Faculty of Mechanical Engineering Sarajevo, Vuka Karadžića 30, BH, RS,
zdravko.bozickovic@gmail.com

²University of Banja Luka - Faculty of Mechanical Engineering Banja Luka, Vojvode Stepe Stepanovića 75, BH, RS,
ranko.radonjic@unibl.rs

³University of Banja Luka - Faculty of Mechanical Engineering Banja Luka, Vojvode Stepe Stepanovića 75, BH, RS,
rankob@teol.net

Abstract: The paper presents and analyzes the problems that appear in the process of discontinuous bending of round conical tube. Because of the variable tool radius (stamp and die) it leads to various gaps (“holes”) at the point where the tube will be longitudinally welded after bending, which is a significant problem in manufacturing. Based on previously defined data, tool geometry was created by CATIA software. In order to determine the optimum shape of tools FE numerical simulation of forming tubes with a software package simufact.forming has been derived. For this analysis a constant coefficient of friction between tin and tools is taken, and forming speed is defined to match the speed of movement of the executive machinery. The results of the distribution of effective strain and effective stress have been analyzed.

Key words: tin bending, strain, stress, numerical simulation

1. INTRODUCTION

Tin structures based on round conical tubes are specific by their aesthetic appearance, simplicity of transport, installation and quick replacement of damaged parts due to external factors. This is important when we use poles for public lighting and public telecommunications. The material quality of round conical tubes are construction steels of S 235 JR and S 355 JR quality (EN 10025 standard). Development of these tubes is done by discontinuous bending of hydraulic press.

2. PROBLEM DESCRIPTION

A problem that often arises in the process of discontinuous bending of round conical tubes with one longitudinal seam is a geometric shape of the final product. For this type of design it often appears a difference in the size of gap at the point where there is a need for welding in further procedure, which is a significant problem in manufacturing [1]. Various gaps (“holes”) appear due to the fact that tools for this product have a variable radius, which directly affects the size of the elastic return as well as different stress-strain state in a work piece. It is possible to use numerical simulations to determine the optimal form of tools which will enable that in the process of discontinuous bending we get a work piece to be able to undergo the following operation (the operation of longitudinal welding) in a defined technological process. In addition to the variable tool radius, the size of the gap at the joint point of tubes is

affected by developed preform shape as well as mechanical characteristics and deformability parameters for work piece material. The development technology of round conical tubes is shown in Fig. 1 [2].

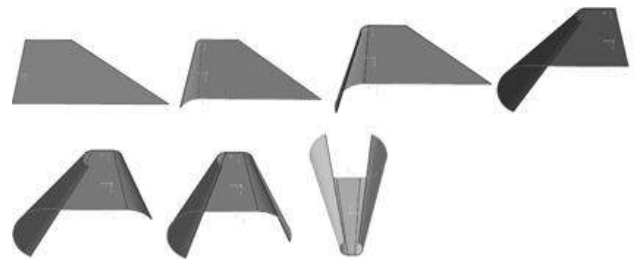


Fig.1. Development technology of round conical tubes

It should also be noted that the preforms for the conical tube are made of tin rolls in two phases:

- unwinding and flattening of tin on corresponding processing systems
- cutting a developed shape of preform on circular shearing machines.

It can be seen that in the process of making a preform there is an impact on the change of stress-strain and structural state of material, especially around the edges where the cutting was done. In addition, due to unequal cooling of rolls in the rolling process, mechanical characteristics of tins at the beginning, in the middle and at the end are not the same. The same problem is with mechanical characteristics along, across and at an angle of 45 degrees to the axis of rolling. Therefore it is necessary when purchasing tin in rolls to examine influential factors

on the deformability of materials. The deformability of materials is influenced by mechanical and chemical characteristics of materials, the temperature of processing, delivery condition, the degree and speed of strain.

3. EXPERIMENT

Strain parameters which are examined are:

- stress ratio on the yield point and strength of materials,
- contraction of cross section
- exponent of the curve of strain strengthening
- coefficient of normal anisotropy.

Basic strength characteristics of materials, as well as stress-elongation curve required for stress analysis were obtained from the tensile test of specimen made of samples of steel sheets of S235 JR quality and thickness of 3 mm.

3.1. Determining the mechanical characteristics of materials

The examination procedure and specimen geometry (Fig. 2) are defined by EN 10002-1 standard. Mechanical and chemical characteristics of the basic material are prescribed by EN 10025-2 standard.

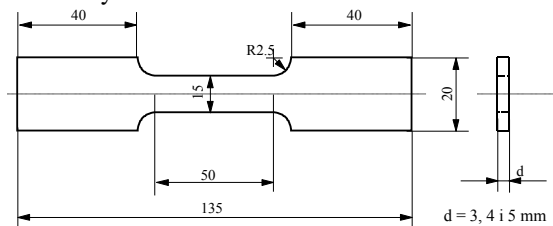


Fig.2. Specimen for determining tensile characteristics

The examination was done on modern electromechanical tearing machine during the load control. Elongation was recorded using extensometer HOTTINGER HK 25 of $\pm 0,001$ mm precision. The results of the determination of tensile characteristics of specimens cut from samples of 3 mm thick steel sheets are given in Table 1 [3].

Table 1. Mechanical characteristics of tin S 235 JR

Tag of specimen	Upper flow stress R_{eH} , MPa	Lower flow stress, R_{eL} , MPa	Tensile strength R_m , MPa	Elongation A, %
Spec. 3-1	331	322	407	28.7
Spec. 3-2	328	321	402	30.2
Spec. 3-3	335	325	412	29.4

The layout of stress-elongation diagrams obtained by testing specimen (tag Spec. 3-1) is shown in Fig. 3. Other diagrams are not given because they show a similar character of the behavior of materials. In order to determine the real modulus of elasticity for S 235 JR steel it is designed the specimen for calibration testing whose layout is given in Fig.4. Cross-section of the specimen: width of 29.5 mm, thickness of 3 mm, cross-sectional area of 88.5 mm^2 .

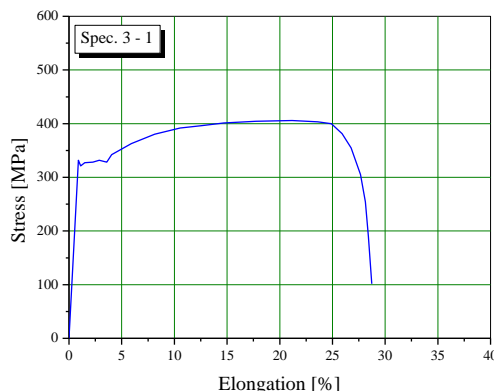


Fig.3. Stress-elongation diagram of the Spec. 3 - 1

The prepared specimen was glued with measuring tape HOTTINGER LY11-10/120 by which the strain is registered depending on the load growth.



Fig.4. Prepared specimen for determination of elasticity modulus

For the determination of elasticity modulus it is required a linear part of stress-elongation curve, the prepared specimen is loaded above the limit of proportionality. The diagram layout of the stress-elongation calibration curve is given in Fig. 5. The value of elasticity modulus of 207.6 GPa was gained by calibration testing, which is for 1.1 % lower than 210 GPa prescribed for this group of steels given in the literature.

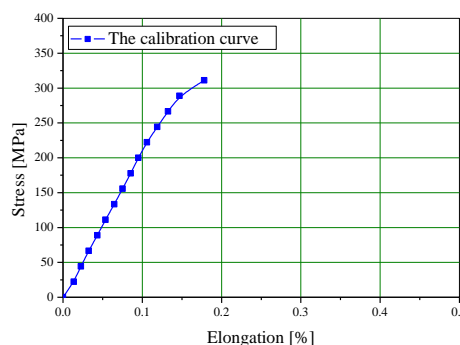


Fig.5. Stress-elongation diagram of a calibration curve

3.2. Determination of deformability parameters

Based on the results of elongation test, the curve of material flow work piece was determined. In fact, in an area of uniform (homogeneous) deformation there is an uniaxial stress state and the correlation between tensile force, the nominal and real stress (which is at the same time equal to the strain resistance and equivalent stress) is determined.

Also, the deformation length (in this case, the largest-first principal strain) presents effective (equivalent) strain.

According to the diagram, Fig. 3, some real stress for the corresponding strain is determined [4]:

$$k_0 = \sigma_v, k_1 = \sigma_1 \cdot (1 + \varepsilon_1) \dots k_M = \sigma_M \cdot (1 + \varepsilon_M) \quad (1)$$

Extrapolation of the real flow curve is done by function [5]:

$$k = C \cdot \varphi^n \quad (2)$$

Logarithmic strains (φ) are calculated using the equation [5]:

$$\varphi_0 = 0, \varphi_1 = \ln(1 + \varepsilon_1) \dots \varphi_M = \ln(1 + \varepsilon_M) \quad (3)$$

C and n are constants which are determined from the condition of volume constancy and maximum force in the tensile diagram. The mean value of flow stress which is determined by examining is $R_{eL} = 322$ MPa. Stress ratio on the edge of flow and tensile strength (Table 1) is 0.7912. Constant $C = k_M / \varphi_M^n$ is obtained from the curve of solidification and is $C = 663.5$ MPa and the exponent of the curve of strain strengthening is $n = \varphi_{eM} = 0.18$. Poisson's number $\nu = 0.3$, Young's elasticity modulus was determined experimentally $E = 2.09 \cdot 10^5$ MPa.

The exponent of the curve of deformation strengthening represents the effective deformation on the border of balanced stretching deformation. Solidification curve (Fig. 6) is represented by the equation:

$$k = 663,5 \cdot \varphi^{0.18} \quad (4)$$

According to the values of factor n i.e. the impact of reinforcement intensity on steel deformability, this material belongs to the group of materials which are poor workable in cold strain.

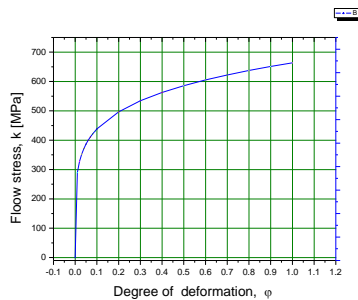


Fig.6. Flow curve for work piece material

4. NUMERICAL SIMULATION

4.1. Modeling

In order to perform simulation of forming processes, it is firstly required to model the process defining all necessary parameters, which should be as close to the value of real process [5]. For this purpose one tool segment is created, that is, a stamp and a die for the upper tube diameter of 155 mm and the diameter of the tube on the bottom base is 165 mm, and a developed preform shape.

The modeling was done in CATIA software package. Taking into account that the simulation was done in the software package *simufact.forming* [6] it was necessary to

save created models of tools and a preform in the appropriate format (eg. stl).

In the modeling stage in *simufact.forming* there are inserted geometrical data of tool, information on mechanical characteristics, deformability parameters of work piece materials. There is also inserted the real (examined) value of the elasticity modulus, since it has a significant influence on the occurrence of elastic return. The simulation was done for the segment of tube with length of 1000 mm, tin thickness of 3 mm (quality of material is S 235 JR according to EN standard. Tool, that is, a stamp and a die are defined as rigid bodies, while the work piece is defined as a deformable body. Flow of metal work piece in numerical simulation is described by flow curve. For discretization of preform in the software Sheetmesher's with Hexahedral's form of final elements was used. Modeling of tubes was performed in seven steps of bending in a tool. This paper presents the stress and deformations of the first and seventh operation.

Model in the first stage of forming tubes is shown in Fig. 7.

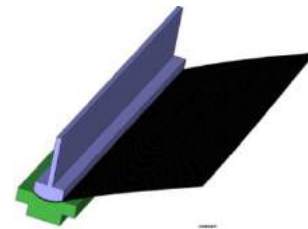


Fig.7. Model of tool and preform in the first phase of bending

The model in the seventh stage of tube formation is shown in Fig. 8.

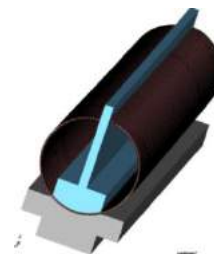


Fig.8. Model of tools and preform in the seventh stage of bending

4.2. Presentation of the distribution of effective stress

The distribution of effective stress along the work piece during bending is shown in Fig. 9 and 10. Stress is in the range from 0.4 MPa to 406.3 MPa. The highest stresses are along the radius of bending work piece and the lowest are found outside the zone of bending. Other distributions of effective stress by bending phases are not shown because they show an almost identical character of behavior.

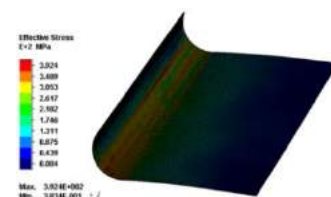


Fig.9. Distribution of effective stress in the first phase of forming tubes

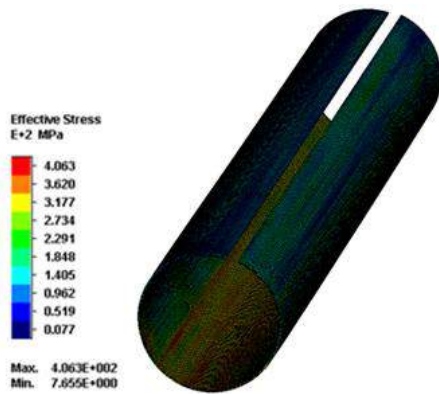


Fig.10. Distribution of effective stress in the seventh phase of forming tubes

4.3. Presentation of the distribution of effective strain

Figures 11 and 12 shows the distribution of effective strain in the first and seventh stage of forming tubes. The analysis results showed that the distribution of effective strain is very symmetric. The strain range is from 0 to 0.66, which represents a small effective strain which is below the allowable limit. The greatest deformation is in the area of contact between the work piece and the tool where there is the smallest radius but there it is also small enough that the treatment is not critical.

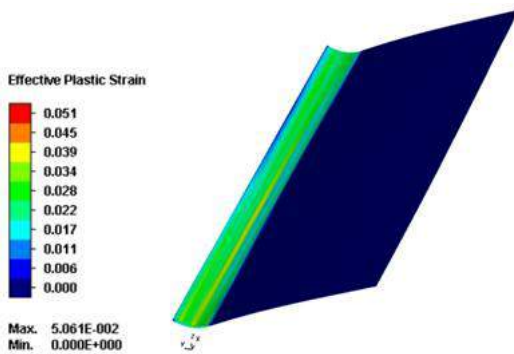


Fig.11. The distribution of effective strain in the first phase of forming tubes

Also, in Fig. 12 it can be seen that the gap value at the point where longitudinal welding of tubes will be conducted is almost the same. On this basis we can conclude that the modeled form of tool is optimal for the defined requirements of forming.

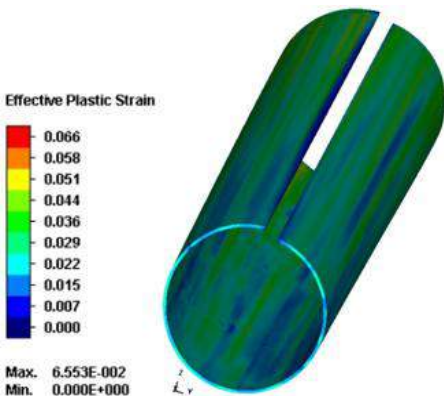


Fig.12. The distribution of effective strain in the seventh phase of forming tubes

4.4. Bending force

Since all stages of bending are carried out in the same tool, the values of strain force are approximately equal. The force in the first stage of bending is shown in the diagram in Fig. 13.

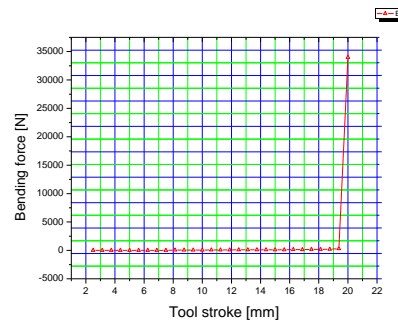


Fig.13. The diagram of force-tool stroke in the first stage of forming tubes

5. CONCLUSION

Discontinuous tin bending in the process of forming round conical tubes is characterized by varying stress-strain state in the work piece, different size of the elastic return and a variable degree of deformation. Applying numerical simulation it is possible to determine the optimal form of tools (stamp and die) by which the production will receive a satisfactory form of tubes, which could be welded without great difficulty in the further process. Based on the simulation results it can be concluded that the modeled tool for the upper tube diameter is 155, while the diameter of the lower base is 165 mm (length of tube is 1000 mm) from the point of satisfying the needs of production. Also, the simulation results can provide that the values of stress and strain in the work piece are within the approved range.

REFERENCES

- [1] Božičković, Z. (1996) *Optimization of discontinuous formation of polygonal tubes on CNC-hydraulic tandem press*, Master's thesis, The Faculty of Mechanical Engineering, Banja Luka, pp. 30-40
- [2] Božičković, Z. (1998) *Optimal design process of discontinuous formation of polygonal tubes with the application on CNC hydraulic tandem press*, DEMI, Banja Luka, pp 26-31
- [3] Božičković, Z. (2010) *Elastic-plastic strains of polygonal tubes with variable cross-section during longitudinal welding*, PhD thesis, The Faculty of Mechanical Engineering, Banja Luka, pp. 90-97
- [4] Plančak, M., Vujović, V. and others (2002) *Practicum of laboratory exercises in the technology of plasticity*, Faculty of Technical Sciences, Novi Sad, pp 58-69
- [5] Mandić, V. (2005) *Modeling and simulation of deformation process*, The Faculty of Mechanical Engineering, Kragujevac, pp. 33-55
- [6] Simufact.forming (2008) *Simulating Manufacturing, User Guide*

EXPERIMENTAL ANALYSIS AND MATHEMATICAL MODELLING OF THE ROLLING FORCE

Milan JURKOVIĆ¹, Zoran JURKOVIĆ², Asim JUŠIĆ¹, Vesna MANDIĆ³

¹Technical faculty, University of Bihać, Irfana Ljubijankića bb., Bihać, Bosnia and Herzegovina

²Faculty of Engineering, University of Rijeka, Vukovarska 58, Rijeka, Croatia

³Mechanical Engineering Faculty, University of Kragujevac, S. Janjić 6, Kragujevac, Serbia
 mi.jurkovic@gmail.com, zoran.jurkovic@riteh.hr, asimjusic@hotmail.com, mandic@kg.ac.rs

Abstract: This paper deals with experimental determination of rolling force, mathematical modelling, analytical calculation and verification of rolling force. The results of performed research indicate that the mathematical-experimental modelling can be successfully used to define the rolling force and the technological parameters of the rolling process. In this paper the mathematical model of rolling force $F = f(\Delta h, \varepsilon, \delta, k)$ has been defined. Main achievements are: original experimental identification of rolling force, original of measuring sensor for measurement of rolling force and mathematical model for defining the rolling force.

Key words: experimental analysis, mathematical modelling, rolling force, process, model

1. INTRODUCTION

The objectives of this paper are to define mathematical model of rolling force in dependence of the basic influential parameters. This paper is based on experimental results for the rolling force on the line for rolling with three machining modules, where the measurement equipment and measurement system are used for measuring the rolling force. The initial data are: cold rolling strip material (DIN St 14), initial thickness $h_0 = 2,5$ mm and width $b_0 = 350$ mm. Diameters of rolls on machining modules are: $D_1 = 207,9$ mm; $D_2 = 175,7$ mm and $D_3 = 157,9$ mm. Parameters of the rolling process are: absolute deformation Δh , relative degree of deformation ε , coefficient δ and yielding of materials k .

In this paper has been presented plan of the experiments and its results for the rolling force, procedure of modelling, testing adequacy of the model, analysis result of the modelling and experiment, comparison of experimental force and modelling force, and at the end simulation of the rolling force [1,2,3,4,5,6,7,8,9].

2. EXPERIMENTAL RESEARCH OF ROLLING FORCE

The experimental analyses of rolling process are made in the aim of measuring the rolling forces which are used for modelling and simulation of the rolling process (Fig. 1). Original experiments have carried out in the industrial conditions (plant "Krajinametal" Bihać) under macro project titled: *Research and development of flexible rolling machines* (Bosnia and Herzegovina) and project titled: *Modelling and Simulation Processes by Using Genetic and Stochastic Algorithm* (Croatia).

2.1. Measuring system

By means of special measuring converter with strain gauge (Fig. 2) was realized experimental test mechanical load of rolling machine in process of cold rolling with measuring the rolling forces (Fig. 3).

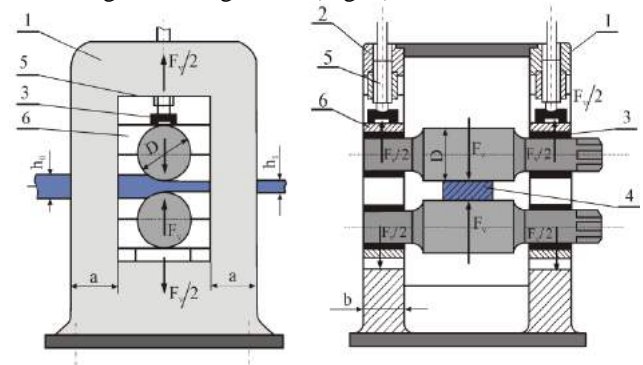


Fig. 1. Frame of rolling machine (1,2), sensor force (3), rolled section-sheet metal (4), thread spindle (5), roller cradle (6)

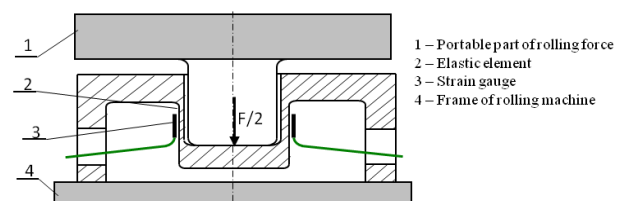


Fig. 2. Converter with strain gauge (measuring element)

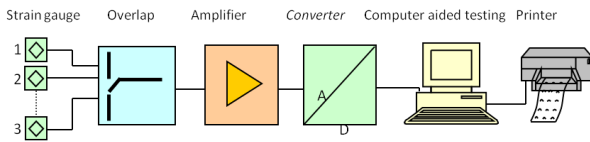


Fig. 3. Measuring system

3. ANALYSIS OF THE INPUT AND OUTPUT VARIABLES (The choice of the process parameters and block scheme)

The force modelling has been performed for the four variables of rolling process (Fig. 4.). The parameters of the rolling process are defined in the following way:

- input variables: absolute deformation Δh (mm), relative degree of deformation ε , coefficient $\delta = 2\mu l/\Delta h$, where $l = \sqrt{\Delta h R}$, $R = D/2$ and yield stress of material k (N/mm²).
- output value – rolling force F_v (kN).

Function of the process state: $F_v = f(\Delta h, \varepsilon, \delta, k)$. A graphic presentation of the input – output values is given in Fig. 4.

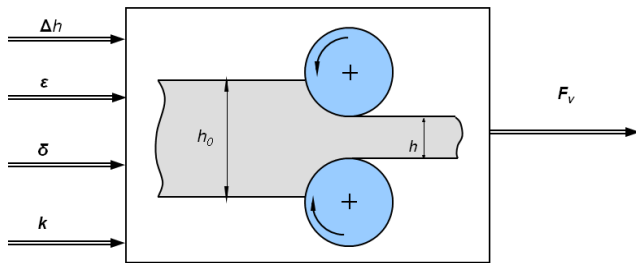


Fig. 4. Scheme for rolling force modelling (input – output values)

The coded and physical values of influential parameters are presented in Table 1.

Table 1. Physical x_{ji} and coded X_{ji} values

Influential factors	Coded and physical input values			
Physical input values	$x_1 = \Delta h$ (mm)	0,5	1,0	1,5
	$x_2 = \varepsilon$	0,20	0,40	0,60
	$x_3 = \delta$	2,0	3,5	5,0
	$x_4 = k$ (N/mm ²)	250	375	500
Coded input values	X_i	-1	0	1

4. EXPERIMENTAL DESIGN AND RESULTS

The experiments were performed by using plan of experiments with $N = 2^k + n_0 = 2^4 + 4 = 20$ tests (Table 2). The design matrix meets the criteria of orthogonality, symmetry and normativity [1].

5. MATHEMATICAL MODELLING OF ROLLING FORCE

For choosing the type of the mathematical model, there is no generally applicable rule, that means, that for each investigated process or system have to be chosen a model and examine its accuracy and adequacy in relation to the real process. On the basis of performed experiment and regression analysis the statistical model is determined by means of real regression coefficients b_i , b_{ii} , b_{im} , b_{imk} so that mathematical model obtains the form:

$$\hat{Y} = \sum_{i=0}^k b_i X_i + \sum_{1 \leq i < m} b_{im} X_i X_m + \sum_{1 \leq i < m < k} b_{imk} X_i X_m X_k \quad (1)$$

$$b_0 = \frac{1}{N} \sum_{j=1}^N X_{0j} Y_j, \quad X_{0j} = 1$$

$$b_i = \frac{1}{N - n_0} \sum_{j=1}^N X_{ij} Y_j, \quad \text{za } i = 1, 2, \dots, k \quad (2)$$

$$b_{im} = \frac{1}{N - n_0} \sum_{j=1}^N X_{ij} X_{mj} Y_j, \quad \text{za } 1 \leq i < m \leq k$$

Taking in attention only significant coefficients of regression, the mathematical model of force has the form:

$$Y = F = 5113,75 + 394,43 X_1 + 406,81 X_2 + 368,56 X_3 + 600,43 X_4 - 118,06 X_1 X_4 - 193,81 X_2 X_3 X_4 + 91,43 X_1 X_2 X_3 X_4 \quad (3)$$

The coefficient of multiple regression $R = 0,982$ shows very good correlation between varying X_i and rolling force. Encoding the mathematical model (3) is obtained the physical mathematical model of the rolling force in the form of:

$$Y = F_v = 992,35 + 2736,62 \Delta h - 2890,73 \varepsilon - 264,70 \delta + 3,15 k - 1353,85 \Delta h \varepsilon - 199,38 \Delta h \delta - 3,40 \Delta h k + 2075,41 \varepsilon \delta + 15,46 \varepsilon k + 1,74 \delta k - 6,25 \varepsilon \delta k + 1,08 \Delta h \varepsilon \delta k. \quad (4)$$

6. ANALYSIS OF MODELLING AND EXPERIMENT RESULTS

6.1. Comparison of the experimental force and modelling force

Rolling force obtained results by the experimental investigation and mathematical modelling were presented on Figure 5. Results comparisons were shown adequacy of the model (4) and its possible using for rolling force prediction. The obtained experimental results (Table 2) and results obtained by mathematical model (4) show very good correlation between each other (Figure 5), also presented by multiple regression coefficient $R = 0,982$. According to that, rolling force model (4) describes accurately enough experimental results within domain of experiment.

6.2. Simulation of rolling force

3D simulation model (4) was shown, on Figure 6, dependence of the rolling force in relation to relative degree of deformation ε and absolute deformation Δh . In the same time other input parameters coefficient δ and yield stress of material k were constant on coded level -1 shown in Table 1.

Table 2. Experimental results

trial run N_j	1	2	3	4	5	6	7	8	9	10
Experimental forces F_j (kN)	3370	4460	3880	4900	3780	4825	5245	6190	4520	5440
trial run N_j	11	12	13	14	15	16	17	18	19	20
Experimental forces F_j (kN)	5795	6140	5880	5924	5828	6730	4790	4868	4890	4820

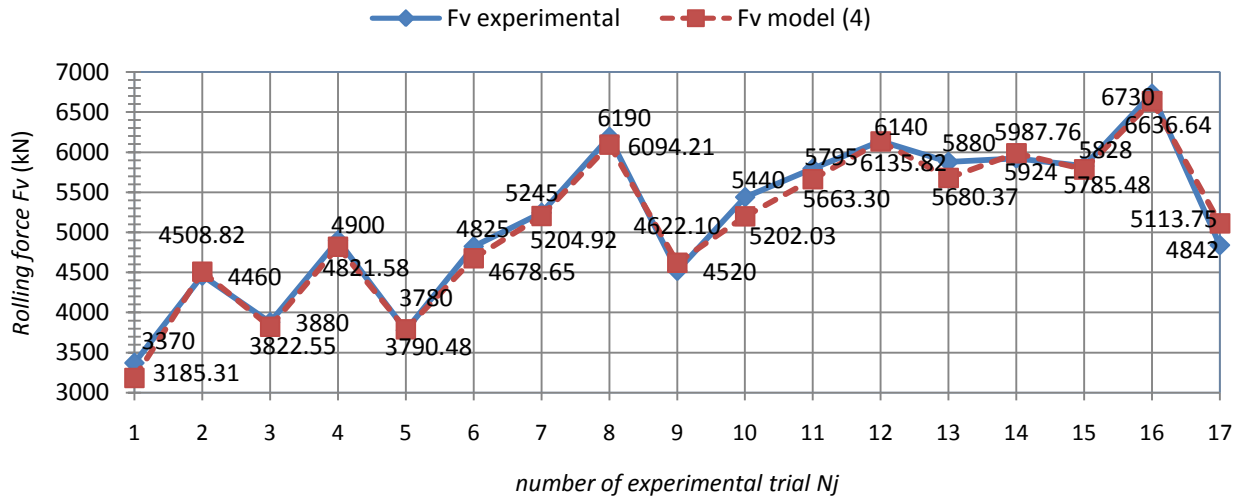


Fig. 5. Comparison of the experimental and modelling force results

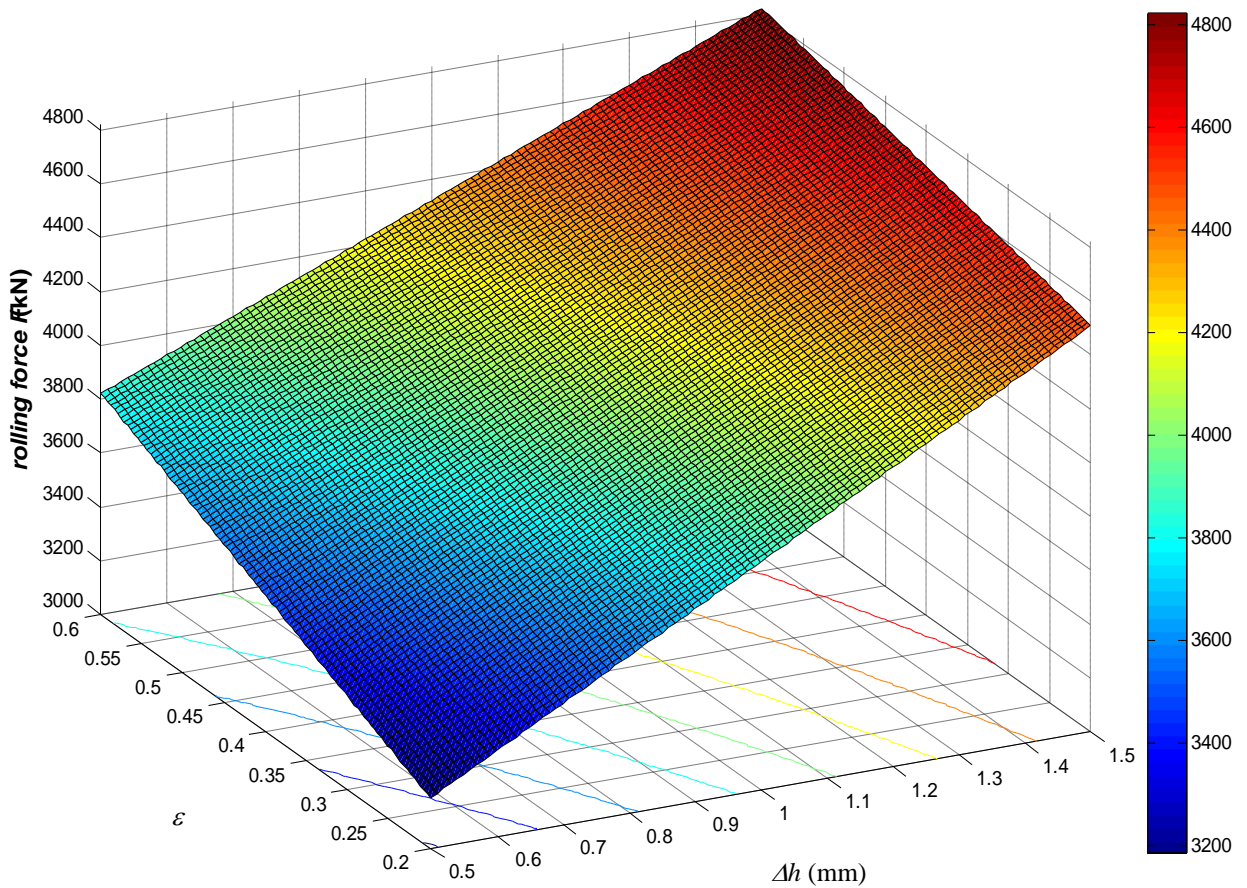


Fig. 6. Response surface for rolling force model (4) depends on relative degree of deformation and absolute deformation with constant values of the coefficient $\delta = 2$ and yield stress of material $k = 250 \text{ N/mm}^2$

7. ONCLUSION

The obtained model of the rolling force enough correctly and reliable describes forming force, that are confirmed with confidence level $P=0.95$ and the coefficient of multiple regression $R=0.982$. On this presented way obtained model is useful to reduce the production cost and achieve desired product quality.

REFERENCES

- [1] JURKOVIĆ, M. (1999) *Mathematical Modelling and Optimization of Machining Processes*, Faculty of Engineering, University of Rijeka, Rijeka.
- [2] LISICYN A.I., OSTRENKO, V. J. A. (1976) *Modelirovanie processov obrabotki metallov davleniem* (in Russian), Tehnika, Kiev.
- [3] MASLOV, V. E., ŠAPOVAL, V. H. (1983) *Eksperimentalnoe issledovanie processov obrabotki metallov davleniem*, (in Russian), Tehnika, Kiev.
- [4] KOBAYASHI, M. (1978) *Influence of Rolling Conditions of Spreading in Flat Rolling of Round Wire*, J. Jap. Soc. Technol. Plast. 210/78.
- [5] LANGE, K. (1974) *Lehrbuch der Umformtechnik, Band 2, Massivumformung*, Springer Verlag Berlin.
- [6] MANDIĆ, V. (2007) *Virtuelni inženjering*, (in Serbian), Mašinski fakultet Kragujevac, Kragujevac.
- [7] JURKOVIĆ, Z., JURKOVIĆ, M., KUZMAN, K. (2002) *Experimental Friction Test by Sheet Metal Deep Drawing Process, 7th International Conference on Technology of Plasticity- ICTP*. The University of Tokyo, Yokohama: Japan Society for Technology of Plasticity. Vol. 1. pp 805-810.
- [8] JURKOVIĆ, M. (1988) *CNC Manufacturing Line for the Profile Rolling*, Inventor/Pronalazač, Vol. 68, No.3, pp 20-22, Sarajevo.
- [9] JURKOVIĆ, Z., JURKOVIĆ, M. (2003) *Modelling and Simulation Application by the Optimization of Deep Drawing Process*. Journal of Technology for Plasticity. Vol. 28, No 1-2, pp 121-134.



NUMERICAL SIMULATION OF UPSETTING OF PRISMATIC BILLETS BY V-SHAPE DIES WITH EXPERIMENTAL VERIFICATION

Dragisa VILOTIC¹, Miroslav PLANČAK¹, Sergej ALEXANDROV², Aljosa IVANISEVIC¹, Dejan MOVRIN¹,
Mladomir MILUTINOVIC¹,

¹Faculty of Technical Science, University of Novi Sad, Trg Dositeja Obradovica 6, Novi Sad, Serbia
vilotic@uns.ac.rs, plancak@uns.ac.rs, aljosa@uns.ac.rs, movrin@uns.ac.rs, mladomil@uns.ac.rs

²Institute for Problems in Mechanics, Russian Academy of Science, 101-1 Prospect Vernadskogo, 119526
Moscow, Russia
sergei_alexandrov@yahoo.com

Abstract: Upsetting processes represent an elementary operation which is often integrated into complex technological processes of cold and hot bulk metal forming. These processes also have significant role in material formability analyses.

In this paper, results obtained by numerical simulation of upsetting of prismatic specimens by V-shape dies in cold condition are presented. Numerical simulation is performed using Simufact Forming program package.

Results obtained by numerical simulation of upsetting of prismatic billets with square section of material C45E steel by V-shape dies with die angle of 120° are verified experimentally.

Key words: Upsetting, Numerical simulation, V-shape dies, Prismatic billets

1. INTRODUCTION

Upsetting processes have an important role in the technology of bulk metal forming. For the upsetting of prismatic or cylindrical billets, flat dies are most often used, although upsetting can be obtained with tools of different geometry.

Given in [1] is the stress analysis in deformation zone in upsetting of workhardening material by cylindrical dies. The load and average pressure as a function of die stroke were determined and compared to results obtained experimentally.

In paper [2] stress analysis of upsetting prismatic billet with concave-curve dies is obtained. Solution of contact stress and forming load, i.e. distribution of contact stress and forming load in upsetting cylinder by conical dies is presented in [3].

Various modes of upsetting of prismatic and cylindrical billets find their application in the analysis of formability of materials. Upsetting with dies of various geometry are presented on Fig.1. [1, 4, 5].

Determination of stress-strain state in the processes of metal forming is one of the most important tasks of the applied theory of plasticity. The knowledge of stress-strain enables determination of the process parameters and analysis of material formability.

There are three groups of methods which enable stress-strain and forming load determination:

- Theoretical
- Experimental
- Numerical

In this paper results obtained by numerical simulation of upsetting of cylinder by V-shape dies in Simufact Forming programming package and the results obtained experimentally are presented.

Experimental part of the paper was conducted in the Laboratory for Technology of Plasticity at the Department of Production Engineering in Novi Sad. The upsetting of prismatic billets made of steel C45E material was performed by V-shape dies on Sack und Kiesselbach hydraulic press of 6,3 MN rated force. Two series of billets with square section were used.

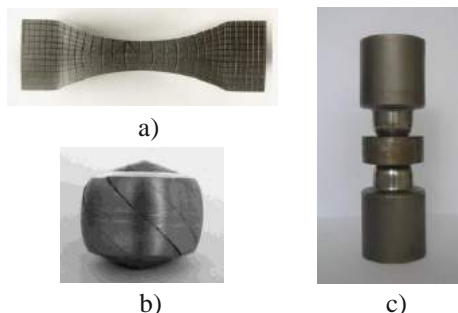


Fig.1. Upsetting with dies of various geometry:

- a) cylindrical dies [1]
- b) conical dies [4]
- c) spherical dies [5]

2. NUMERICAL ANALYSIS OF UPSETTING PRISMATIC BILLETS BY V-SHAPE DIES

Numerical analysis of upsetting of prismatic billets by V-shape dies was performed using the finite element method in Simufact Forming v.10 programming package.

The finite elements method is modern method of numerical analysis and represents a method of direct analysis. Unlike the other numerical methods it is based on physical discretization.



Fig.2. Upsetting by V-shape dies

On Fig.2. beginning of the process of upsetting of prismatic billet by V-shape dies is given. The dies and models in simulation were modeled in CAD package Solid Edge V18 and then imported to the Simufact Forming program. Two series of billets were used and initial dimensions are given on Fig.3. (a, b). SIMesh Tetra mesher with 2mm element size was used, Fig.3. (c). Dies used in simulation were set as rigid bodies and press velocity was 1mm/s.

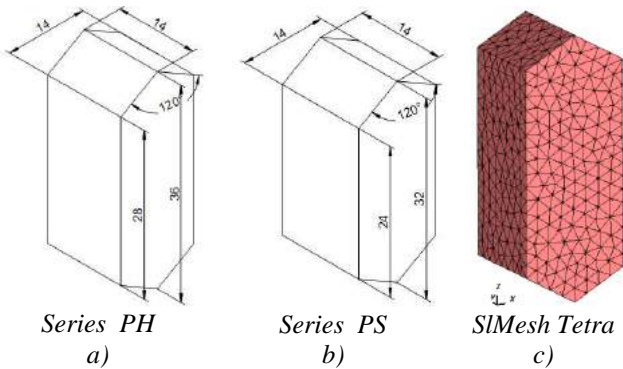


Fig.3. Initial dimension of the billets

2.1. Simulation results

By 3D numerical simulation of upsetting of prismatic part by V-shape dies the information on stress-strain state and forming load diagram as function of die stroke were obtained. In the simulation, the flow curve for C45E steel determined by Rastagaev's technique and approximated by the below equation was used:

$$k = 289,671 + 668,779 \cdot \varphi_{ef}^{0,3184} [MPa] \quad (1)$$

where:

k -flow stress

φ_{ef} -effective strain

Friction between contact surface of dies and billet was defined with coefficient of friction $\mu = 0,12$.

Fig.4. and Fig.5. shows stress distribution at the end of upsetting process for billets series PH and PS. Maximum die stroke for upsetting of the billet series PH was 20mm and for series PS maximum die stroke was 17mm. It can be concluded that maximum effective stress for series PH in the end of the process is 1205MPa, Fig.4., and for series PS that value is 1149MPa, Fig.5. It can be seen that maximum effective stress in both series are concentrated on the contact surface of the billets.

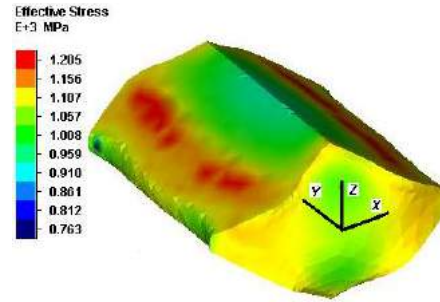


Fig.4. Distribution of effective stress for billets series PH

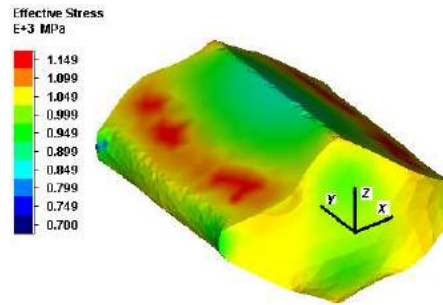


Fig.5. Distribution of effective stress for billets series PS

Distribution of the effective stress inside the billets series PH along x direction is given on Fig.6. and for billets series PS on Fig.7. Planes, in which appropriate effective stresses act, are 5, 10 and 15 mm offitted from the reference point in y direction for series PH and 4, 8 and 12mm for series PS. It can be seen that for both series value of effective stresses decreases with increasing of x coordinate.

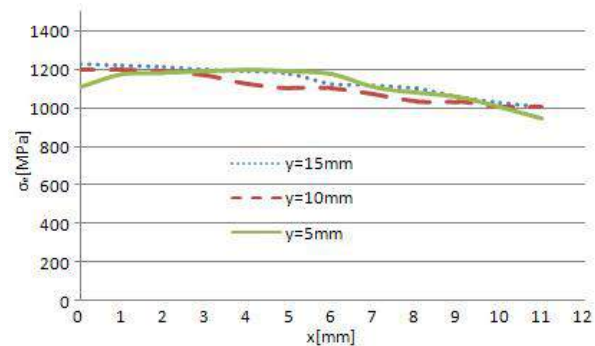


Fig.6. Distribution of effective stress along x direction for billets series PH

Fig.8. shows distribution of effective plastic strain for billets series PH. Distribution of effective plastic strain for billets series PS is given on Fig.9.

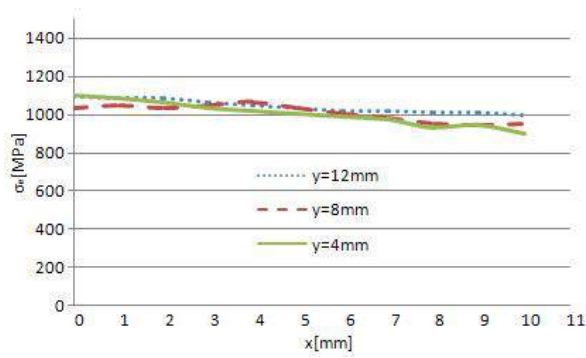


Fig.7. Distribution of effective stress along x direction for billets series PS

From Fig.8. and Fig.9. it can be concluded that for both series maximum plastic strain is concentrated on the contact surface of billet. For billets series PH maximum plastic strain is 1,681 and for billets series PS that value is 1,501.

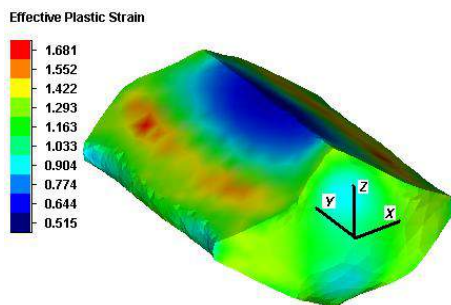


Fig.8. Distribution of effective plastic strain for billet series PH

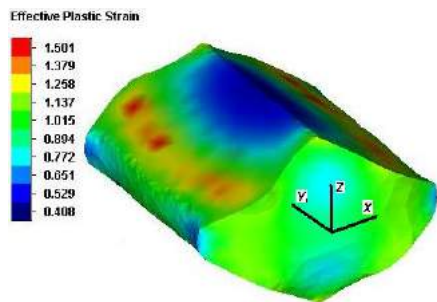


Fig.9. Distribution of effective plastic strain for billet series PS

Forming load diagram as function of die stroke is shown on Fig.12. and Fig.14.

3. EXPERIMENTAL TEST OF FORMING LOAD

Experimental test of changing of forming load depending of the die stroke was conducted on Sack&Kiesselbach hydraulic press of 6,3MN rated force (Fig.10.).

The billets compressed in the experiment were made from C45E steel. Billets geometries performed in experiment were identical to the ones used in simulation, Fig.3 (a, b). The dies used in the experiment were polished and

upsetting was performed with coefficient of friction $\mu = 0,12$.



Fig.10. Sack&Kiesselbach Hydraulic Press

Fig.11. shows billet series PH before and after deformation. From Fig.11. can be seen that the shape of the billets after deformation is the same as shape of billet in the end of simulation process.

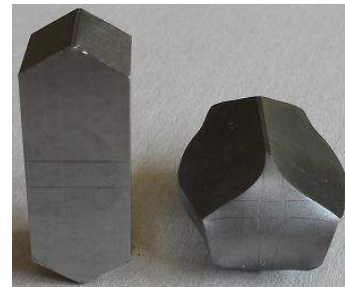


Fig.11. Billet series PH before and after deformation

In the end of the process the billet cracked. The crack appeared on the both lateral sides of billet in y,z plane. Upsetting of the billets series PH was performed with the maximum die stroke of 20mm. From the diagram in Fig.12. it can be concluded that the forming load obtained by simulation is higher than in the experiment, and the difference is approximately 6%. In the last phase, between 18mm and 20mm forming load obtained in simulation is 40% higher than forming load obtain experimentally.

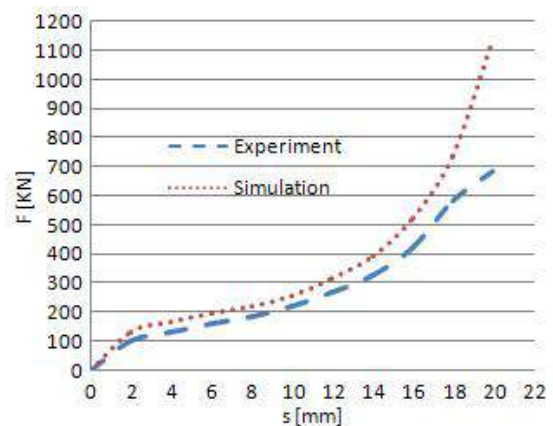


Fig.12. F-s diagram for billets series PH

Billet from second series before and after deformation is given on Fig.13. In the end of the process billet cracked.

Upsetting of the billets series PS was performed with the maximum die stroke of 17mm. From Fig.13 it can be seen that the shape of the billet after deformation is same as shape of billet in the end of simulation process.

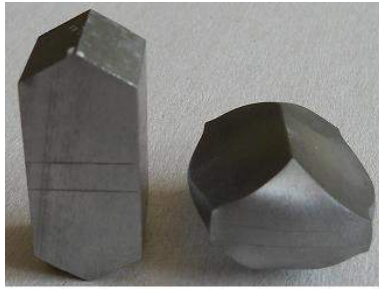


Fig.13. Billet from series PS before and after deformation

Diagram on Fig.14. shows that during the entire process the forming load obtained by simulation was negligible higher than the load obtained by experiment.

From Fig.14. it can be concluded that the forming load obtain by simulation and experiment is almost the same after die stroke of 8mm, but then, from 8mm to the end of the process forming load obtained by simulation is higher than in experiment. Difference between forming load in simulation and experiment in the end of the process is approximately 18%.

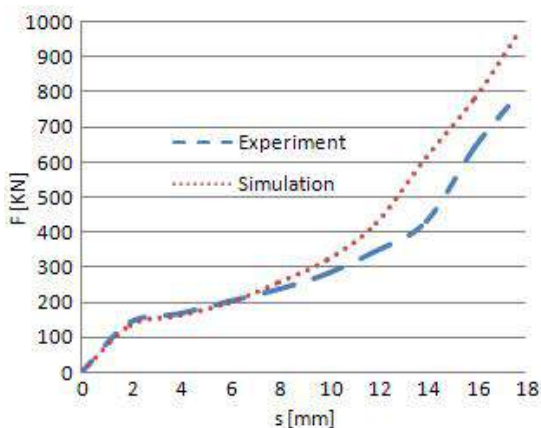


Fig.14. F-s diagram for billets series PS

4. CONCLUSION

Upsetting processes occur as production phases in most technologies for cold and warm bulk forming. They are performed with tools which geometry often differs from the standard plane geometry. Analysis of processes in plastic forming technology requires the stress-strain state to be determined as well as the basic process parameters. For these reasons various method are used, e.g. theoretical, experimental, numerical.

This paper presents a comparative view of results obtained by simulation in Simufact Forming program package and results obtained experimentally. For the experiment and simulation V-shape dies and prismatic billets are used.

From the analysis of presented results it can be concluded that forming load obtained in simulation is negligible

higher than the load obtained in experiment. It should be mentioned that the maximum forming load obtained by simulation is by 6%-18% higher than in experiment, and in one moment that difference reaches 40%. Also, it can be concluded that the effective plastic stress for billets in both series decreases with increasing of x coordinate.

ACKNOWLEDGEMENT

This paper is a part of the investigation within the project EUREKA E!5005 financed by Serbian Ministry of Science and Technological Development. Authors are very grateful for the financial support.

REFERENCES

- [1] VILOTIĆ, D., SHABAIK, A.H. (1985) *Analisis of upsetting with profiling tools*, Journal of Engineering Materials and Technology, Vol. 107, pp. 261-264
- [2] LIN, S.Y. (2002) *Stress analysis of upsetting with concave curve dies*, Journal of Material Processing Technology, Vol. 213, pp 59-68
- [3] VILOTIĆ, D., VUJOVIĆ, V., PLANČAK, M. (1994) *Determination of contact stress in upsetting of cylinder by cone-concave dies*, Metallurgy and New Materials Researches, Vol. II, No. 1-2, pp. 105-113
- [4] VILOTIĆ, D., PLANČAK, M., GRBIĆ, S., ALEXANDROV, S., CHIKANOVA, N. (2003) *An approach to determining the workability diagram based on upsetting test*, Fatigue & Fracture of Engineering Materials & Structures, Vol.26, pp 305-310
- [5] VILOTIĆ, D., CHIKANOVA, S., ALEXANDER, S. (1999) *Disc upsetting between spherical dies and its application to the determination of forming limit curves*, Jurnal of Strain Analysis, Vol. 34, pp
- [6] ROBERT, D. COOK *Finite Element Modeling for Stress Anlysis*, University of Wiskonsin-Madison, 1995.



THE APPLICATION OF ADAPTIVE FEM METHOD TO STRESS AND STRAIN ANALYSIS OF COLD FORGING PROCESS

Milan LAZAREVIC, Dejan LAZAREVIC, Milos JOVANOVIC, Sasa RANDJELOVIC
University of Nis, Faculty of Mechanical Engineering, Nis, Serbia
sassa@masfak.ni.ac.rs

Abstract: *The non-linear adaptive FEM methods are nowadays standard tool for solving practical engineering problems. The researches and development of this methods and their application in non-linear solid mechanics in last decade are focused on creating the most suitable algorithm model for analyse for concrete forming process. These efforts resulted in flexible and adaptable numerical methods which allow following of deformation process through observing of material flow, stress-strain state and many other process parameters for very complex predefined conditions. The analyses and results of this numerical model that approximate real-state forming process with a high level of accuracy is a great advantage of this methods, especially in case of solving problems with large boundary motion in non-linear solid mechanics, for instance, in bulk forging technology. In this papers is presented implementation of adaptive model in real conditions of plastic deformation during cold forging process simulation, with observing of the characteristic areas in stress-strain field in tool cavity, as well as material displacement.*

Key words: *ALE formulation, non linear deformation, mesh distortion, forging technology*

1. INTRODUCTION

An early attempts on creating realistic numerical model of liquid fuel motion in nuclear reactor, with a simultaneous progress of computer method, led to research and development of many different numerical descriptions and FEM methods for solving problems in field of non-linear solid mechanics. Finally, some of these methods, due their similarity, founded application in simulations of metal forming processes.

The classical methods, the pure Lagrangian and the pure Eulerian methods, are usually employed in continuum mechanics. Because of the shortcomings of these methods, such as element entanglement during material distortion in application of Lagrangian method, and convective effects accompanied with requiring a sophisticate mathematical mappings that follows application of Eulerian method, the new approach, which tries to combine the good characteristics of both methods, and in the same time excludes their disadvantages, were developed [1,4].

The arbitrary Lagrangian-Eulerian (ALE) method is based on the arbitrary movement of reference frame, which is continuously rezoned in order to allow a precise description of the moving interface and to maintain the element shape. This method unites a precise definition of the moving boundaries and interfaces without appearing of convective effects from Lagrangian method, with advantage of strong element distortion possibilities from Eulerian method [1,2,3,4].

The ALE method and other approaches used to treat non-linear path - dependent materials need an implicit interpolation technique, which implies a numerical burden

which may lead to uneconomically process, especially in fast-transient dynamic analysis. In comparison with classical Lagrangian method, the ALE method is much more competitive if adequate stress updating technique is implemented. In opposition to the classical methods, where distorted and locally coarse mesh may occur, ALE method shows greater level of adaptivity and adequate meshes with regular shaped elements.

The main challenge for the non-linear FEM methods applied on solid mechanics problems is precise numerical description of boundary conditions in both cases – the free boundary and contact boundary conditions. In the same time, one of the goals is tendention to minimize time costs by avoiding too frequent remeshing during simulation.

The methods used to treat non-linear path-dependent materials usually need an implicit interpolation technique, implies a numerical burden which may be uneconomical, particularly in fast-transient dynamic analysis of solids, where explicit algorithms are usually employed.

2. GOVERNING EQUATIONS IN THE ALE METHOD

The configuration of a continuous medium under motion can be presented by the same material points, and this configuration may change with time. The motion is described by one-to-one mapping relating the material point, X , in its initial position with its actual position, x , at the moment of time, t :

$$d = x(X, t) - X \quad (1)$$

The mapping conditions require that Jacobian

$J = \det \left[\frac{\partial x_i}{\partial X_j} \right]$ is non-vanishing.

The computational frame in the ALE description is a reference independent of the particle motion and it may be moving with an arbitrary velocity [2,3,4].

Material velocity, v_i is defined by:

$$v_i = \frac{\partial x_i}{\partial t} \Big|_x \quad (2)$$

and mesh velocity :

$$\hat{v}_i = \frac{\partial x_i}{\partial t} \Big|_z \quad (3)$$

If the physical property is the spatial coordinate x yield:

$$v_i = \hat{v}_i + w_j \frac{\partial x_i}{\partial \chi_j} \quad (4)$$

or

$$c_i = v_i - \hat{v}_i \quad (5)$$

where is :

$$c_i = w_j \frac{\partial x_i}{\partial \chi_j} - \text{convective velocity}$$

w - material velocity in the reference system,

c - relative velocity of the mesh according reference model.

The relationship between the material time derivative, the referential time derivative and the spatial derivative:

$$\frac{\partial f}{\partial t} \Big|_x = \frac{\partial f}{\partial t} \Big|_z + c_i \frac{\partial f}{\partial x_i} \quad (6)$$

The conservation laws that govern the motion of the continuum in ALE description are written as:

Continuity equation:

$$\frac{\partial \rho}{\partial t} \Big|_z + c_j \frac{\partial \rho}{\partial x_j} = -\rho \frac{\partial v_j}{\partial x_j} \quad (7)$$

Momentum balance equation :

$$\rho \frac{\partial v_i}{\partial t} \Big|_z + \rho c_j \frac{\partial v_i}{\partial x_j} = \frac{\partial \sigma_{ij}}{\partial x_j} + b_i \quad (8)$$

Energy conservation:

$$\rho \frac{\partial e}{\partial t} \Big|_z + \rho c_j \frac{\partial e}{\partial x_j} = \sigma_{ij} \frac{\partial v_i}{\partial x_j} + \rho a - \frac{\partial}{\partial x_i} \left(k_{ij} \frac{\partial \theta}{\partial x_j} \right) \quad (9)$$

where is : ρ - density ; σ - Cauchy stress tensor; θ - thermodynamic temperature; b - body force per unit of volume; e - specific internal energy, a – work of internal force; k - thermal conductivity tensor [1].

The right hand side of ALE conservation laws equations are written inclassical Eulerian form, and the arbitrary motion of the mesh is presented on the left hand side.

The purpose of using material time derivatives, referential time derivatives and spatial derivatives in the same

equation is to relate Cauchy stresses and thermal conductivity with conservation laws.

2.1. Boundary conditions

One of the main application of the adaptive FEM methods, as well as ALE method, is large boundary motion problems which are directly related with a momentum equation. It is usually assumed that values of velocities and heat flux or temperature are given. The velocities vary with time and extra equation is needed to determine (the unknown position of the free surface).

In the ALE formulation are employed the same boundary conditions used in Eulerian and Lagrangian descriptions because boundary conditions depend on concrete problem configuration and not the applied method. Along the domain boundaries must be defined kinematic and dynamic conditions. Usually this is presented as:

$$v_i = g_i \text{ in } \partial R_x^g \quad (10)$$

$$\sigma_{ij} n_{xj} = h_i \text{ in } \partial R_x^h \quad (11)$$

where g and h are given boundary velocity and pressure, respectively, n_x is the outward unit normal to ∂R_x and ∂R_x the piecewise smooth boundaries of spatial domain R_x ([4], [5]).

Cauchy stress tensor is defined as a function of temperature, density and velocity fields:

$$\sigma = s(\theta, \rho, v) \quad (12)$$

While its material time derivative by means of stress field and knowledge :

$$\frac{\partial \sigma}{\partial t} \Big|_x = r(\theta, \rho, v, \sigma) \quad (13)$$

Any of the commonly used constitutive equations can be written in the previous manner. Therefore, the application of such models is moving in a wide range of problems of deformation of solids, from small deformation linear elasticity in the area, to large deformations in viscoplasticity. For example, any plastic material can be defined as to behave as follows:

$$\frac{\partial \sigma_{ij}}{\partial t} \Big|_x = \Delta \sigma_{ij}^c + W_{ik} \sigma_{kj} + \sigma_{ik} W_{kj} \quad (14)$$

where is: $\Delta \sigma_{ij}^c$ the objective or real increase of stress and represent part of the actual stress σ due to the deformation of material - "pure strain", eg.:

$$\Delta \sigma_{ij}^c = C_{ijkl} v_{(k,l)} \quad (15)$$

where C is reaction of material which depend from stress σ , $v_{(k,l)}$ is velocity components of extension tensor

$$v_{(i,j)} = \frac{1}{2} \left(\frac{\partial v_i}{\partial x_j} + \frac{\partial v_j}{\partial x_i} \right).$$

Generalization of viscoplastic materials commonly used by defining a yield surface and assuming that the strain rate can be linearly divided into elastic and plastic components. It is important to note that hardening rule explicitly defines the evolution of yielding surface is usually written in incremental form.

The remeshing techniques are concerning with the definition of mesh velocity \hat{v} , for example, if $\hat{v} = 0$ using Eulerian method and but if $\hat{v} = v$ using Lagrangian method. Evidently that trying to find the best choice for applied description of material and mesh velocity, and a low cost algorithm for updating the mesh constitute represent main task of ALE method.

There are two cases of boundary conditions. The first assumes that all domain boundaries have a known position at every instant which include Euler's internal and external boundaries of the flow, with prescribed movement of material surfaces and solid-wall boundaries. The second refers to the unknown free surface at the boundary of the domain (or generally the material surface) and will be reduced to the previous position when the free surface is known. These equations is used for surface identified as Lagrange, $c = w = 0$ is useful for solving problems of structural mechanics problems.

3. COLD FORGING SIMULATION OF VALVE HOUSING

Analysis of metal plastic deformation by finite element method and its results largely depend on the choice of software package in which it is performed, and the choice of mathematical models that describe the specific problem. The results of such a complex analysis depend on the scope and accuracy of entering a large number of parameters of real processes.

One of the more complex examples of successive volume of cold forging technology, in four phases, is shown in the figure below. Steel cylindrical phosphate workpiece, AISI 1010, weighing 29 g, you get the valve body (Fig. 1).



Fig 1. Forging workpiece and final part after four operations

The first phase include the initial forming of workpiece where it does not get any final geometry of the finished work but it gets the final contours of technology for the next stage of forging. Especially in the third stage of forging will come to the fore the accuracy of the spherical surface to enable better contact with the tool to the material flowed in the right direction [5,6] (Fig. 2).

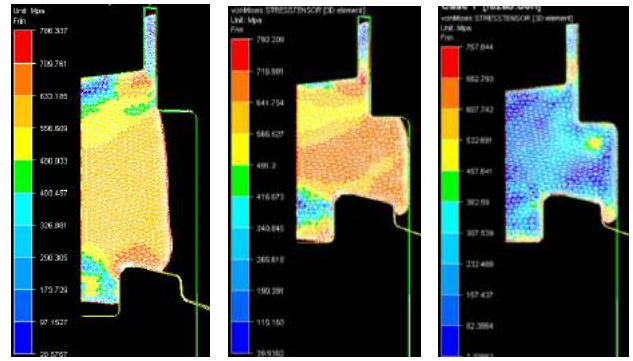


Fig. 2. Flow of material at third operation

The case of unknown free surface is reduced to one where all the domain boundaries are fixed or given prescribed motion. The continuous generation of new mesh - remeshing is fully defined when the mesh velocity \hat{v} is given within the domain.

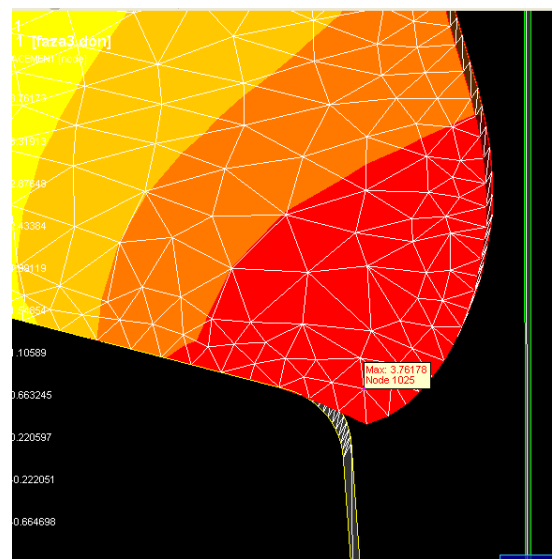
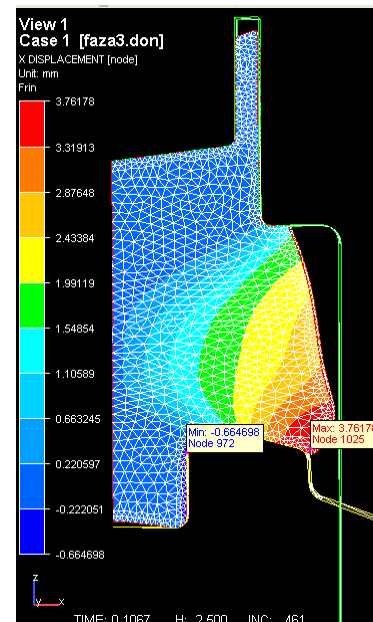


Fig. 3. Meridian cross section of workpiece and a die during deformation process with locally refined mesh presented

This can be done by simple ad hoc formula, solving equations of potential that maintain element regularity or any other mesh generation algorithm to conserve the element connectivity. Most of these remeshings method are based on defining the new position of nodes (Fig.3), and then calculate mesh velocity by finite difference approximation [7,8,9,10].

4. CONCLUSION

The overall impression of the ALE method, which was presented here show the applicability and effectiveness of this method to solve the problem of continuum mechanics. This method increases the main advantages of the finite element method for modeling complex geometries and boundary conditions of surfaces. It allows a smooth and easy processing and closing of borders and boundaries with a moving free surfaces, and excellent flexibility in the movement generated mesh model. The result is a very flexible modeling method that allows adjustment of high distortions of the continuum and moving boundary surface, computational efficiency (in terms of computational cost of data processing simulation), and numerical modeling of precision especially in the functions of copying material surfaces, and interpolation along the enrichment of specific areas.

ACKNOWLEDGEMENT

This paper is supported by Project Grant III44004 (2011-2014) financed by Ministry of Education and Science, Republic of Serbia.

REFERENCES

- [1] ATZEMA E. H, HEUTNIK J, *Finite element analysis of forward – backward extrusion using ALE techniques*", University of Twente, Department of Mechanical Engineering, The Netherlands.
- [2] BAAIJENS F. P. T, *An U-ALE formulation of 3D unsteady viscoelastic flow*, International Journal for Numerical Methods in Engineering, vol. 36, pp. 1115-1143, 1993.
- [3] HUERTA A, DIEZ P, "*Error estimation including pollution assessment for nonlinear finite element analysis*", Computer Methods in Applied Mechanics and Engineering, vol. 181, 2000. pp. 21-41
- [4] LIU W. K, CHEN J. S, BELYTSCHKO T, ZHANG Y. F, *Adaptive ALE finite elements with particular reference to external work rate on frictional interface*, Computer Methods in Applied Mechanics and Engineering 93, North-Holland, 1991. pp. 189-216
- [5] RANDJELOVIC S, STOILJKOVIC V, BOGDANOV Lj, "*Metal flow Modeling at the Forward Extrusion in the Shape Changing Area*", The 13th International DAAAM symposium "Intelligent Manufacturing &Automation: Learning from Nature", 23-26th, October 2002, Vienna, Austria.
- [6] FLITTA I, SHEPPARD T, *Material flow during the extrusion of simple and complex cross-sections using FEM*, J. Mater. Science and Technol, 2005 Vol. 21 No. 6, pp. 648-656.
- [7] HALVORSEN F, AUKRUST T, *Studies of the mechanisms for buckling and waving in aluminium extrusion by use of a Lagrangian FEM software*, Int Journal of Plasticity 2006, 22, pp. 158–173.
- [8] GANG F, JIE Z, DUSZCZYK J, *Effect of pocket design on metal flow through single-bearing extrusion dies to produce a thin-walled aluminium profile*, J Mater Process Technol 2008; 99, pp. 91 – 101.
- [9] KRUMPHALS F., SHERSTNEV P., MITSCHKE S., RANDJELOVIC S, SOMMITSCH C., *Physically Based Microstructure Modelling of AA6082 during Hot Extrusion*, Key Engineering Materials (Vol. 424) pp. 27-34, 2009.
- [10] RANDJELOVIC S, MILOSAVLJEVIC P, SOMMITSCH C, *Hot extrusion technology generation on the basis of FEM and FMEA analysis*, Strojarstvo, vol. 52, pp. 43-50, No1, 2010, ISSN 0562-1887



METAL FORMING TECHNOLOGIES IN DENTAL COMPONENTS PRODUCTION

¹Mladomir MILUTINOVIĆ, ¹Dragiša VILOTIĆ, ²Tatjana PUŠKAR, ²Dubravka MARKOVIĆ,
¹Aljoša INAVIŠEVIĆ, ²Michal POTRAN

¹Department for production engineering, Faculty of technical sciences, University of Novi Sad, Novi Sad, Serbia

²Department of dentistry, Medical faculty, University of Novi Sad, Novi Sad, Serbia

mladomir@uns.ac.rs, vilotic@uns.ac.rs, tatjanapuskar@yahoo.com, dubravkamarkovic@yahoo.com,
aljosaivanisevic@gmail.com, michalpotran@gmail.com

Abstract: In the recent years, a lot of efforts have been made with goal of improving manufacturing technologies for the production of dental components used to replace missing biological structures, support of a damaged biological structure, or to enhance an existing biological structure. Due to complex geometry and demands for high mechanical properties, accuracy and reliability in use dental devices (implants, frames, bridges, orthodontic appliances, denture base plates etc..) are predominately produced by application of advanced manufacturing technologies in combination with computer-aided techniques (CAD, CEA, CAM...).

In this paper the possibility of application of metal forming and shaping technologies in fabrication of the dental components will be presented.

Key words: Metal forming technology, dental components,

1. INTRODUCTION

In the past dental devices (implants, frames, bridges, orthodontic appliances, denture base plates etc.) were conventionally produced primarily from metal materials by using casting techniques. But over the last two decades dentistry and dental techniques have been undergoing a radical and rapid shift in terms of employing advanced manufacturing technologies such as: CNC machining, metal forming, precision casting, sintering, surface engineering, rapid prototyping, and rapid manufacturing [1]. At the same time diagnostic tools have become increasingly more sophisticated and medical imaging technology can now present patient data with high precision [2].

Advanced manufacturing technologies usually combine novel manufacturing techniques and machines with the application of computer-aided techniques (CAD, CEA, CAM, RE...). It has enabled not only the improvements of the existing manufacturing process, but also process automation, design of greater variety of complex products with increased accuracy and reliability in use, as well introduction of innovative, state-of-the-art dental services, visualization, analyze and optimization of the dental devices and dental procedures, development of the new materials and dental procedures, time and money saving of dental treatments etc.

The selection of the suitable technique for the manufacturing of a certain product is a very complex problem. It implies multicriteria decision, depending on several factors. The most important are: component design and complexity, material processing ability, desired accuracy and quality, mechanical and physic properties, production quantity, and cost. In case of dental devices this issue is even more emphasized due to a

number of specific demands regarding materials characteristics and the fact that in most cases production is related to creation of tailor-made components. Material used in dentistry must be biocompatible and meet the general requirements of biomedical engineering, such as: nontoxicity, good corrosion and oxidation resistance, high specific strength, hardness and toughness, the appropriate modulus of elasticity etc. As a rule, most of biocompatible materials (Stainless steel, Titanium and its alloys, etc) exhibit poor or modest processability, when traditional technologies are employed.

Modern metal forming technologies are promising way for processing of these materials and manufacturing of numerous medical and dental devices. This paper reviews metal forming and shaping methods applied in dentistry.

2. APPLICATION of METAL FORMING TECHNOLOGIES IN DENTISTRY

The use of forming technologies in medicine and dentistry is increasing permanently. According to [3] forming is one of the leading technologies applying to production of the metallic implants. Key features of forming technology are:

- enhanced mechanical properties of formed part (strength, hardness, fatigue resistance, toughness)
- high accuracy and surface quality
- close tolerances and high repeatability of part geometry
- cost saving due to a considerable reduction of process times and material waste.
- complex shapes are produced in simple way

In addition, new developed and refined forming technologies make it possible to produce parts ready-to-assembly (net shape forming-NSF) or parts which require

finishing machining only on some surfaces, most of which are non-active (near net shape forming-NNSF). Majority of metal materials used for manufacturing of dental devices can be processed by forming technology. Due to low formability some of these metals must first be heated so they can be transformed into final shape (warm and for forming), while other metals are naturally more processable and can be shaped at room temperature (cold forming). Forging, rolling, drawing, and punching are traditional forming technologies, used the most often in dentistry. However, recently introduced forming and hybrid processes such as severe plastic deformation (SPD), superplastic forming (SPF), metal injection molding (MIM), thixoforming, incremental forming etc. are becoming highly attractive option when the manufacturing way of dental devices is considered. These technologies have further increased the efficiency of the forming techniques in terms of getting dental components with more complex geometry, possibility to shape hard to deform materials, material structural improvements etc.

2.1 Forging

Forging is the most common metal forming process used for production of implants applied to orthopaedic surgery and traumatology [3]. It is because forging yields components with greater strength than those produced by any other metalworking process. Joint replacement implants made from stainless steel were the first forged implants in the mid of last century [4]. During the 1970s and 1980s, stainless steel has been replaced by Titanium. As stainless steel forgings, early Titanium implants required heavy post-processing machining as well hand belting and polish finishing. Typical tolerances of those implants were in the range 0,25-0,5mm[4]. Advancements in equipment, process design, and technology enabled later the development of NNSF and NSF forging implants [5]. Apart from Titanium and its alloys forged implants today may be produced from differ materials such are: Cobalt, Chrome, Molybdenum, and Zirconium [5].

Techniques for forging of Titanium are essentially the same as for low-alloy steels [6]. Forging process of mostly used Ti6Al4V Titanium alloy takes place in the temperature range 800-1000°C. Forging temperature, strain velocity, and die preheating have the crucial influence on the properties of the forged components. Because of the rapid cooling and the fairly narrow hot working range, the chilling effect of dies should be reduced to a minimum by keeping contact time as short as possible. When forging Titanium and its alloys very intensive friction occurs between die and deformed material that together with low thermal conductivity result in structure and property inhomogeneity of forged part. Diffusion of Oxygen, Nitrogen and Hydrogen causes the changes at product surface both in chemical composition and microstructure. In order to minimize these phenomena heating of workpiece should be carried out with protective atmosphere and proper lubricants applied. As it said before forging of Titanium implants is mainly related to orthopedics field i.e. for producing of large sized implants. On the other hand, implants smaller in size as those used in dentistry (tooth implants, artificial

denture, connection plates, orthodontic apparatus etc.) were exclusively produced by cutting processes. General problem of forging micro components and parts with small volume is the low heat capacity of specimen compared to the cooling caused by surrounding air and dies and therefore the traditional hot forging procedure is not applicable. Also, when considering micro forming, some size effects need to be taken into account.

In the past it was not possible to micro forge Titanium. Recent works have confirmed that it is feasible to forge micro-components instead of using traditional cutting methods [7]. The solution is found in indirect heating and design of warm tooling setup that allows permanent heating of specimen (Fig. 1)

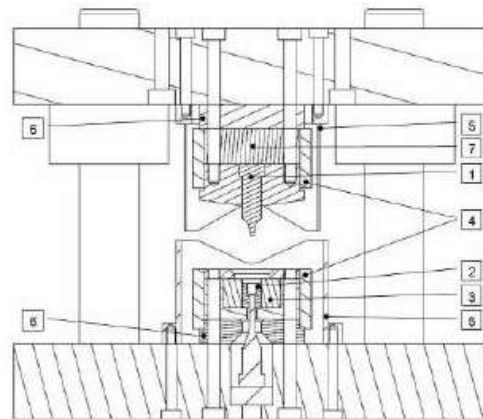


Fig.1 The tool-set for micro warm forming [8]
1) punch 2) die insert 3) stress ring, 4) heaters
5) thermal shield 6) isolation 7) load distributor

Fig.2a shows 3D model and dimensions of a Titanium dental implant (abutment). Until now this component featuring complex geometry, high production volumes and advanced material is primarily manufactured by turning, the HEX key and flank on the side and the holes through is done by milling and drilling respectively [7]. Newly developed warm-forging (350-400°C) procedure enables complete part geometry to be obtained in only two steps (Fig 2b) [9].

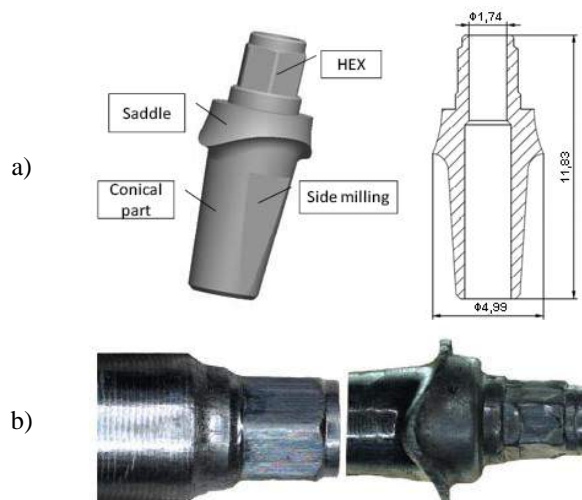


Fig.2 a) 3D Model of dental abutment and
b) photograph of the formed specimens after the first (left) and second (right) operation [9]

2.2 Sheet metal forming

Sheet metal technologies are also applied to produce a variety of medical implants as well dental components (cold-pressed denture base plates, dental prosthesis etc).

Sheet forming of Titanium, especially of Ti6Al4V alloy, is much more demanding and more difficult process to perform than processing steel sheets. Therefore cold-rolled titanium sheets which are used as starting material must first be annealed. Sheet forming of Titanium can be realized both as cold and warm process. Advised temperature for warm sheet-titanium forming is 350-400°C, but in some cases, such as deep drawing operation, higher temperature is applied in order to decrease the amount of operations and to obtain better dimensional accuracy of the drawn-parts through lower spring-back [3]. Usually, both titanium blanks and dies are warmed up. During the cold processes it is necessary to apply intermediate annealing. An annealing process is very often required after the processing in order to remove internal stresses of the final products.

Titanium and its alloys are characterized by poor drawability. Limit drawing coefficient, $m=d/D$, as one of the criteria for evaluating sheet ability to deep drawing operations, in case of cold process of Ti6Al4V titanium alloy is $m=0,83-0,76$ while during the warm processing is $m=0,71-0,63$. Similar to forging, strain velocity significantly affects the sheet forming process of Titanium, and therefore it is advised to form titanium sheets on the hydraulic presses with the velocity lower than 0,25m/s [3]. Corner radiuses and clearance between a punch and die are also very important. Since Titanium is very prone to galling process and formation of Titanium "build-ups" on the tool surfaces it is essential to ensure the effective separation of the contact surfaces.

2.3. Superplasticity forming

Superplastic forming (SPF) is a net-shape forming process used with superplastic materials, a unique class of materials that has the ability to undergo extraordinarily large tensile deformation. Ductilities of 1000–2000% are commonly observed in metallic superplastic materials although, commercially, elongations of 300% is sufficient to form even the most complex component [10]. High ductility is also encountered in superplastic alloys during torsion, compression, and indentation hardness testing. Phenomenon of superplasticity appears in many materials including ceramics and composites [10]. There are two essential requirements for the occurrence of superplasticity: 1) high temperature, usually greater than half of the melting point, 2) stable microstructure, with fine grain size, high-angle grain boundaries and grain boundary diffusion [11]. The major advantages of SPF process are: excellent accuracy and fine surface quality of final part, absence of springback phenomena and residual stresses, large and complex workpieces can be shaped in only one operation, less tooling costs, and cost and weight saving.

Computer aided simulation is an important part of the SPF process that enables design and analyze of the various aspects issues of the process. The most critical issues of SPF are related to material behavior during

forming (limited predictive capabilities of material deformation and failure) and low production rate.

The pioneer work and driving force for future developing of superplastic applications in dentistry and maxillofacial surgery was the manufacture of dental implants using high-strength, mill-annealed titanium alloy [12]. Since then, the range of applications has expanded and now includes: lower and upper complete and partial denture frameworks, implant-retained over dentures, cleft palate plates and hollowed-bulb obturators in dentistry with further studies on maxillofacial applications [11]. Unlike the application of SPF technology in the industry which usually means the production of standardized elements in large quantities, dental components (like dental prosthesis) are tailor product made to fit a patient's oral shape. Therefore, one of the basic conditions for economical application of this technology in dentistry is to find the way for cost-effective die production. A possible solution is the application of ceramic dies.

In Fig.3 the scheme of superplastic dental prosthesis forming process of Ti6Al4V alloy by Argon gas pressure developed by Curtis et al. [12] is given. The ceramic die insert (7) used to produce a dental prosthesis is made first based on a mould of the patient's oral shape taken by the dentist. In the next step the die assembly (steel furnace chamber and ceramic die insert) is mounted on hydraulic press and induction heated to 900°C.

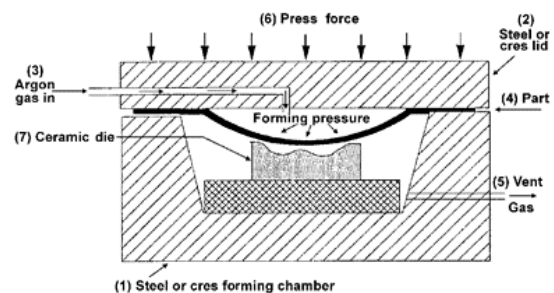


Fig.3 Scheme of die assembly for SPF [13]

Once a Titanium alloy plate (140 mm diameter and 3 mm thickness) has been inserted into the die set, it takes approximately 90 min to reach the sheet insertion temperature, somewhere between 800 and 900 °C. A low clamping pressure is applied at this stage to maintain Argon gas (3) flows above and below the forming sheet to protect against oxygen contamination. During forming process clamping force of about 60kN is applied, as the workpiece is shaped by Argon gas at pressures of up to 4,2MPa. It needs up to 3 hours to complete forming process. Fig.4 shows a dental prosthesis made by SPF.



Fig.4 Partial upper denture-Ti6Al4V shaped by SPF [11]

2.4 Severe plastic deformation

Severe plastic deformation (SPD) is a term describing a group of metal forming techniques in which an ultra-large plastic strain is introduced into a bulk metals and alloys without any significant changes in the overall dimensions of the specimen [14]. The components obtained by SPD exhibit high strength ductility and fatigue resistance. This process causes the formation of ultrafine grained microstructure (submicron or nano-size) in the initial material. In order to gain such microstructure, starting (grained) material must have predominantly high angle boundaries, the structure must be uniform over the billet volume and the large plastic strains may not have generated internal damage or cracks [15]. A few procedures have been developed within SDP technology: Equal channel angular pressing (ECAP), High pressure torsion (HPT), Accumulative roll bonding (ARB), Reciprocating extrusion-compression (REC), Cyclic close die forging (CCDF), cyclic extrusion compression (CEC), Repetitive corrugation and straightening (RCS), severe torsion straining (STS), super short multi-pass rolling (SSMR). The schemes of the principal SPD methods are presented in Fig 5.

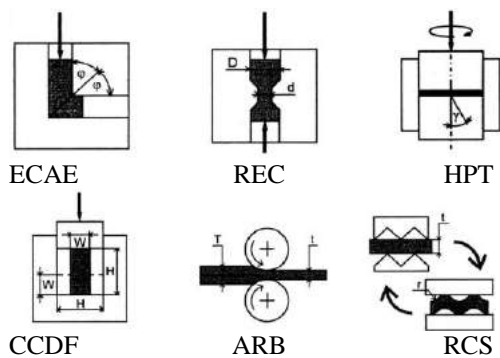


Fig.5 Illustration of some SPD processes [16]

The main areas of application of SPD technologies are aerospace, aircraft, and automotive industry as well medicine. Today, many medical and dental devices including hip, knee and dental implants, various screws, plates and meshes used in orthopedic applications are being produced by SDP [15]. Predominant materials used in these applications are cobalt-chrome alloys, stainless steel and titanium alloys.

3. CONCLUSION

This paper has discussed metal forming technologies and their applications in dentistry. It was shown that metal forming technologies have been substantially employed in dental area for producing components such as dental implants, denture base plates, dental prosthesis etc. Tremendous time and material savings, improved functionality, mechanical properties, high accuracy, and quality of dental devices, are some of reasons why in the future we could expect these technologies to be more frequent applied in dentistry.

Acknowledgement

Results of investigation presented in this paper are part of the research realized in the framework of the project

“Research and development of modeling methods and approaches in manufacturing of dental recoveries with the application of modern technologies and computer aided systems”–TR 035020, financed by the Ministry of Science and Technological Development of the Republic of Serbia

REFERENCES

- [1] GIBSON I., (2005), Advanced Manufacturing Technology for Medical Applications, Wiley ed.,
- [2] VANDENBROUCKE B, KRUTH J.P, (2007) "Selective laser melting of biocompatible metals for rapid manufacturing of medical parts", Rapid Prototyping Journal, Vol. 13, Issue 4, pp.196 – 203
- [3] ADAMUS J, (2007) Forming of the Titanium implants and medical tools by metal working. Archives of Materials Science and Engineering, Vol.28, Issue 5, pp. 313-316.
- [4] WALL A, HEFFRON P (2004), Forgings and orthopaedic implants, Bonezone, Vol. 3, pp.37-39
- [5] ZUZULA J, SULEK M, MILLER M, (2004), Net-Shape Forging - Orthopaedic Implants Move from “Rough” to “Precision” Bonezone, Vol 3, pp.45-47
- [6] <http://www.titaniumprocessingcenter.com/>
- [7] Eriksen R. S. et al. (2009) Micro forming of titanium, International Journal of Material Forming, Vol. 2 Suppl. 1, pp 601–604
- [8] ARENTOFT M, et al. (2008) Microforming of lightweight metals in warm conditions, International journal of material forming, Vol. 1, pp. 435-438.
- [9] ARENTOFT M, et al. (2011), Towards the first generation micro bulk forming system. CIRP Annals - Manufacturing Technology. Vol. 60, pp 335-338.
- [10] CURTIS R.V. et al. (2009) Dental biomaterials Imaging, testing and modeling, Wookhead Publishing ISBN 978-1-84569-424-1 (e-book)
- [11] BONET J et al, (2002), Numerical simulation of the superplastic forming of dental and medical prostheses, Biomechan. Model Mechanobiol. Vol. 1, pp.177 – 196
- [12] CURTIS R.V, et al, (2000), Dental implant superstructures by superplastic forming. Superplasticity in Advanced Materials, ICSAM-2000. Trans Tech Publications Inc., Zurich, Switzerland, pp. 47–52.
- [13] SANDERS D.G, (2004) Reinforced ceramic dies for superplastic forming operations, J.of Materials Eng. and Performance, Vol 13(6), pp. 753-757
- [14] AZUSHIMA A et al. (2008) Severe plastic deformation (SPD) processes for metals, CIRP Annals - Manufacturing Technology, Vol. 57, pp 716–735
- [15] VERLINDEN B, (2005), Severe plastic deformation of metal, Proc. 2nd Int. Conference on Deformation Processing and Structure of Materials, pp 3-18
- [16] ZRNIK J. et al. (2008), Processing of metals by severe plastic deformation (SDP) – structure and structure and mechanical properties respond. METALURGIJA 47, pp. 211-216.

34th INTERNATIONAL CONFERENCE ON PRODUCTION ENGINEERING



SECTION H

**RAPID PROTOTYPING
REVERSE ENGINEERING**



SOME ASPECTS OF RAPID PROTOTYPING APPLICATIONS IN MEDICINE

Miroslav PLANČAK¹, Tatjana PUŠKAR², Ognjan LUŽANIN¹, Dubravka MARKOVIĆ²,
Plavka SKAKUN¹, Dejan MOVRIN¹

¹ Faculty of Technical Sciences, University of Novi Sad, Trg Dositeja Obradovica 6, Novi Sad, Serbia

² Medical faculty Novi Sad, Department of dentistry, Hajduk Veljkova 12, Novi Sad, Serbia
plancak@uns.ac.rs., tatjanapuskar@yahoo.com, luzanin@uns.ac.rs, dubravkamarkovic@yahoo.com,
plavkas@uns.ac.rs, movrin@uns.ac.rs

Abstract: Rapid prototyping (RP) is a term which encompasses a number of modern technologies for manufacturing of physical models directly from CAD files. Concept of RP offers essential advantages and benefits in development of a new product: quick transition from first idea to final product (short „time to market”), lower production costs, improved (optimized) product quality. Application range of RP covers different fields: production and civil engineering, architecture, medicine etc. Medical RP models are built mainly by stereolithography, fuse deposition modeling, selective laser sintering and inkjet systems. Main application in medicine is in orthopedics, soft tissue modeling, dentistry and maxillofacial surgery. As regard dentistry, RP models enable quick and reliable fabrication of medical devices, visualization, prosthesis fabrication, implant design and manufacture etc. Current paper gives insight into the RP techniques which are most commonly employed in dentistry. Furthermore, some new RP techniques and trends are discussed, while main specificities of RP in dental application are presented.

Key words: rapid prototyping, medicine, dentistry

1. INTRODUCTION

The basic idea underlying Rapid prototyping (RP) technologies is the possibility of rapidly building prototypes of a new product designed in a CAD environment. Prototype making is an important part of development and manufacturing of products. It helps testing product design (form, functionality, etc.) before significant investment in tooling is made. In the past, model or prototype making was expensive and time consuming process, which did not allow many modifications of design. The result of this were products which were seldom optimised [1], [2], [3].

When RP technologies were developed, primary fields of application were engineering and design. Applications of RP in medicine came later, with the development of modern imaging modalities (Computed Tomography - CT or Magnetic Resonance Imaging MRI) which provided input data for model generation in RP [4], [5], [6].

In this paper some RP technologies and their application in medicine and dentistry are presented.

2. RP IN MEDICINE

RP technologies in medicine and manufacturing differ. In manufacturing, models are usually designed in CAD environment and then converted to 3D model while in medicine and dentistry objects of interest usually exist in physical form [7], [8]. To create a medical model it is necessary to acquire data for model building. There are

several ways for data acquisition. Most common are CT – Computed Tomography and MRI - magnetic resonance imaging, although CT are widely applied for RP because image post-processing is less complex. Some other imaging modalities which can be used for data acquisition are MDCT – Multidetector Computed Tomography, CBCT – Cone Beam Computed Tomography, PET – Positron Emission Tomography, SPECT – Single Photon Emission Computed Tomography and US – Ultrasonography [5].

After data acquisition, the next step is image post-processing which provides data for RP techniques, where the STL file format is commonly used.

There are a number of RP techniques which can be used in medicine: Stereolithography (SL), Selective Laser Sintering (SLS), Fused Deposition Modeling (FDM), Laminated Object Manufacturing (LOM), Inkjet printing techniques etc.

Among numerous possible applications of RP in medicine are:

- possibility to improve diagnostic quality and help in pre-surgical planning. Simulating complicated surgical steps in advance using prototype model can help foresee complications during operation which may result in reduced procedure time.
- use for implant and tissue design, both for bone reconstruction and replacement of soft tissues, as rapid prototyping can be applied on a variety of materials.
- opportunities for scientific research
- use in medical training and education.

Numerous papers have dealt with application of RP in medicine. In [4], the authors used stereolithography models in diagnosis and the precise preoperative simulation of skeleton modifying interventions for several cases of maxillo-cranio-facial surgery.

A 3D model generated by fused deposition modelling and used for planning and verification of a surgical procedure was described in [8]. In this case, the patient required replacement of left hip joint.

Several applications of RP technologies in soft tissue facial prosthetics are presented in [15], [16]. Examples included orbital prosthesis, auricular prosthesis, nasal prosthesis, etc. Examples were analysed from various aspects related to RP application: quality, economic influence and clinical implications.

3. RP IN DENTISTRY

According to [7] there are several areas in dentistry in which RP can be implemented. Those areas are:

- Manufacture of dental devices – due to a number of advantages, the most prominent of which is complex geometry, RP models allow additional functionalities to dental devices.
- Visualization, diagnostics and education – RP models offer realistic visual and tactile information and are used by surgeons to gain knowledge of anatomical structure. This, in turn, facilitates communication in surgical teams and between doctors and patients. In addition, medical students can use RP models to efficiently learn and practice surgical procedures
- Surgical planning – RP models allow surgeons to efficiently plan intricate operations. Moreover, they can also be used as templates and guides in operation rooms. Not only real surgical tools can be applied on these models to significantly reduce operation time, but also surgeons are able to see actual location, size and shape of the problem area in hand. Finally, anatomical structure can be visualized by using transparent and/or multicoloured models.
- Customized implant design – In the past, implant parts used to be selected from standard size parts provided by manufactures. Thus, in cases of special requirements, that are outside standard range or between sizes due to disease or genetics, problems occurred. Standard implants had to be customized for that specific case, which prolonged operating time and increased risks of the surgical complication. Besides, there was also a chance that the implant did not fit well. RP allows design of individual dental implants, eliminating majority of the discussed problems.
- Orthotics – RP model can be used to design orthotic devices with the specific patient's tooth alignment.
- Prosthetics – So far, dental prosthesis (coping, crown, bridge, fixture etc.) fabrication has greatly depended on the skills of dentists and technicians. RP techniques are increasingly changing this situation for the better, eliminating the influence of individual skills on the final result.

- Forensics – RP is a valuable tool in various types of investigations. Being sufficiently accurate to present effects of the wounds, RP models can be used to preserve evidence.
- Biologically active implants – This is a new area of RP application. Dentistry can successfully exploit RP technologies to manufacture biologically active implants such as jawbones that might be damaged or malformed due to disease.

4. APPLICATION EXAMPLES

As mentioned before, there are many different areas in dentistry where RP techniques can be applied and numerous examples can be found in literature related to this subject.

In [7] a design of a drill guide is presented. In some cases holes have to be drilled in the patient's jawbone in order to position dental implants. A drill guide's function is to guide surgeon's drill to the planned implant location. CT scan data of the jaw are converted into 3D model which enables a dentist to go virtually through the jawbone to search for the best location for the proposed implants. Once the designing process is finished, the CAD model of the drill guide is transferred to an RP system to fabricate the real drill guide. In addition, the model of the jawbone is usually fabricated, so the fit of the drill guide and the treatment planning can be checked and verified. Fig. 1 depicts a bone-supported drill guide, while Fig.2 shows an RP jawbone model (stereolithography) with mounted drill guide.

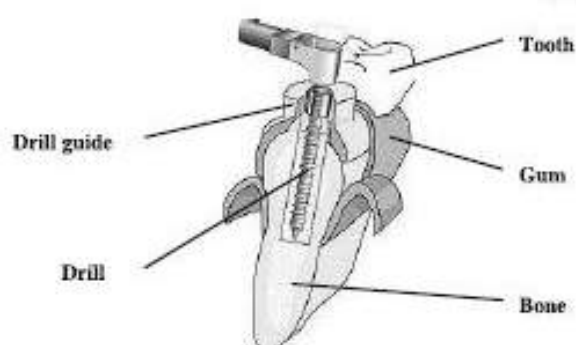


Fig. 1 Schematic of bone-supported drill guide[7]



Fig. 2 Model of jawbone with a mounted drill guide, manufactured by stereolithography[7]

Stereolithography has also been used for building 3D models for educational purposes. Teaching cube was constructed as a teaching device in an operative dentistry

course [9]. At the learning exercise it is required from students to demonstrate the ability to evaluate simulated cavity preparation for which purpose the cube was used. (Fig 3). CAD model of the cube allows changing shape, number, position and sizes of cavities and making new RP model for different types of learning exercise.



Fig. 3 The teaching cube [9]

Application of 3D printing in design and fabrication of dental prosthesis were presented in [7]. Traditional crown fabrication includes seven steps (tooth grinding, imperssion taking, treated tooth extraction, assembly of biting set, wax pattern making, centrifugal investment casting with finishing and porcelain sintering and resin polymerization) and all of these steps depend significantly on the skills of dental technician. A computer-aided crown fabrication process simplifies the traditional fabrication process and accelerates the production period by using 3D imaging, CAD and RP. In this process CAD packages are used to construct a crown model, while an RP system generates the crown model. This procedure includes four steps: crown inner and outer surface preparation, CAD crown model construction, crown model fabrication and investment casting and finishing. By the inner surface one understands the surface of the tooth after the preparation or the surface of the standard die if the tooth is missing, while the outer surface represents the original surface of the damaged tooth or teeth. There are two methods for deriving the geometry of the outer surface. The first method relies on standardized teeth which are digitized, while in the second method the surface based on the geometry of the neighboring and opposite teeth is designed. Construction of the crown model is performed by combining the inner and outer surface.

A novel method of pattern fabrication for the investment casting was proposed by the Liu at al, [11]. They investigated ice pattern fabrication by rapid freeze prototyping (RFP). In the investement casting, which has found application in manufacturing of dental devices, a wax pattern is usually used. The use of wax patterns is connected with some technical difficulties such as the wax pattern expanding, ceramic shell cracking etc. This new technology employs investement casting with ice patterns. For that purpose new process and equipment for RP were developed. In this process, selective depositing and freezing of the material (water) layer by layer is used to produce parts. Basically, two methods are used to deposit water: continuous deposition and drop-on-demand. deposition (Fig.4).

The build environment is kept at a low temperature which is below water freezing point. Pure water or colorized water is extruded or ejected from the nozzle and deposited

on the previously solidified ice surface. The most important advantages of the RFP process are: the process is cheaper and cleaner, it has potential to build accurate ice parts with excellent surface roughness, sufficient layer binding, easiness and no residue for part removal in molding process, no shrinkage, and, finally, easiness of material expansion compensation.

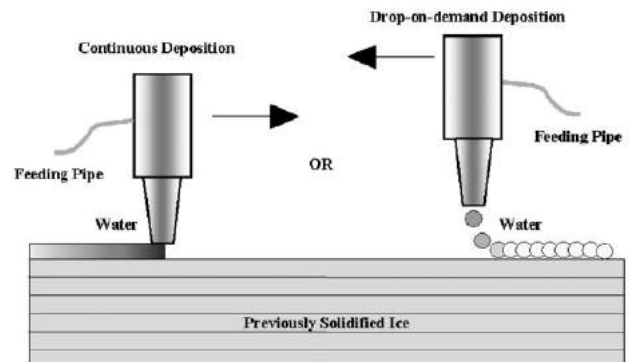


Fig. 4 Principle of rapid freeze prototyping [11]

Another new technique developed for metal parts, termed Selective Laser Melting, is reported in paper [14]. Designed primarily for making non machinable complex parts for direct use, this technology also found its application in medical industry. In this process, fully dense parts are manufactured, creating a fluid phase which is also known as the 'melt pool'. SLM is a laser welding process and for that reason all related phenomena, such as pores, cracks, distortion, warping, and residual stress, must be taken into consideration. To avoid or reduce these negative effects to a minimum, optimization of the basic machine parameters such as the laser diameter has to be performed. Dental crowns and bridges can be produced by this method.

5. RP SOFTWARE TECHNOLOGIES

As already noted, application of RP technologies demands the use of dedicated software and hardware through all the main stages: (i) design, (ii) process planning, and (iii) manufacture. Regardless of the particular type of RP technology, which could be either conventional or novel, the basic data processing flow remains virtually unchanged.

The first stage of the data processing flow consists of 3-D modelling using some of the commercially available CAD software. Alternatively, model geometry data can be obtained through reverse engineering, medicinal CT-scans, or mathematical modeling.

In order to be efficiently used as input information into various RP processes, model data must be pre-processed into some of the neutral data formats. Despite its intrinsic deficiencies, stereolithography (STL) format is a *de facto* standard which is widely accepted by the industry. However, as a result of intensive research in the domain of product and model data exchange, numerous alternative data formats have been developed, such as STH (Surface Triangles Hinted Format), CFL (Cubital Facet List), RPI (Ransellaer Polytechnic Institute format), G-WoRP (Geometric Workbench for RP), STEP

(STandard for the Exchange of Product data - AP203), etc.

The process planning stage consists of a number of specialized tasks which are also performed using dedicated software solutions: verification of 3-D model and correction of errors, compensation of STL file, definition of the direction in which the material shall be applied, packaging of models into machine's workspace, detection of unsolidified residuals, generation of props and supports, slicing, generation of scanning path, and generation of control information data file which is subsequently fed into RP machine's control unit.

On today's market there exist numerous dedicated software tools capable of efficiently performing the required tasks, such as *Bridgeworks (Solid Concepts, Inc, USA)*, *MagicsSG (Materialise, Belgium)*, *Vista (3D Systems)*, etc.

6. CONCLUSION

This paper focused on a review of prototyping applications in medicine with emphasis on dentistry, i.e., dental replacements. An increasing demand for flexible, cost-effective, and efficient technologies for manufacture of various types of anatomical replacements in medicine in general, and dentistry, has stimulated development of a vast array of rapid prototyping technologies with the ultimate goal of re-creating them *de novo*. Presented in this paper was a succinct review of the state of the art in this field, accompanied by some relevant application examples. In the near future, one should expect that the existing array of RP technologies which still accentuate the use of predominantly engineering materials such as polymers, powdered metals, etc., will be augmented by a nascent technology termed bioprinting. This shall allow layered manufacturing of various replacements based on biological materials, thus adding new quality to the ever expanding domain of rapid prototyping technologies used in medicine.

REFERENCES

- [1] PHAM, D.T., GAULT, R.S. (1998) *A comparison of rapid prototyping technologies*, International Journal of Machine Tools & Manufacture, Vol. 38, pp 1257-1287
- [2] KRUTH, J.P., LEU, M.C., NAKAQAWA T. (1998) *Progress in Additive Manufacturing and Rapid Prototyping*, Annals of the CIRP, Vol. 47/2, pp 525-540
- [3] ROSOCHOWSKI, A., MATUSZAK A. (200) *Rapid tooling: the state of the art*, Journal of Materials Processing Technology 106, pp 191-198
- [4] PETZOLD, R., ZEILHOFER, H.-F., KALENDER, W.A. (1999) *Rapid prototyping in medicine – basics and application*, Computerized Medical Imaging and Graphics, Vol. 23, pp 277-284
- [5] RENGIER, F., MEHNDIRATTA, A., VON TENGG-KOBLIGK, H., ZECHMANN, C.M., UNTERHINNINGHOFEN, R., KAUCZOR, H.-U.,

GIESEL, F.L. (2010) *3D printing based on imaging data: review of medical applications*, Int J CARS

- [6] MAGNE, P. (2007) *Efficient 3D finite element analysis of dental restorative procedures using micro-CT data*, Dental materials 23, pp 539-548
- [7] LIU, Q., LEU, M.C., SCHMITT, S.M. (2006) *Rapid prototyping in dentistry: technology and application*, Int J Adv Manuf Technology, Vol 29, pp 317-335
- [8] SCHENKER, R. at al. (1999) *Novel combination of reverse engineering and rapid prototyping in medicine*, South African Journal of Science 95, pp 327-328
- [9] CHAN, D at al. (2004) *Application of Rapid Prototyping to Operative Dentistry Curriculum*, Journal of Dental Education, Vol.68, No 1 , pp 64-70
- [10] PAPANAYIDAKOS, P., LAL, K. (2008) *Complete implant rehabilitation using subtractive rapid prototyping and porcelain fused to zircon prosthesis: a clinical report*, The Journal of Prosthetic Dentistry, Vol. 100, issue 3
- [11] LIU, Q., SUI, G., LEU, M.C. (2002) *Experimental study on the ice pattern fabrication for the investment casting by rapid freeze prototyping (RFP)*, Computers in industry, Vol.48, No 3, pp 181-197
- [12] ZHANG, W., LEU, M., JI, Z., YAN, Y. (1999) *Rapid freezing prototyping with water*, Materials and Design 20, pp 139-145
- [13] LEU, M.C., ZHANG, W., SUI, G. (2000) *An experimental and analytical study of ice part fabrication with rapid freeze prototyping*, Annals of the CIRP, Vol. 49/1, pp 147-150
- [14] GEBHARDT, A. at al. (2010) *Additive Manufacturing by Selective Laser Melting The Realizer Desktop Machine and its Application for the Dental Industry*, Physics Procedia
- [15] BIBB, R., EGGBEER, D., EVANS, P. (2010) *Rapid prototyping technologies in soft tissue facial prosthetics: current state of the art*, Rapid Prototyping Journal 16/2, pp 130-137
- [16] BIBB, R., WINDER, J. (2010) *A review of the issues surrounding three-dimensional computed tomography for medical modelling using rapid prototyping techniques*, Radiography 16, pp 78-83

Acknowledgement

Results of investigation presented in this paper are part of the research realized in the framework of the project "Research and development of modeling methods and approaches in manufacturing of dental recoveries with the application of modern technologies and computer aided systems" – TR 035020, financed by the Ministry of Science and Technological Development of the Republic of Serbia.



ART AND DESIGN OPTIMIZED 3D PRINTING

Nenad GRUJOVIĆ¹, Jelena BOROTA¹, Milan ŠLJIVIĆ², Dejan DIVAC³, Vesna RANKOVIĆ¹

¹Faculty of Mechanical Engineering, University of Kragujevac, Sestre Janjic 6, 34000 Kragujevac, Serbia

²Faculty of Mechanical Engineering, University of Banjaluka, Vojvode Stepe Stepanovica 75, 78000 Banja Luka, B&H

³Jaroslav Černi Institute for the Development of Water Resources, Jaroslava Černog 80, 11226 Pinosava, Serbia
gruja@kg.ac.rs, jborota@gmail.com, milansli@yahoo.com, ddivac@Eunet.com, vesnar@kg.ac.rs

Abstract: The 3D printing belongs to rapid prototyping (RP) technology and is an extremely versatile and rapid process accommodating geometry of varying complexity in various applications, and supporting many types of materials. Besides commercial manufacturing and production process, RP technology can be successfully applied in art and industrial design. The major objective of the study presented in this paper is to provide a high-quality procedure for the optimal and most appropriate application of RP to realization of artistic items. Special attention is devoted to the relation between conceptual design in art and 3D printing, with representation of experiences gained in practice.

Key words: rapid prototyping, art, design

1. INTRODUCTION

Digital art is a new form of expression in contemporary art of the 20th century. With this term is described the various artistic works created using digital technology. Depending on the application of technical resources, software or hardware, there are different kinds of digital art, which continue to evolve with the development of computer technology. In the early seventies the concept of digital art is trying to gain its true definition. New media art is term that actually defines digital art. Digital technology has changed and transformed traditional activities (painting, drawing, sculpture) in entirely new forms, such as pixel art, digital installation, computer games, and created a new artistic practices. [1]

With the appearance of software for three-dimensional graphical representation, modern artists are able to express their creativity by using it as a form of expression. By this software, artists design 3D models, which are a mathematical representation of 3D object, but without the possibility of materializing their work. Three-dimensional printing facilitates the transfer from the virtual to the material world. In this way, digital art gets one additional site.

Nowadays, there are many art students who are using 3D printing technology, especially in the design of ornaments, jewellery, furniture, sculpture, etc. Among other, 3D printing technology is used to visualize future piece of art, make copies of them, and can be used in creating the conceptual design of piece of art.

3D printing technology is commonly used for rapid and far cheaper, by conventional means, production of prototypes and testing samples and is classified as production technologies, which belong to a large family

of additive technology, ie. production technology by adding.



Fig.1. The application of 3D printing in digital art – Torolf Sauermann [2]

2. 3D PRINTING TECHNOLOGY

Three-dimensional printing technology is a new additive technology, which, based on 3D digital models, generates a workpiece by adding material in thin layers. There are two types of 3D printing technology: direct printing and printing binder.

In the process of direct printing, base material is applied to the work surface using a print head, after which material is curing by UV radiation. On the other hand, in the process of binder printing, print head is used for applying binder (adhesive) onto the surface of the powder material (substrate), which is the basic material.

Figure 2 shows the printing procedure for printing a single layer [3]. ZCorp 3D printer parts are shown

schematically: 1 powder bed, 2 feed piston, 3 roller mechanism, 4 bridge with inkjet print head, 5 build piston, 6 build platform and 7 gate for excess material.

The first operation shows a bridge that carries feed piston and print head and moves from left to right. Direction of movement feed piston is shown in the picture, and by its moving feed piston applies a certain amount of powder. In second step, powder extends in a thin layer over the previously-made layer in the build platform. At the end of the walk to the right side, feed piston removes the excess powder to the gate for excess material. In the next step, bridge is moving from the right to the left side, while the inkjet print head printing the cross-section of actual layer. Upon the bridge arrival at the left end position, the powder bed for the addition of materials is raised by one step, while the build platform goes down for the thickness of the layer, and for each new layer of the cycle is repeated.

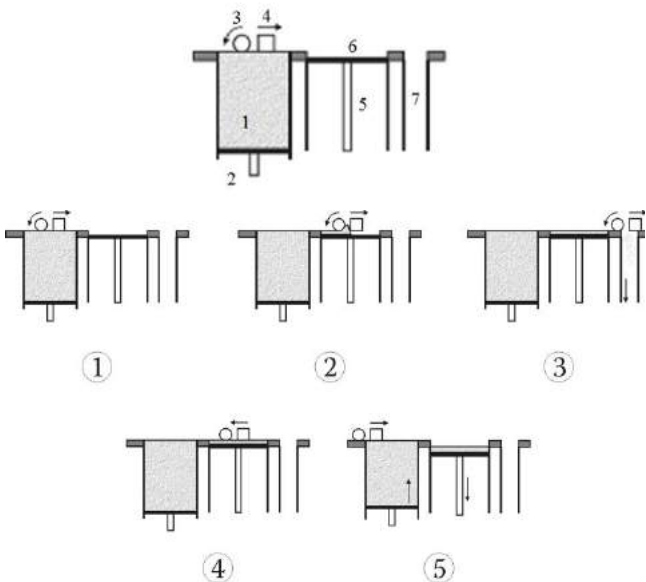


Fig.2. The 3D printing procedure on the printer ZCorp

Powder, which is not connected with binder, serves as a support. When the procedure is completed, finished part is surrounded with the support powder. Build piston is raised, and supporting powder removes very carefully with sophisticated vacuum cleaner. The rest of the powder, that is sucked, can be reused for creating new model. After short drying, model may ready for using.

But post processing is necessary, if model wants to be used in the purpose of design and functionality. Start of using 3D printing process in commercial purposes is connected with establishment of ZCorporation Company in 1994 in Massachusetts, USA. In the 1997th, based on patented technology [4], which is developed at the Institute of Technology, Massachusetts (MIT), this company has developed and commercialised its first 3D printer – Z402 system [5]. This technology is one of the procedures with the pulverized material, and it use the principle of binding printing technology.

Choice of binder is limited, but the principle is versatile, and new applications are constantly appearing. On the other hand, same as 2D inkjet printers, it can be made objects in colour, which is a unique opportunity in the world of RP techniques [6].



Fig.3. ZCorporation ZPrinter 310 System in the Center for Information Technology Mechanical Engineering in Kragujevac

ZCorporation is constantly improving material for 3D printing process. New material on the market place does not require infiltration of cyanoacrylate or epoxy adhesive, because the mechanical properties are satisfactory. Also, it is working on researching for moulding materials and materials for making iron casting cores. The fastest RP system today is Spectrum 510 3D printer. It has increased resolution in the horizontal plane, and thus provides a better surface quality and development of more precise details of the printing parts.



Fig.4. Prototypes made at the Center for Information Technology (CIT) Faculty of Mechanical Engineering in Kragujevac

Applications of 3D printed parts made are numerous, and constantly growing [7]. Various post-processing features can easily be the model of the desired shape and characteristics. Some applications are: improvement of the geometry and functionality of parts, conceptual design, functional testing, FEM visualization (Finite Element Method) and visualization of thermal changes, development patterns for casting and more.

Center for Information Technology at Faculty of Mechanical Engineering in Kragujevac, since 2006, was among the first in the region who is began to research in this area.

Figure 4 shows some of the prototypes for engineers and construction designers in the field of construction (segment of the tunnel for Corridor 10), in the field of bioengineering (prototype of inhaler for company "Prizma" - Kragujevac), in the field of automobile engineering (mechanical assembly of door handles) and mechanical engineering (model of anchor machine) that are made at the Center for Information Technology, Faculty of Mechanical Engineering in Kragujevac.

3. PROCEDURE FOR MAKING MODEL IN 3D PRINTER

In the Center for Information Technology at Faculty of Mechanical Engineering in Kragujevac is in use ZPrinter 310 System ZCorporation. ZPrinter 310 System use ZPrint Software applications for printing prototypes, Figure 5.

ZPrint Software supports several file formats for 3D printing, such as PLY, 3DS, VRML, but the most famous is the STL format. During import of STL file, it may cause problems, because errors that occurred during modelling. These errors in the STL file can be removed Zprint Software, but only a simple one. Serious problems must be solved by special applications, such as CATIA, SolidWorks, AutoCAD and more. The parameters, that are important for the printing process, are: layer thickness, saturation (parameters related to the amount of binder), pour compensation binder and anisotropy scaling.

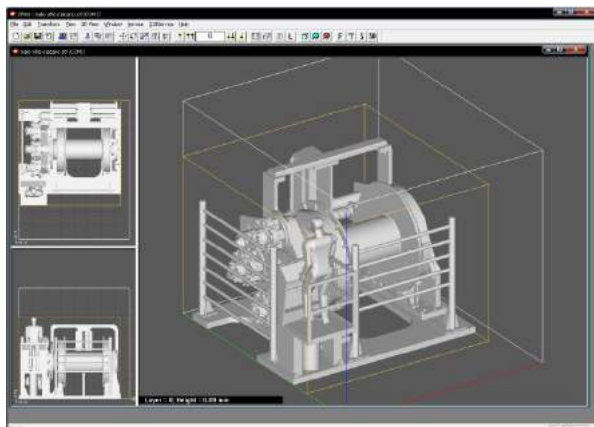


Fig.5. Model in ZPrint software

During the determination of part orientation in the software, sensitive details should be arranged in a vertical direction. The supports can set up for particularly sensitive areas by using the "Fixture".

Basic post-processing process consists in removing excess powder from the printing part and carefully taking out of the working chamber. After that, excess powder shall be removed from the printing part in air pressure chamber. The next process is drying printing part (freely or in an oven at 90 ° C) and the strengthening with sophisticated infiltrators. Model is infiltrated with cyanoacrylate adhesives, or for persistent models, epoxy adhesives. After all post-processing process, parts can be treated by sandblasting, coloring or metallizing for better visual effect. By the combination of the basic material and urethane infiltrate can become the flexible parts. [8] [9]

4. EXAMPLE OF APPLICATION

In addition to a wide variety of applications in the field of industrial design, special attention is paid to the application of RP in a complex project of making a giant art sculptures. The basic idea for creating sculptures Ultrasaurusa (called "Luna Park") in his life-size belongs to the couple Ivan and Heather Morrison. Model, 16 high and 20 meters long, is designed to decorate the park in Portsmouth (UK). For this occasion, artistic couple is made a documentary art movie "An Unreachable Country - a long way to go," which shows the birth process of this sculpture, which is designed and fabricated by Serbian experts in Kragujevac, under the direction of Goran Krstic, mechanical engineer [10]. 3D model, that was printed in the CIT, Faculty of Mechanical Engineering in Kragujevac, has found its place in the early stages of conceptual design, then in the process of contracting, performance at a competitive public tender, and then in the final design and construction.

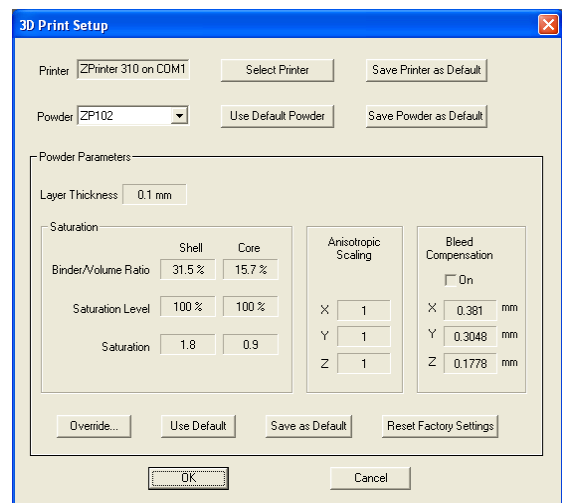


Fig.6. Parameters for printing with ZPrint software

For the corresponding CAD model Ultrasaurusa height of 16m and 20m in length, it was necessary, by using 3D printing, to produce smaller Ultrasauros model, measuring 16cm x 20cm, in order to more easily perform optimization in conceptual design. To enable 3D printing

of this model, it was necessary to generate the STL file based on this model with parameters control.

The resulting STL file is loaded into a ZPrint software application. During the 3D printing process, layer thickness was set on 0.09 mm, and printing process lasted 2 hours and 25 minutes, Figure 7. After printing, the part is removed from the powder, cleaned and put in oven to dry, which lasted 1 hour. Finally, the infiltrate was applied on final model to improve the mechanical properties and quality of the model surface.

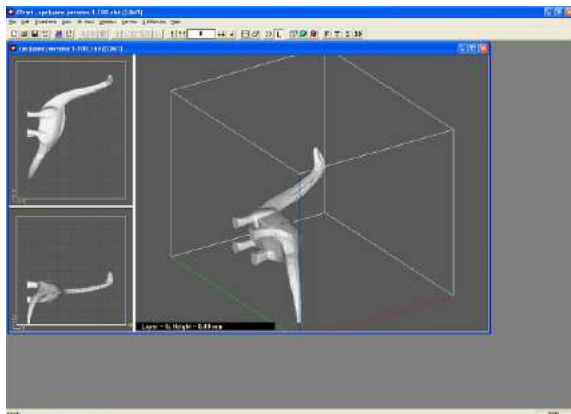


Fig.7. Model ready for printing with ZPrint software

The material used for printing the ZP102 in combination with binder ZB56, as recommendation by the company ZCorp.



Fig.8. Model after 3D printing

5. CONCLUSION

Thanks to the advantages of RP technology, designers can create complex parts, saving time and money. Depending on customer needs, optimisation of product design is easier and with minor limits.

Easy for of use, affordable and high-speed of manufacturing, 3D printing technology now enjoys great popularity both in industry circles and in the world of design, modern art, etc. Prediction says, that the price of these devices and production costs soon will increase their use.

There is only one limit in the application of 3D printer and this is user's imagination. It is possible, with proper preparation, printing also very large models, dividing them into parts and assembling them as children's blocks.

Models can be sanded, polished, metallized, coated, etc. In any case, this kind of printing present the future that must be wisely used.

Due to other circumstances in the same location in Kragujevac is a multidisciplinary environment between Faculty of Mechanical Engineering and Faculty of Art. It is a pity that there are not joint projects between them, but presented the result is one step in that direction.



Fig.9. Ultrasaurus at Luna park, Portsmouth, United Kingdom

REFERENCES

- [1] http://en.wikipedia.org/wiki/Digital_art
- [2] <http://www.mbhonaker.com/sauermann.html>
- [3] GRUJOVIĆ N. (2005), *Brza izrada prototipova – Rapid Prototyping* (In Serbian), Mašinski fakultet, Kragujevac, s. 53-60
- [4] LAUDER A., CIMA M.J., SACHS E., FAN T. (1991), *Three Dimensional Printing: Surface Finish and Microstructure of Rapid Prototyped Components*, Synthesis and Processing of Ceramics: Scientific Issues, Boston, MA, USA, s. 331-336.
- [5] VENUVINOD P.K., MA W. (2005), *Rapid Prototyping – Laser-based and Other Technologies*, Kluwer Academic Publishers, (ISBN 1-4020-7577-4), Norwell, MA, USA, s. 294-300.
- [6] GEBHART A. (2003), *Rapid Prototyping*, Hanser, (ISBN 3-446-21259-0), München, Germany, s. 178-183
- [7] PHAM D.T., GAULT R.S. (1998), *A comparison of rapid prototyping technologies*, International Journal of Machine Tools and Manufacture, Elsevier Science, (ISSN 0890-6955), Volume 38, Number 10, October 1998, s. 1257-1287
- [8] ZPRINTER 310 USER MANUAL (2003), ZCorporation, September 2003.
- [9] TRAJANOVIĆ M., GRUJOVIĆ N., MILOVANOVIĆ J., MILIVOJEVIĆ V. (2008) *Računarski podržane brze proizvodne tehnologije*, Mašinski fakultet, Kragujevac, 2008
- [10] <http://www.artscouncil.org.uk/news/luna-parks-16-metre-dinosaur-comes-southsea-common/>

ACKNOWLEDGMENT: The part of this research is supported by Ministry of Science in Serbia, Grants III41007.



3D PRINTING TECHNOLOGY IN EDUCATION ENVIRONMENT

Nenad GRUJOVIĆ¹, Milan RADOVIĆ¹, Vladimir KANJEVAC¹, Jelena BOROTA¹, George GRUJOVIĆ²,
Dejan DIVAC³

¹Faculty of Mechanical Engineering, University of Kragujevac, Sestre Janjic 6, 34000 Kragujevac, Serbia

²IBM UK Limited, 76/78 Upper Ground, South Bank, London SE1 9PZ, United Kingdom

³Faculty of Civil Engineering, University of Belgrade, Bulevar Kralja Aleksandra 73, 11000 Belgrade, Serbia
gruja@kg.ac.rs, radovic.milan@gmail.com, vkanjevac@gmail.com, jborota@gmail.com, GeorgeAG@ATT.biz,
ddivac@eunet.rs

Abstract: This paper presents a result of a decade of teaching and research with students of Faculty of Mechanical Engineering in Kragujevac, Serbia, in an environment established for the course of Rapid Prototyping (RP). The environment is based on the 3D printing and 3D scanning technologies, and their relationship with other technologies. Special attention is devoted to "RepRap", an open source project, and "RapMan", a 3D printer based on that technology. The printer has been assembled, tested and brought to production form in Center for Information Technology located at the Faculty of Mechanical Engineering in Kragujevac. Experience gained in educational environment in Serbian faculty corresponds to reports of the printer use as an educational tool in many schools all over the Europe, in the first place in United Kingdom.

Key words: rapid prototyping, education

1. INTRODUCTION

Rapid Prototyping (RP) process can be represented as a succession of additive technological processes which allow the construction of complex objects. The input of the RP process is a 3D digital geometrical model [1] that can be realized either with a CAD program or via Reverse Engineering (RE) [3]. The RE is performed in two steps. First a 3D scan of an existing object is taken and then the results of the scan are appropriately elaborated.

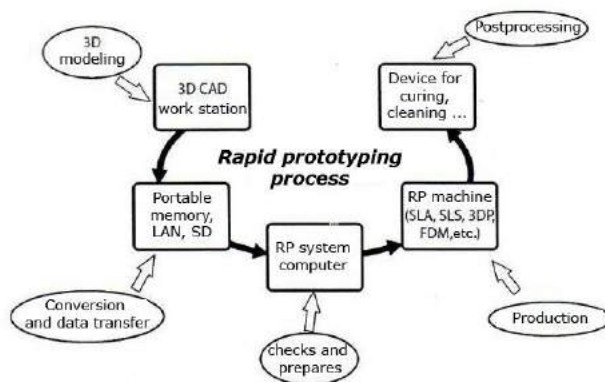


Fig.1. Basic steps of an RP process

The RP processes are now widely used in the industry because of their many advantages. An important characteristic of the RP processes is their relation to the RE which allows to replicate the existing parts of a product or a product in its integrity for which no technical documentation is available. The basic steps of every RP process are represented in the Figure 1: 3D modelling,

data conversion and storage, data control and preparation, realization of the prototype and post processing. These steps can be repeated until a satisfactory level of quality is achieved.

2. 3D PRINTING TECHNOLOGY

In 2005 the company "Bits From Bytes" built the first release of their 3D printer RapMan which was soon upgraded into the Release 2.1 [6]. The RapMan printer was based on a technology developed at the University of Bath as part of a project called RepRap. The first releases of the printer were made of a mechanical part only leaving to the end user to realize the control of the mechanical part based on the various solutions proposed by the RepRap project. In 2009 Bits From Bytes built the Release 3.0 of the printer RapMan which included also the electronic part that made it ready to print [7]. Shortly after the RapMan was adopted as part of the educational program in over 200 schools in the UK.

3D objects are made of layers of melted material laid on top of each other modelled to create the final object.

The materials that are most frequently used for 3D printing are ABS and PLA. ABS is derived from the petroleum (as the majority of the polymers) and PLA is derived from the starch and it can biodegrade under certain conditions (at 60 C in a slightly acid compost). Other materials that can be used are LDPE, HDPE, PP, uPVC, PVC, Nylon6, PMMA and many others.

The RapMan is a Computer Numerical Control (CNC) machine based on the extrusion of the plastic. The

temperature at which the extrusion is performed depends on the type of the material used for the 3D printing. The extruded material has a shape of a thin “thread”. The 3D object is printed with the thread which draws the object layer by layer.

The figure 2 represents the process of 3D printing. The extruder carries the material used for printing up to the heater by pressing mechanism where the material is heated to reach the operating temperature and extruded to form a layer of the 3D object on the platform. The extruder can move along XY surface. After the first layer has been drawn, the platform is lowered in Z direction by the amount of the thickness of the drawn layer and everything is ready for the next cycle. The extruder and the platform are powered by a stepper motor whose movements are controlled by a set of parameters which define the temperature and the position of the heater, the extrusion speed, the layer thickness etc.

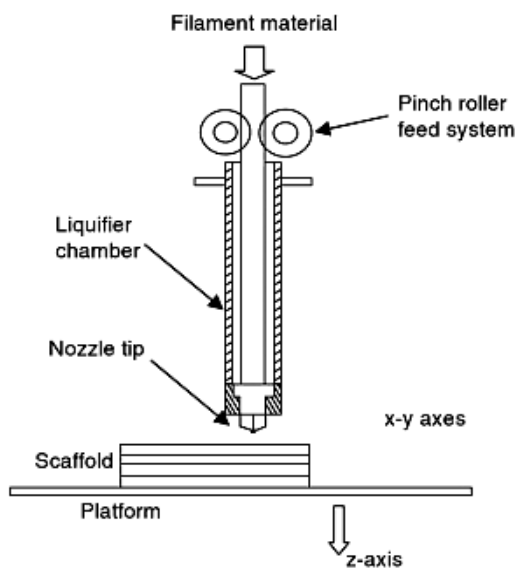


Fig.2. 3D printing process of one layer [8]

The figure 3 shows the 3D object while the last layer is being printed. The objects realized via this process can be easily replicated and used in different ways [9]. It is also possible to enhance the hardness of the printed object the cyanoacrylate glue application.

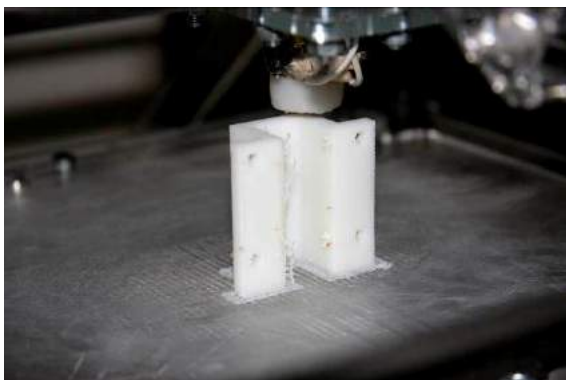


Fig.3. Scaffold - 3D printing process



Fig.4. Parts printed at CIT, Kragujevac

The figure 4 shows some of the 3D objects printed in the Centre for Information Technology at the University of Kragujevac. Both the technic of 3D printing as well as the materials used in the printing are continuously being improved. The BFB 3000 represents the state of the art in the 3D printing and it has three extruders which can use three different materials.

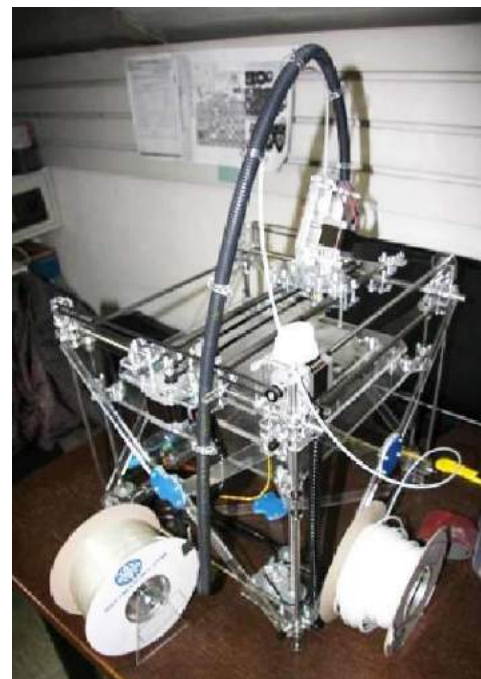


Fig.5. BitsFromBytes RapMan 3.1 at CIT, Kragujevac

3. PROTOTYPES CONSTRUCTION WITH 3D PRINTERS

The printing process of the RapMan printer needs to be prepared by CAM program. The CAM program analyses the 3D object and based on this analysis prepares the commands in G-Code language that will control the RapMan. There are two versions of CAM program for the RapMan. The first one is called Skeinforge [10] and is completely open-source. The Skeinforge is interoperable with all the operative systems used today and offers great possibilities for customisation in 3D printing. The drawback is its complexity and that it does not have any user interface defined. The second one is AXON [7] which is available free of charge by BitsFromBytes.

The AXON is based on the Skeinforge program and it has its own GUI. The drawback is that the AXON is interoperable only with Microsoft Windows Operative System.

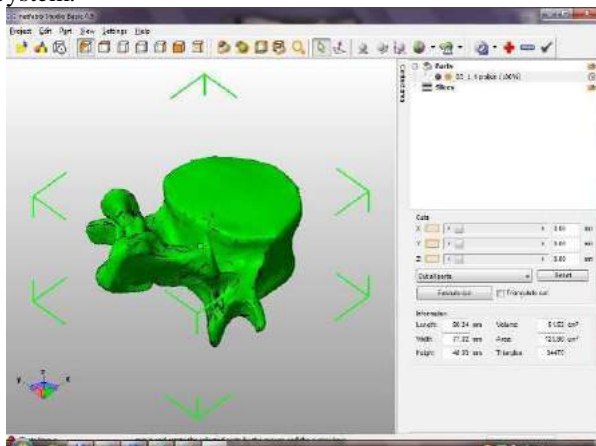


Fig.6. STL file at Netfabb Studio basic

The steps of prototypes construction are usually as follows: firstly a 3D model is built and stored in some format supported by the CAM packets (STL), all the imperfections are corrected and the format is translated by the CAM packet in the G-code. The model is eventually printed with the 3D printer.

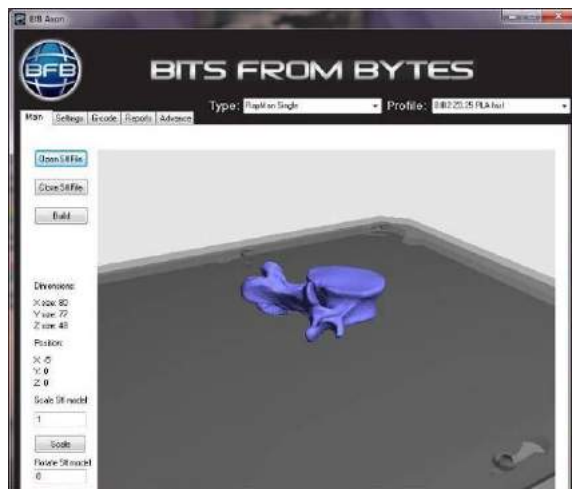


Fig.7. STL file at Axon Software

The AXON SW supports the STL format. The STL file may contain some errors caused by mistakes made during the phase of the 3D object modelling. These errors can be corrected with the application called Netfabb Studio shown in the picture 6 (the basic version of the application is free of charge whereas the professional version needs to be purchased). The basic version of Netfabb Studio can be used for correcting some simple errors in the STL files. For more complex problems errors the professional version is required [7]. After the STL file has been corrected, the file is imported in the AXTON SW (shown in the picture 7). The most important parameters that can be regulated by the AXTON SW are Layer Thickness, Temperature (at which the material is extruded) and Support Option (the support for printing of

the objects in the air). The support is shown in the picture 8 in green.

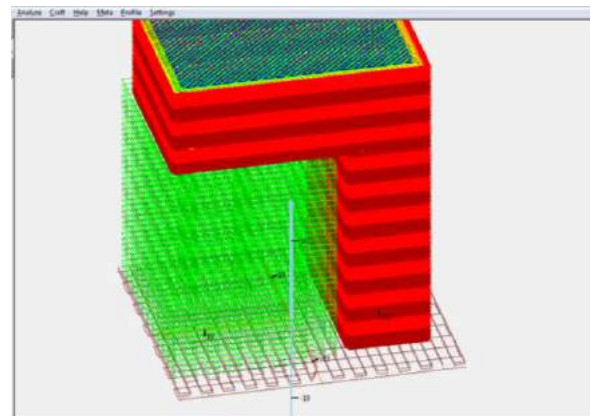


Fig.8. Model generated at CAM Skeinforge

When all the printing parameters are properly set, the STL file is translated in G-code which is stored on the SD card which is plugged in the 3 D printer. The 3D printer used in the Centre for the Information and Technology (CIT) at the University of Kragujevac is 3D printer RapMan 3.1. The 3D models are made in CAD starting from the reference models realised using the Reverse Engineering (RE) methods (i.e. by post processing of the Computer Tomography (CT) scans). The picture 9 shows the 3D print of the vertebra realised at the CIT as part of the course “Brza Izrada Prototipova” (Fast Prototypes Construction) [4]. The print is realised with the biodegradable material PLA. The time required for its construction was around 4.5 hours. After removing scaffold from platform, basic post-processing consists in careful removing its support. The dimensions of the printed objected were compared with the dimensions of the model generated with the SW and the comparison showed that the dimensions matched perfectly.



Fig.9. Model of vertebra made at Center for Information Technology at Faculty of Mechanical Engineering, University of Kragujevac

The 3D prints built in this way can be used as both conceptual as well as functional parts. The 3D printers used at the CIT as part of classes of “Fast Prototypes Construction” course are RapMan 3.1 as well as ZPrinter 310 shown in the picture 10. The ZPrinter 310 [11] is an

expensive professional 3D printer and requires greater costs for maintenance and material used in printing as well as longer printing time. Unlike the ZPrinter 310, the RapMan requires much lower costs but at the same time provides good basis of learning the techniques used for 3D printing which makes it a very interesting educational tool.

4. CONCLUSION

The modern RP systems have been developed based on the proven and improved technologies and therefore can be widely used in the industry. On the other side, the so called open source solutions such as RapMan are more suitable for the research work and the education. Despite being a relatively new technology in the industry, the RapMan technology played a big role in reaching some important targets dictated by the modern market such as shortening the length of TTM (Time To Market) and lowering the cost of the final product which made this technology much more interesting to the industry and created a need for skilled engineers in the fields of RP and RE.



Fig.10. ZPrinter 310 System at CIT, Kragujevac

The course “Rapid Prototyping” created at the University of Kragujevac has been awarded as the best course in Serbia as part of WUS Austria CDP program because of its importance and quality [4].

There are great potentials for application of this technology in many other even non-technical fields such as art and design, geography etc. This makes it a very interesting subject to be thought in schools the same way it was done in the past with the Information Technology. The co-authors of this paper are the students and lecturers at the University of Kragujevac.

REFERENCES

- [1] HARRISON P. (2003), *Rapid Prototyping user guide*, Faculty of computing Sciences and Engineering, De Montfort University, Leicester.
- [2] TRAJANOVIĆ M., MANIĆ M., MIŠIĆ D., VITKOVIĆ N. (2005), *Expert system for selection of 3D scanning methods of physical objects* (In Serbian), YU info 2005, Kopaonik
- [3] TRAJANOVIĆ M., MANIĆ M., MIŠIĆ D., VITKOVIĆ N. (2006), *The use of reverse engineering techniques on the example of swindler spoon* (In Serbian), YU info 2006, Kopaonik
- [4] GRUJOVIĆ N. (2005), *Brza izrada prototipova-rapid prototyping* (In Serbian), WUS Austria CDP+ 141-2004, Faculty of Mechanical Engineering, Kragujevac
- [5] TRAJANOVIĆ M., GRUJOVIĆ N., MILOVANOVIĆ J., MILIVOJEVIĆ V. (2008), *Računarski podržane brze proizvodne tehnologije* (In Serbian), Faculty of Mechanical Engineering, Kragujevac
- [6] www.reprap.org
- [7] www.bitsfrombytes.com
- [8] GIBSON I, ROSEN DW, STRUCKER B. (2009), *Additive Manufacturing Technologies: Rapid Prototyping to Direct Digital manufacturing*, s.143-156. Springer New York Heidelberg Dordrecht, London
- [9] PHAM D.T., GAULT R.S. (1998), *A comparison of rapid prototyping technologies*, International Journal of Machine Tools and Manufacture, Elsevier Science, (ISSN 0890-6955), Volume 38, Number 10, October 1998, s. 1257-1287
- [10] <http://fabmetheus.crsndoo.com/>
- [11] www.zcorp.com

ACKNOWLEDGMENT: The part of this research is supported by Ministry of Science in Serbia, Grants III41007.



AUGMENTED REALITY ASSISTED PART REMOVAL FOR POWDER-BASED 3D PRINTING SYSTEMS

Nikola MILIVOJEVIĆ¹, Nenad GRUJOVIĆ², Dejan DIVAC¹, Vladimir MILIVOJEVIĆ¹, Jelena BOROTA²

¹Jaroslav Černi Institute for the Development of Water Resources, 80 Jaroslava Černog St., Begrade, Serbia

²Faculty of Mechanical Engineering, University of Kragujevac, 6 Sestre Janjić St., Kragujevac, Serbia

nikola.milivojevic@gmail.com, gruja@kg.ac.rs, ddivac@eunet.rs, vladimir.milivojevic@gmail.com, jborota@gmail.com

Abstract: 3D printing generally refers to a set of technologies that create 3D physical prototypes by solidifying layers of base material using various binding techniques. By definition 3D printing is an extremely versatile and rapid process accommodating geometry of varying complexity in hundreds of different applications, and supporting many types of materials. Powder-based processes, such as ZCorp 3DP provide great versatility and speed. But there are several bottlenecks related to human factor. When the 3D printing process completes, loose powder surrounds and supports the part in the build chamber. Users remove the part from the build chamber after the materials have had time to set, and return unprinted, loose powder back to the feed platform for reuse. The problem is that entire build area is filled with powder so the user cannot perceive exact position of parts. Usually it is more effective to position several parts within build volume using printing software and print them in one cycle. This increases the risk of damaging the parts while removing them. This paper presents the system for augmented reality assisted part removal, which helps the user to see printed parts through unbound powder. The virtual image of printed parts is generated using data from printing software 3D document that contains both parts geometry and their position within build chamber. This way the risk of damaging the parts during their removal is greatly reduced.

Key words: 3D printing augmented reality, visualization, ZCorp.

1. INTRODUCTION

Rapid Prototyping (RP) refers to a broad set of additive manufacturing technologies used in various stages of product development, with significant application in arts, education, and medicine [1]. By using any of these technologies in traditional processes, time and cost of modeling and planning is greatly reduced. The fastest RP systems today are based on powder binding processes, such as 3D printing by ZCorporation and SLS by 3D Systems. Still, considerable time is required for parts post-processing, thus overall efficiency of RP system may be reduced. One of required steps in powder-based systems is removing produced parts from loose powder, which is usually performed by trained person using vacuuming system. Nevertheless, vacuuming and cleaning must be done with great caution, because the parts are buried in loose powder and gradually appear during the extraction. Usually, the whole of build chamber is used for parts, in order to increase efficiency. Not only this is time consuming process, but parts may also be damaged while extracting, which requires RP process to be repeated. It would be of great benefit if some visual aid would be provided for operating technician, so that part extraction can be accelerated and risks of damaging parts diminished.

Recent advances in augmented reality applications provide cheap and effective solutions for marker-based

systems with wearable displays [2]. Such system is presented in this paper as an aid for part extraction procedure in 3D printing process. The main idea is to help operating technician by visualizing the position of parts within build chamber, while they are still buried in loose powder. The system relies on printing setup generated by proprietary software, and the use of fiducial markers applied on top surface of 3D printer.

2. 3D PRINTING

ZCorporation was founded in 1994, in Massachusetts, USA. Based on MIT-patented technology [3], this company developed and commercialized their first 3D printer, Z402 System, in 1997. 3D printing is RP powder-based technology that uses liquid binder for layer generation.

The binder is applied on powder via printing head, using the same process as in thermal inkjet printing. This also allows for printing to be performed using multiple binder liquids in various colors. Figure 1 illustrates fabrication of a single layer[4]. The following parts are of main interest: on the left-hand side is reservoir chamber with feed piston at the bottom, the gantry with roller are depicted as circle and square, respectively, in the middle is build chamber with build piston at the bottom, while on the right-hand side is overflow chute. The gantry traverses from left to right side, and vice versa, while the print head it carries

travels along the gantry, allowing the binder to be printed on whole top surface of the build chamber.

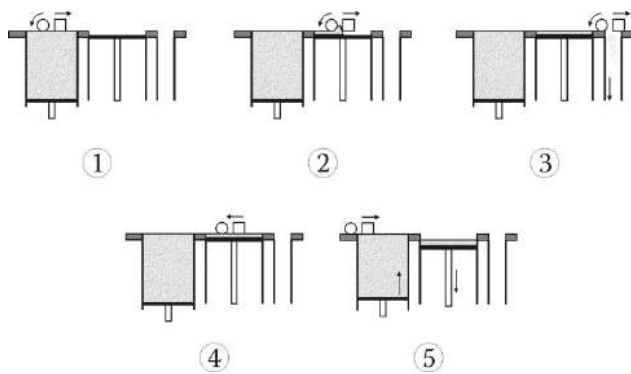


Fig.1. The process of 3D printing

At first, the feed piston is raised, so that the powder is slightly over the top of reservoir chamber. The gantry then moves from left to right over reservoir chamber, while the roller picks up free powder. The second step is spreading this powder over build chamber. The build piston is already lowered for height of one layer, so that the powder could be spread evenly. At the rightmost position, the excess powder is dropped through the chute to overflow bin, so it can be recycled later. The fourth step is actual printing of layer, where the print head applies binding liquid on new layer of powder in build chamber, and thus binds this layer to previously printed layers. The final step is at leftmost position of gantry, where the feed piston is raised and the build piston is lowered, and the whole process is repeated.

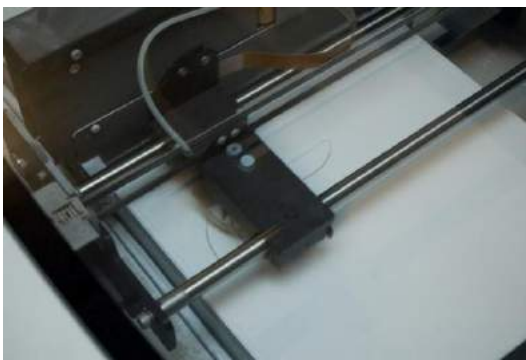


Fig.2. Fabrication of single layer

This way, the model is built, layer by layer, and the whole process results in solid part buried in unbound powder. The unbound powder also provides support for printed parts, so that complexity of geometry is not an issue. The loose powder is removed usually by vacuuming and may be used for printing (Figure 3a). After initial cleaning, the parts usually undergo post processing, such as depowdering (removing remains of unbound powder by blowing), curing (drying in an oven at around 100°C), and infiltrating (e.g., strengthening the surface of the part with epoxy)[5].



Fig.3. Part removal: a) vacuuming loose powder; b) damaged part due to improper extraction

One of the main problems is how to extract printed parts from unbound powder. The reason for this is that usually multiple parts are printed in one batch, in order to utilize the whole build volume and reduce print times. Even if a single part is printed, but one with complex geometry or thin features (Figure 3b), the operating technician may damage the part if he is not aware of its actual position within build chamber.

The presented augmented reality system is designed to provide technicians visual aid by superimposing parts layout within build chamber.

3. AUGMENTED REALITY

Augmented Reality (AR) is the synthesis of real and virtual imagery[6]. In contrast to Virtual Reality (VR) in which the user is immersed in an entirely artificial world, augmented reality overlays extra information on real scenes: typically computer generated graphics are overlaid into the user's field-of-view to provide extra information about their surroundings, or to provide visual guidance for the completion of a task. In its simplest form, augmented reality could overlay simple highlights, arrows or text labels into the user's view - for example, arrows might guide the user around a foreign city. More complex applications might display intricate 3D models, rendered in such a way that they appear indistinguishable from the surrounding natural scene.

Major advantages of AR are ease of collaboration, intuitive interaction, integration of digital information,

and mobile computing. AR enables a user to work in a real world environment. At the same time user can receive additional computer-generated information. Until recently, AR has been mainly engaged in scientific visualization and gaming environments, but the latest investigations are aimed at supporting activities like surgery, training and collaborative work[7]. Some early uses of AR in architecture were for sketching.

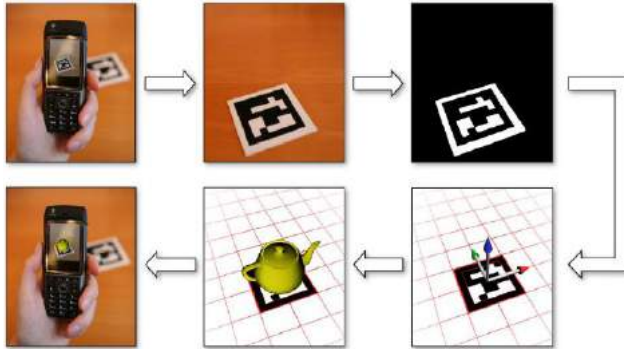


Fig.4. Pipeline of AR system

Figure 4 illustrates the pipeline of AR system[8]: the user points image capturing device to a marker; the image is captured and converted to black-and-white format; the marker is located in the image and coordinate system is computed based on position and orientation of marker; using computed coordinate system, an image of 3D object is rendered; the resulting image is overlaid on device display. The process is near real-time, depending on hardware capabilities of the system.

4. AR ASSISTED SYSTEM FOR PART REMOVAL

The solution presented here is designed to visually assist technicians in part removal procedure using marker-based AR that supports both handheld and head-mounted devices. The parts layout in build chamber setup by technician using ZPrint software represents input for visualization. The platform for AR is ARToolKit, a reliable GNU library for single-camera applications.

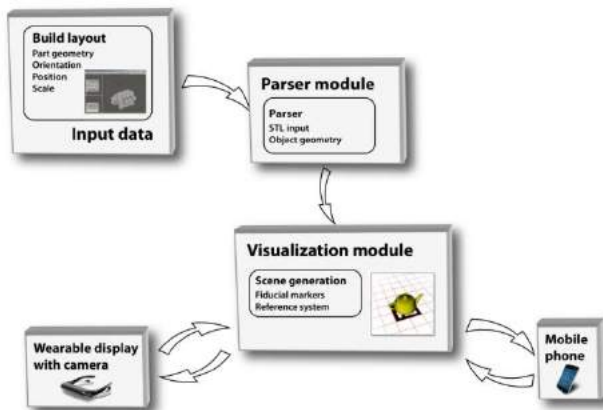


Fig.5. Structure of the system

The structure of the system is illustrated in Figure 5. The central part is the visualization module, which can be hosted both on head-mounted or handheld devices. This module uses data from parser module to generate scene for rendering based on marker orientation and position. The parser module is used to convert build layout to geometry data used in visualization module.

A build batch consists of multiple parts arranged within build volume. It holds information on part geometry and layout. Since native format for saving build in ZPrint software is undocumented binary file, the technician needs to export the build to STL file, using menu command File > Export STL. The resulting file represents input data for the parser module, which converts triangle list into object geometry used by visualization module.



Fig.6. AR assisted part removal

Up to 4 fiducial markers may be used by visualization module, so that the technician can freely move while extracting printed parts. It is only necessary that at least one marker is always in field of view, so marker placement is important when preparing the system. By using special markers, it is possible to calibrate the system through guided procedure. The calibration is performed in order to establish reference coordinate system for visualization. Once reference coordinate system is established, the system will require subsequent calibration only if the marker placement changes.

The system supports the use of either head-mounted or mobile AR devices. When using head-mounted AR device, the technician is free to move while extracting printed parts. The overlaid image of printed parts guides the technician in process of part removal, thus reducing the risk of damaging the parts buried in loose powder. When using the mobile AR device, the technician needs to periodically check part layout because using the AR device interferes with handling the other equipment. Nevertheless, for more complex build layouts even sporadic use of AR helps the technician to plan the part removal and reduce the associated risks.

5. SUMMARY AND CONCLUSION

The presented system for AR assisted part removal in 3D printing provides new way of helping technicians in sensitive operation of printed part extraction. The risk of damaging printed parts in the process of removal from

loose powder is greatly reduced through use of such a system, especially with use of head-mounted AR which enables technician to keep visualized build layout constantly in field of view, while the use of mobile AR device provides periodical checks of layout. The best results can be achieved when building layouts that are relatively complex or when printing delicate parts.

Further work on this system will be directed mostly to visualization manipulation, since visualizing of complex builds in some cases proves to be distracting to the operating technician. The tools for manipulation of AR visualization that will be developed are cutting plane and object visibility. The technician will be able to hide objects through selection of visible objects or by means of moveable cutting plane. By hiding already extracted parts, AR visualization may provide better compliance with progress of removal operation, while cutting plane also resembles the process of removing loose powder from top to bottom of the build chamber.

The application of system for augmented reality assisted part removal, in presented state and with further improvements, will improve productivity and lessen the manufacturing costs in powder-based 3D printing services.

REFERENCES

- [1] JACOBS, P.F. (1992) *Rapid Prototyping & Manufacturing– Fundamentals of StereoLithography*, Society of Manufacturing Engineers, (ISBN 0-87263-425-6), Dearborn, MI, USA, s. 4-23
- [2] AZUMA, R., BAILLOT, Y., BEHRINGER, R., FEINER, S. MACINTYRE, B. (2001) *Recent advances in augmented reality*. Computers & Graphics, IEEE, November/December, 21, 6, 34-47.
- [3] LAUDER, A., CIMA, M.J., SACHS, E., FAN, T. (1991) *Three Dimensional Printing: Surface Finish and Microstructure of Rapid Prototyped Components*, Synthesis and Processing of Ceramics: Scientific Issues, Boston, MA, USA, s. 331-336.
- [4] ZPrinter 310 User Manual (2003), ZCorporation,.
- [5] TRAJANOVIĆ, M., GRUJOVIĆ, N., MILOVANOVIĆ, J., MILIVOJEVIĆ, V. (2008) *Računarski podržane brze proizvodne tehnologije*, monografija, Mašinski fakultet, Kragujevac
- [6] FEINER, S.K. (2002) *Augmented reality: a new way of seeing*. Scientific American, Vol. 4 No.24, 48-55.
- [7] POUPLYREV, I., TAN, D.S., BILLINGHURST, M., KATO, H., REGENBRECHT, H. TETSUTARI, N. (2002) *Developing a generic augmented-reality interface*. IEEE Computer, 35, 3, 44-50.
- [8] WAGNER, D., SCHMALSTIEG, D. (2007) *ARToolKitPlus for Pose Tracking on Mobile Devices*, Computer Vision Winter Workshop 2007, Graz Technical University

ACKNOWLEDGMENT: The part of this research is supported by Ministry of Science in Serbia, Grants III41007.



APPLIED RAPID PROTOTYPING TECHNOLOGY AND MODELING IN THE SPECIFIC PATIENT DAMAGE HIP REPLACEMENT

Dalibor NIKOLIĆ¹, Branko RISTIĆ³, Milovan RADOSAVLJEVIĆ^{2,4}, Nenad FILIPOVIĆ^{1,2}

¹Bioengineering Research and Development Center, BioIRC, 34000 Kragujevac, Serbia

²Faculty of Mechanical Engineering, University of Kragujevac, 34000 Kragujevac, Serbia

³Medical Faculty in Kragujevac, University of Kragujevac, 34000 Kragujevac, Serbia

⁴High Technical School, 34000 Kragujevac, Serbia

markovac85@kg.ac.rs, fica@kg.ac.rs

Abstract: *The missing part of the pelvic bone that was destroyed by artificial hip replacement and further destroyed by infection was constructed and analyzed. To successfully cure infection it is necessary to completely "close" the bone, i.e. free space in the bone with the bone cement in combination with antibiotic.*

We implemented a rapid prototyping technology for the object embedded in the patient's bone damage in order to cure the patient from an infection and the process of bone destroying. This technology could be very useful in cases of complex cases which require reconstruction. Digital data acquired during C.T. scan is fed into our software application system, which generates the bone model depicting the pathology. This model is used to plan the surgical strategy where the errors during the surgery are minimized.

Key words: *artificial hip, implants;*

1. INTRODUCTION

Improper posture, a variety of diseases, injuries and other factors cause bone defects in human's hip, requiring surgery and installation of an artificial hip [1-4]. There is bone infection in 1- 2% of cases after patient surgery which destroy the bone. In such cases it is necessary to perform a hip replacement and remove the infection treated with antibiotics [5-8]. Unfortunately the treatment of such infections is long, sometimes even years are necessary without any visible improvement. During the treatment of infections the patients have to be rested because their movements could be very difficult and painful. Although it seems that this disease comes up very rarely, some people are facing with this problem, which can continue for many years. Therefore, there is a need to find different solution to cure this problem.

2. SOFTWARE TOOL DESCRIPTION

In order to solve this clinical problem we developed a software tool which consists of several independent applications in sequence, where the output of the previous application is input for next application (Fig. 1).

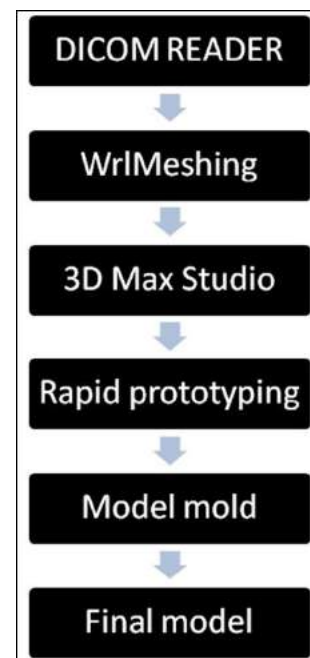


Fig.1. Graphic model of the software application

2.1. Dicom reader

The first software module is used for the recognition objects from DICOM images (DICOM reader). It is a very useful tool developed in a way that gives a great application with minimal modifications [9-10]. It is guided by the fact that DICOM format is used in almost all fields of the medicine and in almost all medical devices.

This software is used to load DICOM - medical images (*. DCM), to identify the contours of the slices (Fig. 2), and to convert these slices into the PNG black and white images. The outlined in the recording mark (the object of interest) is denoted with white color and the black color denotes the outer part (Fig. 3).

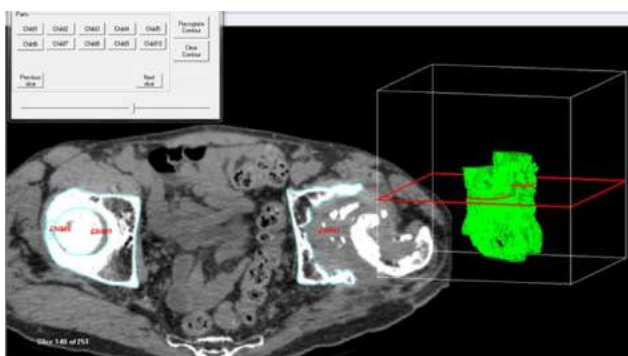


Fig.2. DICOM reader application

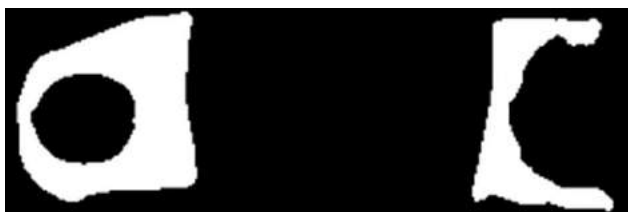


Fig.3. Selected objects from the DICOM images (objects of interest)

2.2. WrlMeshing

The next software module in a series of software application is WrlMeshing. This algorithm was developed at the Center for Bioengineering, Faculty of Mechanical Engineering in Kragujevac. Its function is that of a series of 2D PNG (black and white) images to create three-dimensional model by using an algorithm to "uplift" pixels and thus creating a "voxel". With a small modification of the source code this tool was used to obtain a 3D model of the left and right pelvic bones with a series of 2D images obtained using the previous software module. In this way we created the pelvic bones of the left side (healthy hip) and right pelvic bones (destroyed hip) in the Fig. 4.

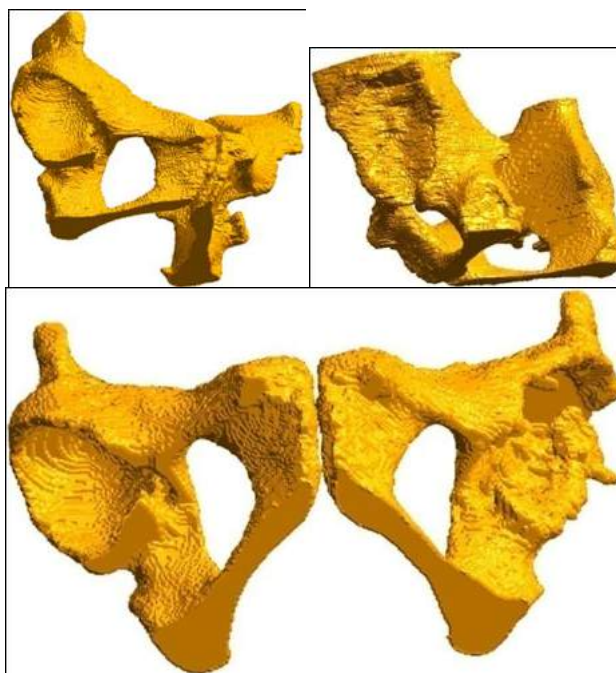


Fig.4. 3D model of the pelvic bone (healthy and diseased)

2.3. Autodesk 3D MaxStudio®

For further manipulation of the model the commercial 3D software Autodesk MaxStudio was used. Software modules DICOM READER, WrlMeshing, are designed and used as a converter from DICOM images into 3D format that can be further treated with CAD or other graphics software. (*.DCM -> *.STL)

Since the left and right pelvic bone can be considered as a model and its representation in the mirror, to obtain the missing part of the injured (right) pelvic bone, we used the healthy (left) with rotation the bone as a mirror [11-12]. Then we have these two bones overlapping as it is presented in Figure 5. By using Boolean operation we removed the parts that overlap and we obtained a difference of healthy and diseased bone (Figure 6).

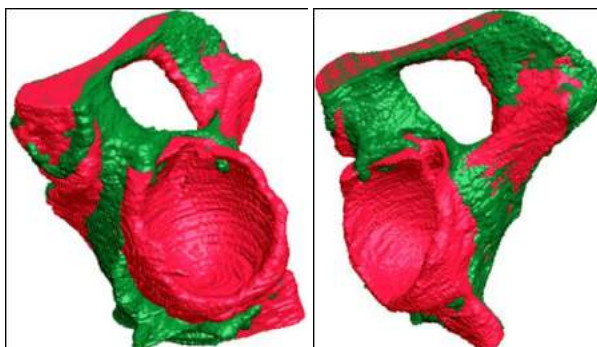


Fig.5. Overlapped healthy and damaged pelvic bone

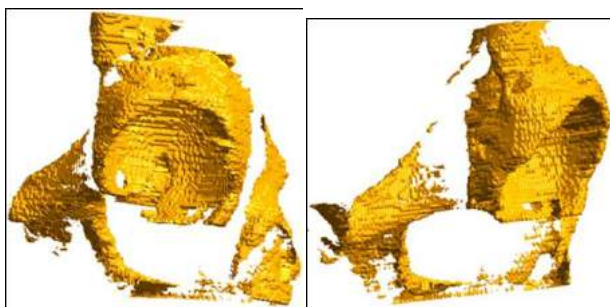


Fig.6. Model after subtraction Boolean operations

After overlap procedure there was a lot of additional objects which we do not need and they represents an error in the symmetry of the pelvic bone. Also we have taken into account that left and right bones do not have completely the same shape and dimensions. The excess objects are removed. The final 3D model is obtained in Figure 7. It is now possible to create a realistic model, which will later be incorporated into the patient.

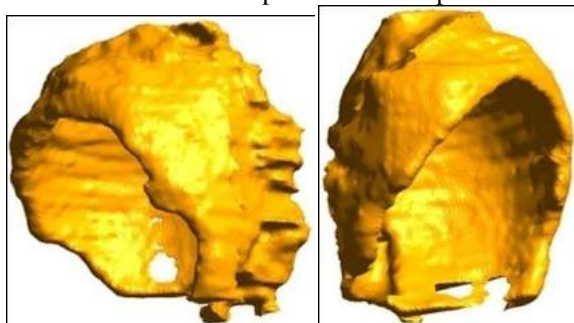


Fig.7. Final model of the missing part

3. APPLICATION OF THIS METOD

Based on this final model we created real model in the mold (Figure 8) of Plexiglas on the 3D milling machine, which was implemented in the surgical hall be cast model. The mold was made of several parts that can easily be obtained by extraction of casting and mold sterilization as it has been shown in Fig. 9. The sterilization temperature was applied at the mold plexiglass material.



Fig.8. Model in the mold is ready for installation in the patient (picture from surgical rooms)

The model is poured into a mold which was prepared before surgery, so within the real time surgical intervention the surgeon can estimate model preparation (melting point 160°C).



Fig.9. Different 2D cross-sections of Plexiglas material produced on the 3D milling machine

4. CONCLUSION

In this paper we demonstrated the software solution which already started to be applied in the clinical practice in Clinical Center in Kragujevac. These software tools simplified and make cheaper the diseases diagnosis and treatment.

Computer three-dimensional reconstruction and modeling of the damaged part of the pelvic bone from the 2D images obtained by CT scanner can be easily and accurately implemented in real patient. The aim is that on the basis of computer models to create a mold for casting. The model then can be implemented in real-sterile surgical hall. In this way, we improved approach to planning and carrying out serious surgery on the patient, and even shorten the duration of the surgical intervention. The results of this particular example emphasized the strengths of the medial prototyping process in preparing hip models for pre-surgery planning. Rapid prototyping models can provide assistance as a surgical planning tool in complex cases, especially in improving surgical results and disease treatment. Considering the novel findings of broad improvements in accuracy and time, a new field of research is emerging, serving both virtual surgery applications and physical implant generation.

REFERENCES

- [1] ALBINANA, J., MORCUENDE, A., DELGADO, E., WEINSTEIN, L. (1995) *Radiologic pelvic asymmetry in unilateral late-diagnosed developmental dysplasia of the hip.*, J Pediatr Orthop Vol. 15 No 6, pp 753-762.
- [2] BECK, M., LEUNIG, M., ELLIS, T., SLEDGE, B., GANZ, R. (2003) *The acetabular blood supply: implications for periacetabular osteotomies.* Surgical Radiol Anat. Vol. 25, No 5-6, pp 361-367.

- [3] BROWN, A., FIROOZBAKHS, K., DECOSTER, A., REYUNA, R., MONEIM, M. (2003) *Rapid prototyping: The Future of Trauma Surgery*. J Bone Joint Surg. Vol. 85A (Supplement 4), pp 49-55.
- [4] BROWN, A., WILLIS, M., FIROOZBAKHS, K., BARMADA, A. (2001) *Computed tomography image guided surgery in complex acetabular fracture*. Clin Orth Vol. 370, pp 219-261
- [5] WOHLERS, T.(2004) *Rapid Prototyping, Tooling and Manufacturing State of the Industry Report*. Wohlers Report
- [6] HOPKINSON, N., HAGUE, R., DICKENS, P. (2006) *Rapid Manufacturing: An Industrial Revolution for the Digital Age*, Wiley.
- [7] WINDER, J., Bibb, R. (2005) *Medical Rapid Prototyping Technologies: State of the Art and Current Limitations for Application in Oral and Maxillofacial Surgery*. J Oral Maxillofac Surg, Vol. 63, No 7, pp 1006-15.
- [8] PRAMANUK, S., AGARWAL, K., RAI, N. (2005) *Chronology of total hip joint replacement and materials development*. Trends Biomater. Artif. Organs, Vol. 19, No 1, pp 15-26.
- [9] FISHER, J. (2001) *Biomedical Applications*. Modern Tribology Handbook, Vol. Two: Materials, Coating and Industrial Applications, edited by Bharat Bhushan. Florida: CRC Press, Boca Raton, pp 1593-1609.
- [10] KALPAKJAN, S., SCMID, R. (2003) *Manufacturing processes for engineering materials*, 4th edition: Prentice Hall, pp 610-619.
- [11] WALKER, H., MESWANIA, J., MUIRHEAD-ALLWOOD, K., CATTERALL, T. (1988) *The role of 3D image reconstruction and rapid prototyping models in total hip arthroplasty*, Phidias-EC Funded network project on rapid prototyping in medicine.
- [12] CALLISTER, D. (2006) *Materials Science and Engineering: An Introduction*, 7th edition: McGraw-Hill, pp 728-735.



APPROACHES TO AUTOMATED CREATION OF TISSUE ENGINEERING SCAFFOLDS

Milan TRIFUNOVIĆ, Jelena MILOVANOVIĆ, Miroslav TRAJANOVIĆ, Nikola KORUNOVIĆ,
Miloš STOJKOVIĆ

Faculty of Mechanical Engineering, University of Niš, Aleksandra Medvedeva 14, Niš, Serbia
milant@masfak.ni.ac.rs, jeki@masfak.ni.ac.rs, traja@masfak.ni.ac.rs, nikola.korunovic@masfak.ni.ac.rs,
miloss@masfak.ni.ac.rs

Abstract: *Tissue engineering (TE) is a relatively new field in biomedical engineering that is receiving much attention among the scientific community and the general public. One approach to promote the regeneration of new tissue is application of scaffolds as a template to guide the proliferation, growth and development of cells appropriately. Scaffolds internal structure plays an important role for this purpose. The process of creating customized scaffolds includes definition of the internal architecture suitable for the development of the desired tissue and creation of external geometry to match the geometry of fragment being replaced. This paper analyzes the approaches which aim to simplify and automate the process of creating customized scaffolds.*

Key words: *tissue, engineering, scaffold*

1. INTRODUCTION

Tissue engineering is an interdisciplinary field that applies the principles of engineering and the life sciences toward the development of biological substitutes that restore, maintain, or improve tissue function [1]. One approach to tissue engineering involves the use of scaffold as a structure which allows cells attachment, proliferation, differentiation and migration. After seeding the cells into a scaffold they are cultured in vitro until the scaffold is ready to be implanted. Along with the process of tissue regeneration scaffold is gradually degrading leaving newly formed tissue in place. Three primary requirements for scaffolds are [2]: (1) to define anatomic shape and volume, (2) to provide temporary mechanical support, and (3) to enhance tissue regeneration through delivery of cells, genes, and/or proteins.

Initial research has shown that the internal microstructure of scaffolds in terms of shape, pore sizes and pore networks influences the proliferation, differentiation as well as the angiogenesis of the forming tissue [3]. Scaffolds made with conventional fabrication techniques have a number of shortcomings. They are primarily reflected in lack of mechanical strength, nonuniformity in terms of size and distribution of pores and arbitrary pore shape. This is because conventional fabrication techniques offer minimal control over the internal architecture of scaffold. With the advent of rapid prototyping technology it has become possible to create complex scaffolds and control of the internal architecture of the scaffolds. Fabrication of scaffolds using rapid prototyping technologies implies the existence of scaffold CAD model.

Problem of creating customized scaffolds to meet patients requirements is very complex. On one hand it is necessary

to generate the appropriate internal geometry that will be suitable for the development of different types of tissues, while on the other hand it is necessary to ensure that the external geometry corresponds to the outer geometry of the organ or organ part that is to be replaced. There are several approaches to solving this problem which simplify and automate the process of creating scaffolds. These approaches offer to the user possibility to choose internal geometry that provides the desired scaffold properties and then perform automated scaffold creation. This paper provides an overview and comparison of existing approaches to automated scaffold creation. It also aims to consider possibilities for their improvement.

2. ANALYSES OF APPROACHES

Naing and his collaborators developed system called Computer aided system for tissue scaffolds (CASTS) which provides the users with a database of designs to choose from, generates scaffolds with desired parameters and properties, and customises scaffolds according to patients requirements [4]. System operates on a graphics workstation which runs ProENGINEER. CASTS has three separate modules, namely, an input module, a designer's toolbox and an output module.

Input module is used to convert raw patient data obtained through magnetic resonance imaging (MRI) and computed tomography (CT) scan to surface model in IGES format. The conversion is carried out using image processing software MIMICS.

Designers toolbar has several functions. Firstly the appropriate unit cell is selected depending on porosity, surface area to volume ratio and strength requirements from the parametric library developed by the creators of the system [5]. Parametric library contains 11 unit cells

(Fig.1.) – polyhedral shapes – that can be divided into two categories: cells that can fill space (without leaving gaps) and cells that can span space (leaving gaps). After selecting the unit cell designer can change its size to conform to pore size requirements and defines the overall dimensions of the scaffold using sizing routines. The next step is the automated generation of scaffold of given size using a specially developed algorithm [6]. Output values, such as pore sizes, surface area to volume ratio and porosity of the scaffold are calculated and displayed also.

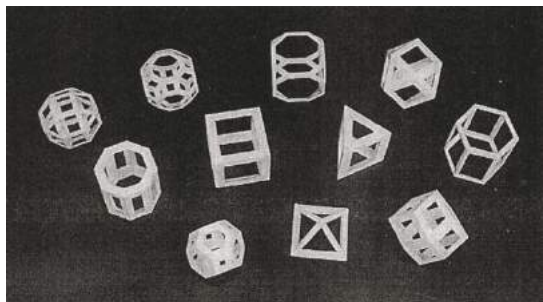


Fig.1. The 11 unit cells

To ensure better ingrowth of cells the authors have come up with an approach where created scaffold is cut by using developed routines into layers that can be seeded separately and then assembled prior to implantation (Fig.2.).

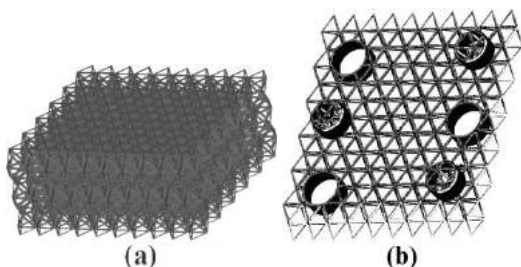


Fig.2. (a) Rectangular scaffold block model (b) Sliced scaffold model with orientation features

Output module is used to create customized scaffold through applying Boolean operation on previously generated scaffold and solid model of a part of patients bone which was created based on surface model. The final output is scaffold structure in near net shape of the patients defect represented by model in STL format.

For validation purposes authors generated and fabricated patient specific scaffold using CASTS system. Octahedron-tetrahedron space filling system was used for scaffold generation (Fig.3.). The length of strut in each unit of the scaffold was set to 2.5mm which gave a porosity of 93 per cent with a macro pore size of 1.193mm. SLS fabricated femur scaffold with the scaffold model and the surface profile are shown in Fig.4.. Under the light microscope, the scaffold was found to exhibit regular pre-designed microarchitecture, proving the effectiveness of the system.

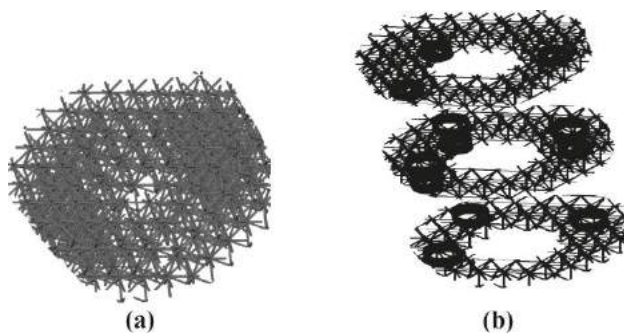


Fig.3. Femur scaffold model (a) before and (b) after slicing

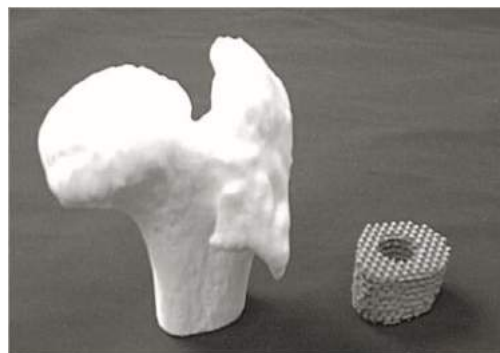


Fig.4. A femur segment (left) and the fabricated customized scaffold (right)

Another approach to automated creation of tissue engineering scaffolds is the result of the work of Ramin and Harris [7]. It involves the use of library of routines that interact with the CAD software and enable automated creation of geometric elements. The authors have chosen multi section solid (curved rod) as a geometric element because it is the most suitable form for the creation of trabecular bone (Fig.5.) like structure that was their area of interest. The resulting geometry is represented by a network of irregular and interconnected rods and corresponds to geometry of the regenerated tissue. Scaffold is obtained by representing the multi section solid in reverse form using the appropriate routines as a channel in the reference volume.

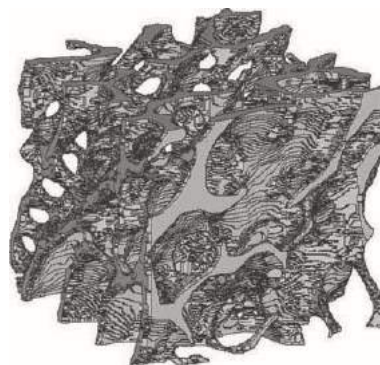


Fig.5. Example of an STL representation of human trabecular bone structure from a μ CT scan of a femoral neck

Multi section solid is defined with one or two cross sections while the path is defined by a straight or curved line in space (Fig.6.). Curved paths are defined by three control points. The authors have chosen pore size, pore shape, number and orientation of pores as design variables.



Fig.6. Example of a multi section solid

Pore size is controlled by planar curve that is defined by a number of control points (Fig.7.), while the shape of the pore is controlled by the values of the tangents at the control points. Authors used five control points to define a pore section, with the first and the fifth vertex coincide and each control point was positioned as a vertex of an ideal square. Pore interconnectivity and porosity are calculated as output from the system. Pore location was defined by the absolute coordinates of the centre of the enclosed square on the surface. All design parameters can be set as either constant or variable.

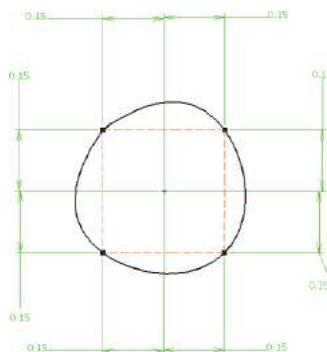


Fig.7. Definition of pore size

In order to prove validity of this approach five cubic scaffolds were created. They had interconnecting pore channels that range from 200 to 800 μm in diameter, and each was with an increasing complexity of the internal geometrical arrangement. One of them is presented in Fig.8.

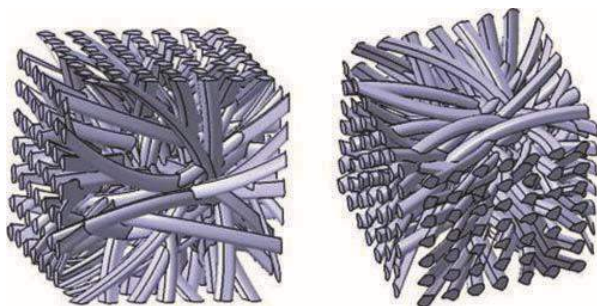


Fig.8. Details of some curved paths and their random connections

Authors also presented a clinical case study where they integrated one of the geometries generated for cubic scaffolds with the craniofacial implant (Fig.9.) [8].

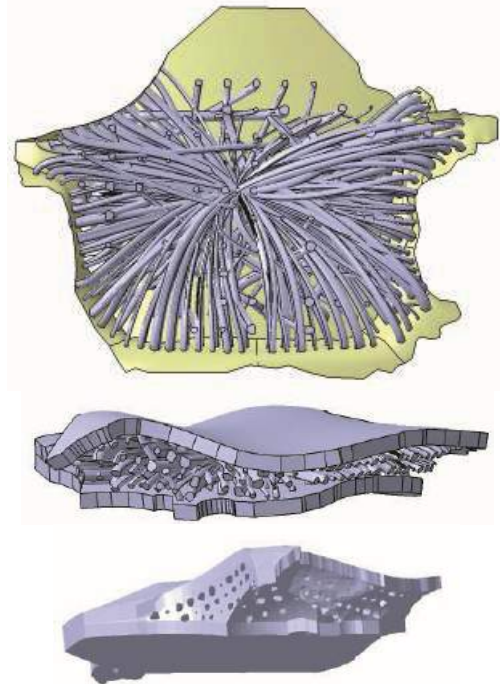


Fig.9. (up) Global network of rods enclosed by the surfaces surrounding the craniofacial implant (middle) Simulated trabecular and compact bone structures (down) Scaffold geometry for the craniofacial implant analysed

3. DISCUSSION

One of the advantages of the CASTS system compared to Ramins approach is that the size and shape of the pores are defined more precisely. CASTS system has also undergone validation in terms of fabricating customized scaffolds. In one case [9] scaffold fabricated using this system was used for culturing C2C12 myoblast cells in vitro for 21 days in order to determine its suitability for cardiac tissue engineering. High density of cells was recorded after 4 days of culture. Fusion and differentiation of C2C12 were observed as early as 6 days in vitro. A steady population of cells was then maintained throughout 21 days of culturing.

Ramins approach provides creating irregularities in the scaffold structure which is a feature that is found in the structure of trabecular bone. The advantage of this approach compared to the CASTS system is that it does not imply the use of Boolean operations when creating customized scaffolds. The main reason is that the application of these operations makes the process of generating scaffold ineffective in cases when the geometries to be merged are very complex and irregular. Time savings when creating scaffolds using this approach ranges from 75 to 90% compared to the manual creation [7]. With this approach it is also possible to define that input variables are changed by a mathematical function in

order to mimic the different gradients of density that exist in bone structure. On the other hand Ramins approach does not involve the analysis of mechanical properties of the scaffold, and the porosity is not defined as an input parameter but is calculated as output value after the creation of geometry.

Scaffolds are aimed to temporarily replace and promote growth of biological structures which are usually inhomogeneous. Having this in mind it could be useful to further improve existing systems or develop a completely new one with the possibility to create heterogeneous scaffold both structurally and in terms of materials. Another direction in which the research in this field can be directed is attempt of further automation of the system that would ensure automatic selection of unit cell and generation of scaffold structure with appropriate parameters, all based on specifications defined by the tissue engineer.

4. CONCLUSION

Although different approaches were analysed, their main advantage is that they do not rely on the users skill for creation of customized scaffold. Automation of processes in these approaches is the key factor that ensures the design of a large number of geometric elements in a short time, while maintaining a high level of flexibility. These systems represent significant scientific contribution on which further investigations in this field can be based on.

ACKNOWLEDGEMENT

This paper reports on the research which is undertaken in the scope of project "Virtual human osteoarticular system and its application in preclinical and clinical practice" (project id III 41017) funded by the Ministry of Education and Science of Republic of Serbia for the period 2011-2014.

REFERENCES

- [1] Langer, R., Vacanti, J.P., (1993) Tissue engineering, *Science*, Vol. 260, No. 5110, pp. 920-926
- [2] Hollister, S.J., Lin, C.Y., (2007) Computational design of tissue engineering scaffolds, *Computer Methods in Applied Mechanics and Engineering*, Vol. 196, No. 31-32, pp. 2991-2998
- [3] van Tienen, T.G., Heijkants, R.G., Buma, P., de Groot, J.H., Pennings, A.J., Veth, R.P., (2002) Tissue ingrowth and degradation of two biodegradable porous polymers with different porosities and pore sizes, *Biomaterials*, Vol. 23, No. 8, pp. 1731-1738
- [4] Naing, M.W., Chua, C.K., Leong, K.F., Wang, Y., (2005) Fabrication of customised scaffolds using computer-aided design and rapid prototyping techniques, *Rapid Prototyping Journal*, Vol. 11, No. 4, pp. 249-259
- [5] Chua, C.K., Leong, K.F., Cheah, C.M., Chua, S.W., (2003) Development of a tissue engineering scaffold structure library for rapid prototyping. Part 1: Investigation and classification, *The International*

Journal of Advanced Manufacturing Technology, Vol. 21, No. 4, pp. 291-301

- [6] Chua, C.K., Leong, K.F., Cheah, C.M., Chua, S.W., (2003) Development of a tissue engineering scaffold structure library for rapid prototyping. Part 2: Parametric library and assembly program, *The International Journal of Advanced Manufacturing Technology*, Vol. 21, No. 4, pp. 302-312
- [7] Ramin, E., Harris, R.A., (2009) Advanced computer-aided design for bone tissue-engineering scaffolds, *Proceedings of the Institution of Mechanical Engineers, Part H: Journal of Engineering in Medicine*, Vol. 223, No. 3, pp. 289-301
- [8] Ramin, E., (2010) Automated design of trabecular structures, Ph.D. Thesis, Loughborough University
- [9] Yeong, W.Y., Sudarmadji, N., Yu, H.Y., Chua, C.K., Leong, K.F., Venkatraman, S.S., Boey, Y.C., Tan, L.P., (2010) Porous polycaprolactone scaffold for cardiac tissue engineering fabricated by selective laser sintering, *Acta Biomaterialia*, Vol. 6, No. 6, pp. 2028-2034



3D DIGITIZING FREE FORM SURFACES BY OPTICAL TRIANGULATION LASER SCANNING

Radomir VUKASOJEVIĆ, Željko RAIČEVIĆ, Simo ŠALETIĆ

University of Montenegro Faculty of Mechanical Engineering, Cetinjska br.2, Podgorica, Crna Gora

vukas@ac.me, zeljko.raicevic@t-com.me

Abstract: *The paper provides an overview of the developed system of digitization and determines their suitability to interact with other subsystems of the computer integrated manufacturing.*

The developed systems for digitization which are based on modern semiconductor laser, CCD camera and the original algorithms for detection, correction and transformation of points from the surface of the object, creating a cloud of surface points and exchange data with the software package Pro / ENGINEER are presented in the paper.

The success of the developed system is given over digitalization of more complex shapes objects.

Key words: 3D digitizing, optical triangulation, 3D laser scanning

1. INTRODUCTION

Commercially is available a wide range of 3D digitizing technology based on a variety of applications that allow processing of objects in a large range of sizes. Often used terms: 3D scanning, laser digitizing and digital shape sampling and processing forms.[1]

Applications of surfaces generation from data points captured from real objects, by optical 3D scanners and other technologies include reverse engineering, quality assurance in industry, medicine, art., metrology, product design etc.

Data obtained from 3D digitizing technologies are often far from being perfect, and results are usually point clouds.

One scanning process will not lead to a complete model for most of objects. It is necessary several scanning processes from different directions in order to obtain information from all sides of the objects. Scan must be brought into a common reference system, and then create a complete model. [2]

Reconstruction of the shape of object, often, is done by processing a wide range of data obtained by laser scanning. Algorithms processed cloud points through a polygonal approximation mesh. Procedures that enable the direct optimization and evaluation of the scanned data is accelerated and improved. There are more surface meshing concepts: Marching-Cubes, Delaunay triangulation/tetrahedrization, and the fitting of parametric surfaces (e. g., B-Splines or Bézier representations) etc.

3D digitizing methods can be classified into passive and active. Passive methods, in most cases, do not require special hardware. The accuracy of these methods depends mainly on the resolution of the system for imaging and possibility to identify shapes in the picture. Passive 3D technology generally uses one of three techniques of measuring length: measurement based on photogrammetric, stereoscopically and techniques of reconstruction. [3]

Active methods have two approaches: contact and noncontact. Contact method is characterized by a contact object and the sensor. Noncontact methods, in general, are based on the reflection of radiation or light and recording reflection or transmission of energy. Reflection methods can be optical and non-optical, and transmission methods, are mainly based on X-rays.

3D laser scanning is an active, non-contact, non-destructive technology that captures the shape of physical objects using laser light. Laser scanning system works on principles of acquisition data of points or generation 3D point cloud from the surface of the object. For most 3D applications point clouds are not directly acceptable, and they have to be converted to triangle mesh models, NURBS surface models, or CAD models. Recording and measuring the spatial structure, in general, can be achieved by: triangulation, measurement based on time and phase shift. There are and other hybrid technology or combination of technologies for scanning, three-dimensional linear laser interferometry, Conoscopic holography and so on.

Non-optical methods work on the principle of determining distances by measuring the time needed to get light to the object and to return. Optical methods obtain shape by measuring the reflection of light projected on the object. Optical methods are not suitable for translucent surfaces.[4]

2. DATA PROCESSING

In analyzing data obtained by laser scanning is usually necessary to be processed millions of points. Processing point cloud of real objects generated with 3D digitalization process contains a certain level of errors. Reconstruction based on raw, data points will result in inadequate CAD model, which degrades the accuracy of the reconstruction of object surface.

Depending on the applied 3D digitalization technology there are various problems with results derived from the measurement procedure, the geometric complexity of the object, purpose of models etc. Regardless of 3D digitalization technique appear errors related to the point cloud, such as the presence of noise, outliers, gaps, large number of data points, disorganization and a lack of data.[5]

The presence of noise, points out of range etc. requires the elimination of errors and regulates the data points. Pre-processing enables filtering of errors, arranging and reduction of data points.

3. LASER TRIANGULATION

Noncontact systems process geometric 3D data from complex surfaces. It is possible to obtain commercial devices based on wide variety of 3D optical sensing techniques, such as: laser scanning triangulation (3D Scanners, Cyberware, Digibotics, Laser Design, Vitronic); Moiré Fringe Contouring (Wicks and Wilson, Breuckmann, InSpeck); Phase Measuring Profilometry ([TC]) Digital Stereo Photogrammetry (TCTi).

Laser triangulation is a reliable noncontact technology for digitizing surface. Development of CCD optical sensors appliance of laser triangulation technique increased significantly.[7] Laser triangulation is an active stereoscopic technique where the distance from the object is calculated by the directional light source and video camera. The laser beam is deflected from a mirror on the scanned object. The object scatters the light, which is then collected by a video camera located at a known distance from the laser. Using trigonometry, calculate the 3D space coordinates (X, Y and Z) of the points, figure 1.

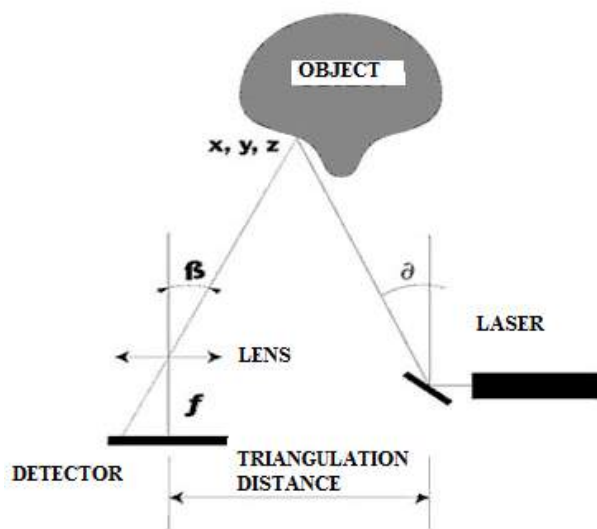


Fig. 1. 3D laser triangulation

Since the illuminated area on the optical sensor sees a group of pixels with different intensity of light, it is necessary with specific functions determine the position of points on the picture. From algorithm for determining

the position of the point, depends the accuracy of digitization.[6]

Scanning method determines the relative motion of objects and light sources. It is possible that an object do not move, and that the laser-camera system, or just the laser, moving transversely, or that the object and light source are stationary and movable mirrors control direction of light which is registered by the optical sensor.

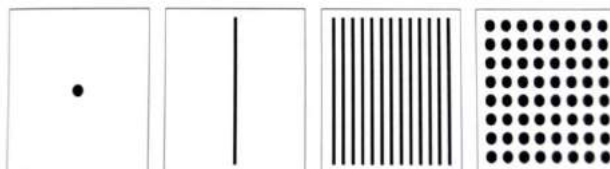


Fig. 2. Types of laser light for scanning objects [6]

The light emitted by lasers and falling on the object may have a different geometric form like point, line, set of lines or points, figure 2.[6] Beam of light outlines the mark on the object what making it possible to obtain information about the distance of reference points. For the measuring of complete surfaces, the projection of single points is very time consuming. If light on the object is in the form of line it is possible to determine distance of more points in a single recording, which speeds up and simplify the process, figure 3.

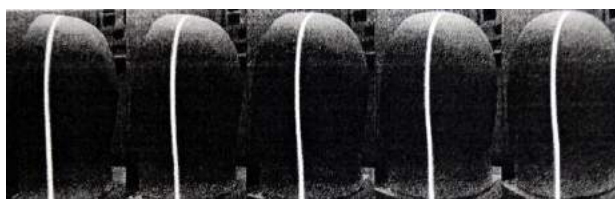


Fig. 3. Object illuminated by light in the form of line

Using lightening forms with a set of lines or dots increases the efficiency of data acquisition. In these three ways of lightening the optical sensor must be in form of CCD matrix.

The movement of the light source and/or optical sensor can be with constant speed or periodically. When moving is at a constant speed optical sensor detects the position of the light area on the object in fixed time intervals. In periodic motion sensor detects the position of lightening area in moment when the light source is not moving.

Scanner software calculates the value of a series of depth, which can be converted to 3D position of points in the scanner coordinate system, using a calibrated position and orientation of light sources and sensors. [7]

Standard methods for data retrieval based on optical triangulation scanning are suitable only for planar objects of uniform reflectance. Curved, unconnected and surfaces with different reflections cause a systematic distortion of the data range. Analysis of space-time can be corrected by each of the objects and achieve much higher accuracy using existing technology. When coherent light is used,

such as lasers, however, appear certain places, stains, which represent the limit for the accuracy of triangulation.

3.1. CAD modeling

From digitized point cloud, obtained by measurement techniques, appropriate algorithm creates surfaces that define border of the scanned object and from topological interior creates a solid model. Modeling objects, in computer graphics, means creation of objects (models) using computers that is, further, may be used for: making constructive documentation, various graphic designs, technological preparation of production (CAP / CAPP / CAM) and engineering analysis.

The process of creating geometrical model consists of: defining the basic geometry of objects and its storage in database. Modeling is process of selection of basic geometric primitives and their primitives, and with connection and composing, by 2D and 3D operations model is formed.

The CAD modeling procedure defines: geometric, functional, material, aesthetic and other properties of objects. Computer graphics uses three types of geometric models: wire frame, surface and volume.

Wireframe model present a set of vertex points and border edges that define the basic characteristic of an object: contour, orientation in relation to the environment and function. Surface model is described by the vertex points, border edges and surface, which enables to define the visibility of graphical entities, creation of clear technical documentation and assemblies. Volume model is described by the apex points, border edges, and adjacent areas of the affected their capacity-solid model.

Basis of presentation of computer graphics, which gives high accuracy model, is approximation of real curved surface by Bézier's surface. Views of geometric models derived approximations of curved surfaces with flat polygons, called Facet models.

4. INTERACTION OF 3D DIGITIZING SYSTEM WITH CIM

The concept of obtaining 3D data depends of technical capabilities and available equipment, which determines the technology of digitization; individual components and corresponding algorithms in the implementation.

Faculty of Mechanical Engineering from Podgorica develops non-contact digitizing systems. The 3D Center on the Faculty, through the "Machine Vision in Automation and Quality Control", for characteristic objects, develops specific software to define the models, and after that their production.

As a source of coherent light for scanning is used semiconductor laser, laser diode K52-267. manufacturers EDMUND Scientifics, with characteristics: power broadcasting 2.5 mW, wavelength 760.1 nm, beam diameter $0.7 \div 1.4$ mm; scattering angle 60° , dimensions $\varnothing 11 \times 62$ mm. On the laser diode is placed generator of line which inlet beam of laser light transfer in the plane at specific angle.

Line generator allows that light falls on the scanned object in the form of line as geometric shapes. Generally the body of laser diode allows putting in the special stand, which can be moving in all three coordinate directions.

For detection of the reflected laser light from the object is used CCD sensor R3GB CFA in digital camera TMC 9700, manufacturers PULNIX AMERICA. The camera is powered by electricity with 110/12V AC adapter, connected to the transformer 220/110V, type MA4150, manufacturer NeBo Electronics.

Camera features: size CCD 8.9×6.7 mm, resolution CCD 768×484 pixels; dimension cell 11.6×13.6 μm . The camera lens is a COMPUTAR G13-85, manufacturer Sigma.

The camera is placed on a stand that allows precise positioning in relation on the workpiece and the laser diode.

As a rotating stand for workpieces is used rotating worktable VMR-320 of universal milling FGU-32, manufacturer MZT Skopje, dimension $\varnothing 320$ mm. By adding a special aluminum strips with the appropriate measures increases positioning accuracy 20 times.

Processing is done on HMC 500/40 Horizontal Machining Center.

Laser is set so that the emitted light line passes through the vertical axis of the rotating base, and camera is positioned from the workpiece at a distance depending on the desired resolution of imaging.

Computer for data acquisition and data processing Compaq Deskpro, with Frame Grabber graphics card ULTRA II RGB, manufacturer Coreco Ltd., connected with the camera over the PCI interface. Image acquisition application is TCi Professional, manufacturer Coreco Ltd. Application allows online display and freeze image from camera.

Effective image analysis and filtering data was performed by rejecting pixels with intensity less than preset level, i.e. setting the intensity of light pixels to zero for all pixels with intensity lower then $P=200$.

Convex surface of the object can cover reflected laser light from the camera lens, it leads to gaps in the images and the absence of digitization.

Light rays passing through the camera lens leads to their unequal refraction on spherical boundary surfaces, which results in deformation of the image. Only the light beam that matches with the optical axis is not distort. In addition, the reason for the deformation can be and construction of CCD sensors. Cells in CCD have rectangular shape. Therefore, it appears compressing images in the direction of smaller size CCD matrix cells, with the coefficient equal one to another dimension of the cells.

Software that provides detection, correction and transformation of coordinates for the purposes of digitalization is Pro/ENGINEER with Pro/SURFACE, Pro/SCAN-TOOLS, Pro/MFG and Pro/NC-POST MODULS, and specific application, developed in 3D Centre Faculty of Mechanical Engineering. This application allows analyzing pictures, forming shapes of surface points, correction, filtration and optimization of data to be used in Pro/ENGINEER software.

Correction of digitized coordinates of points is the inverse process of forming. Deformation covers all pixels, from pictures. But, essential to process are only points that represent the coordinates of the points of structure, which shortens the process of correction.

Coefficient of image correction is the process of determining the validation by which the deformed image pixel transform into pixel non-deformed image. Deformation may occur due to eccentricity axis of optical lens to the center of the CCD sensor.

Images of scanned object with flat surfaces, is shown on figure. 4, and cylindrical surface figure 5. Image processing was performed through a specific algorithm steps: detection of point coordinates, interpolation and correction coordinates of points and optimization of the number of points.



Fig. 4 Visualization of the reconstructed flat surface



Fig. 5 Visualization of reconstructed cylindrical surface

Transformation of coordinates is a process that position of points in a polar-cylindrical coordinate system translated into a rectangular coordinate system.

Reconstruction Program Pro/SCANTOOL as input accepts files created in formats IGES and VDA. Post processing program allows transfer to the control unit of operating the machine.

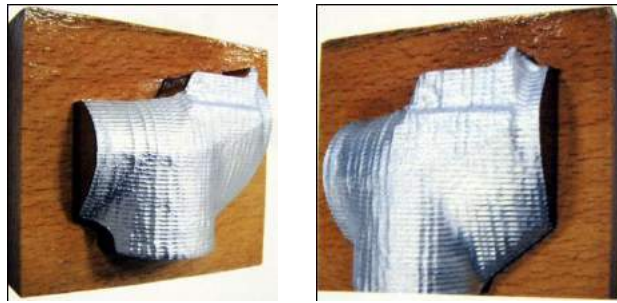


Fig. 6. Processed segment of surface fuel unit

For processing on HMC 500/40 HORIZONTAL Machining Center using three sequences: *Profile Milling* processing by cylindrical cutter; *Conventional Surface - rough surface reconstruction* and *Conventional Surface - finish surface reconstruction*.

5. CONCLUSION

Digitization is used for systematic and accurate collection and processing of data. 3D model represents group of data used to show an object in the 3D virtual space. 3D modeling means the use of polygons or NURBS. Product of 3D laser scanning and photogrammetric scanning is 3D measurable model in the form of cloud points in which every point has a spatial coordinate. For digitalization may be used commercial devices, available equipment and software packages with appropriate customization which guarantee the accuracy of the data collected.

REFERENCES

- [1] Lee K.H., Woo H., Suk T. (2001) *Data Reduction Methods for Reverse Engineering*, The International Journal of Advanced Manufacturing Technology, Vol.17, Springer-Verlag London Limited,
- [2] F. Bernardini and H. Rushmeier (2002) *The 3D Model Acquisition Pipeline*, IBM Thomas J. Watson Research Center, Yorktown Heights, New York, USA, Volume 21
- [3] C. Teutsch (2007) *Model-based Analysis and Evaluation of Point Sets from Optical 3D Laser Scanners*, volume 1, Shaker Verlag
- [4] Schwenke, H. et al. (2002.) *Optical Methods for Dimensional Metrology in Production Engineering*, Annals of the CIRP, 51/2
- [5] Huang M.- C., Tai C.-C. (2000) *The Pre-Processing of Data Points for Curve Fitting in Reverse Engineering*, The International Journal of Advanced Manufacturing Technology 16:635-642, Springer- Verlag London Limited
- [6] Otto K., Wood K. (2001) *Product evaluation: A reverse engineering and the redesign methodology*, Reserch in Engineering Design, Springer, Verlag, London, 1998.
- [7] S. Zhang, P. Huang (2006) *High-resolution, real-time 3-D shape measurement*, Optical Engineering



QUALITY 3D SURFACE RECONSTRUCTION BASED ON POINT CLOUD GENERATED BY OPTICAL MEASURING TECHNIQUES

Milan BLAGOJEVIĆ¹, Miroslav ŽIVKOVIĆ¹, Bojana ROSIĆ²

¹ Faculty of Mechanical Engineering, University of Kragujevac, Sestre Janjić 6, Kragujevac, Serbia
blagoje@kg.ac.rs, zile@kg.ac.rs

² Technical University of Braunschweig, Institut für Wissenschaftliches Rechnen, Hans Sommer Strasse 65,
Braunschweig, Deutschland
bojana.rosic@tu-bs.de

Abstract: *The new products or tools development are often based on already existing products, prototypes or physical models, mostly very complex shapes. Such free form surface can be accurately reconstructed only on the basis of a large number of measuring points. By the classic measuring methods, it is very difficult or impossible to measure sufficient number of points. The digitization is realized by and ATOS measurement systems. A result of digitization with optical measuring system ATOS is detailed polygonized mesh or point cloud.*

Depending on application, creating of the model's surface is carried out with introduction of certain assumptions and approximations, based on knowledge of processing technology of model whose geometry is reconstructed. All commands necessary for reconstruction are placed in CATIA Workbenches under group Shape. The presented procedure is hardware- and time-consuming. It generates accurate digitized object's surface, mathematically defined by NURBS.

Key words: *Optical 3D digitization, 3D surface reconstruction, Reverse Engineering, Product development, CAD/CAM/CAE*

1. INTRODUCTION

In order to satisfy contemporary requirements in the functional, aesthetic and ergonomic reasons products are complex shapes. Tools or new products development are often based on already existing products, prototypes or physical models. In the parts processing, especially in fabrication of pressed parts, sub-areas of the surface resulting from flat sheet metal panels are not transformed in the precisely defined mathematical surface. They should be reconstructed in one of the CAD program in order to obtain a computer model suitable for further design, construction of tools and production preparation.

In this paper, emphasis is specifically placed on accurate reconstruction of the surface of physical model. Number of surface areas is in fact a free form surfaces. From the standpoint of Reverse Engineering (RE), we are trying to describe a lot of sub-areas of the surface by the basic geometric entities: planes, sphere parts, cylinder parts, cones, etc.

Through the shown process, we extract the digital shape of any physical object [1-4]. The physical model of the surface is reconstructed and very accurately describes the complex geometry of manufactured items.

The importance of their implementation is very noticeable in the finite element method, in which the use of these areas to create models that describe the geometry is made, not the ideal obtained by 3D modeling. In practice, it is known that very often geometric imperfections of the real model cause events that would not be caught observing the idealized model - CAD model.

2. 3D DIGITIZING PROCESS

Classic measuring methods provide insufficient number of points for precise products surface reconstruction, because such free form surface can be accurately reconstructed only on the basis of a large number of measuring points. Non contact digitizing is done through optical measuring systems [5], [6], which captures hundreds of thousands of points in a single shot of the object. These measuring results provide very accurate computer reconstruction of shape, and so reduce development time and increase product quality. Reconstruction problems of this sort occur in diverse scientific and engineering application domains.

2.1. Theoretical Background

In order to digitize a 3D surface, at least two different views of the object's surface are necessary. Using the knowledge of the projection matrix of the cameras, it is possible to generate a depth estimate by triangulation. The process of triangulation is well understood, and is fairly straight forward. The accuracy of the triangulation is higher if the angle between the rays is increased, this means that ideally the cameras generating the stereo images should be very far apart. The problem is the finding of the same point on the surface in both images. This is known as the correspondence problem. The correspondence problem is one of the main problems in stereo vision, and there are no fool proof ways around the problem for unassisted vision. By assisting the vision process by using structured light, the correspondence

problem can be greatly reduced though. The structured light method uses a technique where the surface to be digitized is lit by a light source emitting light in a known pattern. This can be achieved by using a projector emitting for example a checker pattern on the surface. This method is most effective when the emitted light is the only light source, and this is often not the case for real environments, and certainly not for outdoor use.

Dense stereo is a relatively simple way to do stereo vision. In its simplest form it tries to match every pixel in one of the stereo images to every pixel in the other picture. This simple form is very ineffective, and is never used in practice. Matches are typically sought on what are called epipolar lines in the pictures. The use of this technique requires that the cameras are mounted side by side, since it assumes that point on the surface will be at the same height on both stereo images. Another way to generate stereo data is sparse stereo, this approach tries to minimize the number of pixels that has to be checked for correspondences, and thereby the correspondence problem by only looking at parts of the images that are likely to be recognizable from one image to another. One such method is looking at the perceived edges or lines in the images.

The main difference between dense and sparse stereo, is that in sparse stereo, comparison is not done on a pixel by pixel basis, but groups of pixels defining a feature. An edge of an object in the image would for example be defined by at least two pixels. The fact that more pixels are involved reduces the correspondence problem, since the comparison is based on more data.

There are several issues that makes problem of finding points in the stereo images that corresponds to the same point on the surface of an object difficult. It is likely that the surface looks different from different angles, this is typically caused by the fact that views from different angles are subject to different lighting conditions. Shiny object for example can look very different from different angles because of the highlight effect on the surface. This problem can be a limiting factor on the distance the stereo cameras can be placed from each other, and thereby the achievable depth accuracy.

In order to convert 2D coordinates in the stereo images to 3D coordinates, a method for intersection of 3D lines has to be used. As long as the correspondence problem is solved, the 2D to 3D conversion should be a fairly simple problem to solve, since it's only a matter of solving simple linear equations.

Once the 3D surface points have been tracked over individual measurements, and their relative positions have been determined to an acceptable level, the collections of tracked points needs to be combined in a way that can represent the surface that is spanned between them.

One representation of the surface is a mesh spanned by the tracked points. In order to generate this mesh, triangles have to be spanned between the tracked points, in a way that fills out the surface between the points. One can think of spanning a graph between the point nodes.

Another simpler method is to augment a quadratic mesh of a given number of nodes, by the known surface points. This could be done by interpolating the mesh points between the known surface points, and on essence wrapping the mesh around the known points.

2.2. 3D Digitizing Workflow by System ATOS

As example, we consider automotive industry part.

In order to meet requirements defined by optical measuring system, object is properly prepared for 3D digitization process. In this measuring project, measuring object is prepared from the point of its application for accurate generation of a point cloud. Measuring project must provide a precise determination of the rotational axis, and allow the determination of the position ATOS sensor in all individual measurements necessary to digitize the complete surface. As the measuring object is not painted, its direct exposure to light source (projector) causes the appearance of too large illuminated (overexposed) areas of measuring images. In order to resolve this problem, the surface is sprayed by material which reduces the degree of reflection. This is done by applying spray titanium-dioxide (TiO₂) on the surface of the object to be digitized.

Based on dimensions of measuring object, required accuracy, and density of the point cloud, it is chosen appropriate measuring volume. The measuring volume is part of the space in front of the measuring sensor where whole measuring object or its part, is placed during the digitization, Figure 1.

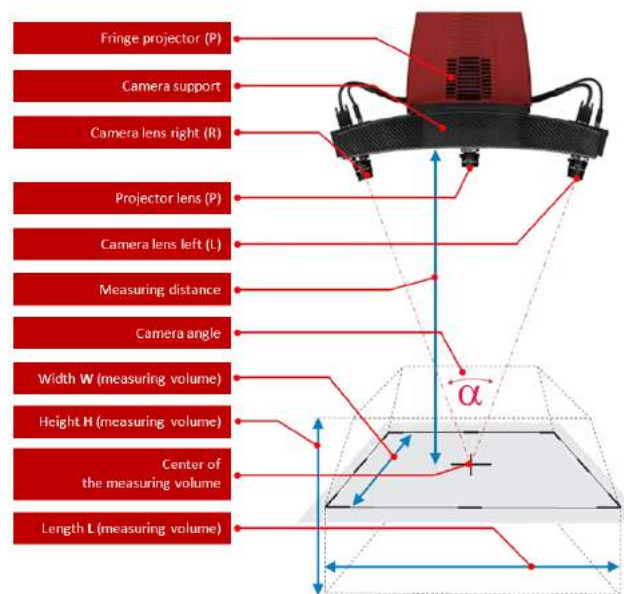


Fig.1. Measuring Volume of Optical Measuring System

ATOS (Advanced Topometric Sensor) [7] is an industrial, high resolution, optical 3D scanner. Instead of measuring single points, full part geometry is captured in a dense point cloud or polygon mesh describing the object's surface and primitives precisely. The ATOS system is a white light optical scanner which scans three-dimensional objects and converts the images to high density point clouds. This allows accurate measurement and capture of the shape and size of the visible surface of almost any 3D object. The scanning is based on optical triangulation and stereo-viewing. A projector is used to project striped fringe patterns onto the object's surface. These images are captured simultaneously by the two measurement cameras from different angles. Throughout multiple individual measurements the entire area is recorded. ATOS digitizing sensor calculates its 3D coordinates based on visible reference objects - uncoded reference points. This

stereo-setup supports an easy and very accurate 3D capturing of the reference objects. Reference point diameter and strategy of points applying to object's surface are function measuring volume used. With the help of digital image processing, 3D-coordinates are computed fast and with high accuracy for up to 4 million camera pixels using the supplied high end System PCs. The captured scan data is then automatically integrated in the predefined reference marker framework.

The additional data captured with two cameras of the ATOS system are used to verify the calibration of the system, detect movements and high ambient light changes during the measurement and verify the matching accuracy of the individual scans into the global coordinate system. Configuration of measuring system for 3D digitizing ATOS, used in digitizing, is given in Table 1.

Table 1. Configuration of Digitizing System

Item	Property
Optical Measuring System	ATOS IIe 400
Sensor Configuration	Measuring volume: 250x200x200 [mm x mm x mm] Reference point size: 3 [mm] Projector lens, focal length: 17 [mm] Camera lenses, focal length: 23 [mm]
Calibration Object	Calibration Panel 250 CP20/MV250x200mm ² , SN: CP20/250/D05470, Aluminium 22.9x10 ⁻⁶ mmK ⁻¹
Application software	ATOS v602

Measuring process is carried out through sufficient number of individual measurements. All individual measurements are made at an angle 45°-60° relative to the plane in which lies the measuring object.

3. 3D SURFACE RECONSTRUCTION

Broadly speaking, the class of problems we are interested in can be stated as follows: Given partial information of an unknown surface, construct, to the extent possible, a compact representation of the surface.

Depending on application, creating of the model's surface implies the introduction of certain assumptions and approximations, based on knowledge of processing technology of model whose geometry is reconstructed. The process of generating NURBS surface consists of procedures for point cloud processing (importing and filtering of points in point cloud, mesh generation, smoothing, cleaning, filling of holes on mesh, decimation and optimization), and procedures for generating smaller surface areas (creating and joining of 3D curves, basic patch creating, creating of surface's parts over patches, filleting, blending and joining of surface's parts).

3.1. Point Cloud Processing

Point cloud is imported in Open Source software MeshLab. Cleaning of mesh, removing spikes, discontinuities and other errors in point cloud is done in

order to make regular mesh. Next, polygonized mesh is generated, over resulting point cloud. Triangulated mesh consists of 42570 points and 85140 triangles, Figure 2. In many cases the reconstructed model contains too many elements (triangles, edges, vertices) to be amenable for further processing. A widely used method decimates the model by contracting edges with their incident triangles.

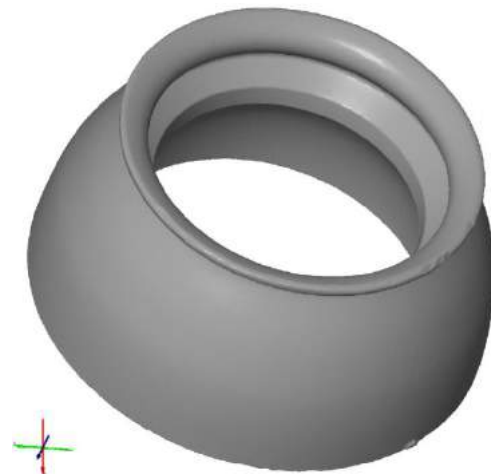


Fig.2. Point Cloud generated by Optical Measuring System ATOS

All these phases include some distortion in working data, so software ATOS and MeshLab have possibility to compare mesh with source point cloud (which very precisely describes digitized surface) in form of labels, sections or complete deviation field.

Point Cloud generated by Optical Measuring System ATOS is located in random coordinate system, Figure 2. Model transformation in an appropriate coordinate system is performed using 3-2-1 transformation, Figure 3.

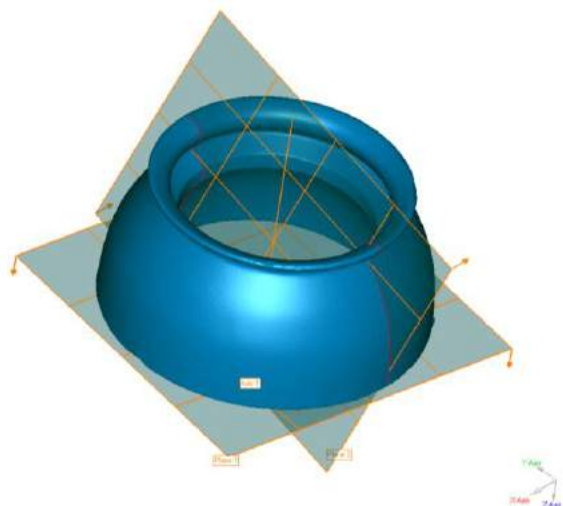


Fig.3. 3-2-1 Transformation

3.2. 3D Surface Generating

The creation of the accurate surface approximation is a complex task, and therefore fairly hard to solve. 3D surface reconstruction is performed in software CATIA V5. All significant commands are placed in Workbenches under group Shape (Digitized Shape Editor, Quick Surface Reconstruction, Generative Shape Design, Free

Style, ICEM Shape Design, and Automotive Class A). Fully Reverse Engineered model is depicted in Figure 4.



Fig.4. Reconstructed NURBS surface based on digitized data

Since surface was then modeled using a combination of 3D CAD packages, to make sure the CAD data fit the scan data in the needed tolerance ATOS software built-in quality checking tools provide immediate visual quality control. Deviation checking between surfaces or curves and underlying polygon mesh is performed, Figure 5. Deviation is calculated as shortest (normal) distance between reconstructed and scanned surface.

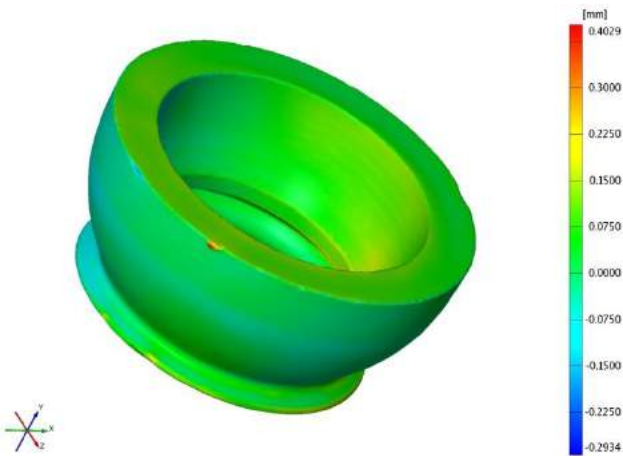


Fig.5. Deviation of as built to the Reverse Engineered Surface as a color coded cloud of data

4. CONCLUSION

The world's leading PLM software integrate modules for handling and processing of the point cloud, and then generating of the surface over the cloud. This fact points to the importance of this topic in the industry and R&D.

This article presented the development of a model to fit 3D surfaces to point clouds acquired by a non-contact optical sensor. In other words, problem is to digitize outlines and reconstruct the three-dimensional surface of the structure of interest.

It is presented and discussed a technique to generate 3D surfaces from point clouds by using parametric NURBS

surfaces in CATIA software. The construction of a proper 3D triangulated mesh has essential impact on reconstruction process.

This method offers: (a) Quick and accurate data capture (even of a relatively large object), (b) Confidence that the data reflects the "as built" state, (c) Data that can readily be imported into the desired CAD software for planning and design purposes, and (d) Savings in time and cost compared to more traditional methods.

The integration of ATOS in industrial development and production processes helps: (a) Reduce production start-up times, (b) Optimize component quality, (c) Speed up the time to production, (d) Maintain high level of quality assurance throughout the entire manufacturing process, (e) Establish early trend analysis within series production processes, (f) Reduce rejects and rework, thus saving valuable time and money, and (g) Automated quality control; improving overall quality assurance, requiring fewer personnel and considerably increasing performance. Results showed that the system accuracy is fairly enough to guarantee excellent quality with sub-micron errors.

ACKNOWLEDGMENTS

The part of this research is supported by Ministry of Education and Science, Republic of Serbia, Grants TR32036 and III41007.

REFERENCES

- [1] Živković M., Blagojević M., Rakić D., (2007), (2008), (2009), (2010) *The annual report on the use of received and installed capital equipment: 3D Digitization Systems ATOS Iie and TRITOP*, Ministry of Science and Technological Development of the Republic of Serbia, Faculty of Mechanical Engineering in Kragujevac, Kragujevac
- [2] Živković M., Blagojević M., Rakić D., (2007) *Report on the performed digitization of assemblies by 3D Digitization Systems ATOS Iie and TRITOP*, Zastava Auto, Faculty of Mechanical Engineering in Kragujevac, Kragujevac
- [3] Blagojević M., Rakić D., Živković M., Bogdanović Z., (2008) *Digitizing and Optical Measuring in Automotive Industry*, International Congress Motor Vehicles and Motors 2008, Kragujevac
- [4] Blagojević M., Živković M., (2011) *Algorithm for 3D Surface Reconstruction based on Point Cloud generated by Optical Measuring Techniques*, Mobility and Vehicle Mechanics, Vol.37, No.1, pp. 63-77, ISSN 1450-5304
- [5] ATOS User Information, ATOS Iie and ATOS Iie SO (as of Rev. 01) Hardware, (2008) GOM mbH, Braunschweig, Germany
- [6] ATOS User Manual Software, ATOS v6.01, (2008) GOM mbH, Braunschweig, Germany
- [7] Blagojević, M., (2009) *Application of optical measuring systems in modeling and simulation (in Serbian)*, Faculty of Mechanical Engineering, University of Kragujevac



TOWARDS DIGITAL TEMPLATE FOR ARTIFICIAL HIP IMPLANTS SELECTION

Goran DEVEDŽIĆ¹, Suzana PETROVIĆ¹, Saša ĆUKOVIĆ¹, Branko RISTIĆ^{2,3}, Zoran JOVANOVIĆ³, Miloš ĆIROVIĆ¹

¹Faculty of Mechanical Engineering, Sestre Janjić 6, Kragujevac, Serbia

²Faculty of Medicine, Svetozara Markovića 69, Kragujevac, Serbia

³Clinical Centre Kragujevac, Clinic for Orthopedics and Traumatology, Zmaj Jovina 30, Kragujevac, Serbia

devedzic@kg.ac.rs, suzana.petrovic@mfgk.rs, cukovic@kg.ac.rs, branko.ristic@gmail.com,

zjovanovic@medf.kg.ac.rs, cirovic.milos@gmail.com

Abstract: Technology of so-called “digital templating” is based on 3D parametric models of femur and endoprosthesis of hip. It is aimed in pre-operative planning, primarily for artificial hip implants selection, as well as visualization tool for other surgical activities planning. Parametric master model of a femur is developed from a series of 2D and 3D images obtained by different scanning methods, which include both X-ray based and optical. In that course, for the initial model we use optically scanned 3D images of cadaveric bones and their educational replica. Generated clouds of points are optimized during reconstruction process to ensure proper polygonization and creation of surface and solid models. Parametric definition of a femur uses a set of cross-sectional parameters that provide anatomically consistent individualization (customization) of the master model. Family tables for different designs of endoprosthesis are also developed. The process of artificial hip implants selection assumes automatic positioning of a stem into femoral channel during which developed control mechanism calculates both the overlapping volume and the clearance between cortical bone and the stem. Depending on individual characteristics of a patient and orthopedic surgeon preferences the system ranks the alternatives and visualizes the correspondent data and solutions.

Key words: Free-form modeling, reverse engineering, femur, endoprosthesis

1. INTRODUCTION

Planning of the surgery and the choice of type and size of the implant is a very important part of preoperative preparation of patients prior to installation hip arthroplasty. Total hip replacement (THR) is one of the most applied surgical operations today, aiming in elimination of pain and restoring gait capabilities. In a total hip replacement, both acetabular and femoral head are replacing by metal and plastic parts [1]. Traditionally, orthopedic surgeon uses transparent foils of the stem and acetabular cup together with X-ray film for selection of proper implant type and sizes [1], [3]. Extensive development of the computer assisted surgery (CAS) techniques brings new abilities and much more precise procedures [4], [7-9]. We present new approach to so-called *digital templating* of the THR preoperative planning, based on 3D parametric model of the proximal femur and hip endoprosthesis.

2. PARAMETRIZATION OF FEMUR AND PROSTHETIC IMPLANTS

2.1. Femur reconstruction

The approach to the reconstruction of the scanned object's surfaces depends on their geometrical regularity, i.e. whether these have proper shapes or represent free-form (sculptured) shapes. The algorithm of sculptured surface

reconstruction is shown in Fig. 1. and consists of three complementing phases: the points phase, the polygon phase, and the surface phase.

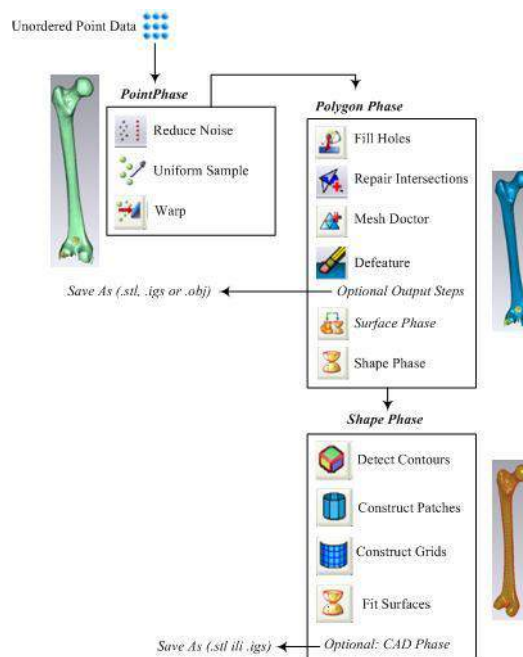


Fig.1. The algorithm of sculptured surfaces reconstruction

During scanning process a measurement system generates cloud of points that represents the shape of the scanned object. We used ATOS IIe optical measurement system. Points phase usually involves optimization and reduction of the number of discrete shape samples in order to simplify the representation of an object for further application, keeping its consistency and meaningfulness [2], [6].

Conversion of optimized cloud of points generates polygonal model of the shape. This phase ensures the detection, removal, repair and relaxation of the set of polygons (triangles) and determines the level of smoothness of the polygonal surface through noise reduction.

The surface phase results in the creation of NURBS-based surface model using the smoothed grid of the polygonal model. After the refinement, surface model is ready for further application, which includes solid modeling, analysis, etc. [4-5], [7-8].

2.2. Definition of femur axes

Parameterization of a femur is based on determination of characteristic cross sections and the set of sufficient number of the parameters that describe femur's shape in anatomically consistent way. We present the approach to femur axis determination that uses the set of the centers of gravity for the each characteristic femoral cross section (Fig.2). The femur axis consists of the two counterparts, namely shaft's axis and neck's axis, which are fitted to the set of characteristic points and smoothed.

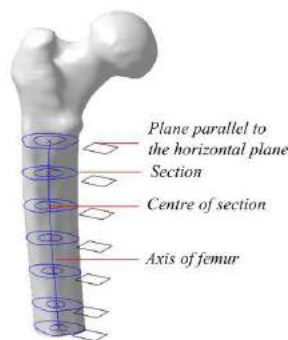


Fig.2. Axis of a femur's shaft

From the anatomical point of view, femoral head has spherical shape. Determination of the neck and head axis requires the point of the head's center, as well as the set of other spatial geometrical entities shown in the frontal (Fig.3) and horizontal planes (Fig.4).

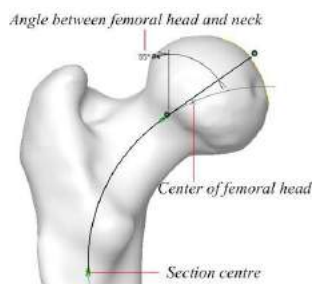


Fig.3. Axis of a femur's neck in the frontal plane

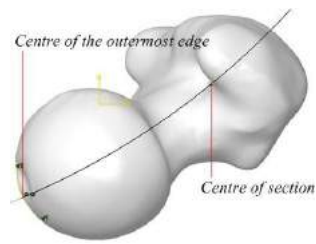


Fig.4. Axis of a femur's neck in the horizontal plane

2.3. Parameterization of the femur

The femoral axis is the support for the cutting planes that generate cross sectional profiles. The cutting planes are normal to the smoothed axis in the points of the aforementioned characteristic set (Fig.5).

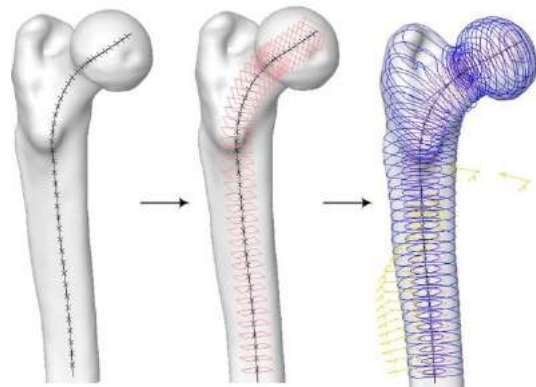


Fig.5. Femoral cross sectional profiles

In order to provide individualization (customization) of the master model the appropriate scaling is required. Analyzing the anatomical features given in the [3], [4], [5], [7] we have adopted the parameters, their values and ranges. Using the ranges and the extreme values in the characteristic femoral cross sections we have calculated scaling coefficients shown in the Table 1. To prevent violation of anatomical consistency during customized scaling we introduce the set of rules that have the role of control mechanism.

Table 1. Scaling coefficients in the characteristic cross sections

	Region and scale factor
	Neck shaft angle (ACD)
	Offset (TAC)
	Head diameter (A)
	RA: from 0.79 to 1.50
	Metaphyseal width (D)
	RD: from 0.71 to 1.56
	Metaphyseal width (G)
	RG: from 0.59 to 1.41
	Metaphyseal width (E)
	RE: from 0.76 to 1.79
	Metaphyseal width (F)
	RF: from 0.78 to 1.83
	Intramedullary diameter (B)
	RB: from 0.56 to 1.77
	Extramedullary diameter (B')
	RB': from 0.82 to 1.47

3D parametric-based geometry of a femur, which creates so-called master model capable to adapt to customized anatomic values of each individual patient, results from blending operation applied to cross sectional profiles along femoral axis under rules of control mechanism. Figure 6 shows outer 3D geometries of femoral cortical (a) and trabecular (b) bone.

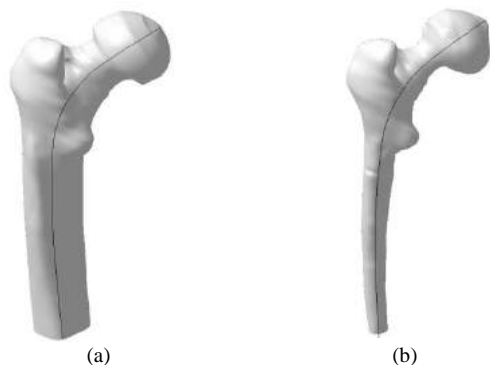


Fig.6. 3D geometry of cortical (a) and trabecular (b) bone

2.4. Implants parameterization

The model of an implant is defined by the set of parameters, which directly affect the selection process [3-5], [7], [8]. The most influential are stem shaft diameter (A), length (B), neck length (D), and offset (C) (Fig.7). These parameters, together with other ones that completely describe implant design, define the family table, i.e. the set of implants' models available on the market, specific for a particular manufacturer, or the most frequently used in a certain clinic.

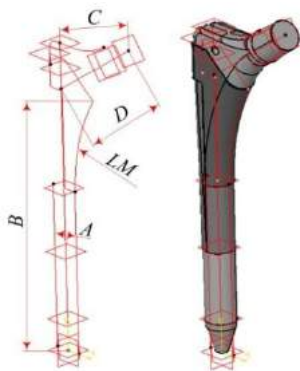


Fig.7. Skeleton model of a stem

The same procedure is applied for other parts of artificial hip prosthesis.

3. DIGITAL TEMPLATE

The implant selection by comparing the radiological images and implant film, although the most frequently used, has its own deficiencies. One of the main drawbacks relates to the enlargement in radiographs, which may not

necessarily be in proportion to the real case, causing mismatching during the operation. Development of 3D digital template aims in more precise and reliable pre-operational planning.

Prior the implantation of a stem medullary cavity is reamed in order to extract the marrow and properly shape the stem shaft intramedullary seat. Reamed medullary cavity has straight axis that matches implant's axis, while intramedullary canal matches spatial femoral axis. Hence, spatial axis of metaphysis should be approximated by a straight line, and additionally set user defined planes that define femoral anteversion angle required for proper implant insertion (Fig.8).

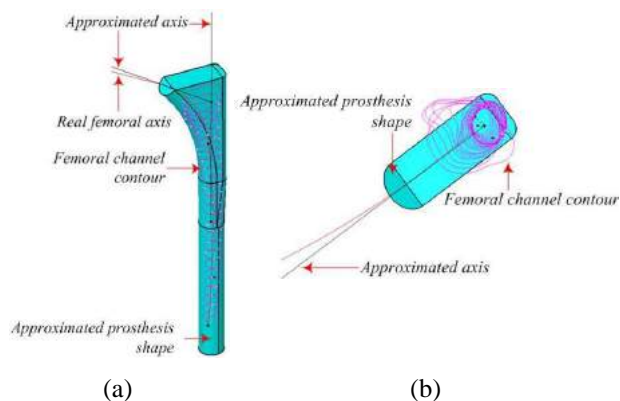


Fig.8. Profile of intramedullary canal and the model of a reamer: a) isometric view, b) horizontal plane view

Since the reamer has the regular shape, in the contrary to intramedullary canal that has irregular shape, one of the important criteria in reamer shape and size selection is to satisfy that the reamer profile tightly circumscribe the canal's contour edges (Fig.9). This criterion should be fulfilled at as many cross sections along femoral axis as possible. Control mechanism performs the optimization of the selection process.

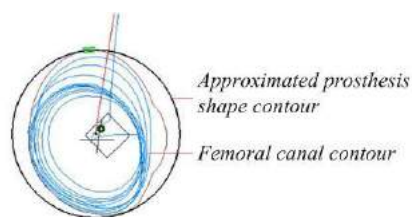


Fig.9. Matching reamer size

Customization of the generic model of a femur requires inputting parameters' values (Tbl.1) by measuring correspondent distances on radiographs (film or digital format) (Fig.10a). According to the rules of the control mechanism, the master model regenerates the master models of femur and implant (Fig.10b,c).

Selection process uses implants' family table to choose between available alternatives that suits current parameter

¹ Goran Devedžić, PhD, Faculty of Mechanical Engineering, Sestre Janjić 6, Kragujevac, Serbia, devedzic@kg.ac.rs

² Suzana Petrović, PhD student, Faculty of Mechanical Engineering, Sestre Janjić 6, Kragujevac, Serbia, suzana.petrovic@mfkg.rs

³ Saša Ćuković, PhD student, Faculty of Mechanical Engineering, Sestre Janjić 6, Kragujevac, Serbia, cukovic@kg.ac.rs

⁴ Branko Ristić, PhD, Faculty of Medicine, Svetozara Markovića 69, Kragujevac, Serbia, branko.ristic@gmail.com

⁵ Zoran Jovanović, Clinical Centre Kragujevac, Clinic for Orthopedic and Traumatology, Kragujevac, Serbia, zjovanovic@medf.kg.ac.rs

⁶ Miloš Ćirović, PhD student, Faculty of Mechanical Engineering, Sestre Janjić 6, Kragujevac, Serbia, cirovic.milos@gmail.com

values and surgeon preferences. In addition, rules of the control mechanism check for other constraints and anatomical/surgical consistency – for instance, an average clearance between walls of intramedullary canal and stem body should be within preferred value (Fig.11). By comparing the geometry of customized femur and intramedullary canal shape the built-in rules search for optimal size and shape of the implant. Finally, the control mechanism provides the alternatives ranking.

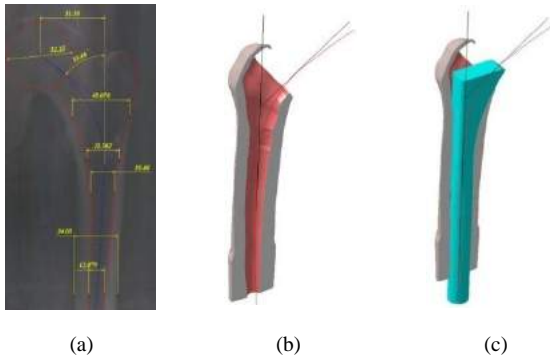


Fig.10. Regeneration of the master models: a) radiograph of a proximal femur, b) master model of femur, c) matching master models of femur and implant



Fig.11. Checking the implant alternative

Confirmation of the optimality of selected implant is performing by analysis of stem fitness in different cross sections along femoral axis, in horizontal and/or frontal plane (Fig.12).

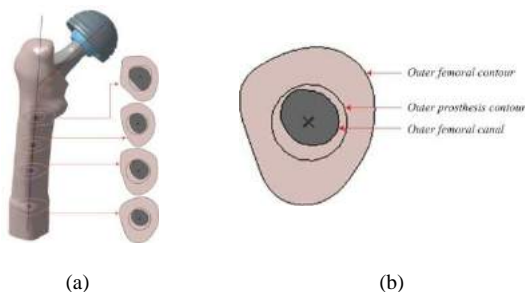


Fig.12. Stem fitness in different cross sections

Final stage of implant selection involves analysis of estimated bone mass that will be removed during reaming and medullary cavity preparation for stem insertion. Figure 13 shows an estimated bone mass of 9 grams, as well its distribution along the intramedullary canal.

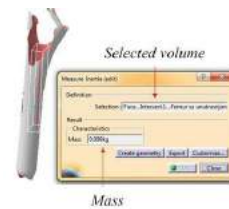


Fig.13. Estimated removed bone mass and its distribution

4. CONCLUSION

Technology of so-called digital templating provides more precise preoperative planning of total hip arthroplasty. The methodology uses master (generic) parametric models of femur and implants that automatically regenerate upon entering customized anatomical values of the proximal femur parameters. Automated procedure for the analysis of shape and size of the prosthesis provides its optimal selection in each individual case. Furthermore, the analysis may yield to determination of an implants' ideal shape and size that supports the custom-based prosthesis manufacturing.

In addition, the whole methodology may be used in solving biomechanical problems (stress analysis, deformations), prosthesis production, and education.

ACKNOWLEDGMENT

The results of this research are the part of the project supported by Ministry of Science of Serbia, Grant III-41007.

REFERENCES

- [1] WIESEL W.S., DELAHAZ N.J. (2007) *Essentials of Orthopedic Surgery*, Springer, London
- [2] GONZÁLES C.R., WOODS E.R. (2008) *Digital image processing*, Prentice Hall
- [3] BREUSCH J.S., MALCHAU H. (2005) *The Well – Cemented Total Hip Arthroplasty*, Springer, Berlin
- [4] SCHONNING A., OOMMEN B., IONESCU I., CONWAY T. (2009) Hexahedral mesh development of free-formed geometry: The human femur exemplified, *Computer-Aided Design*, Vol.41, pp.566-572.
- [5] LAINE H.J., LEHTO M.U.K., MOILANEN T. (2000) Diversity of Proximal Femoral Medullary Chanal, *The Journal of Arthroplasty*, Vol. 15
- [6] PARK H. (2005) A hybrid approach to smooth surface reconstruction from 2- D cross sections *Int J Adv Manuf Technol*, Vol 25, pp 1130 - 1136
- [7] ADAM F., HAMMER D. S., PAPE D., KHON D. (2002) Femoral anatomy, computed tomography and computer – aided design of prosthetic implants, *Arch Orthop Trauma Surg* Vol122, pp 262 – 268
- [8] GRACIA et al. (2010). Study of bone remodeling of two models of femoral cementless stems by means of DEXA and finite elements, *BioMedical Engineering OnLine*, pp. 9-22.
- [9] Stojkovic M., Trajanovic M., Vitkovic N., Milovanovic J., Arsic S., Mitkovic M. (2009) Referential geometrical entities for reverse modeling of geometry of femur, *Computational Vision and Medical Image Processing - VipIMAGE 2009*, Porto, Portugal, 14.-16. October.



METHODS FOR CREATING GEOMETRICAL MODEL OF FEMUR ANATOMICAL AXIS

Nikola VITKOVIĆ¹, Jelena MILOVANOVIĆ¹, Miroslav TRAJANOVIĆ¹, Nikola KORUNOVIĆ¹, Miloš STOJKOVIĆ¹, Miodrag MANIĆ¹

¹ University of Niš, Faculty of Mechanical Engineering in Niš, A. Medvedeva 14, Niš, Serbia
vitko@masfak.ni.ac.rs, jeki@masfak.ni.ac.rs, nikola.korunovic@masfak.ni.ac.rs, traja@masfak.ni.ac.rs, miloss@masfak.ni.ac.rs, mmanic@masfak.ni.ac.rs

Abstract: *The two methods for creation of the CAD model of the anatomical axis of femur will be presented in this paper. These methods are: GCM (Gravity Center Method), and CPM (Curve Projection Method). Both methods enable creation of femur anatomical axis geometrical model, which is based on data acquired from the medical imaging devices (CT, MRI, X-Ray). The basic difference between these two methods and the other applied for the geometrical modeling of femur anatomical axis is in the manner of generating the points through which 3D curve passes (or goes near). The technique applied is developed considering the natural shape of the femur bone, and not just by using standard CAD techniques for geometrical modeling which are common in standard engineering. The application of these methods can be extended to other bones in human body as in the fast creating of the model for the use in planning orthopedic operations, the input models for rapid prototyping, designing of implants, etc.*

Key words: *Anatomical axis, femur shaft, surface, curve, geometrical model*

1. INTRODUCTION

The main goal of this research is to develop CAD modeling method which enables creation of accurate geometrical model of the anatomical axis of femur (3D curve). The other important goal is to cultivate a method which is easy and quick to perform. Previous studies show that it is difficult to achieve these goals simultaneously, as the realization of one may obstruct the realization of the other. This paper presents two different methods which attempt to accomplish the appointed goals to the greatest extent possible. These methods are:

- GCM (Gravity Center Method) which conforms to the anatomical, morphological and geometrical properties of the femur,
- CPM (Curve Projection Method) which conforms to the position, topology and geometrical properties of the femur.

1.1. The geometrical analysis and construction

The geometrical analysis of the femur (shaft) is based on the reverse modeling of the scanned samples by CAD (computer-aided design) software. The reverse modeling begins with importing the coordinates of the points of scanned tissue (from CT) into the appropriate CAD software. The next step is to create a valid polygonal model by using CAD software features and to define referential geometrical entities (detailed explanation of RGE in [1] by Milos et al.). The final step is to apply methods for the creation of valid geometrical model of femur anatomical axis.

1.2. The comparative values

To check the integrity of the developed method adequate dimensions were chosen, and the comparison was made with the already established and determined values in anatomy, orthopedic surgery and practice (presented by Cong-Feng Luo in [2]). For this analysis three angles were measured and compared:

- Anatomical Axis – Neck axis (AN), mean value about 126°
- Distal condylar angle – (DC), mean value about 81°
- Anatomical axis – Mechanical axis (AM), mean value about 6° - 8°

Angles were measured in Anterior Posterior plane [1] of the femur bone model. These angles were chosen since they are often used in clinical anatomy and surgery to determine the proper position and orientation of lower limb bones.

1.3. The possible benefits

The developed methods can have multiple benefits (or uses) in medicine and technology. The geometrical model (3D curve) of the anatomical axis of femur can be used for the creation of the femur shaft surface model, or to define femur geometry, position and orientation, as it is presented in [3] by Cong-Feng Luo et al. The latter can be used to create a 3D solid model for the purpose of studying different aspects of stresses on the femur itself, by a finite element analysis, as presented in [4] by Hsu RWW et al.

Besides that, the 3D curve and the surface model of the femur shaft can be used to analyze the use of different aspects of implants in surgery of the skeletal system.

1.4. The current research in this field

The methods for developing femur anatomical axis are presented and adequately described by Cong-Feng Luo in [2], and Morland JR et al. in [5]. These methods use two points for anatomical axis definition. One point is defined as the center of the knee, while other can be the center of the knee, or the point which is 10 cm away from the surface of knee joint, midway between the medial and lateral surfaces [2]. The line created between two points is always linear, thus, it does not follow the shape of the femur shaft in a natural way. Presented methods use more points on the femur shaft for the creation of the 3D curve, and enable creation of a more natural anatomical axis. Of course, a 3D curve created in this manner can have complex shape, but it can be approximated with the linear curve which can be more precise than the line created only through two points.

The creation of solid models from data acquired from medical imaging methods (in this case MRI) is well described in [6] by Stephen Fening. The principles described in that thesis, are general principles for geometrical modeling based on medical data, and they can be applied for various types of models creation, as it is the case in this research.

2. MATERIALS AND METHODS

The geometry analysis of the femur shaft included 10 scans of femur samples. Samples were scanned by computer tomography (CT) in the resolution of 0.5mm. The samples were obtained from European adults, intentionally including different gender and age: 4 women samples, both right and left, age 25, 33, 45, 67, 6 men samples, both right and left, age from 22 to 72. It was assumed that this diverse set of samples could present quite a diverse morphology of the very same bone.

2.1. GCM (Gravity Center Method)

This method uses same principle as the one described in [2], although with some differences. Instead of using only two points for anatomical axis creation, more points are used in this method. These points are gravity centers of the femur's body cross-sections, Fig 1. The procedure for creating anatomy axis of the femur is somewhat complex, and contains several steps, which are:

1. Creating basic RGE's (Referential Geometrical Entities) on the femur model. This procedure is described in [1] in more detail,
2. Creating plane of intersection (POI) which is plane normal to the AP (Anterior Posterior) plane. The process of creating AP plane is explained in [1],
3. Creating femur's body cross sections, which are cross sections between planes parallel to POI and femur's polygonal model, Fig 1, 2,

4. Defining gravity centers of each cross section, Fig 1.,

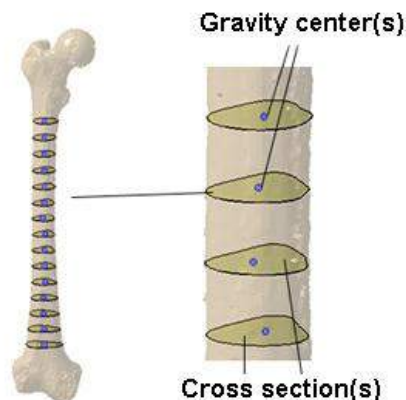


Fig 1. Femur body cross sections for the GCM

5. Creating 3D spline curve using near operator, with gravity center points as reference, Fig 2.

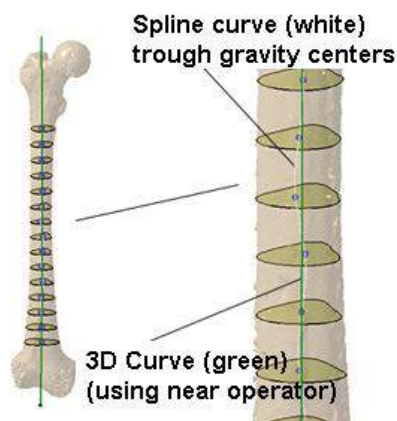


Fig 2. 3D spline curve (anatomical axis) for the GCM

6. Extrapolating curve at end points towards the hip and tibia (tangent extrapolation).

The result of this process is a 3D spline curve which is actually the model of femur anatomical axis in 3D space. The measuring of three angles is done in AP plane, with projected anatomical and mechanical axis. AN angle is measured between the projected neck axis and the line tangent to the anatomical axis projection in AP plane. AM angle is measured between the projected mechanical axis and the line tangent to the anatomical axis in the point of its intersection with the mechanical axis. DC angle is measured between the tangential line of distal femur and the projected anatomical axis, Fig 3. To confirm that this method is usable, the procedure is performed on ten femur specimens. The values for three defined angles are presented in the Table 1.

Data in Table 1. show that angles are in the appropriate range (compared to study in [2]). Conclusion follows that this is an adequate procedure for creation of the femur's anatomical axis. For some bone models there is a possibility for vast angle(s) deviation; however, this is usually the case when a bone model is inadequate, perhaps due to: bone illness, wrong input data, osteoporosis, etc.

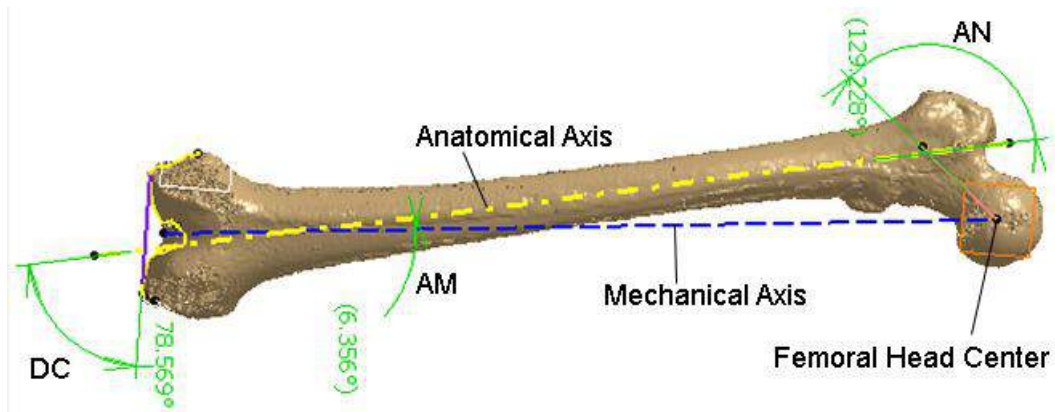


Fig 3. Adequate Femur dimensions (angles) defined on the femur polygonal model

Table 1. Angle values for different femur models (GCM)

Angle\Femur	1	2	3	4	5	6	7	8	9	10	Mean
AN	127.1	129	127	127	126	124.9	127.2	126.4	127.20	129.23	127.10
AM	8.36	7.61	7.86	8	3.4	7.8	8	7.6	7.56	6.36	7.26
DC	81	80.54	82.22	78.96	80.86	79.9	79.7	82	80.33	78.57	80.41

2.2. CPM (Curve Projection Method)

This method uses a different procedure for defining femur's anatomical axis than standard methods do, as it is described in [1-3, 5]. Generally, the idea for this procedure emanated from the CPM method when cross sections geometry was analyzed. The analysis shows that topology and geometry of cross section curves are very similar to the deformable ellipsis, Fig2. Using that as a starting point for analysis, one can say that cross sections can be projected into two normal planes. These planes contain axes of ellipse, and they are normal to the cross section plane. In the normal plane, cross section is projected as a line, which is actually the axis of ellipse. Middle point of the line is actually the center of ellipse, and end points are the end points of the ellipse axes in appropriate directions, Fig 4. The procedure for this method is:

1. Defining position and orientation for the plane of intersection (POI). This plane is one of the initial planes (PX, PY, PZ) of the imported polygonal model.
2. Creating femur's body cross sections, which are cross sections between planes parallel to POI and femur's polygonal model, Fig 4,
3. Projecting cross section curves to the two perpendicular planes,
4. Finding middle points of the projected curves (lines),
5. Creating 2D spline curves in the normal planes using near or through operator (which depends on quality of curves) with middle points as reference, Fig 4,
6. Extrapolating 2D curves in tangent directions, Fig 5,
7. Creating surfaces as extended 2D spline curves in directions normal to the perpendicular planes, Fig 5,
8. Defining 3D spline curve as a result of the surfaces intersection, Fig 5.

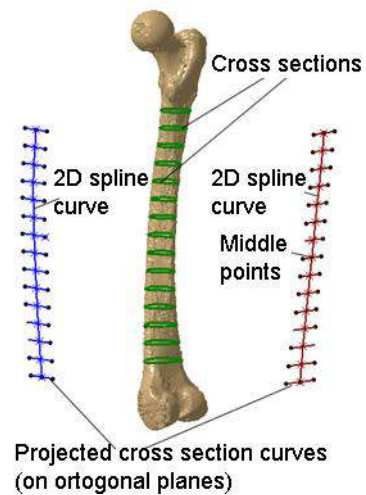


Fig 4. 2D Spline curves and projected cross section curves (on orthogonal planes)

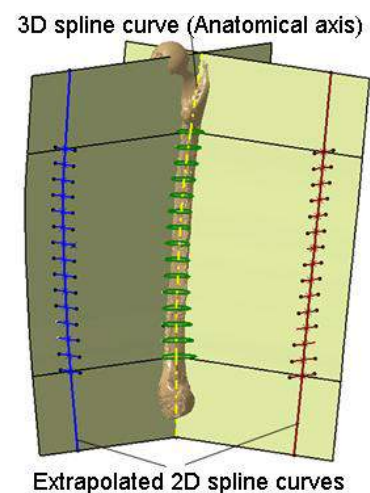


Fig 5. 3D spline curve (anatomical axis) for the CPM

Table 2. shows that angles are in the adequate range, with some deflections (compared to study in [1]). Conclusion follows, that this method is appropriate for anatomical axis creation.

Table 2. Angle values for different femur models (CPM)

Angle\Femur	1	2	3	4	5	6	7	8	9	10	Mean
AN	129.93	131.14	126.93	137.56	133.59	124.9	127.2	126.4	128.12	132	129.78
AM	6.36	8.78	11.21	8.85	5.94	7.8	8	7.6	7.82	9.6	8.20
DC	78.27	79.4	79.47	78.12	78.31	79.9	79.7	82	79.12	79.5	79.38

3. RESULTS AND DISCUSSION

Table 1. and Table 2. show different values for defined angles of ten femurs. It can be seen from the tables, that values are in good range, but there are some deviations. For example in Table 2, there is a major digression in AN angle, 137.56 (CPM). This kind of digression can occur with some femurs due to: a defective femur model, an unhealthy or a deformed femur, etc. That’s why arithmetic mean is used for calculating angle values, since it can describe general case, and not an individual occurrence. According to the measurement results (Table 3.), a conclusion follows that GCM method has an advantage in Anatomical axis – Neck axis angle, and in Distal Condylar Angle (but much less difference compared to the Anatomical axis – Neck axis angle). The angle between Anatomical axis and Mechanical axis has a similar value in either method. The general conclusion follows that both methods can be applied. However, if precision is the most important condition, then the first method is a better choice, while if the speed of creation is the main factor, then the second method ought to be used (there is no need for RGE’s definition, which is a time consuming process).

Table 3. Angle mean values for GCM and CPM

Angle \ Method	GCM	CPM
AN	127.10	129.78
AM	7.26	8.20
DC	80.41	79.38

4. CONCLUSION

The presented research describes a new approach that will help to clearly comprehend the geometry of the femur’s shaft region (especially the cross section geometry) and, therefore, the geometry of the femur, too. Furthermore, this can improve the design of new implants, taking into consideration their anatomical landmarks, structure and distribution of their bony tissue, and stresses. Finally, the new way of looking at femur shaft can improve the surgery preparation and make it more efficient [7-9]. The methods described in this paper will be tested on more femur specimens, and this does not imply only the amount of specimens, yet, their more comparative values (dimensions), different geographical region, various age groups, etc.. The main reason for further testing is the possibility for creation of one universal method for femur anatomical axis definition, which will produce accurate results regardless of the input data.

ACKNOWLEDGEMENT

The paper presents a case that is a result of application of multidisciplinary research in the domain of bioengineering in real medical practice. The research

project (Virtual Human Osteoarticular System and its Application in Preclinical and Clinical Practice) is sponsored by the Ministry of Science and Technology of the Republic of Serbia - project id III 41017 for the period of 2011-2014.

REFERENCES

- [1] Stojkovic, M., Trajanovic, M., Vitkovic, N., Milovanovic, J., Arsic, S., Mitkovic, M. (2009) Referential Geometrical Entities for Reverse Modeling of Geometry of Femur, Vip Image 2009, Porto, Portugal.
- [2] Cong-Feng, Luo. (2004) Reference axis for reconstruction of the knee, The Knee, Vol.11, No 4, pp 251– 257
- [3] Cong-Feng, Luo., Koshino, T., Takeuchi, R., Saito T. (2001) Reliability of the transepicondylar line as a parameter of femoral axial alignment, Journal of Orthopaedic Science, Vol. 6, No 5, pp 373 – 377.
- [4] Hsu, RWW., Himeno, S., Coventry, MB., Chao, EY. (1990) Normal axial alignment of the lower extremity and load-bearing distribution at the knee, Clinical Orthopaedics and Related Research, Vol. 255 pp 215– 227.
- [5] Morland, JR., Bassett, LW., Hanker, GJ. (1987) Radiographic analysis of the axial alignment of the lower extremity, Journal of Bone and Joint Surgery, Vol. 69, No 5, pp 745-749.
- [6] Fening, S. (2003) The creation of solid models of the human knee from Magnetic resonance images, Doctor thesis, The faculty of the Fritz J. and Dolores H. Russ College of Engineering and Technology of Ohio University, pp 41
- [7] Kharwadkara, N., Kent, R.E., Shararab, K.H., Naiquec, S. (2006) 5° to 6° of distal femoral cut for uncomplicated primary total knee arthroplasty : Is it safe?, The Knee, Vol.13, No 1, pp 57 - 60
- [8] Dargel, J., Joern, M., Feiser, J., Ivo, R., Koebke, J. (2010) Human Knee Joint Anatomy Revisited: Morphometry in the Light of Sex-Specific Total Knee Arthroplasty, Journal of Arthroplasty, Vol. 26 , No 3, pp 346 - 353
- [9] William, M., Boyle, J., Clark, L., Krackow, Kenneth A. (2005) The Variability of Intramedullary Alignment of the Femoral Component During Total Knee Arthroplasty, Journal of Arthroplasty ,Vol. 20, No 1, pp 25 - 28



METHOD FOR CREATING 3D SURFACE MODEL OF THE HUMAN TIBIA

Marko VESELINOVIC¹, Dalibor STEVANOVIC¹, Miroslav TRAJANOVIC¹, Miodrag MANIC¹, Stojanka ARSIC², Milan TRIFUNOVIC¹, Dragan MISIC¹

¹Faculty of Mechanical Engineering, University of Nis, Aleksandra Medvedeva 14, 18000 Nis, Serbia

²Faculty of Medicine, University of Nis, Blvd. Dr Zorana Djindjica 81, 18000 Nis, Serbia
veselinovic_marko@yahoo.com, dalibor.stevanovic85@gmail.com, traja@masfak.ni.ac.rs,
miodrag.manic@masfak.ni.ac.rs, stojanka@medfak.ni.ac.rs, draganm@masfak.ni.ac.rs

Abstract: This paper presents the application of geometric modeling techniques in the process of creating 3D surface model of the human tibia. In order to create valid CAD (computer-aided design) model, the accurate definition of geometry and topology of tibia's entity is essential. Therefore, geometrical model was created based on anatomical and morphological properties of the human tibia. Proposed process of creation tibia's geometrical model contains several steps: importing and editing the CT (computer tomography) model in CAD software, recognition and defining of geometrical entities, and creation of adequate surface model. From the morphometric point of view this approach allows creation of more accurate models than the use of standard modeling techniques.

Key words: 3D surface model, tibia, reverse modeling, reverse engineering, CAD

1. INTRODUCTION

In orthopedic surgery, but also in all other sub-branches of surgery, where the need for creation of customized implants or fixators exists, there is a specific requirement to know the exact geometrical model of the human bone. Therefore, it is very important to create geometry of the bone rapidly and accurately. Usually, the techniques of reverse modeling (RM) are used to define the exact geometrical model of bones. Having such models, it is possible to build customized bone implants and fixators using rapid prototyping technologies.

There are few different approaches for creating 3D surface model of human bones. Some of them are applied for creating 3D surface model of bones other than tibia, e.g. femur. Nevertheless, they are presented in this paper, because method used for one human bone, can be used for some other.

First approach is based on deforming the sample of the human bone shape according to an input X-ray image. In this example template shape is solid model, but the same method could be used for creating 3D surface model. Disadvantages of this method are about dealing with X-ray images, e.g. inaccurate patient positioning, and possible less accurate 3D model than by using CT [7,8]. 3D model (solid or surface) created with this approach does not have precisely defined geometric entities (points, planes, spline curves, etc.). This is the main disadvantage of this method compared with method used in this paper. Furthermore, using method with defined geometric entities, accuracy of the 3D surface model can be controlled (if there are more planes for cross-sections, more spline curves will be created, and obtained model will be more precise).

Second approach for creating 3D surface model is by using curves which are in relation with CT slices [9,10]. This is disadvantage of the second approach compared with method from this paper, which can use differently oriented curves (curves which are not strictly linked to CT slices).

For creating 3D model of femur, approach defined in [11] use curves obtained from different cross-sections. In this paper curves are obtained from cross-sections which are in relation with mechanical axis and 3 main parts of tibia (proximal end, tibial shaft or distal end).

In this paper the method of characteristic regions for creating 3D surface model of the human tibia is presented. This method is based on anatomical and morphological properties of the bone.

2. INPUT DATA

The radiology image of the bone, which is often called raw data in CAD terminology, represents input data for RM. The sample of tibia was scanned by CT in resolution of 0.5mm. The raw data, that is coordinates of the points of scanned bone, were imported into appropriate CAD software for reverse modeling. The CT scans were obtained fast, but in a low resolution (in terms of RM). That affected on accuracy of some details in the 3D digital model, but not on accuracy of the total bone morphology. In addition, CT scans contained internal bone tissue structures, as well as the other type of the surrounding soft tissues. That is the reason why these scans required considerable time for model post processing ("for cleaning and healing the model").

3. REVERSE MODELING

Reverse modeling of a human bone's geometry using CAD software means generating digital 3D model of bone's geometry from radiology image (X-Ray, CT, MRI). In this particular case, CATIA V5 R19 CAD software and its modules were used. Importing the raw data into the CAD system results in generating of one or more clouds of points (discrete points of the bone, which are scanned by some of radiology methods). In the next phases of reverse modeling, the geometrical features of higher order (curves and surfaces) are designed.

The process of creating model of tibia was based on the processes that are described in [1,2].

1. Importing and editing (filtering, aligning, etc.) of clouds of points.
2. Tessellation of polygonal model (mesh) by creating a huge number of small triangular planar surfaces between the points in the cloud, as well as editing of polygonal model.
3. Recognition and defining the Referential Geometrical Entities (RGEs) and it's correlation with tibia anatomy (Fig. 2).
4. Creating anatomical points and spline curves in the defined planes (Fig. 3).
5. Creating the 3D surface model of tibia using obtained spline curves (Fig. 4).

4. THE 3D SURFACE MODEL OF THE HUMAN TIBIA

Situated at the medial side of the leg, tibia, excepting the femur, is the longest bone of the skeleton. It has a body and two extremities, proximal and distal. Proximal end of the tibia has a broad superior articular surface which articulates with the femur. The shaft has prismoid shape with three surfaces and three margins. The anterior margin, the most prominent of the three, commences above at the tuberosity, and ends below at the anterior margin of the medial malleolus. Distal end of the tibia, much smaller than the upper, is prolonged downward on its medial side as a strong process, the medial malleolus. Its inferior articular surface is quadrilateral, and smooth for articulation with the talus [3,4] (Fig. 1).

4.1. Recognition and defining the RGEs

In the case of the tibia, the mechanical axis is a line from the center of the tibial plateau (interspinous intercruciate midpoint) extending distally to the center of the tibial plafond. [5]

The tibial plateau (proximal/superior articular surface) was approximated with ellipse, which was best solution compared with all other tested entities: circles, spline curves, etc. The first point of mechanical axis is center of the ellipse, which is approximately equal with center of tibial spines notch [5]. Second point is center of the tibial plafond (distal/inferior articular surface) which was approximated with adequate lower cross-section of distal end of tibia (Fig. 2).

Next step was creation of ten planes based on mechanical axis and anatomical landmarks of tibia. These planes were used for the creation of the cross-sections.

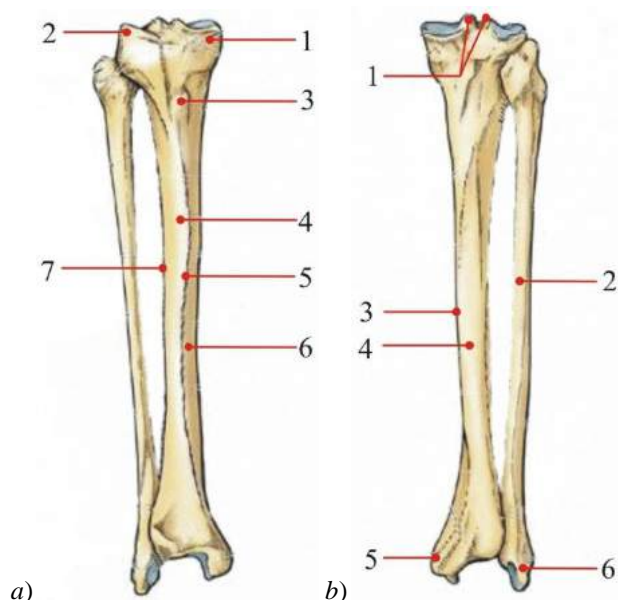


Fig.1. Right tibia and fibula, a) Anterior view, 1. Medial condyle, 2. Lateral condyle, 3. Tibial tuberosity, 4. Lateral surface, 5. Anterior margin of tibia, 6. Medial surface, 7. Lateral margin of tibia, b) Posterior view, 1. Intercondylar tubercles of intercondylar eminence, 2. Fibula, 3. Medial margin of tibia, 4. Posterior surface, 5. Medial malleolus, 6. Lateral malleolus [3]

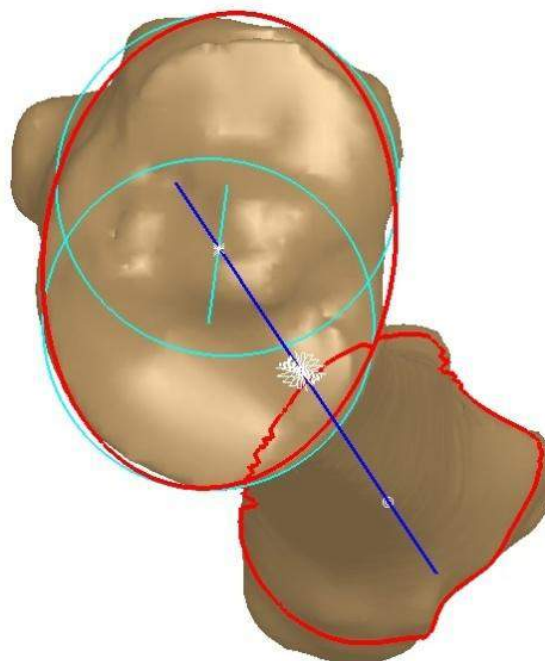


Fig.2. RGEs on polygonal model of the right tibia

4.2. Creating anatomical points and spline curves

The intersections of planes and polygonal model of tibia produces contour curves (cross-section contour). These curves were used for creating points and spline curves (Fig. 3).

Obtained spline curves were used for creation of the proximal end of tibia surface model (Fig. 4). The

expanded proximal end is a bearing surface for body weight, which is transmitted through the femur. It consists of medial and lateral condyles, with intercondylar eminence and anterior and posterior intercondylar area between and the tibial tuberosity, on the anterior surface [6].

The same procedure was applied for creation of 3D surface model for the distal end of tibia (Fig. 6). The slightly expanded distal end of the tibia has anterior, medial, posterior, lateral and distal surfaces. It projects inferomedially as the medial malleolus. The distal end of the tibia, when compared to the proximal end, is laterally rotated (tibial torsion). The short thick medial malleolus has a smooth lateral surface with a crescentic facet that articulates with the medial surface of the talus [6].

For tibial shaft (Fig. 5), set of nineteen planes was used. These planes are perpendicular to the mechanical axis. The shaft is triangular on the cross section and has three surfaces: medial, lateral and posterior, separated with three margins: anterior, lateral and medial [6].



Fig.3. Points and spline curves on proximal end of tibia

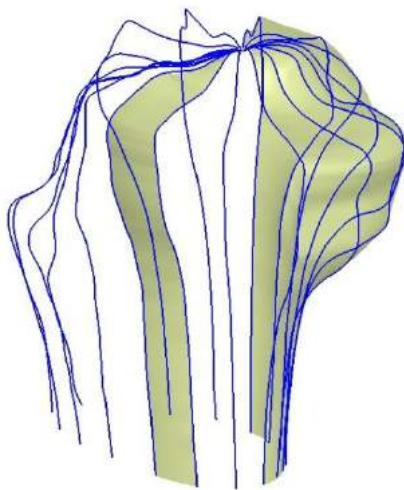


Fig.4. Creation of the 3D surface model of the proximal end of tibia

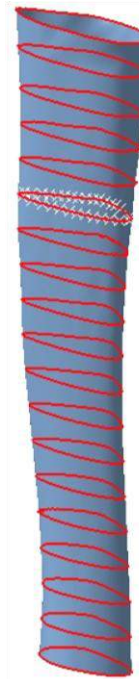


Fig.5. 3D surface of shaft of tibia

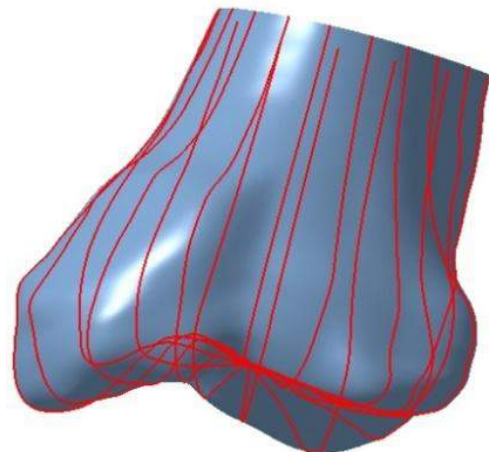


Fig.6. 3D surface of the distal end of tibia

4.3. Creating 3D surface model of tibia

3D surface model of tibia was created by merging 3D surfaces of proximal end, shaft and distal end of tibia (Fig. 7).

Problem with this approach is alignment of these tibial parts during merging. This requires approximations of 3D surface models of tibial parts on places where they should be connected.

5. CONCLUSION

Reverse modeling and reverse engineering provide all necessary tools for design of 3D surface model of bone and rapid prototyping of customized implants and fixators.

Application of bone reverse modeling method based on RGEs, enables building of high quality 3D surface model using CT scans as raw data. It is necessary to know

anatomy of the bone for recognition and defining the RGEs.

Disadvantage of the method of characteristic regions is bad alignment of created 3D surface models of tibial parts during merging.

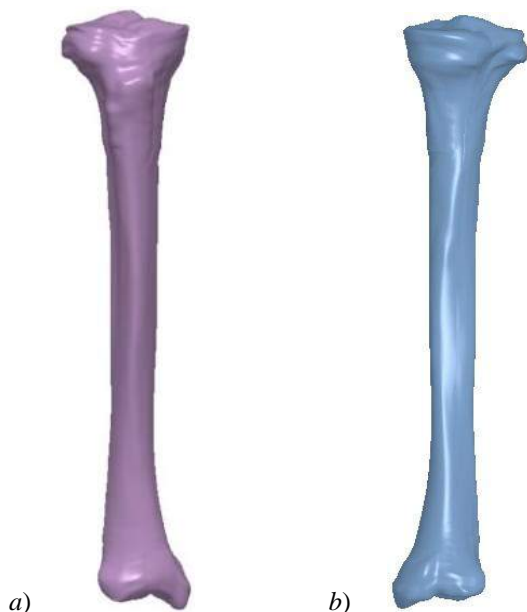


Fig.7. 3D surface model of the right tibia, a) anterior view, b) posterior view

ACKNOWLEDGMENTS

This paper is part of project III41017 Virtual human osteoarticular system and its application in preclinical and clinical practice, funded by the Ministry of Education and Science of Republic of Serbia, for the period of 2011-2014.

REFERENCES

- [1] STOJKOVIC, M., TRAJANOVIC, M., VITKOVIC, N., MILOVANOVIC, J., ARSIC, S., MITKOVIC, M. (2009) *Referential Geometrical Entities for Reverse Modeling of Geometry of Femur*, WIPIMAGE, Porto, Portugal, Proceedings, pp 189-194
- [2] VITKOVIC, N., TRAJANOVIC, M., MILOVANOVIC, J., KORUNOVIC, N., ARSIC, S., ILIC, D. (2011) *The geometrical models of the human femur and its usage in application for preoperative planning in orthopedics*, 1st - International Conference on Internet Society Technology and Management / ICIST, Kopaonik, pp 13
- [3] MOORE, K., DALLEY, A., AGUR, A. (2010) *Tibia*, Clinically Oriented Anatomy, 6th Edition, pp 520-521
- [4] BROWN, P. *The tibia and fibula*, The online skeleton, Forensic Anthropology, pp 60-61, <http://www-personal.une.edu.au/~pbrown3/oskel.html>

- [5] COOKE, D., SLED, E., SCUDAMORE, A. (2007) *Frontal Plane Knee Alignment: A Call for Standardized Measurement*, The Journal of Rheumatology, Vol.34, No 9, pp 1796-1801
- [6] STANDRING, S. (2008) *Tibia*, Gray's Anatomy, 40th Edition, Chapter IX
- [7] GUNAY, M., SHIM, M.-B., SHIMADA, K. (2007) *Cost- and time-effective three-dimensional bone-shape reconstruction from X-ray images*, The international journal of medical robotics and computer assisted surgery, Vol.3, pp 323-335
- [8] FILIPPI, S., MOTYL, B., BANDERA, C. (2008) *Analysis of existing methods for 3D modelling of femurs starting from two orthogonal images and development of a script for a commercial software package*, Computer methods and programs in biomedicine, Vol.89, pp 76-82
- [9] TARNITA, D., POPA, D., TARNITA, D. N., GRECU, D. (2006) *CAD method for three-dimensional model of the tibia bone and study of stresses using the finite element method*, Romanian Journal of Morphology and Embryology, Vol.47, pp 181-186
- [10] JIANG, T., LIN, F., KALTMAN, S. I., SUN, W. (2009) *Anatomical modeling and rapid prototyping assisted surgical reconstruction*, Proceedings of the Eleventh Solid Freeform Fabrication Symposium, University of Texas Austin, pp 555-564
- [11] VICECONTI, M., ZANNONI, C., PIEROTTI, L. (1998) *TRISOLID: an application of reverse engineering methods to the creation of CAD models of bone segments*, Computer Methods and Programs in Biomedicine, Vol.56, pp 211-220



COMPUTER BIOMECHANICAL ANALYSIS OF SPECIFIC TOOTH FOR DIFFERENT APPLIED LOADING

Dejan PETROVIĆ¹, Marko ANDJELKOVIĆ², Ljiljana TIHAČEK-ŠOJIĆ², Nenad FILIPOVIĆ^{1,3}

¹Bioengineering Research and Development Center, BioIRC, 34000 Kragujevac, Serbia

²Dental School in Belgrade, University of Belgrade, 11000 Beograd, Serbia

³Faculty of Mechanical Engineering, University of Kragujevac, 34000 Kragujevac, Serbia
racanac@kg.ac.rs, fica@kg.ac.rs

Abstract: Dental roots restored with posts are subjected to the risk of failure under loads, particularly in cases of small dentin thickness. This study adopted the finite element analysis to compare the elastic stress distribution for particular tooth geometry with different applied loads. Under normal load, von Mises equivalent stress was determined for the different regions of the tooth, periodontal ligament, compact and sponge bones. The results demonstrated that stress concentrations occurred mainly in the enamel region model. The model presented stress concentration in a region limited to the enamel material adjacent to its apical end, thus preserving the root dentin damaged.

Key words: dental biomechanics, stress analysis;

1. INTRODUCTION

Stress/strain redistributions occurring within compact and sponge bone as a result of prosthodontic treatments are highly complex and an understanding of the biomechanical factors (strains) initiating bone remodelling due to prosthodontic procedures has not been conclusive so far [1]. For this reason an in-depth understanding of the biological activity in the supporting abutments and bone structures is required as a means for possible improving the outcomes of such restorations. Therefore a detailed biomechanical model becomes essential, especially in typical clinical cases, in order to develop a computational biomechanical simulation capable of identifying the quantitative mechanical response to fixed prosthodontic treatment. Although some studies [2] indicate that intra-radicular posts reinforce pulpless teeth, recent investigations [3-7] have demonstrated that root post transmit masticatory loads to the tooth root and supporting structures.

In this study we evaluated displacements and effective stress distribution in the tooth for different applied loading: 50N, 100N, 150N, ... , 500N.

2. METHODS

We modeled the lower first premolar tooth which has been shown in Figure 1.

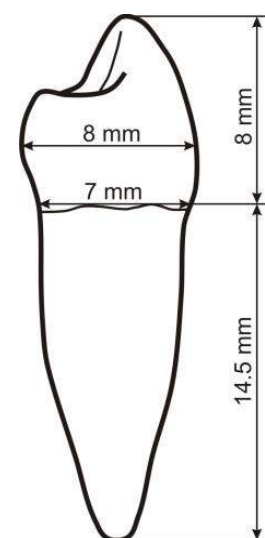


Fig. 1 Modeled tooth geometry

Detailed tooth geometry with tissue layers is presented in Figure 2. The outer layer of tooth called enamel is separated from the inner layer called dentine, as it is shown in Figure 2 (right). The middle part of tooth is the dental pulp, with no impact on the stress distribution and it is modeled as the empty space. The right side in the Figure 2 is tooth appearance viewed from the side of the cheeks or tongue.

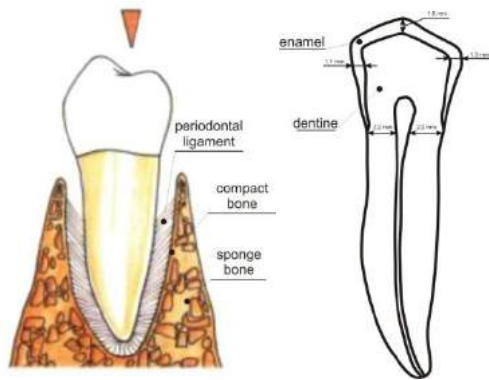


Fig. 2 Geometry and tissue layers

Between the teeth and compact bones is periodontal ligament which has average thickness about 0.25 mm. Around periodontal ligament is a thin strip of compact bone, with thickness of 0.3 mm and the rest is sponge bone. Applied load direction is acting parallel to the longitudinal axis of the tooth. The tissue material characteristics are shown in Table 1. The two-dimensional finite element mesh is shown in Figure 3.

Table 1. Tissue material properties

Tissue	E – Young's modulus	ν – Poisson's ratio
Enamel	84100 MPa	0,20
Dentine	18600 MPa	0,31
Periodontal ligament	70,3 MPa	0,45
Compact bone	15000 MPa	0,30
Sponge bone	1500 MPa	0,30

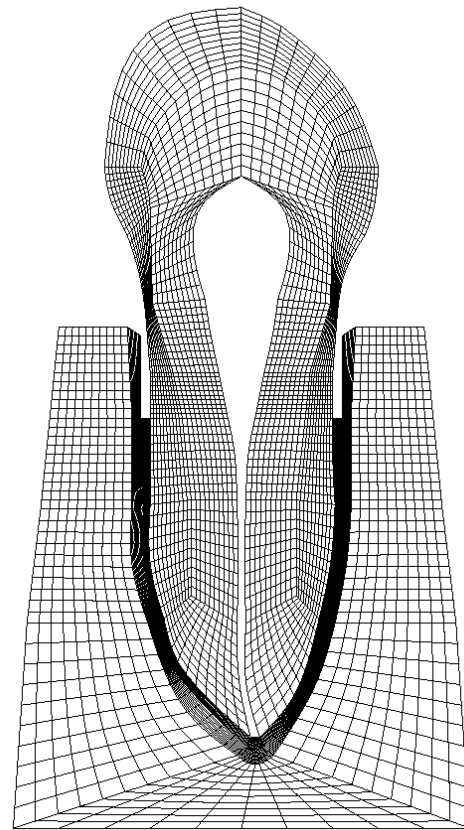


Fig. 3 Generated finite element mesh

3. RESULTS

Figure 4 shows the displacement and von Mises stress distributions for applied load of 50 N. The von Mises stress distributions and displacement for 500 N applied force is presented in Fig. 5. It can be seen that the maximal stress always appears at the enamel zone where actually load is applied. Obviously enamel and dentine bring much more force than periodontal ligaments and sponge and compact bone. Also it can be seen that there is very small displacement of the periodontal ligaments within the order of $4e^{-7}$ mm which can be estimated by using computer simulations.

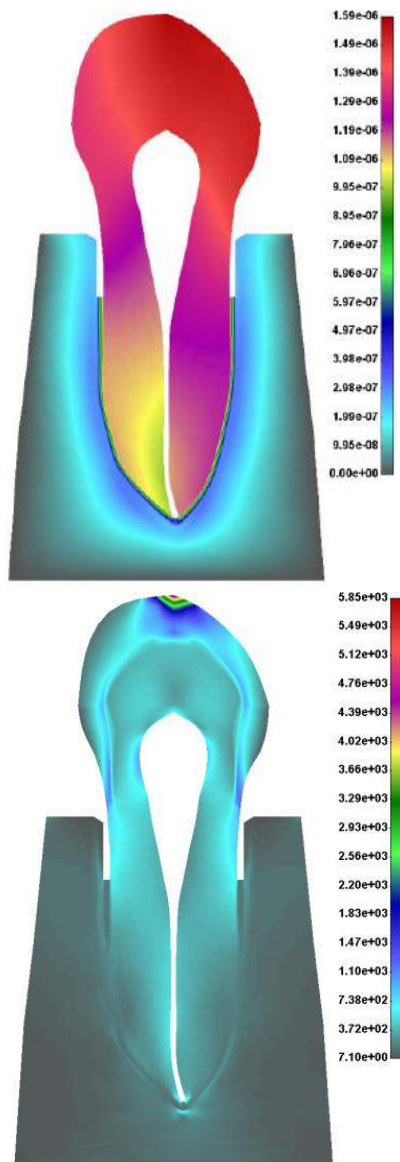


Fig. 4 Displacement and von Mises stress distribution for 50N force applied

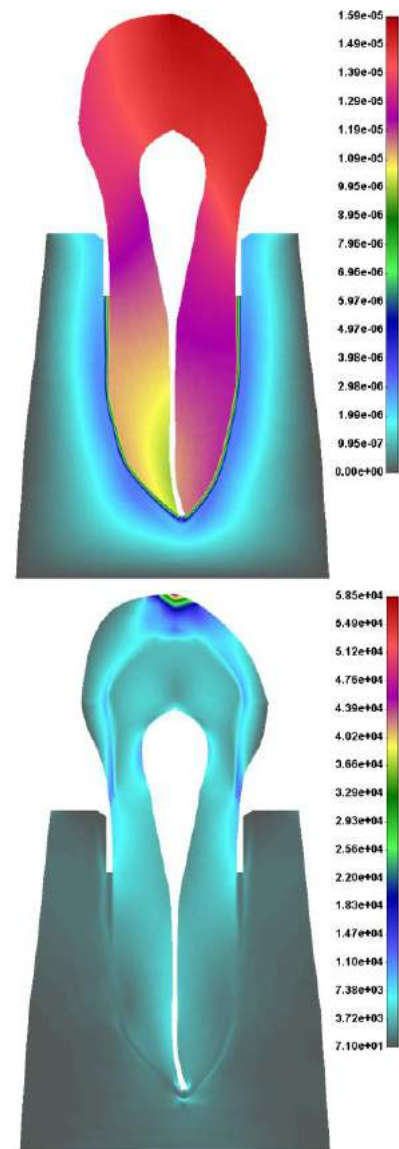


Fig. 5 Displacement and von Mises stress distribution for 500 N force applied

4. CONCLUSIONS

Finite element analysis has been used extensively to predict the biomechanical performance of various dental implant designs as well as the effect of clinical factors on the success of implantation. The present study defines the initial biomechanical responses for applied loads of 50 up to 500 N for a specific single tooth within surrounding periodontal ligament, compact and sponge bones. It has been shown that the maximal stress distribution occurs in the area of enamel material which can be a high potential for damaged structure. Future work will include more study on a specific-patient based material estimated from real patient and geometrical data will be provided from CT scanner.

REFERENCE

- [1] YAMASHITA, J., WANG, Q., DECHOW, P., C. (2006) *Biomechanical effects of fixed partial denture therapy on strain patterns of the mandible*, The Journal of Prosthetic Dentistry, Vol.95, No 1, pp 55-62
- [2] KO, C.,C., CHU, C.,S., CHUNG, K.,H., LEE M.,C. (1992) *Effect of posts on dentin stress distribution in pulpless teeth*, The Journal of Prosthetic Dentistry, Vol.68, No 3, pp 421-427
- [3] REINHARDT, R.,A., KREJCI, R.,F., PAO Y.,C., SRANNARD J.,G. (1983) *Dentine stresses in post-reconstructed teeth with diminished bone support*, Journal of Dental Research, Vol.62, No 9, pp 1002-1008
- [4] ASMUSSEN, E., PEUTZFELDT, A., SAHAFI, A. (2005) *Finite element analysis*

- of stresses in endodontically treated, dowel-restored tooth*, The Journal of Prosthetic Dentistry, Vol.94, No 4, pp 321-329
- [5] PIERRISNARD, L., BOHIN, F., RENAULT, P., BARQUINS, M. (2002) *Coronoradicular reconstruction of pulpless tooth: A mechanical study using finite element analysis*, The Journal of Prosthetic Dentistry, Vol.88, No 4, pp 442-428
- [6] HO, M.,H., LEE, S.,Y., CHEN, H.,H., LEE, M.,C. (1994) *Three-dimensional finite element analysis of the effects of posts on stress distribution in dentin*, The Journal of Prosthetic Dentistry, Vol.72, No 4, pp 367-372
- [7] MORGANO, S.,M. (1996) *Restoration of pulpless teeth: application of traditional principles in present and future contexts*, The Journal of Prosthetic Dentistry, Vol.75, No 4, pp 375-380

34th INTERNATIONAL CONFERENCE ON PRODUCTION ENGINEERING



SECTION I

**AUTOMATIZATION, ROBOTIZATION AND MECHATRONICS
IT AND ARTIFICIAL INTELIGENCE IN PRODUCTION ENGINEERING**



WIRELESS SENSOR NETWORK APPLICATION IN MONITORING OF MACHINING OPERATIONS

Zivana JAKOVLJEVIC^a, Miroslav PAJIC^b, Dragan ALEKSENDRIC^c, Dragan MILKOVIC^c

^aDepartment of Production Engineering, Faculty of Mechanical Engineering, University of Belgrade, Kraljice Marije 16, 11 000 Belgrade, Serbia, ^bDepartment of Electrical and Systems Engineering, University of Pennsylvania, PA 19104, USA, ^cFaculty of Mechanical Engineering, University of Belgrade, Kraljice Marije 16, 11 000 Belgrade, Serbia
zjakovljevic@mas.bg.ac.rs, pajic@seas.upenn.edu, daleksendric@mas.bg.ac.rs, dmilkovic@mas.bg.ac.rs

Abstract: The scope of this paper is the research of the possibilities of application of Wireless Sensor Networks (WSNs) for monitoring of machining operations. Due to the limited battery lifetime, WSNs are energy constrained networks and energy efficiency of the network is a very important issue. Since communication requires significantly more energy than processing, instead of sending raw data through the network, data processing and decision making should be performed in the node. Consequently, as a basis for WSN design we consider IEEE 802.15.4 Wireless Networking Standard, created for low data rates and very low power consumption which makes it suitable for remote monitoring and control. In this paper, a prototype of the node, designed for acceleration monitoring, has been developed. The node has been created at the Faculty of Mechanical Engineering in Belgrade and it is based on low power Atmel Atmega16 microcontroller and IEEE 802.15.4 compatible transceiver.

Key words: Wireless sensor networks, machining operations monitoring

1. INTRODUCTION

In-situ sensor monitoring of machining operations has attracted significant attention in the last decade. During machining, cutting forces, vibrations, acoustic emission, temperature, audible sound, etc. are influenced by cutting tool state and conditions of the material removal process. The aforementioned process quantities can be measured and acquired signals can be processed to extract features correlated with the process and tool condition. These features carry information for on-line decision making and diagnosis of the cutting process state. After the diagnosis, the appropriate actions are executed by human operator or control system. A number of techniques for tool condition and process parameters monitoring using the described procedure have been proposed [1]. Nevertheless, the industrial application of on-line condition-based monitoring systems is still sporadic.

The most significant limiting factors for implementation of the proposed techniques are sensor deployment and wiring. It is necessary to place the sensor very close to the cutting zone; on the tool would be the best. Nevertheless, the tools are placed in spindles or on moving platforms, which makes them difficult or impossible to access by wiring. Besides, when wiring is feasible, its cost is estimated to 10-100\$ per sensor [2].

Recent developments in wireless technology have opened up new possibilities. Communication between the sensor and the supervisory or control system can be wireless, which enables sensor placement at very inaccessible locations, such as tool (Fig. 1). In this scenario, the sensor operates as a node in a Wireless Sensor Network (WSN). It has embedded processor and radio transceiver. The

node is battery charged and energy efficient operation of the sensor is of critical importance.

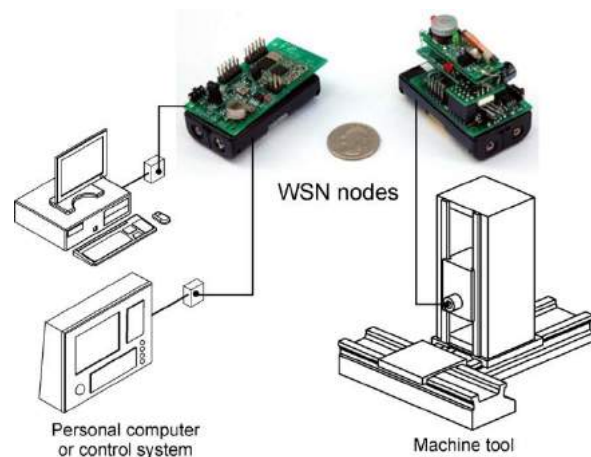


Fig. 1. Mounting of the wireless sensor to the tool

It is worth noting that radio communication (including both transmissions and receptions) of a sensor node is significantly more energy consuming than in-node computation. To exploit benefits of wireless communication, the sensor should be made intelligent. It should carry out not only the measurements, but also data acquisition, signal processing, features generation and decision making. Instead performing a batch wireless transmission of the raw signal and the processing at central computer, the whole diagnosis process should be performed at the node. In this case, only the information about the decision (diagnosis) should be transmitted.

Machining operations monitoring assumes high sampling rates. Sensor integrated tooling for monitoring of tool vibration and temperature in milling using wireless communication was studied in [3]. Nevertheless, contrary to the above given observation, instead of in-node signal processing, the raw data (20KHz) were sent to PC using intensive Bluetooth (IEEE 802.15.1) communication. In [4], the machine tool vibrations were monitored using wireless accelerometer. The less communication intensive IEEE 802.15.4 wireless standard was used for raw signal transmission to the PC. Signal processing and decision making were carried out in PC. Due to the bandwidth constraint, the sampling rate was restricted to only 1000 Hz. In both applications, the communication is very intensive which has repercussions on battery lifetime.

The utilization of wireless sensors assumes the in-node signal processing using low-power microcontrollers. There have been some approaches [5, 6] that used microcontroller based systems for tool breakage detection in end milling. Instead of transmitting a large amount of data, the signal is analyzed at the node. On abnormal event (tool breakage) detection, the message is sent to the PC using SMS [5] or wired communication (Ethernet) [6]. Bluetooth (IEEE 802.15.1) and IrDA are designed for high data rate applications such as voice, video and LAN communication. They are very communication intensive and thus suffer from high energy consumption, making them unsuitable for wireless sensor applications such as one at hand. GSM and GPRS are even less appropriate. The energy consumption is also very high and there are additional costs related to the GSM or GPRS modules (~100\$) and SIM card purchase and operation. On the other hand, IEEE 802.15.4 standard offers low data rate and low power. It is characterized by long battery life. For these reasons this standard is used as a basis for WSN.

In this paper, the possibilities to employ WSNs in machining operations monitoring have been investigated. An overview of WSN was presented as well as a prototype node developed at Faculty of Mechanical Engineering, University of Belgrade (FME). The node is employed in tool acceleration measurements in turning. In this example, the decision making is carried out at the node and only the information about significant event is transmitted to the coordinator.

2. INTRODUCTION TO WSNs

In a Wireless Sensor Network (WSN) each node has one or more sensors, embedded processors and low-power radio. All the nodes coordinate in order to perform a common task. In-network data processing greatly reduces the energy consumption. It can be additionally reduced by applying appropriate communication protocols. IEEE 802.15.4 can operate at star or peer to peer topology. IEEE 802.15.4 has three operating frequency bands with different number of channels and transfer rates: 868 MHz → 1 channel – 0 (20Kb/s); 915 MHz → 10 channels – 1-10 (40Kb/s); 2.4 GHz → 16 channels – 11-26 (250Kb/s). In the IEEE 802.15.4 architecture three layers can be distinguished (Fig. 2). These are: 1) Physical (PHY) layer, 2) Medium Access Control (MAC) layer and 3) Network and Application layer.

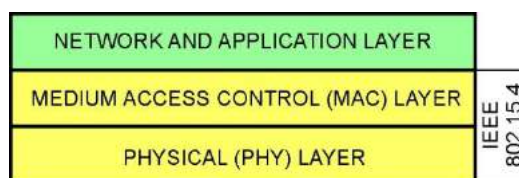


Fig. 2. IEEE 802.15.4 architecture

Physical layer has the following functionalities [7]: 1) activation and deactivation of the radio transceiver, 2) energy detection within the current channel, 3) link quality indication for received packets, 4) clear channel assessment (CCA), 5) channel frequency selection, 6) data transmission and reception. PHY frame structure of transmitted data is shown in Fig. 3.

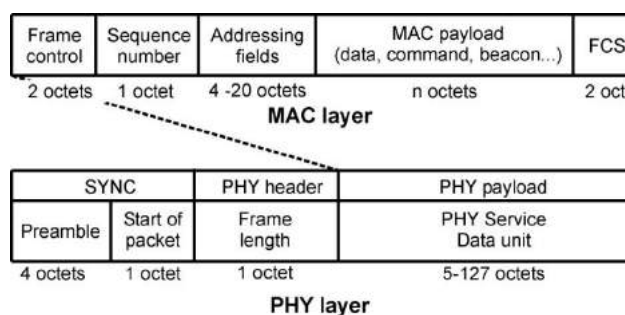


Fig. 3. PHY frame structure [7]

In IEEE 802.15.4 MAC layer two modes of operation are defined: 1) beacon enabled network, 2) non-beacon enabled network. In the beacon mode (Fig. 4a) the device waits for the coordinator's beacon to start transmission. When the transmission is complete, the coordinator schedules the next beacon and the device goes to sleep. All the devices in the network know when to communicate with each other. The timing circuits of the nodes have to be synchronized. In the non-beacon mode all nodes, except the coordinator, are almost always 'asleep'. The device wakes up on event and sends a message to the coordinator. Beacon mode is used when sink runs on batteries, while non-beacon is preferred when the sink is non energy constrained (in this mode the coordinator has to always 'listen').

IEEE 802.15.4 MAC layer enables the creation of different MAC protocols that define the communication procedure between nodes. The MAC protocols must be energy efficient. There are many sources of energy waste in WSN, and the most important are [8]: 1) **Collided packets**: when more than one packet is sent to a node at the same time; since the receiver can not receive both packets, these packets are rejected and should be retransmitted; 2) **Overhearing**: node receives packets intended to other nodes; 3) **Control packet overhead**: minimal control packets should be used in transmission; 4) **Idle listening**: listening of the idle channel to receive possible traffic; 5) **Overmitting**: sending the message when the destination node is not ready.

There are many different MAC protocols [8]: B-MAC, Sensor-MAC, WiseMAC, Traffic Adaptive MAC protocol, D-MAC, etc. Nevertheless, no MAC protocol is accepted as a standard and it is application dependant. In monitoring operations, communication is usually triggered by a sensing event. Therefore, if no sensing

event occurs the nodes could stay idle for a long time. To preserve energy, radio transceivers are programmed to stay in the sleep mode, thus avoiding idle listening. This can be easily implemented in star topologies, where all nodes communicate with the coordinator (i.e., gateway) in a single hop. Nevertheless, the reach and the presence of obstacles in the node's vicinity usually demand the multi-hop between the sensor node and the sink (i.e., gateway), with minimum latency, while consuming the minimal amount of energy.

B-MAC protocol [9], used in this paper, is designed for monitoring operations. It provides nodes with duty cycle mechanism in order to eliminate idle listening which is very important in multi-hop networks. It is convenient for monitoring of machining operations as well as for machine tools control.

Radio duty cycling [9] is very important for the reliable data transmission with low latency. In B-MAC it is carried out by periodic channel sampling. Normally, a node is in the sleep mode. It wakes up after a predefined time has elapsed and checks for the network activity. If activity is detected, the node powers up and stays awake to receive the incoming packet. After the reception the node returns the sleep mode. If no packet is received after timeout, the node goes back to sleep as well.

Before sending the data, the transmitter sends a preamble. To reliably receive the data the preamble should be at least as long as the interval between two subsequent checking for channel activity. The length of the preamble has to give enough time to node to wake up, detect the activity in the channel, and receive the preamble. After receiving the preamble, the node receives the message. If the node wakes up and there is no activity at the channel, the idle listening occurs only for a short duration of time. The length of the period between two subsequent channel activity sampling is the result of the trade-off between the latency and the energy efficiency of the network.

3. DEVELOPMENT OF WIRELESS NODE

The block diagram of the experimental nodes developed at FME is shown in Fig. 4. It is based on low power Atmel Atmega16 microcontroller [10] and Microchip MRF24J40 radio transceiver [11].

Atmega16 [10] is 8-bit microcontroller with 1 KB SRAM and 16 KB of program memory. It is a low power microcontroller with power consumption of 1.1mA in the active mode at (frequency) 1MHz, (voltage) 3V and (temperature) 25°C, and 0.35mA in the idle mode. Furthermore, the microcontroller has 8 single ended channels for 10-bit ADC, 32 bidirectional DIO, one 16-bit and two 8-bit timer/counters with compare modes. The oscillator frequency is up to 16MHz. In our platform 8MHz has been used.

MRF24J40 [11] transceiver is compliant with IEEE802.15.4 standard. Its operating frequency band is 2.4GHz and the data rate is 250 Kb/s. It has integrated 20MHz oscillator. Its typical power consumption is 19mA in receive (Rx), 23mA in transmit (Tx) and 2µA in the sleep mode. Thus, the transceiver's power consumption in active modes (Tx or Rx) is around 20 times higher than the power consumption of the microcontroller.

MCF24J40 operates within Mikroelektronika ZigBee3 development board.

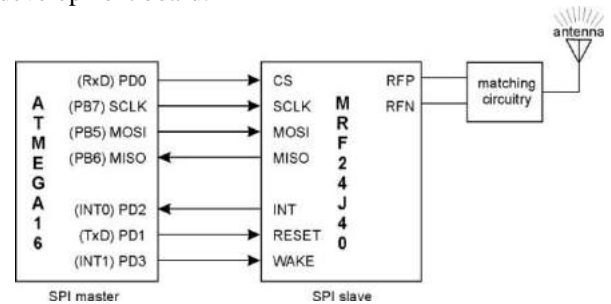


Fig. 4. FME WSN node

The communication between the microcontroller and the transceiver is carried out using 4-wire SPI interface. SPI functions in full duplex master/slave configuration. The microcontroller (master) sends data to the transceiver through MOSI, and the transceiver (slave) sends data to the microcontroller on MISO line. Serial clock (SCLK) is output from the master. SPI is used not only for data transfers, but also for transceiver programming using protocol defined by the manufacturer.

Besides SPI lines, there are three additional lines between the microcontroller and the transceiver. These are RESET, WAKE and INT. RESET and WAKE are used for transceiver reset and wake. Using INT line MRF24J40 transceiver can signal one of 8 available interrupts to the microcontroller. The most interesting interrupts for our application are receive interrupt and transmit interrupts for normal transmission and guaranteed time slots transmissions in a beacon mode.

4. EXPERIMENTAL VALIDATION

The described wireless node, developed at FME, has been implemented for acceleration monitoring in turning. Fig. 5 shows the experimental setup. The accelerometer is mounted on a tool holder and it is wired to the wireless node that is placed on toolpost. The other node is connected to the PC via DIO. Since the sink (PC) is mains powered and there is no need for multi-hop configuration, the non-beacon mode of operation has been chosen. Although not used in this setup, B-MAC protocol was implemented to allow extensions to multi-hop configurations (i.e., topologies) in industrial environments where physical constraints prohibit use of a single-hop communication between the sensor and the gateway.

ADXL311 Analog Devices dual-axes measurement system, with measuring range $\pm 2g$ was used. It is powered from microcontroller by 5V. In our setup, only vertical acceleration component is measured. Accelerometer signal is linked to microcontroller port A0. Microcontroller performs 10-bit ADC. In the given installation the maximum sampling rate is 15kHz.

Acceleration measurements have been widely used for tool condition monitoring and a number of methods for tool breakage and tool wear have been proposed [1]. These methods were usually based on Discrete Wavelet Transform, Hilbert-Huang Transform and other sophisticated techniques. Nevertheless, in this paper the WSN are in focus, rather than diagnosis techniques. This

is the reason that it was decided to simply employ in-node signal thresholding.

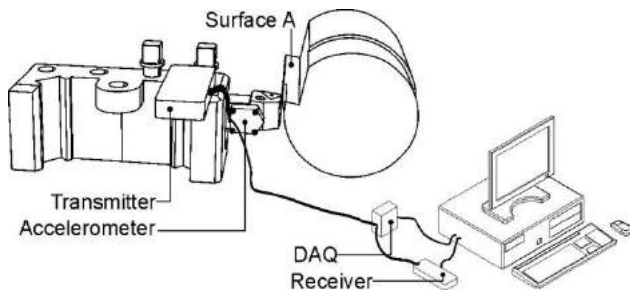


Fig. 5. Experimental setup

To provide a significant change of acceleration on the tool holder, we use intermittent turning of grooved part (Fig 5). On the cutting process stop at surface A the high vibrations occur. In the given setup the acceleration signal below the value that corresponds to 2.71V is considered as the event which has to be detected. On this event the microcontroller wakes up the transceiver and sends a message containing the signal value (2 bytes) and the number of occurrences (1 byte). In order to avoid the detection of transients after the cutting process stops, we introduce a waiting period of 50ms after an event is detected, before we allow the detection of the next event. At least 50ms have to pass between two subsequent events regardless of the value of the acceleration signal. On data reception, the sink node puts the port D high and keeps it high for 20ms. To verify the performance of nodes, the voltage level of port D and acceleration signal are acquired using DAQ with 500Hz sampling rate. In this setup, the DAQ is used as a kind of digital oscilloscope. The sent data package contains only 3 bytes of data, while the whole frame for sending the data package contains 22 bytes (Fig. 3). The short addresses that give the addressing field of 8 bytes are used. The data transmission assumes SPI communication (2Mbps) of these bytes between microcontroller and transceiver on both (Rx and Tx) sides, as well as radio communication (250 Kb/s). Besides, the microcontroller and the transceiver exchange control sequences via SPI. This leads to latency of event detection of 4ms on the receiver's side.

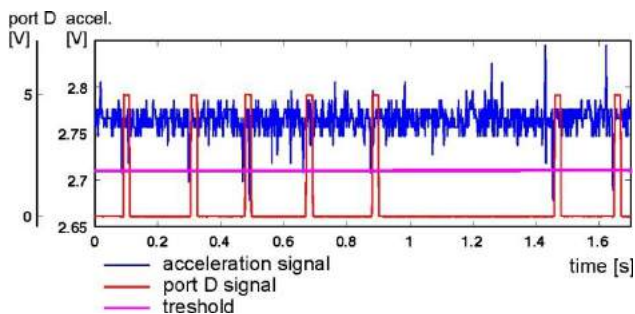


Fig. 6. Experimental results

Fig. 6 shows the accelerometer signal (acquired by DAQ) along with the voltage level on the port D of the receiver. A number of experiments were carried out on Hasse & Werde lathe. In the experiment shown in Fig. 6 the cutting parameters were: $n=300\text{rpm}$, $s=0.05\text{mm/r}$ and $a=0.7\text{mm}$. The experimental results indicate a reliable performance of the developed wireless node.

5. CONCLUSION

In this paper, the application of WSN in machining operations monitoring has been investigated. Initially, the communication reliability was questioned. The concern was that a huge amount of ferrous materials in the communication area could lead to electro-magnetic disturbances, causing communication failures and packet drops. Nevertheless, the experiments have shown that the communication was reliable. As the distance between the nodes (connected to the sensor and to the PC) was 2m, there was no need for multi-hop network deployment. Using WSNs the placement of sensors at otherwise inaccessible/difficulty accessible locations such as tool or even workpiece becomes easily feasible. This opens up the new possibility in machining process monitoring and control.

Acknowledgement: The authors express the gratitude to the Serbian Ministry of Education and Science, research grants TR35007, TR35020, TR35045, TR35030.

REFERENCES

- [1] TETI, R., JEMIELNIAK, K., O'DONNELL, G., DORNFELD, D. (2010) *Advanced monitoring of machining operations*, CIRP Annals – Manufacturing Technology, Vol. 59, pp 717-739
- [2] TIWARI, A., LEWIS, F., L., GE, S., S. (2008) *Wireless Sensor Network for Machine Condition Based Maintenance*, 8th Int. Conference on Control, Automation, Robotics and Vision, pp 461-467
- [3] SUPROCK, C., A., NICHOLS J., S. (2009) *A Low Cost Wireless High Bandwidth Transmitter for Sensor-Integrated Metal Cutting Tools and Process Monitoring*, International Journal of Mechatronics and Manuf. Systems, Vol. 2, No. 4, pp 441-454
- [4] WRIGHT, P., DORNFELD, D., OTA, N. (2008) *Condition Monitoring in End-Milling using Wireless Sensor Networks (WSNs)*, Transactions of NAMRI/SME, Vol. 36, pp 177-183
- [5] PRICKETT, P., SIDDIQUI, R., A., GROSVENOR, R., I. (2011) *A microcontroller-based end milling cutter monitoring and management system*, International Journal of Advanced Manufacturing Technology, doi 10.1007/s00170-010-3135-z
- [6] SIDDIQUI, R., A., AMER, W., AHSAN, Q., GROSVENOR, R., I., PRICKETT, P. (2007) *Multi-band infinite impulse response filtering using microcontrollers for e-monitoring applications*, Microprocess and Microsystems, Vol. 31, pp 370-380
- [7] IEEE 802.15.4 Standard
- [8] DEMIRKOL, I., ERSOY, C., ALAGROEZ, F. (2006) *MAC Protocols for Wireless Sensor Networks: a Survey*, IEEE Communications Magazine, Vol. 44, No. 4, pp 115-121
- [9] POLASTRE, J., HILL, J., CULLER, D. (2004) *Versatile Low Power Media Access for Wireless Sensor networks*, SenSys '04 Proceedings of the 2nd international conference on Embedded networked sensor systems, pp 95-107
- [10] Atmel (2010) Atmega16 Datasheet
- [11] Microchip (2008) MRF24J40 Datasheet.

IMPLEMENTATION OF PALLET LOADING METHOD AND VIRTUAL REALITY TO THE NEW SOFTWARE PRODUCT

Dušan KRAVEC, Marián TOLNAY, Ondrej STAŠ, Michal BACHRATÝ

Faculty of mechanical engineering, Slovak University of Technology, Nám. Slobody, Bratislava, Slovak republic
dusan.kravec@stuba.sk, marian.tolnay@stuba.sk, ondrej.stas@stuba.sk, michal.bachraty@stuba.sk

Abstract: This article describes software which is usable in a process of palletization. It uses virtual reality to simulate process of palletization, especially process of loading objects to the pallet. In this software, several methods are implemented for creating optimal layout for prism and cylinder shaped objects. Software output contains coordinates and orientation of each object. This is a closer look inside of it, its functions, main idea of the program and also pictures of its GUI (Graphical User Interface).

Key words: pallet, palletization software, deployment, virtual reality

1. INTRODUCTION

Testing new deployment methods of objects on the palette requires flexible software to directly communicate with the control unit of SCARA robot. Workplace consists of robot useful in palletization process (SCARA construction), belt conveyor, pallets, vision system and computer. In this article is introduced a new software product that coordinates robot. This software was created in the Java and Visual Basic programming language. It contains three modules: deployment of the objects module, virtual reality module and control module. Characteristics of each module are described in the next chapters of this article.

2. DEPLOYMENT OF OBJECTS

The main task of the software is to design optimal layout of objects on the pallet. Thanks to implemented methods of deployment user can choose the best layout. The first step to generate results is to enter this input data:

- Pallet dimensions (length, width and maximum height of load)
- Type of object (Box or cylinder)
- Object dimensions (length, width, height of the box / height and diameter of the cylinder)

Each type of an object has its picture preview with basic dimensions. Analysis can start after entering all necessary input data. Software evaluates this entered data and chooses the optimal deployment method thanks to implemented algorithms [1]. Optimality criterion is the highest number of objects stored on one pallet. Deployment method that can store up maximum of objects is chosen. If the user is not satisfied with automatically selected result then he can manually select deployment type of method.

For box – shaped objects are well known following methods:

- 1 block, 2 block and 3 block method
- Steudls 4 block method
- Smith and DeCanis 4 block method

For box – shaped objects are well known these deployment methods:

- “Raster” method
- “Cross” method

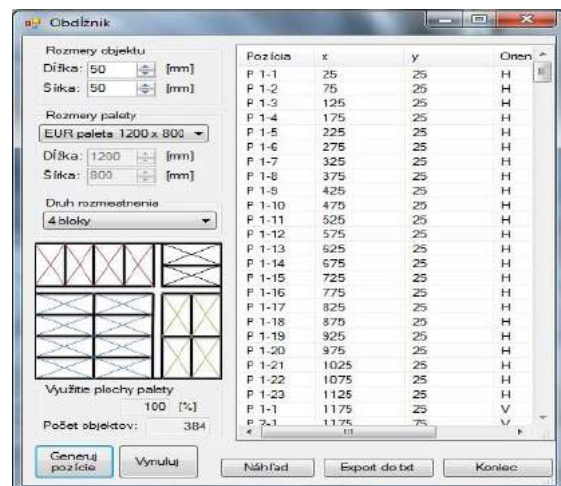


Fig.1. Deployment of objects module

The next step is calculation of coordinates. Outputs from this step are three coordinates (x, y and z) and orientation (horizontal / vertical) of the object. For each object are generated three coordinates and one orientation. The list of all coordinates can be found in the table of this form. Data from table can be saved to external text file on a hard disc of a computer. It is necessary for communication with the robot control program which is described in a chapter number three.

In the following sections are described well known deployment methods of objects on the pallet.

2.1. Single block, 2 block and 3 block method

A method using a single block is the simplest method for resolving the pattern of boxes on the pallet. There are only two possible options to place the boxes: *vertical* or *horizontal*. Block dimensions are identical to the dimensions of pallets [4]. Calculation of coordinates for horizontally oriented boxes is (1):

$$P_{i,j} = \left[\frac{l}{2} + l(i-1); \frac{w}{2} + w(j-1); H \right] \quad (1)$$

Calculation of coordinates for horizontally oriented boxes is (2):

$$P_{i,j} = \left[\frac{w}{2} + w(i-1); \frac{l}{2} + l(j-1); V \right] \quad (2)$$

Where:

L – the length of the pallet l – the length of the box
 W – the width of the pallet w – the width of the box
 With this conditions: $L \geq W$ and $A \geq B$

Method for using 2 or 3 blocks is basically an extension of single block method. In the method of 2 blocks we are trying to find the best combination of vertically and horizontally oriented boxes along the length of the pallet. Optimum combination contains smallest unused space between boxes. We can also use the third block to fill an empty area above the second columns (columns of vertically oriented boxes) using inverted boxes [4].

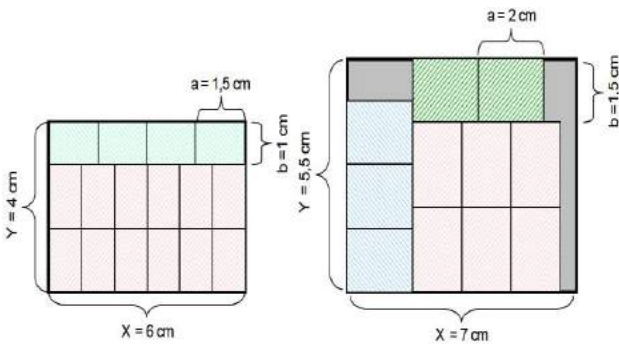


Fig.2. Two – block and three – block deployment

Analogically we can use this method for the width of the pallet and find the best solution for placing the boxes. The advantage of these methods is the simplicity and clarity. The disadvantage is that it does not provide an optimal solution for every problem.

2.2. Steudls 4 block method

This method divides storage area for four blocks located in the corners of the pallet. These blocks are rotated, depending on the direction of stored objects (horizontal or vertical). This method was described by Harold J. Steudl in 1979, therefore it is also known as

Steudl algorithm. It is a recursive method and uses dynamic programming. Dynamic programming is used to optimize process. It divides a big problem on a little sub problems. These sub problems are solved and results for future potential use are stored [6].

The first step of this method is finding an efficient combination of horizontally and vertically oriented boxes on a circuit of pallet. In other words, we are trying to find the smallest gap between combination of horizontal and vertical oriented boxes stored in length (width) of pallet. [6] We can do this by using this objective function (3):

$$F_n(S_n) = Max[X_n * l + Y_n * w + F_{n-1}(S_{n-1})] \quad (3)$$

$$X_n * l + Y_n * w \leq D_n$$

$$n = 1, 2, 3, 4$$

Where:

$F_n(S_n)$ – max sum of horizontally and vertically oriented boxes on the n side with state variable S_n at the beginning of the side.
 X_n – number of objects of length L placed along the side n
 Y_n – number of objects of width W placed along the side n
 D_n – length of the pallet
 S_n – is a state variable that defines the initial conditions for the side n .

This state variable can take these three values:

- Boxes are only horizontally oriented along the side n of the pallet
- Boxes are only vertically oriented along the side n of the pallet
- Boxes are vertically and horizontally oriented along the side n of the pallet

Objective function is calculating each combination of three values from S_n . For the three possible values of S_n and four blocks of boxes we can use this calculation: $3^4 = 81$. So we have to choose the best result from 81 results. Objective function $F_n(S_n)$ can be described as maximizing the utilized length of each side. However we have to include the pattern of boxes on the previous side. It can also be defined as minimizing the unused circuit of the pallet.

In the second step we have to fill the unused area. This step is linked by 2 problems. The first one is filling of empty area which can hold one or more boxes. The second problem is overlap of individual blocks which can be identified for example in this case (4):

$$D_1 - X_1l < X_3l \text{ and } D_4 - X_4l < X_2l \quad (4)$$

Steudls method is very good for creating efficient pattern of boxes on pallet, but we have to be careful not to create an overlapped area.

2.3. Smith and Decanis 4 block method

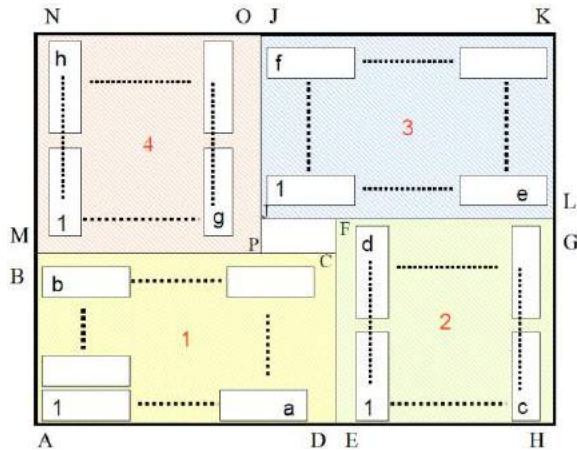


Fig.3. Smith and DeCanis deployment method

The picture shows the layout of boxes on a pallet according to Smith and Decani. It is investigating all possible combinations of the shown layout. On a first sight, this method is similar to Steudl method, but the number of objects in the blocks 1-3 and 2-4 is not equal. The principle of determining the number of objects across the width and length of each block is different. The first step is to define the first block. The second block needs to be higher than the first block. The third block need to be wider than the second block and fourth block is created in the remaining empty space. All possible dimensions of the first block and also dimensions of the other blocks are calculated. Then we can choose the best solution for our dimensions of boxes and pallet. This solution contains the highest number of boxes which we can store on one pallet [3].

Objective function for this method is (5):

$$MaxZ = a * b + c * d + e * f + g * h \quad (5)$$

Optimization is finished after generating all possible combinations. This method does not allow overlapping of blocks, as it can occur in Steudl method, but we can find more unused space between blocks. This problem can be solved either by adding another block or several blocks into this empty space.

2.4. Cylinders

In terms of methodology, the deployment cylinders are the easiest shape for planning the layout on the pallet. On figure 7 are two simple layouts of cylinders, which are not so difficult. In the first case we can see losses among cylinders. In the latter case we are trying to eliminate these losses but not always successfully. This case is effective only if the number of cylinders in the first row equals to the number of cylinders in the second row. We cannot say which of these layouts is more efficient because sometimes the number of cylinders on the pallet is equal in both of them. More advanced software can evaluate both layouts and give the best solution to the user [5].

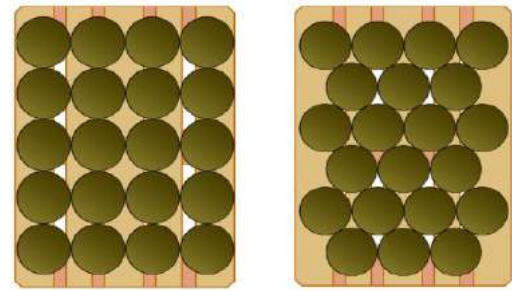


Fig.4. Deployment patterns of cylinders

Calculation of coordinates for „raster” alignment of cylinders (6):

$$P_{i,j} = \left[\frac{d}{2} + d(i-1); \frac{d}{2} + d(j-1) \right] \quad (6)$$

Calculation of coordinates for „cross” alignment of cylinders (7):

$$P_{i,j} = \left[\begin{array}{l} d - \frac{d}{2} \left(2 * \left\lfloor \frac{j}{2} \right\rfloor - j \right) + d(i-1); \\ \frac{d}{2} + d * \frac{\sqrt{3}}{2} (j-1) \end{array} \right] \quad (7)$$

After resolving the question of layout, it is necessary to answer the question of stability. Between the layers of cylinders the pads are inserted that enhance the stability of the whole system. It is inappropriate to combine both types of layout between layers. To ensure stability, we are using different accessories, such as walls, fences, packing washers, belts, etc.

3. VIRTUAL REALITY

Coordinates of the end effector position do not provide excellent idea of the chosen solutions. Therefore it was necessary to incorporate the graphic element to the program which would indicate a solution in three – dimensional (3D) preview. Two – dimensional (2D) rendering would be sufficient when we are analyzing only one layer of the load. For multilayer solutions are better 3D models, so it is necessary to use virtual reality interface. There are many interfaces that can provide rendering of the objects in space. We chose OpenGL interface, because is mainly used for modeling components, technical applications and technical product development. It can provide rendering the object in space and allows to manipulation with it. It is also used in computer games and simulations. This interface can be controlled by programming languages like C++ and Java. Before starting the program we have to install the GLUT library. From this library OpenGL reads the forms, shapes, functions, materials, scenes, movements, calculations, etc.

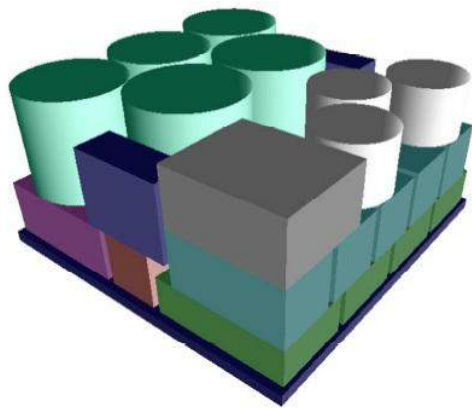


Fig.5. Virtual reality 3D model

Dimensions of the object, dimensions of the pallet and coordinates with the rotations of objects are used as input data to the model. After drawing the solution into a virtual reality model user can rotate and control the load by mouse. This module can draw static or dynamic model of the load. Static model has no movements but we can control it with the mouse. Dynamic model is still rotating.

4. ROBOT CONTROL

Inevitable function of this software is his communication with the SCARA robot. The control system knows several commands for controlling the movements of the robot, for example: MOVE 100, 100, 90, 50 (go to coordinates 100, 100, 90, 50). Serial link is used for sending the individual commands and also for receiving the answers from the control system. This connection is made by the USB port. We have created a simple window to control the robot from our computer. It contains a text line to send a simple commands and a text box to write the entire program for the robot. Another text field is used for writing the answers from the robot control system. If we will send the entire program from the first text box to the control system, the error will occur because a buffer will be full. The buffer of control system can handle only 50 lines of the program at once, so it is necessary to send the entire program line after line to it. To solve this problem we created two synchronized threads. The first thread sends individual commands to the control system of the robot (output) and the second thread is reading replies from it (input). Thread output is inactive until the thread input does not catch the answer from control system of the robot. After catching the answer, the next line of the program is sent by thread output and again waits for the response. The whole process will repeat until the entire program will be send line by line. The second problem was the automatic generation of the commands for robot. So we have created a template commands to store only the one basic object. To this template are placed the variables on places of coordinates. These variables are automatically changed after each cycle of storage.

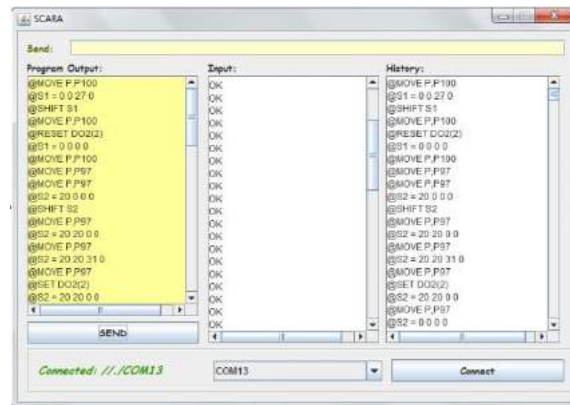


Fig.6. Robot control module

Control program is reading them from a text file that imposed a program for planning the layout of objects. Each coordinate has a characteristic variable. According to a number of lines in this text file is determined a number of cycles. If an error occurs in the control program of the robot we can start it again from the last performed command. The last part of the window is a line that informs the connection status to robot control system via USB. If connection is ok, then the green sign CONNECTED is shown. If an error occurs then the red sign DISCONNECTED is shown. Refreshing the connection can be done through the CONNECT button.

5. CONCLUSION

Knowledge of methods used for two-dimensional layout is essential for creating three-dimensional and mixed loads. Mixed load consists of one or more shapes. Many software products have implemented these methods in their algorithms. They use them for evaluation, calculation and creating optimal layout of objects on the pallet. When three – dimensional distribution is used then it is necessary to create a virtual reality model of pallet load. Thanks to this model we can analyze load and fill the empty area using methods for two – dimensional loading. This problem is solved in VEGA project.

REFERENCES

- [1] CORMEN, T. (2009) *Introduction to algorithms*, Massachusetts Institute of technology.
- [2] HAJDUK, M. (2008) *Robotické bunky*, SjF,Košice.
- [3] HEINZE, A. (2006) *Optimisation of BMW Group Standardised Load Units via the Pallet Loading Problem*, Linköping.
- [4] KUHN, T. (1999) *Automatisierte Palettierung mit Mehrfachgreifern*, Universität Hannover, Berlin.
- [5] NELISSEN, J. (1993) *New Approaches to the Pallet Loading Problem*, Aachen.
- [6] YANG, M. (1993) *Multi-layer palletization of multi-size boxes for 2D and 3D problems*, Montreal

LAYOUT DESIGN OF VACUUM EFFECTOR HEAD FOR MANIPULATION WITH FLOPPY MATERIALS

Ján SLAMKA, Marián TOLNAY, Michal JEDINÁK

USETM, Slovak University of Technology, Nám. Slobody 17, Bratislava, Slovakia
 jan.slamka@stuba.sk, marian.tolnay@stuba.sk, michal.jedinak@stuba.sk

The article deals with the selection of appropriate vacuum holding components and their localization in the handling system that is to hold and move rectangular plates. In this article the method of designing and creating the calculation and the program that will enable the automatic selection of the suction elements, as well as their optimal localization in relation with the permitted deflection of the handled object. The calculation is verified by FEM modeling.

Keywords: effector, gripper, suction gripper, suction cups, construction of gripping effectors, object handling.

1. METHOD PROPOSITION FOR THE SELECTION AND DEPLOYMENT OF VACUUM COMPONENTS OF THE HOLDING SYSTEMS

The proposed solutions and the calculation were done for items intended for the manipulation of the vacuum effectors according to the following conditions: manipulated object is flat - sheet metal or metal plate, or a part of it, with a maximum dimension of 2000 x 1200, material - steel plate thickness of 0.2 to 7 mm.

The selection of the required size (diameter) and the number of effectors is such to ensure the safe manipulation with the object and the optimal deployment is done according to the permitted deflection of the manipulated object, where this value is entered into the program by the user [1,2]. In the case of solving one vacuum effector, we can simplify the manipulated object to a circular plate held at the center D_p .

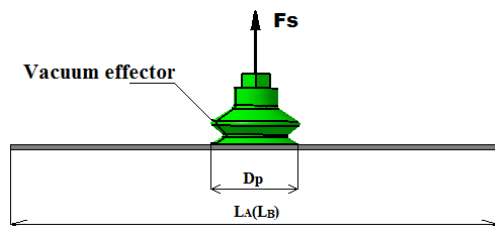


Fig. 1: Using one effector

For the deflection of the plate is true that [4]:

$$Y = \frac{-0,53 + 1,53 \left(\frac{2D}{D_p}\right)^2 - \frac{0,94}{\left(\frac{2D}{D_p}\right)^2} - 3,21 \cdot \ln\left(\frac{2D}{D_p}\right) - 3,55 \left(\ln\left(\frac{2D}{D_p}\right)\right)^2 - \frac{0,89}{2} \ln\left(\frac{2D}{D_p}\right)}{1,3 \left(\frac{2D}{D_p}\right)^2 + 0,7} \frac{\rho(D/2)^4}{Eh^3} \quad (1)$$

The case of holding with several effectors, where the object handled is of circular shape of radius R we

suggest the deployment of the effectors on a circle of diameter R_u .

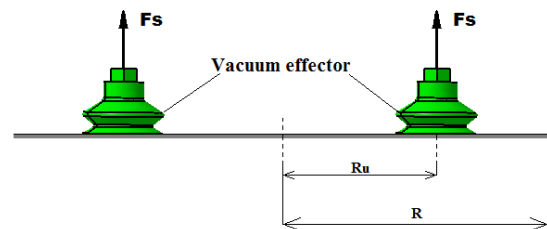


Fig. 2: Using several effectors

Solving the following equations we get the equation of deflection on the perimeter [4].

$$Y_Y = \frac{239 R^4 \cdot \rho \cdot g}{208 B \cdot h^2} - \frac{141 R^2 \cdot R_u^2 \cdot \rho \cdot g}{104 B \cdot h^2} + \frac{43 R_u^4 \cdot \rho \cdot g}{208 B \cdot h^2} + 3 \frac{R_u^2 \cdot R^2 \cdot \rho \cdot g}{B \cdot h^2} \ln \frac{R_u}{R} \quad (2)$$

And the deflection of the plate in the center is:

$$Y_S = \frac{143 R_u^4 \cdot \rho \cdot g}{208 B \cdot h^2} + \frac{R^2 \cdot R_u^2 \cdot \rho \cdot g}{B \cdot h^2} \left(\frac{57}{104} - \frac{3}{2} \ln \frac{R}{R_u} \right) \quad (3)$$

The total deflection of the circular plate is then expressed as the sum of those two deflections:

$$Y = Y_Y + Y_S \quad (4)$$

The problem of rectangular plates can be solved with sufficient accuracy, by representing the rectangle as two circular plates with diameters responding to the lengths of the sides of the rectangle (Fig. 3) [3].

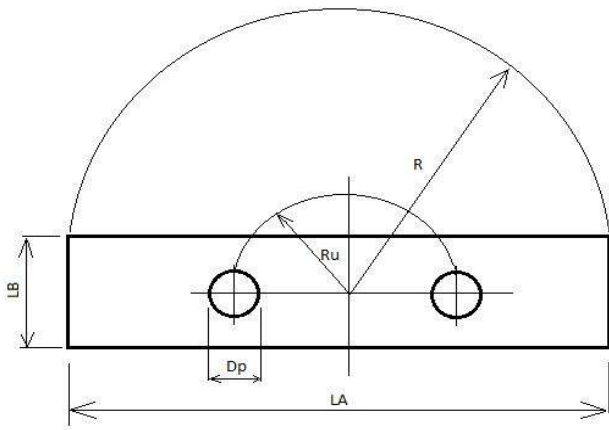


Fig .3: Substitution of rectangular plates by circular ones

2. PROPOSAL FOR AUTOMATED SELECTION AND DISTRIBUTION OF VACUUM COMPONENTS IN THE HOLDING SYSTEMS

In this study, the software used was the 2009 version of SolidWorks software with an integrated program SolidWorks Simulation used for solving model situations. This sub-program operates on the principle of FEM. Following the establishment of a network of elements, it calculates the parameters in nodes by applying specified material properties. The accuracy of the calculation is then given by the delicacy of the network. Therefore, for these relatively simple cases the criteria selected are very strict in addition to the controlled formation of a curvilinear grid. The force action is represented by the acceleration of gravity.

Material that was used:

Metal 11 343.0 heat rolled

Modul of elasticity $E = 2 \cdot 10^5$ MP

Poisson's ratio $\mu = 0,28$

Modul of shear stress $G = 8 \cdot 10^4$ MPa

Density $\rho = 7,80$ g/mm³

Tensile strength $R_m = 325$ MPa

Yield strength $R_e = 180$ MPa

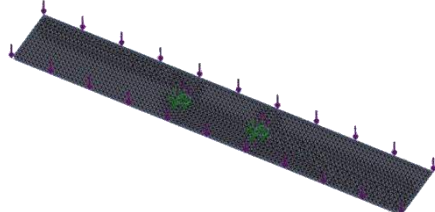


Fig. 4: Volume network of the plate

2. 1 ANALYSIS OF DEFLECTION USING ONE VACUUM EFFECTOR

This simple situation gives us an initial idea of the deformations and tensions in the material. The used structure resulted in 82,576 computing nodes and 45,879 elements. The resulting effect is accentuated by the deformation ratio of 4:1 (Fig. 5). In this case, we can control the deflection only by changing the effector diameter.

Input Data:

- Diameter of the effector $D_U = 40$ mm
- Central deployment
- Semi-product 350 x 600 x 0,5 mm

Output Data:

- The deflection of the free end (corners) $Y = 15$ mm
- Maximum stress in the areas marked red is 59.8 MPa

Table 1. Deflection Values of semi-product 350x600

Dimensions: 350 mm x 600 mm						
thickness [mm]	0,5	1	1,5	2	5	7
deflection[mm]	15,08	3,78	1,70	0,87	0,12	0,053

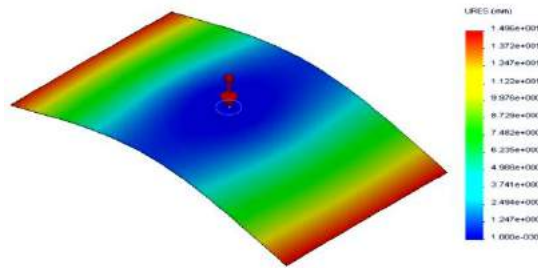


Fig. 5: The course of deformation show in scale 4:1

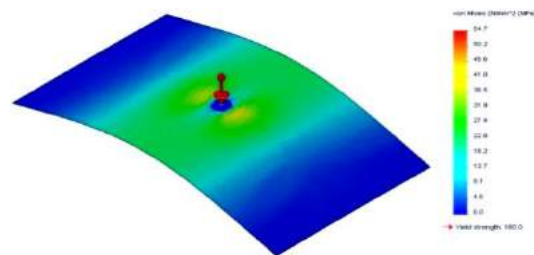


Fig. 6 The course of stress

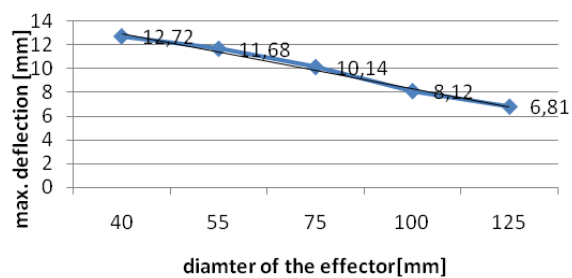


Fig. 7: The relation between deflection Y and the diameter of the effector D_p

2.2 DEFLECTION ANALYSIS IN THE CASE OF USING TWO OR MORE VACUUM EFFECTORS

In the case of using two effectors deployed along the length of the axis, the regulation of the deflection of the free ends was done by changing the distance separating the effectors from each other. The contours of the effectors are represented in the images below as circles.

Input Data:

- Diameter of effector $D_p = 40$ mm
- Number of effectors $n = 2$
- Diameter of the pitch circle $D_u = 90,125$ mm
- Semi-product $650 \times 1000 \times 0,5$ mm
- Permitted deflection 100 mm

Output Data:

- Deflection $Y = 109$ mm $> Y_{DOV} = 100$ => doesn't meet required conditions

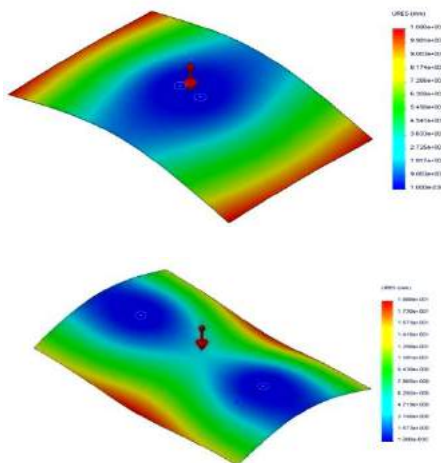


Fig. 8: Using two effectors a, b

To highlight the benefits of using multiple mounting in cases with high strain, dependence was obtained between the deflection of the free end and distances separating the holding elements. The calculation was performed for semi-product of dimensions $1200 \times 750 \times 1,5$ mm. When using an element with a diameter of 125 mm, we calculated 26 mm of deflection and tension in the critical areas reached values up to 100 MPa. As the chart shows the change in distance, results in an exponential decrease of the value of the deflection.

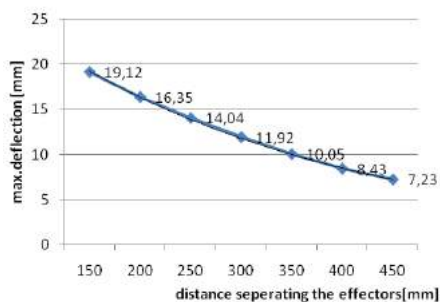


Fig. 9: The relation of the deflection Y and the distance between the effectors.

When using several vacuum effectors, whether because of force-stress on the elements or due to the reduction of the deflection, after consideration the solution should be chosen in, so that it best meets the requirements of no additional costs. And chosen a solution that will best meet the requirements of no additional costs to deal with. This confirms the dependence shown in Fig. 10th The result confirms that the arrangement of elements in the form of a ring, affects the deflection only by the use of 4 effectors.

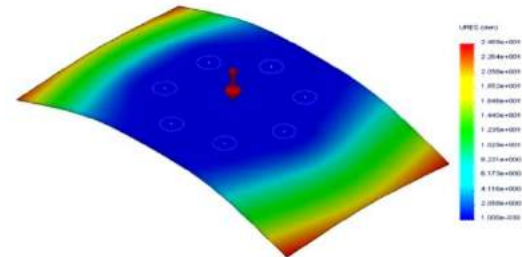


Fig. 10: Holding using more several effectors

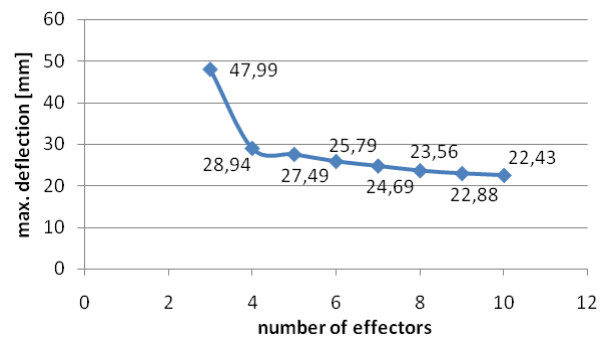


Fig. 11: The relation between the deflection Y and the number of effectors n arranged in a circle n

2.3 EFFECT THE ARRANGEMENT OF ELEMENTS ON THE DEFORMATION

This example illustrates the different deformation patterns at different ends of the plate and the way it is deformed in relation to different arrangements of the effectors. Choice between these arrangements depends on the requirements, like which side should enter the forming machine. Choosing the right arrangement is evident from Fig. 12 and Fig. 13.

Input data:

- diameter of the effector $D_p = 125$ mm
- number of effectors $n = 3$
- diameter of pitch circle $D_u = 516,0775$ mm
- semi-product $1200 \times 2000 \times 1,5$ mm

Output Data:

- difference of deformation of opposite corners $\Delta = 47,2$ mm
- difference of deformation of opposite corners $\Delta = 54$ mm

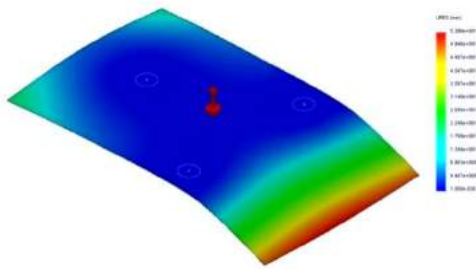


Fig. 12: Deformation with a symmetrical longitudinal arrangement

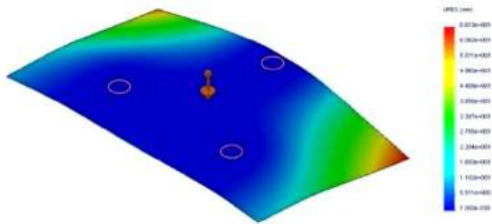


Fig. 13: Deformation with diagonal symmetrical arrangement

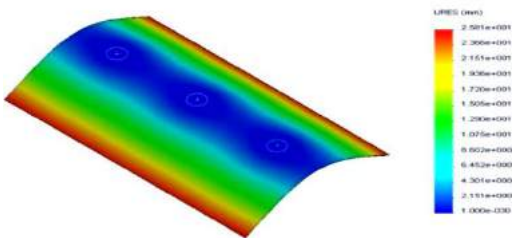


Fig. 14: Deformation with linear arrangement along the larger dimension

3. CONCLUSION

The research presented in this paper was to obtain visual images, and numerical values while examining the handling process when manipulating a metal sheet plate in the form of a rectangle. The results obtained are in the form an image, which shows the plate as well as the place it s holded from and colors showing the intensity of the deflection and stress all over the plate. Numerical values represented the extreme stresses and deformations of the material.

In the second part of the presented research results in the case of one gripping element, the impact of variations of the diameter of the vacuum effectors on the resulting deflection. In all the cases studied, the deformations occurring where only elastic deformations. The case of using two vacuum effectors was analyzed, were the dimensions f the vacuum components where chosen in such a way to satisfy the force requirements for ensuring a safe grip on the manipulated object. In the last part our attention goes to the issue of using more effectors arranged in a defined circle. Based on the values obtained, it can be argued that it is economically advantageous to use the maximum number of four elements. Further an increase the value of the deflection significantly doesn't appear. Additionally, the effect of rotating the trio of elements with an angle of 45° and the linear arrangement on the value of the deflection.

The presented approach helps to simplify the work of a designer in the design of the vacuum grips. It helps the user to select the correct size and number of effectors in handling a steel sheet as well as choosing the best location. In the calculations, the dynamic page of the problem in hand has not been solved or calculated. The safe grip of the object was ensured and secured by a safety factor.

Practical Application of the new methodology of appropriate deployment of the holding elements is used to manipulated and handle materials with large diameters and perimeters and of small thickness. In these cases it is possible to replace the intuitive deployment calculation method described in this paper. The result is a rational determination of the size and number of the vacuum effectors.

REFERENCES

- [1] PALKO, A., SMRČEK, J.: *End-effectors for industrial and service robots.*(In Slovak) Košice: TU, 2004. ISBN 80-8073-218-3.
- [2] TOLNAY, M., ABRAMOVIČ, R.: *Motion model application in manipulation and transportation device design.* In: Proceedings of Mechanical Engineering 2007, Bratislava: STU, 2007. ISBN 978-80-227-2768-6.
- [3] KUBA, F.: *Theory of elasticity and selected applications,* (InCzech) Praha, SNTL, 1982
- [4] SYČ- MILÝ, J. a kol.: *Flexibility and strength: Solved examples* (In Slovak). 1. vyd. Bratislava: ALFA, 1988.
- [5] TOLNAY M., Olšavský, V., Brody, M.: *The layout of manipulation effector.* In: Proceedings of 9th ASME Engineering Systems Design and Analysis Conference. ESDA 2008, jul 2008, Haifa, Israel, ISBN 0-7918-3827-7, Order No. 1794 CD, ESDA 2008



DC SERVO MOTORS CONTROL OF CNC MACHINES BY SLIDING MODE

Vladislav BLAGOJEVIĆ¹, Miodrag STOJILJKOVIĆ², Milorad RANČIĆ³

¹Faculty of Mechanical Engineering, University of Niš, Aleksandra Medvedeva 14, Niš, Serbia

²Faculty of Mechanical Engineering, University of Niš, Aleksandra Medvedeva 14, Niš, Serbia

³High Technical School, Đorđa Stratimirovića 23, Zrenjanin, Serbia

vlada@masfak.ni.ac.rs, misa@masfak.ni.ac.rs, rancicmil@ptt.rs

Abstract: Nowadays, the DC servo motors are used to power CNC machines. Accuracy and positioning of CNC machine is directly conditioned by the good and exact control of servo motors. There are many different control algorithms. This paper presents a new algorithm for servo motor control that uses the theory of variable structure system with sliding working mode. In this paper, all the advantages of the proposed control algorithm, compared to conventional PID controllers are presented by computer simulation.

Key words: CNC, digital control, DC servo motor, sliding mode

1. INTRODUCTION

Machine tools are an important part of many manufacturing processes with a growing demand of part quality and cost reduction. To achieve these objectives, machine tools have incorporated technology to automatize the process and the introduction of the first Computer Numerical Control (CNC) machine was in the early 1970's, when most of the digital hardware from the Numerical Controlled (NC) machine was replaced by a dedicated computer.

The control architecture of a modern machine tool can be divided in three levels:

- servo control,
- interpolation, and
- adaptive control,

as figure 1 shows [1].

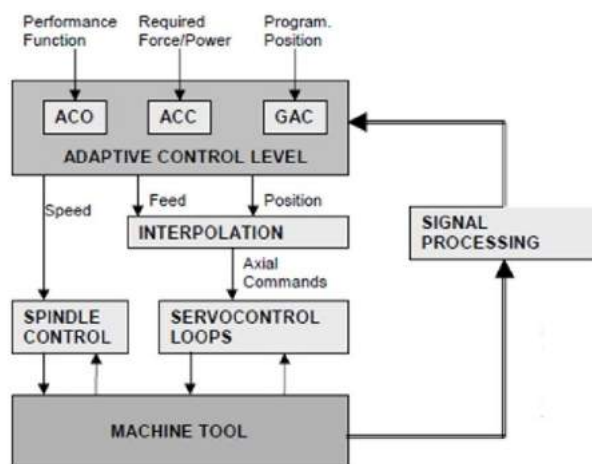


Fig.1. Good quality figure with clear lettering

Adaptive control sets the programmed parameters (feeds and speeds) in order to pursue a given criterion or to minimize a given cost function using measured or predicted output process variables (force, power, and surface roughness among others).

The interpolator level sets the coordinated movements among the axes of motion in order to achieve the tool trajectory. The desired trajectory is divided in discrete points using a given criterion at the interpolation level and then the command for each axis is generated. The interpolation level can be classified as Linear Interpolation, Circular Interpolation, and Complex Surface Interpolation.

Servo control loops control the axes of the machine based on requirements of velocity, position and acceleration. Traditionally, the dynamics of each axis in a machine tool is represented as a second order system for which well-known techniques are applied, such as PID (Proportional-Integral-Derivative) controllers [1]. However, the action of these simple controllers can be degraded by process perturbations, model uncertainties and non-linearities, which require sophisticated techniques and innovative hardware to achieve higher control requirements.

The main goal of this paper is exploration of the possibility of applying the algorithm of control of the variable structure with sliding working mode to the problem of CNC machine axes control by DC servo motors control. The motives for this paper are to be found in numerous publications dedicated to the application of sliding modes to various control tasks [2], which confirm the superiority of such systems over classic solutions. The basic features of sliding modes, known to a small circle of experts in the field of automatic control, are:

- theoretical invariance to the external load and internal perturbations (parameters uncertainty) if machining conditions are satisfied [3] and practical robustness;
- the character of the system's movement is known in advance;

- the movement does not depend on the object's parameters and control, but only on control parameters;
- what is necessary is not exact knowledge of the object's parameters, but only of the range of their possible change;
- it is easier to ensure the system's stability by decomposing the problem of stability into two simpler sub-problems;
- lowering the order of the differential equation which describes movement.

Apart from the above listed features, systems with a variable structure with sliding working modes have shortcomings. There are two basic of these:

- the necessity of measurability of the full state of the controlled object;
- the occurrence of vibration in the control signal, which may cause excitation of non-modelled dynamics of the object and undesired movement in the area of the predicted trajectory.

The first shortcoming can successfully be solved by the application of the observer, which partly alleviates the second, too. However, algorithms which solve one or both these problems have also been developed.

This paper makes use of a digital algorithm of control of the variable structure, which was applied for the first time to the problem of controlling the generator of waveforms [4] and detailed explained in [5].

The paper is organized in the following way: the second part presents an outline of the digital control algorithm with sliding mode on the basis of [5]. The third part presents the mathematical model of DC servo motor that is used in CNC machines. The fourth part presents the effects of the application of the above-mentioned algorithm of control in comparison with conventional PID controllers by means of computer simulation.

2. ALGORITHM OF DIGITAL CONTROL WITH SLIDING MODE

The algorithm of control, whose application to the problem of CNC machine axes control by DC servo motors control is examined in this paper, belongs to the group of digital algorithms of control of variable structure. The goal of synthesis of control is to achieve movement of the system in the space of state on a pre-given hyper-surface, in systems of the higher order, i.e. on a line (most frequently a straight line), in systems of the second order. To do so, what must be ensured is the transfer of the system's state from any initial state to the given hyper-surface and its subsequent movement on it in the sliding regime. This means that the system's phase trajectories all go into the given hyper-surface. Since it is selected so that it passes through the outcome of the space of state, which represents the state of equilibrium, asymptotic stability of the system is also ensured. In this way, the system is brought into equilibrium according to a pre-given trajectory, which may also have attributes of optimality. To summarize, the movement of these system has three phases [5,6]:

- I. the phase of reaching the hyper-surface;
- II. the phase of the sliding regime;
- III. the phase of steady state.

If the sliding hyper-surface is marked as $s(x)$, the conditions are met by satisfying the inequality.

$$s(\mathbf{x})\dot{s}(\mathbf{x}) < 0 \quad (8)$$

This condition can be satisfied by applying various algorithms of control. However, they must contain a relay component of type, which may give rise to parasitic movements (chattering) in the area of the hyper-surface $s(x)=0$ even in the steady state. Such movements are especially intrusive in electromechanical systems

$$U_0 \operatorname{sgn}\{s(\mathbf{x})\}, U_0 > 0 \quad (9)$$

The algorithm applied in this paper eliminates or minimizes the problem of vibration to a tolerable level. The control is formed so that it has two components: a relay component, which ensures safe and quick transfer of the system's state near the sliding hyper-surface without intersecting it, and a linear component, which brings the system's state into $s(x)=0$ in the following step (during one discretization period).

In shortest, the applied algorithm, which is described in [5] in detailed, can be represented in the following way.

For a given controllable and observable dynamic system

$$\dot{\mathbf{x}} = \mathbf{A}\mathbf{x} + \mathbf{b}u, \quad \mathbf{x} \in R^n, \quad u \in R^1, \quad \mathbf{A}_{n \times n}, \quad \mathbf{b}_{n \times 1} \quad (10)$$

Since the control will be digitally implemented, it is necessary to perform time-discretization of the model (3).

If T denotes the discretization period and

$$\mathbf{A}_\delta(T) = \frac{e^{AT} - \mathbf{I}_n}{T}, \quad \mathbf{b}_\delta(T) = \frac{1}{T} \int_0^T e^{A\tau} \mathbf{b} d\tau, \quad (11)$$

the discrete-time state-space model of the nominal system, by using δ -transform, can be expressed in the form:

$$\delta \mathbf{x}(kT) = \mathbf{A}_\delta(T)\mathbf{x}(kT) + \mathbf{b}_\delta(T)\mathbf{u}(kT) \quad (12)$$

The well known scalar switching function $s(\mathbf{x})$ in sliding mode control systems that defines a sliding surface in the state space ($s=0$), along which the sliding mode is organized, is chosen as

$$s = \mathbf{c}_\delta(T)\mathbf{x} \quad (13)$$

Where $\mathbf{c}_\delta(T)$ is the switching function vector of appropriate dimension.

Detailed control design procedure of selected digital sliding mode control algorithm is given by Golo and Milosavljević [4,5]. Here, only the important relations will be briefly recounted.

The positioning control law is obtained as:

$$u = -\mathbf{c}_\delta(T)\mathbf{A}_\delta(T)\mathbf{x}(k) - \Phi(s(k), \mathbf{X}(k)) \quad (14)$$

The switching function vector $\mathbf{c}_\delta(T)$, which exclusively defines system dynamics in sliding mode, is selected according to the relation:

$$\mathbf{c}_\delta(T) = [\mathbf{c}_1(T) \mid 1]\mathbf{P}_1^{-1}(T) \quad (15)$$

where:

$$\mathbf{P}_1(T) = [\mathbf{b}_\delta(T) \dots \mathbf{A}_\delta^{n-1}(T)\mathbf{b}_\delta(T)] \begin{bmatrix} a_1(T) \dots a_{n-1}(T) & 1 \\ a_2(T) \dots & 1 & 0 \\ \vdots & \ddots & \vdots \\ 1 & \dots & 0 & 0 \end{bmatrix} \quad (16)$$

$$\delta_i(T) = \frac{e^{-\alpha_i T} - 1}{T}, \quad \alpha_i > 0, \quad i \neq j \Rightarrow \alpha_i \neq \alpha_j, \quad i, j = 1, \dots, n-1 \quad (17)$$

$$c_i(T) = \frac{1}{(i-1)!} \frac{d^{i-1} \prod_{j=1}^n (\delta - \delta_j(T))}{d\delta^{i-1}} \Big|_{\delta=0} \quad (18)$$

Function $\Phi(s, X)$ is defined as:

$$\Phi(s, X) = \Phi(s) = \min \left(\frac{|s|}{T}, \sigma + \rho |s| \right) \text{sgn}(s); 0 \leq \rho T < 1, \sigma > 0 \quad (19)$$

Parameters σ and ρ defines sliding mode reaching dynamics and should be chosen to provide as short as possible reaching phase [5,6,7,8].

3. DC SERVO MOTOR MATHEMATICAL MODEL

The DC servo motor circuit diagram [9] is presented in figure 2, where $i_a(t)$ is armature current, L_a is armature inductance, R_a is armature resistance, $V_a(t)$ is input voltage, $E_b(t)$ is back emf., T_L is load moment, T_m is motor moment and ω is motor angular velocity.

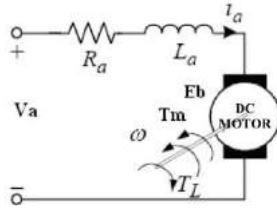


Fig.2. DC servo motor circuit diagram

The velocity and position of the DC servo motor, is controlled by changing the supply voltage. According to this theory, the state-space representation of servomotor in space matrix could be expressed in this form:

$$\begin{bmatrix} \dot{x}_1(t) \\ \dot{x}_2(t) \end{bmatrix} = \begin{bmatrix} 0 & 1 \\ 0 & -M \end{bmatrix} \begin{bmatrix} x_1(t) \\ x_2(t) \end{bmatrix} + \begin{bmatrix} 0 \\ N \end{bmatrix} V_a(t) \quad (20)$$

$$M = \frac{D_m R_a + k_b k_t}{J_m R_a} \quad (21)$$

$$N = \frac{k_t}{J_m R_a} \quad (22)$$

where $x_1(t) = \theta$ is angular position of the rotor shaft, $x_2(t) = \omega$, D_m is equivalent viscous density by the motor [10], k_b is back-emf constant, k_t motor torque constant, J_m is equivalent inertia by the motor.

4. SIMULATION RESULTS

In order to verify the theoretically obtained results, a simulation is carried out. The control plant is a DC servo motor with parameters $k_b=0.02113$ Vs/rad, $k_t =0.04686$ Nm/A, $J_m=0.00003$ Kgm², $R_a=2.2$ Ω , and its state space model for these purposes is:

$$\begin{bmatrix} \dot{x}_1 \\ \dot{x}_2 \end{bmatrix} = \begin{bmatrix} 0 & 1 \\ 0 & -15 \end{bmatrix} \begin{bmatrix} x_1 \\ x_2 \end{bmatrix} + \begin{bmatrix} 0 \\ -710 \end{bmatrix} u \quad (23)$$

$$x_1 = \theta_d - \theta, \quad x_2 = -\omega \quad (24)$$

where θ_d and θ are desired and actual angular position of the rotor shaft and u is the control signal by input voltage V_a .

The simulation was performed with $T=0.4$ ms and parameter $\alpha=15$ s⁻¹. The desired angle of rotor shaft was $\theta_d=120$ rad. The controller parameters have been selected as: $\sigma = 25$, $\rho = 0$, $c_\delta(T) = [-0.028141 \ -0.001407]$, $c_\delta(T)A_\delta(T) = [0 \ -0.007014]$.

In figure 3, the results of positioning of the DC motor rotor shaft when digital control with sliding mode and traditional PID controller with gain $K_P = 1.2$, $K_I = 0.5$ and $K_D = 0.1$ are used, are shown.

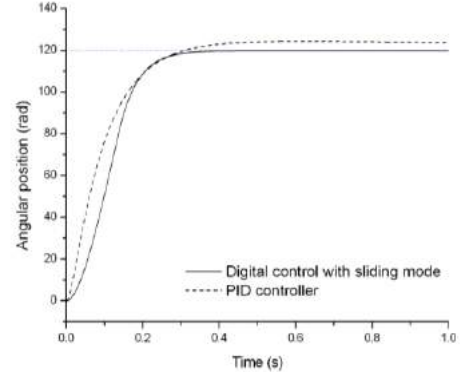


Fig.3. Diagram of the rotor shaft position

In figure 4, the result of phase portrait of nominal system when digital control with sliding mode is used, is shown.

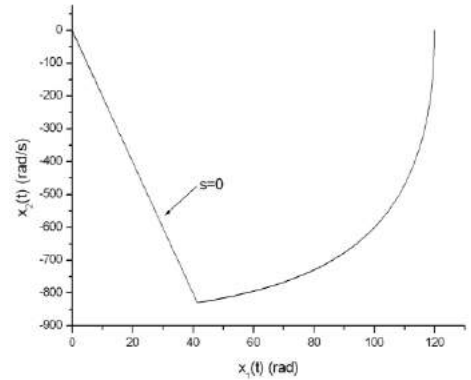


Fig.4. Phase portrait of nominal system

In figure 5, the diagram of digital control law with sliding mode is shown.

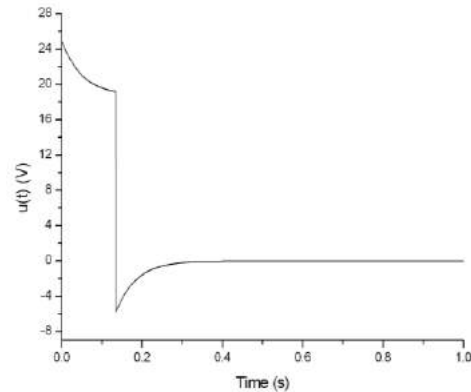


Fig.5. Diagram of digital control law with sliding mode

The results of position show that digital control with sliding mode of the DC motor rotor shaft exhibits superior performance in comparison with the case when conventional PID controller is used. The digital control with sliding mode approach successfully achieves the desired positions of the rotor shaft. For the same conditions, traditional PID controller shows much bigger positioning errors

The switching function $s(x)$, which is one of the main parts of the digital sliding mode control, is shown in figure 6.

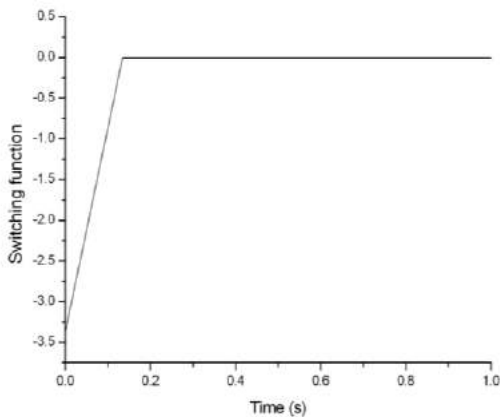


Fig.6. Diagram of switching function

All previous diagrams show the advantages and simplicity of proposed digital control with sliding mode in comparison with traditional PID controller. One of the most important advantages is exact control and abstinence of position error in steady state.

5. CONCLUSION

The paper discusses the positioning problem of the DC servo motor rotor shaft in CNC machines. Digital control with sliding mode is employed in solving this problem. The designed digital sliding mode controller performs its task successfully, since it ensures robustness, quick reaching of the desired position without overshoot and oscillation. The advantages of this nonlinear type of control are shown in Chapter 4, where its performance is compared with the PID controller. The position error when digital control with sliding mode is used is less and equal to zero than in case of traditional PID controller, for the same conditions.

It may be concluded that application of digital control with sliding mode strategy in positioning of DC servo motor rotor shaft in CNC machines is justified due to much better response and greater robustness.

ACKNOWLEDGEMENT

This paper is part of project TR35034 The research of modern non-conventional technologies application in manufacturing companies with the aim of increase efficiency of use, product quality, reduce of costs and save energy and materials, funded by the Ministry of Education and Science of Republic of Serbia.

REFERENCES

- [1] KOREN, Y. (1997) *Control of Machine Tool*, Journal of Manufacturing Science and Engineering, Vol. 119, pp 749-755
- [2] UTKIN, V. I. (1992), *Sliding Modes in Control and Optimization*, Springer Verlag
- [3] DRAZENOVIC, B. (1969) *The Invariance Condition in Variable Structure Systems*, Automatica, Vol. 5, pp 287-295
- [4] GOLO, G., MILOSAVLJEVIĆ, Č. (1997) *Two-phase Triangular Wave Oscillator Based on Discrete-time Sliding Mode Control*, Electron. Lett., Vol. 33, pp 1838-1839
- [5] GOLO, G., MILOSAVLJEVIĆ, Č. (2000) *Robust discrete-time chattering free sliding mode control*, ELSEVIER Systems & Control Letters, pp. 19-28
- [6] BLAGOJEVIĆ, V., (2004) *Synchronization of the Work of Pneumatic Executive Organs in Technological Processes*, Magistar Thesis, Faculty of Mechanical Engineering, University of Nis
- [7] BLAGOJEVIĆ, V., (2010), *Contribution to the Development of Efficient Control of Pneumatic Executive Organs*, Ph D Thesis, Faculty of Technical Sciences, Novi Sad
- [8] BLAGOJEVIĆ, V., MILOSAVLJEVIĆ, Č., RADOVANOVIĆ, M., STOJILJKOVIĆ, M. (2003), *Improvement of the Work of the Pneumatic Machine for Bending By Using the Digital Sliding Mode*, Facta Universitatis series Mechanical Engineering, Vol. 1, No. 10, pp 1347-1354
- [9] MEHMET, A., İSMAİL, T. (2007) *Motion Controller Design for the Speed Control of DC Servo Motor*, International journal of applied mathematics and informatics, Vol. 1, pp 131-137
- [10] RAHMAT, F., RAMLI, S. (2008) *Servomotor Control Using Direct Digital Control And State-Space Technique*, Journal Teknologi, Vol. 49, pp 45-60



COMPLIANCE MODELING AND IDENTIFICATION OF 5-AXIS VERTICAL ARTICULATED ROBOT FOR MACHINING APPLICATIONS

**Dragan MILUTINOVIC, Milos GLAVONJIC, Nikola SLAVKOVIC, Sasa ZIVANOVIC,
Branko KOKOTOVIC, Zoran DIMIC**

University of Belgrade, Faculty of Mechanical Engineering, Kraljice Marije 16, Belgrade, Serbia
LOLA Institute, Kneza Viseslava, Belgrade, Serbia

dmlutinovic@mas.bg.ac.rs, mglavonjic@mas.bg.ac.rs, nslavkovic@mas.bg.ac.rs, szivanovic@mas.bg.ac.rs,
bkokotovic@mas.bg.ac.rs, zoran.dimic@li.rs

Abstract: This paper describes analytically and experimentally based compliance modeling and identification of 5-axis vertical articulated machining robot. The conventional method for the calculation of Cartesian space compliance based on joint compliances and Jacobian matrix is expanded and used for experimental 5-axis machining robot. Analytical analysis was conducted for effects of compliances of each joint individually on Cartesian space robot compliance. Experimentally, the Cartesian space compliance is obtained by direct measurement of the absolute displacements evoked by static forces along 3-orthogonal directions at the tool tip in the robot workspace for the case of 3-axis machining.

Key words: robot, machining, compliance modeling

1. INTRODUCTION

Industrial robots are promising cost-effective and flexible alternative for certain multi-axis milling applications. Compared to machine tools, robots are cheaper and more flexible with larger workspace. It is well known that poor accuracy, stiffness and complexity of programming are the most important limiting factors for wider adoption of robotic machining in machine shops [1]. In order to contribute to efficient use of robots for machining applications, research and development of reconfigurable robotic machining system were initiated [2]. The research and development comprise two groups of problems: the realization of a specialized 5-axis machining robot with integrated motor spindle in order to improve robotic machining accuracy, and the development of the machining robot control and programming system which can be directly used by CNC machine tool programmers and operators [2].

This paper describes analytically and experimentally based compliance modeling and analysis of 5-axis machining robot. The conventional method for the calculation of Cartesian space compliance based on joint compliances and Jacobian matrix [3-5] is expanded and used. Analytical analysis was conducted for effects of compliances of each joint individually on Cartesian space robot compliance. Experimentally, the Cartesian space compliance is obtained by direct measurement of the absolute displacements evoked by static forces along 3-Cartesian directions at the tool tip in the robot workspace for the case of 3-axis milling.

2. PROBLEM STATEMENT

A basic module of the proposed concept of the robotic machining system [5] is the specialized 5-axis robot, Fig.

1a, with integrated motor spindle and with larger workspace, higher payload and stiffness.

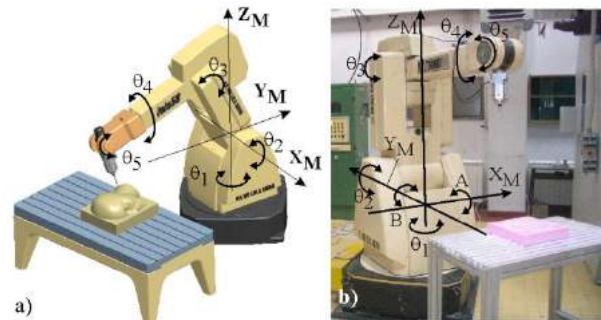


Fig.1. 5-axis machining robot

Due to its advantages in respect of stiffness and singularities, such robot would operate as a specific vertical 5-axis milling machine (X, Y, Z, A, B) spindle-tilting type. The development of specialized 5-axis vertical articulated machining robot is a joint project with robot manufacturer. For the development of control and programming system as well as for the analysis and development of the mechanical structure of 5-axis machining robot from Fig. 1a, a 6-axis vertical articulated robot with payload of 50kg, Fig. 1b, was used as a testbed, in a way that the sixth axis was blocked. The robot is equipped with high speed motor spindle with maximum speed of 18,000 min⁻¹.

The focus of current research, one part of results being presented in this paper, is related to compliance modeling and analysis of the experimental 5-axis machining robot, which includes:

- Analytically based robot compliance modeling.
- Experimentally based robot compliance modeling.
- Machining experiments.

3. JACOBIAN MATRIX AND WORKSPACE

As it was mentioned, the 5-axis robot from Figure 1a will be considered below as a specific configuration of the 5-axis vertical milling machine (X, Y, Z, A, B) spindle-tilting type. Figure 2 represents a geometric model of the robot.

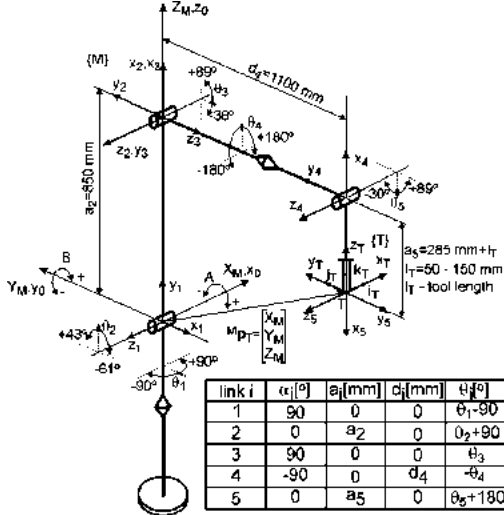


Fig.2. D-H link coordinate frames and kinematic parameters

The robot reference frame {M} has been adopted according to the standard of this machine type and coincides with the robot based frame (x_0, y_0, z_0) . The tool frame {T} is attached to the milling tool tip T in a way that axis z_T coincides with tool axis and also coincides with axis of the last link of the robot to which motor spindle is attached. The thus configured machining robot, where machining is performed on a work table in front of the robot as well as limited motions in joints relative to the reference position allows for: taking into account only one solution of inverse kinematic, avoiding the robot singularities, conveniences related to the stiffness.

Joint coordinates vector for this 5-axis vertical articulated robot is represented as $\theta = [\theta_1 \ \theta_2 \ \theta_3 \ \theta_4 \ \theta_5]^T$ where θ_i are scalar joint variables controlled by actuators. Given that the robot has 5 DOF, only the direction of tool axis z_T is controllable, while axes x_T and y_T will have uncontrollable rotation about it. The position and orientation of the tool frame {T} relative to robot reference frame {M} is described by world coordinates vector expressed as $\mathbf{x} = [X_M \ Y_M \ Z_M \ A \ B]^T$.

To model the robot, the Denavit-Hartenberg (D-H) notation [6] was used. To perform kinematic analysis, first coordinate frames are rigidly attached to each link. The homogeneous transformation describing the relation between one link and the next link is traditionally referred to as an A matrix. Matrix ${}^{i-1}A$ designates D-H transformation matrix relating frame (i) to frame $(i-1)$. Figure 2 shows D-H coordinate frames and link kinematic parameters for the experimental 5-axis robot from Figure 1b i.e. Figure 2 in the reference position taking into account the ranges of joint motions.

After the D-H coordinate frame is assigned to each link, the transformation between successive frames $(i-1)$ and (i) is described as follows:

$${}^{i-1}A = Rot(z, \theta_i) \cdot Trans(z, d_i) \cdot Trans(x, a_i) \cdot Rot(x, \alpha_i) = \begin{bmatrix} {}^{i-1}i_i & {}^{i-1}j_i & {}^{i-1}k_i & {}^{i-1}p_{Oi} \\ 0 & 0 & 0 & 1 \end{bmatrix} \quad (25)$$

Substituting D-H parameters of the links in equation (1) the transformation matrices ${}^{i-1}A$ are obtained first. As noticeable from Figure 2 the frame {T} can be described relative to the frame (x_5, y_5, z_5) by homogeneous transformation matrix as 5_7T [2]. Now, as it is well-known [6], the tool position and orientation i.e. the position and orientation of frame {T} with respect to the robot reference frame {M}, Figure 2, for the given joint coordinates vector θ and specified link parameters can be determined as

$${}^M_7T = {}^0_1A \cdot {}^1_2A \cdot {}^2_3A \cdot {}^3_4A \cdot {}^4_5A \cdot {}^5_7T \quad (26)$$

The position and orientation of arbitrary frame i attached to the link i with respect to the robot reference frame {M} i.e. robot based frame (x_0, y_0, z_0) can be expressed as

$${}^O=iT = {}^0_1A \cdot {}^1_2A \cdot \dots \cdot {}^{i-1}A = \prod_{j=1}^i {}^{j-1}A = \begin{bmatrix} {}^{i-1}i_i & {}^{i-1}j_i & {}^{i-1}k_i & {}^{i-1}p_{Oi} \\ 0 & 0 & 0 & 1 \end{bmatrix} \quad (27)$$

for $i = 1, 2, 3, \dots, n = 5$ where n is number of joints.

The robot Jacobian matrix relates joint velocities to Cartesian velocities of the tool tip. The mapping between static forces applied to the end-effector and resulting torques at the joints can also be described by Jacobian matrix [6,9]. Considering that the robot consists of five revolute joints, the Jacobian matrix has as many rows as there are degrees of freedom and the number of columns is equal to the number of joints

$$J = [J_1 \ J_2 \ \dots \ J_n] \quad (28)$$

with column vectors

$$J_i = \begin{bmatrix} {}^i\mathbf{k}_{i-1} \times ({}^0\mathbf{p}_n - {}^0\mathbf{p}_i) \\ {}^0\mathbf{k}_{i-1} \end{bmatrix} \quad (29)$$

Substituting vectors from equation (3) in equation (5) Jacobian matrix columns J_i , $i = 1, 2, 3, \dots, n = 5$ are obtained.

Workspace for 3-axis machining is shown in Fig. 3.

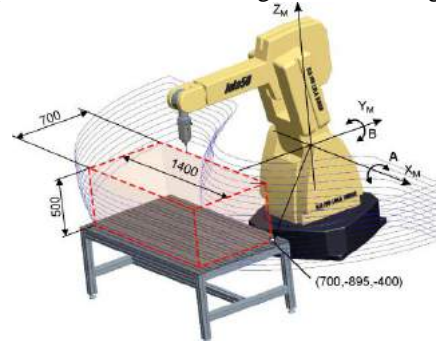


Fig.3. Workspace in the case of 3-axis machining ($A=0^\circ, B=0^\circ$)

4. COMPLIANCE MODELING

As stated in [1,5,7,8] elastic properties of robot segments are insignificant, so there follows below the analysis of compliance model in Cartesian space based on joint compliances. The analysis will be conducted on the existing experimental machining robot from Fig. 1b. Based on the principle of virtual work, the convectional formulation for the mapping of joint compliance matrix C_θ into the Cartesian space compliance matrix $C_X(\theta)$ [3-5] is expressed as

$$C_X(\theta) = J(\theta) \cdot C_\theta \cdot J(\theta)^T \quad (30)$$

where C_θ is the compliance matrix in joint space which has the diagonal form as

$$C_\theta = \text{diag}(C_{\theta 1}, \dots, C_{\theta n}) \quad (31)$$

and $J(\theta)$ is Jacobian matrix.

Equation 6 is practically used in [4] to determine the robot compliance center and in [5] for machining robot compliance analysis where it is stated how suitable it is, for it allows mapping of the joint compliance matrix C_θ into Cartesian compliance matrix $C_X(\theta)$ without calculating any inverse kinematic functions. Since C_θ is diagonal, the Cartesian space compliance matrix $C_X(\theta)$, Eq. 6, is the sum of the joint compliances associated with each individual joint as

$$C_X(\theta) = C_{X1}(C_{\theta 1}) + \dots + C_{Xn}(C_{\theta n}), \quad n = 5 \quad (32)$$

where

$$C_{Xi}(C_{\theta i}) = C_{\theta i} \cdot \mathbf{J}_i \cdot \mathbf{J}_i^T, \quad i = 1, 2, \dots, n, \quad n = 5 \quad (33)$$

while \mathbf{J}_i are column vectors of Jacobian matrix $J(\theta)$.

Equations 8 and 9 provide insight into the impact of compliance of each joint individually on the Cartesian space compliance. This means that impact of the corresponding joint is obtained incorporating in the Eq. 8 only its compliance, while the other joints are considered stiff. This is of crucial importance for the present paper, because it can be useful for robot manufacturer's experts in the design of specialized machining robot.

For an articulated robot, $C_X(\theta)$ is symmetric non-diagonal and configuration dependent matrix. Thus, if C_θ can be experimentally determined, the Cartesian space compliance matrix C_X , Eq. 6 and the linear displacement of robot tool tip under external static force vector $\mathbf{F} = [F_x \ F_y \ F_z]^T$ at any location in the workspace can be estimated as

$$\delta \mathbf{x} = C_X(\theta) \cdot \mathbf{F} \quad (34)$$

Table 1 shows the experimentally identified compound joint compliances.

Table 1. Experimentally identified joint compliances

Joint number i	1	2	3	4	5
$C_{\theta i} [\text{rad/Nm}] \cdot 10^{-7}$	7.14	10.12	12.30	17.32	91.35

Using experimentally determined compound joint compliances, the Cartesian space compliance matrix is calculated in workspace shown in Fig. 3.

Figure 4 shows the distributions of analytically determined compliances in the $Z_M = 0$ plane.

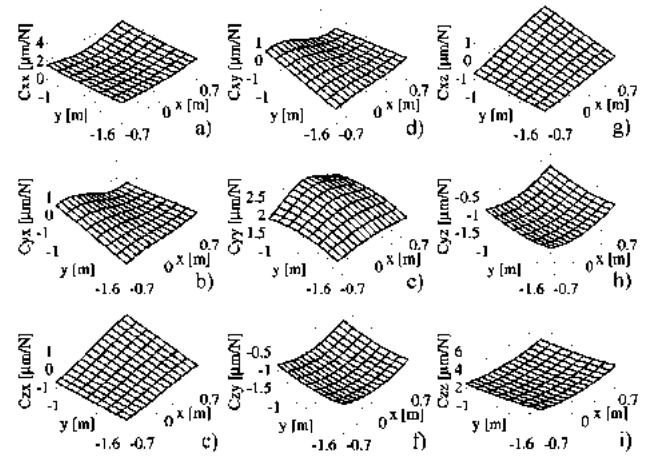


Fig.4. Distributions of analytical compliances in the plane $Z_M=0$

The distributions of direct-compliances C_{xx}, C_{yy} and C_{zz} are presented in Figs. 4a, 4e and 4i respectively. The distributions of cross-compliances C_{yx}, C_{zx} and C_{zy} are given in Figs. 4b, 4c and 4f respectively. Figure 4 can be also viewed as the Cartesian space compliance matrix $C_X(\theta)$ in the $Z_M = 0$ plane in the workspace shown in Fig. 3.

The distributions of dominant components of direct-compliances originating from individual joints are shown in Fig. 5.

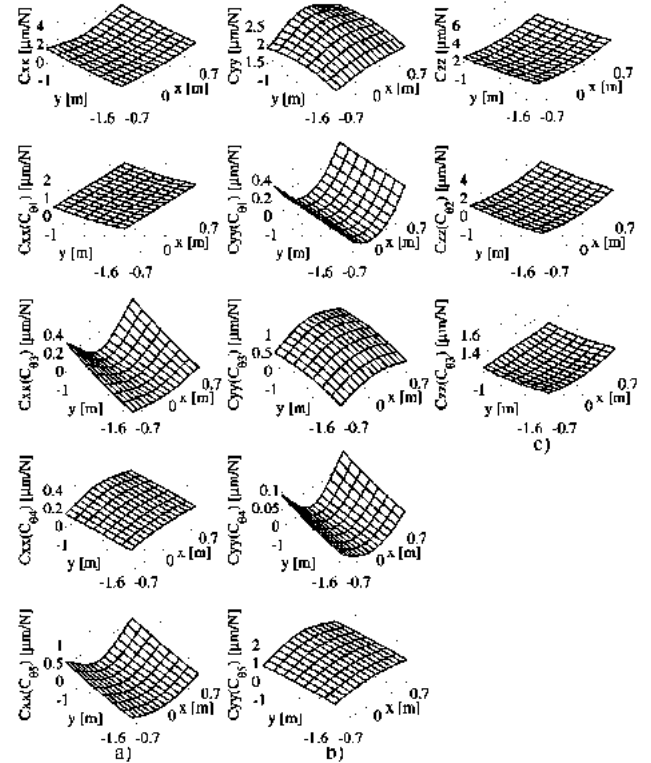


Fig.5. Distributions of dominant direct-compliance components

5. EXPERIMENTAL COMPLIANCE

Another approach to obtain the Cartesian compliance of the machining robot is the direct measurement of the absolute displacement evoked by a load at the tool tip.

The elements of the experimental setup are shown in Fig. 6. The original and deformed positions of sphere-tip tool caused by deadweight of 250N are measured with FARO Portable CMM 3D, from which translational displacements δx , δy and δz are calculated.

Displacements of the sphere-tip tool are measured in the workspace shown in Fig. 3 at 40 points with the fixed X_M - and Y_M -coordinates in 6 Z_M -levels ($Z_M = -400mm$ to $Z_M = 100mm$). Experimental compliances are determined based on sphere-tip tool displacements evoked by static amount of the milling force of 250N in all 3 Cartesian directions. Figure 6 shows an example of displacements measurement for the case of robot loading in Y_M - direction.



Fig.6. Experimental setup of robot loading and displacements measurement

Figure 7 shows the distributions of experimentally obtained compliances in the $Z_M = 0$ plane. The distributions of experimental direct-compliances C_{xx} , C_{yy} and C_{zz} are shown in Figs. 7a, 7e and 7i, respectively.

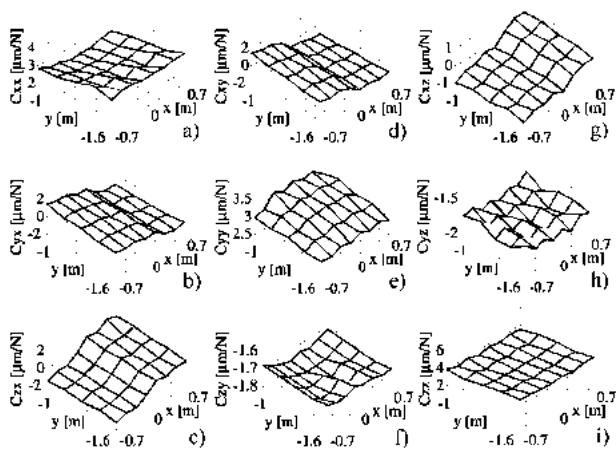


Fig.7. Distributions of experimental compliances in the plane $Z_M=0$

Experimental cross-compliances are presented in Figs. 7b, 7c and 7f, respectively. Comparing them with analytically determined compliances, Fig. 4, it can be inferred that the character of their distributions is similar, but

experimentally determined compliances are slightly higher. Higher values of experimentally determined compliances compared to those determined analytically originate from compliances of structure elements, motor spindle and tool itself.

6. CONCLUSION

The paper presents analytically and experimentally based compliance modeling and analysis of 5-axis machining robot based on conventional approach for the mapping of joint compliances into robot Cartesian space compliance. By expanding this modeling approach, it has been shown that it is possible to analyze each joint compliance impact on robot Cartesian space compliance. Satisfactory correlation between analytically and experimentally determined robot Cartesian space compliances confirms the usability of each joint compliance effects on tool tip displacements. Suitable model of the process forces and compliance model proposed in this paper also enable the development of virtual robotic machining system for further research. The present research has laid foundations for an advanced design method for one machining robot as well as for the development of strategy for real-time tool tip displacement compensation based on captured process forces.

REFERENCES

- [1] PAN, Z., ZHANG, H. (2008) *Robotics machining from programming to process control: a complete solution by force control*. Industrial Robot: An International Journal, Vol. 35, No 5, pp 400-409
- [2] MILUTINOVIC, D., GLAVONJIC, M., SLAVKOVIC, N., DIMIC, Z., ZIVANOVIC, S., KOKOTOVIC, B., TANOVIC, LJ. (2011) *Reconfigurable robotic machining system controlled and programmed in a machine tool manner*. Int J Adv Manuf Technol, Vol.53, No 9-12, pp 1217-1229
- [3] HUDGENS, J.C., HERNANDEZ, E., TESAR, D. (1991) *A compliance parameter estimation method for serial manipulator DSC*. Applications of Modeling and Identification to Improve Machine Performance ASME, Vol. 29, pp 15-23
- [4] MILUTINOVIC, D., MILACIC, V. (1996) *Micro Scara Robot as Universal Adaptive Compliant Wrist*. Annals of the CIRP, Vol.45, No1, pp 31-34
- [5] ABELE, E., WEIGOLD, M., ROTHENBUCHER, S. (2007) *Modeling and identification of an industrial robot for machining applications*. Annals of the CIRP Vol. 56, No1, pp 387-390
- [6] CRAIG, J.J. (1989) *Introduction to robotics: mechanics and control, 2nd ed.* Addison - Wesley
- [7] ABELE, E., ROTHENBUCHER, S., WEIGOLD, M. (2008) *Cartesian compliance model for industrial robots using virtual joints*, Prod. Eng. Res. Devel Vol. 2, No3, pp 339-343
- [8] ALICI, G., SHIRINZADEH, B. (2005) *Enhanced Stiffness Modeling, Identification and Characterization for Robot Manipulators*, IEEE Transactions on Robotics, Vol. 21, No 4, pp 554-564
- [9] SCIAVICCO, L., SICILIANO, B. (2000) *Modelling and Control of Robot Manipulators, 2nd ed.* Springer-Verlag.



INVESTIGATION AND ADAPTIVE NEURO-FUZZY ESTIMATION OF MECHANICAL/ELECTRICAL PROPERTIES OF CONDUCTIVE SILICONE RUBBER

Dalibor PETKOVIĆ, Nenad D. PAVLOVIĆ

University of Niš, Faculty of Mechanical Engineering, Aleksandra Medvedeva 14, 18000 Niš, Serbia
daliborc@gmail.com, pavlovic@masfak.ni.ac.rs

Abstract: *Conductive silicone rubber has great advantages for strain sensing applications. The electrical behavior of the elastomeric material is rate-dependent and exhibit hysteresis upon cyclic loading. Several constitutive models were developed for mechanical simulation of this material upon loading and unloading. One of the successful approaches to model the time-dependent behavior of elastomers is Bergstrom-Boyce model. The paper summarizes the results of investigations on the conductive silicone rubber as strain sensor. An experimental investigation of the sensors subjected to different time-dependent strain histories is presented. Three different tests have been developed to measure time-dependent and strain-dependent behavior of the rubber. To investigate the electrical properties, the resistance of silicone was measured during the mechanical tests. An adaptive neuro-fuzzy inference system (ANFIS) is used to approximate correlation between these measured features of the material and to predict its unknown future behavior. ANFIS has unlimited approximation power to match any nonlinear function arbitrarily well on compact set and to predict a chaotic time series.*

Key words: *conductive silicone rubber, adaptive neuro fuzzy, prediction, strain sensor*

1. INTRODUCTION

Artificial neural networks (ANNs) are flexible modeling tools with capabilities of learning the mathematical mapping between input and output variables of nonlinear systems. One of the most powerful types of neural network system is adaptive neuro fuzzy inference system (ANFIS). ANFIS shows very good learning and prediction capabilities, which makes it an efficient tool to deal with encountered uncertainties in any system. Fuzzy Inference System (FIS) is the main core of ANFIS. FIS is based on expertise expressed in terms of 'IF-THEN' rules and can thus be employed to predict the behavior of many uncertain systems. FIS advantage is that it does not require knowledge of the underlying physical process as a precondition for its application. Thus ANFIS integrates the fuzzy inference system with a back-propagation learning algorithm of neural network. An ANFIS model has been established in this study to predict the voltage changing of conductive silicone rubber during compression tests. The experimental results were obtained from many compression strain tests to make accurate representation of the material behavior.

In this study, based on our experimental measurements, an constitutive model was developed. This model was made by using ANFIS. So far, experimental investigation of mechanical and electrical properties of conductive silicone rubber was performed in [1]. There are many studies of the application of ANFIS for prediction and real-time identification of many different systems. In [2] the effectiveness of predicting non-uniformity of the wafer surface with ANFIS was investigated under conditions of the three process parameters. A developed finite element method was used to obtain the training data

and testing data about non-uniformity on wafer surface. An ANFIS model is developed in [3] to forecast the energy requirements of different types of buildings having different properties. A neuro-fuzzy model was utilized to predict the hardness and porosity of shape memory alloy in [4]. The purpose of that study is estimation of porosity and hardness of the produced samples. Paper [5] presented an improved ANFIS with self-feedback for the applications of time-series prediction. An ANFIS model is applied to predict the flow stress in hot deformation process of Ti6000 alloy in [6]. In [7] optimum cure time of the rubber compounds are predicted using ANFIS model. Various principles of the neural network approach for predicting certain properties of polymer composite materials are discussed in [8]. The applicability of ANFIS for prediction of carbon dioxide solubility in polymers was showed in [9]. In paper [10] was developed a micromechanism theory that successfully captures many of the time-dependent characteristics of filled rubber.

An ANFIS model will be established in this study to predict the voltage changing of conductive silicone rubber during compression tests. Many compression tests of conductive silicone rubber has been conducted at different strain rates and strains to characterize the voltage changing behavior and understand the deformation mechanisms during the deformation process. The constructed ANFIS model exhibits a high performance for predicting voltage changing of the conductive silicone rubber during compression tests. The results obtained in this work indicate that ANFIS is effective method for prediction of voltage changing in conductive silicone rubber and have better accuracy and simplicity compared with the classical methods.

2. MATERIAL AND METHOD

2.1. Experimental Measuring

The carbon-black filled silicone rubber is electrically conductive and its resistance changes by deformation. These properties make this material suitable to develop force or deformation sensors. The characteristics of voltage and stress were represented as function of deformation and time. Various compression tests of the silicone were performed. The specimens were made by press-curing from carbon-black filled silicone rubber (Elastosil R570/70, Shore A 70), as shown in Figure 1. The changing of electrical resistance of silicone rubber specimens were measured with the help of special compression tool and electrodes vulcanized on the top bottom side of the specimens. Measurement electrode was cured on those sides of silicone rubber specimens. The electrodes were made from soft copper weave since it makes good electrical contact. Wires were soldered on the electrodes with connectors to connect to the measurement instrument.



Fig.1. Raw conductive silicone rubber Elastosil R570/70 and one cubic sensor-specimen

Zwick ProLine material-testing machine Z005, shown in Figure 2, was used to measure the mechanical and electrical properties of the sensor-elements. Throughout the mechanical tests, the resistance-deformation and force-deformation diagrams were recorded and automatically drawn via the software testXpert II. As input voltage for electrical source 5V were used according to initial resistance of the sensor-elements during the compression test.

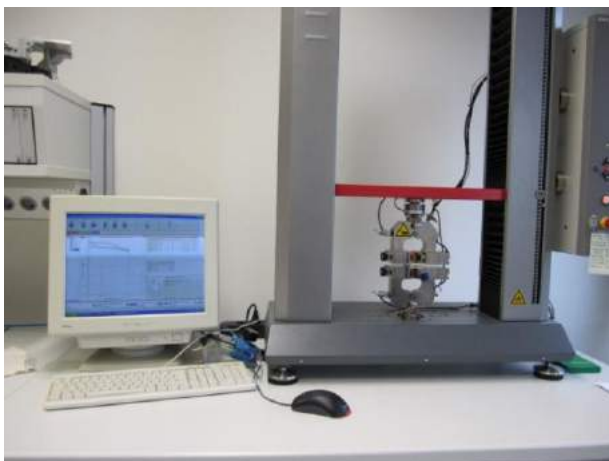


Fig.2. Experimental setup for ProLine material-testing machine

2.2. Adaptive Neuro Fuzzy Inference System

Adaptive neuro fuzzy system (ANFIS) was suggested by Jang [11]. ANFIS can serve as a basis for constructing a set of fuzzy 'if-then' rules with appropriate membership function to generate the stipulated input-output pairs. The membership functions are tuned to the input-output data. ANFIS is about taking an initial fuzzy inference (FIS) system and tuning it with a back propagation algorithm based on the collection of input-output data. The basic structure of a fuzzy inference system consists of three conceptual components: a rule base, which contains a selection of fuzzy rules; a database, which defines the membership functions used in the fuzzy rules; and a reasoning mechanism, which performs the inference procedure upon the rules and the given facts to derive a reasonable output or conclusion. These intelligent systems combine knowledge, technique and methodologies from various sources. They possess human-like expertise within a specific domain – adapt themselves and learn to do better in changing environments. In ANFIS, neural networks recognize patterns, and help adaptation to environments. Fuzzy inference systems incorporate human knowledge and perform interfacing and decision-making.

Here the training data is obtained by many compression tests of the silicone specimens. One half of the data are used for training while the other half is used for checking and validation of the model. With a proper training scheme and fine filtered data-sets, ANFIS is capable of predicting voltage values quite accurately since it learns from training data. This measurement-free architecture also makes it immediately available for operation once they are trained.

In time series prediction the past values of voltage changing up to time "t" are used to predict the value at some point in the future "t+p". The standard method for this type of prediction is to create a mapping from D points of the time series spaced "Δ" apart; that is $[x(t - (D - 1)\Delta) \dots x(t - \Delta), x(t)]$ to predict a future value $x(t + p)$, where $D = 4$ and $\Delta = p = 6$ are used. For off-line learning data is updated and predicted only after presentation of entire data set, or only after an epoch. The number of times the entire data set is used to check and validate the prediction is called epoch number. Matlab's Fuzzy logic toolbox is used for the entire process of training and evaluation of FIS.

In order to build an ANFIS that can predict $x(t + p)$ from the past values of voltage changing, the training data format is $[x(t - 18), x(t - 12), x(t - 6), x(t); x(t + 6)]$. As can be seen, there are four inputs and one output. The inputs are $x(t - 18), x(t - 12), x(t - 6), x(t)$ and the output is $x(t + 6)$. There are two membership functions on each input since this structure has fast training procedure. In this study we have chosen bell-shaped membership functions with maximum equal to 1 and minimum equal to 0. This type of functions has best characteristics for fuzzing the inputs. Experimental results of voltage changing are shown in Figure 3. To avoid slow training procedure, the experimental data were trimmed. The first 10 seconds of the data are ignored to avoid the transient portion of the data. Training and checking data are shown

in Figure 4 and input bell-shaped membership functions for training are shown on Figure 5. One half of the data are used for training while the other is used for checking and therefore the number of rules is $2^4=16$ rules. In the generating FIS matrix the number of fitting parameters is 104, including 24 non-linear parameters and 80 linear parameters. Most of the fitting is done by the linear parameters. The non-linear parameters are mostly used for fine tuning for further improvement. We applied the hybrid learning algorithms to identify the parameters in the ANFIS architectures. This algorithm has a forward and a backward pass which results in very good and fast learning error decreasing.

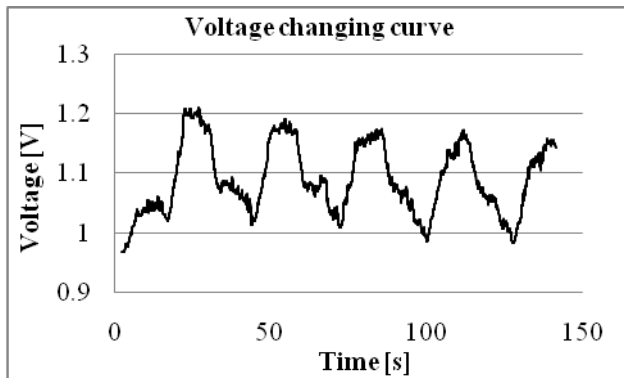


Fig.3. Voltage changing curve from experimental measurements

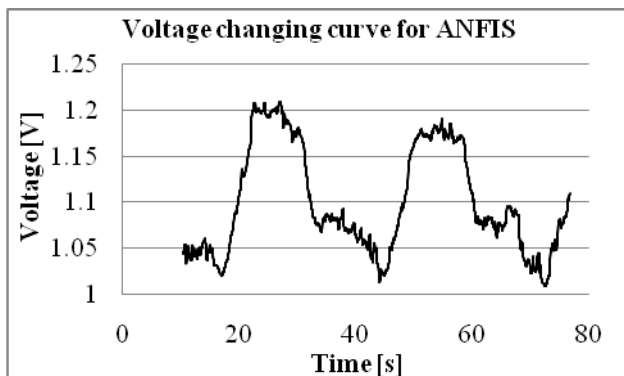


Fig.4. Training and checking data used for ANFIS prediction

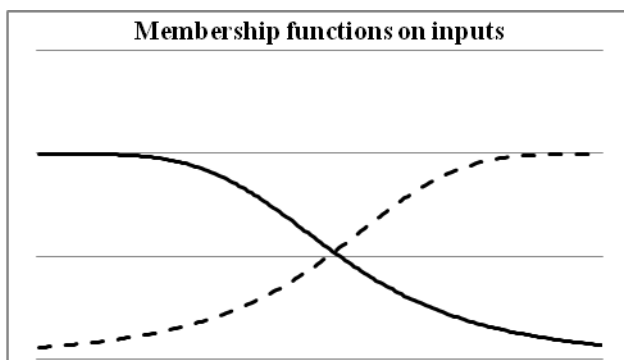


Fig.5. Initial membership functions on inputs

3. RESULTS

The error curves for both checking and training data are shown in Figure 6. Training error was represented by circles and checking error by squares. It can be noted that training error is higher than checking error, which is common process in non-linear regression. It could indicate that the training process is not close to finished yet. It can be also seen that the training procedure was lasted for 10 epochs. Figure 7 shows the time series prediction of voltage changing obtained using ANFIS. The ANFIS prediction results were represented by dotted line and experimental results by solid line. Here the difference between predicted values and measured values is negligible. Figure 8 shows the prediction error. It is found that the maximal error is 0.06V which does not result any change in the control signal since this conductive silicone rubber cannot be used for accurate measurements because of strong non-linearity. Selection of number of membership functions, training data and epoch are obtained by trial and error. For further improvements, the number of membership functions have to be increased which results in slower training procedure. Fuzzy Logic Toolbox of MATLAB was used to develop the ANFIS model with four inputs and single output as given in Figure 9.

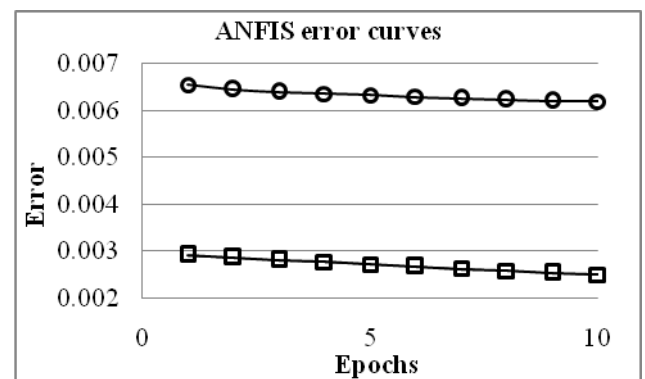


Fig.6. Error curves: training error (circle), checking error (square)

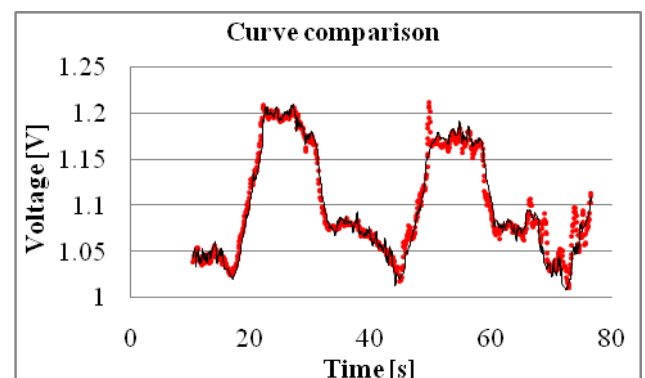


Fig.7. Voltage changing curve predicted by ANFIS (dotted line) and curve obtained by measuring (solid line)

¹Dalibor Petković, dipl.ing. Faculty of Mechanical Engineering Niš, Aleksandra Medvedeva 14, 18000 Niš, dalibortc@gmail.com.

²Nenad D. Pavlović, Prof. dr., Faculty of Mechanical Engineering Niš, Aleksandra Medvedeva 14, 18000 Niš, pavlovic@masfak.ni.ac.rs.

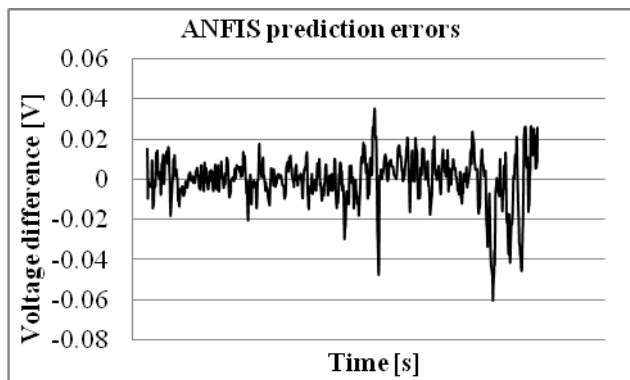


Fig.8. ANFIS prediction errors

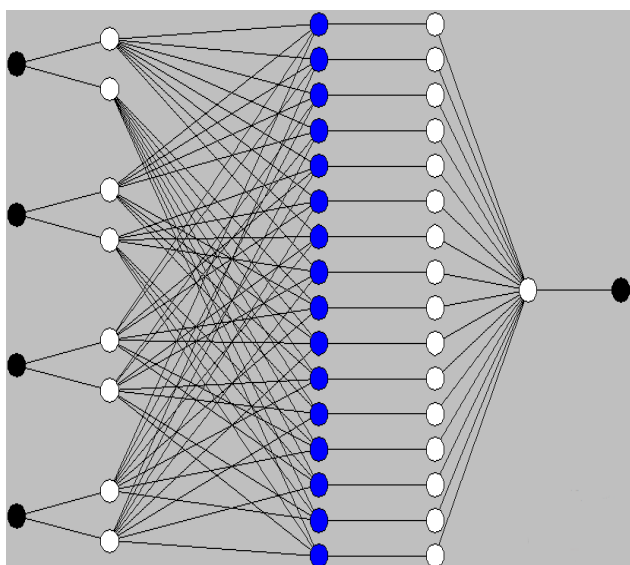


Fig.9. ANFIS structure

4. CONCLUSION

In this paper a new constitutive model was presented that allows predictions of the voltage changing behaviour of elastomeric materials. The most important advantage of such a model is the ability of real time identification of conductive silicone rubber electrical behavior, which can be used for strain sensing structure or other applications of this material. ANFIS is used to approximate correlation between measured features of the material and to predict its unknown future behaviour for voltage changing. The implementation of ANFIS model is less complicated than that of sophisticated identification and optimization procedures. Compared to fuzzy logic systems, ANFIS has automated identification algorithm and easier design and compared to neural networks it has less number of parameters and faster adaptation. The non-linear characteristics of the conductive silicone rubber can be tolerably handled in the proposed system. This prediction could be utilized as input for the strain sensing control system. Possibility to reduce the number of sensors and connections improve the performance of control strategy. The ANFIS based time series prediction model for voltage changing of conductive silicone rubber is unique and novel as it is simple, reliable and easily accessible for different compression conditions.

ACKNOWLEDGEMENTS

This paper is supported by Project Grant III44004 (2011-2014) financed by Ministry of Education and Science, Republic of Serbia.

REFERENCES

- [1] VALENTA, L. (2008) *Mechanical and Electrical Testing of Electrically Conductive Silicone Rubber*, Material Science Forum, Vol.4, pp 179-184
- [2] LO, S.-P., LIN Y.-Y. (2005) *The prediction of wafer surface non-uniformity using FEM and ANFIS in the chemical mechanical polishing process*, Journal of Materials Processing Technology, Vol.168, pp 250-257
- [3] EKICI, B.-B., AKSOY, U.-T. (2011) *Prediction of building energy needs in early stage of design by using ANFIS*, Expert Systems with Applications, Vol.38, pp 5352-5358
- [4] KHALIFEHZADEH, R., FOROUZAN, S., ARAMI, H., SADRNEZHAAD, S.K. (2007) *Prediction of the effect of vacuum sintering conditions on porosity and hardness of porous NiTi shape memory alloy using ANFIS*, Computational Materials Science, Vol.40, pp 359-365
- [5] VAIRAPPAN, C., TAMURA, H., GAO, S., TANG, Z. (2009) *Batch type local search-based adaptive neuro-fuzzy inference system (ANFIS) with self-feedbacks for time-series prediction*, Neurocomputing, Vol.72, pp 1870-1877
- [6] HAN, Y., ZENG, W., ZHAO, Y., QI, Y., SUN, Y. (2011) *An ANFIS model for the prediction of flow stress of Ti600 alloy during hot deformation process*, Computational Materials Science, Vol.50, pp 2273-2279
- [7] KARAAGAC, B., INAL, M., DENIZ, V. (2011) *Predicting Optimum Cure Time of Rubber Compounds by Means of Anfis*, Materials & Design, Article in Press
- [8] ZHANG, Z., FRIEDRICH, K. (2003) *Artificial neural networks applied to polymer composites: a review*, Composites Science and Technology, Vol.63, pp 2029-2044
- [9] KHAJEH, A., MODARRESS, H., REZAEI, B. (2009) *Application of adaptive neuro-fuzzy inference system for solubility prediction of carbon dioxide in polymers*, Expert Systems with Applications, Vol.36, pp 5728-5732
- [10] BERGSTROM, J.S., BOYCE, M.C. (2000) *Large strain time-dependent behavior of filled elastomers*, Mechanics of Materials, Vol.32, pp 627-644
- [11] JANG, J.-S.R. (1993) *ANFIS: Adaptive-Neural-based Fuzzy Inference Systems*, IEEE Trans. On Systems, Man, and Cybernetics, Vol.23, pp 665-685



TOWARDS A CONCEPTUAL DESIGN OF AN INTELLIGENT MATERIAL TRANSPORT BASED ON MACHINE LEARNING AND AXIOMATIC DESIGN THEORY

Milica PETROVIĆ¹, Zoran MILJKOVIĆ¹, Bojan BABIĆ¹, Najdan VUKOVIĆ², Nebojša ČOVIĆ³

¹ University of Belgrade – Faculty of Mechanical Engineering, Production Engineering Department, Kraljice Marije 16
11120 Belgrade 35, Republic of Serbia:

mmpetrovic@mas.bg.ac.rs, zmiljkovic@bg.ac.rs, bbabic@mas.bg.ac.rs

² University of Belgrade-Faculty of Mechanical Engineering, Innovation Center, Kraljice Marije 16 11120
Belgrade 35, Republic of Serbia:

nvukovic@mas.bg.ac.rs

³ Company FMP d.o.o. - Belgrade, Lazarevački drum 6, 11030 Belgrade, Republic of Serbia:

nebojsa.covic@fmp.co.rs

Abstract: *Reliable and efficient material transport is one of the basic requirements that affect productivity in sheet metal industry. This paper presents a methodology for conceptual design of intelligent material transport using mobile robot, based on axiomatic design theory, graph theory and artificial intelligence. Developed control algorithm was implemented and tested on the mobile robot system Khepera II within the laboratory model of manufacturing environment. Matlab[®] software package was used for manufacturing process simulation, implementation of search algorithms and neural network training. Experimental results clearly show that intelligent mobile robot can learn and predict optimal material transport flows thanks to the use of artificial neural networks. Achieved positioning error of mobile robot indicates that conceptual design approach can be used for material transport and handling tasks in intelligent manufacturing systems.*

Keywords: *intelligent manufacturing systems, conceptual design, axiomatic design theory, neural networks, mobile robot*

1. INTRODUCTION

For the last thirty years manufacture concepts have had several redefinitions. In the eighties and nineties, the concept of flexible manufacturing systems (FMS) was introduced to develop a new family of products with similar dimensions and constraints [1]. The manufacturing enterprises of the 21st century are in an environment where markets are frequently shifting, new technologies are continuously emerging, and competition is globally increasing. Rapid changes in product demand, product design, introduction of new products and increasing global competition require manufacturing systems to be highly flexible, adaptable and responsive [1].

A methodology that includes the technological migration [1] from established flexible manufacturing systems (FMS) to intelligent manufacturing system (IMS) is presented in this paper. For needs to be addressed at the design stage of new manufacturing system with all intelligent characteristics, this paper would like to present a methodology for conceptual design of manufacturing systems using axiomatic design approach.

Beside axiomatic design methodology, the mentioned requirements cannot be fulfilled without artificial intelligence. According to the literature published by CIRP and other manufacturing periodicals during the past decade, nearly 34 modern manufacturing systems and

production modes have been proposed and 35 mathematical methods have been used for building intelligent systems [2]. The wide application of these intelligent mathematical methods or their combinations in manufacturing will definitely enhance the development of manufacturing system modelling and provide the new solutions. Some of the methods are: machine learning, artificial neural networks, heuristic search, and graph theory, etc. Evolutionary computation (i.e. genetic algorithms, genetic programming, evolutionary programming, and evolutionary strategies) and artificial neural network are the most widespread [3]. Intelligent material transport implies solving path generation problem and control movement of an intelligent agent - a mobile robot. The graph algorithms are used to generate path and artificial neural networks for prediction of duration of manufacturing operations. In [4] different graph search algorithms are presented.

2. AXIOMATIC DESIGN THEORY

Axiomatic design theory is an attempt at synthesis of the basic principles of design in various engineering fields and in all phases of design. This design methodology is based on identifying customer needs and their transformation into correspondent functional requirements

in the physical domain. According to [5], going from one domain to another is called mapping and it happens in the each design phase: conceptual, product and process design phase, respectively. Furthermore, the design

process is done through the iterative mapping between the functional requirements (FRs) in the functional domain, and the design parameters (DPs) in the physical domain, for each hierarchical level (Fig.1).

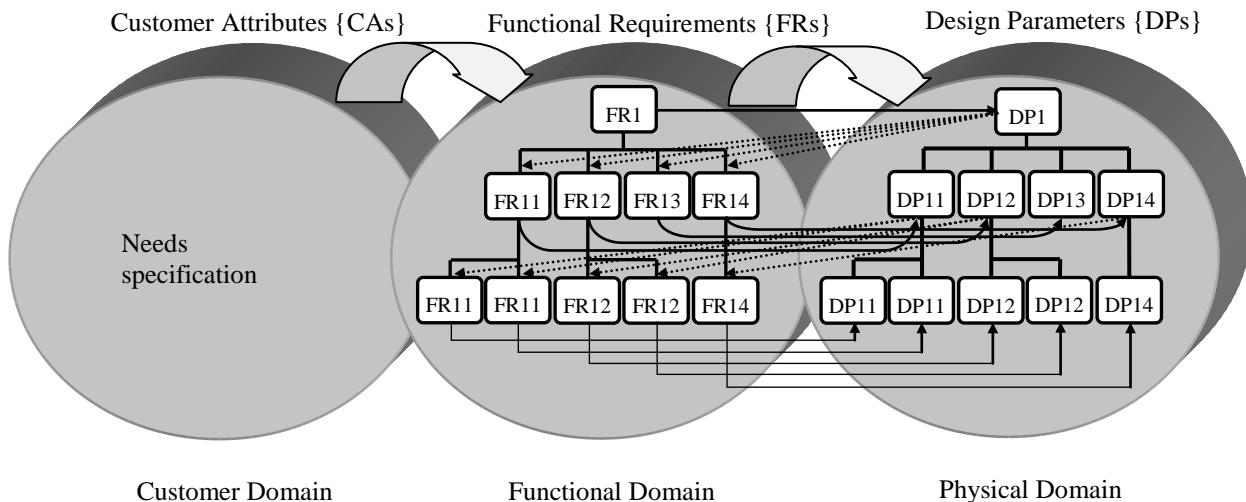


Fig.1. Concept of domain, mapping and axiomatic decomposition

In mathematical terms, the relationship between the FRs and DPs is expressed as [5]:

$$\{FR\} = |A| \cdot \{DP\} \quad (35)$$

where $\{FR\}$ denotes the functional requirement vector, $\{DP\}$ denotes the design parameter vector, and $|A|$ denotes the design matrix that characterizes the design process. The structure of the matrix $|A|$ defines the type of design being considered and for the three hierarchical

levels particular design matrices $|A|$ are presented in the Table 1. It can be concluded that $|A|$ matrix in the second hierarchical level is triangular and for that reason we can change some DPs to set some other FRs without affecting the rest of FRs [5]. Such a design is called a decoupled design. In the third hierarchical level $|A|$ matrix is diagonal and each of the FRs can be satisfied independently by means of one DP. Such a design is called an uncoupled design.

Table 1. List of the functional requirements, correspondent design parameters and correspondent $|A|$ matrices

	DP1: Mobile robot	DP11: Odometry motion model	DP12: Path planning module	DP13: Manufacturing process simulation	DP14: Neural networks	DP111: Sensory information from encoders	DP112: Sensory information from the camera	DP121: Path planning algorithms	DP122: Control algorithms	DP141: Parameters for neural networks training
FR1: Intelligent material transport	X									
FR11: Determining mobile robot position and orientation		X	X	X	X					
FR12: Path planning		0	X	X	X					
FR13: Prediction of manufacturing process parameters		0	0	X	X					
FR14: Machine learning of material transport flows		0	0	0	X					
FR111: Determining parameters in motion model						X	0	0	0	0
FR112: Determining position and orientation of the characteristic objects in the environment						0	X	0	0	0
FR121: Generating path nodes						0	0	X	0	0
FR122: Path following						0	0	0	X	0
FR141: Getting expected performance of IMS						0	0	0	0	X

3. MOBILE ROBOT IN A MANUFACTURING ENVIRONMENT

To explain mobile robot motion and actions in manufacturing environment, five modules are developed.

3.1. Motion model

The position of the mobile robot is determined by the system state vector $x_t = (x, y, \theta)$, where x and y are the components that define the position vector, and θ is the angle orientation. Mathematical formulation for mobile robot odometry is given by (2):

$$\begin{bmatrix} x' \\ y' \\ \theta' \end{bmatrix} = \begin{bmatrix} x \\ y \\ \theta \end{bmatrix} + \begin{bmatrix} \Delta s \cos(\theta + \Delta\theta / 2) \\ \Delta s \sin(\theta + \Delta\theta / 2) \\ \Delta\theta \end{bmatrix} \quad (36)$$

where x' , y' and θ' are the components of the state vector at time t' , x , y and θ components at time t ; Δs the incremental path lengths [6].

3.2. Material flow analysis

Material transport analysis in manufacturing environment was recognized as the first task in a path planning module. First of all, flow line layout design is adopted. After that, the data about machines, parts and time duration of operations should be gathered and analyzed. Table 2 presents a list of machines, and Table 3 presents a list of parts.

Table 2. List of machines in manufacturing plant

Machine	Machine type
M#1	Shearing machine
M#2	CNC punch press for punching and blanking
M#3	Hydraulic punch press
M#4	Punch press for punching and blanking
M#5 and M#6	Pillar drill (bench drill)
M#7	Circular saw
M#8	Whetting machine
M#9	Line for machining parts made of cooper

Table 3. List of representative parts in manufacturing plant

Part	Description
P#1	Transport fuse
P#2	Mainbusbar support
P#3	Support d800
P#4	Busbar 2 L1

After defining number of parts and machines, we need to define quantitative relations between them. In general, this dependence can be presented with matrix M_{DM} , which

is written using matrix M (matrix of machines) and D (matrix of parts) [7].

$$M_{DM} = \begin{bmatrix} p_{11} & \cdots & p_{1j} & \cdots & p_{1NM} \\ \vdots & \ddots & \cdots & \cdots & \vdots \\ p_{i1} & \cdots & p_{ij} & \cdots & p_{iNM} \\ \vdots & \cdots & \cdots & \ddots & \vdots \\ p_{ND1} & \cdots & p_{NDj} & \cdots & p_{NDNM} \end{bmatrix} \quad (37)$$

If we need time dependence between machines and parts, we put the time duration of machine operation to a correspondent machine instead of parameter p_{ij} . At the end, using graph theory, we define matrix of distances between machines (R) [6].

3.3. Path planning algorithms

Three algorithms are developed and implemented for the mobile robot path planning task. The first one is A* search algorithm, that is used for finding the shortest path between start and goal points. It combines *Dijkstra algorithm* and *bread-first* search algorithms. Using M_{DM} matrix, the second algorithm determinates sequence of machines for each representative part and chooses machine the robot should visit, according to a minimal distance criteria. Finally, the third algorithm is used for determining the order of machines in accordance to manufacturing process. This algorithm generates characteristic time parameters of the manufacturing process (the duration of the operation on the machine) and time parameters related to part transport to the machine (time needed for mobile robot to travel between machines).

3.4. Prediction of manufacturing process parameters

It is known that engineering processes generally do not have deterministic nature. The processes that are important for the material transport task in terms of duration are the machining process and the process of robot movement between the defined nodes (machines). Considering the fact that these processes have stochastic nature, we can conclude that nominal time duration of operations, as well as time of transport from one node to another, are different for each part. For that reason, uniform distribution is chosen to model stochasticity of the nominal time duration.

3.5. Neural Networks for prediction of duration of manufacturing operations

Implementation of the neural networks (NN) to model various problems in production engineering goes back to the 20th century. According to [8], there are three basic categories of their use: classification, prediction and functional approximation. Prediction of the next node (machine) in the path, where robot needs to go and deliver the part, is based on past values of the system state (in this case the time parameters of the process and the time of robot movement between the machines) and the current values of the system state (the node where the robot is

currently located). For NN training the Matlab Neural Network Toolbox is used, with supervised learning algorithm (Levenberg-Marquardt) [8] and the sigmoid activation function.

4. EXPERIMENTAL RESULTS

The experimental model of manufacturing environment is static and positions of machines are *a priori* known. Experimental model and the *Khepera II* mobile robot are shown in Fig. 2. The first goal is test accuracy of path following. During tracking the trajectory, the robot has to deliver part to machines, according to manufacturing process, defined by matrix M_{DM} . Coordinates of start and goal point is known. While executing the transport task, the robot optimizes the path between the machines using A* algorithm [6]. The mean position errors during the first experiment in x and y directions are $\Delta x=0.5598$ [cm] and $\Delta y=1.4624$ [cm].

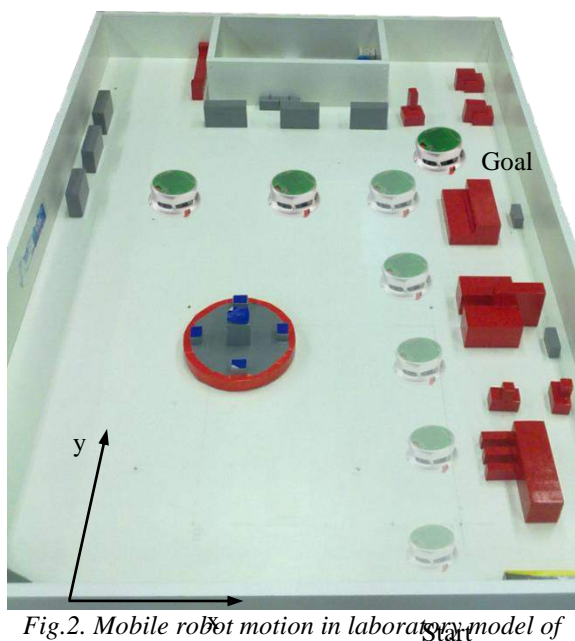


Fig.2. Mobile robot motion in laboratory model of manufacturing environment

The next experiment is conducted in same conditions, but the coordinates of the goal point are not known at the beginning. This parameter depends on the time robot needs to travel from one machine to another. When the robot finishes transport of the last representative part to machine for the first operation, its current pose is passed to NN. Based on this information, NN predict the nearest machine where manufacturing operations are completed and generate information about the future robot actions.

5. CONCLUSION

This paper presents a method for conceptual design of mobile robot material transport in intelligent manufacturing system. Intelligent mobile robot, with *a priori* known static obstacles in the environment, has the ability to generate an optimal motion path in accordance with the requirements of the manufacturing process and priority servicing of machine tools. Mobile robot learns the optimal transport routes and sequence of manipulation

by using neural network [6]. Neural network was developed to predict the parameters of manufacturing process and to learn characteristic time parameters of the process. For the purposes of the simulation we used the nominal time parameters (estimated using empirical data) of the manufacturing process, and its stochastic nature is modeled according to uniform distribution [6]. Search algorithms and neural network models are developed in Matlab environment and implemented on a *Khepera II* mobile robot. Achieved positioning error of mobile robot indicates that conceptual design approach based on axiomatic design theory and neural networks can be used for material transport and handling tasks in intelligent manufacturing systems.

ACKNOWLEDGMENTS

This paper is part of the project: *An innovative, ecologically based approach to implementation of intelligent manufacturing systems for production of sheet metal parts*, financed by the Ministry of Education and Science of the Serbian Government, Grant TR-35004.

REFERENCES

- [1] REVILLA, J., CADENA, M. (2008) *Intelligent Manufacturing Systems: a methodology for technological migration*, Proceedings of the World Congress on Engineering, Vol II, London U.K, pp. 1257-1262.
- [2] QIAO, B., ZHU, J. (2000) *Agent-Based Intelligent Manufacturing System for the 21st Century*, International Forum for Graduates and Young Researches of EYPO, Hannover, The World Exposition in German.
- [3] BREZOCNIK, M., BALIC, J., BREZOCNIK, Z. (2003) *Emergence of Intelligence in Next-generation Manufacturing Systems*, Journal Robotics & Computer-Integrated Manufacturing, Vol. 19, pp. 55-63.
- [4] SIEGWART, R., NOURBAKHSH, I. R., (2004) *Introduction to Autonomous Mobile Robots*, MIT Press, Cambridge, Massachusetts.
- [5] SUH, N. P. (1990) *The Principles of Design*, Oxford University Press, New York.
- [6] PETROVIĆ, M., MILJKOVIĆ, Z., BABIĆ, B., ČOVIĆ, N. (2011) *Artificial neural networks and axiomatic design theory in conceptual design of intelligent material transport*, Proceedings of the 37th JUPITER CONFERENCE with foreign participants, Belgrade, pp. 3.72-3.79, (in Serbian).
- [7] MILJKOVIĆ, Z., BABIĆ, B. (2005) *Machine-Part Family Formation by Using ART-1 Simulator and FLEXY*, FME Transactions, New Series, Vol.33, No.3, pp. 157-162.
- [8] MILJKOVIĆ, Z., ALEKSENDRIĆ, D. (2009) *Artificial Neural Networks – Solved Examples With Short Theory Background*, Faculty of Mechanical Engineering, University of Belgrade, Belgrade, (in Serbian)

SOFTWARE SOLUTION OF REENGINEERING MODEL OF TECHNOLOGICAL PROCESSES OF SMALL ENTERPRISES

Milan D. ERIĆ, Miladin Ž. STEFANOVIĆ, Branko U. TADIĆ, Slobodan R. MITROVIĆ
 Faculty of Mechanical Engineering, Sestre Janjića 6, Kragujevac, Srbija
ericm@kg.ac.rs, miladin@kg.ac.rs, tadic@kg.ac.rs, boban@kg.ac.rs

Abstract: Constantly expanding market demands in terms of product range and product quality, price reduction and delivery times, are the basic requirements of small enterprises. How small business can respond to these requirements, or how fast, at a lower price and make the product quality, i.e. reduce the time and cost of processing, the answer is requested in the application of information technology and reengineering. The paper presents a software solution of reengineering model of technological process of small enterprises, and justification for its implementation. This solution enables reviewing the goals, minimizing time and cost of processing and maximizing productivity.

Key words: software solution, reengineering model, small enterprises

1. INTRODUCTORY REVIEW

In domestic written and electronic media, at professional meetings on which different topics regarding solving issues of small enterprises survival in uncertain business environment are being discussed, reviews could often be read or heard, upon which the conclusion is drawn that small enterprises usually do not have their own development, and even if they do, they invest very little in it. That is resulting in the inability to adequately adapt to the environment demands, that is to say, the enterprises are unable to, on existing method of quality, quickly and efficiently respond those demands. In the enterprise the problems are created, related to both new product and technologies development and therefore technological processes as well, and also for redesign or restyling of already existing products and improvement or reengineering of already implemented technologies and technological processes. One way to solve the problem of development and reengineering of not only technological processes of small enterprises is in establishing innovation center, or knowledge incubator. The function and the main task of the center or incubator is solving problems in development and reengineering faced by small enterprises, as well as development of their own businesses and transfer of contemporary technologies, methods and procedures and adapting to domestic conditions, Fig.1. In small enterprises, as well as business systems, there are more or less different problems. They may be related to product design (design, modeling, engineering analysis, visualization etc.), procurement and supply, marketing, finance, informational systems, implementation of quality systems, design of technological processes, technology, etc. Many generated problems small enterprises solve by their own resources. However, huge number of problems, especially problems related to new product and technology development (and therefore the technological processes), remains unsolved

what directly affects the competitiveness of small enterprises. Unsolved problems (●), from systematic point of view, seek for solution outside the space borders of small enterprises (●) and forming one new systematic space (●), space problem.

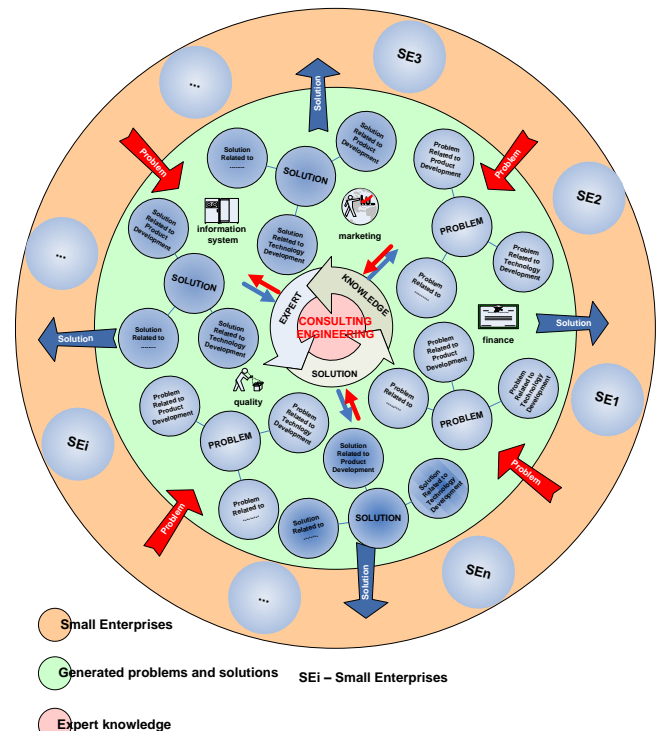


Fig.1. Space model architecture of generated problems and solutions

Part of system space problem, are also problems of improving the already developed products or reengineering of technological processes. For the solutions of these problems, systematic and expert knowledge are required (●) which are concentrated in Scientific-research Institutions. In the centers and

incubators of scientific institutions, along with experts from different fields, the solutions are generated (●) which fill in the space solution (●). From the space generated solutions, small enterprises use those solutions for their already generated problems.

Small enterprises in connection with research institutions (innovation centers (IC) and knowledge incubators (KI)) should find the way for profit implementation through results implementation of scientific and development researches, should find the way to solve not only problems of development and reengineering of technological processes, but also development problem of new product, improvement of existing one, they should find the way to solve the problem of professional training, etc. Basic advantage of this solution is not to solve the same problem in several places that small enterprises do not invest in development that is extremely expensive, to establish expert base for different fields in one place, and to take advantages of innovation centers and knowledge incubators.

A methodology for reengineering of technological processes has been developed for proposed solution [1]. Software "IM2RTP" has been developed for methodology (Informational development model and Reengineering of technological processes) with basic architecture and logical data model which are represented in work [2].


2. DESCRIPTION OF SOFTWARE SOLUTION


Three parts are combined through the module. OLTP (*On-Line Transaction Processing*) part of the software provides transactional data processing regarding technological data base, through function of input, alteration and review. GUI (*Graphic User Interface*) part of the software provides visual reengineering, designing variants of technological procedures and "piggybacking". OLAP (*On-Line Analytical Processing*) part of the software provides analytical processing of dimensional data. After starting software, the first (initial) form is shown (Fig.2.)




Fig.2 Initial software form

in which the icons are noticed:

 for starting module to work with technological data base,

 for starting module to work with technological procedures,

 for starting assistance, and text box with basic information about software,



for competition of software work.

The same icon function as „PROCESS“ and „BASES“ also have cards „TECHNOLOGICAL PROCESS“ and „TECHNOLOGICAL BASES“. By choosing card „TECHNOLOGICAL BASES“ the form in the shape of control board is displayed (Fig.3.). Cutting tools, measuring tools, tool machines, accessories, SHP, auxiliary time, preparatory finish time, and additional time are possible choices of this navigational form.



Fig.3. Navigational form of „TECHNOLOGICAL BASE“

This navigational form at the same time reflects the structure of technological data base. By choosing options “Cutting tools”, the new form of MDI structure “Cutting tools” is obtained (Fig.4.). This is at the same time the mask for the input of basic data for cutting tools. Drop-down list “Type of processing” defines the type of tools. Other data that could be entered by using this mask are: Tolls marking, Standard, Technological marking, Name of tool, Tools name, Price (dinar and EUR), Number of sharpening, or number of cutting edges, Sharpening time if the tool is being sharpened, Time to change tools, Tools endurance, Personal income of workers, Marking of material and tool coating, Tools manufacturer marking. Keys **Add**, **Modify**, **Delete** start the functions for adding new tool, editing and deleting existing tool. The delete function performs also the cascade deleting of other data concerning geometry of chosen tool. Key **Other** calls up a new form (Fig.5.) for defining geometry of chosen tool.

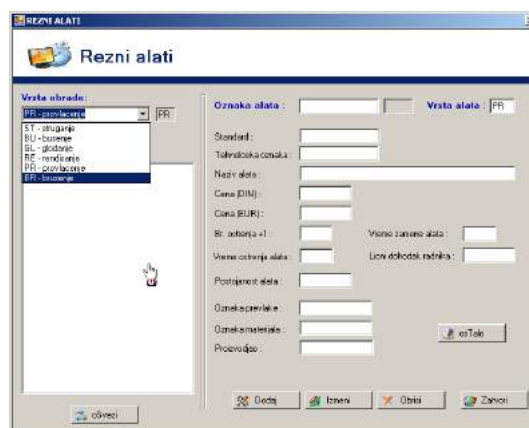


Fig.4. Form appearance of „Cutting tools“

For the type of milling processing, the data concerning geometry are: nominal diameter, Length of milling cutter, Breast angle, Back angle, Angle of the spiral, Cone angle, Width of milling cutter, Length of cutting part of milling

cutter, Number of milling cutter teeth, and Image or sketch of milling cutter.



Fig.5. Form appearance of „Cutting tools - MILLING“

According to the same principle, the forms for other type of processing have been done (scraping, drilling, grinding, broaching, and planing). The tool geometry for chosen type of processing is defined on each form.

The remaining sections related to OLAP, GUI and the remaining part of OLTP, are chosen by using navigational form „TECHNOLOGICAL PROCESS“. This navigational form includes following options: „The object of processing“ (OLTP); „Technological process“ (OLTP); „Variations of technological process“ (GUI); „Technological process based on existing one“ (GUI) and „Variations analysis“ (OLAP). Options „Operation list of technological process“ and „Operations cards of technological process“ form technological documentation. The form „Technological process“ (Fig.6.) is the first in a row of MDI forms by which the technological procedure is defined. From the drop-down list „Technological process“, that includes data: Marking_TP, Variation_TP, Type_variation_TP, Marking_PO, the technological procedure that could be changed is being chosen. For new technological procedure in the field „MARKING“, the new marking of TP is entered and in the field „VARIATION“ the variant of TP is entered. Pressing the key „NEW“ the new form to input other data, related to TP Description of technological procedure and the date of forming technological procedure, is being opened.

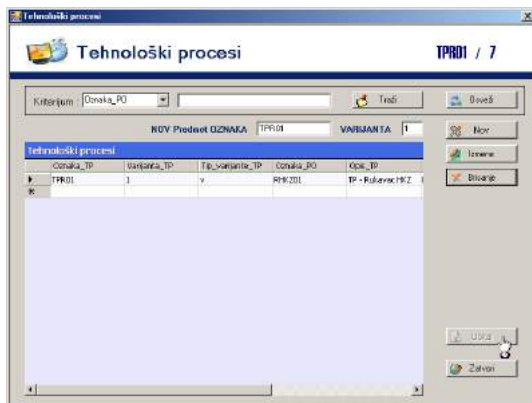


Fig.6. Appearance of form „Technological process“

Using the key „Operation“ the new form „Operation“ is opened (Fig.7.) by which operations of technological procedure is defined. The data being inputted are Marking

and Operation name, and the quantity of SHP, if used in performing operation. The overlapping coefficient of the main time has the value 1 for orderly performance of the operations, with parallel and combined its value is less than 1. With click on the key „Image“ the new form is opened by which the joining of image/sketch of operation is being performed (processing scheme). The image of the operation is a target model of technological model, and can be downloaded from CAD base of technological models.

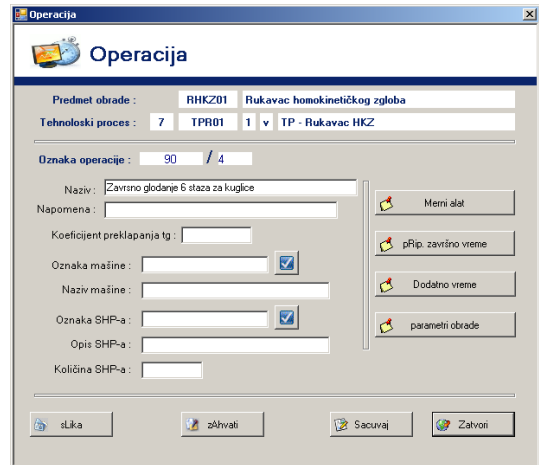


Fig.7. Appearance of form „Operation“

The form is showed in Fig.8 obtained by click on the key „Processing parameters“ of form „Operation“. This form is used to display and input the data necessary for calculation of processing expenses. The data defined in technological data bases will be displayed and the remaining data are inputted through this form.

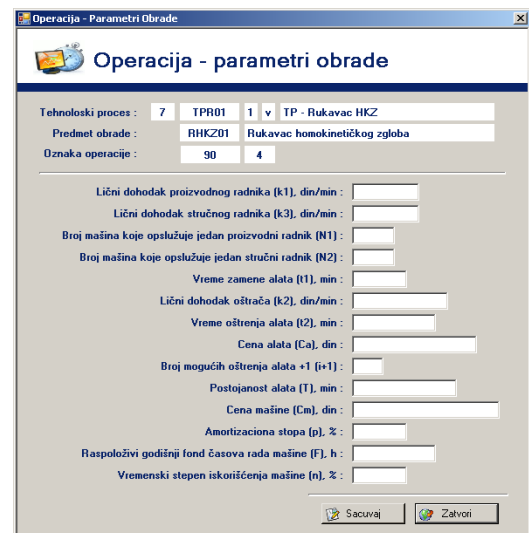


Fig.8. Form appearance for entering parameter values necessary for calculation of processing costs

The key „Procedures“ of form „Operation“ opens new form „Procedures“ Fig.9. The data entered are Process marking, and in the drop-down list Type of processing is defined as type of processing as well as Process description. By checking field , all tools are shown for chosen type of processing. Appropriate tool is chosen from drop-down list by checking. The main processing time and auxiliary time are defined with forms of clicking on the keys



Fig.9. The appearance of form for defining operation

On Fig.10. is shown the form for defining of processing parameters and calculation of the main processing time. The appearance of forms is depending on the type of treatment. In function Save (Sacuvaj) is built a mathematical model for calculating the main processing time depending on the type of treatment. In this case this function in addition to the role of storing data in the database has an function calculation.

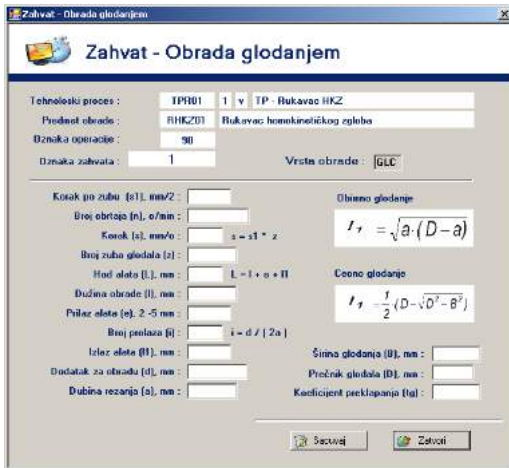


Fig.10. The appearance of form for defining processing parameters

Part of the software with GUI interface and visual modeling is realized through the option "Versions of technological processes" and "The technological process based on existing", Fig.11.

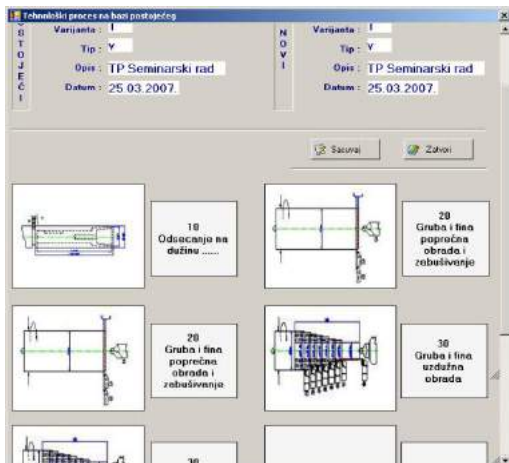


Fig.11. The appearance of form "The technological process based on existing"

OLAP software component is implemented through the "Analysis of variations". Choice of production process for the three variants of its graphic display three-dimensional data as follows: During the processing, production and processing costs, Fig.12. In this way he realized the concept of multidimensional databases.

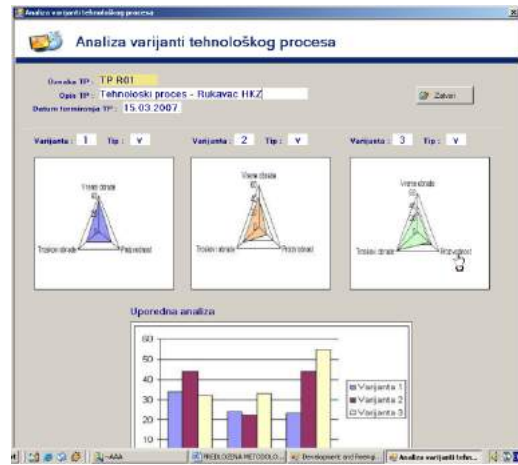


Fig.12. Output from the multidimensional database technology

Technological documentation, which is the carrier of technological information, is formed by using the "List of the operation of technological processes" and "Maps of the operation of technological processes".

3. EFFECTS OF APPLICATION OF THIS SOFTWARE SOLUTION

Showing a software solution that supports the design and engineering and reengineering of the technological process has four primary objectives:

- reduction of manual work in the business of making the technological process that causes stress to the production engineers and experienced designers of technological processes,
- improvement / optimization of existing technological processes through the use of available information on the machines, tools, accessories, workability, etc.
- systematization of the best observed processes for families of components within an enterprise, thus ensuring the transfer of knowledge and experience of experienced designers,
- systematization of production time and costs as a precondition for the techno-economic analysis.

Advantages of the system, which allows the design of new and re-engineering of existing technological processes, are:

- reduction of design time,
- lower cost of designing and manufacturing,
- enables the design of technological processes of the same validity, quality,
- development of rational technological processes,
- increased productivity and so on.

Measurement of results is based on changes in values of those parameters, which are marked as the most influential for a given technological process, based on analysis of Ishikawa diagram, Fig.13.. On the basis of the projected software by reviewing the

goals (to minimize time and cost of processing and maximizing productivity), using feedback and the appropriate models at the level of treatment and operation.

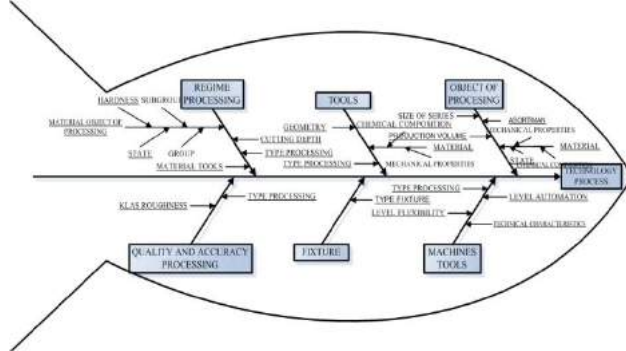


Fig.13. Ishikawa's diagram of technological process

In doing so, to change the corresponding parameter can be without any effect, with limited effect and with significant effect and the effect, which will provide a significant advantage over the other variants. Cost Benefit Analysis (analysis of cost-benefit) (C / B analysis) or cost-effectiveness analysis is an economic method of assessment of relative value changes to

existing or proposed projects or situations, or to the methods of economic analysis that compares and evaluate the merits and shortcomings of a Project cost analysis (cost) and benefits (benefit). In this case, Cost-benefit analysis is to estimate the effect of using this model (re) engineering of the technological processes of small businesses that use software solutions "IM2RTP". On the one hand with the advantages (benefits) of the proposed model, and the other analyzes the costs and any potential negative consequences (cost) in order to assess the rationality of using this model. Affirmation of the need to prove that the benefits are large enough to justify the cost. In order to do C / B analysis using this software, defined as factors in the qualitative and quantitative terms should reflect certain changes (Table 1). That the final grade unified measurable and immeasurable factors are introduced weights or weight or importance factor (Z), (which is the sum of all the factors 1) which is multiplied by the subjective assessment (SA) which ranges from 1 to 5 Subjective value is defined for the case before and after application software and the technological complexity of different parts.

Table 1 Ratings factor cost of application software "IM2RTP"

Factors	Importance of Factors (Z)	Part/The technological complexity of part											
		A 0.7				B 0.8				C 0.9			
		Before		After		Before		After		Before		After	
		SA	SA * Z	SA	SA * Z	SO	SA * Z	SA	SA * Z	SA	SA * Z	SA	SA * Z
The share of the manual work	0.05	5	0.25	1	0.05	5	0.25	1	0.05	5	0.25	1	0.05
Information availability	0.10	2	0.2	5	0.5	2	0.2	5	0.5	2	0.2	5	0.5
Systematization of solutions	0.05	2	0.1	5	0.25	2	0.1	5	0.25	2	0.1	5	0.25
The transfer of knowledge and experience	0.05	2	0.1	3	0.15	2	0.1	3	0.15	2	0.1	3	0.15
Assumptions for the techno-economic analysis	0.05	2	0.1	3	0.15	2	0.1	3	0.15	2	0.1	3	0.15
The quality of technical documentation	0.10	2	0.2	5	0.5	2	0.2	5	0.5	2	0.2	5	0.5
Design time	0.30	2	0.6	2.1	0.63	2.8	0.84	3.5	1.05	3	0.9	4	1.2
The costs of designing	0.30	2	0.6	2.1	0.63	2.8	0.84	3.5	1.05	3	0.9	4	1.2
Σ	1.00		2.15		2.86		2.63		3.7		2.75		4

Graphic representation of the results is given on Fig.14.

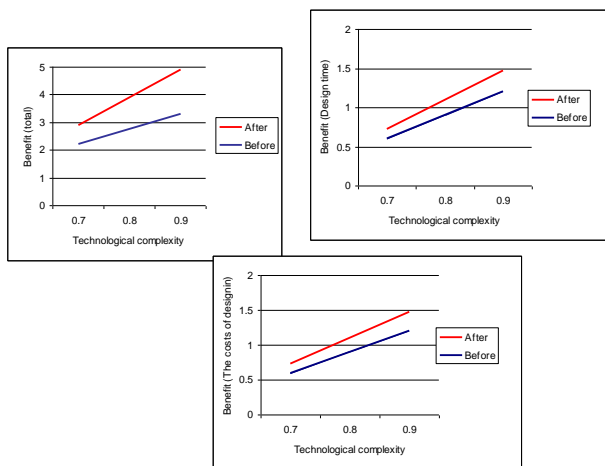


Fig.14. Graphic representation of dependence C/B of technological complexity

On the basis of cost-benefit analysis, three parts (A, B, C) with varying technological complexity (Part A has the lowest technological complexity is estimated at 0.7, part B is 0.8 and part of C has the highest technological complexity of 0.9), is concluded that the all three cases, it payable to use the proposed model, and that the greatest benefits are in the case of C. Based on the value of total benefits for at least part of the technological complexity of the cost of application software "IM2RTP" and about 33%, the middle part of the technological complexity of the cost of application software is about 40%, and the technologically most complex part of the cost of application software is 45%. If factors are considered during the design and cost savings would be at least for part A, 5%, then the middle part of the technological complexity of B about 25% and the technological complex of about 33% (Fig.15).

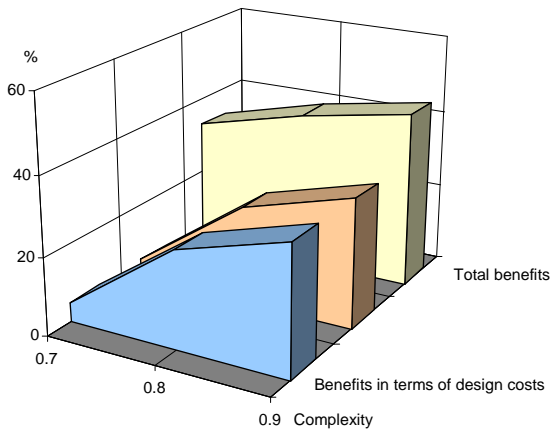


Fig.15. Graphic representation of cost-effectiveness of software in relation of technological complexity

Finally, we can conclude the following: the technological complexity of parts produced by small firms is higher, the higher cost of using the software.

4. CONCLUSION

Software solution, "IM2RTP", is intended for engineers, designers and technologists engaged in the development and reengineering of the technological processes. The basic idea related to this software is that it is a tool for engineers, who will in a simple and intuitive way for a relatively short time, through a very usable user (graphical) interface to develop a technological process, to implement re-engineering an existing or define a new technological process reengineering of existing and all fully documented. At the same time the projected database make it possible to preserve the experiential knowledge of designers as knowledge of the company internally.

REFERENCES

- [1] ERIC M., TADIĆ B., STEFANOVIĆ M. (2008) *Model of Reengineering of Technological Processes*, XXXII Conference on Production engineering, Novi Sad, pp 615-618
- [2] ERIC M., STEFANOVIĆ M., TADIĆ B. (2009) *Architecture of Information Model for Reengineering of Technological Processes for Small Enterprises*, 10th International Scientific Conference on Flexible Technologies, Novi Sad, pp 198-210
- [3] LONGENECKER J., MOORE C., PETTZ W. (2003) *Small Business Management*, Thomson Learning, Mason, Ohio
- [4] RIORDAN R. (2005) *Designing Effective Database Systems*, Addison-Wesley
- [5] POLIŠČUK J. (2007) *Projekovanje informacionih sistema*, EF, Podgorica



ONTOLOGY-BASED SUPPLY CHAIN PROCESS CONFIGURATION

Milan ZDRAVKOVIĆ, Miroslav TRAJANOVIĆ, Hervé PANETTO, Alexis AUBRY, Mario LEZOCHÉ
Faculty of Mechanical Engineering in Niš, University of Niš, Niš, Serbia
{milan.zdravkovic, traja}@masfak.ni.ac.rs
Research Centre for Automatic Control (CRAN – UMR 7039), Nancy-Université, CNRS, Nancy, France
{Herve.Panetto, alexis.aubry, mario.lezoche}@cran.uhp-nancy.fr

Abstract: *The complexity of the inter-organizational collaboration processes is one of the main concerns of the supply chain management. SCOR (Supply Chain Operation References) process reference model addresses those concerns by providing a process implementation roadmap, consisting of workflows, best practices, systems and performance metrics. In this paper, we use SCOR framework to develop knowledge-based solution for rapid supply chain process configuration. We describe the semantic application for supply chain process configuration, algorithms for process selection and generation of a SCOR thread diagram, describe its indented use and argue about its potential benefits.*

Keywords: *Supply Chain Management, Ontology, Semantic Technologies, Business Process Management*

1. INTRODUCTION

Supply chain is a complex, dynamic networked environment which consists of a number of different actors, assets, goals, competencies, functions and roles. The interest in creating a new discipline of supply chain management was developed in the early '60s with the initial motivation to investigate the increase in demand fluctuation (known as "bullwhip effect") which occurred in deeper levels of the manufacturing supply tree [1]. With the development of processing power in the '90s, it became possible to quantify and manage this effect.

However, despite the technology development, it appears that Supply Chain Management (SCM) paradigm is adopted unexpectedly slow. Some of the main reasons are: lack of feasible technology support; inconsistency of supply chain and individual enterprises' business strategy; and difficulties in change management, from internal and external perspective. We relate these issues to the three pillars of supply chain management: objectives, IT systems and business functions.

Any inter-organizational collaborative form is characterized by a singular objective, expressing the common interest of involved parties to collaborate. Where supply chain has a singular objective, its actors are individually characterized by different objectives, not necessarily compatible with the overall one. This misalignment may have a negative impact on the capability of an enterprise to act upon its business strategy, when the enterprise is involved in more than one supply chain.

Advances in ICT have great impact on social, economic and technical aspects of doing business. However, rapid progress also resulted in increasing complexity and heterogeneity of systems, having a negative effect on realization of one of the fundamental requirements for

ICT applications - enterprise integration capability and interoperability [2].

Besides different integration challenges imposed by inter-organizational collaboration requirements, the lack of internal, horizontal integration still remains the issue in many enterprises. Weaknesses of isolated business functions become critical when enterprise-wide information systems, such as ERP system, are implemented. This is evident from the proportion of change management uptake in ERP implementation, in overall, sometimes as high as 70% [3]. Using standard processes included in an ERP is considered as valuable implementation tool. These processes are often seen as "best practices" - collective, organized and empirically validated knowledge, enabling increase in company performance, and providing a powerful tool for change management [4].

Many researches are trying to show that the effective solution for all three classes of SCM problems is related to the use of knowledge-based technologies. Cross-functional, horizontal enterprise integration often relies on the existing body-of-knowledge, commonly represented by standards and reference models. Mainstream research of interoperability of applications focuses on federation, where mapping is done at the semantic level [4], with the use of interfaces, reference models or ontologies. Finally, the coherence between local and global objectives is enabled by ensuring the consistency of system-wide decision making, a concept of enterprise integration in the frame of enterprise modeling [5]. For the reasons above, SCM researchers today are shifting towards the exploration of semantic web technologies, where they are based on the use of so-called Ontologies.

Ontology is considered as the logic theory for explicit, full or partial description of conceptualization [6]. Its use is expected to facilitate the definition of perceptual and

formal meaning of information. While the representation of common perceptions on specified domain enables efficient communication, avoiding unwanted interpretations and use of terms, the definition of formal meaning can enable reasoning of implicit facts and improve systems interoperability [7], in general. OWL (OWL 2 Web Ontology Language) is a family of knowledge representation languages, which provides the syntax for authoring and exchanging the ontologies among relevant tools and applications.

While semantic tools are candidates for technical aspect of the SCM solution, the common denominator problem of above issues is the notion of business process. In this paper, we propose ontology-based solution for the problem of supply chain process configuration. This solution is based on the Supply Chain Operation Reference (SCOR) model.

In order to gain real benefits from Supply Chain Management, information systems must span full horizontal organization of enterprises and beyond – its customers and suppliers. For dealing with the complexity of such environment, reference models played an important role. Supply Chain Operations Reference (SCOR) [8] is a standard approach for analysis, design and implementation of changes required for the improvement of five core, integrated processes in supply chains: plan, source, make, deliver and return. SCOR is implemented from the perspective of an individual enterprise and resembles all interactions and transactions of physical resources in radius of two levels downstream and upstream in its supply chain.

For the ontology-based supply chain process configuration, we use our ontological framework [9] which is based on SCOR-KOS OWL model – OWL representation of the implicit SCOR model. Its competency is validated by using following questions: 1. Which process elements constitute one SCOR process and in which order? 2. What are the input and output resources for the selected process element? 3. What are the metrics and best practices for the selected process element? 4. Which systems can facilitate the improvement of the selected process element and/or process category?

The SCOR-KOS OWL model is mapped to what we call a problem ontology – a formal representation of the domain problem which is used as a meta-model by specific semantic application. In this case, the role of problem ontology is played by SCOR-CFG OWL model, and it is exploited by the application for supply chain process configuration.

2. APPLICATION OF THE SKOR-KOS OWL MODEL FOR SUPPLY CHAIN PROCESS CONFIGURATION

In this section, we demonstrate the use of the SKOR-KOS OWL model for supply chain process configuration, namely, the inference and presentation of a SCOR thread diagram – configuration of source, make and deliver processes, on basis of asserted product topology, participants and production strategies for each component.

For this purpose, a semantic web application is developed, which relies on the application ontology – SCOR-CFG OWL model. Use of the application involves assertion of the product configuration, namely principal product topology and manufacturing strategies for each of the components and invocation of the algorithm for rendering SCOR thread diagram. Different process patterns (and roles) are applied in each of the three possible manufacturing strategies: made-to-stock, made-to-order or engineered-to-order. The approach is demonstrated on a case of production of residential evaporative cooler product, which is made to stock. Cooler is assembled from 39 components, supplied by 10 vendors, including fan, pump, nozzles, water inlets and feeds, chamber and reservoir, aluminium frame, safety mesh, louvres, casters, nuts, bolts, etc.

First, product information is acquired by using software application and corresponding meta-model for product acquisition in inter-organizational networks [10]. Then, product configuration is asserted in the SCOR-CFG OWL model. This model consists of following concepts: SC_project, SC_product, SC_production_type, SC_process (with child concepts, corresponding to different process types) and SC_participant. Relations between concepts are established by following properties:

```
hasPrincipalProduct(SC_project, SC_product)
isComponentOf(SC_product, SC_product)
employsStrategy(SC_product,
SC_production_type)
employsProcess(SC_production_type,
SC_process)
owns(SC_participant, SC_project)
precedes(SC_process, SC_process)
produces(SC_participant, SC_product)
```

Initially, the SCOR-CFG OWL model is asserted with instances of production strategies (SC_production_type object) and processes (SC_process object). Properties employsStrategy and employsProcess are defined as subproperties of the transitive employs. These relations enable the inference of make and delivery processes involved in manufacturing of the component of specific strategy.

When product configuration is saved, new statements are asserted in the SCOR-CFG OWL model. The generation of a SCOR thread diagram is done by selecting (and rendering) participants of supply chain project, its products (components) and, finally, processes, in exact order. Participants of selected supply chain project are inferred by using a SPARQL query, represented by following DL query:

```
(produces some
(isComponentOf some
(isPrincipalProductOf value
<selected_project>)))
or
(produces some
(isPrincipalProductOf value
<selected_project>))
```

In order to enable inference of participants in the infinite number of levels of supply and demand from the main

participant, isComponentOf property is defined as transitive.

Next, for each participant, its components of a principal product are inferred by query:

```
producedBy value <participant>
and (
isComponentOf some
(isPrincipalProductOf value
<selected_project>)
or
(isPrincipalProductOf value
<selected_project>))
```

Employed processes are inferred on basis of asserted precedes relations, which determine possible transitions of SCOR process categories, within participants (Sx-My-Dy) or between them (D1-S1, D2-S2,

D3-S3). The latter, cross-participant asserted transitions are valuable for the inference of source processes, on basis of principal product topology. For the selected product, employed processes are inferred by query:

```
SC_process and
(((preceededBy some
(employedBy some
(isComponentOf value <product>)))
and SC_source_process)
or
(employedBy value <product>))
```

Figure 1. shows the generated SCOR thread diagram. It is generated by application script, on basis of data collected from OWL file by SPARQL queries, represented with DL queries above.

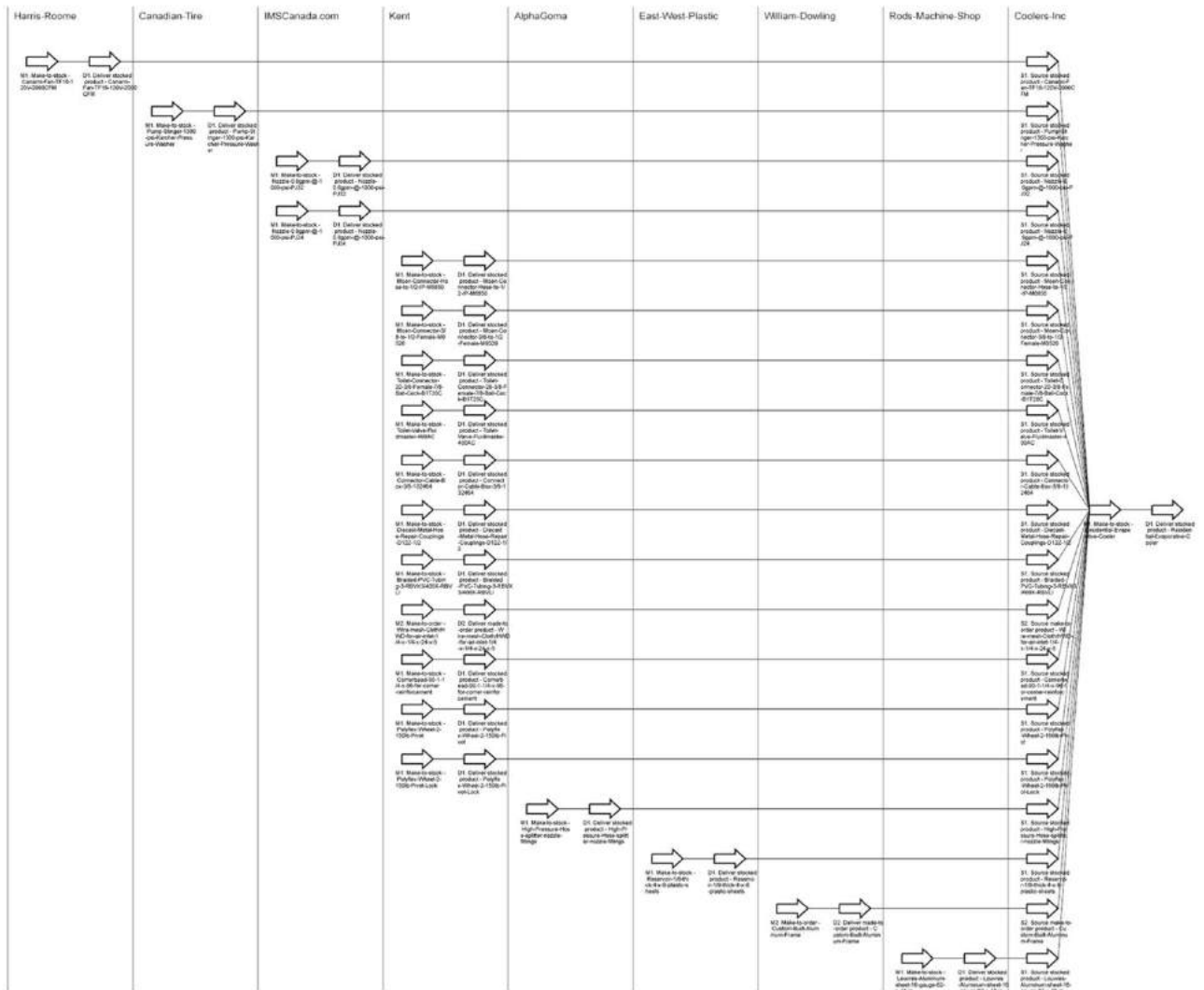


Figure 1. Generated SCOR thread diagram (partial)

Using the semantics Fact-Oriented Model enriching process expressed in [11] the SCOR thread diagram can benefit of an increasing number of specialized concepts from the enterprises domains and the result can gain in precision.

The SCOR thread diagram is a conceptual map of supply chain, built on basis of rules, asserted in SCOR-CFG OWL, prescribed by the SCOR framework. Developing conceptual models means specifying the essential objects or components of the system to be studied, the

relationships of the objects that are recognized and what kinds of changes in the objects or their relationships affect the functioning of the system and in which ways.

It enables the visual representation of high-level processes (process categories), roles and basic flows of information and resources between supply chain participants. Some of the features of the presented application are: development of complex thread diagrams, generation of process models and workflows and generation of implementation roadmap. These are elaborated below.

Example above shows only interactions and collaborations between 2 levels of a supply chain: principal customer and its first-tier suppliers. The number of visualized levels depends on the submitted product topology: if detailed product topology is entered, full supply chain would be represented by the resulting SCOR thread diagram, with the number of tiers corresponding to the depth of a principal product topology. Horizontal organization of individual supply chain actors can be represented in more detail, by inferring additional participants for different manufacturing strategies: warehouses (D, S), plants (M) and headquarters (P).

A SCOR thread diagram is not a process map. In fact, it is just a representation of supply chain configuration. However, full process model can be generated by adding new rules for configuration of the SCOR PLAN activities and by exploiting alignment relations between the SCOR-KOS and SCOR-CFG OWL models.

Alignment relations between the SCOR-KOS and SCOR-CFG OWL models also provide opportunities for the generation of a detailed implementation roadmap, consisting of proposed best practices, relevant systems (or their modules, capabilities, intended use, etc.) for their execution, resource tracking (SCOR Inputs and Outputs) and environment for measuring the performance of a supply chain, by using the SCOR metrics.

3. CONCLUSIONS

The compliance to industry (community) standards is a competitive advantage of a single enterprise, especially if it depends on multiple supply chains. It is beneficial for dealing with horizontal integration, interoperability of systems and flexible governance, as critical success factors for collaborative enterprises. However, these benefits are realistic only if the compliance is managed in a manner which enables a seamless acquisition, effective use and re-use and continuous evolution of knowledge, which represent the standards themselves.

In this paper, we addressed the issues of supply chains configuration and, partially coordination. Understanding and using the SCOR reference model is a competitive advantage of a single SME, as it provides structured collaboration capability. Still, like most of the domain reference models, SCOR is a complex and dynamic set of concepts and, hence, very hard to implement and maintain, especially at bottom tiers of supply chains.

The application based on the SCOR-CFG and SCOR-KOS OWL models is expected to demonstrate the positive impact of using knowledge-based systems for SCOR implementation, in segments of supply chain configuration (by enabling generation of SCOR thread diagrams), coordination (by enabling generation of XPDL process models) and continuous improvement (by enabling generation of process implementation roadmaps). The approach relies on and builds upon widely accepted industry practice, represented in its native format. The native representation is expected to gain attention and understanding of SCM expert's

community and, hence, facilitate the transition towards using more sophisticated, knowledge-based tools in the domain. Its mapping and alignment to higher-level ontologies will enable a structured support in other SCM processes, such as partners' selection, performance tracking, exceptions handling, etc. Also, it is expected to contribute to further development and/or refinement of the SCOR reference model.

REFERENCES

- [1] J.W. Forrester, *Industrial Dynamics*, The M.I.T. Press, Cambridge, MA, (1961).
- [2] H. Panetto, A. Molina, Enterprise integration and interoperability in manufacturing systems: Trends and issues, *Computers in Industry*, 59 (7) (2008) 641-646.
- [3] J. Motwani, R. Subramanian, P. Gopalakrishna, Critical factors for successful ERP implementation: exploratory findings from four case studies, *Computers in Industry*, 56 (6) (2005) 529-544.
- [4] B. Grabot, *Process Alignment or ERP Customisation: Is There a Unique Answer?*, Springer Series in Advanced Manufacturing, ERP Systems and Organisational Change, Springer, London, (2008) 139-156.
- [5] F. B. Vernadat, F.B., 2002, Enterprise Modeling and Integration (EMI): Current Status and Research Perspectives, *Annual Reviews in Control*, 26 (2002) 15-25.
- [6] N. Guarino, P. Giaretta, Ontologies and knowledge bases – towards a terminological clarification, In N. Mars (Ed.), *Towards very large knowledge bases: knowledge building and knowledge sharing*, IOS Press, Amsterdam, (1995) 25-32.
- [7] D. Fensel, Ontologies: Dynamic networks of formally represented meaning, In: *Proceedings of the 1st Semantic web working symposium*, July 30th-August 1st, 2001, Stanford, USA (2001)
- [8] G. Stewart, Supply-chain operations reference model (SCOR): the first cross-industry framework for integrated supply-chain management, *Logistics Information Management* 10 (2) (1997) 62–67.
- [9] Zdravković, M., Panetto, H., Trajanović, M., 2010, Towards an approach for formalizing the supply chain operations, In *Proceedings of the 6th International Conference on Semantic Systems*, Graz, Austria, September 1-3, 2010
- [10] Zdravković, M., Trajanović, M., 2009, "Integrated Product Ontologies for Inter-Organizational Networks", *Computer Science and Information Systems (COMSIS)*, ISSN: 1820-0214, Vol.6, No.2, pp.29-46
- [11] Lezoche, M., Aubry, A., Panetto, H., 2011, "Conceptualisation approach for Cooperative Information Systems interoperability", *ICEIS 2011*, Beijing, China, June 8-11, 2011.



PREDICTION OF THE NONLINEAR STRUCTURAL BEHAVIOUR BY DIGITAL RECURRENT NEURAL NETWORK

Vesna RANKOVIĆ¹, Nenad GRUJOVIĆ¹, Dejan DIVAC², Nikola MILIVOJEVIĆ², Konstantinos PAPANIKOLOPOULOS³, Jelena BOROTA¹

¹Faculty of Mechanical Engineering, University of Kragujevac, Sestre Janjić 6, Kragujevac, Serbia

²Jaroslav Černi Institute for the Development of Water Resources, Jaroslava Černog 80, Belgrade, Serbia

³Institute of Structural Analysis and Seismic Research, National Technical University of Athens, Iroon Polytechniou 5, GR-157 80 Zographou, Athens, Greece

vesnar@kg.ac.rs, gruja@kg.ac.rs, ddivac@eunet.rs, nikola.milivojevic@gmail.com, kpapani@mail.ntua.gr
jborota@gmail.com

Abstract: *The dynamical systems contain nonlinear relations which are difficult to model with conventional techniques. Nonlinear models are needed for system analysis, optimization, simulation and diagnosis of nonlinear systems. In recent years, computational-intelligence techniques such as neural networks, fuzzy logic and combined neuro-fuzzy systems algorithms have become very effective tools to identification nonlinear plants. The problem of the identification consists of choosing an identification model and adjusting the parameters such that the response of the model approximates the response of the real system to the same input. This paper investigates the identification nonlinear system by Digital Recurrent Neural Network (DRNN). A dynamic backpropagation algorithm is employed to adapt weights and biases of the DRNN. Mathematical model based on experimental data is developed. Results of simulations show that the application of the DRN to identification of complex nonlinear structural behaviour gives satisfactory results.*

Key words: *identification, structural behaviour, digital recurrent network*

1. INTRODUCTION

Nonlinear system identification and prediction is a complex task. All the processes in nature are nonlinear. In large number of processes, the nonlinearities are not prominent, so their behavior can be described by the linear model. In the linear systems theory there exist a large number of methods that can be applied for obtaining the linear model of processes. The nonlinear model must be chosen when the nonlinearity is strongly exhibited.

Neural network modelling and identification from experimental data are effective tools for approximation of uncertain nonlinear dynamic system. Neural networks are classified into two major categories: feedforward and recurrent. Most of publications in nonlinear system identification use feedforward networks, for example multilayer perceptrons, [1]. The feedforward neural networks trained with a standard back-propagation algorithm can be used for the identification of nonlinear dynamic systems [2]. Chen [3] explained neural network-based method for determining the dynamic characteristic parameters of structures from field measurement data. Conventional back-propagation is used to train the neural network. However, the conventional back-propagation algorithm has the problems of local minima and slow rate of convergence.

An improvement to the back-propagation algorithm based on the use of an independent, adaptive learning rate parameter for each weight with adaptable nonlinear function is presented in [4]. Adaptive time delay neural

network structures was utilized in [5], for nonlinear system identification. Nonlinear system on-line identification via dynamic neural networks is studied in [6]. Reference [7] studied the modeling and prediction of NARMAX- (nonlinear autoregressive moving average with exogenous inputs) model-based time series using the fuzzy neural network methodology.

This paper investigates the identification nonlinear structural behaviour system by digital recurrent neural network. Dynamic backpropagation algorithm is used to adapt weights and biases.

2. METHODS FOR THE IDENTIFICATION OF NONLINEAR DYNAMIC SYSTEMS

Different methods have been developed in the literature for nonlinear system identification. These methods use a parameterized model. The parameters are updated to minimize an output identification error.

$$y_m(k) = f_m(\varphi(k), \theta) \quad (1)$$

where $y_m(k)$ is the output of the model, $\varphi(k)$ is the regression vector and θ is the parameter vector.

Depending on the choice of the regressors in $\varphi(k)$, different models can be derived:

NFIR (Nonlinear Finite Impulse Response) model –

$$\boldsymbol{\varphi}(k) = (u(k-1), u(k-2), \dots, u(k-n_u)),$$

where n_u denotes the maximum lag of the input.

NARX (Nonlinear AutoRegressive with eXogenous inputs) model:

$$\boldsymbol{\varphi}(k) = (u(k-1), u(k-2), \dots, u(k-n_u), \\ y(k-1), y(k-2), \dots, y(k-n_y))$$

NARMAX (Nonlinear AutoRegressive Moving Average with eXogenous inputs) model:

$$\boldsymbol{\varphi}(k) = (u(k-1), u(k-2), \dots, u(k-n_u), \\ y(k-1), y(k-2), \dots, y(k-n_y), \\ e(k-1), e(k-2), \dots, e(k-n_e))$$

where $e(k)$ is the prediction error and n_e is the maximum lag of the error.

NOE (Nonlinear Output Error) model-

$$\boldsymbol{\varphi}(k) = (u(k-1), u(k-2), \dots, u(k-n_u), \\ y_m(k-1), y_m(k-2), \dots, y_m(k-n_y))$$

NBJ (Nonlinear Box-Jenkins) model- uses all four regressor types.

In this paper, NOE model (Fig. 1) is used for representation of nonlinear systems.

outputs $y_m(k-1), y_m(k-2), \dots, y_m(k-n_y)$ are multiplied by weights $\omega_{y_{ij}}$ and summed at each hidden node. Then the summed signal at a node activates a nonlinear function. The hidden neurons activation function is the hyperbolic tangent sigmoid function. In Fig. 2, ω_i represents the weight that connects the node i in the hidden layer and the output node; b_i represents the biased weight for i -th hidden neuron and b is a biased weight for the output neuron.

The output of the network is:

$$y_m(k) = \sum_{i=1}^{n_H} \omega_i v_i + b \quad (2)$$

where n_H is the number of hidden nodes and:

$$v_i = \frac{e^{n_i} - e^{-n_i}}{e^{n_i} + e^{-n_i}} \quad (3)$$

$$n_i = \sum_{j=1}^{n_u} u(k-j) \omega_{u_{ij}} + \sum_{j=1}^{n_y} y_m(k-j) \omega_{y_{mij}} + b_i \quad (4)$$

The difference between the output of the plant $y(k)$ and the output of the network $y_m(k)$ is called the prediction error:

$$e(k) = y(k) - y_m(k) \quad (5)$$

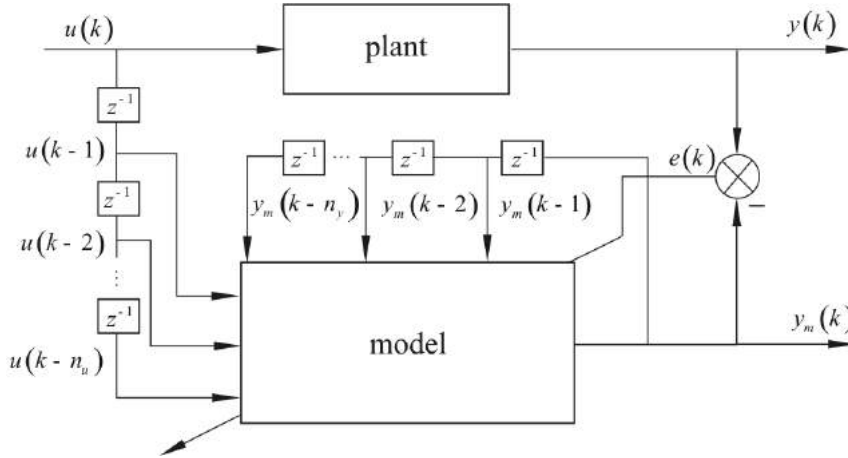


Fig. 1. The general block schema of the NOE model

3. DRN NEURAL NETWORK FOR NONLINEAR SYSTEM IDENTIFICATION

Fig. 2 is an example of a DRN. The output of the network is feedback to its input. This is a realization of the NOE model. The output of the network is a function not only of the weights, biases, and network input, but also of the outputs of the network at previous points in time. In [7] dynamic backpropagation algorithm is used to adapt weights and biases.

DRN network is composed of a nonlinear hidden layer and a linear output layer. The inputs $u(k-1), u(k-2), \dots, u(k-n_u)$ are multiplied by weights $\omega_{u_{ij}}$,

This error is used to adjust the weights and biases in the network via the minimization of the following function:

$$\mathcal{E} = \frac{1}{2} [y(k) - y_m(k)]^2 \quad (6)$$

Using the gradient decent, the weight and bias updating rules can be described as:

$$\omega_{u_{ij}}(k+1) = \omega_{u_{ij}}(k) - \eta \frac{\partial \mathcal{E}}{\partial \omega_{u_{ij}}} \quad (7)$$

$$\omega_{y_{mij}}(k+1) = \omega_{y_{mij}}(k) - \eta \frac{\partial \mathcal{E}}{\partial \omega_{y_{mij}}} \quad (8)$$

$$b_i(k+1) = b_i(k) - \eta \frac{\partial \mathcal{E}}{\partial b_i} \quad (9)$$

$$b(k+1) = b(k) - \eta \frac{\partial \varepsilon}{\partial b} \quad (10)$$

where:

$$\frac{\partial \varepsilon}{\partial \omega_{u_{ij}}} = \frac{\partial^e \varepsilon}{\partial y_m} \frac{\partial y_m}{\partial \omega_{u_{ij}}}; \quad \frac{\partial \varepsilon}{\partial \omega_{y_{ij}}} = \frac{\partial^e \varepsilon}{\partial y_m} \frac{\partial y_m}{\partial \omega_{y_{ij}}};$$

$$\frac{\partial \varepsilon}{\partial b_i} = \frac{\partial^e \varepsilon}{\partial y_m} \frac{\partial y_m}{\partial b_i}; \quad \frac{\partial \varepsilon}{\partial b} = \frac{\partial^e \varepsilon}{\partial y_m} \frac{\partial y_m}{\partial b}$$

where the superscript e indicates an explicit derivative, not accounting for indirect effects through time.

The terms $\frac{\partial y_m}{\partial \omega_{u_{ij}}}$, $\frac{\partial y_m}{\partial \omega_{y_{ij}}}$, $\frac{\partial y_m}{\partial b_i}$ and $\frac{\partial y_m}{\partial b}$ must be propagated forward through time, [8].

$$\varphi(k) = (u_1(k-1), u_2(k-1), y_m(k-1))$$

where u_1 is water level, $u_2 = \frac{2\pi j}{365}$ is the season varying

between 0 and 2π , j represents the number of days since January 1st.

A data set includes 783 data samples. The available set of data was divided into two sections as training and test set. The MATLAB Neural Network Toolbox is applied for the implementation of the digital recurrent network network. Different DRNN models were constructed and tested in order to determine the optimum number of neurons in the hidden layer. The two-layer network with a tan-sigmoid transfer function at the hidden layer and a linear transfer function at the output layer were used. The optimal network size was selected from the one which resulted in maximum correlation coefficient for the training and test sets, Table 1. Based on Table 1, it was concluded that the optimal number of hidden neurons is 27. The total number

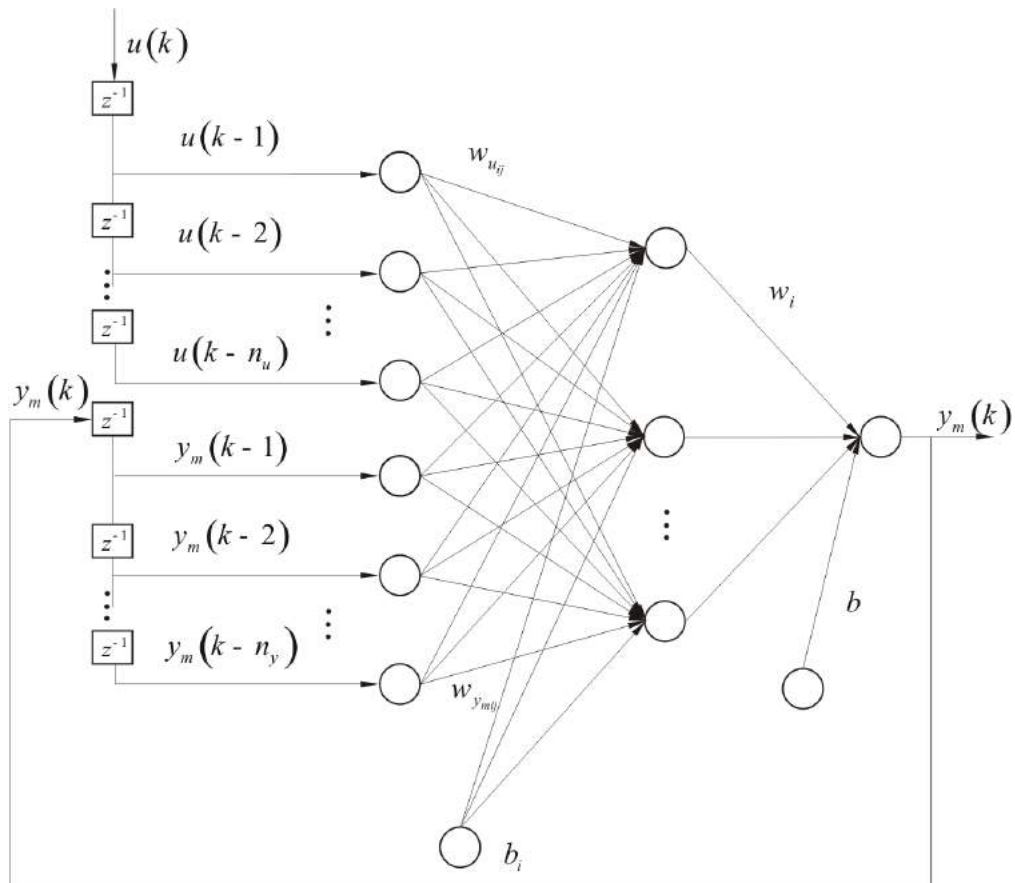


Fig. 2. Digital Recurrent Network

4. SIMULATION RESULTS

The major objective of the study presented in this paper is to construct DRNN model to predict the radial displacement of arch dam. The DRNN model was developed and tested using experimental data which are collected during eleven years.

It is considered the behaviour of nonlinear dynamic system with two input and one output.

The model input vector is defined by:

of the parameters of DRN network is 136. In the learning processes, the weights (108) of the neural networks were adapted as well as the biases (28).

Table 1. Correlation coefficient for the training and test sets.

DRNN- structure	3-20-1	3-24-1	3-27-1	3-30-1
Training	0.889	0.936	0.974	0.966
Test	0.877	0.943	0.972	0.965

Figure 3 shows the measured and models computed values in training +test set.

[2] NARENDRA, K.S., PARTHASARTHY, K. (1990)

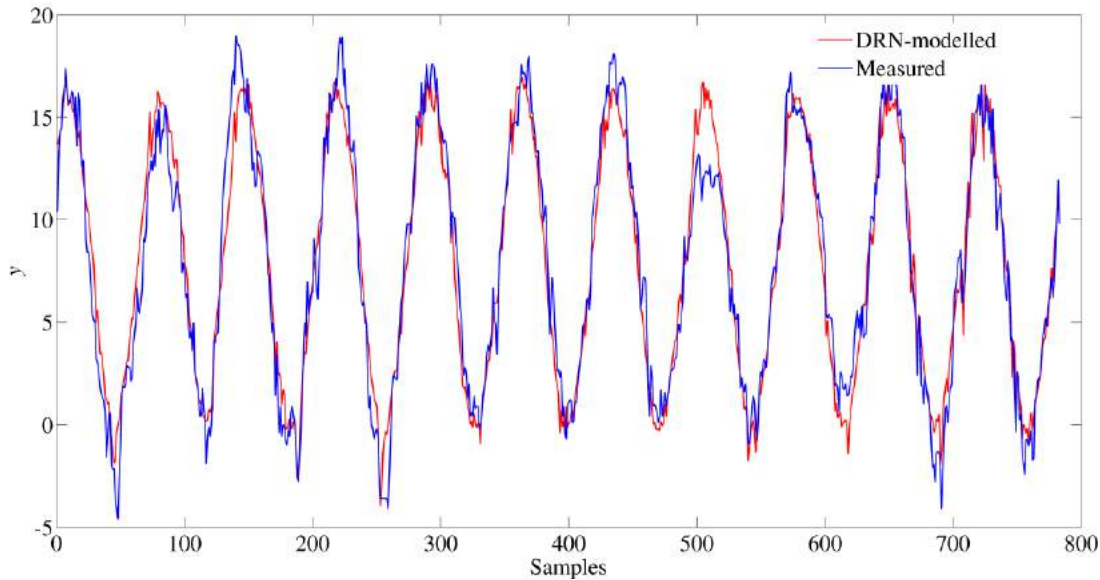


Fig. 3. The measured and modelled values in training +test set.

5. CONCLUSION

The dynamical systems contain nonlinear relations which are difficult to model with conventional techniques. In this paper, DRN has been successfully applied to unknown nonlinear system identification and modelling. The real-data set was used to demonstrate the effectiveness of the proposed approach. Comparing the modelled values by DRNN with the experimental data indicates that soft computing model provides accurate results. In the designing of neural network model, the problem is how to determine an optimal architecture of network.

The determination of the values of n_u and n_y is an open question. Large time lags result in better prediction of the NN. However, large n_u and n_y also result in large number of parameters (weights and biases) that need to be adapted. In considered example, satisfactory results were obtained for $n_{u1} = n_{u2} = n_y = 1$.

REFERENCES

[1] YU, W., (2004) *Nonlinear system identification using discrete-time recurrent neural networks with stable learning algorithms*, Information Sciences, Vol. 158 No. 1, pp 131-147.

Identification and control of dynamical systems using neural networks, IEEE Trans. Neural Networks, Vol. 1, No. 1, pp 4-27.

- [1] CHEN, C.H. (2005) *Structural identification from field measurement data using a neural network*, Smart materials and structures, Vol. 14, No. 3, pp S104-S115.
- [2] GUPTA, P., SINHA, N. K. (1999) *An improved approach for nonlinear system identification using neural networks*, Journal of the Franklin Institute, Vol. 336, No. 4, pp 721-734.
- [3] YAZDIZADEH, A., KHORASANI, K. (2002) *Adaptive time delay neural network structures for nonlinear system identification*, Neurocomputing, Vol. 47, No. 1-4, pp 207-240.
- [4] YU, W., LI, X. (2001) *Some New Results on System Identification with Dynamic Neural Networks*, IEEE Transactions on Neural Networks, Vol. 12, No. 2, pp
- [5] GAO, Y., ER, M.J. (2005) *NARMAX time series model prediction: feedforward and recurrent fuzzy neural network approaches*, Fuzzy Sets and Systems, Vol. 150, No. 2, pp 331-350.
- [6] HAGAN, M., JESUS, O. D., SCHULTZ, R. (1999) *Training Recurrent Networks for Filtering and Control*, Chapter 11 of *Recurrent Neural Networks: Design and Applications*, L.R. Medsker and L.C. Jain, Eds., CRC Press, pp 325-354.

ACKNOWLEDGMENT: The part of this research is supported by Ministry of Science in Serbia, Grants III41007 and TR37013.



ERP IMPLEMENTATION STRATEGIES FOR MANUFACTURING COMPANIES IN E-BUSINESS ENVIRONMENT

Darko STEFANOVIĆ, Andraš ANDERLA, Cvijan KRSMANOVIĆ, Aleksandar IVIĆ

Faculty of Technical Sciences, University of Novi Sad, Trg Dositeja Obradovića 6, Novi Sad, Serbia
darkoste@uns.ac.rs, andras@uns.ac.rs, cvijan@uns.ac.rs, ivicaca@gmail.com

Abstract: *In response to the growing global competition, many manufacturing companies have embarked upon enterprise resource planning (ERP) implementation. An ERP system as an integrated software solution spans the range of business processes that enables companies to gain a complete view of its business. While ERP organizes information within the company, e-business disseminates that information far and wide. The purpose of these new technologies is to enable the extended value chain, and companies that are able to plug their internal information systems into the information chain that parallels the physical goods value chain will prosper.*

This paper presents possible options of ERP implementation in e-business environment for a new manufacturing company with no history of information systems ("Greenfield" company) and for a company with nonintegrated information systems which has no rapid and meaningful data exchange between its internal systems that record business events ("Nonintegrated Systems" company).

Key words: *Enterprise Resource Planning, Information System, Implementation, E-business*

1. INTRODUCTION

Organizations today are constantly in search for ways to achieve better business performance and sustain competitive advantages through effective deployment of resources and business processes. In order to be more efficient, many companies rely on extensive use of ICT, often by installing Enterprise Resource Planning (ERP) systems [1]. The ERP system is an integrated set of programs that provides support for core business processes, such as production, input and output logistics, finance and accounting, sales and marketing, and human resources. An ERP system helps different parts of an organization to share data, information to reduce costs, and to improve management of business processes [2]. According to Wier, Hunton, and HassabElnaby, ERP systems aim to integrate business processes and ICT into a synchronized suite of procedures, applications and metrics which goes over companies' boundaries [3].

2. ERP EVOLUTION AND DEFINITIONS

The evolution of ERP has often been used in the academic literature to describe the concept of Enterprise Systems (ES) [4], [5], [6], [7]. Enterprise Systems, also commonly referred to as ERP systems [4], have their origin in the early 50's. It was with the introduction of computers into the business that the first applications began to emerge. At first these applications were used for automating manual processes like bookkeeping and inventory management. The use was expanded during the 60's to Inventory Control Systems (ICS) and Bill-of-Material (BOM)

planning which in turn gradually became standardized into Material Requirements Planning (MRP). During the 70's new software systems were introduced with the emphasis on the optimization of the manufacturing processes. These systems synchronized the material requirements with the production requirements and became known as Manufacturing Resource Planning (MRP II) systems. The manufacturing process optimization was developed in the form of the Computer-Integrated Manufacturing (CIM) concept in the 80's. The increased scope of information systems paved the way for ERP systems, which provide a software package designed to integrate the internal value-chain of an enterprise, covering business processes from manufacturing to transportation as well as secondary processes like accounting and finance. In the late 90's suppliers began to add more modules and functionality to the core modules of the ERP systems. These extensions to the ERP system include Advanced Planning and Scheduling (APS), Customer Relationship Management (CRM) and Supply Chain Management (SCM). The core ERP modules combined with the aforementioned extensions became known as Extended Enterprise Resource Management (X-ERP) [8] or ERP II [9], [7].

Currently we are seeing that ERP II is still evolving. Bond describes the reason for this evolution as: "Enterprises are starting to transform themselves from vertically integrated organizations focused on optimizing internal enterprise functions to more agile, core competence based entities that strive to position the enterprise optimally in the supply chain and the value network" [9]. The positioning of the enterprise should be considered in a

broader context than just dyadic relations in the form of B2C or B2B. Instead, the collaborative commerce definition as given by Gartner Research Group should be taken into account. It states that “C-commerce involves the collaborative, electronically enabled business interactions among an enterprise’s internal personnel, business partners and customers throughout a business or trading community” [9]. In essence, this means enterprises position themselves optimally in the supply chain and the value network by means of electronic auctions and other one-to-many or many-to-many relations [10].

ERP II can be seen as the successor to ERP or as Moller puts it: “ERP II is essentially componentized ERP, e-business and collaboration in the supply chain” [11].

Moller has created a conceptual framework for ERP II (see Figure 1) in which he defines four layers; the foundation, process, analytical and portal layer. With this model we can see that ERP II is more than just an information system, it is a complete concept of how to manage all enterprise (information) systems. When consulting other literature on ERP II, like Weston who speaks of the ERP II “umbrella” [12], all concepts described there can be placed in the conceptual framework by Moller. Taking this model as a basis for the ERP II definition, a number of possibilities were found in the academic literature.

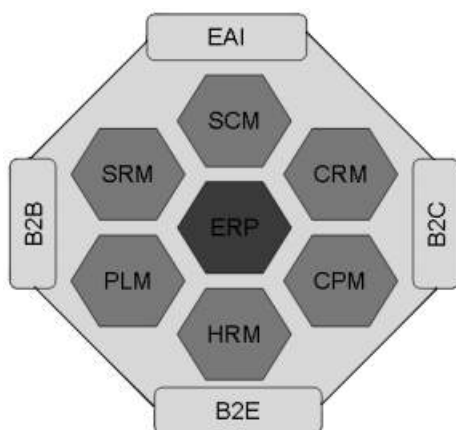


Figure 1: Conceptual framework ERP II

Gartner Research Group defined ERP II as: A business strategy and a set of industry domain-specific applications that build customer and shareholder value by enabling and optimizing enterprise and inter-enterprise collaborative operational and financial processes.

This definition by GRG is based on the idea of creating value for the organization. Another definition uses integration and collaboration as a basis: ERP II supports the evolution of an organization towards becoming a link in a value collaboration network by creating a business web in which web services play an important role in regard to integration and collaboration both on a personal and business process level.

Both of these approaches to ERP II are valid. They are linked together, collaboration is the essence of ERP II when compared to ERP but business value is the main driving force behind the application and development of ERP II. To accommodate both visions on ERP II, this paper uses a combination of both approaches: ERP II is a concept of value-chain oriented information systems which use database technology to manage and utilize both business processes and data, including customer, product, employee, supplier, and financial data with the purpose of creating customer and shareholder value.

This definition will be used in this paper from this point on and be referred to as “ERP”. The term ERP is used because it is hard to use any other term, simply because there is no general consensus about any other terminology. This is also pointed out by McGaughey in his article: “While some companies are expanding their ERP system capabilities (adding modules) and still calling them ERP systems, others have started to use catchy names like enterprise suite, E-commerce suite, and enterprise solutions to describe their solution clusters that include ERP among other modules/capabilities” [7].

3. ERP AND E-BUSINESS RELATIONSHIP

Since the late 1990s, companies have increasingly turned to Internet and Web based technologies, but they found that without ERP software, sharing accurate information with their trading partners is impossible. ERP organizes information within the enterprise, e-business disseminate that information far and wide. In short, ERP and e-business technologies supplement each other.

In order to make rational decisions about how to use the resources of the company to improve operations and increase its market share, any implementation of ERP, e-business, or both, companies must be aware of their starting positions and have a clearly defined desired, the final state. Figure 2 shows the areas in which the company can be found depending on the level of integration of ERP and e-business technologies in their business. [13], [14].

Integrated Enterprise ERP					
Integrated Business-Unit ERP					
Limited/Single-Function ERP					
Nonintegrated System					
Greenfield					
	No E-Business Capabilities	Channel Enhancement	Value-Chain Integration	Industry Transformation	Convergence

Figure 2: ERP/e-business matrix

The five possible ERP spaces for the company on the matrix are:

- Greenfield – Start up company, no system are in place, the cultural impact of any decision to move to another ERP scenario is low. It is possible for company in this space to jump immediately to any one of the five positions along the e-business landscape. A company in this ERP scenario is in the best possible position to define an e-business-based business model.
- Nonintegrated Systems – Company operating in the legacy environment, has a large number of nonintegrated information systems with many different platforms and operating systems, numerous applications programs and competing languages. Many of these information systems are unique to a particular corporate function and exchange of data between them is insufficient and slow. Such an environment has enormous ongoing maintenance costs and might be characterized as „worst in class“. For such a company, e-business might be viewed as a way to fix the system without having to actually fix its pieces.
- Limited-Single-Function ERP – Company has successfully installed one or more basic ERP modules (usually finance, human resources and / or manufacturing modules) across a business unit, looking at the level of the entire company has remained incompletely optimized.
- Integrated Business Unit ERP – Company has successfully integrated ERP solution in one or more business units, ideally, such a company operates as a holding company.
- Integrated Enterprise ERP – Company that is fully integrated ERP solution throughout the company.

Spaces in which the company can be found to overlaps in a way that borders are not stressed and do not have all the pieces of the company located in the same area, especially when it comes to multi business unit companies. Moreover, in the real world, companies are often located somewhere between or over multiple space described [15].

4. POSSIBLE OPTIONS OF ERP IMPLEMENTATION IN E-BUSINESS ENVIRONMENT

Most companies recognize the importance of becoming e-enabled. However, many companies take a haphazard approach with disconnected project teams, disjointed technological investments, and unclear strategic objectives. Several steps, like determine where the company is going, assess organizational capabilities to get there, plan and implement the route forward, are required to undertake an appropriate migration from any starting point on the ERP/e-business matrix to one of the desired destination points.

On the route forward, a company might legitimately stop at any point, consolidate its efforts before moving on, and possibly decide not to move any further. A migration path

strategy should be redefined every six months, as business conditions in a particular industry warrant.

A company on the Greenfield ERP axis has a number of possible options (see Figure 3). It can implement ERP and e-business simultaneously, moving from its starting point to either an integrated business unit or integrated enterprise ERP at the same time it moves one, two, or three snapshots across the e-business landscape. Also, the company can decide not to implement ERP and move across e-business panorama, hoping that technology will become available to allow it to process transaction and manage internal information without the need for ERP technology. A start-up company would very rarely implement an integrated ERP system prior to moving along the e-business landscape.

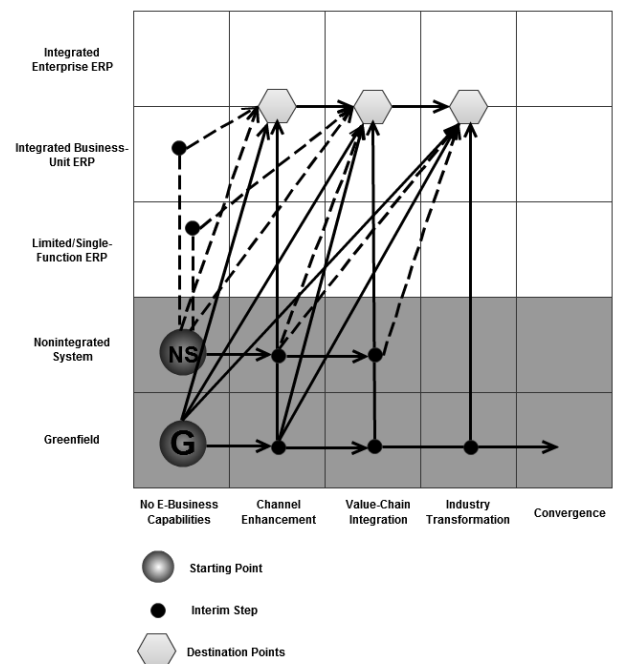


Figure 3: Greenfield & Nonintegrated System ERP Migration Options

The company starting with nonintegrated internal systems has similar options as the Greenfield company but is constrained by its starting position. Such a company can seek to get its house in order and implement ERP before beginning its e-business journey. Or it can develop some e-business skills first and then move to implement ERP, but it cannot move too far across the e-business landscape before it becomes necessary to implement ERP (see Figure 3). A company on the Nonintegrated Systems ERP axis may be forced to implement ERP by a stronger partner in the developing value network.

5. CONCLUSION

The blending of Internet technologies and traditional business concerns is impacting all industries and is really the latest phase in the ongoing evolution of business. An ERP system is one of the most inclusive technologies in organizations thus far. The decision to implement an ERP

system in a company usually has a profound impact on the organization and on all members of the supply chain. There must be a clear and documented understanding of the impact of an ERP implementation on each business process and on the supply chain. In the e-world, the focus is no longer just on how well an application can store and manage data and move it around within the enterprise. It is now on both adding value to that data to turn it into information and knowledge, and on moving that data and information across enterprises to create knowledgeable extended enterprises.

Each company's situation will be unique. But efforts must be managed in a systematic manner, as befits any strategic initiative. Specifically, this means that these efforts must be controlled at a senior leadership level and coordinated appropriately across the enterprise. Senior executives must now become even more familiar with and engaged in technology to make their companies successful.

REFERENCES

- [1] OLSEN, K. O., and SÆTRE, P. (2007) IT for Niche Companies: Is an ERP System the Solution? *Information System Journal*, 17, 1, 37-58.
- [2] ALADWANI, A. M. (2001) Change management strategies for successful ERP implementation, *Business Process Management Journal*, 7 (3), pp. 266-275.
- [3] WIER, B., HUNTON, J. and HASSABELNABY, H. R. (2007) Enterprise resource planning systems and non-financial performance incentives: The joint impact on corporate performance, *International Journal of Accounting Information Systems*, 8 (3), pp. 165-190.
- [4] DAVENPORT, T.H. (1998) Putting the enterprise into the enterprise system. *Harvard Business Review*, July/August, pp. 121-31.
- [5] CHEN, I.J. (2001) Planning for ERP systems: analysis and future trend. *Business Process Management Journal*, Vol. 7 No.5, pp.374-386.
- [6] WORTMANN, J.C. (1998) Evolution of ERP systems. *Strategic Management of the Manufacturing Value-chain*, Kluwer Academic Publishers, Amsterdam.
- [7] MCGAUGHEY, R.E. & GUNASEKARAN, A. (2007) Enterprise Resource Planning (ERP): Past, Present and Future. *International Journal of Enterprise Information Systems*, Vol. 3, Issue 3, pp. 23-35.
- [8] RASHID, M.A., HOSSAIN, L. & PATRICK, J. (2002) The Evolution of ERP Systems: A Historical Perspective. *Enterprise Resource Planning: Global Opportunities, Challenges and Solution*, Idea Group Publishing, USA, ISBN: 1-930708-36-X. pp. 1-16.
- [9] BOND, B., GENOVESE, Y., MIKLOVOC, D., WOOD, N., ZRINSEK, B. and RAYNER, N. (2000) ERP Is Dead—Long Live ERP II. *Gartnergroup*, New York, NY.
- [10] MARKUS M.L., PETRIE D. & AXLINE S. (2000) Bucking the Trends: What the future may hold for ERP packages. *Information Systems Frontiers*, Volume 2, Number 2, pp. 181-193.
- [11] MOLLER, C. (2005) ERP II: a conceptual framework for next-generation enterprise systems? *Journal of Enterprise Information Management*, Volume 18, Number 4, pp. 483-497.
- [12] WESTON, F.C. (2003) ERP II: The extended enterprise system. *Business Horizons*, Volume 46, Number 6, November 2003, pp. 49-55.
- [13] NORRIS, G., HURLEY, J. R., HARTLEY, K. M., DUNLEAVY, J. R., BALLS, J. D. (2000) "E-Business and ERP: Transforming the Enterprise", PricewaterhouseCoopers
- [14] DEISE, M. V., NOWIKOW, C., KING, P., WRIGHT, A. (2000) "Executive's Guide to E/ Business: From Tactics to Strategy, New York: John Wiley & Sons
- [15] STEFANOVIĆ, D., ANDERLA, A., RAŠIĆ, D., MIRKOVIĆ, M., STEFANOVIĆ, N., MILISAVLJEVIĆ, S. (2011) Investigation Of Conditions For The Integration Of Modern ICT In Operations Of Production Systems, *InfoTeh-Jahorina* Vol. 10, Ref. E-IV, p. 659-662

Research for this article was conducted under the project "Improving the competitiveness of Serbia in the process of joining the European Union, Ministry of Science of Serbia, no. 47028, for the period 2011th-2014th year.

34th INTERNATIONAL CONFERENCE ON PRODUCTION ENGINEERING



SECTION J

NONCONVENTIONAL TECHNOLOGIES (ADVANCED MACHINING TECHNOLOGIES)



SURFACE ROUGHNESS AT ABRASIVE JET ENGRAVING OF GLASS PARTS

Laurențiu SLĂTINEANU¹, Margareta COTEATĂ¹, Miroslav RADOVANOVIĆ², Ștefan POTĂRNICHE¹,
Lorelei GHERMAN¹, Irina BEȘLIU³

¹“Gheorghe Asachi” Technical University of Iași, Blvd. D. Mangeron, Iași, Romania

²University of Niš, Faculty of Mechanical Engineering in Niš, Serbia

³University “Ștefan cel Mare” of Suceava, Universității Street, Suceava, Romania

slati@tcm.tuiasi.ro, mcoteata@tcm.tuiasi.ro, mirado@masfak.ni.ac.rs, potarnichestefan@yahoo.com,
lo_drey@yahoo.com, grigorasirina_sv@yahoo.com

Abstract: Essentially, the main machining processes applied to the glass parts are the cutting, the drilling and the engraving. Nowadays, one of the techniques used to transfer drawings or inscriptions on the glass parts is the abrasive jet engraving. This machining method is based on the effects generated at the impact of the abrasive particles transported by means of a compressed air jet with the surface layer of the machined part. The main characteristic which changes as consequence of the abrasive jet engraving is the surface roughness. The paper includes some considerations concerning the phenomena able to affect the surface roughness parameters during the abrasive jet engraving. An experimental research was developed to study the evolution of the surface roughness parameters for a variation of some experimental work conditions (average dimension of the abrasive particles, distance between the nozzle and the test piece flat surface, the angle between the direction of the abrasive jet and the test piece flat surface). Some empirical mathematical models were thus determined and analyzed, to better highlight and understand the influence exerted by the work conditions on the surface roughness parameters in the case of the abrasive jet engraving of the glass parts.

Key words: glass parts, abrasive jet engraving, surface roughness, empirical model, influence factors

1. INTRODUCTION

The glass is an amorphous material characterized by a high mechanical resistance and hardness, by brittleness, transparency and low dilatation coefficient. The common glass contains 75% silica (SiO₂), Na₂O, CaO and several minor additives. For long time, the glass was used especially in windows and drinking vessels; nowadays, the glass is used also in various industrial fields [1-3]. The main machining processes applied to glass workpieces are cutting, drilling, and engraving [2-5]. The engraving could be defined as a machining method which allows the transfer of inscriptions and drawings on parts surfaces. There are many types of engraving methods applied to the glass workpieces, but they could be included in two main groups: *chemical methods* and *cutting methods*. The chemical engraving methods use chemical reactions developed on the surfaces which are not protected between the chemical active substances and the glass. The cutting methods could be materialized by means of solid tools (abrasive wheels or drills, small diamond tipped burrs) or abrasive particles; these last methods could be considered as *abrasive jet machining methods*. The abrasive jet engraving uses the effects generated at the contact of the abrasive particles with the workpiece surface layer: if in the case of metallic workpieces this machining method supposes the changing of the surface aspect as result of plastic deformation, microcracking and

microcutting effects, in the case of the glass workpiece it is expected that the machined surface aspect changes especially due to the material removal by microcracking effects. Glass engraving is a form of decorative glasswork that involves engraving a glass surface or object. Adjouadi et al. studied the phenomena of light scattering in the case of glass test pieces eroded by sandblasting; during the experiments, they varied the projected sand mass, the opening of the light beam and the distance sample-receptor [2]. A decrease of the optical transmission from 91.6 to 13 % and an increase of the surface roughness from 0.035 up to 2.27 μm as consequence of the sandblasting process were highlighted. Ismail et al. investigated the erosion phenomenon in glass by experimental research and simulations by finite element method; they highlighted the influence exerted by the particle size and velocity on the material removal in the sandblasting process [3]. The material removal in the case of a single impact was determined by means of a profilometer; the authors appreciated that there is a good correspondence between the results obtained by simulation and by experimental research about the craters sizes.

2. SURFACE ROUGHNESS AT ENGRAVING

It is known that the surface roughness is one of the parameters (together with the shape errors and the

waviness) used to define the geometry of a machined surface; there is a convention to consider as roughness the assembly of asperities characterized by a ratio between the wave length and height lower than 50. Many factors exert influence on the roughness parameters of the machined surface; chemical composition and mechanical properties of the workpiece material, sizes of the machining parameters, geometry of cutting tool active part, rigidity of the machining system, presence and type of the cooling liquids etc. On the other hand, nowadays there are many parameters used to characterize the surface roughness of the machined surface; in accordance with the actual standards, some groups of the profile parameters are the following: amplitude parameters which take into consideration the prominences and gaps, amplitude parameters which consider the average ordinate, pitch parameters and hybrid parameters. Each of these parameters could be useful for a certain destination of the machined surface.

When the glass workpieces are sandblasted or engraved by means of the abrasive jet, a certain roughness will characterize the obtained surface and some parts properties (transparency, friction coefficient etc.) will depend on the surfaces roughness; for this reason, it is important to know which is the influence exerted by various factors on the roughness parameters of to the surfaces machined by means of the abrasive jet.

Initially, the abrasive particles directed to the workpiece surface have a kinetic energy W_i :

$$W = \frac{m_p v_i^2}{2}, \quad (1)$$

where m_p is the abrasive particle mass and v_i – the initial speed of the abrasive particle, before the impact.

During the impact of the abrasive particle with the workpiece surface layer, a part of their kinetic energy is transferred to this layer, and transformed in other types of energy. After the impact, the abrasive particle may continue its motion, but with a diminished speed v_f . The difference ΔW between the initial kinetic energy and the kinetic energy of the abrasive particle after impact represents the energy which contributed to the development of some specific phenomena in the workpiece surface layer:

$$\Delta W = \frac{m_p (v_i - v_f)^2}{2}, \quad (2)$$

v_f being the final speed of the abrasive particle.

Generally, as consequence of the abrasive particle impact with the workpiece surface layer, effects of elastic deformation, plastic deformation, microcracking and microcutting could be highlighted.

The abrasive particle must develop a local pressure higher than the workpiece material strength, to generate permanent deformations, microcracks and microchips.

Due to the high brittleness of the glass, it is expected that the material removal and the changing of the blasted surfaces aspect in comparison with the initial one develop especially as result of the microcracking (fig. 1); if some close microcracks join or the pressure exerted by the abrasive particles is high enough, small particles from the glass workpiece could be removed. The machined surface

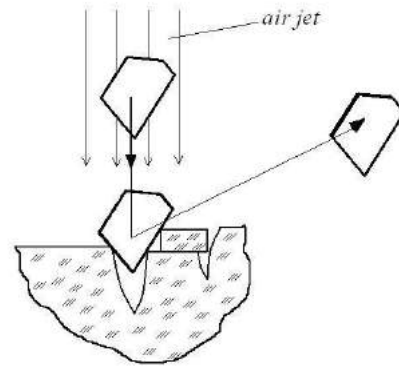


Fig. 1. Phenomena of microcracking and material detaching as result of the engraving process

could be considered as a concatenation of the microcavities resulted by material detaching or of deformed small zones; at the same time, this surface is the result of the statistic distribution of the impact phenomena on the workpiece surface.

3. EXPERIMENTAL RESEARCH

In order to verify the validity of the above mentioned hypotheses and to obtain more information concerning the influence exerted by various factors on the roughness of the surface affected by the action of the abrasive jet, some experimental research were designed and developed.

With this aim in view, a common blasting gun (type 650R, Prodif Air comprimé - France) was connected by adequate tubes to a usual compressor ($p=0.588$ MPa) and to the recipient containing the abrasive particles (sand). In order to determine empirical models able to highlight the influence of some operating parameters on the sizes of the surface roughness parameters, a factorial experiment with three variables at two levels was designed and materialized.

A schematical representation of the sandblasting

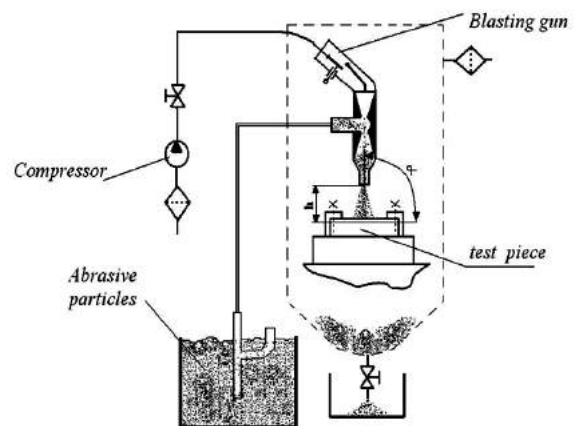


Fig. 2. Schematic representation of the equipment for abrasive jet engraving

equipment is included in figure 2. Essentially, the sand is absorbed from a recipient by the depression generated in the blasting gun by the circulation of the compressed air. The abrasive particles are directed to the workpiece surface by means of a nozzle. After their impact with the workpiece surface, the abrasive particles arrive in a conical zone of the sandblasting precinct, from which they could be periodically removed.

The average size g of the abrasive particles, the distance h between the nozzle of the sandblasting gun and the flat surface of the workpiece, and the angle α of inclination between the abrasive jet axis and the workpiece flat surface were considered as independent variables. The sizes of the surface roughness parameters were measured by means of a surface roughness meter type Mitutoyo, which allowed the measurement of arithmetic mean deviation of the profile Ra , maximum height of the profile Ry (determined as sum of height Yp of the highest peak from the mean line and depth Yv of the deepest valley from the mean line), ten-point height of irregularities Rz and root-mean-square deviation of the profile Rq . The sizes of the parameters which define the experimental conditions and the experimental results were inscribed in table 1. In the columns 2, 3 and 4 of the table 1, the sizes of the input parameters corresponding to each experiment were included; three sizes of each surface roughness used parameter (Ra , Ry , Rz , Rq) were measured. In distinct columns, the average sizes of the surface roughness parameters were mentioned.

The experimental results were mathematically processed

by means of software based on the method of the last squares [6] and taking into consideration only the average dimensions of the sizes corresponding to each surface roughness parameter. The software allowed establishing the most adequate mathematical relation for the determined experimental data, on the basis of the Gauss's criterion. However, accepting the hypothesis that the considered factors (the average dimension g of the abrasive particles, the distance h and the inclination angle α) exert a monotonous influence (without maximum and minimum points) on the output factors, functions type power were preferred, because these functions offer a direct image on the significance of the influence exerted by each considered factor.

In the above mentioned conditions, the following empirical models were determined:

$$Ra = 3.554g^{0.392}h^{-0.00473}\alpha^{0.124} \quad (3)$$

$$Ry = 30.884g^{0.309}h^{0.00217}\alpha^{-0.0559} \quad (4)$$

$$Rz = 21.927g^{0.334}h^{-0.00809}\alpha^{0.0939} \quad (5)$$

$$Rq = 4.459g^{0.390}h^{-0.00498}\alpha^{0.120} \quad (6)$$

By examining the empirical models, one may notice that the most important influence exerted on the studied surface roughness parameters corresponds to the average dimension g of the abrasive particles, because the exponents attached to this size have the highest sizes in the empirical models. The second factor able to influence

Table 1. Experimental conditions and results

Exp. no.	Input parameters			Surface roughness parameter Ra , μm				Surface roughness parameter Ry , μm			
	g , mm	h , mm	α , degrees	Ra_1	Ra_2	Ra_3	Average value for Ra , μm	Ry_1	Ry_2	Ry_3	Average value for Ry , μm
1	2	3	4	5	6	7	8	9	10	11	12
1	0.35	10	15	3.37	3.93	3.71	3.67	27.05	31.79	28.52	29.120
2	0.35	10	90	4.48	3.83	3.98	4.10	37.87	29.7	29.67	32.413
3	0.35	40	15	2.94	2.91	3	2.95	21.18	27.05	24.54	24.257
4	0.35	40	90	4.2	4.05	3.61	3.95	23.7	24.9	22.43	23.677
5	1.6	10	15	5.59	7.17	4.54	5.77	33.55	44.91	37.87	38.777
6	1.6	10	90	5.81	7.53	7.62	6.99	40.03	40.6	38.04	39.557
7	1.6	40	15	5.86	6.14	5	5.67	38.96	51.99	30.95	40.633
8	1.6	40	90	6.59	8.96	8.44	8.00	55.24	55.45	56.87	55.853
Exp. no.	Input parameters			Surface roughness parameter Rz , μm				Surface roughness parameter Rq , μm			
	g , mm	h , mm	α , grade	Rz_1	Rz_2	Rz_3	Average value for Rz , μm	Rq_1	Rq_2	Rq_3	Average value for Rq , μm
1				21.06	22.42	22.92	22.13	4.31	4.79	4.74	4.61
2	0.35	10	15	24.64	23.42	24.2	24.09	5.44	4.86	4.96	5.09
3	0.35	10	90	17.68	18.73	17.62	18.01	3.68	3.68	3.74	3.70
4	0.35	40	15	20.99	22.5	18.82	20.77	5.05	4.9	4.31	4.75
5	0.35	40	90	29.6	36.32	25.61	30.51	6.82	8.55	5.6	6.99
6	1.6	10	15	36.41	37.96	35.43	36.60	7.94	9.26	9.14	8.78
7	1.6	10	90	31.89	33.74	24.56	30.06	7.28	7.79	5.98	7.02
8	1.6	40	15	40.21	43.32	42.98	42.17	8.54	10.62	10.27	9.81

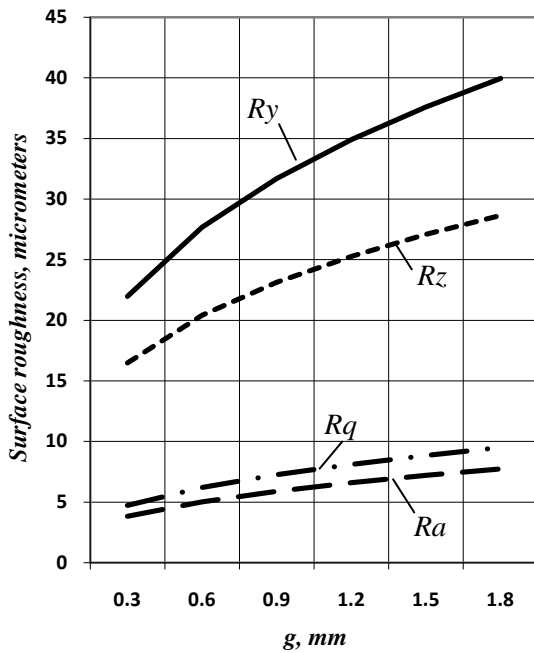


Fig. 3. Influence exerted by the average dimension of the abrasive particles on the sizes of the surface roughness parameters

the surface roughness parameters is the angle α of inclination between the axis of the abrasive jet and the flat surface of the workpiece, but this influence is significant only in the cases of the parameters Ra and Rq . For the other situations, the sizes of the exponents are very low and this fact shows that the considered parameters practically do not exert influence on the surface roughness parameters; this is the situation of the angle α in the case of roughness parameters Ry and Rz and of the distance h for all four considered surface roughness parameters.

The graphical representation from figure 3 shows the influence exerted by the average dimension g on the surface roughness parameters Ra , Ry , Rz and Rq , on taking into consideration the empirical relations (3), (4), (5) and (6).

To better highlight the change of the surface profile as consequence of the sandblasting process, the profilogram from the figure 4 can be used; in this profilogram, the left zone correspond to the blasted surface, while the right zone represents the surface which was not affected by the blasting process.

4. CONCLUSIONS

The study of glass parts sandblasting could highlight either the resistance of the glass parts at erosion process or the change of the optical properties of these parts. Essentially, during the process of glass sandblasting, the material removing develops as consequence of microcracking phenomena. The roughness of the surfaces affected by sandblasting process depends essentially on the abrasive particles and workpiece material properties, on the operating parameters, on the parameters which characterize the compressed air circulation. Some theoretical considerations were formulated about the

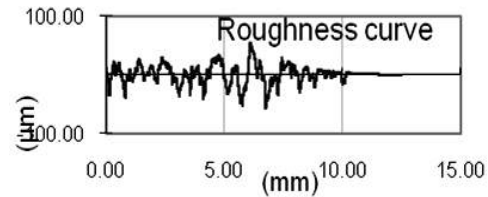


Fig. 4. Roughness profile for the initial surface (right) and the sandblasted surface (left) of the glass part

developing of the glass sandblasting process. A factorial experiment with three variables at two levels allowed the establishing of some empirical relations type power which show the influence exerted by the average dimension of the abrasive particles, the distance between the nozzle of the sandblasting gun and the flat surface of the test piece and by the angle of inclination between the abrasive jet axis and the same flat surface of the workpiece on the surface roughness parameters Ra , Rz , Ry and Rq . In the future, there is the intention to extend the investigation of the influence exerted also by other factors on the parts surface layers properties as result of applying the sandblasting process.

REFERENCES

- [1] CAN, A., KANTÜRER, T. (2010) *Theoretical and experimental study for the drying process of glass colour according to mass transfer laws*, Strojarsstvo, Vol. 52, No. 5, pp 501-506
- [2] ADJOUADI, N., LAOUAR, N., BOUSBAA, C., BOUAOUADJA, N., FANTOZZI, G. (2007) *Study of light scattering on a soda lime glass eroded by sandblasting*, Journal of the European Ceramic Society, Vol. 27, No. 10, pp 3221-3229
- [3] ISMAIL, J., JAIRI, F., NAIT-ABDELAZIZ, M., BOUZID, S., AZARI, Z. (2011) *Experimental and numerical investigations on erosion damage in glass by impact of small-sized particles*, Wear, in press, accepted manuscript, available at http://www.sciencedirect.com/science?_ob=MIimg&_imagekey=B6V5B-52HJNWX-4-1&_cdi=5782&_user=5286814&_pii=S0043164811001840&_origin=search&_zone=rslt_list_item&_coverDate=04%2F01%2F2011&_sk=999999999&wchp=dGLzVtb-zSkzS&md5=52edf632e2ccaf836836bca93c077bee&ie=/sdarticle.pdf, accessed at 3.05.2011
- [4] DODUN, O. (2001) *Nonconventional technologies. Machining with materialized tools* (in Romanian), Chișinău, Publishing House Tehnica Info
- [5] RADOVANOVIC, M., MANIC, M., MARINKOVIC, V. (2007) *Cutting speed prediction by abrasive waterjet of stainless steel*. Optimum technologies, technologic systems and materials in the machines building field. TSTM-13, No. 1, Bacău, pp. 6-11
- [6] CREȚU, G. (1992) *Fundamentals of the experimental research. Handbook for laboratory activities* (in Romanian), Polytechnic Institute of Iași, Romania



THE RESEARCH OF DISCHARGE ENERGY IN EDM PROCESS

Marin GOSTIMIROVIC, Pavel KOVAC, Milenko SEKULIC, Borislav SAVKOVIC

Department of Production Engineering, Faculty of Technical Science, University of Novi Sad, Trg D. Obradovica 6,
21000 Novi Sad, Serbia

maring@uns.ac.rs, pkovac@uns.ac.rs, milenkos@uns.ac.rs, savkovic@uns.ac.rs

Abstract: In electrical discharge machining (EDM) material is removed through periodical electrical discharges between the tool and workpiece. The electrical discharge energy which in the discharge zone is transformed into heat is of key importance in EDM process. Characteristics of discharge energy define the technological performances of EDM. Therefore, principle of EDM and characteristics of discharge energy parameters are analyzed in this paper. In addition, thermal properties of discharge energy were experimentally investigated and their influence on material removal rate, gap distance and surface roughness. The experiments were conducted on manganese-vanadium tool steel using copper tool electrode. Researches conducted in this paper allow efficient identification of relevant discharge energy parameters for the selection of optimal EDM machining conditions.

Key words: EDM, discharge energy, material removal rate, gap distance, surface roughness

1. INTRODUCTION

Electrical Discharge Machining (EDM) is one of the most important non-conventional machining processes. It is primarily used for machining difficult-to-machine materials and complex geometry parts for which **traditional** techniques are not applicable. **Moreover, this** process is only available for machining metals (hardened alloy steel, high speed steel, cemented carbide) and materials that offer a minimum electrical conductivity.

In EDM, material is removed through periodical electrical discharges between the tool and workpiece [1]. EDM requires the tool and workpiece to be submerged in a liquid dielectric at a small distance, and they are connected through an electronic switch to a DC power source. Upon establishing the voltage, a strong magnetic field is established between the tool and workpiece. Due to attractive force of the magnetic field, at the shortest local distance between the tool and workpiece there is a build-up of particles from the machining process which float in the dielectric fluid. This forms the plasma channel and the electrons begin to move towards the positively charged electrode. On their way, the accelerated electrons collide with the neutral particles from the machining process and the dielectric liquid. There is a chain reaction in which a large number of negative and positive ions are generated. The ionization initiates creation of electro-conductive zone between the workpiece and tool, thus causing electrical discharge.

Disruption of current supply annihilates the discharge zone, causing abrupt cooling which results in an explosive flushing of melted matter and solid particles off the workpiece surface. A series of discharges results in a number of small craters which increase surface roughness.

Between the periodical discharges there is a deionization of dielectric liquid and the products of machining are evacuated from the work zone. This process provides stability of pulse discharge by preventing the continuous current flow and generation of electric arc or a short circuit. Shown in Fig. 1 is principle of EDM process, input parameters (workpiece, tool, machine and dielectric) and output technological performances (material removal rate, machining accuracy and surface integrity).

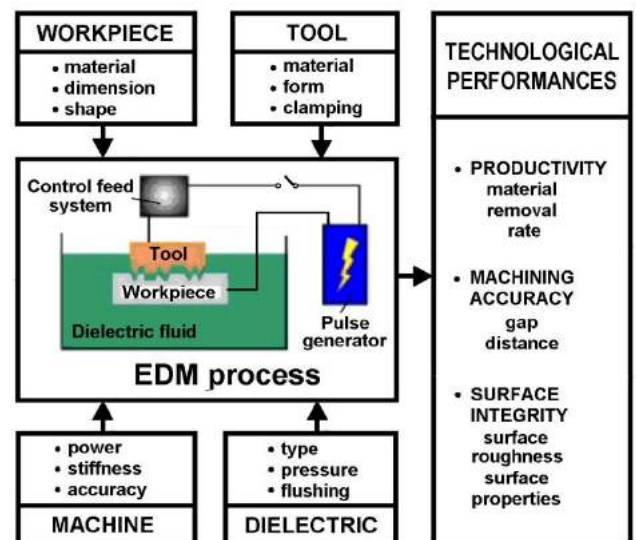


Fig.1. Electrical Discharge Machining

Based on the previously mentioned, efficiency of EDM directly depends on the discharge energy which is transformed into heat in the machining zone [2]. The

generated thermal energy leads to high temperatures which result in local melting and evaporation of workpiece material. However, the high temperature also impacts various physical and chemical properties of tool and workpiece. This is why research of discharge energy is of key importance in EDM process.

2. DISCHARGE ENERGY

The discharge energy is the mean value of electric parameter which is transformed into heat during discharge, and can be expressed by a following equation:

$$E_e = \int_0^{t_e} u_e(t) \cdot i_e(t) \cdot dt \cong U_e \cdot I_e \cdot t_e \quad (1)$$

where U_e is the discharge voltage, I_e is the discharge current and t_e is the discharge duration.

As can be seen from Eq. (1), the discharge energy is directly influenced by the characteristics of electric pulses. Their influences are interconnected and depend on the rest of the machining parameters [3].

The discharge voltage depends on the paired electrode materials and machining conditions. It ranges between 15 and 30 V. It can be indirectly influenced by the choice of tool material. Inherent to the tool material are thermal properties and the speed of deionization of machining are, so that for every tool/workpiece material combination there is a corresponding discharge voltage. Practically all kinds of electro-conductive materials can be used for tools. Generally, most popular are materials with low electrical resistivity and high melting point, among which are copper, graphite, wolfram, and their alloys.

The discharge current directly impacts the discharge energy. However, the impact of discharge current is limited by the tool surface area which is interfacing the workpiece, i.e. the current density. In case when the current density oversteps the limit for the given machining conditions (approximately 10 A/cm²), the removed material per unit area is such that it cannot be efficiently evacuated by circulation of dielectric liquid. This deteriorates the process of deionization of machining are, thus reducing the efficiency of EDM.

The discharge duration is another parameter which allows direct control of discharge energy. However, here too the independent regulation of process parameters is limited. It is known from experience that discharge duration must be limited for a particular discharge current. Otherwise, a DC arcing occurs which damages the surfaces of tool and workpiece.

The material removal process in EDM is associated with the erosive effects which occur as a result of an extremely high temperature due to the high intensity of discharge energy through the plasma channel, Fig. 2. The material removal rate and the surface integrity correspond to the adjusted crater profile that is defined by a through the radius. For that reason, the material removal models were mainly based on the electro-thermal mechanism.

Therefore, several simplifying assumptions are used for the modeling of the material removal EDM process [4]. The material of the workpiece is homogeneous and isotropic. Flushing efficiency is considered to be ideal. The molten of the workpiece material in the discharge zone is removed completely. Only one crater occurs per electrical discharge. The crater radius is assumed to be a function of discharge energy.

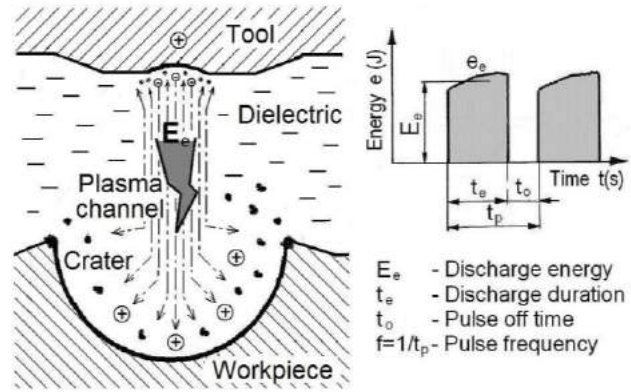


Fig.2. Model of material removal process in EDM

Based on the previous discussion, now it can be logically assumed that the material removed volume of a single electric pulse would be proportional to the discharge energy:

$$V_e = C_V \cdot E_e \quad (2)$$

where C_V is the constant that depends on the workpiece material.

The material removal rate represents the average volume of material removed over the machining time. By using Eq. (2), as well as Eq. (1), there follows the expression for material removal rate:

$$V_w = V_e \cdot f = \frac{V_e}{t_e + t_o} = C_V \cdot U_e \cdot I_e \frac{t_e}{t_e + t_o} \quad (3)$$

where f is the pulse frequency and t_o is the pulse off time. On the other hand, the material removal in a single pulse discharge is determined by computing the volume of the crater supposed to be hemispherical with a radius equal to R_{max} :

$$V_e = \frac{2}{3} \pi \cdot R_{max}^3 \quad (4)$$

In Eq (4), R_{max} is defined as the maximum surface roughness observed over maximum height of irregularities.

From the Eq. (4) also using Eq. (2) and (1), one derives expression for maximum height of irregularities:

$$R_{max} = \left(\frac{3}{2\pi} C_V \cdot U_e \cdot I_e \cdot t_e \right)^{1/3} \quad (5)$$

In practical, the surface quality is defined over the surface roughness R_a . The surface roughness is defined as the

arithmetic average deviation of the assessed profile (ISO 4287), and it is given as:

$$R_a \cong \frac{1}{4} R_{\max} \quad (6)$$

Theoretical, dependence of the gap distance on the discharge energy is given by equation:

$$a_e = C_a \cdot E_e^m \quad (7)$$

where C_a and m are the constants that depend on the machining conditions.

3. EXPERIMENTAL PROCEDURES

Experimental investigation was conducted on EDM machine tool "FUMEC – CNC 21" of South Korea ($I_e=0\div 100$ A, $t_e=0\div 1000$ μ s and $t_o=0\div 100$ μ s). The material used in the experiment was manganese-vanadium tool steel, DIN 90MnV8 (0,9% C, 2% Mn, and 0,2% V), hardness 62 HRC. The tool was made of electrolytic copper with 99,9 % purity, 20×10 mm cross-section. The dielectric was petroleum. Due to small eroding surface and depth, natural flushing was used.

The machining conditions included variable discharge current and discharge duration. The rest of the parameters

were held constant, according to manufacturer's recommendations.

The experiments were conducted according to the specified experiment plan. Input parameters were varied and the resulting machining parameters of EDM process were monitored and recorded. Measured parameters were material removal rate V_w , gap distance a , and surface roughness R_a .

Material removal rate (ratio of removed material volume and the effective machining time) was measured indirectly, by monitoring the machining time for the set eroding depth. The depth and time of eroding were monitored using the machine tool CNC control unit. Gap distance was calculated as the half of difference between the tool and workpiece contour dimensions. Measurements were conducted using electronic callipers (precision: 0,001 mm). Surface integrity was assessed by measuring surface roughness and research of the surface layer properties. "PERTHOMETER S5P" of Mahr, Germany was used to measure the surface roughness.

4. RESULTS AND ANALYSIS

Table 1 shows the results of experimental investigation for the selected machining conditions. For various discharge currents and discharge durations, following process parameters are shown: material removal rate, gap distance and surface roughness.

Table 1. The results of experimental investigation

Level	Machining conditions		Machining state	Technological performances of EDM		
	Discharge current	Discharge duration	Discharge energy	Material removal rate	Gap distance	Surface roughness
	I_e (A)	t_e (μ s)	E_e (μ J)	V_w (mm ³ /min)	a (mm)	R_a (μ m)
Low	5	1	100	3,22	0,09	3,9
		2	200	4,16	0,095	4,2
		5	500	6,47	0,10	5,1
		7	700	4,31	0,105	5,1
Middle	20	5	2000	24,49	0,20	10,2
		7	2800	31,82	0,22	10,4
		10	4000	26,70	0,23	10,8
		20	8000	17,11	0,24	11,2
High	50	10	10000	46,36	0,28	11,8
		20	20000	66,83	0,30	12,5
		50	50000	72,92	0,31	13,2
		100	100000	60,60	0,33	13,4

Figure 3 shows the influence of discharge energy on the material removal rate. Shown are comparative results for low, medium, and high discharge current, for copper tool electrode. The diagram shows that the increase of discharge current results in increased discharge energy, which ultimately leads to higher material removal rate. However, for every discharge current there is an optimal value of discharge energy which results in maximum material removal rate. This efficiently precludes us from unambiguous determination of the influence of discharge energy on

material removal rate. The analytical considerations presented in this paper confirm that the increase of discharge current increases the material removal rate (Eq. 3), and optimal influence of discharge durations on material removal rate. In real conditions, lengthy pulses cause enormous concentration of removed material, as well as the increase of gas bubbles in the machining area. Due to impaired evacuation of machining products, a portion of the discharge energy is spent on re-melting and evaporation of solidified metal particles. The remaining, larger, portion of

discharge energy takes place in a gaseous environment, thus being lost irreversibly. Such impaired process stability affects the EDM productivity.

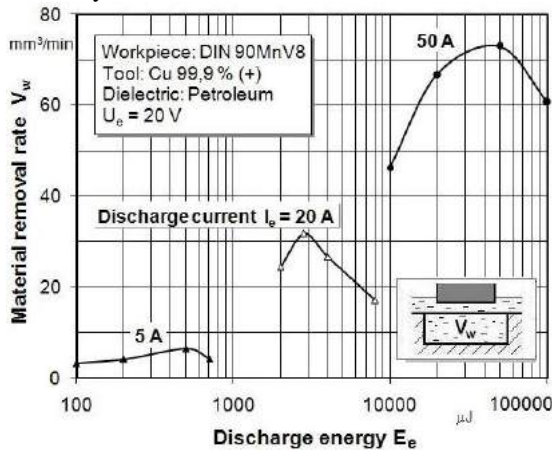


Fig. 3. Dependence of the material removal rate on the discharge energy

Shown in Fig. 4 is the dependence of gap distance on the discharge energy. Somewhat, the increases of discharge current and discharge duration values results in a uniform increase of gap distance. It is evident that the gap distance follows the discharge energy in order to maintain stability of EDM. Otherwise, the deionization of machining are would be affected, which could result in lower productivity. The experimental results confirm the analytical assumptions.

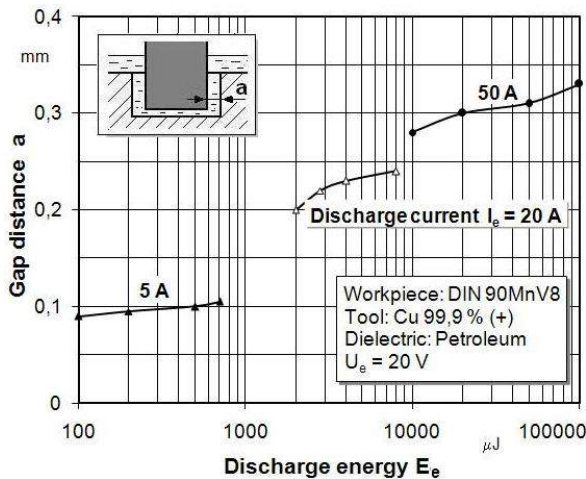


Fig. 4. Dependence of the gap distance on the discharge energy

The relationship between the surface roughness and discharge energy, for various parameters of discharge energy, is shown in Fig. 5. As the discharge energy increases, so do the heat concentration and workpiece surface temperature, which results in larger craters, i.e. greater surface roughness. Moreover, is a slight increase of surface roughness with the discharge duration, while the discharge current has a more pronounced influence on the surface roughness. The machined surface consists of a number of craters of various dimensions, while the roughness is even in all directions.

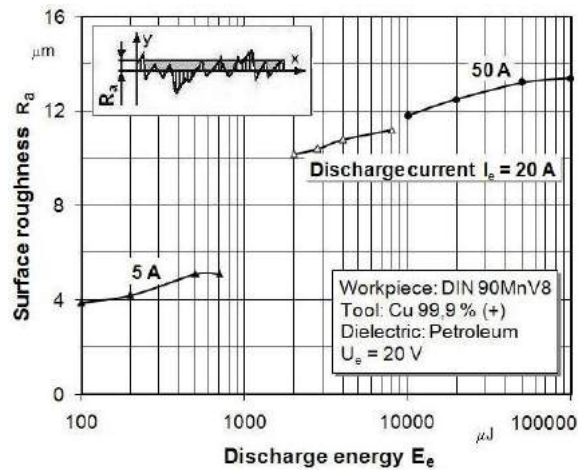


Fig. 5. Dependence of the surface roughness on the discharge energy

5. CONCLUSION

The discharge energy is the most important parameter of EDM process. The discharge energy directly depends on the discharge current and the discharge duration. Characteristics of the discharge energy define the technological performances of EDM.

The results of experimental investigation show that, there is an optimal discharge energy which yields maximum material removal rate. The material removal rate increases with the increase of discharge current for an optimal discharge duration. The discharge energy causes uniform increase of gap distance. When the discharge energy is increased the gap distance exerts greater influence on accuracy of EDM. Surface roughness directly depends on the discharge energy. Moreover, the discharge current is more significant than the discharge duration.

REFERENCES

- [1] KONIG, W. (1979) *Fertigungsverfahren, Band 3 Abtragen*, VDI-Verlag GmbH, Dusseldorf
- [2] LIN, Y.C., HWANG, L.R., CHENG, C.H., SU, P.L. (2008) *Effects of electrical discharge energy on machining performance and bending strength of cemented tungsten carbides*, J Mater Process Technol., Vol. 206, pp. 491-499
- [3] WONG, Y.S., RAHMAN, M., LIM, H.S., HAN, H., RAVI, N. (2003) *Investigation of micro-EDM material removal characteristics using single RC-pulse discharges*, J Mater Process Technol., Vol. 140, pp. 303-307
- [4] SINGH, A., GHOSH, A. (1999) *Thermo-electric model of material removal during electric discharge machining*, Int J Mach Tool Manu., Vol. 39, pp. 669-682



THE EFFECTS OF SHOT PEENING ON THE FATIGUE LIFE OF MACHINE ELEMENTS

Dragan ADAMOVIĆ, Milentije STEFANOVIĆ, Branislav JEREMIĆ, Srbslav ALEKSANDROVIĆ
Faculty of Mechanical Engineering in Kragujevac, S. Janjic 6, 34000 Kragujevac, Serbia
adam@kg.ac.rs, stefan@kg.ac.rs, bane@kg.ac.rs, srba@kg.ac.rs

Abstract: For increasing the resistance to fatigue and wear, different methods for improvement of contact layers properties are used. First of all, the improvement of properties is realized by heat treatment (induction and flame hardening), chemical-heat treatment (carburizing and nitriding) and plastic surface forming (surface forming by rolls, disks and balls, as well as shot-peening). The paper gives detailed explanation of the shot peening procedure, which involves the ejection of shots at high speed onto the forming object. The intensity of impact is the function of the kinetic energy and angle at which the shot hits the forming object. Thereat, smaller or larger increase of hardness occurs on surface layers, remaining stresses are made, surface topography is changed, and, in some cases, the structural changes are possible (disintegration of remaining austenite). This all leads to increase of fatigue life of elements subjected to shot-peening. The influence of specified effects on the increase of fatigue life depends on strength of material subjected to shot-peening but also on conditions at which the shot-peening process is performed. This paper will present the influence of shot peening on the increase of fatigue life of different parts.

Key words: Shot Peening, Fatigue Life, Machine Elements

1. INTRODUCTION

The shot-peening process involves the ejection of shots at high speed onto the forming object. Each shot which hits the object seems like the blow of a tiny hammer. The intensity of impact is the function of the kinetic energy and angle at which the shot hits the forming object. Thereat, smaller or larger increase of hardness occurs on surface layers, residual stresses are made, surface topography is changed, and, in some cases, the structural changes are possible (disintegration of residual austenite). This all leads to increase of dynamic strength of elements subjected to shot-peening. The influence of specified effects on the increase of dynamic strength depends on strength of material subjected to shot-peening, but also on conditions at which the shot-peening process is performed.

Unlike shot blasting, which is used for cleaning surface of parts by tiny sand particles, shoot-peening is used for strengthening part surface. It is performed with small hard balls, which can be made of steel, cast iron, glass or ceramics.

2. THE INFLUENCE OF SHOT-PEENING EFFECTS ON DYNAMIC STRENGTH

It is well known that forming by spray of balls can improve fatigue of metal materials. That improvement is reflected in one of the two possible ways: increase of stress for constant life or increase of life for constant stress, as shown in figure 1 [1]. However, it is also possible to reduce part mass for the same loading and life,

which can be extremely important, especially in airline, car and military industry.

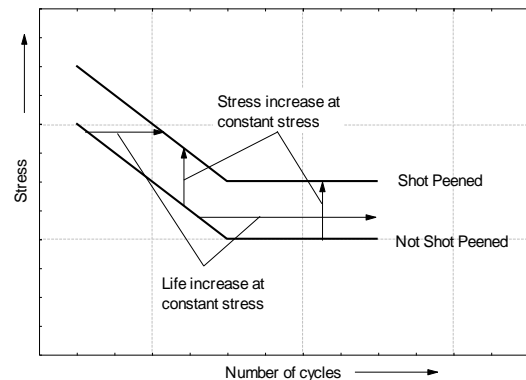


Fig.1. Influence of shot peening on material fatigue behavior

Hardening by shot peening can be done by variation of many parameters, enumerated in the first column in Figure 2, [2], which represents conditions in which the peening process is done.

The shot stream affects the condition of surface layers or the working piece. In certain cases the following changes can occur:

- breaking or removing of the protective layers, e.g., oxide layers,
- change of the surface topography ΔR_t ,
- hardening or softening of surface layers, represented as changes in hardness ΔHV ,
- changes of the residual stresses $\Delta \sigma^{RS}$ in layers close to the surface, due to creation of certain distribution

- of residual stresses in surface layer of relatively small thickness,
- phase transformations in layers close to the surface, e.g., transformation of the retained austenite ΔRA in quenched steels,

- formation of cracks in the case of the machining by the shot stream of high intensity.
- Intensity of changes of various characteristic parameters of material status depends also on initial values of these parameters before the shot peening, what is shown in the second column of Figure 2 by short symbols.

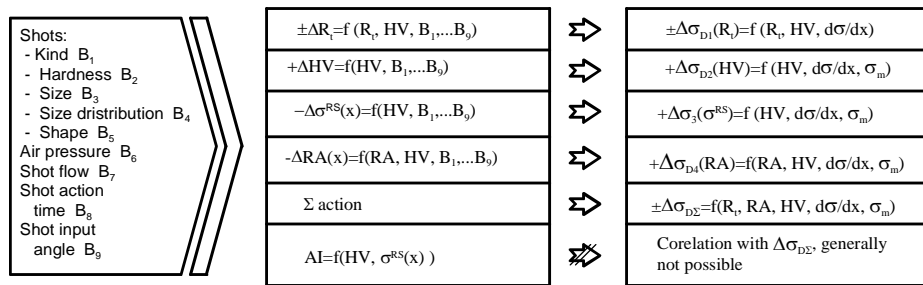


Fig.2. Mutual influence of shot peening conditions and fatigue strength

Each change of the surface conditions reflects, in some way, on fatigue behavior, for instance, the fatigue strength. In that the magnitude of influential parameters effect is different, depending on type and status of material, as well as on type of fatigue straining. These influences are shown in the last column of Figure 2. Under the simplified assumption that changes of fatigue strength, due to individual influences of different factor, superimpose cumulatively, the total status can be represented by the following equation:

$$\pm \Delta \sigma_{D,\Sigma} = -\Delta \sigma_{D,1}(+\Delta Rt) + \Delta \sigma_{D,2}(+\Delta HV) + \Delta \sigma_{D,3}(-\sigma^{ZN}) + \Delta \sigma_{D,4}(-\Delta RA) \quad (1)$$

Now it is quite clear how the very complicated dependence of the fatigue strength increase due to multiple possible influences arises. Optimal conditions of shot peening, depending on type and status of material, shapes and size of element (part), as well as on type of stress, can be very different.

3. APPLICATION AND BASIC CRITERIA FOR APPLYING THE SHOT-PEENING PROCEDURE

The shot-peening procedure is widely applied for parts strengthening (dynamically loaded parts in car, airline and military industry). Shot-peening is performed on steel and non-ferrous metal parts. The percentage of increase of dynamic strength, i.e. fatigue life, can be various and depends on type of material, shot-peening conditions and machine part shape. The literature [3,4] includes a lot of data which indicate the effects of various parts strengthening. In figure 3, according to [4], the percentage of dynamic strength increase for different parts groups is shown. The increase is the largest for spring elements. Compression coil springs are, most probably, the parts which are most often subjected to shot-peening. They are used not only in car industry, but also in other industry sectors; therefore, the annual production coil springs amounts to hundreds of millions. Coil springs should always be subjected to shot-peening from both the outer and inner side, because the largest fatigue life is obtained only in such a case [5]. In the course of shot-peening of springs, particular attention is given to the selection of

shot-peening intensity, because too intense shot-peening can cause the change of static properties of the spring [6].

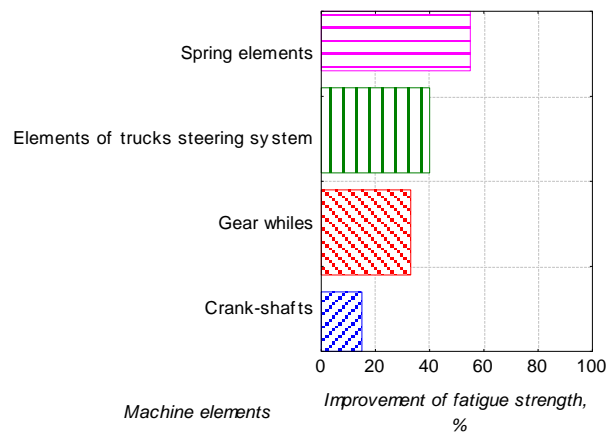


Fig.3. Increase in fatigue life of some machine elements as a result of shot peening [4]

For parts loaded only with direct variable loading, with the aim of increasing lifetime in relation to conventional shot peening, stress-peening, i.e. strain-peening is applied. This means that the part is shot in strained state, which provides higher compressive residual stress in relation to stresses obtained by normal shot-peening. Compression coil springs are very convenient for strain-peening. According to [5], if springs subjected to strain-peening are applied, it is possible to save about 25 kg of an airplane mass, which is not to be neglected in airline industry.

The initial material for manufacture of coil springs is hot rolled, drawn, peeled or abraded steel. Each of the surfaces obtained in such a way, especially on rolled material, has small errors (caused by rolling), boundary decarburisation and certain roughness. Anomalies in structure, caused by melting (segregation) and non-metal inclusions should also be taken into consideration. If located near surface, these anomalies can have negative effects on fatigue behaviour of springs. In such cases, shot-peening increases fatigue life for 30 - 180% [7]. Leaf springs, if loaded by one-sides bending, are subjected to shot-peening only from one side. If, in the course of performance, the spring is two-sidedly bent, shot-peening is performed on both sides.

One of the main causes of significant reduction of leaf and spiral steel springs life is the presence of decarburised surface layer, formed in the course of technological manufacture procedure. It was established that surface decarburisation leads to significant reduction of resistance to fatigue, due to both smaller strength of surface layer and the creation of tensile residual stresses in decarburised layer [8].

The procedure of strengthening by shot-peening is also often used for shafts and axes. Shot-peening is performed either on the entire surface or only on locations of grooves for the pins and transition radii. There are many papers [4,5] which indicate the significant increase of fatigue life of shafts and axes, caused by shot-peening.

Gears are the machine elements which are, also, often subjected to shot-peening. It has been determined that the procedure of shot-peening leads to formation of surface topography which enables creation of tiny oil tanks [5], which provides better lubrication and decrease of working temperature in the course of performance. Shot-peening of gears with low manufacture tolerance can lead to intrusion during the performance. In such cases, shot-peening is performed only in the area of tooth root, while gear tooth sides are protected.

Gears are also often subjected to shot-peening after cementation. Fatigue life of cemented gear, at maximal stress of 560 MPa, was increased from 270000 to 3 millions of cycles, after shot-peening [5]. It is recommended to use balls of increased hardness for that procedure, because they provide higher values of compressive residual stresses.

Heat zones made by welding are always under tensile stresses which reduce fatigue life of welded joints. The shot-peening procedure leads to creation of compressive stresses in surface layer and increase of fatigue life of welded joints.

Electrolytic coatings of soft metals, such as cadmium, lead, tin and zinc have minor influence on dynamic strength, unlike coatings of hard metals (nickel or chrome). Reduction of dynamic strength, in the course of coating by chrome and nickel, is the result of creation of tensile stresses in the surface layer. If a small crack appears in the coating, it continues to spread into the basic material. If the basic metal surface was subjected to shot-peening before coating procedure, the compressive residual stresses which arise prevent spreading of cracks in the coating.

The paper [9] has shown that shot-peening after chrome and nickel coating leads to increase of fatigue resistance. Coatings adhere much better to surface subjected to shot-peening than to abraded surface.

Shot-peening can also be performed only on one part of some machine element surface. Untreated surface is usually protected (masked) by stripes of good adhesion properties which are sufficiently elastic to absorb shots impacts. Masking is most often performed on points where dimensional accuracy and smooth surface are needed. This procedure is often used on crankshafts, where only radius is subjected to shot-peening, while sleeves for slide bearings are protected. One should bear in mind that masking increases the costs of machine element manufacture. That is why it is used only when it is necessary.

On materials such as stainless steel, manganese steel, stellites, nickel alloys etc., significantly higher hardness of surface layer is obtained by shot-peening procedure [5]. This is very important for parts which cannot be thermally treated, and which are required to have high resistance to surface wear.

In the course of shot-peening, it is possible to perform the correction of parts with relatively thin cross section. Such treatment annuls unfavourable tensile residual stresses which lead to machine element bending. According to data provided by Metal Improvement Company [5], it is possible to carry out, successfully, the correction of different parts, such as shafts, pipes, rings, ring gears, piston rods, discs etc.

Shot-peening can also be used for cleaning a metal surface (shot-blasting). Shot-blasting is much better than sandblasting, because during sandblasting, small notches, which represent stress concentrators, are made, which is not the case with shots.

Shot-peening procedure can eliminate the porosity of cast and welded junctions to a large extent. In many cases, shot-peening is much more reliable and economical than vacuum impregnation.

In addition to strengthening dynamically loaded parts, shot-peening procedure is also used for forming large dimension parts (peen-forming). This forming is used, almost exclusively, in airline industry and is based on the same physical foundations as the shot-peening focused on strengthening. Shot-peening intensity should be sufficient for change of macro-geometry of part being subjected to it.

In addition to strengthening parts made of steel, significant increase of dynamic strength is accomplished by using shot-peening on parts made of alloys of aluminium, magnesium, titan, as well as bronze and brass [5].

The endurance of machine elements can be increased by proper selection of materials, rational part construction, suitable technological forming procedures or combination of all those possibilities. Thereat, the main aim is to form the product of the highest quality level and acceptable price.

For parts subjected to variable stresses during the performance, material selection is based on fatigue properties. In practice, they selection is more often performed on the basis of static strength (flow limit and tensile strength). Up to a certain limit, the selection based on tensile hardness represents a satisfactory criterion. However, in some other cases (corrosion fatigue and strength at limited number of cycles) that selection does not give satisfactory results. Certain increase of tensile strength leads to limited increase of dynamic strength, because the material sensitivity to stress concentration and creation of fatigue cracks increases. In those cases, the selection of material should be made based on dynamic strength of the material.

Numerous factors, which can influence the resistance to material fatigue, should already be influenced in the phase of constructing parts, sets, devices etc. In most cases, the appearance of fatigue cracks can be prevented by adequate and optimal selection of the material and development of quality constructions. Such approach provides more possibilities for increasing the dynamic

strength compared with other available procedures. One of the most important tasks is the reduction of stress concentration. For complex shape parts, it is difficult to obtain theoretical solutions, and experimental analysis is often complicated and long. In those cases, it is more useful to rely on the results of fatigue investigations, because in that way the majority of loaded zones can be identified as well as the influence of additional factors (manufacture defects, residual stresses, corrosion and friction). For reduction of stress concentration, it is necessary to avoid sharp shifts of cross section, openings and notches. Sometimes, in order to make the entire construction functional, solutions which lead to dynamic strength reduction are used. In those cases, it is necessary to search for other methods and procedures for increasing dynamic strength.

The technological procedure of manufacture has a considerable influence on dynamic strength of machine elements. Machine forming procedures, in which considerable roughness and tensile compressive stresses are created in the surface layer, lead to significant reduction of parts resistance to fatigue. The increase of resistance to fatigue is accomplished by selection and adequate defining of technological manufacture procedures, especially of parts exposed to dynamic loadings in the course of performance. Some mechanical forming procedures (scraping, milling and grating) do not provide high resistance of parts to fatigue. Dynamic strength of parts is, to a large extent, increased by the grinding procedure, first of all by polishing. The procedures of surface plastic forming of parts can increase resistance to fatigue significantly. The procedure of shot-peening of surface by beam of balls is particularly convenient. Thermal and chemical-thermal surface forming can increase (induction hardening, cementation, nitriding) or reduce (normalisation, annealing, chrome-coating) dynamic strength.

Exploitation conditions, such as working temperature, type of loading and frequency, also have significant influence on fatigue behaviour of machine parts.

Parts of weapons and tools should provide functionality, be of small dimensions and be able to bear very high dynamic loadings. The increase of dynamic strength, i.e. the resistance to fatigue of such parts, cannot be achieved by increasing dimensions, but only by some other solutions and procedures. Procedure of shot-peening of critical points or complete parts offers the needed possibility for realising that increase. To that purpose, it is especially convenient to use, for example, the finite elements method or other ones, even experimentally, in order to carry out the stress analysis of the part, and only after that to perform the shot-peening procedure on points of largest tensile stresses. For a large number of dynamically loaded elements of weapons and tools, the value of limited dynamic strength is important, because those elements change during the exploitation, after particular exploitation period.

The proper selection and preservation of shot-peening parameters values throughout the forming process and improvement of resistance to fatigue life can be multiple. When selecting the procedure of part forming by shot-peening, certain limitations should be born in mind, such as:

- Impossibility to preserve tolerated dimensions after treatment,
- Impossibility to carry out shot-peening on locations with small opening and covered surfaces,
- At too intensive shot-peening of small cross section parts, permanent deformations may occur, which would disrupt part functionality etc.

Due to all this, it is necessary to be well aware of potential consequences, caused by shot-peening procedure and to have particular experience in practical application of this procedure.

4. CONCLUSION

The procedure of shot-peening by steel balls beam represents one of the methods for strengthening dynamically loaded parts by plastic surface forming which is applied on materials such as: steel, regardless of thermal treatment, cast steel and cast iron, copper alloys, aluminium alloys, titan alloys and some other metals. In addition to that, this procedure can also be applied for: cleaning machine elements, previous forming of elements for galvanisation and metallisation, protection against corrosion destruction, stress corrosion, pitting and erosion, sheet metals forming and correction of parts of small cross section.

During the shot-peening performance, quantitative and qualitative changes occur in surface layer. Those changes are: creation of compressive residual stresses in surface layer, change of surface layer hardness, change of surface topography and change of surface layer structure.

ACKNOWLEDGMENT

The part of this research is supported by Ministry of Education and Science, Republic of Serbia, Grant TR32036 .

REFERENCES

- [1]. D. ADAMOVIĆ, et all. (1995) Shot Peening, JTA, Kragujevac (in Serbian)
- [2]. H. WOHLFAHRT (1981) Kugelstrahlen und Dauerschwingverhalten, ICSP1, Paris, p. 675-694.
- [3]. A. NIKU-LARI (1981) Overview on the Shot-Peening process, ICSP1, Paris,
- [4]. A. NAKONIECZNY (1981) The effect of Shot-Peening on the Fatigue life of machine elements, ICSP1, Paris, p. 45-50.
- [5]. Shot-Peening applications, Metal Improvement Company, Inc., Ninth edition, (2005).
- [6]. WEI BAAO, et all. (1987) Effect of Shot-Peening on fatigue behavior of compressive coil springs, Advances in Surface Treatments, volume 3, Pergamon Press, Oxford, p. 215-219.
- [7]. J. CHAMPAIGNE (2001) Shot Peening Overview, Electronics Inc., Mishawaka
- [8]. S. SATO, et all. (1981) The effect of Shot-Peening to decarburized spring steel plate, ICSP1, Paris, p. 303-312.
- [9]. J. O. ALMEN (1951) Fatigue loss and gain by electroplating, Prod. Engineering, No22, p.109



ENERGY BALANCE OF THE PLASMA ARC CUTTING PROCESS

Andjela LAZAREVIC, Miodrag MANIC, Dragoljub LAZAREVIC

Ministry for Infrastructure and Energy, Nemanjina 22-24, Belgrade, Serbia
Faculty of Mechanical Engineering, University of Nis, Aleksandra Medvedeva, Nis, Serbia
andjela.lazarevic@mre.gov.rs, mmanic@masfak.ni.ac.rs, dlazarevic@masfak.ni.ac.rs

Abstract: *Consideration of the Manufacturing Plant's Energy Balance, together with all its processes, represents an important aspect that needs to be controlled and which could contribute to the rational and efficient use of energy.*

In order to determine energy balance of the plasma arc cutting process, each of the power components (power contributions) for cutting process should be calculated or assessed. Distribution of these components depends of the process input parameters, and its consideration is very complex. Taking into consideration different approaches to the calculation or assessment of the power components by various authors, this paper represents generalized and systemized results of the different authors' researches, through combination of experimental and theoretical results.

After determination of the power components, process energy balance was represented, additionally illustrated by experimental research and by thermal imaging of the workpiece by thermo-vision camera, few seconds after cutting process terminated.

This approach to the plasma arc cutting provided better understanding of the Heat Affected Zone, as well as identification of the potential inefficiencies of the plasma cutting process.

Key words: *Plasma Arc Cutting, Energy Balance, Heat Affected Zone, Temperature Fields*

1. INTRODUCTION

Plasma characteristics, available to the human perception, are its heating and light energy. Intensity of heating and light energy depends of the energy quantity used for gas ionization, during plasma formation. Energy used results in releasing internal energy of the atoms and, through the energy balance, influence plasma characteristics, which could have directed and limited impact. Depending of the plasma gas and plasma arc composition at given cutting current, lower or higher energy quantity is distributed at particular plasma arc length.

In order to determine energy balance of the plasma arc cutting process, each of the power components (power contributions) for cutting process should be calculated or assessed. Distribution of these components depends of the process input parameters, and its consideration is very complex. There are different approaches to the calculation or assessment of the power components, however, it usually represents combination of empirical and theoretical considerations, as well as calculation of the power components based on the measured temperatures and other relevant plasma characteristics. The various authors' considerations are represented here by generalization and systematization of their results.

Plasma temperature metering is particularly difficult. Spectroscopic method represents one of the most applicable methods for plasma temperature

determination. Although it is important to know temperatures during plasma cutting, for the practical use and additional shaping of the material, particularly in terms of metallographic structure and hardness changes, it is important to know temperature distribution in the workpiece after cutting process terminated, when the intense source of heating energy was eliminated, providing monitoring of the workpiece cooling during time. This is the reason why after the identification of the power components, energy balance was represented, additionally illustrated by experimental research and by thermal imaging of the workpiece by thermo-vision camera, few seconds after cutting process terminated [1].

2. INTERNAL PLASMA ENERGY

Based on the molecular-kinetic theory, internal energy of the body is higher if the velocity of its particles (composing the body) is higher. The movements in gases comprise of translational and rotational movements of its molecules and inter-molecular vibrations of its atoms. Result of these three types of movements is kinetic energy of molecules and atoms. Additionally there is potential energy, resulting from the forces of attraction acting between molecules. Total internal energy of the body represents sum of the internal thermal energy, internal chemical energy and internal nuclear energy.

Internal thermal energy of plasma comprises of the kinetic energy of chaotic movements of its particles,

representing the sum of internal energy of the ideal gas (u_{ig}) and average energy of the electrostatic interactions between particles (u_e) [2]. Therefore, internal energy is: $u = u_{ig} + u_e$. Internal energy changes in an ideal monatomic gas is $\Delta u = 3/2 R \Delta T$, specific heat capacity at constant volume is $c_v = 3/2 R$, therefore $\Delta u = c_v \Delta T$. For the beginning stage at temperature $T_0 = 0$ K there is zero internal energy u_0 , therefore $u_{ig} = u_0 + c_v T$.

Part of the internal energy of plasma related to the energy of electrostatic interactions between particles (u_e) can be determined from the general electrostatic equations and amounts $u_e = -NE^2/d$, where E is particles charges, N is number of particles of the same kind at the volume V and d Debye length of the penetration of external electrostatic field into plasma. Total plasma energy amounts: $u = u_0 + c_v T - NE^2/d$.

Mutual interactions between plasma particles are changed in accordance with the Coulomb's law. However, it was experimentally determined that average energy of the Coulomb's mutual interactions of particles E^2/r (r is average separation distance between particles) is low comparing to the heating energy of the particles movements, which is proportional to the Boltzmann's constant and absolute temperature. There is an inequation $E^2/r < kT$, which represents the condition of rarefied plasma.

This means that, in order to generate fully ionized plasma, the gas should be heated at the temperature T , so that the average heating energy of the particles movements is equal or higher than its ionization energy (I), that is $kT \geq I$, which at the same time represents the condition of the fully ionized plasma [3].

Since there are different plasma gases, it is important to take into account that ionization potential of molecular gases is always higher than ionization potential of atomic gases. Namely, ionization of the two atomic gases comes after its dissociation therefore there is high quantity of energy in its plasma, proportional to its dissociation and ionization temperature. For example, ionization potential of Hydrogen atom is 13.59 eV, while this energy for Hydrogen molecule is 15.44 eV. Ionization potentials of the valence electrons (I_1) and electrons of other orbits (I_i) differ. For example, Helium ionization potential is $I_1 = 24.58$ eV, while $I_2 = 54.2$ eV.

For double and triple atoms ionization, the energy of around 100 eV should be used, while for full ionization this energy amounts 1,000 eV. If the ionization potential is lower, higher ionization degree X could be reached, at lower temperatures, i.e. lower energy used. For Hydrogen ($I_1 = 13.59$ eV) the highest ionization degree $X \approx 1$ could be reached at temperature of 24,000 K, while for Helium ($I_1 = 24.58$ eV) the highest ionization degree $X \approx 1$ could be reached at temperature of 50,000 K. In order to generate high temperature plasma arc, high ionization degree should be reached [4].

2.1. Basic power components of the plasma cutting process

When plasma jet reaches the workpiece material, ionized gas cools. During cooling, when gas goes back through the field of thermal dissociation, a large amount of heat comes to the workpiece and increases the efficiency of heat transfer [5].

Due to the contact of the high temperature plasma jet and workpiece, different phase transformations of the material occurs, followed by the set of phenomena such as conduction and convective heat transfer, radiation etc.

Workpiece material absorbs heat quantity at the thickness which is typically much less than a millimetre. Part of the plasma jet heat melts workpiece material, coming up with the solid-liquid phase transformation in the area close to the heat source. When material melts, latent heat is absorbed without further temperature increasing. Plasma jet penetrates through the workpiece at constant speed, while high flow plasma gas removes melted material from the kerf. While material cools so called solid-solid phase transformation occurs. Namely, some parts of the material heats at the very high temperature, but lower than material melting temperature, which leads to the formation of one phase (e.g. austenite structure), which could be later changed to some other phase (e.g. perlit or martensite structure) after cooling the material. It is also important to observe that the type of plasma gas influence the phase transformation of the contact surfaces, on its chemical composition and mechanical properties.

Total power of the plasma cutting process (Q_{tot}), taking into account that it comes from the direct electric current passing from electrode (cathode) to the workpiece (anode), is equal to the voltage (U) multiplied by cutting current (I): $Q_{tot} = UI$.

When plasma jet comes out of the nozzle, some losses occur due to the interactions of the free part of the plasma jet and outer atmosphere. Part of the heat flux is lost due to the radiation of the free part of the plasma jet (Q_{rad}), while part is used for the workpiece surface heating ($Q_{surface}$). According to this, when plasma jet comes to the workpiece surface during plasma cutting process, workpiece is already heated at the temperature which can amounts a few hundreds K. Sum of this two power components is denoted as $Q_{lost-up}$ and represents sum as follows: $Q_{lost-up} = Q_{rad} + Q_{surface}$.

In order to make considerations easier, it could be assumed that plasma jet entrance the workpiece through the surface A , which is equal to the surface of the plasma jet, at the part where it entrance the workpiece. Therefore, out of the total power of the process, after losses of the free part of the plasma jet, heat flux Q_{kerf} entrance the workpiece, so that the equation for the total power could be represented as follows: $Q_{tot} = UI = Q_{lost-up} + Q_{kerf}$

Total power available for the plasma cutting now comprises of the available power brought by the plasma arc inside the kerf (Q_{kerf}) and power dissipated by the exothermal oxidation reaction (Q_{oxy}), if plasma gases are oxygen or air (during oxidation certain

amount of energy is released), therefore the following equation could be represented: $Q_{\text{available}} = Q_{\text{kerf}} + Q_{\text{oxy}}$. However, this power available is not equal to the power used for the material melting in the kerf. Namely, only part of the available power is used for material melting (Q_{melt}), while the rest represents heat conduction losses inside the workpiece (Q_{HCL}) or energy losses due to the energy brought by the ejected slag ($Q_{\text{lost-down}}$). Therefore, the equation of the power available to the process could be also written by the following equation: $Q_{\text{available}} = Q_{\text{kerf}} + Q_{\text{oxy}} = Q_{\text{melt}} + Q_{\text{HCL}} + Q_{\text{lost-down}}$.

Figure 1 represents previously explained power components participation in the plasma cutting process. Blue arrows represent power available for the plasma cutting process, while yellow arrows represents power/heat flux used during the process, both for material melting and losses

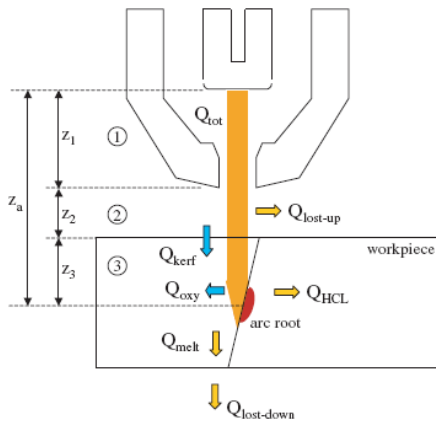


Fig. 1 Power components of the plasma cutting process

Heat flux of the plasma jet which passes through the area A (Q_{kerf}) consist of the electrical power transported by the plasma (Q_{elec}), power carried by convection through area A (Q_{cv}), power given by conduction through area A (Q_{cd}) and power radiated through area A ($Q_{\text{rad} \rightarrow A}$), as it is represented by following equation: $Q_{\text{kerf}} = Q_{\text{elec}} + Q_{\text{cv}} + Q_{\text{cd}} + Q_{\text{rad} \rightarrow A}$

Taking into account all mentioned above, the equation for the power available for the process could be written as follows: $Q_{\text{kerf}} = Q_{\text{elec}} + Q_{\text{cv}} + Q_{\text{cd}} + Q_{\text{rad} \rightarrow A} + Q_{\text{oxy}}$

It is also necessary to observe which part of the power available is used for material melting. Taking into account that the transferred arc is considered, it could be assumed that to whole electric power (Q_{elec}) is used for material melting, via anode attachment, transferred to the front side of the kerf. Other components of the available power/ heat flux which participate in material melting with some its percentile share are represented by the following equation:

$$Q_{\text{melt}} = Q_{\text{elec}} + x\% (Q_{\text{cv}} + Q_{\text{cd}} + Q_{\text{rad} \rightarrow A} + Q_{\text{oxy}})$$

2.2. Energy Balance of the Plasma Cutting Process

In order to determine energy balance of the plasma arc cutting process, each of the power components (power contributions) for cutting process should be calculated or assessed. Knowledge of the temperature and mass

flow is essential for calculation of the particular power components [6] and [7].

Power component used for melting material (Q_{melt}) can be obtained calculating the energy needed to melt 1 m³ of material (E_{melt}):

$$E_{\text{melt}} = \left[\left(\int_{T_p}^{T_1} c_p(T) dT \right) + L_f \right] \rho$$

where T_p is workpiece temperature, T_1 is melting temperature of the workpiece material, c_p is specific heat capacity, L_f is latent heat of the material melting and ρ is material density.

Based on the calculated energy needed for the material melting, power component used for melting material (Q_{melt}) could be calculated using the following equation:

$$Q_{\text{melt}} = E_{\text{melt}} \cdot V \cdot v_{\text{torch}}$$

where V is volume of the kerf passed by plasma jet at the particular moment in time and v_{torch} – torch speed.

Power dissipated by the exothermal oxidation reaction (Q_{oxy}) can be calculated using the following equation:

$$Q_{\text{oxy}} = \frac{0.45 \cdot D_{O_2} \cdot \Delta H}{M_{O_2}}$$

where D_{O_2} is mass flow of oxygen and M_{O_2} is molar mass of oxygen.

In the exothermal oxidation reaction, reaction of the iron and oxygen is dominant, while the heat quantity released (ΔH) is equal to 549.2 kJ/mol. Usually, only no-dissociated oxygen reacts with workpiece material, which leads to the assumption that only part of the plasma jet which has temperature higher then 3,500 K (temperature of the oxygen dissociation) reacts with the workpiece material. At these temperatures plasma jet densities are higher comparing to the same plasma jet at higher temperatures. This is why approximately 90 % of the plasma gas flows through the outer part of the plasma jet, where the temperatures are lower than 3,500 K. Out of this part of the plasma jet, only front part reacts with the frontal side of the kerf, which means that only 45 % of total oxygen is effectively involved in the oxidation reaction.

Heat flux brought by the plasma arc through the surface A (Q_{kerf}) is assessed by calculation of its individual components.

The electrical power transported by the plasma jet (Q_{elec}) could be calculated by the following equation:

$$Q_{\text{elec}} = \int_A q_{zelek} dS$$

The power carried by convection through area A (Q_{cv}) could be calculated by the following equation:

$$Q_{\text{cv}} = \int_A K \frac{\partial T}{\partial z} dS$$

The power given by conduction through area A (Q_{cd}) could be calculated by the following equation:

$$Q_{\text{cd}} = \int_A \rho h v_z dS$$

The power radiated through area A ($Q_{\text{rad} \rightarrow A}$) could be calculated by the following equation:

$$Q_{\text{rad} \rightarrow A} = \int_A q_z dS$$

The power needed for melting material increase with the cutting speed, therefore the quantity of melted material ejected from the kerf per time unit increase as well. However, increase of the cutting speed decrease

the total amount of ejected melted material per length unit.

Ratio of the power used for material melting and available power represents important indicator of the plasma cutting process efficiency. It was determined that this ratio is lower than 0.6 for low speed plasma cutting processes, while the rest of the heat flux is related to the losses due to the energy brought by the ejected slag ($Q_{lost-down}$) and heat conduction losses inside the workpiece (Q_{HCL}). It is considered that Q_{HCL} represents around 30 % of the power needed for material melting Q_{melt} and that it decreases with the speed increase.

At higher cutting speeds, the ratio of the power used for material melting and available power varies depending of the material thickness i.e. it is higher if the material thickness is higher, since the quantity of melted material ejected from the kerf is higher.

When plasma gas flow increases, power dissipated by the exothermal oxidation reaction (Q_{oxy}) increases as well. This is the reason why the total available energy for the plasma cutting process increases. At the same time, the power used for material melting decreases (Q_{melt}), since increase of the plasma gas flow increase the melted material ejection from the kerf. This leads to the important increase in the heat flux, which is lost due to the energy brought by the ejected slag ($Q_{lost-down}$).

Energy Balance of the plasma cutting process could be represented by Sankey's diagram, as it is shown at figure 2.

The power brought by the plasma arc inside the kerf (Q_{kerf}) and power dissipated by the exothermal oxidation reaction (Q_{oxy}) are represented as the input powers to the process i.e. power available in the workpiece for the cutting process and are represented by the blue arrows. The share of the power used for material melting (Q_{melt}), heat conduction losses inside the workpiece (Q_{HCL}) and energy losses due to the energy brought by the ejected slag ($Q_{lost-down}$) represent the ways of using the available energy, represented by violet arrows.

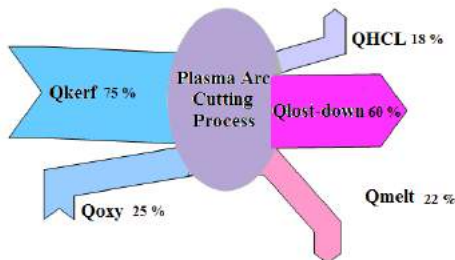


Fig. 2 Energy Balance of the plasma cutting process represented by Sankey's diagram

Power used for material melting (Q_{melt}) was previously represented by the following equation: $Q_{melt} = Q_{elec} + x\% (Q_{cv} + Q_{cd} + Q_{rad \rightarrow A} + Q_{oxy})$.

It could be split at the components, which separate shares should be examined. In order to simplify the analysis, part of this power is related to the power

given by conduction through area A (Q_{cd}), power carried by convection through area A (Q_{cv}) and power radiated through area A ($Q_{rad \rightarrow A}$), and their separate shares were not considered. Therefore, the previous equation could be written as follows: $Q_{melt} = Q_{elec} + x\% (Q_{other} + Q_{oxy})$.

3. CONSIDERATION OF THE TEMPERATURE FIELDS CHANGES AT THE WORKPIECE

During plasma cutting process high temperatures of the plasma jet and workpiece are developed. Moving the heat source i.e. the plasma cutting torch in respect to the workpiece surface contributes to the high oscillations of the temperature at the relatively narrow area of the kerf. For example, material heating and cooling velocities at 0.1 mm from the top kerf edge could reach values between 1,000 and 2,000 K/s.

Plasma jet temperature metering is particularly difficult. One of the most usually used methods is spectroscopic method for plasma jet temperature determination. Although it is important to know temperatures during plasma cutting, for the practical use and additional shaping of the material, particularly in terms of metallographic structure and hardness changes, it is important to know temperature distribution in the workpiece after cutting process terminated, when the intense source of heating energy was eliminated, providing monitoring of the workpiece cooling during time [8].

Experimental research of the plasma cutting process was done at the CNC machine, type HPM Steel Max 6.25. Plasma cutting unit was Hypertherm HPR130. This machine was placed at the workshop of the company EM DIP d.o.o. from Nis, dealing with engineering and production of the electro-mechanic industrial equipment and parts [1].

The workpiece material used for the experimental research was stainless steel: X10CrNiMn-16-10-2 (EN 10025), with the following chemical composition: 0.1 % C; 16 % Cr; 10 % Ni i 2 % Mn.

Workpiece temperature metering was done after the cutting process terminated using the infrared thermo-vision camera, aiming to meter and represent thermal energy radiated by the particular body. Namely, infrared thermo-vision camera measures temperatures without direct contact with the object of metering, providing the visualization of the infrared radiation, making it available to the human senses by the eye sense. Infrared radiation is transformed, proportionally to the body temperature, to the images or thermographs, representing the relative temperature difference, each with the particular colour.

In this specific case, thermo-vision camera used was type *Varioscan resolution*, for the spectrum from 8 to 12 μm length waves, i.e. in the lengths of the infrared radiation. The continuous metering was done starting from 2 until 17 s after the cutting process was terminated. The temperature fields for two material thicknesses were examined: 12 i 15 mm [1].

For the material thickness of 12 mm the temperature fields recording were done first through the material thickness, since the material was cut 10 mm from the outer side of the workpiece, 2 s after the plasma cutting process was terminated, as represented at figure 3.

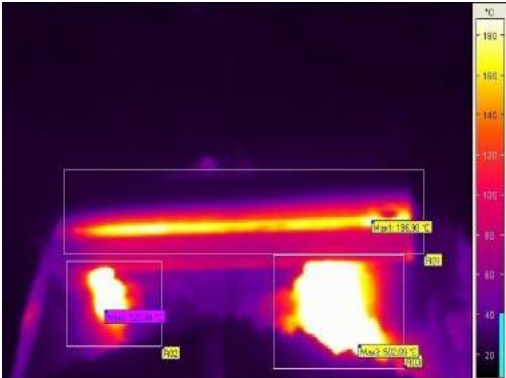


Fig. 3a Thermograph for the material thickness of 12 mm, 2 s after the plasma cutting process was terminated

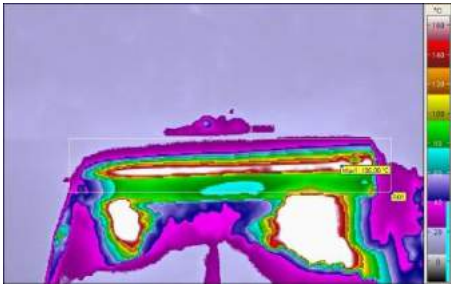


Fig. 3b Isotherms for the material thickness of 12 mm, 2 s after the plasma cutting process was terminated

The highest temperatures are below the workpiece, at the coordinate table. From the figures it could be observed that the highest temperature is 2 seconds after the cutting process terminated, 525.84 °C. This could be used to explain the previous observation that 60 % of the total available power for the plasma cutting process is lost due to the energy brought by the ejected slag.

Figure 4 represents thermographs with respective temperature profiles 17 seconds after the cutting process was terminated.

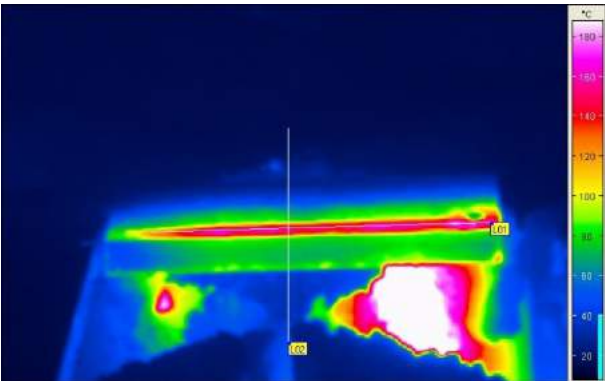


Fig. 4a Thermograph 17 s after the plasma cutting process was terminated, thickness 12mm

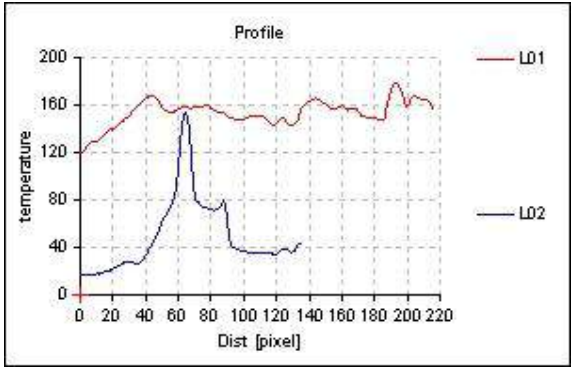


Fig. 4b Temperature profiles 17 s after the plasma cutting process was terminated

Good agreement of the experimental research of the temperature fields and energy balance of the process done at this paper with the theoretical considerations and empirical results of other authors could be observed good.

4. CONCLUSION

Taking into consideration the existing trend of increasing energy efficiency in all energy consumption sectors, all companies have to begin behave responsible toward energy usage in its manufacturing processes. This is the reason why consideration of the Manufacturing Plant's Energy Balance, together with all its processes, represents an important aspect that needs to be controlled and which could contribute to the rational and efficient use of energy. The potential inefficiencies of the plasma cutting process were identify in this paper, through the consideration of the overall process energy balance. The diminishing of these inefficiencies could considerably improve the manufacturing processes.

In this paper, power components contributing to the plasma cutting process were determined, calculated or assessed, in order to generate the energy balance of the process. Theoretical and experimental research that led to the energy balance preparation were additionally illustrated by experimental research and by thermal imaging of the workpiece by thermo-vision camera, few seconds after cutting process terminated.

This allowed the consideration of the temperature fields' changes during the workpiece cooling, through the length and thickness of the workpiece. It was shown that highest share of energy was lost due to the energy brought by the ejected slag, since the temperatures of the coordinate table were much higher than the workpiece temperatures. Namely, ratio of the power needed for the material melting and available power for the process represents important indicator of the plasma cutting process efficiency. It was determined that this ratio is lower than 0.6 for low speed plasma cutting processes, while the rest of the heat flux is related to the losses due to the energy brought by the ejected slag and heat conduction losses inside the workpiece.

In this sense, further research should be focus on the possibilities and ways for more efficient use of the energy during plasma cutting process, i.e. increasing of the process energy efficiency. The instalment of the equipment and units for additional use of the thermal energy, otherwise lost by the ejected slag, should be considered. To be more precise, system of pipes with the high flow of fluid could be installed under the coordination table. The system of pipes should be installed on the way to follow the movements of the torch, providing that the heat source is always close to the transport media.

REFERENCES

- [1] LAZAREVIC, A. (2010) *Modeliranje korelacija tehnoloških parametara rezanja plazmom i analiza toplotnog bilansa korišćenjem metoda veštačke inteligencije*, Doktorska disertacija, Masinski fakultet u Nisu.
- [2] GRANT, R. M. (2005) *Contemporary Strategy Analysis*, Blackwell Publishing.
- [3] MALIC, D., (1967) *Termodinamika i termotehnika*, Gradjevinska knjiga, Beograd.
- [4] FROLOV, V. V., VINOKUROV, V. A., VOLČENKOV, V. N. (1979) Teoretičeskie osnov svarki, Высшая школа
- [5] ILIC, G., RADOJKOVIC, N., STOJANOVIC, I. (1996) *Termodinamika II - Osnove prostiranja toplote*, Masinski fakultet u Nisu.
- [6] FRETON, P., GONZALEZ, J. J., GLEIZES, A., CAMY PEYRET, F., CAILLIBOTTE, G., DELZENNE, M. (2002) *Numerical and experimental study of a plasma cutting torch*, Journal of Physics D: Applied physics 35, pp. 115-131.
- [7] TEULET, PH., GIRARD, L., RAZAFINIMANANA, M., GLEIZES, A., BERTRAND, PH., CAMY PEYRET, F., BAILLOT, E., RICHARD, F. (2006) *Experimental study of an oxygen plasma cutting torch: II. Arc-material interaction, energy transfer and anode attachment*, J. Phys. D: Appl. Phys. 39, pp. 1557 – 1573.
- [8] GLEIZES, A., GONZALEZ, J. J., FRETON, P. (2007) *Thermal plasma modelling*, Journal of Physics D: Applied physics 38 R153-R183.

MODEL FOR OPERATING COSTS OF PLASMA CUTTING

Srdjan T. MLADENOVIC, Miroslav R. RADOVANOVIC

University of Nis, Faculty of Mechanical Engineering, Nis, Serbia
maki@masfak.ni.ac.rs, mirado@masfak.ni.ac.rs

Abstract: Operating costs of plasma cutting should form the basis for evaluating its profitability. Acceptable cut quality, increased traverse speed and lower cost per meter of the cut together with cheaper equipment and possibility of cutting various materials assure wider application of this procedure. Optimizing a plasma cutting operation based on operation cost is typically a trial-and-error process that is usually inspired in recommendations given by manufacturers of plasma cutting tools and consumables. The operating costs for plasma cutting are presented in this paper.

Key words: Advance machining, Plasma Cutting, Operating Cost

1. INTRODUCTION

The plasma-arc process had its origin almost 70 years ago. In 1941 the U.S. defence industry was looking for better ways of joining light metal together for the war effort and, more specifically, for the production of airplanes. Out of this effort, a new welding process was born. An electric arc was used to melt the metal, and an inert gas shield around the arc and the pool of molten metal was used to displace the air, preventing the molten metal from picking up oxygen from the air. This new process "TIG" (Tungsten Inert Gas) seemed to be a perfect solution for the very specific requirement of high-quality welding.

By 1950, TIG had firmly established itself as a new welding method for high-quality welds on exotic materials. While doing further development work on the TIG process, scientists at Union Carbide's welding laboratory discovered that when they reduced the gas nozzle opening that directed the inert gas from the TIG torch electrode (cathode) to the work piece (anode), the properties of the open TIG arc could be greatly altered. The reduced nozzle opening constricted the electric arc and gas and increased its speed and its resistive heat. The arc temperature and voltage rose dramatically, and the momentum of the ionised and non-ionised gas removed the molten puddle due to the higher velocity. Instead of welding, the metal was cut by the plasma jet.

In Figure 1, both arcs are operating in argon at 200 amps. The plasma jet is only moderately constricted by the 3/16 inch (4.8 mm) diameter of the nozzle orifice, but it operates at twice the voltage and produces a much hotter plasma arc than the corresponding TIG arc. If the same current is forced through a nozzle with an even smaller opening, the temperature and voltage rise. At the same time, the higher kinetic energy of the gas leaving the nozzle ejects the molten metal, creating a cut.

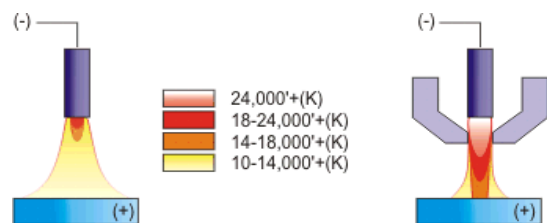


Fig.1. TIG arc and plasma arc

2. PLASMA CUTTING

Plasma cutting is a process that is used to cut steel and other metals of different thicknesses (or sometimes other materials) using a plasma torch. In this process, an inert gas (in some units, compressed air) is blown at high speed out of a nozzle; at the same time an electrical arc is formed through that gas from the nozzle to the surface being cut, turning some of that gas to plasma. The plasma is sufficiently hot to melt the metal being cut and moves sufficiently fast to blow molten metal away from the cut.

The characteristics of the plasma jet can be altered greatly by changing the gas type, gas flow rate, arc current, arc voltage and nozzle size. For example, if low gas flow rates are used, the plasma jet becomes a highly concentrated heat source ideal for welding. Conversely, if the gas flow rate is increased sufficiently, the velocity of the plasma jet is so great that it ejects molten metal created by the hot plasma arc and cuts through the workpiece.

Plasma cutting is an industrial process that is essentially controlled by the operators' empirical mind-set, which is typically inspired in recommendations given by the manufacturers of the cutting torches that are to be used. Those recommendations, however, reflect the point of view of the manufacturers' business, which includes not

only selling the cutting torches but also the consumables. Yet, the manufacturers' recommendations usually lead to solutions that are technically sound in terms of cutting quality, but do not necessarily correspond to the most cost-effective solutions on the user's point of view.

As a result, the user customarily attempts to optimize the cutting operations by trial-and-error every time it is needed to setup the existing equipment for a new different task.

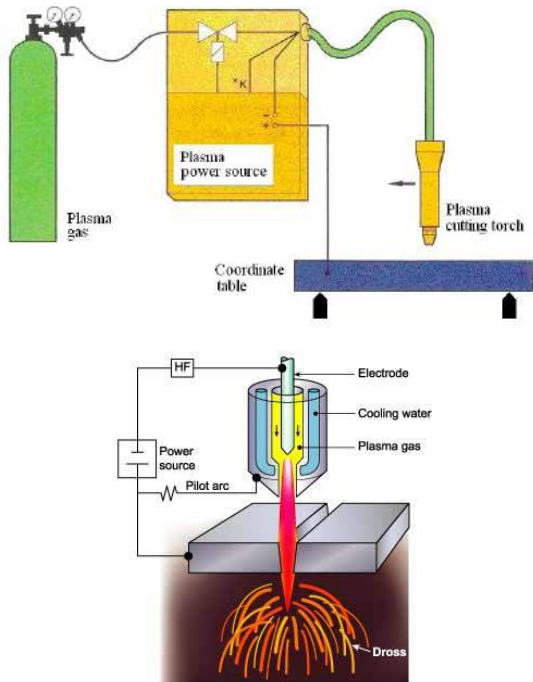


Fig.2. Plasma cutting

In an industrial point of view, general contributions for the systematization of knowledge on the plasma cutting is an industrial process that is plasma cutting process appear to be out of question essentially controlled by the operators' empirical since plasma torches and respective nozzles come in a mind-set, which is typically inspired in recommenda-wide range of sizes. Additionally, the topology of operations given by the manufacturers of the cutting complete plasma cutting systems varies from the torches that are to be used. Those recommendations, simple hand-held torches to complex CNC machines however, reflect the point of view of the manufacture-of different shapes and sizes.

There are several methods of plasma cutting. The well-known are: conventional plasma cutting, dual flow plasma cutting, air plasma cutting, oxygen plasma cutting, underwater plasma cutting and other.

In Table 1 are shown gas quality and pressure requirements for machine HyPerformance plasma HPR130.

In Table 2 are shown gas types and amperage of current for material types of plasma cutting.

In Table 3 is shown power supply machine.

Table 1. Gas quality and pressure requirements

Plasma gas	Quality	Pressure +/- 10%	Flow rate
O ₂ Oxygen	99.5% pure Clean, dry, oil-free	827 kPa / 8.3 bar	4250 l/h
N ₂ Nitrogen	99.9% pure Clean, dry, oil-free	827 kPa / 8.3 bar	7080 l/h
Air	Clean, dry, oil-free	827 kPa / 8.3 bar	7080 l/h
H35 Argon-hydrogen	(H35 = 65% Argon, 35% Hydrogen)	827 kPa / 8.3 bar	4250 l/h
F5 Nitrogen-hydrogen	(F5 = 95% Nitrogen, 5% Hydrogen)	827 kPa / 8.3 bar	4250 l/h

Table 2. Gas types and amperage of current for material types

	Plasma	Shield
Mild steel / Stainless steel / Aluminium		
Gas types	Plasma	Shield
Cutting 30 to 45 A	O ₂ / N ₂ & F5 / Air	O ₂ / N ₂ / Air
Cutting 80 A	O ₂ / F5 / -	Air / N ₂ / -
Cutting 130 A	O ₂ / N ₂ & H35 / H35 & Air	Air / N ₂ / N ₂ & Air

Table 3. Power supply

General	
Maximum OCV (U ₀)	311 VDC
Maximum output current (I ₂)	130 Amps
Output voltage (U ₂)	50 – 150 VDC
Duty cycle rating (X)	100% @ 19.5 kW, 40°C
Ambient temperature/Duty cycle	Power supplies will operate between -10°C and +40°C
Power factor (cosφ)	0.88 @ 130 ADC output
Cooling	Forced air (Class F)
Insulation	Class H
Input power (input voltage (U₁) X input current (I₁))	
200/208 VAC, 3-PH, 50-60 Hz, 62/58 Amps	
400 VAC CE, 3-PH, 50-60 Hz, 32 Amps	

3. COST OF PLASMA CUTTING

How to calculate cost of operation and establish metrics for improvement? There are many costs associated with a mechanized plasma-cutting machine beyond the capital equipment purchase. There are general overhead costs, maintenance costs, service call charges, gas costs, consumable and torch costs, and electricity charges. The plasma-profiling machine is also likely to have a host of auxiliary equipment that may also be considered: material handling equipment, environmental control equipment, safety gear etc. The labor component for plasma cutting may include machine operators, helpers, maintenance personnel, secondary operation workers and others. The intent of this article is to review the most significant variables affecting annual cost of operation and to establish metrics for improvement.

In typical plasma cutting operations there are four major ongoing costs: cost of power, gas, cost of consumables, and cost of labor.

Productivity can be regarded as being the ratio between production speed and cost. For plasma cutting, productivity can be defined by an expression of the type

$$P = \frac{V_C}{C_H} \quad (2)$$

Where V_C is the traverse speed and C_H is the cutting cost per unit time.

Both V_C and C_H depend on several process variables and productivity can be improved either by increasing the traverse speed, or decreasing the cutting cost per unit time, or both.

For a given torch, the main process variables in plasma cutting are the amperage the current, the traverse speed V_C , the pressure of the cutting gas, and the pressure of the protective gas. There are four major factors for the production cost in typical plasma cutting operations: electrical power, gases and torch consumables [1].

$$C_H = C_E + C_P + C_S + C_M \quad (3)$$

Where C_E , C_P , C_S and C_M are respectively: the cost per unit time of the electrical power, the cost of the cutting gas (plasma), the cost of the compressed air that is used as protective gas (shield) and cost of the torch consumables. All the costs are expressed in €/h.

Cost of the electrical power can be defined by expression:

$$C_E = c_E \cdot P_E = c_E \cdot (P_P + P_T) \quad (4)$$

Where c_E is unit cost of electric energy (EUR/kWh), P_E is electric power consumption (kW), P_P is electric power of aggregate the plasma, P_T is electric power of working table.

Cost of the cutting gas (plasma) and the cost of the compressed air that is used as protective gas (shield) can be defined by expressions:

$$C_P = c_P \cdot Q_P \quad (5)$$

$$C_S = c_S \cdot Q_S \quad (6)$$

Where c_P and c_S is unit cost of plasma gas and shield gas (EUR/m³), Q_P is gas consumption (m³/h).

Cost of the torch consumables C_M to set a monthly or year monitoring of consumption, and later this value is translated into cost per time.

4. OPERATING COSTS

The major power consumer in a cutting machine is the DC power supply. Most of the energy consumed by the system is put directly to work on the material in a very hot energy-dense arc. To get a rough idea of the power consumption of plasma system is multiply the amperage output by the average operating voltage. To calculate kilowatts of input consumed, multiply by a power supply efficiency factor of around 85%. Example an 80A plasma system has an average operating voltage of about 100V. This means the power supply puts out 6.8 kW (8kVA x 0.85 = 6.8 kW).

To arrive at daily or yearly power consumption multiply times the average up-time or arc-on time in a day. Arc-on time is the amount of time actually spent cutting over a given time interval. This can be measured by a pierce and arc-on time counter, or calculated from programming distances and speeds and daily throughput. Arc-on time will vary with material type and thickness, size of cut pieces, material handling, machine speed, torch height control speed, and many other factors. Most shops average about 55% actual arc-on time. That means in a given 8-hour shift only 4.4 hours are spent cutting. In the year we have 1144 hours are spent cutting (260 days).

Plasma systems use as plasma gas: oxygen, air, nitrogen, argon-hydrogen, and other gases. The consumption rate varies with the size of the plasma system and various operating conditions. Generally the operations manual will provide consumption rates in cubic meter per hour for a given nozzle size and operating pressure or flow tube setting. For example an 80A oxygen plasma system consumes 2 m³/hours of oxygen when cutting. To find the cost of operation multiply the consumption rates of plasma gas by the arc-on time and cost of the gas, which is often measured in EUR per m³. The same system may use 8.5 m³/hours of shield air. Shop air is generally considered free other than associated maintenance costs to keep it clean. But shield gases such as nitrogen O₂, and mixes can be costly and should be calculated as above.

Consumable costs can be tracked on a weekly, monthly or yearly basis. These costs vary widely depending not only on the cost of the parts but on the performance and life of the parts, which is dependent on many factors. Consumable and plasma torch life varies with application, operating parameters, duration of cuts, number of pierces, operator skill etc. The best way to capture and begin to control consumable costs is to keep daily logs of parts life measured in number of pierces and arc hours. Over time,

in a production environment, it is possible to closely track the number of pierces and the total arc-hours for a given set of parts on a given cutting job. If a plasma torch is operated and maintained correctly the annual cost of torches, gas swirling devices, shields, retaining caps and other parts should be low compared to the nozzle and electrode cost. But the reality in many shops is that overall consumable cost is 2 X the nozzle and electrode cost.

In Table 4 are shown consumption of the power, cutting and shield gas in m³ per hour and consumable in EUR per day.

Table 4. Consumption of power, cutting and shield gas and consumable

Factors		Mild Steel	Stainless Steel	Aluminium
Power (current 80A)	kWh	8.2	7.5	10.2
Cutting gas (plasma gas)	O ₂	2	-	-
	N ₂	-	0.8	-
	F5	-	0.4	-
	H35	-	0.3	1.5
Protective gas (shield gas)	O ₂	0.5	-	-
	N ₂	-	4.5	2
	Air	8	-	6
Consumable	EUR	10	10	10

In Table 5 are shown operating costs for one month if cutting machine works 25 days (110 hours). A price of 0.105 EUR/kWh was used for the electricity costs. The following gas prices were taken as the basis for calculating the plasma gas costs: N₂ – 1.5 EUR/m³, O₂ - 1.5 EUR/m³, F5 - 2 EUR/m³ and H35 - 2 EUR/m³. Air is generally considered free, but consumption of air compressor during compression to 6-8 bar is about 2 kWh.

Table 5. Operating costs for one month

Factors		Mild Steel	Stainless Steel	Aluminium
Power		95	86.5	118
Cutting gas (plasma)	O ₂	330	-	-
	N ₂	-	132	-
	F5	-	88	-
	H35	-	66	330
Shield gas	O ₂	82.5	-	-
	N ₂	-	990	330
	Air	23	-	20
Consumable		250	250	250
Overall	EUR	780.5	1612.5	1048

The table shows that the operating costs of a plasma cutting are big, and it is therefore necessary to optimize the machine and several recommendations are given in the conclusion.

5. CONCLUSION

Plasma cutting is a process that is used to cut steel and other metals. Here are some recommendations for

optimizing plasma cutting machine to lower cost of operation and increase productivity:

1) Maximize up-time on the machine. A cutting machine should be cutting. Preventative maintenance is essential to prevent costly downtime for repairs. Material handling solutions such as multiple cutting beds, overhead cranes, and plate handlers can minimize manual loading and offloading and keep the operator focused on the cutting process. Motion matters as well: If the torch height controls or machine traverse speed is slow the machine spends more time positioning the torch than cutting metal.

2) Minimize secondary operations: Controlling costs of secondary options is achieved by optimizing cut quality. To do this requires not only a well-maintained machine but also a well-trained operator. The highly skilled operator produces more cut pieces, of higher quality, with less scrap material and less rework down the line. Getting good cut quality from the plasma arc cutting process requires careful control over process parameters and attention to detail.

3) Control consumable costs: Controlling consumable costs, like controlling cut quality is part equipment and part operator. A good operator will get the most out of a set of parts and prevent catastrophic failures.

ACKNOWLEDGEMENT

This paper is part of project TR35034 "The research of modern non-conventional technologies application in manufacturing companies with the aim of increase efficiency of use, product quality, reduce of costs and save energy and materials", funded by the Ministry of Education and Science of Republic of Serbia.

REFERENCES

- [1] COOK D., (2000), *Cost of Operation in Mechanized Plasma Cutting*, Magazine "Welding Design & Fabrication", Ohio, USA.
- [2] FERREIRA P., MELO I., GONÇALVES-COELHO A., MOURÃO A., (2009), *Plasma cutting optimization by using the response surface methodology Extending the C-K design theory*, The annals of "DUNĂREA DE JOS", University of Galați, Galați, Romania, pp 213-218
- [3] RADOVANOVIĆ M., (2005), *Plasma Cutting of Metals*, 7th International Conference on Accomplishments of Electrical and Mechanical Industries - DEMI 2005, University of Banjaluka, Faculty of Mechanical Engineering, Banjaluka, Bosna and Hercegovina, pp.165-170
- [4] RADOVANOVIĆ M., (2005), *Determining of Cutting Data by Plasma Cutting*, Seventh International Scientific Conference "Smolyan-2005", University of Plovdiv "Paissiy Hilendarski", Technical College-Smolyan, Smolyan, Bulgaria, pp. 235-239
- [5] RADOVANOVIĆ M., (2004), *Comparison of abrasive water jet cutting and plasma cutting*, International scientific conference UNITECH'04, Technical University of Gabrovo, Gabrovo, Bulgaria, pp. II-137-II-142



CUT QUALITY IN ABRASIVE WATER JET CUTTING

Predrag JANKOVIĆ¹, Miroslav RADOVANOVIĆ², Jelena BARALIĆ³

University of Niš, Faculty of Mechanical Engineering, A. Medvedeva 14, Niš, Serbia

¹jape@masfak.ni.ac.rs, ²mirado@masfak.ni.ac.rs

³University of Kragujevac, Technical Faculty Čačak, Serbia, jbaralic@tfc.kg.ac.rs

Abstract: Abrasive water jet cutting process is defined by many influencing factors, which determinate cut quality. Substantial efforts has been made in understanding effects of individual process parameters, like: diameters of water and abrasive nozzle, water pressure, size and flow rate of abrasive, distance of cutting head from material surface, feed rate, etc.

Process optimization, as a background of its successful application, is achieved through correct choice of process parameters. A series of water jet cutting experiments were conducted for identification and understanding of process influencing factors. In this Article are presented results of investigation of factors influencing cut quality by abrasive water jet cutting process of aluminium alloy. The experimental results indicate that the cutting head feed rate and abrasive flow rate have a significant influence on the cut surface topology.

Key words: Abrasive Water Jet Cutting, Abrasive Water Jet Cutting Process Influencing Factors, Cut Quality, Surface Roughness

1. INTRODUCTION

Each day reveals new materials that could be applied in different areas of mechanical engineering. In most of these materials processing by conventional methods is a major problem due to breakage and tool wear, uneconomical or even impossibility of processing.

The problem of cutting difficult-to-machine materials used in the aerospace industry, aircraft industry and automobile industry, led to the development and application of today the most attractive technology for contour cutting - Abrasive Water Jet cutting (AWJ). The first commercial water jet cutting system was built to cut laminated paper tubes in 1971. Since then, water jet technology has experienced a steady growth. In the early 80's, the idea of entraining abrasive into water jet was promoted and commercial abrasive water jet systems became available in 1983.

In the last ten years, the AWJ technology has shown a rapid development due to its remarkable advantages and its capability to extend to new fields of application. It is able to cut any kind of material, carry out complex profiles, prevent thermal and mechanical damages on the target material, and reduce the burr formation and the delamination phenomena. Abrasive water jet cutting is an appropriate and cost effective machining process for a number of applications and materials and is applied in nearly all areas of modern industry, such as: automotive industry, aerospace industry, construction engineering, environmental technology, chemical process engineering, and industrial maintenance [1].

However abrasive water jet cutting belongs among complicated dynamical and stochastic processes with incomplete information about mechanism and side effects

character. In AWJ cutting, the final cut surface roughness and the dimensional accuracy depend on the process parameters including the water pressure, the abrasive mesh number, the abrasive mass flow rate, the feed rate, and the orifice and abrasive nozzle diameters [2-3].

In this paper, an experimental investigation of the cut quality of EN AW-6060 aluminium alloy sheets machined by abrasive water jets is presented.

2. ABRASIVE WATER JET CUTTING PROCESS

The technology of water jet cutting uses either pure water or a mix of water and a fine abrasive material to form an abrasive water jet for use on harder workpieces. The list of materials that can be cut using a pure water jet includes Styrofoam, fiberglass, PVC, nylon, rubber and food products such as fish, meat, bread and cakes. The abrasive water jet differs from the pure water jet in just a few ways. In pure water jet, the supersonic stream erodes the material. In the abrasive water jet, the water jet stream accelerates abrasive particles and those particles, not the water, erode the material. With abrasive added to the water jet, virtually any material can be cut, including metals such as aluminum, carbon steel and stainless steel, high-nickel alloys and brittle materials such as marble, reinforced composites and honeycomb and sandwiched materials. Modern machine shops now use abrasive water jet machines side by side with other traditional or non-traditional machine tools to cut 2D parts out of all kinds of materials and profit from the use because of their productivity, quick turn-around time, and relative low cost [4].

At its basic, water flows from a pump, through the pipe, and out of the cutting head (Fig. 1). The energy required for cutting materials is obtained by pressurizing water to high pressures and then forming a high-intensity cutting stream by focusing this water through a small orifice.

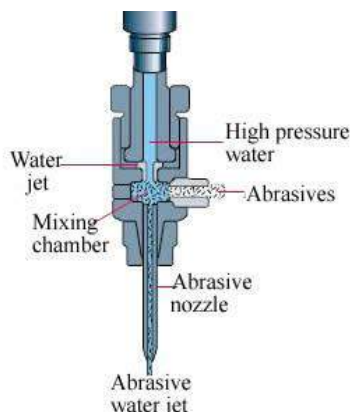


Fig.1. Abrasive water jet cutting head

The use of the abrasive materials with water jet for cutting is based on the principle of erosion of the material upon which the jet hits [5]. Each hard abrasive particle acts like a single point cutting tool. Because of the size of the abrasive particles the impact on the workpiece of an individual particle is small but together the large total number of particles erode the material in significant volume.

3. CUT QUALITY

For the AWJ cutting process evaluation the greatest influence has a group of geometric characteristics, as determined by the geometric layout of the part. The group of geometric characteristics of objects is: dimensional accuracy, shape accuracy and cut quality [6].

There is a difference between the workpiece accuracy and precision of machine elements moving in relation to the workpiece lying on the desk. The accuracy of the workpiece is a combination of, machinery, process parameters and workpiece stability. The biggest errors were the result of the process parameters influence.

In the abrasive water jet cutting "cut quality" is a term that describes the combination of characteristics such as geometry of cut (kerf width, kerf taper) and cut surface quality (cut surface roughness). Standards for describing the cut quality, resulting in abrasive water jet cutting, are not yet established [7]. Parameters that define the cut quality (geometric characteristics of cut quality and cut surface quality) in abrasive water jet cutting are shown in Figure 2.

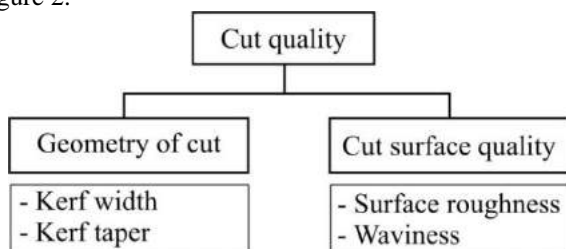


Fig.2. Characteristics of cut quality

Kerf width is the distance between the cut surfaces. For the kerf width is taken smaller value of width in the upper and lower section of the cut. When cutting with abrasive water jet kerf is usually wider at the upper, but the lower section (Fig. 3). The reason is that the cut get deeper, the energy of jet drops. The result is the appearance of "kerf taper".

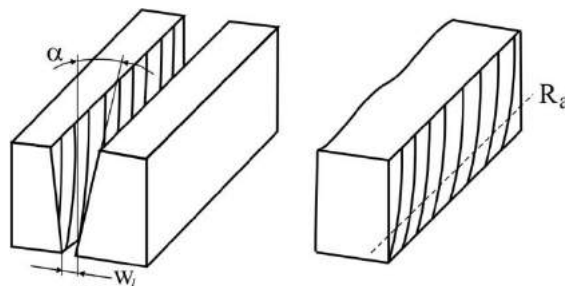


Fig.3. Cut geometry and surface quality

Kerf taper (Fig. 3) is of interest because it provides an idea of the perpendicularity of part across the contact surface of the cut, that is, whether the additional processing required. It is defined by the value of the taper (α), corresponding to the corner of the cut surface that is tilted relative to the vertical plane [8].

The **surface roughness** is used to describe the cutting surface and gives an indication of whether the subsequent machining required. It is defined using the value of roughness average R_a . Cut surface can never be ideally smooth. It consists of small, finely spaced surface irregularities (micro irregularities - roughness) formed in the course of treatment. Additionally, there are surface irregularities of grater spacing (macro irregularities - **waviness**), which may be periodically repeatable (Fig. 3).

4. EXPERIMENTAL WORK

Although AWJ cutting involves a large number of variables and virtually all these variables affect the cutting results (kerf width, taper and surface roughness), only few major and easy-to-adjust dynamic variables were considered in the present study (Fig. 4).

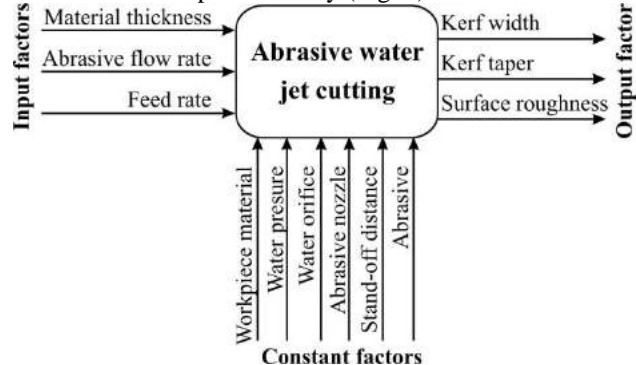


Fig.4. Factors influencing cut quality

4.1. Experimental set-up

A series of water jet cutting experiments were conducted using a Byjet 4022 abrasive water jet cutting machine (Bystronic AG, Switzerland). It is equipped with a dual intensifier high output pump with power of 37 kW and a

five axis positioning system. The machine was used to cut 40 mm long slots on 700×50 mm test specimens with thickness of 6 mm and 10 mm.

The main process parameter varied in the cutting operation was the feed rate (the speed at which the cutting head moves along workpiece during cutting operation). In this study the material thickness and the abrasive flow rate were also varied. For each level of the material thickness ($s=6$ mm and 10 mm) and abrasive flow rate ($q=300$ and 400 g/min), six levels of feed rates ($v=200, 300, 400, 500, 800$ and 1000 mm/min) were used at a single level of the water pressures of $p=400$ MPa, stand-off distance of 2 mm and a single level of impact angle of 90° . The other parameters were kept constant using the system standard configuration, that is: the orifice diameter was $d_0=0.30$ mm, the abrasive nozzle diameter was $d_A=1.02$ mm and the length of abrasive nozzle was 78 mm. Commercial grade garnet was used as the abrasive material. The garnet was sieved through an 80 mesh size before use, which meant that the average particle diameter was 180 μm .

As workpiece material, aluminium alloy AA-ASTM 6060 (EN: AW-6060; ISO: Al MgSi) was used. Alloy 6060 is one of the most popular of the 6XXX series alloys. Typical uses include architectural sections, sections fit for forming processes and automotive parts. The aluminium alloy was chosen as a workpiece material because the material is very attractive, possess resistance to corrosion and can provide significant value for the end user. Also, aluminum and its alloys are characterized by high reflectivity and thermal conductivity. This makes them relatively difficult to cut with lasers. Abrasive water jet cutting, which does not create an observable heat affected zone, is much more useful for cutting aluminum for modern applications.

To measure the geometry of the cut is used an optical microscope, a product of "Konus Diamond" company from Italy, with a CMOS camera. Image is recorded with the camera resolution 1280×1024 points, and wide field of view of 5.4 mm. The measurement was performed with an accuracy of 0.01 mm.

The surface roughness was measured with a digital, stylus type measuring instrument Mitutoyo SJ-301. Precision of measurement was 0.01 μm .

4.2. Experimental results and discussion

The kerf geometry of a through cut generated by abrasive water jets may be described as in Fig. 5.

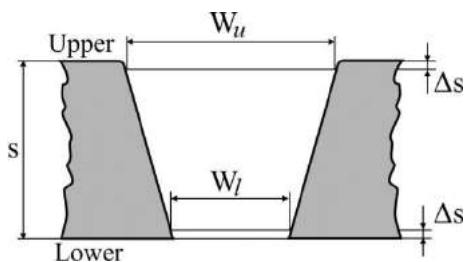


Fig.5. Schematic representation of kerf geometry

The kerf geometry (kerf widths on upper and lower section of the cut) was measured from the optical microscope images. These measurements were taken for

each cut away from the ends of the slots (by a distance Δs , related to material thickness) to eliminate any effect of the cutting process at the jet entry and exit.

Fig. 6 and Fig. 7 show some typical and representative trends and relationships between the kerf geometry (upper kerf width W_u and lower kerf width W_l) and the cutting parameters.

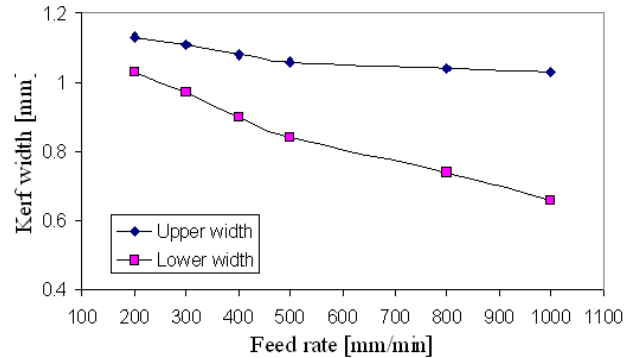


Fig.6. The effect of feed rate on the kerf width

From the Fig. 6 it can be seen that the feed rate has a negative effect on both the upper and lower kerf widths. The negative effect of the feed rate on both the upper and lower kerf widths is because a faster passing of abrasive water jet allows fewer abrasives to strike on the jet target and hence generates a narrower slot.

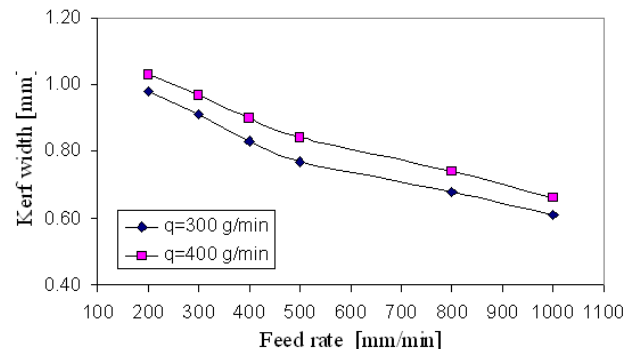


Fig.7. The effect of abrasive flow rate on the lower kerf width

By increase of abrasive flow rate the larger number of abrasive particles share in machining process, which has positive effect on kerf geometry. From Fig. 7. it can be seen that higher abrasive flow rate produce greater kerf widths, especially lower kerf width.

Whilst surface roughness is a common phenomenon in all machining operations, striation or waviness is a special feature of cuts with beam cutting technology, such as AWJ cutting. It is formed when the ratio between the available energy of the beam and the required energy of the destruction becomes comparatively small [9]. Surface roughness obtained in AWJ cutting application is determined by striations caused by jet at the lower region of the cut surface. Typical cut surface of 10 mm thick aluminium alloy sample is presented in Fig. 8.

The cut surface has better quality at upper region (entrance area) of the jet. From the middle of the thickness downwards, the surface quality deterioration is observed. Surface quality deteriorates as the material thickness increase. As the penetration depth of abrasive water jet increases, the jet loses its energy due to the jet-

material interaction, mutual particle impacts, etc. This situation results in rougher surface characteristics at the lower region of the cut surface.



Fig.8. Cut surface generated in AWJ cutting of aluminium alloy sample

The results of determining surface roughness at lower region of the cut surface with respect to the material thickness, feed rate and abrasive flow rate are graphically represented on Fig 9.

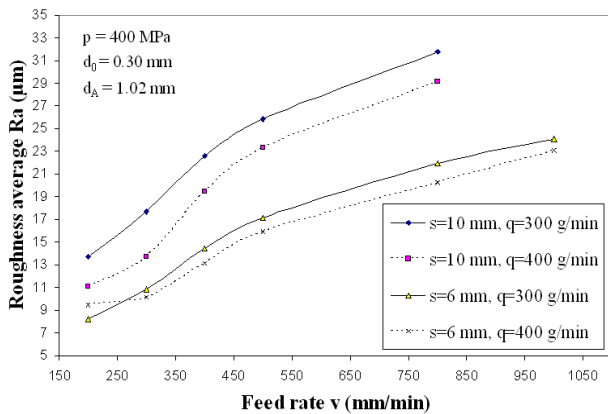


Fig.9. Roughness average Ra in dependence of material thickness, feed rate and abrasive flow rate

The influence of abrasive flow rate is found to be less significant on surface roughness. The increase in the number of impacting particles contributes to the improved surface finish. A high number of abrasive particles involved in mixing increases the probability of particle collision that decreases the average diameter of the impacting particles, so the roughness decreases with an increase of the abrasive flow rate.

5. CONCLUSION

In abrasive water jet cutting the final cut surface roughness and the dimensional accuracy depend on the many process parameters. Experimental study shows that, among others, the most important factors influencing the cut surface quality of aluminium alloy are feed rate and abrasive mass flow rate. Summarizing the main features of the experimental results, the following conclusions may be drawn:

- As the feed rate increases, the AWJ cuts narrower kerf. This is because the feed rate of abrasive water jet allows fewer abrasives to strike on the jet target and hence generates a narrower slot.
- Higher abrasive flow rate produce greater kerf width, especially lower kerf width because the larger number

of abrasive particles share in machining process which has positive effect on kerf geometry.

- The surface has better characteristics in the region that starts from the upper point where abrasive water jet begins to cut to the middle of the thickness. From the middle of the thickness downwards, the surface quality deterioration is observed.
- With an increase in the abrasive flow rate, the roughness is reduced. For high abrasive mass flow rates, the roughness is less sensitive to changes in the feed rate.

ACKNOWLEDGMENTS

Paper is result of technological project TR35034 "The research of modern non-conventional technologies application in manufacturing companies with the aim of increase efficiency of use, product quality, reduces of costs and save energy and materials" which is supported by Ministry of Education and Science of the Republic of Serbia.

REFERENCES

- [1] MOMBER W, KOVACEVIC R. (1998) *Principles of Abrasive Water Jet Machining*, Springer, London, New York
- [2] HLOCH S, FABIAN S. (2006) *Qualitative analysis of AWJ factors affecting the surface roughness*, Wissenschaftliche Beitrage, TFH Wildau, Germany, pp. 113-119
- [3] LEBAR A, JUNKAR M. (2004) *Simulation of abrasive water jet cutting process*, Modeling Simul. Mater. Sci. Eng. 12, pp. 1159-1170
- [4] ZENG J, OLSEN J, OLSEN C. (199) *The Abrasive Water Jet as a Precision Metal Cutting Tool*. In: Proceedings of the 10th American Water Jet Conference, Houston, Texas, August 14-17, pp. 829-843.
- [5] NEDIĆ B, BARALIĆ J. (2010) *The Wear of the Focusing Tube and the Cut-Surface Quality*, Tribology in industry, Vol. 32, No 2, 2010, pp. 38-43
- [6] MAROS Z. (2003) *Quality and efficeincey at abrasive waterjet cutting of an aluminium alloy*. Proceedings of the 6th International MTeM Conference, Cluj-Napoca, Romania
- [7] JANKOVIĆ P, RADOVANOVIĆ M. (2008) *Characteristics of Part Accuracy and Errors by Abrasive Water Jet cutting*. 8th International Conference "Research and Development in Mechanical Industry" RaDMI 2008, Užice, Serbia, s. 215-222
- [8] GUO N. S, LOUIS H, MEIER G. (1993) *Surface structure and kerf geometry in abrasive water jet cutting: formation and optimization*. Proceedings of 7th American Water Jet Conference, St. Louis, Vol. 1, s. 1-25
- [9] CHEN L, SIORES E, WONG W.C.K. (1996) *High-pressure abrasive waterjet erosion process*, Proc. Pacific Conf. on Manufacturing, Seoul, Korea, pp. 642-647

THE COMPLEXITY OF DEFINING THE QUALITY OF LASER CUTTING

Bogdan NEDIĆ, Jelena BARALIĆ, Miroslav RADOVANOVIĆ

Faculty of mechanical engineering, Kragujevac, Technical faculty, Čačak, Faculty of mechanical engineering, Niš
 nedic@kg.ac.rs, jbaralic@tfc.kg.ac.rs, mirado@masfak.ni.ac.rs

Abstract: Laser cutting is thermal cutting process based on melting or evaporation of workpiece material in zone of cut. Cut quality is very important characteristic of laser cutting that ensures the advantage in regard on other contour cutting processes. The paper presents results of research on the effects of laser cutting parameters on surface quality by laser cutting. In laser cutting, the edges of the workpiece have a characteristic grooved pattern. Groove lag refers to the greatest distance between two drag lines in the direction of the cut. This paper gives mathematical model to define drag line depending on the laser cutting parameters.

Key words: Laser, laser cutting, quality of laser cut, modeling of drag line

1. INTRODUCTION

Laser cutting is an attractive process for contour cutting of plate. It is the most accurate and cost-effective process and for some the only way to create new products. Laser cutting is thermal cutting process. Laser is generator of light beam. Laser beam is a high intensity beam of light. It can be focused into a very small spot (0.1-0.2 mm in diameter) on the workpiece surface by a lens or focusing mirror. The intensity of the focused laser beam typically is 10^7 - 10^8 W/cm². High concentrated light energy in the spot of the focused laser beam melts or evaporates almost any material in a fraction of a second. In laser cutting, highly concentrated light energy obtained by laser radiation is used for cutting of workpiece material in zone of cut. The laser beam is a new universal cutting tool that can cut almost all known materials. Laser cutting is an economical alternative to many other methods of cutting. Speed, flexibility and precision, which are the main features of laser cutting, reduce production costs significantly and quickly return investments. ([2], [3], [4])

2. LASER CUT QUALITY

The quality of the cutting laser treatment is determined by the size and shape accuracy and surface quality of cut. Assuming that the accuracy of the shape and dimensions of the features desk axis CNC laser cutting machines, quality control unit and a precision engineered parts, we can conclude that the quality of treatment reduces the quality of the cut. The quality of the cut refers to the geometry section, the parameters of the topography and physical-chemical characteristics of the material in the surface layer. The geometry of laser cut is defined by the cut width (s_r), the cut slope (β), the curve of the cutting edges (r) and the appearance of slag (h_s), figure 1 [1].

Visual observation of the laser cut surface may be noticed two zones: upper, in the area of the input laser beam, which is surface-treated with a fine regular grooves at the

distance 0.1-0.2 mm, and the lower zone, in the area of output laser beam, in which the cut surface roughened with grooves relating whether due to solvents and slag from the cutting zone. For this reason was adopted to measure the surface roughness of laser cut at a distance of one third of the thickness of the upper edge of the cut. The topography of the cut grade includes roughness, waviness and shape variations. It differs from the roughness of the cut in the direction of the laser beam axis and the roughness of the laser beam in the direction normal to the axis of the laser beam and the direction of the workpiece movement. Physical and chemical characteristics of the material in the surface layer section refer to the surface layer formed in the laser cutting and thermal effect of laser beam on the workpiece material. In doing so, we observe the microstructure of materials, hardness, appearance and size of residual stresses the oxide layer [1].

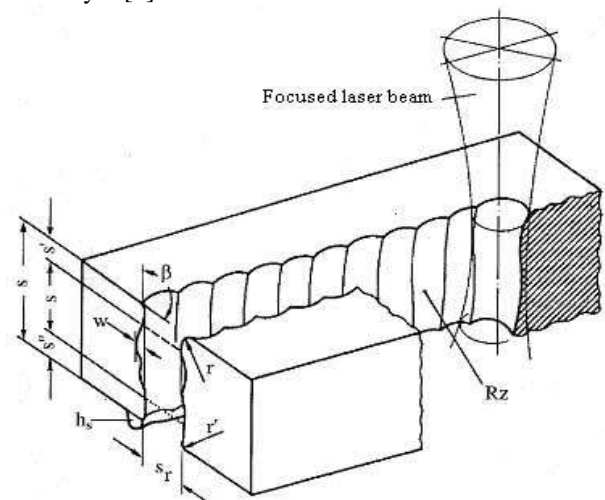


Fig. 1. Schematic view of the laser cut [1]

In laser cutting, surfaces of cut have a characteristic grooved pattern. At low cutting speeds, the grooves run

almost parallel to the laser beam. As the cutting speed increases, the grooves bend away from the direction of cutting. Groove lag refers to the greatest distance between two drag lines in the direction of the cut. The groove lag is evaluated visually. The evaluation is carried out on a picture of cut with the aid of a magnifying glass or microscope. These grooves or furrows are result from the regular shape forms a focused laser beam, the speed of movement of the workpiece and the process of creation, of relating and curing the incisional solvents.

The quality of processing in laser cutting process is influenced by many factors. All these factors can be grouped into effects:

1. The influence of laser cutting machines:
 - the influence of the laser source (wavelength, laser power, mode, polarization, stability and power mode)
 - the influence of optical transmission systems for laser beam (quality of mirrors)
 - the influence of cutting head:
 - The focusing system (lens quality, focal length, diameter of the focused beam, the depth of the focus);
 - Nozzle (shape, diameter hole, position relative to the workpiece);
 - Sensor positioning;
 - The influence of coordinate work table (accuracy of positioning, static and dynamic stiffness);
 - the influence of power supply systems (electrical power, gas supply, cooling system);
 - the influence of control units (increments of management, reliability).
2. The influence of laser beam (beam diameter, divergence, monochromatic, coherence, polarization).
3. The influence of workpiece:
 - influence of workpiece material (type, absorption, diffusion coefficient, coefficient of thermal conductivity, melting temperature, temperature of evaporation);
 - influence of workpiece geometry (shape, dimensions, tolerances);
 - surface quality and surface coatings;
4. The influence of the assist gas (type, purity)
5. The influence of processing parameters (laser power, cutting speed, assist gas pressure).

From these numerous factors have the greatest impact: laser power, material properties of the workpiece, cutting speed, type, purity and pressure of assist gas, laser beam characteristics and time stability of laser power, laser beam adjusting processing parameters, process of cutting and others. The most important characteristic which makes estimates of the machine is power laser radiation. Since the laser cutting process is heat, the amount of heat produced an influential factor which depends on the ability of the laser cutting. Having that other things being equal, increasing power of laser radiation allows cutting thicker materials and increased cutting speeds. Stable power, fashion and concentrating the energy of laser radiation (spatial and temporal) is a key factor for the application of lasers in materials processing technology. Cutting speed is the speed of the workpiece or the laser beam on the surface of objects. Can be determined

experimentally or by using the known dependence in which represented laser power density and properties of the material is cut. More parameters affect the speed of cutting: laser power, mode, size, light stains, the type and thickness of the workpiece, the initial melting and evaporation energy and so on. Taking into account the quality of cut and cutting speed by observing the function of the thickness of the workpiece can be useful to define the area of the cutting speed is limited by upper and lower curve. Outside of this area is an area of incomplete cutting. Within the area of usable cutting speed by changing the speed of cutting is done changing the cut quality (appearance and size of the slag, roughness, etc.). A variation of the focus position relative to the surface of the workpiece shows different characteristics on the quality of the cut. Depending on the type of material and thickness of the work focus is positioned at or slightly below the surface of the workpiece.

Assist gas in the area leads through the machining process in which the head has to be coaxial with the focused laser beam. Using assist gas to blow the melted and vaporized material of the work more easily drained from the cutting zone, which directly affects the purity and quality of cut. In addition, the melted material can not be re-cut and pre-hardened workpiece weld. Using assist gas to blow also prevents binding of slag on the back of the cut, and cutting speed can be increased to 40%. The task of the assist gas is in the process of cutting to protect the lens from the vaporized and melted material of the workpiece. For some metals is used reactive gas, oxygen, because it helps the exothermic reaction. Using oxygen as assist gas increases the total energy used in the process 40% of cutting so that it is possible to increase cutting speed by 25% compared to the cutting speed at which the air is assist gas. Besides the type of assist gas and purity of the assist gas have very significant impact on the processing parameters and quality of cut. Assist gas pressure affects the cutting speed and the speed of relating melted and vaporized material to the appearance of slag at the edges of origin section. Pressure decreases when increasing the thickness of the workpiece or the cutting speed is reduced. In the action of laser radiation on the workpiece in the formation of various vapors that are in the ground state or united with the ingredients of atmospheric air can be deposited on optical surface of the focusing element. This reduces laser radiation. In cases where the deposited layer of large, laser radiation can act on it as the material of the workpiece, and how it is on the lens, will cause damage. Larger particles are vaporized or molten material that can cause uncontrollable burst permanent damage to optical elements. A stream of assist gas which is directly in front of the lens blow protects it from damage. ([5], [6], [7])

3. EXPERIMENTAL TESTS

Experimental study was aimed to determine the influence of processing parameters on the quality of laser cut. It was examined the effects of laser power, cutting speed, assist gas pressure, and focus position on the surface quality, especially to grooves and drag lines.

Tests were performed at Bystronic laser cutting machine - BYSTAR 3015, in company "Metal Systems - Process Processing" of Kragujevac.

The material of the work is S235 JRG2 (Č0361), 15 mm of thickness. The material properties of samples are shown in Table 1.

Table 1. The material properties of samples

Type of material	Chemical composition			Mechanical properties
	C, %	Mn, %	Si, % P, S, %	R _e , N/mm ²
S235 JRG2 (Č0361)	≤ 0.17	≤ 1.40	0.03 - 0.30 ≤ 0.045	≥ 235

Testing refers to the quality of the optimal values of cutting parameters for material processing S235 JRG2 (Č0361) 15 mm of thickness, with varying processing parameters. Varying one parameter is taken by its maximum and minimum recommended value while other parameters have optimum values recommended by the manufacturer of laser machines for a given material.

Roughness measurement was carried out on the measuring device Talysurf-6. Using this measurement system parameter values were obtained by the surface topography of processed material.

This study was conducted with the following parameters:

- Laser power (kW): P = 4.3, 4.5, 5.1
- Cutting speed (mm/min): V_p = 1200, 1400, 1700
- Assist gas: O₂
- Pressure of assist gas (bar): p = 0.5, 0.7, 0.8
- Focus position (mm): f = 0.4, 0.5, 0.6

When testing was done cutting the panels 15 mm thick sections measuring 50 x 50 mm.



Fig. 2. Form of samples

Optimal values of the parameters regime, recommended by the manufacturer of machines, material thickness 15 mm are:

- Laser power (kW): 4.5
- Cutting speed (mm/min): 1400
- Assist gas O₂ pressure (bar): 0.7
- Focus position (mm): 0.5

Sample 1 was processed with these regimes.

The analysis of test results show that influence of laser cutting parameters on surface quality can conclude the following:

1. Increasing the distance from the focus of the work negatively affect the surface roughness, or you get worse surface quality,

2. Increase speed of movement of support slightly affects the quality of treatment within certain limits, provided that a significant increase in speed leads to weld site incision and drainage of molten material impossibility,
3. Increasing the power of the laser beam affecting the surface quality,

The influence of assist gas pressure is negligible.

After measurement, surface topography, carried out the measurement deviations from the line of cut a straight line, as figure 3. These measurements were aimed at determining the influence of laser cutting regimes on grooves and the drag lines and to determining the equations of drag lines.

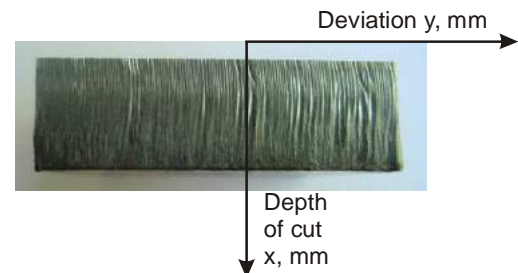


Fig. 3. The position of the coordinate system for measuring deviations of drag lines

To determine the equation, was determined by measuring variations in each 3 mm. As the best shape that represents the wrong line of cut adopted in equation

$$y = a x + b x^2 \quad (1)$$

In Figures 4, 5 and 6 are shown the surface obtained by laser cutting and cut the curve represented mathematically depending on the parameters of laser cutting regimes.

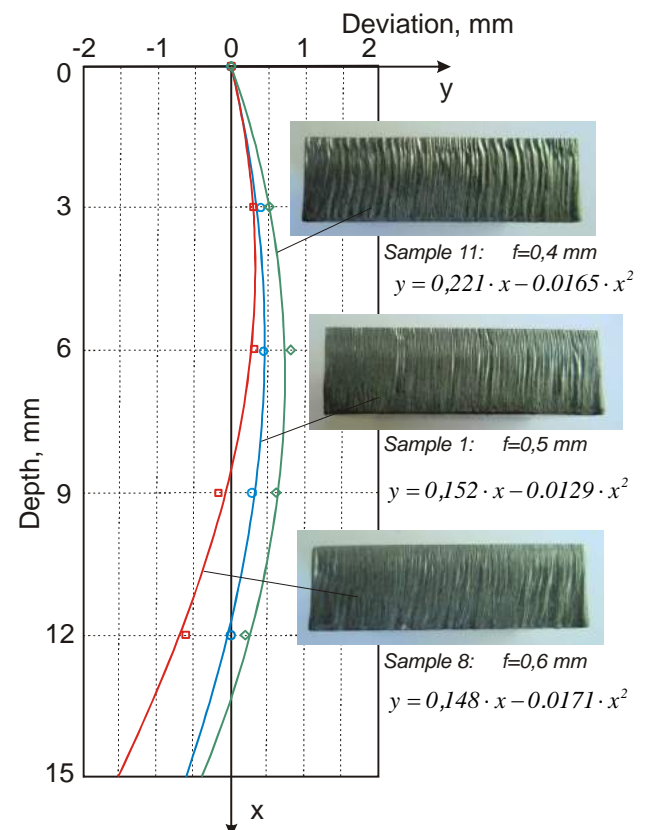


Fig. 4. Drag lines in dependence of focus position

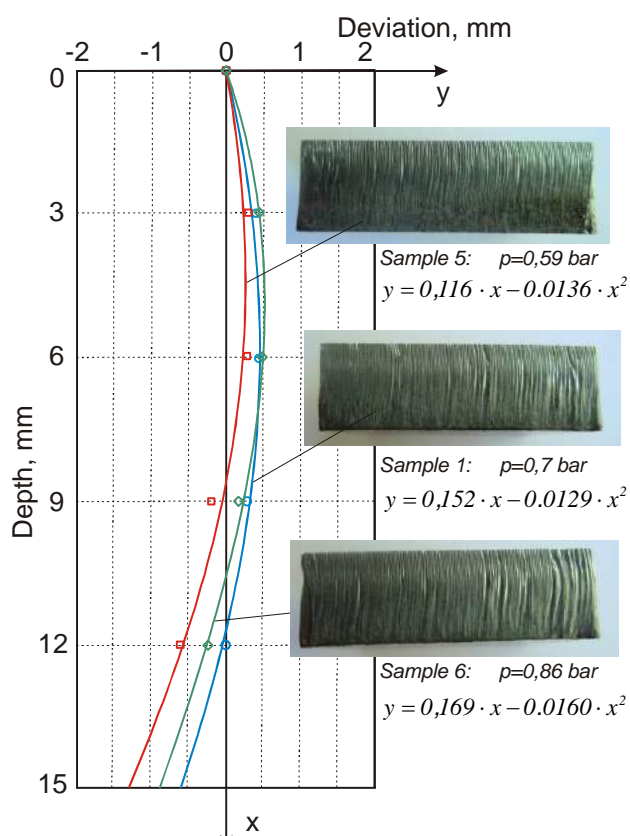


Fig. 5. Drag lines in dependence of pressure of assist gas O_2

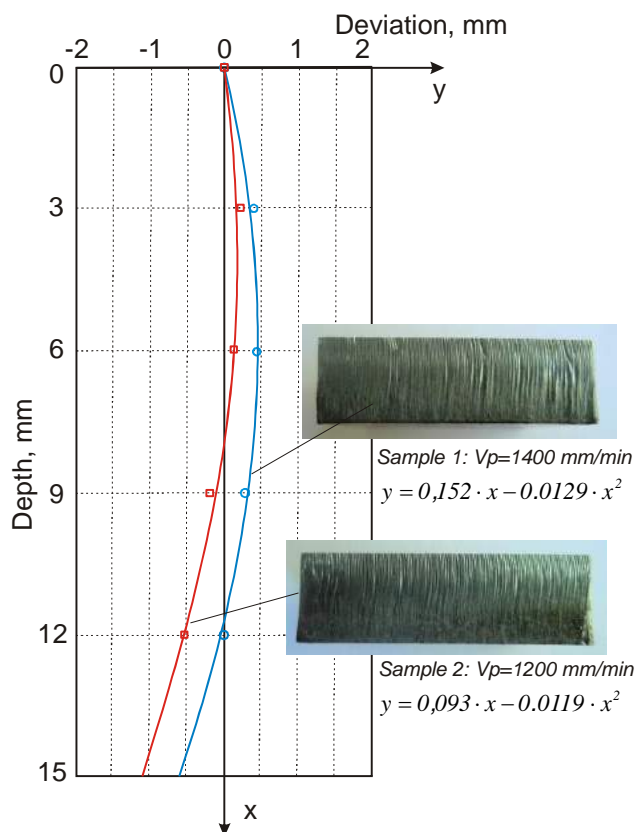


Fig. 6. Drag lines in dependence of cutting speed

4. CONCLUSION

Technological problems related to the application of laser machines for cutting materials have insufficient knowledge of the application of laser techniques and non-existence of a lack of reliable information and practical knowledge of the influential parameters on the process of treatment. Knowledge of the laser cutting process, and its dependence on various factors, make it possible to achieve the required quality of cut and at the same time achieve maximum productivity. By establishing the legality of the processing quality and treatment process of influential factors is necessary to build the appropriate database. Integrating knowledge and data in computer-supported preparation of production achieved maximum technical and economic effects.

Experimental study was aimed to determine the influence of processing parameters on the quality of laser cut. Experimental researches related to surface quality of carbon steel S235 JRG2 (Č0361) and were performed at Bystronic laser cutting machine - BYSTAR 3015. It was examined the effects of focus position, pressure of assist gas and cutting speed on the grooves and drag lines.

Applied experimental studies have shown that the curvature of drag lines can be represented by a mathematical curve in the form of $y = ax + bx^2$.

The analysis of test results shows that the parameters of laser cutting have influence to form of curvature of drag lines. It can be concluded that some parameters have significant influence. Drag line may well be present by mathematical second-order polynomial model. To establish the drag line equations depending on the regime of laser cutting parameters it is needed one extensive investigation with the exact definition of the beginning of the defined parameters.

ACKNOWLEDGEMENT

This paper is part of project TR35034 "The research of modern non-conventional technologies application in manufacturing companies with the aim of increase efficiency of use, product quality, reduce of costs and save energy and materials", funded by the Ministry of Education and Science of Republic of Serbia.

REFERENCES:

- [1] RADOVANOVIĆ, M., (2003), *Features of laser cut surface*, 3th International Conference RaDMI 2003, Herceg Novi, Serbia&Montenegro, pp. 486-491
- [2] ČURČIĆ, S., (2005), *Non-conventional machining processes*, Technical Faculty, Čačak.
- [3] MILIKIĆ, D., (2002), *Non-conventional machining processes*, Faculty of technical Engineering, Novi Sad.
- [4] LAZIĆ, M. (1990), *Non-conventional machining processes*, Mechanical Engineering, Kragujevac, 1990.
- [5] TRAJKOVSKI, S., DUDESKI, LJ., (1999), *Nekonvencionalni metodi na obrabotka*, Mašinski fakultet, Skopje.
- [6] <http://sr.wikipedia.org/sr-el/Laser>
- [7] <http://www.esabcutting.com/cutting/en/process/laser-cut-quality.cfm>



MACHINING PARAMETERS EFFECT ON THE JET RETARDATION IN ABRASIVE WATER JET MACHINING

Jelena BARALIĆ¹, Bogdan NEDIĆ², Predrag JANKOVIĆ³

University of Kragujevac, Technical Faculty Čačak, Serbia, jbaralic@tfc.kg.ac.rs
University of Kragujevac, Faculty of mechanical engineering, Serbia, nedic@kg.ac.rs
University of Niš, Faculty of Mechanical Engineering, Serbia, jape@masfak.ni.ac.rs

Abstract: Abrasive water jet machining is frequently used in industry. It is one of the most versatile processes in the world. Very different materials can be machined using this method. The basic advantage of abrasive water jet machining is that no heat affected zones or mechanical stresses are left on a abrasive water jet cut surface. The main disadvantages of abrasive water jet machining are irregularities on the machined surface such as differences in surface roughness at the top and bottom, and the appearance of curved lines - jet retardation. The machining parameters have a great influence on these phenomena. The aim of this paper is to investigate the effect of machining parameters on appearance of curved lines-jet retardation. Č4580 (AISI 304) was machined by abrasive water jet under varying traverse speeds, water jet pressures and abrasive flow rates. The machined surfaces were examined and jet retardation was measured. The experimental results indicate that there is firm correlation between water jet retardation and referred machining parameters.

Key words: abrasive water jet, traverse speed, jet retardation, surface roughness

1. INTRODUCTION

If all you have is a hammer, everything looks like a nail. This saying best explains our traditional view of the machining, where the cutting tools are made of hard material and must have at least one cutting edge. More than fifty years ago a new machining procedure appeared. The tool was quite different from the conventional understanding. In the early seventies the first machine for this machining was produced. This procedure was the water jet machining, and the tool was a clean water jet. In the eighties, this method was enhanced by adding abrasive material into the water jet and thus a new procedure for machining (abrasive water jet machining) was created.

Abrasive water jet proved to be ideal for processing of very hard and brittle materials, and easy to handle fragile materials. It is also good for machining in cases that have limitations in terms of clamping force [6].

Abrasive water jet belongs to a group of contour processes. However, it fails to achieve satisfying accuracy and quality of the cut. The main causes for inaccuracy are taper of the cut and jet retardation. The taper can be compensated, but the problem of the jet retardation has not yet been solved.[3]

2. ABRASIVE WATER JET MACHINING

With abrasive water jet cutting, the water jet serves primarily as an energy transmission medium for accelerating the abrasive. The higher the speed with which the solid particles hit against the material to be cut, the higher the removal rate is.

The most common operations that can be performed with abrasive water jet machining are: cutting, surface polishing, surface cleaning, etc.. In all cases, the processing mechanism is based on erosion. [4]

Figure 1 shows the installation for abrasive water jet machining on which the experiment has been carried out.



Fig.1. Installation for abrasive water jet machining

Modern installations for the abrasive water jet machining work with water pressure over 5000 bar, where the water jet reaches speed up to 1400 m/s.

Schematic of abrasive water jet machining is shown in Figure 2.

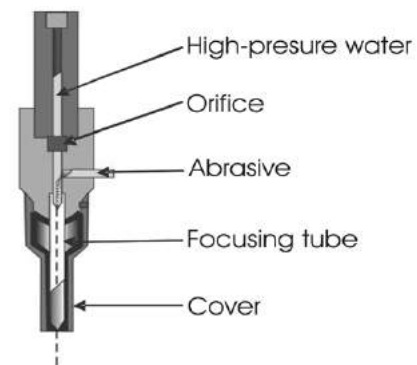


Fig.2. Schematic of abrasive water jet processing

Abrasive water jet machining shown in Figure 2 is the classic variant – abrasive injector water jet machining. Abrasive water jet machining works with water jet that is accelerated across the orifice. In the mixing chamber, the high speed water jet generates a vacuum with which the abrasive is mixed with the water jet. This mixture is accelerated and focused in the focusing tube.

3. SURFACE MACHINED WITH ABRASIVE WATER JET

The largest problem with abrasive water jet machining, is a disparity in quality of the machined surface. This disparity is manifested at different parameters of surface roughness, machined surfaces deviation from the vertical plane-taper of the cut and the appearance of curved lines on machined surface-jet retardation. All these phenomena significantly affect the restrictions of using abrasive water jet machining.

Figure 3 shows the appearance of the surface machined with abrasive water jet and the change of quality of the machined surface, i.e. the change of the roughness of the machined surface for different depths of the cut.

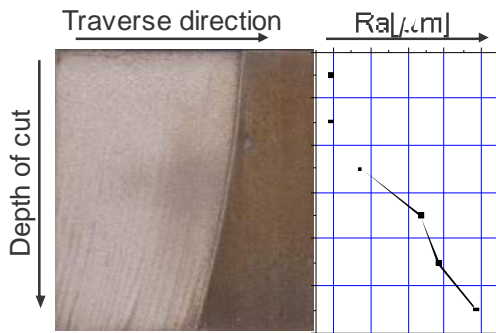


Fig.3. Changes of appearance and quality of machined surfaces by abrasive water jet, depending on the depth of cut

Surface roughness and its changes depending on the depth of cut is the most important parameter to evaluate the effect of certain machining parameters on the quality of the machined surface. [6]

Various cut qualities and degrees of precision can be created with abrasive water jet cutting. Workpieces cut with the abrasive waterjet are divided into five quality levels, Figure 4.

- Q1 – theoretical separation cut: the workpiece was (with high traverse speed) just roughly parted. It requires additional force to separate the workpiece.
- Q2 – separation cut: the workpiece was also just roughly parted. Due to a slight reduction of the traverse speed, the separation cut displays increased process stability.
- Q3 – production cut: the production cut is a quality level selected for economic reasons. It offers good quality with economical traverse speed.

- Q4 – quality cut: the quality cut distinguishes itself through high precision of the workpiece and low surface roughness.
- Q5 – the highest quality: the highest precision of the workpiece and the lowest surface roughness, but produced with very low traverse speed.

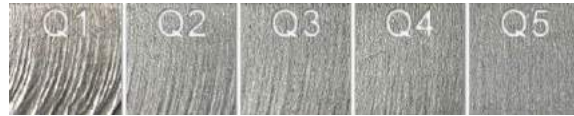


Fig.4. Five characteristic surface qualities

On the surfaces machined with abrasive water-jet in almost all stated surface qualities, curved lines typical for abrasive water-jet machining can be detected. The lines in the upper zone of the machined surface are almost vertical, whereas in the lower zone they are curved. End of the upper zone is commonly called limit zone of fine machining. After this limit, appearance of curved lines is becoming ever more prominent and the increase of the surface roughness is significant.

The curved lines can be more easily discerned on the surfaces in the lower qualities (Q1 and Q2) which occur during machining at high traverse speeds.

This phenomena can be related to the jet loss of energy during the cutting process, i.e. retardation of the cutting front of the abrasive water jet in material. Retardation of the cutting front shows the jet direction through workpiece material. The jet loss of energy causes the change of quality of the machined surface and the abrasive water jet retardation–jet retardation–Yret, Figure 5.



Fig. 5. Jet retardation

The jet retardation results in diversion on the exit edge, which cause geometry errors especially on corners and radius, Figure 6.

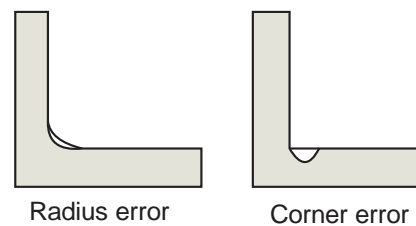


Fig. 6. Radius and corner error

The jet retardation can also result in imprecision at the beginning and at the end of cut, as well.

4. MACHINING PARAMETERS EFFECT ON THE JET RETARDATION

All irregularities on the machined surface, obtained either by the standard or unconventional treatment processes (laser, plasma, abrasive water jet), are machined surface characteristics, and they are precisely standardized [6]. The object of interest of this research is the effect of machining parameters on the retardation of the abrasive water jet. The quality of the surface machined by the abrasive water jet can be influenced by machining parameters such as traverse speed, waterjet pressure, abrasive flow rate, standoff distance, depth of cut and angle of cutting [1], [2]. Influence of individual parameters is different. The largest number of authors agree that the most influential are traverse speed, waterjet pressure and the abrasive flow rate [3].

This paper presents an analysis of traverse speed, water jet pressure and abrasive flow rate effect on the jet retardation for stainless steel Č4580 (AISI 304).

Figure 7 shows the appearance of machined surfaces of 30 mm thick Č4580 for different traverse speeds.

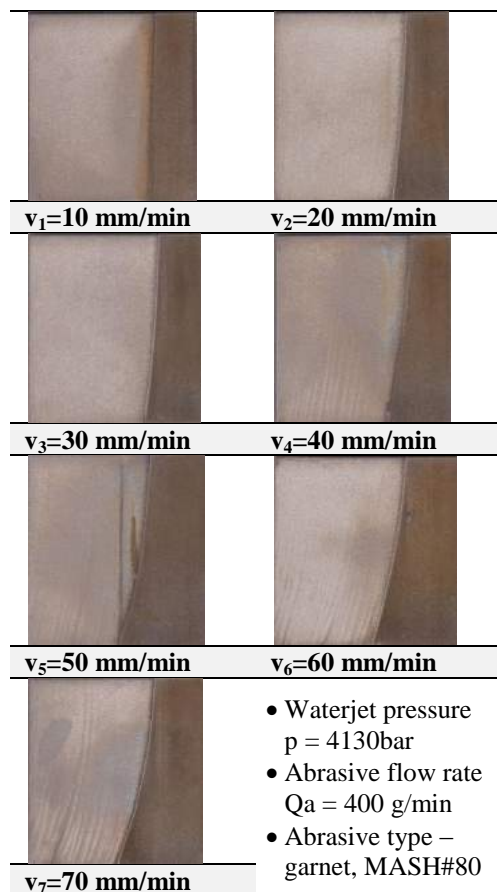


Fig.7. Appearance of machined surface depending on traverse speed [6]

The Figure 7 indicates that during machining process at traverse speed of 10 mm/min, no significant difference in quality of the machined surface occurs. During machining process, with higher traverse speeds, the difference in quality of the machined surface is more distinct and it varies depending on depth of the cut. Also, jet retardation compared to the vertical line is increasing. Figure 8 shows

the appearance of machined surfaces of 30 mm thickness Č4580 for different water jet pressure.

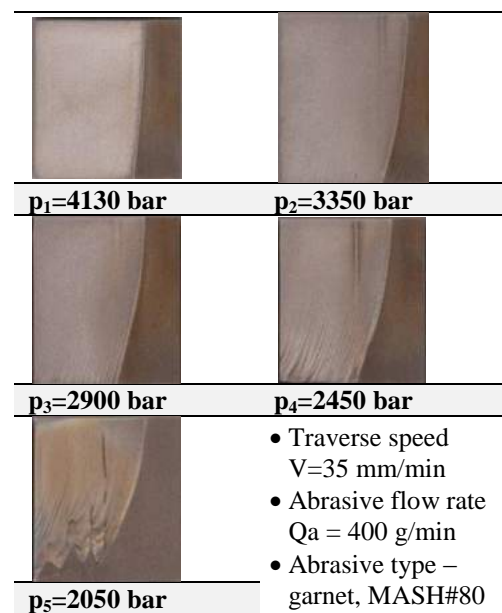


Fig.8. Appearance of machined surface depending on water jet pressure

The Figure 8 indicates that during machining process at water jet pressure of 4130 bar, no significant difference in quality of the machined surface occurs. Also, jet retardation compared to the vertical line is insignificant. During machining with lower water jet pressures difference in quality of the machined surface is more distinct and jet retardation is considerable. Machining with water jet pressure of 2050 bar was not possible.

The Figure 9 shows the appearance of machined surfaces of 30 mm thickness Č4580 for different abrasive flow rates.

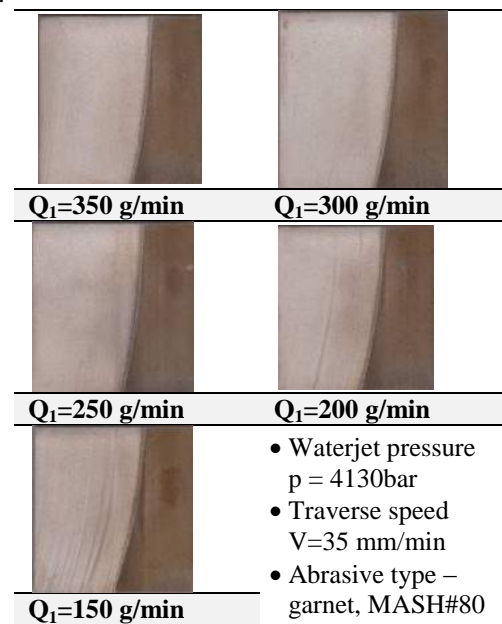


Fig.9. Appearance of machined surface depending on abrasive flow rate

Figure 9 shows that during machining with higher values of abrasive flow rate – 400 g/min the difference in quality of the machined surface and jet retardation is not

significant. Machining with lower abrasive flow rates results in increase of difference in quality of the machined surface and increase of jet retardation.

In order to observe the differences more carefully, the deviation of the line of cut - jet retardation from the vertical line, at different depths of cut has been measured. These measurements were performed at 10 points at depth of cut (every 3 mm).

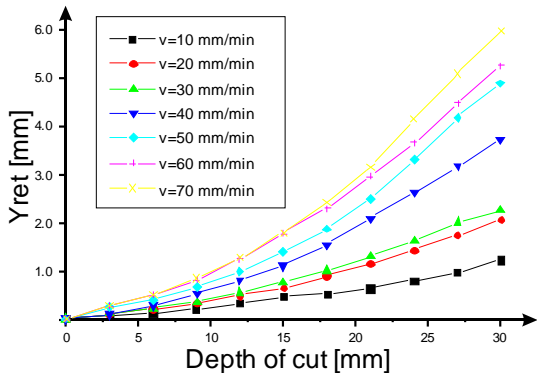


Fig.10. Jet retardation for different traverse speed

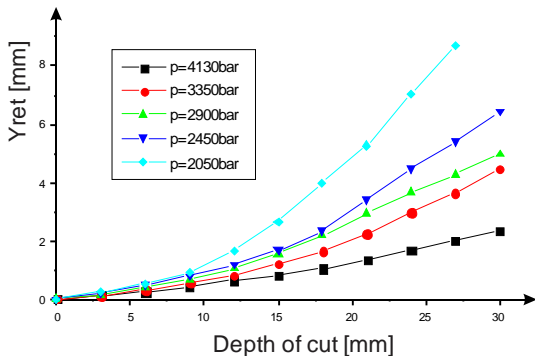


Fig.11. Jet retardation for different water jet pressures

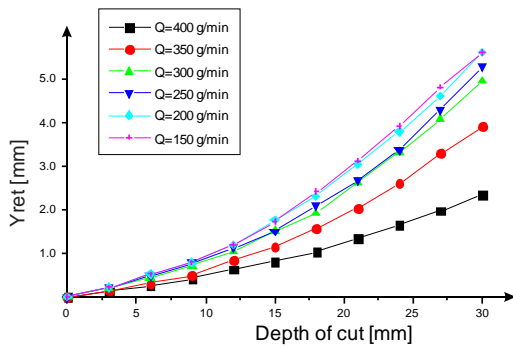


Fig.12. Jet retardation for different abrasive flow rates

Figures 10, 11 and 12 shows changes in jet retardation as function of traverse speed, water jet pressure and abrasive flow rate. Figure 10 infers the rise of the water jet retardation with the rise of traverse speed. Figures 11 and 12 infer decrease of the water jet retardation with increase of water jet pressure and abrasive flow rate. This clearly suggests firm correlation between water jet retardation and referred machining parameters .

5. CONCLUSION

The paper presents the results of the research concerning the machining parameters effect on the change of the abrasive water jet retardation.

The effect of the traverse speed on the jet retardation is evident. Higher values of the traverse speed cause higher retardation of the abrasive water jet. It has also been observed that the increase of abrasive water jet pressure causes the decrease in the abrasive water jet retardation. Also, abrasive flow rate has a significant influence on the retardation of the abrasive water jet. Higher values of abrasive flow rate cause lower water jet retardation.

It is also a significant influence of the depth of cut on the retardation of the jet. With the increasing depth of cut the retardation of the jet increases.

Therefore, high quality of the machined surface can be achieved through the machining with abrasive water jet by selecting the machining parameters.

Choosing appropriate combination of machining parameters, significant water jet retardation can be avoid. In this way errors in contour cutting with abrasive water jet machining can be reduced.

ACKNOWLEDGEMENT

This paper is part of project TR35034 The research of modern non-conventional technologies application in manufacturing companies with the aim of increase efficiency of use, product quality, reduce of costs and save energy and materials, funded by the Ministry of Education and Science of Republic of Serbia.

REFERENCES

- [1] HASHISH, M. (1984) *A modelling study of metal cutting with abrasive waterjets*, J. Eng. Mater. Technol., Vol. 106, pp. 88-100
- [2] VALIČEK, J., HLOCH, S., KOZAK, D. (2009) *Surface geometric parameters proposal for the advanced control of abrasive waterjet technology*, Adv. Manuf. Technol., 41, pp. 323-328
- [3] ORBANIC, H., JUNKAR, M. (2008) *Analysis of striation formation mechanism in abrasive water jet cutting*, Wear, 265, pp. 821-830
- [4] MOMBER, A.W., KOVACEVIC, R.,(1998) *Principles of Abrasive Waterjet Machining*, Springer
- [5] JANKOVIĆ, P., RADOVANOVIĆ, M., (2010) *Identifikacija i klasifikacija faktora koji utiču na proces sečenja abrazivnim vodenim mlazom*, IMK-14, istraživanje i razvoj, broj 35, Srbija, s.71-76
- [6] BARALIĆ, J., NEDIĆ, B., JANKOVIĆ, P., (2011) *The traverse speed influence on surface roughness in abrasive waterjet cutting applications*, Proceedings of the 12th International Conference on Tribology, SERBIATRIB, Kragujevac, 11-13. Maj, 349-353

34th INTERNATIONAL CONFERENCE ON PRODUCTION ENGINEERING



SECTION K

**JOINING AND CASTING TECHNOLOGIES
PROCESSING OF NONMETAL MATERIALS (PLASTIC, WOOD, CERAMICS, ...)**



ANALYSIS AND DESIGN OF HIGHLY EFFICIENT METHODS OF TREATMENT

Michael KHEIFETZ, Natalia POZILOVA, Alexander PYNKIN, Leonid AKULOVICH

The State Scientific and Production Amalgamation "Center" of the National Academy of Sciences of Belarus,
Nezavisimosti Avenue, 66, Minsk, Belarus
kheifetz@presidium.bas-net.by, mlk-z@mail.ru

*Belarusian State Agricultural Technical University, Nezavisimosti Avenue, 99, Minsk, Belarus

Abstract: Analysis of the self-organization processes in deposition, thermal treatment, deformation, and cutting of surface layers of items, as well as in combined methods of treatment, i.e. in deposition of coatings and thermal treatment combined with deformation and cutting, shows that a technological complex can work continuously and stably in an automatic mode requiring no external control. This gives reasons for the technological complexes designed as autonomous flexible production modules to be used for combined electromagnetic and thermomechanical treatment of workpieces.

Key words: self-organization, processes of deposition, thermal treatment, technological complex

1. INTRODUCTION

Development and adoption of new methods of treatment based on combination of different types of energy or effects on the treated material is a promising trend in machine building.

Generally, a system model of technology [1] is represented by a combination of three input flows: substance, energy, information. It may be reasonable to consider the use of energy and information subsystems for these purposes. The first supplies and converts energy necessary to affect an intermediate product in order to change its physical and mechanical properties, to remove or to deposit material. It is specified by the form of treatment. The second controls the flows of energy and substance, providing them in the required quantities to the prescribed place of the working volume so that to ensure the certain form, size and properties of the workpiece surface.

2. FORMATION OF A SURFACE LAYER BY METHODS OF TREATMENT

It is expedient to consider the process of treatment as some energy system affecting an intermediate product so that transition from one state to another corresponding to a new quality is provided [2]. This effect is achieved in several stages. At the first stage, the supplied energy is converted to working energy, E_w , by technological equipment. At the second stage, the working energy is converted to the energy of the effect, E_{eff} , on the treated object. At the third stage, the energy of the effect leads to the formation of physicochemical mechanisms, $M_{ph.-ch.}$, of treatment of the intermediate product that are a main element of the method of treatment parameters formation (efficiency, energy consumption, quality of the surface, etc.).

Thus, the process of treatment (PT) represents a chain of energy conversion

$$PT = \{E_w \Rightarrow E_{eff} \Rightarrow M_{ph.-ch.}\}. \quad (1)$$

Processes of shaping (Sh) are characterized by the components [2]

$$Sh = \{M_{e,s}, F_{d,e}, K_{sch.t}\} \quad (2)$$

and features of them: point, linear, surface, volumetric sources for $M_{e,s}$; continuous, oscillating, pulse effect for $F_{d,e}$; rectilinear, rotary, two rectilinear, rotary-translational motion or its absence for $K_{sch.t}$.

As a result, all methods are first subdivided into three classes: with removal, without removal, and with deposition of the material. Second, subclasses which characterize the types of energy used in treatment of the material are distinguished for each class. Third, there exist differences in the character of the physicochemical effect and, fourth, in the type of instrumentation used and the kinematics of treatment [1].

On the basis of this classification, there are suggested the generalized models of the method of treatment (MT), which are usually represented [2] by analytical expression of the form

$$MT = \{N_{m,t}, RA_{m,t}, E_w, E_{eff}, M_{ph.-ch.}, K_{sch.t}, F_{d,e}, M_{e,s}, S, G\}, \quad (3)$$

where $N_{m,t}$ is a name of the method of treatment; $RA_{m,t}$ is a range of application of the method of treatment; S is a scheme of location and fastening of intermediate product; G is a treating instrument.

Formulas (1) - (3) give a rather complete and clear idea about the structure and composition of the processes of treatment and shaping components. It would be convenient to use them for the new technological procedures and methods of shaping development, yet they are of no effect when any logical operations and transformations are needed. To formalize the conditions of target-oriented formation of new methods of treatment, each aggregate of like components r_i is described as some

set of technological solutions R_i . This approach [3] allows each method of treatment $r_{m,t}$ to be represented in the form of a procession

$$PT = \{E_w \Rightarrow E_{\text{eff}} \Rightarrow M_{\text{ph.-ch}}\}. \quad (4)$$

where r_{surf} is a treated surface of workpiece; r_{mat} is the treated material; r_t is a type of the method of treatment application area; $r_{\text{eff.mat}}$ is the means to effect the material of intermediate product; $r_{e,s}$ is a type of energy supplied to the working zone; $r_{m.e.s}$ is the means of energy supply to the working zone; $r_{e,\text{sour}}$ is an energy source; $r_{e,m}$ is an energy mode of treatment; r_i is the treating tool; r_k is a type of kinematic scheme of treatment; r_{st} is a static scheme of treatment.

Each element of procession (4) is a component of the corresponding set of technological solutions, i.e., $\{r_i\} = R_i$ or $r_i \in R_i$.

The presence of a specific property α in a technological solution r_i is expressed by the corresponding predicate

$$E_\alpha(r_i), \quad (5)$$

which confirms that the technological solution r_i possesses the property α .

Each property α can acquire many values θ_α . Then the expression

$$E_\alpha(r_i) \wedge \theta_\alpha \quad (6)$$

indicates that the technological solution r_i possesses the property α and the value of the latter is θ_α .

Predicate (5) allows one to choose a technological solution with a given property, the value of which is determined by formula (6).

In general, a technological solution r_i is characterized by a number of properties $\alpha, \delta, \dots, \gamma$, each of which can acquire different values; this is expressed by the formula

$$\forall r_i \exists \alpha \exists \delta \dots \exists \gamma \{ [E_\alpha(r_i) \wedge (\bigvee_{j=1}^n \theta_{\alpha j})] \wedge [E_\delta(r_i) \wedge (\bigvee_{k=1}^m \theta_{\delta k})] \wedge \dots \wedge [E_\gamma(r_i) \wedge (\bigvee_{p=1}^q \theta_{\gamma p})] \}.$$

Certain relationships can exist between the values of the properties of the solution r_i and not every combination of them is admissible, i.e., the technological solution r_i possesses the property α with the value $\theta_{\alpha n}$ and the property δ , the value of which is determined by the set $\theta_{\delta p j}$. This situation is described by the relation

$$\exists \alpha \exists \delta \forall r_i [E_\alpha(r_i) \wedge \theta_{\alpha n} \rightarrow E_\delta(r_i) \wedge (\bigvee_{j=1}^k \theta_{\delta p j})].$$

We assume that if any two components of the method of treatment possess at least one common property, then a relationship of commonality of properties exists between them. This makes it possible to organize the selection of technological solutions by equivalency and preference [3]. Unlike solutions, with the combinations of their properties corresponding to each other, are chosen by the first characteristic:

$$\exists \alpha \forall r_i \forall r_j [E_\alpha(r_i) \wedge E_\alpha(r_j) \wedge (\theta_\alpha^{r_i} = \theta_\alpha^{r_j}) \rightarrow (r_i \approx r_j)] \quad (7)$$

and like solutions possessing the best values of the required properties are chosen by the second characteristic

$$\exists \theta_\alpha \forall r_{i1} \forall r_{i2} [E_\alpha(r_{i1}) \wedge E_\alpha(r_{i2}) \wedge (\theta_\alpha^{r_{i1}} h \theta_\alpha^{r_{i2}}) \rightarrow (r_{i1} \approx r_{i2})]. \quad (8)$$

According to (7), (8), this approach allows one to formalize the search for a technological solution r_i by the specific value of the determined criterion of selection t_q :

$$\theta_\alpha^{r_i} h t_q, \quad (9)$$

where h is a symbol of preference ratio, which can acquire values $>, \geq, <, \leq$.

Then a combination of predicates of the type (9) allows one to select the solution r_i by several criteria of selection $t_{q1}, t_{q2}, \dots, t_{qn}$, which correspond to n different properties of the solution r_i . In this case the condition of selection of the solution r_i takes the form

$$\bigwedge_{j=1}^n (\theta_{\alpha j}^{r_i} h_j t_{qj}) \quad (10)$$

Use of expression (10) in problems of selection of unlike technological solutions possessing different but mutually dependent properties α and δ (i.e., the condition $E_\alpha(r_i) \rightarrow E_\delta(r_j)$ is valid) allows one to organize the selection of solutions

$$\exists \theta_\alpha \forall r \forall r_j [E_\alpha(r_i) \wedge E_\delta(r_j) \wedge (\theta_\alpha^{r_i} h_1 t_1) \wedge (\theta_\delta^{r_j} h_2 t_2) \rightarrow (r_i \approx r_j)]. \quad (11)$$

However, in general, condition (11) is not valid, since the interrelations of the properties $E_\alpha(r_i) \rightarrow E_\delta(r_j)$ of the solutions r_i and r_j are often unknown. Moreover, in substantiating the selection of technological solutions and the synthesis of combined methods one must allow for stability of formation of the parameters of the quality of treatment and consider the mechanisms of control over stability of the technological process using feedback [4]. Therefore, it is suggested to use criteria of self-organization as an object function instead of specific values of the combination of the criteria of selection $t_{q1}, t_{q2}, \dots, t_{qn}$, since the conditions providing self-organization of surface phenomena and stabilization of formation of the parameters of the quality of treatment are a consequence of an excess structural composition of the considered technological system [5].

3. ANALYSIS OF SELF-ORGANIZATION OF SURFACE PHENOMENA

Interrelated processes of motion and exchange of material and information flows in a technological system are described by the entropy [6, 7]

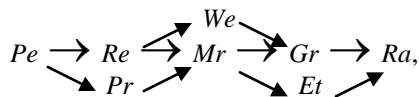
$$\varepsilon = -k \int_0^\infty p \ln p dp,$$

where ε is an entropy; k is a constant factor; p is a density of the subsystem probable states distribution.

The production of entropy $\sigma = d\epsilon / dt$ makes it possible to consider the criteria describing different states of the working zone of the technological system.

A study of the state of the working zone and investigation of self-organization of technological processes in combined methods of treatment [8] allowed one to consider the model of analysis of the articles formation processes.

Analytical model of the structural changes and phase conversions of the treated material, establishes the sequence of the structures and phases formation with increase of the power of effects by the criteria of transfer



where Pe – Peclet number; Re – Reynolds number; Mr – Marangoni number; Gr – Grashof number, Ra – Rayleigh number; We – Weber number; Pr – Prandtl number; Et – thermoelectrical number.

Use of the criteria of the structures and phases formation greatly decreases the volume of experimental studies of the processes of a surface layer formation in highly efficient methods of treatment.

In cases when the physicochemical mechanisms of a surface layer formation are unknown, it is suggested to describe the processes by the laws of distribution of random quantities rather than by a system of balance equations [8].

The Romanowski relation [9]

$$R = (\lambda_p^2 - k) / \sqrt{2k}, \quad (12)$$

where λ_p^2 is the Pierson criterion; k is the number of degrees of freedom used in calculation of theoretical distribution of statistical characteristics, allows one to judge the degree of correspondence of the statistical data to the selected law of distribution.

A statistical analysis of the parameters of quality of the studied methods of treatment makes it possible to distinguish the most substantial technological factors and to reveal the interrelations between them. Formation of technological rules of the studied methods of treatment only from narrow ranges of the modes restricted by the conditions of self-organization provides conditions for stabilization of the parameters of quality of a surface layer.

In selecting the number of elements and processes realized by a technological complex it is expedient to consider the interrelation of conflicting requirements to a production system on its reliability and plausibility. The reliability-stability and flexibility-adaptivity relationship can serve as a criterion which allows one to decide on a rational structure of a technological complex.

In self-organizing systems one can control flexibility and reliability by changing the number of subsystems [4]. Each subsystem i has a strictly defined q_1 and a fluctuating with scattered characteristics q_2 . The total yield of the system to a first approximation with account for the additivity of the material and information flows is

$$q^{(i)} = q_1^{(i)} + q_2^{(i)}. \quad (13)$$

Assuming that under the conditions of production $q^{(i)}$ is an independent random quantity, we present the total yield as

$$Q = \sum_{i=1}^n q^{(i)} \quad (14)$$

Total yield (14), according to the central limit theorem [4], increases in proportion to the number of subsystems n , whereas the degree of scattering increases in proportion to the square root \sqrt{n} , similar to relation (12). These estimates are based on an analysis of linear relation (13); in fact, the feedback inherent leads to even more substantial suppression of scattering of the characteristics. Thus, it is expedient to create technological complexes of highly efficient treatment providing stabilization of the parameters of quality of a part and automatic control over technological processes with self-organization of surface phenomena as key factor.

4. MATCHING OF PROCESSES IN COMBINED METHODS

Simultaneous use of several energy fluxes transferred to the working zone by both a technological medium and instrumentation with control elements sharply increases the efficiency of technological operations [8]. However, in the combined use of several fluxes there arise technological limits to stability of combined processes. Therefore, principally new technological complexes for combined treatment can now be created on the basis of self-organization in technological systems [10].

To produce articles by technological complexes, the thermomechanical and electromagnetic flows of substance and energy can be used, since the processes of the production objects surface formation, up to micron accuracy, have basically a thermomechanical character, and electromagnetic flows (due to their simplicity of formation and convenience of monitoring) are most technological.

We consider the whole range of technological operations: deposition, thermal treatment, deformation and cutting of surface layers of treated articles, and the principal combinations of them which should be realized by technological complexes in combined electromagnetic and thermomechanical treatment of articles. The method of electromagnetic fusion is used for deposition of a surface layer, in which particles of ferromagnetic powder are aligned with electrode chains in a constant magnetic field, and, as a result of electric-arc discharges, are welded to the surface of the blank. This method enables to deposit coatings of only a certain thickness; then the formed layer loses stability, and protrusions formed on the surface are destroyed in subsequent discharges. The processes of surface formation are controlled by electromagnetic flows, which, besides the fixation of ferropowder particles, provide intense heat release at the joints and, regardless of the powder used, control the weld layer thickness, changing its electric resistance.

Local inductive electric-contact heating or electric-spark discharge, which, besides heating, alloy the surface layer of the treated articles using ferropowder particles or additives put to lubricating and cooling fluids, are used

for surface thermal treatment of products. Electromagnetic flows in the working zone allow to control both the depth and degree of surface layer strengthening in thermal treatment.

Ball rollers are used in technological complexes to strengthen the deformation and change the form of surface layers. In surface plastic deformation, additional degrees of freedom allow the ball, as a result of interaction with the treated surface, to rotate as well as to swing. Without additional heating, the degree of deformation is small and the trajectory of the ball has a loop-like character. In heating, the treated material goes to a plastic state, thus making the degree of deformation and the coefficient of friction increased. This impedes rotation and decreases the length of, first, the peak-like and, then, sinusoidal trajectory of the ball, thus leading to a decrease in the intensity of plastic deformation. So, the process of surface plastic deformation can be controlled by a thermal effect and additional rotation of the ball.

A technological complex makes cutting by traditional cutters, milling cutters, emery disks, and a free abrasive in a magnetic field.

When cutting by traditional cutting tools during treatment with preheating, the equilibrium of intensities of temperature weakening and deformation strengthening is violated, and the zone of chip formation loses stability and begins to shift, changing the shear angle. In this case the process of chip formation can be controlled by additional displacement of the rotating tools, which prevents frozen metal fastening to the blade and restores the working part of the cutting edge, thus excluding a jump of temperature in a localized zone of chip formation. When grinding by an emery disk, with an increase in depth of cutting in incision or oscillations of the allowance, the forces of cutting and friction increase, which facilitate active crumbling-out of abrasive particles of the disk. Due to this, the disk wear and the velocity of transfer of crumbled heated particles increase. As a result, the forces of cutting and friction decrease, thus decreasing the intensity of the crumbling process. These oscillations of intensity, by restoring the abrasive particles of the disk, enable to control the process of grinding.

Treatment of viscous and plastic materials by an emery disk leads to its greasing, thus impeding self-sharpening. In this case the process of grinding is controlled by electromagnetic flows in magneto-abrasive treatment in which metal is removed by unfastened grains of abrasive powder with a ferromagnetic coating under the effect of a constant magnetic field.

5. CONCLUSION

Analysis of the self-organization processes in deposition, thermal treatment, deformation, and cutting of surface layers of items, as well as in combined methods of treatment, i.e. in deposition of coatings and thermal treatment combined with deformation and cutting, shows that a technological complex can work continuously and stably in an automatic mode requiring no external control. This gives reasons for the technological complexes designed as autonomous flexible production modules to be used for combined electromagnetic and thermomechanical treatment of workpieces.

REFERENCES

- [1] PODURAEV, V. (1985) *Technology of Physicochemical Methods of Treatment* [in Russian], Moscow.
- [2] RYZHOV, E., AVERCHENKOV, V. (1989) *Optimization of Technological Processes of Mechanical Treatment* [in Russian], Kiev.
- [3] GOLODENKO, B., SMOLENTSEV, V., (1994) Vestn. Mashinostr., No. 4, pp 25-28
- [4] KHEIFETZ, M., CHEMISOV, B., AKOULOVICH, L., et al., (2002) *Intellectual Production* [in Russian], Novopolotsk.
- [5] ARTOBOLEVSKII, I., ILINSKII, D. (1983) *Principles of Synthesis of Systems of Automatic Machines* [in Russian], Moscow.
- [6] EBELING, V. (1979) *Structure Formation in Irreversible Processes: Introduction to the Theory of Dissipative Structures* [Russian translation], Moscow.
- [7] HAKEN, G. (1980) *Synergetics* [Russian translation], Moscow.
- [8] KHEIFETZ, M., KOZHURO, L., MROCHEK, J. (1999) *The Processes of Self-organization at the surface formation* [in Russian], GomeI.
- [9] PASKHVER, I. (1974) *Law of Large Numbers and Statistical Regularities* [in Russian], Moscow.
- [10] VASILEV, A., DALSKII, A., KHEIFETZ, M., et al., (2002) *Technological principles of details treatment* [in Russian], Minsk.



34th INTERNATIONAL CONFERENCE ON
PRODUCTION ENGINEERING
28. - 30. September 2011, Niš, Serbia
University of Niš, Faculty of Mechanical Engineering



**DESIGN OF TECHNOLOGICAL COMPLEXES FOR HIGHLY EFFICIENT
TREATMENT**

Vladimir BORODAVKO, Victor GAIKO, Viacheslav KRUTSKO, Michael KHEIFETZ, Elena ZEVELEVA

The State Scientific and Production Amalgamation "Center" of the National Academy of Sciences of Belarus,
Nezavisimosti Avenue, 66, Minsk, Belarus

engine@presidium.bas-net.by, mlk-z@mail.ru, kheifetz@presidium.bas-net.by

*Polotsk State University, Bloshin Street, 29, Novopolotsk, Belarus
e.zeveleva@mail.ru

Abstract: *The structural synthesis of technological complexes for highly efficient combined thermomechanical and electromagnetic treatment of surfaces of revolution and end and flat surfaces showed the expediency of setting up universal technological complexes in the form of a flexible production module that consists of unified units that carry out principal, additional, and adjusting movements of the parts and tools and provide their mounting and fastening. Unification of combined treatment of surfaces of revolution and flat surfaces using additional units permits the creation of flexible treatment centers.*

Key words: *technological complexes, thermomechanical and electromagnetic treatment, flexible treatment centers*

1. INTRODUCTION

One of the ways to improve the efficiency of machine building is to create the complexes of technological, transport, energy, and information machines and apparatuses which realize the work process as a logically complete part of the production cycle. Such a combination of machines has come to be known as a technological complex [1, 2]. Therefore, shortening the time for the new technological complexes creation and implementation is a pressing problem of modern machine building industry.

Principles of optimum design of a technological complex have been developed by Artobolevskii [1] and Koshkin [2]. A two-stage design was proposed:

- 1) structural synthesis in which principal schemes of solutions that are in conformity with initial technological conditions are considered;
- 2) parametric synthesis in which a schematic solution is embodied in a structural form as a combination of specific mechanisms, blocks, devices, and elements of the technological complex.

Analysis of the technological complexes grouping involve the following [3]:

- 1) study of the structure and preselection of the types of grouping;
- 2) study of the effect of the latter on quality, rigidity, accuracy, and wear resistance of the elements and consideration of the methods of their optimization.

Methods of analysis and optimization of selection of groupings [4] for automated assembly technological complexes [1, 2], aggregate machines [5, 6], automatic rotor lines [2, 7], and multioperation machines [3, 5, 8] are presently known. However, the problems of structural

and parametric synthesis in design of technological complexes implementing processes of highly efficient combined treatment have not been studied as yet.

By virtue of this, development of the methodology of synthesis of technological complexes of highly efficient treatment, strengthening, and recovery of articles is of primary importance. It includes:

- a) giving reasons for choice of highly efficient combined methods of treatment which provide the resource saving and repair of machine elements;
- b) design of the structure of a universal technological complex for highly efficient treatment, strengthening, and recovery of machine elements;
- c) optimization of the parameters of the processes implemented by a technological complex of highly efficient treatment.

Shortening the design time for the new advanced technological processes involving the use of tools, assembly units and systems, machines, and modules that form a single technological complex, is among topical problems of modern machine building industry.

A key problem in designing a technological complex is the setting up of a structure that provides smooth operation and flexible readjustment of a complex for highly efficient treatment [9].

Rational reliability and adaptivity are provided in structural synthesis based on analysis of elements and study of corteges of the technological complex [1].

2. ANALYSIS OF ELEMENTS OF TECHNOLOGICAL COMPLEXES

A technological complex in the general case is considered as a hierarchical «man-machine» system [1] that

comprises the following levels:

- I) functional elements that implement the principal movement, the feeding movement, and the tool movement;
- II) functional subsystems in the form of assembly units;
- III) functional systems that provide operational and transport movements, feeding and removal, and maintenance;
- IV) technological modules or assembly machines, and power and information machines;
- V) automatic and semiautomatic lines and sections that form the technological complex.

Each subsystem of the n -th level is an element of a subsystem of the $(n + 1)$ -th level. The makeup of the technological complex and each functional system and subsystem that are involved in a technological module and the functions of their constituent elements comply with the intention of the technological operations for which the given technological complex is set up.

In the general case each subsystem consists of several elements whose naming involves the names of the functions (movements) performed. During the technological process, a subsystem of a given type performs a certain typical function, i.e., a typical technological operation.

Plants for highly efficient turning, milling, and abrasive treatment, rotational cutting [10], electromagnetic facing [11, 12] with plastic surface deformation [12], and magnetic-abrasive polishing [11] that have been designed to date are functional systems with a set of various subsystems.

The makeup and number of interlevel links of the elements of technological complexes for combined electromagnetic and thermomechanical treatment are analyzed using a two-digit numbering of the constituent systems and elements. The first digit corresponds to the level of the constituent: 1, denotes functional elements; 2, functional subsystems; 3, functional systems; 4, technological machine; 5, technological complex. The second digit is the ordinal number of each constituent of the given level.

Thus, the following code numbering is obtained for constituents of the fifth level: 51, technological complex for combined electromagnetic and thermomechanical treatment for surfaces of revolution; 52, the same for end surfaces; 53, the same for flat surfaces.

We consider a technological complex for combined electromagnetic and thermomechanical treatment of pans with surfaces of revolution.

The fourth level of technological complexes is made up of technological modules by the method of treatment: 41, turning treatment; 42, abrasive treatment; 43, rotational cutting; 44, electromagnetic facing with plastic surface deformation; 45, magnetic-abrasive polishing.

The third level represents functional systems: 31, operating system that includes elements needed for fulfilling the designated purpose of the functional system; 32, auxiliary system that effects adjusting movements of the tool and the workpiece; 33, servicing system that provides replacement of the workpiece and the tool and filling of the facilities for feeding the powder and the lubricating fluid.

The second level is functional subsystems: 21, of the workpiece movement; 22, of the tool movement; 23, of the feeding movement; 24, of the electromagnetic system movement; 25, of additional heating of the treated surface; 26, of feeding of the lubricating fluid; 27, of the powder feeding; 28, of the tool adjusting movements that can coincide with the principal movements; 29, of replacement of the workpiece and the tool.

The first level involves functional elements that implement: 11, principal movement of the workpiece (111, rotational movement; 112, translational movement); 12, principal movement of the tool (121, rotational movement; 122, translational movement); 13, additional movement of the tool (131, rotational movement; 132, translational movement); 14, feeding (inward) movement (141, lengthwise movement; 142, lateral movement; 143, movement perpendicular to the plane of the lateral and lengthwise movements); 15, movement of the electromagnetic system: 16, movement of the facility for feeding the powder; 17, adjusting movement of the workpiece (171, lengthwise movement; 172, lateral movement; 173, movement perpendicular to the plane of the lateral and lengthwise movements); 18, adjusting movement of the tool (181, lengthwise movement; 182, lateral movement; 183, rotational movement).

On the basis of an analysis of the sets of constituent functional systems, functional subsystems, and functional elements, which are called corteges [1], we determine links between them.

3. STRUCTURAL SYNTHESIS OF CORTEGES OF TECHNOLOGICAL COMPLEXES

Study of the graphs of corteges (Fig. 1) permits establishment of the number of interconnections between the various levels that make up the technological complex.

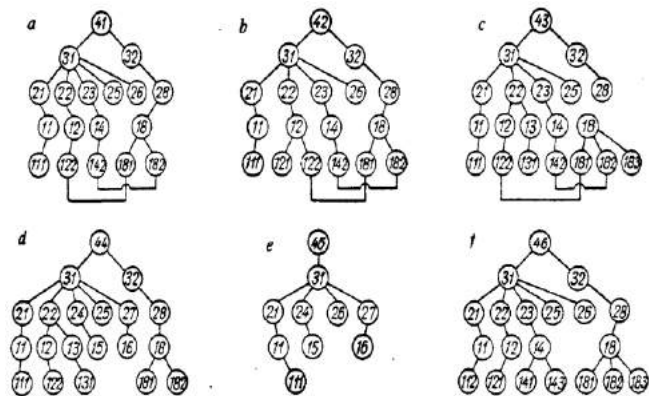


Fig. 1. Graphs of corteges of: turning treatment (a), abrasive treatment (b), rotational cutting (c), electromagnetic facing with plastic surface deformation (d), magnetic-abrasive treatment (e), milling treatment (f)

All technological modules (the IV level) include functional systems (the III level) 31 and 32 (operating and auxiliary), except for technological module 45.

Functional subsystem 22 (tool movement) is absent in technological module 45; functional subsystem 23 (feeding and inward movement), in technological modules 44 and 45; functional subsystem 24 (movement of the electromagnetic system), in technological modules 41, 42, 43, and 46; functional subsystem 25 (additional heating), in technological modules 42 and 45; functional subsystem 26 (feeding of the lubricating fluid), in technological modules 43 and 44; functional subsystem 27 (dispenser), in technological modules 41, 42, 43, and 46; functional subsystem 28 (adjusting movements), in technological module 45.

Thus, in most cases technological complexes involve: functional subsystem 21 (workpiece movement) - rotation (111); functional subsystem 22 (tool movement) - translational movement (122); functional subsystem 22 (additional movement of the tool) - rotation (131); functional subsystem 23 (feeding or inward movement) - lateral movement (141); functional subsystem 28 (adjusting movements of the tool) - lengthwise and lateral movement (181, 182).

To design a universal technological complex for combined thermomechanical and electromagnetic treatment, we unify corteges and determine coincident links and functional elements. The match of corteges (Fig. 2) reveals the expediency of setting up a universal technological complex that combines highly efficient thermomechanical and electromagnetic methods of treatment of surfaces of revolution.

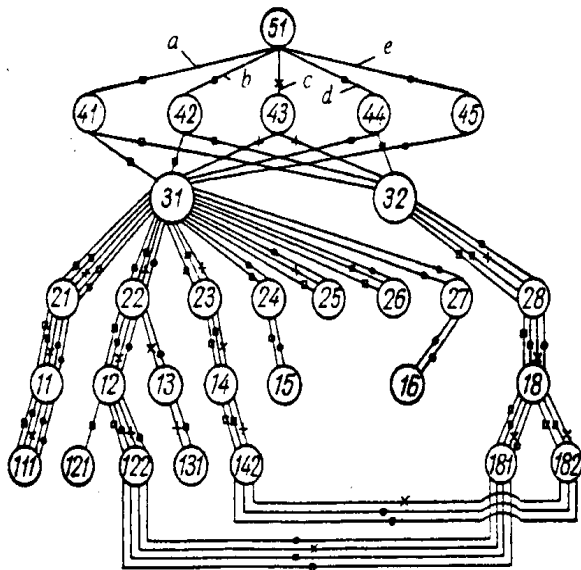


Fig. 2. Graphs of corteges of a technological complex for treatment of surfaces of revolution: turning treatment (a), abrasive treatment (b), rotational cutting (c), electromagnetic facing with plastic surface deformation (d), deformation treatment (e)

The structural synthesis of the elements based on the considered links permits identification of a number of unified units in the makeup of the technological complex: 1) of principal movement, which provides workpiece rotation about the horizontal axis; 2) of the tool drive: a, of translational movement along the axis of rotation of the workpiece and inward movement and b, of rotational

movement, whose velocity is determined from the forces applied during the treatment; 3) of feeding: a, of the powder for facing or polishing and b, of the working lubricating-cooling fluid; 4) of the drive of the electromagnetic system, which are used for: a, control over the technological process and b, control and regulation of the treatment quality; 5) that serve for: a, energy supply and b, control over the energy actions on the surface layer of the treated workpiece.

Unit 2, a can be made in the form of a lathe support, and unit 2, b is fastened to unit 2, a, which offers the opportunity to use the existing mechanisms of unit 2, a to implement some of the tool movements.

Let us consider the links (Fig. 3) between functional elements of a technological complex for treatment of end surfaces.

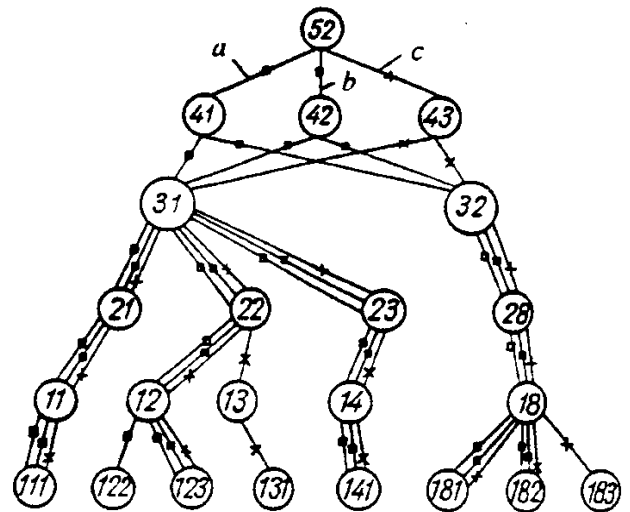


Fig. 3. Graphs of corteges of a technological complex for treatment of end surfaces: turning treatment (a), abrasive treatment (b), rotational cutting (c).

The match of corteges indicates that the units of the complex for treatment of surfaces of revolution are totally suited for treatment of end surfaces except that the principal movement should be replaced by tool feed (the translational movement should be replaced by lateral movement).

We next consider the links (Fig. 4) between functional elements of a technological complex for treatment of flat surfaces.

The match of corteges of the technological modules for treatment of flat surfaces shows the following: 1) the unit of workpiece movement provides translational movement, 2) the unit of tool movement provides rotational movement, and 3) the translational movement of the tool in the technological module for magnetic-abrasive polishing can be replaced by feeding movement, and therefore, the unit will carry out one movement.

An analysis of the match of corteges of the technological complexes for treatment of surfaces of revolution and end and flat surfaces revealed that, for carrying out combined thermomechanical and electromagnetic processes, the operating functional system should be provided with the principal movement, feeding movement, adjusting movement, and additional movement.

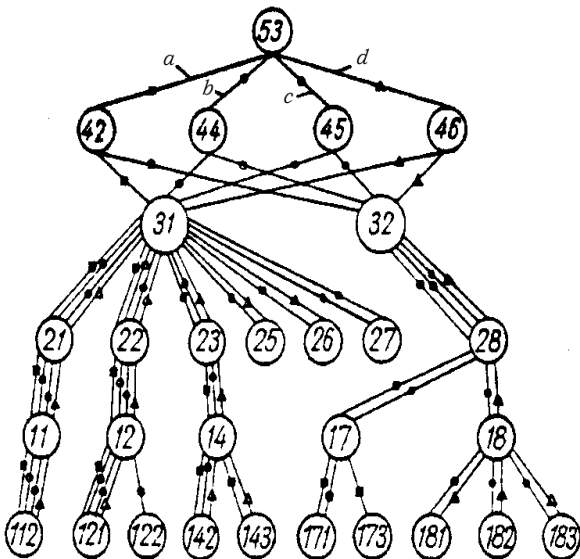


Fig. 4. Graphs of corteges of a technological complex for treatment of flat surfaces: abrasive treatment (a), electromagnetic facing with plastic surface deformation (b), magnetic-abrasive treatment (c), milling treatment (d).

In the general case, for carrying out the set of movements, it is advisable to construct the technological complex from unified blocks that effect: 1) rotational movement of the workpiece, 2) rotational movement of the tool, 3) three mutually perpendicular translational movements of the table, 4) additional rotational movement of the tool, 5) adjusting turning movement of the axis of the rotational tool, 6) mounting of the work-piece on the table in treatment of flat surfaces, and 7) fastening of the tool in turning treatment.

Units 1 and 2 can be structurally united with the units that carry out adjusting movements for regulating the distance between the axis of rotation and the frame (table) of the complex, and units 4 and 5 can be integrated.

4. CONCLUSION

The structural synthesis of technological complexes for highly efficient combined thermomechanical and electromagnetic treatment of surfaces of revolution and end and flat surfaces showed the expediency of setting up universal technological complexes in the form of a flexible production module that consists of unified units that carry out principal, additional, and adjusting movements of the parts and tools and provide their mounting and fastening.

Unification of combined treatment of surfaces of revolution and flat surfaces using additional units permits the creation of flexible treatment centers.

REFERENCES

[1] ARTOBOLEVSKII, I., ILINSKII, D. (1983) *Principles of Synthesis of Systems of Automatic Machines* [in Russian], Moscow.
 [2] KOSHKIN, L. (1982) *Rotor and Rotor-Conveyor Lines* [in Russian], Moscow.

[3] VRAGOV, Yu. (1978) *Analysis of Arrangements of Metal-Cutting Machine Tools: Principles of Arrangement* [in Russian], Moscow.
 [4] BUSLENKO, N. (1964) *Simulation of Production Processes* [in Russian], Moscow.
 [5] GEBEL, H. (1969) *Arrangement of Aggregate Tools and Automatic Lines* [Russian translation], Moscow.
 [6] DASHCHENKO, A. (1970) *Theory of Automatic Machines* [in Russian], Moscow, pp. 75-84
 [7] KLUSOV, I., SAFARYANTS, A. (1969) *Rotor Lines* [in Russian], Moscow.
 [8] MATALIN, A., DASHEVSKII, T., KNYAZHITSKII, I. (1974) *Multiooperation Machine Tools* [in Russian], Moscow.
 [9] FROMENT, B. and LESAGE, J.-J. (1984) *Production: Les techniques de l'usinage flexible*, Paris.
 [10] KOZHURO, L., MROCHEK, J., KHEIFETZ, M., et al. (1997) *Treatment of the wear resistance coatings* [in Russian], Minsk.
 [11] YASHCHERITSYN, P., ZABAVSKII, M., KOZHURO, L., AKULOVICH, L. (1988) *Diamond-Abrasive Treatment and Hardening of Workpieces in a Magnetic Field* [in Russian], Minsk.
 [12] KOZHURO, L., CHEMISOV, B. (1995) *Treatment of Machine Parts in Magnetic Field* [in Russian], Minsk.

INFLUENCE OF PRODUCTION PROCESS ON FATIGUE PROPERTIES OF HEAVY CASTINGS - A CASE STUDY

Radivoje MITROVIĆ¹⁾, Dejan MOMČILOVIĆ²⁾, Olivera ERIĆ³⁾, Ivana ATANASOVSKA³⁾

¹⁾Faculty of Mechanical Engineering, University of Belgrade, Kraljice Marije 16, Belgrade, SERBIA

²⁾Institute for Testing of Materials, IMS, Bulevar vojvode Mišića 43, Belgrade, SERBIA

³⁾Institute Kirilo Savic, Bulevar vojvode Stepe 51, 11000 Belgrade, Serbia,

rmitrovic@mas.bg.ac.rs, dejanmomcilovic@yahoo.com, olivera.eric@iks.rs, ivatanasov@yahoo.com

Abstract: This paper describes the analysis of production process on failure of heavy flange casting of hydro turbine shaft. Special emphasize on metallurgical failure analysis of in-service crack initiation is presented in this paper. The presence of dendrite structure points to incomplete or irregular flange heat treatment. Testing the mechanical properties of the material, revealed slight discrepancies between the experimental results and the requirement of the specification for the production of the flange material. The conclusion of this research shows that production process resulted of inhomogeneous microstructure and subsequent data scatter. This indicated that the heat treatment regime, as a part of production process, had some influence in the fatigue fracture of flange casting.

Key words: casting, microstructure, fatigue, fracture

1. INTRODUCTION

This paper describes the partial investigation of turbine shaft Kaplan's 28 MW bulb turbine failure. The bulb turbine generator's horizontal shaft, Fig. 1, is made by joining the forged and cast parts by slag welding, Fig. 2. The shaft is manufactured as hollow, housing a servomotor inside it, for shifting the runner blades. The flange, on which the crack occurred, is made of steel casting of 20GSL designation, according to GOST 977-88, [1]. The operating speed of turbine shaft was 62.5 rpm. The fact that cracks were found on heavy casting (approx weight 20 tons) raised question of origin of failure in casting and subsequent heat treatment process.

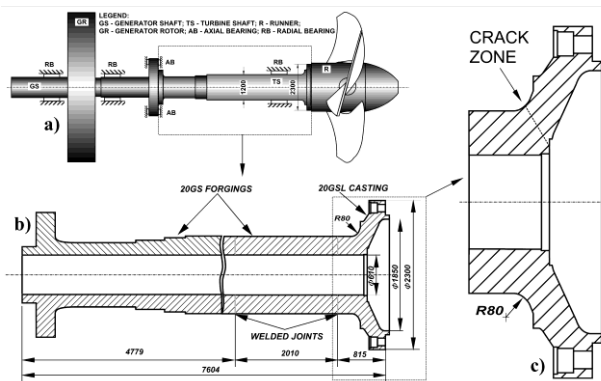


Fig 1. Position of crack on general assembly of hydraulic turbine shaft

General appearance of the cracked zone of 20GSL heavy casting is given at Fig 2. The close view of zone with cracks is given at the Fig 3.



Fig. 2. General appearance of the cracked zone

2. EXPERIMENTAL RESULTS

2.1. Chemical Composition and Mechanical test

Table 1 shows the chemical composition of flange material in accordance with the requirements of the reference standard, [1]. The testing determined that the chemical composition meets standard's requirements.

Table 1. Chemical composition of flange

	%C	%Si	%Mn	%S	%P
Min	0,16	0,60	1,00	-	-
Max	0,22	0,80	1,30	0,030	0,030

During cutting of samples for the chemical, mechanical and metallographic tests, numerous gas holes and pores were detected that resulted from the casting process, Fig. 4. Gas pores and holes were not perceived around the crack initiation location, i.e. around the outer shaft surface, but exclusively in the casting volume. The testing of casting meets standard's requirements, [1]. The zone of cutting out of all samples for the mechanical and metallographic tests was 20 mm below to the external shaft surface. The results of mechanical test are given at the Table 2.

Table 2. Average and required mechanical properties at room temperature of the 20GSL steel casting, [1].

	Average values	Required (GOST 977) - min. values
Yield strength (MPa)	310	294
Tensile strength (MPa)	509	540
Elongation, in 2 in. (%)	17.6	18
Reduction of area (%)	35.2	30
Brinell hardness HB	153	-
Charpy-V notch, +20°C (J)	74.4	23.4

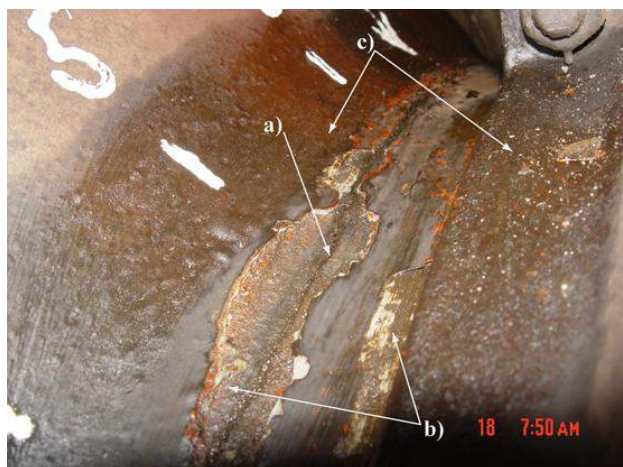


Fig. 3. Close view of the transient flange radius after detecting the crack
 a) Main crack, b) anti-corrosive protection layer, c) oil residue on corrosion pits

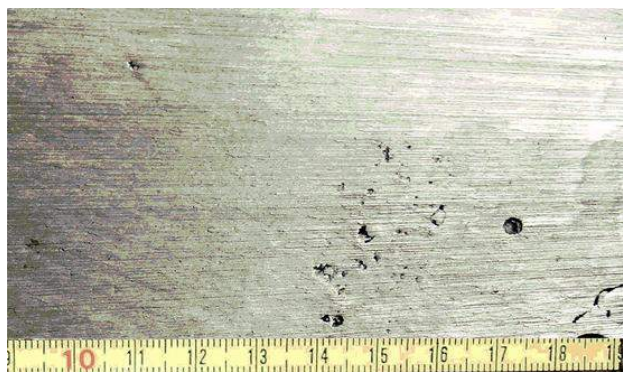


Fig. 4. Gas holes and shrinkages on casting, zone near flange radius R80

2.2. Fatigue properties

Testing of the fatigue strength was completed according to the requirements of standard, [1], in open-air conditions, at the +20°C, at load ratio $R = -1$. Fatigue limit S_{FL} of the shaft flange material was tested on ZWICK ROELL HB 250 and it is 168.0 MPa. The results of fatigue tests are shown on table 3, and the S-N diagram on Figure 5.

Table 3. Average and reference fatigue values of the 20GSL flange steel casting, [1].

Fatigue limit S_{FL} (MPa)	Average values	Reference values	
		on air	in water
	168	225	140

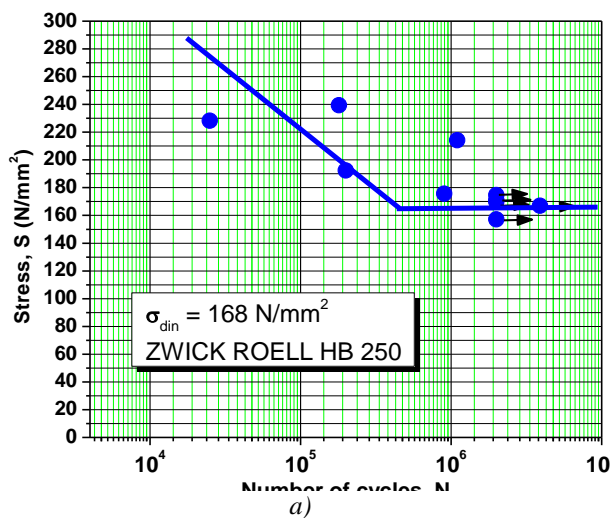


Figure 5. S-N diagram for 20GSL Casting
 a) S-N diagram
 b) Position of samples on testing machine

2.3. Metallographic inspection

By reviewing the original documentation from the time of delivering and installing of the shaft, it was discovered that heat treatment of the shaft was done by applying the regime shown of Fig. 6:

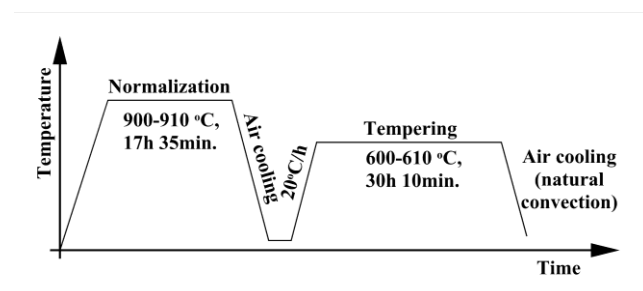


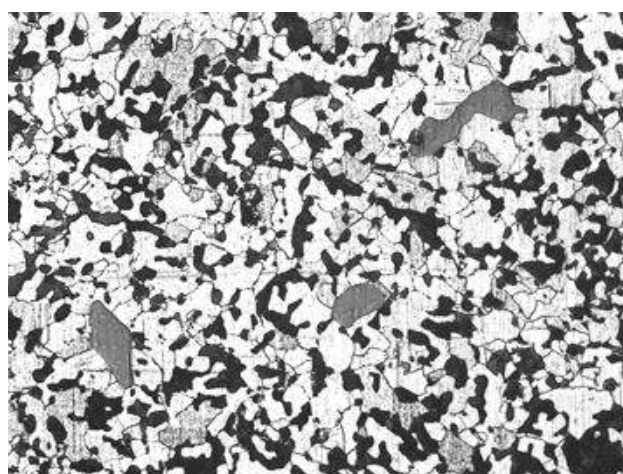
Fig 6. Applied heat treatment regime

Such a heat treatment regime indicates that complete austenization was done, with complete breaking of the microstructure that had remained from the casting process.

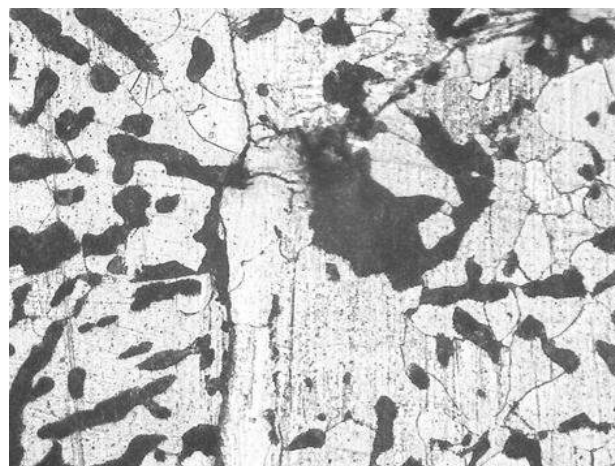
However, the microstructure of the material is the cast ferrite-pearlite one, with oxide type non-metallic inclusions and with minimal participation of dendrite structure, Fig. 7a). Dendrite structure presence points to the possibility of incomplete or irregularly executed shaft flange heat treatment, which explains the observed scatter of results in all the mechanical tests. It was also determined that there were large non-metallic oxide inclusions in the structure, which occurred in sequences. The fine micro cracks were found in microstructure, Fig 7 b). The results of quantitative metallography are given at the Table 4.

Table 4. Results of quantitative metallography

Standard	Grain size - scale	Number of grains/mm ²	Grain diameter
ISO 643:2003	7	1204	32μm
GOST 5639-82	8	2048	22μm



a)



b)

Fig. 7. Microstructure of flange material

- a) Cast, ferrite-pearlite microstructure, x 200, 5% nital
- b) Micro cracks emanating from shrinkage, x 500, 5% nital

3. DISCUSSION

The chemical composition of the tested shaft flange material corresponds to the requirements of the GOST 977-88 standard, [1]. The fact that some of the obtained elongation values were lower than the minimal required, shows that there are locations in the microstructure that have reduced ability for plastic deformation. So, in these locations easier occurrence of initial cracks can be expected.

The established tensile properties, specifically tensile strength and elongation values, are lower than required ones, i.e. the tested steel casting sample does not fully meet the tensile characteristics requirements stated in the GOST 977-88 standard, [1].

From the point of view of toughness, the presented and analyzed results of testing the notch impact strength shows that the material meet the requirements of the reference standard, [1].

The results of micro-structural analysis in light microscope show that the microstructure was cast fine grained, ferrite-pearlite microstructure with non-metallic oxide-type inclusions and with sporadic dendrite-structure participation. The presence of micro cracks is also noticed.

According to the heat treatment regime stated by the shaft manufacturer, it could be expected that complete austenization was done, with breaking the dendrite microstructure that had remained from the casting process. However, the obtained microstructure test results, shown on Fig 7, demonstrate that some portion of residual dendrite microstructure has remained. The presence of dendrite structure points to incomplete or irregular flange heat treatment. Moreover, microstructure and subsequent data scatter indicated that the heat treatment regime had some influence in the fracture process.

Such non-homogeneous microstructure, together with the observed porosity and micro cracks, has contributed to faster propagation of the fatigue crack, compared with the

case of the flange material that completely fulfill requirements, [1]. The fact that was spotted significant data scatter, shown on Fig 5a), also indicates the influence of casting defects on fatigue properties of casting. On Fig 8, it is shown one of fatigue test specimens with cracks, prematurely cracked during fatigue test. This figure clearly demonstrates that the casting defects was the weak links during fatigue crack growth on flange. The result of few specimens like the specimen shown on Fig 8, was not incorporated into diagram on Fig 5a).



Fig. 8. Premature failure of test specimens due to casting defect - tested by liquid penetrants

According to [1], fatigue limit at $R=-1$ in open air is 225 MPa, and 140 MPa in water. However, by testing the shaft material samples, the value of 168 MPa of fatigue limit in open air was obtained, which is $\approx 25\%$ less than the reference value of 225 MPa.

4. CONCLUSIONS

The chemical composition of flange casting met requirements of the relevant standard.

The fact that 20GSL flange casting mechanical properties does not completely fulfilled the requirements [1,2], indicate that there is a gap in production process, casting and heat treatment that led to lower properties compared to required ones.

Fine grained microstructure indicate that heat treatment was done properly, which points to casting process as a major point which induce lower mechanical properties.

However, the reasons for the premature failure can't be completely attributed to the material quality and the heat treatment.

The shaft failure occurred due to the combination of several factors:

- inappropriate corrosion protection in the zone of critical radius and lack of procedures of renewing corrosion protection of turbine shaft.
- high stresses during start/stop cycles and during regular operating regime in the zone of R80 radius for "wet" environment.

The following suggestions emerged from this production process based failure analysis:

- Redefining of procedures for periodical non-destructive inspection of the shaft-flange transition zone status, with increased frequency,

- Periodical renewal of the anticorrosive protection on the shaft flange, especially in the shaft-flange transition zone,
- Keeping the start/stop cycles at minimal values as it is possible,
- The key recommendation is the improvement of general technical conditions of delivery for flange material upon a new commissioning [3, 4].

Acknowledgements

This research was supported by the Serbian Ministry of Education and Science, Project TR 35029 - Development of Methodology for Improvement of Operational Performance, Reliability and Energy Efficiency of Machine Systems used in the Resource Industry

REFERENCES

- [1] GOST 977-88, *Steel Castings. General Specification*
- [2] ТРОЩЕНКО, В.Т. (1987) *Сопротивление усталости металлов и сплавов*, Наукова думка, pp 668-670 (in Russian)
- [3] MARICIC, T., HABER, D., PEJOVIC, S. (2007) *Standardization as Prevention of Fatigue Cracking of Hydraulic Turbine-Generator Shaft*, IEEE Electrical Power Conference, Montreal, CD
- [4] ATANASOVSKA, I., MITROVIĆ, R., MOMČILOVIĆ, D. (2011) *FEM model for calculation of Hydro turbine shaft*, *Proceedings – the Sixth International Symposium KOD 2010*, 29-30.09.2010., Palić, Serbia, Published by Faculty of Technical Science – Novi Sad, Serbia, pp.183-188



MODELLING DATABASE OF QUALIFIED WELDERS ACCORDING TO STANDARD SRPS EN 287-1:2008

Dusan JOVANIC, Zeljko EREMIC, Milos JOVANOVIĆ

Technical College of Applied Sciences in Zrenjanin, Dj. Stratimirovica 23, Zrenjanin, Serbia
Technical College of Applied Sciences in Zrenjanin, Dj. Stratimirovica 23, Zrenjanin, Serbia
Welding Institute of Slovenia, Ptujška 19, Ljubljana, Slovenia
jovanickosta@gmail.com, zeljko.eric@vts-zr.edu.rs, milos.jovanovic@i-var.si

Abstract: Database of qualified welders provides improvement of the quality of welding process and meeting the requirements of the standard ISO 3834 – Quality requirements for fusion welding of metallic materials, regarding keeping and systematic updating of the appropriate documentation.

The qualified welders database was designed by means of the Visual Studio 2008 and MS SQL Server 2008 Express as DBMS.

The appearance and the contents of the output document, i.e. the welder qualification entirely meet the requirements of the SRPS EN 287-1:2008 - Qualification test of welders- fusion welding, part 1: Steels.

Key words: welding management, welder qualification, database.

1. INTRODUCTION

According to the ISO Standard 3834 – Quality requirements for fusion welding of metallic materials, a manufacturer must have a sufficient number of competent staff available in order to plan, perform, monitor and research welding production to meet the said requirements.

All welders must have a valid certificate - Qualification test of welders in accordance with the standard SRPS EN 287-1:2008.

The database of certified welders provides manufacturers with electronic data processing and management, which offers an accurate and fast insight regarding number, validity and range of qualification of welders.

2. PREREQUISITES FOR APPLICATION DEVELOPMENT

Prior to development of application to support training and certification of welders in Banat, it is necessary to provide environment for its development. Visual Studio 2008 environment was used to develop this application while Microsoft SQL Server 2008 Express was used as a database management system and Crystal Reports to create reports.

3. DESCRIPTION OF THE APPLICATION

The application contains a system for working with user accounts which requires users to log in to be able to work on the system. If a user wants to log in for working on the system, he must type in the account name and password. There are two types of users: administrators, who have access to all menu options, and ordinary users (operators) who cannot view the menu option “Administration”. The

observed application will be analyzed in this paper through menu options it offers.

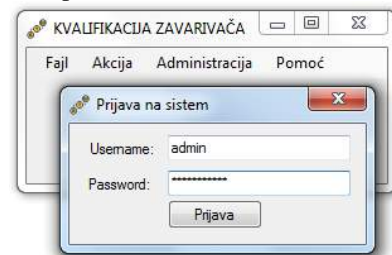


Fig.1. System login form and login form in the background

3.1. File

The menu bar button “File” contains two options: Log out (to log out actual user account, but without exiting the application) and exit (to close up the application). If a user is logged out of his account, it is possible to access the system again by entering any valid user account name and password.

3.2. Action

Action is a menu bar button used for direct work with certificates and it contains the following options:

- Certificate
- Certificate database

Certificate is used to open the basic form for a new certificate entry and it is called “Certificate”.

Welder's qualification test certificate

Welder: JMBG: 0202902850005 No: 1
 Welder's name: Petar Petrović Stamp: 02 Place of birth: Zrenjanin
 Date of birth: 02.02.1982 Identity card No: 123456 Issued in: Zrenjanin
 Employer: Begaj

WPS - Reference: A (D1/WPS-03-2) Code/Testing Standard: EN 287-1

Data	Test piece	Range of qualification
Welding process (root):	311	311
Welding process (fill):	311	
Type of weld:	BW	BW, FW
Base material - group:	1.1	1.1, 1.2, 1.4
Material thickness (mm):	56	>= 28.50
Outside pipe diameter (mm):	57.00	
Welding position:	H1.045	PA, PB, FC, PD, PE, PF (Plate), PF (Pipe), HH-045
Welding consumable:	nm	nm
Shielded gas - type:	Ar	Ar
Product type (plate or pipe):	T	T
Job knowledge:	<input checked="" type="checkbox"/>	Acceptable
Weld details:	ee nb	ee nb, sa mb, be, si, ni
Preheating (°C):	-1	
Additional heat treatment (°C):	-1	Procedure: Koljenje
This certificate is valid for two years, starting from:	04.04.2011	
Designation (s):	EN 287-1:311 T BW 1.1 nm1560 057 00 H1.045 sa nb	
Signature (s):	04.04.2011	
Expire:	D. Jovanović, dipl. inšp. in MANAGER	mr M. Rančić, dipl. inšp.

Fig.2. Form for a new certificate entry

TextBox components are used for textual data entry (which are in some cases, like for JMBG-personal identification number, limited to numbers only), DateTimePicker components are used for date entry, ComboBox lists, which are linked to appropriate data from the database, are used for data entry from a certain domain, while CheckBox control is used for logical data types entry.

In a part of the form which refers to data of "test piece" automatic updating of values is provided at the moment of its change. For example, if a chosen value is in the field "material group 1.1" in the column "range of qualification", the value „1.1, 1.2, 1.4“ is immediately updated as well, etc. Similarly to value controls, the field "Designation" is automatically updated as well.

Certificate database contains a list of recently entered certificates which is in the list on the right-hand side of the form. Changes in a selected certificate can be done by selecting the appropriate item in the list which opens form with identical interface as the interface used for entering a new certificate and its fields are loaded with the data about the selected certificate previously stored in the appropriate database tables. For the purpose of a more effective work, this form offers filtration of the list of existing certificates by the following criteria:

- certificate ID
- welder's name
- welder's company
- period of certificate validity

A click on the reset button enables to return the list of all recorded certificates.

Baza Sertifikata

Kriterijumi pretrage:

ID Sertifikata: []
 Ime zavarivača: []
 Kompanija: []
 Datum izdavanja: []

Rezultat pretrage - nadani sertifikati:

ID Sertifikata	Ime zavarivača	Kompanija	Datum izdavanja
1	Zeljko Eremic	Begaj	4/4/2011

Forma: N/A
 Datum izdavanja od: 14.05.2011
 Datum izdavanja do: 14.05.2011

Resetuj Pretragu
 Pretraga

Fig.3. Certificate database form

3.3. Administration

Administration is an item which is can be viewed only by the users having a status of administrator and it contains the following items:

- Settings
- Dictionary
- Range of qualification
- Account management

The form "Settings" controls settings of connection string used for connecting with the existing database. SqlConnection is a sub-class of ADO.NET class called Connection. It is designed to handle connections with databases of "SQL Server" [1]. If connecting with database fails when application is started, a new form shows up where a user may enter a correct connection string. Certificate template is a path leading to the report template. The application supports possibility to print the same data in different ways provided that there are several report templates. This form is also a place where application interface language can be changed.

Podešavanja

Konekcionni string: log=welding_certificate:Integrated Security=True Ažuriraj

Šablon sertifikata: E:\DataForBackup\VTSSS\djovanic\CODE\VTSSS_PPK

Jezik interfejsa: Srpski Engleski

Fig.4. Settings form

The item "Dictionary" opens a form which enables adjusting of those attributes which use values from a domain. An appropriate codebook should be selected first and then it is possible to add new items or modify and delete the existing items of a selected codebook. Codebook values are usually used in ComboBox lists of the form for certificate manipulation.

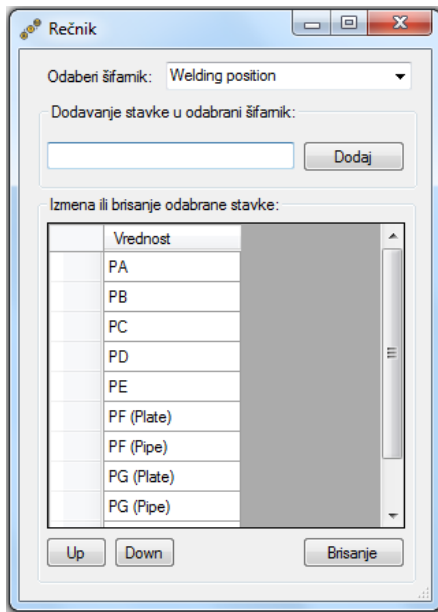


Fig.5. Dictionary form

Range of qualification is the item which opens a form for connecting independent values from used values section with dependent values from range of qualification section. Like in the case of the previous form, a codebook whose elements are used to create dependency links is selected. In the list on the left-hand side there are independent elements of the codebook and on the right-hand side there are potentially dependent codebook elements. Dependency links of selected independent element, if any, are given in the bottom field. In this form, new dependency links may be created or the existing ones modified.

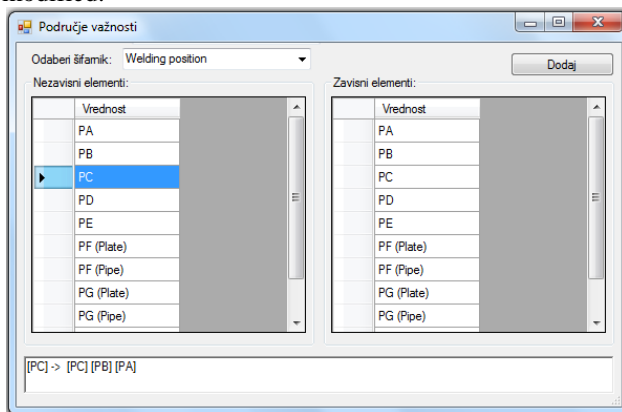


Fig.5. Range of qualification form

Accounts management is a form which provides adding new accounts or managing the existing ones. Only administrators have access to this form because it is found within the item Administration.

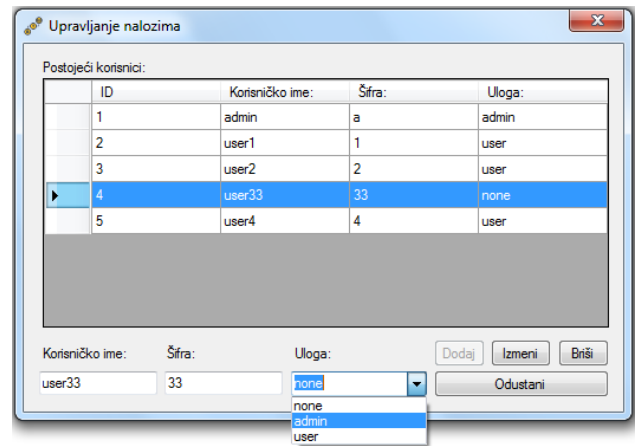


Fig.6. Accounts management form

3.4. Assistance (Help)

This item contains items “About us” and short assistance (help) guidelines for using this system.

4. DATABASE

Application database contains several tables with stored data. The table “dictionary_type” contains a list of codebooks used in the system which even the administrator cannot access because it is received completed after installation and its content is unchangeable. The table “dictionary” which contains the codebook elements is linked to it. Each codebook element must be linked to its codebook through values in the field “type_id“. The table “dependency“ contains codebook element pairs, one of them being dependant, the other independent. Data are stored in this table through range of qualification form. The table “welder“ contains information about the welder who is awarded the certificate. The table “weldingcertificate“ is linked to the appropriate row in the table “welder“ through the field “welder_id“ and it contains information about the certificate awarded to a welder it is linked to. The data about the users who can log in for the work on the system (their username, password, and type of account – administrator or user, operator) can be found in the table “user“.

Certain fields in the tables “welder“ and “weldingcertificate“ contain codes of elements from the table “dictionary“. Those are the fields in the form “certificate” realized by using ComboBox list. This is an advantage in the situations when a codebook element changes its name because this change is automatically updated and in all linked certificates and welders. If, for example, a company entered into the codebook changed its name, it would be enough to change its name only in the codebook to have it changed with all recorded welders of that company.

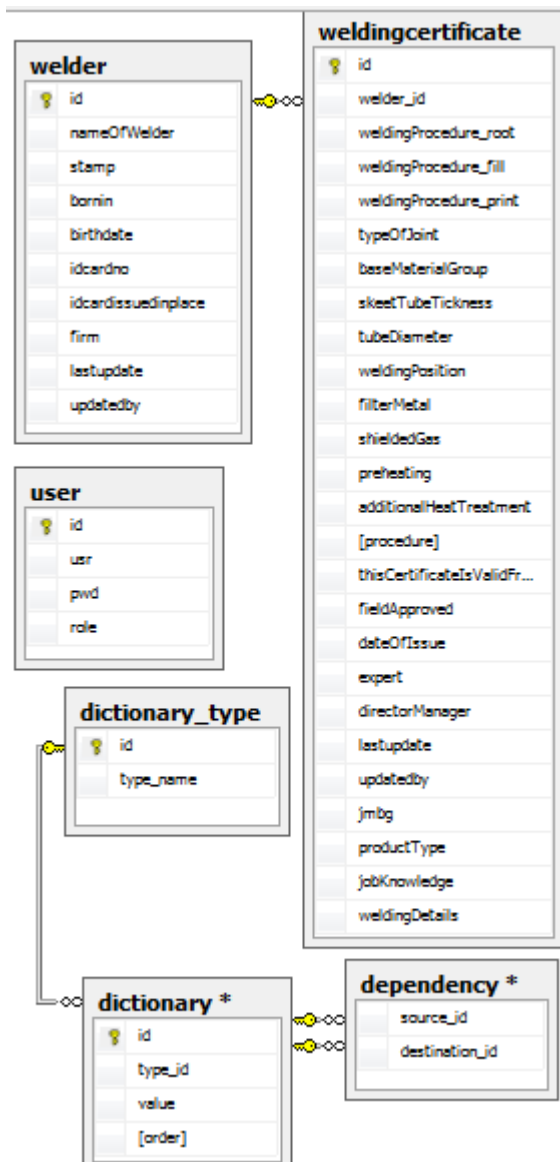


Fig.7. Database diagram

5. DATA OPTIMIZATION AND SYNCHRONIZATION

Optimization and synchronization of the application is done by using DataSet collection of data and Properties namespace. DataSet object memorizes the changes made to syllables stored in it. Owing to that, DataSet object can be used to update syllabus in the database. The main principle is very simple: at the beginning DataSet object will be filled in with data and than the changes will be entered in one or more syllables. After that the changes should be transferred into the database by means of DataAdapter object [2].

When the application is started the required information from the database is loaded in DataSet which is in operating memory. After that, the application communicates during operation with the data in DataSet collection which is in operating memory; DataSet synchronization in the databases is done occasionally and with the application at the end of the operation. Thus the interaction with the database is minimized which positively affects the application performances.

Setting of application parameters from the Settings form are saved between two application startups by using "Properties namespace". "Connection string" is imported from this "namespace" when the application is started and then the link to the base is established and the data sending from the base in DataSet could start.

6. CONCLUSION

Database of qualified welders provides a fast and simple browse and selection of the most adequate staff for welding activities and hence, the quality of products is improved.

Besides, a database of qualified welders is created in accordance with the requirements prescribed by the standard SRPS EN 287-1 Qualification test of welders-fusion welding, part 1: Steels in the area of report appearance, and in accordance with standard ISO 3834 for creating and systematic updating of documentation.

REFERENCES

- [1] John Sharp, "Microsoft Visual C# 2008: Korak po korak", CET Computer Equipment and Trade ; Beograd, Sr.; Novembar 2009.
- [2] Matthew MacDonald, „ASP.NET 3.5 sa C# 2008 od pocetnika do profesionalca“, Kompjuter biblioteka ; Cacak, Sr.; Juni 2009.
- [3] SRPS EN 287-1:2008- Qualification test of welders-fusion welding, part 1: Steels.

ACKNOWLEDGEMENTS



The paper is the part of the RSEDP2 program project: **Welders` training and certification in Banat**
The project is financed by EU





34th INTERNATIONAL CONFERENCE ON
PRODUCTION ENGINEERING
28. - 30. September 2011, Niš, Serbia
University of Niš, Faculty of Mechanical Engineering



**MECHANICAL PROPERTIES OF WELDED JOINTS AT STEEL
TUBES WITH SQUARE CROSS SECTION**

Andreja ILIĆ¹, Danica JOSIFOVIĆ¹, Vukić LAZIĆ¹, Lozica IVANOVIĆ¹

Faculty of Mechanical Engineering, University of Kragujevac, Sestre Janjić 6, 34000 Kragujevac, Serbia,
Phone: +381-34-335990, Fax: +381-34-333192

gilic9@sbb.rs , danaj@kg.ac.rs , vlazic@kg.ac.rs , lozica@kg.ac.rs

Abstract: *Welded construction working properties are highly influenced by the stress and strain distribution in welded joints zones. Stress and strain distributions are determined by stress concentration provoked by geometrical discontinuities and heterogeneous of material. Stress concentration changed the stress distribution, position of maximal stresses and, by that, the position of danger cross section zone which act as damage and integrity safety risk.*

This paper deals with experimental determination of stress concentration influence on welded constructions integrity. The experimental procedure was done on welded joints models in static load conditions on samples made of commonly used steel tube with square cross section. Experimental procedure was conducted on existing testing devices in Welding Laboratory and Material Testing Laboratory at Faculty of Mechanical Engineering in Kragujevac. The models of welded joints at steel tubes were loaded to bending and maximal bending force was determined. Additional stress concentrator was introduced to the models, as circular hole in axis, to determine the influence of multiple stress concentration to maximal obtained bending force.

The aim of this paper is to analyze influence of stress concentration to the resistance of welded structures. Stress concentration were analyzed by experimental approach objected to include as much influential factors as it is possible. The main objective of stress state distribution is creating the precise analytic model and to obtain the relevant data and information for constructions evaluating and optimizations, so as to perform integrity, safety and reliability analysis. This paper pointed out the necessity of analyzing the welded constructions on different dimension levels. Further investigations in this area have to be continued by development of numerical model of the welded construction which will, in involvement with adequate software, complete the experimentally obtained results.

Key words: *welded joint, multiple stress concentration, bending*

1. INTRODUCTION

Welding is most dominant method of forming permanent joints in mechanical constructions which provide essential role in fabrication of wide range components and structures. Welded joints due to other joining methods provide higher efficiency, lighter weight, smooth joint appearances, easy alteration and addition are possible, less expensive. The technology procedures of welding are continually developing due to application of the newly obtained results in fundamental scientific disciplines, as well as in the other disciplines to meet the modern demands. But, as consequence of applied technology processes, zones of welded joints are the zones of high level of residual stresses and high degree of material inhomogeneity. The welding process is based on localized heating and cooling, which creates irregular temperature field. The process of welding provoked disrupted expansion and contraction during heating and cooling. Welded joints zones are zones with high thermal and structural stresses, which derive from the process of welding and represent their own stresses which do not depend on the external load. Other structural discontinuities in those zones, such as stress concentrators

additionally complicate the stress state. The indicated facts point out that properties of welded joints are key element of structural integrity of the welded constructions. Welded structure is a complex system that can be considered from many aspects. Safety and reliability requirements for welded construction point out that welded joint zones have to be considered adequately. The essence of determining the present stress state in zones of welded joints is the formation of the more accurate analytical model of welded constructions. Capacity calculations analyze and prove mechanical resistance and stability of welded structures for the expected loads and exploitative conditions. The multiple stress concentrations at zones of welded joint and mechanical properties of welded joints are major dominant factor to precision of analytical models used for calculations. Data obtained from exploitation of welded constructions showed that mechanical properties of welded joints due to its nature were not adequately take in consideration in present analytical models and capacity calculations.

2. OBJECT AND METHODOLOGY OF EXPERIMENTAL TESTING

In order to test the mechanical properties of welded joints at steel tubes with square cross section due to its wide usage and significance, the experimental testing in two stages was done. The experimental testing of mechanical properties was done on welded joints models in static load conditions on mechanical loading device with automatic registering the force dependence on elongation, firstly without additional stress concentrator in welded joints zones, and after that, with introducing it as circular holes in axis. The samples were made, by defined welding procedure, of commonly used steel tube with square cross section. Experimental procedure was done using testing devices in Welding Laboratory and Material Testing Laboratory at Faculty of Mechanical Engineering in Kragujevac. The joint models of steel tubes were loaded to bending and maximal bending force was determined. The operation of mechanical loading machine was achieved through the worm transmission and the winding spindle. Winding spindle is in relation to moving jaws of the machine. The machine is equipped with a device for registering force dependence on elongation. Mechanical loading machine was loaded in the range up to 5 kN with a force increase speed adequate for static tests 10 mm/min during testing (Fig.1.).



Fig.1. Loading principle during testing

For preparation of models, steel tubes of commonly used structural steel with square cross section were welded with wire electrode ESAB AUTROD 12:51, $d = 1$ mm, the specification EN 440, from ESAB producers, Sweden using welding device VARMIG 400 D 42 in protective atmosphere of CO_2 with flow rate 9 l / min. Welding parameters were: welding current $I = 105$ A, welding voltage $U = 21$ V and welding speed $v_z = 28$ m/h. Circular holes in axis were introduced to the models as additional stress concentrators to determine the influence of multiple stress concentration to maximal bending force. Tested models were prepared with proper geometrical similarity to real welded constructions. Testing was done according to pre-defined procedure on a series of five specimens. Firstly, models of welded joints at steel tubes

with square cross section loaded to bending were tested. The shapes and dimensions of tested models, are shown in Fig.2.

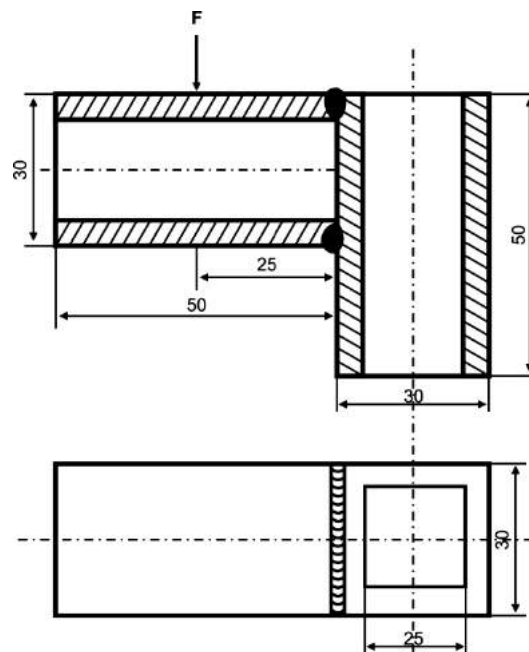


Fig.2. Shape and dimensions of tested specimens

Force dependence on elongation were register and maximal bending force were determined (Fig.3.). The obtained results show small relative variations and can be taken as relevant for further analysis.

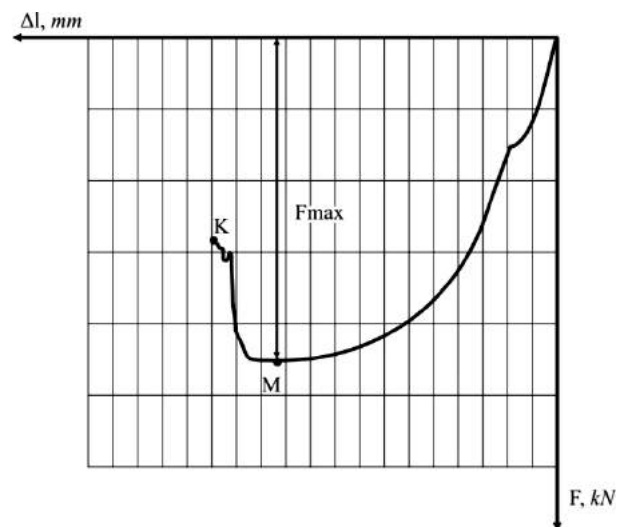


Fig. 3. Force dependence on elongation for tested specimens

Second stage of experimental testing were done on the models with additional stress concentrators in zones of welded joints for qualitative determination of multiple stress concentration to mechanical properties. Testing was done according to pre-defined procedure on a series of five models of welded joints at steel tubes with square cross section and circular holes in axis loaded to bending. The shapes and dimensions of tested models during the second stage of testing are shown in Fig.4. Force

dependence on elongation were registered automatically on testing device and maximal bending force were determined. The obtained results are shown at Fig.5. and show very small relative variations, so can be taken as relevant for further analysis.

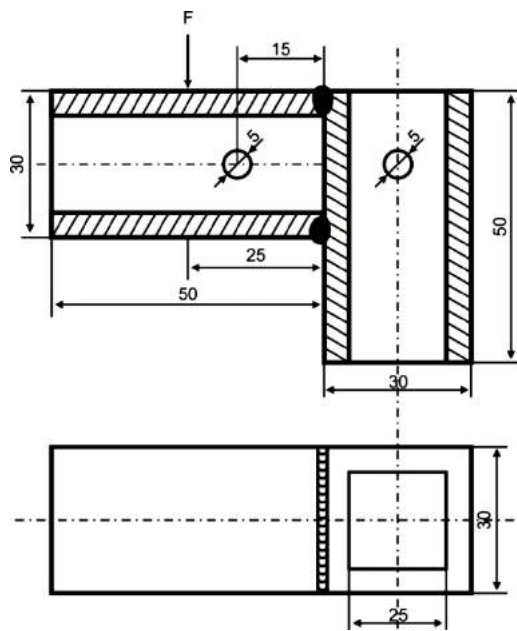


Fig.4. Shape and dimensions of tested specimens

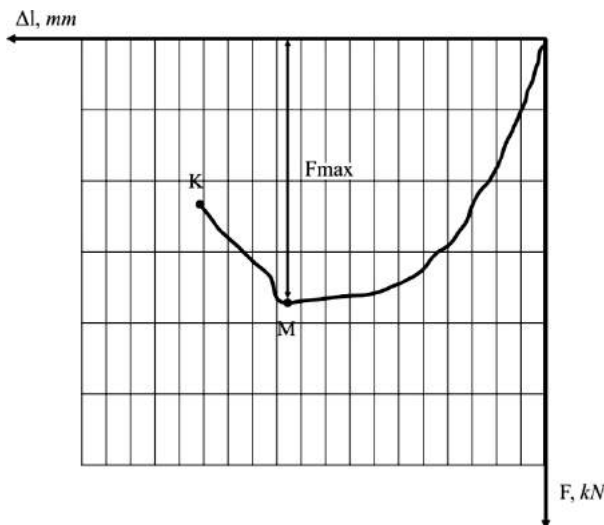


Fig. 5. Force dependence on elongation for specimens with holes

The presented diagrams (Fig.3 and Fig.5.) showed different material behavior due to different multiple stress concentration within tested samples. Complex stress state provoked by multiple stress concentration conditioned the different answers to loading. Furthermore, maximal bending forces obtained on two tested types of models were different. Mechanical properties comparisons of tested specimens are shown in Fig.6. The trend of decline in mechanical properties of tested models is obvious at Fig.6. The diameters of holes in tested models were a few times smaller than dimensions of cross section of square tubes, but provoked stress concentrations were significant to mechanical properties of models. It is important to note

that provoked stress concentrations would be severally higher in dynamic load conditions.

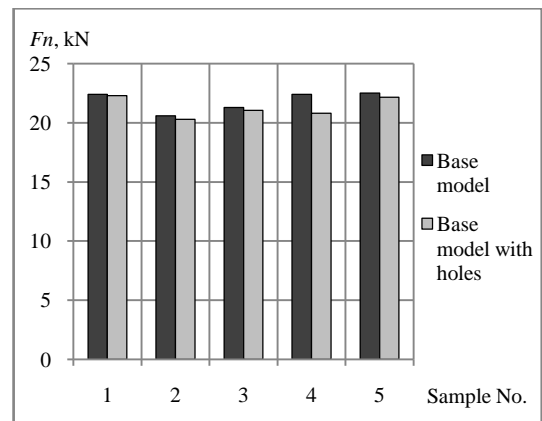


Fig.6. Mechanical properties comparisons of tested models

3. EVALUATIONS OF OBTAINED RESULTS

The material used for tested models preparation is widely used structural steel of commercial quality that fully meets the required mechanical properties, which was experimentally confirmed. Mechanical properties of welded joint, during testing, remain within the limits of base material. By that, it can be concluded that by the appropriate choice of parameters for technological welding process, good utilization of the base material can be achieved. The appearance of models made of steel tubes with square cross section and welded joints loaded to bending after testing is shown at Fig.7.



Fig. 7. Appearance of models with holes after testing

The position of breaking zone shows that the highest stress concentration occurred in the area welded joints. All tested models break at zones of highly loaded weldment. The obtained results are in agreement with other literature sources that analyze the stress concentration and stress-strain state of metallic materials in zones with high degree of inhomogeneity. The comparisons of maximal obtained bending force showed that multiple stress concentration provoke decline in mechanical properties of welded joints at steel tubes with square cross section. The self obtained experimental result is in accordance with relevant literature sources related to this area.

Different behavior of tested models during loading showed that mechanical properties of tested models were highly influenced by stress state distribution in zones of welded joints. Diagrams of dependence force on elongation for two types of models showed that stress concentration due to holes additionally complicate the stress state, but high levels of stresses were obtained in zones of weldments. The experimental results are in accordance with the results shown in the literature related to this area.

4. CONCLUSION

Welding is widespread joining method in mechanical constructions. Due to applied technology, it introduced high level of residual stresses and high degree of material inhomogeneity. Mechanical properties of welded joints are dominant influential factor to properties, safety and reliability of whole welded structures.

Experimental testing of mechanical properties of welded joints has become vital factor in the successful way of engineering and manufacturing, research and development of welded structures. Only with appropriate consideration of nature of welded joints, the benefits of this joining method can be fully realized. On the other hand, welded construction must be analyzed on different dimension levels. Development of mathematical models and finite element methods in analysis of welded construction bring higher degree of flexibility in design, but experimental determinations of mechanical properties of welded joints are essential. Experimental determination of mechanical properties of welded joints is not only a verification tool for analytical and numerical models. It is a method to establish phenomenological relationship in zones of welded joints.

The application areas of welded constructions and its roles become more and more important according to the modern demand in mechanical engineering. Furthermore, present safety and reliability demands become more and more stricter. The modern welded structures must have lower weight, better performance and reduced energy consumption. This facts support the use of efficient and more accurate design methods. The design methods must be linked to safety, reliability and quality requirements which must be based on full understanding of nature of welded joints. Also, welding without any improvement gives rise to local stress concentration, residual stresses and different types of defects. These features combined with high level of load give rise danger of failure and loss of structural integrity. However, the stress distribution for a complex welded structure is usually not known, and conservative assumptions are made of the residual stress distribution and stress concentration when life predictions are assessed.

Finally, the challenge, in order to obtain design and manufacture of lightweight and effective welded structures with appropriate safety and reliability, may be recognized as applying local design methods with evaluating of residual stress fields and stress concentrations. Those design methods must be related to nature of welded joints zones in relation to its positions, load and real exploitation conditions.

REFERENCES

- [1] JOSIFOVIĆ, D. (2000) *Examinations of mechanical construction I*, Faculty of Mechanical Engineering in Kragujevac (in Serbian).
- [2] JOVANOVIĆ, M., ADAMOVIĆ, D., LAZIĆ, V. (1996) *Welding technology*, Faculty of Mechanical Engineering, Kragujevac (in Serbian).
- [3] JOVANOVIĆ, M., LAZIĆ, V (2008) *MMA, MAG/MIG welding - manual*, Faculty of Mechanical Engineering in Kragujevac (in Serbian)
- [4] ILIĆ, A. (2007) *Application of 3D photoelastic analysis for determination of stress state in mechanical constructions*, Master degree thesis, Faculty of Mechanical Engineering, Kragujevac (in Serbian).
- [5] ILIĆ, A., JOSIFOVIĆ, D. (2008) *Design of the welded construction on the base of the photoelastic residual stress examinations*, 5th International Symposium „KOD 2008“, Proceedings of papers, pp. 359 – 364, Serbia.
- [6] ILIĆ, A., JOSIFOVIĆ, D., LAZIĆ, V. (2009) *Experimental determination of the construction form influence on stress concentration in welded joints*, 8th Youth Symposium on Experimental Mechanics, Proceedings of extended abstracts, pp. 6 – 7, Hungary.
- [7] ILIĆ, A. (2010) *Stress concentration and welded construction form influence on its durability*, PhD entrance thesis, Faculty of Mechanical Engineering, Kragujevac (in Serbian).
- [8] ILIĆ, A., JOSIFOVIĆ, D., LAZIĆ, V., IVANOVIĆ, L. (2011) *Experimental determination of stress concentration influence on welded constructions stability*, The 7th International Conference Research And Development Of Mechanical Elements And Systems IRMES 2011, Proceedings of papers, pp. 219 – 224, Serbia.
- [9] DALLY, J. W., RILEY, W. F. (2008) *Experimental Stress Analysis*, McGraw-Hill Book Company, USA.
- [10] JAMES, F. D. (2004) *MODERN EXPERIMENTAL STRESS ANALYSIS completing the solution of partially specified problems*, John Wiley & Sons Ltd, England.
- [11] DAVIES, C. (2003) *The Science and Practice of Welding*, Vol. 2, Cambridge University Press, England.
- [12] ENV 1993-1-1. Eurocode 3: *Design of steel structures - Part 1-1*. CEN 1992.
- [13] LUDWIG, M. J. (2000) *Design of Welded Connections*, American Welding Society, USA.
- [14] DAVID, S. A., DEBROY, T., DUPONT, J., KOSEKI, T., SMARTT, H. (2008) *Trends in Welding Research*, Proceedings of the 7th International Conference, American Welding Society, USA.
- [15] GROTE, K. H., ANTONSSON, E. K. (2009) *Springer Handbook of Mechanical Engineering*, Springer London, England.



DETERMINATION OF OPTIMUM TEMPERING TEMPERATURE IN HARD FACING OF THE FORGING DIES FOR WORKING AT ELEVATED TEMPERATURES

Vukić LAZIĆ, Dragan MILOSAVLJEVIĆ, Srbislav ALEKSANDROVIĆ, Rajko ČUKIĆ, Božidar KRSTIĆ, Gordana BOGDANOVIĆ

Faculty of Mechanical Engineering, Sestre Janjić 6, 34000 Kragujevac, Serbia
vlazic@kg.ac.rs, dmilos@kg.ac.rs, srba@kg.ac.rs, jbcukic@ptt.rs, bkrstic@kg.ac.rs, gocab@kg.ac.rs

Abstract: In this paper is presented only a part of the complex procedure that must be conducted in order to successfully regenerate damaged forging dies by hard facing. After identification of the type and cause of the dies damage, we have selected the procedure and parameters of hard facing, that were further corrected by test hard facing on models. In that way, we were able to relate the output results with the repairing technology. This made possible selection of optimum hard facing technology for the adopted procedure and the filler material, as well as for the chosen regime of thermal treatment.

Key words: forging tools, hard facing, tempering brittleness, toughness.

1. INTRODUCTION

The forging dies are in exploitation subjected to numerous cyclic loads, thus, after certain operating time, the impression damages occur, and the tool has to be replaced or repaired [1, 2]. Statistical investigations of the damaged dies have shown that main causes of their removing from exploitation could be: change of dimensions and form of impressions due to friction and wear, cracks all over the die due to thermal fatigue, and micro cracks caused by action of the stress concentrators [3, 4, 5, 6].

Besides the thermal stresses, caused by temperature gradient, also appear the structural stresses, which depend on chemical composition of steel, kinetics of austenite transformation, and of the cooling speed. Due to influence of cyclic variation of thermal stresses, the initial cracks can also appear on the material surface.

In the present case, we analyzed the forging dies aimed for manufacturing parts in car and trucks making industry. During the excessive monitoring of dies in exploitation, it was noticed that failures could be due to following reasons: increase of the forged pieces dimensions due to worn die, deformation of the thin-walled portions of the die, appearance of cracks at certain parts of the die, and local fractures.

The aforementioned damages are remedied primarily by application of the manual metal arc welding (MMA) procedure, and machining is mainly done by grinding, depending on the application of the filler material. In

order to select the optimum technology of forging dies hard facing, numerous test were conducted at the model whose sizes were determined according to the similarity theory principle, namely the non-dimensional analysis.

For the quality criterion of the performed hard facing was adopted the change of hardness and structure in the zones of the hard faced layer, namely in the heat affected zone and beneath it, as well as the resistance of the deposited layers to wear.

Hard facing of dies aimed for operation at elevated temperatures as an objective has generally their repairing by compensating losses caused by friction or crumbling.

2. MATERIALS FOR FORGING DIES MANUFACTURING AND THEIR CHARACTERISTICS

Refractory steels are used for temperatures above 300°C. Here we speak of small, medium and large dies, for hot forming, tools for pressing and extrusion of non-ferrous metals at elevated temperatures, tools for hot trimming, dies for pressurized casting of pure Al, Zn and Mg.

In the considered case, all experiments were conducted on forging dies made of steel Č5742 (DIN 17350 56NiCrMoV7) and Č4751 (DIN 17350 X38CrMoV51). Chemical composition, mechanical characteristics and microstructure of these steels are given in Tables 1 and 2 [1, 2].

Table 1. Chemical composition and comparative marks of steels Č5742 and Č4751

No.	Mark by YUS	Chemical composition, %									Relation to other standards	
		C	Si	Mn	P	S	Cr	Ni	Mo	V	DIN	UNI
1.	Č5742	0.55	0.3	0.7	0.035	0.035	1.1	1.7	0.5	0.12	56NiCrMoV7	U52NiCrMo6KU
2.	Č4751	0.40	1.0	0.4	0.025	0.025	5.0	-	1.3	0.4	X38CrMoV51	UX35CrMo05KU

Table 2. Mechanical characteristics and microstructure of steels Č5742 and Č4751

No.	Mark by YUS	Soft annealing			Tempering temperature			Preheating temperature, T_p , °C	Microstructure B.M.
		t, °C	HV _{max}	R _m , MPa	t, °C	HRC	R _m , MPa		
1.	Č5742	670-700	250	850	400-700	50-30	1700-1100	≈ 300	M + B (Interpass)
2.	Č4751	800-830	250	850	550-700	50-30	1700-1100	≈ 300	M + B (Interpass)

Since blacksmith workshops use forging dies in thermally tempered state (quenching and high tempering), we subjected all the samples to that treatment, to come as close as possible to real exploitation conditions. On selected samples (models) we measured hardness after thermal treatment and it was 40-42 HRC for Č5742 and 41-49 HRC for Č4751. The softening annealing was not performed (though HV>350) since mainly grinding was used for machining.

Since the samples of thicker cross sections were also hard faced (s = 40-45 mm), made of steels prone to self-hardening (C>0.35%), the preheating was necessary. The preheating temperature was determined according to Seferian formula [7], obtaining $T_p \approx 300^\circ\text{C}$.

3. SELECTION OF PROCEDURE, TECHNOLOGY AND FILLER MATERIAL

Hard facing of chosen samples was performed in Laboratory of Zastava cars, by application of cored electrodes. Technological parameters of hard facing were determined according to [1, 7, 8, 9, 10], and hard facing was performed in two and three passes to decrease the degree of mixing (dilution), i.e., to obtain declared characteristics supplied by the manufacturer of electrodes. We measured the velocity of hard facing during each pass, and we also, prior to applying another layer, checked the preheating temperature, i.e., the interpass

temperature. The digital-measuring device Tastoherm D1200 was used for measurements, which is supplied with a thermocouple NiCr-NiAl with a measuring range from - 50°C to 1200°C.

As a filler material there were applied highly alloyed basic electrodes UTOP 38 (DIN 8555 - E3-UM-40T, Ø3.25 mm) and UTOP 55 (DIN 8555 - E6-UM-60T, Ø5.00 mm). The filler materials were aimed for hard facing of dies

that are used for forming of steels and other metals both in hot and cold state, like ingot mold, steel molds, dies and pressing mandrels. Hard faced layers are tough, resistant to wear and impact. The hard faced layers hardness is constant up to temperature of 600°C [1].

This basic electrodes were dried prior to application according to the following regime: heating up together with the furnace up to temperature of 350-400°C, keeping for 2 hours at the drying temperature, and cooling in the furnace for 1 hour, while the temperature did not fall below 150°C. Thus heated electrodes were used for hard facing of the preheated samples, with decreasing the level of diffusive hydrogen and eliminating the possibility appearance of hydrogen induced cracks.

In Tables 3 and 4 are presented the hard facing parameters (hard facing current was for about 10% lower than at welding), as well as properties of the filler material [1].

Table 3. Parameters of the MMA hard facing

No.	Electrode mark		Core diameter, mm	Hard facing current, A	Voltage, V	Hard facing velocity, cm/s	Heat input energy, J/cm
	Iron plant SŽ Jesenice	DIN 8555					
1.	UTOP 38	E3-UM-40T	3.25	115	26	≈ 0.28	8543
2.	UTOP 55	E6-UM-60T	5.00	190	29	≈ 0.25	17632

Table 4. Filler material properties

No.	Electrode mark		Chemical composition, %					Type of current	Hard face layer hardness, HRC	Application
	Iron plant "Fiprom"	DIN 8555	C	Cr	Mo	V	W			
1.	UTOP 38	E3-UM-40T	0.13	5.0	4.0	0.20	+	= (+)	36-42	Hard facing of dies for operation at elevated and normal temperatures
2.	UTOP 55	E6-UM-60T	0.50	5.0	5.0	0.60	+	= (+)	55-60	- II -

Order of hard faced layers deposition is given in Figure 1.a, where prior to each pass, the layer of slag was removed with a steel brush. The following layers were also applied according to this scheme (the second - Figure 1.b and the third - Figure 1.c).

The width of a pass hard faced with the $\varnothing 3.5 \text{ mm}$ electrode was $b \approx 10\text{-}12 \text{ mm}$, the height of the faced layer was $h \approx 1.5 \text{ mm}$, and with the $\varnothing 5.00 \text{ mm}$ electrode measures were $b \approx 16\text{-}18 \text{ mm}$ and $h \approx 2.1 \text{ mm}$ [1].

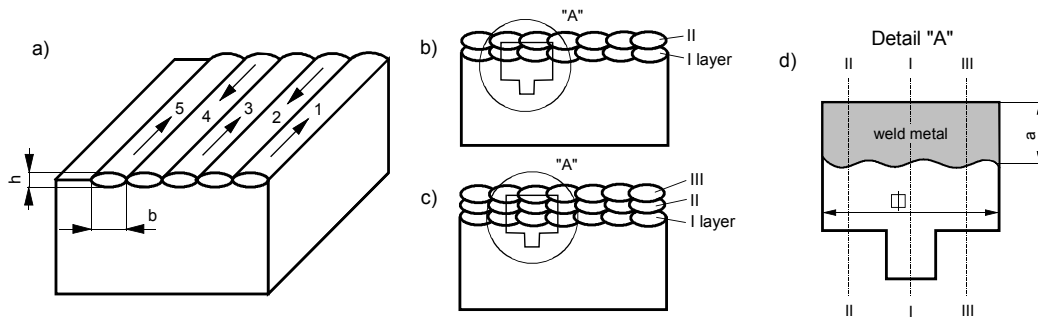


Figure 1. Order of hard faced layers deposition: a - 1st layer, b - 2nd layer, c - 3rd layer, d - pin appearance

4. PHENOMENON OF TEMPERING BRITTLENESS

4.1 Theoretical considerations

During hard facing of hardening prone steels aimed for forging dies, in the vicinity of the hard faced layer, appear brittle unfavorable structures, the residual stresses increase occur, which frequently surpass the yield strength. From all these reasons, it is necessary to perform tempering, after the forging dies hard facing, in order to decrease the level of residual stresses, and to transfer martensite structures into the upper bainite (feathery) structures, with preservation of good mechanical properties. Frequently, in real manufacturing conditions, arises a problem of selecting the optimum annealing temperatures, which in fact represents the compromise between the presented requirements.

It was noticed that, in some steels that were alloyed with Mn or Cr, i.e., Cr-Mn or Cr-Ni, during annealing can appear a damaging phenomenon of the so called "tempering brittleness". Tempering should be avoided from temperatures in zones in which is recorded the increased hardness, so it is recommended that tempering starts even from higher temperatures. In cases when tempering is performed from higher temperatures, the rapid cooling is recommended through the critical temperatures region, i.e., undercooling, what prevents diffusion as an essential factor for appearance of tempering brittleness [1, 11].

On the other hand, for some classes of steels, the decrease of toughness is possible to notice also by metallographic methods [1, 11], while for reduction of hazard that this phenomenon occurs it is strongly recommended to alloy these steels by molybdenum (up to 0.6%), by tungsten (up to 1.5%), as well as by niobium. During tempering, these elements exhibit positive effects, since they are slowing segregation. On the contrary, carbon and phosphorus contribute to appearance of the tempering brittleness. The assumption is that the negative effect of phosphorous initiates already at small amounts ($\approx 0.005\% \text{ P}$) [1, 11]. Influence of phosphorus is related to its expressed tendency to segregation. Also, about very important influence of phosphorus on this phenomenon, displays the

fact that carbides, extracted from steel in brittle condition, are richer with phosphorus than carbides extracted from steels that possess normal toughness. The mentioned phenomenon of toughness decrease is reversible, which means that it will reappear after later heating over 520°C , and slow cooling.

Sensitivity of material to tempering brittleness can be established by testing the steel for impact toughness, in the wide temperature range, as well as by determination of the steel transition temperature from ductile to brittle fracture. Tendency of different steels to appearance of tempering brittleness depends mainly on their chemical composition, manufacturing procedure and processing.

In the present case, we have investigated influence of the tempering temperature of hard faced tools on hardness distribution across the hard faced layer cross section. To do that, we varied tempering temperatures from 370 to 670°C , taking 30°C as the temperature interval. Time of keeping the sample at certain temperature was two hours, with slow cooling down to room temperature. In Figure 2 are presented hard faced layer and base metal hardness variation as a function of the tempering temperature. It can be noticed that at temperature $\approx 520^\circ\text{C}$ an increase of hardness occurs, what points to possibility of tempering brittleness that was caused by martensite decomposition, and residual austenite in the structure. Function of hardness variation of the hard faced layer, obtained by experiments, is in agreement with data from literature for the base metal [12, 13], since the chemical composition of the filler material, approximately corresponds to base metal.

4.2 Presentation of obtained results

In order to investigate the cooling speed influence to the tempering brittleness, we heated new samples up to 520°C , then heated through for two hours, and in one case cooled slowly together with the furnace, and in the other in the quiet air. The HV1 hardness was measured on those samples in the I-I direction (Figure 1d), starting from different distances from the hard faced layer surface. In Figure 2a,b are given diagrams as representation of the hardness variation.

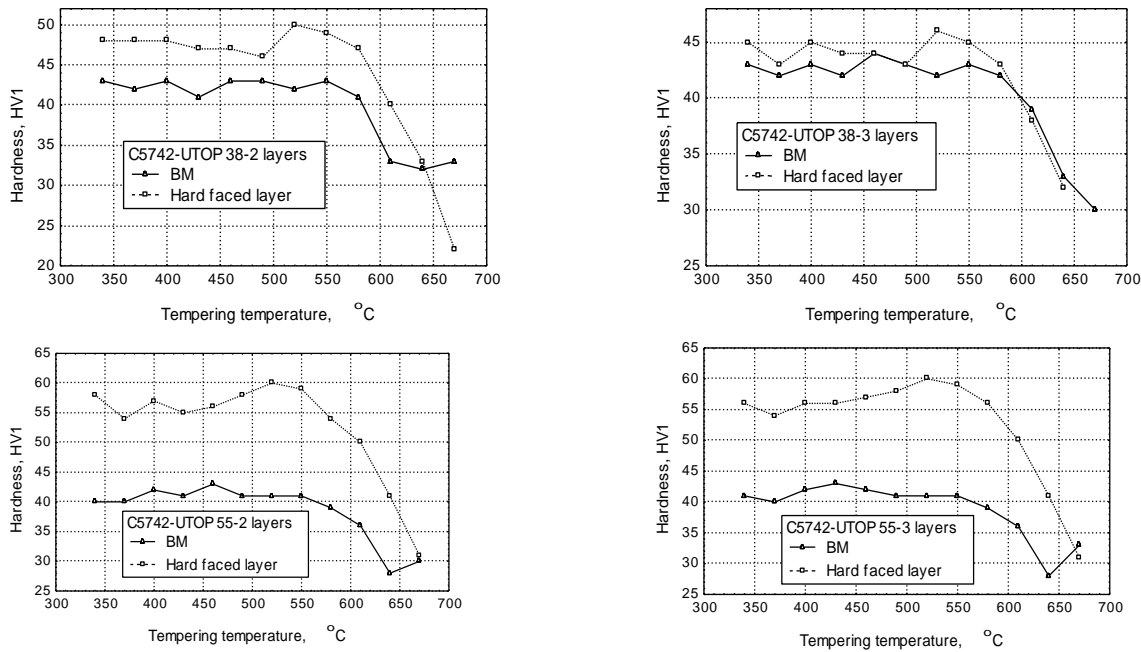


Figure 2. Hardness variation as a function of tempering temperature

5. CONCLUSION

In the paper we have shown that successful hard facing of forging dies is possible only after detailed investigation on models. Besides the corresponding technology of hard facing, it is also necessary to determine experimentally the thermal treatment regime which will ensure that the reparation procedure, proposed here, produce satisfactory results also in exploitation conditions. Besides requirements that are related to mechanical properties of the hard faced layer, the resistance to wear and thermal fatigue, also needed is proper toughness and favorable microstructure, as well as good machinability. These contradictory requirements can be fulfilled only by appropriate selection of the reparation procedure and corresponding filler metal, then by selection of optimum hard facing technology, including also as cheap as possible final machining of the repaired part.

All these point out the fact that the reparation tasks can be successfully performed only in specialized plants, which have at their disposal, the adequate equipment and corresponding expert staff, and in no case can that be done in improvised workshops.

REFERENCES

- [1] LAZIĆ, V. (2001) *Optimization of hard facing process from the aspect of tribological properties of hard faced metal and remaining stresses*, (PhD thesis), Faculty of Mechanical Engineering in Kragujevac, (in Serbian).
- [2] LAZIĆ, V., et al. (2005):: *Selection of the optimum technology of the forging dies reparation from the aspect of tribological characteristics*, TRIBOLOGIA – TEORIA I PRAKTIKA, ROK XXXVI, NR 2 (200), pp. 11-31.
- [3] DZIUBINSKI, J., KLIPMEL, A. (1985) *Napawanie i natryskiwanie cieplnie*, Wydawnictwa Naukowo-Techniczne, Warszawa, (in Polish).
- [4] WERNOSKI, A. (1983) *Zmeczenie cieplne metali*, Wydawnictwa Naukowo- Techniczne, Warszawa, (in Polish).
- [5] GIERZYNSKA, M. (1983) *Tarcie zużycie i smarowanie w obróbce plastycznej metali*, Wydawnictwa Naukowo-Techniczne, Warszawa, (in Polish).
- [6] BELJSKI, E., I. (1975) *Stoikost kuznečenih štamпов*, Izdatelstvo "Nauka i tehnika", Minsk, (in Russian).
- [7] JOVANOVIĆ, M., ADAMOVIĆ, D., LAZIĆ, V. (1996) *Technology of hard facing - handbook*, self-edited by authors, Kragujevac, (in Serbian).
- [8] LAZIĆ, V., et al. (2010) *Theoretical-experimental determining of cooling time ($t_{8/5}$) in hard facing of steels for forging dies*, Thermal science, Vol. 14, No. 1, pp. 235-246.
- [9] LAZIĆ, V., et al. (2009) *Reparation of damaged mallet for hammer forging by hard facing and weld cladding*, Tehnical Gazete Vol. 16, No. 4, pp. 107-113.
- [10] LAZIĆ, V., et al. (2010) *Energetic analysis of hard facing and weld cladding of an air powered drop hammer damaged ram*, Thermal science, Vol. 14, Suppl., pp. S269-S284.
- [11] VIDOJEVIĆ, N. (1973) *Thermal treatment of metals*, Faculty of Technology and Metallurgu, Belgrade, 1973. (in Serbian).
- [12] LAZIĆ, V., et al. (2001) *Influence of post surfacing thermal treatment on working characteristics of forging tools*, Welding & welded structure, Vol. 46, No. 1-2, pp. 5-11, (in Serbian).
- [13] CATALOGUES: Verkaufsgesellschaft M.B.H., Vosen-dorf., SŽ Jesenice, Bohler-Kapfenberg, Messer Griesheim-Frankfurt am Main, Lincoln Electric-SAD, etc.

SELECTION OF THE WELDING TECHNOLOGY OF RELIABLE ASSEMBLIES USING GMAW PROCESS

Vukić LAZIĆ, Dragan MILOSAVLJEVIĆ, Srbslav ALEKSANDROVIĆ, Rajko ČUKIĆ, Božidar KRSTIĆ,
 Gordana BOGDANOVIĆ

Faculty of Mechanical Engineering, Sestre Janjić 6, 34000 Kragujevac, Serbia
vlazic@kg.ac.rs, dmilos@kg.ac.rs, srba@kg.ac.rs, jbcukic@ptt.rs, bkrstic@kg.ac.rs, gocab@kg.ac.rs

Abstract: In this paper it will be given a procedure of determination of optimized shielded gas welding technology of the high reliable assemble built-up of the massive pipes on plate. Determination of welding regime, besides of welding method choosing, welding joint and welding groove, filler metal and welding equipment, calculating of energy-technological parameters, implies preliminary estimate of the base metal weldability. That estimate can be resumed as evaluation of resistance to cracks in the base metal during welding procedure, as well as determining prior and the follow-up thermal treatment of base metal if needed.

Key words: weldability, welding technology, preheating, GMA welding, cracks.

1. INTRODUCTION

In this paper is exposed only a part of results of determination of welding technology for reliable assembly to be used in Cern research installment in Switzerland. According to Figure 1a, the central pipe (position 1) should be welded for the plate (position 2),

with previously prepared groove according to detail "A" (Figure 1b). After that, it is also necessary to weld the two cut pipes (position 3) with the circular joint to the pipe detail "B" (Figure 1c), as well as longitudinally to the pipe along the two generator lines according the detail "C" (Figure 1d). Here we consider technology of welding of central pipe for plate wall only.

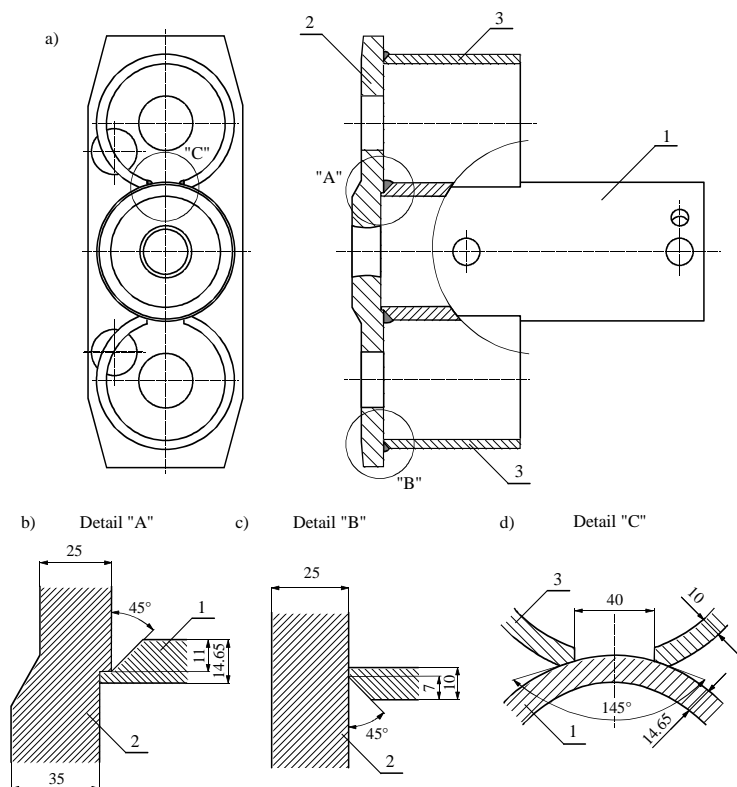


Figure 1. Welding of the central and peripheral pipes to the plate (a) and appearance of the individual grooves (b, c, d)

2. EVALUATION OF THE BASE METALS WELDABILITY

from catalogues and obtained by chemical analysis, are given in Tables 1 and 2, respectively.

Chemical composition and mechanical properties of the base metal (positions 1 and 2) - St 52.0 and C 15, taken

Table 1. Chemical composition and mechanical properties of the welded steel - St 52.0 (DIN 2448/81, DIN 1629/84)

Content of individual elements, %									
	C	Si	Mn	P	S	Cr	Ni	Cu	Al
Catalogue	0.14-0.20	0.40-0.55	1.20-1.50	≤0.04	≤0.04	≤0.30	≤0.30	≤0.03	-
Analyzed	0.17	0.45	1.33	0.008	0.009	-	-	-	0.028
Mechanical properties									
	R _{eH} , MPa		R _m , MPa		A ₅ , %				
Catalogue	min 355		500-650		min 21				
Analyzed	377		577		30.8				

Based on the chemical and metallographic analyses of the welded steel, one can say that here we deal with the small grain C-Mn steel of the increased strength (R_m= 577 MPa,

R_{eH}= 377 MPa, A₅= 30.8%) of the lamellar ferrite-perlite structure.

Table 2. Chemical composition and mechanical properties of the welded steel - C 15 (DIN 17 2109)

Content of individual elements, %									
	C	Si	Mn	P	S	Cr	Ni	Cu	Al
Catalogue	0.12-0.18	≤ 0.40	0.30-0.60	≤0.045	≤0.045	-	-	-	-
Analyzed	0.14	0.02	0.38	0.010	0.008	0.02	0.04	0.05	0.033
Mechanical properties									
	R _{eH} , MPa		R _m , MPa		A ₅ , %		HB		
Analyzed	274		369		37		118		

Based on the chemical and metallographic analyses of the welded steel, one can say that here we deal with the steel of the lamellar ferrite-perlite structure.

According to calculations criteria (given in detail in literature [1, 2, 3, 4, 5, 6, 7]), here we deal with steels of good weldability. Thus, with adequately selected technology, these positions can be successfully welded with different welding procedures (SMAW, GMAW).

The base metals are resistant to both cold cracks, and, especially, to hot cracks, due to negligible content of impurities [3, 5, 8, 9].

3. WELDABILITY OF THE BASE METALS

We selected the metal arc gas welding with gas mixture, at the semi-automatic numerical machine for circular welding. In order to fix the pipe cover for the plate three joints at three points at 120° angles were made. Prior to joining, the perpendicularity of the pipes and the plate was checked, for each assembly. Joining was done with 82% Ar + 18% CO₂ shield, manually (with the wire of diameter 1.6 mm and current of intensity I ≈ 280 A), and the joints' length was about 20 mm. After cooling down to the room temperature, the beginnings and ends of joints on all three joints were fix.

3.1 Calculation of the welding parameters

Technological parameters of metal arc gas welding were calculated according to the following method [5]:

- Groove area: $A_g = 2 \cdot P_{\Delta} = 11 \cdot 11 / 2 = 60.5 \text{ mm}^2$;
- Joint area: $A_j \approx 1.1 \cdot A_z = 1.1 \cdot 60.5 = 66.55 \text{ mm}^2$;
- Single joint layer area: $A_z \approx 33 \text{ mm}^2$;
- The single layer mass per unit length: $M = \rho \cdot A_z \cdot L = 7.85 \cdot 0.33 \cdot 1 = 2.59 \text{ g}$;
- Quantity of the deposited material per time unit: $m_{1.6} = 0.64 + 0.55 \cdot M - 0.055 \cdot M^2 = 1.70 \text{ g/s}$;
- Welding speed: $v_z = \frac{m \cdot 6000}{A_z \cdot \rho} = 0.656 \text{ cm/s}$;
- Wire speed: $v_t = \frac{0.012132 \cdot A_z \cdot v_z}{d^2} = 6.46 \text{ m/min}$;
- Welding current: $I_{1.6} = 378 \cdot \log v_t + 26 = 332 \text{ A}$;
- Operating voltage: $U = 14 + 0.05 \cdot I = 31 \text{ V}$;
- Heat input energy: $q_l = \frac{U \cdot I}{v_z} \cdot \eta = 13336 \text{ J/cm}$;
- Welding depth: $\delta = 0.3 \cdot r = 0.3 \cdot 0.00537 \sqrt{q_l} = 0.186 \text{ cm}$;

- Shielding gas type: mixture (82% Ar + 18% CO₂);
- Shielding gas flow: $q \approx 20$ l/min.

The calculated welding parameters serve as the initial ones for selecting the welding regime in the metal arc gas welding. The same are then compared to ones proposed from experience and, eventually, the correction of calculations is done prior to the welding itself. After testing of the realized joints, those welding parameters are adopted that produce the best results [8].

3.2 Selection of the filler metal

As the filler metal is used the steel (copper plated) wire - VAC 60, $\varnothing 1.6$ mm (DIN 8559/94 - SG-2-CY 4233), aimed for welding in the gas shielded atmosphere. Mechanical properties of the clean welding layer and chemical composition of the wire are given in Tables 3 and 4, respectively [5, 10].

Table 3. Mechanical properties of the clean welded layer

Yield strength R_{eH} , MPa	Tensile strength R_m , MPa	Elongation A_5 , %	Toughness (-40°C) ISO-V, J
410-490	510-590	22-30	> 47

Table 4. Wire chemical composition (Welding current: DC-E. +)

C	Si	Mn	P	S
0.08	0.90	1.50	<0.025	<0.025

3.3 Selection of the welding technology and control of the realized joints

Prior to commencing the continuous welding, for both the test and for real ones, the circular radial deviation of each working piece was checked. This deviation was within the range of 0.1 to 0.2 mm, what was considered as acceptable. In addition, prior to welding, the joint pieces were degreased by washing with the adequate cleanser, and then they were dried.

In order to select the optimum technology, the numerous test welds were performed with the calculated parameters, under the conditions without preheating, in two passes. After these tests, we decided to weld pipes for the plate in two passes and without preheating. Passes were done

immediately one after the other. The capping pass 2 relaxes the root pass 1 what gives better microstructure, the possible brittle zones are avoided, and the level of the residual stresses is decreased. With this way of welding the necessary excess weld metal is formed, which is removed by machining due to final ultrasonic control. From the test joints, the metallographic ground test samples were prepared, at which the micro hardness was measured (HV1) and the microstructure was read off individual zones of the welded layer (Table 5). The welding regime in these tests was the following: $U = 31$ V, $I = 333$ A, $v_z = 0.6$ cm/s, $q_1 = 14624$ J/cm.

Table 5. Measured hardness and read off microstructure of individual joint zones (2-layers, $T_p \approx 20^\circ\text{C}$)

Tested zone	Read off microstructure	Maximum and minimum hardness, HV1
B.M.1	Lamellar perlite-ferrite	185-193
HAZ ₁	Interphase + tempered martensite	210-310
WELDING METAL	Small grain Vidmansteten + granular (globular) perlite + bainite	239-245
HAZ ₂	Needle martensite + bainite + tempered martensite + perlite	289-400
B.M.2	Lamellar perlite-ferrite	175-189

Based on read off microstructure and measured micro-hardness (Table 5), one can notice that in HAZ₂ the hardness is somewhat bigger than the prescribed limit value ($HV \approx 350$). Though it is allowed that in HAZ hardness can be bigger than this value, under the condition that the wire is dry and clean, we did, for the sake of better filing of the groove, nicer appearance of the

weld and somewhat lesser value of the HAZ₂ hardness, correct the welding parameters, and then continued with the test welds. In these additional tests, the welding regime was: $U = 32$ V, $I = 345$ A, $v_z = 0.42$ cm/s, $q_1 = 21300$ J/cm. The measured hardness and microstructure of individual zones of the weld, done by this regime, are shown in Figure 2.

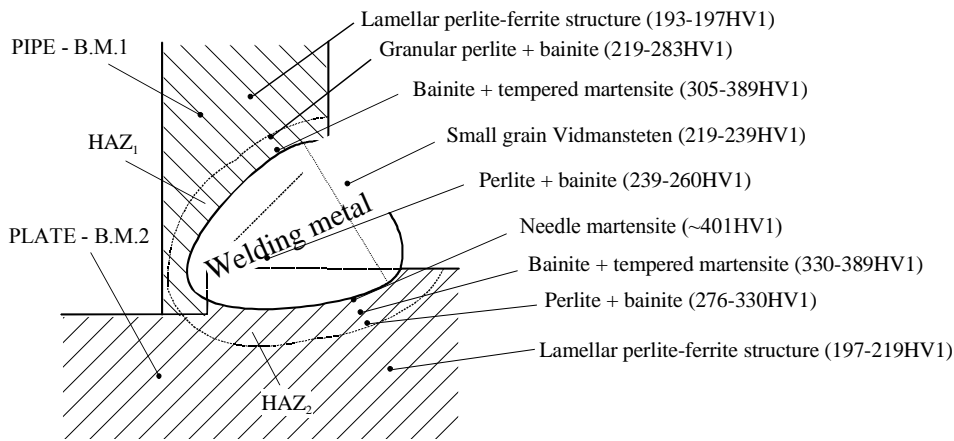


Figure 2. Measured hardness and read off microstructure of individual zones of the weld (2 layers, $T_p \approx 20^\circ\text{C}$)

By comparative analysis of the obtained results on samples with the original and corrected welding regimes, the negligible changes can be noticed, both of hardness and microstructure of individual zones of the weld (especially in the HAZ₂, along the joining line of the weld and the plate). The reason for the increased hardness should be looked for in increased cooling speed due to significantly bigger plate thickness (35 mm) than the pipe of thickness (14.65 mm). Regardless of the fact that the increased hardness could be tolerated due to low level of the diffused hydrogen, we decided to perform the two-pass welding with preheating. Parts were heated in the furnace up to $T_p = 200^\circ\text{C}$, heated through for 2 hours at that temperature and welded. Reason for this is to prevent appearance of the needle martensite in the HAZ₂. Welded assemblies, where the preheating temperature dropped below 150°C , were additionally heated by the gas burner immediately prior to welding. The temperature was there controlled by thermo-chalks.

During performing the two-pass welding the energetic parameters were constantly monitored (I , U and v_w), related to driving power which, in welding of real parts, ranged within limits $q_1 = 14624\text{--}21300 \text{ J/cm}$. This energy, with application of preheating provides for necessary welding in, convenient hardness and microstructure, as well as the adequate output mechanical properties.

4. CONCLUSION

Considering the extensive theoretical and experimental analyses, which are related to weldability of the base metal, the adopted procedure, chosen filler metal, applied technology and metallographic-laboratory control of the welded joints, the following conclusions can be drawn:

- The base metal is from the high steels class and its weldability is good,
- This steel is not prone to forming of cracks and brittle zones during welding by melting,
- Welding can successfully be performed by metal arc gas welding procedure with the proposed technology,
- The two-pass welding is necessary due to construction of the given type of groove,
- Experimental investigations with preheating showed negligible increase of hardness from the prescribed limit value,

- By preheating the danger of forming the brittle phases and appearance of undesirable microstructure were prevented.

REFERENCES

- [1] LAZIĆ, V., et al. (1995) *The contribution to determination of limiting welding parameters of high strength steels*, Faculty of Mechanical Engineering in Kragujevac, Proceedings, Kragujevac, pp. 133-140.
- [2] JOVANOVIĆ, M., et al. (1995) *Review and evaluation of high strength steels weldability*, Faculty of Mechanical Engineering in Kragujevac, Proceedings, Kragujevac, pp. 125-132.
- [3] VULOVIĆ, R., et al. (2005) *Selection of the welding technology of reliable joints using GMAW process*, HEAVY MACHINERY - HM 2005, Kraljevo, Proceedings, pp. II A.5–II A.8.
- [4] LAZIĆ, V., et al. (2005) *Theoretical-experimental determining of cooling time ($t_{8/5}$) in hard facing*, HEAVY MACHINERY - HM 2005, Kraljevo, Proceedings, pp. II A.17–A 20.
- [5] JOVANOVIĆ, M., et al. (1996), *Welding technology – Manual independent author's edition*, Kragujevac, (first edition), (in Serbian).
- [6] MILOSAVLJEVIĆ, M., et al. (1986) *Fundamentals of Steel Constructions*, Gradjevinska knjiga, Belgrade, (in Serbian).
- [7] LAZIĆ, V., et al. (1995) *Validity of some formulae for calculation of cooling time during welding*, Welding & welded structures, Vol. 40, No. 2, pp. 89-94.
- [8] LAZIĆ, V., et al. (2004) *Improvement of the welding procedure of the fire truck rear axle semi housing assembly*, Mobility & Vehicles Mechanics, Vol. 30 No 1, pp. 45-57.
- [9] ITO, Y., BESSYO, K. (1972) *Weld crack ability formula of high strength steels*, J. Iron and Steel Inst., Jap., No. 13, pp. 916-930.
- [10] Catalogues of electrode and electrode materials producers: FEP-Plužine, SŽ Jesenice-Slovenia, Bohler-Kapfenberg, Messer Griesheim-Frakfurt am Main, Esab- Goteborg, Lincoln Electric-SAD, etc.
- [11] STANDARDS: JUS, DIN, ASTM, PN, etc.

AN OVERVIEW ON FRICTION STIR WELDING OF THE AL 2024 T351

Dragan MILČIĆ¹, Aleksandar ŽIVKOVIĆ², Miroslav MIJAJLOVIĆ¹

¹ University of Nis, Faculty of Mechanical Engineering Nis, Aleksandra Medvedeva 14, 18000 Nis, Serbia

² Goša FOM a.d., Industrijska 70, 11420 Smederevska Palanka, Serbia

milcic@masfak.ni.ac.rs, a.zivkovic@gosafom.com, mijajlom@masfak.ni.ac.rs

Abstract: Friction stir welding is a solid state welding technique used for joining soft metals such aluminium and its alloys are. Alloy 2024 is a representative of conventionally unweldable alloys but fully weldable by friction stir welding. In this case, welding is possible only when proper geometry of the welding tool, welding speed etc. are selected. Like for other welding techniques, results of the welding have to be evaluated by testing given by requirements of appropriate standards. However, it is a challenge to select proper parameters and paper presents some successful experimental results on this topic and announces further developments in the technology of the friction stir welding.

Key words: Friction Stir Welding, 2024 aluminium alloy

1. INTRODUCTION

Friction stir welding (FSW) is a solid state welding process predominantly used for joining materials difficult to weld by applying some of conventional processes. Its application is mainly connected with the welding of aluminium alloys and other soft metals/alloys. In comparison to other welding processes, FSW delivers the smallest amount of energy to the base metal, which results in the smallest deformation in the structure of the base metal. However, FSW is still an unconventional welding process because of the complexity of application and the need for long welds in order to have great productivity. FSW is used for plate-shaped parts [1].

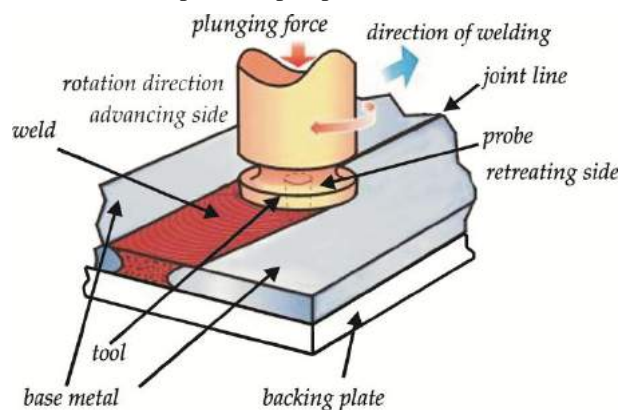


Figure 1 Schematic of the FSW process

In FSW, a cylindrical, shouldered tool (Figure 1) with a profiled threaded probe is rotated at a constant speed and fed at a constant traverse speed into the joint line between two plates, which are butted together. The parts have to be clamped rigidly onto a backing plate to enable welding.

2. WELDING TOOL

Welding tool used in FSW is a specialized rotating component that passes entirely through or partially

through the workpiece(s) along the joint line, and may or may not have a shoulder [1] and the welding tool always has a probe. The probe is usually cone or cylindrical with the thread on the side. It is common to use left sided thread for clockwise rotation of the welding tool or right sided thread for counterclockwise rotation of the welding tool. The type of the thread is various: metric, profiled, oval etc., with changeable/unchangeable thread step. What type of the thread and thread step will be used depends from the material of workpieces (base metal).

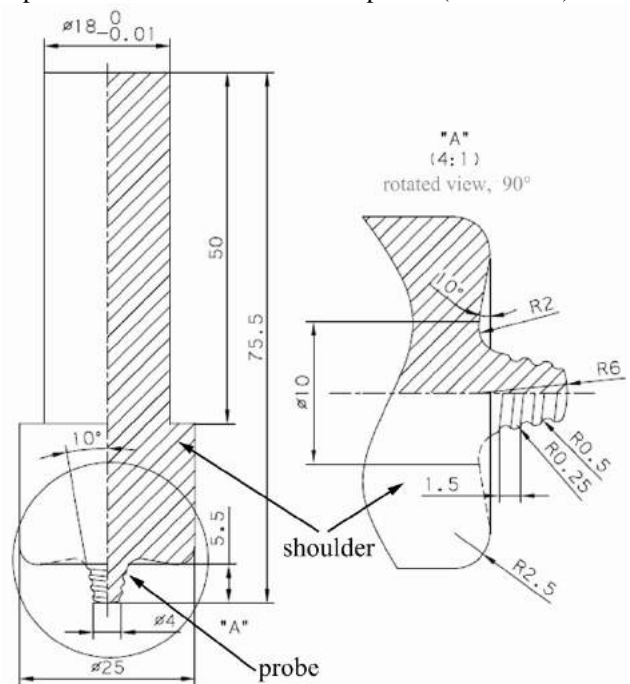


Figure 2 Drawing of the common welding tool [2]

Welding tools must resist high temperatures, and wear and they are manufactured from durable, heat resistant and high strength steels. Active surfaces [1] of the welding tool are usually manufactured by milling or

turning, polished and heat treated after machining – annealed and normalized. Hardness of active surfaces on the welding tool should be at least the same as the hardness of workpieces or higher.

3. WORKPIECES

The first application of FSW was on the groove welds on railway vehicles [1] however it was never intended to be used only for the one type. Development of the FSW was tremendous and it expanded on various fields as well as on application on butt welds, spots welds etc. However, groove welds are primary application of the FSW especially on the plate-shaped parts where pipes are included as well.

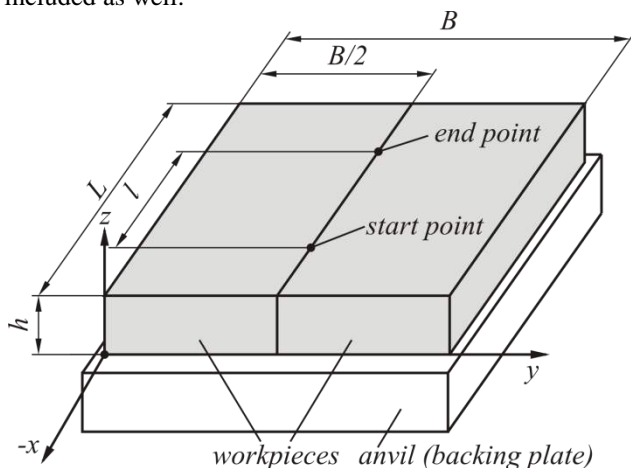


Figure 3 Scheme of the positioned workpieces in position for welding

Before the welding start workpieces are set on an anvil (backing plate), connected to each other on the joint line and clamped to the work table of the machine. Workpieces must be rigidly clamped since forces that appear during welding have to be used for deformation, stirring and mixing of material instead of moving workpieces. Anvil assists in weld root creation and supports workpieces during welding. It has to be manufactured from stiff, rigid, with low thermal conductivity material capable to maintain stability of the system and reduce thermal losses.

3.1. Material of workpieces

FSW is widely used for the joining of softer metals such aluminium and aluminium alloys are. Aluminium alloys are always a challenge for welding, without concern on weldability or unweldability of base metal. Like other arc welding processes, FSW is applicative for welding of 5xxx and 6xxx series of Al alloys but its advantages over other processes are seeable when welding 2xxx class of Al alloy. A representative of the 2xxx class is alloy 2024 and it is widely used in FSW processes.

Aluminium alloy 2024 is an Al alloy, with Cu and Mg as the alloying elements. It is used in applications requiring high strength to weight ratio, as well as good fatigue resistance. It is not weldable, and has average machinability. Due to poor corrosion resistance, it is often clad with Al or Al-Zn for protection, although this procedure may reduce the fatigue strength. It has a density

of 2.73 g/cm³, Young's modulus of 73 GPa across all tempers, and begins to melt at about 500 °C. Due to its high strength and fatigue resistance, 2024 is widely used in aircraft structures, especially wing and fuselage structures under tension. Because the material is susceptible to thermal shock, 2024 is used in qualification of liquid penetrant tests outside of normal temperature ranges.

Table 1. Chemical composition and mechanical properties of alloy EN AW 2024 T351

Chemical composition		Mechanical properties	
Chemical element	Mass %		
Al	~	0.2% Proof Stress $R_{p0.2}$	266-274 N/mm ²
S	0.12		
Fe	0.28		
Cu	4.52	Tensile Strength R_m	404-424 N/mm ²
Mn	0.65		
Mg	1.60		
Cn	0.01	Elongation A_5	22.00%
Zn	0.09		
Ti	0.016		
B	0.009		
N	0.02		

Data in Table 1 is taken from the Approved Certificate data: Alcoa International, inc, No 47831, for sheet of 2100 mm × 6000 mm × 8mm, material EN AW 2024 T351 used for the FSW process (experiments).

4. TECHNOLOGICAL PARAMETERS

FSW is effective and productive only when the right combination of the welding tool (material, geometry, surface condition etc.) is used on proper workpieces (material, geometry, type of joint etc.) with proper technological parameters of the FSW process (travel speed, tool rotation speed, plunging time, dwelling time etc.). Only in that case appear adequate tribological processes and phenomena (contact pressure, friction, wear, lubrication, heat generation, deformation, adhesion, material exchange etc.) which result with monolith joint between workpieces and qualitative weld.

Technological parameters are the few properties of FSW directly changeable and/or adjustable during welding process. However, selection of proper technological parameters, meaning, travel speed v_{ts} and tool rotation speed v_{rot} , as the most important ones is a difficult task. From the beginning of FSW's industrial application (mid 1992.) until present days, selection of travel speed and tool rotation speed is done by 'try and error' principle. Usable data about the technological parameters for specific processes/materials are usually hidden.

In most of the cases technological parameters of FSW are given over the welding step determined as the ration of tool rotation speed and travel speed v_{rot} / v_{ts} .

Živković [2] has estimated that 2024 alloy can be successfully welded for the weld step varying from 30 to 5, where the best results were achieved for parameters given in the Table 2. Welding was performed more than 100 times.

Table 2. Experimental welding step values for successful welding of the 2024 alloy [2]

v_{rot} / v_{ts}			
1180/116=10.17	1180/46=25.65		
750/150=5.00	750/116=6.64	750/93=8.06	750/73=10.27

5. VERIFICATION OF RESULTS

The final result of the FSW has to be a product that must fulfill its projected purpose. Decomposing this statement to the primary level: FSW joint has to be qualitative and should at least maintain properties of the base metal in projected range if not possible to improve them. According to the existing standards in FSW [3], verification of the results and FSW process has to be done by testing of specimens that have to be specially prepared and extracted from the welded structure (Figure 4).

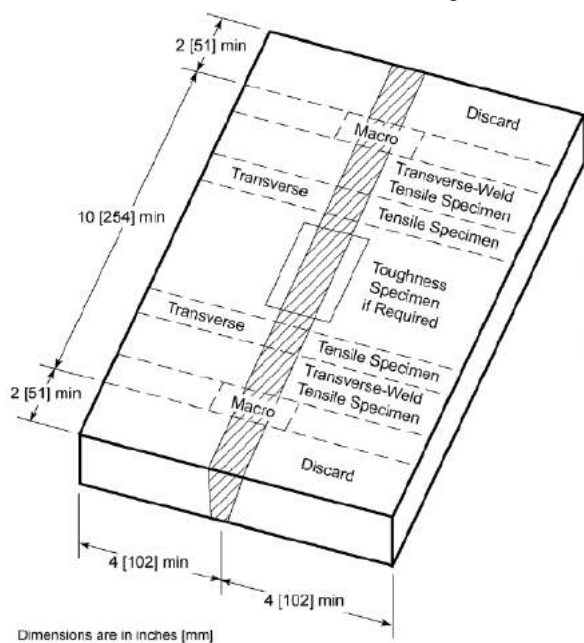


Figure 5 Location of Square Groove Weld Test Specimens—Plate [3]

5.1. Mechanical properties

Welded structures can be overmatched or undermatched from the aspect of the weld joint's strength. FSW process applied on 2024 alloy mostly gives overmatched structures: values of the strength, yield stress, hardness, elongation etc. slightly drop in the area of the weld or heat affected zone (HAZ) (Table 3).

Table 3 Experimental values of mechanical properties of FSW processed 2024 alloy in HAZ [2]

Test N ^o .	$R_{p0.2}$, MPa	R_m , MPa	A_5 , %	v_{rot} / v_{ts}
1	323	398	6,0	1180/116=10,17
2	316	319	7,1	1180/46=25,65
3	324	330	4,8	750/150=5,00
4	318	395	7,5	750/73=10,27
5	/	210	2,2	750/150=5,00
6	313	365	4,2	750/73=10,27

The common hardness diagram of 2xxx class has a specific W-shape: hardness of the material on join (center) line has some median value and distancing from the center line it gradually drops until the center of the HAZ than it rises and stabilizes its value outside the HAZ.

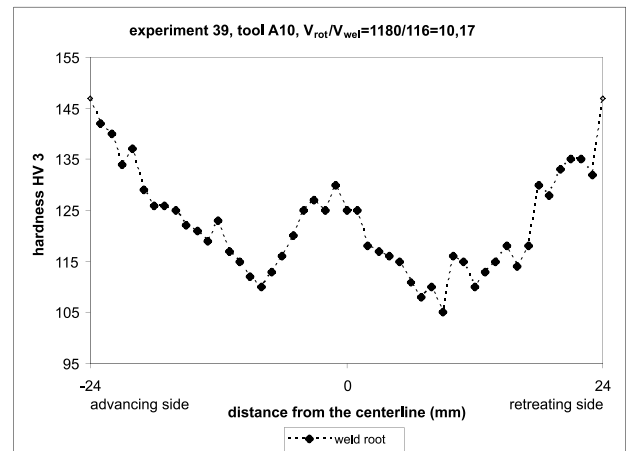


Figure 5 Hardness distribution in FSW, for 2024 alloy [2]

Hardness peak on the centerline is a result of the nugget zone (N). Nugget is the zone of fully recrystallized material that appears on the very center of the joint line and it is a product of intensive plastic deformation initiated by the welding tool and heat treatment of material (during the welding process) (Figure 6).



Figure 6 Macroscopic section on nugget zone of the FSW weld on 2024 alloy [2]

6. FUTURE WORK, DISCUSSION AND CONCLUSIONS

During past 20 years of application of FSW, science has given the great tribute to its improvement and better understanding the process itself. Numerous researches on the FSW application were aimed in recognition of dominant parameters that influence the process and the possibilities of their adjustments in order to reach optimal or desired characteristics of welds [4].

As mentioned earlier, some parameters of the FSW process are adjustable and simple to change since they depend only on possibilities of the system or fabricator. Challenge is to manipulate with other, nonadjustable or difficult to be adjusted parameters that depend not only from the process but from various physical phenomena as well. From the early beginning of application it is recognized that dominant processes in weld creation during FSW are deformation and heating. Literature explains differently these two processes: somewhere this

is stirring and heat generation, somewhere adhesion, diffusion, wear and friction, and some authors explain it as a pure mechanical process with the influence of other processes.

If some accepts any of the proposed explanation to be satisfactory accurate, FSW will still remain elusive from some point of view, either on macro or micro level, and the shade of our (human) no-understanding of the physics keeps us away from perfect design of the FSW. Anyhow, this challenge is overcome by numerous experiments and researches, and analysis of the processes that appear during FSW – good explanation of these processes helps in understanding the FSW in general.

With the goal of better design of the FSW (meaning: proper selection of technological parameters, geometrical parameters of the welding tool, workpieces' preparation etc.) mathematical model for the heat generation during FSW is developed. Heat is a necessity of the FSW process and its tribute in better weld creation lies dominantly in softening of the workpieces and easing the deformation/adhesion/stirring... process during weld creation.

Mathematical model relies on mathematical analysis, theoretical assumptions, state of the art in measuring techniques, recognition of dominant physical phenomena etc (Figure 7).

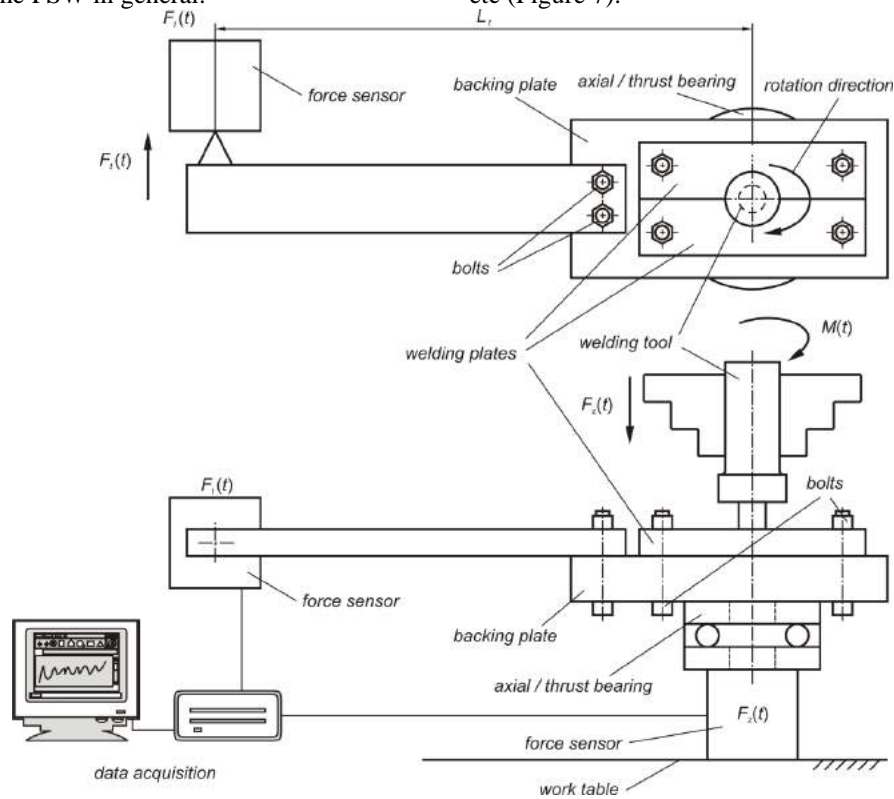


Figure 7 Scheme of the experimental setup for the FSW process

Further research in this area of FSW requires:

1. Recognition and precise determination of active/reactive forces in the system welding tool-workpieces, its influence and possibilities of increase/decrease of their magnitude.
2. Estimation of tribological parameters in contact between welding tool and workpieces (friction coefficient, contact pressure, adhesion, wear, selfaligning, selflubrication etc.)
3. Possibilities of the process efficiency increase (energy consumption, heat losses cuts etc.).

ACKNOWLEDGMENT

The paper presents and preliminary research observations needed for the realization of the research project TR35034 – “An investigation into modern non-conventional technologies: applications in manufacturing companies with the aim of increasing efficiency of use and product quality, of reducing costs and of saving energy and materials”. The project is supported by the Ministry of Education and Science of the Republic of Serbia.

REFERENCES

- [1] Mijajlović, M, Milčić, D, Stamenković, D, Živković, A: Mathematical Model for Generated Heat Estimation During Plunging Phase of FSW Process, Transactions of Famena, Faculty of Mechanical Engineering and Naval Architecture, Zagreb, Croatia, XXXV-1/2011, April 2011, pp 39 - 54, ISSN 1333-1124, UDC 621.791.1.
- [2] Živković, A: Influence of friction stir welding tool geometry on properties of welded joint of alloys Al 2024, PhD thesis, University of Belgrade, Faculty of Mechanical Engineering, 2011.
- [3] AWS D17.3/D17.3M:2010 Specification for Friction Stir Welding of Aluminum Alloys for Aerospace Applications, 2010.
- [4] Thomas W M et al. 1991 Friction stir butt welding International Patent Application No PCT/GB92/02203; Thomas W M et al. 1995 Friction stir butt welding GB Patent Application No 9125978.8; Thomas W M et al. 1995 Friction stir butt welding UP Patent No 5 460 317.



DETERMINATION OF TENSILE PROPERTIES OF WELDED JOINTS – INFLUENCE OF SPECIMEN GEOMETRY

Nenad GUBELJAK¹⁾, Bojan MEDJO²⁾, Jožef PREDAN¹⁾, Marko RAKIN^{2, a)}, Goran RADENKOVIĆ³⁾, Aleksandar SEDMAK⁴⁾

¹⁾ Faculty of Mechanical Engineering, University of Maribor, Smetanova 17, Maribor, Slovenia

²⁾ Faculty of Technology and Metallurgy, University of Belgrade, Karnegijeva 4, Belgrade, Serbia

³⁾ Faculty of Mechanical Engineering, University of Niš, Aleksandra Medvedeva 14, Niš, Serbia

⁴⁾ Faculty of Mechanical Engineering, University of Belgrade, Kraljice Marije 16, Belgrade, Serbia
^{a)} marko@tmf.bg.ac.rs

Abstract: Determination of mechanical properties of welded joints is a very important part of integrity assessment of welded structures. This paper deals with the differences obtained by using two specimen geometries for tensile testing: round tensile (RT) and micro tensile (MTS) specimens. Concerning the strength mismatching level, both overmatched and undermatched joints of high-strength low alloyed steel are considered. It is shown that the two weld metal specimens give somewhat different results, while the base metal specimens do not exhibit significant differences. For overmatched joint, larger values are obtained by MTS specimens, while the opposite situation is observed in the case of undermatched joint. This can be attributed to the influence of material heterogeneity and several zones that are included when cutting the RT specimen from the joint (different fractions of as-welded and reheated microstructures, local spots with different strength, and possibly even a small portion of HAZ). Deformation of the specimens is also examined using the finite element method; RT specimens are modelled as multi-layered structures, to take into account the material heterogeneity within the joint.

Key words: Welded joints, inhomogeneity, tensile testing, round tensile specimen, micro tensile specimen

1. INTRODUCTION

In structures manufactured from metals and alloys, welded joints are often critical locations for fracture initiation, due to different metallurgical or geometrical defects, as well as residual stresses. Having in mind their way of fabrication, welded joints are highly inhomogeneous parts of welded structures, with respect to elastic-plastic deformation and fracture properties. The microstructures, and therefore also mechanical properties, in different regions of a joint can vary significantly. In some applications, i.e. for determining the fracture behaviour, it is very important to know the local values of the yield strength, ultimate tensile strength and other mechanical properties.

It is common practise in fabrication to select the filler material which will ensure overmatching, to protect the weld from localization of plastic strain and hence decrease the risk of failure. Such requirement is most pronounced in case of joints subjected to tension loading normal to the effective area (e.g. girth welds in pipes).

Non-critical components and components exposed to lower loading levels, as well as structures fabricated from high-strength steels may have undermatched joints.

In the absence of the exact properties of HAZ, a flaw assessment procedure using the base metal properties could lead to an unsafe result. Adequate information (not the one based on the hardness values) on the local

material properties can also be useful for optimization of the welding procedure. Therefore, it is recommended to study the behaviour of all regions of the mismatched joint. It is often rather difficult to determine the tensile properties of a heat affected zone, due to its small size, but it is important for a complete understanding of the joint performance.

Micro tensile specimens testing enable the determination of property gradient through the welded joint. This technique was originally developed for property determination of HAZ for multipass welded joints [1]. Other uses of this procedure include the situations when not enough material is available to extract standard specimens. Micro tensile specimens are often used for: determination of gradients in properties, determination of material properties for small weld geometries (laser welds, etc) and determination of mechanical behaviour of micro-components.

Yield strength and tensile strength calculated using the hardness profiles are not adequate for many cases [2]. Also, deformation hardening can not be estimated by such conversion, which is important because only the stress-strain curve adequately describes the tensile behaviour.

Therefore, an experimental investigation on the properties of the entire welded joints is performed by testing flat micro tensile specimens, Figs. 1-3. The results obtained by these tests are compared with standard round tensile

specimens, in order to determine the differences caused by different specimen geometries and dimensions.

2. EXPERIMENTAL PROCEDURE

The analysis is conducted on high-strength low-alloyed (HSLA) steel welded joints. The base metal (BM) is HSLA steel NIOMOL 490; details about the joints fabrication are given in [3]. Overmatched (OM) and undermatched (UM) joints are analysed. Chemical composition of the base metal and filler materials is given in Table 1. Nominal mechanical properties (by producer specification) of the base metal and weld metals are given in Table 2.

Table 1. Chemical compositions (in weight %)

	C	Si	Mn	P	S	Cr	Mo	Ni
OM	0.040	0.16	0.95	0.011	0.021	0.49	0.42	2.06
BM	0.123	0.33	0.56	0.003	0.002	0.57	0.34	0.13
UM	0.096	0.58	1.24	0.013	0.16	0.07	0.02	0.03

Table 2. Mechanical properties of the base metal, overmatched and undermatched consumable (by producer specification)

Mat.	Label	$R_{p0.2}$ MPa	R_m MPa	M	Charpy K_v J
OM	FILTUB 75	700	780	1.37	>40 J at -60°C
BM	NIOMOL 490	510	650	-	>60 J at -60°C
UM	VAC 60	437	556	0.86	>80 J at -50°

The overview of the micro tensile specimens' positions in a welded joint is given in Fig. 1. Dimensions of specimen are given in Fig. 2, while Fig. 3 shows the photograph of block from which they were cut, specimen before the testing and fractured specimen, along with the 1 Eurocent coin.

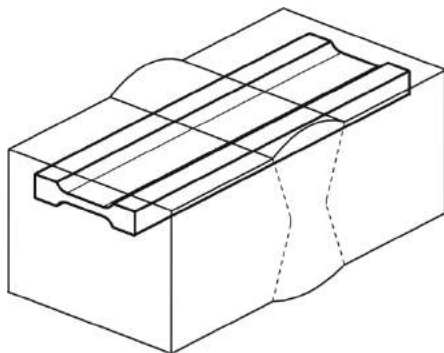


Fig.1. Micro tensile specimens – longitudinal direction

The position of a round tensile specimen for testing the properties of weld metal is given in Fig. 4, with the dimensions of specimen in Fig. 5.

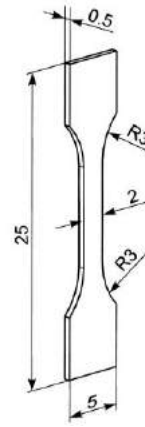


Fig.2. Micro tensile specimen – dimensions

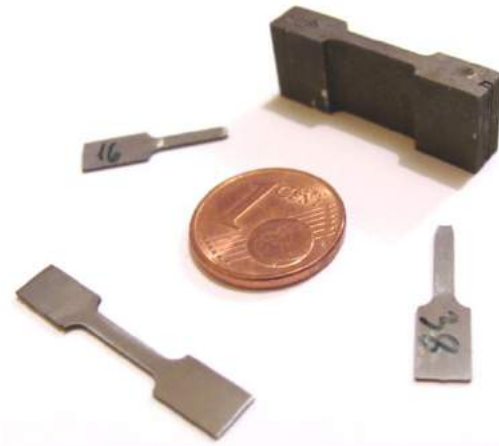


Fig.3. Micro tensile specimens – photograph of the specimens with 1 Eurocent coin

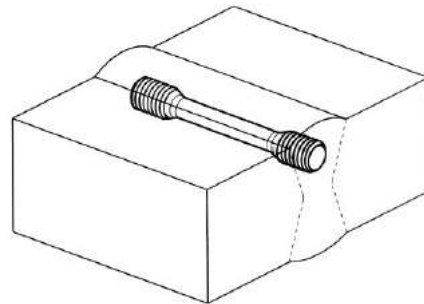


Fig.4. Round tensile specimen – longitudinal direction

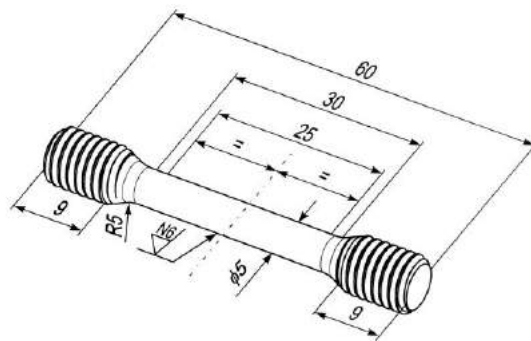


Fig.5. Round tensile specimen – dimensions

3. RESULTS AND DISCUSSION

The welding process has a direct effect on the through-thickness distribution of weld metal and HAZ microstructures. Accordingly, different tensile properties have been measured by the two used specimen geometries. The results (yield strength $R_{p0.2}$ and ultimate tensile strength R_m) obtained by testing the MTS specimens across OM and UM welded joints are given in Figs. 6 and 7, respectively.

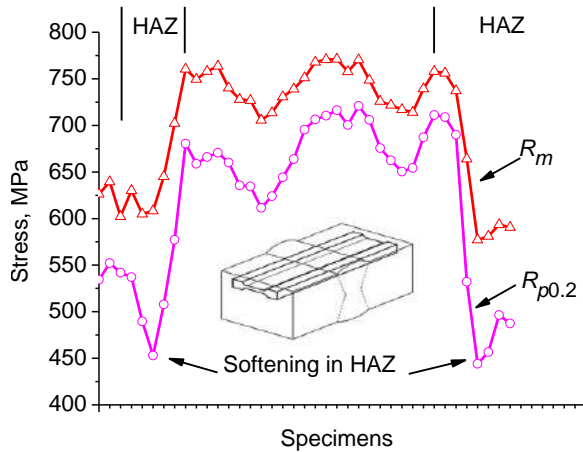


Fig.6. Tensile properties distribution obtained by MTS specimens of overmatching welded joint.

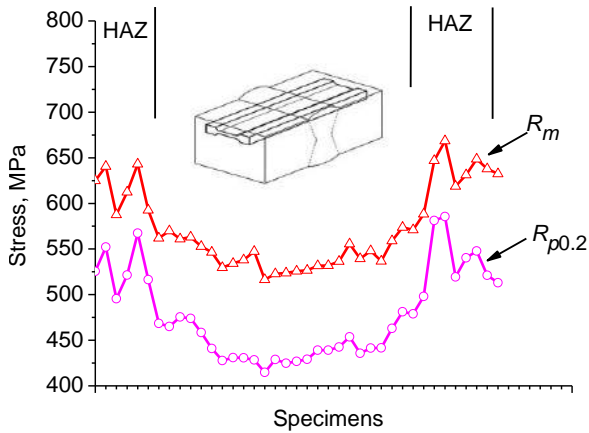


Fig.7. Tensile properties distribution obtained by MTS specimens of undermatching welded joint

To investigate the suitability of two specimen types for determining the mechanical properties of welded joints, both groups of results are compared in Fig. 8. For the base metal, rather similar values of local and global mechanical properties are obtained, which is in agreement with the conclusions from [4, 5]. Such behaviour can be attributed to the relatively homogeneous properties of the base material.

On the other hand, yield strength and ultimate tensile strength of the weld metals exhibit certain differences. For the overmatched joints, larger values are obtained by micro tensile specimens, while the opposite situation is observed in the case of undermatched joint. This can be attributed to the influence of the material heterogeneity,

and many zones that are included when cutting the round tensile specimen from the joint (parts of the weld metal near the fusion line, and maybe even a small portion of HAZ).

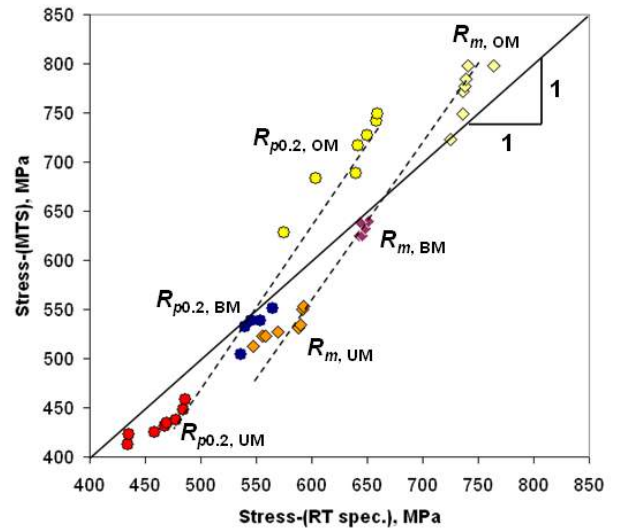


Fig.8. Tensile properties obtained by MTS and RT specimens – comparison

The observed difference is also examined by the finite element method, using the software package Abaqus [6]. A simplified analysis is conducted: material properties were modelled by the several layers approximately corresponding to the actual tensile data given in Figs. 6 and 7. Therefore, the round tensile specimen is analysed as multi layered structure, as shown in Fig. 9. The finite element mesh used for calculations is also given in Fig 9. Due to the examined configuration, three-dimensional model is used, with loading applied as prescribed displacement at one end of the specimen.

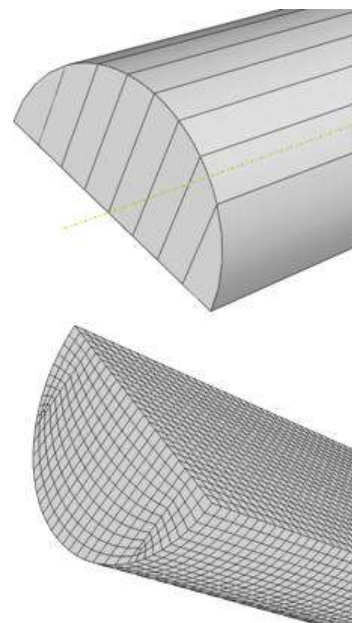


Fig.9. One half of round tensile specimen cross-section – zones with different tensile properties and FE mesh

Distribution of yield strength is shown in Fig. 10, for both overmatched and undermatched joints. A small portion of HAZ is also taken into account, having in mind that it could be a realistic situation for specimens cut from the weld metal.

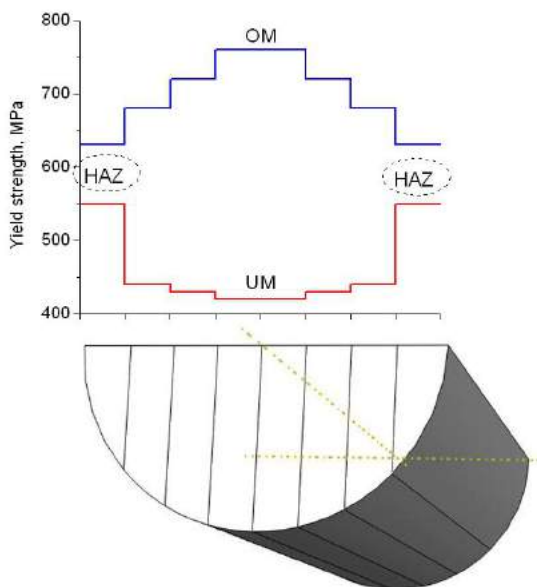


Fig.10. Distribution of yield strength through the specimen cross section

The trends for the two specimen types (Fig. 11) are similar as experimental ones, i.e. RT specimens cut from OM weld metal have lower yield strength in comparison with MTS. Opposite is observed in case of UM RT specimens.

The behaviour of welded joints can also be influenced by local changes in material properties, i.e. occurrence of local weak or strong spots which can change the results of the experimental testing. The usage of micro tensile specimens helps to enhance the knowledge about the local material behaviour, having in mind its small cross-section and different positions within the welded joint.

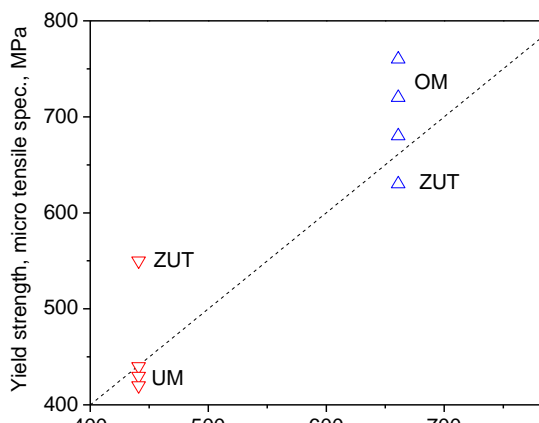


Fig.11. Numerical results for the yield stress of OM and UM weld metal

In addition to differences in strength of the welded joint zones, ductility is also found to be variable. The current work includes determining the influence of ductility and differences in stress field (MTS and RT geometry), which will provide more precise data on mechanical properties of the examined joints.

4. CONCLUSION

Micro-hardness measurements in multiphase welded joints reflects strength (mis-matching) differences, but cannot provide accurate values of mechanical properties, especially those concerning the hardening behaviour. Therefore, tensile properties of the welded joints are determined by both round tensile and flat micro tensile specimens in this paper, and the differences in results are discussed. A simplified numerical analysis using the finite element method confirmed that the tensile strength of the overmatched joint determined on RT specimens is smaller than that from MTS specimens, while the undermatched joint exhibit different behaviour. The properties of base metal determined on both specimens are similar, having in mind the material homogeneity. The results for weld metals can be attributed to the inhomogeneous material properties across the joint, local spots with different strength and possibility that a portion of HAZ exists in the round tensile specimens.

ACKNOWLEDGEMENT

NG and JP acknowledge the support of Slovenian Ministry of Higher Education, Science and Technology under the project E!5348. BM, MR, GR and AS acknowledge the support from the Serbian Ministry of Science under the projects ON 174004 and E!5348.

REFERENCES

- [1] Klausnitzer, E. (1976) *Entwicklung eines verfahrens zur entnahme und prüfung von mikro-flachzugproben aus der WEZ von schweißverbindungen*. Materialprüfung, Vol. 18, No. 11, pp. 411-416
- [2] Dobi, Dj., Junghans, E. (1999) *Determination of the tensile properties of specimens with small dimensions*. Kovine, Zlitine, Tehnologije, Vol. 33, No. 6, pp. 451-457
- [3] Gubelj, N., Scheider, I., Koçak, M., Oblak, M., Predan, J. (2002) *Constraint effect on fracture behaviour on strength mis-matched welded joint*. Proceedings of the 14th European Conference on Fracture, Vol I, pp. 647-655
- [4] Çam, G., Erim, S., Yeni, Ç., Koçak, M. (1999) *Determination of mechanical and fracture properties of laser beam welded steel joints*. Welding Journal, Supplement No. 6, pp. 193-201
- [5] Scheider, I., Brocks, W., Cornec, A. (2004) *Procedure for the determination of true stress-strain curves from tensile tests with rectangular cross-section specimens*. Journal of Engineering Materials and Technology ASME, Vol. 126, pp. 70-76
- [6] Abaqus FEM software package, www.simulia.com



MANUFACTURING AND CHARACTERISATION OF FLAKES MADE BY SOFT LITHOGRAPHY TECHNIQUE

Anka TRAJKOVSKA PETKOSKA

University St. Kliment Ohridski, Bitola, R. Macedonia
anka.trajkovska@uklo.edu.mk

Abstract: In this work shaped Polymer Cholesteric Liquid Crystals (PCLC) flakes have been proposed for novel optical applications. Details of the manufacturing method of shaped micron-sized PCLC flakes by soft lithography technique are given here followed by the flakes' characterization data. Examples of modified flakes' electro-optical properties by the aid of various dopants of different nature (micro- vs. nano-dopants, conductive and non-conductive ones) are presented, as well. Finally, some novel applications utilizing PCLC flakes will be highlighted.

Key words: polymer cholesteric liquid crystals, flakes, soft lithography, electro-optic behaviour, dopants

1. INTRODUCTION

Liquid crystals (LCs) represent a special condensed matter phase that falls between disordered isotropic liquids and ordered solid crystals. They possess the fluidity of a liquid phase, and at the same time, exhibit an orientational and a certain degree of positional order. In general, LC materials consist of rod-like (calamatic) or discotic (disk-like) molecules. The anisotropic molecular shape and the presence of certain degree of order are responsible for the significant anisotropic optical, electrical, magnetic, and mechanical properties, which have found many applications in optics, electronics, and photonics. According to the microscopic order and the interaction between molecules, there are different classes of LCs phases (mesophases), such as *nematic*, *cholesteric* and *smectic* [1-3].

Cholesteric LC (CLCs) exhibit uniaxially-oriented LC molecules within the nematic sublayers with orientation described by the so-called *director*. The director rotates in a helical fashion around an axis perpendicular to the sublayers with a period p (*pitch length*). The rotational direction defines the *handedness* of the cholesteric phase, which can be *left-* or *right-handed*. The pitch length and the helical twist sense together with the refractive index of the cholesteric material determine the optical properties of this mesophase, among which is the selective reflection. The unique optical characteristics of CLCs, such as the selective reflection and circular polarization, have potential in many optical, photonic and electronic applications. Proper molecular design of LC molecules enables CLC materials with varying pitch lengths that can reflect color from deep UV- to far IR- region, as well as ability to be processed easily into large-area, monodomain, defect-free films, which opens wide range of opportunities for many novel applications, such as notch filters, reflectors, polarizers, as well as novel types of displays [4-9]. *Polymer CLC (PCLC)* materials have

been used as films and flakes. PCLC flakes have the potential to be used in numerous passive and active electro-optic applications. The most attractive application of PCLC flakes is as an alternative to existing liquid crystal display (LCD) and particle display technologies, because they can provide number of advantages, viz. *a flexible, thin, multi color, low-power, and low-cost display*.

2. EXPERIMENTAL

2.1. Liquid Crystal Materials

LC materials presented in this work are thermotropic cholesteric LCs [1]. Particularly, PCLC materials are used and techniques for preparation PCLC films and flakes are covered [10,11]. Due to the disadvantages of irregular shaped flakes (random shapes, no control over their dimensions, great variations in thicknesses, sharp edges that causes light scattering, etc., Fig. 1), it is of crucial importance to find a way to shape the PCLC material or film into controllable shaped particles (shaped flakes) with an intention to be a part of new generation of electronic paper applications [12,13].

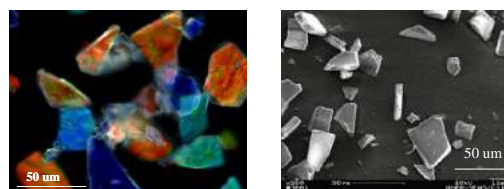


Fig.1. Randomly shaped flakes: a) image taken with polarizing optical microscope (POM) in a reflective mode between crossed polarizers (true color), and b) electron micrograph taken with scanning electron microscope (SEM).

2.2. Shaped PCLC Flakes

To overcome the flake size variations, and consequently, to be able to control and model the flake behavior in an electric field, a method for manufacturing shaped flakes was invented by the author. The new method for making shaped flakes, which has been shown to be very effective, is based on *soft lithography* technique (Fig. 2). Shaped flakes are made in a flexible polydimethylsiloxane (PDMS) mold with a pattern on it. Namely, a patterned silicon wafer is used as a rigid master (template) over which a PDMS elastomeric material is cast (Fig. 2a). After hardening, the PDMS replica is peeled off from the silicon wafer to give an inverse replica of the wafer. Such replica constitutes a flexible mold for making shaped flakes. Depending on the design on the patterned silicon wafer, different shapes of flakes can be manufactured in PDMS molds [13,14].

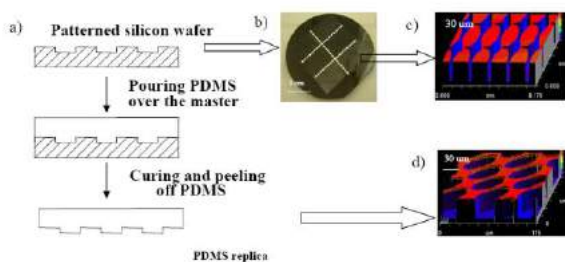


Fig. 2. a) Scheme of the process of making a PDMS mold over a rigid patterned silicon wafer, b) patterned silicon wafer, c) example of ellipsoidal shaped pattern on the silicon wafer scanned with white light profilometer, d) white light profilometer image of a PDMS mold as an inverse replica of the patterned silicon wafer shown in c).

Different techniques were used for characterization of shaped PCLC flakes. Flakes are characterized in terms of their shape, surface structure and uniformity using polarized optical microscopy (POM, Fig. 3), scanning electron microscopy (SEM, Fig. 4), white light interferometry, and other techniques [13,14].

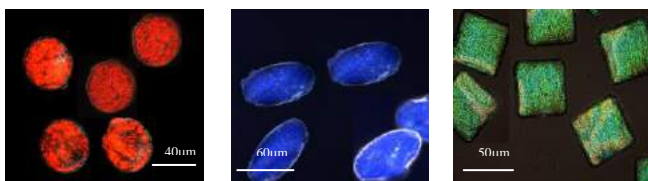


Fig. 3. Shaped flakes characterized by POM in reflective mode, crossed polarizers. [Under illumination at near normal incidence, the three colors (red, blue, green) are apparent in the true color images.]

2.3. Electro-optic behavior of PCLC Flakes

An electro-optic device consists of a cell assembled of two indium tin oxide (ITO) glass substrates, which is filled with suspension made of PCLC flakes in a suitable host fluid (e.g. propylene carbonate). When an alternating

current (AC) field is applied to the test device (shown in Fig. 5a), flakes that initially lie nearly parallel to the cell substrates rotate about 90° about their longest axis. For example, an applied electric field of $\geq 10 \text{ mV}_{\text{rms}}/\mu\text{m}$ (rms : root mean square) between 10 and 1000 Hz, initiates flake reorientation with temporal response on the order of ten to hundreds of milliseconds. Selective reflection colors are shifted and diminished as the flakes rotate (Fig. 5b). Fig. 5c) shows inducing a dipole on a PCLC flake during when an electric field is applied [13,15].

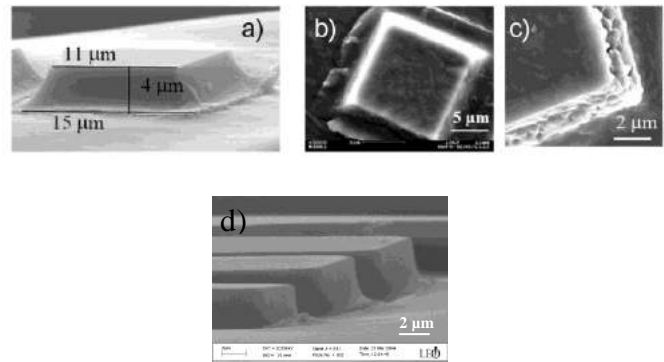


Fig. 4. Shaped flakes characterized by SEM: a) single filling to produce square shaped flake, b) top view of the square flake, c) multiple filling of shaped flake, d) dimensional uniformity of rectangle shaped flakes.

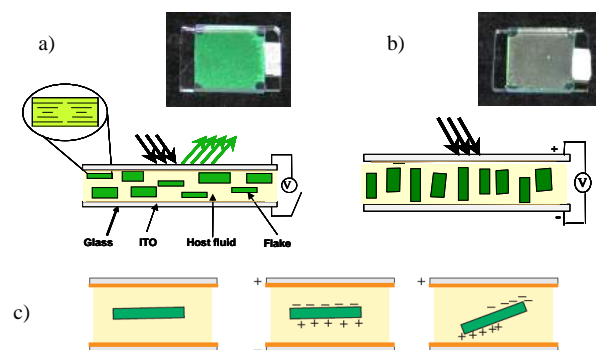


Fig. 5. Typical cell device filled with a suspension of flakes and host fluid: a) before, and b) after application of an electric field. Insets: photos of actual cell devices: before (reflective-bright state) and after application of the field (dark-nonreflective state); c) Generation of a dipole moment on a flake particle when an electric field is applied (Maxwell-Wagner polarization).

2.4. Modified PCLC Flakes

The goal of doping of PCLC was mainly to enhance dielectric properties of this material. Flakes made of dielectrically enhanced PCLC material can be hosted in fluids like insulating silicone oils and show reorientational and translational electro-optic behavior (as it is explained in the previous section 2.3). Variety of dopants to the PCLC material showed different effect. In Table 1 are given dopants used in this work and their

effect on PCLC matrix. All dopants are grouped in three main groups: (1) carbon-based dopants (conductive), (2) metal-based dopants (conductive), and (3) inorganic dopants (nonconductive, exhibiting high dielectric constant [13,16,17]).

Table 1. Dopants used for PCLC modifications

Dopant	Particle size*	Percolation threshold (PT) (vol %)	Conductivity (1 kHz) at PT [S/m]	Dielectric constant (10 kHz) at PT (vol %)
Neat PCLC (no dopant)	–	–	$\sim 1 \times 10^{-9}$	2.1
1) C-based				
CB VPA	17 nm	2	1×10^{-5}	10
CB M	75 nm	6	1×10^{-5}	10
SWNT-1	1.4×2 to $5 \mu\text{m}$	0.7	1×10^{-6}	5
SWNT-2	$1.1 \text{ nm} \times 0.5$ to $100 \mu\text{m}$	0.4	1×10^{-6}	2.2
MWNT	10 to $20 \text{ nm} \times 0.5$ to $200 \mu\text{m}$	0.8	$\sim 1 \times 10^{-3}$	10
2) Metal-based				
CI-HQ	$1.1 \mu\text{m}$	20	1	–
ITO	$3.38 \mu\text{m}$	25	$\sim 1 \times 10^{-4}$	5
Al flakes	$12 \mu\text{m}$	30	$\sim 1 \times 10^{-2}$	20
3) Inorganic				
BT-1	70 nm	–	–	7.7 (27.0)
BT-2	1 to $1.1 \mu\text{m}$	–	–	6.1 (32.0)
BT-3	1.3 to $1.8 \mu\text{m}$	–	–	5.8 (27.0)
TiO ₂ -1	30 nm	–	–	5.2 (54.4)
TiO ₂ -2	$10 \text{ nm} \times 40 \text{ nm}$	–	–	7.5 (22.0)

*Primary average particle dimensions.
Legend: CB VPA – carbon black Vulcan PA90, CB M – carbon black Monarch M120, SWNT-1 is single carbon walled nanotubes (type 1), SWNT-2 is single walled carbon nanotubes (type 2), MWNT – multiwalled carbon nanotubes, CI-HQ – carbonyl iron, ITO – indium tin oxide, BT – barium titanate.

The first class of dopants, *conductive dopants*, consisting of either carbon-based or metallic particles, show large increases in composites' conductivity with percolation thresholds ranging from 0.4 vol % to 30 vol %, depending on the size and shape of the dopant particles (Fig. 6). The conductive dopants, also, introduce a charge (positive or negative) to the flakes. The second class of dopants, *inorganic insulating dopants*, change the dielectric constant from 2 (for neat PCLC) to <10 at dopant levels of ~30 vol % (Fig. 7).

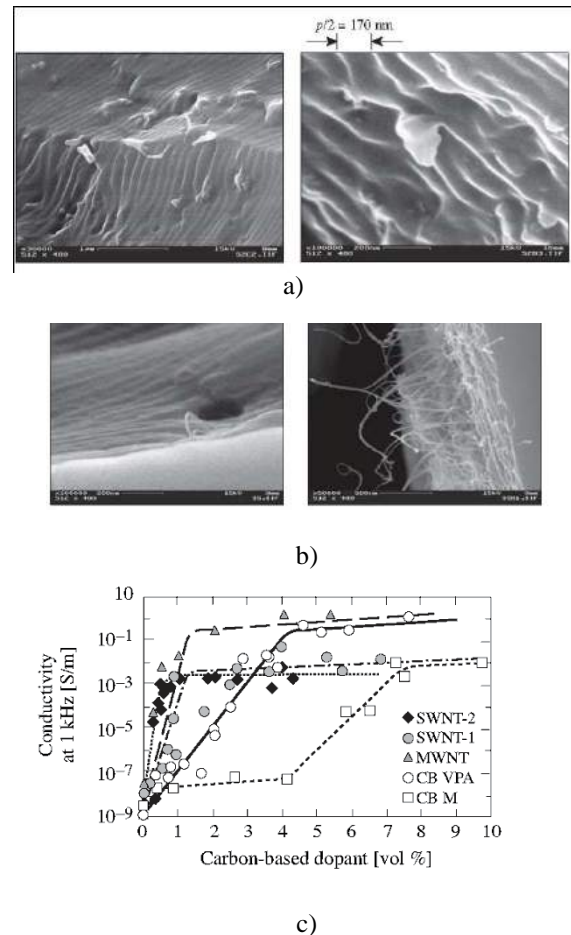


Fig. 6. a) SEM pictures of 5 vol.% CB VPA in PCLC, b) 1.2 vol.% SWNT-1 doped PCLC flakes, c) Carbon-based dopants (CB and carbon nanotubes): comparison of conductivity at 1 kHz vs. dopant concentration.

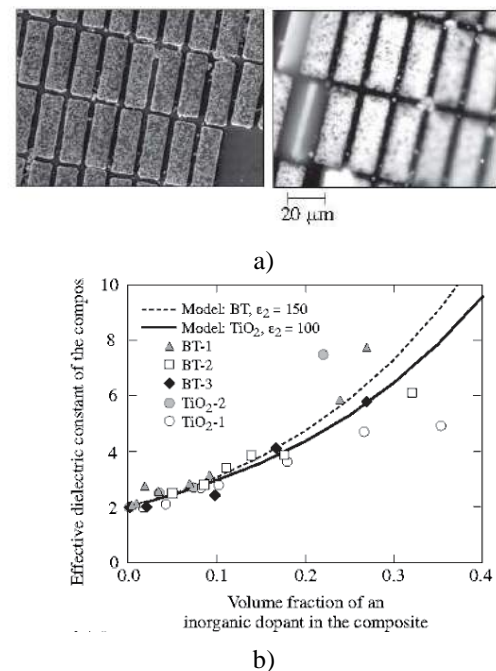


Fig. 7. a) SEM images of BaTiO₃-doped PCLC flakes. b) Comparison of dielectric constant at 10 kHz for PCLC composites using inorganic dopants BaTiO₃ and TiO₂.

The percolation threshold (PT), as the actual insulating-to-conducting transition in the polymer composite, occurs when the conductive dopant concentration exceeds a critical value that is characterized by a sharp jump in the conductivity by many orders of magnitude (Fig. 8). The concentration, at which PT occurs, depends on many factors, such as the nature of both the polymer host and the dopant, the composite porosity, dopants' dispersion and their alignment, chemical interactions, processing method, the presence of surfactants, ionic salts [16,17].

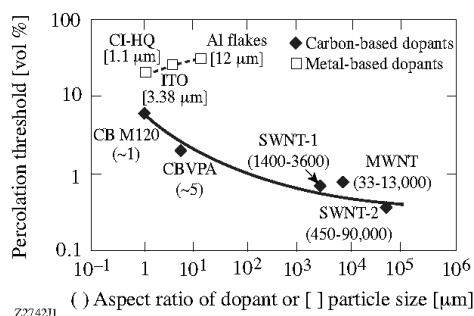


Fig. 8. Percolation threshold vs. dopant average aspect ratio (range given in parentheses) or particle size [given in brackets].

3. SUMMARY

PCLC flakes provide bright, saturated colors without the need for additional color filters and polarizers as a result of their intrinsic selective reflection. Shaped PCLC flakes have many advantages over irregular-shaped or commercial PCLC flakes such as tailor-designed shapes, control over their dimensions and thicknesses, no light scattering from the sharp edges, etc... PCLC flakes in an appropriate host fluid reorient from a bright (reflective) state to a dark (nonreflective) state under an applied ac electric field. Maxwell-Wagner polarization is confirmed as the main mechanism for the flake reorientation (Fig. 5c). This electro-optic effect is created by extrinsic charges that migrate to the surface of the dielectric flake when an electric field is actuated, inducing a dipole moment on the flake. The flake reorientation depends on many factors, such as the dielectric properties of both the flake and the host fluid, the flake geometry, the host viscosity, and the electric field. Modification of PCLC flakes by doping with conductive or dielectric dopants increases the flake conductivity and/or dielectric constant. Doping of PCLC flakes reduces the reorientation time and extends the response to the dc regime. The concept of electronic paper and sensors based on PCLC flakes is very attractive to consumers nowadays. It offers possibility for a thin, reflective, lightweight, flexible devices that uses little power.

REFERENCES

[1] COLLINGS, P., HIRD, P. (1997) *Introduction to Liquid Crystals, Chemistry and Physics*, Taylor and Francis Ltd.

[2] YEH, P., GU, C. (1999) *Optics of Liquid Crystal Displays*, New York: Wiley & Sons.

[3] CHANDRASEKHAR, S. (1977) *Liquid Crystals*, Cambridge University Press.

[4] BLINOV, L.V. (1983) *Electro-optical and magneto-Optical Properties of Liquid Crystals*, J. Wiley & Sons Ltd.

[5] BERREMAN, D. W. (1970) *Phys. Rev. Lett.* 25(9), pp 577-581.

[6] FERGASON, J. L. (1966) *Mol. Cryst.* 1, pp 293-307.

[7] TRAJKOVSKA, A. (2008) *Liquid Crystalline Oligofluorenes-Chiroptical Properties and Photoalignment*, Verlag Dr. Müller, VDM ISBN 978-3-639-07096-5.

[8] SCHADT, M. (1997) *Ann. Rev. Mat. Sci.* 27, pp 305-379.

[9] WU, S. T., YANG, D. K. (2001) *Reflective Liquid Crystal Displays*, J. Wiley & Sons Ltd.

[10] KORENIC, E. M., JACOBS, S. D., FARIS, S. M., LI, L. (1998) *Mol. Cryst. and Liq. Cryst.* 317, pp 197-219.

[11] FARIS, S. M. (1994) *U.S. Patent No. 5,364,557*.

[12] TRAJKOVSKA PETKOSKA, A., JACOBS, S. D., KOSC, T. Z., MARSHALL, K. L. (2007) *U.S. Pat. 7,238,316 B2*.

[13] TRAJKOVSKA PETKOSKA, A. (2008) *Polymer Cholesteric Liquid Crystal Flakes – Their Electro Optic-Behaviour for Potential E-Paper Application*, Verlag Dr. Müller, VDM ISBN 978-3-639-06439-1.

[14] TRAJKOVSKA PETKOSKA, A., VARSHNEYA, R., KOSC, T. Z., MARSHALL, K. L., JACOBS, S. D. (2004) *Adv. Funct. Mater.* 15, pp 217.

[15] TRAJKOVSKA PETKOSKA, A., KOSC, T. Z., MARSHALL, K. L., HASMAN, K., JACOBS, S. D. (2008) Motion of doped polymer cholesteric liquid crystal flakes in a direct-current electric field *J. Appl. Phys.* 103, p 094907.

[16] TRAJKOVSKA PETKOSKA, A., JACOBS, S. D. (2008) Effect of different dopants on polymer cholesteric liquid crystal properties *Mol. Cryst. Liq. Cryst.* 495, p 334

[17] TRAJKOVSKA PETKOSKA, A., JACOBS, S. D., MARSHALL, K. L., KOSC, T. Z. (2010) *U.S. Pat. No. 7,713,436 B1*.

INDUSTRIALIZATION OF EASY BOOM

Rok JUSTIN ¹⁾, Davorin KRAMAR ²⁾, Janez KOPAC ²⁾, Mirko SOKOVIĆ ^{2)*}

¹⁾ Savatech d.o.o., EKO programme, Škofjeloška 6, 4000 Kranj, Slovenia

²⁾ Faculty of Mechanical Engineering, University of Ljubljana, Aškerčeva 6, 1000 Ljubljana, Slovenia

mirko.sokovic@fs.uni-lj.si

Abstract: The paper presents some results of the project of design and implementation of a new type of floating containment boom made of PVC material. The new boom is light weight, highly stable with no inflation system required. Boom has small volume when packed for transport and is simple and quick to deploy. It is made of UV and oil resistant material. The new type of oil boom was tested in clean water and is available for application in oil spill accidents. Also calculations for salt water were made. Boom is suitable for closed waters, rivers and streams, harbours, canals, etc. Product of research and development is original Slovenian PVC floating containment boom marked as Easy Boom.

Key words: floating containment boom, PVC oil boom, manufacturing and processing

1. INTRODUCTION

It is estimated that between 1.5 and 10 million tons of oil end up in oceans and seas. The major problem is caused by sudden spills of greater amounts of oil in smaller restricted areas such as the Adriatic Sea, the part of which is the Gulf of Trieste with the Slovenian coastal region. It is owing to this fact that ports in the northern Adriatic developed very rapidly, which resulted in a highly frequent shipping of various loads. Besides a continual pollution from the mainland, the sea and the coastal area are further endangered by the potential hazard sources such as crude oil and its products, as well as various chemicals in the maritime traffic [1].

Oil spills have a catastrophic impact on the maritime ecosystems and numerous living beings as their survival is threatened either directly or indirectly. Oil spills which reach the coast affect the well-being of the local residents, and can negatively influence the fishing trade, tourism industry, sailing, diving, etc. [2]. A long-lasting negative psychological influence is observable with people, which goes far beyond the elimination of the pollution.

2. OIL ON THE WATER

The physics of oil spills. There are many physical and chemical processes, collectively known as weathering, that changes the oil's properties and behaviour after it is spilled into the ocean, Fig. 1 [3].

Many of these weathering processes happen at the same time, but as time goes on, some processes become less important. When it comes to an oil spill, the competent authorities have to be immediately notified. In compliance with the set procedures they alarm the services and teams who take suitable steps using their know-how and equipment. Immediately after the oil spill is stopped, the priority task is to prevent the oil from spreading further. When the polluted surface grows larger, the cleaning

becomes more difficult and expensive as well as lengthy. Therefore it is urgent to use the so-called "floating containment booms", which form a part of the basic equipment in every such intervention. Containment booms are the first device to be applied in the event of an oil spill and the last one to be eliminated. The market offers many types of floating containment boom; each of them has its specific advantages and disadvantages [4]. The efficiency of every individual boom depends on the weather, the amount and characteristics of the oil spill and the speed of the water current.

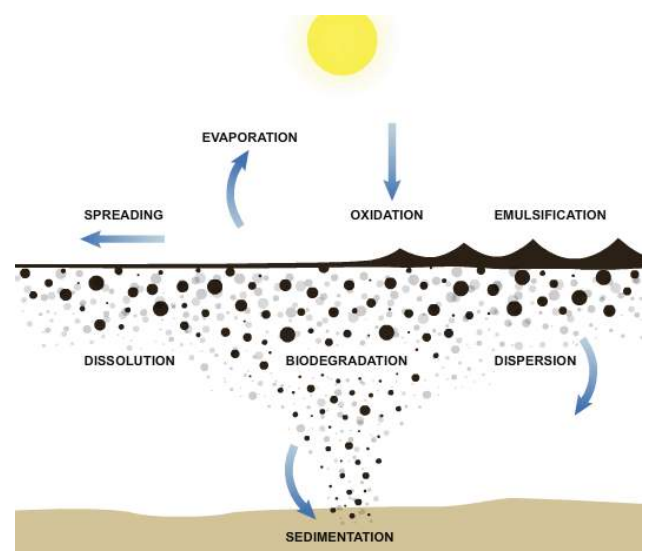


Fig. 1. The physics of oil spills

3. CLASSICAL RUBBER FLOATING BOOM

Savatech d.o.o. has been manufacturing floating booms made of rubber for more than 25 years. During this period has developed different types of floating containment booms with regard to the purpose of application. The

floatable body prevents oil spill to spread across the water surface and assures buoyancy of the boom. The longitudinal bodies should be filled with air before use. In the case of fixed booms, the floatable body is actually formed of longitudinal elements filled with polyurethane foam; therefore the air-inflation system is not required. The underwater part of the boom or the wing of varied lengths with regard to the size of the boom prevents oil from sinking under the sea level.

The main advantage of rubber booms is:

- long service life and
- good resistance to various environmental influences.

Besides the classical containment booms, air-inflated or filled with polyurethane foam, Savatech d.o.o. also manufactures three-stage booms (SGB = Shore Guardian Boom), Fig. 2, and permanent booms (PB = Permanent Boom), Fig. 3, made of rubber [5].



Fig. 2. SGB - Shore guardian boom



Fig. 3. PB900 boom, Koper (2009)

The three-stage booms (SGB) are intended for transiting from the sea to the mainland, for pebble and sandy shores. The boom is made of three elements; the lower two are filled with water and the upper one is filled with air. Such a construction provides for an excellent buoyancy of the entire boom and its perfect adapting and sealing properties at passing from the sea to the shore.

Permanent booms (PB) are intended for use in conditions that require strong and robust booms, which need not be filled. Such booms are suitable for all water surfaces but they prove best effective in the sea water. Their above-water level part comprises 1/3 of the entire boom height. The buoyancy is secured with the in-built buoys, which on their bottom part are weighted.

All boom types can be fitted with connecting elements, which are made in compliance with the ASTM F 962-04 standard, and we can offer special connection with pins, depending on customer requirements.

4. DEVELOPMENT OF PVC BOOMS

Owing to a rising demand in containment booms made from lighter materials (Fig. 4), and, as a result, lower price and faster supply, Savatech d.o.o. has decided to develop a completely new type of oil booms using a new

technology. These new booms are made from the PVC material using the high-frequency welding technology.

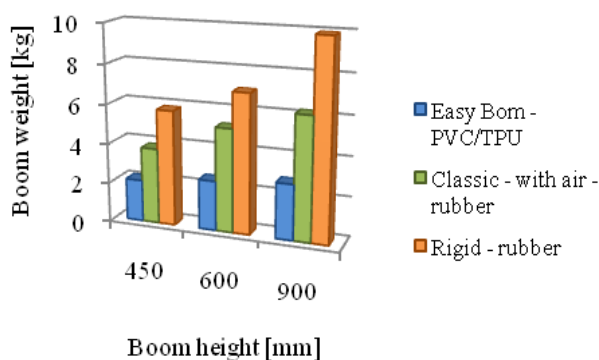


Fig. 4. Weight by different type of boom

The material, from which these booms are made, is a polyester fabric with the PVC/TPU coating. Such coating is better resistant to oil and possesses better UV resistance than the usual PVC-material [6].

The high-frequency welding technology is much faster than the vulcanisation procedure. Two shapes to be welded together are placed on the machine and a suitable electrode is selected. The electrode can be of any shape, however, it has to conduct electricity, and its size should correspond to the working surface of the machine and the required splice type. The electrode is made from aluminium which is very easy to process. The suitable welding time as well as cooling time and pressure, at which the machine presses on the electrode, are set. All settings depend on the materials to be welded. During the welding cycle, the circuit is closed, leading from the machine through the electrode and both shapes to the working table and back to the machine. When electric current passes through both materials, the PVC/TPU coating warms up strongly and it melts where the electrode presses. During a short cooling cycling the material hardens back and the shapes are welded.

The strength of a welded splice depends on the materials used and machine settings, therefore it is recommended to make a test splice and test it on a tearing machine. The strength of splices can be increased by using a ribbed electrode.

The working procedure and boom dimensions are adapted to shorten the procedure time and enhance the yield of material.

4.1. In-house PVC type of a boom

We have decided to manufacture only non-inflatable oil booms from the PVC/TPU-material, which are suitable for interventions, as the competition in the area of inflatable booms made of this material is too tough. The condition was that tensile strength of the material is one half lower than the tensile strength of the vulcanised rubber material, Fig. 5.

Preliminary sketches and calculations were made and three additional goals set:

- all components are built-in in the boom,
- a folded boom occupies minimum space,
- simple manufacture of the boom.

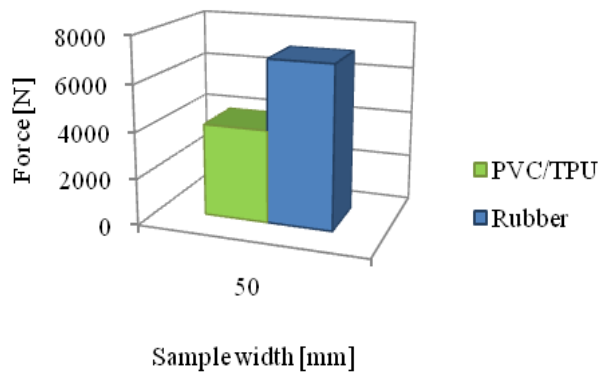


Fig. 5. Tensile strength of PVC/TPU and rubber for oil boom on 50 mm width sample

The majority of manufacturers offer materials which are suitable precisely for floating containment booms. We decided to use materials with a PVC/TPU coating of orange colour. In comparison with the usual PVC coating, this coating is slightly more expensive but provides better resistance to oil and UV-rays. Since it took some time for the first samples to be delivered (manufacturer's capacities were occupied), some preliminary specimens from different materials were made.

Specimens were tested in clean water and it was found out that the buoyancy calculations were correct. The first prototype did badly. The problem was that each separate buoyant body had to be welded on the basic material at a definite distance, which caused many problems in the procedure and was rather time consuming. The floating body had a shape of a square, therefore material wrinkled and, as a consequence, sealing was problematic and it had leaks. As those samples were rejected, new sketches and calculations were prepared. A great deal of attention was devoted to the shape and dimensions of a floating body. Foamed polyethylene in the form of thinner sheets was applied and it proved good. Every meter of a boom contains two such buoys and due to a low thickness, the welding procedure is simplified. The boom is not only pleasant to look at but it folds excellently. In the case of an intervention, it can't become stuck; it is simply pulled into the water and deployed. On its bottom part, the boom is weighted with a properly selected hot-zinc-coated chain to provide for a good stability and higher tensile strength. The boom is connected with a high-capacity zippers (found on the internet), which can be exposed to up to 3000 N/5cm. The main advantage of these zippers is their low weight and a simple use. Specimens of boom were made and tested in fresh water. They proved excellently in every respect. Booms are noted for their low total weight, good buoyancy, simple use, fast manufacture procedure and favourable price. The specimen was released.

All tests and specimens were made in compliance with the ISO 9001 standard.

4.2. Manufacturing of PVC boom

Before introducing the boom into the series production, the specifications were elaborated. The entire set of booms of various heights was specified and

manufactured: 250, 450, 600 and 900 mm. Standard lengths of segments are 3, 5 and 10 m. These sizes can cover the majority of customer requirements; however, it is possible to manufacture custom-made booms as well. Drawings for all types were produced and a working procedure was specified. Furthermore, the control procedure was specified, according to which the quality of the manufactured boom is verified.

Each boom has a waybill in conformity with the ISO 9001 standard, which is to be completed throughout the manufacturing process until its finish. In the waybill, any difficulties at the manufacture and the results of visual test should be noted. The completed and signed waybill is the prerequisite for shipping the boom. Besides the waybill, the test report is to be completed, which actually reports about the work performed. The test report is attached to every manufactured boom and serves as a certificate of quality.

The production process for floating containment boom starts with the preparation of tools and materials. The material is bought and every delivery is supplied with a quality certificate but it is nevertheless checked for quality by the in-house quality control [6]. The basic shapes are then cut and all required lines for folding and welds are marked, Fig. 6.

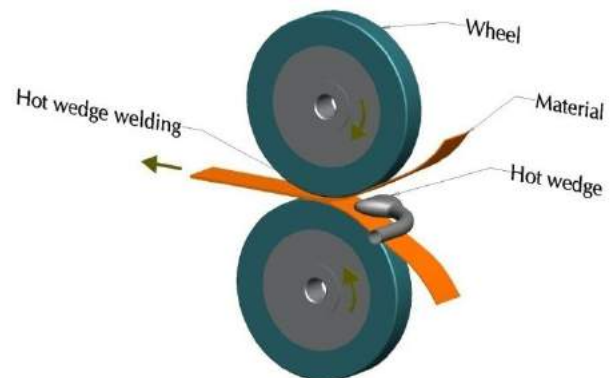


Fig. 6. Hot wedge or hot air welding

A corresponding number of floating bodies from polyethylene foam are cut, as well as handles for transporting the boom. A corresponding number of zippers are prepared. A welding procedure on a high-frequency machine follows. Only a small number of simple welds are required. First, pockets for the chain and steel rope are welded on the upper part, which is then followed by transversal welding of pockets for inserting the foamed polyethylene material and their closing. Finally, a connecting zipper and a label with the data and serial boom number are welded on the material. The chain is inserted in the boom bottom and the steel rope in the upper part. The boom is finished and checked whether it is in compliance with the control specifications, the test report is filled out, the product can now be packed and shipped.

Using this production process and technology, we managed to achieve a yield of material that surpasses 90%. The manufacture of such type is at least three times quicker than the production of booms made of rubber, Fig. 7.

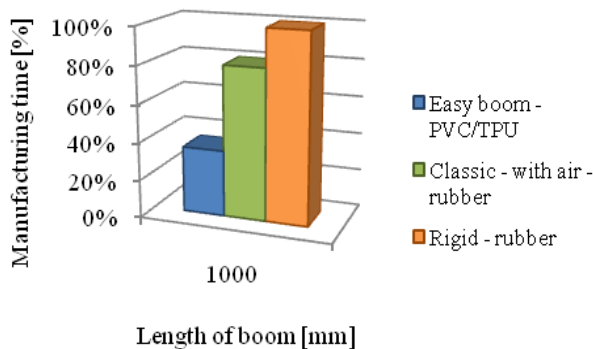


Fig. 7. Manufacturing time of boom

4.3. Test in the field

Tests were carried out in clean water (Fig. 8) and booms proved excellently. We have named it Easy Boom and have already offered it in the market.



Fig. 8. Testing of new type of boom (2010)

The project results have met all set goals. Thus Easy Boom:

- doesn't require an inflation system,
- is used in stagnant (wave less) water and lakes,
- is intended for interventions,
- is made from the material that is good resistant to oil and UV-rays,
- is simple for use thanks to its well-considered and resource-full manufacture,
- light-weight but highly stable,
- occupies little space when folded,
- is noted for its favourable price (Fig. 9).

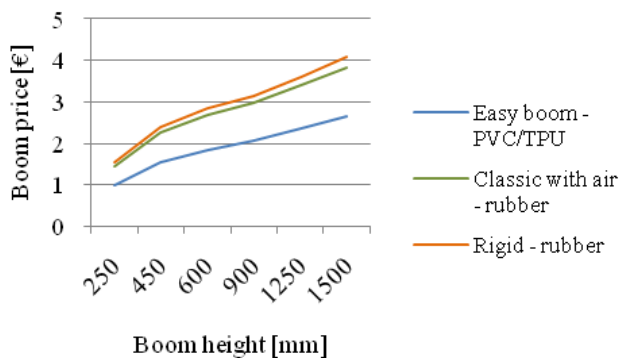


Fig. 9. Price of different type of boom

The offer will be continually rounded with accessories, such as boom fixation onto the shore, boxes for storing, wind-up reels, and we are considering the idea of making a special car trailer for transporting all required equipment needed in this type of interventions.

5. CONCLUSIONS

The result of the project was the design and implementation of a new type of floating containment boom so-called Easy Boom. The new boom is light weight, highly stable with no inflation system required. Boom has small volume when packed for transport and is simple and quick to deploy, (Fig. 10). It is made of UV and oil resistant material.



Fig. 10. Folded Easy Boom 250

Easy Boom has already attracted attention of a Slovene customer who in December 2010 bought 230 m of new developed boom and plans to make further purchases in this year. We are discussing with that customer a purchase of accessories and universal on shore fixation system. The offers have been prepared and we are waiting for a response.

The customer is highly satisfied with our product, and pointed out its light-weight and simple use. Furthermore, he found connecting with zippers highly resourceful, despite being slightly sceptical at first. The boom contains handles used for transporting the boom, and will be used on lakes and slowly flowing rivers.

REFERENCES

- [1] DORČIĆ, I. (1987) *The basics of cleaning oil pollution*, The Croatian Alliance of Chemists and Technologists, INA Research and Development, Society for the water protection of Croatia, Zagreb (in Croatian).
- [2] EFROYMSON, R.A. (2004) Improving Tools for Ecological Risk Assessment at Petroleum-contaminated Sites, *The Oil & Gas Review*, pp 1-5.
- [3] UMEK, T., SOTLER, Z. (1995) *Response to environmental accidents at sea and ashore*, Proceedings, Mišič's water day, Murska Sobota, May (in Slovene).
- [4] Hydrotechnik Lübeck, official web page, <http://www.hydrotechnik-luebeck.de/>, March, 2011.
- [5] Savatech EKO, Interne materials, catalogues 2010, 2011.
- [6] JUSTIN, R., SOKOVIĆ, M. (2011) *Industrialisation of PVC Easy Boom*, Diploma thesis, Faculty of Mechanical Engineering, Ljubljana (in Slovene).

34th INTERNATIONAL CONFERENCE ON PRODUCTION ENGINEERING



SECTION L

TRIBOLOGY



PROPOSAL OF A NEW FRICTION TESTING METHOD FOR BULK METAL FORMING

Miroslav PLANČAK¹, Igor KAČMARČIK¹, Dejan MOVRI¹, Đorđe ČUPKOVIĆ²

¹Faculty of Technical Science, University of Novi Sad, Trg Dositeja Obradovica 6, Novi Sad, Serbia
plancak@uns.ac.rs

²Cimos d. d., C. Marežanskega upora 2, Koper, Slovenia

Abstract: Friction between workpiece and die is an important parameter in most metal forming processes. This undesirable phenomenon affects the forming load and energy, material flow, workpiece quality and tool life. Knowledge of friction magnitude is essential for the analytical analysis and numerical simulation of metal forming processes, as well as for tool and process design. Quantification of actual friction conditions during deformation can be carried out by different methods. The most employed experimental technique for determination of friction during deformation process is ring compression test. It provides an average value of coefficient of friction over the specimen surface. However, ring test does not represent in appropriate way cold bulk metal forming operations in which higher normal stresses and larger surface area expansion take place. For such forming conditions other experimental tests have to be applied. Current paper elaborates the proposal for a new friction testing method for bulk metal forming processes in which more severe conditions prevail. Method is based upon double backward extrusion process. Results are analyzed and compared with results obtained by other measuring techniques. Relevant conclusions are drawn.

Key words: metal forming, friction, testing method

1. INTRODUCTION

Tribology in metal deformation processes plays an important role. Friction between die/workpiece contact surfaces is undesirable phenomenon, as it affects in negative way forming load, material flow, workpiece quality as well as die wear characteristics. Consequently, friction may result in unexpected breakdown, the need for re-adjustment of the die and machine and other disturbances of the whole forming process.

Triboogical conditions in metal forming operations are very complex as they are influenced by many process parameters such as contact pressure, temperature, relative velocity, combination of die/workpiece material, lubrication and surface expansion ratio. Friction is quantified by coefficient of friction “ μ ” or/and friction factor “ m ”. These parameters can be obtained by various experimental models (simulative tests). The most applied method to determine “ μ ” (“ m ”) is ring - compression test [1], [2], [6]. This test has proven to be a simple method which makes possible to obtain an average value of friction coefficient in one forming operation. However, ring - test induces relatively low contact pressure and small surface expansion ratio and therefore is not suitable for cold bulk metal forming operations in which interface die/workpiece pressure may reach values up to 2500 MPa. Due to this reason other experimental trials have been accomplished which comply with more severe forming and tribological conditions.

Following section gives short insight into some of the models for evaluation of friction data in cold bulk metal forming.

EXPERIMENTAL MODELS FOR FRICTION EVALUATION IN METAL FORMING

A number of alternative methods have been developed to evaluate coefficient of friction in metal forming technologies. Most of them are intended for and adjust to specific operations: sheet metal forming, extrusion, hot forging, cold forging, etc.

In open die backward extrusion test (ODBET) [4] cylindrical specimen is placed at flat platen and compressed by top platen which is provided with the hole. During upsetting, material flows horizontally in radial direction and axially upward through the hole. In this way extruded height is generated which is a measure of friction. By creating and using calibration curves coefficient of friction can be obtained.

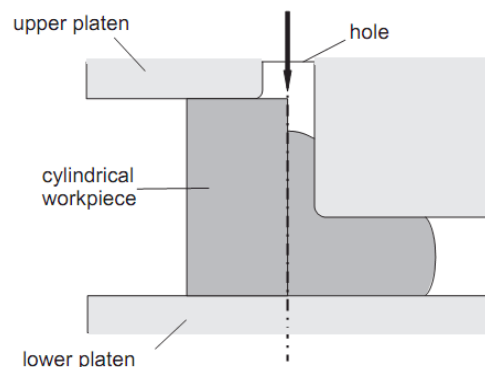


Fig.1. ODBET test [4]

In [3] new T - shape compression test is proposed (Fig. 2.). In this test cylindrical specimen is placed at the die with a V - groove. During upsetting by top flat platen some material flows into the V - groove and some is upset and flows sideways. The height of extruded part is friction sensitive. By FE simulation calibration curves are generated which enables determination of “μ” (“m”).

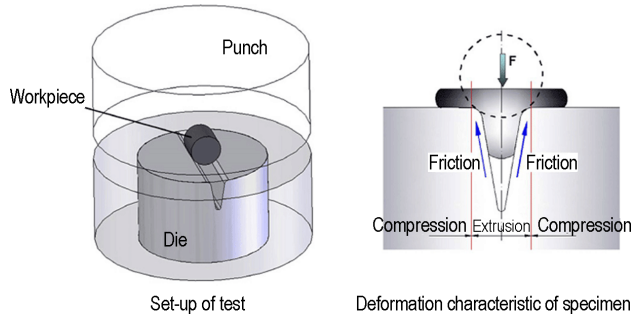


Fig 2. T - shape compression [3]

The sketches of some other experimental methods are given in fig. 3.

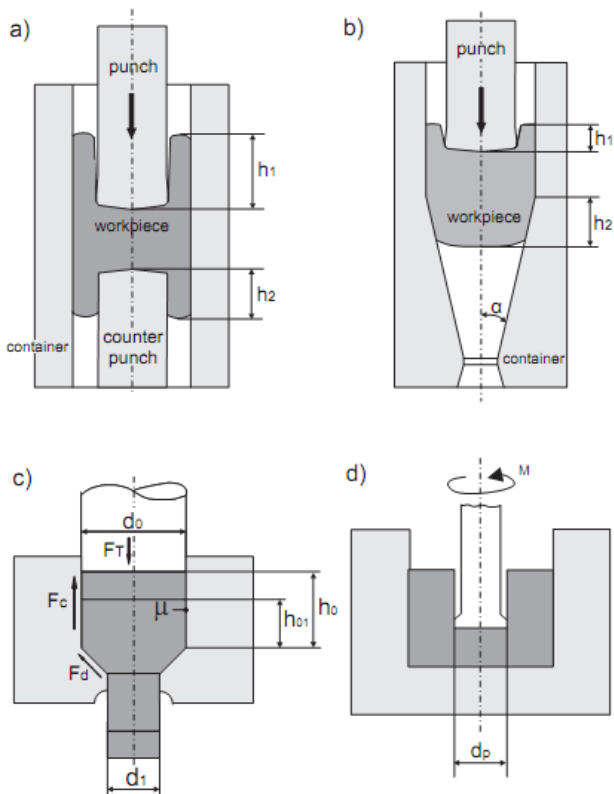


Fig.3. Methods for determining friction magnitude (a - backward - forward hollow extrusion, b - combined forward-backward extrusion, c - forward extrusion and d - backward extrusion with a twist)

In backward - forward hollow extrusion (Fig.3a) material flows in two directions: upwards and downwards. Geometry values h_1 and h_2 , for the same die/tool geometry, depend on the friction coefficient. For the theoretical friction value $\mu = 0$, material flows both upwards and downwards in the same amount. The higher the friction, the more material flows upwards [9].

In combined forward - backward extrusion (Fig.3b) punch for conventional backward extrusion and die for conventional forward extrusion are used. Material flows in both backward and forward directions. Ratio h_1/h_2 determines the friction value. When friction is high, more material flows backwards, and vice versa, low friction results in more forward movement of the workpiece material [8].

Forward extrusion can also be used in friction evaluation. Total extrusion force in this process in this process (F_T) equals to:

$$F_T = F_C + F_d + F_{dd} \quad (1)$$

where F_C , F_d - load required to overpower friction in vertical and conical die/workpiece interface and F_{dd} - load required for deformation in conical segment.

During observed interval, height h_0 decreases to h_{01} and load F_T decreases for ΔF_T . Load reduction ΔF_T is a function of only F_C , as F_d and F_{dd} remain constant during this interval. Therefore, friction coefficient can be calculated from:

$$\mu = \frac{\Delta F_T}{\sigma \cdot \pi \cdot d_0 \cdot \Delta h} \quad (2)$$

where σ is flow stress of the workpiece material [9, 10, 11].

In backward extrusion with a twist (Fig.3d) workpiece is deformed in backward extrusion and then punch is being rotated while die is kept stationary. By using two different punches (with different punch lands) friction can be obtained from:

$$m = \frac{2\sqrt{3}(M_1 - M_2)}{\pi \cdot d_p^2 \cdot h_c \cdot \sigma} \quad (3)$$

where d_p is the diameter of the punch, h_c is the length of the punch land, σ is flow stress of the material and M_1 , M_2 are momentums measured for each punch [5]

2. DOUBLE BACKWARD EXTRUSION

Schematic of the double backward extrusion process is shown in fig.4.

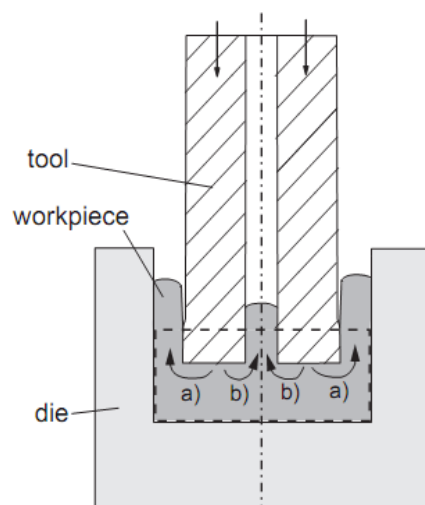


Fig 4. Double backward extrusion (material flows in two directions: “a” and “b”)

A cylindrical billet is backward extruded with a special punch that has an opening through the center. Because of this specific construction of the punch, material flows in two directions:

- a) to the side, between the punch and die (like in conventional backward extrusion process)
- b) to the middle of the punch (through the opening in the punch)

In current work punch shown in Fig.5. is used. This is a standard punch for backward extrusion with a hole $\phi 9$ mm drilled through the center. Inner diameter of the die was $\phi 40,4$ mm and dimensions of the billet were $\phi 40 \times 35$ mm.

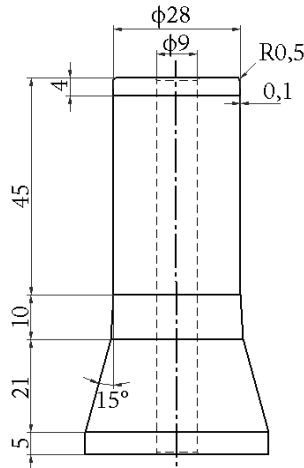


Fig.5. Geometry of the tool used in both FE simulation and experiment

3. FINITE ELEMENT MODELLING BY SIMUFACT FORMING 9.0

The goal of FE simulation was to obtain friction calibration curves that would be used in determination of friction in experiment. The idea of the simulation was to vary friction coefficient and keep other input parameters (billet geometry, material, press velocity...) constant.

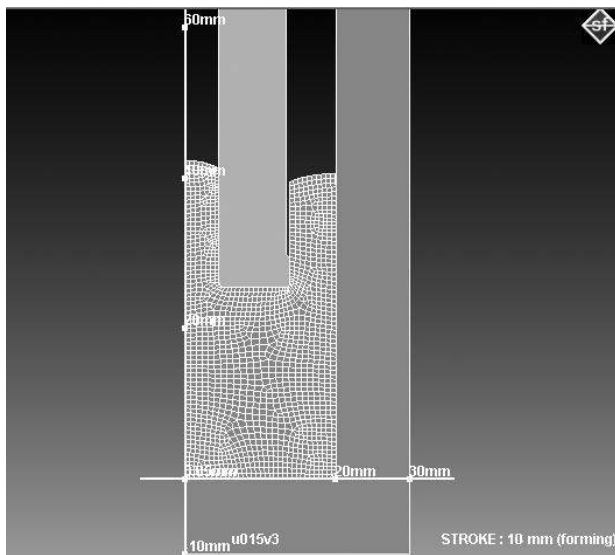


Fig 6. FE simulation in Simufact Forming 9.0

Advanced Front Quad mesher with 0,6 mm element size was used. Punch and die were set as rigid bodies and press velocity was 0,25 mm/s.

Axisymmetric 2D simulation was performed in Simufact Forming 9.0 (SF 9.0) software. Initial billet was a cylinder $\phi 40 \times 35$ mm. Material of the billet was aluminum alloy with stress - strain curve: $K = 315,2 + 117,1 \cdot \phi^{0,2}$.

Stroke of 22 mm was simulated and the height of material that flowed through central opening was measured at every 2 mm of punch increment.

In Fig.8. correlation between material flowed through the central opening and press stroke in terms of specific friction coefficient is shown. It can be noted that in FE simulation, for a given workpiece material and geometry, with an increase of friction coefficient, material flows more through the central opening.

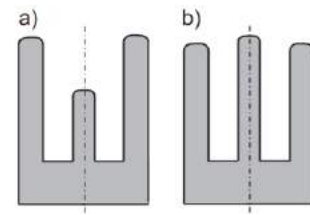


Fig 7. Material flow in (a) low friction conditions and (b) in high friction conditions

Preliminary simulations showed that, unlike in ring – test [1, 2, 6], billet's material has a great influence on material flow.

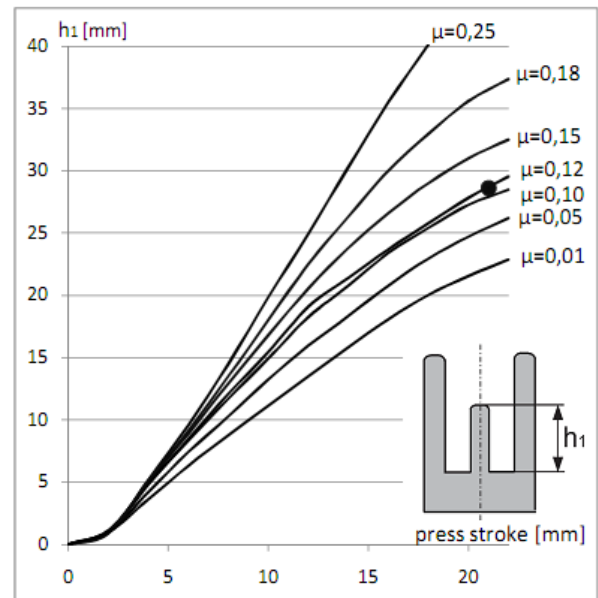


Fig 8. Friction calibration curves for double backward extrusion obtained by simulation in SF 9.0

4. EXPERIMENT

Double backward extrusion experiment was conducted on 6.3 MN hydraulic press Sack & Kiesselbach at Faculty of Technical Science in Novi Sad, Serbia. Cylindrical billet ($\phi 40 \times 35$ mm) was extruded with 22 mm stroke. Billet was lubricated with oil [7].

Same tool and die geometry was used as in simulation (Fig.5.), as well as same billet material (aluminium alloy - $K = 315,2 + 117,1 \cdot \varphi^{0.2}$).



Fig 8. Workpiece after double backward extrusion

Material which flowed through the central opening (height h_1 , Fig.8.) and press stroke (22 mm) were superimposed on friction calibration chart obtained by FE simulation (black dot, Fig.8.). From this chart, it can be concluded that friction in experiment was $\mu \approx 0,12$.

5. CONCLUSIONS

Knowledge of friction magnitude in metal forming is a very important as friction has a great influence on almost all process parameters. There are several methods for determining friction coefficient, such as combined forward – backward extrusion, forward extrusion, backward extrusion, twist test, ect. A brief overview of some of these tests was given in the paper. The most employed method is ring – test. However, in ring – test only low contact pressures occur and, therefore, this test is not adequate for processes where severe contact pressures prevail.

A double backward extrusion method has great possibilities for friction evaluation. During this process large plastic deformations occur.

In this work simulation of double backward extrusion of cylindrical billet was performed in order to obtain friction calibration chart.

Results of the simulation showed that, the higher the friction, the more material flows through the central opening in the punch.

At the end experimental double backward extrusion was performed with the same input parameters as in simulation. By using friction calibration chart obtained from FE simulation, friction coefficient in experiment was determined. Results show that friction coefficient was $\mu \approx 0,12$ which corresponds very good with early expectations, because workpiece was lubricated with oil.

6. ACKNOWLEDGEMENT

This paper is a part of the investigation within the project EUREKA E!5005.

REFERENCES

1. MALE, A.T., COCKROFT, M.G. (1964) *A Method for the determination of the coefficient of friction on metals under conditions of bulk plastic deformation*, Journal of the Institute of Metals, Vol. 93, 65.
2. BURGDORF, M. (1967) *Über die Ermittlung des Reibwertes für Verfahren der Massivumformung durch den Ringstauchversuch*, Industrie Anzeiger, pp15-20.
3. ZHANG, Q. (2009) *Evaluation of friction conditions in cold forging by using T-shape compression test*, Journal of Materials Processing Technologies, Vol 209., pp5720-5729.
4. SOFUOGLU, H., GEDIKLI, H. (2002) *Determination of friction coefficient encountered in large deformation processes*, Tribology International 35, pp27-34.
5. BAY, N., WIBOM, O., NIELSEN, J. AA. (1995) *A new friction and lubrication test for cold forging*, Annals of the CIRP, Vol. 44/1.
6. HAWKYARD, J.B., JOHNSON, W. (1967) *An analysis of the changes in geometry of a short hollow cylinder during axial compression*, Int. J. Sci. Pergamon Press Ltd., Vol. 9, pp. 168-182.
7. CUPKOVIC, DJ. (2005) *Prilog istrazivanju procesa dvostrukog suprotnosmernog istiskivanja*, Novi Sad.
8. KUZMAN, K., PFEIFER, E., BAY, N., HUNDIG, J. (1996) *Control of material flow in a combined backward can – forward rod extrusion*, Journal of Materials Processing Technology 60, 141-147
9. FERESHTEH-SANIEE, F., PILLINGER, I., HARTLEY, P. (2004) *Friction modeling for the physical simulation of the bulk metal forming processes*, Journal of Material Processing Technology 153-154, 151-156.
10. MARINKOVIC V., MARINKOVIC T. (2009) *Odredjivanje koeficijenta trenja u procesima obrade istiskivanjem*, 11th Int. conference on Tribology – Serbiatrib.
11. VILOTIC, D., PLANCAK, M., KUZMAN, K., MILUTINOVIC, M., MOVRIN, D., SKAKUN, P., LUZANIN, O. (2007) *Application of net shape and near-net shape forming technologies in manufacture of roller bearing components and cardan shafts*, Journal for Technology of Plasticity, Volume 32, pp.87-103.



34th INTERNATIONAL CONFERENCE ON
PRODUCTION ENGINEERING
29. - 30. September 2011, Niš, Serbia
University of Niš, Faculty of Mechanical Engineering



COMPARISON OF CONVENTIONAL AND NEW LUBRICANTS FOR COLD FORMING

Plavka SKAKUN¹, Igor KAČMARČIK¹, Tomaž PEPELNJAK², Ognjan LUŽANIN¹ Aljosa IVANIŠEVIĆ¹,
Mladomir MILUTINOVIĆ¹

Faculty of Technical Sciences, University of Novi Sad, Trg Dositeja Obradovica 6, Novi Sad, Serbia
Faculty of Mechanical Engineering, University of Ljubljana, Aškerčeva 6, Ljubljana, Slovenia
plavkas@uns.ac.rs, igorkac@uns.ac.rs, tomaz.pepelnjak@fs.uni-lj.si, luzanin@uns.ac.rs, aljosa@uns.ac.rs,
mladomil@uns.ac.rs

Abstract: Many different tests for determination of friction coefficient in metal forming have been developed. Some of them are general, while the others are specific for certain metal forming methods. One very often used test, particularly for bulk deformation processes is the ring compression test. In this paper ring compression test is used for friction coefficient determination for three different lubricants, two conventional (oil for cold forging and phosphated surface with MoS₂), and one new environmentally friendly lubricant (Bonderlube FL 741). Aim of the test was to prove that new kind of lubricant can achieve good lubricating conditions and can be used as a replacement for conventional environmentally hazardous lubricants.

Key words: ring compression test, environmentally friendly lubricants

1. INTRODUCTION

Main tasks of lubricant in metal forming processes are to reduce friction, lower the deformation force and to prolong tool life. Lubricants in cold bulk metal forming processes, especially in extrusion, must have abilities to withstand some additional requests. These processes have certain characteristics (high normal pressure between workpiece and tool, large surface expansion of the workpiece etc.) and lubricant is subjected to very severe conditions. Lubricating system which can withstand these conditions is phosphate coating with some additional soap based lubricant. It has been in use for a long period of time (since 1930's) because it's ability to obtain good lubricating conditions in processes where high pressures, friction and temperature occur.

Use of phosphate coatings has negative environmental impact because of several drawbacks (large amounts of waste water, bath sludge containing heavy metals etc.), and therefore efforts have been made to improve existing lubricating systems and to develop new.

In this paper values of friction coefficient for different types of lubricants are compared. Both environmentally friendly and environmentally hazardous lubricants were used with the aim to prove that environmentally friendly lubricant can obtain same friction conditions within lubricating system as environmentally hazardous lubricant.

2. CONVENTIONAL TRIBOLOGICAL SYSTEM - PHOSPHATE COATING

Wide application and development of cold extrusion is connected with application of phosphate coating. This coating, usually containing zinc, is lubricant carrier. Because of chemical reaction that occurs between lubricant and coating, lubricant adhesion to the billet is improved.

There are several steps in process of zinc phosphate coating forming and they can be divided in three groups: cleaning of billet, phosphate coating generation and lubrication [7].

First group consists of surface cleaning operations and preparation of surface for phosphate coating. Mechanical cleaning, such as shot blasting and peeling, can prepare surface for better adhesion of the zinc phosphate coating and lubricant, chemical cleaning is applied with the aim to degrease billet, and this is followed by rinsing, pickling, and again rinsing. The pickling operation prepares the surface of the billet for the zinc phosphate coating process, usually sulfuric or hydrochloric acid is used. After this operation billet is rinsed with water in order to neutralize remaining acid.

In the zinc phosphate coating operation, a zinc phosphate coating is formed on the steel surface. It is conversion coating and zinc phosphate is chemically bonded to the metal base. This operation is also followed by rinsing.

The coated part is provided with lubricant by dipping into a hot bath of alkaline soap (e.g. sodium stearate), that reacts with the zinc phosphate to form zinc stearate. Layer of zinc phosphate has crystalline structure which has dual

role, it chemically binds soap to the surface and acts as a physical carrier for the soap. After lubrication, it is necessary to dry the billets.

Although lubricating system with zinc phosphate coating shows many advantages, especial in cold extrusion processes, from mentioned procedure it can be seen that from environmental point of view it has negative impact on the environment [3]. Those negative impacts are: large water requirements in rinse baths, sludge containing heavy metals, necessity of periodic replacement of baths, large amounts of waste waters containing grease, oils, acid and soap etc. In addition to these reasons phosphating process requires longer treatment time than new tribological systems.

3. NEW TRYBOLOGICAL SYSTEMS

New tribological systems which can be used instead of zinc phosphate coating have been developed in two directions: new conversion coatings and lubrication without conversion coating [3].

Basic method for the first group is conversion coating method, only modified and improved comparing to phosphate coating procedure, eliminating many drawbacks related to zinc phosphates. One of these methods is electrolytic phosphate coating. The main advantages of this procedure are: sludge free phosphating bath is obtained, use of acid for pickling may be avoided by electro chemical pickling, cycle time is considerably shortened, working environment is improved. This procedure also makes possible to phosphate high alloyed steels and stainless steel. It can be seen from the Fig. 1, which shows SEM micrographs of conventional, chemical phosphate coating and electrolytic phosphate coating, that electrolytic phosphate coating ensures much more uniform and finer crystalline coating with smaller film thickness.

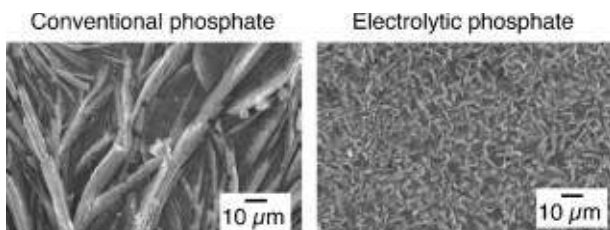


Fig. 1. SEM micrographs of conventional and electrolytic phosphate coating [3]

Another method which belongs to group of new conversion coatings is microporous coating. Different techniques have been developed to produce porous surface layer in which liquid lubricants can be entrapped. Depending on the applied method layer thickness is from 1 µm to 5 µm, and friction coefficient which can be achieved is as low as for phosphate coating plus soap lubrication.

Two concepts of lubrication without conversion coating are presented in paper [3]. First is dual bath system, where base coating is adhering to the workpiece surface on top of which over-coating is formed to reduce friction. Second is single bath system, developed in several

variations. One of them is method called “dry-in-place” where double coating is formed consisting of a lubricant carrier as base with a lubricant film on top. This lubricant consists of an inorganic salt as base component and a wax as a lubricant. Process is simple for application (dip and dry process) and obtained coating can achieve similar lubricating conditions to the coating formed by phosphating and soap. Similar lubricant, Bonderlube FL 741 was used in experiment described in this paper,

4. RING COMPRESSION TEST

Experimental tests for determination of friction coefficient between materials of tool and workpiece within the metal forming processes are numerous. There are tests developed for specific manufacturing processes, (rolling, extrusion, deep drawing etc.,) or tests of general purposes. In this investigation general test was used (ring compression test). Results of the test was used to compare friction coefficient values for different lubricants.

The idea for the ring compression test was first presented by Kunogi [5] and later improved by Mail and Cockcroft [6], Avitzur [1] and many other researches. Basic technique of this test relates dimensional changes of a ring specimen to the coefficient of friction. When a ring specimen is compressed between two flat dies, depending on the value of friction coefficient, value of inner diameter can increase or decrease. High friction coefficient results in inward flow of the material, while low friction coefficient results in an outward flow of the material. To determine friction coefficient it is necessary to measure change in height and in inner diameter of the ring, to calculate percentage value of nominal strains ϵ_h and ϵ_d and to compare $\epsilon_h - \epsilon_d$ curve to calibration curves. In this research calibration curves, calculated according Avitzur's equations [1] were used. In Fig 2 calibration curves are presented.

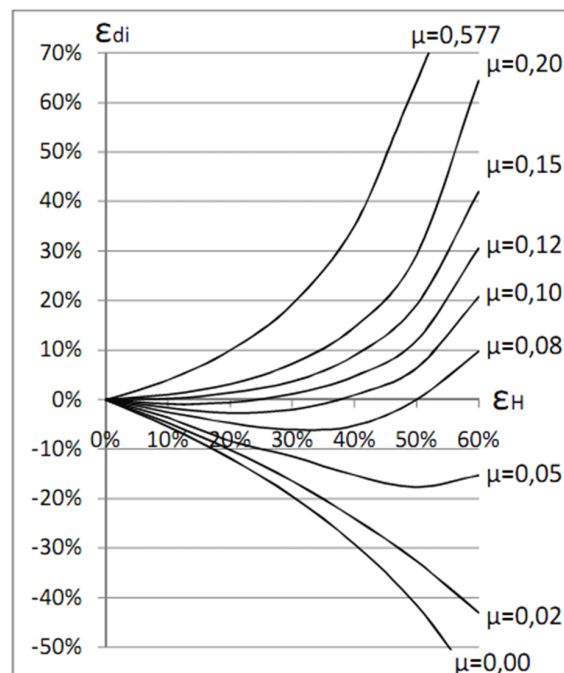


Fig. 2. Calibration curves

5. EXPERIMENTAL DETERMINATION OF FRICTION COEFFICIENT

Ring compression experiment was conducted in order to determine friction coefficient for three different kinds of lubricants, two conventional (oil for cold forging and phosphated surface with MoS_2), and one new environmentally friendly lubricant (Bonderlube FL 741).

5.1. Preparation of specimens

Material of rings was Č4320. Phosphated rings was lubricated with MoS_2 . To apply Bonderlube lubricant at the ring surface certain procedure was followed.

According to the manufacturer instructions phases of the Bonderlube application are: shot blasting, immersion in hot dematerialized water and Bonderlube application followed by hot drying.

If shot blasting can not be applied as a surface preparation, it can be replaced by usual surface preparation for phosphate coating forming.

Before application Bonderlube needs to be diluted by adding demineralized water. Concentration of dilution depends on products types and expected deformation rate, and can be between 60% and 90%. Recommended standard concentration is between 70% and 80%. Temperature of the process is 60°C , during application bath must be gently moved to avoid product stratification. Also localized overheating must be avoided, temperatures over 70°C , lead to product coagulation. Time of application is from 3 to 7 minutes, what depends on workpiece dimensions.

After application of lubricant, workpiece needs to be dried at the 100°C

5.2. Experiment

Common geometry of a ring specimen which is used in this test has proportion of outer diameter to inner diameter to height 6:3:2. This proportion was used in current experimental investigation too. Dimensions of rings were: outer diameter $D = 18\text{ mm}$, inner diameter $d = 9\text{ mm}$ and height $h = 6\text{ mm}$. Ring specimen for compression test is presented at Fig 3. Experiment was conducted on Sack&Kieselbach hydraulic press, nominal force 6.3 MN, using flat dies.

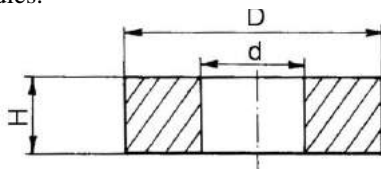


Fig.3. Specimen for ring compression test

At Fig. 4 ring with applied Bonderlube FL 741 lubricant on its surface is presented.

According to experimental values of height and inner diameter for each ring, percentage value of nominal strains ϵ_h i ϵ_d are calculated and $\epsilon_h - \epsilon_d$ curve is compared to calibration curves. At Fig.5 comparison of experimental and calibration curves are presented. Values of

experimentally determined friction coefficients are in table 1.

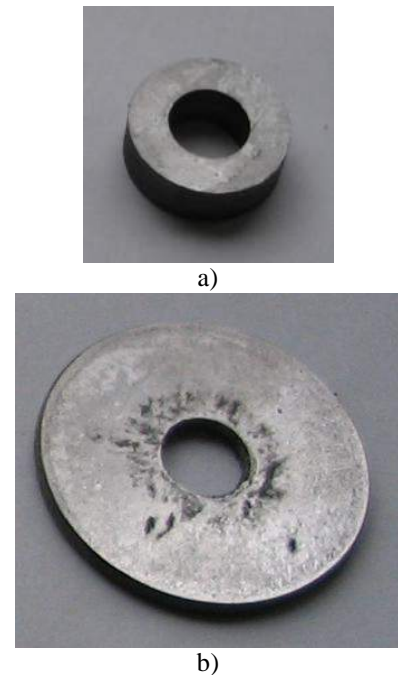


Fig. 4. Ring with Bonderlube FL 741 lubricant on its surface a) before test b) after test

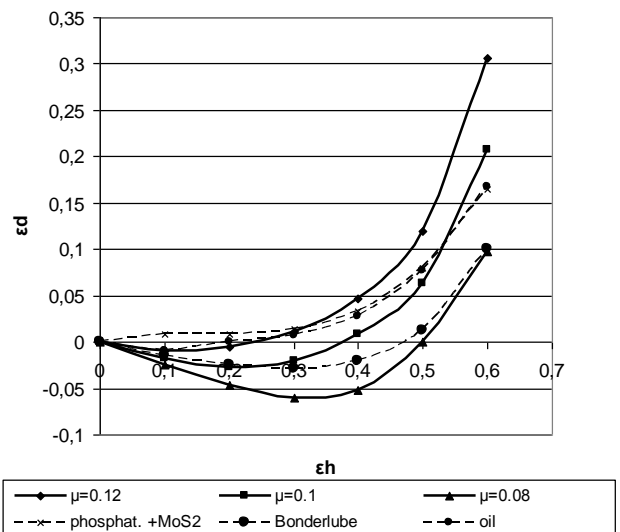


Fig. 5. Calibration and experimental curves

Table 1 Experimentally determined friction coefficient values for different lubricants

No	Lubricant	Friction coefficient
1.	Oil for cold forging	≈ 0.11
2.	Phosphated surface + MoS_2	≈ 0.11
3.	Bonderlube FL 741	≈ 0.09

6. CONCLUSION

Ring compression test was used for determination of friction coefficient for three different types of lubricants.

Two conventional lubricants were used (oil for cold forging, phosphate coating with MoS₂) and one environmental friendly lubricant, Bonderlube FL 741. Comparing with conventional ways of lubrication there are several advantages in both economical and environmental way, when Bonderlube FL 741 lubricant is used. Experimental results showed that value of friction coefficient for Bonderlube lubricant is lower ($\mu \approx 0.09$), compared to conventional lubricants ($\mu \approx 0.11$).

Future work implies determining and comparing friction coefficient of old and new lubricants using test for specific method, e.g. cold extrusion. In this way it would be possible to evaluate lubricant suitability for specific method.

ACKNOWLEDGEMENT

This paper is a part of the investigation within the project EUREKA E!5005

REFERENCES

- [1] AVITZUR, B. (1968). *Metal Forming: Processes and Analysis*. Mc Graw –Hill Book Company, USA.
- [2] KALPAKIJAN, S., SCHMID, S.R. (2008). *Manufacturing Processes for Engineering Materials*. Pearson Prentice Hall, Singapore
- [3] BAY, N., AZUSHIMA, A., GROCHE, P., ISHIBASHI, I., MERKLEIN, M., MORISHITA, M. (2010). *Environmentally Benign Tribo-systems for Metal Forming*. CIRP Annals – Manufacturing Technology, vol. 59, no. 2, p. 760-780.
- [4] ARENTOFT, M., BAY, N., TANG, P.T., JENSEN, J.D. (2009). *A New Lubricant Carrier for Metal Forming*. CIRP Annals – Manufacturing Technology, vol. 58, no.1, p.243-246
- [5] KUNOGI, M. (1956). *A new method of cold extrusion*. Journal of Science Research Institute, vol. 50, p.215
- [6] MALE, A.T., COCKROFT, M.G. (1964/65). *A Method for the Determination of the Coefficient of Friction of Metals under Conditions of Bulk Plastic Deformation*. Journal of the Institute of Metals, vol.93, p.38-46
- [7] GARIETY, M., GRACIOUS, N., ALTAN, T., (2007) *Evaluation of new cold forging lubricants without zinc phosphate precoat*, International Journal of Machine Tools & Manufacture 47, pp 673-681
- [8] YOSHIDA, M., IMAI, Y., YAMAGUCHI, H., NAGATA, S. (2003). *Nihon Parkerizing*, Technical report No 15
- [9] NAKAMURA, T., SUMIOKA, Y., SAGISAKA, Y., ISHIBASHI I., SEKIZAVA, M. (2008). *Lubrication Performance of Environmentally Friendly Lubricants for Forging*. 1st Report Proceedings of 59th Japanese Joint Conference for the Technology of Plasticity, p.579-580
- [10] BAY, N., NAKAMURA, T., SCHMID, S. (2010). *Green Lubricants for Metal Forming*. Proceedings of 4th International Conference on Tribology in Manufacturing Process 2010, p.5-28.
- [11] SKAKUN, P., PLANČAK, M., VILOTIĆ, D., MILUTINOVIĆ, M., MOVRIN, D., LUŽANIN, O. (2011) *Comparative investigation of different lubricants for bulk metal forming operations*, Proceedings of 10th Anniversary International conference on accomplishments in electrical and mechanical engineering and information technology, Banja Luka, BiH, pp 275-280
- [12] KAČMARČIK, I., MOVRIN, D., LUŽANIN, O., SKAKUN, P., PLANČAK, M., VILOTIĆ, D., (2011) *Determination of friction in bulk metal forming processes*, Proceedings of Serbiatrib '11, 12th International conference on tribology, Kragujevac, Serbia, pp 111-116

IMPORTANCE OF TRIBOLOGICAL CONDITIONS AT MULTI-PHASE IRONING

Milentije STEFANOVIĆ¹, Slaviša ĐAČIĆ², Sbrislav ALEKSANDROVIĆ¹, Dragan ADAMOVIĆ¹

¹Faculty of Mechanical Engineering in Kragujevac, s. Janjic 6, 34000 Kragujevac, Serbia

²Coal Mine A.D., Pljevlja, Montenegro,

stefan@kg.ac.rs, djale@t-com.me, srba@kg.ac.rs, adam@kg.ac.rs

Abstract: The importance of tribological conditions in metal forming is well known and equal to other forming process factors – material, machine and tool. The results obtained in investigation of the effects of tribological conditions in cold metal forming are presented in the paper. A typical tribo-model is strip ironed between angled die surfaces. The changes in pressure, friction coefficient and surface topography in single and multi-phase sliding in the conditions of boundary lubrication were investigated. The low carbon mild steel sheet, suitable for plastic forming, was used. In dependence on conditions in contact, it is possible to realize various friction lows. In course of investigation the so called constant low friction has been realized in condition of high contact pressures. The results of multi-phase sliding, which simulates the moving of piece through dies, are especially significant.

Key words: cold forming, multi-phase ironing, friction coefficient, sheet metal

1. INTRODUCTION

In cold metal forming processes, characterized by high pressures, local tool loads, generating of new piece surfaces etc., realisation of the convenient lubrication regime and elimination of micro-welding are of extreme importance. Distribution and intensity of shearing stresses on piece surface influence the possibility for plastic forming, i.e. the size of active force, energy consumption, tool life, piece surface quality etc. Taking into consideration the complexity of specified factors, tribological investigations in MF processes are extremely important and equal with investigations of other forming system segments - machines, tools and materials.

In the closed system tool-lubricant-material numerous tribological factors are present, most of which are variable during the process and are in a particular interaction, which makes the entire problem extremely complex. These factors can be observed from macro-geometrical, rheological or some other aspect. Some factors which are very important are: properties of tool material and material being formed, thermal problems (temperature, heat transfer, ...), micro- and macro-properties of forming process, relation of contact and free surface of the piece, friction properties, lubricant and lubrication method properties, contact surface roughness and its orientation, plasticity, fatigue, adhesion, diffusion, wear, stress and strain distribution, sliding speed, remaining stresses, damages, physical-chemical properties, condition of surface etc [3].

Proper selection of tribological conditions and identification of boundary relations on contact surfaces enables controlled flow in surface layer, whereat this layer has sufficiently lower flow limit than basic material and can be defined without fracture. By combination of main tribo-factors in forming system – speed, load (strain

ratio), type of materials in contact (topography, content), preparation of contact surface and lubricant type, it is possible to realise mixed, i.e. boundary friction. In that way, contact between tool and piece material, tearing of softer material particles and rough disruptions of forming conditions are reduced to minimum.

At ironing, pieces of considerable height in relation to diameter are obtained, with bottom thickness larger than wall thickness. In forming, which is most often multi-phase for one stroke, inner diameter slightly changes. Total thinning, i.e. number of rings and geometrical relations of work surfaces of tool elements are important in forming.

2. CHOICE OF TRIBOLOGICAL MODEL

Modelling of tribological conditions at ironing implies satisfying of the minimum of necessary criteria considering the similarity in stress strain properties, temperature-speed conditions, properties of tools surface and material. Classical scheme of ironing is shown in Fig. 1, and different tribo-models of ironing are shown in Fig. 2.

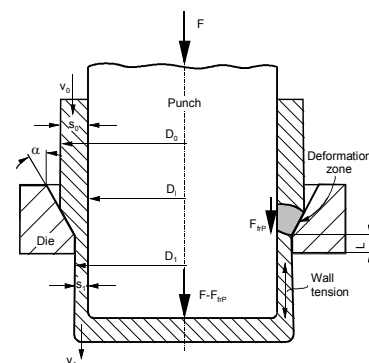


Fig. 1. Scheme of ironing

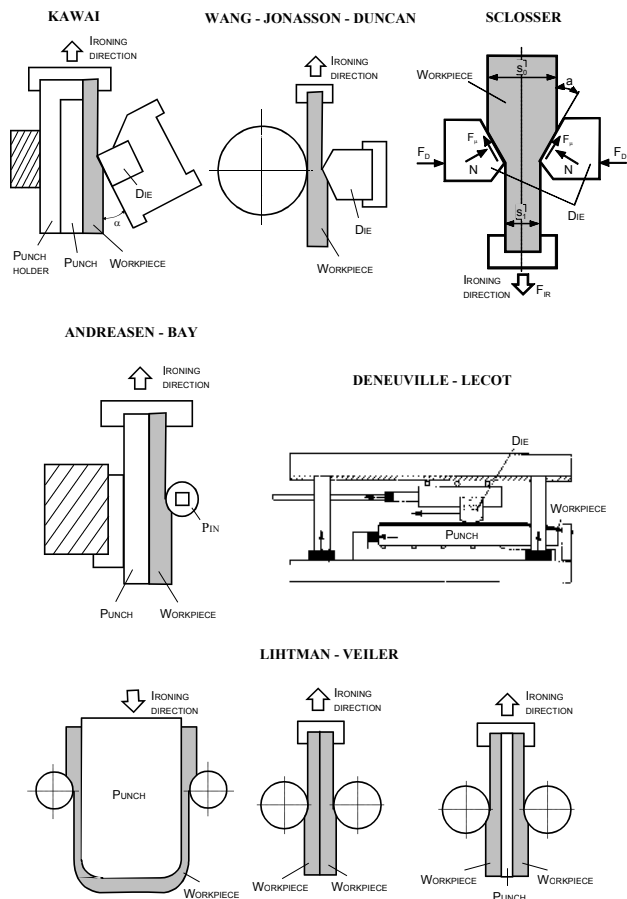


Fig. 2. Tribo-models of ironing

In researches, the results of which are presented in this paper, the basic ironing model, which imitates zone of contact with die with biaxial symmetry, was used as tribo-model, Fig. 3. This is a classical model (*Schlosser*), which enables realisation of high contact pressure and takes into account real geometrical conditions of forming process. It was used in many researches, especially in the area of tribology of stainless steel sheet metals and in Al- alloys forming [1], [2].

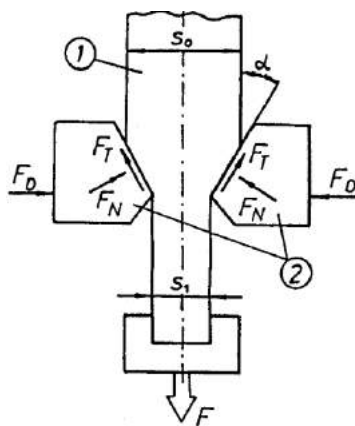


Fig. 3. Scheme of the tribo-model

Model applied in paper, according to fig.3, requires measuring of holder force F_D and drawing-sliding force F . If the test-specimen dimensions and die angle are known, it is possible to determine friction coefficient and average pressure in contact:

$$\mu = \frac{F}{2F_D} - \operatorname{tg} \alpha \quad (4)$$

$$p = \frac{F \sin^2 \alpha + 2F_D \sin \alpha \cos \alpha}{b_0(s_0 - s_1)} \quad (5)$$

where is:

- b_0 - specimen width,
- s_0 - initial test-specimen thickness ,
- s_1 - thickness after drawing.

3. EXPERIMENTAL RESULTS

Ironing is realised in conditions close to plane strain state. The investigated material is low-carbon steel sheet metal of quality DC04, convenient for plastic forming. Mechanical and other properties are specified in Table 1. Dimensions of test-specimen being investigated are: $b_0 \times s_0 \times \text{length} = 20 \times 2,5 \times 200 \text{ mm}$.

Table 1. Material properties

R_p , MPa	R_m , MPa	A, %	r	n
185,2	284,5	35,3	1,68	0,215

Contact pair is made of tool steel, hardness 60 HRC, highly-polished to mean roughness $R_a=0,06 \mu\text{m}$. Gradient angle is $\alpha=10^\circ$, as recommended in literature. Drawing speed is 20 mm/min. In investigations, mineral oil for cold forming was used [3].

The investigations were made on a special device, ERICHSEN 142, according to the model in Fig.3, which was placed on the machine for investigation of sheet-metals,

Side force F_D is realized by a special hydro-device, which enables measuring of the force. In the course of investigation, forces of 5, 10 and 15 kN were given. Drawing force, in dependence on the sliding path, was measured by a special measuring chain.

In dependence on specified conditions, it is possible to carry out certain classification of friction types, taking as a criterion the value and change of friction coefficient and appearance of test-specimen surface after investigation [1]:

- I - constant low friction,
- II - increase of friction after realisation of type I,
- III - constant increase of friction,
- IV - constant high friction.

Proper contact surfaces have the following descriptions:

- flat (smooth)
- lightly polished
- with abrasions
- lightly scratched
- heavily scratched

At drawing at sliding length of 60 mm, there are no changes in friction character, as a rule. In addition, drawing force records at successive investigations are shown, with shorter sliding paths. Dependence of force on

sliding path practically remains constant during investigation period, which corresponds to I friction type. Dependence of drawing force on travel at various working pressures is shown in Fig. 4. Total drawing force consists of friction force and "ideal" forming force which depends exclusively on strain ratio [3], [4]. Sheet metal thinning at the same compression force F_D does not depend on tribological conditions in contact [4, 5]. Increase of the number of drawings worsens the lubrication conditions, which corresponds to real process of drawing through numerous dies-rings, Fig. 5.

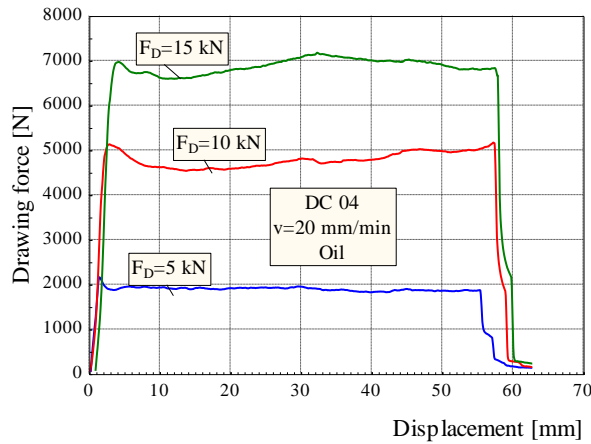


Fig. 4. Change of drawing force for different F_D

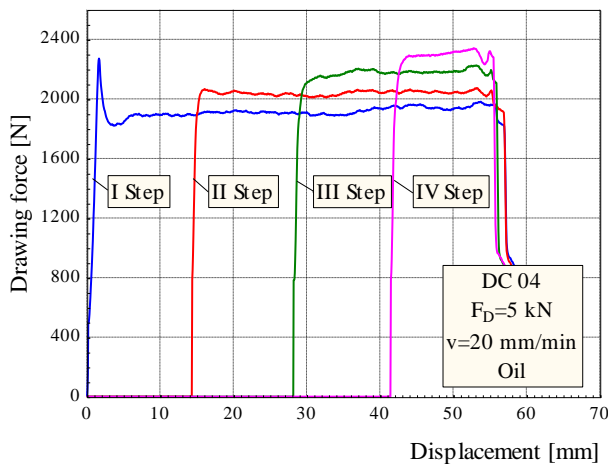


Fig. 5. Change of ironing force at multiphase drawing at $F_D=5\text{ kN}$

Important changes in contact occur in the first and second forming phase, and then the process becomes stationary in the subsequent phases, if friction conditions do not change, Fig. 6.

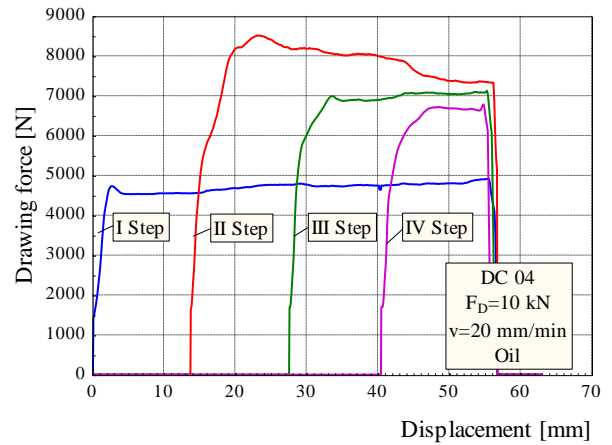


Fig. 6. Change of ironing force at multiphase drawing and $F_D=10\text{ kN}$

By using formula (1), it is possible to determine friction coefficient dependence on experimental conditions, Fig. 7. Due to faster increase of contact surface in dependence on compression force, at bigger F_D forces, smaller pressures are realised and vice versa. By using formula (2), it is possible to determine average contact pressure in sliding zone. Dependence of contact pressure on travel at multiphase sliding is shown in Fig. 8. and Fig. 9.

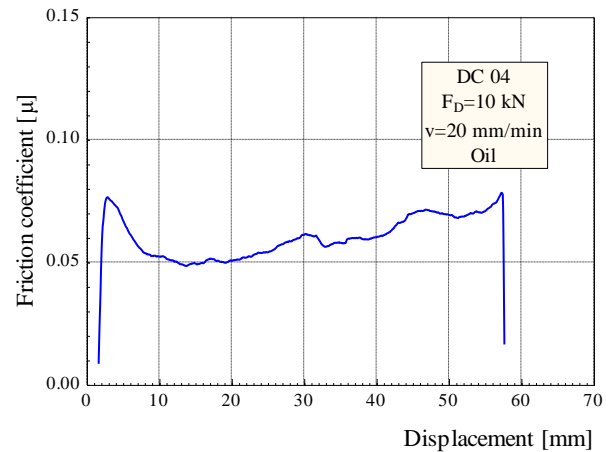


Fig. 7. Change of friction coefficient with sliding path at $F_D=10\text{ kN}$

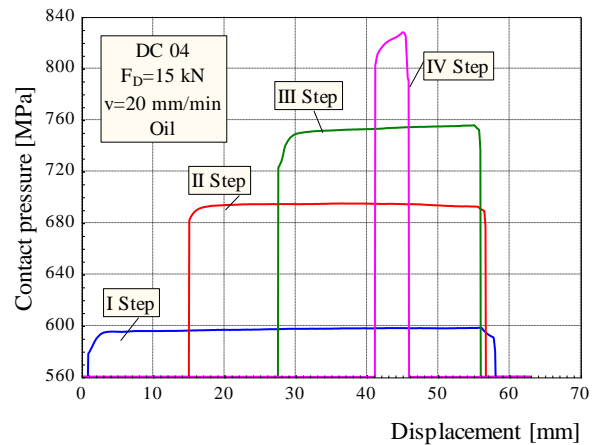


Fig. 8. Change of contact pressure at multiphase drawing and $F_D=15\text{ kN}$

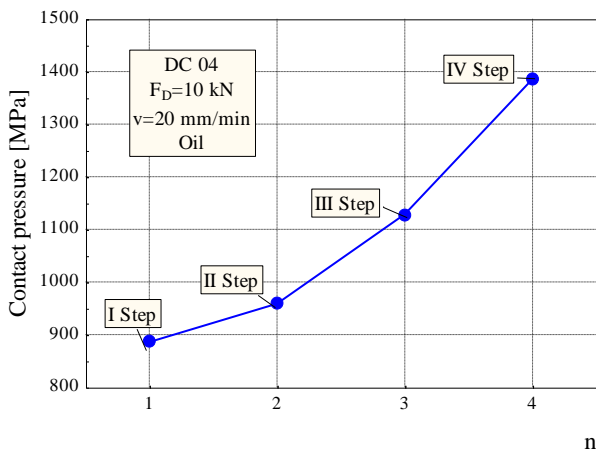


Fig. 9. Change of contact pressure at $F_D=10$ kN and $n=4$ phases of sliding

4. CONCLUSIONS

Cold plastic forming processes are characterized by unity of positive and negative influence of outer friction forces; on some areas of contact of tool and material, friction should be intensified (e.g. on movable die surface in indirect extrusion, on punch surface in ironing, etc.), and in some other zones (in general, on almost all surfaces) friction forces must be reduced by lubrication as much as possible.

At model investigations of ironing, presented in the paper, stationary process with "constant low friction" was realised in conditions of high contact pressure. Friction coefficient values are the lowest at the first drawing and do not depend on sliding length.

At consecutive drawing-sliding, specific pressure in contact increases with the constant holder force, with realisation of boundary friction.

In the course of investigation, a new surface is generated, so the total length of test-specimen is increased.

At sliding lengths that are considerably larger than those in the experiment, the appearance of friction force increase is possible, as well as the appearance of the third or fourth friction type.

REFERENCES

- [1] M. STEFANOVIĆ, D. ADAMOVIĆ (1989) *Characteristics of Constant Low Friction in Testing Sheet Metal by Ironing*, Yutrib 89, Faculty of Mechanical Engineering Kragujevac, Proceed. pp. 177-182.,
- [2] N. BAY, D.D. OLSSON, J.L. ANDREASEN (2008) *Lubricant test methods for sheet metal forming*, Tribology International, Volume 41, Issues 9-10, Pages 844-853
- [3] S.ĐAČIĆ, M. STEFANOVIĆ, S. ALEKSANDROVIĆ, D. ADAMOVIĆ (2008) *Characteristic of Friction in Sheet Metal Sliding with Thickness Reduction*, 12th International Conference on Tribology SERBIATRIB 2011, Kragujevac, Proceed. pp.366-369.
- [4] D. ADAMOVIĆ, M. STEFANOVIĆ, M. ŽIVKOVIĆ, F. ŽIVIĆ (2006), *Investigation of Influence of Tribological Conditions on Friction Coefficient During Multiphase Ironing for Steel and Aluminium Sheet Metal*, *Tribology in industry*, Kragujevac, Vol.28, No 3&4, pp.29-34.
- [5] D. ADAMOVIĆ, M. STEFANOVIĆ, M. PLANČAK, S. ALEKSANDROVIĆ (2008) *Analysis of Change of Total Ironing Force and Friction Force on Punch at Ironing*, *Journal for Technology of Plasticity*, Novi Sad, Vol.33, No1-2, pp.23-38.



34th INTERNATIONAL CONFERENCE ON
PRODUCTION ENGINEERING
28. - 30. September 2011, Niš, Serbia
University of Niš, Faculty of Mechanical Engineering



**EVALUATION OF PHYSICAL AND CHEMICAL CHANGES
IN HYDRAULIC OIL USING ON-LINE SENSORS**

Vito TIČ^{1,2}, Darko LOVREC²

¹Olma d.d., Poljska pot 2, Ljubljana, Slovenia

²University of Maribor, Faculty of Mechanical Engineering, Smetanova 17, Maribor, Slovenia
vito.tic@olma.si, d.lovrec@uni-mb.si

Abstract: *On-line condition monitoring of the entire system or individual components can be used for detection of impending system break-down, at which point, on-line monitoring of the hydraulic fluid plays a decisive role in general on-line condition monitoring.*

Physical and chemical properties of hydraulic oil are changing during its use as a function of many influencing factors, such as increased temperature, friction, wear, water contamination, etc..., which results in accelerated oil oxidation, thermal decomposition of the oil and the increased level of oil contamination (liquid or solid). To determine oil condition, paper presents various physical and chemical changes in hydraulic oil, which can be detected using robust and cost-effective on-line sensors. Understanding the mechanisms of oil ageing and deterioration is crucial, and it is not only necessary for proper interpretation of measured results and taking consequent actions, but it is also important for proper selection of individual sensors or entire condition monitoring system design.

The use of on-line oil condition sensors together with appropriate knowledge of physicochemical changes in oil allows user to have constant overview of the oil quality and its properties. This information can sometimes be crucial to prevent damage and ensure reliable operation of the system.

Key words: *oil ageing, condition monitoring, physical and chemical properties*

1. INTRODUCTION

Latest trends in industrial applications are to increase machine's productivity and reliability and to minimize operating-costs and down-time of the machine. One of the ways to achieve these goals is the use of the predictive maintenance which is based on planned maintenance intervals and condition-based servicing. Due to a widespread availability of robust and cost-effective on-line sensors for measuring various fluid properties, latest developments deal with on-line oil condition monitoring to determine the condition of hydraulic system and fluid. This allows for maintenance work to be carried out based on the detected system condition.

However, measurement of the oil condition is much more complex than measurement of e.g. pressure or temperature. The oil condition cannot be determined with only one single parameter. Several parameters must be observed at the same time. For the best understanding and interpretation of the results we also have to track trends of these parameters.

2. PHYSICAL AND CHEMICAL CHANGES IN HYDRAULIC OIL

The term oil ageing commonly refers to chemical and physical changes in oil properties. Hydrocarbon ageing processes have been intensively studied since the

beginning of the 20th century. During these studies a number of theories have been developed about principle of chemical reactions. Due to the diversity of the base oils, the diversity of additives and the resulting number of components present in the oil, it is impossible to give precise and unique statement of the general mechanisms of oil ageing and ongoing chemical processes – we can only imagine many possible chemical reactions. The great diversity of structures can even be seen in base oils. Additives, even in very low quantities, can have different effects on physicochemical properties of the oil, especially on the ageing process.

Another point, which prevents the prognosis of the individual chemical reaction of oil ageing, is that the chemical reactions depend on the present operating conditions of the machine. The most important influence quantities are temperature and presence of oxygen, water or metal catalysts, which all have a determining influence on the ageing mechanisms. In the past, empirical studies have further explored these influence quantities on hydraulic fluids. Several other parameters also have influence on oil ageing, such as pressure, system volume, shear-rate of long chain molecules, radiation – especially light, etc.

Some of the most important physical and chemical changes in hydraulic oil, which can be detected using robust and cost-effective on-line sensors, are presented below.

2.1. Temperature

Temperature is certainly one of the basic and most important physical quantities, which requires continuous monitoring. Known fact is that the hydraulic fluids age much faster at high operating temperatures because of the accelerated rate of oxidation. It is believed that life expectancy of hydraulic mineral oil is halved for every 10 °C above 60 °C. Moreover, most of the other physical and chemical parameters of hydraulic fluid are highly dependent on the temperature. The temperature also influences viscosity, relative humidity, dielectric constant and electrical conductivity of the hydraulic fluid. Change of each parameter with temperature will be briefly explained below.

2.2. Viscosity

Also, the viscosity is very important physical property of mineral hydraulic oils because it affects the lubrication film and thus the friction and wear. The viscosity value is typically specified in a narrow band for a certain type of oil. However from oil to oil the viscosity might differ. From system and component view certain upper and lower threshold values for the operating viscosity are specified. Changes of the viscosity throughout the operation might result from oil deterioration and contamination with other oils respectively fluids. Thermal oxidation very often leads to an increase of the viscosity, whereas shearstress especially of long chain VI-improver-oils leads to a decrease of viscosity.

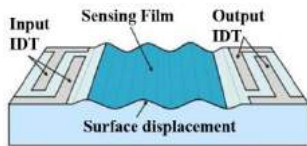


Fig.1. Quartz crystal wave resonator for on-line viscosity measurement

Figure 1 presents the on-line viscosity measurement that can be made by placing the quartz crystal wave resonator in contact with liquid. As the acoustic wave resonator supports a standing wave through its thickness the wave pattern interacts with electrodes on the lower surface (hermetically sealed from the liquid) and interacts with the fluid on the upper surface. Described measurement principle is very sensitive to surface contamination and formation of deposits, which is a common problem of most modern on-line sensors.

Hydraulic oil viscosity varies with pressure and temperature. Since the measurements take place at relatively low and constant pressure, the effect of pressure can be neglected. However, we should not ignore the impact of temperature. With increasing temperature the viscosity is sharply declining. In order to accurately determine the change of viscosity of hydraulic oil through its lifetime is therefore appropriate to take a baseline - the calibration curve, which shows the relationship between temperature and viscosity.

In our test, the viscosity-temperature calibration curve was recorded for hydraulic mineral oil between 10 °C and 90 °C. Acquired data points were mathematically and statistically evaluated.

Figure 2 shows calibration curve obtained experimentally to determine the coefficients a, b and c of Vogel equation:

$$\eta = a \cdot e^{b/(T-c)} \quad (1)$$

where:

a, b, c, d – constants,
 η – dynamic viscosity [Pas],
 T – absolute temperature [K].

The quality of obtained calibration curve (function) is given by the coefficient of determination R^2 .

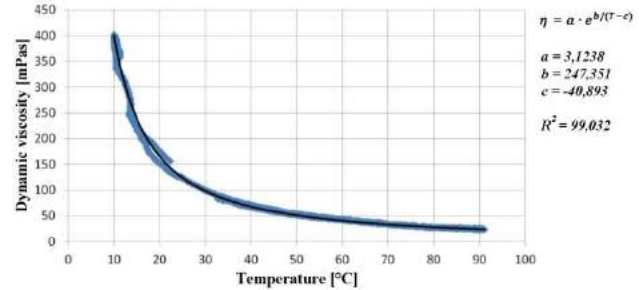


Fig.2. Experimental viscosity-temperature calibration curve

In contrast to conventional laboratory methods, which report oil kinematic viscosity ν at 40 °C in cSt, on-line sensors usually report dynamic viscosity η measured at system temperature (T). To be able to compare both methods, first, we need to normalize measured dynamic viscosity η at system temperature to dynamic viscosity at 40 °C $\eta(40)$. The calculation is done on the basis of experimentally obtained viscosity-temperature calibration curve. After knowing $\eta(40)$ we have two options: we can estimate the increase in dynamic viscosity at 40 °C in percentage, or we can calculate the kinematic viscosity where we assume that the density of the oil is constant. The process is shown below on Figure 3.

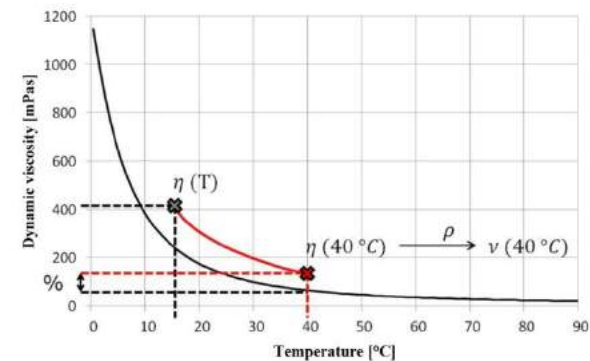


Fig.3. Assessment of viscosity increase

2.3. Relative humidity

Water is in practice one of the greatest threats to the hydraulic and lubricating oil. Lubricant film reduces the load and act as a catalyst in the processes of aging and degradation of oil. Water may be present in dissolved, emulsified or free form.

Relative humidity Φ is defined as the ratio of the absolute humidity e_a and saturation humidity e_n (the highest possible absolute humidity) at a given temperature, expressed as a percentage:

$$\Phi = \frac{e_a}{e_n} \cdot 100\% \quad (2)$$

Changes in relative humidity capacitive sensors detect and show the percentage of saturation of the hydraulic oil. Oil is 100 % saturated if it contains the maximum amount of bound water at a certain temperature and pressure. In addition to a function of temperature and pressure, water solubility also depends on the chemical compatibility of the water and oil. Consequently, the level of saturation can significantly vary depending on the different base oils and various packages of additives [1].

For hydraulic systems is important to know the relative humidity, because it allows us to monitor the point of condensation from the moist when oil starts separating water droplets. This leads to the formation of mild emulsion, and, consequently, accelerated corrosion of components.

2.4. Conductivity

The conductivity of a solution is a measure of its ability to conduct electricity. The electrical conductivity of a solution of an electrolyte is measured by determining the resistance of the solution between two flat or cylindrical electrodes separated by a fixed distance. An alternating voltage is used in order to avoid electrolysis. Typical frequencies used are in the range 1 to 3 kHz. The dependence on the frequency is usually small.

Electrical conductivity of the solution G is inversely proportional to the resistance R : $G = 1/R$. Since the resistance is expressed in ohms Ω , the electrical conductivity is expressed in Ω^{-1} . Electrical conductivity of the sample increases with cross section and decreases with distance:

$$G = \frac{\kappa A}{l} \quad (1)$$

where:

G – electrical conductivity,
 κ – specific electrical conductivity,
 A – cross section area,
 l – length between the electrodes.

Specific fresh oil has its own characteristic conductivity, which is typically lower value. Because conductivity is oil specific it is a criterion for differentiating oils. Also the entry of foreign substances (solid/liquid) can be detected if such entry causes a change in conductivity. Thus oil changes, oil mixtures, and contamination can be detected. In addition conductivity changes due to aging processes so that the course of aging can also be tracked based on conductivity.

2.5. Relative permittivity

The relative permittivity ϵ_r of the fluid is a measure of its polarity. Basic oils and additive packages with different chemistry and from different manufacturers can differ in polarity. Thus polarity of the fluid is a quality factor through which oil changes, oil mixtures and refreshing can be detected.

Moreover, oils change their polarity during the aging process. It is also possible to monitor the trend of aging.

Measurement of relative permittivity ϵ_r is based on a capacitive measurement transformer moistened with oil.

When there are two electrical charges q_1 and q_2 placed in vacuum and are separated with distance r , the potential energy of their interaction equals:

$$V = \frac{q_1 q_2}{4\pi\epsilon_0 r} \quad (3)$$

When these two same charges are placed into media (air, liquid), potential energy of their interaction equals:

$$V = \frac{q_1 q_2}{4\pi\epsilon r} \quad (4)$$

where:

V – potential energy of electrical charges at distance r ,
 q_1, q_2 – electrical charges,
 ϵ – permittivity in media,
 ϵ_0 – permittivity in vacuum,
 r – distance between charges.

Permittivity is usually given as relative static permittivity or dielectric constant, which is dimensionless parameter:

$$\epsilon_r = \frac{\epsilon}{\epsilon_0} \quad (5)$$

where ϵ_r is relative static permittivity or dielectric constant. Dielectric constant of the media is high, if its molecules are polar or highly polarized.

Figure 3 presents temperature dependency of electrical conductivity and dielectric constant for mineral hydraulic oil. Data shown on the figure were obtained experimentally and are further used to normalize temperature dependency of electrical conductivity and dielectric constant.

Like viscosity, the electrical conductivity and dielectric constant are also monitored at 40 °C to neglect the temperature effect on these two parameters. Since they cannot be always measured at 40 °C, they are normalized to 40 °C with post-calculation.

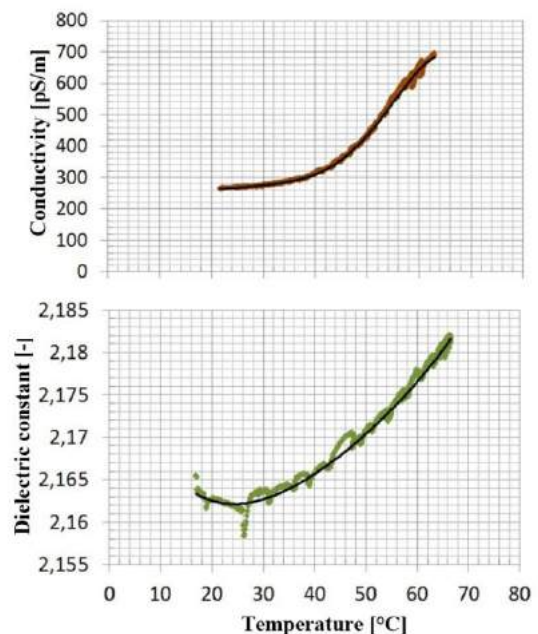


Fig.4. Temperature dependency of electrical conductivity and dielectric constant for mineral hydraulic oil

3. APPLICATION OF ON-LINE CONDITION MONITORING OF HYDRAULIC OIL

The practicality and usefulness of on-line condition monitoring (OCM) methods for hydraulic fluids can be clearly shown on a real industrial application. Figure 5 presents data from OCM of industrial hydraulic system, which is ideal for OCM, since its poor construction design puts high stress on mineral hydraulic oil, which is prone to accelerated oil oxidation and deterioration.

It is very difficult to show the large amount of data in such small picture. That is why only three major parameters are presented:

- temperature (red),
- relative humidity (blue),
- dielectric constant (green).

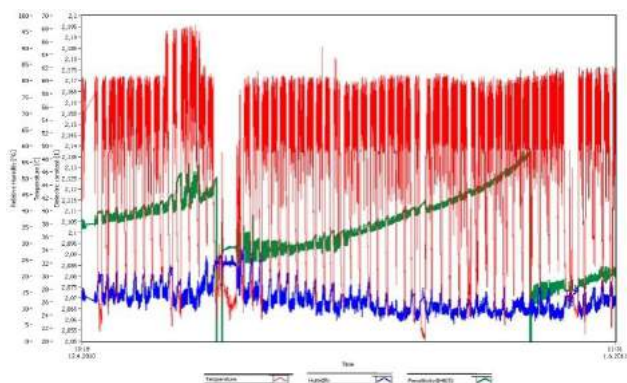


Fig.5. Industrial application of on-line oil condition monitoring system

It can be clearly seen that the dielectric constant (green) is rapidly increasing due to the accelerated oxidation and deterioration of oil and then suddenly drops when the oil replacement has taken place.

It is assumed that dielectric constant is increasing due to the thermal decomposition of oil because there were no other contaminants detected during this time - relative humidity is low and constant. Also, there were no increased oil contamination levels detected (ISO 4406).

Our assumptions were confirmed by parallel chemical laboratory analysis which reported high neutralization number of mineral hydraulic oil and suggested immediate oil change.

4. CONCLUSION

The use of on-line oil condition sensors together with appropriate knowledge of physicochemical changes in oil allows user to have constant overview of the oil quality and its properties. This information can sometimes be crucial to prevent damage and ensure reliable operation of the system.

Long term predictions in the field of condition monitoring certainly include smaller, more sophisticated OCM systems with multiple condition monitoring analysis capabilities, artificial intelligence (expert rules, fuzzy logic, neural network algorithms,...) that will be eventually mass produced.

ACKNOWLEDGEMENT

Operation part financed by the European Union, European Social Fund. Operation implemented in the framework of the Operational Programme for Human Resources Development for the Period 2007-2013, Priority axis 1: Promoting entrepreneurship and adaptability, Main type of activity 1.1.: Experts and researchers for competitive enterprises.



REFERENCES

- [1] STACHOWIAK, G. W., Batchelor, A. W.: Engineering Tribology, 2nd edition, Butterworth-Heinemann, 2001;
- [2] L. R. RUDNICK: Lubricant additives: chemistry and applications, 2nd edition, Taylor & Francis group, 2008;
- [3] ATKINS, P., DE PAULA, J.: Atkins' Physical Chemistry, 8th edition, Oxford University Press, 2006; ISBN 978-0-1987-0072-2
- [4] MEINDORF, T.: New Maintenance Concepts by Continuous Oil Monitoring, Proceedings of OilDoc 2011, Rosenheim, Germany, February 2011
- [5] TIC, V., KAMBIC, M., LOVREC, D.: Uporabnost sistemov za on-line spremljanje stanja hidravličnih olj, Proceedings of SloTrib 2010, Ljubljana, Slovenia, November 2010



USE OF AN ON-LINE CONDITION MONITORING SYSTEM FOR HYDRAULIC MACHINES

Darko LOVREC², Vito TIČ^{1,2},

¹University of Maribor, Faculty of Mechanical Engineering, Smetanova 17, Maribor, Slovenia

²Olma d.d., Poljska pot 2, Ljubljana, Slovenia
d.lovrec@uni-mb.si, vito.tic@olma.si

Abstract: *The increasing investment costs of machines, the demand for longer maintenance intervals and higher system reliability with less downtime and breakdowns, and the desire to shorten the mean-time between failures, ..., is forcing the manufacturers of machines to incorporate condition-monitoring systems within their machine designs. This especially involves machines that operate around-the-clock, under difficult operating conditions and/or away from professional maintenance staff, and is particularly important for machines with built-in hydraulic drive systems, where constant monitoring of equipment status, as well as the hydraulic fluid, is required.*

In comparison with the classical monitoring methods, the paper presents a short-overview of used modern on-line condition monitoring methods suitable for the monitoring of a single hydraulic component, entire hydraulic drive, and for monitoring the used hydraulic fluid as well. In the case of the hydraulic fluid monitoring, special attention is paid to knowledge of the physical and chemical properties of fluids and their changing mechanisms, in particular the fluid-ageing processes.

Key words: hydraulics, oil, fluid ageing, condition monitorings

1. INTRODUCTION

The increasing investment costs of machines, the demand for longer maintenance intervals and higher system reliability with less downtime and breakdowns, and the desire to shorten the mean-time between failures, is forcing the manufacturers of machines to incorporate condition-monitoring systems within their machine designs. This especially involves machines that operate around-the-clock, under difficult operating conditions and/or away from professional maintenance staff, and is particularly important for machines with built-in hydraulic drive systems, where constant monitoring of equipment status, as well as the hydraulic fluid, is required – Figure 1.

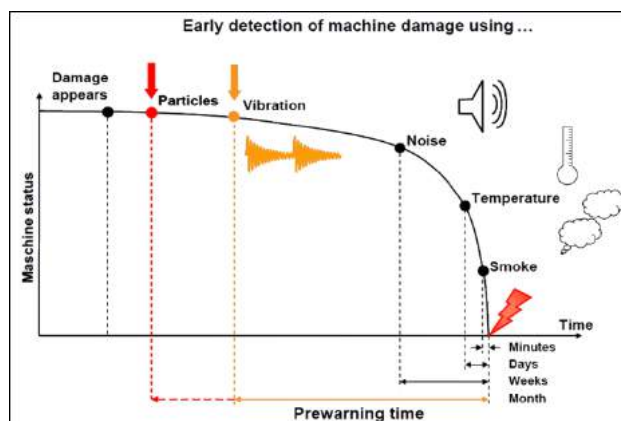


Figure 1 - Pre-warning times for different CM methods [1]

2. MONITORING OF COMPONENTS

Condition monitoring of hydraulic equipment, resp. components, can be arranged in two different groups: into simple measures for component monitoring - simple approach and into measures based on the advanced methods of signal acquisition and conditioning.

2.1. Simple approach for basic components

One of the simplest cases is represented by the continuous monitoring of filter elements within a hydraulic system. It can provide valuable clues to the performance of the filter and the condition of the system.

The warning of filter-bypass is typically afforded by visual or electrical clogging-indicators. These devices indicate when a pressure-drop (Δp) across the element is approaching the opening pressure of the bypass valve (where fitted). In the case of a return-filter, for example, if the bypass valve opens at a Δp of 3 bar, the clogging indicator will typically switch at 2 bar.

This method has been used for a long time and belongs to a signal-based approach. The example is displayed in Figure 2. It shows a typical filter used in all hydraulic systems. As the filter gathers the dirt particles and drains them out of the fluid, they collect in the filter element and over time the pressure-drop across the filter increases. Within this time domain approach, a threshold needs to be set for the pressure-drop across the filter and once it is

exceeded a failure signal can be generated for exchanging the filter element during the next machine maintenance.

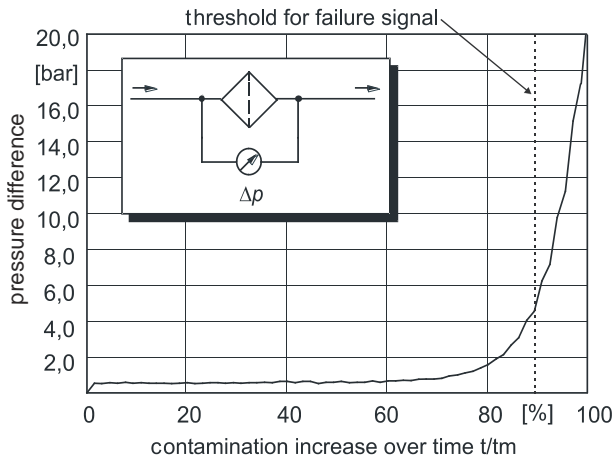


Figure 2: Signal-based condition monitoring

Advanced filter-condition monitoring represents the replacement standard for clogging-indicators using differential pressure gauges or transducers, which enables continuous, condition-monitoring of the filter element. This permits the trending of fluid cleanliness against filter-element pressure-drop, which may be used to optimize oil-sample and filter-change intervals. For example, the optimal change for a return-filter in a particular system could be higher or lower than the clogging indicator switching pressure of 2 bar.

It is well-known fact that the pressure-drop across the filter is also oil-temperature dependent – at low temperatures the oil viscosity increases and, consequently, the pressure-drop. This can lead to a false signal and a missed warning. In order to avoid this, the use of an additional temperature sensor is reasonable.

Continuous monitoring of filter-pressure drop can also provide early warnings of component failures and element ruptures. For example, if the Δp across a pressure filter suddenly increases from 1 to 3 bar (all other things equal), this could be an indication of a component's upstream imminent failure. Similarly, a sudden decrease in Δp could indicate a rupture within the element – something that a standard clogging-indicator will not warn of.

In both these mentioned cases, filter monitoring with additional sensors and the implementation of simple logic, become more complex.

2.2. Advanced approach for complex systems

A more complex approach for condition-monitoring should be used in the cases of more-complex systems, for example hydraulic linear-drive. One possibility is represented by model-based condition diagnosis.

A model of the considered physical system should be built in order to achieve failure detection using this method. When using a detailed-model of the system, we are able to track any-back changes in the system's performance, down to a single parameter that can be directly interpreted by its physics. As an example, the structure of an electro-hydraulic linear-drive in the form of series-connected block models, which can be diagnosed individually or combined with the use of a

model-based failure monitoring system, is shown in Figure 3 (for more details see [3] and [4]).

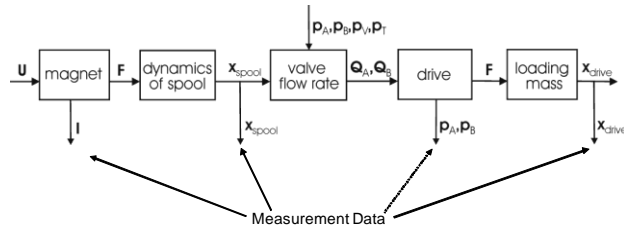


Figure 3: Model-based approach of a hydraulic linear-drive [3]

The condition of a magnetic actuator and the spool dynamics of a digitally-controlled valve can be monitored using available signals such as voltage, current, and a displacement of the valve spool.

We can therefore use different possibilities for the failure diagnostics on a proportional solenoid. When using e.g. a model with distributed parameters [5], we can reconstruct the armature or spool position by the use of current and voltage signals using signal calculation. Due to the high computing power necessary, this needs to be calculated offline, at intervals of about five seconds.

An advantageous structure for the use of these diagnostic functions, is shown in Figure 4. The measuring data needed for the control are made available on the used microcontroller. Decentralized diagnostic functions have access to the internal signals and are capable of exchanging additional information via field bus used [4].

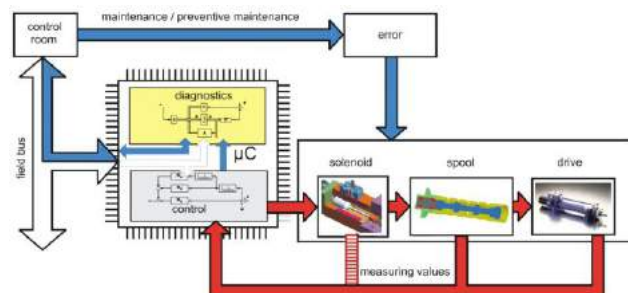


Figure 4: Integration of control and condition-monitoring functions [4]

External inquiries about a component's condition are possible, whilst alternatively recognized safety risks can be signalled by the component itself. Depending on the used sensors and the component's size, different parts of the electro-hydraulic drive can be modelled and used for calculation of leakages or friction at the cylinder, as well as wear around the valve metering edges.

3. CONDITION MONITORING OF FLUID

Whilst temperature, flow, pressure, displacement, and vibration sensors all have their part to play within the condition-monitoring of a simple component or complex drive, for early detection of changes in fluid and lubricant condition, other methods and sensor types should be used (see e.g. [6], [7], [8]).

Hydraulic-fluid contains a lot of information about itself and also about the lubricated machine parts and the contamination level. Quite a few years ago, oil analysis in laboratories established itself as the best-practice for verifying whether hydraulic systems are in good working-

order. Laboratory analysis became a common feature of such systems, initially as robust field measurement devices in temporarily-installed measurement devices, and later in permanently-installed sensors for continuous oil-monitoring.

Over the years, different methods of hydraulic fluid condition-monitoring have been used: from a simple temperature or fluid colour-monitoring, to viscosity, moisture and particles contamination level measurement, through to more complex methods, e.g. measurement of qualitative and quantitative changes of oil-gas phase-composition during oil ageing [9].

Before looking for suitable sensors for the detection of changes within the fluid, any influences on the fluid deterioration process must be known - Figure 5 [2], [3].

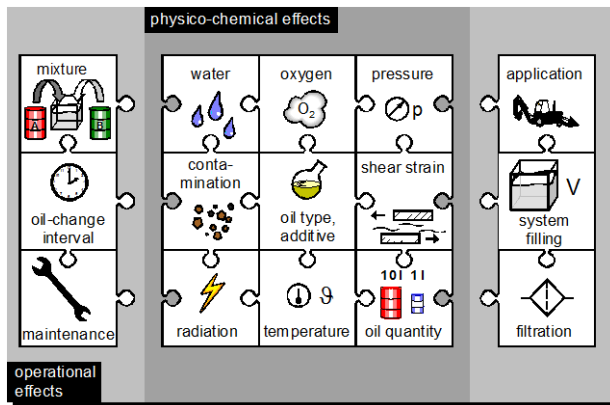


Figure 5: Influences on the oil-deterioration process [2]

In contrast to discrete oil analysis by external laboratory or on-site methods, on-line condition monitoring (OCM) of the fluid allows continuous monitoring and condition-based machine maintenance, which can also detect unexpected machine failures. Such failures could be contamination of the oil by water, mixing with other fluids, usage of the wrong oil, etc.

Today, a variety of on-line sensors are available, which are important parts of laboratory analysis due to their sufficient precision. On-line sensors provide trend-analysis, and the laboratory procedure provides the detailed-information required to analyze the trend. Service and maintenance measures are implemented based on the measurement results.

The most important physical and chemical changes in hydraulic oil can be detected using robust and cost-effective on-line sensors, working on different principles as shown in Figure 6.

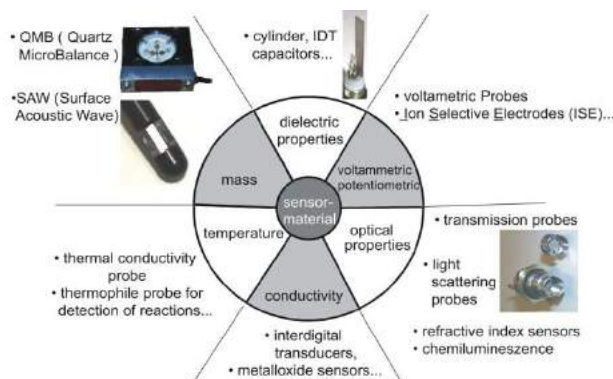


Figure 6: Sensor principles [2]

In order to have the all the more important information about fluid-condition for on-line condition-monitoring built into a machine, the following physic-chemical values should at least be measured:

- *Temperature* as one of the basic and most important physical quantities, which requires continuous monitoring.
- *Fluid cleanliness level*, or changing wear-rate, or wear patterns with on-line particle sensors (particle counters) or wear sensors helping you to make informed maintenance planning decision.
- *Viscosity* as a very important physical property of mineral hydraulic oils, which affects the lubrication-film and thus the friction and wear.
- *Relative humidity* - water is in practice one of the greatest threats to hydraulic and lubricating oils.
- *Relative permittivity* as a measure of fluid-polarity, which depends of the basic oil-type and additive packages. Polarity of the fluid is a quality factor through which oil-changes, oil-mixtures and refreshing can be detected.

Whilst temperature sensors play a basic role within a condition-monitoring sensor package, early detection of changes in oil and lubricant conditions, consistent monitoring of worn-metal debris, and insight into the actual conditions of vital machinery and equipment, need other sensor types. Many manufacturers have developed a range of innovative and practical on-line sensors for oil-condition detection and monitoring.

Figure 7 shows some of the sensor on the market appropriate for OCM installed into an industrial fix mounted or portable OCM device.

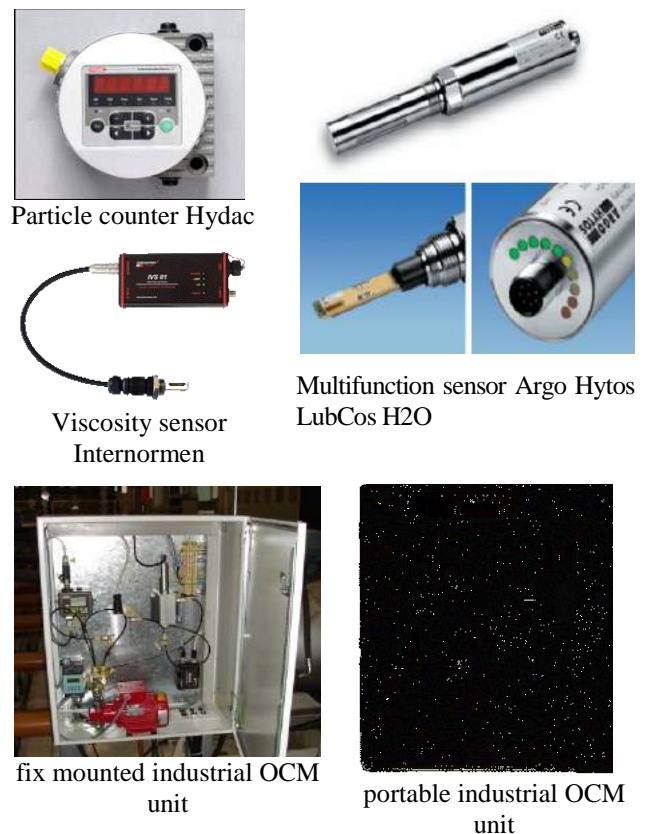


Figure 7: Different OCM sensors and units

The basis of latest research project is the development of a conventional on-line oil condition-monitoring (OCM) system. This system is based on several on-line sensors – see Figure 7, connected to a local data acquisition system. Data collected from several monitored systems, are sent to the central-database and processing system, which was developed using LabView. Figure 8 shows the user-interface panel of developed OCM system, together with real measurements results from industrial application of OCM.

Although the oil-condition data can be accessed at any time from anywhere, and although the measured parameters show some satisfactory trends regarding oil degradation over time, the application itself is universal, robust, user-friendly and a system that can be used by untrained personnel.

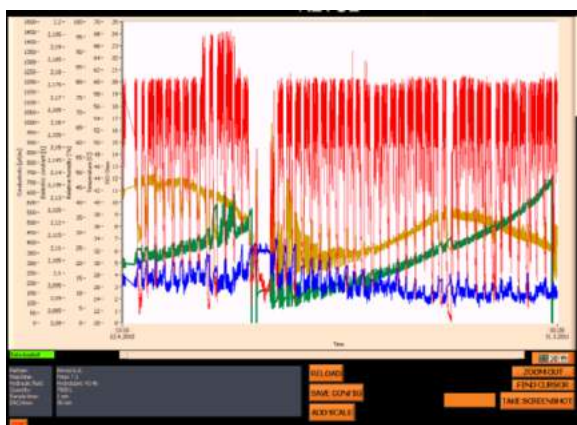


Figure 8: Industrial application of developed on-line oil condition-monitoring system

Even though only a few parameters are shown in Figure 8, we can clearly see, that it is difficult to read and evaluate oil (and machine) condition from displayed charts.

These factors highlight the main weakness of conventional OCM systems:

- alarms can be triggered only within exact predefined limits,
- an expert is needed to extract full information from the measurements,
- there is no plain information on the hydraulic system's status, and the necessary actions to be taken.

In contrast to conventional OCM, a modern OCM system incorporates an automatic diagnosis-system or so-called expert system. Such an automatic diagnosis system allows for a more-detailed look at the measurements, looking for specific damage pattern, and considering operational conditions.

Ultimately, the maintenance manager is disinterested in diagrams or frequency plots. What is required here is a clear report on the hydraulic system's status combined with recommendation for action.

In addition, OCM also enables a better documentation of oil-changes, machine maintenance, and helps to minimize the total cost of ownership by extending maintenance periods and reducing the downtime of the machine.

4. CONCLUSION

This paper focused on benefits and importance of using condition-monitoring systems within modern production machines. By explaining two different approaches in the field of hydraulic-drives it provides a short insight into the use of different possibilities for on-line condition-monitoring methods. Special sensors are required and different sensor principles are discussed, for the monitoring of the fluid.

Real-time monitoring of the root cause of a single component, whole machine or lubricant failure, will allow you to take immediate action at the first indication of change. The use of appropriate on-line sensors and monitoring methods [10] definitely helps you to increase productivity, reduce costs, and improve profitability.

REFERENCES

- [1] KUHL, A.: Condition Monitoring – many options, one goal, Proceedings of OilDoc 2011, Rosenheim, Germany, February 2011
- [2] MURRENHOF, H.: Condition – Monitoring of Hydraulic Drives and its Fluids, Proceedings Fluidna tehnika/Fluid Power 2005, p.p. 141 – 161, Maribor
- [3] MURRENHOF, H., MEINDORF, TH., STAMMEN C.: Condition Monitoring in Fluid Power Technology. Proceedings of 4th International Fluid Power Conference, Vol. 2, Dresden, 2004, pp. 219-244
- [4] STAMEN, C.: Condition Monitoring für intelligente hydraulische Linearantriebe, Dissertation, RWTH Aachen, 2005
- [5] MOSELER, O.: Modellgestuetzte Fehlererkennung an elektromagnetischen Proportionalventilen mit Mikrocontrollern, Oelhydraulik und Pneumatik 44 (2000), Nr.7, p.p. 640 - 648
- [6] MEINDORF, T.: New Maintenance Concepts by Continuous Oil Monitoring, Proceedings of OilDoc 2011, Rosenheim, Germany, February 2011
- [7] TIC, V., KAMBIC, M., LOVREC, D.: Uporabnost sistemov za on-line spremljanje stanja hidravličnih olj, Proceedings of SloTrib 2010, Ljubljana, Slovenia, November 2010
- [8] KRALMANN, J., MANNEBACH H.: Ein Multisensor zur Überwachung von Hydraulikölen. Tagung Landtechnik 2004, Dresden, VDI-Verlag, Düsseldorf, S. 107-113, ISBN 3-18-091855-1
- [9] SEYFERT, C.: Take a smell at your Oil – A New Approach towards on-line Oil Condition Monitoring, Proceedings of 4th International Fluid Power Conference, Vol. 2, Dresden, 2004, pp. 321-330
- [10] TIC, V., LOVREC, D.: Implementation of artificial intelligence within Oil-condition-Monitoring Systems, MOTSP, Rovinj, Croatia, 7-10 June 2011



STUDY ON SURFACE ROUGHNESS MINIMIZATION IN TURNING OF POLYAMIDE PA-6 USING TAGUCHI METHOD

Dragoljub LAZAREVIĆ, Miloš MADIĆ, Predrag JANKOVIĆ, Andela LAZAREVIĆ

Faculty of Mechanical Engineering of Niš, University of Niš, A. Medvedeva 14, Niš, Serbia
dlazarevic@masfak.ni.ac.rs, madic@masfak.ni.ac.rs, jape@masfak.ni.ac.rs, andjelalazarevic@gmail.com

Abstract: In any machining process, it is most important to determine the optimal settings of machining parameters aiming at reduction of production costs and achieving the desired product quality. This paper discusses the use of Taguchi method for minimizing the surface roughness in turning polyamide PA-6. The influence of four cutting parameters, cutting speed, feed rate, depth of cut, and tool nose radius and their interaction on average surface roughness (R_a) was analyzed on the basis of the standard L_{27} Taguchi orthogonal array. The experimental results were then collected and analyzed with the help of the commercial software package MINITAB. Based on the the analysis of means (ANOM) and analysis of variance (ANOVA), the optimal cutting parameter settings are determined, as well as level of importance of the cutting parameters.

Key words: Polyamide PA-6, surface roughness, optimization, Taguchi method, turning

1. INTRODUCTION

Polyamides are thermoplastic polymer composites extensively used in a variety of applications in different fields of engineering, such as aircraft, automobile, robots and machines, due to an excellent property profile, and hence replaced many traditional metallic materials [1]. Even though the polyamides are produced as near net shapes, the machining has to be performed during the final stage of production to get the finished products [2]. However, there are a limited number of papers about machining of polyamides in the literature.

Gaitonde et al. [1] applied Taguchi's quality loss function approach for simultaneously minimizing the power and specific cutting force during turning of both PA6 and PA66 GF30 polyamides. Taguchi's optimization was performed with tool material, feed rate and cutting speed as the process parameters. Gaitonde et al. [2] developed RSM based second-order mathematical models for analyzing the influence of cutting speed and feed rate on machining force, cutting power, and specific cutting pressure during turning of unreinforced polyamide (PA6), and reinforced polyamide with 30% of glass fibers (PA66 GF30). Eriksen [3] examined the influence of cutting parameters (feed rate, cutting speed and tool nose radius) and the fibre orientation on the surface roughness in turning of short fiber reinforced thermoplastic. The results showed that the roughness of the machined surfaces was highly influenced by the feed rate and tool nose radius, whereas the influence of cutting speed was negligible. Marin [4] analyzed the effects of cutting speed, feed rate, and depth of cut on main cutting force in turning of PA 66 polyamide.

In this paper, Taguchi method [5] was applied to optimize cutting parameters in turning of polyamide PA-6 for achieving better surface finish.

2. TAGUCHI METHOD

The Taguchi technique is a methodology for finding the optimum setting of the control factors to make the product or process insensitive to the noise factors [5]. Taguchi's techniques have been used widely in engineering design, and can be applied to many aspects such as optimization, experimental design, sensitivity analysis, parameter estimation, model prediction, etc. The distinct idea of Taguchi's robust design that differs from the conventional experimental design is that of designing for the simultaneous modeling of both mean and variability [5]. Taguchi based optimization technique has produced a unique and powerful optimization discipline that differs from traditional practices. While, traditional experimental design methods are sometimes too complex and time consuming, Taguchi methodology is a relatively simple method.

Taguchi method uses a special highly fractionated factorial designs and other types of fractional designs obtained from orthogonal arrays (OAs) to study the entire experimental region of interest for experimenter with a small number of experiments. This reduces the time and costs of experiments, and additionally allows for an optimization of the process to be performed. The columns of an OA represent the experimental parameters to be optimized and the rows represent the individual trials (combinations of levels).

Traditionally, data from experiments is used to analyze the mean response. However, in Taguchi method the mean and the variance of the response (experimental result) at each setting of parameters in OA are combined into a single performance measure known as the signal-to-noise (S/N) ratio. Depending on the criterion for the quality characteristic to be optimized, different S/N ratios can be chosen: smaller-the-better, larger-the-better, and

nominal-the-better. For example, the S/N ratio for smaller-the-better criterion is employed when the aim is to make the response as small as possible. This category of the S/N ratio is defined as:

$$\eta_i = S / N = -10 \log \left(\frac{1}{n} \sum_{j=1}^n y_{ij}^2 \right) \quad (6)$$

where η_i is S/N ratio in the i-th trial, y_{ij} is the j-th observed value of the response (quality characteristic) in i-th trial, n is the number of individual observations in i-th trial, due to noise factors or repetition of trial. Regardless of the category of the quality characteristic, a higher algebraic value of S/N ratio corresponds to better quality characteristic, i.e. to the smaller variance of the output characteristic around the desired (target) value. A full explanation of the method can be found in many references including [5, 6].

3. EXPERIMENTAL PROCEDURE

3.1. Material and machining conditions

The material used for cutting was unreinforced polyamide PA-6 (commercially DOCAMID 6E) produced by Quattroplast Ltd. (Hungary). The mechanical properties of the work material are: density = 1.14 g/cm³, tensile strength = 80 N/mm², module of elasticity = 3200 N/mm², Charpy impact resistance > 3 KJ/m². The test specimen were in the form of bar, 92mm in diameter and 50mm in length (Figure 1).

The machine used for the experiments was the universal lathe machine “Potisje PA-C30” with a 11 kW power, speed range $n = 20 \div 2000$ rpm, and longitudinal feed rate range $f = 0.04 \div 9.16$ mm/rev. Cutting tool was SANDVIK Coromant tool holder SVJBR 3225P 16 with inserts VCGX 16 04 04-AL (H10) and VCGX 16 04 08-AL (H10). The tool geometry was: rake angle $\gamma = 7^\circ$, clearance angle $\alpha = 7^\circ$, cutting edge angle $\chi = 93^\circ$, and cutting edge inclination angle $\lambda = 0^\circ$.

In the study, the average surface roughness (R_a) was considered. It was measured at three equally spaced positions around the circumference of the workpiece using the profilometer SurfTest Mitutoyo SJ-301.



Fig.1. Experimental setup

Table 1. Experiment plan, results and S/N ratios for the average surface roughness

Trial no	Designation	Cutting speed V_c , (mm)	Feed rate f , (mm/rev)	Depth of cut a_p , (mm)	Tool nose radius r , (mm)	R_a (μm)		η (dB)
1	A ₁ B ₁ C ₁ D ₁	65.03	0.049	1	0.4	1	1.07	0.0000
2	A ₁ B ₁ C ₂ D ₂	65.03	0.049	2	0.8	0.95	0.86	0.8563
3	A ₁ B ₁ C ₃ D ₁	65.03	0.049	4	0.4	1.31	1.42	-1.3292
4	A ₁ B ₂ C ₁ D ₁	65.03	0.098	1	0.4	1.39	1.51	-3.2348
5	A ₁ B ₂ C ₂ D ₁	65.03	0.098	2	0.4	2.05	1.4	-4.8873
6	A ₁ B ₂ C ₃ D ₂	65.03	0.098	4	0.8	2.09	1.67	-5.5370
7	A ₁ B ₃ C ₁ D ₂	65.03	0.196	1	0.8	3.78	3.56	-11.2972
8	A ₁ B ₃ C ₂ D ₁	65.03	0.196	2	0.4	3.46	3.34	-10.6309
9	A ₁ B ₃ C ₃ D ₁	65.03	0.196	4	0.4	3.61	3.51	-11.0299
10	A ₂ B ₁ C ₁ D ₂	115.61	0.049	1	0.8	1.04	1.4	-1.8207
11	A ₂ B ₁ C ₂ D ₁	115.61	0.049	2	0.4	1.04	1.01	-0.2154
12	A ₂ B ₁ C ₃ D ₁	115.61	0.049	4	0.4	1.22	1.12	-1.3716
13	A ₂ B ₂ C ₁ D ₁	115.61	0.098	1	0.4	1.43	1.29	-2.6823
14	A ₂ B ₂ C ₂ D ₂	115.61	0.098	2	0.8	1.25	1.44	-2.5961
15	A ₂ B ₂ C ₃ D ₁	115.61	0.098	4	0.4	1.78	1.63	-4.6429
16	A ₂ B ₃ C ₁ D ₁	115.61	0.196	1	0.4	3.41	3.23	-10.4260
17	A ₂ B ₃ C ₂ D ₁	115.61	0.196	2	0.4	3.41	3.39	-10.6296
18	A ₂ B ₃ C ₃ D ₂	115.61	0.196	4	0.8	6.03	5.74	-15.3976
19	A ₃ B ₁ C ₁ D ₁	213.88	0.049	1	0.4	0.85	0.69	2.2236
20	A ₃ B ₁ C ₂ D ₁	213.88	0.049	2	0.4	1.04	1.16	-0.8408
21	A ₃ B ₁ C ₃ D ₂	213.88	0.049	4	0.8	1.45	1.36	-2.9580
22	A ₃ B ₂ C ₁ D ₂	213.88	0.098	1	0.8	1.37	1.59	-3.4292
23	A ₃ B ₂ C ₂ D ₁	213.88	0.098	2	0.4	1.24	1.45	-2.6008
24	A ₃ B ₂ C ₃ D ₁	213.88	0.098	4	0.4	1.7	1.54	-4.2009
25	A ₃ B ₃ C ₁ D ₁	213.88	0.196	1	0.4	3.33	3.1	-10.1492
26	A ₃ B ₃ C ₂ D ₂	213.88	0.196	2	0.8	5.53	4.94	-14.3921
27	A ₃ B ₃ C ₃ D ₁	213.88	0.196	4	0.4	3.61	3.45	-10.9577

3.2. Experimental plan

In the present study, four cutting parameters, namely, cutting speed (V_c), feed rate (f), depth of cut (a_p), and tool nose radius (r) were considered. The cutting parameter ranges were selected based on machining guidelines provided by workpiece and tool manufacturer's recommendations and previous researches [2, 3].

Three levels for cutting speed, feed rate and depth of cut and two levels for tool nose radius were considered (Table 2). The cutting parameters were arranged in standard Taguchi's $L_{27}(3^{13})$ OA. Cutting parameters V_c , f and a_p were assigned to columns 1, 2 and 5, respectively. Cutting parameter r was assigned to column 12. As tool nose radius had only two levels, the dummy-level technique [4] was used to reassign level 1 to level 3. The plan of experimental layout to obtain average surface roughness (R_a) is shown in Table 1. Following the Taguchi's $L_{27}(3^{13})$ OA, 54 experiment trials were performed at random order to avoid systematic errors.

Table 2. Cutting parameters and their levels used in experiment

Cutting parameter	Level		
	1 (low)	2 (medium)	3 (high)
A – V_c (m/min)	65.03	115.61	213.88
B – f (mm/rev)	0.049	0.098	0.196
C – a_p (mm)	1	2	4
D – r (mm)	0.4	0.8	-

Since the objective of experiment is to optimize the cutting parameters to get better (i.e. low value) of average surface roughness S/N ratio the average S/N ratios for smaller the better for average surface roughness were calculated using the Eq. 1. The S/N ratios are given in Table 1.

4. ANALYSIS AND DISCUSSION

The experimental results were analyzed with analysis of means (ANOM) and analysis of variance (ANOVA). The analyses have been obtained by using the statistical software MINITAB. The calculations of ANOM and ANOVA are described in detail by Phadke [5].

4.1. Analysis of means

ANOM is the process of estimating the factor effects. Based on the ANOM, one can derive the optimum combination of the cutting parameters, with respect to average surface roughness (R_a). The optimum level for a factor is the level that gives the highest value of S/N ratio in the experimental region [5].

The results of ANOM are presented in Figure 2. From the Figure 2, one can observe that the optimal ANN combination of cutting parameter levels is $A_1B_1C_1D_1$. In other words, optimal value of each cutting parameter is (A) cutting speed, 65.03 m/min, (B) feed rate, 0.049 mm/rev, (C) depth of cut, 1 mm, and (D) tool nose radius, 0.4 mm.

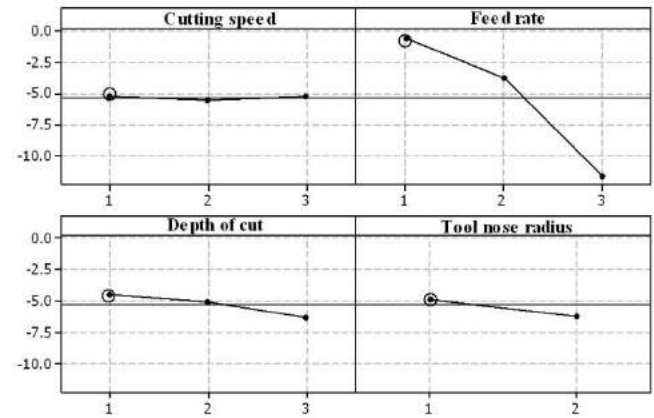


Fig.2. ANOM diagram

4.2. Analysis of variance

The purpose of the analysis of variance is to investigate which cutting parameters significantly affect the surface quality characteristics. ANOVA was performed using the S/N ratios as the response (Table 2). ANOVA is accomplished by separating the total variability of the S/N ratios, which is measured by the sum of the squared deviations from the average of the S/N ratio, into contributions by each of the cutting parameters and the error.

In ANOVA, the ratio between the variance of the cutting parameter and the error variance is called Fisher's ratio (F). It is used to determine whether the parameter has a significant effect on the quality characteristic by comparing the F test value of the parameter with the standard F table value ($F_{0.05}$) at the 5% significance level. If the F test value is greater than $F_{0.05}$, the cutting parameter is considered significant. Table 3 shows the results of ANOVA for average surface roughness.

Table 3. Analysis of variance (ANOVA) for S/N ratios

Source	Degrees of freedom	Sum of squares	Mean square	F
Cutting speed	2	0.497	0.249	0.17
Feed rate	2	583.343	291.671	196.41
Depth of cut	2	16.076	8.038	5.41
Tool nose radius	1	12.077	12.077	8.13
Error	19	28.215	1.485	
Total	26	640.208		

From the ANOVA results, it can be seen that cutting parameters, namely feed rate, depth of cut and tool nose radius are statistically significant for affecting average surface roughness (R_a). The change of the cutting speed in the range given in Table 1 has an insignificant effect on the R_a .

Figure 3 shows the percentage contribution of each cutting parameter to the total variation, indicating their degree of influence on the R_a . Feed rate is the most influential parameter followed by depth of cut and tool

nose radius, whereas the influence of cutting speed is negligible.

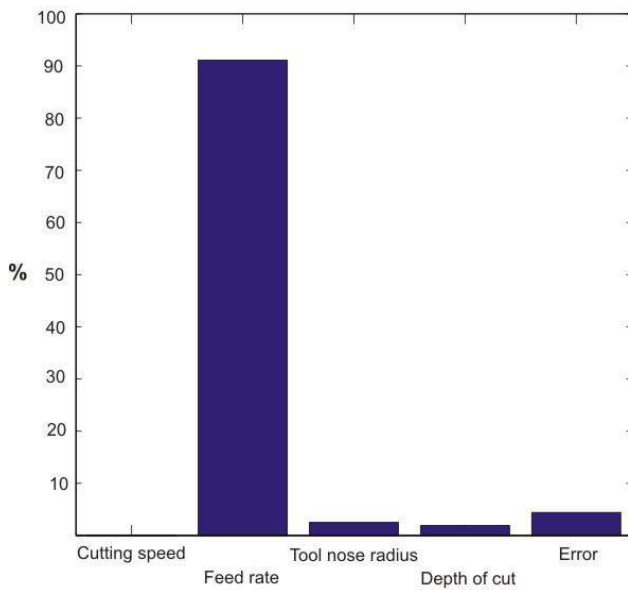


Fig.3. Cutting parameters percentage contribution

It can be seen from Figure 3 that changing the cutting parameters (feed rate, depth of cut, and tool nose radius) between the chosen parameter levels (Table 1) contributes to 95.59 % of the total variation in the R_a . Furthermore, the small percent contribution of error confirms the absence of significant factor interactions.

4.3. Verification

Confirmation testing is necessary and important step in the Taguchi method. Once the optimal combination of cutting parameters is selected, the final step is to predict and verify the expected response through the confirmation test. There is no need to run the confirmation test if the optimal parameter combination is already included in the OA, as in this case. The optimal combination of cutting parameters ($A_1B_1C_1D_1$) corresponds to 1-st trial in Table 1.

Taguchi prediction of S/N ratio under optimum conditions is $\eta_{est} = 0.779205$ dB which is higher than obtained in experiment (Table 1).

In order to judge the closeness of the η_{est} and observed value of S/N ratio, the confidence interval (CI) is determined. The CI is given by [6]:

$$CI = \sqrt{\frac{F_{\alpha(1, f_e)} \cdot V_e}{n}} \quad (7)$$

where $F_{\alpha(1, f_e)}$ is the F value from statistic table at a confidence level of $(1-\alpha)$ at degrees of freedom (DoF) = 1, and error DoF = 19, V_e is the error variance, and n is defined as:

$$n = \frac{N}{1 + v} \quad (8)$$

where N is the total number of experiments and v is the total DoF of all parameters. At the 95% confidence level, the CI is ± 1.388 . Since the prediction error is within CI

value the optimal combination of cutting parameter levels can be validated.

5. CONCLUSIONS

This article has described the application of Taguchi method for optimization of cutting parameter settings for minimizing the average surface roughness in turning of polyamide PA-6. Four cutting parameters, cutting speed, feed rate, depth of cut, and tool nose radius were considered and arranged in the L_{27} OA. From the ANOM and ANOVA results the following conclusions can be drawn:

- combination of low levels of cutting parameters is beneficial for minimizing average surface roughness,
- ANOVA results indicate that the feed rate is far the most significant parameter, followed by tool nose radius, and depth of cut, whereas the influence of cutting speed is negligible. The ANOVA resulted in less than 5% error indicating that the interaction effect of process parameters is negligible.
- Since the cutting speed is not important it could be set at the highest level to obtain higher material removal rate.

The Taguchi method is relatively simple yet a powerful optimization approach that could be efficiently applied for machining optimization problems.

ACKNOWLEDGMENTS

This paper is part of project TR35034 and III41017, funded by the Ministry of Education and Science of the Republic of Serbia.

REFERENCES

- [1] GAITONDE, V.N., KARNIK, S.R., MATA, F., PAULO DAVIM, J. (2008) *Taguchi approach for achieving better machinability in unreinforced and reinforced polyamides*, Journal of Reinforced Plastics and Composites, Vol.27, No 9, pp. 909-924
- [2] GAITONDE, V.N., KARNIK, S.R. MATA, F., PAULO DAVIM, J. (2009) *Study on some aspects of machinability in unreinforced and reinforced polyamides*, Journal of Composite Materials, Vol.43, No 7, pp. 725-739
- [3] ERIKSEN, E. (1999) *Influence from production parameters on the surface roughness of a machined short fibre reinforced thermoplastic*, International Journal of Machine Tools and Manufacture, Vol.39, No 10, pp. 1611-1618
- [4] MARIN, M. (2010) *Studies on the main cutting force in turning polyamide PA 66*, Annals of the Oradea University, Fascicle of Management and Technological Engineering, Vol.IX, No 2, pp 3.162-3.166
- [5] PHADKE, M.S. (1989) *Quality Engineering using Robust Design*, AT&T Bells Laboratory/Prentice-Hall, New Jersey, USA
- [6] ROSS, P. (1988) *Taguchi Techniques for Quality Engineering*, McGraw Hill, New York, USA



WEAR BEHAVIOUR OF HARD Cr COATINGS FOR COLD FORMING TOOLS UNDER DRY SLIDING CONDITIONS

Slobodan MITROVIĆ, Miroslav BABIĆ, Dragan ADAMOVIĆ, Fatima ŽIVIĆ, Dragan DŽUNIĆ, Marko PANTIĆ

Faculty of Mechanical Engineering, Sestre Janjic 6, Kragujevac, Serbia

boban@kg.ac.rs, babic@kg.ac.rs, adam@kg.ac.rs, zivic@kg.ac.rs, dzuna@kg.ac.rs, pantic@kg.ac.rs

Abstract: Cr hard coatings are largely used in industry in metal cutting and cold forming processes; This work on quantitative way represents improvement, in terms of wear resistance, which is obtained by depositing Cr hard coating on foundation material. Wear testing is done on tribometer with block – on – disc contact geometry at sliding contact of Cr hard coated sample with steel disc. Testing was performed in conditions without lubrication at variable value of contact parameters (normal load, sliding speed). Cr hard coatings in all contact conditions show smaller values of wear rate.

Key words: Cr hard coating, Dry sliding, Wear

1. INTRODUCTION

Chrome is metal with huge industrial use and it is used as both protective and decorative coating. When it comes to decorative role, chrome is applied on smooth surfaces (usually nickel) to create a thin and bright layer; the thickness of this layer is about 0.25–0.50 μm . Chromium plating systems are very versatile, allowing to use a variety of substrates (like steel, zinc, copper, aluminum and plastic), and they provide bright and long-lasting appearance to the chromated components, so that they have great use in auto-industry [1,2].

Industrial technologies are advancing and certain mechanical components require the combination of dimension invariability, good technical characteristics, moderate wearing and good corrosion resistance. The solution is in applying thin hard coating, in order to protect the base material with appropriate mechanical characteristics and adequate wear resistance. Hard chromium has a greater thickness than bright chromium and has a large variability, going up to 100 μm . Thanks to the good corrosion and wear resistances, with an excellent compromise in high hardness and fracture toughness, hard chromium is a material adopted in many industrial fields [3–6].

One of the main purposes for which this coating is chosen, is the production of very hard surfaces, resistant to pressure, impacts and wear; many types of tools can be made. as gauges, mechanical components, rolls of many kinds [7]

Hard chromium plating is very widespread technique of improving the resistance of components to wear and corrosion, and it is used in many situations where resistance to abrasive wearing is of vital importance. Hard chromium can be electrodeposited to a considerable thickness with relatively simple equipment. Nevertheless, a great drawback of the electroplating process is the presence of hexavalent chromium (Cr^{6+}) in the electrolyte,

which is environmentally harmful. In order to solve this problem, electrolytes containing Cr^{6+} are now substituted by Cr^{3+} . [8].

The aim of this study was to quantify the influence of hard chromium coatings to extend the service life of tools in metal forming applications. The tests were conducted in dry sliding conditions and at different values of contact load and speed skating. Results of testing samples at different values of contact load and sliding speed are presented in the form of graphs and histograms in order to highlight the benefits of hard Cr coating compared to uncoated material.

2. EXPERIMENTAL

The steel X165CrMoV12 is taken as the foundation on which the coating is being deposited and it is often used for tool making in processing of metal forming. When defining tribological tests, it was taken into consideration that contact conditions, as much as possible, correspond to real exploitation condition. Also, based on a few sample tests, the contact parameters are being defined so that there is no penetration of coating, because the primary goal of testing is the tribological potential of hard Cr coatings. Work on quantitative way represents effects of depositing these coatings on lifetime of tools in metal forming applications in conditions without lubrications.

2.1. Material

Contact pairs are made of alloy tool steel with great toughness and hardness, label X165CrMoV12. This steel is wear resistant and scheduled to work on cold. Hardening in oil and loosening were done before mechanical grind processing. Mechanical characteristics are given in Table 1, and chemical composition in Table 2.

In order to test them, the samples were coated with hard Cr coating. It should be pointed out that the substrate was heat-treated alloy tool steel X165CrMoV12.

Hard chroming procedure is performed in ZCZ – Zastava Tools. Chromic coating thickness before final processing by grinding and polishing was about 0.2 mm, and after final processing was 30µm. Surface defects on these groups of samples, before performed tests, are not noticed.

Table 1. Mechanical characteristics of alloy tool steel X165CrMoV12

Hardness after soft annealing HB max	Tensile strength after soft annealing MPa max	Hardness after hardening in oil and loosening HRC	Measured hardness on the used tool HRC
250	830	57-65	58-63

Table 2. Chemical composition of alloy tool steel X165CrMoV12

Chemical element	%
C	~ 1.65
Si	~ 0.30
Mn	~ 0.30
P max	~ 0.035
S max	~ 0.035
Cr	~ 12.0
Ni max	~ 0.25
Mo	~ 0.60
V	~ 0.10
W	~ 0.50

2.2. Tribological test

Tribological tests are performed on a block-on-disc sliding wear testing machine with the contact pair geometry in accordance with ASTM G 77-83. A schematic configuration of the test machine is shown in Fig. 1. The test block was loaded against the rotating steel disc. This provides a nominal line contact Hertzian geometry for the contact pair.

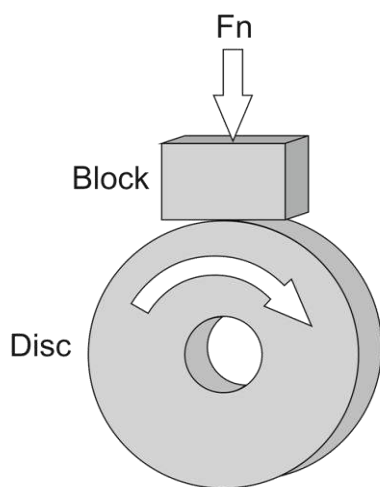


Fig.1. The scheme of contact pair geometry

The test blocks (6.35x15.75x10.16 mm) were prepared from tool steel X165CrMoV12, while one part of the samples is coated with hard Cr coating. The values of surface roughness were measured on the prepared

samples before and after depositing of coating. Measuring of surface roughness was done on Talysurf 6 device and appearance of material layout in surface layer on referent length $l=1.2\text{mm}$. Measured value of surface roughness for samples of tool steel and samples on which hard Cr coating is being deposited is $Ra=0.01\mu\text{m}$ and $Ra=0.01\mu\text{m}$ respectively. Surface profilometer of these surfaces are shown in Fig.2 and Fig.3.

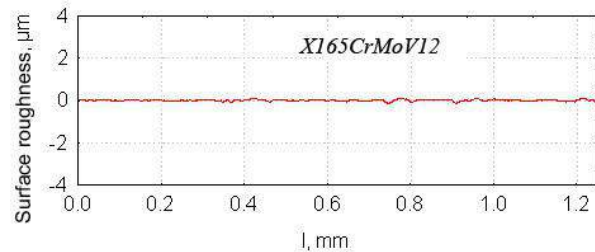


Fig.2. Surface profile X165CrMoV12

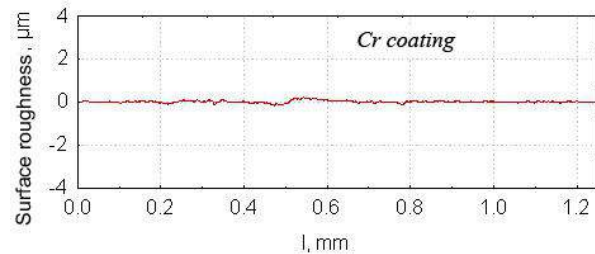


Fig.3. Surface profile X165CrMoV12 + Cr

More detailed description of the tribometer is available elsewhere [9]. The wear behavior of the block was monitored in terms of the wear scar width - h (Fig. 4). Using the wear scar width and geometry of the contact pair the wear volume (in accordance with ASTM G77-05) and wear rate (expressed in mm^3) were calculated. The repeatability of the results for replicate tests was found as satisfactory (variation of wear scar width was under 5%).

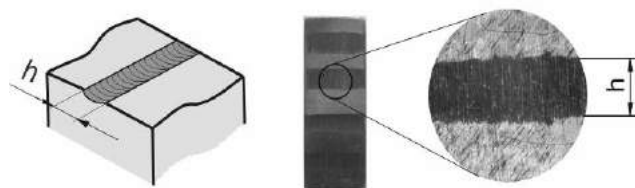


Fig.4. Wear scar

3. RESULTS AND DISCUSSION

Tribological tests of two groups of prepared samples are performed. The first group is base material, steel, of marking X165CrMoV12, while the second group are samples with hard Cr coating applied on base material. Prepared samples are tested in conditions without lubrication, with varying values of sliding speed and normal load. Sliding speed in contact was taking three values 0.25, 0.5 and 1ms^{-1} . The normal load value also had three values 10, 20 and 30N during the tests. During each test these values have remained constant. The normal load values are selected to avoid coating perforation during the testing, which was achieved.

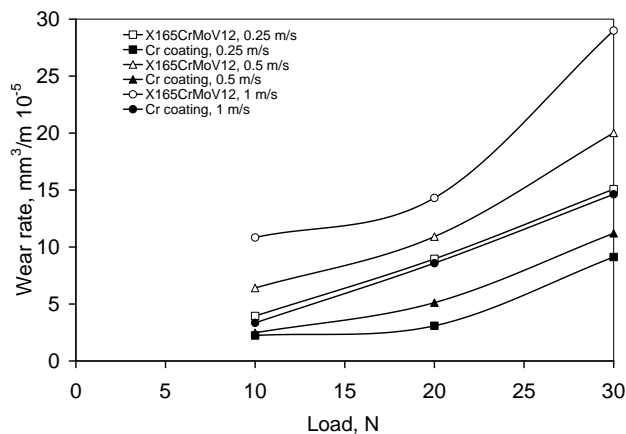


Fig.5. Wear rate dependence of tested samples on the normal load value (10, 20 and 30N)

The Figure 5 represents wear rate dependence of the normal load value, at constant speed sliding values. The diagrams shows, that in all contact conditions, the wear rate value of hard Cr coating is lesser in comparison to wear rate value of the sample without coating. Also, it is noticed that with increase of normal load value in the contact zone there is increase of wear rate value, which is accordant to theoretical patterns.

Figure 6 displays wear rate dependence of tested samples on changing sliding speed value in contact zone, at constant normal load value. Presented diagram shows increase of wear rate with increase of sliding speed, the only exception represents the wear curve referring to wear value obtained at the smallest normal load value of 10N. Based on this, we can say that at normal load values of 10N, the change of sliding speed does not influence the wear rate. This could be due to the way the contact is achieved. Because of small contact loads, can be said that the contact is achieved only on the peaks of asperities, about which the wear rate values witness and they are in this occasion very small.

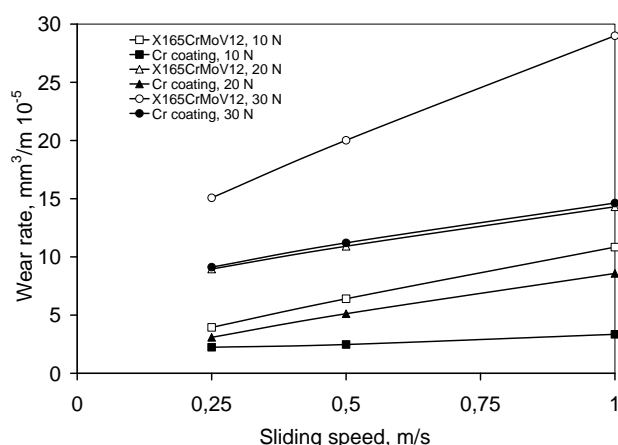


Fig. 6. Wear rate dependence of tested samples on sliding speed (0.25, 0.5 and 1ms⁻¹)

The work of L.H. Chiu has showed the stability and satisfactory wear resistance of hard Cr coating (7 μm thick), in the long run, at contact pressures up to 11 MPa [10]. In our case, the contact pressures in initial moments,

when the contact is achieved along the line, were, depending on the load, within the range of 30 to 60 MPa. With the wear development the contact pressure decreases, and then the contact is achieved on the surface.

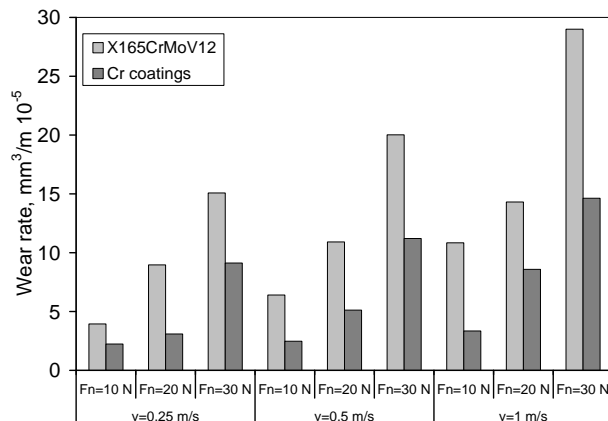
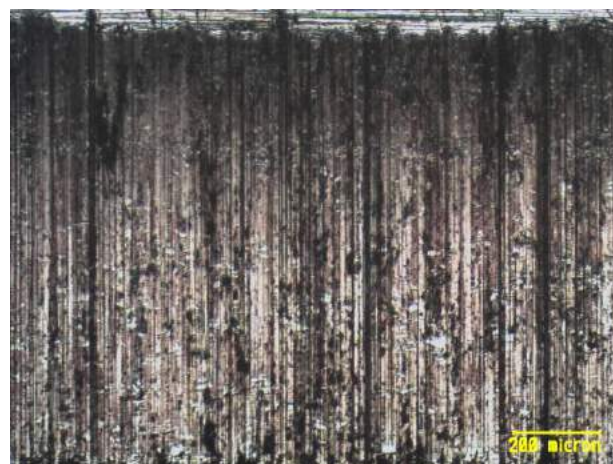
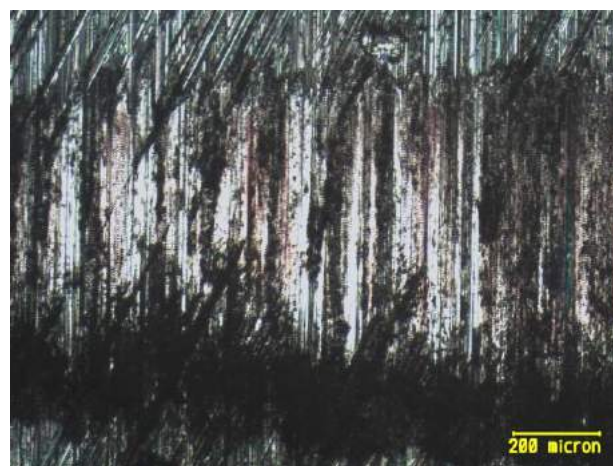


Fig.7. Histogram display of wear rate value for tested samples



a)



b)

Fig.8. Wear tracks after sliding road of 200m, normal load value of 30N and sliding speed of 1ms⁻¹ a) without coating; b)hard Cr coating.

Histogram display (shown on fig.7) enables to perceive, from quantitative aspect, the advantages of material with hard Cr coating in comparison to the material without

¹ Slobodan Mitrović, Ph.D., Faculty of Mechanical Engineering, Kragujevac, boban@kg.ac.rs

² Miroslav Babić, Ph.D., Faculty of Mechanical Engineering, Kragujevac, babic@kg.ac.rs

coating. It can be seen that, when considering wear rate, the material with coating has slightly smaller wear values in comparison to the material without coating. The difference in wear rate value is in the range of 40-60%. The most uniform difference in percentages in wear rate value of these two groups of samples is 0.5m/s at sliding speed.

Primarily we should say that adhesive wear occurs when the contact pressure between sliding surfaces is high enough to cause local plastic deformation and welding between the contacting asperities. Abrasive wear, however, occurs between two hard sliding surfaces when hard debris particles are indented and make grooves in the sliding surface of the material. Both kinds of wear can be lessened by either a decrease on the contact pressure or an increase in the mechanical strength of the material itself. Figure 8 presents wear tracks of tested samples in the conditions without lubrication and after sliding road of 200m. Displayed tracks in Figure 8 are created in condition of the highest sliding speeds and maximum normal load in this test. Based on the appearance of wear tracks, we can conclude that the dominant wear mechanism is abrasive wear.

At the very beginning of making contact we can talk about adhesive wear, which is the consequence of contact block-on-disc, or high contact pressures which appears when contact is achieved only on the peaks of asperities. With further development of the wear, contact passes from linear into contact on the surface, when the domination of abrasive wearing begins.

4. CONCLUSION

Tested samples coated by hard chrome coating showed bigger wear resistance in comparison to the samples without coating, samples of tool steel. Comparative display of measured wear rate value of both materials shows that wear of hard Cr coating samples is for 40-60% less. Based on this we can conclude that by depositing of hard Cr coatings on steel base, the lifetime of tool in metal forming application could be considerably prolonged.

Also, hard Cr coatings have shown durability and wear resistance at contact pressure of 60MP, which is the consequence of the line contact and normal load value of 30N.

Based on the Figures of wear tracks of tested samples we can conclude that the dominant wear mechanism is abrasive wear.

REFERENCES

- J.M. Tyler: Automotive Application for Chromium, Metal Finishing, pp 11-14, (1995).
- H. Silman, G. Isserlis and A.F. Averill: Protective and decorative coatings for metals, Surface Technology, Volume 8, Issue 5, , Pages 451-452 (1979).
- A. Darbeida, J. von Stebut, M. Barthole, P. Belliard, L. LeLait, G. Zacharie: Comparative tribological study of chromium coatings with different specific

hardness, Surface and Coatings Technology, 68/69, 582—590, (1994).

- G.A. Lausmann: Electrolytically deposited hardchrome, Surface and Coatings Technology, 86-87 , 814-820 (1996).
- G.E. D'Errico, E. Guglielmi, G. Rutelli: A study of coatings for end mills in high speed metal cutting, Journal of Materials Processing Technology, 92-93, 251-256, (1999).
- Andreas Wank a,□, Bernhard Wielage, Hanna Pokhmurska, Eduard Friesen, Guido Reisel: Comparison of hardmetal and hard chromium coatings under different tribological conditions, Surface & Coatings Technology, 201, 1975–1980 (2006).
- D.T. Gawne, T.F.P. Gudyanga: Durability of chromium plating under dry sliding conditions, Tribology International, Volume 17, Issue 3 , Pages 123-128, (1984)
- K.C. Walter, J.T. Scheuer, P.C. McIntyre, P. Kodali, N. Yu, M. Nastasi : Increased wear resistance of electrodeposited chromium through applications of plasma source ion implantation techniques, Surface and Coatings` Technology, Volume 85, 1-2, pp 1-6. (1996).
- Babic M., Mitrovic S., Jeremic B.: The Influence of Heat Treatment on the Sliding Wear Behavior of a ZA-27 Alloy, Tribology International Volume 43, Issues 1-2, 16-21 (2010)
- L.H. Chiu, C.F. Yang, W.C. Hsieh, A.S. Cheng: Effect of contact pressure on wear resistance of AISI H13 tool steels with chromium nitride and hard chromium coatings, Surface and Coatings Technology 154, 282–288 (2002)



INFLUENCE OF WEAR OF CUTTING ELEMENTS OF CONVEX MILLING CUTTERS ON PROCESSED SURFACE TOPOGRAPHY

Ivan SOVILJ-NIKIĆ, Bogdan SOVILJ, Stanislaw LEGUTKO, Sandra SOVILJ-NIKIĆ, Ivan SAMARDŽIĆ,
Ivan KOLEV

Faculty of technical science, University of Novi Sad, Trg Dositeja Obradovića 6, Novi Sad, Serbia
diomed17@gmail.com, bsovilj@uns.ac.rs, legutko@sol.put.poznan.pl, sandrasn@eunet.rs, ivan.samardzic@sfsb.hr,
kolev@ru.acad.bg

Abstract: *The actual area of contact is the basic size and starting point for investigation and interpretation of tribological processes, and its determination is one of the primary tasks of research. This paper presents the results of experimental research on the impact of wear of cutting elements of convex milling cutter on the processed surface topography.*

Key words: *cutting element, convex milling cutter, wear, cutting speed, feed, processed surface topography*

1. INTRODUCTION

In the process of cutting contact of convex milling cutter with a workpiece material is achieved between scraped and face area, as well as between back surface of the cutting element and processed surface [2,3,4].

Tribological processes that occur in the process of cutting on both surfaces of the tool cutting element are developed under specific conditions. Research of wear process of convex milling cutter on characteristics of the state and output effects of machining process is very important. Quantifying the actual contact area is linked with a number of unresolved issues when it comes from methodology and instrumentation.

One of the future procedures for determining the actual area of contact is based on its topography. Due to the existence of a higher order surface roughness and the existence and development of tribological processes in this area, it is necessary to improve methodologies that define the topography.

Topography parameters of contact surfaces of elements of tribo-mechanical systems are result of previous and final operations of machining process [1,6,8].

The geometrical parameters of contact surfaces are significantly changed under the influence of plastic deformation, the efforts by other structures and destruction of the structure by friction. Starting topography, caused by processing technology, is continuously changed during the cycle of exploitation.

The contact surface of tribo-elements, after finish processing, is never absolutely smooth. Numerous irregularities resulting from previous and final operations may have different geometric parameters and induce more or less irregularities of tribo-elements.

Characteristic parameters, inherited during the technological process, define macro and micro geometry of contact areas. For the correct analysis of tribological processes and tribologically correct construction,

roughness of contact surfaces is very important. To complete the picture of contact surface topography is necessary to define the roughness precisely. Based on a complex research of milling process, in this paper a part of the research results related to the processing of surfaces using convex milling cutter is given.

2. BASIC OPERATIONS OF PROCESS OF MILLING PROCESSING

Modern milling is a very universal machining method. During the past few years, hand-in-hand with machine tool developments, milling has evolved into a method that machines a very broad range of configurations.

Production operations of milling cutter processing are classified according to type and shape of milling used for processing into: facing cutter milling, end-milling cutter milling, side and face cutter milling etc (fig.1) [5,7,9].

An effective usage of working means in metal industry demands knowledge of current parameter process. The technological parameters which influence tool wear take an important place in the process. Together with parameters for determination of process economy they effect the realization of optimal parameter of cutting regime.

Important precondition for the process economy is the possession of actual cutting information. The need for this information is growing with increased application of computer in the process control and automated systems. The number of data is larger at milling due to process complexity and due to variety of milling possibility. Insight into the milling process is more complicated due to following facts:

- tool is periodically in the contact with the material
- changeable number of cutters in contact with material
- changeable component width

- possible changes of input and output angle due to different relation between tool and workpiece.

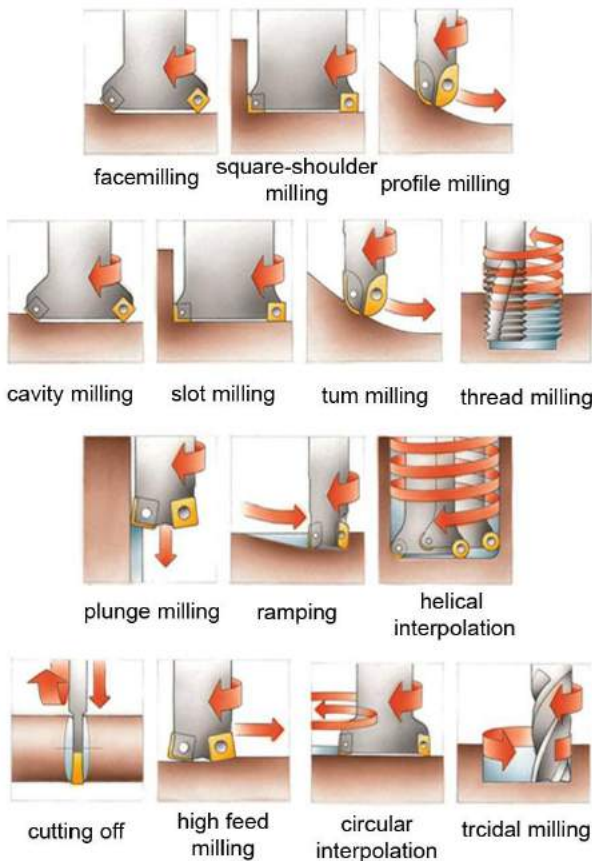


Fig.1. The main types of milling operations

Observing of surface quality at the workpiece has been performed by means of roughness parameters (R_{max} , R_z , R_a , R_s , R_t , $R_{3z_{max}}$, R_{3z}) in dependence of cutting length (L).

3. RESEARCH RESULTS

Table 1. Conditions of experiment realization

Experiment – tool tag	Machine		Tool		Working piece	
	GU-2		Convex milling cutter 063(R5) HS6-5-2-5		1C45 23HRC	
	Cutting depth (mm)	Feed (mm/min)	No. of rotations (rot/min)	Radial runout (mm)	Milling procedure	No. of milling cutters
I-G1	5	125	100	0.10	Opp. direc.	1
II- G2	5	125	160	0.15	Opp. direc.	2
III-G3	5	200	160	0.08	Opp. direc.	3
IVG4	5	200	100	0.20	Opp. direc.	4
V-G5	5	160	125	0.12	Opp. direc.	5
VI-G6	5	160	125	0.16	Opp. direc.	6
VII-G7	5	160	125	0.12	Opp. direc.	7

Milling process is, in comparison to the other working processes, a specific one. During milling process not only one tooth takes part in the process but as many teeth as the tool has it. Radius of every tooth can vary and this can influence the process in significant way. It means that some of the teeth will be involved much more in the process. The cutting load at those teeth is also much higher, the milling process is more intensive. Therefore, the radial eccentricity has been measured at milling tools which are in assembly with the machine, i.e. radial eccentricity relative to rotation axe and not relative to milling tool axe.

Investigations were realized in real conditions as follows:

- a) working piece: material **1C45**, improved, chemical composition(table), dimensions 475x250x65

Table 1. Chemical composition of the working piece

C(%)	Si(%)	Mn(%)	P(%)	S(%)
0.50	0.35	0.80	0.045	0.045

- b) tool: convex milling cutters $\phi 63$, material **HS6-5-2-5**, tooth number $z=12$

- c) machine: universal milling machine GU-2

Measuring of wearing zone width was realized at tool microscope ZEISS. Research was consisted of development of wear process at various cutting speeds and feeds.

Table 1 shows conditions of experiment realization and figures 2-8 shows measured values of parameters of roughness.

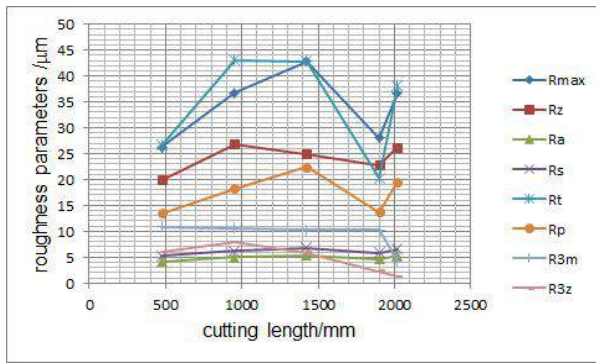


Fig.2. Dependence of wear parameters on length of cutting by tool G1

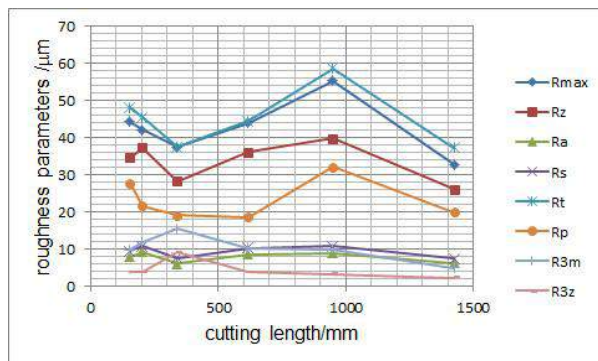


Fig.3. Dependence of wear parameters on length of cutting by tool G2

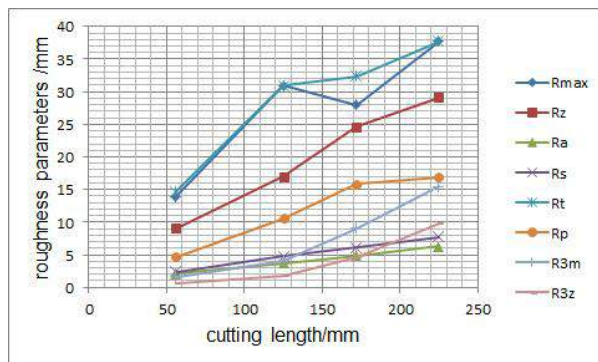


Fig.4. Dependence of wear parameters on length of cutting by tool G3

Based upon investigation results from experiment I and IV; and II and III it can be concluded:

- at constant cutting speed and with feed increase, milling cutter life significantly decreases at constant feed
- with speed increase milling cutter life decreases for 30-40 %

the smallest milling cutter life was obtained for mean values of speed and feed (experiments V-VII)
Analyzing the diagrams on figures 2-8, it can be concluded that wear parameters, almost for all tools, increase in the beginning of processing and afterwards they decrease. Also, the tool lives are different for different processing regimes.

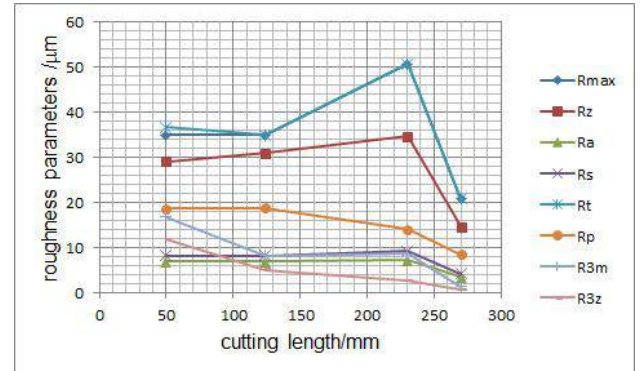


Fig.5. Dependence of wear parameters on length of cutting by tool G4

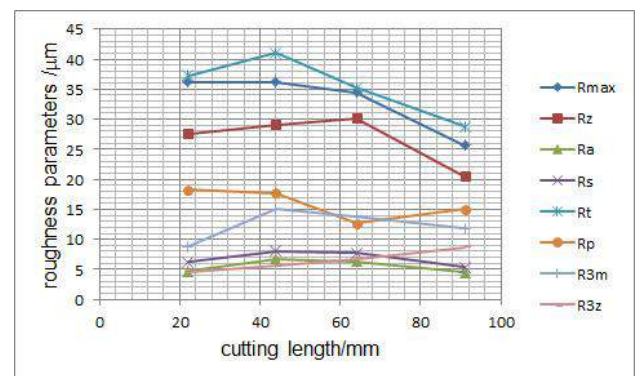


Fig.6. Dependence of wear parameters on length of cutting by tool G5

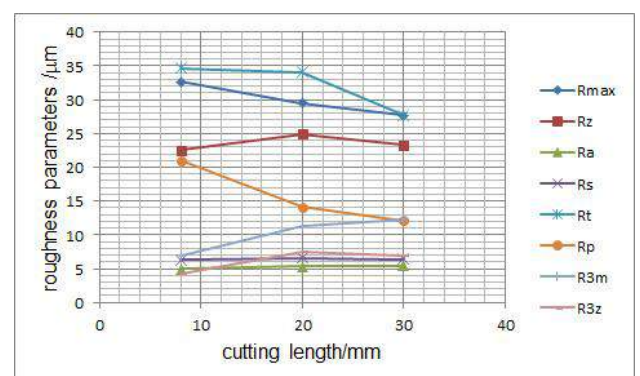


Fig.7. Dependence of wear parameters on length of cutting by tool G6

¹ Ivan Sovilj-Nikić, PhD student, FTN, Trg Dositeja obradovića 6 and diomed17@gmail.com.

² Bogdan Sovilj, Prof. dr, FTN, Trg Dositeja obradovića 6 and bsovilj.

³ Stanislaw Legutko, Prof. dr hab, Politechnika Poznanska, Piotrowo 3. and stanislaw.legutko@put.poznan.pl.

⁴ Sandra Sovilj-Nikić, PhD student, FTN, Trg Dositeja obradovića 6 and sandrasn@eunet.rs.

⁵ Ivan Samardžić, Prof. dr, Mechanical Engineering Faculty, Trg Ivane Brlić Mažuranić 2 and Ivan.Samardzic@sfsb.hr

⁶ Ivan Kolev, Assoc.Prof, "Angel Kanchev" University of Ruse, R&DS, Studentska 8. and kolev@ru.acad.bg

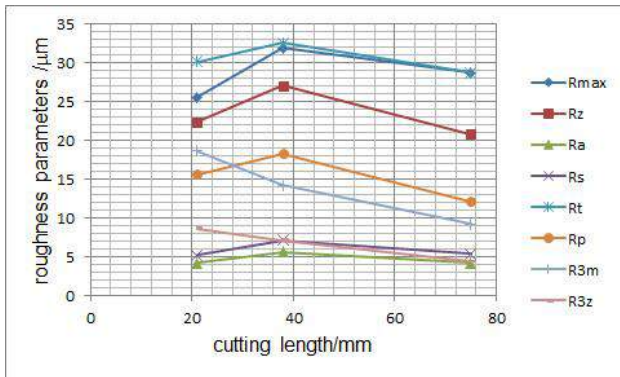


Fig.8. Dependence of wear parameters on length of cutting by tool G7

4. CONCLUSION

Based on obtained research results it can be concluded that the wear of cutting elements of the convex milling cutter has a direct impact on the topography of processed surface. This relationship between the wear of tool cutting edges and topography parameters allows determination of the tooth wear criteria of convex milling cutters.

REFERENCES

- [1] IVKOVIĆ, B., RAC, A. (1995) *Tribologija*, Jugoslovensko društvo za tribologiju
- [2] SOVILJ, B. (1988) *Identifikacija triboloških procesa pri odvalnom glodanju*, Univerzitet u Novom Sadu
- [3] KOLEV, I. (2009) *Rjazane na materialite*, RU "Angel Kincev"
- [4] DUDAS, I. (2003) *Gepgyartas-teccnologia III*, Miskolci egytemy kiado
- [5] NESLUSIN, M., et all (2007) *Experimentalne metody v trieskovom obrabani*, Zilinska univerziteta v Ziline
- [6] TANASIJEVIĆ, S. (2004) *Tribološki ispravno konstruisanje*, Mašinski fakultet u Kragujevcu
- [7] ČUŠ, F. (2009) *Postopki odrezavanja*, Univerza v Mariboru
- [8] SOVILJ, B., et all (2010) Identification and methods of measuring tribological characteristics of materials, *Scientific Journal of Agricultural Engineering*, Vol. 36, No. 3, pp 295-304
- [9] SANDVIK COROMANT (2005), *Metalcutting technical guide*, Sandvik Coromant



INFLUENCE OF FRICTION COEFFICIENT ON WORKPIECE ROUGHNESS IN RING UPSETTING PROCESS

Marko VILOTIĆ, Damir KAKAŠ, Aleksandar MILETIĆ, Lazar KOVAČEVIĆ, Pal TEREK
Faculty of Technical Sciences, University of Novi Sad, Trg Dositeja Obradovića 6, Novi Sad, Serbia
markovil@uns.ac.rs, kakasdam@uns.ac.rs, miletic@uns.ac.rs, lazarkov@uns.ac.rs, terekpal@gmail.com

Abstract: In forming processes contact friction significantly influence metal flow, stress-strain state and process parameters. Furthermore, tribological conditions influence workpiece surface quality and its dimensional precision.

This paper presents results of the influence of contact friction coefficient on a workpiece surface quality in ring upsetting by flat plates. Workpiece surface roughness is measured using atomic force microscope. Ring upsetting experiments are conducted with ion implanted and nonimplanted dies.

Key words: ring upsetting, ion implantation, nanoroughness, AFM, friction coefficient

1. INTRODUCTION

Quality of a metal forming process is often controlled by the interfacial friction between the contacting die and workpiece surfaces. If the interfacial friction forces are large enough, the strain condition and formability of the workpiece may deteriorate and the energy required to form the part may be unacceptably high [1].

A basic premise of the theory of friction is that apparently flat, smooth surfaces are not so smooth when viewed on a microscopic scale. Surfaces of metals are actually rough, and asperities representing the roughness of the surface are present in surfaces of metals. Workpieces, dies and tools are characterized by surface roughness. Until all asperities are flattened, surface roughness has an influence on the friction properties of those surfaces, especially at the beginning of metal forming processes. During forming process asperities plough into each other, and thus a small sliding always exists. At the beginning of the process, since the tool is in contact just with the peaks of the asperities, the friction properties depend on the distribution of asperities, on their height and their deformation during the process, e.g. on the roughness of the contact surface. With the flattening of asperities the contact with the tool gets larger and this leads to varying friction properties [2, 3, 4, 5].

Such friction produces a tangential (shear) force at the interface between die and workpiece which restricts movement of the material and results in increased energy and press forces. The magnitude of the shear friction stress influences the deformation pattern, the temperature rise, the tool deflection and the total force in metal-forming [6]. The prediction of how quick the die will failure is an important objective to guarantee good output from a cold forging process. The failure of a tool does not only require it to be replaced but it also stops production, causes rejection of the workpieces, and requires new adjustment of the machine. The replacement of the dies

planned according to a predictive maintenance program less affects productivity than unexpected stops [7].

2. FRICTION IN METAL FORMING PROCESS

During metal forming process working surface of the die is in continuous contact with the workpiece surface. In the contact between the die and workpiece high values of normal and tangential stresses are present together with the displacement and sliding of material. Contact surfaces of the die and workpiece have initial roughness which changes during metal forming process.

Contact friction corresponds to a resistance of relative movement between two bodies in contact, with normal stress present in between them (fig. 1).

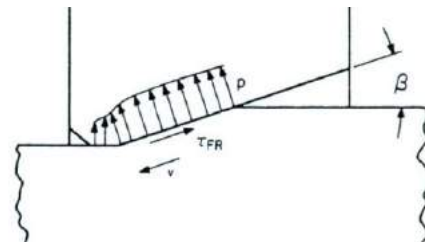


Fig. 1. Contact between workpiece and die [4]

In between those surfaces lubrication is present which lowers contact friction. During metal forming process removal of workpiece's material and wear process initiates on the surface of the die and workpiece, which modifies initial tribological conditions in forming process. Since relative movement between die and workpiece is always present in metal forming process, friction is integral part of every metal forming process (with an exception of uniaxial tension). Contact friction is negative event since it causes an increase of required force and

work, die wear and nonuniform deformation. Rolling process is exception, since friction is required for process to be carried out.

During metal forming process peaks of asperities found on workpiece and die are in contact, while other areas of the contact surface are separated by lubricant (fig. 2).

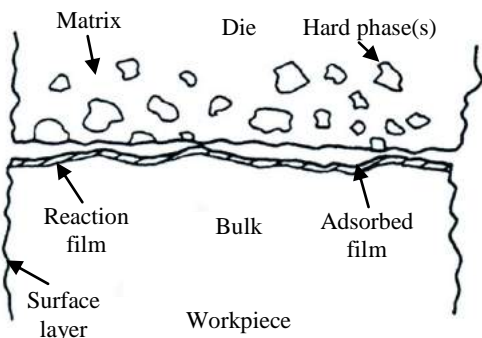


Fig. 2. Peaks in contact [4]

Composition of anti-friction material is changing during metal forming process, because friction generate workpiece and die wear, oxidation and corrosion of metal which affects friction and lubrication conditions.

Surface roughness of tools and final parts is important for adequate lubrication and it also stands as a wear criterion in the metal forming process. Surface profile consists of many peaks and valleys that get deformed in the forming process. Those deformed peaks and valleys affect lubricant film sustainability and because of that surface topography affect the maintenance of lubricant film. For this reason, the surface topography is very important in metal forming processes.

According to [2] friction coefficient increases with surface roughness decrease except when samples were made of brass. For samples made of aluminum and steel, highest friction coefficient values are obtained in case of polished surface, while lowest values are obtained for machined only surface.

Tab. 1. Friction coefficient and factor values [2]

Trial no.	Deformation ratio (%)		Friction coefficient
	x_1	x_2	
1	19.2	1.85	0.08
2	19.3	1.75	0.09
3	39.4	2.20	0.08
4	42.8	2.25	0.12
5	58.0	2.05	0.13
6	59.0	2.09	0.12

Since the contact area between die and workpiece is smallest at machined samples, and highest for polished samples, the lowest friction coefficient values were obtained on samples whose surface is only machined.

Various instruments are being used for measuring surface topography and for topography measurements in nano and micro scale atomic force microscopy can be successfully used.

As universal method for friction coefficient measurement in bulk metal forming processes, ring upsetting by flat plates (dies) have been used [4, 7, 8].

3. RING UPSETTING EXPERIMENT

Fig. 3 shows contact friction coefficient determination by ring upsetting method.

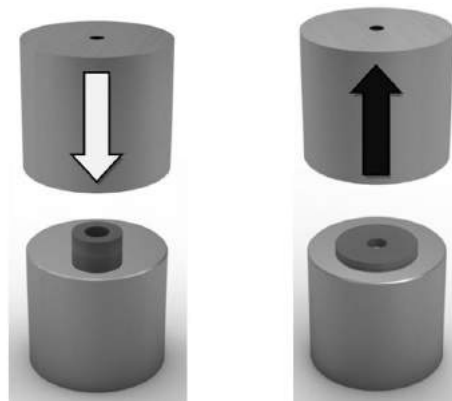


Fig. 3. Ring upsetting method

Method consists of establishing the dependence between deformation of inner ring's diameter and ring's height. This dependence is taken into etalon chart and compared with existing within the chart.

Ring upsetting has been performed incrementally, with a height deformation around 10%. After each upsetting stage ring's dimensions were measured. Incremental upsetting has been carried out until total deformation of the ring's height has reach around 70%.

Once the ring upsetting has been completed, deformation of the ring's inner diameter and deformation of the ring's height has been calculated for each upsetting increment. By connecting all the pairs of height and inner diameter deformation curve was defined.

In order to find the friction factor for the completed upsetting process, it is necessary to compare the curve with an existing ones from the etalon diagram.

Ring upsetting has been carried out with two different pairs of dies. One pair of dies has been grinded, polished and ion implanted with $2 \cdot 10^{17} \text{ N}^+ 50 \text{ keV}$, while another pair of dies has not been ion implanted. Dies were made of X210Cr12 cold work tool steel (Č.4150) with dimensions $\phi 50 \times 45 \text{ mm}$. Rings were made of Ck15 unalloyed carbon steel (Č.1221) with initial dimensions $D_2:D_1:h=18:9:6 \text{ mm}$. Hardness of the dies was 58+2 HRC, while hardness of the ring upset with nonimplanted dies was 167 HV-10 and hardness of the ring upset with implanted dies was 161 HV-10. Upsetting was done without contact surface lubrication.

4. RESULTS

4.1 Ion implantation simulation by SRIM software

In order to ensure successful ion implantation into X210Cr12 steel, SRIM simulation software was used to evaluate the effect of $2 \cdot 10^{17} \text{ N}^+ 50 \text{ keV}$ ion implantation into die's surface. As it can be seen from fig. 4, ion implantation depth was around 100 nm. For the convenience, SRIM simulation on fig. 4 was completed with 10000 ions.

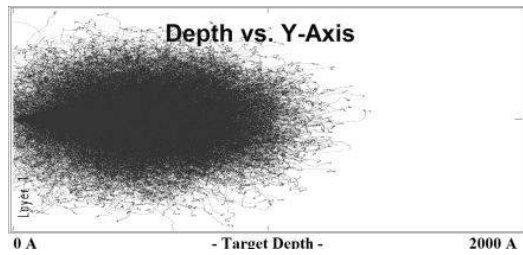


Fig. 4. SRIM simulation of ion implantation into steel

Based on the results of simulation, ion implantation of the dies has been carried out in Institute of Nuclear Sciences “Vinča”.

4.2 Ring upsetting – contact friction coefficient

Fig. 5 shows comparison of friction factors obtained from a ring upsetting experiment while tab. 2 shows friction factors and friction coefficients values. Friction calibration curves were obtained by Avitzur [9] and Hawyard and Jonson [10] by using only theoretical analysis. These authors assumed that in ring uniform deformation (no barreling) and constant interface frictional shear factor take place.

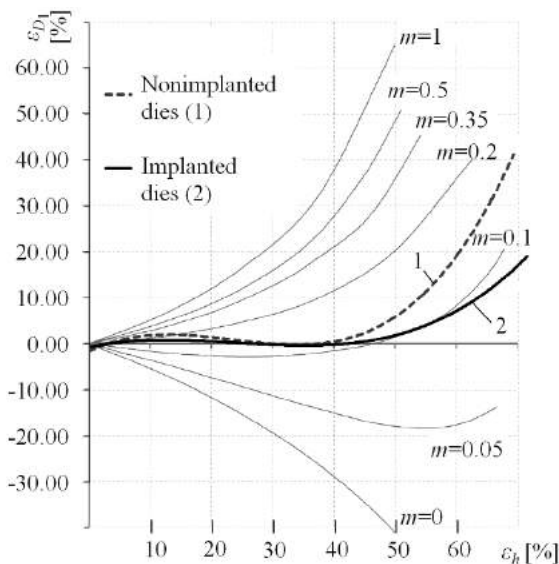


Fig. 5. Comparison of friction factors for rings upset with implanted (2) and nonimplanted dies (1) [8, 9, 10]

Tab. 2. Friction factors and friction coefficients for rings upset with implanted and nonimplanted dies

Dies	Friction factor (m)	Friction coefficient (μ)
Nonimplanted	0.15	0.087
Implanted	0.11	0.064

4.3 Measurement of ring’s surface roughness change

Purpose of die and workpiece topography measurement prior and after ring upsetting was to determine the influence of die’s surface ion implantation on friction and dimensional accuracy, i. e. workpiece surface quality at metal forming processes. By comparing the roughnesses

between corresponding rings, influence of die’s surface ion implantation on ring’s quality and accuracy can be established.

Topography of the ring was measured with VEECO “di CP II” atomic force microscope.

To evaluate the effect of die surface ion implantation on ring’s surface roughness during upsetting, ring roughness has to be determined before upsetting was carried out. Fig. 6 displays topography of the ring that hasn’t been upset with dies and tab. 3 shows average roughness values of rings before upsetting.

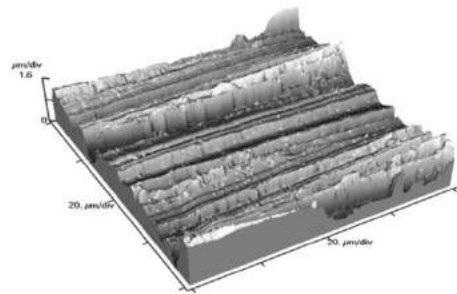


Fig. 6. Topography of the ring’s surface before upsetting

Tab. 3 Average values of R_a for ring before upsetting

Ring for upsetting with	R_a [nm]
ion implanted dies	126.75
nonimplanted dies	137.65

Fig. 7 shows measuring points where surface roughness was measured using atomic force microscopy, while tab. 4 shows average ring’s roughness values after upsetting. Distance between measuring points on the rings is approximately 1 mm.

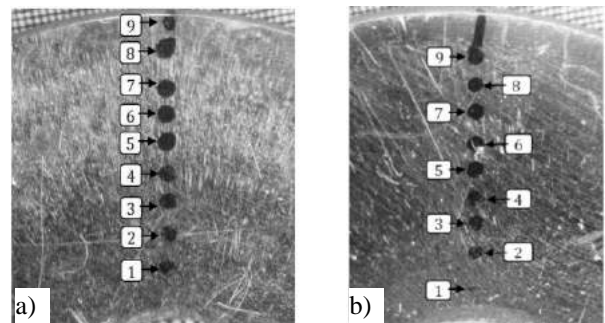


Fig. 7 Measuring points on the ring upset with a) nonimplanted dies, b) implanted dies

Tab. 4 Average values of R_a for ring after upsetting

Ring upset with	R_a [nm]
ion implanted dies	11.11
nonimplanted dies	23.79

Fig. 8 shows topography of the ring upset with nonimplanted dies at measuring point 7 (see fig. 7), while fig. 9 shows topography of the ring upset with implanted dies also at measuring point 7.

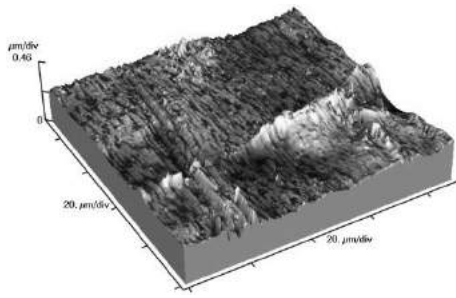


Fig. 8. Topography of the ring upset with nonimplanted dies measured at point 7

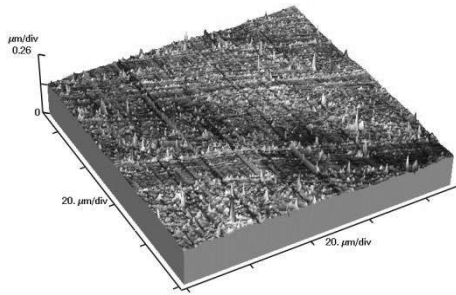


Fig. 9. Topography of the ring upset with ion implanted dies measured at point 7

Fig. 10. shows roughness comparison between the rings upset with nonimplanted and ion implanted dies.

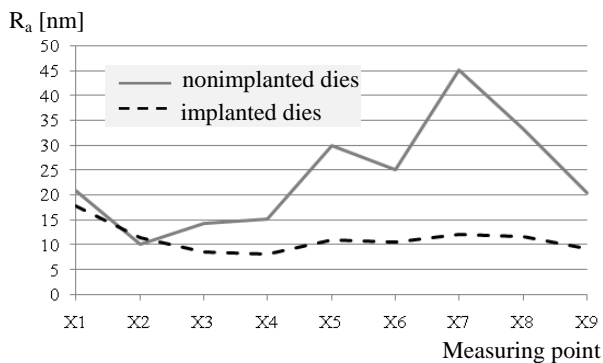


Fig. 10. Roughness comparison between the rings upset with nonimplanted and ion implanted dies

5. DISCUSSION

It is evident from diagram (fig. 5) that ion implantation has influence on friction coefficient in ring upsetting process, since friction coefficient is 1.36 times lower in case of upsetting with ion implanted dies.

According to tab. 4 ring upset with ion implanted dies has average roughness (R_a) that is 2.14 times lower than ring upset with nonimplanted dies. Also, it is obvious from fig. 8 and 9 that rings upset with ion implanted dies has smoother surface compared to ring upset with nonimplanted dies.

Diagram on fig. 10 shows that ring upset with ion implanted dies has roughness in narrower range compared to ring upset with nonimplanted dies.

6. CONCLUSION

Based on the results presented in this paper, it can be concluded that ion implantation can reduce the friction coefficient and improve surface roughness and quality at bulk forming process. AFM application is essential for researching surface nanomorphology in bulk forming processes. Results obtained in this paper contribute to development of ultraprecision engineering.

ACKNOWLEDGEMENTS

This paper is a part of research included into the project “Project TESLA: science with accelerators and accelerator technologies”, financed by serbian Ministry of Science and Technological Development. The authors are grateful for the financial support.

REFERENCES

- [1] LOVELL, M. R., DENG, Z. (2001) *Characterization of interfacial friction in coated sheet steels: influence of stamping process parameters and wear mechanisms*, Tribology International, Vol. 35, pp 85-95.
- [2] SAHIN, M., CETINARSLAN, C. S., AKATA, H. E. (2007) *Effect of surface roughness on friction coefficients during upsetting processes for different materials*, Materials and Design, Vol. 28, pp 633-640
- [3] DIETER, G. (1984) *Mechanical metallurgy. second ed*, Japan: McGraw-Hill International Book Company.
- [4] LANGE, K (1985) *Handbook of metal forming*, USA: McGraw-Hill International Book Company.
- [5] MALE, A., COCKROFT, M. (1964) *A method for the deformation of coefficient of friction of metals under bulk plastic deformation*, J. Ins. Met, Vol. 93, pp 38-46.
- [6] BEHRENS, A., SCHAFSTALL, H. (1998) *2D and 3D simulation of complex multistage forging processes by use of adaptive friction coefficient*, Journal of Materials Processing Technology, Vol. 80-81, pp 298-303.
- [7] SCHEY, J. (1972) *Metal Deformation Processes: Friction and Lubrication*, Marcel Dekker Inc, New York.
- [8] PLANČAK, M., VILOTIĆ, D. (2003) *Tehnologija plastičnog deformisanja*, Fakultet tehničkih nauka, Univerzitet u Novom Sadu, Novi Sad.
- [9] AVITZUR, B. (1968) *Metal Forming Processes and Analysis*, McGraw-Hill.
- [10] HAWKYARD, J.B., JOHNSON, W. (1967) *An analysis of the changes in geometry of a short hollow cylinder during axial compression*, Int. J. Sci. Pergamon Press Ltd., Vol. 9, pp 168-182.



34th INTERNATIONAL CONFERENCE ON
PRODUCTION ENGINEERING
28. - 30. September 2011, Niš, Serbia
University of Niš, Faculty of Mechanical Engineering



FRICION FORCE MICROSCOPY OF DEEP DRAWING MADE SURFACES

Bozica BOJOVIC, Dusan KOJIC, Zoran MILJKOVIC, Bojan BABIC, Milica PETROVIC

University of Belgrade, Kraljice Marije 16, 11120 Belgrade, Republic of Serbia

bbojovic@mas.bg.ac.rs, dkojic@mas.bg.ac.rs, zmiljkovic@mas.bg.ac.rs, bbabic@mas.bg.ac.rs,
mmpetrovic@mas.bg.ac.rs

Abstract: Aim of this paper is to contribute to micro-tribology understanding and friction in micro-scale interpretation in case of metal beverage production, particularly the deep drawing process of cans. In order to bridging the gap between engineering and trial-and-error principles, an experimental AFM-based micro-tribological approach is adopted. For that purpose, the can's surfaces are imaged with atomic force microscopy (AFM) and the frictional force signal is measured with frictional force microscopy (FFM). In both techniques, the sample surface is scanned with a stylus attached to a cantilever. Vertical motion of the cantilever is recorded in AFM and horizontal motion is recorded in FFM. The presented work evaluates friction over a micro-scale on various samples gathered from cylindrical, bottom and round parts of cans, made of same the material but with different deep drawing process parameters. The main idea is to link the experimental observation with the manufacturing process. Results presented here can advance the knowledge in order to comprehend the tribological phenomena at the contact scales, too small for conventional tribology.

Keywords: Frictional force microscopy, Deep drawing process, Friction force, Micro-tribology

1. INTRODUCTION

Theories and methods currently engaged in deep drawing process cannot satisfy engineering needs and, in practice, for engineering design and production control, they have to use the trial-and-error method through repeated testing, simulating and trouble-shooting to reach the quality requirements pointed out in [1]. Previous researchers studied the material flow influence and distribution of deformation, improving the deep drawability, determining the optimal blank shape and estimating the required drawing force, explained in [2]. An examination of some of the objectives is performed in FE simulations of the process [3, 4]. However, the effectiveness of the results from numerical simulations is strongly connected to the correct modeling of the complex contact conditions, i.e. the frictional coefficient μ and material anisotropy effects. In order to model the friction between the flange and die and blankholder properly, the global value of the frictional coefficient has to be replaced by a variable frictional coefficient.

Since friction forces are largely dependent on the contact geometry [5], the influence of surface topography on friction is significant in micro and nano-scale, compared to the macro scale, where the surface roughness readily changes due high applied loads [6]. Therefore, investigations required to permit a more effective modeling of the frictional phenomenon during deep drawing operations imply studding of tribological

phenomena at very small contact scales that AFM-based techniques can provide. AFM-based tribological studies are used for interacting surfaces behavior investigation on the micro and nano-scales. Micro-tribology is the bridge between classical macro-tribology and nano-tribology. Micro-tribology offers a reliable characterization of frictional properties of materials as it involves larger contact size and also provides high sensitivity comparable to nano-tribology techniques proved in the study [7].

Investigation becomes more complex in case of coated materials as pre-painted and lacquering tin plate used in food beverage production being our scope of interest. Pre-painted steel sheets are complex systems made of several layers whose global properties are evaluated by scratch and indentation tests in studies [4, 8]. The aim of this study is to evaluate friction over a micro-scale on samples gathered from cans made by deep drawing. This study, by explanation of the frictional force signal gathered by frictional force microscopy tends to contribute fundamental understanding of friction of engineering surfaces, in general.

2. MATERIALS AND METHODS

Mass production of cans is performed by a sheet feed press CEPEDA (component of automated manufacturing line) by deep drawing. Cans are made of various tin plates, but we used DR550 for the experiment, regarding its widespread. Double Reduced Tinplate Sheets (DR

550) are made of cold rolled and tin coated steel with high strength and sufficient ductility. This kind of tin plate, before deep drawing, is exposed to lithography and lacquering processes. Samples for the experiment are taken from the cylindrical, rounded and bottom part of seven different cans after deep drawing with the various process parameters.

A commercial scanning probe microscope (JSPM 5200, JEOL, Japan) is used for this investigation. Commercial probe produced by MikroMasch, Estonia, CSC37/AIBS for general purpose is used for contact mode scanning. The probe is a three-lever chip that contains long cantilevers with a Single-Crystal Silicon tip that has conical shape. Typical uncoated tip radius is less than 10 nm, height 15-20 μm , full angle cone is less than 40° and the typical force constant is 0.3–0.65 N/m. Resulting tip curvature radius is 40nm due 30nm aluminum back coating. All experiments are performed at room temperature. For topography and friction scanning the AFM operates in constant force mode. In AFM the tip is in permanent contact with the sample surface and due to its topography, the cantilever is deflected in the Z-direction. In FFM the torsion of the cantilever due to friction force between tip and sample is detected via photo-diode. AFM and FFM recorded images of samples are analyzed by WinSPM software.

The friction signal (recorded in Volt) is indicative of the friction force, and therefore, the identification of the dominating parameter that affects the change in the friction signal is the aim of this paper.

3. RESULTS AND DISCUSSION

Out of 41 successfully gathered AFM and FFM scans, 24 are selected and analyzed in WinSPM Ver.2.15 software, specialized for SPM data processing. The scan area is of the same size $10 \times 10 \mu\text{m}$, $5 \times 5 \mu\text{m}$, $3 \times 3 \mu\text{m}$ and $2 \times 2 \mu\text{m}$ considered as a group of FFM images. Within each of group the span of relative values of the friction signal are calculated and shown in Table 1.

Table 1. Span of friction signal relative values

Group No.	Scan area [μm]	Span of friction signal relative values [V]
4.	10×10	$1.2 \div 5.4$
5.	5×5	$0.9 \div 2$
6.	3×3	$0.6 \div 2$
7.	2×2	$0.7 \div 2$

For a scan area of $5 \times 5 \mu\text{m}$ and smaller, the friction signal spans are almost equal, according to Table 1. Scans gathered for $1 \times 1 \mu\text{m}$ area also confirm this trend. Aside to these values, the span of friction signal for $10 \times 10 \mu\text{m}$ area is evidently larger. Similar values are found for few scans

performed on $25 \times 25 \mu\text{m}$. Results shown in Table 1 indicate that the scan area size influences the friction force signal value in a manner that relative values are higher for larger scan areas. Consequently the specific size of the scan area should be determined before friction force evaluations and comparison.

The friction signal span shown in Table 1 has lower and upper value which correlates to sample position on can. Samples taken from the cylindrical part have upper values and those taken from the rounded part have approximate but smaller values for all analyzed FFM images. Opposite to those, samples taken from the bottom part have lower values.

The images which belong to groups $5 \times 5 \mu\text{m}$, $3 \times 3 \mu\text{m}$ and $2 \times 2 \mu\text{m}$ of scan area sizes are investigated in detail. The regions of interest are the locations where the topography of the specimen changes, namely, near the grooves and elevations which can be observed in Figure 1 as line-like structures and in Figure 3 as wide light region spreading diagonally.

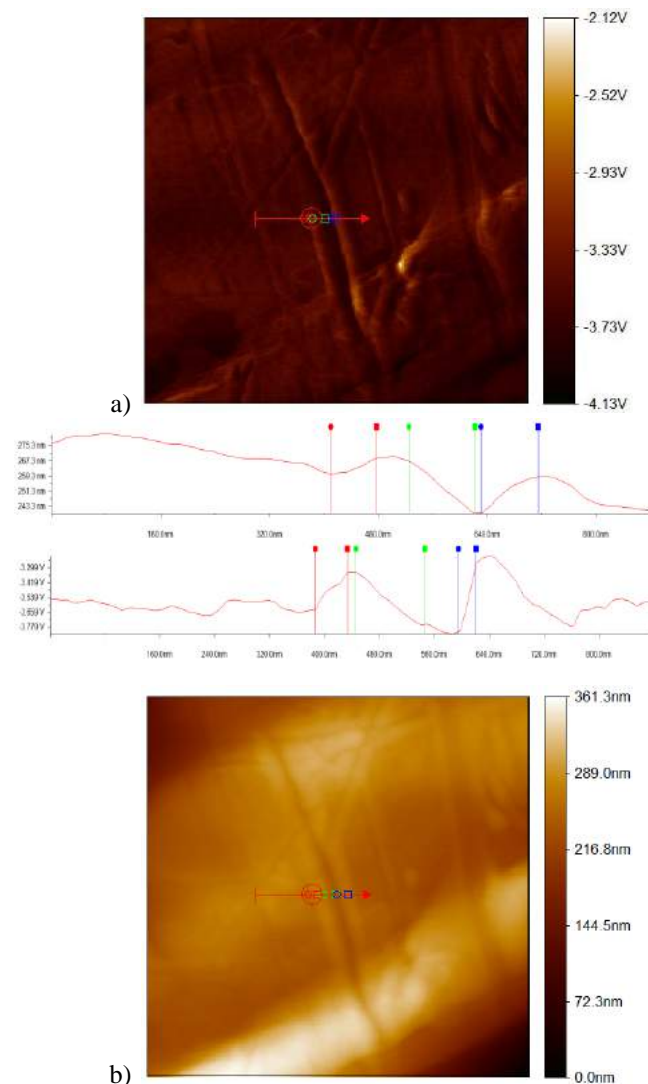


Fig.1. Comparison of AFM (a) and FFM (b) data for scan along the same line of the specimen for surface area $3 \times 3 \mu\text{m}$ (slide direction from left to right)

Figure 1 shows that surface topography significantly affects friction signal values. AFM (a) and FFM (b) data for the scan along the same line of the specimen, gathered in the slide direction from right to left, exhibit spatial shift between the friction signal and the corresponding topography. Friction signal goes ahead compare to topography features. This observed bias is result of the beforehand contact that occurs with conical shape tip resulting curvature radius of 40nm. Observation cannot be admitted by conclusions from [9] due different measure conditions. Bhushan showed that AFM and FFM images spatial shift between the peaks in the lateral force and those in the corresponding topography are resulting from an atomic-scale stick-slip process.

The tip passes across the groove from left to right side (opposite to arrowed line). Friction signal decreases when the tip is moving down the groove (between blue markers in Figure 1), which is in accordance to the step model explanation given in [10]. The explanation is that the friction decreases during sliding down and increases by moving up the step. Recorded friction signal increases when the tip is moving up the pile that formed along the groove (between green markers) and it decreases again (between red markers) when it moves down the pile.

By observing the difference in slope in the friction signal segments between blue and red markers it may be concluded that the friction depends on the surface slope of the roughness profile. Steeper asperities cause a larger slope, as blue marked frictional signal confirms compared to the friction signal segment bordered with red markers. Explanation is given in [11] where the ratchet mechanism theory of friction is described. The friction force depends on the surface slope of the roughness profile and the sensitivity of the variation in the friction force is much higher for relatively larger slopes. This is due to the nature of the tangent function where the value increases gradually, for small angles, and drastically, for relatively large angles. Figure 2 illustrates the ratchet mechanism.

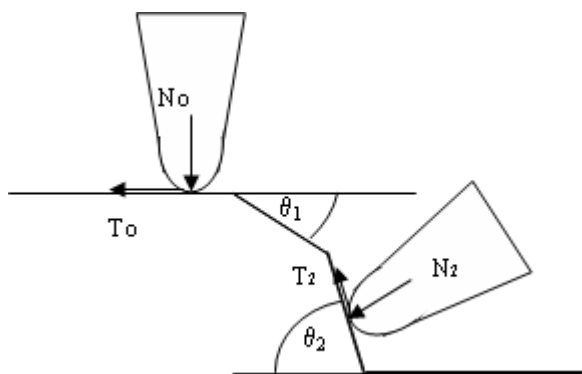


Fig.2. Ratchet mechanism theory of friction (schematic illustration)

In order to prove the effect of surface geometry variation on the friction force, the following equations are given in [12]. Friction force and applied load have different indices in this paper compared to the source.

$$T_n = T_0 \pm N_0 (\operatorname{tg} \theta_n - \operatorname{tg} \theta_{n-1}) \quad (9)$$

where the friction force for a flat surface T_0 , applied load N_0 and friction force on slope surface T_n , normal force N_n . The angles in (1) θ_n, θ_{n-1} are defined as absolute values of slope angle which neighbor each other. The plus sign is assigned for positive slope, and the minus sign for negative slope.

Taking into account that the friction force signal is shifted and for further analyses, images presented in Figure 3 show the friction signal profile (b), and adjusted to roughness profile (a).

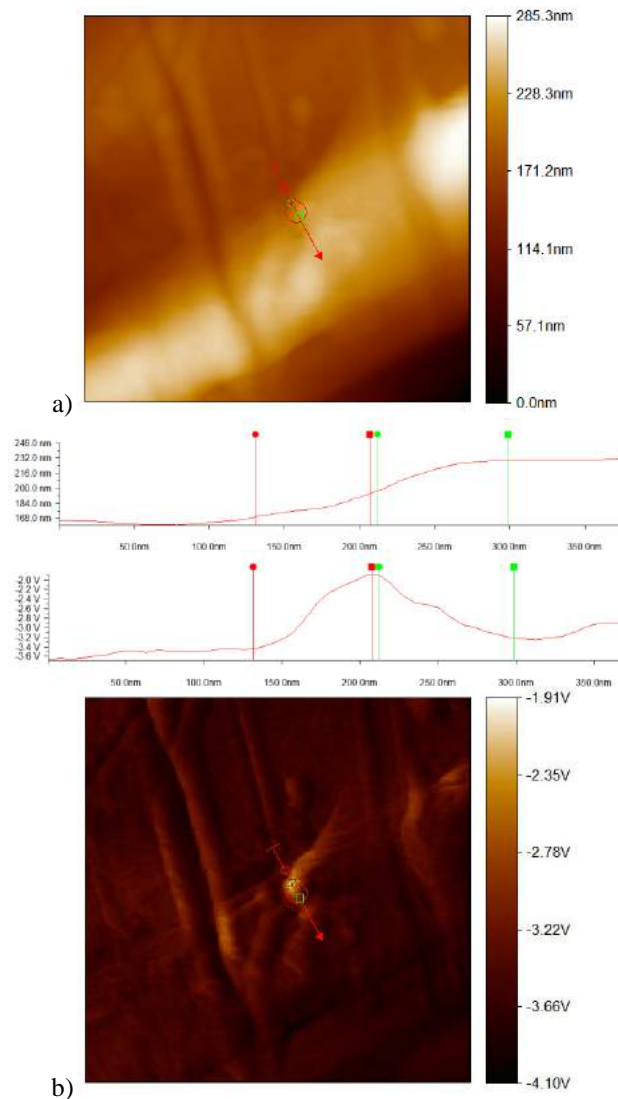


Fig.3. Comparison of AFM (a) and FFM (b) data for scan along the same line of the specimen for surface area $2 \times 2 \mu\text{m}$

It can be seen in Figure 3 that the friction signal becomes higher if the tip moves up – elevates (between red markers). The friction signal is supposed to increase all way upward, but suddenly it decreases. In Figure 3 the change in friction signal is significant between green markers, where the degree of slope decreases. Furthermore, the change in the force signal is evident in the FFM image (Figure 3b) and does not match any change in surface topography except the negative change

of slope. Such findings have already been observed in [12] and explain the frictional behavior where the variation in the friction force depends on the change in slope rather than the magnitude.

4. CONCLUSION

This paper presents frictional force signal deviation scanned by frictional force microscopy. Sample images are gathered from cans made by deep drawing from the cylindrical, rounded and bottom part of seven different cans. The major conclusions are:

- Scan area size influences the friction force signal value in a manner that relative values are higher for larger scan areas. Consequently the specific size of the scan area should be determined before friction force evaluations and comparison.
- The regions where significant changes in the friction signal are evident are locations where the topography of the specimen changes, namely, near grooves and elevations.
- Scans along the same line of the specimen, exhibit spatial shift between the friction signal and the corresponding topography due to the tip geometry.
- Friction depends on the surface slope of the roughness profile. Friction signal decreases during sliding downward and increases while sliding upward due to the nature of tangent function.
- Unexpected frictional behavior is observed where the change in slope, rather than the magnitude, causes the variation in the friction force.

The friction force signal recorded by FFM gathered from an engineered surface produced by deep drawing process exhibits behavior determined by surface topology. All findings presented here are in accordance to investigations presented in [6-12] regardless that those experiments were prevalent conducted on structured surfaces, with an asperity defined geometry. It is essential for good understanding of tribological processes at the micro and nano scales, regarding real engineered surfaces made by conventional manufacturing processes.

The presented work is the start of a four-year project. As concluded in this paper, the friction force values defined by Amonton's law should be used with caution in material selection, in simulations, and in theoretical modeling. Embedding the deviation of friction force into CAD/CAE/CAPP can provide more efficient and accurate, low cost engineering solutions for deep drawing engineering and production.

ACKNOWLEDGEMENT

The paper is a part of the research financed by The Serbian Government, The Ministry of Science and Technological Development. Project title: *An innovative, ecologically based approach to implementation of intelligent manufacturing systems for production of sheet metal parts* (TR-35004).

REFERENCES

- [1] Colgan, M., Monaghan, J. (2003) *Deep drawing process: analysis and experiment*, Journal of Materials Processing Technology Vol. 132, pp 35–41
- [2] Xu, Y. (2004) *Universal formability technology and applications*, Journal of Materials Processing Technology Vol. 151, pp 119–125
- [3] Zhang, S., Hodgson, P.D., Cardew-Hall, M.J., Kalyanasundaram, S. (2003) *A finite element simulation of micro-mechanical frictional behaviour in metal forming*, Journal of Materials Processing Technology Vol. 134, pp 81–91
- [4] Lee, J.M., Ko, D.C., Lee, K.S., Kim, B.M. (2007) *Identification of the bulk behavior of coatings by nano-indentation test and FE-analysis and its application to forming analysis of the coated steel sheet*, Journal of Materials Processing Technology Vol. 187-188, pp 309–313
- [5] Lee, B.H., Keum, Y.T., Wagoner, R.H. (2002) *Modeling of the friction caused by lubrication and surface roughness in sheet metal forming*, Journal of Materials Processing Technology Vol. 130-131, pp 60–63
- [6] Sung, I.H., Lee, H.S., Kim, D.E. (2003) *Effect of surface topography on the frictional behavior at the micro/nano-scale*, Wear Vol. 254 1019–1031
- [7] Achanta, S., Liskiewicz, T., Drees D., Celis, J.-P. (2009) *Friction mechanisms at the micro-scale*, Tribology International Vol. 42, pp. 1792–1799
- [8] Rudermann, Y., Iost, A., Biggerelle, M. (2011) *Scratch tests to contribute designing performance maps of multilayer polymeric coatings*, Tribology International Vol. 44, pp. 585–591
- [9] Bhushan, B. (2005) *Nanotribology and nanomechanics*, Wear Vol. 259, pp. 1507-1531
- [10] Santner, E., Klaffke, D., Meine, K., Polaczyk, Ch., Spaltmann, D. (2006) *Demonstration of topography modification by friction processes and vice versa*, Tribology International Vol. 39, pp. 450–455
- [11] Achanta, S., Liskiewicz, T., Drees D., Celis, J.-P. (2009) *Friction mechanisms at the micro-scale*, Tribology International Vol. 42, pp. 1792–1799
- [12] Sung, I.H., Lee, H.S., Kim, D.E. (2003) *Effect of surface topography on the frictional behavior at the micro/nano-scale*, Wear Vol. 254, pp. 1019–1031

34th INTERNATIONAL CONFERENCE ON PRODUCTION ENGINEERING



**PREVIOUS WINNERS OF THE CHARTER AND PLAQUE
"Professor dr Pavle Stanković"**



**PREVIOUS WINNERS OF THE CHARTER AND PLAQUE
"Professor dr Pavle Stanković"**

For 1983

Prof. dr Rudolf Zdenković, dipl. ing., Fakultet strojnictva i brodogradnje, Zagreb
Prof. dr Vladimir Šolaja, dip. ingl., Mašinski fakultet, Beograd
Prof. dr Julije Kirner, dipl. ing., Fakultet tehničkih nauka, Novi Sad

For 1984

Prof. dr Janez Peklenik, dipl. ing., Fakultet za strojnictvo, Ljubljana
Prof. dr Binko Musafija, dipl. ing., Mašinski fakultet, Sarajevo

For 1985

Prof. dr Predrag Popović, dipl. ing., Mašinski fakultet, Niš
Prof. dr Vladimir Milačić, dipl. ing., Mašinski fakultet, Beograd

For 1986

Prof. dr Branko Ivković, dipl. ing., Mašinski fakultet, Kragujevac
Prof. dr Strezo Trajkovski, dipl. ing., Mašinski fakultet, Skoplje

For 1987

Prof. dr Svetislav Zarić, dipl. ing., Mašinski fakultet, Beograd
Prof. dr Iosip Hribar, dipl. ing., Fakultet strojnictva i brodogradnje, Zagreb

For 1988

Prof. dr Branislav Deverdzić, dipl. ing., Mašinski fakultet, Kragujevac
Prof. dr Elso Kuljanić, dipl. ing., Mašinski fakultet, Rijeka
Prof. dr Zoran Seljak, dipl. ing., Fakultet za strojnictvo, Ljubljana

For 1992

Prof. dr Jozef Rekecki, dipl. ing., Fakultet tehničkih nauka, Novi Sad
Prof. dr Sava Sekulić, dipl. ing., Fakultet tehničkih nauka, Novi Sad
Prof. dr Joko Stanić, dipl. ing., Mašinski fakultet, Beograd
Prof. dr Vlado Vujović, dipl. ing., Fakultet tehničkih nauka, Novi Sad

For 1994

Mile Benedetić, dipl. ing., LOLA Institut, Beograd
Prof. dr Vuko Domazetović, dipl. ing., Mašinski fakultet, Podgorica
Prof. dr Milenko Jovičić, dipl. ing., Mašinski fakultet, Beograd



34th INTERNATIONAL CONFERENCE ON
PRODUCTION ENGINEERING
29. - 30. September 2011, Niš, Serbia
University of Niš, Faculty of Mechanical Engineering



For 1996

Prof. dr Milisav Kalajdžić, dipl. ing., Mašinski fakultet, Beograd
Prof. dr Dragutin Zelenović, dipl. ing., Fakultet tehničkih nauka, Novi Sad

For 1998

Prof. dr Ratko Gatalo, dipl. ing., Fakultet tehničkih nauka, Novi Sad
Prof. dr Vučko Mečanin, dipl. ing., Mašinski fakultet, Kraljevo

For 2000

Prof. dr Mihailo Milojević, dipl. ing., Mašinski fakultet, Kraljevo
Prof. dr Dragoje Milikić, dipl. ing., Fakultet tehničkih nauka, Novi Sad

For 2002

Prof. dr Vojislav Stoiljković, dipl. ing., Mašinski fakultet, Nis
Prof. dr Ilija Ćosić, Fakultet tehničkih nauka, Novi Sad

For 2005

Prof. dr Dragan Domazet, dipl. ing., Mašinski fakultet, Niš
Prof. dr Pavao Bojanić, dipl. ing., Mašinski fakultet, Beograd

For 2006

Prof. dr Miroslav Plančak, dipl. ing., Fakultet tehničkih nauka, Novi Sad
Prof. dr Ratomir Ječmenica, dipl. ing., Tehnički fakultet, Čačak

For 2008

Prof. dr Dragan Milutinović, dipl. ing., Mašinski fakultet, Beograd
Prof. dr Milentije Stefanović, dipl. ing., Mašinski fakultet, Kragujevac

For 2009

Prof. dr Sergey A. Klimenko, dipl. ing., Mechanical and Technological Department of the
Bryansk Transport Machine-Building Institute
Prof. dr Velibor Marinković, dipl. ing., Univerzitet u Nišu, Mašinski fakultet u Nišu
Prof. dr Velimir Todić, dipl. ing., Fakultet tehničkih nauka, Novi Sad



Prof. Dr. Sci. (Eng.) Sergey A. Klimenko



S. A. Klimenko was born in 1956 in Bryansk (Russian Federation). In 1973 he finished school and entered the Mechanical and Technological Department of the Bryansk Transport Machine-Building Institute (at present – the Bryansk State Technical University), which he graduated in 1978 with an honour. S. A. Klimenko got qualification of the mechanical engineer on speciality «Technology of machine-building, metalcutting tools and instruments».

In August 1978 S. A. Klimenko started working career in the Institute of Superhard Materials of UkrSSR Academy of Sciences (at present – the V. Bakul Institute for Superhard Materials of the National Academy of Sciences of Ukraine), where he has been working as an engineer-probationer, engineer, junior researcher, researcher, senior researcher, Head of the Department. Since February 2006 up to now he has been a Deputy Director of Science of the V. Bakul Institute for Superhard Materials of the National Academy of Sciences of Ukraine.

In September 1986 S. A. Klimenko defended his Cand. Sci. dissertation, in April 1999 – Doctor Science (Engineering) dissertation.

In 1993 he was assigned the academic rank «Senior researcher».

Since 1999 he has also worked as a lector of the Zhytomyr State Technological University. In 2003–2004 he worked as a lector of the National Technical University of Ukraine “Kyiv Polytechnic Institute”, since 2006 to 2010 – as a lector of the Donbass State Machine-Building Academy.

In 2003 he was awarded the academic rank “Associate Professor”, in 2006 – the academic rank «Professor». In the same year S.A. Klimenko was elected the Full Member (Academician) of the Academy of Technological Sciences of Ukraine.

Since 2005 he has been the Head of the State Examination Commission of the National Technical University of Ukraine “Kyiv Polytechnic Institute”.

Four doctoral dissertations on engineering sciences have been written and defended under his direct supervision.

Since 1993 up to present S. A. Klimenko has been – the CEO of the All-Ukrainian public organization “Association of machine-building technologists of Ukraine”. In 1996 he has become an Academic Secretary of the specialized section “Machine-building and transport” of the Committee of State Prizes of Ukraine.

S.A. Klimenko is member of Editorial Council of the number of scientific and technical journals of Belarus, Russia, Serbia, Ukraine.

S. A. Klimenko is a laureate of the Prizes of the National Academy of Sciences of Ukraine, The National Academy of Sciences of Belarus, The Academy of Sciences of Moldova (2008). The Union of scientific institutes of machine-building of Serbia acknowledged him with the Diploma and Sign of «Prof. Dr. Paul Stankovic» (2009).

S.A. Klimenko was awarded with the State Prizes in science and technology of Ukraine for his scientific achievements (2008).

The results of his studies are published in more than 650 scientific publications, among which there are 17 monographs and text editions, 40 patents of the USSR, Belarus, Russia, Serbia, Ukraine.



34th INTERNATIONAL CONFERENCE ON
PRODUCTION ENGINEERING
29. - 30. September 2011, Niš, Serbia
University of Niš, Faculty of Mechanical Engineering



Prof. Velimir Todić, PhD, mech. eng.

Dr. Velimir Todić was born on 30.10.1946. in Donja Podgorija, Mrkonjic Grad, Republika Srpska, Bosnia-Herzegovina. He finished primary school in 1961 in Barači and secondary technical-mechanical school in 1965 in Bečej. He enrolled at Faculty of Mechanical Engineering in Novi Sad in academic year 1965/66 where he graduated on 20.10.1970 at the Department of production engineering. He defended his master's thesis in 1978 at the Faculty of Technical Sciences in Novi Sad, and the PhD dissertation in 1987 at the same university.



After graduation he obtained the degree of dipl. eng. and on 01.01.1971 started working as a research assistant at the Institute of Mechanical Engineering in Novi Sad. After military service, on 01.09.1972 he was elected as teaching assistant at the Faculty of Engineering in Novi Sad, teaching the subject Manufacturing processes and tools. On 03.11.1988 he was elected the assistant professor, on 15.11.1993 associate professor, and full professor on 01.07.1998. He has held classes at undergraduate level, teaching the following subjects: Manufacturing processes and Techno-economic optimization and a part of the course Accessories and Measurement and control. At master's degree studies he was involved in teaching of the subjects Techno-economic optimization theory, Automation of manufacturing processes design and Techno-economic optimization and partly in subjects Automaton of product design and Optimization of product design. Now he holds a course in Design of manufacturing processes, Technological logistics and entrepreneurship, Integrated CAPP systems and Manufacturing database, Internet technology in production engineering, Entrepreneurship in small and medium enterprises and a part of course in Computer integrated manufacturing, Tool manufacturing technologies for plastics, Information technology in the plastic processing industry.

At the Department of computer aided manufacturing systems and design processes he introduced the subjects Techno-economic optimization, Logistics and manufacturing entrepreneurship, Integrated CAPP systems and manufacturing database, Internet technology in production engineering, Entrepreneurship in small and medium enterprises and a module from the subject of Computer integrated manufacturing, Technology of plastic tools manufacturing, Information technology in plastic processing industry.

During his teaching activity prof. Todić mentored over 80 graduate and undergraduate-master works and participated in the defense of over 300 works. He was a mentor to two master's theses and participated in committees for defense of a number of theses at the Faculty of Technical Sciences in Novi Sad and other mechanical faculties in the country. He now mentors three doctoral dissertations, and he also participated in the evaluation committees and in the defense of several doctoral dissertations at the Faculty of Technical Sciences.

As a researcher and manager he participated in over 50 projects in the field of production engineering. He has published over 200 scientific papers in scientific and professional conferences in the country and abroad and in domestic and international journals, especially in the field of design and optimization of manufacturing processes and automation of manufacturing processes design. He is the author of three university textbooks and one scientific publication.

Professional work of Dr. Todić is contained in more than 30 research projects, expert reviews, prototypes, new methods, software and solutions to improve existing products and technologies, of which the largest number is made for the industry. He was on a study visit to Germany in 1983, where he visited a number of university centers of this country. He was the organizer of a number of scientific conferences in the country. He is a member of the Executive Board of the Community of scientific and research institutions of production engineering in Serbia. He was for many years the president of the jury of the Metalworkers competition of Novi Sad, Serbia.

He was Vice Dean for Development, scientific research and Finance, at Faculty of Technical Sciences, Associate Director of the Institute for Production Engineering. Member of the Teaching and Research Council of the Faculty of Engineering and Head of the Department of computer aided systems and manufacturing processes in the last three mandates. He received the Plaque and the Charter Dr. Pavle Stankovic.



34th INTERNATIONAL CONFERENCE ON
PRODUCTION ENGINEERING
29. - 30. September 2011, Niš, Serbia
University of Niš, Faculty of Mechanical Engineering



Prof. Velibor Marinković, PhD, mech.eng.

Velibor Marinkovic, PhD, dipl.ing., was born on April 2, 1947. in Krezbinac, Paracin municipality, Serbia. Since 1966. he lives and works in Nis. He finished technical school in Svetozarevo (Jagodina) in year 1966th. In same year he enrolled at the Faculty of Engineering (Mechanical Department), University of Nis. He completed the studies in time and successfully defended his bachelor work on July 1, 1971.



In academic year 1972/73 he started the postgraduate studies in the field of production engineering. He finished the studies by defending his master thesis in year 1978. at the Faculty of Mechanical Engineering in Niš.

His defended the doctoral thesis entitled: "The research of material flow in the cold bulk forming processes" at Faculty of Mechanical Engineering in Nis in year 1982, in front of the Committee consisting of: Prof. Dr. Predrag Popovic, Prof. Branislav Devedžić, Prof. Vlado Vujovic.

Dr. Velibor Marinkovic was elected as an assistant at the Department of Production Engineering Mechanical Engineering in Nis in year 1971. As the assistant professor for the course of Machining he was elected in 1983., at the same University. From March 1996 he is the owner of the title of full professor.

Since April 1974 until April 1975 he was on military service. In 1975 he spent a month at the Technical College in Chemnitz, Germany.

Scientific and technical research by Velibor Marinkovic include the following areas: metal forming technologies, metal cutting technologies, theory of experiment desing and metrology, tribology of machining processes, modeling and optimization of machining processes and artificial neural networks.

As a teacher he was engaged in teaching of the following subjects: machining; measurement and quality control, machine tools I, production technologies I, production technologies II and modeling and optimization of production processes.

He was also engaged in teaching of a number of subjects at post-graduate studies at Production engineering profile and now at the accredited doctoral studies.

Under his direction about a hundred graduate works, one master's theses and one doctoral dissertation have been done. He was also a member of a number of the evaluation committees for the defense of master's theses and doctoral dissertations, at the faculty of Mechanical Engineering in Niš and other faculties in the country.

As the author he has published more than 40 papers in international and domestic journals and proceedings of international and national scientific and professional meetings and conferences, and dozens of papers in the role of co-author. He took part in 16 annual production engineering conferences of Yugoslavia / Serbia.

He is the author of one monograph and three textbooks. He is also a reviewer of two monographs, four textbooks and numerous scientific papers for journals. He has also reviewed the projects financed by the Ministry of Science and Technology of the Republic of Serbia. He participated in the realization of numerous scientific research and innovation projects, as well as commercial ones.

In addition to his scientific and professional activities, prof. Velibor Marinkovic was engaged in other activities and functions, such as: Head of the Chair for Production Engineering in two mandates, head of the Laboratory for Machine tools and machining, a member of the Scientific and Expert Council for technical and technological sciences at University of Nis, a member of the Council of Faculty of Mechanical Engineering in Nis, a member of the Executive Board of the Community of scientific-research institutions of production engineering in Yugoslavia / Serbia, a member of the Jury of the competition of Metalworkers of Serbia and so on.

For the results achieved during his work, Dr. Velibor Marinković won many awards: Plaque and the Charter of the University of Nis for the success at the studies, Little plaque of University of Nis for his contribution to the development of Faculty of Mechanical Engineering and the University of Nis, Silver plaque of Faculty of Mechanical Engineering in Nis for outstanding contribution to the development of faculty and others.

34th INTERNATIONAL CONFERENCE ON PRODUCTION ENGINEERING



AUTHOR INDEX



AUTHOR INDEX

A

Aco ANTIC	65
Adrian GHIONE	205
Aleksandar IVIĆ	407
Aleksandar MILETIĆ	79, 83, 527
Aleksandar SEDMAK	481
Aleksandar TODIĆ	99
Aleksandar ŽIVKOVIĆ	65, 477
Alexander PYNKIN	449
Alexis AUBRY	399
Alin Dan JURCHELA	75
Aljoša INAVIŠEVIĆ	309
Aljosa IVANISEVIC	301, 499
Anđela LAZAREVIĆ	425, 515
Andraš ANDERLA	407
Andreja ILIĆ	465
Anka TRAJKOVSKA PETKOSKA	485
Asim JUŠIĆ	297
Atanas KOČOV	175

B

B. SREDANOVIC	117
Baila DIANA	49
Bato KAMBEROVIĆ	155
Biljana SAVIĆ	103
Boban CVETANOVIĆ	223
Bogdan ĆIRKOVIĆ	99, 121
Bogdan NEDIĆ	87, 439, 443
Bogdan SOVILJ	523
Bojan BABIĆ	389, 531
Bojan MEDJO	481
Bojan RANČIĆ	163, 267, 281, 285
Bojana ROSIĆ	343
Borislav SAVKOVIC	417
Bozica BOJOVIC	531
Božidar KRSTIĆ	469, 473
Branislav JEREMIĆ	421
Branislav SREDANOVIĆ	197
Branka DIMITRIJEVIĆ	239
Branko KOKOTOVIC	381
Branko PEJOVIĆ	99
Branko RADIČEVIĆ	151
Branko RISTIĆ	331, 347, 189
Branko ŠKORIĆ	79, 83
Branko STRBAC	143
Branko U. TADIĆ	393

C

Cristian TARBA	205
Cvijan KRSMANOVIĆ	407
Cvijetin MLAĐENOVIĆ	113

D

Dalibor NIKOLIĆ	331
Dalibor PETKOVIĆ	385
Dalibor STEVANOVIĆ	355
Damir KAKAŠ	79, 83, 527
Danica JOSIFOVIĆ	465
Darko LOVREC	253, 507, 511
Darko STEFANOVIĆ	407
Davorin KRAMAR	489
Dejan ČIKARA	99
Dejan DIVAC	319, 323, 327, 403
Dejan LAZAREVIC	305
Dejan LUKIĆ	109
Dejan MOMČILOVIĆ	457
Dejan MOVRIN	301, 315, 495
Dejan PETROVIĆ	359
Desimir JOVANOVIĆ	87
Dijana NADAREVIĆ	53
Dorian MARJANOVIĆ	13
Dragan ADAMOVIĆ	277, 289, 421, 503, 519
Dragan ALEKSENDRIĆ	365
Dragan DŽUNIĆ	519
Dragan MARINKOVIĆ	201
Dragan MILČIĆ	477
Dragan MILKOVIĆ	365
Dragan MILOSAVLJEVIĆ	469, 473
Dragan MILUTINOVIĆ	381
Dragan MISIĆ	243, 355
Dragan RAJNOVIC	91, 231
Dragan TEMELJKOVSKI	267, 281
Dragisa VILOTIĆ	301, 309
Dragoljub LAZAREVIC	425, 515
Dragoljub ŽIVKOVIĆ	159
Dragutin LISJAK	125
Dubravka MARKOVIĆ	309, 315
Dusan JOVANIC	461
Dusan KOJIC	531
Dušan KRAVEC	369

Đ

Đorđe ČIČA	117, 197
Đorđe ČUPKOVIĆ	495
Đorđe VUKELIĆ	213



34th INTERNATIONAL CONFERENCE ON
PRODUCTION ENGINEERING
29. - 30. September 2011, Niš, Serbia
University of Niš, Faculty of Mechanical Engineering



E, F

Elena ZEVELEVA	453
Emil VEG	103
Fatima ŽIVIĆ	519
Franc CUS	29

G, H

G. LAKIĆ-GLOBOČKI	117
George GRUJOVIC	323
Gheorghe BRABIE	273
Goran DEVEDŽIĆ	189, 235, 347
Goran MLADENOVIC	41
Goran RADENKOVIĆ	69, 481
Goran SLAVKOVIĆ	257
Gordana BOGDANOVI	469, 473
Gordana GLOBOČKI LAKIĆ	197
Gordana LAKIĆ GLOBOČKI	87
Guenther POSZVEK	263
Hervé PANETTO	3, 399

I

Igor BEŠIĆ	185
Igor BUDAK	143
Igor KAČMARČIK	495, 499
Ilare BORDEASU	75
Ile MIRCHESKI	227
Ioan TĂNASE	205
Ion MITELEA	75
Ionuț GHIONEA	205
Irina BEŠLIU	413
Ivan DANILOV	217
Ivan KOLEV	523
Ivan MATIN	213
Ivan MILICEVIC	193
Ivan SAMARDŽIĆ	523
Ivan SOVILJ-NIKIĆ	523
Ivana ATANASOVSKA	457
Ivica ČAMAGIĆ	99, 121

J

Ján SLAMKA	373
Jan STRBKA	133
Janez KOPAČ	489
Janko HODOLIC	143, 185, 213
Jasmina ČALOSKA	175
Jasna RADULOVIĆ	95
Jelena BARALIĆ	435, 439, 443
Jelena BOROTA	319, 323, 327, 403
Jelena MICEVSKA	175, 227
Jelena MILOVANOVIĆ	209, 335, 351
Jelena VIDAKOVIĆ	129
Jozef BARNA	181

Jozef NOVAK-MARCINCIN	181
Jozef PETERKA	61
Jožef PREDAN	481

K, L, Lj

Konstantinos PAPANIKOLOPOULOS	403
Krzysztof STĘPIEN	147
L. KOVAČEVIĆ	83
Laurențiu SLĂTINEANU	413
Lazar KOVAČEVIĆ	79, 527
Lenka CEPOVA	133
Leonid AKULOVICH	449
Leposava SIDJANIN	231
Leposava SIDJANIN	91, 231
Lorelei GHERMAN	413
Lozica IVANOVIĆ	465
Lj. TANOVIĆ	33, 41
Ljiljana TIHAČEK-ŠOJIĆ	359
Ljubinko CVETKOVIĆ	151

M

M. MILUTINOVIĆ	33
Manfred ZEHN	201
Marek ZVONČAN	61
Margareta COTEAȚĂ	413
Marián TOLNAY	369, 373
Marin GOSTIMIROVIC	57, 417
Mario LEZOCHÉ	399
Marko ANDJELKOVIĆ	359
Marko KOVAČEVIĆ	45
Marko PANTIĆ	519
Marko POPOVIC	193
Marko RAKIN	481
Marko VESELINOVIC	355
Marko VILOTIĆ	79, 83, 527
Martin KOVÁČ	61
Michael KHEIFETZ	449, 453
Michal JEDINÁK	373
Michal POTRAN	309
Michele FIORENTINO	189
Mihajlo POPOVIC	41
Mijodrag MILOŠEVIĆ	109
Miladin Ž. STEFANOVIĆ	393
Milan BLAGOJEVI	139, 343
Milan ERIĆ	235, 393
Milan DELIĆ	155
Milan JURKOVIĆ	297
Milan KOLAREVIĆ	151
Milan LAZAREVIC	305
Milan RADOVIĆ	323
Milan ŠLJIVIĆ	319
Milan TRIFUNOVIĆ	209, 335, 355
Milan ZDRAVKOVIC	243, 399



34th INTERNATIONAL CONFERENCE ON
PRODUCTION ENGINEERING
29. - 30. September 2011, Niš, Serbia
University of Niš, Faculty of Mechanical Engineering



Milan ZELJKOVIĆ	65, 113, 117	P	
Milenko SEKULIĆ	417	Pal TEREK	79, 83, 527
Milentije STEFANOVIĆ	277, 289, 421, 503	Pavao BOJANIĆ	41
Milica DAMJANOVIĆ	231	Pavel KOVAČ	57, 417
Milica PETROVIĆ	389, 531	Peđa MILOSAVLJEVIĆ	159
Milorad RANČIĆ	377	Petar PETROVIĆ	15, 217
Miloš ĆIROVIĆ	235, 347	Petar ĐEKIĆ	267
Milos GLAVONJIC	381	Plavka SKAKUN	315, 499
Milos JOVANOVIĆ	305, 461	Predrag ĆOSIĆ	125
Miloš MADIĆ	45, 69, 515	Predrag	
Miloš RISTIĆ	223	JANKOVIĆ	159, 163, 281, 285, 435, 443, 515
Miloš STOJKOVIĆ	209, 335, 243	Predrag PETROVIĆ	95
Milovan RADOSAVLJEVIĆ	331	Predrag POPOVIĆ	267
Miodrag HADŽISTEVIĆ	57, 143, 213	R	
Miodrag MANIĆ	223, 235, 351, 355, 425	Rade IVANKOVIĆ	37
Miodrag STOJILJKOVIĆ	377	Radivoje MITROVIĆ	457
Miomir VUKIĆEVIĆ	151	Radmila JOVANOVIĆ	155
Mircea Octavian POPOVICIU	75	Radomir RADIŠA	193
Mirko SOKOVIĆ	53, 489	Radomir SLAVKOVIĆ	103, 193
Miroslav BABIĆ	519	Radomir VUKASOJEVIĆ	339
Miroslav JANAK	181	Radovan ĆIRIĆ	103
Miroslav MIJAJLOVIĆ	477	Radovan PUZOVIĆ	41
Miroslav PAJIC	365	Rajko ČUKIĆ	469, 473
Miroslav PILIPOVIĆ	217	Ranko BOŽIČKOVIĆ	293
Miroslav PLANCAK	301, 315, 495	Ranko RADONJIĆ	293
Miroslav R.		Ratko GATALO	113
RADOVANOVIĆ	69, 413, 431, 435, 439	Remigiusz LABUDZKI	171
Miroslav TRAJANOVIĆ	209, 243, 335, 355, 399	Robert CEP	133
Miroslav VASIĆ	129	Rok JUSTIN	489
Miroslav ŽIVKOVIĆ	139, 289, 343	S	
Mišo BJELIĆ	151	S. BOROJEVIĆ	117
Mladimir MILUTINOVIĆ	301, 309, 499	Sandira ELJŠAN	249
Najdan VUKOVIĆ	389	Sandra SOVILJ-NIKIĆ	523
Natalia POZILOVA	449	Saša ĆUKOVIĆ	189, 235, 347
Nebojša ČOVIĆ	389	Sasa RANDJELOVIĆ	305
Neculai NANU	273	Sasa ZIVANOVIĆ	381
Nedim GANIBEGOVIĆ	249	Sebastian BALOS	91, 231
Nemanja VASIĆ	121	Sergej ALEXANDROV	301
Nenad D. PAVLOVIĆ	385	Simo ŠALETIĆ	339
Nenad FILIPOVIĆ	331, 359	Slavenko M. STOJADINOVIC	167
Nenad GRUJOVIĆ	319, 323, 327, 403	Slaviša ĐAČIĆ	289, 503
Nenad GUBELJAK	481	Slaviša PLANIĆ	163
Nikola KORUNOVIĆ	209, 335, 351	Slobodan MITROVIĆ	519, 393
Nikola LUKIĆ	217	Slobodan TABAKOVIĆ	113
Nikola MILIVOJEVIĆ	327, 403	Sofija SIDORENKO	227
Nikola SLAVKOVIĆ	381	Srbislav	
Nikola VITKOVIĆ	209, 243, 351	ALEKSANDROVIĆ	277, 289, 421, 469, 473, 503
O		Srdan MLADENOVIĆ	159, 163, 431
Obrad SPAIĆ	37	Srdan VULANOVIĆ	155
Ognjan LUŽANIN	315, 499	Stanislaw LEGUTKO	523
Olivera ERIĆ	91, 231, 457	Štefan POTÂRNICHE	413
Ondrej STAŠ	369		



34th INTERNATIONAL CONFERENCE ON
PRODUCTION ENGINEERING
29. - 30. September 2011, Niš, Serbia
University of Niš, Faculty of Mechanical Engineering



Stevo BOROJEVIĆ	197
Stojanka ARSIC	355
Suzana PETROVIĆ	189, 235, 347

T, U

Tadej TAŠNER	253
Tanja LUKOVIĆ	189
Tatjana PUŠKAR	309
Tatjana PUŠKAR	185, 315
Tomaž PEPELNJAK	499
Tomislav TODIĆ	99
Tomislav VUJINOVIC	277
Uros ZUPERL	29

V

Valentina LATIN	125
Velibor MARINKOVIĆ	45, 285
Velimir KOMADINIĆ	129
Velimir TODIĆ	109
Veronika FECOVA	181
Vesna MANDIĆ	297
Vesna RANKOVIĆ	319, 403
Viacheslav KRUTSKO	453
Victor GAIKO	453
Vid JOVIŠEVIĆ	197
Vidosav D. MAJSTOROVIĆ	5, 167
Vito TIĆ	507, 511
Vladan RADLOVAČKI	155
Vladimir BORODAVKO	453
Vladimir ČARAPIĆ	129
Vladimir KANJEVAC	323
Vladimir KVRGIĆ	129
Vladimir MILIVOJEVIĆ	327
Vladimir R. MILACIC	15
Vladimir SIMIĆ	239
Vladislav BLAGOJEVIĆ	377
Vukić LAZIĆ	277, 465, 469, 473

Z, Ž

Zdravko BOŽIČKOVIĆ	293
Zdravko KRIVOKAPIĆ	37
Zoran DIMIC	381
Zoran JOVANOVIĆ	347
Zoran JURKOVIĆ	57, 297
Zoran MILJKOVIĆ	389, 531
Zoran SPIROSKI	175
Zvonimir JUGOVIĆ	103, 193
Zvonko GULIŠIJA	289
Žarko SPASIĆ	257
Željko EREMIC	461
Željko RAIČEVIĆ	339
Živana JAKOVLJEVIC	365

CIP - Каталогизација у публикацији
Народна библиотека Србије, Београд

621.7/.9(082)

621.7/.9:669(082)

681.5(082)

005.6(082)

004.896(082)

INTERNATIONAL Conference on Production
Engineering (34 ; 2011 ; Niš)

Proceedings / 34th International
Conference of Production Engineering,
September 28-30. 2011, Niš, Serbia ;
[organizer by] University of Niš, Faculty of
Mechanical Engineering, Department for
Production, IT and Management ; [editor,
glavni i odgovorni urednik Miroslav
Trajanović]. - 1. izd. = 1st ed. - Niš :
Mašinski fakultet = Niš : Faculty of
Mechanical Engineering, 2011 (Niš :
Unigraf-x-copy). - XX, 548 str. : ilustr. ;
30 cm

Tekst štampan dvostubačno. - Tiraž 150. -
Str. VII: Foreword / Miroslav Trajanović,
Velibor Marinković. - Sergey A. Klimenko:
str. 539. - Velimir Todić: str. 540. -
Velibor Marinković: str. 541. - Napomene i
bibliografske reference uz tekst. -
Bibliografija uz svaki rad. - Registar.

ISBN 978-86-6055-019-6

1. Mašinski fakultet (Niš)

a) Производно машинство - Зборници b)

Метали - Обрада - Зборници c) Системи

аутоматског управљања - Зборници d)

Управљање квалитетом - Зборници

COBISS.SR-ID 186256140